

Parametric study of cyclic loading effects on the creep behavior of polymers and polymer based composites

by Shane Christian Schumacher

A thesis submitted in partial fulfillment of the requirements for the degree of Master of Science in Mechanical Engineering

Montana State University

© Copyright by Shane Christian Schumacher (2000)

Abstract:

An investigation of the cyclic loading effects on the time dependent response of Nylon 6/6 and a piezoelectric Polyvinylidene Fluoride (PVDF) based composite material is presented. A consistent experimental program has been developed with the main objective to determine the creep behavior of the materials under cyclic loading conditions. An extensive testing procedure employed in this study has involved multiple experimental stages consisting of tensile stress-strain tests, constant load creep tests, and tests under sustained tensile loads with superimposed harmonic oscillations. The creep behavior of Nylon 6/6 and the PVDF based composite has been investigated depending on three loading parameters, mean stress, vibration frequency and amplitude. The study has been performed over a wide range of temperature conditions. The results of this investigation have provided a general view on the cyclic creep response of the materials under investigation, where Nylon 6/6 is a solid polymer and PVDF is an electroded polymer. Nonlinear creep effects induced by cyclic loading conditions have been observed in both materials. The results of the study have demonstrated the limitations of linear viscoelastic theory and have served as a basis for constitutive model development and microstructural analyses of polymers subjected to asymmetric cyclic loading regimes.

PARAMETRIC STUDY OF CYCLIC LOADING EFFECTS ON THE CREEP BEHAVIOR OF POLYMERS AND POLYMER BASED COMPOSITES

by

Shane Christian Schumacher

A thesis submitted in partial fulfillment
of the requirements for the degree

of

Master of Science

in

Mechanical Engineering

Montana State University
Bozeman, Montana

July 2000

© Copyright

by

Shane Christian Schumacher

2000

All Rights Reserved

N378
Sch849

APPROVAL

of a thesis submitted by

Shane Christian Schumacher

This thesis has been read by each member of the thesis committee and has been found to be satisfactory regarding content, English usage, format, citations, bibliographic style, and consistency and is ready for submission for the College of Graduate Studies.

Dr. Aleksandra Vinogradov _____ (Signature) July 17, 2000 Date

Approved for the Department of Mechanical and Industrial Engineering

Dr. Vic Cundy _____ (Signature) 7/17/00 Date

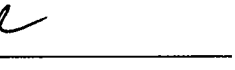
Approved for the College of Graduate Studies

Dr. Bruce McLeod _____ (Signature) 7-19-00 Date

STATEMENT OF PERMISSION TO USE

In presenting this thesis (paper) in partial fulfillment of the requirements for a master's degree at Montana State University, I agree that the Library shall make it available to borrowers under the rules of the Library.

If I have indicated my intention to copyright this thesis (paper) by including a copyright notice page, copying is allowable only for scholarly purposes, consistent with "fair use" as prescribed in the U.S. Copyright Law. Request for permission for extended quotation from or reproduction of this thesis (paper) in whole or in parts may be granted by the copyright holder.

Signature 

Date 7-17-00

Table of Contents

Page

1. INTRODUCTION 1

2. PROPERTIES OF POLYMERS 4

Physical Properties of Polymers 4
Instantaneous Elastic Behavior of Polymers 8
Creep Behavior of Polymers 12
Fatigue Behavior of Polymers 25

3. OVERVIEW OF RESEARCH ON THE CYCLIC RESPONSE OF POLYMERS AND POLYMER BASED COMPOSITES 29

4. GOALS AND OBJECTIVES 33

5. GENERAL APPROACH TO A PARAMETRIC STUDY OF CYCLIC LOADING EFFECTS OF POLYMERS 34

Material Selection 34
Experimental Stages 34
Tensile Testing 35
Constant Load Creep Testing 35
Vibrocreep Testing 36
Post Cyclic Testing 36
Testing Methodology 37
Tensile and Post Cyclic Testing 37
Constant Load Creep Testing 38
Vibrocreep Testing 40
Vibrocreep Criteria 44

6. EXPERIMENTAL PROGRAM AND RESULTS FOR NYLON 6/6 47

Properties and Applications of Nylon 6/6 47
Experimental Program 47
Instrumentation, Equipment, and Data Acquisition 47
Tensile Testing of Nylon 6/6 48
Constant Load Creep Testing of Nylon 6/6 49
Vibrocreep Testing of Nylon 6/6 51
Testing Procedure 55
Tensile Testing Procedure for Nylon 6/6 55
Constant Load Creep Testing Procedure for Nylon 6/6 56

Table of Contents - Continued

Page

Vibrocreep Procedure for Nylon 6/6 56
Post Cyclic Testing Procedure for Nylon 6/6 57
Experimental Results 57
Tensile Testing at 23 °C 57
Constant Load Creep Testing at 23 °C 58
Vibrocreep Testing at 23 °C 59
Post Cyclic Testing at 23 °C 65
Tensile Testing at Elevated Temperatures 67
Constant Load Creep Testing at Elevated Temperatures 69
Vibrocreep Testing at Elevated Temperatures 70
Post Cyclic Testing at Elevated Temperatures 79
Conclusions 82

7. EXPERIMENTAL PROGRAM AND RESULTS FOR PVDF 87

Properties and Applications of PVDF 87
Experimental Program 88
Instrumentation, Equipment, and Data Acquisition 88
Tensile Testing of Nylon PVDF 89
Constant Load Creep and Vibrocreep Testing of PVDF 89
Testing Procedure 92
Tensile Testing Procedure for PVDF 94
Constant Load Creep Testing Procedure for PVDF 94
Vibrocreep Procedure for PVDF 94
Experimental Results 95
Tensile Testing at 23 °C 95
Constant Load Creep Testing at 23 °C 98
Vibrocreep Testing at 23 °C 100
Constant Load Creep Testing at Low Temperatures 104
Vibrocreep Testing at Low Temperatures 107
Conclusions 116

8. STATISTICAL ANALYSIS 118

9. DISCUSSION 121

10. CONCLUSION 127

11. FURTHER RESEARCH 130

Table of Contents - Continued

Page

REFERENCES CITED 131

APPENDICES 138

Appendix A Tensile and Constant Load Creep Testing Results for Nylon 6/6 139
Appendix B Frequency Effects from Vibrocreep Testing of Nylon 6/6 158
Appendix C Amplitude Effects from Vibrocreep Testing of Nylon 6/6 231
Appendix D The Influence of the Parameter μ from Vibrocreep Testing of Nylon 6/6 301
Appendix E Mean Stress Effects from Vibrocreep Testing of Nylon 6/6 329
Appendix F Temperature Effects from Tensile, Constant Load Creep and Vibrocreep Testing of Nylon 6/6 371
Appendix G Post Cyclic Testing Results 404
Appendix H Tensile and Constant Load Creep Testing Results for PVDF 407
Appendix I Frequency Effects from Vibrocreep Testing of PVDF 414
Appendix J Amplitude Effects from Vibrocreep Testing of PVDF 433
Appendix K Mean Stress Effects from Vibrocreep Testing of PVDF 460
Appendix L Temperature Effects from Tensile, Constant Load Creep and Vibrocreep Testing of PVDF 477
Appendix M Statistical Results 502
Appendix N Data Acquisition Programs 539
Appendix O Macros For Data Management 597
Appendix P Manufacture Material Data for Nylon 6/6 and PVDF 606
Appendix Q Instron 1350 Environmental Chamber Design 612
Appendix R Tensile and Creep Environmental Chamber Design 633
Appendix S Creep Testing Equipment Design 643
Appendix T Creep and Vibrocreep Test Fixture for Thin Films 656
Appendix U Ongoing Microstructure Analysis and Model Development Based on Current Work 670

List of Tables

Table		Page
Table 1	Crystal Melt Temperatures of Some Polymer Materials	7
Table 2	Glass Transition Temperatures of Some Polymers	8
Table 3	Testing Summary	37
Table 4	Preliminary Test Matrix for Creep Testing	39
Table 5	Preliminary Test Matrix for Vibrocreep	42
Table 6	Tensile Properties for Nylon 6/6 at 23 °C	58
Table 7	Batch Comparison at 23 °C	58
Table 8	Test Matrix for Nylon 6/6 Vibrocreep Testing at 23 °C	59
Table 9	Tensile Testing of Nylon 6/6 Specimens after Cyclic and Constant Loading at 23 °C	66
Table 10	Tensile Testing of Nylon 6/6 Specimens after Cyclic and Constant Loading at 23 °C	67
Table 11	Tensile Properties of Nylon 6/6 at 23 °C and Elevated Temperatures	68
Table 12	Test Matrix for Nylon 6/6 Vibrocreep Testing at Elevated Temperatures	71
Table 13	Tensile Testing of Nylon 6/6 Specimens after Cyclic and Constant Loading at 41 °C	80
Table 14	Tensile Testing of Nylon 6/6 Specimens after Cyclic and Constant Loading at 41 °C	81
Table 15	Tensile Testing Results for PVDF at 23 °C	96
Table 16	Test Matrix for Vibrocreep Testing of PVDF at 23 °C	100
Table 17	Test Matrix for Vibrocreep Testing of PVDF at -25 °C	108

List of Figures

Figure		Page
Figure 1	Lamella Formation	4
Figure 2	Fibril Formation	5
Figure 3	Spherulite Formation	6
Figure 4	Brittle and Ductile Comparison	9
Figure 5	Temperature Effects on Elastic Modulus of Some Polymer Materials	9
Figure 6	Strain Effects of Strain Rate on Polymer Materials	9
Figure 7	Deformation of spherulites in a Crystalline Structure	10
Figure 8	Lamella Deformation Within a Spherulite	10
Figure 9	Deformation of Molecular Chains in a Amorphous Material	11
Figure 10	Fibril and Lamella Interconnection before Failure	12
Figure 11	Maxwell Model	13
Figure 12	Creep Curve of the Maxwell Model	13
Figure 13	Relaxation Curve of the Maxwell Model	14
Figure 14	Kelvin Model	14
Figure 15	Creep Curve of the Kelvin Model	15
Figure 16	Relaxation Curve of the Kelvin Model	16
Figure 17	Burger Model	16
Figure 18	Creep Curve of the Burger Model	17
Figure 19	Relaxation Curve of the Burger Model	17

List of Figures - Continued

Figure		Page
Figure 20	Step Load History and Resulting Strain	18
Figure 21	Continuous Loading History and Resulting Strain	19
Figure 22	Creep Curves of the Same Polymer at Different Stress Levels	20
Figure 23	Normalized Creep Curves Showing Linear Viscoelasticity	21
Figure 24	Periodic Strain and Stress	22
Figure 25	Creep Strain at Multiple Temperatures	24
Figure 26	Shifting the Temperature Curves to the Reference Temperature	24
Figure 27	Stress Amplitude vs. Cycles to Failure	28
Figure 28	Periodic Stress	43
Figure 29	Periodic Strain	44
Figure 30	Resulting Hysteresis Loop	44
Figure 31	Loading Diagram for Vibrocreep	45
Figure 32	Vibrocreep Effect Above or Below the Linear Viscoelastic Limit	45
Figure 33	Normalized Vibrocreep Effect Within the Linear Viscoelastic Limit	46
Figure 34	Creep Test Fixture for Nylon 6/6	51
Figure 35	Vibrocreep Test Fixture for Nylon 6/6	54
Figure 36	Constant Load Creep of Nylon 6/6 at 23 °C	61

List of Figures - Continued

Figure		Page
Figure 37	Vibrocreep Response of Nylon 6/6 at Different Frequencies at 23 °C	62
Figure 38	Vibrocreep Response of Nylon 6/6 at Different Amplitudes at 23 °C	63
Figure 39	Vibrocreep Response of Nylon 6/6 at Different Mean Stresses at 23 °C	64
Figure 40	Tensile Testing of Nylon 6/6 Specimens after Cyclic and Constant Loading at 23 °C	65
Figure 41	Tensile Testing of Nylon 6/6 Specimens after Cyclic and Constant Loading at 23 °C	66
Figure 42	Tensile Testing of Nylon 6/6 at Different Temperatures	67
Figure 43	Yield Stress and Elastic Modulus vs. Temperature	68
Figure 44	Constant Load Creep of Nylon 6/6 at Different Temperatures	70
Figure 45	Vibrocreep Response of Nylon 6/6 at Different Frequencies at 35 °C	72
Figure 46	Vibrocreep Response of Nylon 6/6 at Different Amplitudes at 41 °C	73
Figure 47	Vibrocreep Response of Nylon 6/6 at Different Mean Stresses at 35 °C	74
Figure 48	Vibrocreep Response of Nylon 6/6 at Different Temperatures	76
Figure 49	Vibrocreep Response of Nylon 6/6 at Different Frequencies and Temperatures	77

List of Figures - Continued

Figure		Page
Figure 50	Vibrocreep Response of Nylon 6/6 at Different Amplitudes and Temperatures	78
Figure 51	Vibrocreep Response of Nylon 6/6 at Different Mean Stresses and Temperatures	79
Figure 52	Tensile Testing of Nylon 6/6 Specimens after Cyclic and Constant Loading at 41 °C	80
Figure 53	Tensile Testing of Nylon 6/6 Specimens after Cyclic and Constant Loading at 41 °C	81
Figure 54	Thermal and Mechanical Dominated Failure Zones	83
Figure 55	Vibrocreep Response of PVDF with ω*a = 100 at 23 °C	84
Figure 56	Vibrocreep Response of Nylon 6/6 with μ=4 at 23 °C	86
Figure 57	Vibrocreep and Creep Testing Fixture for PVDF	90
Figure 58	PVDF Test Sample	96
Figure 59	Tensile Test of PVDF Direction 1 at 23 °C	97
Figure 60	Tensile Test of PVDF Direction 2 at 23 °C	97
Figure 61	Constant Load Creep of PVDF at 23 °C	99
Figure 62	Vibrocreep Response of PVDF at Different Frequencies at 23 °C	101
Figure 63	Vibrocreep Response of PVDF at Different Amplitudes at 23 °C	103
Figure 64	Vibrocreep Response of PVDF at Different Mean Stresses at 23 °C	104
Figure 65	Constant Load Creep of PVDF at -25 °C	105

List of Figures - Continued

Figure		Page
Figure 66	Constant Load Creep of PVDF at Different Temperatures	107
Figure 67	Vibrocreep Response of PVDF at Different Frequencies at -25 °C	109
Figure 68	Vibrocreep Response of PVDF at Different Amplitudes at -25 °C	110
Figure 69	Vibrocreep Response of PVDF at Different Mean Stresses at -25 °C	111
Figure 70	Vibrocreep Response of PVDF at Different Temperatures	112
Figure 71	Vibrocreep Response of PVDF at Different Frequencies and Temperatures	113
Figure 72	Vibrocreep Response of PVDF at Different Amplitudes and Temperatures	114
Figure 73	Vibrocreep Response of PVDF at Different Mean Stresses and Temperatures	115
Figure 74	Vibrocreep Response of PVDF with ω^*a = 100 at 23 °C	117

Abstract

An investigation of the cyclic loading effects on the time dependent response of Nylon 6/6 and a piezoelectric Polyvinylidene Fluoride (PVDF) based composite material is presented. A consistent experimental program has been developed with the main objective to determine the creep behavior of the materials under cyclic loading conditions. An extensive testing procedure employed in this study has involved multiple experimental stages consisting of tensile stress-strain tests, constant load creep tests, and tests under sustained tensile loads with superimposed harmonic oscillations. The creep behavior of Nylon 6/6 and the PVDF based composite has been investigated depending on three loading parameters, mean stress, vibration frequency and amplitude. The study has been performed over a wide range of temperature conditions. The results of this investigation have provided a general view on the cyclic creep response of the materials under investigation, where Nylon 6/6 is a solid polymer and PVDF is an electroded polymer. Nonlinear creep effects induced by cyclic loading conditions have been observed in both materials. The results of the study have demonstrated the limitations of linear viscoelastic theory and have served as a basis for constitutive model development and microstructural analyses of polymers subjected to asymmetric cyclic loading regimes.

INTRODUCTION

At present, along with the increasing demand for materials with novel or improved characteristics, there is a growing concern regarding material longevity. In this regard, two major factors are of immediate importance: time-dependent material properties and operating conditions involving cyclic loading regimes. The former represents an intrinsic material characteristic known as creep, which manifests itself through the development of time-dependent deformations under sustained loads. The second factor is associated with the loading conditions that cause material deterioration due to progressive damage processes. Apparently, certain interaction modes of these seemingly independent phenomena tend to produce qualitatively new effects altering the overall response and, ultimately, the life expectancy of materials.

The interaction effect of superimposed cyclic loads upon nonzero mean loads is a problem of immediate practical interest. This problem has been well studied in metals at high temperatures, however, fewer corresponding studies in polymers have been reported, and are practically non-existent in polymer based composites.

In the thesis, an experimental investigation of the time dependent response of Nylon 6/6 and a Polyvinylidene Fluoride (PVDF) based composite is presented. Experimental results and preliminary microstructural observations obtained in the course of the study provide new experimental evidence regarding

cyclic loading effects on the long-term behavior of the materials under consideration.

The second chapter provides background information regarding the properties of polymers, in particular, their time dependent behavior. The microstructure and physical properties of polymers are described and a theoretical background of the fundamental concepts of linear viscoelastic theory is provided.

The third chapter provides a review of previously published results on creep and vibrocreep of polymers. Emphasis has been placed upon the cyclic loading effects on the creep response of polymers.

The fourth chapter outlines the main objectives of the project. The goals are stated and progression toward these goals is set forth within the thesis.

The fifth chapter describes the general approach to a parametric study of cyclic loading effects on the behavior of polymers. The study involves the material selection, experimentation, and the criteria for vibrocreep analysis.

The sixth chapter describes the developed experimental program and provides a summary of the experimental results obtained from the experiments of Nylon 6/6 (DuPont Zytel® 42A NC010 Polyamide 66).

The seventh chapter describes the experimental program and provides a summary of the experimental results obtained from the experiments of Polyvinylidene Fluoride (PVDF) based composite laminate.

The eighth chapter contains the statistical analysis of the experimental data. The ninth chapter provides a general discussion of the results for both Nylon 6/6 and PVDF. The discussion leads to a number of conclusions formulated in the tenth chapter. The eleventh chapter describes further research directions.

PROPERTIES OF POLYMERS

The development of an understanding of polymer materials can be achieved through the analysis of the physical properties and microstructure. The microstructure and the process by which the material has been created govern the physical properties. The physical properties dictate how the material will perform in a working environment.

Physical Properties of Polymers

The broad class of polymers involves thermoplastics and thermosets that have different molecular structure and characteristics. The products necessary to form a thermoplastic or thermoset are raw materials such as coal, petroleum, and natural gas. The formation of polymers from monomers results in a microstructure with an amorphous form, crystalline form, or a combination of these two forms. The first stage of polymer development is characterized by the formation of lamella, small crystals, and molecular chains that align themselves in a zigzag pattern, Figure 1, Ref[16].

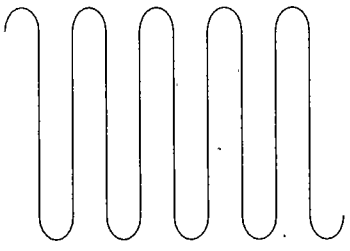


Figure 1 Lamella Formation

The lamellas have a random orientation in all polymer materials. To promote the lamellas growth, the temperature of the polymer is held just below the melt temperature. Once the lamella has started to grow, the second stage starts. The lamella interacts with other lamella, forming long chain branches or fibrils from the remaining molecular chain, Figure 2, Ref[16].

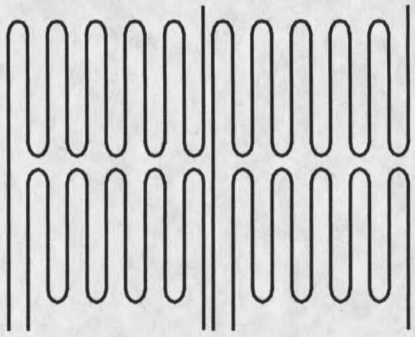


Figure 2 Fibril Formation

The fibrils form of inter lamella connections. As the lamellas interconnect the fibrils fill the gaps between the lamella as shown in Figure 2. The fibrils can be said to "tie a knot" between each other and initiate the third stage of the formation of spherulites, Figure 3, Ref[16].

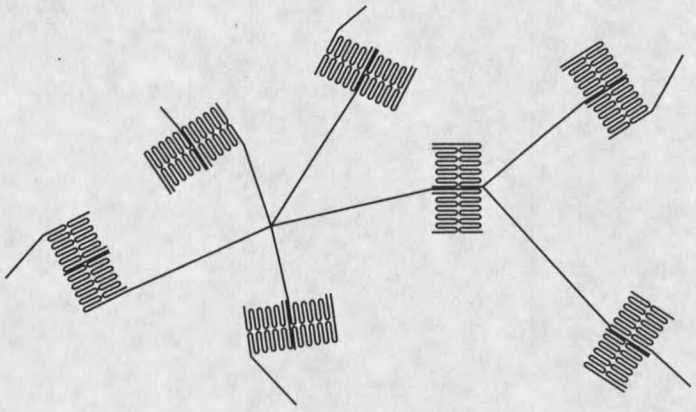


Figure 3 Spherulite Formation

The latter form, a large crystal that develops in radial directions. The final crystallization of the polymer is also dependent upon the temperature at this stage. As the temperature is lowered, spherulites begin to form. The amount of their growth is dependent once again on the hold time at a constant temperature. Once the polymer material is said to be past the glass transition temperature, then all movement of the molecular chains stops. The change in the specific volume of the polymer under the decreasing temperature makes the chains less mobile.

The development of crystals within these three stages determines the degree of crystallinity and orientation of the molecular structure. When microstructural analysis is performed lamella, fibrils, and spherulites can be observed. The orientation of spherulites or large crystals is dependent on hold times and additional mechanical means of molecular chain alignment. The molecular alignment and regularity directly depend on the degree of

crystallization in a polymer material. Mechanical processes such as annealing the polymer material can be performed to promote the alignment of molecular chains. Without molecular regularity and proper alignment of molecular chains the polymer becomes amorphous. Such amorphous regions are voids or gaps between lamella and spherulites due to the fact that the fibrils or remaining parts of molecular chains could not align themselves within the process described above. The amorphous region is about 85% less dense then crystalline regions.

As the polymer cools from the melt temperature, the polymer progresses through thermal transitions. Purely crystalline polymers experience only a melt transition.

Table 1 Crystal Melt Temperatures of Some Polymer Materials, Ref[52]

Polymer	T_m (°C)
Low Density Polyethylene	95-130
High Density Polyethylene	120-140
Polypropylene	168
Polyformaldehyde	181
Nylon 6	216
Polyethylene Terephthalate	245
Nylon 6/6	265
Polytetrafluoroethylene	327

When a polymer develops amorphous (semi-crystalline or mostly amorphous) regions, then the polymer tends to undergo three other transitions between the melt and glass temperatures. The first state of the polymer below the melt temperature is a viscofluid state. In this state the polymer exhibits properties of a viscous fluid with molecular chains having a high degree of mobility. The second

state is the rubbery state, in which the polymer is said to have segment mobility, but does not have molecular mobility. The final state of the polymer below the glass transition temperature is a glassy state, in which the motion of molecular chains cease to exist.

Table 2 Glass Transition Temperatures of Some Polymers, Ref[52]

Polymer	T_g (°C)
Polyethylene	-120
Polyisoprene	-73
Polyformaldehyde	-50, -85
Polypropylene	-10, -18
Nylon 6/10	40
Polyvinyl Chloride	87
Polystyrene	100
Polycarbonate	150

Instantaneous Elastic Behavior of Polymers

The instantaneous elastic properties of polymers depends upon temperature and strain rate. For example, a polymer material at a high temperature tends to exhibit properties of a ductile material, whereas a polymer exhibits brittle properties at lower temperatures, Figure 4. The effects of temperature are graphically shown in Figure 5, Ref[16]. Note that where the curve knees represents a transition temperature such as the glass transition temperature of the polymer. The effect of increasing strain rate is also shown in Figure 6, Ref[49]. It is important that experiments with polymers must be

performed according to ASTM testing specifications that dictate the prescribed temperature and strain rates.

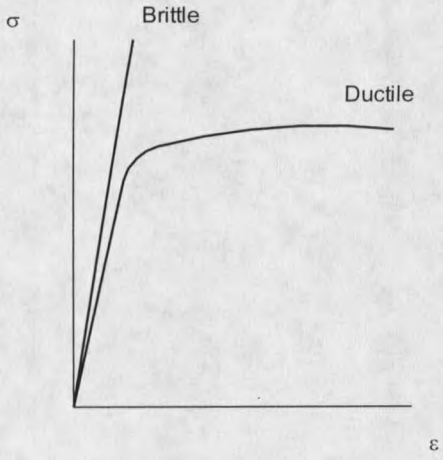


Figure 4 Brittle and Ductile Comparison

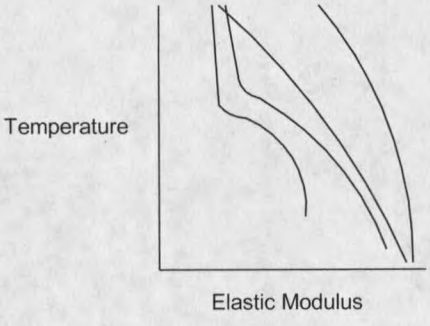


Figure 5 Temperature Effects on Elastic Modulus of Some Polymer Materials

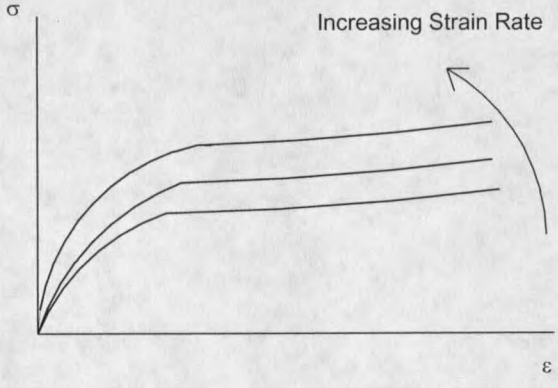


Figure 6 Strain Effects of Strain Rate on Polymer Materials

The elastic response of a crystalline polymer or crystalline region within a polymer material is stiff or brittle and does not produce large deformations. When deformation does occur the spherulites change in shape as a whole and not individually, Figure 7, Ref[16].

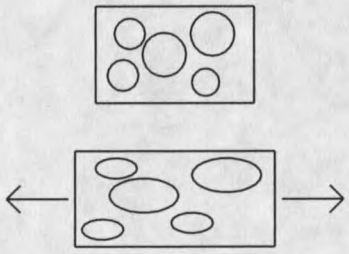


Figure 7 Deformation of spherulites in a Crystalline Structure

Amorphous polymers or regions in a polymer deform elastically by stretching of the bonds between the molecules in the molecular chain. The lamellas start to unfold within the spherulite, and tilt to align with the applied load, Figure 8, Ref[16].

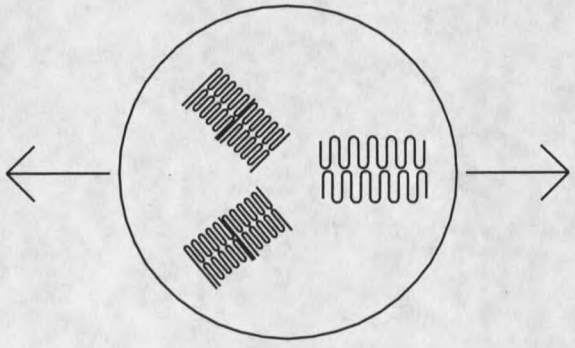
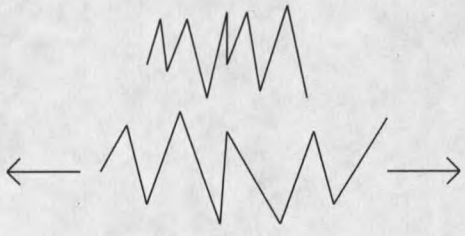
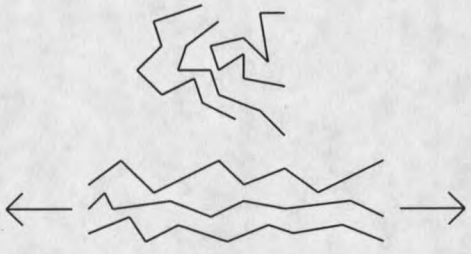


Figure 8 Lamella Deformation Within a spherulite

Thus, an amorphous polymer material or amorphous regions of a polymer deform by alignment and lengthening of the molecular chains, Figure 9, Ref[16].



Elongation of Bonds



Chain Alignment

Figure 9 Deformation of Molecular Chains in an Amorphous Material

The chain lengthening continues until molecular chains fail and the spherulites no longer exist, Figure 10, Ref[16].

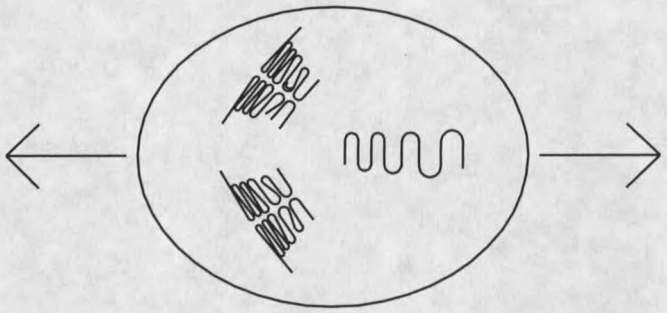


Figure 10 Fibril and Lamella Interconnection before Failure

Creep Behavior of Polymers

A polymer material that has properties with strain or stress rate dependence is considered to be viscoelastic, since it behaves as a viscous fluid or viscoelastic solid. Two types of tests can be performed to represent the viscous behavior of polymers, a creep test or relaxation test. A creep test is performed under a constant stress allowing strain to change over time, whereas a relaxation test is performed under a constant strain allowing stress to change in time. Models that represent the creep and relaxation behavior of a linear viscoelastic solid have been developed using linear springs and dashpots. An example of such a model is the Maxwell model shown in Figure 11, where σ = applied stress or ε = applied strain, E_m, = linear elastic spring coefficient, and η_m = viscosity coefficient.

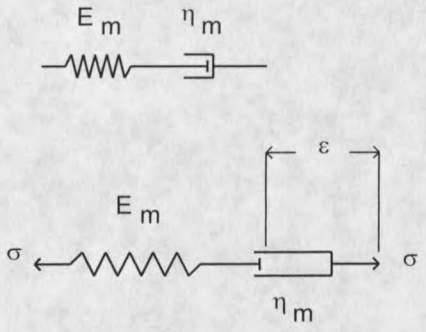


Figure 11 Maxwell Model

The creep and relaxation responses of the Maxwell model are shown in Figure 12, and Figure 13. Equations 1 and 2 represent the constitutive law, respectively, for creep and relaxation of the Maxwell model.

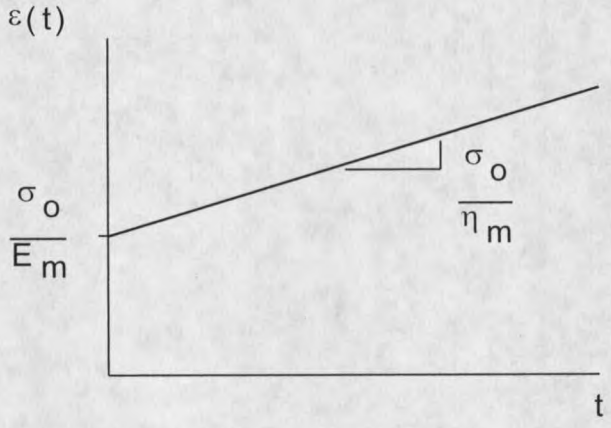


Figure 12 Creep Curve of the Maxwell Model

$$\varepsilon(t) = \frac{\sigma_o}{E_m} + \frac{\sigma_o}{\eta_m}$$

Equation 1

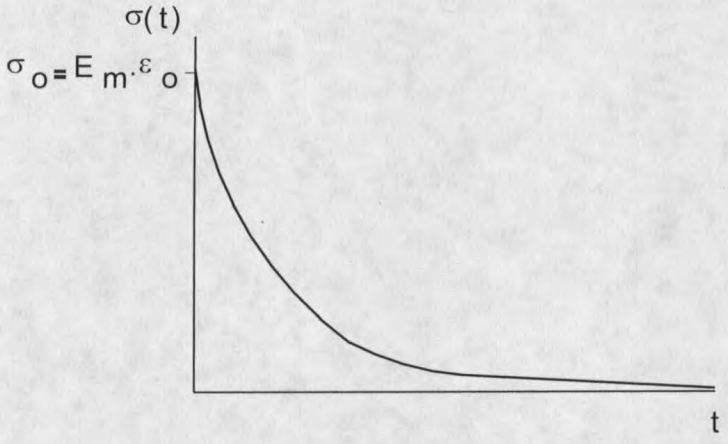


Figure 13 Relaxation Curve of the Maxwell Model

$$\sigma(t) = E_m \cdot \varepsilon_o \cdot e^{\frac{-t}{\tau}}$$

Equation 2

Another viscoelastic material model is the Kelvin model shown in Figure II.14, where σ = applied stress or ε = applied strain, E_k = linear elastic spring coefficient, and η_k = viscous coefficient.

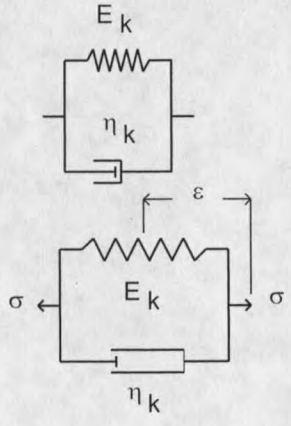


Figure 14 Kelvin Model

The Kelvin model represents creep behavior but cannot represent the relaxation behavior of polymers. The creep and relaxation curves produced by the Kelvin model are shown in Figure 15, and Figure 16, respectively. The constitutive law for creep and relaxation of the Kelvin model are provided in Equations 3 and 4.

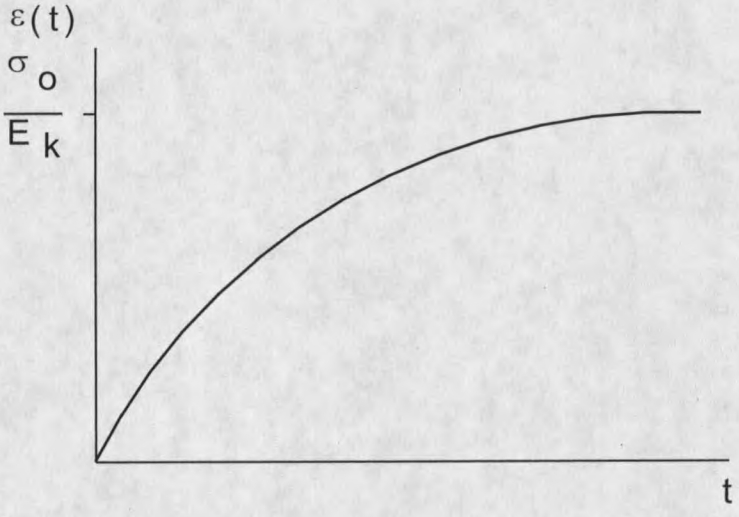


Figure 15 Creep Curve of the Kelvin Model

$$\varepsilon(t) = \frac{\sigma_o}{E_k} \cdot \left(1 - e^{\frac{-t}{\tau_k}}\right)$$

Equation 3



Figure 16 Relaxation Curve of the Kelvin Model

$$\sigma(t) = \varepsilon \cdot \left(E_K \cdot H(t) + \eta_K \cdot \delta(t) \right)$$

Equation 4

The third, more realistic viscoelastic model is the Burger model that represents a linear viscoelastic solid shown in Figure 17, where σ = applied stress or ε = applied strain, E_m = Maxwell linear elastic spring coefficient, E_k = Kelvin linear elastic spring coefficient and η_k = Kelvin viscous coefficient

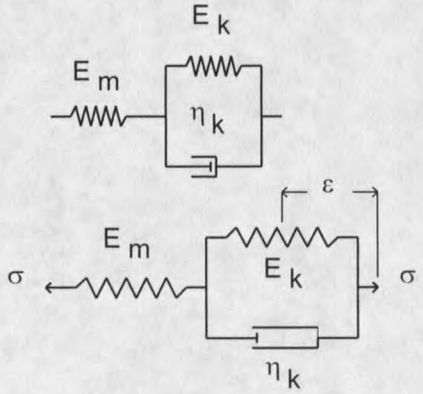


Figure 17 Burger Model

The creep and relaxation curves for the Burger model are shown in Figure 18, and Figure 19, respectively. The constitutive law are provided in Equations 5 and 6, respectively.

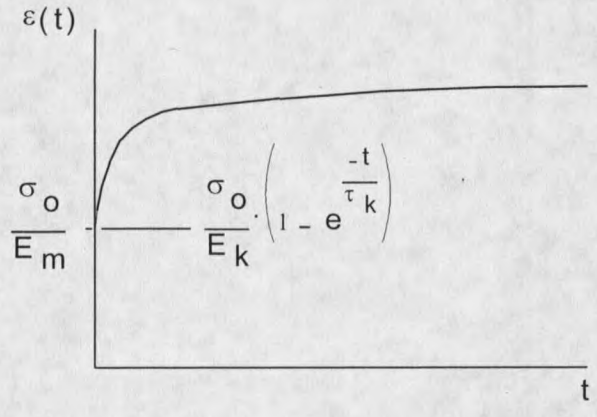


Figure 18 Creep Curve of the Burger Model

$$\varepsilon(t) = \frac{\sigma_o}{E_m} + \frac{\sigma_o}{E_k}\cdot\left(1 - e^{\frac{-t}{\tau_k}}\right)$$

Equation 5

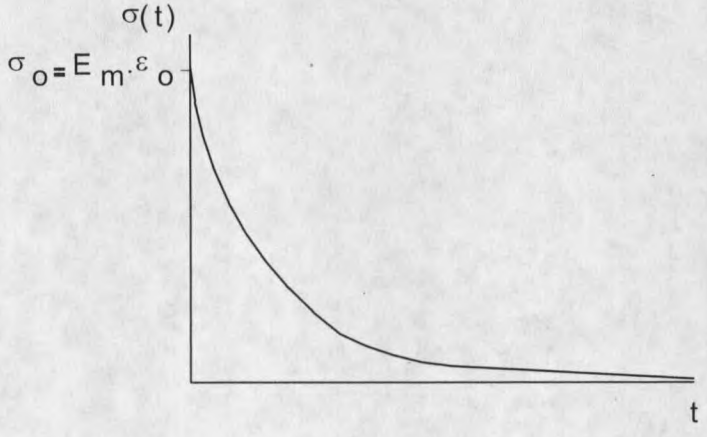


Figure 19 Relaxation Curve of the Burger Model

$$\sigma(t) = E_m \cdot \varepsilon_o \cdot e^{\frac{-t}{\tau}}$$

Equation 6

A more complex model representing the response of polymers is based on the Boltzmann superposition principle which states that the response of a material to a complex loading history can be presented as the sum of individual increments at each load step. This principle applies to loading histories involving both step load increments and continuos loading function as shown in Figures 20-21, Ref[49,24].

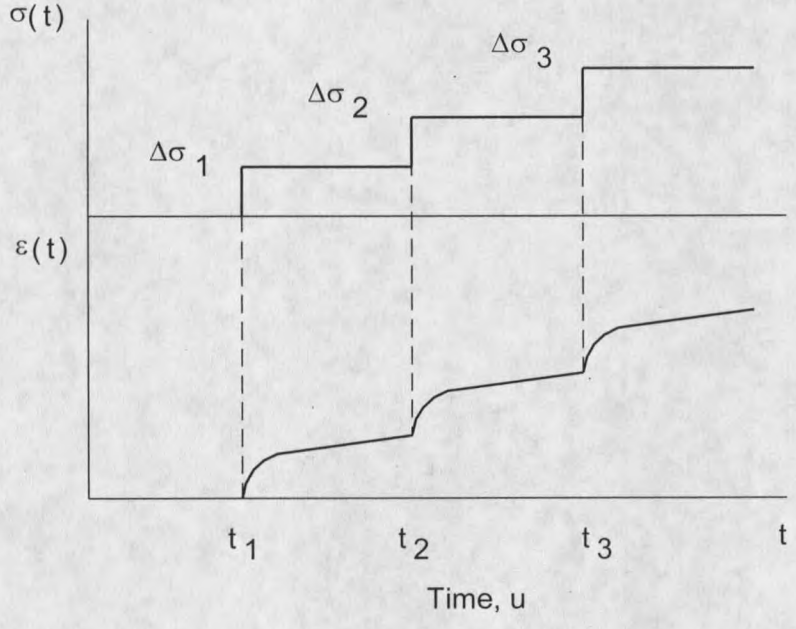


Figure 20 Step Load History and Resulting Strain

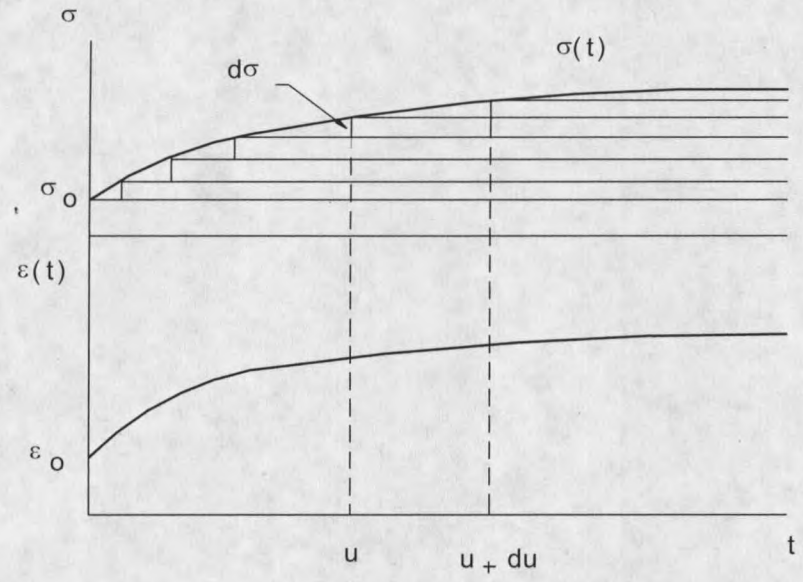


Figure 21 Continuous Loading History and Resulting Strain

For a step load history, the material response in terms of strain is defined in the form of Equation 7, Ref[12]. For a continuous loading history the strain deformation in time is represented by the hereditary integral, in the form of Equation 8 and 9 for creep and relaxation, respectively, Ref [12].

$$\varepsilon(t) = \sum_{i=0}^{n} \sigma_i \cdot \frac{1}{E(t - u_i)}$$

Equation 7

$$\varepsilon(t) = \int_{-\infty}^{t} \frac{1}{E(t-u)} \cdot \frac{d}{du} \sigma(u)\, du$$

Equation 8

$$\sigma(t) = \int_{-\infty}^{t} E(t-u) \cdot \frac{d}{du} \varepsilon(u)\, du$$

Equation 9

Through creep testing a variety of creep curves can be generated at different stress levels, Figure 22.

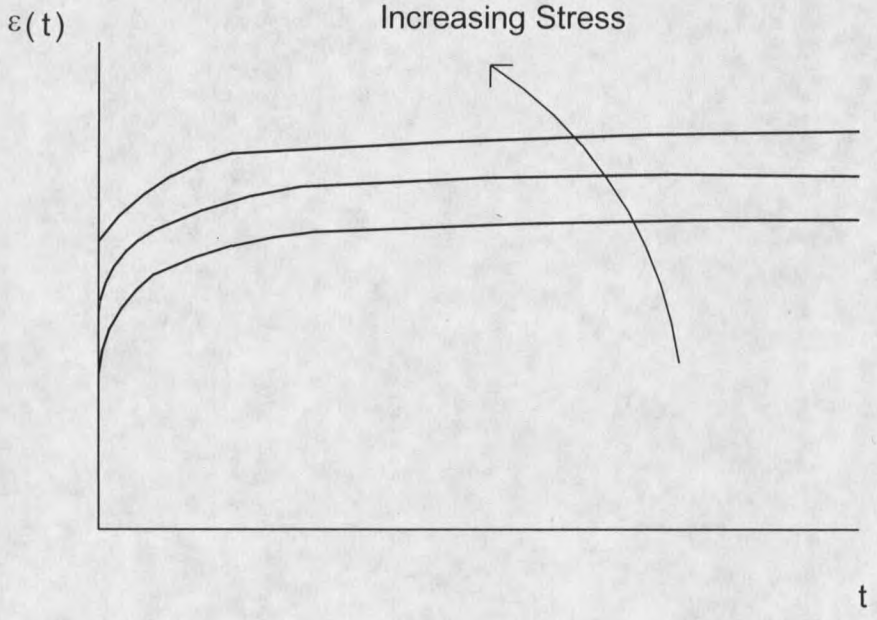


Figure 22 Creep Curves of the Same Polymer at Different Stress Levels

Once the data is generated, the normalization process is performed to determine the linear viscoelastic limit and the creep compliance. In the linear viscoelastic range, normalized creep curves at different stress levels produce one single curve defined as the creep compliance, Figure 23.

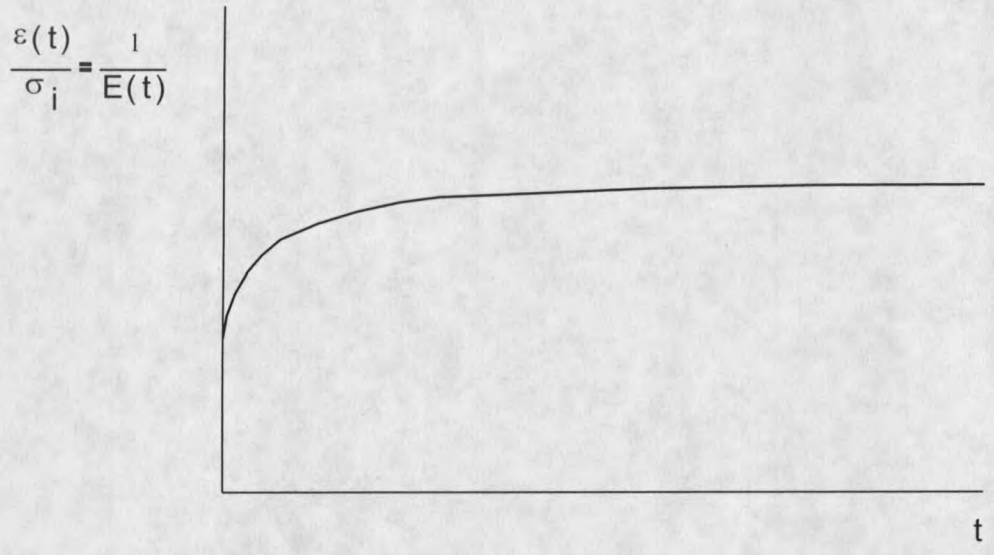


Figure 23 Normalized (Creep Compliance) Creep Curves Showing Linear Viscoelasticity

The single normalized creep curve indicates that the creep behavior of the material is stress independent. In the case of stress dependency of the creep response of polymers, nonlinear viscoelastic theories are required to adequately represent the material behavior.

Typically, dynamic testing methods are being used to characterize linear viscoelastic properties of polymers Ref[13,61]. Dynamic tests are generally performed by applying a sinusoidal strain and measuring the respective stress. The phase shift between the stress and strain sinusoidal waves represents the amount of viscous damping in the material, Figure 24.

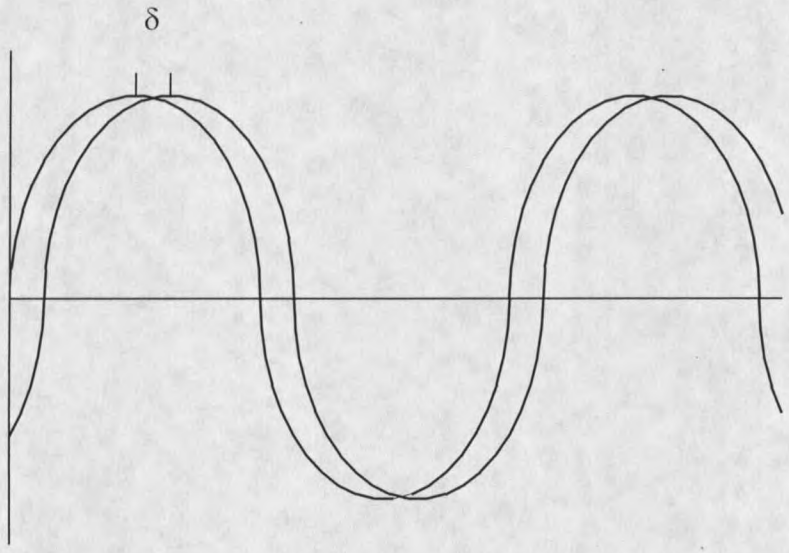


Figure 24 Periodic Strain and Stress

On this basis, the relaxation, storage moduli and compliances are determined in the form illustrated by Equations 10 and 11, Ref[21], where σ_o = stress amplitude and ε_o =strain amplitude.

$$E_p = \frac{\sigma_o}{\varepsilon_o} \cdot \mathrm{Cos}(\delta)$$

$$E_{pp} = \frac{\sigma_o}{\varepsilon_o} \cdot \mathrm{Sin}(\delta)$$

$$\frac{E_p}{E_{pp}} = \frac{\frac{\sigma_o}{\varepsilon_o} \cdot \mathrm{Sin}(\delta)}{\frac{\sigma_o}{\varepsilon_o} \cdot \mathrm{Cos}(\delta)} = \mathrm{Tan}(\delta)$$

Equations 10

$$D_{pp} = \frac{\frac{1}{E_{pp}}}{1 + (\mathrm{Tan}(\delta)^2)^{-1}} \qquad D_p = \frac{\frac{1}{E_p}}{1 + \mathrm{Tan}(\delta)^2}$$

Equation 11

The storage, loss moduli, and compliances calculated above are defined in the frequency domain. The material behavior in the time domain can be characterized in terms of relaxation function and creep compliance by using the following equations, Ref[21], where ω = frequency.

Creep $\quad E(t) = E_p(\omega) - .4 \cdot E_{pp}(.4 \cdot \omega) + .014 \cdot E_{pp}(10 \cdot \omega)$

Relaxation $\quad D(t) = D_p(\omega) + .4 \cdot D_{pp}(.4 \cdot \omega) - .014 \cdot D_{pp}(10 \cdot \omega)$

Equation 12

The time-temperature analogy is used to characterize the response of thermorheologically simple materials. By using a temperature dependent shift factor that relates the properties of the material at any temperature T to the properties at a reference temperature T_o, the curves at different temperatures are shifted by a factor ($a_T(T)$) coinciding with the reference curve at temperature T_o as shown in Figure 25-26.

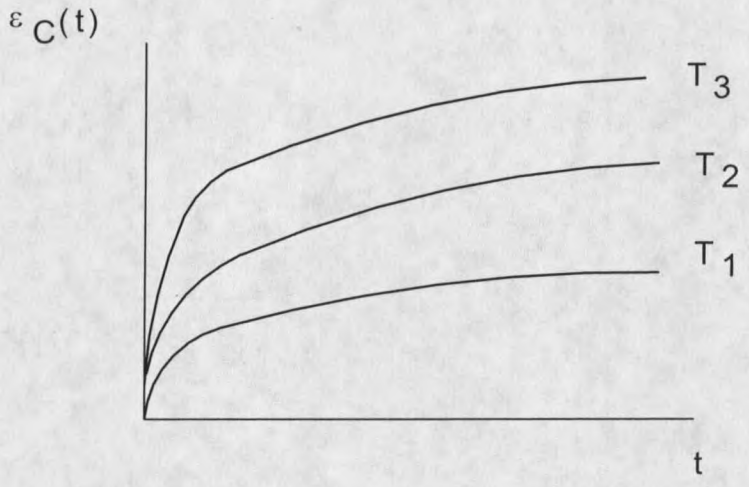


Figure 25 Creep Strain at Multiple Temperatures

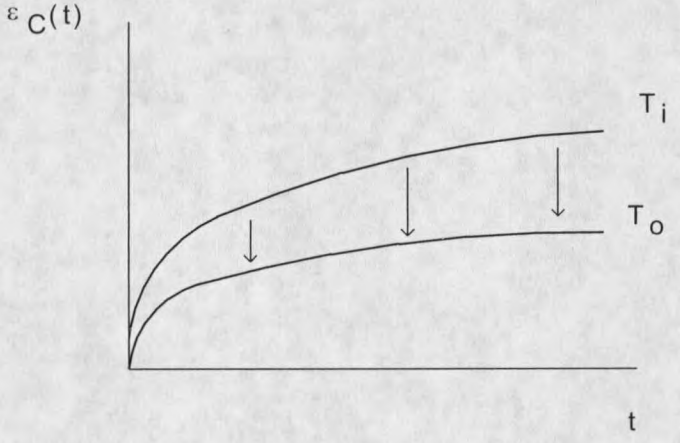


Figure 26 Shifting the Temperature Curves to the Reference Temperature

Note that in Figures 25 -26, $\varepsilon_C(t)$ denotes the creep strain, defined by Equation 13, where ε_T is the total strain, ε_C is the creep strain, and ε_E is the instantaneous elastic strain

$$\varepsilon_T(t) = \varepsilon_C(t) - \varepsilon_E$$

Equation 13

Fatigue Behavior of Polymers

Fatigue testing of polymer materials is conducted by two test methods, stress controlled experiments or strain controlled experiments. A stress controlled test is performed by applying cyclic stress in tension, compression, or both, whereas a strain controlled system is performed by applying cyclic strain in tension, compression, or both. The variables of stress controlled experiments are:

- Cyclic Stress $\Delta\sigma$
- Corresponding $\Delta\varepsilon$
- $_m$ Level
- Corresponding ε_m, Level
- Frequency
- Wave Form (sine, square, etc.)
- Temperature
- Specimen Size

The influence of the above fatigue test variables on a molecular level within a polymer material is broken into seven categories.

- Molecular Characteristics
- Chemical Changes
- Elastic Deformation
- Non Elastic Deformation
- Morphological Changes
- Transition Phenomena
- Thermal Effects

The molecular characteristics of polymer materials are dictated during the formation of the polymer, molecular weight, molecular composition, etc. The molecular characteristics influence the effects of fatigue testing on the remaining categories. The chemical changes in a polymer incorporate bond breaking and

stress cracking. Bond breaking (mainly C-C bonds) can be produced by crack propagation or induced during processing, flaw creation. Bond breaking energy in relation to fracture energy is more significant in crystalline (10^2 -10^3 J/m^2) or thermoset polymers than in amorphous polymers (.1 J/m^2). Even though the total energy due to bond breakage makes up about 10% of the fracture energy in a crystalline polymer, the distribution of the stresses due to bond breakage is of consideration. A crystalline or thermoset polymer transfer the stresses to neighboring molecules or crystals while an amorphous polymer has the ability to transfer the stress through entanglements of chains thus allowing an improved stress distribution. Stress cracking within a polymer is due to environmental effects. A good example of this is a dashboard within a car, where cracks are induced due to sunlight effecting the polymer material.

Elastic deformation is the elastic behavior of the polymer under cyclic stresses. The elastic behavior being that the material can recover all deformation, elastic and visco-elastic, or strain if the testing has stopped. Non elastic deformation would include plastic and visco-plastic deformation, where the deformation is not recoverable if the fatigue testing were stopped. The nonelastic deformation is shown in a polymer by the formation of crazes or shear bands. Crazing develops at a 0° angle relative to the applied load where shear bands develop at 38°- 45° angles to the applied load. The two differ in that crazing develops cavitation with molecular chain orientation, and shear banding develops molecular chain orientation only. If the stress is applied in a manner of

which the material is unloaded for duration of time, then the material is allowed to relax. The relaxation period allows molecular chain alignment preventing deformation during the next cycle. Consequently if the stress is applied in a manner in which relaxation cannot occur, then the cycles to failure is greatly increased.

Morphological changes in a polymer material dictate the history of the processing of the polymer. The changes are noted by thermal and mechanical histories, by which drawing, chain orientation promotion techniques, or crystallization dictate the polymers history, in the case of PVDF polymer heating and stretching of the polymer creates a thermal and mechanical history. The thermal and transition properties of polymers during fatigue testing are of high importance. The effects of fatigue, mechanical deformations due to cyclic stresses, induce energy into a polymer material that is partially transformed into thermal energy, called hysteric heating. The hysteretic heating process produces accelerated failure of a polymer material due to low thermal the thermal conductivity of polymers Figure 27, Ref[29].

The thermal energy produced is highly dependent upon the varied stress, frequency, wave pattern, and specimen size. High varied stresses and high frequencies develop the highest mechanical energy input into the polymer, thus elevating the probability of hysteric heating. Changing the wave pattern of the applied stress by allowing the polymer to rest or dissipate heat between cycles decreases hysteric heating. The specimen size, large surface area and small

thickness, contributes to the ability of a polymer to dissipate the heat generated. Through the heating of a polymer, a transition from glassy to rubbery phases may occur. For a crystalline or thermoset, the polymer may simply just melt away.

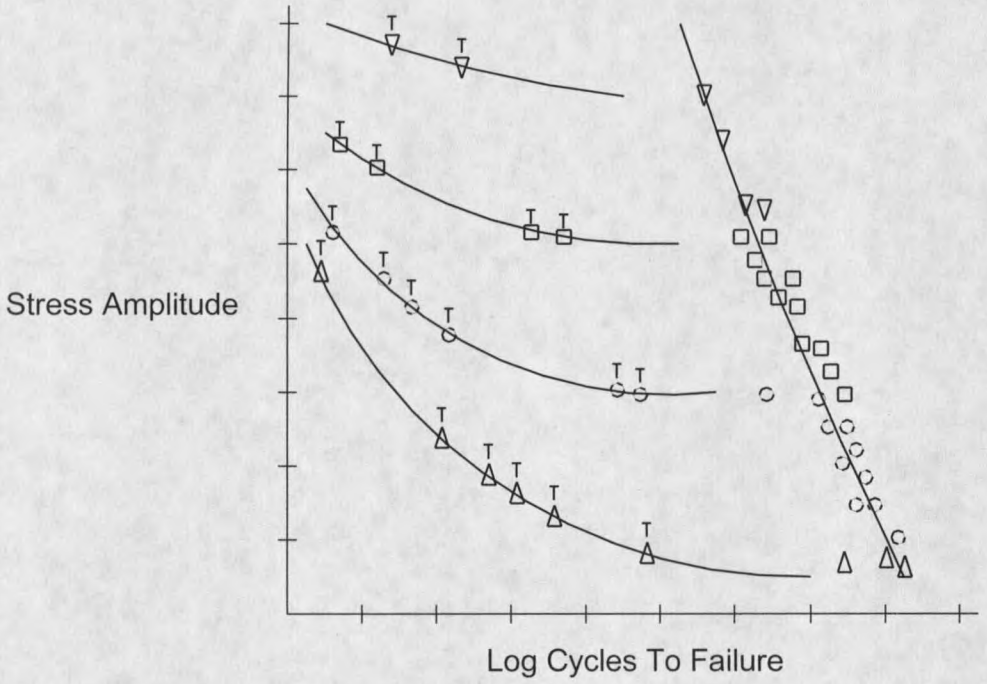


Figure 27 Stress Amplitude vs. Cycles to Failure, Ref[29]

Where $\nabla \rightarrow \square \rightarrow o \rightarrow \Delta$ is an increase in frequency.

Failure of the material is dependent upon the rate at which the stress is applied and temperature, as described above in tensile properties. A high stress rate at low temperatures, promotes brittle type of failure, whereas a low stress rate and high temperature dictate ductile failure. If a crack is developed during fatigue, then the thermal energy within the polymer may allow mobility of molecular chains to prevent further crack propagation. The molecular chains may reduce the stress concentration at the crack tip.

OVERVIEW OF RESEARCH ON THE CYCLIC RESPONSE OF POLYMERS AND POLYMER BASED COMPOSITES

The effects of creep and cyclic load interaction for polymers and polymer matrix composites has not been investigated to the same degree as for metals at high temperatures, Ref[59]. These effects lead to a phenomena defined as vibrocreep, Ref[46, 47]. Ref[46], the vibrocreep effect is quantified using a specific parameter defined as vibrocreep coefficient to predict vibrocreep from experimental data. With the increased use of polymers, such as PVDF, Ref[62] in vibration environments, the characterization of cyclic creep effects in polymers and polymer matrix composites is particularly important. The vibrocreep effect in glass fiber reinforced composites has been studied in Ref[66]. The effect of creep on polymers and polymer matrix composites has been investigated in Ref[21, 24]. Recent aspects of creep analysis are aimed at new polymers and polymer matrix composites, Ref[25, 31, 38, 41, 44, 47]. The same techniques are used to characterize the new materials. Recent advances in creep assessment involve the use of damage analysis to predict creep in structures, Ref[8].

Multiple authors have addressed the effect of cyclic loading on the response of polymer materials. The effect of creep in cyclic loading conditions has been investigated by Ref[22] for an Poly(Dimethylsiloxane) elastomer where the results contradicted the Boltzmann Superposition Principle. In Ref[54, 57], various factors are considered that determine the cyclic behavior of polymers.

Such as wave form, frequency, geometry, etc.. It has been observed that the effect of high stresses and frequencies lead to thermal failure, of polymers, whereas crack initiation and propagation results in mechanical failure. Research has been performed in the thermal failure regime through observations of hysteresis heating of polymers, Ref[30, 65], along with model development in Ref[51]. It has been observed that an increase of cyclic frequency lead to accelerated deformation and shorter fatigue life of polymers. The results shown in Ref[14], indicate that thermal failure has been observed at an increased frequency in glass fiber composite materials. The effect of frequency has been analyzed in Ref[72] in regard to a polyethylene copolymer. An increase in frequency was observed to increase the number of cycles to failure up to a certain frequency limit beyond which the number of cycles to failure decreased. In Ref[53], it has been observed that an increase of frequency in the sonic region produced increased deformation rate of several polymers. An increase in amplitude of the cyclic load has produced similar effects as frequency increases, Ref[36]. The problem of fatigue crack propagation rates in polymers depending on the cyclic frequencies has been studied in Ref[17]. The increase of the amplitude and frequency under cyclic loading conditions is also seen in Ref[68]. The effects of amplitude and frequency combined are quantified and related to the shear rate of deformation under relaxation conditions. The effect of the mean stress upon the deformation and failure of polymer materials is discussed in Ref[60]. It has been observed that under fully reversed cyclic conditions an

increase in the mean stress results in a increase in the number of cycles to failure. These results have been also analyzed using microscopic techniques to assess the formation and propagation of crack growth. Other researchers have analyzed the effects of temperature under cyclic loading conditions. In Ref[70], the assessment of crack growth showed that the crack propagation and initiation are highly temperature dependent. In Ref[43], the combined effect of temperature and humidity are analyzed. The increasing temperature and humidity has lead to a decrease in the strength, stiffness and fatigue life of polymers, under cyclic loading conditions.

Ref[4, 58] further verifies the alignment of the molecular structure during deformation within a polymer material. The alignment of the molecular structure during deformation within a polymer material is further verified by the result of molecular nonhomogenities and surface microcracks due to processing, Ref[17]. From the initial material defects, crazing initiation and propagation occurs first, Ref[45, 56, 42], until crack formation and propagation begins. Once the crack propagates, the crack generally arrests repeating the process Ref[11]. Methods to represent the behavior of crack growth under cyclic conditions have been performed by many researchers Ref[20, 29, 48, 71]. The damage accumulation due to the craze formation and crack growth under cyclic loading conditions has been studied by Ref[55, 63, 64].

In Ref[39], it is shown that the effect of cyclic deformation leads to softening in the thermal dominated regime, whereas hardening is shown in the

mechanical dominated regime for Nylon 6/6. Strain rate analysis has been performed using impact testing to asses response of Nylon 6/6, Ref[1]. The results are used to compare to the cyclic loading tests using linear elastic fracture mechanics. The effects of the crystallinity and molecular weight are analyzed in Ref[67]. The results show that the crystallinity showed effects upon the strength and stiffness of the material, while the molecular weight showed effects upon the ultimate strength. The effect of the residual strain is described as the effect of the Van der Waals and covalent bonding. The increase in strength and stiffness is a result of the molecular alignment where the covalent bonds are aligned about the loading direction adding reinforcement. The effect of the crystallinity was also studied in Ref[37]. The effect of time and temperature are also analyzed for a Nylon 6/6 glass fiber reinforced polymer composite under tension-tension cyclic loading, Ref[35]. The effects of crystallinity as related to the effect increasing amplitude where the increase in amplitude resulted in the crystalline deformation and amorphous regions.

GOALS AND OBJECTIVES

It is well known that polymeric systems tend to exhibit creep behavior at room temperature that can be accurately predicted within the linear range of stress-strain relations based on linear viscoelastic theory. However, the synergistic interactions of creep and damage evolution processes in these materials are far from being well understood. The goal of the thesis is to bridge this gap and enhance the understanding of the cyclic loading effects on the time dependent behavior of polymers and polymer based composites.

GENERAL APPROACH TO A PARAMETRIC STUDY OF CYCLIC LOADING EFFECTS ON POLYMERS

Material Selection

In order to conduct a parametric study of vibrocreep effects in polymers, material selection has been performed based on three criteria. The first criteria concerning the applications of a material in industry and/or research. The second criteria takes into account the physical properties of the candidate material. The third criteria is based on the material.

The first criteria involves two questions:

- Is the material used in a wide range of applications where the cyclic loading effects might be considerable?
- Why is this material more significant that any other in a cyclic loading environment?

The second criterion involves a evaluation of the physical properties through reference materials, Ref[2, 3, 6, 10, 16, 18, 19, 23, 27, 28, 34, 69]. The third criterion involves considerations of properties of polymers such as molecular network crystallinity, transition temperatures, etc..

Experimental Stages

The following experimental stages have been implemented in the developed experimental program.

Tensile Testing

The objective of the tensile testing is to assess the instantaneous mechanical properties of polymer materials. The strength and stiffness characteristics obtained from the tensile testing are related to creep and vibrocreep testing. The temperature influences on the strength and stiffness of the material can also be analyzed through tensile testing. The experimental standards for tensile testing are outlined by the American Society for Testing and Materials. For solid polymers and thin plastic sheeting the ASTM standards are D638-96 and D882-95a, respectively. Tensile testing requires at least 5 test specimens for analysis. The magnitude of the elastic modulus determined is somewhat approximate due to the presence of creep effects. The degree of these effects depend upon the material chosen. Note, the best methodology for determination of the elastic modulus of polymers is by dynamic methods.

Constant Load Creep Testing

In this program, the objectives of creep testing of polymer materials are the determination of the linear viscoelastic limit and the creep compliance. The knowledge of the linear viscoelastic limit allows reference to the applicability of linear viscoelastic theory. With the knowledge of linear viscoelastic limit, vibrocreep testing can be performed within the linear bounds. The verification of the vibrocreep phenomena requires creep testing to assess the degree of the

vibrocreep effect and also the determination if the effect is present in the behavior of a particular polymer.

Vibrocreep Testing

In this program, the objectives of the vibrocreep testing are to assess the effect of the four parameters, frequency, amplitude, mean stress and temperature on the response of the polymer. The degree of influence that each parameter has on the creep behavior of polymers vibrocreep is the main objective of the parametric study conducted within this program. The influence of each parameter separately may help determine the intensity of the vibrocreep effect. Ultimately the vibrocreep effect may be classified by the influence of these parameters separately or combined.

Post Cyclic Testing

In this program, following the stages of creep and vibrocreep testing material specimens are further tested in tension at the same feed rate as that maintained at the stage of tensile testing. The objective of the post cyclic tests are to determine the changes in material properties due to creep deformations under constant and cyclic loading conditions.

The experimental stages described above are summarized in Table V.3. This table also provides information regarding the objectives of each experimental stages, the number of samples tested in each individual experiment and the result obtained at each stage.

Table 3 Testing Summary

Test Type	Motivation	# of Specimens to Represent One Curve	Information Obtained
Tensile	Instantaneous Material Response	5	Yield Stress, Elastic Modulus, and Maximum Stress
Constant Load Creep	Viscoelastic Properties	5	Linear Viscoelastic Limit and Creep Compliances
Cyclic Load Testing	Vibrocreep Effect	3	Frequency, Amplitude, Mean Stress and Temperature Effects
Post Cyclic Testing	Monitor Changes in the Instantaneous Properties	3 or 5	Yield Stress, Elastic Modulus, and Maximum Stress

Testing Methodology

Tensile Testing and Post Cyclic Testing

The results of the tensile test data are averaged and condensed using the tensile and tensile average macros in Excel provided in Appendix O. The final result is strain at every .01 mm/mm. This result is plotted instead of a large number of data points at once to provide a clear and accurate representation of the test data.

Non contact strain and temperature measurements are strongly encouraged through the development of the creep and vibrocreep experimental procedures. The influence of attachments on the test specimens is not a variable

that needs to be added to the study of vibrocreep. All strain measurements are calculated from position measurements a LVDT, position transducer, etc. Temperatures are measurements of the atmospheric temperature about the test specimen except for the infrared temperature measurement system for monitoring the surface temperature of the polymer materials.

Constant Load Creep Testing

The experimental program for creep testing requires two stages, preliminary and final creep testing. The preliminary creep testing is designed to scan a material for the linear viscoelastic limit and more importantly be used for comparison to vibrocreep testing. The specimen geometry should be kept consistent throughout the testing procedure, for tensile, creep and vibrocreep testing. The test specimens chosen for solid polymer testing abide by the tensile testing ASTM D638-96 and for thin plastic sheeting D882-95a for thin films.

The preliminary testing matrix is shown below in Table 4. Typically one specimen is used for each test at the preliminary stage of the program. Assessment of an approximate linear viscoelastic limit can be made and also comparison of the vibrocreep effect can be assessed. The second stage of creep testing requires verification of the linear viscoelastic limit approximated at the preliminary stage. The tests are performed about the linear viscoelastic limit with the addition of 4 specimens to compose a total of 5 specimens. Once the linear limit is verified, stress levels for vibrocreep need to be analyzed for testing

below or above the linear viscoelastic limit. To verify the vibrocreep phenomena, testing within the linear viscoelastic limit is performed to show that the vibrocreep phenomena cannot be analyzed with linear viscoelastic theory. Creep testing above the linear viscoelastic limit provides reassurance of the linear viscoelastic limit and also allows approximation of the effect of the vibrocreep effect.

Table 4 Preliminary Test Matrix for Constant Load Creep Testing

Creep Testing
10% of Yield Stress
20% of Yield Stress
30% of Yield Stress
40% of Yield Stress
50% of Yield Stress
60% of Yield Stress
70% of Yield Stress
80% of Yield Stress
90% of Yield Stress
100% of Yield Stress

The results of the creep test data are therefore averaged and condensed using the 5 Sample and Average 5 macros in Excel provided in Appendix O. The final results are expressed in time at every 12 min. This result is therefore plotted instead of a large number of data points at once to provide a clear and accurate representation of the test data.

A few comments about the application of the static load to produce a creep test are needed. In theory, the load is fully applied at the time t = 0. This is physically impossible, since impacting the test specimen will occur. If the load is applied at a slower rate, then the initial elastic response may not be correct.

Efforts to perform a perfect creep test only become more complicated at lower stress levels. Non contact strain and temperature measurements are strongly encouraged through the development of the creep and vibrocreep experimental procedures. The influence of attachments on the test specimens is not a variable that needs to be added to the study of vibrocreep. All strain measurements are calculated from position measurements a LVDT, position transducer, etc. Temperatures are measurements of the atmospheric temperature about the test specimen except for the infrared temperature measurement system for monitoring the surface temperature of the polymer materials.

Vibrocreep Testing

The experimental program for vibrocreep testing also requires two stages, preliminary and final creep testing. The preliminary creep testing is designed to scan a material for the vibrocreep phenomena and approximate the effect of frequency, amplitude, and mean stress. The specimen geometry should be kept consistent throughout the testing procedure, for tensile, creep and vibrocreep testing. The test specimens chosen for solid polymer testing abide by the tensile testing ASTM D638-96 and for thin plastic sheeting D882-95a for thin films.

The preliminary testing matrix is shown below in Table 5. Typically one specimen is used for each test at the preliminary experimental stage. Assessment of each of the parameters can therefore be analyzed for the direction testing should be pursued in the second stage or if testing should

cease. The second stage of vibrocreep testing requires the decision of testing below or above the linear viscoelastic limit. If testing is performed within the linear viscoelastic limit, then the maximum stress should not exceed this limit. Mean stress and amplitudes must be selected to not violate this condition. Hysteresis heating effects may occur with the selection of the testing amplitude and frequency. If thermal or mechanical dominated failure regions are of particular interest, then the selections of the amplitude and frequency should be selected accordingly. Three test specimens are used to represent a mean stress, amplitude, frequency, and temperature. Three specimens reduce testing time since multiple parameters are being analyzed. The temperature effects upon the vibrocreep phenomena need to be analyzed by keeping the mean stress, amplitude, and frequency constant over a chosen temperature range. A reference temperature should be chosen for comparison. Typically the room temperature is taken since special equipment is not needed such as environmental chambers to test at this temperature, but another reference temperature may be chosen. Once these parameters are held constant, the linear limit may be violated at higher temperatures other than the reference temperature, since the linear viscoelastic limits decrease relative to reference temperature. Decreasing the temperature may be assumed to have the opposite effect with an increase in the linear viscoelastic limit relative to the reference temperature.

Table 5 Preliminary Test Matrix for Vibrocreep Testing

Mean Stress	Amplitude	Frequency
20% of Yield Stress	+-20% of Yield Stress	10Hz
40% of Yield Stress	+-20% of Yield Stress	10Hz
60% of Yield Stress	+-20% of Yield Stress	10Hz
80% of Yield Stress	+-20% of Yield Stress	10Hz
20% of Yield Stress	+-20% of Yield Stress	20Hz
40% of Yield Stress	+-20% of Yield Stress	20Hz
60% of Yield Stress	+-20% of Yield Stress	20Hz
80% of Yield Stress	+-20% of Yield Stress	20Hz
20% of Yield Stress	+-10% of Yield Stress	10Hz
40% of Yield Stress	+-10% of Yield Stress	10Hz
60% of Yield Stress	+-10% of Yield Stress	10Hz
80% of Yield Stress	+-10% of Yield Stress	10Hz
20% of Yield Stress	+-10% of Yield Stress	20Hz
40% of Yield Stress	+-10% of Yield Stress	20Hz
60% of Yield Stress	+-10% of Yield Stress	20Hz
80% of Yield Stress	+-10% of Yield Stress	20Hz

The results of the vibrocreep test data are therefore averaged and condensed using the 3 Sample Dynamic and 3 Average Dynamic macros in Excel provided in Appendix O. The final results are expressed in time at every 12 min. This result is therefore plotted instead of a large number of data points at once to provide a clear and accurate representation of the test data.

Non contact testing for strain and temperature measurements is strongly encouraged through the development of the creep and vibrocreep experimental procedures. The influence of attachments on the test specimens is not a variable that needs to be added to the study of vibrocreep. All strain measurements are calculated from position measurements using a LVDT, position transducer, etc.

Temperatures are measurements of the atmospheric temperature about the test specimen except for the infrared temperature measurement system for monitoring the surface temperature of the polymer materials

Knowledge of the hysteresis loop is necessary to obtain the proper mean strain values. If the hysteresis loop is "wide" then the mean strain will not be recorded properly. This is due to acquiring many data points and searching for the maximum and minimum values using the techniques described above. Other methods of acquiring the mean strain value during periodic loading have been investigated, but computer runtime becomes a factor. If the hysteresis loop is wide then averaging of the maximum and minimum strain values is only applicable if the hysteresis loop is symmetric. This technique is shown in Figures 28-30. These are simple guidelines for vibrocreep testing that have been developed from experience.

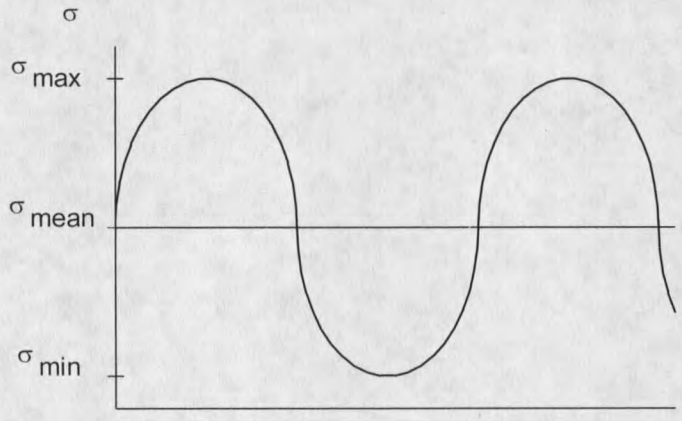


Figure 28 Periodic Stress

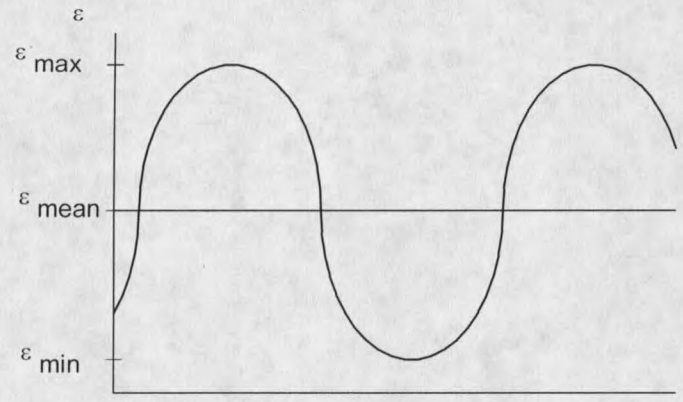


Figure 29 Periodic Strain

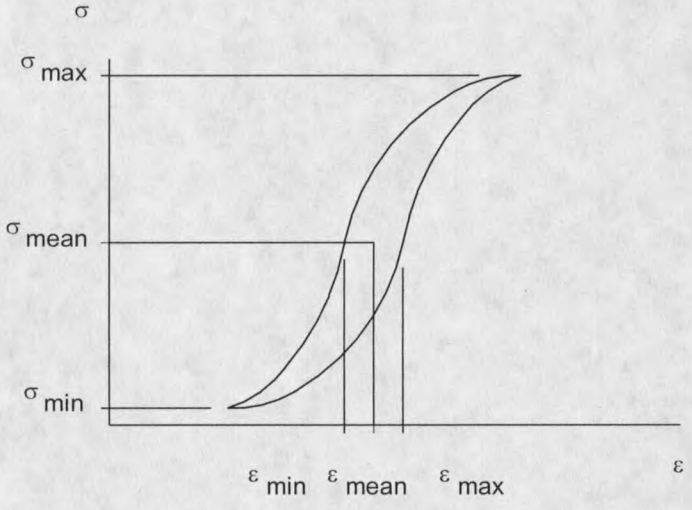


Figure 30 Resulting Hysteresis Loop

Vibrocreep Criteria

The criteria used to detect the presence of vibrocreep effects are illustrated in Figures 30-31, and in particular, if the mean strain from vibrocreep testing resides between the minimum and maximum resulting creep stain curves the vibrocreep effect does not exist. Alternatively, the vibrocreep effect is present if positioned above the creep curve obtained under maximum constant

stress. Normalization of the creep and vibrocreep results, further emphasizes the vibrocreep effect in the linear viscoelastic regime only. Specifically, the normalized vibrocreep curve that deviates from the creep compliance of the material indicates the presence of vibrocreep results shown in Figure 32. The normalization calculation for the vibrocreep result is shown by Equation 14.

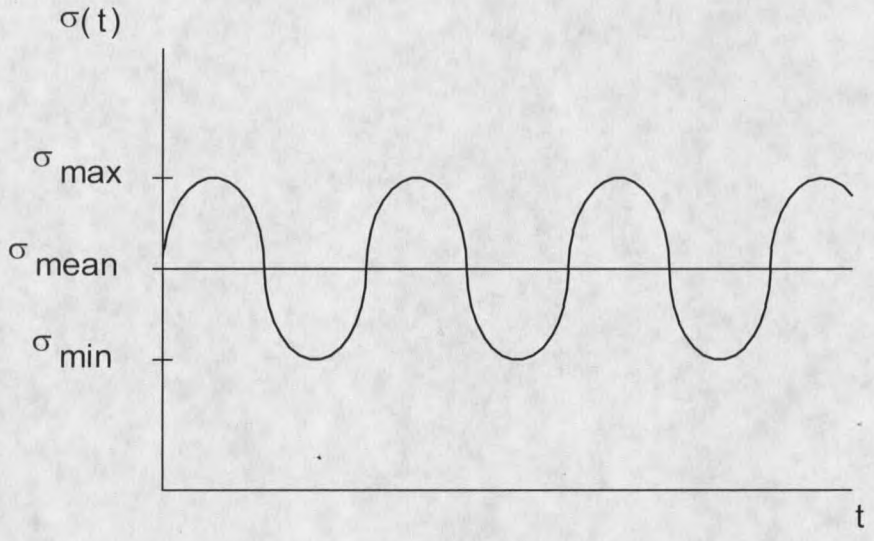


Figure 31 Loading Diagram for Vibrocreep

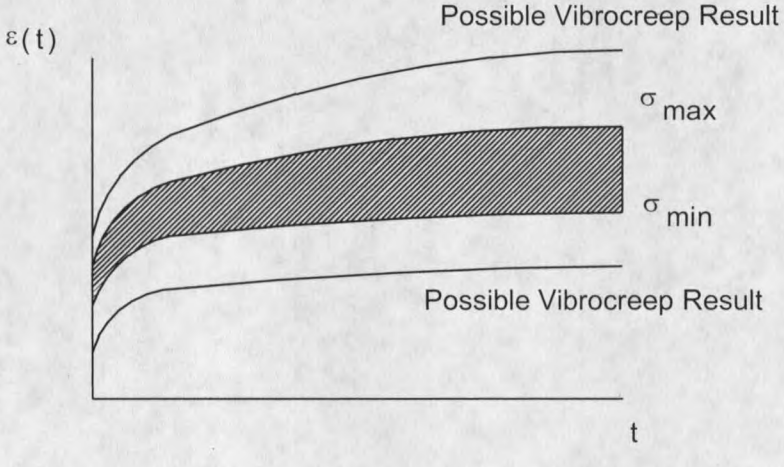


Figure 32 Vibrocreep Effect Above or Below the Linear Viscoelastic Limit

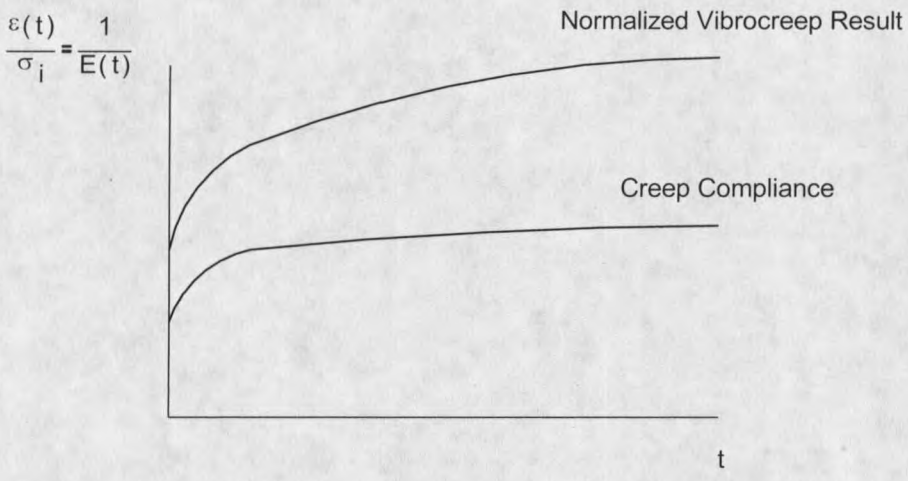


Figure 33 Normalized Vibrocreep Effect within the Linear Viscoelastic Limit

$$\frac{\varepsilon(t)}{\sigma_{mean}} = \frac{\varepsilon_{mean}(t)}{\left(\frac{\sigma_{max} + \sigma_{min}}{2}\right)}$$

Equation 14

EXPERIMENTAL PROGRAM AND RESULTS FOR NYLON 6/6

Properties and Applications of Nylon 6/6

In this study, Nylon 6/6 (DuPont Zytel® 42A NC010 Polyamide 66) has been selected as a test material since it is commonly used in engineering applications. Typical applications of Nylon 6/6 are gears, bearings, bushings, sprockets, and housings for power tools, Ref[12]. Recently, Nylon 6/6 has been used as a matrix in glass reinforced composites for application in automotive transmission gears, Ref[35].

Nylon 6/6 exhibits superior physical properties of stiffness, strength and fracture toughness. General and physical properties of Nylon 6/6 used in this program are described in Appendix P. In general, Nylon 6/6 can be characterized as a highly crystalline thermoplastic polymer.

Experimental Program

Instrumentation, Equipment, and Data Acquisition

In this program, computer aided data acquisition has been performed using National Instruments signal conditioning equipment and windows based data acquisition programming, LABView, version 5.0. The National Instruments signal conditioning equipment involves the following components:

- SCXI 1000 Chassis

- SCXI 1200 module with SCXI 1302 attachment
- SCXI 1100 module with SCXI 1303 attachment
- SCXI 1121 module with SCXI 1321 attachment

The signal conditioning system allows data sampling at 333,000 samples per second with 12 bit resolution. This system provides excitation and the ability to monitor all types of components. The LABView program for data acquisition provided the interface between the measured voltage and the final experimental data.

Tensile Testing of Nylon 6/6. Tensile testing of Nylon 6/6 has been performed using an Instron 4206 screw type tensile testing machine. The displacements have been measured and converted to strain using the crosshead displacement. The load was measured using the 30,000 lbf load cell connected to signal conditioning equipment. The mechanical grips that are used for the creep testing of polymer materials are used is conjunction with the round specimen attachments of the testing apparatus to accommodate the environmental chamber. The environmental chamber was not designed for use with the Instron 4206, so revisions were made. The environmental conditions are monitored using type J thermocouples with an Instron 3111 environmental chamber. The signal conditioning equipment is connected through the control panel of the Instron 4206 test machine. The environmental conditions have been monitored using data acquisition equipment. The position and load are

connected to the SCXI 1321 attachment channels 0 to 1 respectively. The thermocouples are connected to the SCX1 1303 attachment.

The post cyclic testing of solid polymers is performed using the Instron 1350 test machine. The instrumentation and equipment is exactly the same as in vibrocreep testing of polymer materials. The only changes that are performed is output from the 8500 plus control panel which is switched to 12.7 mm/Volt (.5 in/Volt) to accommodate the longer movement required during the tensile test.

The data acquisition program for tensile and post tensile cyclic loads has been programmed to record displacement and load over the duration of the tensile test. The program reads the displacement voltage and converts the reading into strain and the strain is then recorded. The load reading has also been converted from voltage to a load value and recorded. Temperature measurement have been performed using a simple temperature data acquisition program that is executed before the tensile test to verify the steady state temperature conditions in the environmental chamber. An environmental chamber has been used for testing at elevated temperatures.

Constant Load Creep Testing of Nylon 6/6. Creep testing of solid polymers has been performed using an in house built test fixture that has allowed the application of high static loads for testing of Nylon 6/6. Test specimen grips for creep testing of Nylon 6/6 were specially designed and built in order to

provide a high clamping force and axial alignment. Working drawings of the grips and load trays are provided in Appendix S.

A Pentium 120 computer with 40 MB of RAM and a 500 MB hard disk has been used to performed the data acquisition. The data acquisition program has been written for load and displacement measurements. The load has been measured by an Interface 1210 2225 N (500 lbf.) load cell connected to the SCXI 1121 with the SCXI 1321 attachment. Displacement has been measured using a LVDT built by Data Instruments connected to the SCXI 1200 with the SCXI 1302 attachment. The test fixture has been modified to incorporate the environmental chamber. Four thermocouples have been used to measure the environmental conditions. Three thermocouples have been located inside the environmental chamber and the fourth has been used to measure the atmospheric temperature. National Instruments SCXI 1100 with the SCXI 1303 attachment has been used to measure the type J thermocouple voltage. One of the two environmental chambers designed and built by Shane Schumacher, has been used for creep testing and tensile testing using the Instron 4206 screw type testing machine. Working drawings are provided in Appendix Q.

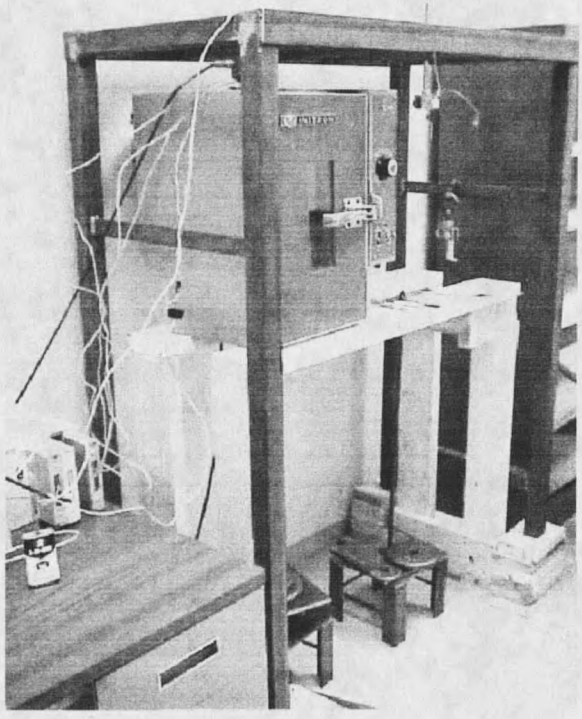


Figure 34 Creep Test Fixture for Nylon 6/6

Vibrocreep Testing of Nylon 6/6. The vibrocreep testing of Nylon 6/6 has been performed using an Instron 1350 servo hydraulic fatigue apparatus with an 8500 Plus control system update from Instron. The Instron 8500 Plus control system has the capability of measuring four test variables. A Pentium 120 computer with 40 MB of RAM and a 500 MB hard disk has been used to performed the data acquisition. The load and displacement have been measured by a data acquisition system at 889 N/Volt (200 lbf/Volt) and 5.08 mm/Volt (.2 in/Volt) respectively using outputs on the 8500 Plus control system control panel. The displacement has been recorded via channel 0 and load has been recorded via channel 1 of the SCXI 1100 attachment. Displacement measurements have

been taken in 3 parts, maximum, mean, and minimum. The displacement data has been converted into strain data and recorded. An initial offset for displacement, approximately 25.4 mm (1 in.), has been found to be necessary since the displacement of failure exceeds the 50.8 mm (2 in.) downward stroke from 0 of the 1350 Instron testing machine allowing a total displacement of 76.2 mm (3 in.) downward movement. The load followed a path similar to that of the displacement, respectively the maximum and minimum values are recorded. An environmental chamber has been designed and built specifically for testing using the Instron 1350 test machine by Shane Schumacher. The environmental chamber did not surround the hydraulic grips, but rested between them, heating the test specimen only. The environment remained constant by forced convection. The environmental chamber requires two holes, top and bottom, for specimen placement in the grips. There was a possibility for a temperature gradient due to the exposure to the atmosphere, therefore thermocouples are placed near the holes, and the temperature difference from the center to either hole does not fluctuate by more than .2 °C. Working drawings of the environmental chamber are provided in Appendix Q.

The monitoring of the environmental conditions and specimen conditions has been performed with infrared temperature measurement, a humidity transmitter, and type J thermocouples. The infrared temperature measurement system has been manufactured by Omega engineering (Model OS65 complete NEMA system). The IR measurement system has provided a 3:1 field of view to

focus a 6.35 mm (.25 in) spot size at 25.4 mm (1 in). The output was measured in terms of volts (0 to 5 volts) over a temperature range of -57 to 250 °C. The humidity transmitter has been also manufactured by Omega Engineering. The transmitter (Model HX92V) that provides an output from 0 to 1 Volt over a range of 0 to 100% relative humidity. The infrared temperature measurement system connects to channel 2, and the humidity transmitter connects to channel 3 of the SCXI 1100 attachment. The temperature measurement of the sample from the IR system has been converted from voltage to °C and recorded. The humidity transmitter measured the relative humidity of the testing room and has also been converted from voltage measurements to % relative humidity and recorded. The type J thermocouples have been used to measure the temperature within the environmental chamber channels 0 to 2 and the thermocouple at channel 3 measures the testing room temperature. The type J thermocouples allow temperature measurement from 0 to 750 °C.

The programming of the data acquisition system using LABView has been accomplished through the development of case structures, similar to a "Do Loop" where the loop control represents the execution of a task. A case structure was needed to separate the gathering of data from the separate modulus, since data must be acquired form each module separately. The dynamic testing of solid polymers requires two case structures, one to control data acquisition of the hysteresis loops and the second to monitor the displacement, load and environmental changes in time. The hysteresis case structure has been

executed every 100 cycles of the second case structure, thus monitoring the changes in the hysteresis loop approximately every hour. The second structure has been designed to monitor the change in strain approximately every 30 seconds. A 30 second execution of the second case structure is controlled by a Do While loop while a time wait function has been used to control the accumulation of data. The Do while loop is also the control for the initial case structure that is executed every 100 cycles. The time to execute the case structures has been recorded along with the wait time to obtain readings with an accuracy of .001 sec..

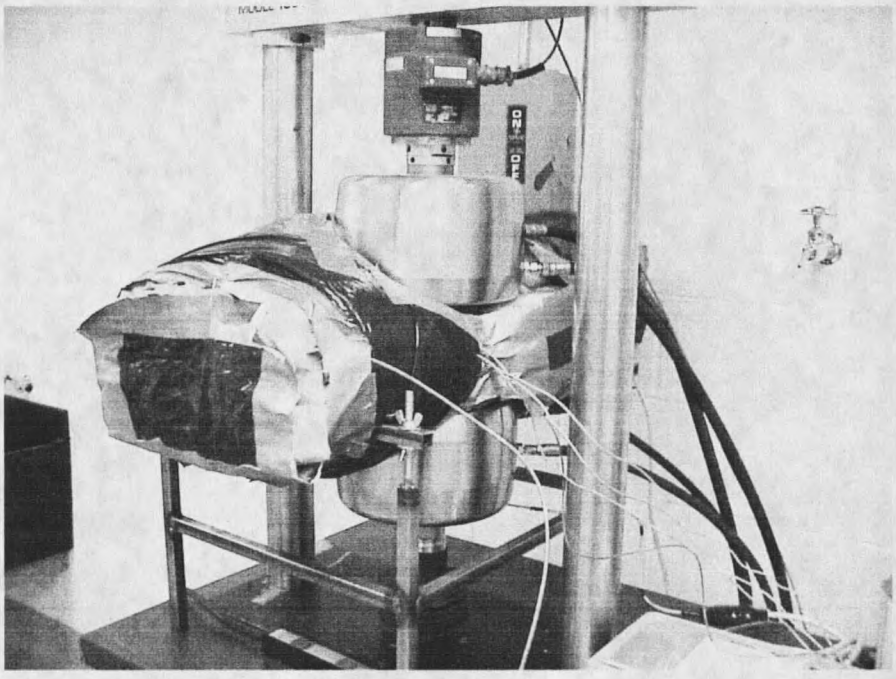


Figure 35 Vibrocreep Test Fixture for Nylon 6/6

Testing Procedure

The specimen geometry used in all experiments has been completed according to ASTM D638-96 Type II standards. All test specimens have been prepared using a CNC milling machine by Technical Services at Montana State University, Bozeman. The material has been purchased from Laird Plastics with the properties shown in Appendix P. Nylon 6/6 has not necessarily been purchased from the same batch of processed material, therefore the effects of batch sensitivity may have effected some results. Testing temperature has been varied from room temperature of 23 °C to 50 °C, with increments of 9 °C. Once the environmental chamber for vibrocreep testing was designed and built, the temperature chamber maintained a temperature of 35 °C with the blower fan in operation by conduction of heat from the motor to the environmental chamber. Nylon 6/6 was first tested in tension to determine the strength and stiffness properties, secondly creep tests were performed, and thirdly the vibrocreep and post cyclic testing were completed.

Tensile Testing Procedure for Nylon 6/6. Tensile testing has been performed at a strain rate of .875 mm/mm * min (in/in * min) or a feed rate of 44.45 mm/min (1.75 in/min) for all temperatures ranging from .5 min at 23 °C to 5 min at 68 °C abiding by the ASTM 638-96 standard. The strength and stiffness calculations are also performed according to the ASTM D638-96 standard.

Constant Load Creep Testing Procedure for Nylon 6/6. The preliminary creep testing for Nylon 6/6 has been performed for 24 hrs. Further creep tests have been performed at a minimum of 9 hours where at least five test specimens were used to represent each resultant curve. The linear viscoelastic range has been determined for each temperature at 23 °C, 35 °C, 41 °C, 50 °C, 59 °C, and 68 °C. The environmental chamber used for tensile testing of Nylon 6/6 was also used for creep testing of Nylon 6/6 with a temperature fluctuation of not more than +-.5 °C. At 23 °C creep testing was performed for 10%, 20%, 30%, 40%, and 50% of the yield stress. The cross-section was considered to remain constant as the material deformed in time (engineering stress). The feed rate during loading of the test specimen was controlled by the use of a hydraulic jack.

Vibrocreep Procedure for Nylon 6/6. The sample geometry was kept the same as in the previous test cases (ASTM D638-96 Type II). The relative humidity was monitored during vibrocreep with readings of 15% +-5% during testing. Approximately in the middle of the vibrocreep testing, the test machine was relocated to another room. The humidity levels remained the same between the two rooms. All testing of Nylon 6/6 was performed in tension-tension mode within the linear viscoelastic regime of the polymer determined from the above creep testing except at elevated temperature, where testing was performed at stress levels relative to the yield stress at 23 °C. Nylon 6/6 specimens have been also monitored for the effects of hysteresis heating where thermal effects

can contribute to deformation over time. Hysteresis heating was not observed, so the deformation of the polymer was considered to be in the mechanically dominated regime.

Post Cyclic Testing Procedure for Nylon 6/6. After creep and vibrocreep programs had been completed, specimens were tested in tension at the same feed rate as that of the initial tensile testing described above. The vibrocreep specimens were tested in tension directly after cyclic tests using the 1350 Instron, where creep test specimens were stored and tested in tension later on the same testing machine. The effect of recovery was initially of great concern for the creep test specimens, but the effect of recovery (testing immediately after completion of a creep test or after storage for weeks or months) did not show an effect on the post tensile properties of the material at 23 °C. At higher temperatures the effect of recovery upon the test specimens has not been investigated

Experimental Results

Tensile Testing Experimental Results at 23 °C

Tensile testing of Nylon 6/6 provided the values of the instantaneous elastic modulus, yield strength, and ultimate strength of the polymer. Nylon 6/6 that was used for the project is an isotropic material, therefore directionality of

the tensile testing relative to the microstructure was not necessary. The results of the tensile testing are provided in Table 6.

Table 6 Tensile Properties of Nylon 6/6 at 23 °C

	Yield Stress (MPa)	Maximum Strength (MPa)	Elastic Modulus (GPa)	Yield Strain (mm/mm)
23 °C	70	78	1.42	.0642

Tensile testing of Nylon 6/6 has been performed for two separate batches of material from Laird Plastics. The feed rates have been kept consistent for all samples. A comparison of the material properties depending on the particular batch is provided in Table 7.

Table 7 Batch Comparison

	Yield Strength (MPa)	Elastic Modulus (GPa)
Batch 1	70	1.42
Batch 2	72	1.42

Constant Load Creep Test Results of Nylon 6/6 at 23 °C

As indicated in the previous chapter, the objectives of creep testing have been to determine the vibrocreep effect, and the linear viscoelastic limit. The results have been also used for the vibrocreep model development. After the preliminary creep testing of Nylon 6/6, the linear viscoelastic limit has been determined to be 30% the yield stress at 23 °C, shown in Figure 36. The complete results of the creep testing at 23 °C are provided in Appendix A.

Vibrocreep Experimental Results at 23 °C

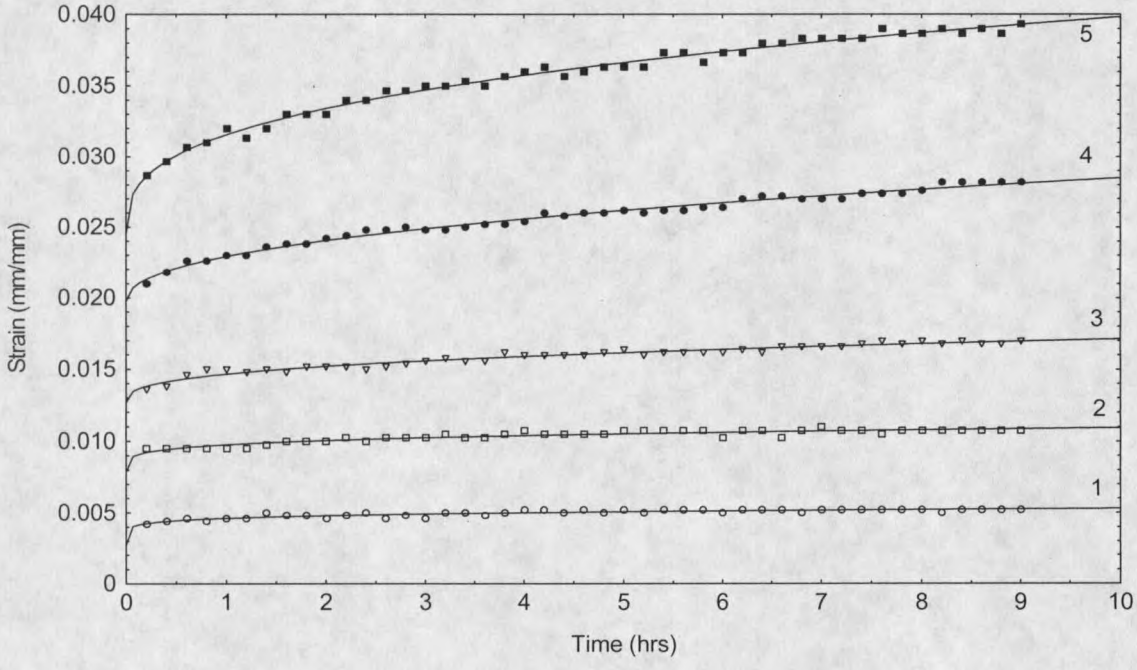
The vibrocreep results for Nylon 6/6 have been divided into three categories that determine the influence of frequency, amplitude, mean stress, respectively. The preliminary vibrocreep testing was performed for 24 hrs. The tests have been used for verification of the vibrocreep in the selected polymer. Nylon 6/6 has demonstrated the effect of vibrocreep, therefore testing was pursued further. A parametric study of vibrocreep effects has been conducted following the test program summarized in Table 8.

Table 8 Test Matrix for Nylon 6/6 Vibrocreep Testing at 23 °C

Mean Stress (% of σ_y)	Superimposed Cyclic Load									
12	Stress Amplitude (% of σ_y)	4			7.5			10		
	Frequency (Hz)	1	10	20	1	10	20	1	10	20
16	Stress Amplitude (% of σ_y)	4			7.5			10		
	Frequency (Hz)	1	10	20	1	10	20	1	10	20
20	Stress Amplitude (% of σ_y)	5			7.5			10		
	Frequency (Hz)	1	10	20	1	10	20	1	10	20

The testing matrix shown is a compact representation of the experimental loading conditions performed. For example, testing was performed at 12%±4% of the yield stress at 1, 10, and 20 Hz to describe frequency effects. Testing is also performed at 12%±7.5% and ±10% of the yield stress at 1, 10, and 20 Hz to further investigate the frequency effects. Once these tests were completed, the

mean stress was changed from 12% to 16% and the same sequence was executed, then from 16% to 20%. Once the testing has been completed, amplitude and mean stress effects can also be investigated with substantial supporting data. All test matrices within the thesis are provided in this format with similar interpretation. The influence of the frequency in the vibrocreep effect shown in Figure 37. The complete results of the frequency effects at 23 °C are provided in Appendix B.



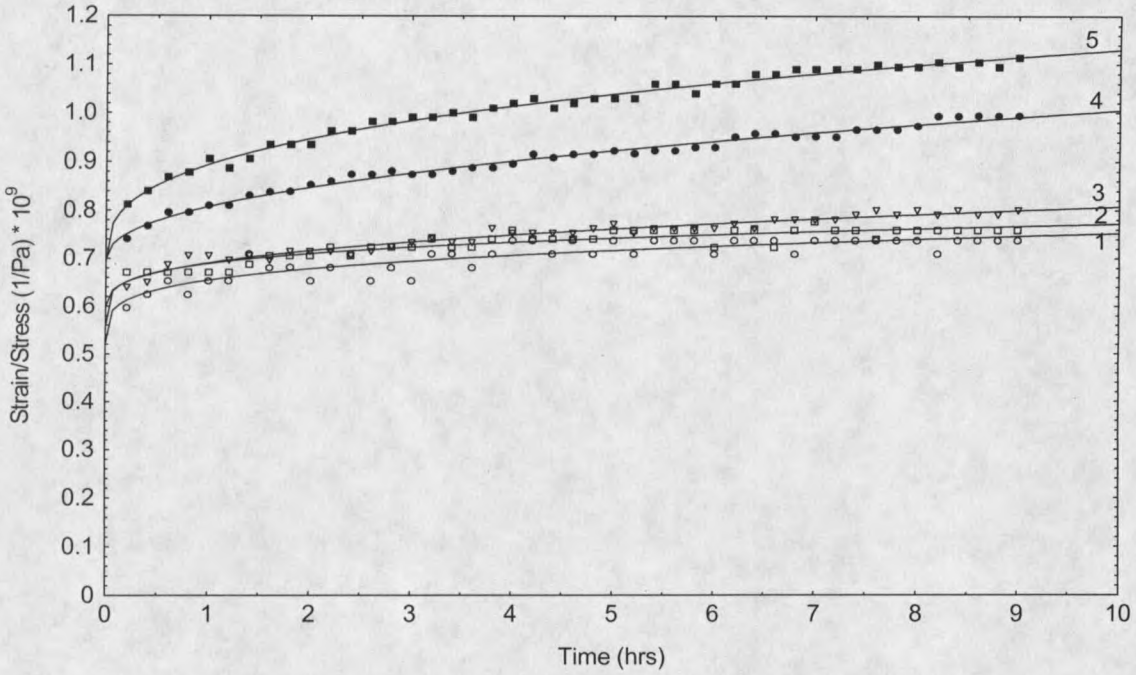
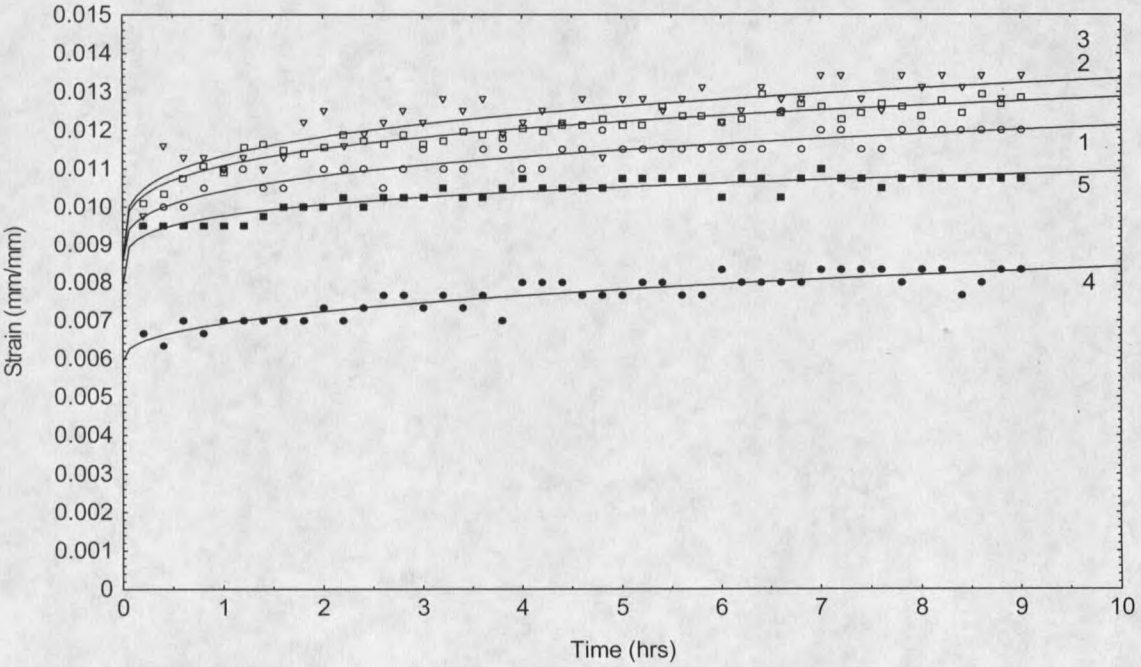


Figure 36 Constant Load Creep of Nylon 6/6 at 23 °C
1- $(0.10)\sigma_y$; **2**- $(0.20)\sigma_y$; **3**- $(0.30)\sigma_y$; **4**- $(0.40)\sigma_y$; **5**- $(0.50)\sigma_y$;
σ_y = 70 MPa at 23 °C



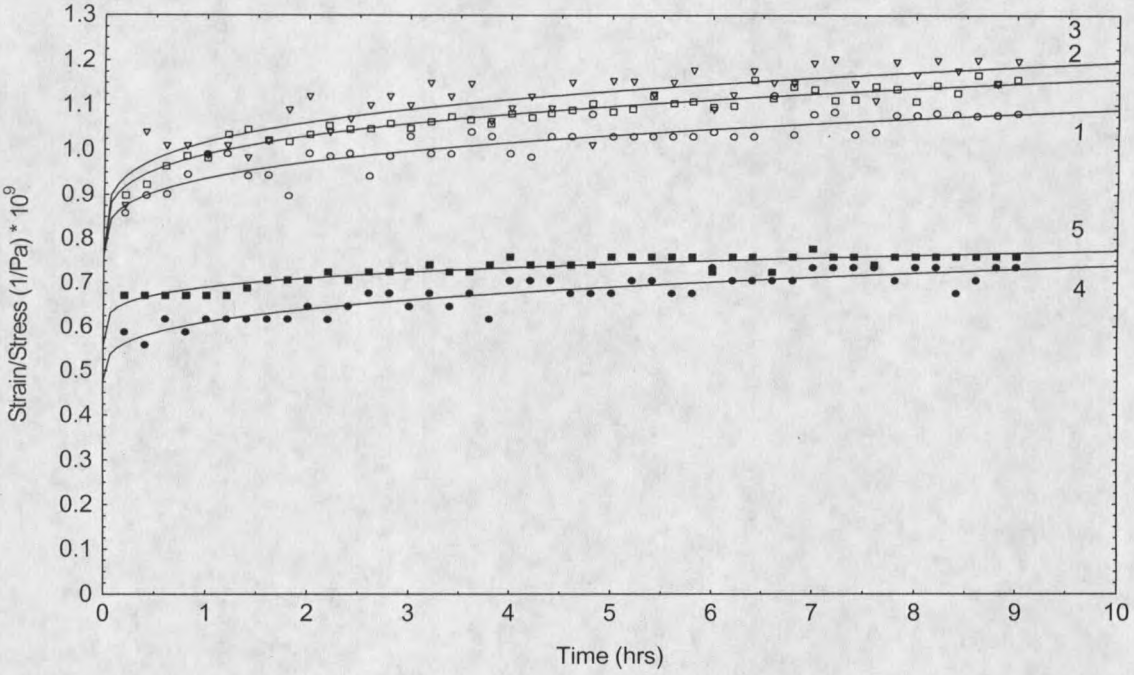


Figure 37 Vibrocreep Response of Nylon 6/6 at Different Frequencies at 23 °C
Vibrocreep: $(0.16\pm0.075)\sigma_y$; **1**- 1 Hz, **2**- 10 Hz, **3**- 20 Hz;
Constant Load Creep : **4**- $(0.16)\sigma_y$, **5**- $(0.20)\sigma_y$;
σ_y = 70 MPa at 23 °C

It has been shown that an increase in the loading frequency resulted in an increase in the vibrocreep effect. An increase in amplitude has also resulted in an increase in the vibrocreep effect, as shown in Figure 38. Complete results of the amplitude effects at 23 °C are provided in Appendix C. The effect of the mean stress upon the creep behavior of Nylon 6/6 is not apparent. As an example, the influence of the mean stress can be observed in Figure 39. Complete results of the mean stress effects at 23 °C are provided in Appendix E.

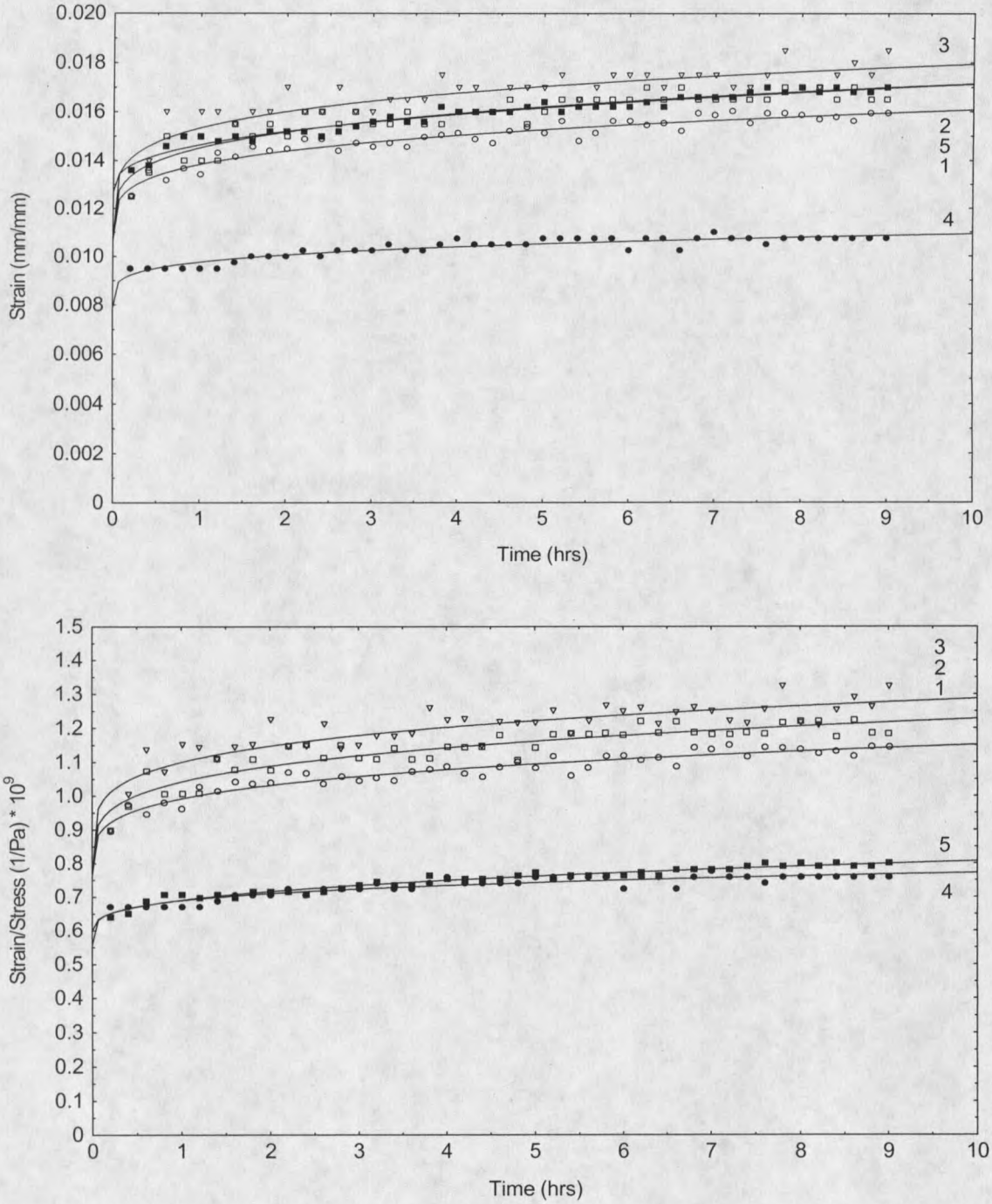


Figure 38 Vibrocreep Response of Nylon 6/6 at Different Amplitudes at 23 °C
Vibrocreep: **1**- $(0.20\pm0.05)\sigma_y$, **2**- $(0.20\pm0.075)\sigma_y$, **3**- $(0.20\pm0.10)\sigma_y$, at 20 Hz;
Constant Load Creep : **4**- $(0.20)\sigma_y$, **5**- $(0.30)\sigma_y$;
σ_y = 70 MPa at 23 °C

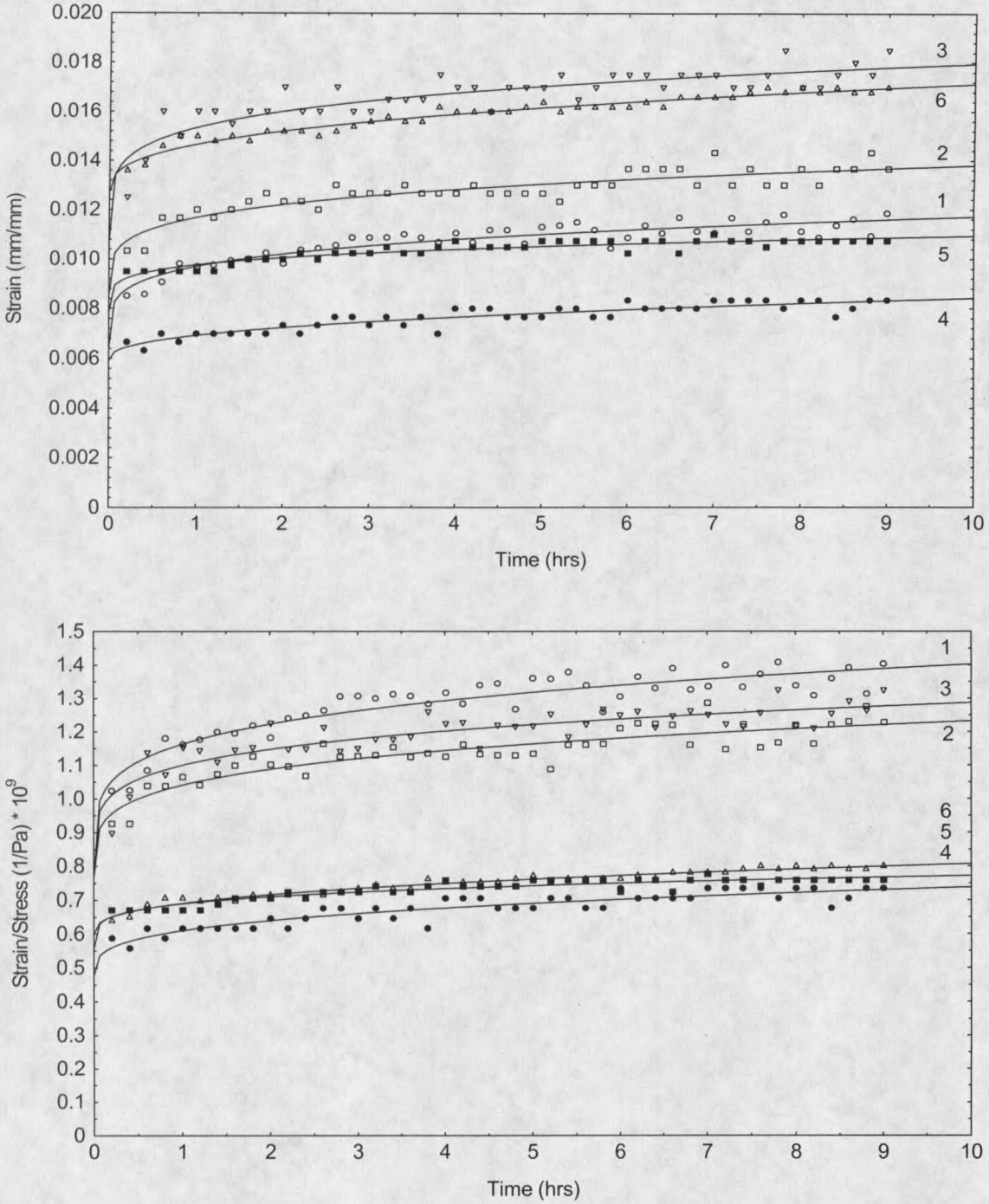


Figure 39 Vibrocreep Response of Nylon 6/6 at Different Mean Stresses at 23 °C

Vibrocreep: **1-** $(0.12\pm0.10)\sigma_y$, **2-** $(0.16\pm0.10)\sigma_y$, **3-** $(0.20\pm0.10)\sigma_y$, at 20 Hz;
Constant Load Creep : **4-** $(0.16)\sigma_y$, **5-** $(0.20)\sigma_y$, **6-** $(0.30)\sigma_y$;
σ_y = 70 MPa at 23 °C

Post Cyclic Testing at 23 °C

The post cyclic testing is described as tensile testing following creep and vibrocreep experiments. The result is a measure of the changes in the material properties in the polymer due to cyclic loading effects. Testing has been performed for all test specimens with an example shown in Figure 40 and the results summarized in Table 9.

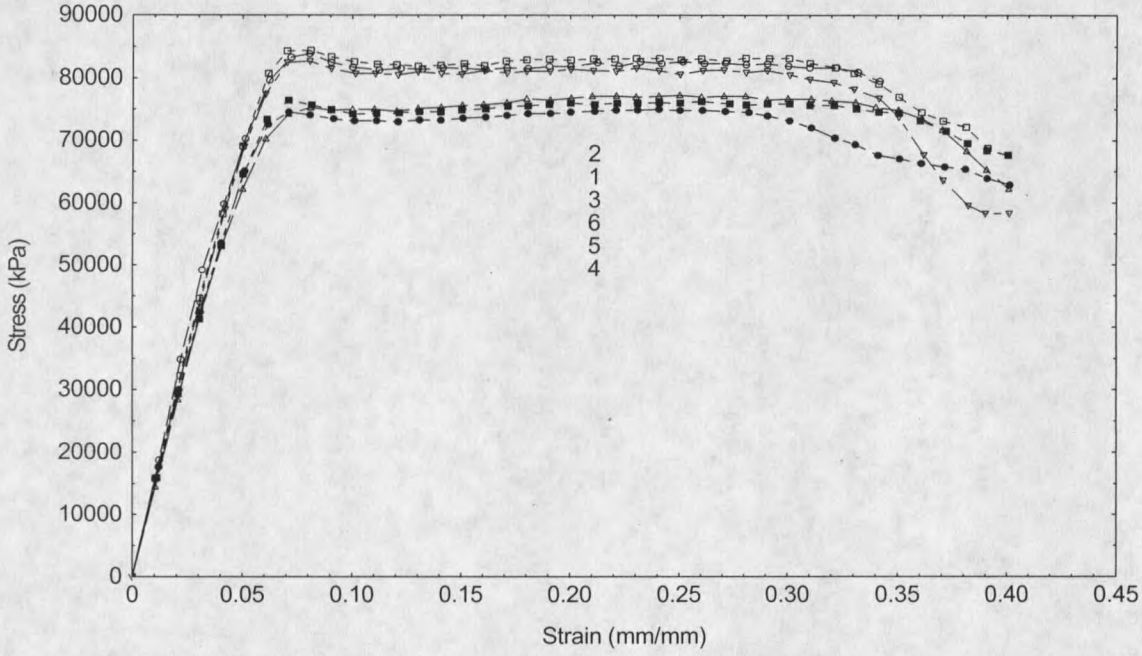


Figure 40 Tensile Testing of Nylon 6/6 Specimens After Cyclic and Constant Loading at 23 °C
Vibrocreep: $(0.16\pm0.075)\sigma_y$, **1**- 1 Hz; **2**- 10 Hz; **3**- 20 Hz;
Constant Load Creep : **4**- $(0.16)\sigma_y$, **5**- $(0.20)\sigma_y$; **6**- Virgin Specimens;
σ_y = 70 MPa at 23 °C

Table 9 Tensile Testing of Nylon 6/6 Specimens After Cyclic and Constant Loading at 23 °C

Curve #	Yield Stress (MPa)	Yield Strain (mm/mm)	Maximum Stress (MPa)	Elastic Modulus (GPa)
1	79.697	.06164	83.877	1.56
2	80.754	.06042	84.414	1.47
3	77.394	.06105	82.676	1.44
4	65.567	.06515	74.543	1.33
5	63.171	.06885	76.427	1.35
6	70	.06420	78.000	1.42

As shown in Figure 40, the strength and stiffness of the material can be seen to increase after the cyclic testing. The effects of recovery after vibrocreep testing has also been determined using post cyclic testing as shown in Figure 41 and summarized in Table 10.

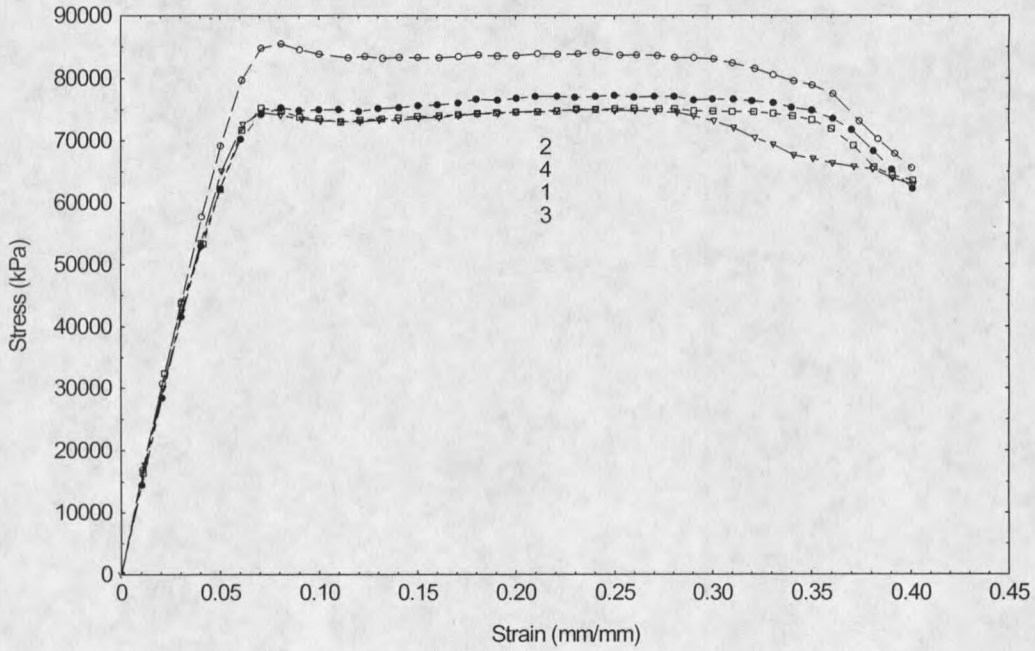


Figure 41 Tensile Testing of Nylon 6/6 Specimens After Cyclic and Constant Loading at 23 °C
Vibrocreep: $(0.16\pm0.10)\sigma_y$, 10 Hz; **1**- Recovered, **2**- Immediate;
Constant Load Creep : **3**- $(0.16)\sigma_y$; **4**- Virgin Specimens;
σ_y = 70 MPa at 23 °C

Table 10 Tensile Testing of Nylon 6/6 Specimens After Cyclic and Constant Loading at 23 °C

Curve #	Yield Stress (MPa)	Yield Strain (mm/mm)	Maximum Stress (MPa)	Elastic Modulus (GPa)
1	71.718	.06104	75.233	1.44
2	82.397	.06593	85.779	1.49
3	65.567	.06515	74.543	1.33
4	70	.06420	78.000	1.42

After approximately one month of recovery, specimens tested under cyclic loading conditions have shown marginal changes in the tensile properties over that of the constant load creep and virgin specimens.

Tensile Testing Results at Elevated Temperatures

Tensile test results at elevated temperatures are shown in Figure 42.

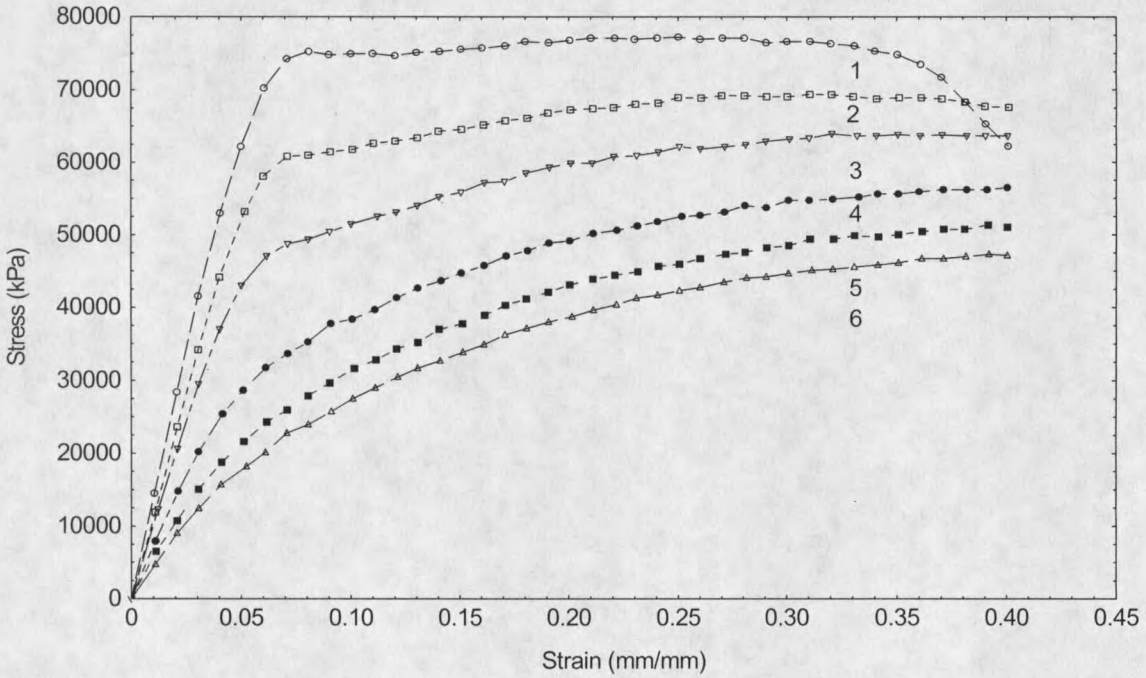


Figure 42 Tensile Testing of Nylon 6/6 at Different Temperatures
1- 23 °C; **2-** 35 °C; **3-** 41 °C; **4-** 50 °C; **5-** 59 °C; **6-** 68 °C;

All calculations of the strength and stiffness have been performed according to the ASTM 638-96 standard. The elastic modulus, yield stress, and ultimate stress are tabulated in Table 11.

Table 11 Tensile Properties of Nylon 6/6 at 23 °C and Elevated Temperatures

	Yield Stress (MPa)	Ultimate Stress (MPa)	Elastic Modulus (GPa)	Yield Strain (mm/mm)
23 °C	70	78	1.42	.0642
35 °C	55.2	70.2	1.21	.0544
41 °C	44.9	65	.96	.0551
50 °C	22	57.5	.708	.0332
59 °C	19	52.4	.548	.0368
68 °C	10	48.9	.459	.0238

The strain values at the given temperatures are provided in engineering strain. The results of the tensile testing of virgin specimens at different temperatures are shown in Figure 43. Complete results of the tensile testing of Nylon 6/6 are provided in Appendix A.

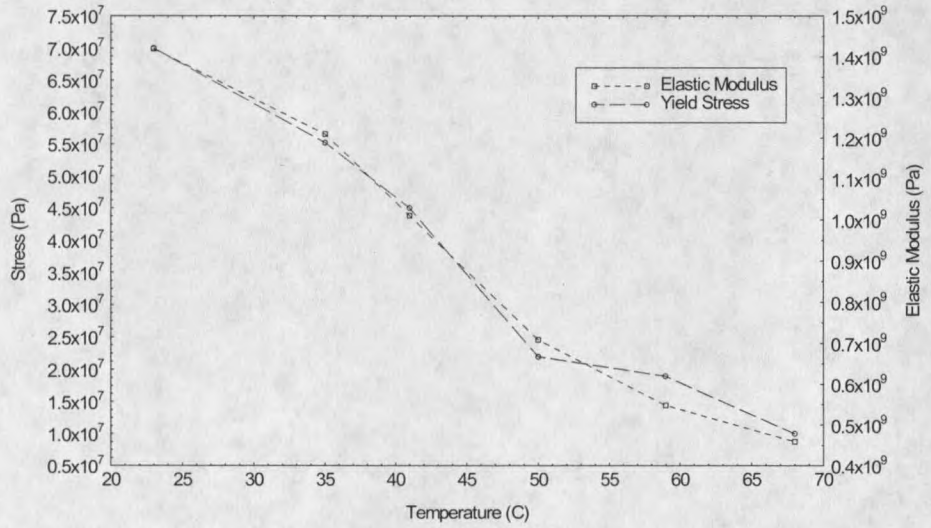
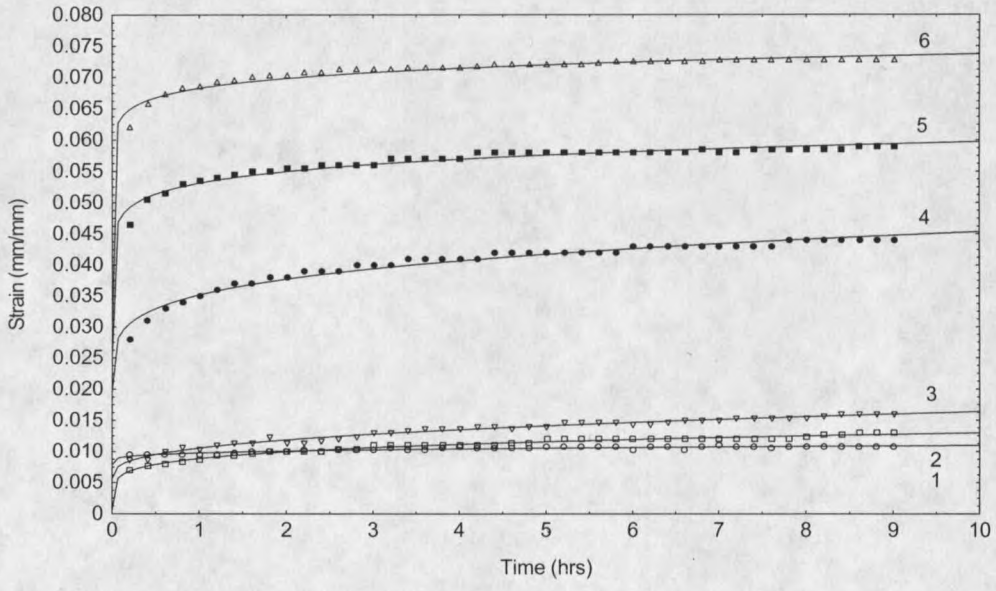


Figure 43 Yield Stress and Elastic Modulus vs. Temperature

Constant Load Creep Testing Results at Elevated Temperatures

The creep tests at elevated temperatures has been performed at 20%, 30%, 40% and 50% of the yield stress at the respective temperature. Complete creep testing results for Nylon 6/6 are provided in Appendix A. As stated above the cross section of the test specimen is assumed to remain constant through the duration of the test (engineering stress) even at elevated temperatures. The linear viscoelastic limit remains at an approximate 30% of the yield stress at their respective temperature.

For Nylon 6/6, stress levels of 16% and 20% with respect to the yield stress at 23 °C is performed at each temperature. The effect of temperature on creep at 20% relative to the yield stress at 23 °C can be observed in Figure 44. From the figure shown, the creep rate is shown to increase with increasing temperature. Complete results of the temperature effect for Nylon 6/6 are provided in Appendix F.



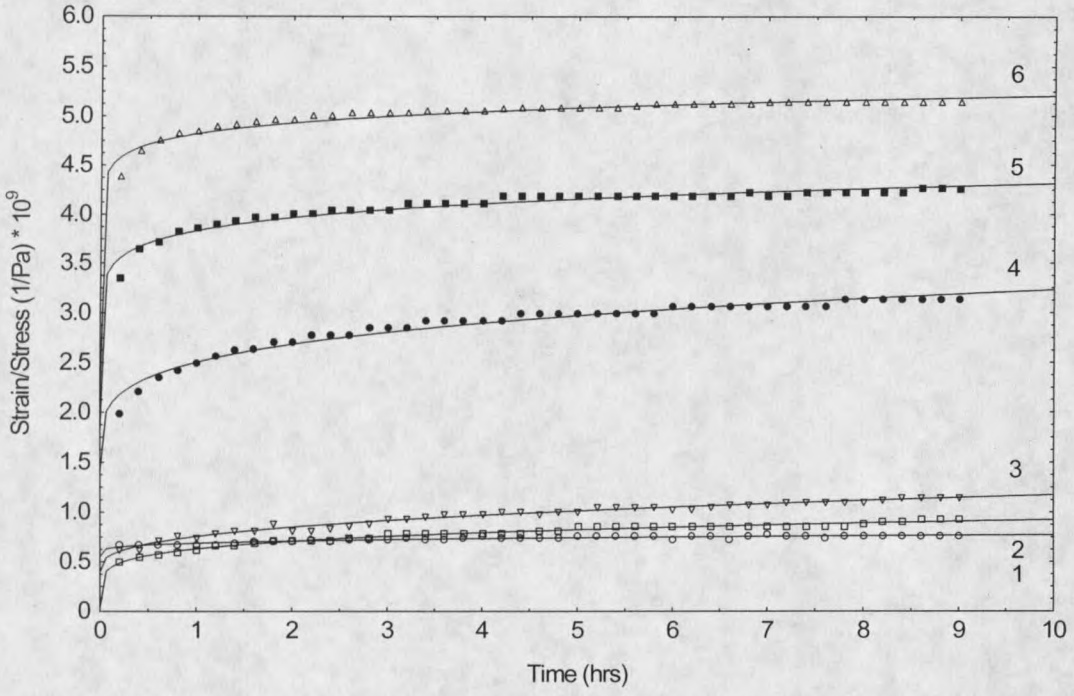


Figure 44 Constant Load Creep of Nylon 6/6 at Different Temperatures
1- $(0.20)\sigma_y$ at 23 °C; **2**- $(0.20)\sigma_y$ at 35 °C; **3**- $(0.20)\sigma_y$ at 41 °C;
4- $(0.20)\sigma_y$ at 50 °C; **5**- $(0.20)\sigma_y$ at 59 °C; **6**- $(0.20)\sigma_y$ at 68 °C;
σ_y = 70 MPa at 23 °C

Vibrocreep Testing Results at Elevated Temperatures

Two test temperatures have been used to characterize the vibrocreep effects, 35 °C and 41 °C at elevated temperatures. The temperatures chosen allowed testing in the linear viscoelastic regime of Nylon 6/6. Testing at stress levels relative to the test temperature is not easily accommodated at the higher temperatures, since amplitude loads at and below 100 N (22.5 lbf) are not executable due to testing machine limitations. Therefore at 41 °C, 4% amplitude relative to the yield stress at 41 °C was not executable.

The remainder of the testing within the linear viscoelastic regime provided the same results for all temperatures. The influence of temperature resulted in a decrease in the vibrocreep effect where the stress level is held constant over the temperature range. The results of the temperature effect for Nylon 6/6 are provided in Appendix F. The effect of the frequency at 35 °C at the yield stress relative to 35 °C and 23 °C upon the vibrocreep effect can be shown in Figure 45. The results of the frequency effects at 35 °C and 41 °C are provided in Appendix B. The effect of increasing amplitude at 41 °C at the yield stress relative to 41 °C and 23 °C is shown in Figure 46. The results of the amplitude effects at 35 °C and 41 °C are provided in Appendix C. The effect of the mean stress at 35 °C at the yield stress relative to 35 °C and 23 °C is shown in Figure 47. The results of the mean stress effects at 35 °C and 41 °C are provided in Appendix D.

Table 12 Test Matrix for Nylon 6/6 Vibrocreep Testing at Elevated Temperatures

Mean Stress (% of σ_y)	Superimposed Cyclic Load				
16	Stress Amplitude (% of σ_y)	4		10	
	Frequency (Hz)	1	10	1	10
20	Stress Amplitude (% of σ_y)	5		10	
	Frequency (Hz)	1	10	1	10

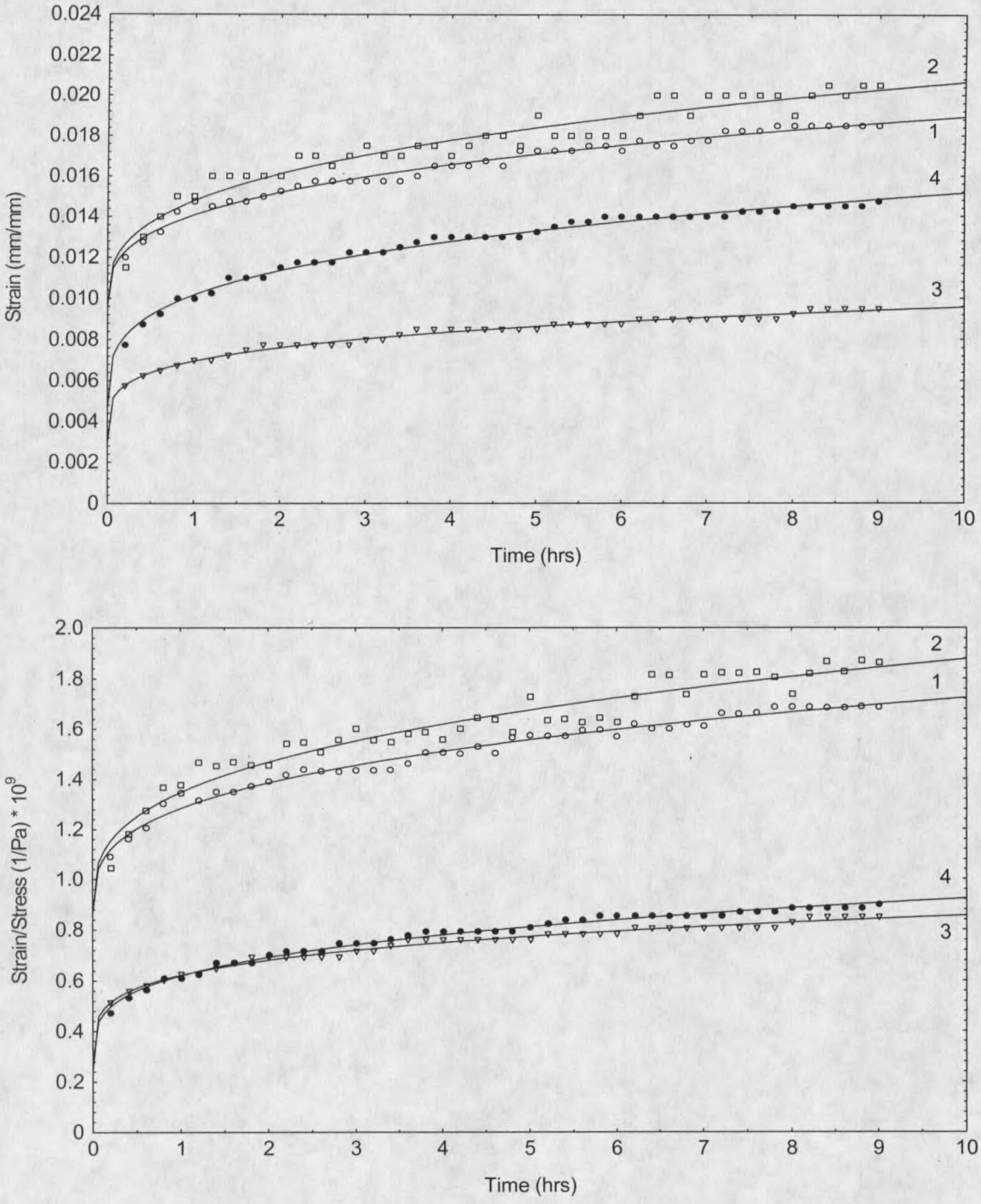


Figure 45 Vibrocreep Response of Nylon 6/6 at Different Frequencies at 35 °C
Vibrocreep: $(0.20\pm0.10)\sigma_y$, **1**- 1 Hz, **2**- 10 Hz;
Constant Load Creep: **3**- $(0.20)\sigma_y$, **4**- $(0.30)\sigma_y$;
σ_y = 55 MPa at 35 °C

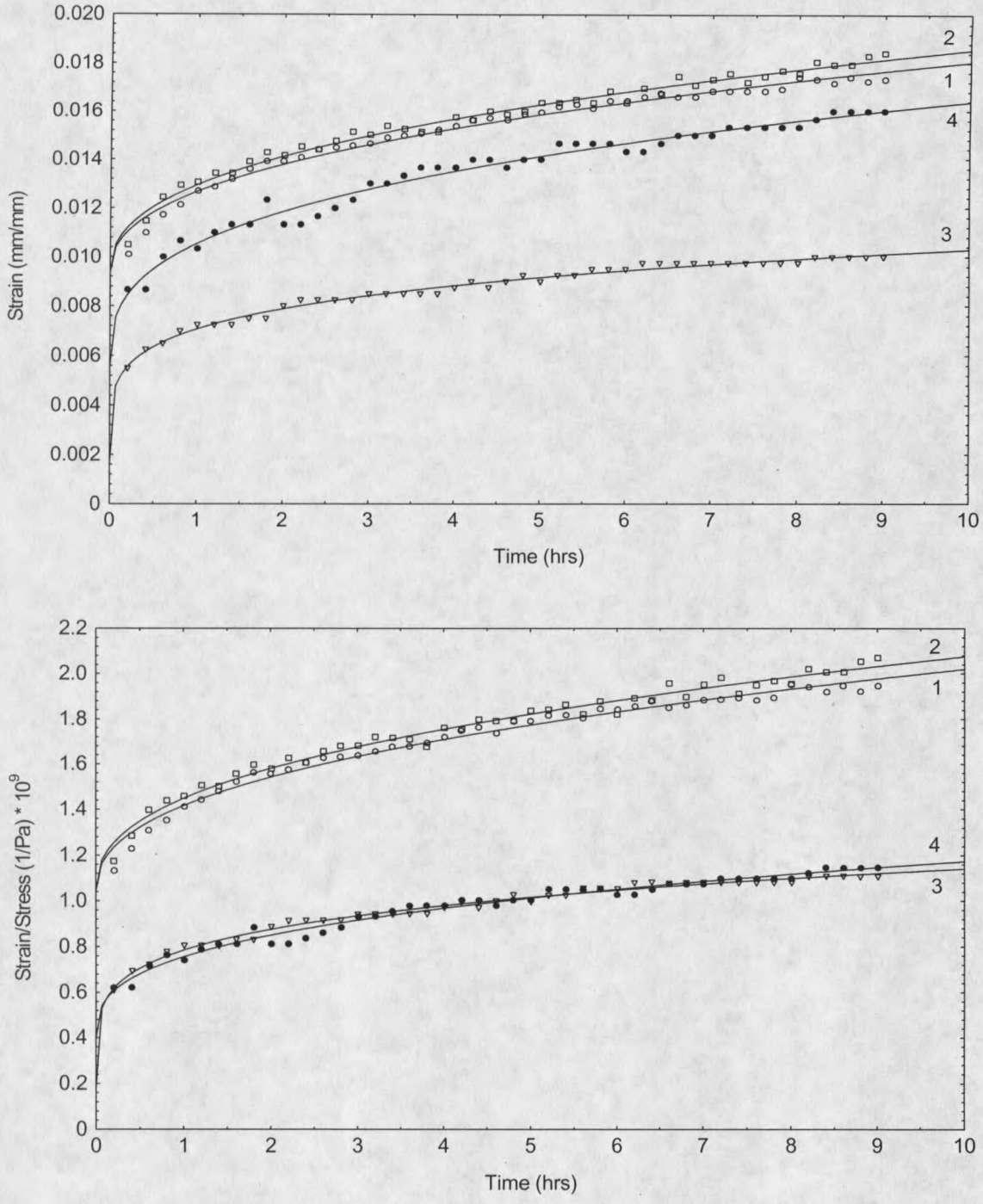


Figure 46 Vibrocreep Response of Nylon 6/6 at Different Amplitudes at 41 °C
Vibrocreep: **1-** $(0.20\pm0.05)\sigma_y$, **2-** $(0.20\pm0.010)\sigma_y$, at 10 Hz;
Constant Load Creep: **3-** $(0.20)\sigma_y$, **4-** $(0.30)\sigma_y$;
σ_y = 45 MPa at 41 °C

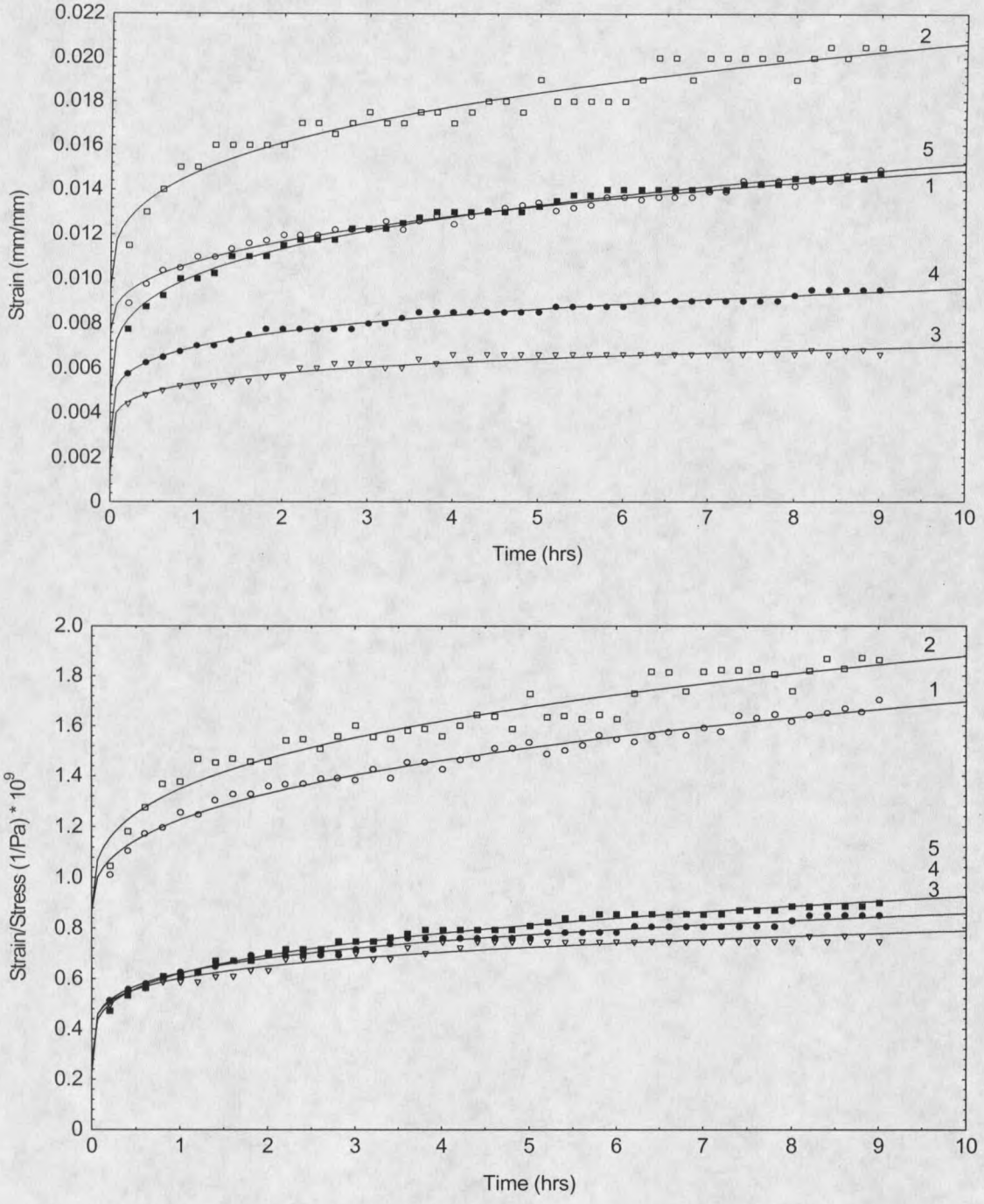


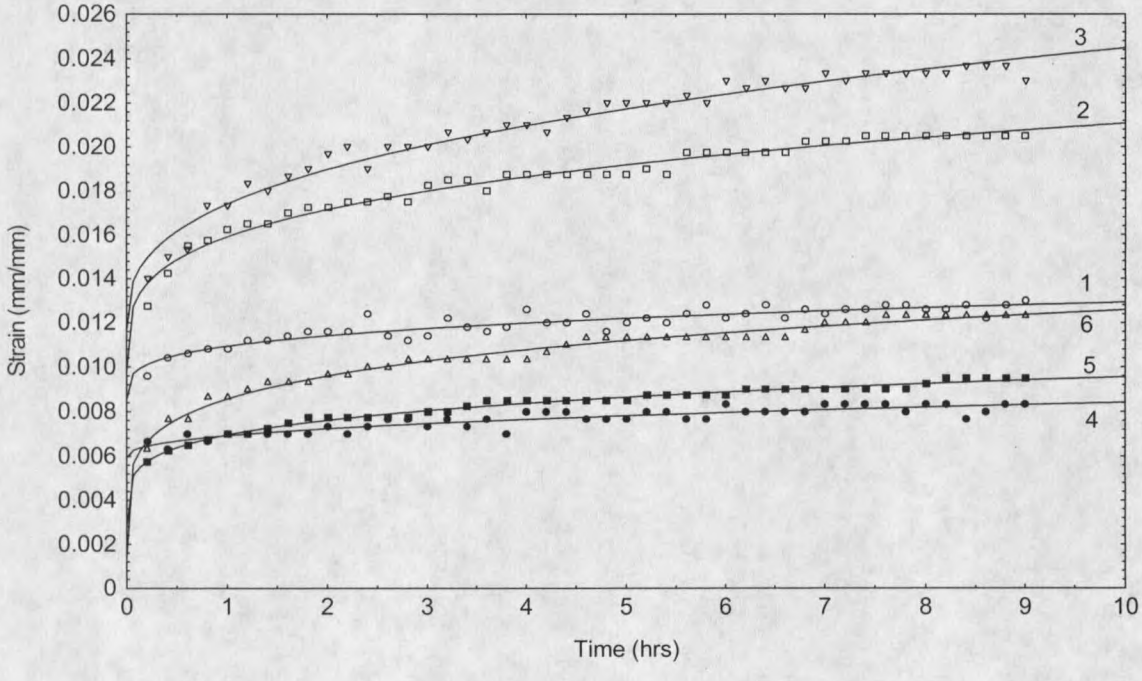
Figure 47 Vibrocreep Response of Nylon 6/6 at Different Mean Stresses at 35 °C

Vibrocreep: **1**- $(0.16\pm0.10)\sigma_y$, **2**- $(0.20\pm0.10)\sigma_y$, at 10 Hz;

Constant Load Creep: **3**- $(0.16)\sigma_y$, **4**- $(0.20)\sigma_y$, **5**- $(0.30)\sigma_y$;

σ_y = 55 MPa at 35 °C

From the results shown in the figures above, the effect of increasing frequency, amplitude, and mean stress show similar results as seen from testing at 23 °C. Through the temperature range this effect is emphasized at the stress levels where the yield stress is relative to the test temperature, but is not evident at the higher stress levels where the yield stress is relative to the 23 °C. The influence of temperature is evident from Figure 48. The result of the temperature effects are provided in Appendix F. An example of the influence of the frequency, amplitude, and mean stress where the yield stress is relative to 23 C is shown in Figures 49-51. From the results, the influence of these parameters has been analyzed above and below the linear viscoelastic limit, and also the influence of temperature.



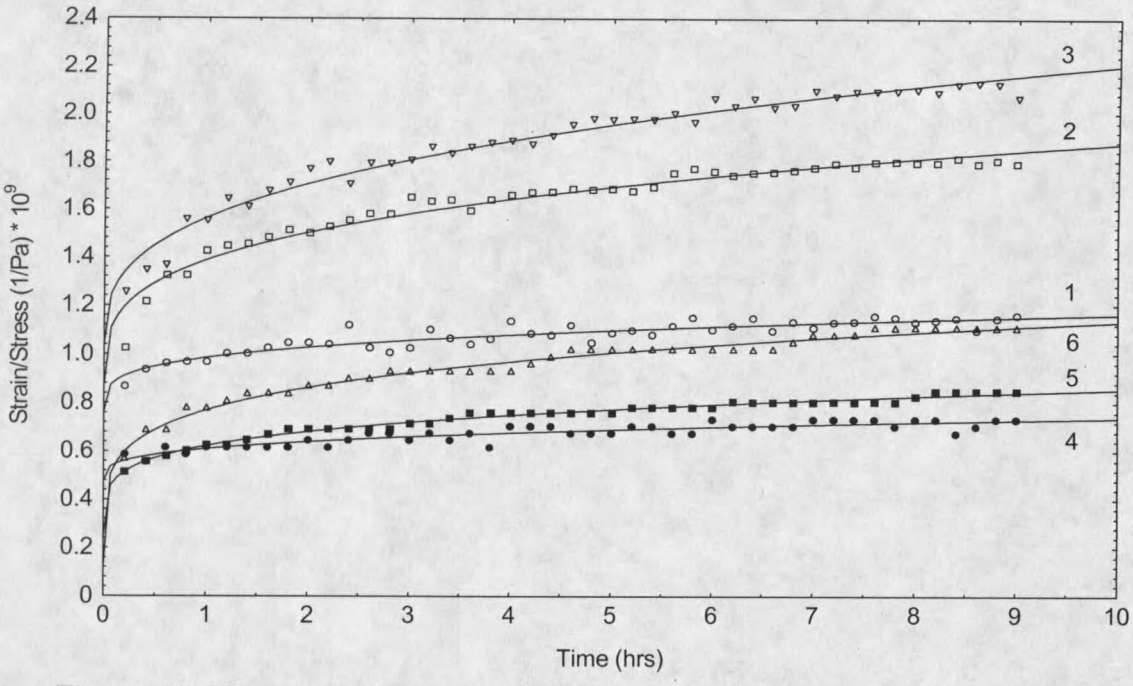
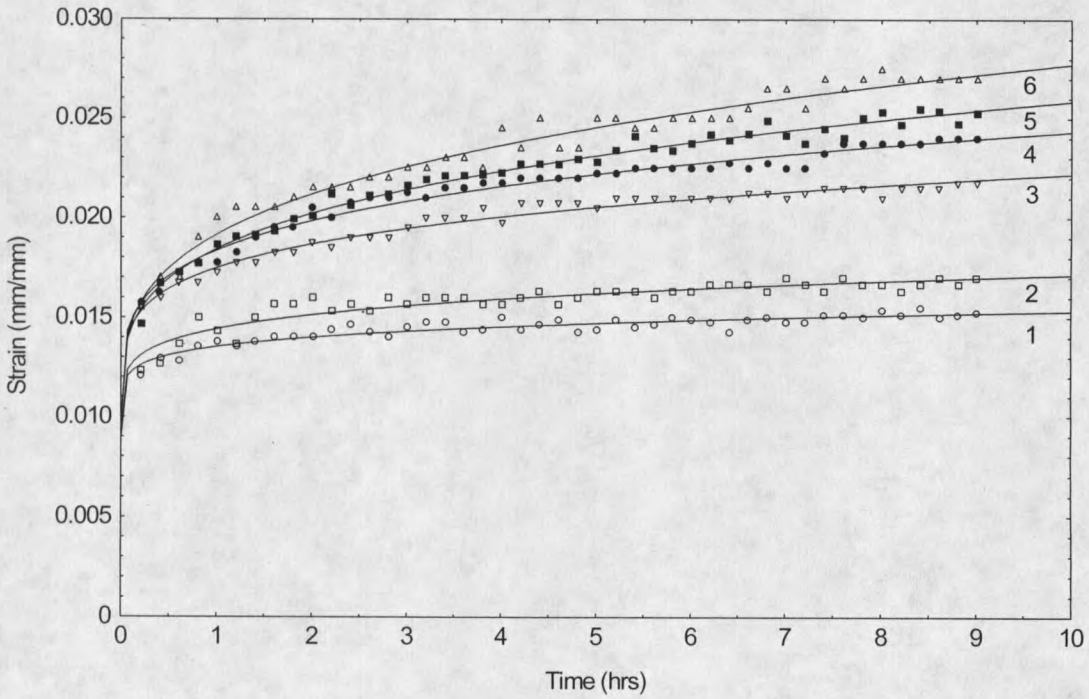


Figure 48 Vibrocreep Response of Nylon 6/6 at Different Temperatures
Vibrocreep: $(0.16\pm0.10)\sigma_y$, 10 Hz, **1**- 23 °C, **2**- 35 °C, **3**- 41 °C;
Constant Load Creep: $(0.16)\sigma_y$, **4**- 23 °C, **5**- 35 °C, **6**- 41 °C;
σ_y = 70 MPa at 23 °C



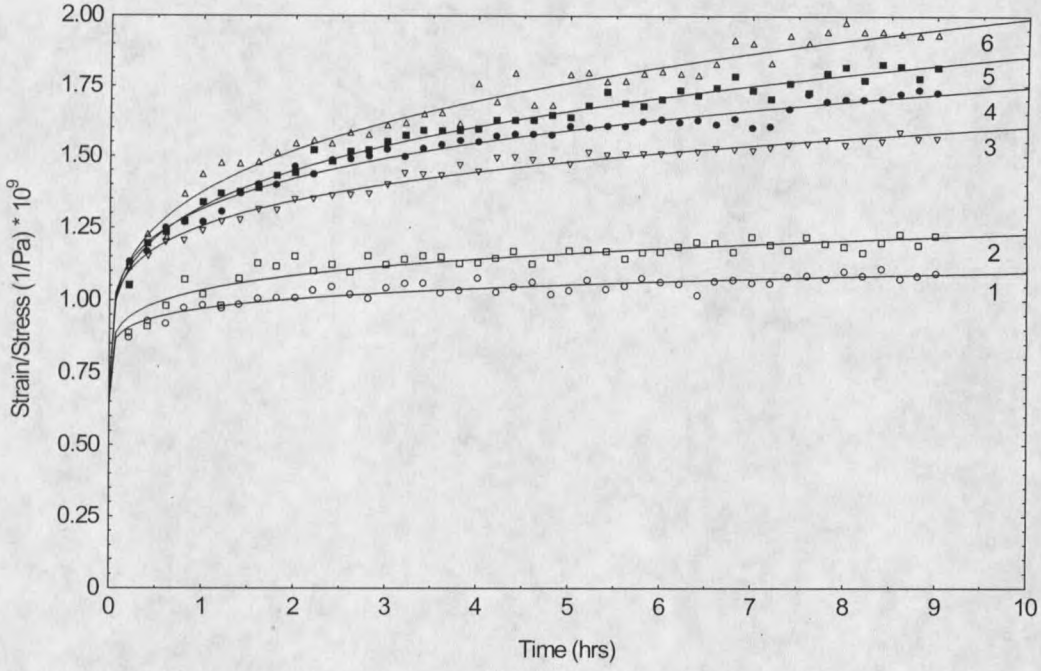
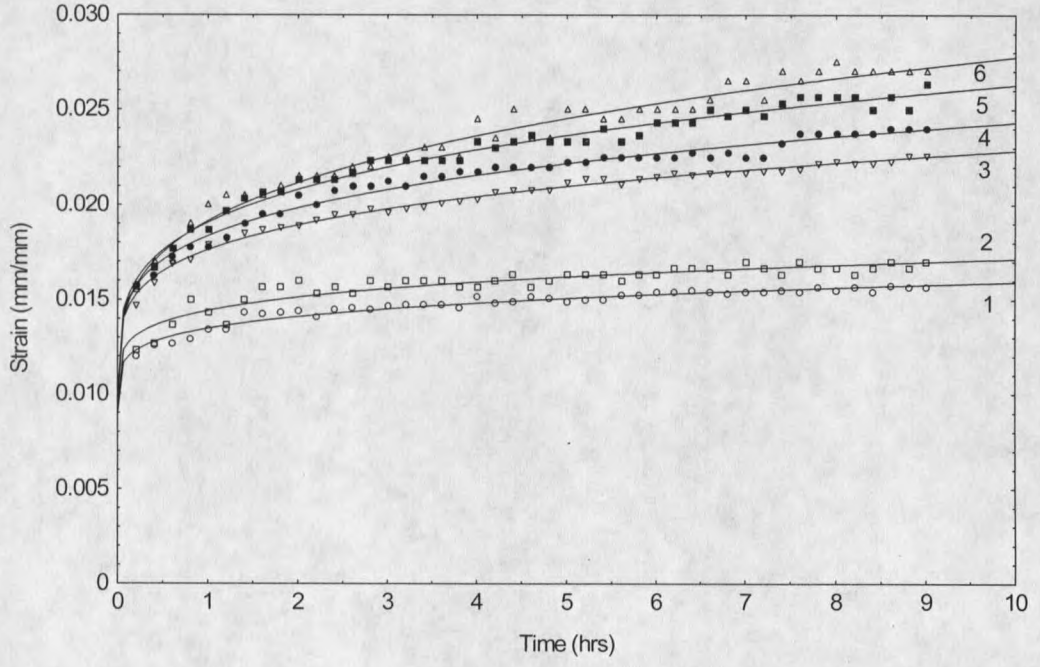


Figure 49 Vibrocreep Response of Nylon 6/6 at Different Frequencies and Temperatures

Vibrocreep: $(0.20\pm0.10)\sigma_y$, **1**- 1 Hz at 23 °C, **2**- 10 Hz at 23 °C;
3- 1 Hz at 35 °C, **4**- 10 Hz at 35 °C, **5**- 1 Hz at 41 °C, **6**- 10 Hz at 41 °C
σ_y = 70 MPa at 23 °C



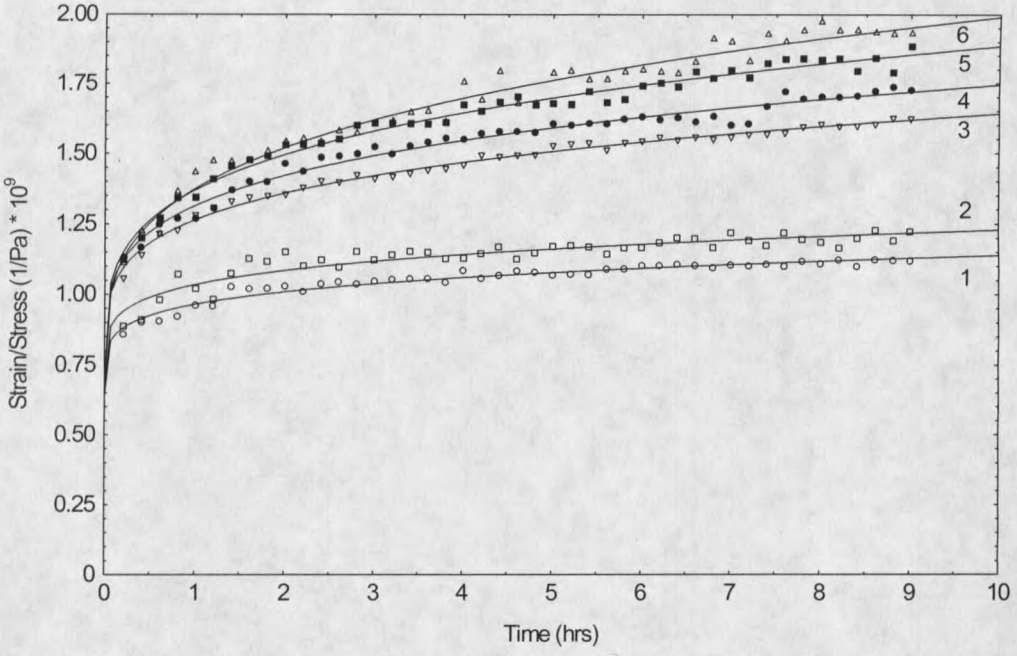
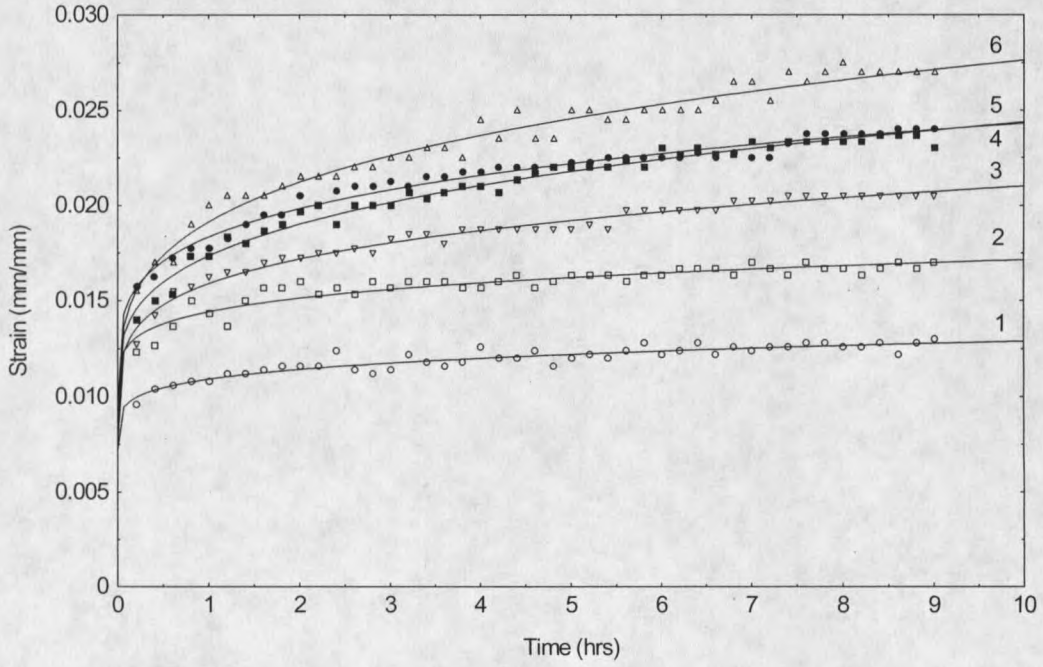


Figure 50 Vibrocreep Response of Nylon 6/6 at Different Amplitudes and Temperatures

Vibrocreep: **1**- (0.20±0.05)σ_y, at 10 Hz, 23 °C, **2**- (0.20±0.10)σ_y, at 10 Hz, 23 °C;
3- (0.20±0.05)σ_y, at 10 Hz, 35 °C, **4**- (0.20±0.10)σ_y, at 10 Hz, 35 °C;
5- (0.20±0.05)σ_y, at 10 Hz, 41 °C, **6**- (0.20±0.10)σ_y, at 10 Hz, 41 °C;
σ_y = 70 MPa at 23 °C



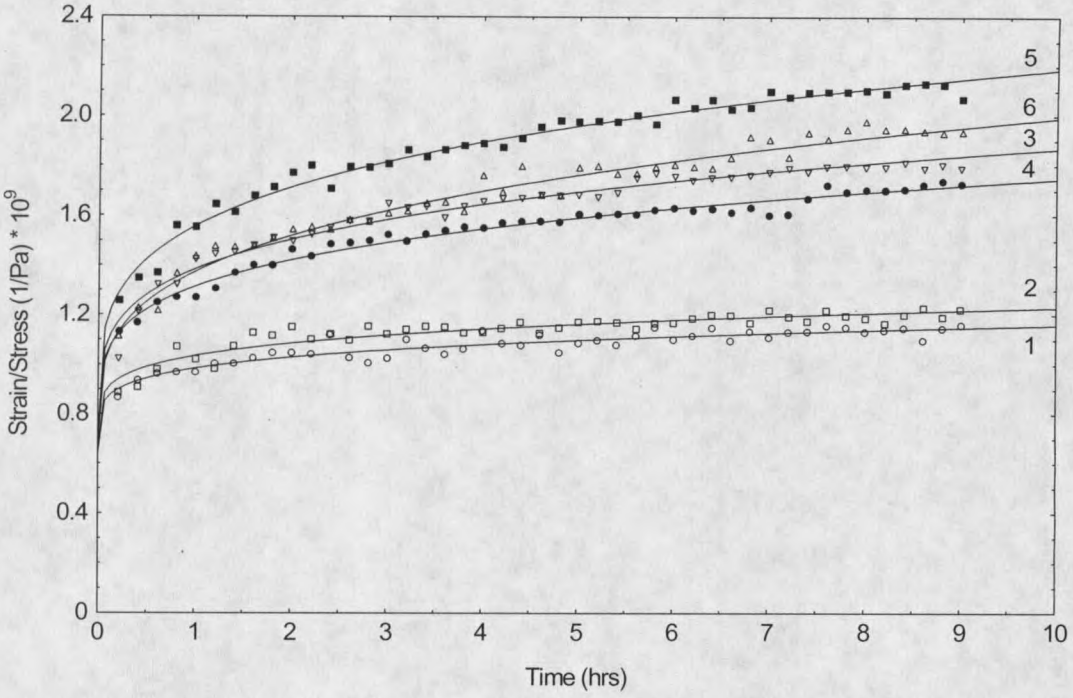


Figure 51 Vibrocreep Response of Nylon 6/6 at Different Mean Stresses and Temperatures
Vibrocreep: **1**- $(0.16\pm0.10)\sigma_y$, **2**- $(0.20\pm0.10)\sigma_y$, at 10 Hz 23 °C;
3- $(0.16\pm0.10)\sigma_y$, **4**- $(0.20\pm0.10)\sigma_y$, at 10 Hz 35 °C;
5- $(0.16\pm0.10)\sigma_y$, **6**- $(0.20\pm0.10)\sigma_y$, at 10 Hz 41 °C;
σ_y = 70 MPa at 23 °C

In Figures 49-50, an increase in temperature with an increase in frequency or amplitude resulted in an increase in the vibrocreep effect. In Figure 51, the effect of increasing mean stress is shown to have a decrease in the vibrocreep effect.

Post Cyclic Testing at Elevated Temperatures

The post cyclic testing is performed for all test specimens at 35 °C and 41 °C. The effect of recovery was not tested for higher temperatures, since this is not possible with the current test equipment. The specimen would be cooled and then reheated. Therefore storage of the creep test specimens is justified. An

example of the post tensile testing at 41 °C at the yield stress relative to 41 °C and 23 °C is summarized in Tables 13-14 and shown in Figures 52-53, respectively.

Table 13 Tensile Testing of Nylon 6/6 Specimens after Cyclic and Constant Loading at 41 °C

Curve #	Yield Stress (MPa)	Yield Strain (mm/mm)	Maximum Stress (MPa)	Elastic Modulus (GPa)
1	66.541	.06424	68.399	1.32
2	65.318	.05940	68.372	1.31
3	57.034	.05005	64.950	1.27
4	44.600	.05510	65.000	.96

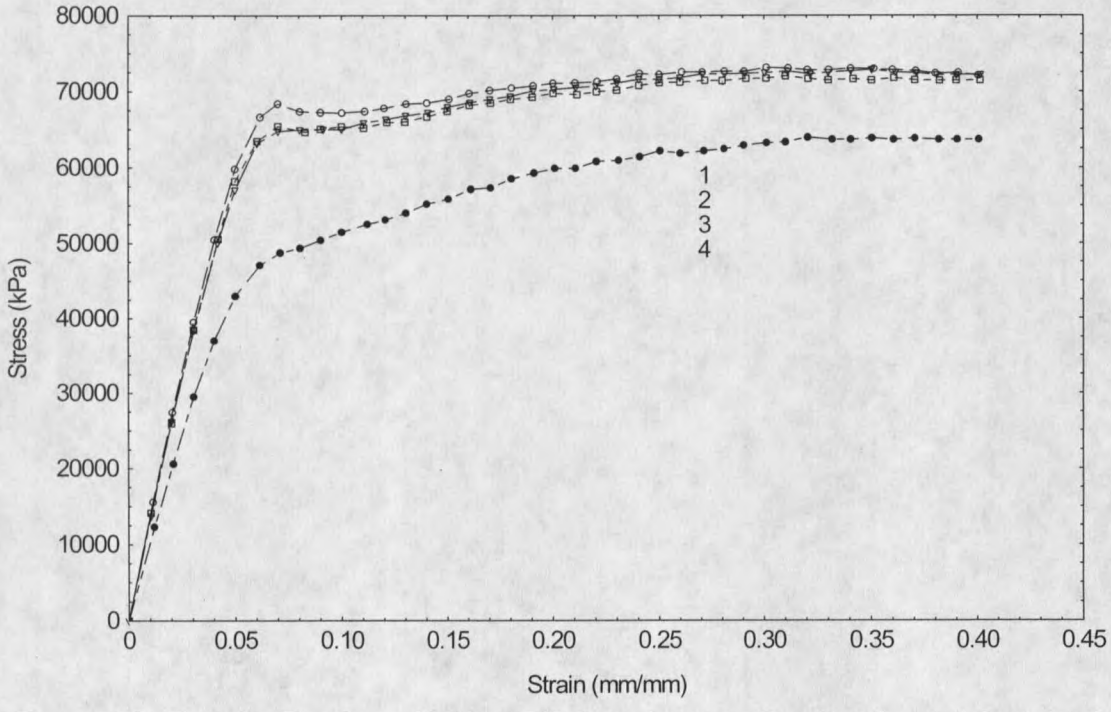


Figure 52 Tensile Testing of Nylon 6/6 Specimens after Cyclic and Constant Loading at 41 °C

Vibrocreep: **1-** $(0.20\pm0.05)\sigma_y$, **2-** $(0.20\pm0.10)\sigma_y$, at 10 Hz;
Constant Load Creep: **3-** $(0.20)\sigma_y$; **4-** Virgin Specimens;
σ_y = 45 MPa at 41 °C

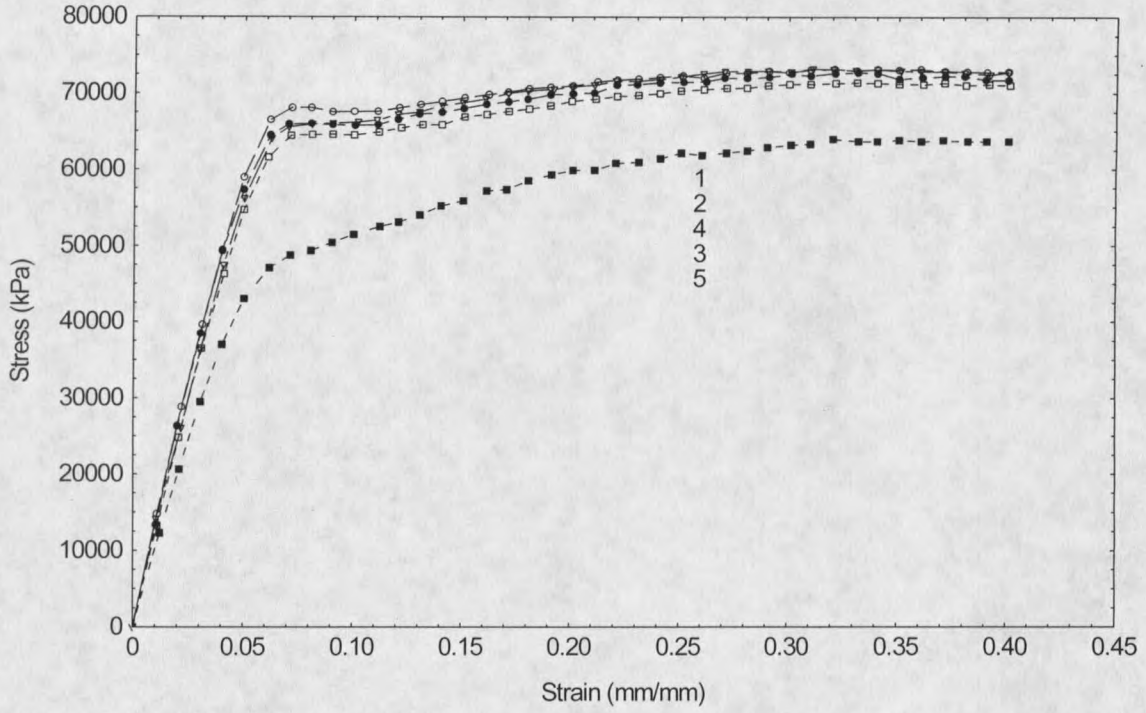


Figure 53 Tensile Testing of Nylon 6/6 Specimens after Cyclic and Constant Loading at 41 °C

Vibrocreep: **1**- $(0.16\pm0.04)\sigma_y$, **2**- $(0.16\pm0.10)\sigma_y$, at 10 Hz;

Constant Load Creep: **3**- $(0.16)\sigma_y$, **4**- $(0.20)\sigma_y$; **5**- Virgin Specimens;

σ_y = 70 MPa at 23 °C

Table 14 Tensile Testing of Nylon 6/6 Specimens after Cyclic and Constant Loading at 41 °C

Curve #	Yield Stress (MPa)	Yield Strain (mm/mm)	Maximum Stress (MPa)	Elastic Modulus (GPa)
1	65.360	.06073	67.891	1.29
2	66.485	.06185	68.080	1.29
3	52.006	.04425	65.787	1.23
4	57.299	.05005	64.950	1.27
5	44.6	.05510	65.000	.96

In the figures shown, at elevated temperatures the strength and stiffness of the constant load creep and cyclic experiments have similar results. The yield stress is lower, but the elastic moduli have marginal differences.

Conclusion

Vibrocreep effects in Nylon 6/6 are evident from the results obtained in this study. Vibrocreep effects have been obtained at the temperatures of 23, 35 and 41°C, above and below the linear viscoelastic limit. The observable difference between creep and vibrocreep of Nylon 6/6 demonstrates that the vibrocreep phenomena is not predictable by current viscoelastic theories.

Tensile test results of Nylon 6/6 show a definite dependence upon test temperature. Increases of 9 °C have a dramatic effect on the tensile properties of the polymer in terms of decreasing elastic modulus and yield stress. The viscoelastic linearity limit remained at approximately 30% of the yield stress over the experimental temperature range. A correlation between stress and temperature effects on the creep behavior of Nylon 6/6 has been observed in all experiments leading to the belief that the material response can be modeled with time-temperature and stress-time analogies. An effect of the glass transition temperature has been shown in Figure 43 over the temperature range.

The degree of vibrocreep effects depending on the mean stress, frequency, amplitude, and temperature of the cyclic loading has been determined. The vibrocreep effect has been shown to increase with increasing frequency or amplitude. Alternatively, the vibrocreep effect has been shown to decrease with increasing mean stress and temperature range below the linear viscoelastic limit.

Typically, polymers have either thermally or mechanically dominated regimes or a combination of the two when subjected to cyclic loading condition, Figure 54, Ref[29]. In the case of Nylon 6/6, hysteresis heating of the polymer has not been observed within the experimental test range studied. This indicates that the observed vibrocreep effects result from damage development and evolution due to the presence of cyclic loading.

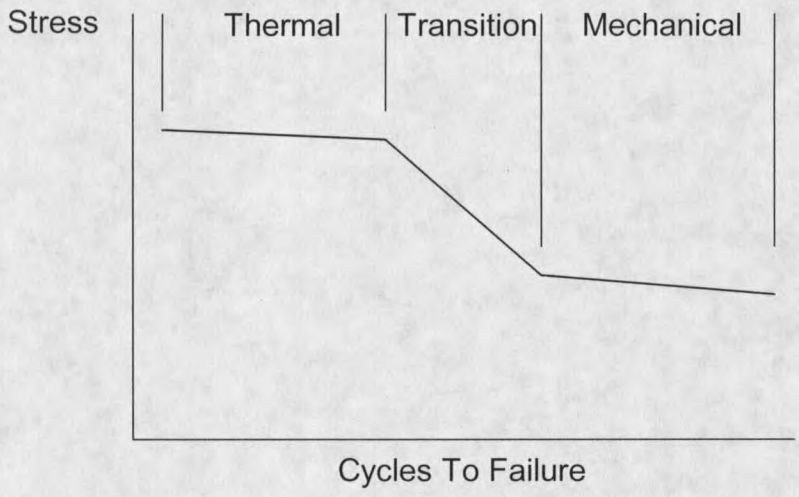


Figure 54 Thermal and Mechanical Dominated Failure Zones

The vibrocreep effects appear to be directly dependent upon the product of the amplitude and frequency of the cyclic load. As shown in Equation 15, this product defines the amplitude rate of loading. As can be observed from Figure 55, vibrocreep effects are directly dependent on the product of the frequency and amplitude.

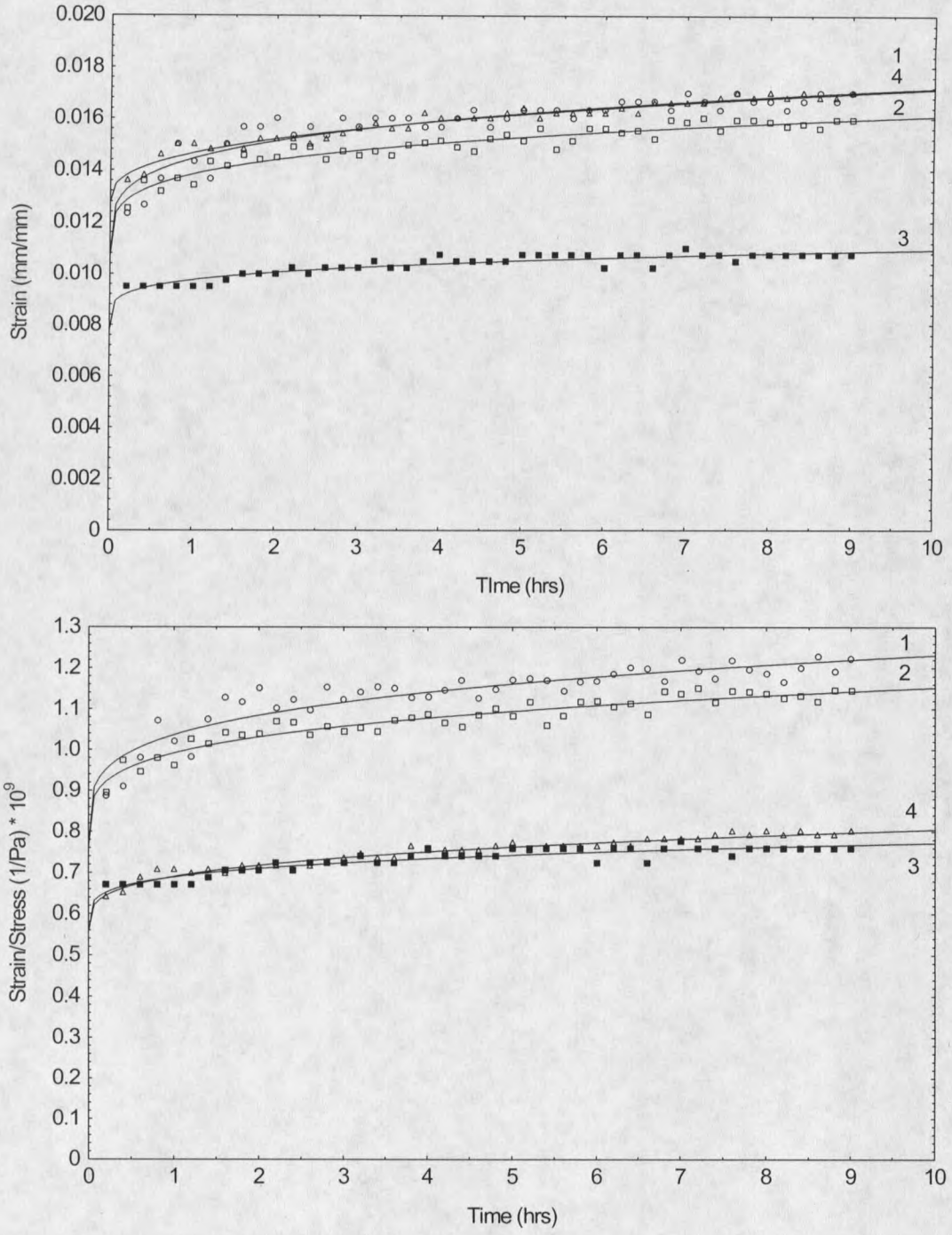


Figure 55 Vibrocreep Response of Nylon 6/6 with ω*a = 100 at 23 °C
Vibrocreep: **1**- $(0.20\pm0.10)\sigma_y$, at 10 Hz; **2**- $(0.20\pm0.05)\sigma_y$, at 20 Hz;
Constant Load Creep : **3**- $(0.20)\sigma_y$, **4**- $(0.30)\sigma_y$;
σ_y = 70 MPa at 23 °C

$$\sigma(t) = \sigma_m + \sigma_a \cdot \mathrm{Sin}(\omega \cdot t)$$

$$\frac{d}{dt}\sigma(t) = \left(\sigma_a \cdot \omega\right) \cdot \mathrm{Cos}(\omega \cdot t)$$

Equation 15

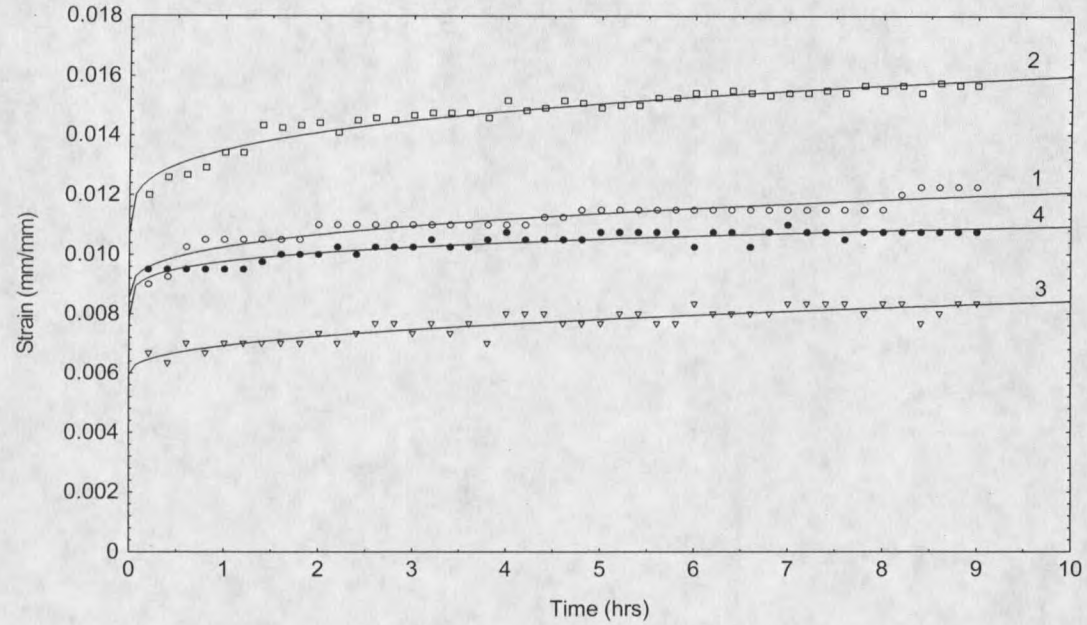
Another factor considered in this study represents the ratio of the mean stress to the amplitude of the cyclic load. This factor can be related to the R ratio typically considered in the studies of fatigue, Equations 16.

$$\mu = \frac{\sigma_{mean}}{\sigma_{amp}} = \frac{\frac{\sigma_{max} + \sigma_{min}}{2}}{\frac{\sigma_{max} - \sigma_{min}}{2}} = \frac{1 + \frac{\sigma_{min}}{\sigma_{max}}}{1 - \frac{\sigma_{min}}{\sigma_{max}}} = \frac{1 + R}{1 - R}$$

$$R = \frac{\sigma_{min}}{\sigma_{max}}$$

Equations 16

The result of this correlation factor combines the amplitude and mean stress effects together as shown in Figure 56. From this figure, $\mu = 4$, an increase in mean stress and amplitude correlates with approximately the same difference between the creep and vibrocreep creep compliance curves. The results of $\mu=4$ for Nylon 6/6 are provided in Appendix D.



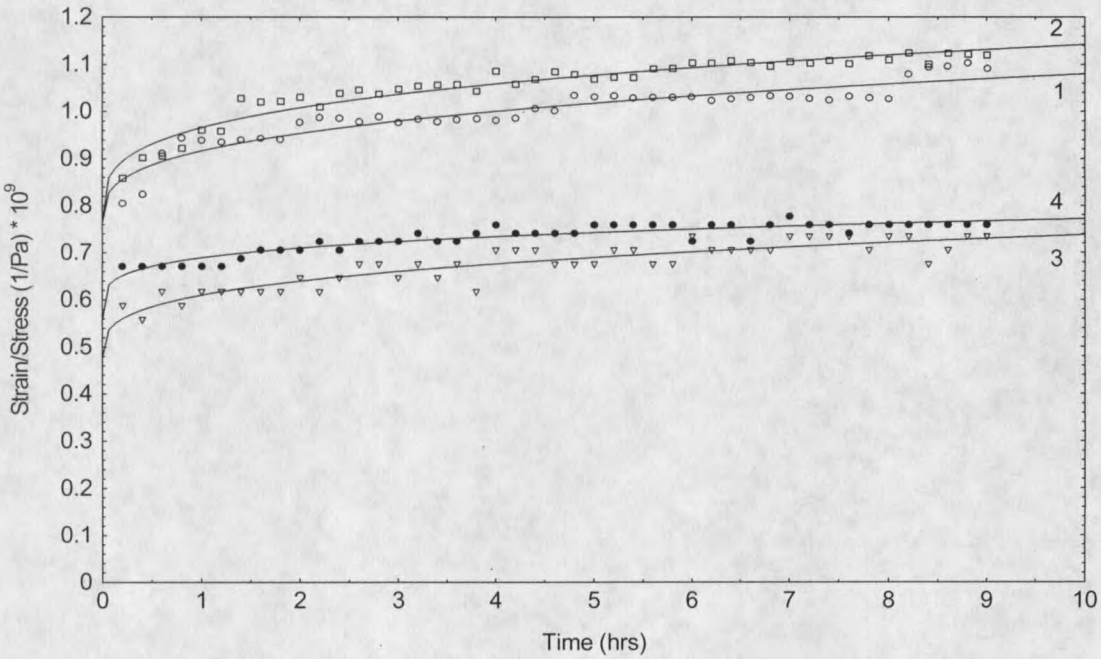


Figure 56 Vibrocreep Response of Nylon 6/6 with μ=4 at 23 °C
Vibrocreep: **1**- $(0.16\pm0.04)\sigma_y$, 10 Hz; **2**- $(0.20\pm0.05)\sigma_y$, 10 Hz;
Constant Load Creep : **3**- $(0.16)\sigma_y$, **4**- $(0.20)\sigma_y$;
σ_y = 70 MPa at 23 °C

EXPERIMENTAL PROGRAM AND RESULTS FOR PVDF

Properties and Applications of PVDF

Polyvinylidene Fluoride (PVDF) is a piezoelectric polymer used extensively for sensors and actuators in dynamic environments, Ref[61]. PVDF material is considered a sandwich composite where the PVDF polymer lies between two surface layers of electrode for electrical connection, thus making a laminate composite.

PVDF testing is performed with the electrodes since this is the most widely used form of the material. Piezoelectric properties of PVDF are produced by deforming a polymer material resulting in a permanent dipole polarization within the polymer, through mechanical deformation of the molecular orbitals. The deformation process is performed above the glass transition temperature, where the dipoles are constrained after cooling and dissipation of the dipole is less likely to occur.

In this study, PVDF is chosen for its physical properties, applications, and microstructure. The material is anisotropic, due to drawing the material to obtain piezoelectric properties, therefore the strength and stiffness of PVDF is dependent upon the loading direction. General and physical properties are provided from the manufacturer in Appendix P. The glass transition temperature of is about -50 °C, therefore the polymer is in the rubbery region at room temperature of 23 °C. The microstructure of PVDF is semi-crystalline. PVDF is

the first commercial piezoelectric material on the market, and there is a high demand for characterization of its properties. The investigation of cyclic loading effects for PVDF has not been performed even though the material is used in cyclic loading environments.

Experimental Program

Instrumentation, Equipment, and Data Acquisition

Computer aided data acquisition is performed with National Instruments signal conditioning equipment and windows based data acquisition programming language called LABView. The National Instruments signal conditioning equipment consists of the following:

- SCXI 1000 Chassis
- SCXI 1200 module with SCXI 1302 attachment
- SCXI 1100 module with SCXI 1303 attachment
- SCXI 1121 module with SCXI 1321 attachment

The signal conditioning system allows data sampling at 333,000 samples per second with 12 bit resolution. This system provides excitation and the ability to monitor all types of components. The LABView program for data acquisition provides the interface between voltages and usable data. The version of LABView is 5.0, which is used for all of the data acquisition programming.

Tensile Testing of PVDF. The tensile testing of PVDF was also performed on the 4206 Instron where a 20 lbf load cell is placed in series with the existing load cell. The mechanical grips from the creep and vibrocreep test fixture are used, since position transducer attachments are required along with provisions for the alternate load cell. A Data Instruments FS1000 Fastar A/C transducer monitors the displacement. The transducer is connected to a SP200A signal processor that allows zero and span setting and temperature compensation. The load cell is provided with excitation and monitored through the data acquisition system. The SCXI 1321 module is used with channel one connected to the displacement and channel two connected to the load. The Instron testing machine provided the constant strain rate necessary to abide by the ASTM 882-95a standards.

Constant Load Creep and Vibrocreep Testing of PVDF. Frank Halloway, a former graduate student, first built the test fixture for relaxation testing of thin films. Extensive modification has been done to the test fixture for creep testing. A pulley system was incorporated to apply the static load or mean load. The second modification was the attachment of a crosshead for axial alignment. The crosshead is adjustable and rolls on rails with steel ball bearings. At the interface of the steel rails and steel ball bearings friction is further minimized with light weight oil. The test fixture was found to have a static frictional force of .45 N. With the use of a dynamic shaker, the sinusoidal waveform could be

superimposed on the static load. Adjustable legs were installed on the dynamic shaker for proper axial alignment. The test fixture is easily portable for the purpose of testing in small rooms such as offices or cold rooms. An environmental chamber manufactured by Instron 3111 is also used for room and high temperature testing. This test fixture is diverse, in that creep and vibrocreep testing can be performed with one fixture instead of two.

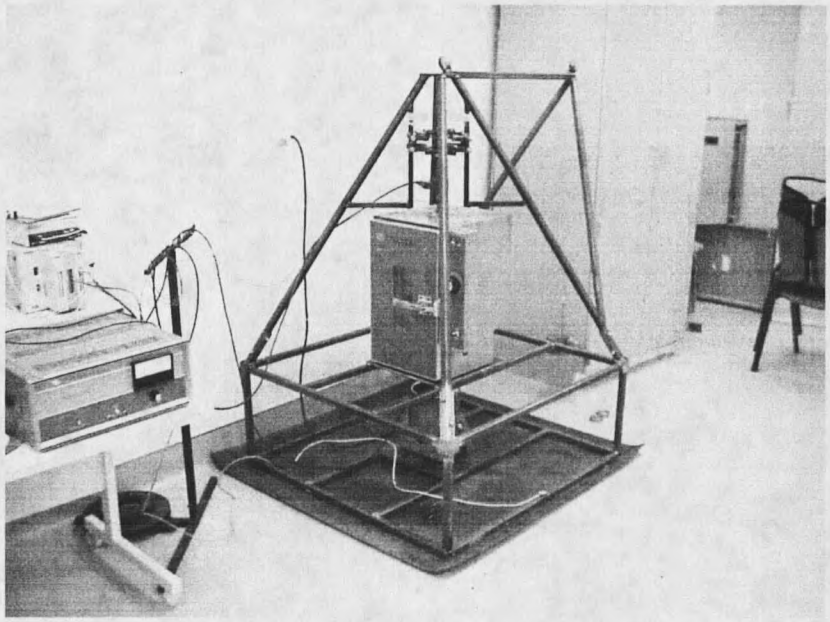


Figure 57 Constant Load Creep and Vibrocreep Testing Fixture for PVDF

Data acquisition for the creep testing of PVDF has been performed with a Gateway 486 computer with 32 MB of RAM and a 2.1 GB hard disk. The components for acquiring data for PVDF are a load cell, position transducer, accelerometer, and thermocouples. The displacement voltage is measured using a Data Instruments FS1000 Fastar A/C transducer. The transducer is connected to a SP200A signal processor that allows zero and span setting and

temperature compensation. The transducer and signal processor allows static and dynamic measurements from 0 to 15,000 Hz. The output voltage is +10 Volts to -10 Volts, therefore a circuit was built to reduce the voltage to +5 Volts to -5 Volts to connect SCXI data acquisition system. The position measurement is connected to channel 0 of the 1321 SCXI attachment and converted to mm and then recorded. The load measurements are acquired from an 88.9 N (20 lbf) fatigue rated Interface load cell model 1500. A gain of 100 is necessary to receive the greatest resolution from the load cell. The load cell is connected to the SCXI 1321 attachment and also excited with 10 Volts from this attachment. The voltage measurement is converted to load and recorded. The influence of outside vibration is measured with a +10 g to - 10 g Sensotec JTF flat pack accelerometer perpendicular to the base or floor. The accelerometer is connected to channel 2 of the 1321 SCXI attachment and also excited with 10 Volts from this attachment. The voltage measurement is converted to g's and then recorded. The environmental temperature was measured using type T thermocouples. Type T thermocouples allow temperature measurement from -270 to 400 °C. The thermocouples are connected to channels 0 to 1 of the SCXI 1100 attachment. One thermocouple measures the temperature within the Instron 3111 environmental chamber, and the other measures the testing room temperature.

The programming of the data acquisition system with LABView is accomplished through the development of case structures. The creep testing of

PVDF only requires one case structure. The time calculations and time wait functions are calculated along with the necessary physical measurements of load, position, acceleration and temperature. The vibrocreep testing of PVDF requires two case structures, one to control data acquisition of the hysteresis loops and the second to monitor the displacement, load and environment changes in time. The hysteresis case structure is executed every 100 cycles of the second case structure; thus monitoring the changes in the hysteresis loop approximately every hour. The second structure is designed to monitor the change in strain approximately every 30 seconds of clock time. A 30 second execution of the second case structure is controlled by a Do While loop. A time wait function is used to control the accumulation of data. The Do while loop is also the control for the initial case structure that is executed every 100 cycles. The time to execute the case structures is recorded along with the time wait to accurately record time to a 1 thousandth of a second.

Testing Procedure

PVDF material was the first material to be investigated for the vibrocreep effect. The first step was the selection of the sample size for the material. Tensile and creep testing has been performed on 7.62 mm x 76.2 mm specimens with an aspect ratio of 10:1, abiding by the ASTM D882-95a standard. This sample geometry has been therefore adopted for all testing of PVDF, tensile, creep and vibrocreep. PVDF thin film have been produced by Measurement

Specialties, Inc. with a continuous electrode pattern over an area of 8.5 in x 11 in. The PVDF film is 28-31 microns thick with approximately 10 microns of silver electrode on each face, thus making the film thickness an average of 51 microns. The copper electrode film was also 28-31 microns of PVDF, but the copper electrode on each face is only approximately 1 micron. The copper electrode film provided a much more challenging task of thickness measurement; therefore a thickness of 31 microns is used to represent the film and electrodes. The PVDF film used for all testing is produced from the same batch of Bulk polymer, thus minimizing batch sensitivity problems.

To reduce the grip effects, the PVDF material was tabbed with posterboard. The tabbed test specimen provides three benefits for testing of the material, the first being the ability to reduce the grip effects, the second allowing measurement of gage length of the test specimen with a caliper, and finally insulating the polymer from the metallic grips.

The material chosen for creep and vibrocreep testing is the silver electroded PVDF. Reasons for choosing the silver electroded material over the copper is that batch sensitivity did not exist for the silver where the copper was questionable. Also, the NASA micro-g group was also using the silver electrode PVDF, therefore the experimental results would benefit the group. Testing temperatures for PVDF are 23 °C and –25 °C. The room temperature of 23 °C was chosen, as a base for the vibrocreep study, since special testing equipment would not be required at this temperature. The temperature of –25 °C was

chosen since cooling the material allowed closer proximity to the glass transition temperature of –50 °C. The cold room allowed the testing apparatus to be moved within the room where the instrumentation and testing apparatus were cooled to the temperature of –25 °C. Recalibration of the instruments was necessary, but all instruments had the ability to work properly at –25 °C.

Tensile Testing Procedure for PVDF. The tensile testing was performed at a strain rate of .5 mm/mm * min of 38.1 mm/min (1.5 in/min) according to the ASTM D882-95a for both material directions. The strength and stiffness determination for PVDF in both directions of the material has been performed abiding by the ASTM 882-95a standard stated above.

Constant Load Creep Procedure for PVDF. The creep testing was performed at stresses 30%, 45%, and 60% of the yield stress at 23 °C and at temperatures of 23 °C and –25 °C. The same specimen geometry has been used for creep testing as in the tensile and vibrocreep testing of PVDF. After months of experimentation, the test fixture proved to be accurate and reliable.

Vibrocreep Testing Procedure for PVDF. The vibrocreep testing was performed at the same means stresses as in creep testing, and at multiple amplitudes, frequencies, and at the temperatures 23 °C and –25 °C. The same specimen geometry used for tensile and creep testing has been also used for vibrocreep testing of PVDF. The vibrocreep testing of PVDF proved to be

challenging also. The limitations of the combination of frequency and amplitude within the testing fixture proved to be the greatest challenge. Unlike an Instron or MTS testing machine, the load and frequency are controlled through the manual application of electromagnetic motion and weight. The lowest amplitude and frequency that the test fixture can accommodate is 5% and 5 Hz respectively. Below these values, the electromagnetic shaker that provides the oscillatory motion does not work properly. An amplitude and frequency to high will also pose a problem, since the crosshead will "jump". When the settings are too high, PVDF emits a sound of a twanging guitar string. The colder temperature within the cold room simply magnified the limitation, but high and low amplitude and frequency limitations did not pose as large limitation as can be seen from the data.

Experimental Results

Tensile Testing Results at 23 °C

Tensile testing has been performed to calculate the strength and stiffness of PVDF. The tensile testing of PVDF was performed on both the silver and copper electrode materials. PVDF is an anisotropic material, therefore tensile testing in two directions was performed. A diagram of the directionality is shown in Figure 58.

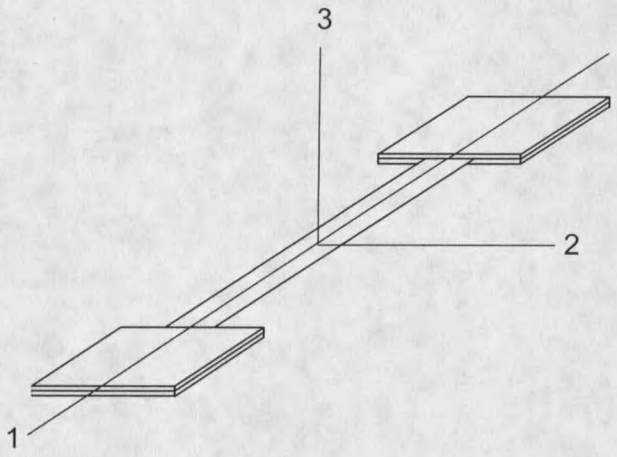


Figure 58 PVDF Test Sample

The results of the tensile testing for both the silver and copper electrode PVDF are shown in Table 15.

Table 15 Tensile Testing Results for PVDF at 23 °C

		Yield Stress (MPa)	Elastic Modulus (GPa)
Silver Electrode			
	Direction 1	30.428	1.96
	Direction 2	23.498	1.69
Copper Electrode			
	Direction 1	46.568	3.42
	Direction 2	37.935	2.84

The results of the tensile testing of the silver electrode PVDF are shown in Figure 59 for direction 1 and Figure 60 for direction 2.

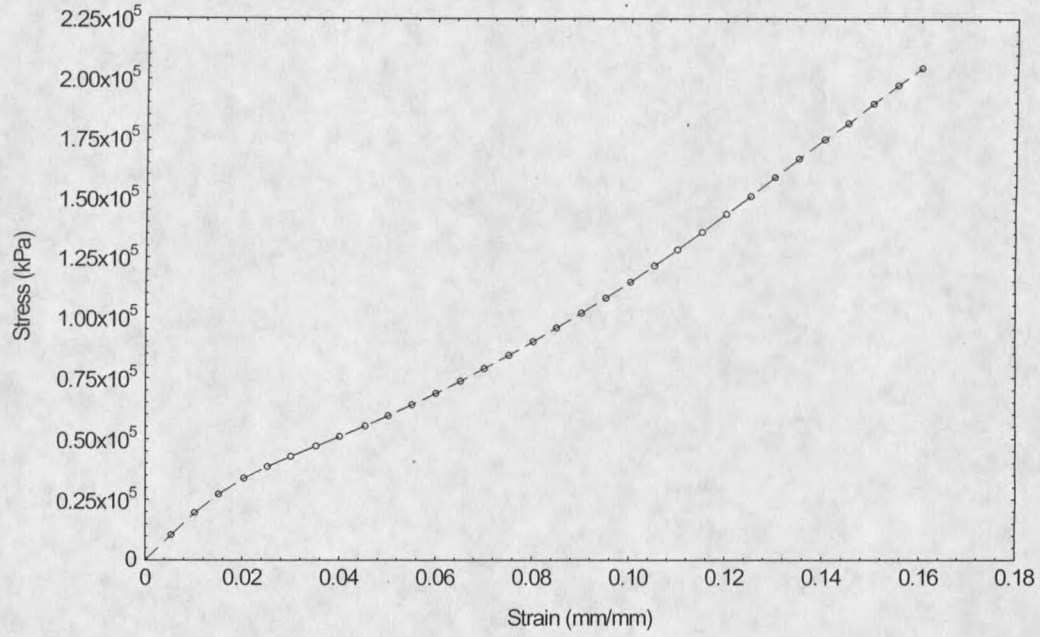


Figure 59 Tensile Test of PVDF Direction 1 at 23 °C

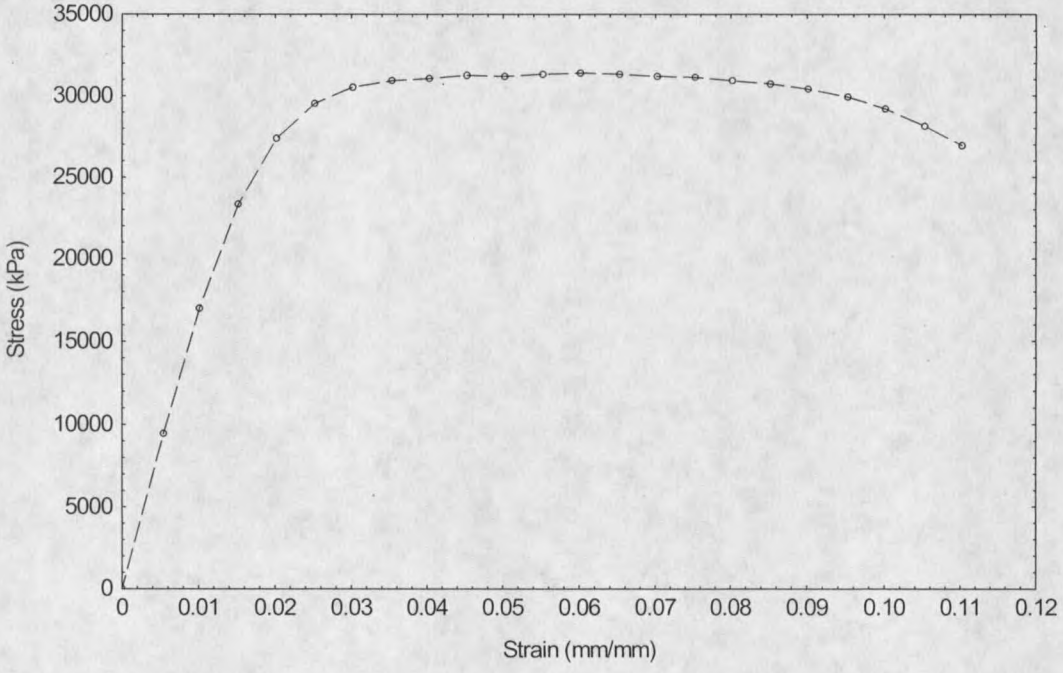


Figure 60 Tensile Test of PVDF Direction 2 at 23 °C

From the figures shown above, the anisotropic behavior of the material can be easily seen. During the tensile testing of PVDF along direction 1, shear banding is not seen through the deformation process, but in direction 2, shear bands occur once the stress level surpasses the yield stress. Complete results of the tensile testing for PVDF are provided in Appendix H. Tensile testing at –25 °C was not performed for PVDF, since the temperature could not be accurately controlled with the present equipment.

Constant Load Creep Testing Results at 23 °C

The test specimen geometry used for creep testing was also the test specimen used for the tensile testing of PVDF, therefore geometric effects can be neglected. The same batch of PVDF from Measurement Specialties is also used in the creep testing. The stress levels used for creep testing are 30%, 45% and 60% of the yield stress at 23 °C for all temperatures. The linear viscoelastic limit was found to be 60% by a former graduate student Frank Halloway. Verification of the linear viscoelastic limit was performed since the materials were not from the same batch of material and the specimen geometry was also different. The results of the creep testing are shown below in Figure 61. Complete results of the creep testing for PVDF at 23 °C is provided in Appendix H.

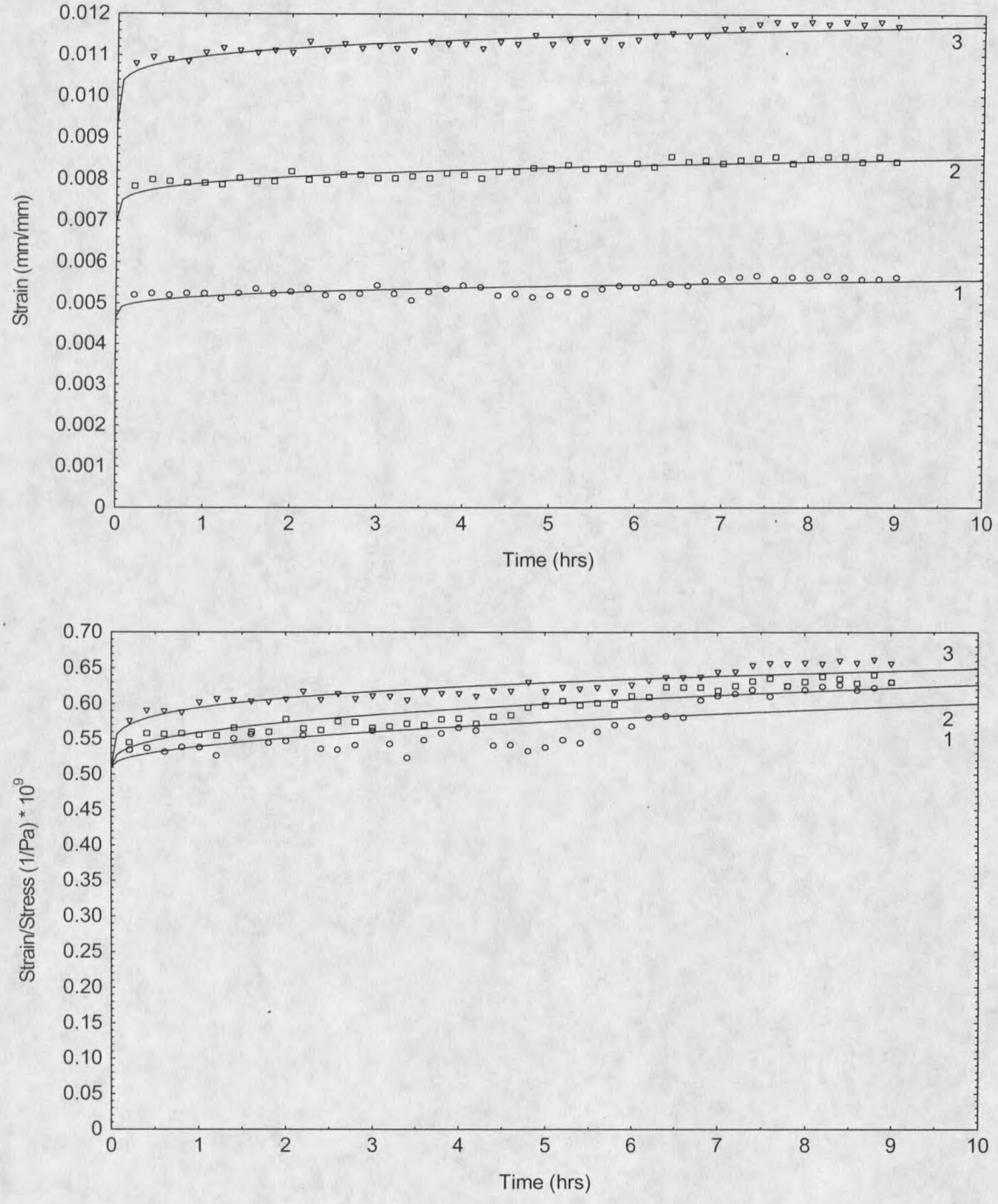


Figure 61 Constant Load Creep of PVDF at 23 °C
1- $(0.30)\sigma_y$; **2**- $(0.45)\sigma_y$; **3**- $(0.60)\sigma_y$;
σ_y = 30.428 MPa at 23 °C

Through creep testing, verification of the linear viscoelastic limit of at least 60% is shown. The normalization techniques are similar to that of Nylon 6/6 where the strain is divided by the stress to test for stress dependence. Complete results of the creep testing for PVDF are provided in Appendix H.

Vibrocreep Testing Results at 23 °C

The vibrocreep testing of PVDF is performed after the creep testing where one test fixture is used for the testing of creep and vibrocreep testing. The test matrix for vibrocreep testing is shown in Table 16.

Table 16 Test Matrix for Vibrocreep Testing of PVDF at 23 °C

Mean Stress (% of σ_y)	Superimposed Cyclic Load								
30	Stress Amplitude (% of σ_y)	10			20				
	Frequency (Hz)	5	10	20	5	10	20		
45	Stress Amplitude (% of σ_y)	10			20			35	40
	Frequency (Hz)	5	10	20	5	10	20	5	10
60	Stress Amplitude (% of σ_y)	10			20			40	50
	Frequency (Hz)	5	10	20	5	10	20	5	10

The amplitudes and frequencies are chosen by the capabilities of the testing fixture. Testing at higher frequencies such as 100 Hz and 5% amplitude has been performed, but lower frequencies were chosen to correlate with Nylon 6/6.

The frequency effect can be seen from Figure 62. Complete results of the frequency effect for PVDF at 23 °C are provided in Appendix I.

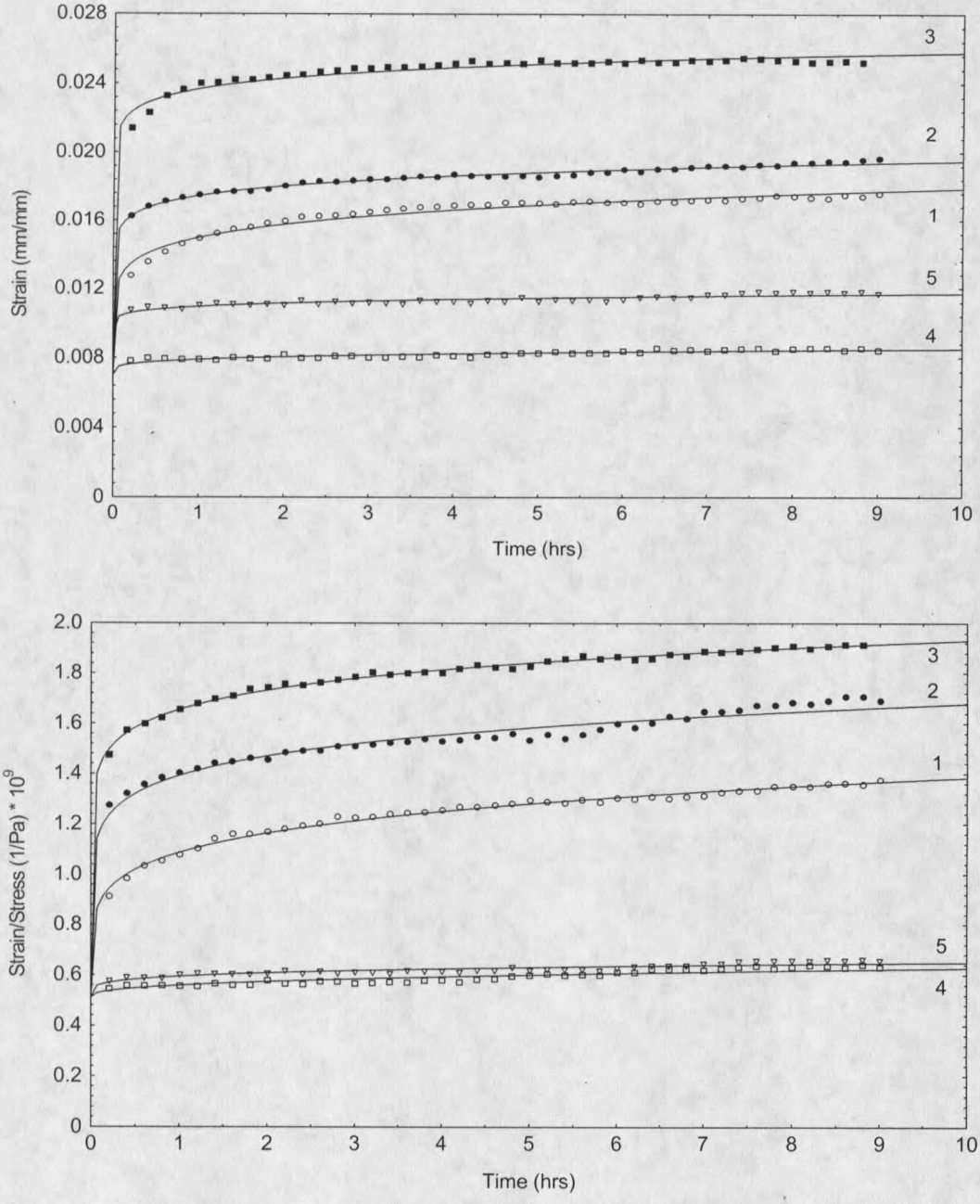
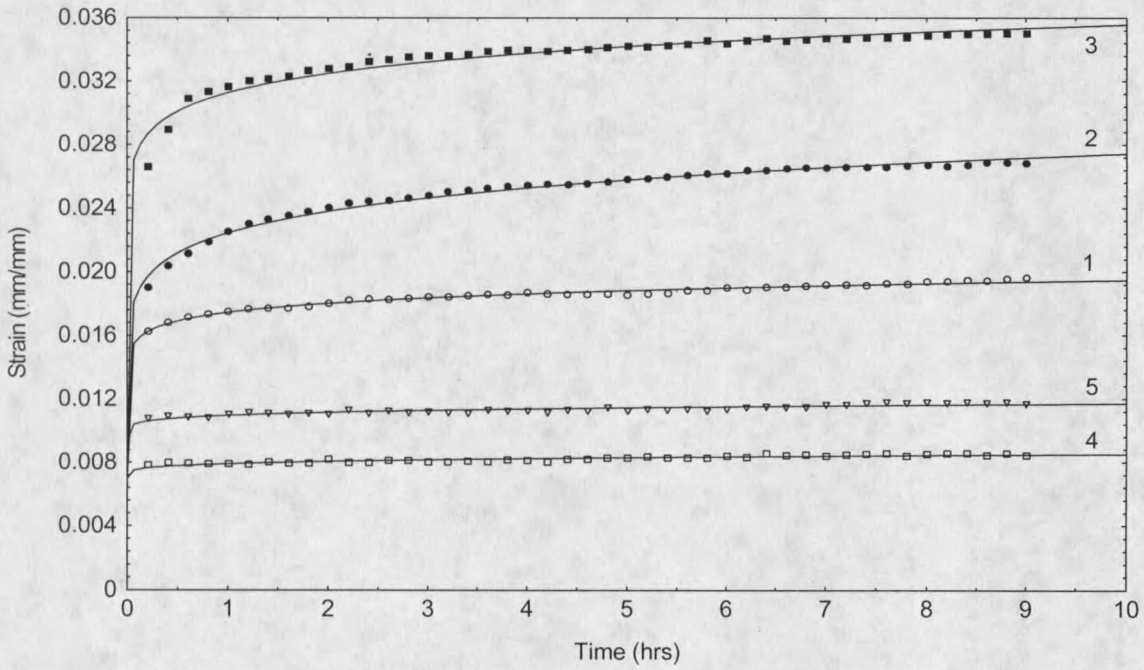


Figure 62 Vibrocreep Response of PVDF at Different Frequencies at 23 °C
Vibrocreep: $(0.45\pm0.10)\sigma_y$; **1**- 5Hz; **2**- 10 Hz; **3**- 20 Hz;
Constant Load Creep; **4**- $(0\ .45)\sigma_y$, **5**- $(0.60)\sigma_y$;
σ_y = 30.428 MPa at 23 °C

At 23 °C the amplitude of 10% is included to further verify the vibrocreep effect and allow for further testing within the linear viscoelastic limit of PVDF. Testing outside of the linear viscoelastic limit can also be seen from the test amplitudes chosen. As can be seen from Figure 63, the vibrocreep effect is increased with increasing amplitude. Complete results of the amplitude effect for PVDF at 23 °C are provided in Appendix J. The effect of mean stress on PVDF can be seen from Figure 64. The vibrocreep effect is seen to increase with an increasing mean stress. Complete results of the mean stress effect for PVDF at 23 °C are provided in Appendix K.



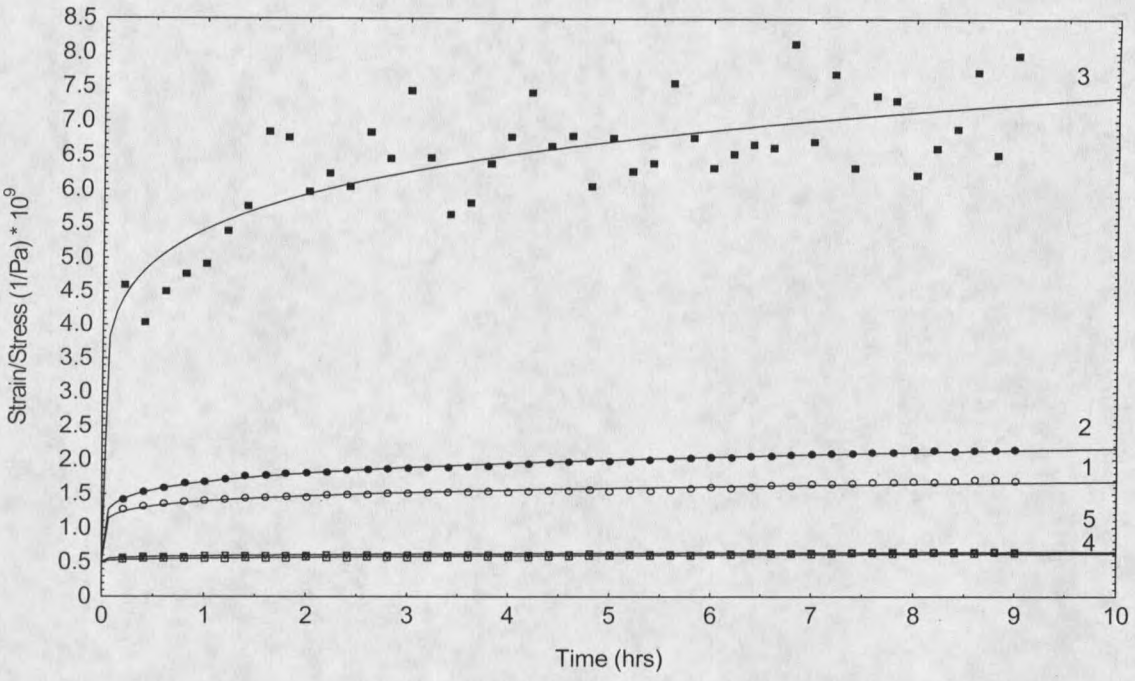
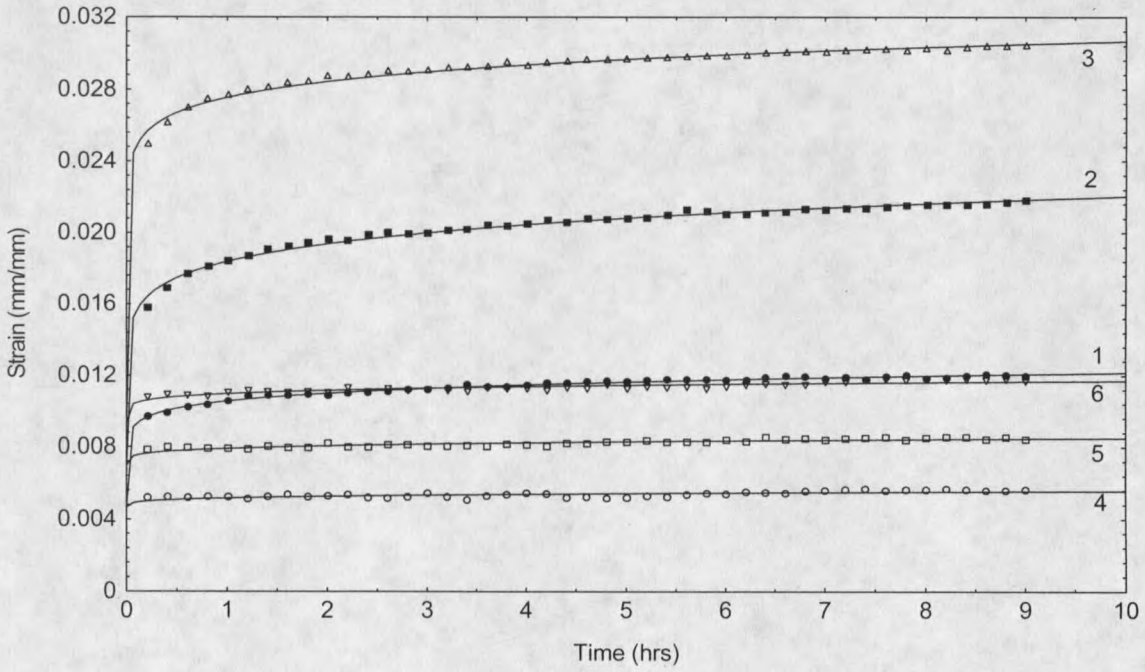


Figure 63 Vibrocreep Response of PVDF at Amplitudes at 23 °C
Vibrocreep: **1**- $(0.45\pm0.10)\sigma_y$; **2**- $(0.45\pm0.20)\sigma_y$; **3**- $(0.45\pm0.35)\sigma_y$, at 10 Hz;
Constant Load Creep; **4**- $(0.45)\sigma_y$, **5**- $(0.60)\sigma_y$;
σ_y = 30.428 MPa at 23 °C



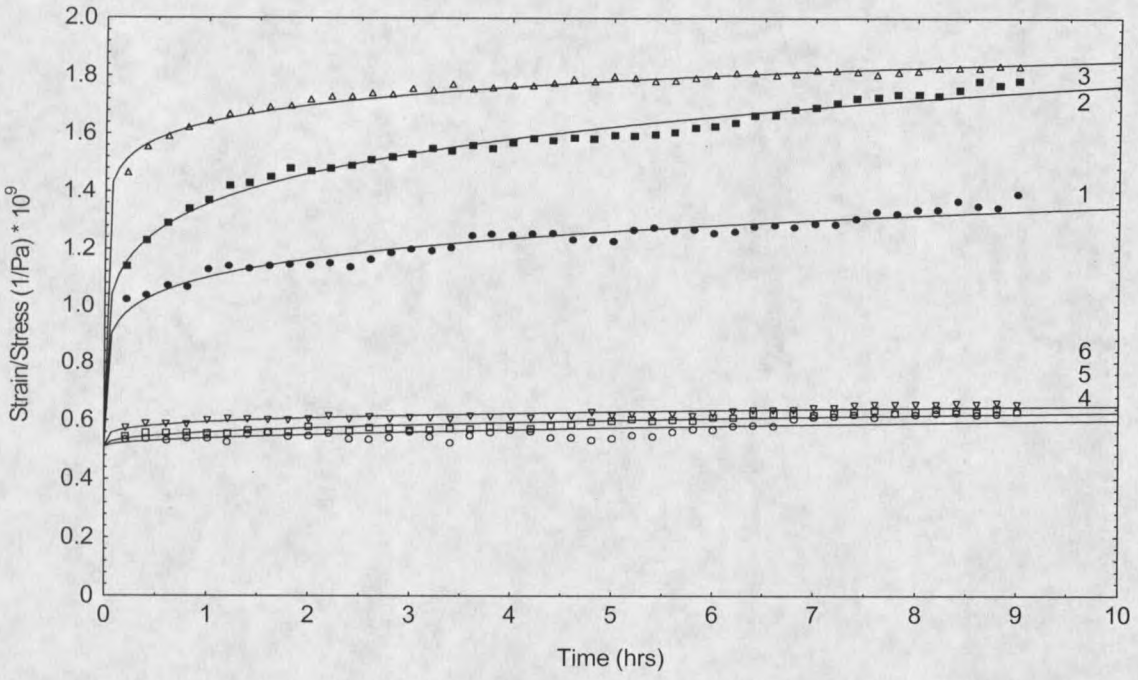


Figure 64 Vibrocreep Response of PVDF at Different Mean Stresses at 23 °C
Vibrocreep: **1**- $(0.30\pm0.20)\sigma_y$, **2**- $(0.45\pm0.20)\sigma_y$, **3**- $(0.60\pm0.20)\sigma_y$, at 5 Hz;
Constant Load Creep; **4**- $(0.30)\sigma_y$, **5**- $(0.45)\sigma_y$, **6**- $(0.60)\sigma_y$;
σ_y = 30.428 MPa at 23 °C

Constant Load Creep Testing at Low Temperatures

The experiments were performed in the cold room provided by the Civil Engineering Department at Montana State University. Creep testing at a lower temperature proved to be challenging since the test fixture provided resistance to axial motion. The crosshead, which contains the load cell and upper grip, showed a frictional resistance in the cold room. The crosshead rolls on ball bearing guides, but frost created a rough path of travel not seen at 23 °C. The effect can be easily seen in Figure 65. The results of creep tests for PVDF at -25 °C are provided in Appendix H. The results shown form testing at –25 °C show a

"jump" in the strain due to a constant creep rate and a development of frost.

From the figures in appendices G-K, over time the material recovers the

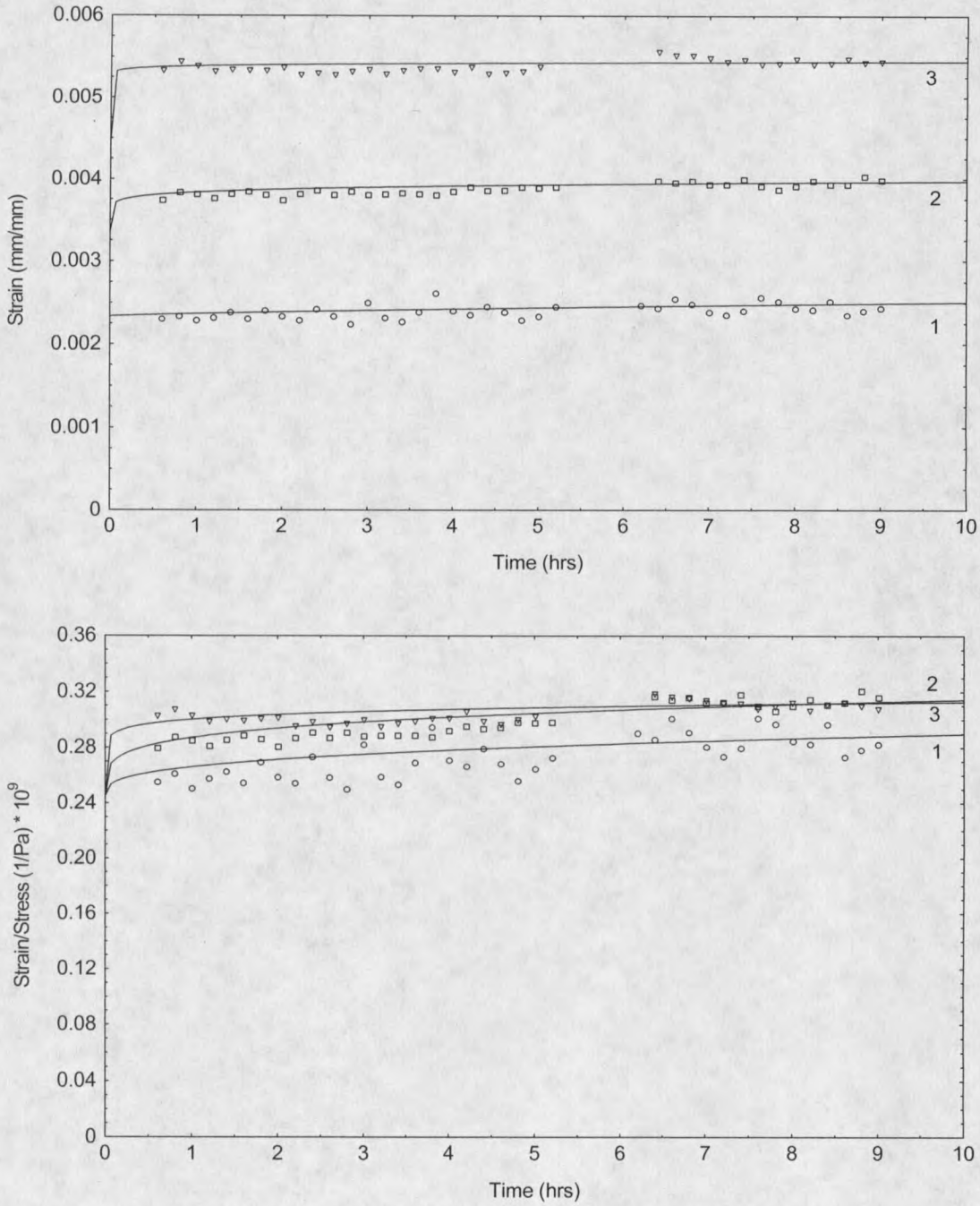
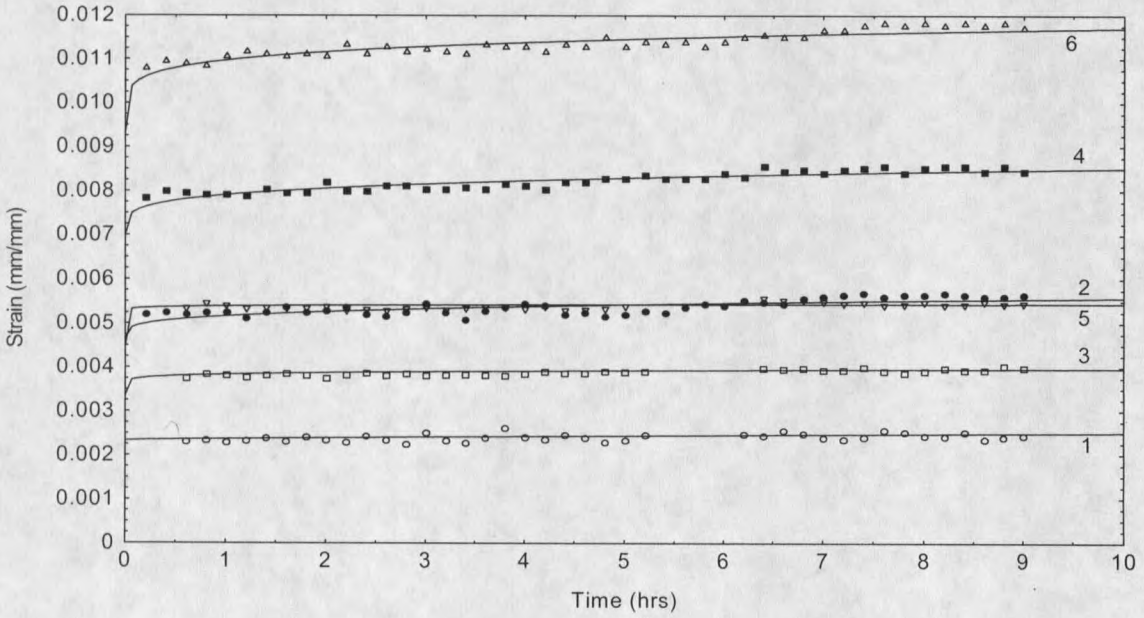


Figure 65 Constant Load Creep of PVDF at -25 °C
1- $(0.30)\sigma_y$; **2**- $(0.45)\sigma_y$; **3**- $(0.60)\sigma_y$;
σ_y = 30.428 MPa at 23 °C

sudden jump in the load. The jump has been removed from the data by deleting the data points since this can be done by using the temporal elastic strain due to the friction in the test fixture. The linear viscoelastic limit should increase relative to 23 °C if the material is cooled even though creep testing at -25 °C was kept at the same stress levels relative performed at 23 °C. Testing relative to the yield stress at –25 °C was not performed since the yield stress was never determined. Through literature the value may be found, but the effects of the geometry, batch, sensitivity, etc. may play a role in the determination of the yield stress. The temperature effect on the creep of PVDF is shown in Figures 66, where a decrease in the temperature greatly decreases the creep rate in PVDF. The results of the temperature effects upon the creep testing for PVDF are provided in Appendix L.



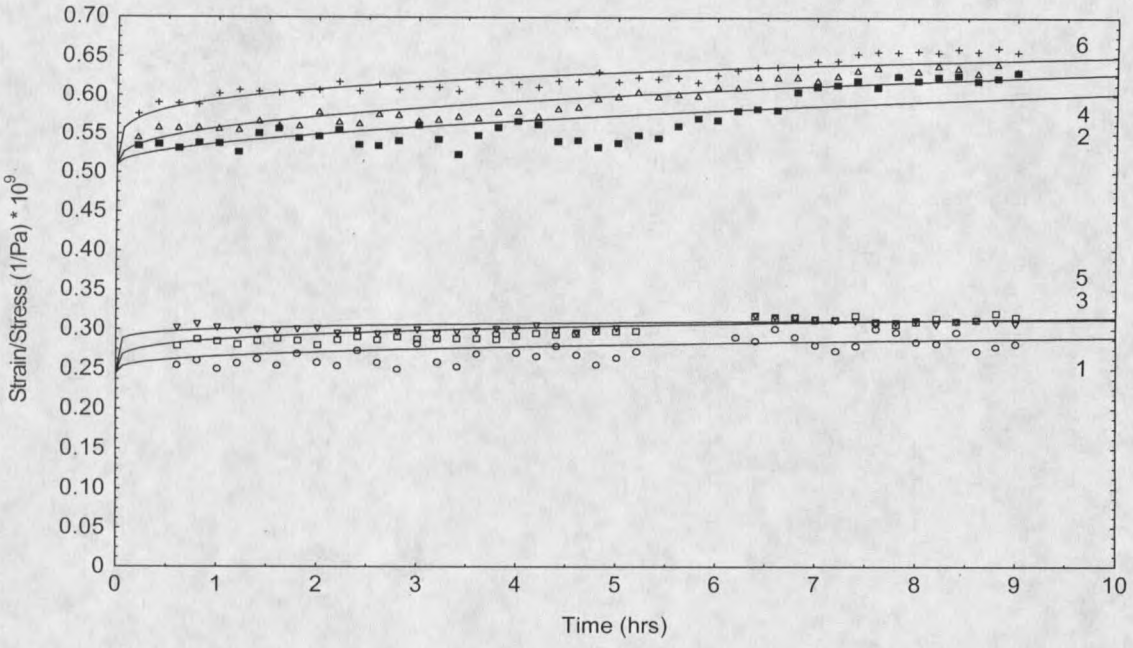


Figure 66 Constant Load Creep of PVDF at Different Temperatures
1- $(0.30)\sigma_y$ at -25 °C; **2**- $(0.30)\sigma_y$ at 23 °C;
3- $(0.45)\sigma_y$ at -25 °C; **4**- $(0.45)\sigma_y$ at 23 °C;
5- $(0.60)\sigma_y$ at -25 °C; **6**- $(0.60)\sigma_y$ at 23 °C;
σ_y = 30.428 MPa at 23 °C

Vibrocreep Testing at Low Temperatures

The vibrocreep testing of PVDF at -25 °C has been performed following the creep testing. The test matrix for vibrocreep testing is shown in Table 17. The effect of increasing frequency at -25 °C is shown in Figure 67. Complete results of the frequency effect for PVDF at -25 °C are provided in Appendix I. The amplitudes chosen at –25 °C were dependent on the test fixture. The effect of increasing amplitude at -25 °C is shown in Figure 68. Complete results of the amplitude effects for PVDF at -25 °C are provided in Appendix J. The effect of the mean stress at -25 °C is shown in Figure 69. Complete results of the

amplitude effects for PVDF at -25 °C are provided in Appendix K.I. The effect of temperature can be seen in Figure 70. The differences in temperature greatly effect the creep rate of the PVDF. The results of the temperature effects for PVDF are provided in Appendix L. In Figures 71-73, the effect of decreasing temperature is shown with increasing frequency, amplitude, and mean stress.

Table 17 Test Matrix for Vibrocreep Testing of PVDF at -25 °C

Mean Stress (% of σ_y)	Superimposed Cyclic Load					
30	Stress Amplitude (% of σ_y)	20				
	Frequency (Hz)	5	10	20		
45	Stress Amplitude (% of σ_y)	20			35	40
	Frequency (Hz)	5	10		5	10
60	Stress Amplitude (% of σ_y)	20			40	50
	Frequency (Hz)	5	10		5	10

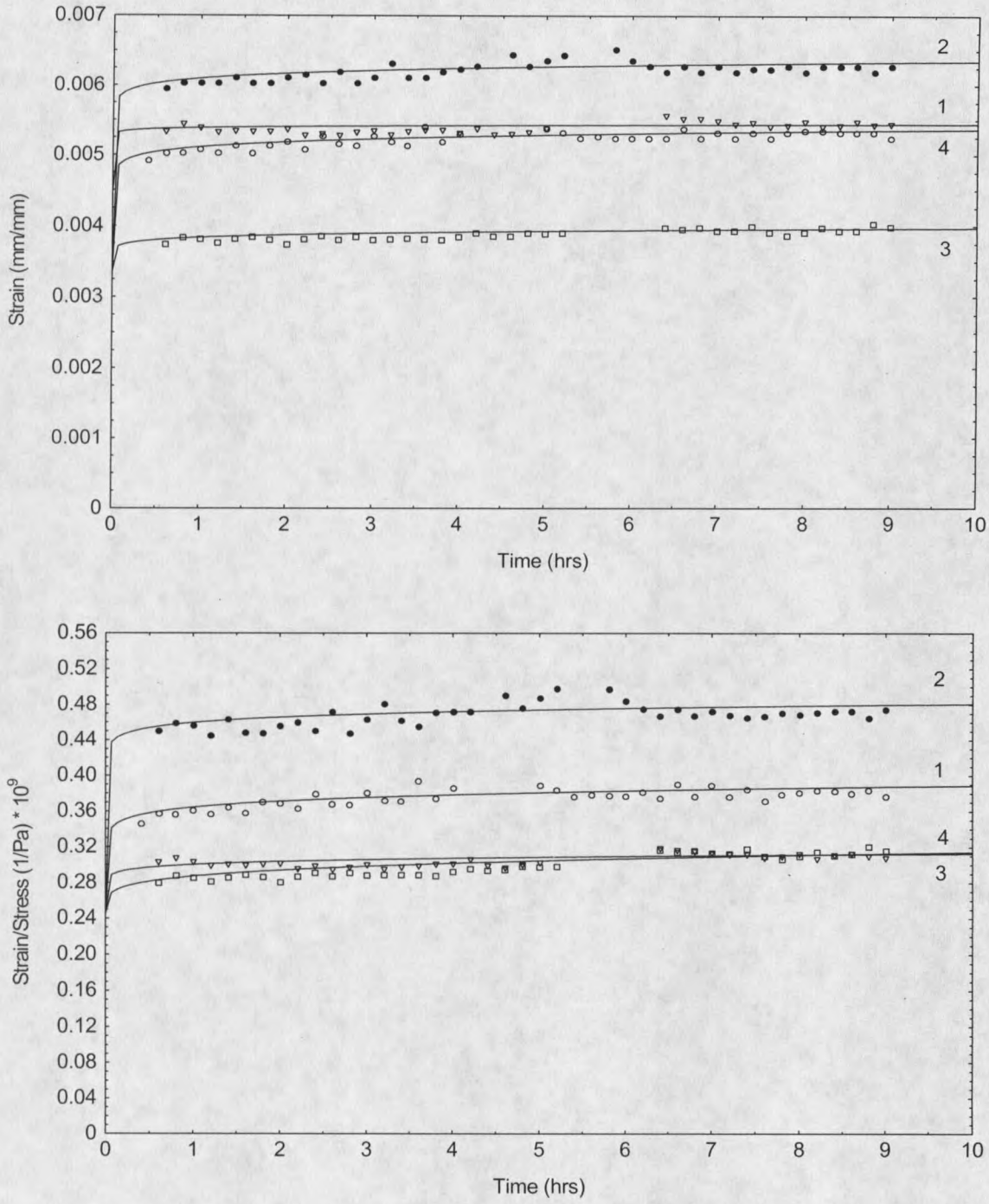


Figure 67 Vibrocreep Response of PVDF at Different Frequencies at -25 °C
Vibrocreep: $(0.45\pm0.20)\sigma_y$, **1**- 5 Hz, **2**- 10 Hz;
Constant Load Creep: **3**- $(0.45)\sigma_y$, **4**- $(0.60)\sigma_y$;
σ_y = 30.428 MPa at 23 °C

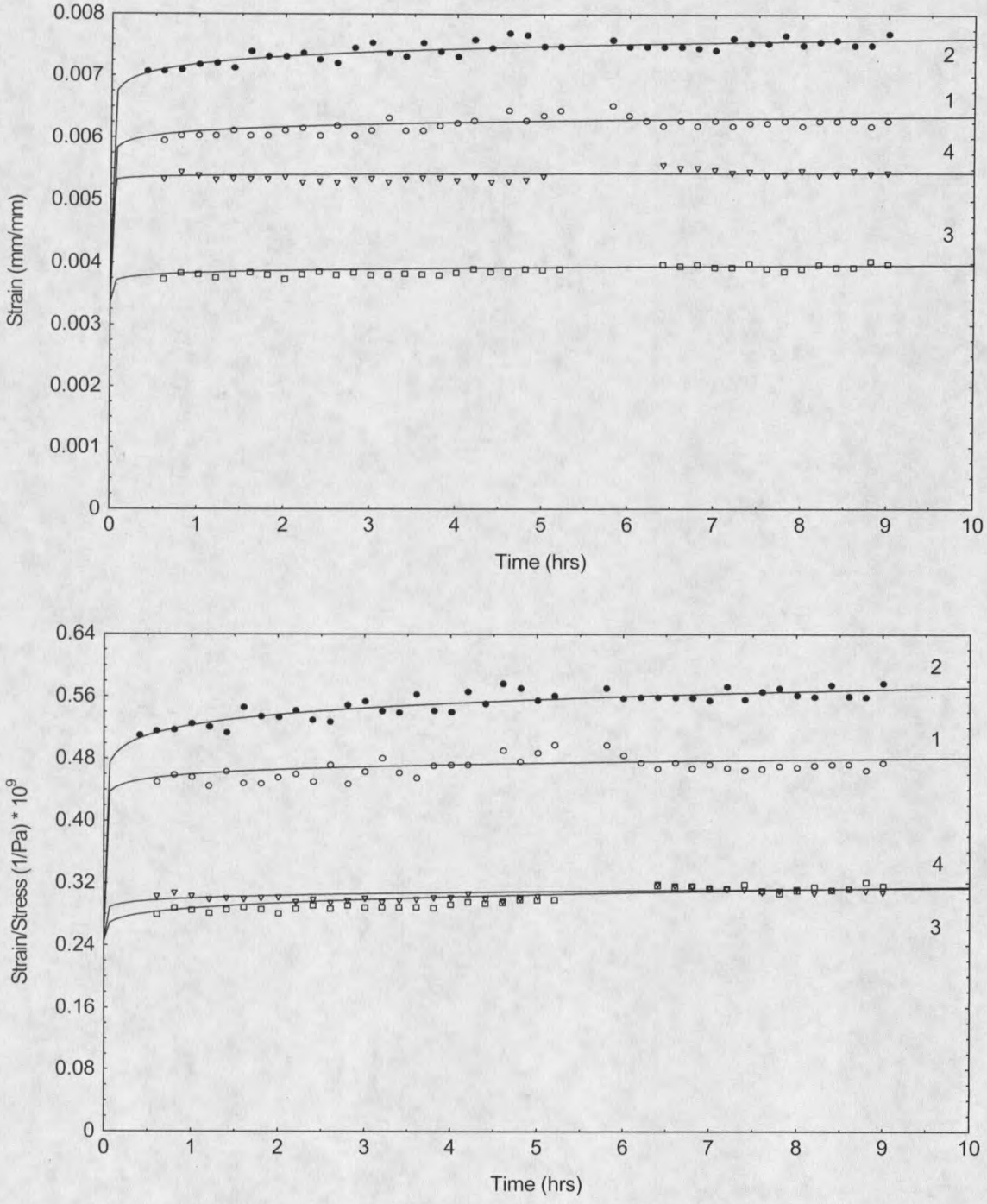


Figure 68 Vibrocreep Response of PVDF at Amplitudes at -25 °C
Vibrocreep: **1**- $(0.45\pm0.20)\sigma_y$, **2**- $(0.45\pm0.40)\sigma_y$, at 10 Hz;
Constant Load Creep: **3**- $(0.45)\sigma_y$, **4**- $(0.60)\sigma_y$;
σ_y = 30.428 MPa at 23 °C

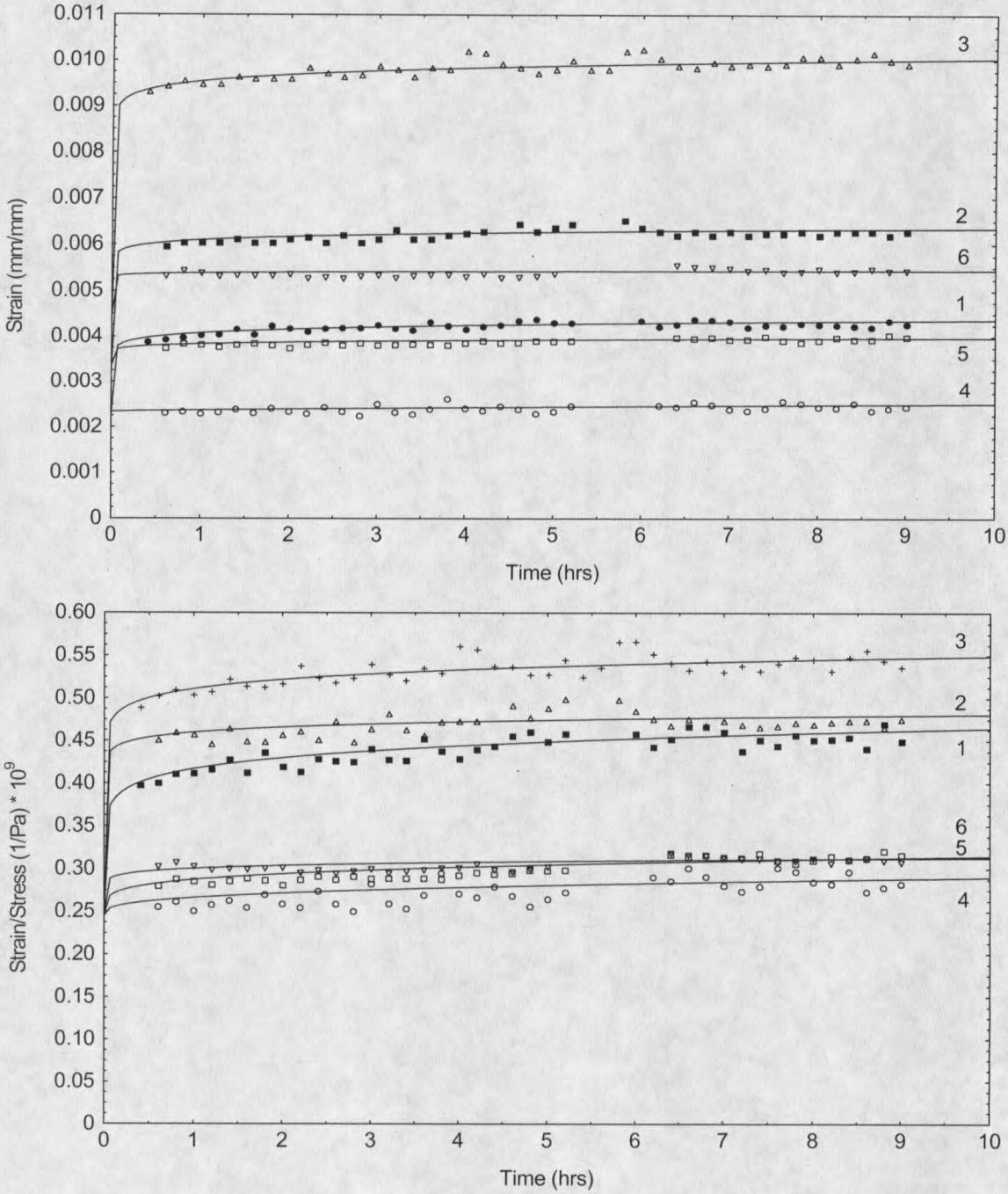


Figure 69 Vibrocreep Response of PVDF at Different Mean Stresses at -25 °C

Vibrocreep: **1**- $(0.30\pm0.20)\sigma_y$, **2**- $(0.45\pm0.20)\sigma_y$, **3**- $(0.60\pm0.20)\sigma_y$, at 10 Hz;
Constant Load Creep: **4**- $(0.30)\sigma_y$, **5**- $(0.45)\sigma_y$, **6**- $(0.60)\sigma_y$;
σ_y = 30.428 MPa at 23 °C

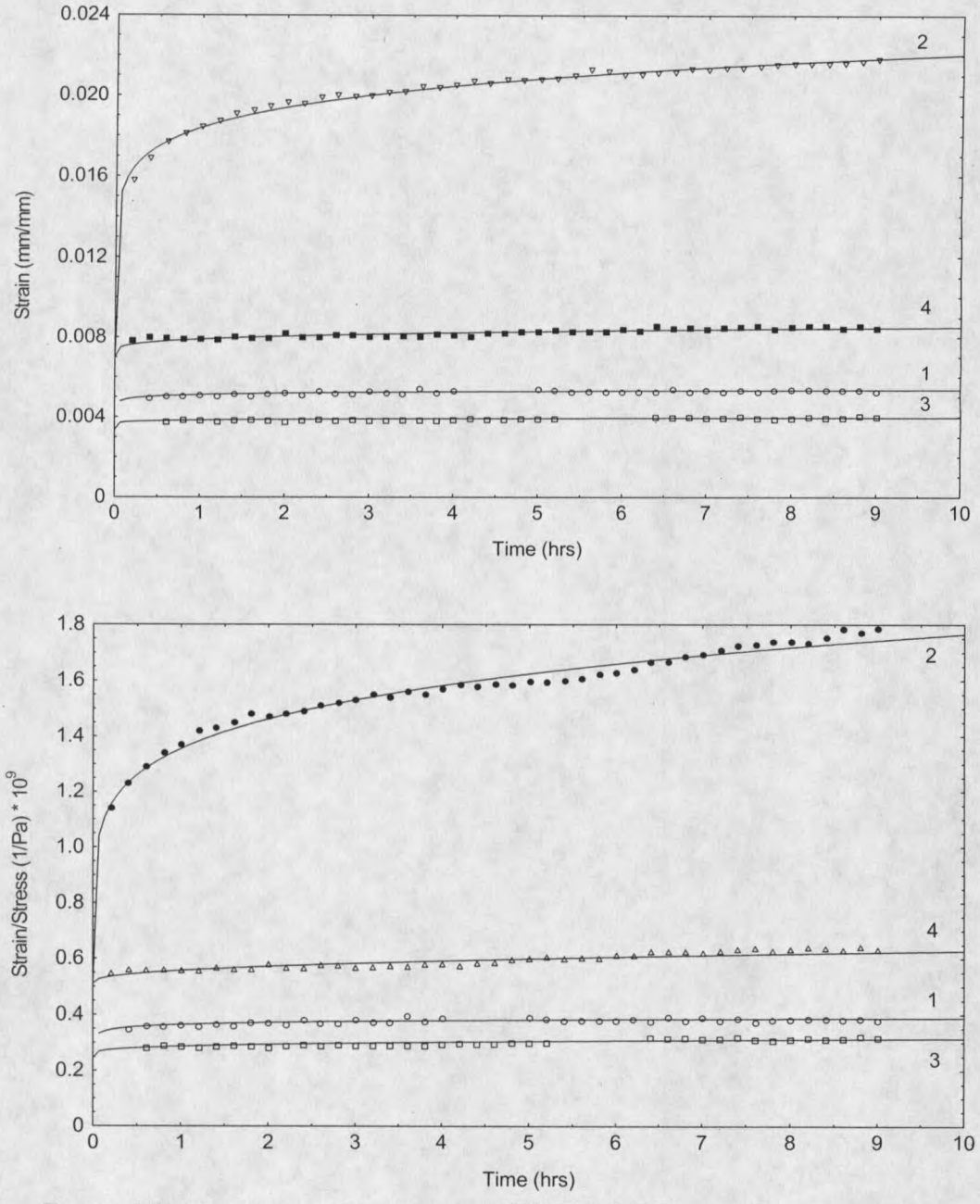


Figure 70 Vibrocreep Response of PVDF at Different Temperatures
Vibrocreep: **1**- $(0.45\pm0.20)\sigma_y$, 5 Hz at -25 °C; **2**- $(0.45\pm0.20)\sigma_y$, 5 Hz at 23 °C;
Constant Load Creep: **3**- $(0.45)\sigma_y$ at -25 °C, **4**- $(0.45)\sigma_y$ at 23 °C;
σ_y = 30.428 MPa at 23 °C

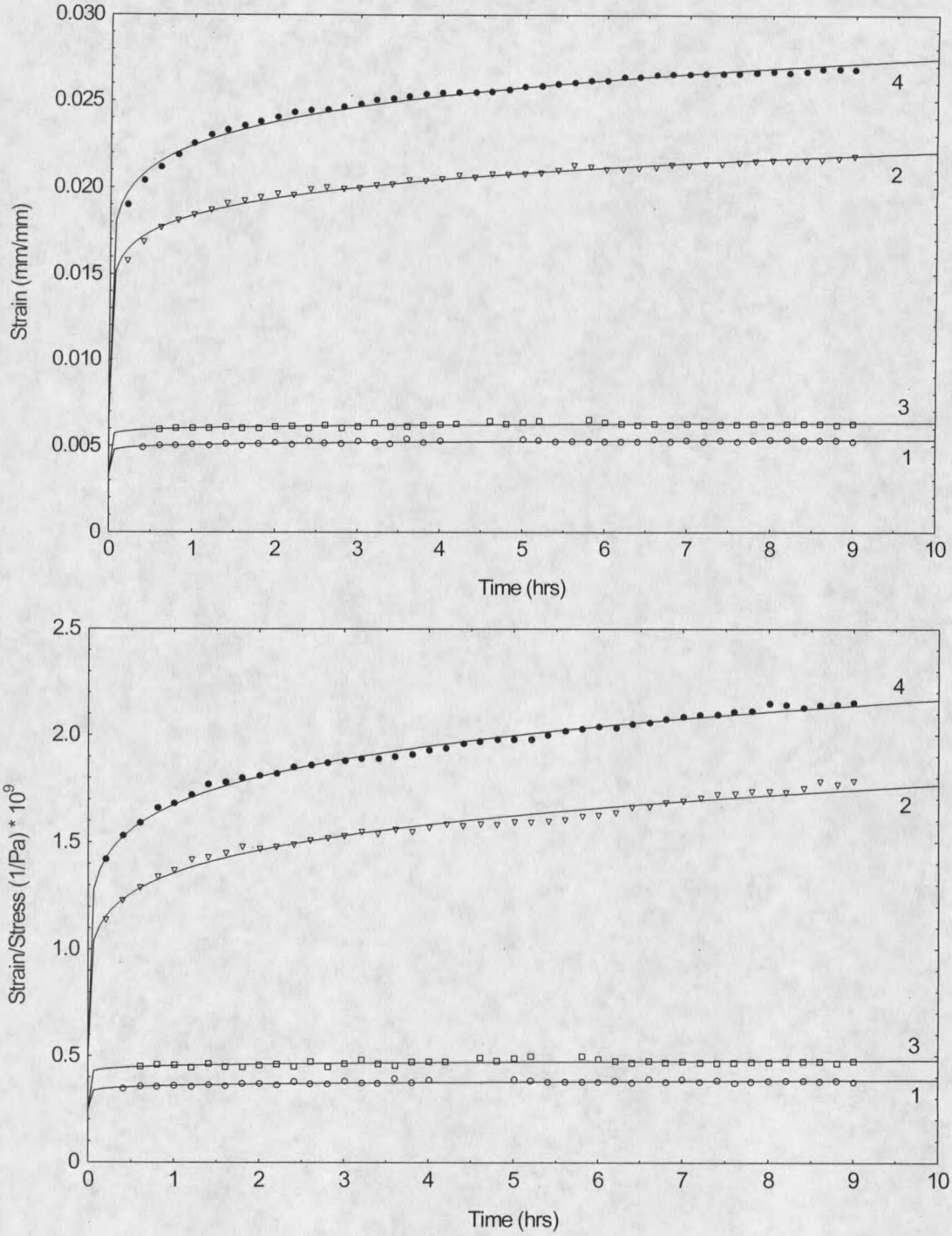


Figure 71 Vibrocreep Response of PVDF at Different Frequencies and Temperatures
Vibrocreep: $(0.45\pm0.20)\sigma_y$, **1**- 5 Hz -25 °C, **2**- 5 Hz 23 °C, **3**- 10 Hz -25 °C, **4**- 10 Hz 23 °C;
σ_y = 30.428 MPa at 23 °C

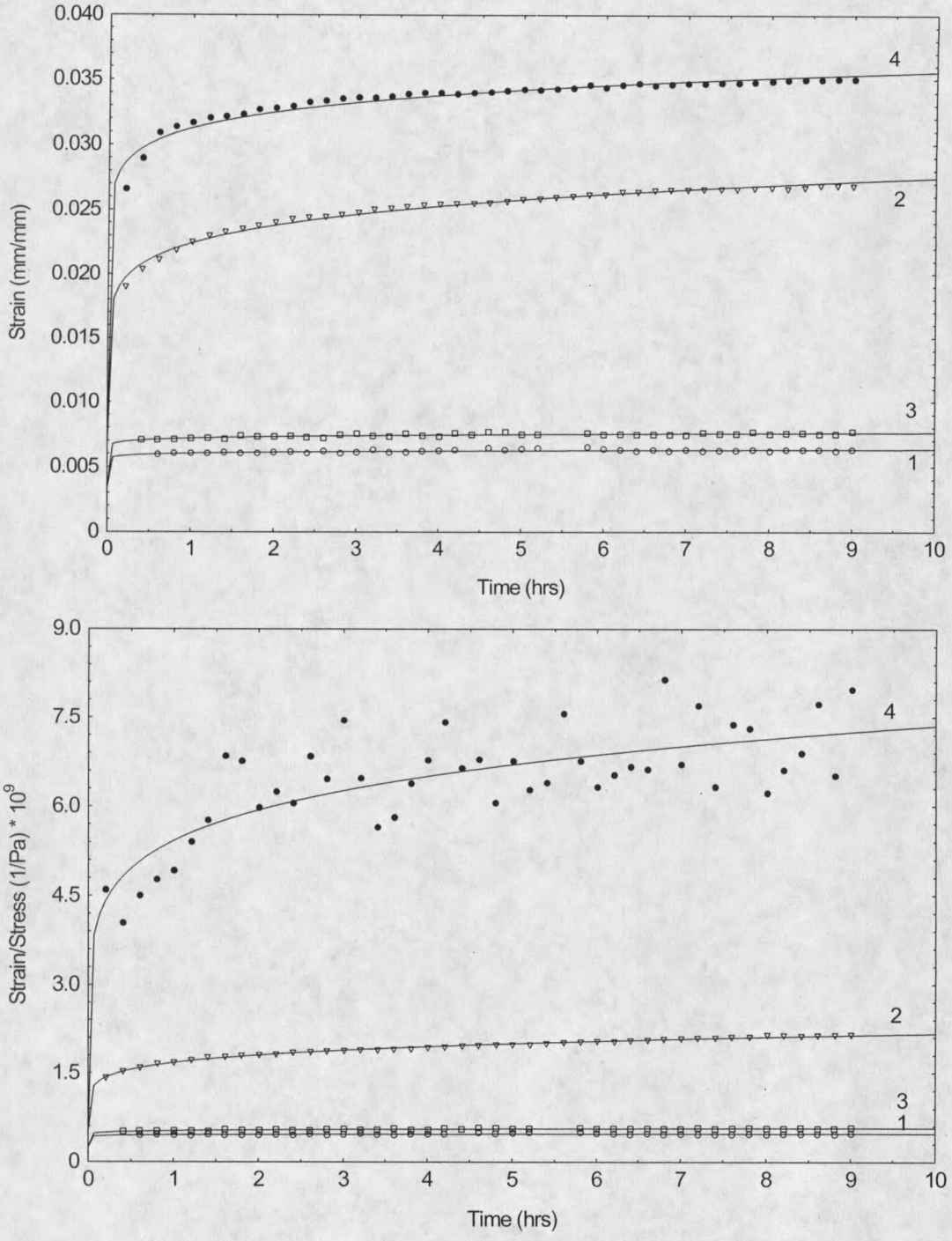


Figure 72 Vibrocreep Response of PVDF at Different Amplitudes and Temperatures

Vibrocreep: **1**- $(0.45\pm0.20)\sigma_y$, at 10 Hz -25 °C, **2**- $(0.45\pm0.20)\sigma_y$, at 10 Hz 23 °C **3**- $(0.45\pm0.40)\sigma_y$, at 10 Hz -25 °C, **4**- $(0.45\pm0.40)\sigma_y$ at 10 Hz 23 °C; σ_y = 30.428 MPa at 23 °C

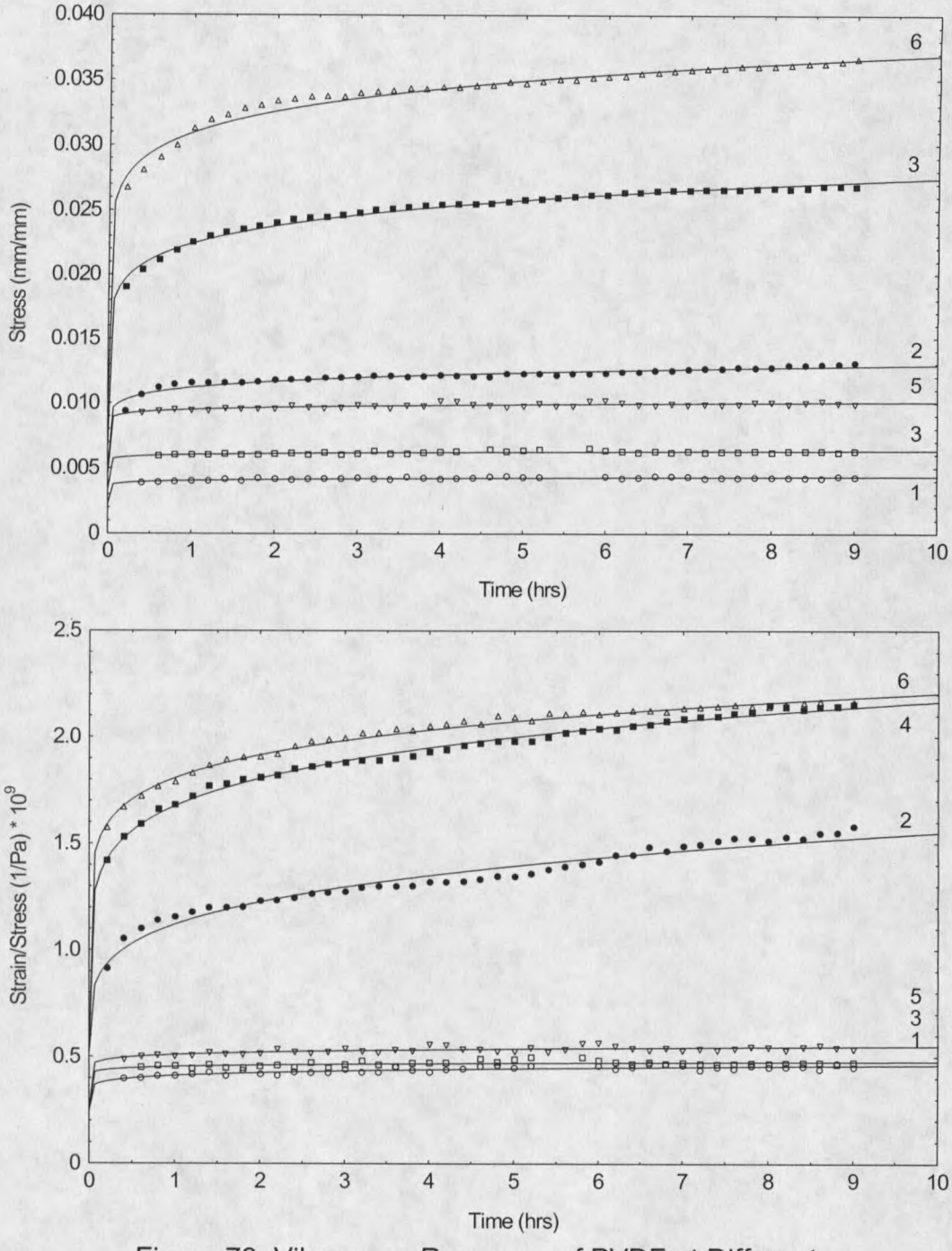


Figure 73 Vibrocreep Response of PVDF at Different Mean Stresses and Temperatures

Vibrocreep: **1**- $(0.30\pm0.20)\sigma_y$, at 10 Hz -25 °C, **2**- $(0.30\pm0.20)\sigma_y$, at 10 Hz 23 °C **3**- $(0.45\pm0.20)\sigma_y$, at 10 Hz -25 °C, **4**- $(0.45\pm0.20)\sigma_y$ at 10 Hz 23 °C; **5**- $(0.60\pm0.20)\sigma_y$, at 10 Hz -25 °C, **6**- $(0.60\pm0.20)\sigma_y$ at 10 Hz 23 °C; σ_y = 30.428 MPa at 23 °C

Conclusion

The effect of cyclic loads on the time-dependent behavior of PVDF can be seen in the figures shown in Appendix H-L. From the figures, it is clear that linear viscoelastic theory can not be used to characterize the vibrocreep phenomena in PVDF. The need for nonlinear material characterization of PVDF is evident from the increase in creep once an oscillatory load is combined with the constant load. The vibrocreep effect has been shown to increase with increasing frequency, amplitude, mean stress and temperature range below the linear viscoelastic limit.

Similarly to Nylon 6/6, the vibrocreep effects appear to be directly dependent upon the product of the amplitude and frequency of the cyclic load, Equation 17. As can be observed from Figure 74, vibrocreep effects are directly dependent on the product of the frequency and amplitude. The product of the two therefore can also be used to correlate other vibrocreep curves at the same mean stress as shown.

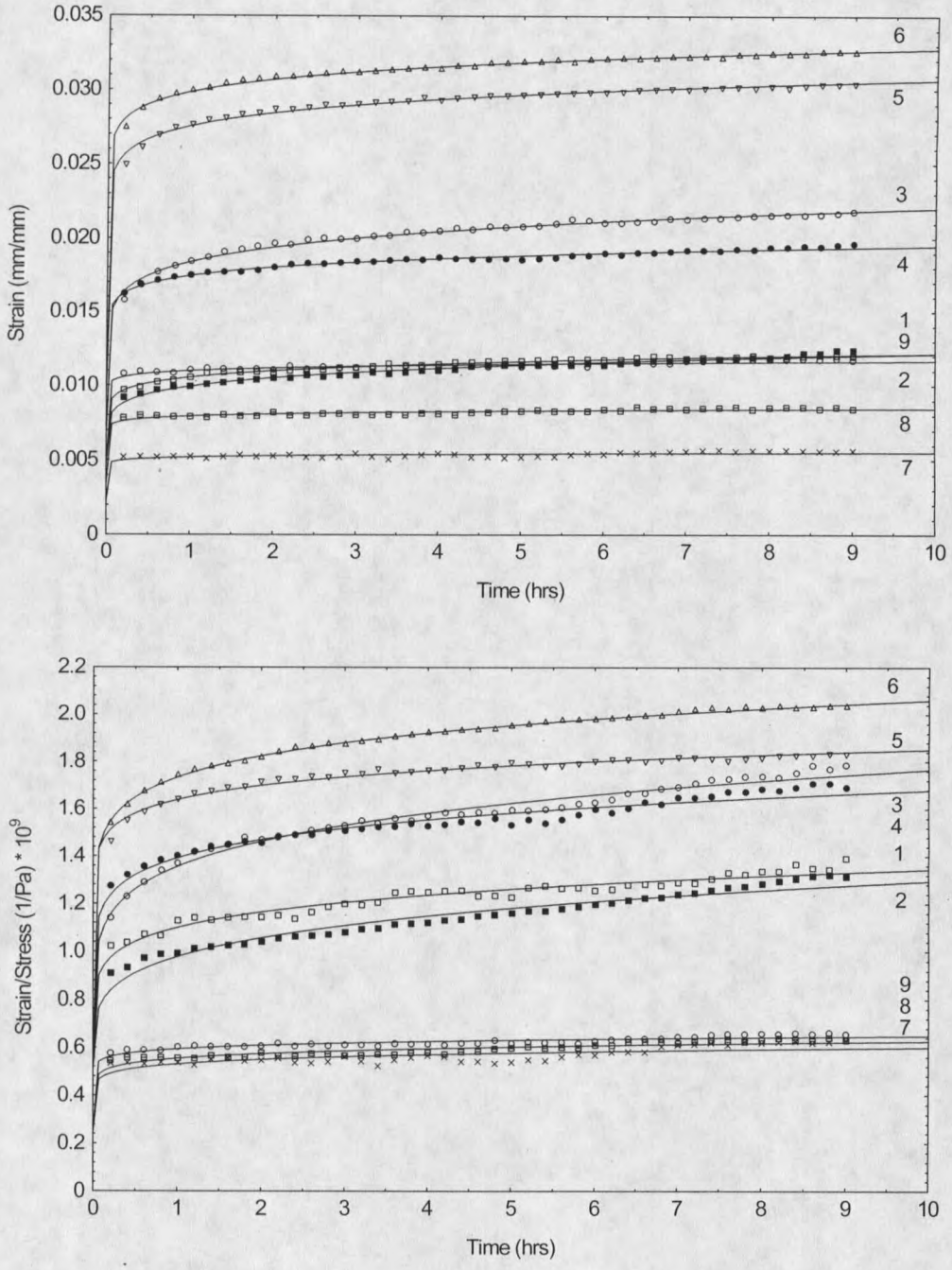


Figure 74 Vibrocreep Response of PVDF with ω*a = 100 at 23 °C
Vibrocreep: **1**- $(0.30\pm0.20)\sigma_y$, at 5 Hz; **2**- $(0.30\pm0.10)\sigma_y$, at 10 Hz;
3- $(0.45\pm0.20)\sigma_y$, at 5 Hz; **4**- $(0.45\pm0.10)\sigma_y$, at 10 Hz;
5- $(0.60\pm0.20)\sigma_y$, at 5 Hz; **6**- $(0.60\pm0.10)\sigma_y$, at 10 Hz;
Constant Load Creep: **7**- $(0.30)\sigma_y$, **8**- $(0.45)\sigma_y$, **9**- $(0.60)\sigma_y$;
σ_y = 30.428 MPa at 23 °C

STATISTICAL ANALYSIS

The use of statistics to predict error and/or uncertainty is widely used. The difficulty is in the testing requirements to develop a population of samples that a handful can be taken from. In the aspect of material testing, developing a population of tensile specimens is not uncommon, but for creep and vibrocreep of polymer materials a high number of samples is usually unattainable since creep testing requires long periods of time Ref[5,50].

In order to assume a Gaussian statistical distribution, etc, 30 samples are needed to represent each curve. The use of small sample theory is therefore used, where the assumption of a statistical distribution is not done. The sample size used for vibrocreep is 3 and for tensile and creep tests is 5. The level of confidence that is typically used by researchers for their experimental statistical representation, is 20:1 (95%). The equation for statistical prediction of the data is provided in Equation 18, Ref[5], where μ = mean population or mean strain at the particular time, $t_{\alpha/2,\nu}$ = t distribution value, α = confidence interval, c = confidence, ν = degrees of freedom, n = number of samples, and S_x = Standard Deviation.

$$\mu - t_{\frac{\alpha}{2},\nu} \cdot \frac{S_x}{\sqrt{n}} < \mu < \mu + t_{\frac{\alpha}{2},\nu} \cdot \frac{S_x}{\sqrt{n}}$$

$$\alpha = 1 - c \qquad \nu = n - 1$$

Equation 18

The statistical representation of the curve fit equation is pursued in a different manner since a large number of data points are used to correlate to the curve fit equation. For all curves, the power law approximation to represent the data is used. The results of the curve fit parameters are provided in Appendix M. For the creep curves, data was reduced for from 600 data points to 45 data points per test. Since 5 tests make up a representative curve, then 225 samples generate the representative creep curve. The representative curve is therefore curve fitted to an approximate model, and the statistical analysis is performed with 225 n number of samples. For the vibrocreep curves, 135 n number of samples is used instead since the number of tests to for a representative curve is at least 3. The same odds of 20:1 (95%) are used to statistically predict the mean of the data. A Gaussian distribution is assumed for the curve fit relation since this is usually assumed for experimental data. The equation for statistical analysis of the curve fit equation is provided below in Equation 19, where t = particular time, a, b, and c = curve fit parameter, $z_{\alpha/2}$ = z distribution value, α = confidence interval, c = confidence, n = number of samples, $\sigma_{\Delta\varepsilon}$ = deviation, and $\Delta\varepsilon$ = mean strain at the particular time.

$$\left(a\cdot t^{b}+c\right)-z_{\frac{\alpha}{2}}\cdot\frac{\sigma_{\Delta\varepsilon}}{\sqrt{n}}<\left(a\cdot t^{b}+c\right)<\left(a\cdot t^{b}+c\right)+z_{\frac{\alpha}{2}}\cdot\frac{\sigma_{\Delta\varepsilon}}{\sqrt{n}}$$

$$\sigma_{\Delta\varepsilon}^{2}=\frac{\sum_{i=1}^{n}\left[\Delta\varepsilon-\left(a\cdot t^{b}+c\right)\right]^{2}}{n-1} \qquad \alpha=1-c$$

Equation 19

The statistical analysis for Nylon 6/6 and PVDF is provided in Appendix M. The representation of the data is shown with 95% confidence intervals. The confidence interval allows the prediction of the mean of the data to be within the bound shown. Statistical analysis is only performed on one representative test. The small sample theory method assumes that the data at each point are independent and they are not, therefore large confidence intervals are a result of this assumption. For a small population, small sample theory is applicable. For Nylon 6/6, the statistical analysis of the tensile, creep, vibrocreep, and post cyclic test results are provided. The statistical analysis of the curve fit equation is also provided within Section I of Appendix M. For PVDF, the statistical analysis is shown for both testing temperatures, since the testing machine is cooled in the cold room or warmed at 23 C. The effects of the temperature on the testing machine provided difficulties such as friction, etc. that are not seen in the testing of Nylon 6/6, therefore more testing was required. The statistical analysis of PVDF is shown in the Section II of Appendix M. The tensile, creep and vibrocreep results are shown with 95% confidence interval at each temperature. The curve fit relations are also shown within the section with 95% confidence intervals.

DISCUSSION

The development of an experimental program and the quantification of the cyclic loading effects on time dependent polymers and polymer based composites have been accomplished. The experimental program involves different testing procedures for assessing the cyclic loading effects. As a result of the experimental program the vibrocreep effect has been investigated on the basis of a consistent parametric study.

The developed experimental program incorporates tensile, constant load creep, and vibrocreep testing. The experimental program involves evaluation of a polymer material by performing preliminary testing to initially verify that the cyclic loading effects can be observed according to the criteria outlined in the experimental program, Figures 31-33. The vibrocreep testing program has focused on the loading conditions below the linear viscoelastic limit of the material. Tensile testing of the polymer material has been used to determine the instantaneous elastic response or the tensile properties. Instantaneous material properties including yield stress and elastic modulus have been determined.

The second part of the experimental program involves creep testing under sustained constant loading conditions. The program has provided the information regarding the linear viscoelastic limit of the material and the respective creep compliances. These results have been used to investigate vibrocreep effects.

The third part of the experimental program, the cyclic loading effects or vibrocreep testing has been investigated using a parametric study. The study evaluates the change in loading parameters, thus assessing their effects upon the vibrocreep phenomenon. The parameters of interest are the frequency, amplitude, mean stress, and temperature. By varying each of the variables independently, the vibrocreep effect has been investigated. The testing required the use of non contact instrumentation and measurement. The use of computerized data acquisition has been developed and performed for all data measurements.

Cyclic loading effects have been examined for Nylon 6/6 through the development of the experimental program and the parametric study described above. Nylon 6/6 has been selected since this material has been used expensively in industry under cyclic loading conditions. Testing of Nylon 6/6 has involved tensile testing of the polymer at room temperature. The test specimen for all testing is the ASTM 638-96 Type II. The results provided a yield stress of 70e6 Pa and an elastic modulus of 1.41e9 Pa. Additional testing at 23 °C allowed the comparison of two different material batches to address nonhomogenities in the material processing, Table 7. Tensile testing was also performed at the temperatures of 35, 41, 50, 59, and 68 °C, Figure 42. After tensile testing had been completed, the preliminary creep and vibrocreep testing is pursued using only one test specimen for each test. The vibrocreep effect was

evident in Nylon 6/6 by the vibrocreep criteria, therefore further testing was pursued.

By testing the material at multiple stress levels, a database of testing results has been developed and used subsequently for constitutive model development. The linear viscoelastic limit has been determined to be approximately 30% at room temperature of 23 °C, Figure 36. The vibrocreep testing was started at 23 °C with mean stresses and amplitudes selected below the linear viscoelastic limit, Table 8. The frequency selection is based upon previous literature where hysteresis heating has been seen, Ref[39]. At least three test specimens have been tested to obtain the vibrocreep results at a particular stress level, frequency and temperature. From the parametric study of the cyclic loading of Nylon 6/6 at 23 °C, the results demonstrate an increase in the vibrocreep effect with increasing frequency and amplitude, Figure 37-38. A decreasing vibrocreep effect is observed with increasing mean stress, Figure 39, and temperature below the linear viscoelastic limit.

At elevated temperatures similar effects have been observed. The results show that an increase of frequency and/or amplitude also increases the vibrocreep effect, Figures 45-46. The cyclic loading effects are also tested outside of the linear viscoelastic limit with the increase in temperature and stress levels relative to 23 °C. The effects of mean stress and temperature can be further seen from Figure 47 and Figures 48-51 respectively, where an increase in temperature decreased the vibrocreep effect below the linear viscoelastic limit.

The effect of mean stress and temperature can be explained as the effect of the creep properties in the material becoming more dominate than the damage development.

The evaluation of the vibrocreep effect is seen from the two different combinations. The first factor, a ratio of the mean stress to the amplitude of the cyclic load can be related to the R ratio typically considered in the studies of fatigue. The result of this correlation factor combines the amplitude and mean stress effects together as shown in Figure 56. From this result an increase in mean stress and amplitude correlates with approximately the same difference between the creep and vibrocreep creep compliance curves. A second comparison where the vibrocreep effects appear to be directly dependent upon the product of the amplitude and frequency of the cyclic load, observed from Figure 55.

The post tensile testing results for Nylon 6/6 show an increase in stiffness and strength of the material that is recoverable from the vibrocreep testing only at 23 °C, Figure 40. The constant load creep test specimens did not result in a significant amount of residual strength until the temperatures are increased, Figure 52-53. The increase in the strength and stiffness may be due to the creep effects which are reduced after creep and vibrocreep testing since the material has been creeping for approximately 12 hrs, therefore the contribution due to creep during the tensile test would be reduced showing an increase in stiffness and strength.

The testing of PVDF has been performed in the same manner as that of Nylon 6/6 with the tensile testing, constant load creep testing, and vibrocreep testing. PVDF was selected due to its wide application in vibration environments. Through testing of PVDF, a methodology of testing thin films has been developed. Test specimen is prepared according to ASTM 882-95a standard. The results of the testing of PVDF show the material to be highly anisotropic. The highest strength and stiffness are found to be along the 1 direction of the material, Table 96. Testing has been performed in the 1 direction. The constant load creep testing results provide the linear elastic limit of at least 60% of the yield stress at 23 °C, Figure 61. The creep testing has been performed at mean stresses of 30%, 45%, and 60%. The selection of the mean stresses and amplitudes has allowed testing within the linear and nonlinear viscoelastic regimes. An additional temperature closer to the glass transition temperature was also selected. Testing within the cold room proved to be challenging, since friction in the pulley and bearing application of the load was considerable.

An increasing vibrocreep effect has been observed with an increasing frequency, amplitude, or mean stress at both temperatures. For 23 °C the results are shown in Figures 62-64 and for -25 °C, Figures 67-69. From the comparison of the two temperatures an increase in the vibrocreep effect with an increasing temperatures is observed in Figures 70-73. The results show that the linear viscoelastic regime does not effect through evaluation of each parameter individually. The product of the frequency and amplitude was therefore used as

a parameter to quantify the test results. The results have shown the product to be quite interesting, Figure 74. The vibrocreep effects appear to be directly dependent upon the product of the amplitude and frequency as seen from the Nylon 6/6 experimental results.

The statistical analysis of the test data is performed on the test data and also on the curve fit of the data. The statistical analysis of the data is based on small sample theory, where the data does not follow a distribution. The results show to be very conservative and as a result the confidence intervals are enormous. The theory applied does not take into account for the interaction of the data on the time scale, but the simple one event in time. Therefore the analysis is not entirely complete since the population is small. Typically statistical analysis is not performed on creep tests since the amount of time required generally results in a small sample population. The statistical analysis of the curve fit equation is done considering the relationship of the data points in time and the differences between the specimens. The curve fit statistical analysis uses the new mean value determined from the fit equation and relates the new mean to the data specimens. The statistical analysis shows that the confidence intervals are much smaller demonstrating the goodness of fit between the data and the curve fit model.

CONCLUSION

Through the development of this study the goals of the project have been met. With the development of an experimental program for testing and characterization of vibrocreep effects, the understanding of the response of polymers under the conditions of superimposed constant and cyclic loads over a range of temperatures has been enhanced.

The results of the investigation indicate that the materials under consideration, i.e. Nylon 6/6 and a piezoelectric PVDF based composite, exhibit accelerated creep rates under the conditions of superimposed constant and cyclic loads. Creep acceleration due to cyclic loading effects has been observed in both materials even in the range of stresses well below their respective viscoelastic linearity limits. It is clear that these effects are essentially nonlinear, as the response of the materials to cyclic loading conditions does not represent a simple superposition of the responses to constant and fully reversed cyclic loads applied separately.

Experiments consistently demonstrate an increase of creep rates in both polymers as frequencies and amplitudes of vibration tended to increase. However, no consistent results have been obtained in regard to the effects of mean stresses on the cyclic creep behavior of the polymers.

It is important to note that the effects of cyclic loading conditions on the long-term response of polymers have been discussed in the literature primarily in

the context of creep-fatigue interaction Ref[29] and Ref[12]. As indicated in the latter publications, failure of polymers subjected to superimposed constant and cyclic loads depends on the relation between the mean stress and stress amplitude of the loading cycle. At higher mean stresses and low amplitudes, the cyclic response of polymers is dominated by creep processes, whereas as mean stresses tend to decrease, progressive damage evolution in polymers becomes the major factor leading to brittle failure. Hertzberg and Manson, Ref[29] have observed that, as a result of the interaction between different deformation and damage mechanisms depending on mean stresses, in some polymers, "surprisingly beneficial influence of mean stress on fatigue crack propagation behavior is not without precedent".

Based on the experimental study reported in this paper, it is clear that the behavior of polymers subjected to superimposed constant and cyclic loads involves nonlinear effects that depend on the interaction between creep and damage evolution processes. Apparently, the character of these processes in the presence of cyclic loads is different than that typically for constant load creep. Thus, the latter is characterized by continuously uniform microstructural changes in the material until the onset of tertiary creep, at which stage progressive damage localization tends to develop. In contrast, during cyclic creep, there is an extended damage initiation process followed by an advanced stage of crack propagation. The onset of these damage mechanisms in polymers depends on a

number of factors such as temperature, strain rate, hydrostatic pressure, and strain induced crystallization.

The effect of increasing mean stress within the linear viscoelastic regime shows decreasing vibrocreep effect for Nylon 6/6 with an increasing effect for PVDF, but above the linear viscoelastic limit an increasing mean stress decreases the vibrocreep effect for both materials. An increasing vibrocreep effect has been shown for both materials, Nylon 6/6 and PVDF, with an increasing frequency and amplitude. The result of increasing temperature on the cyclic loading tests has shown a decrease in the vibrocreep effect for Nylon 6/6 and an increasing effect in PVDF. This difference may be contributed to the glass transition temperature, where cyclic load testing was performed below the glass transition temperature for Nylon 6/6, and above the glass transition temperature for PVDF.

For both Nylon 6/6 and PVDF, the cyclic loading effect showed similar results in regard to the product of two parameters, frequency and amplitude of the cyclic load. Another combination that has been investigated was the combination of the mean stress to the amplitude of the cyclic load that can be further related to the R ratio typically considered in the studies of fatigue. In Nylon 6/6, an increase in mean stress and amplitude correlates with approximately the same difference between the creep and vibrocreep creep compliance curves.

FURTHER RESEARCH

Further research should be performed in four areas. The first area of needed research is the development of a damage model for the assessment of the craze formation on the surface of polymers. The can be verified through material testing and analyzed on microscopic level to develop a damage model in time. The value of such a model would be enormous. The prediction of fatigue life of viscoelastic materials may be an outcome of such a model. The second area of further research is the analysis of the piezoelectric properties of PVDF under vibrocreep conditions. Efforts to perform such tests have been tried, but the test material needs to be custom made in order to prevent arcing of the PVDF material. The data acquisition system, testing equipment described in this document can be used. The third area of further research is the product of frequency and amplitude that needs to be further investigated. The fourth and final area of further research is the development of statistically significant effects for the evaluation of the vibrocreep phenomena in polymers. With the limitations of instrumentation and the testing methods outlined, further research may or may not be feasible.

REFERENCES CITED

1. Arad, S., Radon, J. C. and Culver, L. E., Strain Rate Dependence on Failure Processes in Polycarbonate and Nylon, Journal of Applied Polymer Science, 1973, Vol. 17, pp. 1467-1478

2. ASM International Engineering Plastics Vol 2. © 1988 ASM International, U.S.

3. ASM International Composites Vol 1. © 1988 ASM International, U.S.

4. Bareishis, I. P., The Mechanism of Fatigue Failure of Plastics, Mechanics of Composite Materials, 1996, Vol. 32, No. 2

5. Beckwith, Marangoni, and Lienhard, Mechanical Measurements, © 1993 Addison-Wesley Publishing Company, Inc. U.S.

6. Berins, Michael, Plastics Engineering Handbook, ©1991 Van Nostrand Reinhold, New York

7. Bikales, Norbert M., Mechanical Properties of Polymers, ©1971, John Wiley and Sons Inc. New York

8. Bodnar, A., Chranowski M., and Latus, P., Lifetime Evaluation of Creeping Structures, Proceedings of the Fifth International Conference on Creep of Materials, Lake Buena Vista, Florida USA, May 18-21, 1992

9. Bouda, V. and Staverman, The Effects of Cyclic Loading on Polymers in the Glassy State, Journal of Polymer Science, 1976, Vol. 14, pp. 2313-2323

10. Brandrup, J. and Immergut, E.H., Polymer Handbook, © 1979 John Wiley and Sons, New York

11. Broek, David, Elementary Engineering Fracture Mechanics, © 1986 Kluwer Academic Publishers, Dordrecht

12. Crawford, R. J., Plastics Engineering, ©1987, Pergamen Press, Elmsford, New York

13. Crissman, J.M., and Zapas, L. J., Dynamic Mechanical Behavior of Polyethylene During Creep to Failure in Uniaxial Tension, Journal of Applied Physics, October 1977, Vol. 48, No. 10, pp. 4049-4051

14. Cessna, L. C., Levens, J. A., and Thomson, J. B., Flexural Fatigue of Glass-Reinforced Thermoplastics, Polymer Engineering and Science, 1969, Vol. 9, No. 5, pp. 339-349

15. Constable, I., Williams, J. G., and Burns, D. J., Fatigue and Cyclic Thermal Softening of Thermoplastics, Journal of Mechanical Engineering Science, 1970, Vol. 12, No. 1, pp. 20-29

16. Daniels, C.A., Polymers: Structure and Properties, ©1989 Technomic Publishing Co., Lancaster, Pennsyvania

17. Dentsoras, A. J., and Kouvaritakis, E. P., Effects of Vibration Frequency on Fatigue Crack Propagation of a Polymer at Resonance, Engineering Fracture Mechanics, 1995, Vol. 50, No. 4, pp. 467-473

18. Ebbing, Darrell D. General Chemistry, ©1993 Houghton Mifflin Company, Boston

19. Elias, Hans-Georg, An Introduction to Plastics, VCH, New York

20. Feltner, C. E. and Morrow, Jo Dean, Microplastic Strain Hysteresis Energy as a Criterion for Fatigue Fracture, Journal of Basic Engineering, March 1961, pp. 15-22

21. Ferry, John D. Viscoelastic Properties of Polymers, ©1980, John Wiley and Sons New York

22. Fitzgerald, J.J., Martellock, A.C., Nielson, P., and Schillace, R.V., The Effect of Cyclic Stress on the Physical Properties of a Poly(Dimethysiloxane) Elastomer Polymer Engineering and Science, 1992, Vol. 32, No. 18, pp. 1350-1357

23. Flinn, Richard A., Trojan, Paul K., Engineering Materials and Their Applications, ©1990 Houghton Mifflin Company, Boston

24. Flugge, Wilhelm, Viscoelasticity, ©1967 Blaisdell Publishing Company, Waltham, Massachutes

25. Gates, Thomas, Veazie, David R., and Brinson, Catherine L., A Comparison of Tension and Compression Creep in a Polymeric Composite and the Effects of Physical Aging on Creep, NASA Langley Research Center, August 1996

26. Halford, G.R. Fatigue in the Creep Range-Material Testing, Documentation and Interpretation, NASA Lewis Research Center, September 1975

27. Harper, Charles A., Handbook of Plastics, Elastomers, and Composites, ©1996 McGraw-Hill, New York

28. Hans-George, An Introduction to Plastics, ©1993, VCH, New York

29. Hertzberg, Richard W. and Mansen, John A., Fatigue of Engineering Polymers, ©1980, Academic Press, New York

30. Higuchi, Masakazu, and Imai, Yasufumi, Rheological Interpretation of Heat Generation Associated with Fatigue of Polycarbonate, Journal of applied Polymer Science, 1970, Vol. 11, pp. 2377-2383

31. Holloway, Frank, Material Characterization of Poly(vinylidene flouride): a Thin Film Piezoelectric Polymer, M.S. Thesis, April 1997, Montana State University

32. Incropera, Frank P. and Dewitt, David P., Introduction of Heat Transfer, ©1996 John Wiley and Sons, Inc., U.S.

33. Ives, G. C. and Mead, J.A., Handbook of Plastics Test Methods ,©1971 CRC Press, Cleveland Ohio

34. Jenkins, A.D., Polymer Science, Vol 1 ©1972 American Elsevier Publishing Co. Inc., New York

35. Jia, Nanying, and Kagan, Val A., Effects of Time and Temperature on the Tension-Tension Behavior of Short Fiber Reinforced Polyamides, Polymer Composites, August 1998, Vol. 19, No. 4, pp. 408-414

36. Jo, Nam-Ju, and Koh, Kwang-Nak, Relationship Between Fatigue Behavior and Nonlinear Dynamic Viscoelasticity for High Density Polyethylenes with Different Aggregation States, Journal of Polymer Engineering, 1998, Vol. 18, No. 1-2, pp. 63-82

37. Jo, Nam-Ju, Takahara, Atsushi, and Kajiyama, Tisato, Effect of Aggregation Structure on Non-Linear Dynamic Viscoelastic Characteristics or Orientated High Density Polyethylenes Under Cyclic Fatigue, Polymer, 1997, Vol. 38. No. 20, pp. 5195-5201

38. Jones, Robert M., Mechanics of Composite Materials, © 1975 Scripta Book Company, Washington D.C.

39. Lesser, Alan J., Changes in Mechanical Behavior During Fatigue of Semicrystalline Thermoplastic, Journal of Applied Polymer Science, 1995, Vol. 58, pp. 869-879

40. Letton, Alan, Farrow, Allan, and Strganac, Thomas, Viscoelastic Characterization of Thin-Film Polymers exposed to Low Earth Orbit

41. Lynch, Christopher S., Polyvinylidene Fluoride (PVDF) Elastic, Piezoelectric, Pyroelectric, and Dielectric Coefficients and their Non-Linearities, Ferroelectrics, 1993, Vol. 0, pp. 1-11

42. Kausch, H., H., Crazing in Polymers Vol. 2, © 1990 Springer-Verlag Berlin Heidelberg, Germany

43. Kawabe, Hiromitsu, Higo, Yakichi, Natsume, Yoshitaka, and Nunomura, Shigetomo, Influence of Environmental Conditions on the Fatigue Strength of Plastics, JSME International Journal, 1994, Series A., Vol. 37, No. 1, pp. 31-36

44. Krishnamachari, S.I., Applied Stress Analysis of Plastics , © 1993 Van Nostrand Reinhold New York

45. Mackay, M. E., Teng, T. G., and Schults, J. M., Craze Roles in the Fatigue of Polycarbonate, Journal of Material Science, 1977, Vol. 14, pp. 221-227

46. Maksimov, R. D., and Urzhumtsev, Yu. S., Vibrocreep of Polymeric Materials, Institute of Polymer Mechanics, July-August 1970, No. 4, pp. 643-647

47. Makismov, Robert D., and Kubat, Josef, Time and Temperature Dependent Deformations of Poly(ether ether ketone) (PEEK), Institute of Polymer Mechanics, November-December 1998, No. 6, pp. 734-746

48. Martin, G. C., and Gerberich, W. W., Temperature Effects On Fatigue Crack Growth in Polycarbonate, Journal of Material Science, 1976, Vol. 11, pp. 231-238

49. McCrum, N. G., Buckley, C. P., and Bucknall, C.B., Principles of Polymer Engineering, © 1988 Oxford University Press, New York

50. Miller, Irwin, R, Freud, John, E., and Johnson, Richard, Probability and Statistic For Engineers, © 1990 Prentice Hall Inc., Englewood Cliffs, New Jersey

51. Molinari, A., and Germain, Y., Self Heating and thermal Failure of Polymers Sustaining a Compressive Cyclic Loading, International Journal of Solid Structures, 1996, Vol. 33, No. 23, pp. 3439-3462

52. Moore G.R., Kline, D.E., Properties and Processing of Polymers for Engineers, Prentice-Hall, USA

53. Nurmukhametov, F. N., Dashevskii, V. G., Askadskii, A. A., and Slonimskii, G. L., Study of the Effect of Vibration in the Sonic Frequency Region on the Stress Relaxation Process in Polymers, Polymer Mechanics, 1976, Vol. 12, No. 4, pp. 519-529

54. Opp, D.A., Skinner, D. W., and Wiktorek, R. J., A Model For Polymer Fatigue, Polymer Engineering and Science, March 1969, Vol. 9, No.2, pp. 121-130

55. Phoenix, Leigh S. Modeling the Statistical Lifetime of Glass Fiber/Polymer Matrix Composites in Tension, Composite Structures, 2000, 48, pp. 19-29

56. Rabinowitz, S., Krause, A. R., and Beardmore, P. Failure of Polystyrene in Tensile and Cyclic Deformation, Journal of Material Science, 1973, Vol. 8, pp. 11-22

57. Riddell, M. N., Koo, G. P., and O'Toole, J. L., Fatigue Mechanisms of Thermoplastics, Polymer Engineering and Science, October 1966, pp. 363-368

58. Sakurai, Shinichi, Mokuwa, Sastoshi, Morimoto, Masato, Shibayama, Mitsuhiro, and Nomura, Shunji, Changes in Structure and Properties Due to Mechanical Fatigue for Polyurethanes Containing Poly(dimethyl siloxane), Polymer, 1994, Vol. 35, No. 3

59. Sanders, B. P., Mall, S., and Pittman, R. B. The Effects of Frequency and Temperature on the Fatigue Behavior of a Unidirectional Titanium-Matrix Composite, Composite Science and Technology, 1999, 59, pp. 583-591

60. Sauer, J. A., McMaster, A. D., and Morrow, D. R., Fatigue Behavior of Polystyrene and Effect of Mean Stress, Macromolecular Science and Physics, 1979, B12(4), pp. 535-562

61. Strganac, Thomas W., Letton, Alan, Payne, Debbie Flowers, and Biskup, Bruce A., Characterization of Nonlinear Viscoelastic Behavior Using a Dynamic Mechanical Approach, AIAA Journal, May 1995, Vol. 33, No. 5, pp. 904-910

62. Sunar, M., and Rao, S. S., Recent Advances in Sensing and Control of Flexible Structures via Piezoelectric Materials Technology, Applied Mechanics Review, January 1999, Vol. 52, No. 1, pp. 1-16

63. Takahara, Atsushi, Yamada, Kenji, Kajiyama, Tisato, and Takayanagi, Motowo, Evaluation of Fatigue Lifetime and Elucidation of Fatigue Mechanism in Plasticized Poly(vinyl Chloride) in Terms of Dynamic Viscoelasticity, Journal of Applied Polymer Science, 1980, Vol. 25, pp. 597-614

64. Talreja, Ramesh, Fatigue of Composite Materials, © 1987 Technomic Publishing Company, Lancaster Pennsylvania

65. Tauchert, T. R., The Temperature Generated During Torsional Oscillations of Polyethylene Rods, International Journal of Engineering Science, 1967, Vol. 4 pp. 353-365

66. Turtin'sh, R. P., Influence of Vibration in Creep in Glass-Fiber-Reinforced Plastic in a Complex State of Stress, Institute of Mechanics of Polymers, March-April 1974, No. 2, pp. 358-360

67. Vincent, P. I., The Tough-Brittle Transition in Thermoplastics, Polymer, July, No 1, 1960, pp. 424-444

68. Vinogradov, G. V., Yanovskii, Yu. G., and Isaev, A. I., The Effect of Vibrations (Cyclic Deformations of Large Amplitude) on the Viscoelastic Properties of Polypropylene Melts, International Chemical Engineering, April 1971, Vol. 11, No. 2, pp. 309-313

69. Ward, I.M. and Hadley, An Introduction to the Mechanical Properties of Solid Polymers, ©1993, John Wiley and Sons, England

70. Weaver, Judith L., and Beatty, Charles L., The Effect of Temperature on Compressive Fatigue of Polystyrene, Polymer Science and Engineering, 1978, Vol. 18, No. 14, pp. 1117-1126

71. Williams, J.D., Fracture Mechanics of Polymers, © 1984 Ellis Horwood Limited, Chichester

72. Zhou, Ying-Qiu, and Brown, Norman, The Mechanism of Fatigue Failure in a Polyethylene Copolymer, Journal of Polymer Science, 1992, Vol. 30, pp. 477-487

APPENDICES

APPENDIX A

Tensile and Constant Load Creep Results for Nylon 6/6

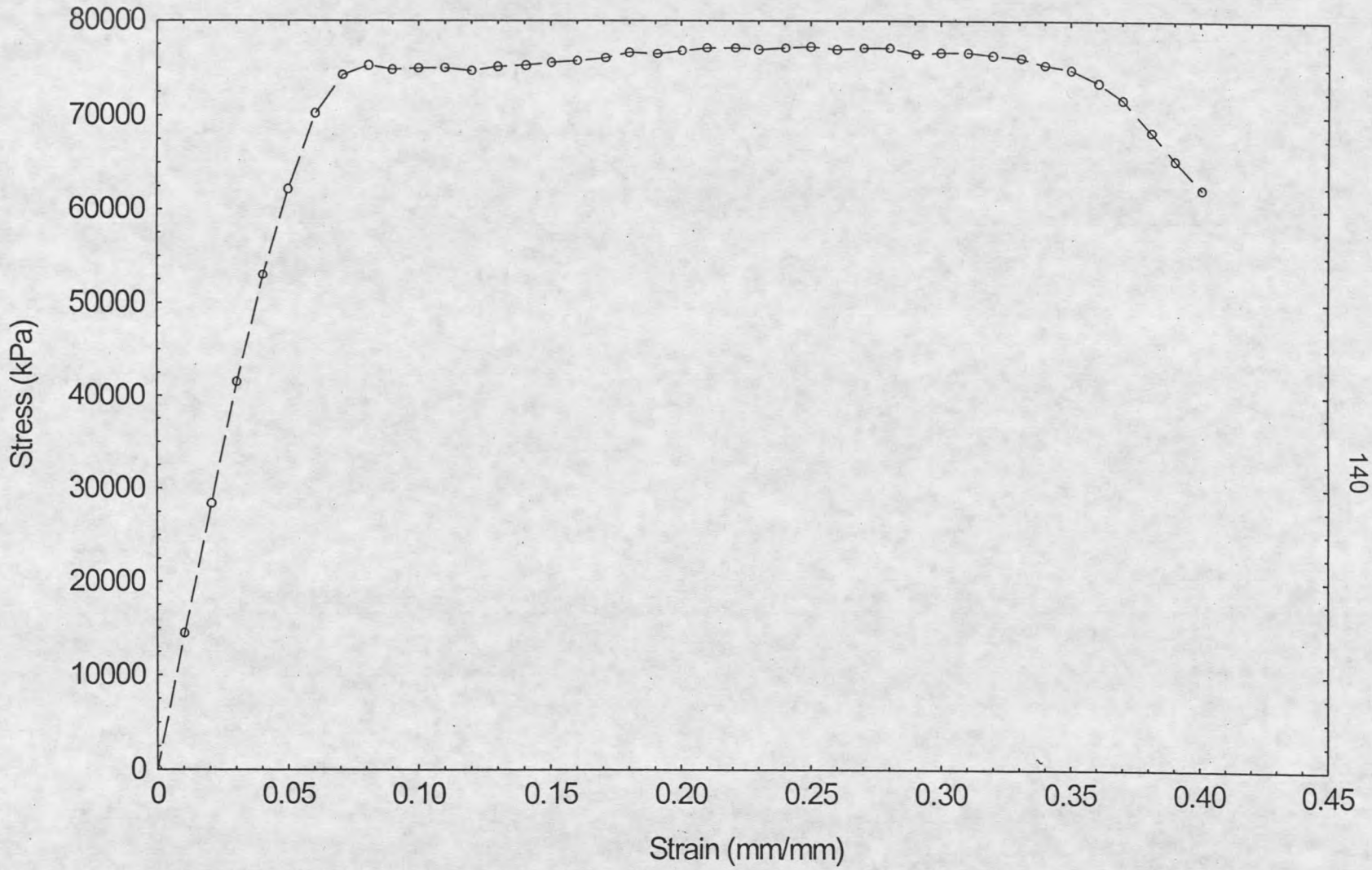


Figure A.I.1 Tensile Testing of Nylon 6/6 at 23 °C

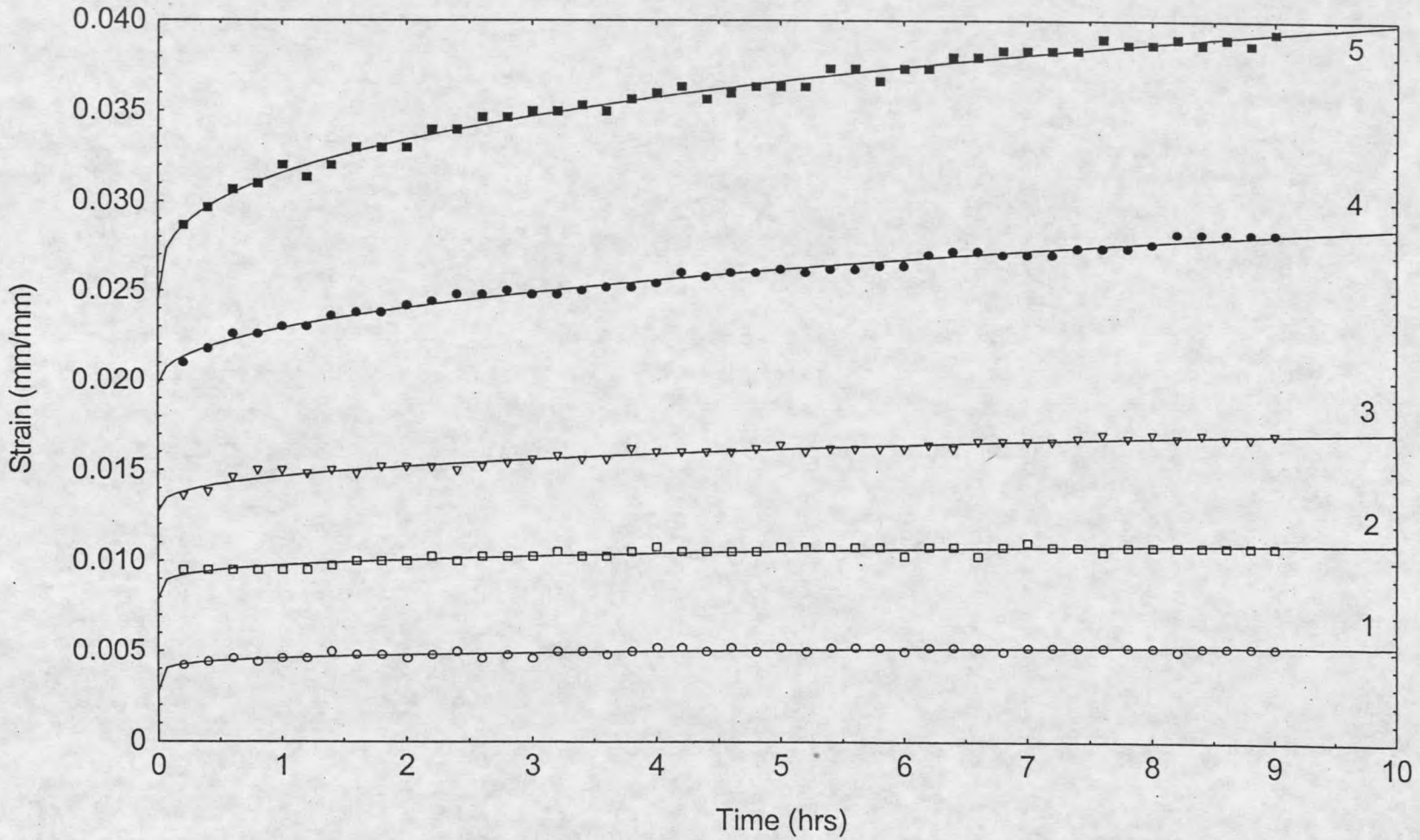


Figure A.I.2 Constant Load Creep of Nylon 6/6 at 23 °C
1- $(0.10)\sigma_y$; 2- $(0.20)\sigma_y$; 3- $(0.30)\sigma_y$; 4- $(0.40)\sigma_y$; 5- $(0.50)\sigma_y$;
σ_y = 70 MPa at 23 °C

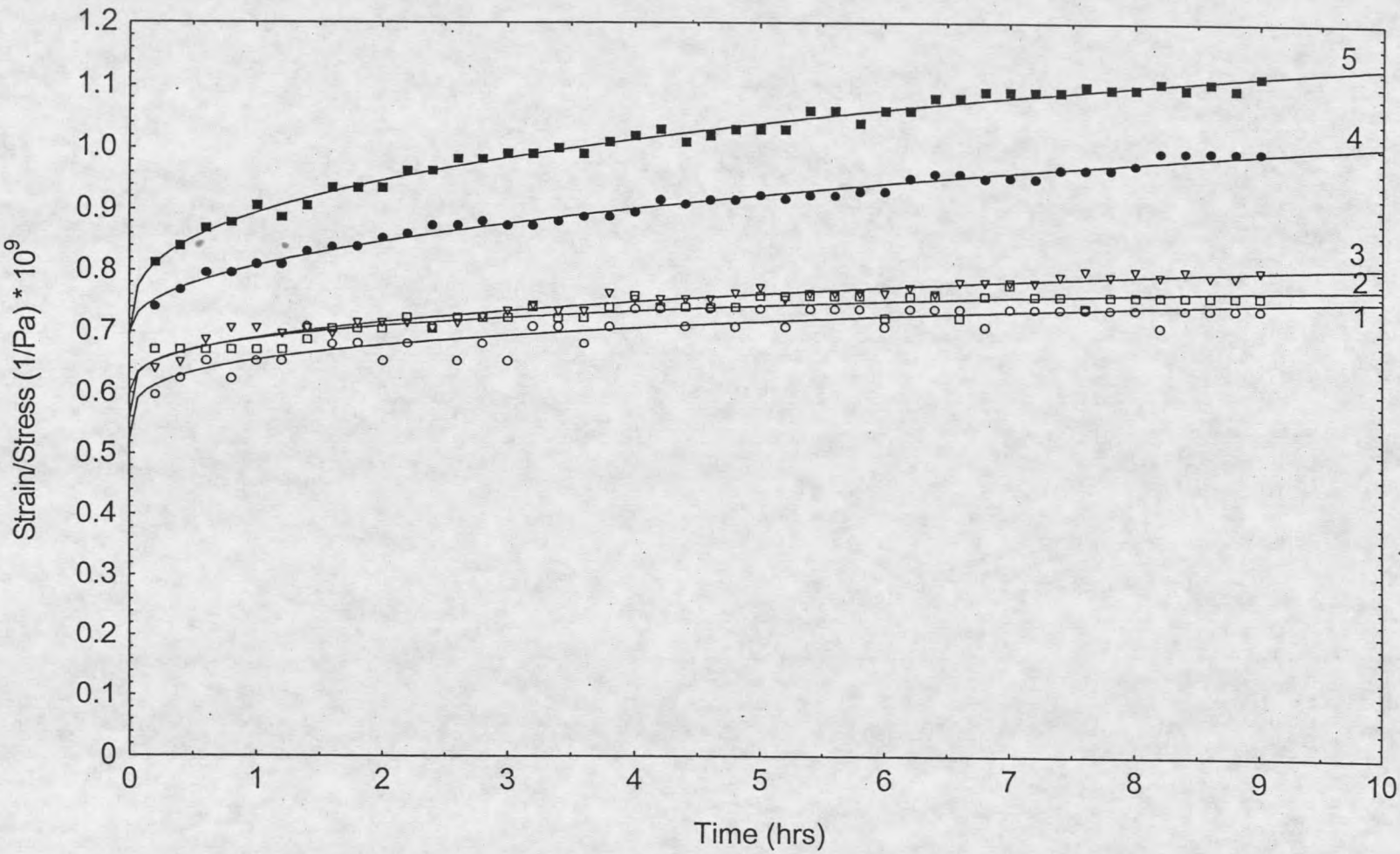


Figure A.I.3 Normalized Constant Load Creep of Nylon 6/6 at 23 °C
1- $(0.10)\sigma_y$; 2- $(0.20)\sigma_y$; 3- $(0.30)\sigma_y$; 4- $(0.40)\sigma_y$; 5- $(0.50)\sigma_y$;
σ_y = 70 MPa at 23 °C

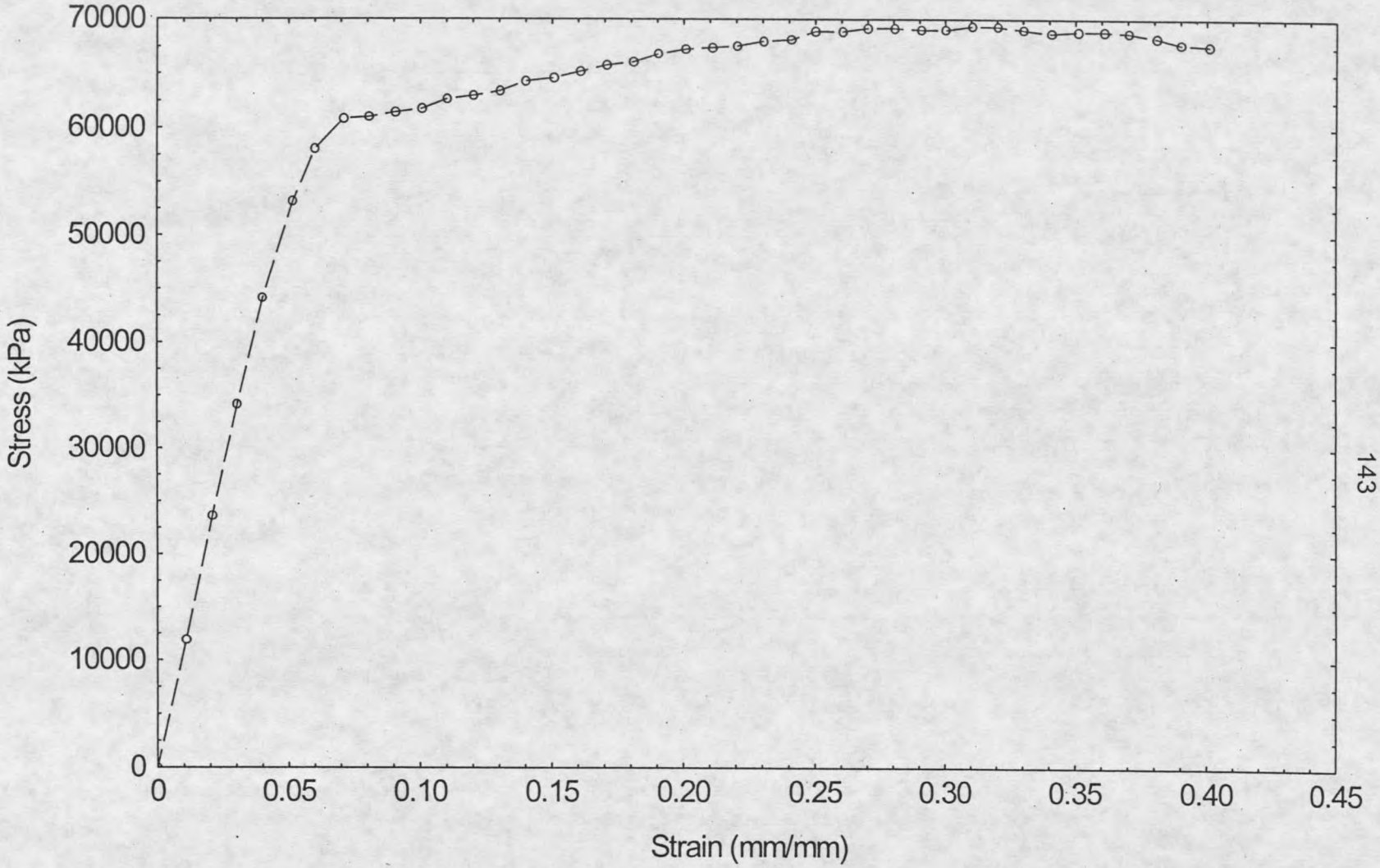


Figure A.II.1 Tensile Testing of Nylon 6/6 at 35 °C

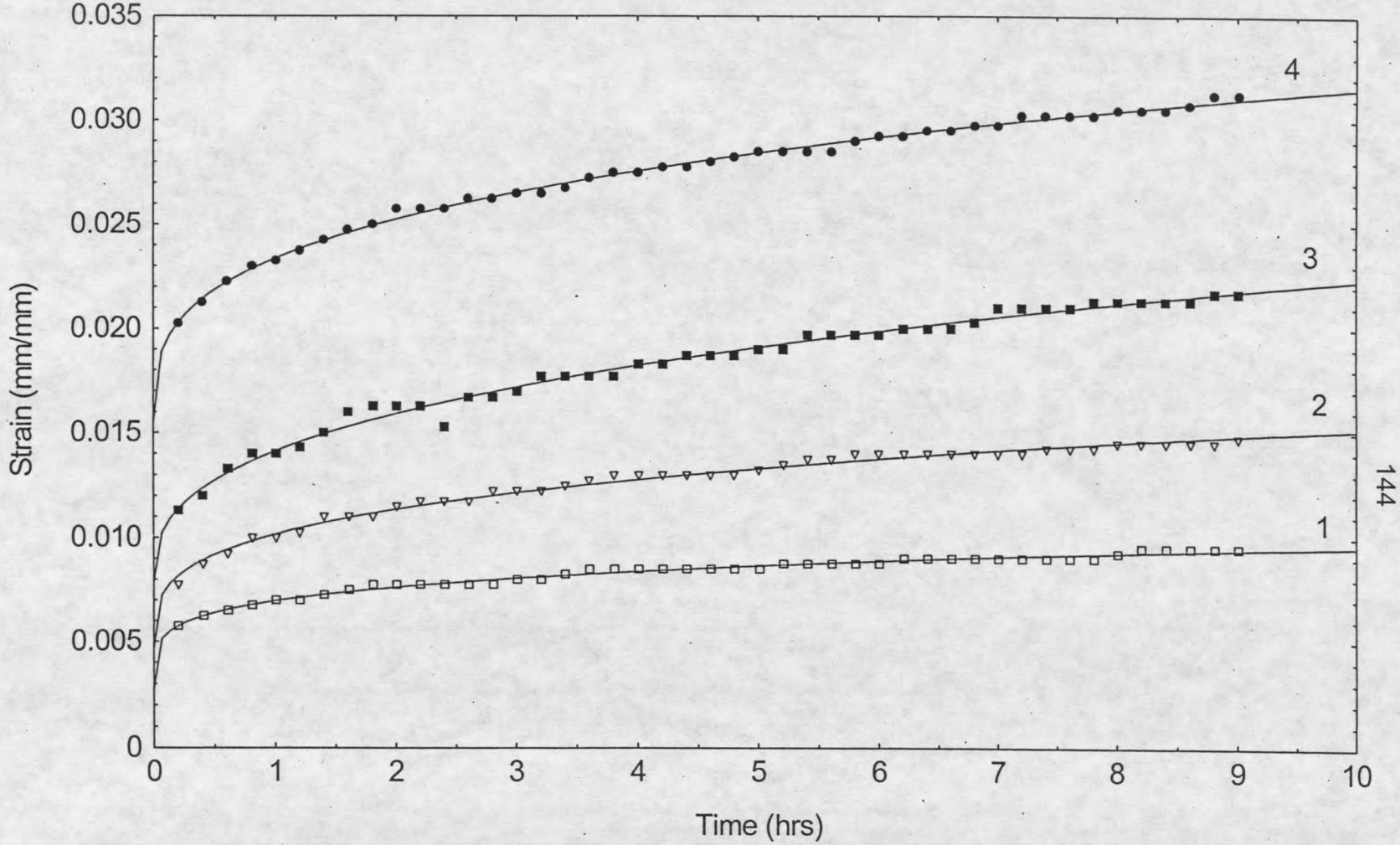


Figure A.II.2 Constant Load Creep of Nylon 6/6 at 35 °C
1- $(0.20)\sigma_y$; 2- $(0.30)\sigma_y$; 3- $(0.40)\sigma_y$; 4- $(0.50)\sigma_y$;
σ_y = 55 MPa at 35 °C

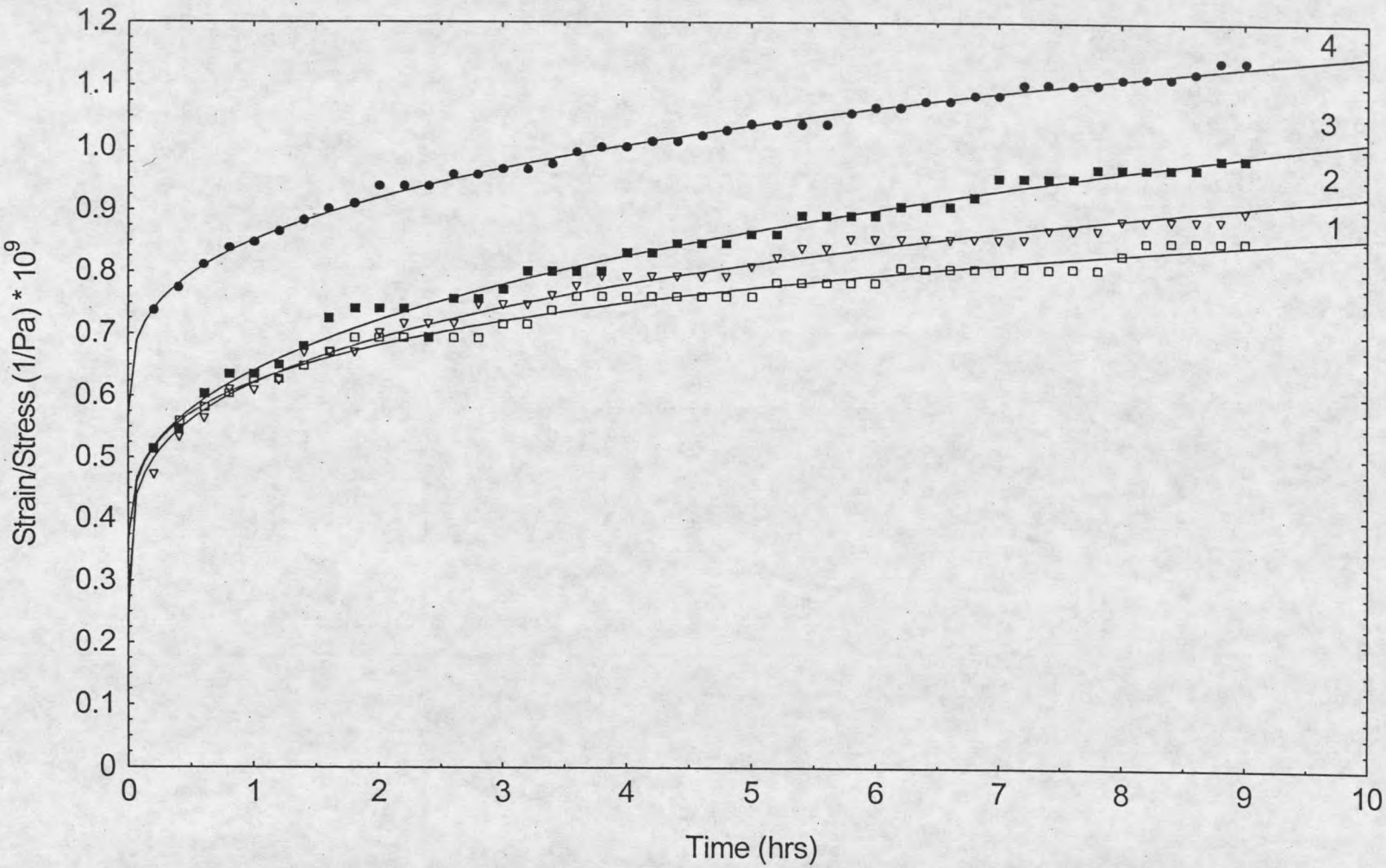


Figure A.II.3 Normalized Constant Load Creep of Nylon 6/6 at 35 °C
1- $(0.20)\sigma_y$; 2- $(0.30)\sigma_y$; 3- $(0.40)\sigma_y$; 4- $(0.50)\sigma_y$;
σ_y = 55 MPa at 35 °C

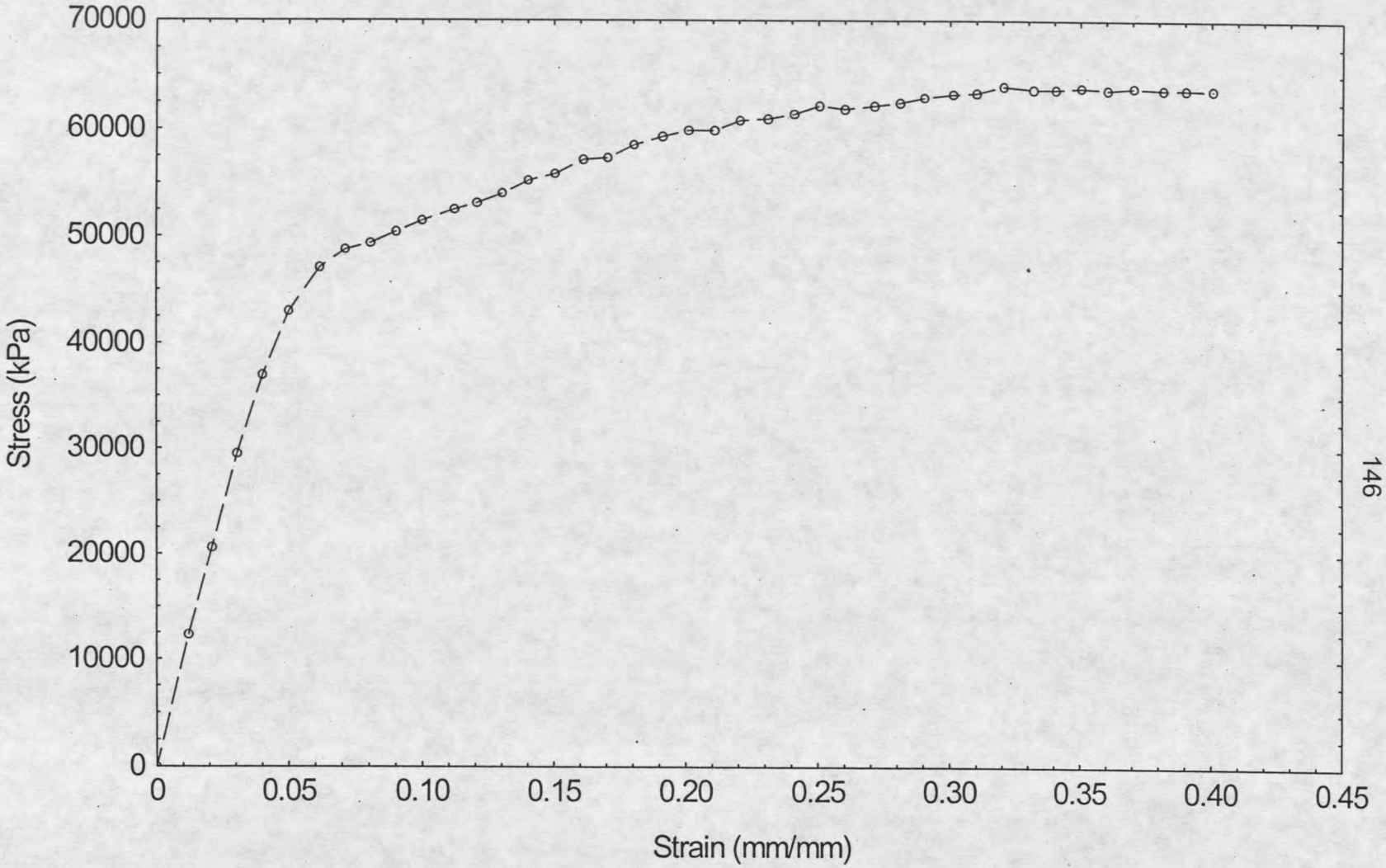


Figure A.III.1 Tensile Testing of Nylon 6/6 at 41 °C

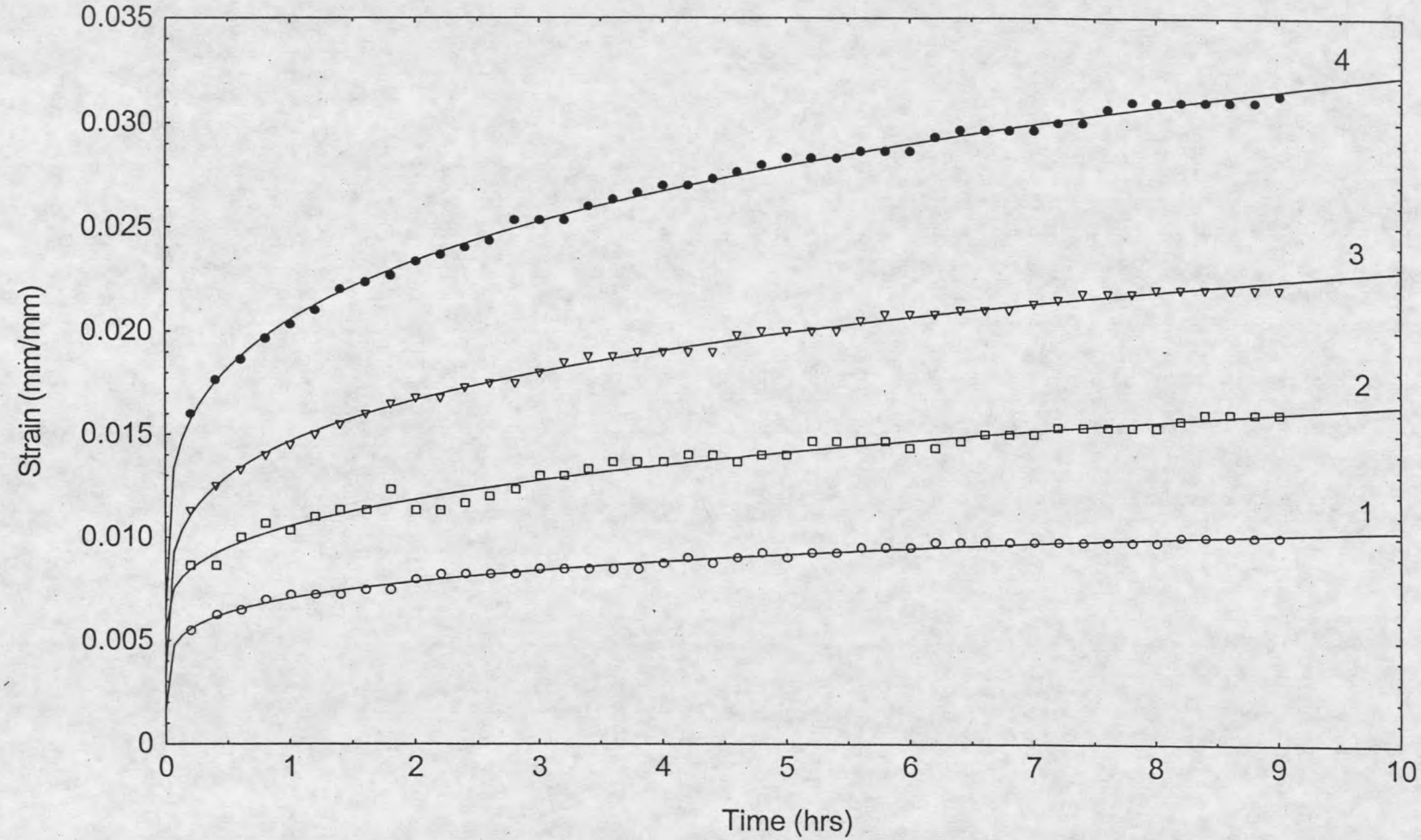


Figure A.III.2 Constant Load Creep of Nylon 6/6 at 41 °C
1- $(0.20)\sigma_y$; 2- $(0.30)\sigma_y$; 3- $(0.40)\sigma_y$; 4- $(0.50)\sigma_y$;.
σ_y = 45 MPa at 41 °C

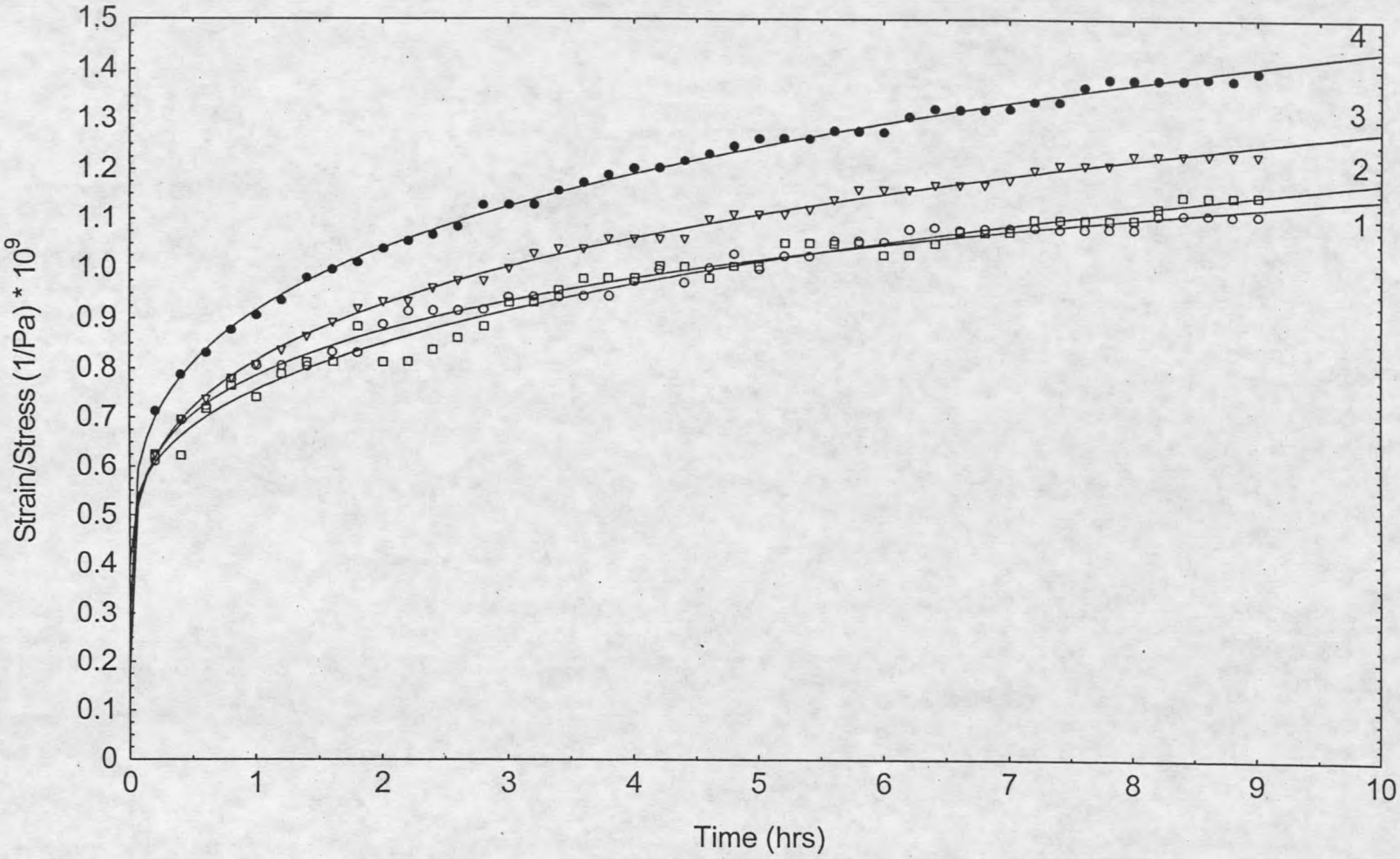


Figure A.III.3 Normalized Constant Load Creep of Nylon 6/6 at 41 °C
1- $(0.20)\sigma_y$; 2- $(0.30)\sigma_y$; 3- $(0.40)\sigma_y$; 4- $(0.50)\sigma_y$;
σ_y = 45 MPa at 41 °C

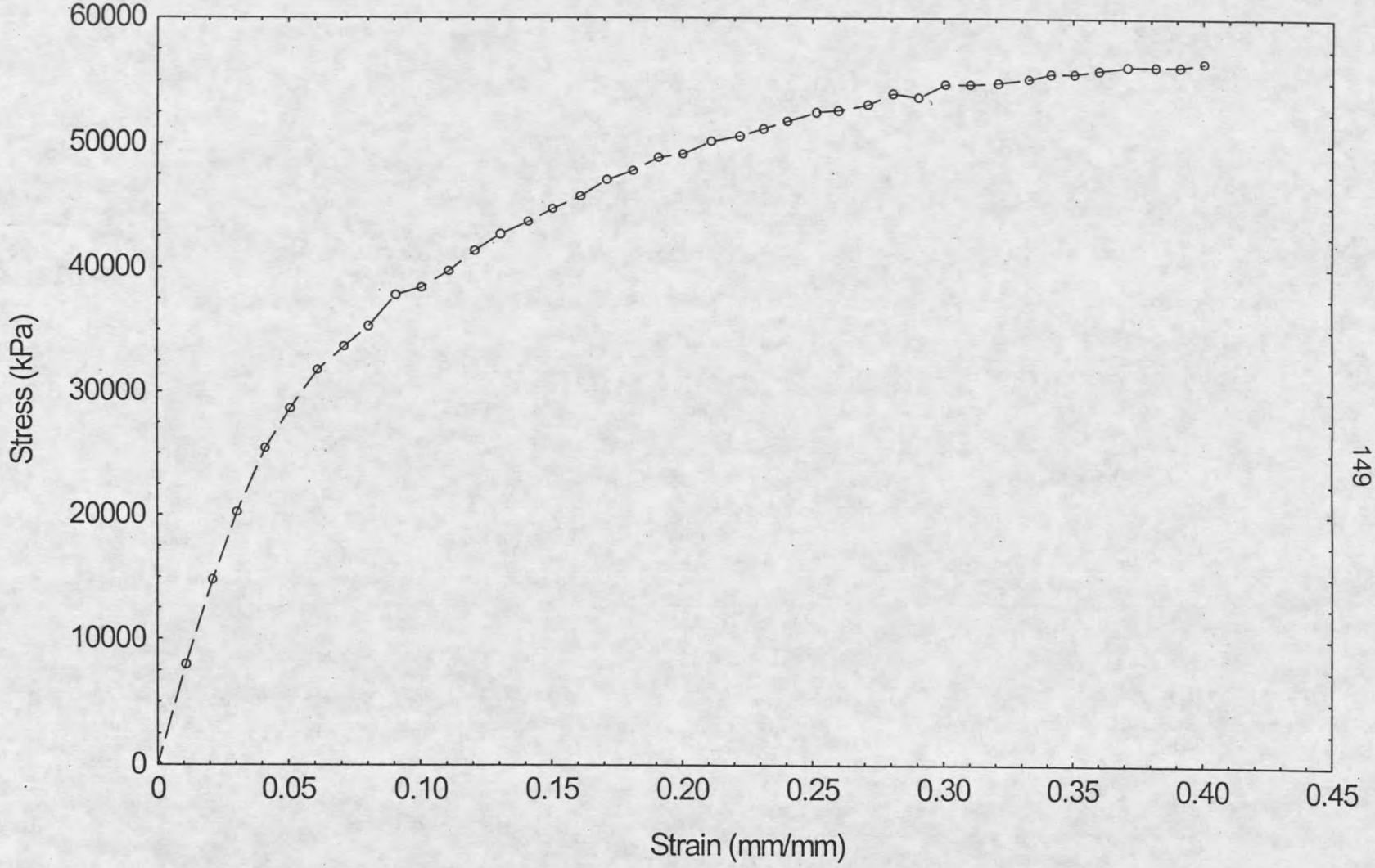


Figure A.IV.1 Tensile Testing of Nylon 6/6 at 50 °C

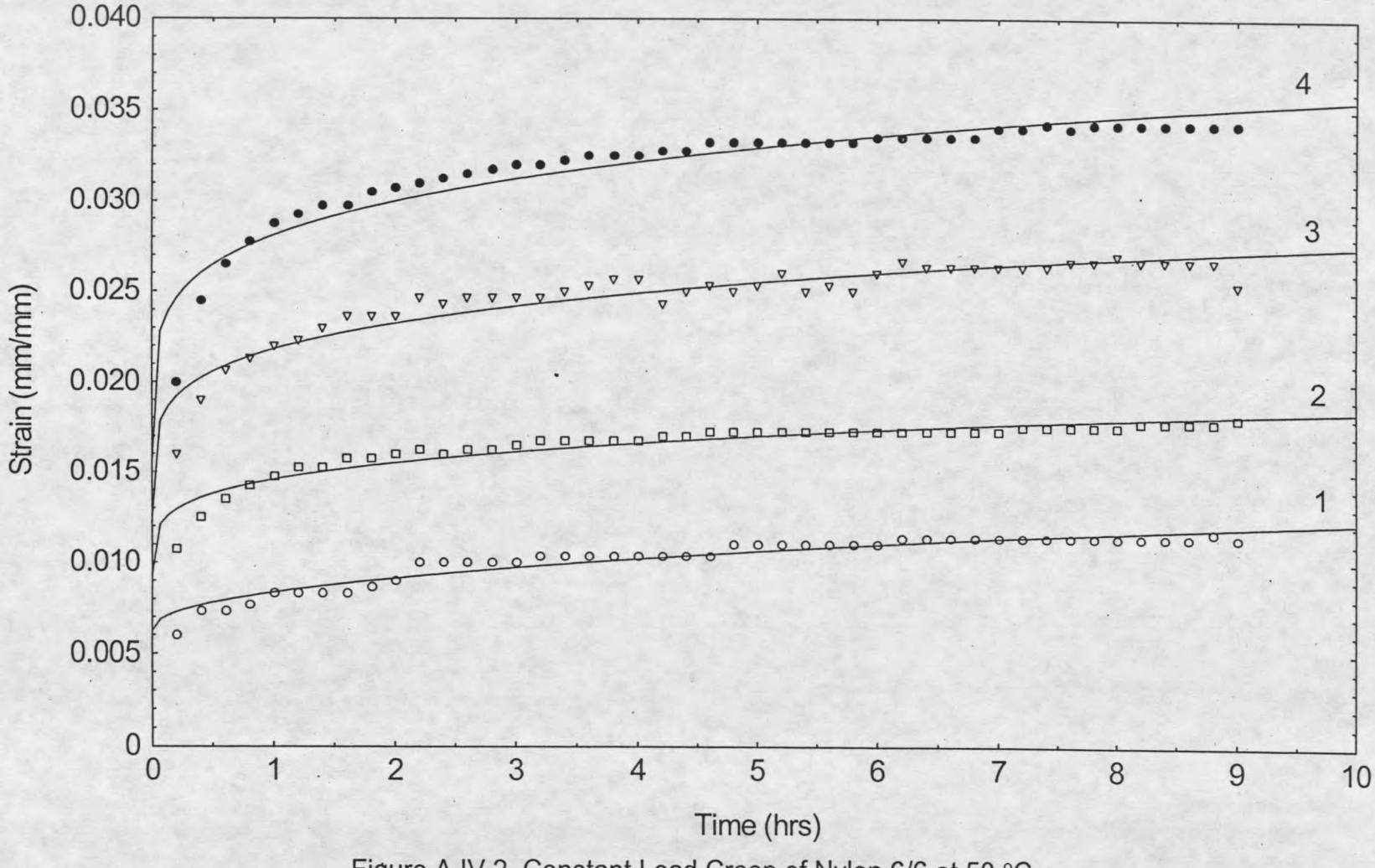


Figure A.IV.2 Constant Load Creep of Nylon 6/6 at 50 °C
1- $(0.20)\sigma_y$; 2- $(0.30)\sigma_y$; 3- $(0.40)\sigma_y$; 4- $(0.50)\sigma_y$;
σ_y = 22 MPa at 50 °C

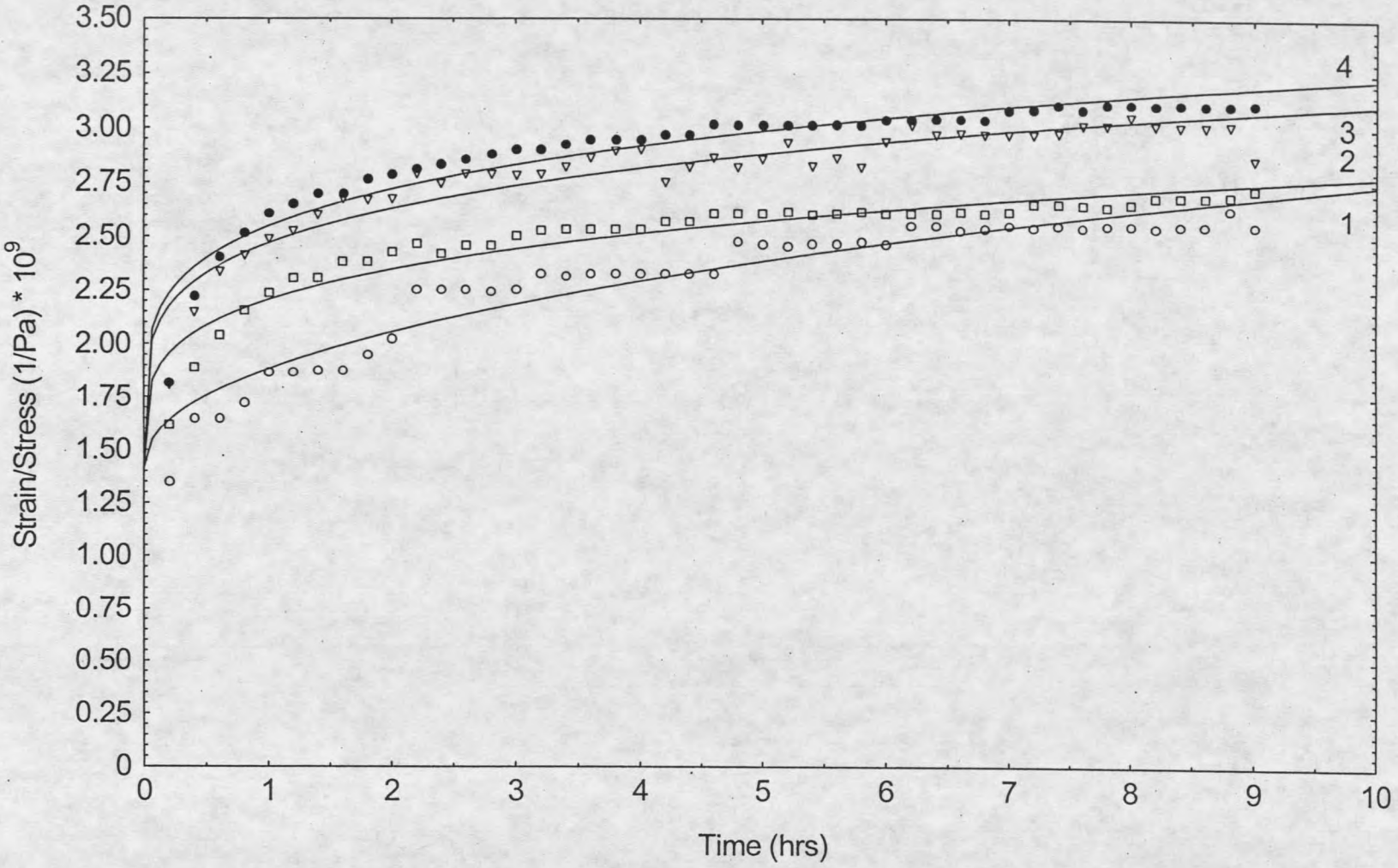


Figure A.IV.3 Normalized Constant Load Creep of Nylon 6/6 at 50 °C
1- $(0.20)\sigma_y$; 2- $(0.30)\sigma_y$; 3- $(0.40)\sigma_y$; 4- $(0.50)\sigma_y$;
σ_y = 22 MPa at 50 °C

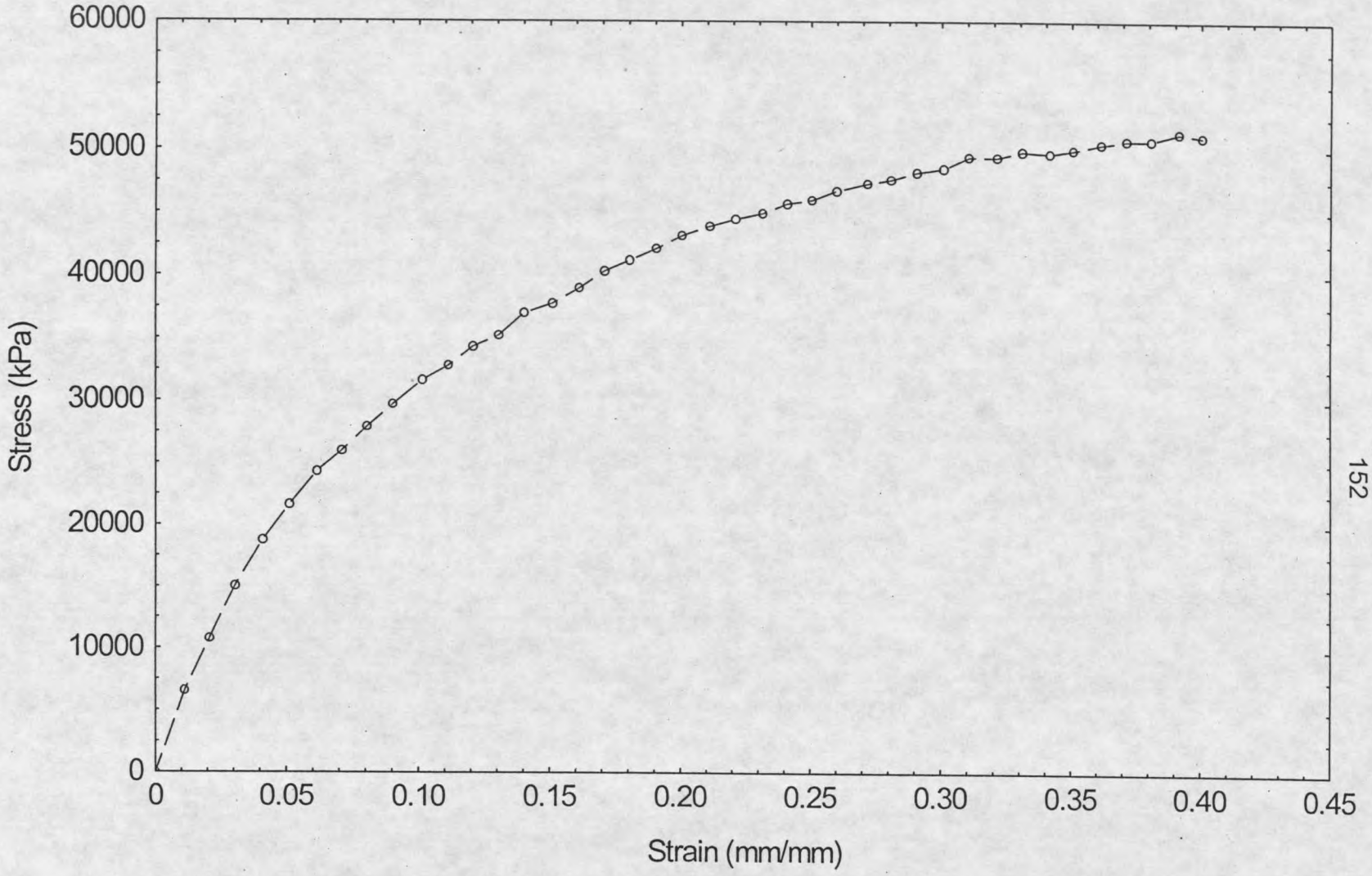


Figure A.V.1 Tensile Testing of Nylon 6/6 at 59 °C

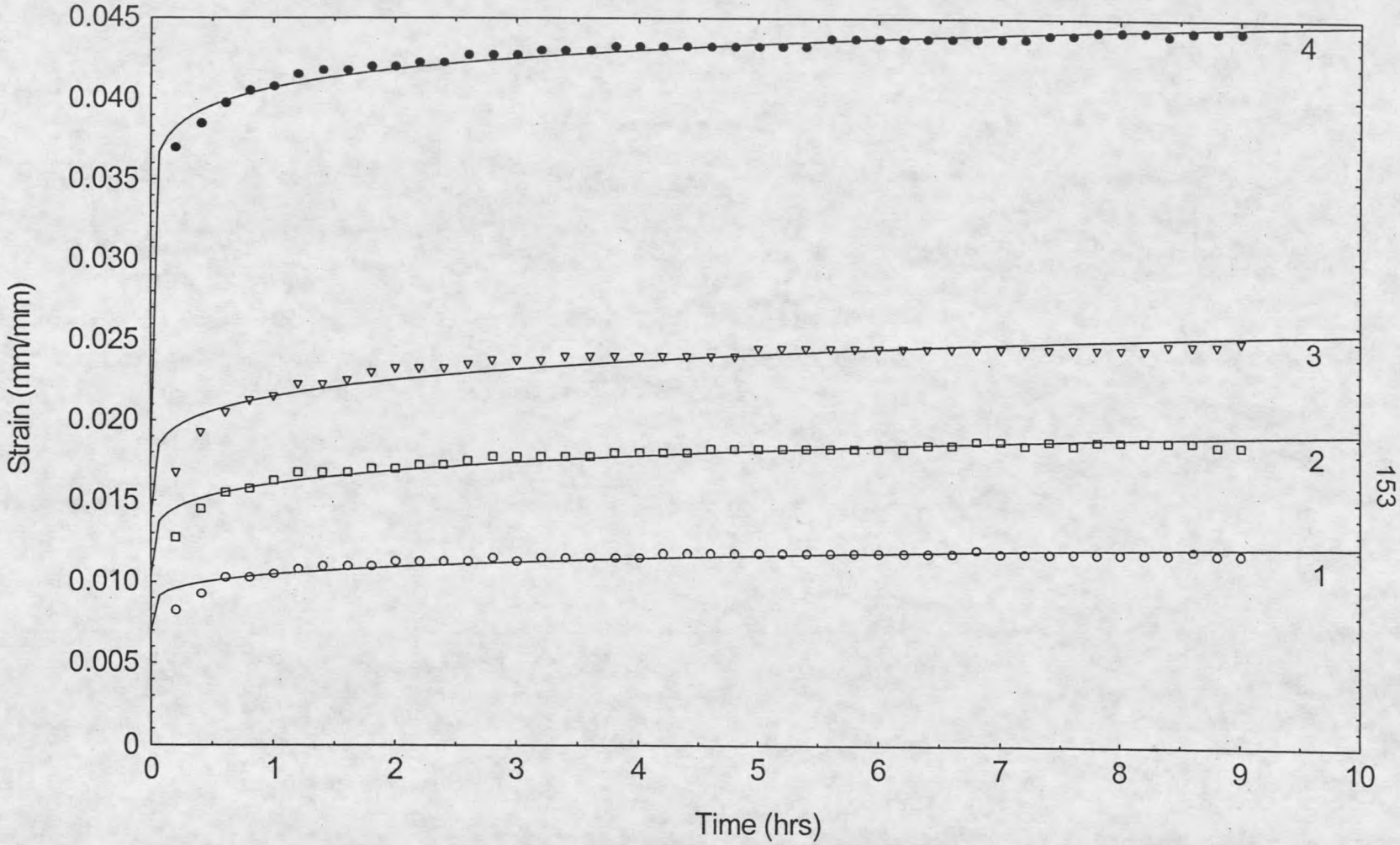


Figure A.V.2 Constant Load Creep of Nylon 6/6 at 59 °C
1- $(0.20)\sigma_y$; 2- $(0.30)\sigma_y$; 3- $(0.40)\sigma_y$; 4- $(0.50)\sigma_y$;
σ_y = 19 MPa at 59 °C

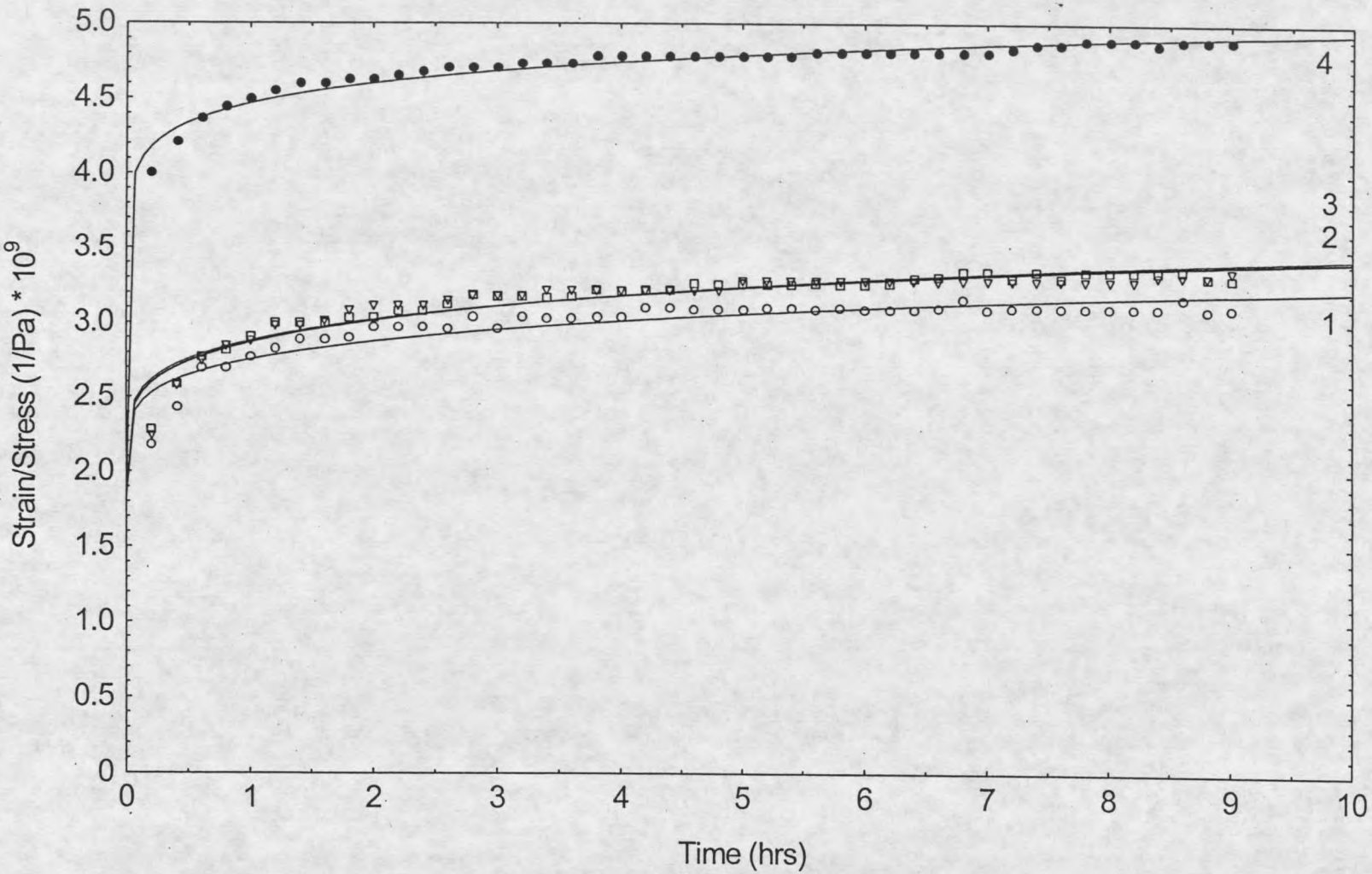


Figure A.V.3 Normalized Constant Load Creep of Nylon 6/6 at 59 °C
1- $(0.20)\sigma_y$; 2- $(0.30)\sigma_y$; 3- $(0.40)\sigma_y$; 4- $(0.50)\sigma_y$;
σ_y = 19 MPa at 59 °C

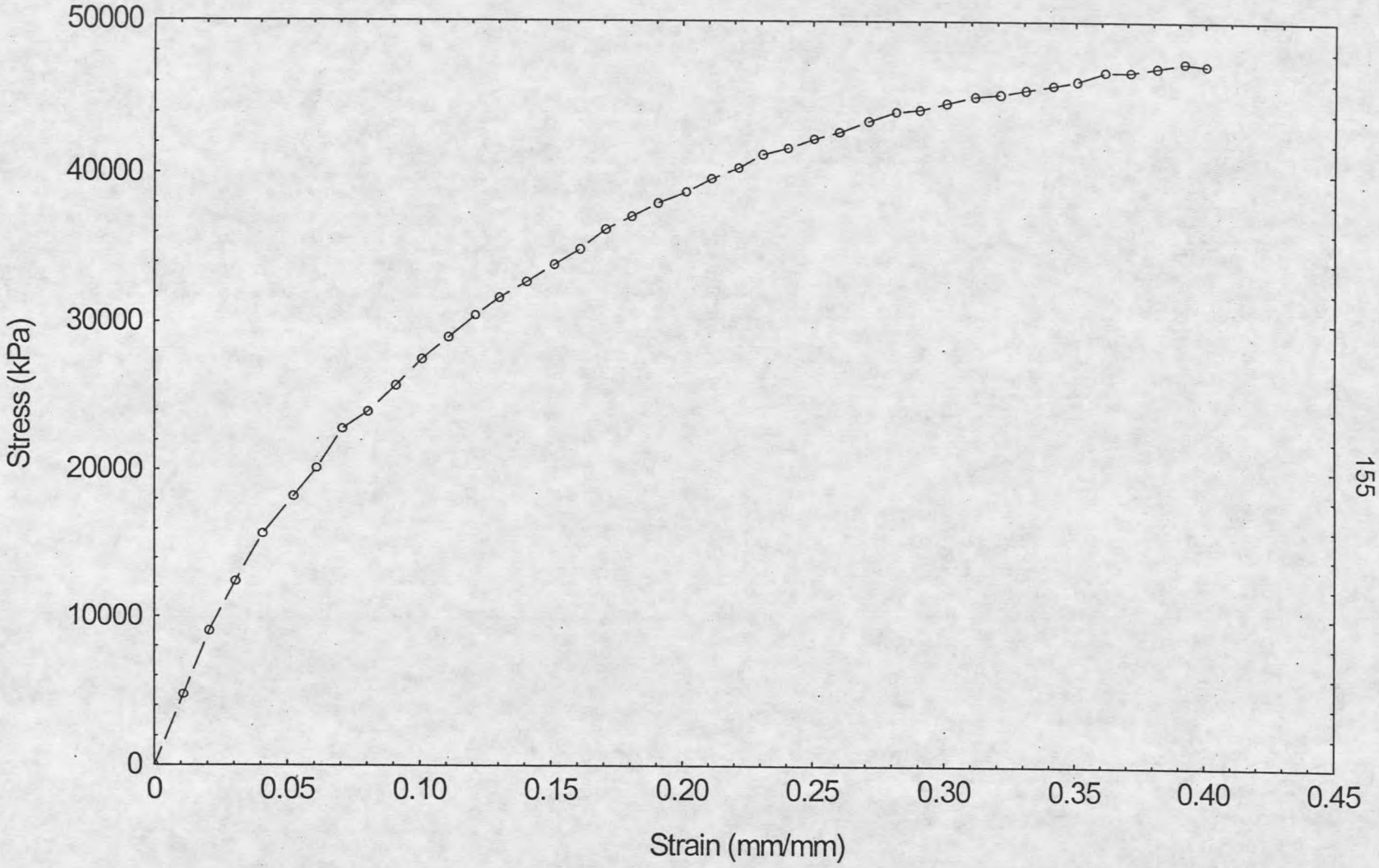


Figure A.VI.1 Tensile Testing of Nylon 6/6 at 68 °C

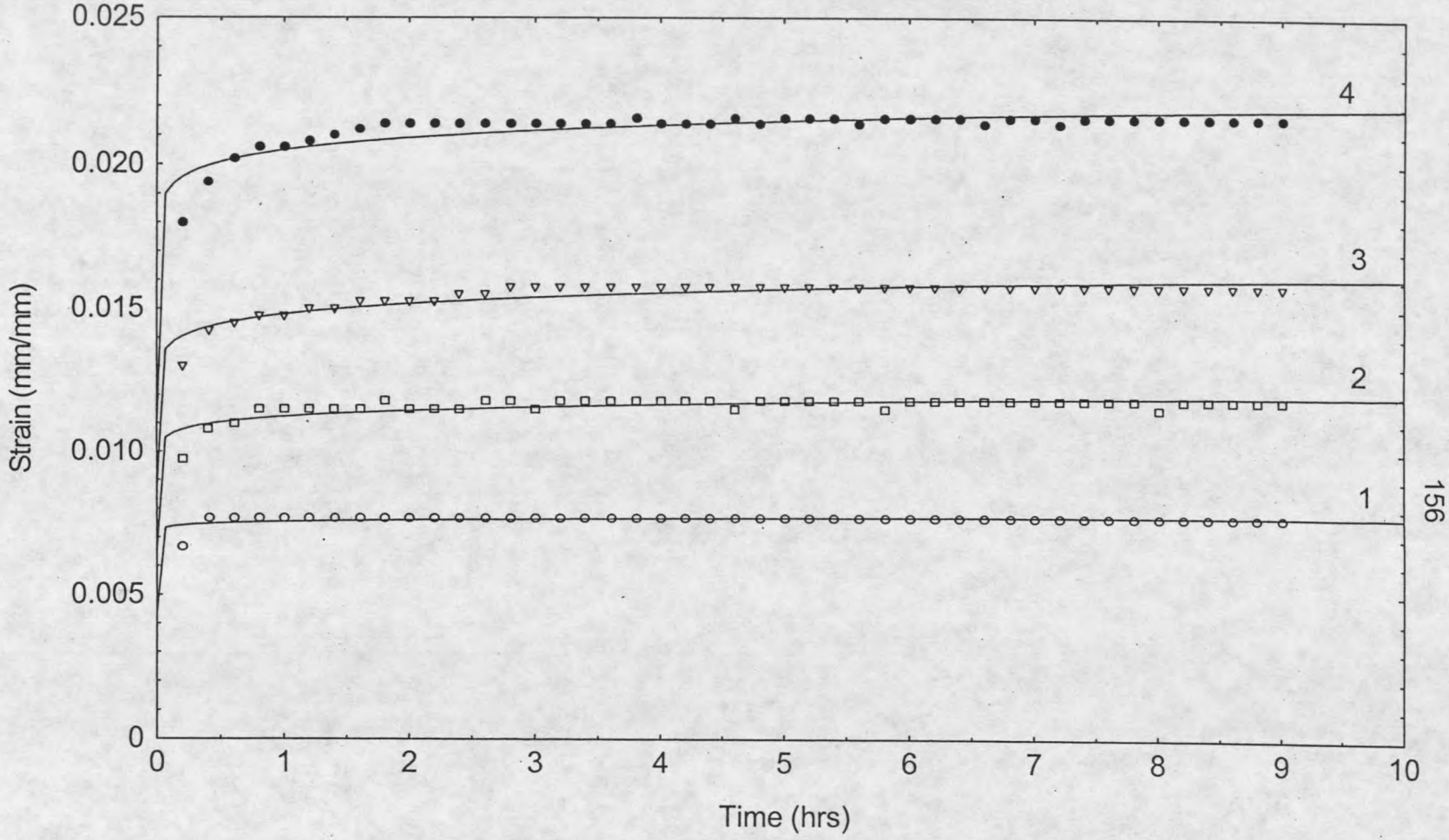


Figure A.VI.2 Constant Load Creep of Nylon 6/6 at 68 °C
1- $(0.20)\sigma_y$; 2- $(0.30)\sigma_y$; 3- $(0.40)\sigma_y$; 4- $(0.50)\sigma_y$;
σ_y = 10 MPa at 68 °C

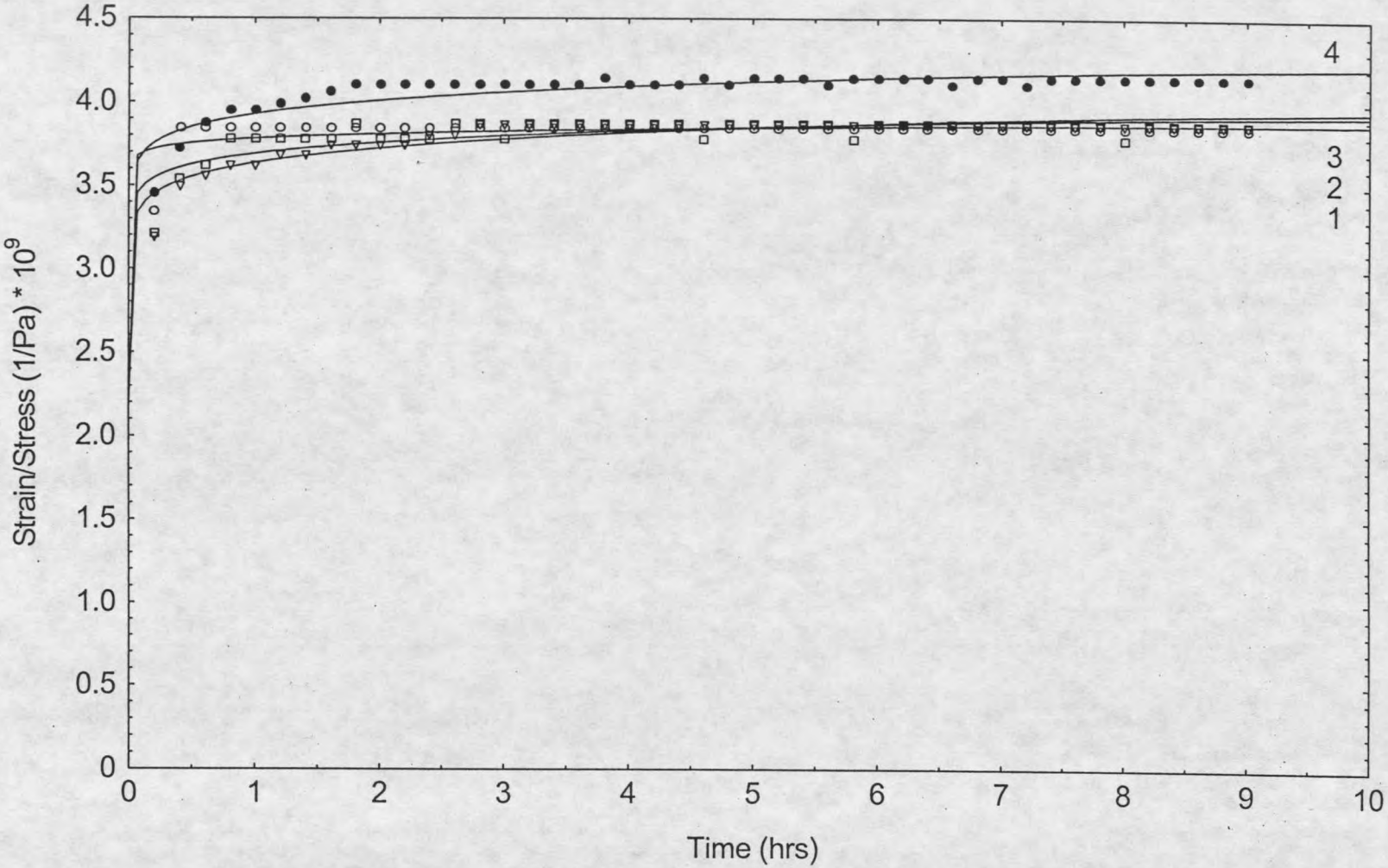


Figure A.VI.3 Normalized Constant Load Creep of Nylon 6/6 at 68 °C
1- $(0.20)\sigma_y$; 2- $(0.30)\sigma_y$; 3- $(0.40)\sigma_y$; 4- $(0.50)\sigma_y$;
σ_y = 10 MPa at 68 °C

APPENDIX B

Frequency Effects from Vibrocreep Testing of Nylon 6/6

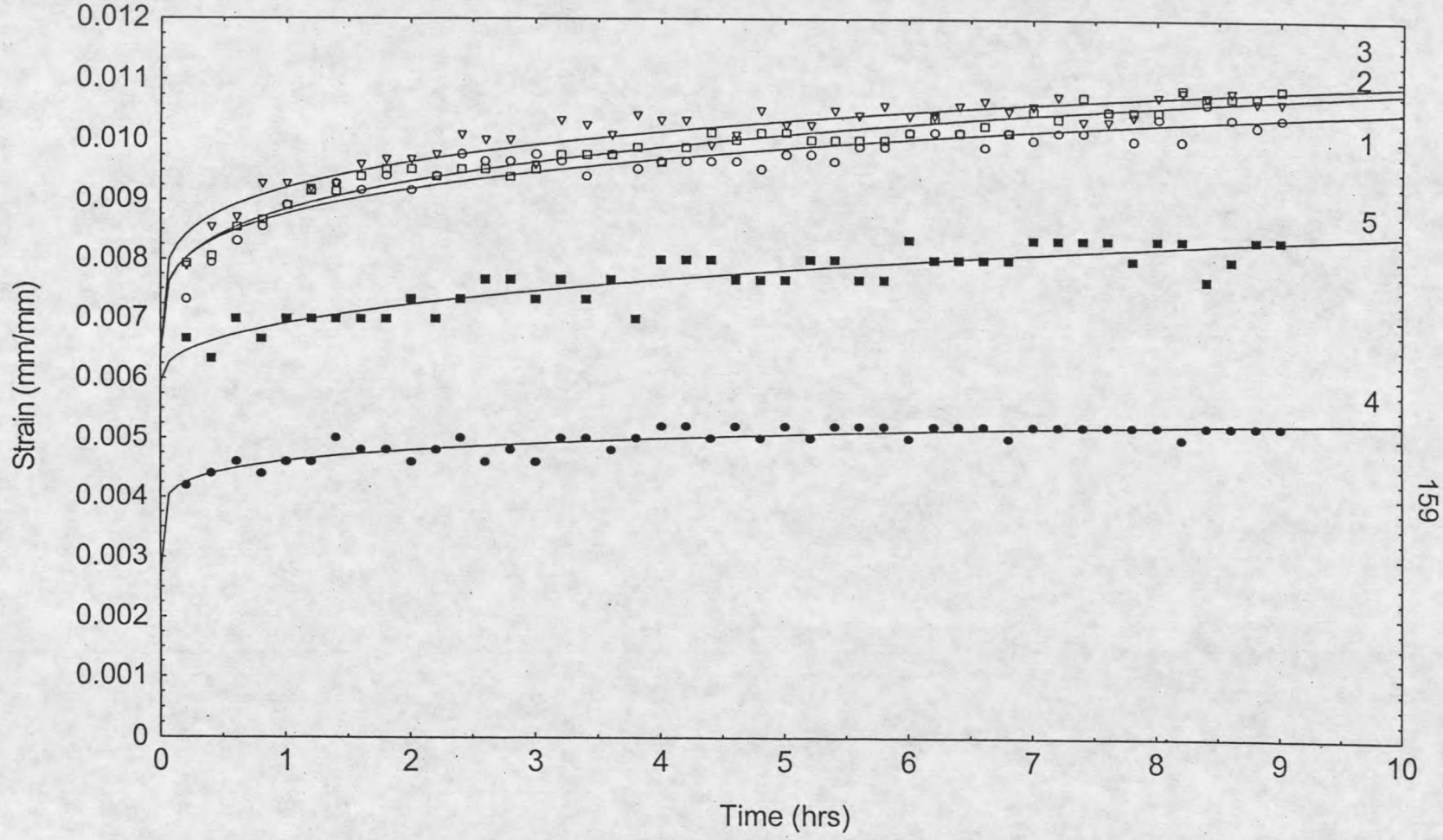


Figure B.I.1 Vibrocreep Response of Nylon 6/6 at Different Frequencies at 23 °C
1- $(0.12\pm0.04)\sigma_y$, 1 Hz; 2- $(0.12\pm0.04)\sigma_y$, 10 Hz; 3- $(0.12\pm0.04)\sigma_y$, 20 Hz;
4- $(0.10)\sigma_y$, 5- $(0.16)\sigma_y$, Constant Load Creep;
σ_y = 70 MPa at 23 °C

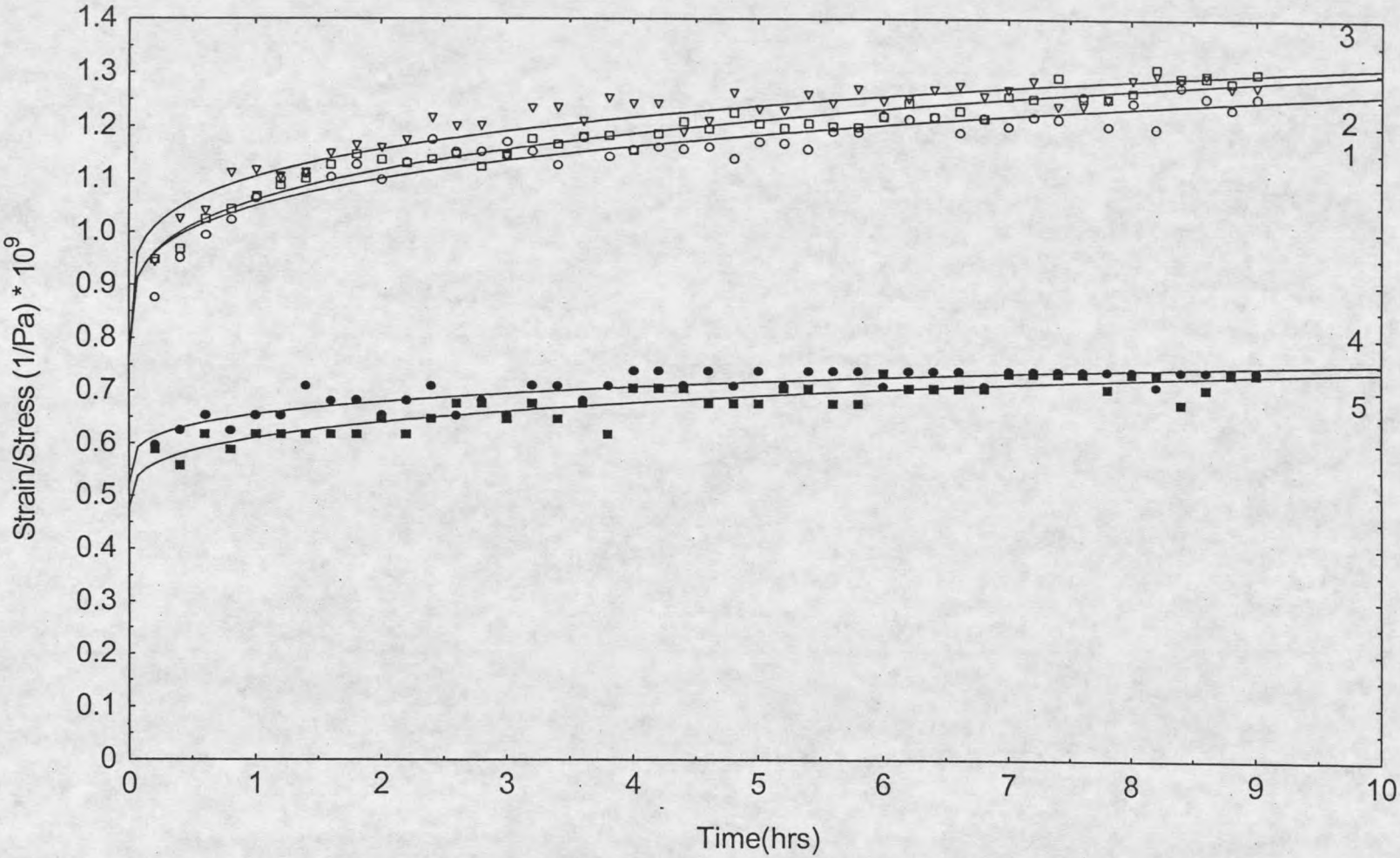


Figure B.I.2 Normalized Vibrocreep Response of Nylon 6/6 at Different Frequencies at 23 °C
1- $(0.12\pm0.04)\sigma_y$, 1 Hz; 2- $(0.12\pm0.04)\sigma_y$, 10 Hz; 3- $(0.12\pm0.04)\sigma_y$, 20 Hz;
4- $(0.10)\sigma_y$, 5- $(0.16)\sigma_y$, Constant Load Creep;
σ_y = 70 MPa at 23 °C

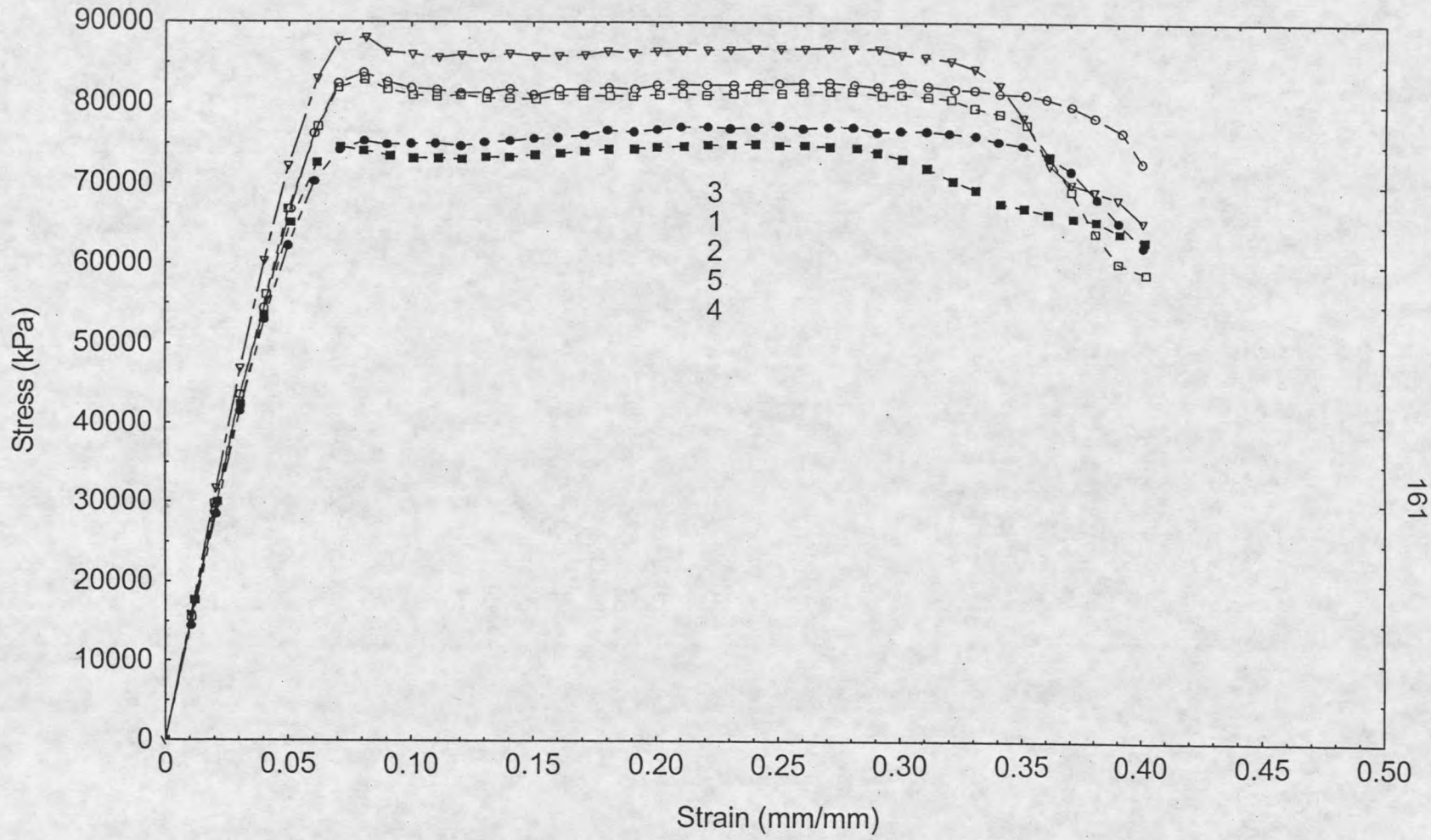


Figure B.I.3 Tensile Testing of Nylon 6/6 Specimens After Cyclic and Constant Loading at 23 °C
1- $(0.12\pm0.04)\sigma_y$, 1 Hz; 2- $(0.12\pm0.04)\sigma_y$, 10 Hz; 3- $(0.12\pm0.04)\sigma_y$, 20 Hz;
4- $(0.16)\sigma_y$, Constant Load Creep; 5- Virgin Specimens;
σ_y = 70 MPa at 23 °C

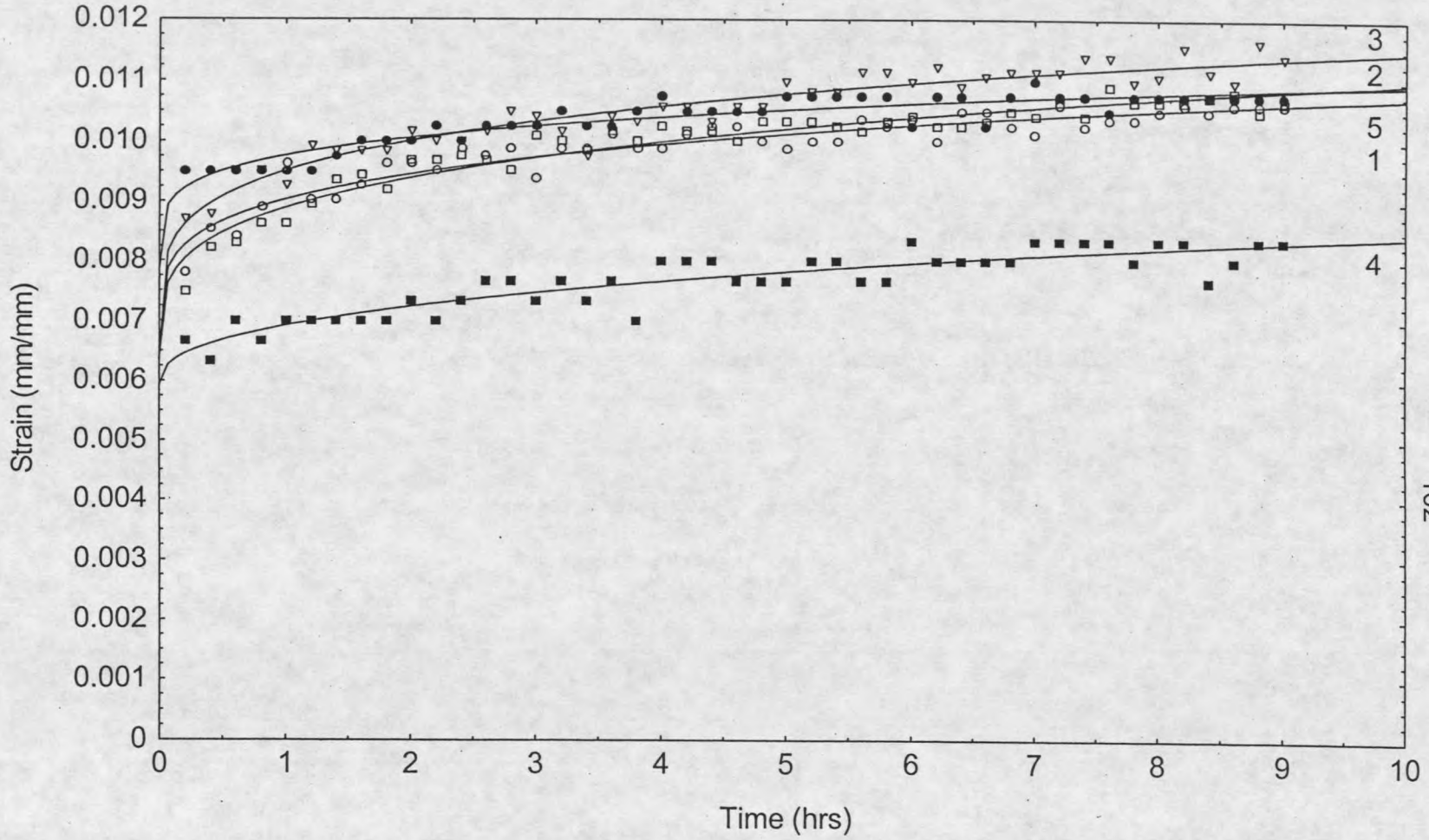


Figure B.I.4 Vibrocreep Response of Nylon 6/6 at Different Frequencies at 23 °C
1- $(0.12\pm0.075)\sigma_y$, 1 Hz; 2- $(0.12\pm0.075)\sigma_y$, 10 Hz; 3- $(0.12\pm0.075)\sigma_y$, 20 Hz;
4- $(0.16)\sigma_y$, 5- $(0.20)\sigma_y$, Constant Load Creep;
σ_y = 70 MPa at 23 °C

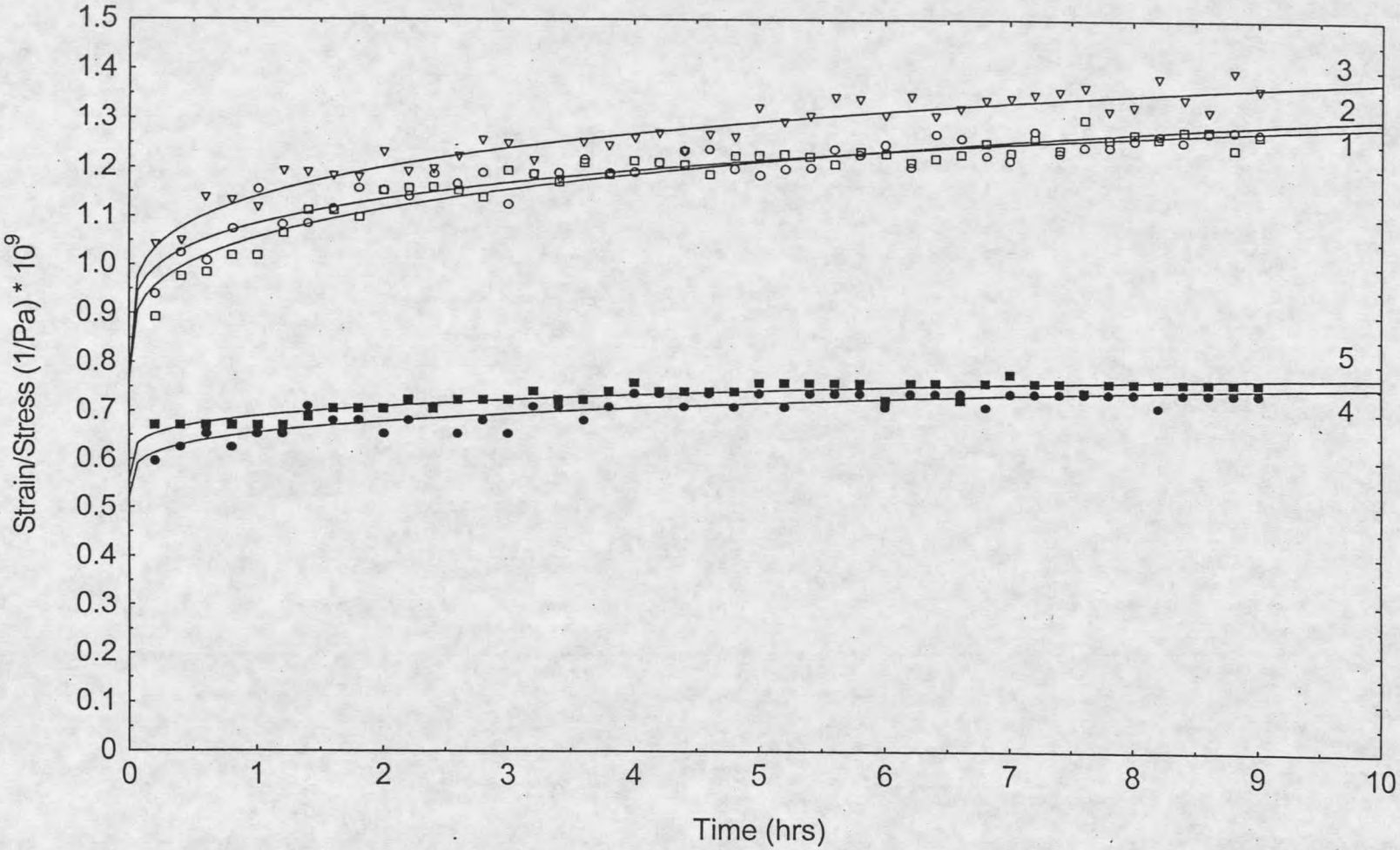


Figure B.I.5 Normalized Vibrocreep Response of Nylon 6/6 at Different Frequencies at 23 °C
1- $(0.12\pm0.075)\sigma_y$, 1 Hz; 2- $(0.12\pm0.075)\sigma_y$, 10 Hz; 3- $(0.12\pm0.075)\sigma_y$, 20 Hz;
4- $(0.16)\sigma_y$, 5- $(0.20)\sigma_y$, Constant Load Creep;
σ_y = 70 MPa at 23 °C

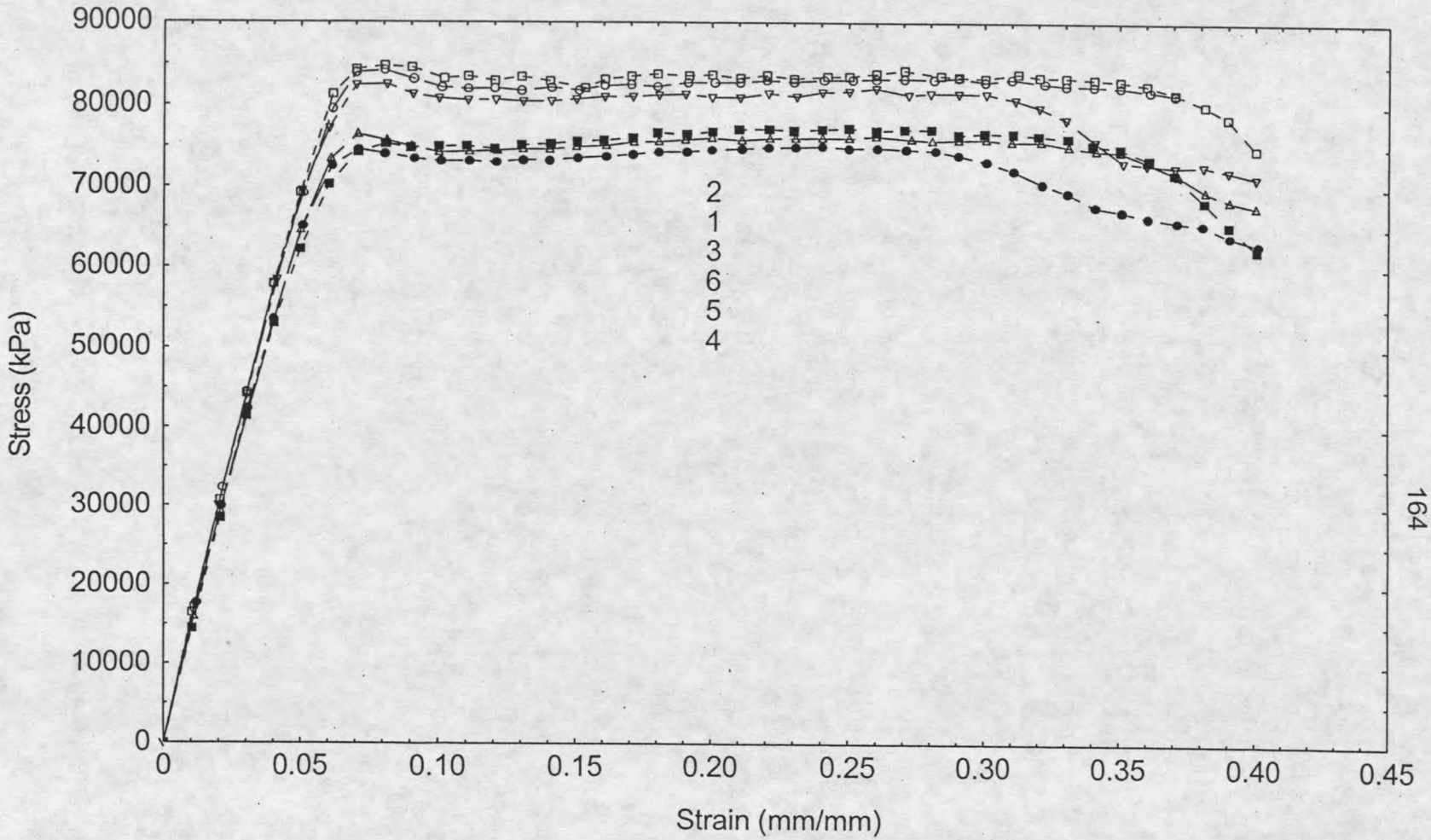


Figure B.I.6 Tensile Testing of Nylon 6/6 Specimens After Cyclic and Constant Loading at 23 °C
1- $(0.12\pm0.075)\sigma_y$, 1 Hz; 2- $(0.12\pm0.075)\sigma_y$, 10 Hz; 3- $(0.12\pm0.075)\sigma_y$, 20 Hz;
4- $(0.16)\sigma_y$, 5- $(0.20)\sigma_y$, Constant Load Creep; 6- Virgin Specimens;
σ_y = 70 MPa at 23 °C

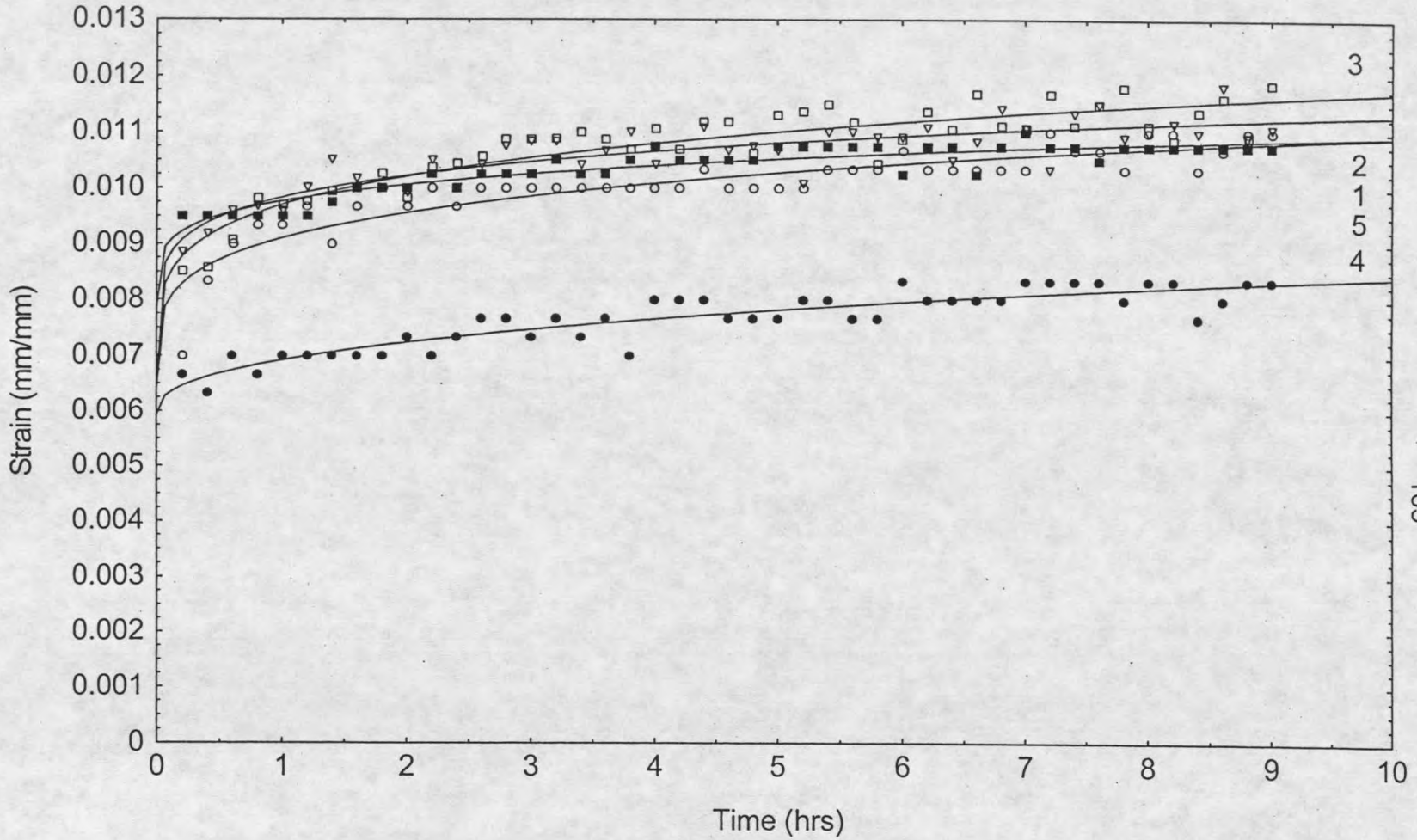


Figure B.I.7 Vibrocreep Response of Nylon 6/6 at Different Frequencies at 23 °C
1- $(0.12\pm0.10)\sigma_y$, 1 Hz; 2- $(0.12\pm0.10)\sigma_y$, 10 Hz; 3- $(0.12\pm0.10)\sigma_y$, 20 Hz;
4- $(0.16)\sigma_y$, 5- $(0.20)\sigma_y$, Constant Load Creep;
σ_y = 70 MPa at 23 °C

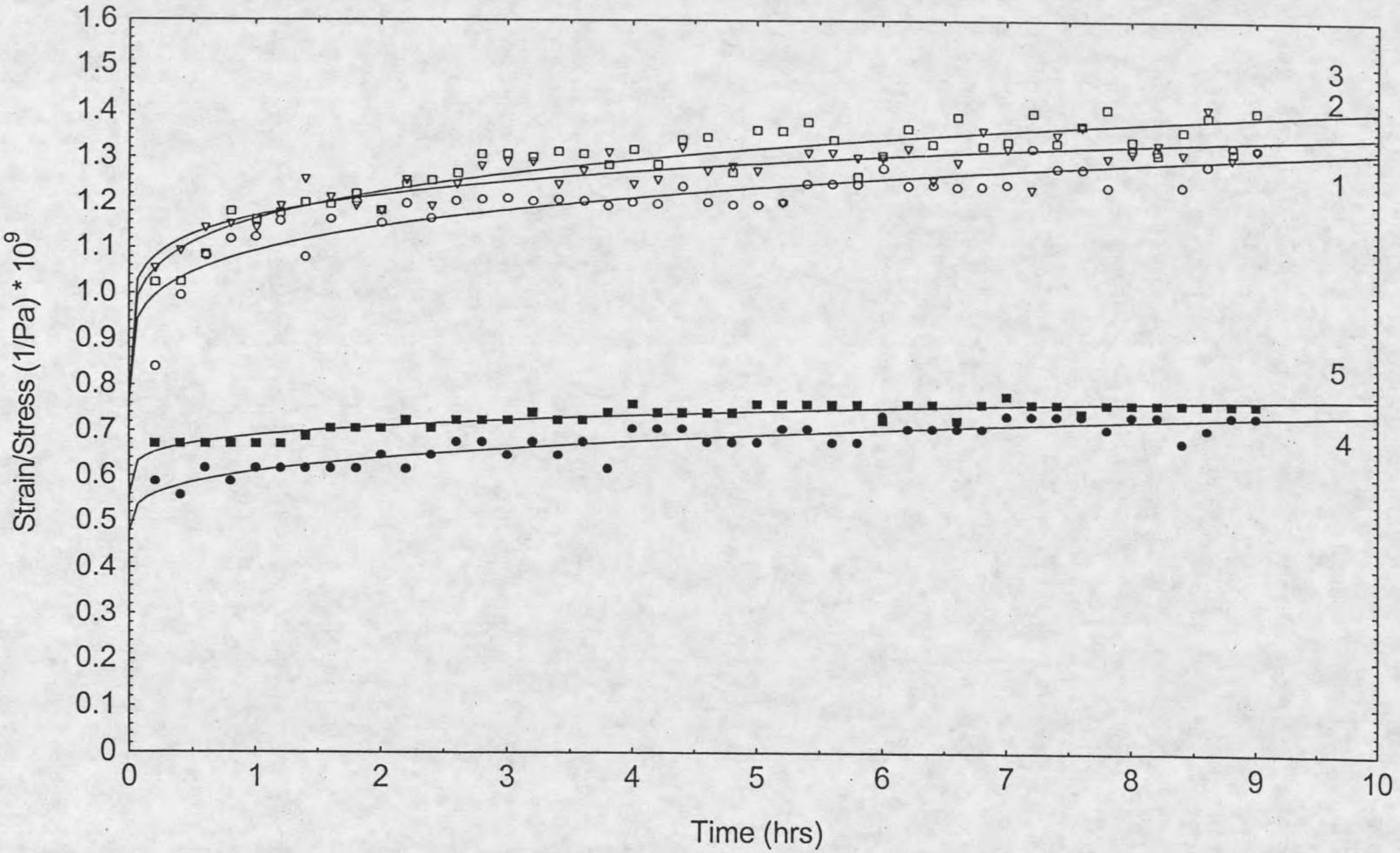


Figure B.I.8 Normalized Vibrocreep Response of Nylon 6/6 at Different Frequencies at 23 °C
1- $(0.12\pm0.10)\sigma_y$, 1 Hz; 2- $(0.12\pm0.10)\sigma_y$, 10 Hz; 3- $(0.12\pm0.10)\sigma_y$, 20 Hz;
4- $(0.16)\sigma_y$, 5- $(0.20)\sigma_y$, Constant Load Creep;
σ_y = 70 MPa at 23 °C

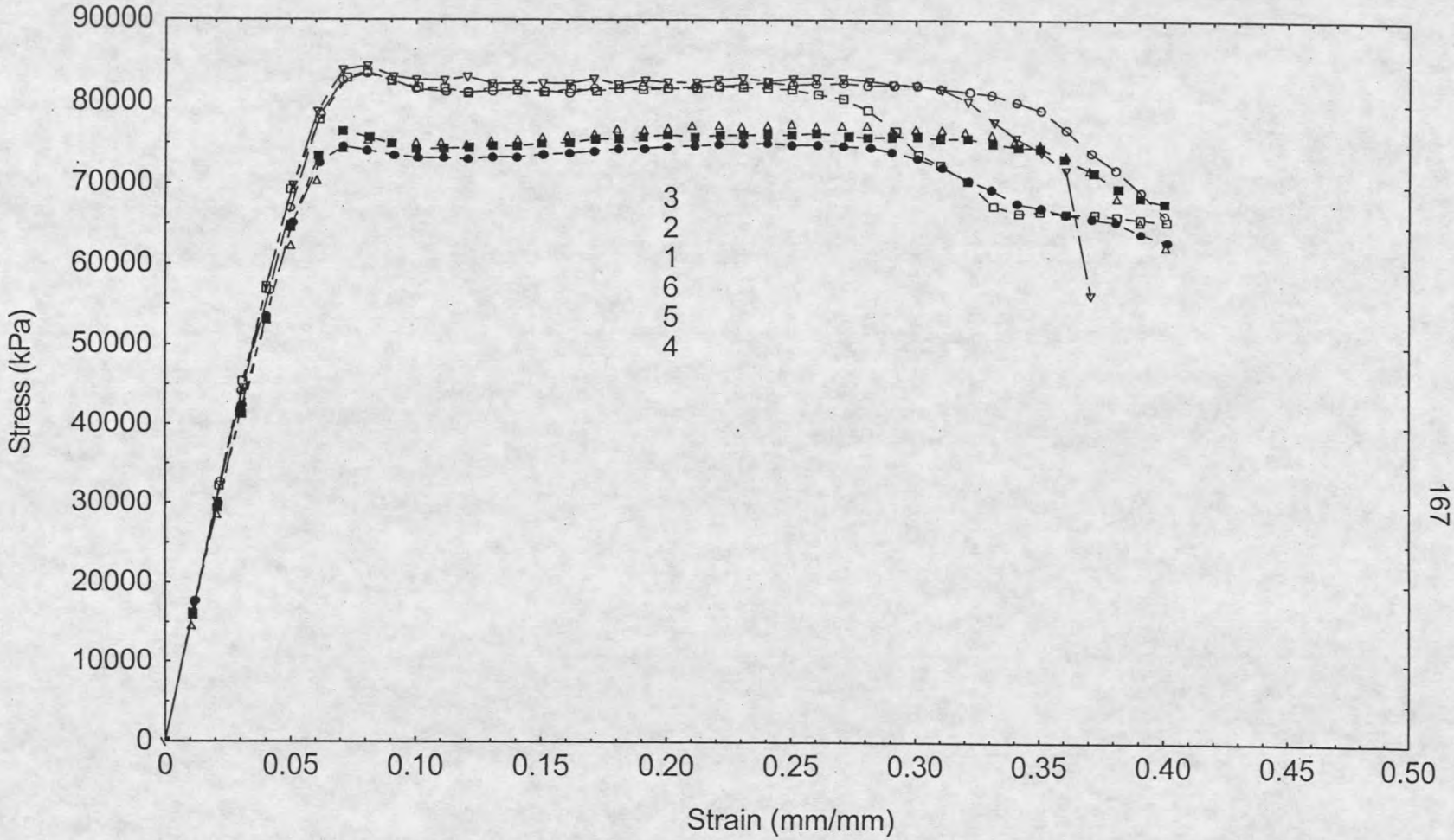


Figure B.I.9 Tensile Testing of Nylon 6/6 Specimens After Cyclic and Constant Loading at 23 °C
1- $(0.12\pm0.10)\sigma_y$, 1 Hz; 2- $(0.12\pm0.10)\sigma_y$, 10 Hz; 3- $(0.12\pm0.10)\sigma_y$, 20 Hz;
4- $(0.16)\sigma_y$, 5- $(0.20)\sigma_y$, Constant Load Creep; 6- Virgin Specimens;
σ_y = 70 MPa at 23 °C

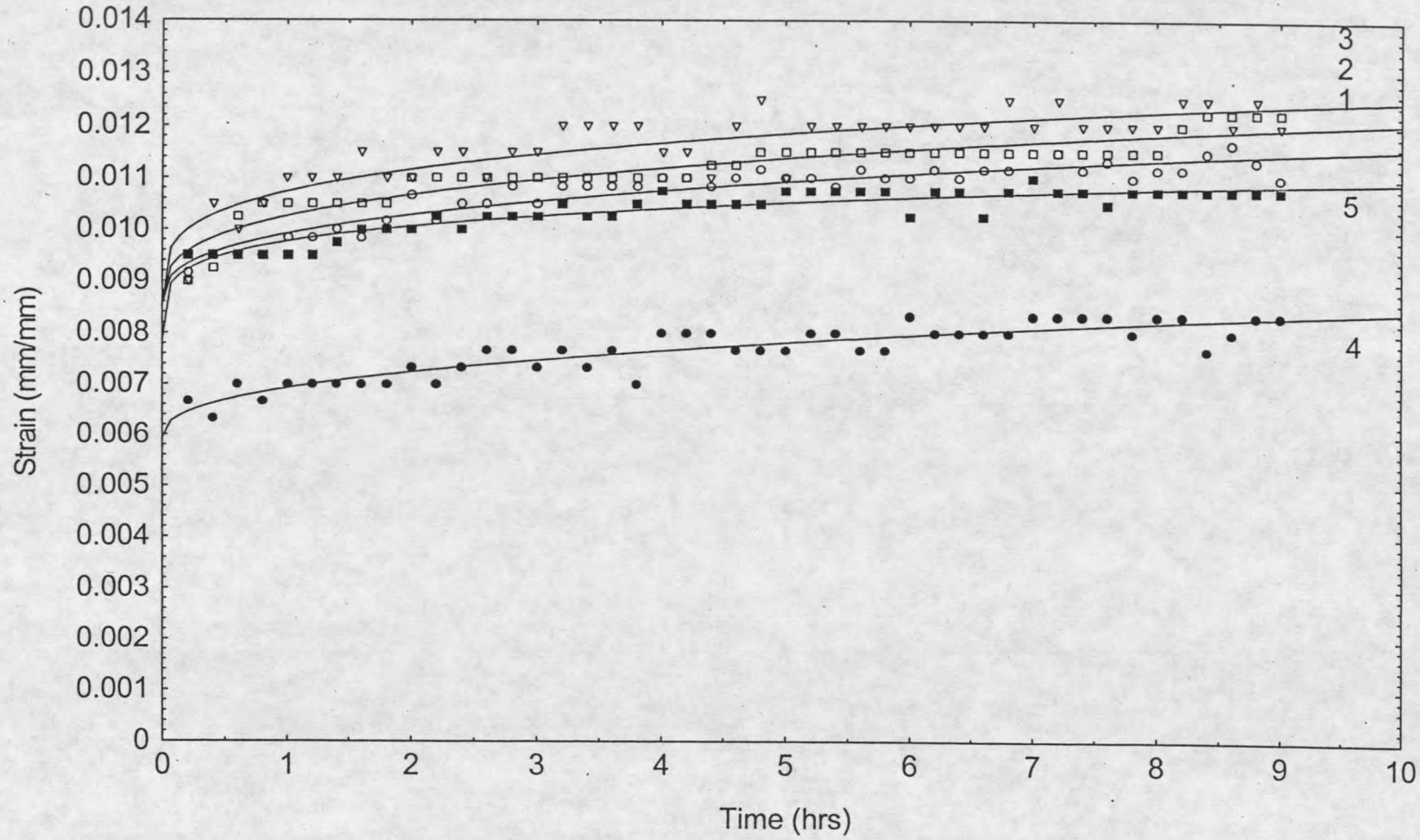


Figure B.I.10 Vibrocreep Response of Nylon 6/6 at Different Frequencies at 23 °C
1- $(0.16\pm0.04)\sigma_y$, 1 Hz; 2- $(0.16\pm0.04)\sigma_y$, 10 Hz; 3- $(0.16\pm0.04)\sigma_y$, 20 Hz;
4- $(0.16)\sigma_y$, 5- $(0.20)\sigma_y$, Constant Load Creep;
σ_y = 70 MPa at 23 °C

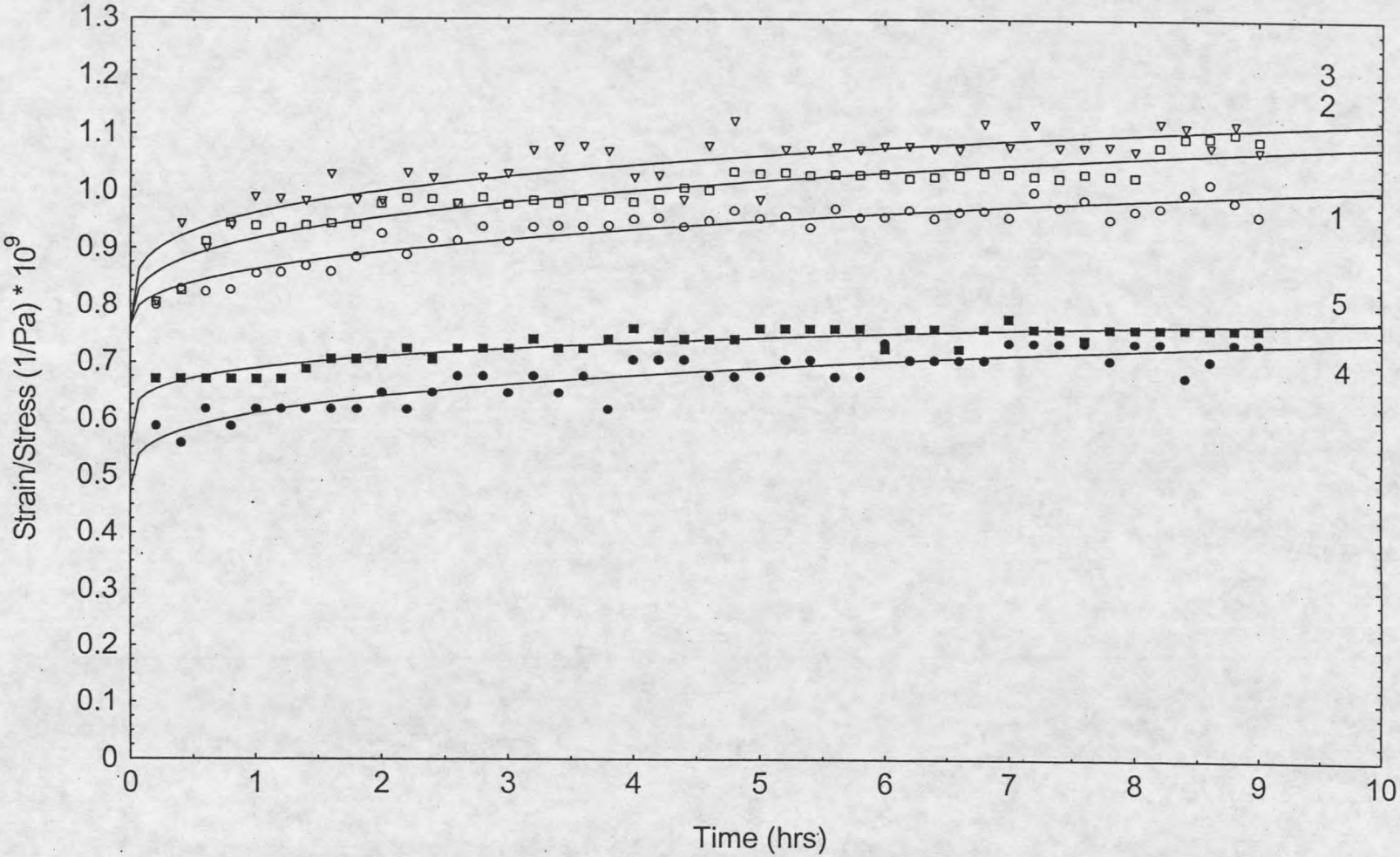


Figure B.I.11 Normalized Vibrocreep Response of Nylon 6/6 at Different Frequencies at 23 °C
1- $(0.16\pm0.04)\sigma_y$, 1 Hz; 2- $(0.16\pm0.04)\sigma_y$, 10 Hz; 3- $(0.16\pm0.04)\sigma_y$, 20 Hz;
4- $(0.16)\sigma_y$, 5- $(0.20)\sigma_y$, Constant Load Creep;
σ_y = 70 MPa at 23 °C

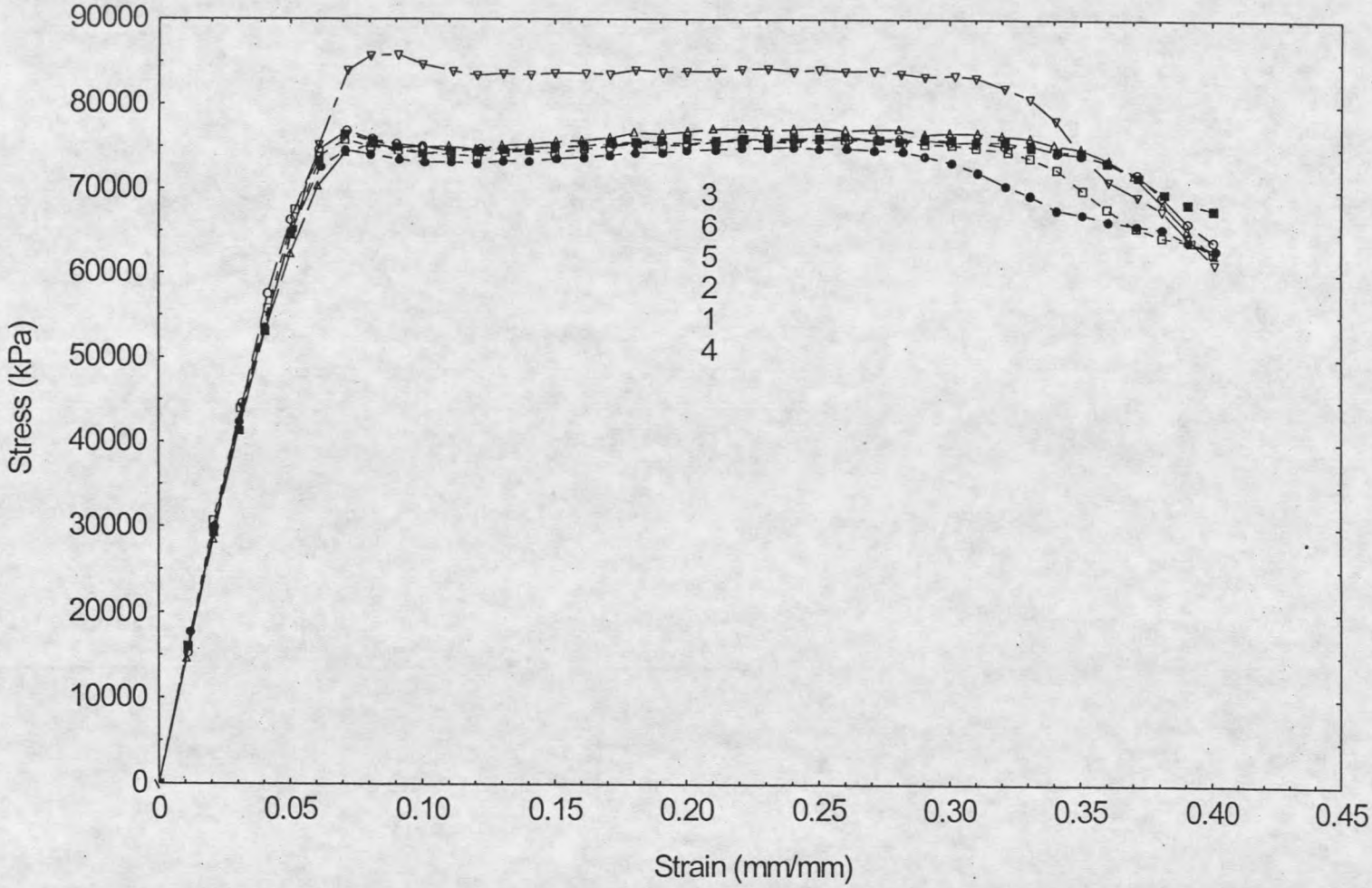


Figure B.I.12 Tensile Testing of Nylon 6/6 Specimens After Cyclic and Constant Loading at 23 °C
1- $(0.16\pm0.04)\sigma_y$, 1 Hz; 2- $(0.16\pm0.04)\sigma_y$, 10 Hz; 3- $(0.16\pm0.04)\sigma_y$, 20 Hz;
4- $(0.16)\sigma_y$, 5- $(0.20)\sigma_y$, Constant Load Creep; 6- Virgin Specimens;
σ_y = 70 MPa at 23 °C

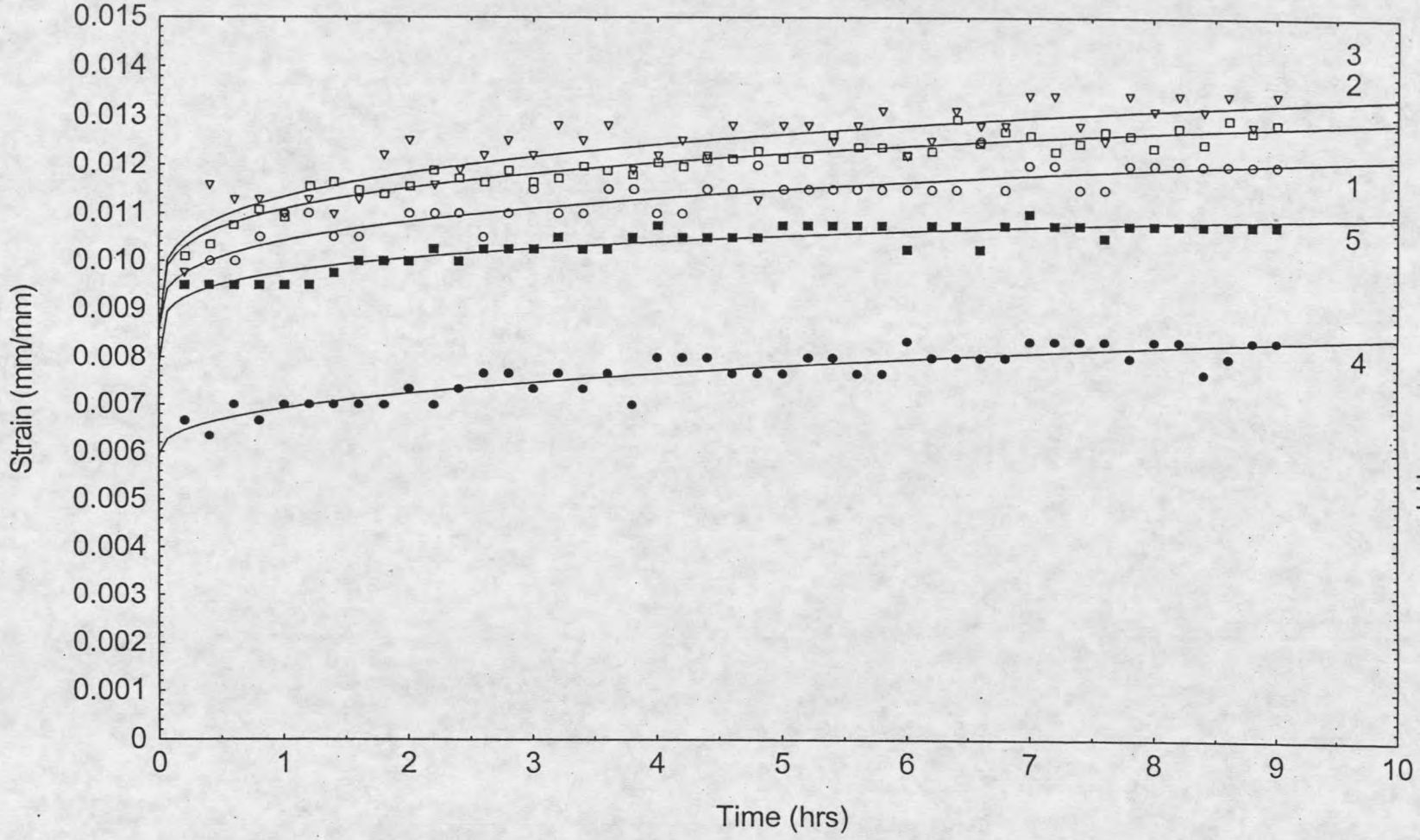


Figure B.I.13 Vibrocreep Response of Nylon 6/6 at Different Frequencies at 23 °C
1- $(0.16\pm0.075)\sigma_y$, 1 Hz; 2- $(0.16\pm0.075)\sigma_y$, 10 Hz; 3- $(0.16\pm0.075)\sigma_y$, 20 Hz;
4- $(0.16)\sigma_y$, 5- $(0.20)\sigma_y$, Constant Load Creep;
σ_y = 70 MPa at 23 °C

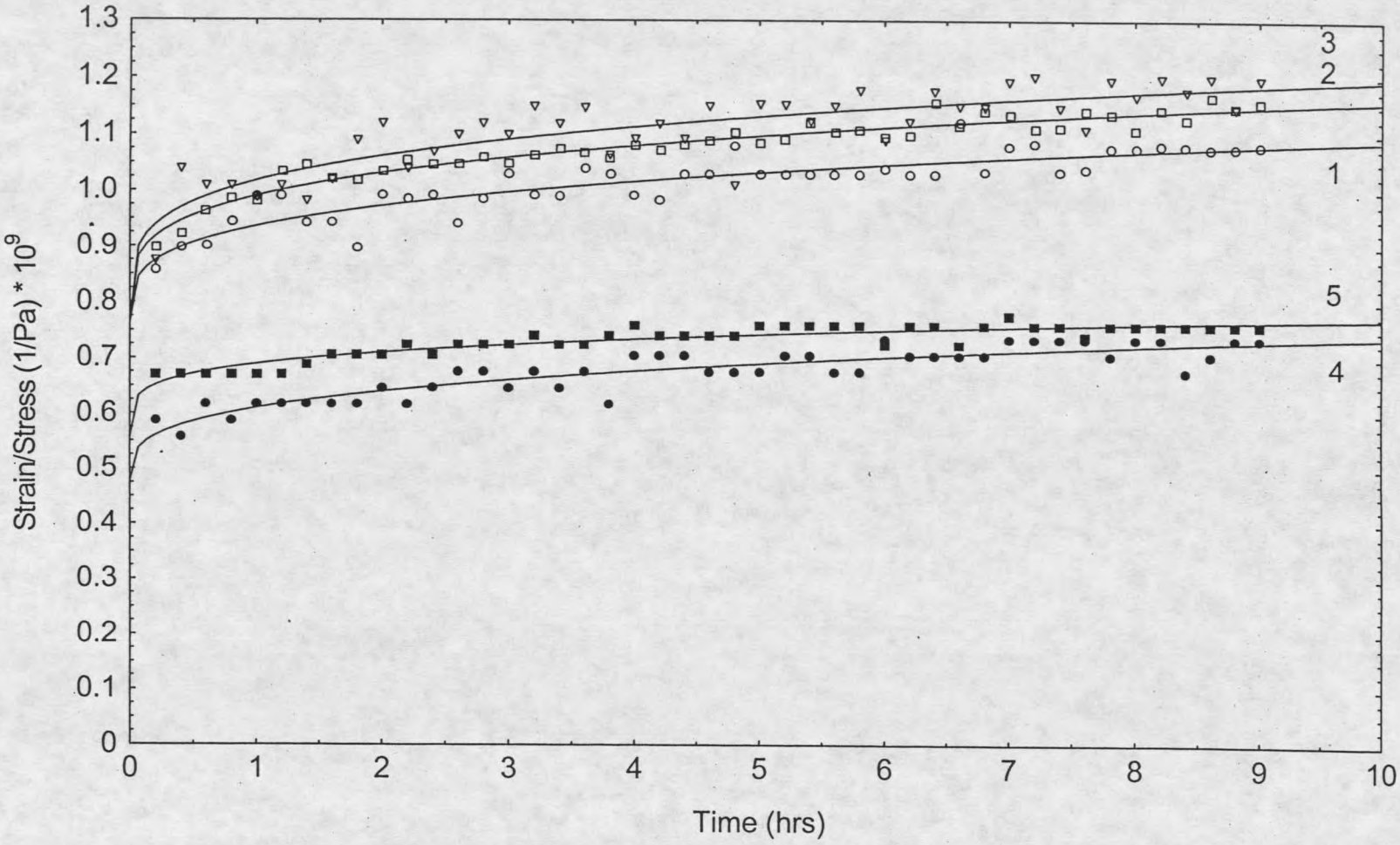


Figure B.I.14 Normalized Vibrocreep Response of Nylon 6/6 at Different Frequencies at 23 °C
1- $(0.16\pm0.075)\sigma_y$, 1 Hz; 2- $(0.16\pm0.075)\sigma_y$, 10 Hz; 3- $(0.16\pm0.075)\sigma_y$, 20 Hz;
4- $(0.16)\sigma_y$, 5- $(0.20)\sigma_y$, Constant Load Creep;
σ_y = 70 MPa at 23 °C

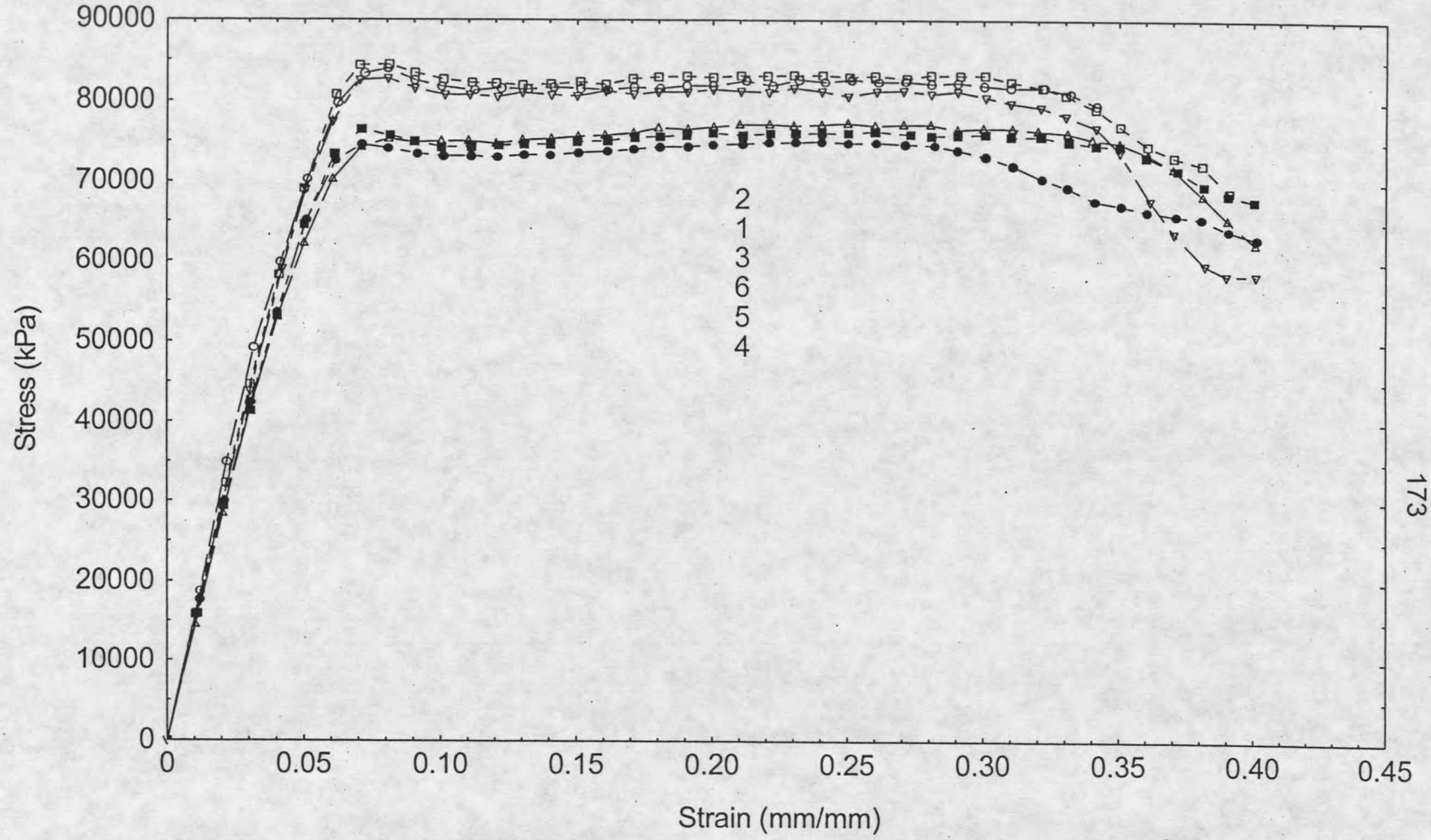


Figure B.I.15 Tensile Testing of Nylon 6/6 Specimens After Cyclic and Constant Loading at 23 °C
1- $(0.16\pm0.075)\sigma_y$, 1 Hz; 2- $(0.16\pm0.075)\sigma_y$, 10 Hz; 3- $(0.16\pm0.075)\sigma_y$, 20 Hz;
4- $(0.16)\sigma_y$, 5- $(0.20)\sigma_y$, Constant Load Creep; 6- Virgin Specimens;
σ_y = 70 MPa at 23 °C

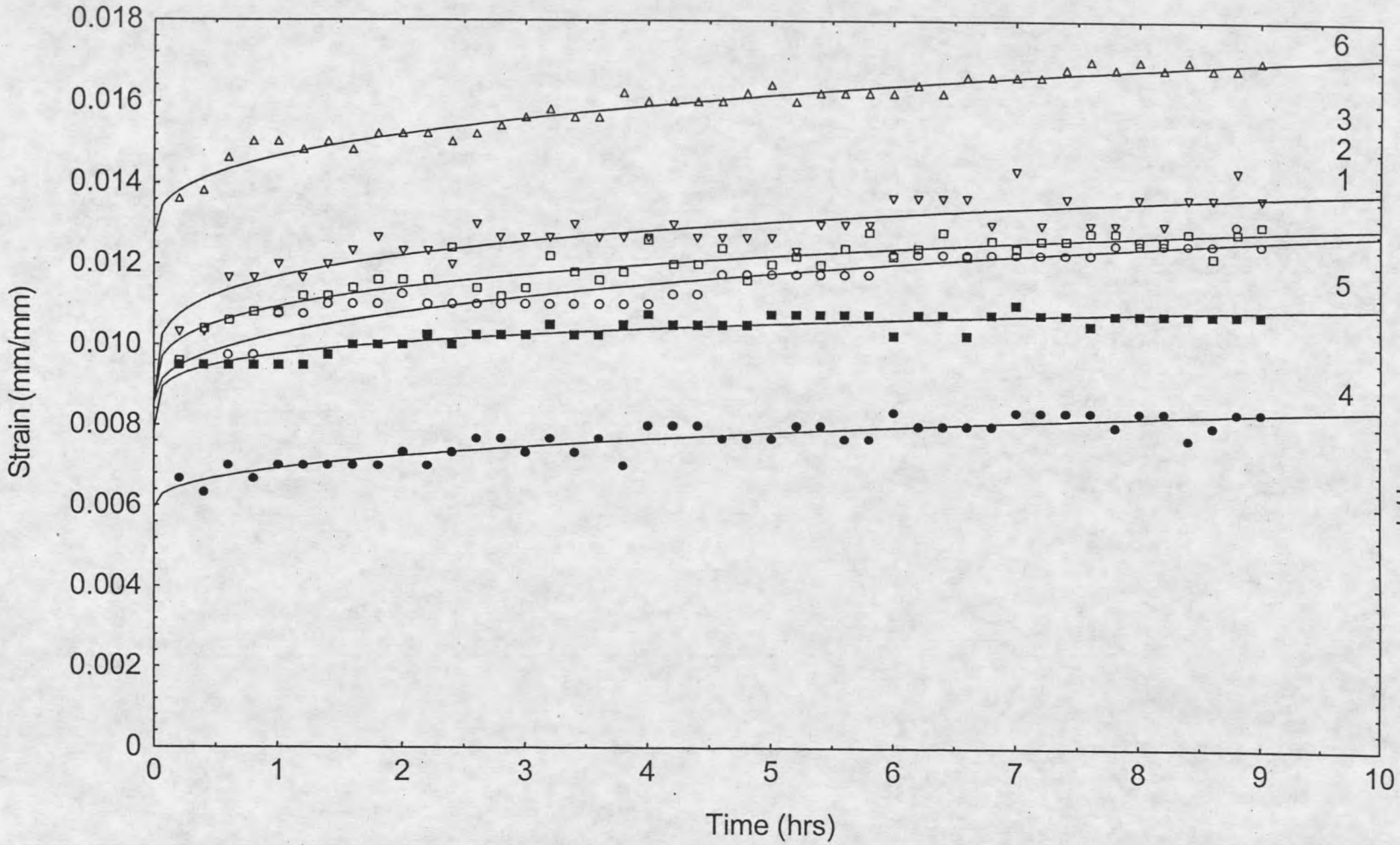


Figure B.I.16 Vibrocreep Response of Nylon 6/6 at Different Frequencies at 23 °C
1- $(0.16\pm0.10)\sigma_y$, 1 Hz; 2- $(0.16\pm0.10)\sigma_y$, 10 Hz; 3- $(0.16\pm0.10)\sigma_y$, 20 Hz;
4- $(0.16)\sigma_y$, 5- $(0.20)\sigma_y$, 6- $(0.30)\sigma_y$, Constant Load Creep;
σ_y = 70 MPa at 23 °C

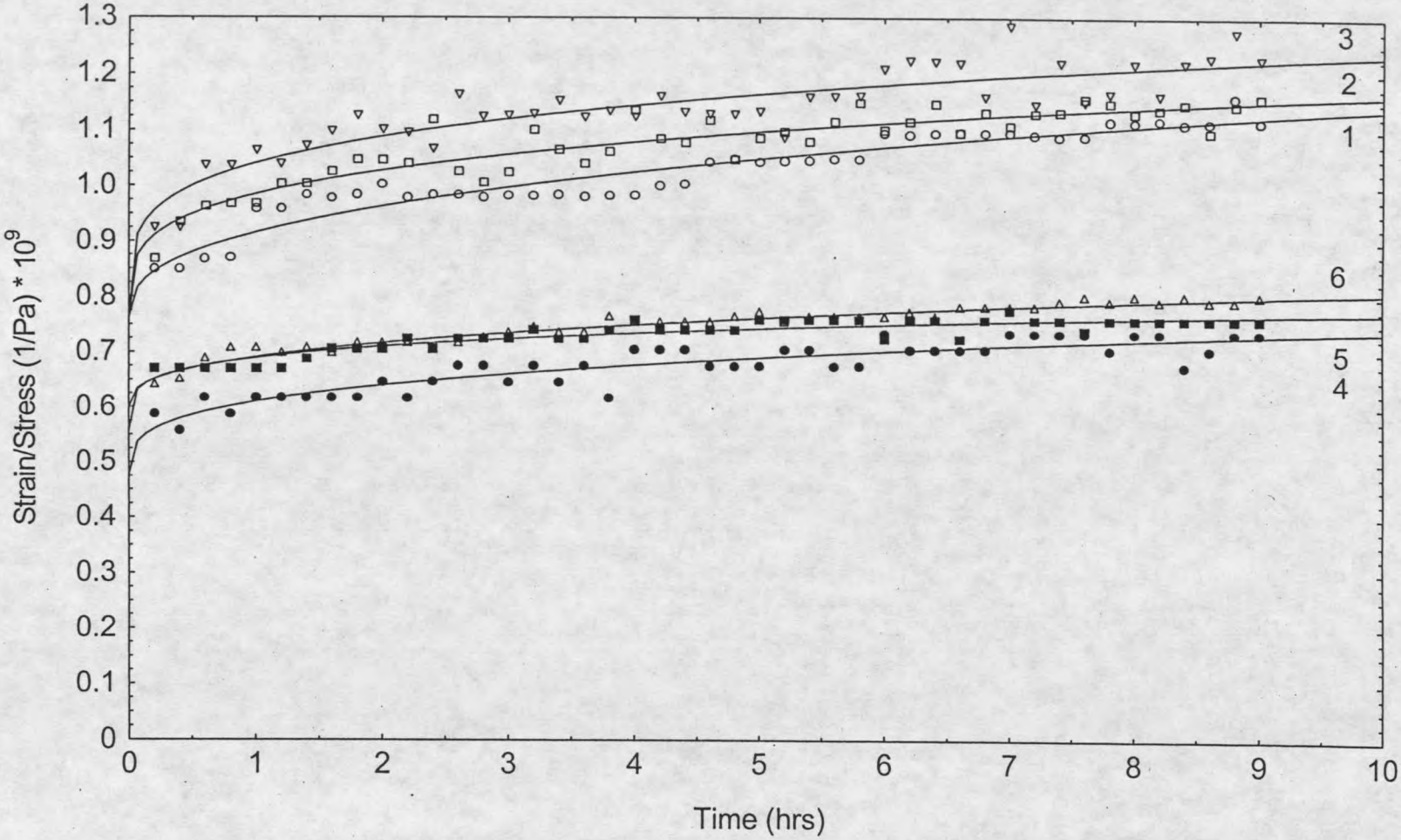


Figure B.I.17 Normalized Vibrocreep Response of Nylon 6/6 at Different Frequencies at 23 °C
1- $(0.16\pm0.10)\sigma_y$, 1 Hz; 2- $(0.16\pm0.10)\sigma_y$, 10 Hz; 3- $(0.16\pm0.10)\sigma_y$, 20 Hz;
4- $(0.16)\sigma_y$, 5- $(0.20)\sigma_y$, 6- $(0.30)\sigma_y$, Constant Load Creep;
σ_y = 70 MPa at 23 °C

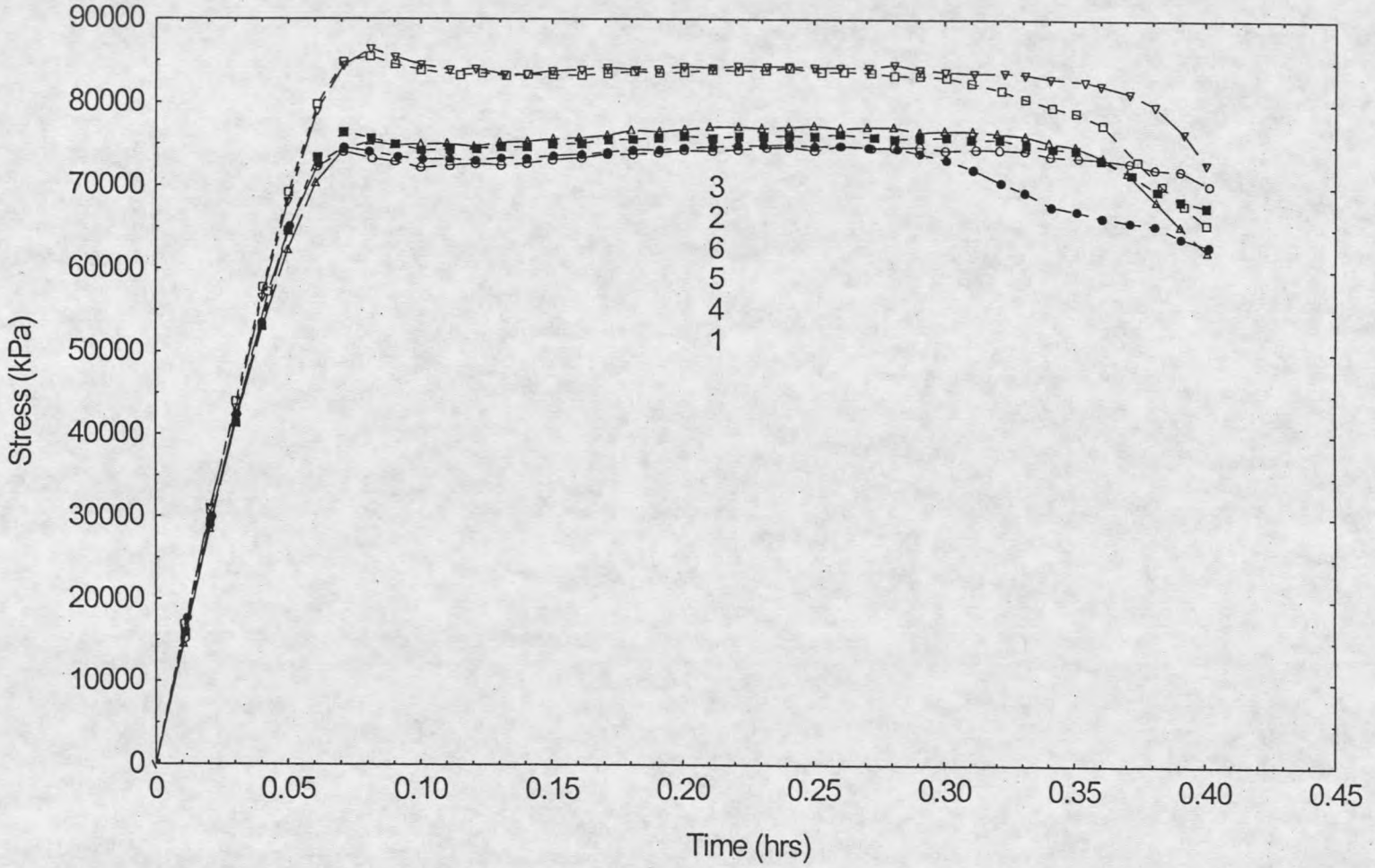


Figure B.I.18 Tensile Testing of Nylon 6/6 Specimens After Cyclic and Constant Loading at 23 °C
1- $(0.16\pm0.10)\sigma_y$, 1 Hz; 2- $(0.16\pm0.10)\sigma_y$, 10 Hz; 3- $(0.16\pm0.10)\sigma_y$, 20 Hz;
4- $(0.16)\sigma_y$, 5- $(0.20)\sigma_y$, Constant Load Creep; 6- Virgin Specimens;
σ_y = 70 MPa at 23 °C

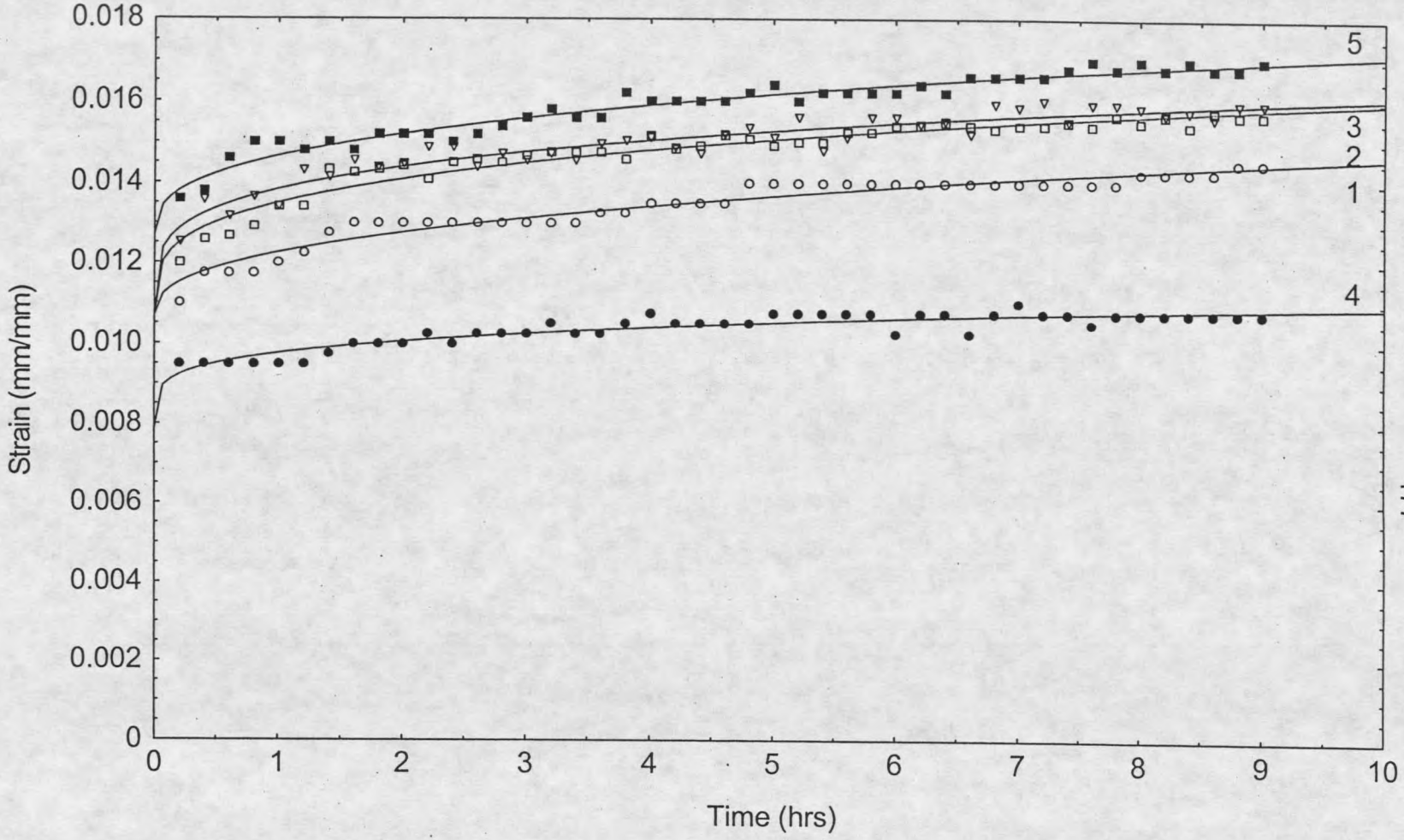


Figure B.I.19 Vibrocreep Response of Nylon 6/6 at Different Frequencies at 23 °C
1- $(0.20\pm0.05)\sigma_y$, 1 Hz; 2- $(0.20\pm0.05)\sigma_y$, 10 Hz; 3- $(0.20\pm0.05)\sigma_y$, 20 Hz;
4- $(0.20)\sigma_y$, 5- $(0.30)\sigma_y$, Constant Load Creep;
σ_y = 70 MPa at 23 °C

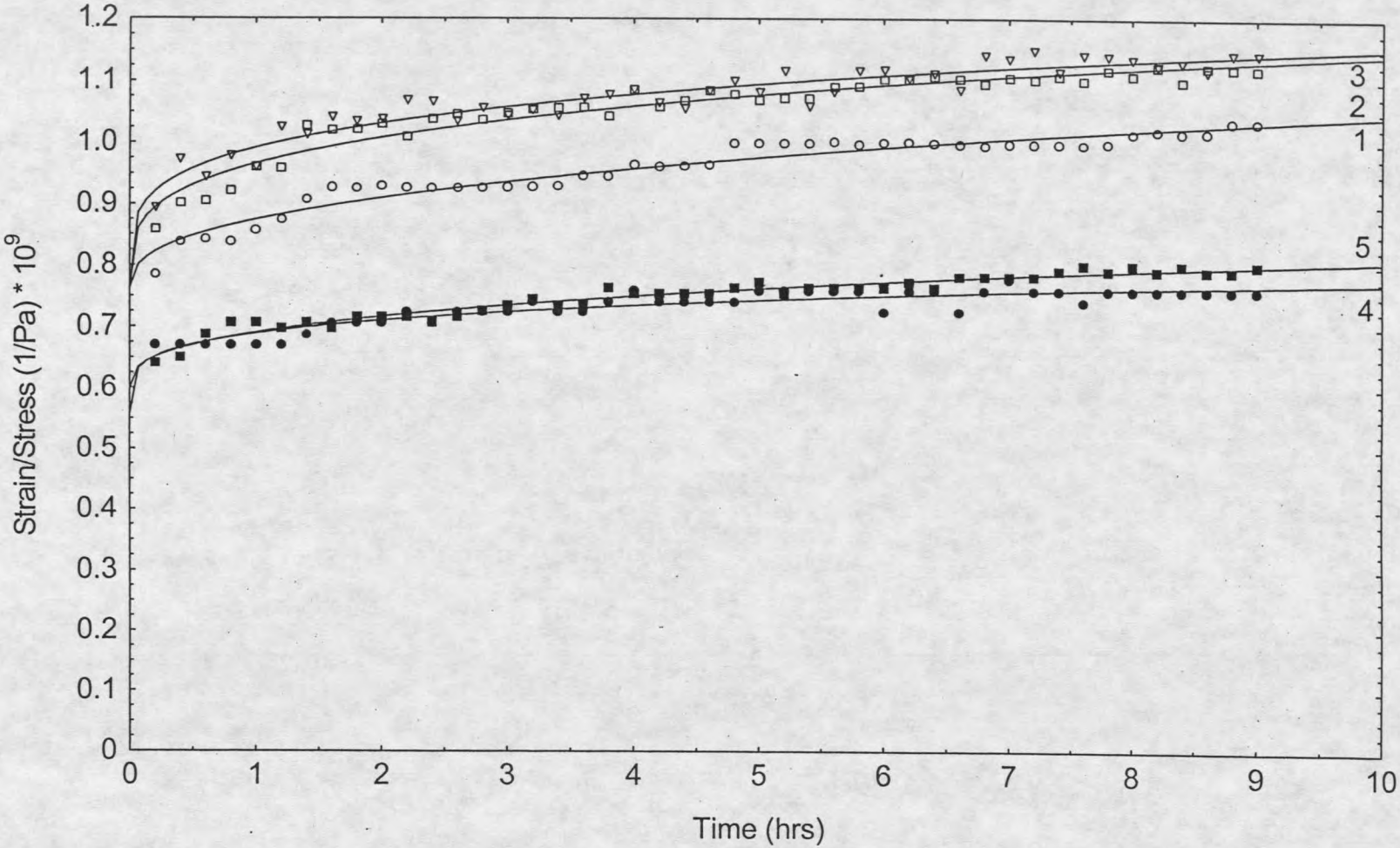


Figure B.I.20 Normalized Vibrocreep Response of Nylon 6/6 at Different Frequencies at 23 °C
1- $(0.20\pm0.05)\sigma_y$, 1 Hz; 2- $(0.20\pm0.05)\sigma_y$, 10 Hz; 3- $(0.20\pm0.05)\sigma_y$, 20 Hz;
4- $(0.20)\sigma_y$, 5- $(0.30)\sigma_y$, Constant Load Creep;
σ_y = 70 MPa at 23 °C

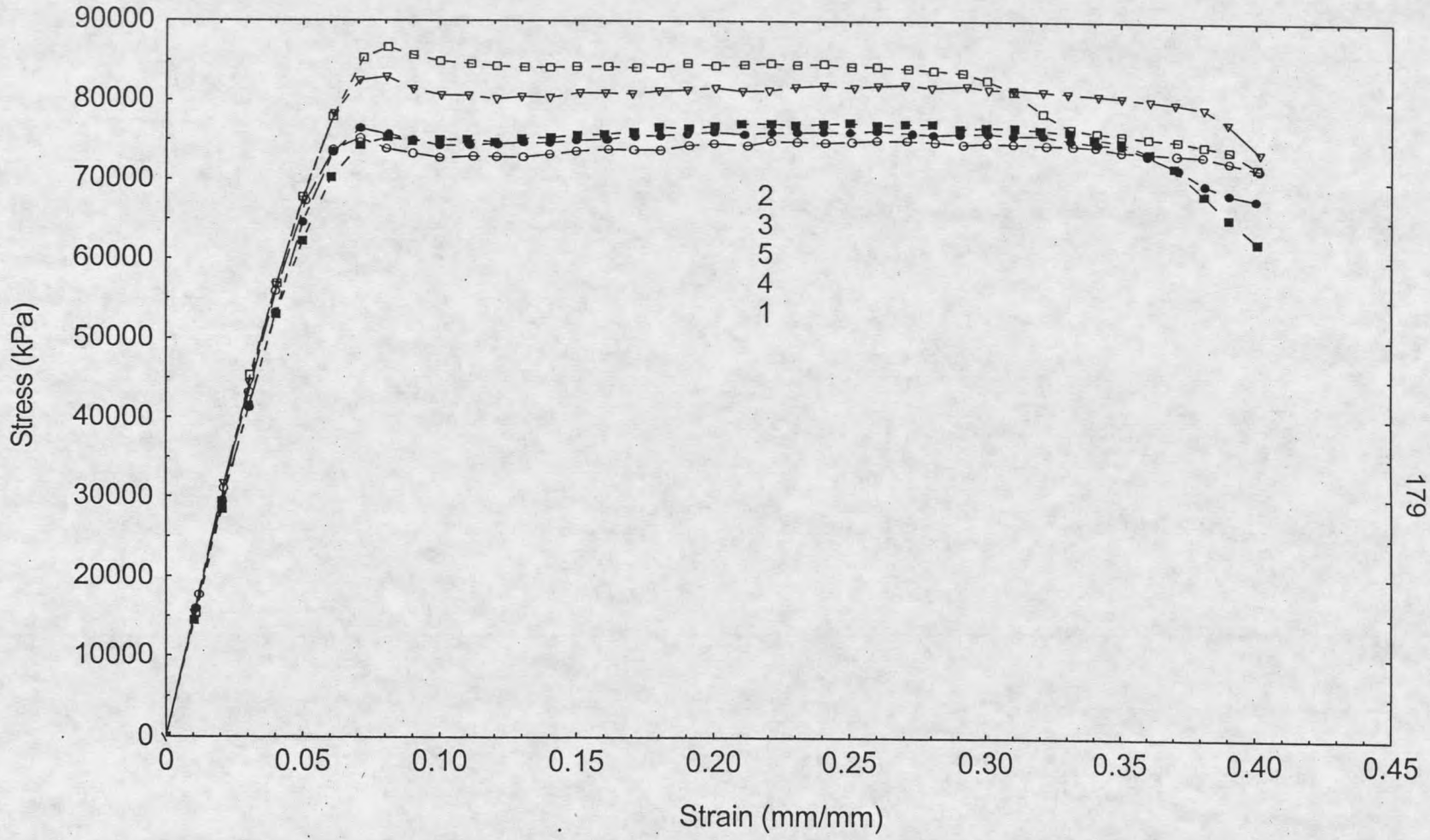


Figure B.I.21 Tensile Testing of Nylon 6/6 Specimens After Cyclic and Constant Loading at 23 °C
1- $(0.20\pm0.05)\sigma_y$, 1 Hz; 2- $(0.20\pm0.05)\sigma_y$, 10 Hz; 3- $(0.20\pm0.05)\sigma_y$, 20 Hz;
4- $(0.20)\sigma_y$, Constant Load Creep; 5- Virgin Specimens;
σ_y = 70 MPa at 23 °C

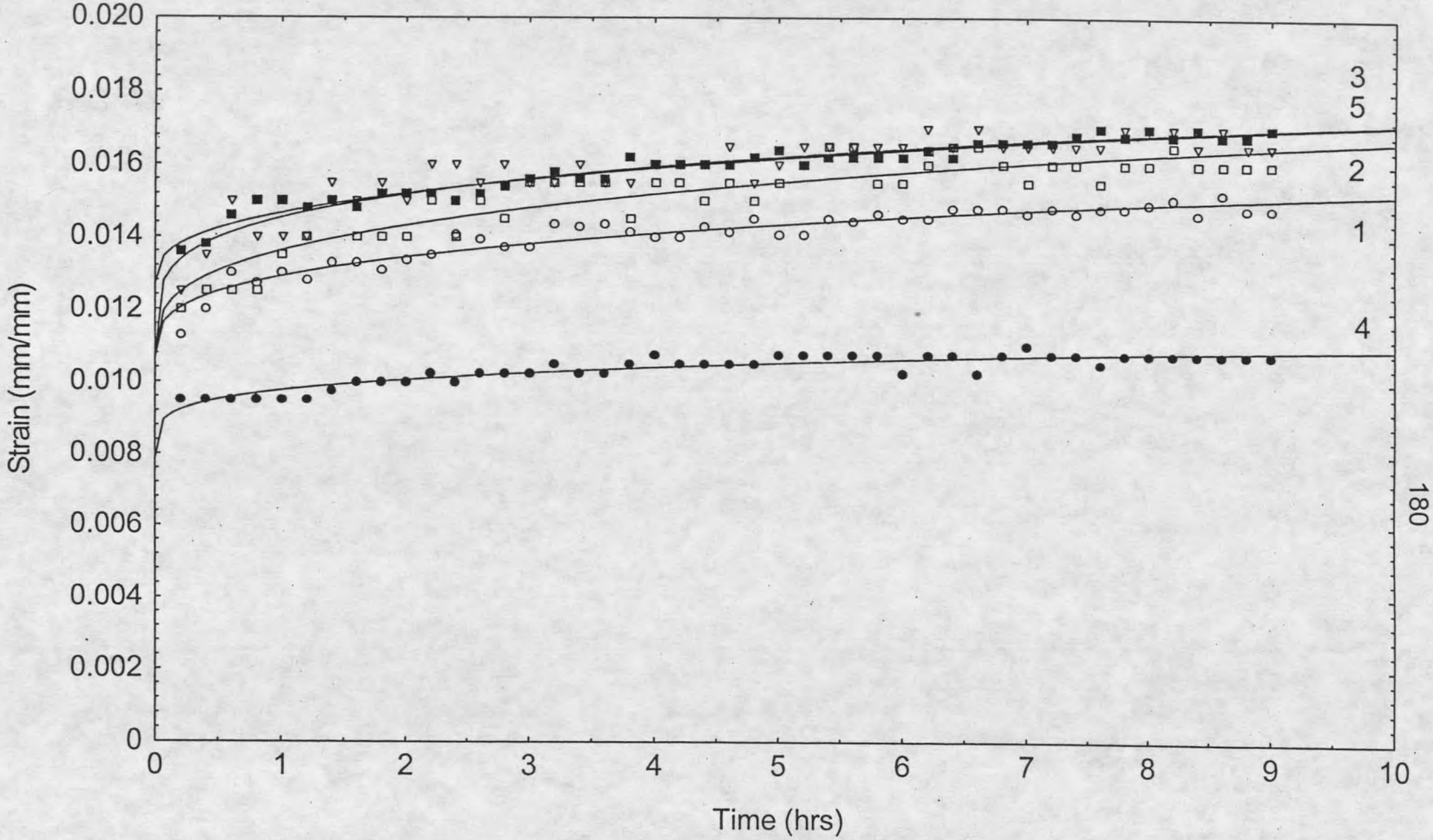


Figure B.I.22 Vibrocreep Response of Nylon 6/6 at Different Frequencies at 23 °C
1- $(0.20\pm0.075)\sigma_y$, 1 Hz; 2- $(0.20\pm0.075)\sigma_y$, 10 Hz; 3- $(0.20\pm0.075)\sigma_y$, 20 Hz;
4- $(0.20)\sigma_y$, 5- $(0.30)\sigma_y$, Constant Load Creep;
σ_y = 70 MPa at 23 °C

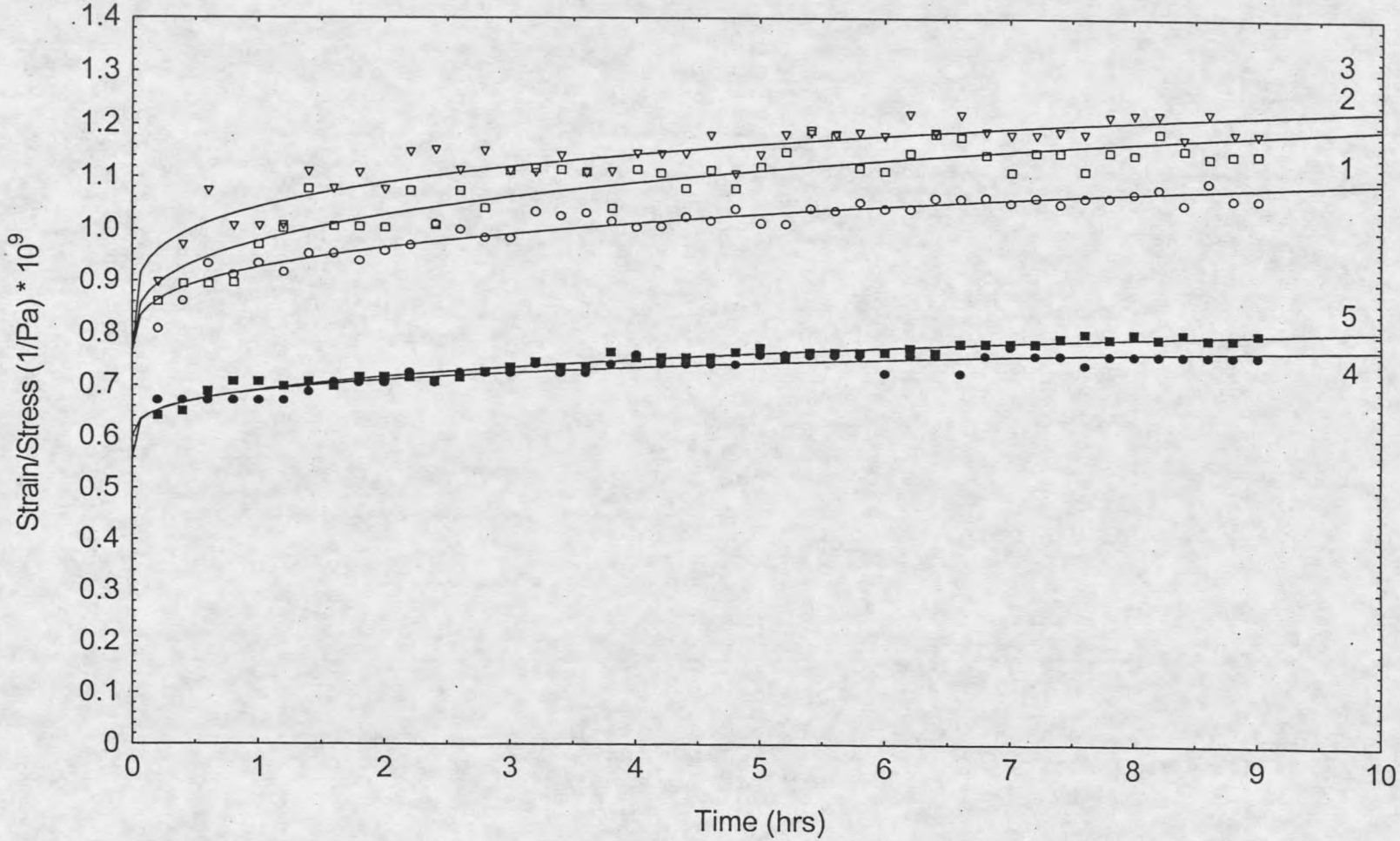


Figure B.I.23 Normalized Vibrocreep Response of Nylon 6/6 at Different Frequencies at 23 °C
1- $(0.20\pm0.075)\sigma_y$, 1 Hz; 2- $(0.20\pm0.075)\sigma_y$, 10 Hz; 3- $(0.20\pm0.075)\sigma_y$, 20 Hz;
4- $(0.20)\sigma_y$, 5- $(0.30)\sigma_y$, Constant Load Creep;
σ_y = 70 MPa at 23 °C

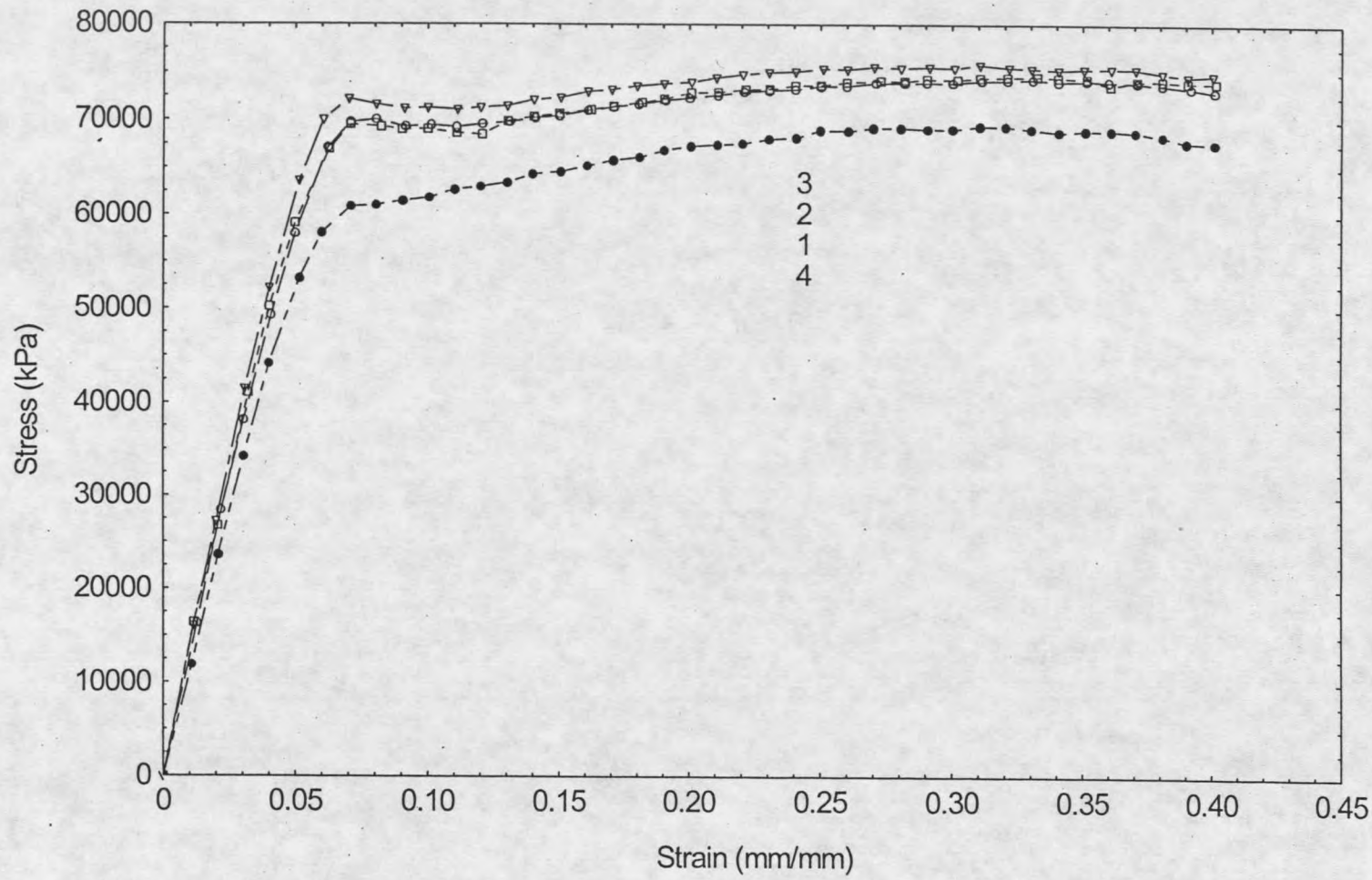


Figure B.I.24 Tensile Testing of Nylon 6/6 Specimens After Cyclic and Constant Loading at 23 °C
1- $(0.20\pm0.075)\sigma_y$, 1 Hz; 2- $(0.20\pm0.075)\sigma_y$, 10 Hz; 3- $(0.20\pm0.075)\sigma_y$, 20 Hz;
4- $(0.20)\sigma_y$, Constant Load Creep; 5- Virgin Specimens;
σ_y = 70 MPa at 23 °C

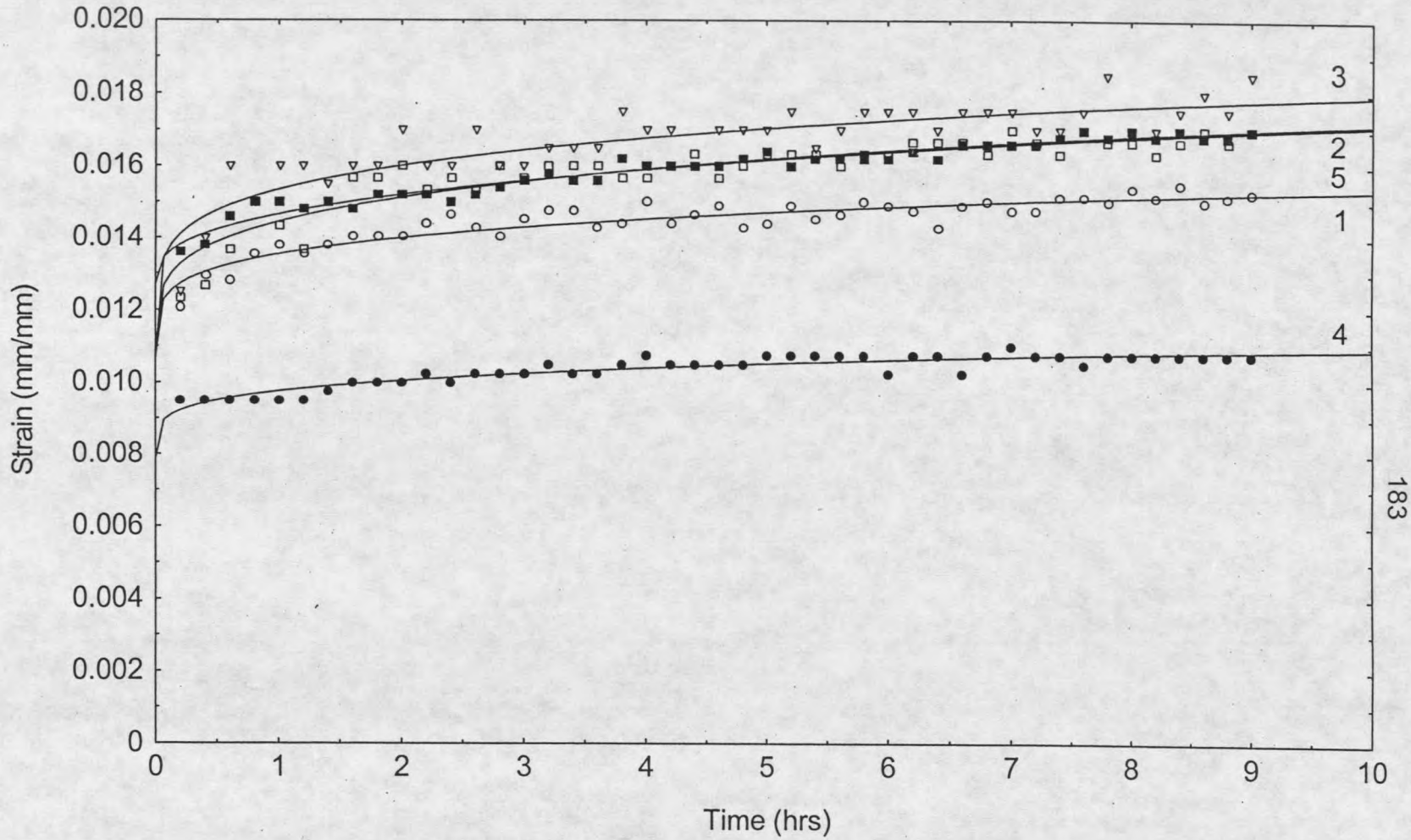


Figure B.I.25 Vibrocreep Response of Nylon 6/6 at Different Frequencies at 23 °C
1- $(0.20\pm0.10)\sigma_y$, 1 Hz; 2- $(0.20\pm0.10)\sigma_y$, 10 Hz; 3- $(0.20\pm0.10)\sigma_y$, 20 Hz;
4- $(0.20)\sigma_y$, 5- $(0.30)\sigma_y$, Constant Load Creep;
σ_y = 70 MPa at 23 °C

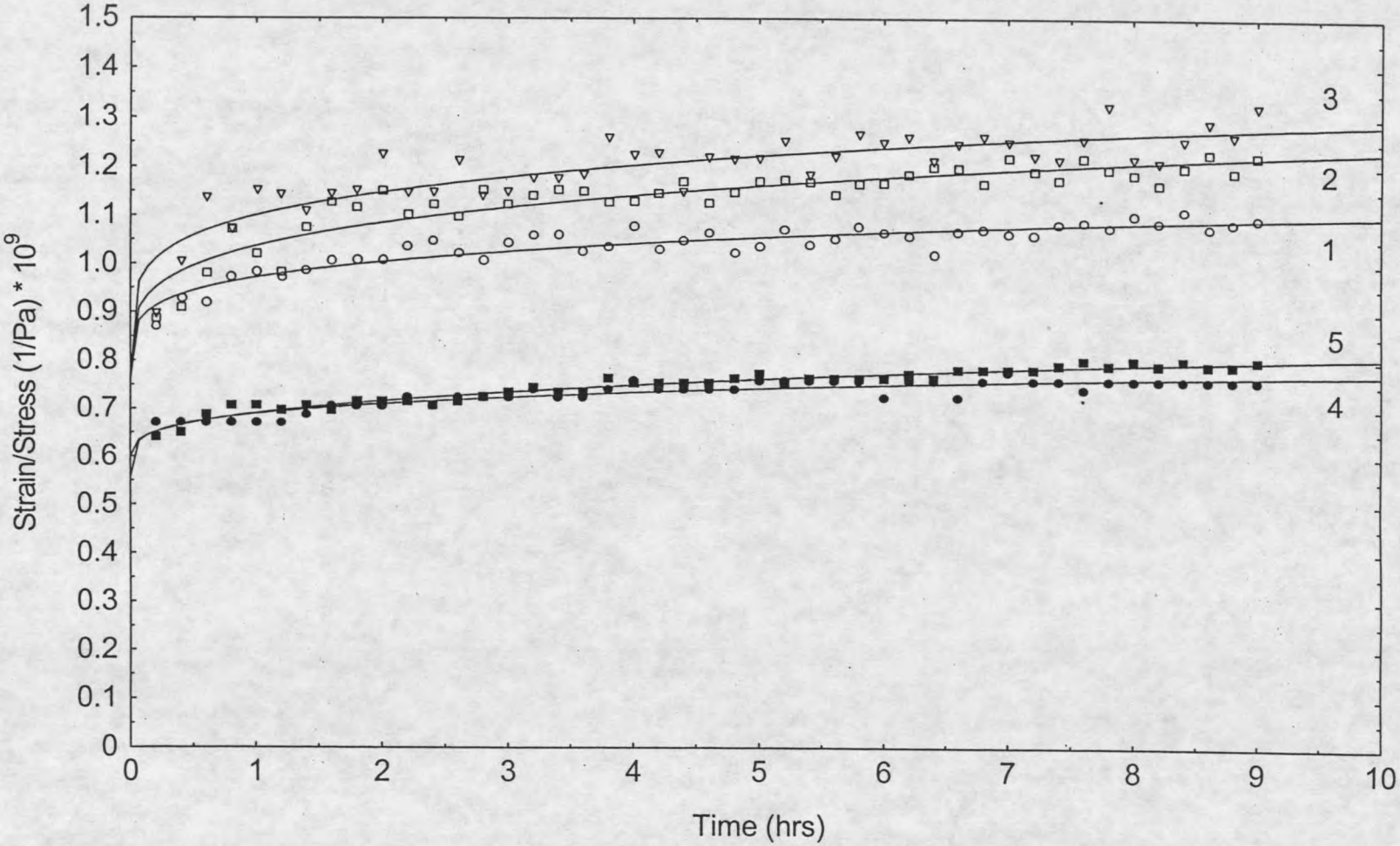


Figure B.I.26 Normalized Vibrocreep Response of Nylon 6/6 at Different Frequencies at 23 °C
1- $(0.20\pm0.10)\sigma_y$, 1 Hz; 2- $(0.20\pm0.10)\sigma_y$, 10 Hz; 3- $(0.20\pm0.10)\sigma_y$, 20 Hz;
4- $(0.20)\sigma_y$, 5- $(0.30)\sigma_y$, Constant Load Creep;
σ_y = 70 MPa at 23 °C

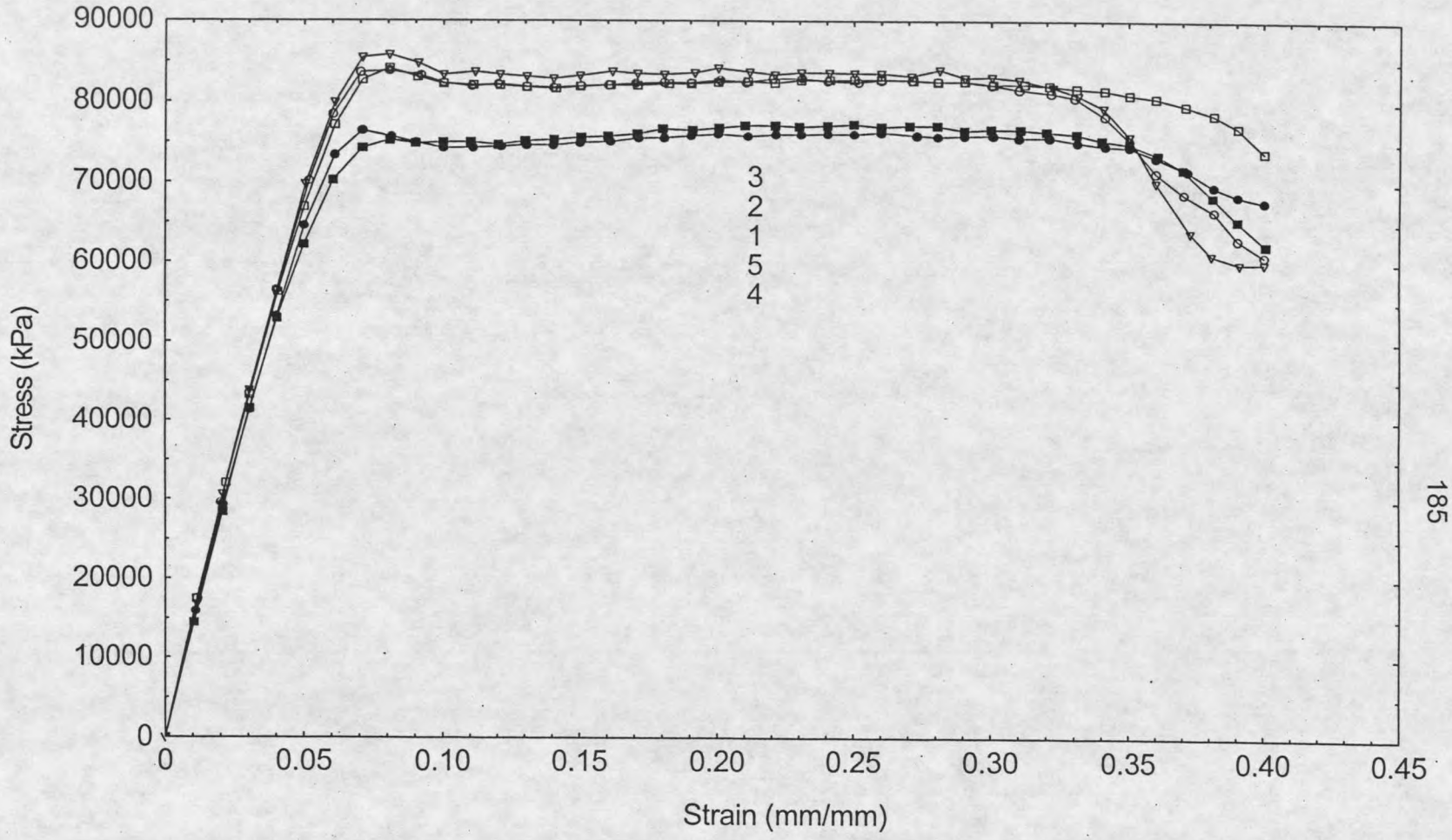


Figure B.I.27 Tensile Testing of Nylon 6/6 Specimens After Cyclic and Constant Loading at 23 °C
1- $(0.20\pm0.10)\sigma_y$, 1 Hz; 2- $(0.20\pm0.10)\sigma_y$, 10 Hz; 3- $(0.20\pm0.10)\sigma_y$, 20 Hz;
4- $(0.20)\sigma_y$, Constant Load Creep; 5- Virgin Specimens;
σ_y = 70 MPa at 23 °C

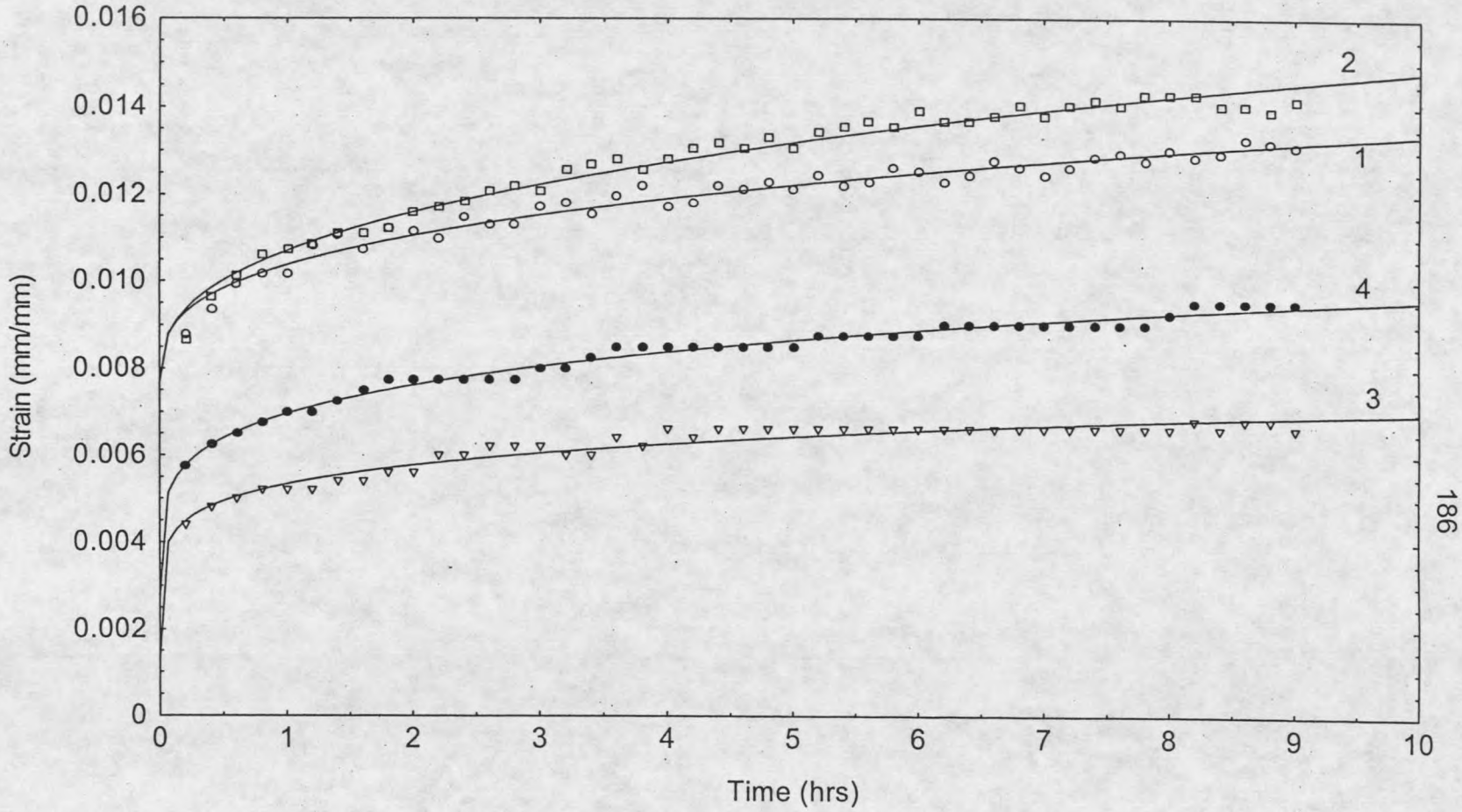


Figure B.II.1 Vibrocreep Response of Nylon 6/6 at Different Frequencies at 35 °C
1- $(0.16\pm0.04)\sigma_y$, 1 Hz; 2- $(0.16\pm0.04)\sigma_y$, 10 Hz;
3- $(0.16)\sigma_y$, 4- $(0.20)\sigma_y$, Constant Load Creep;
σ_y = 55 MPa at 35 °C

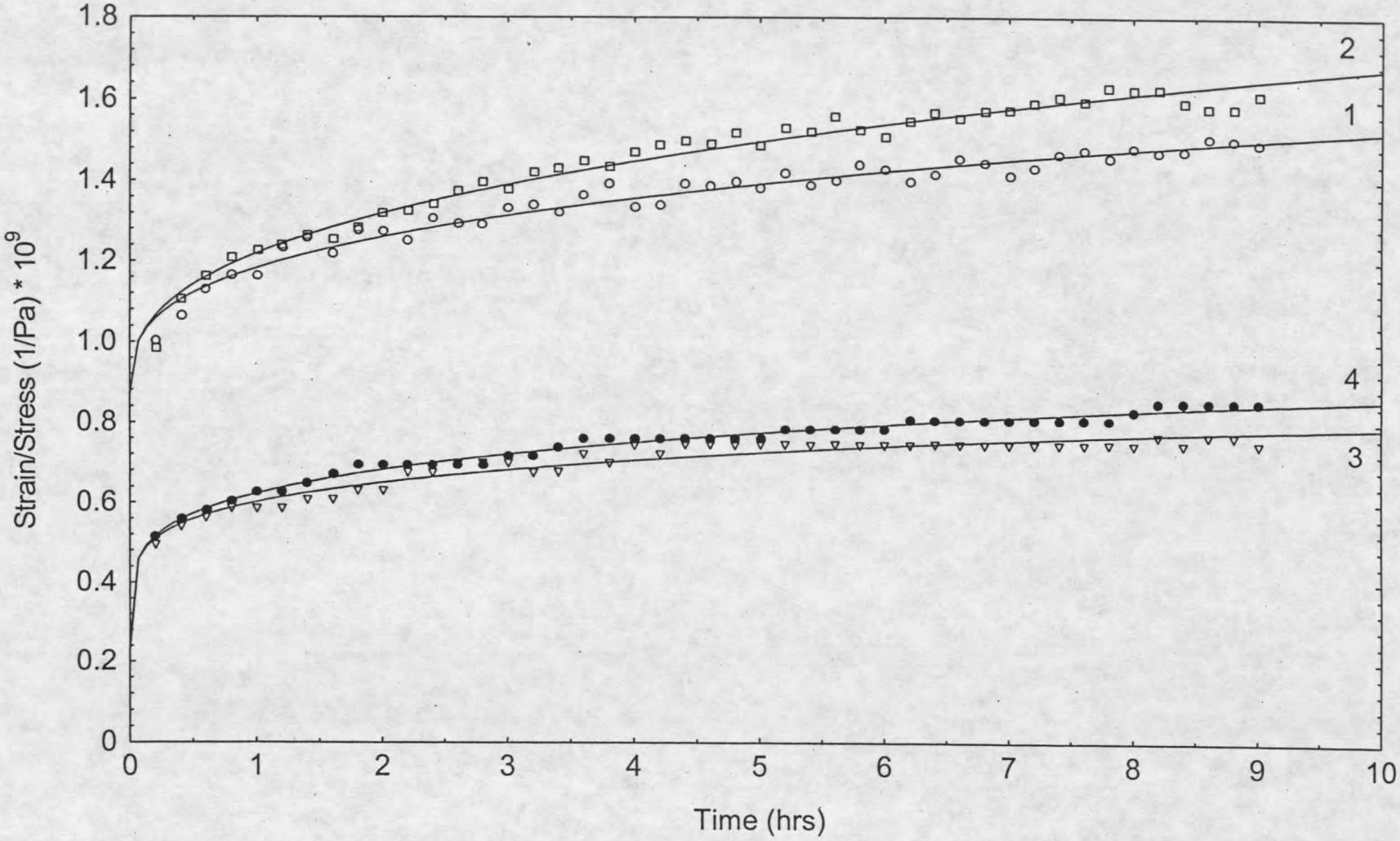


Figure B.II.2 Normalized Vibrocreep Response of Nylon 6/6 at Different Frequencies at 35 °C
1- $(0.16\pm0.04)\sigma_y$, 1 Hz; 2- $(0.16\pm0.04)\sigma_y$, 10 Hz;
3- $(0.16)\sigma_y$, 4- $(0.20)\sigma_y$, Constant Load Creep;
σ_y = 55 MPa at 35 °C

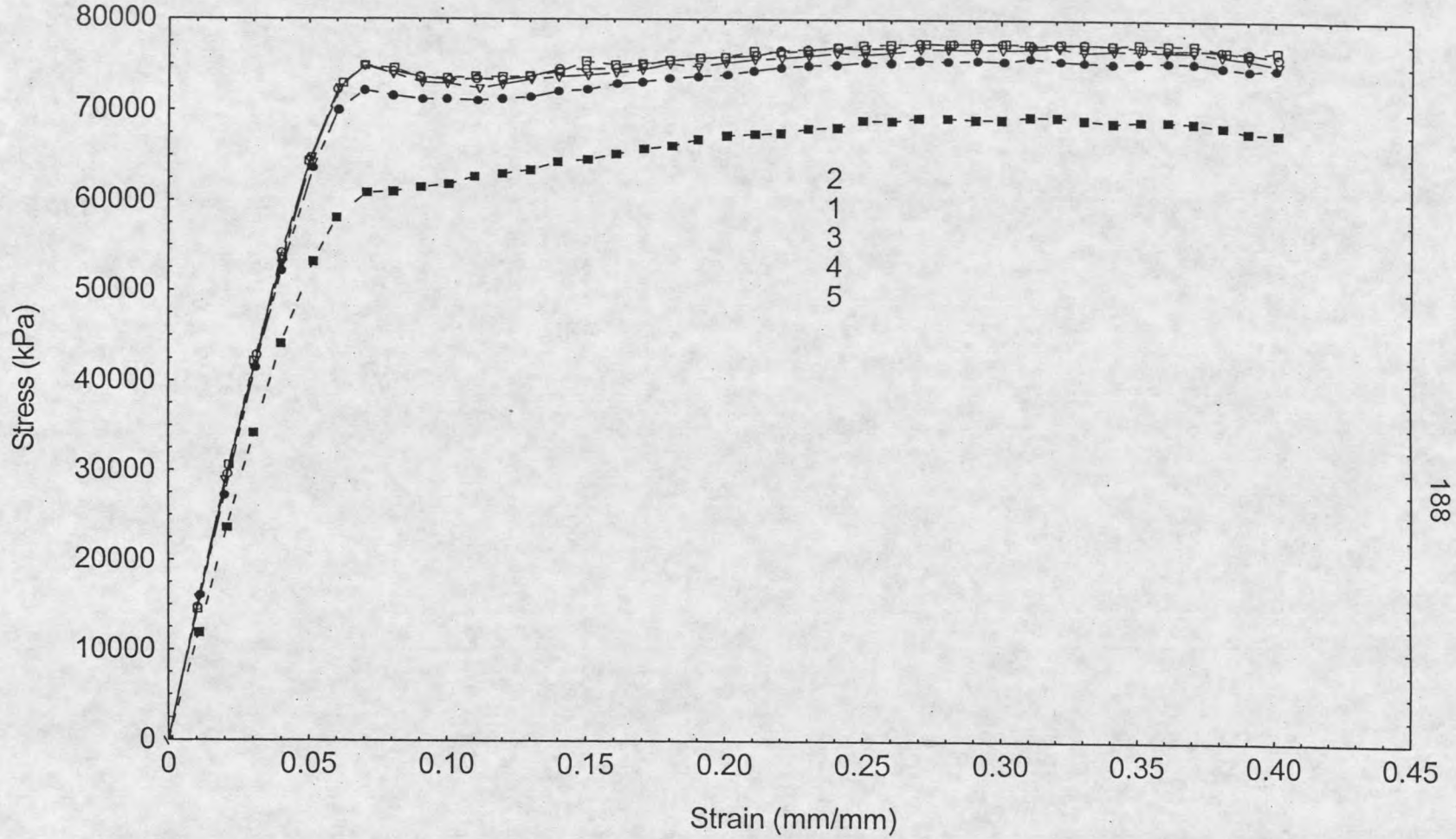


Figure B.II.3 Tensile Testing of Nylon 6/6 Specimens After Cyclic and Constant Loading at 35 °C
1- $(0.16\pm0.04)\sigma_y$, 1 Hz; 2- $(0.16\pm0.04)\sigma_y$, 10 Hz;
3- $(0.16)\sigma_y$, 4- $(0.20)\sigma_y$, Constant Load Creep; 5- Virgin Specimens;
σ_y = 55 MPa at 35 °C

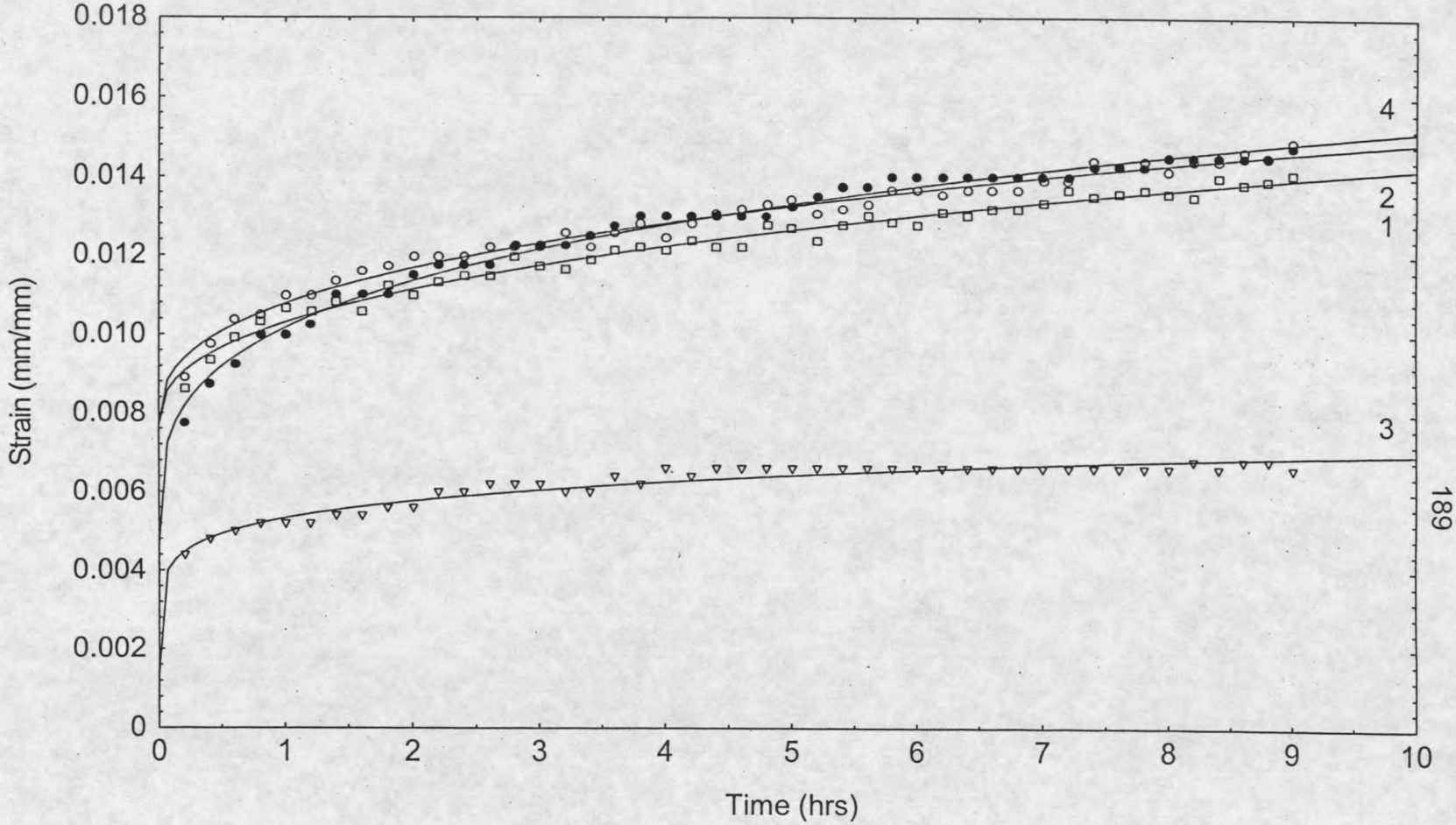


Figure B.II.4 Vibrocreep Response of Nylon 6/6 at Different Frequencies at 35 °C
1- $(0.16\pm0.10)\sigma_y$, 1 Hz; 2- $(0.16\pm0.10)\sigma_y$, 10 Hz;
3- $(0.16)\sigma_y$, 4- $(0.30)\sigma_y$, Constant Load Creep;
σ_y = 55 MPa at 35 °C

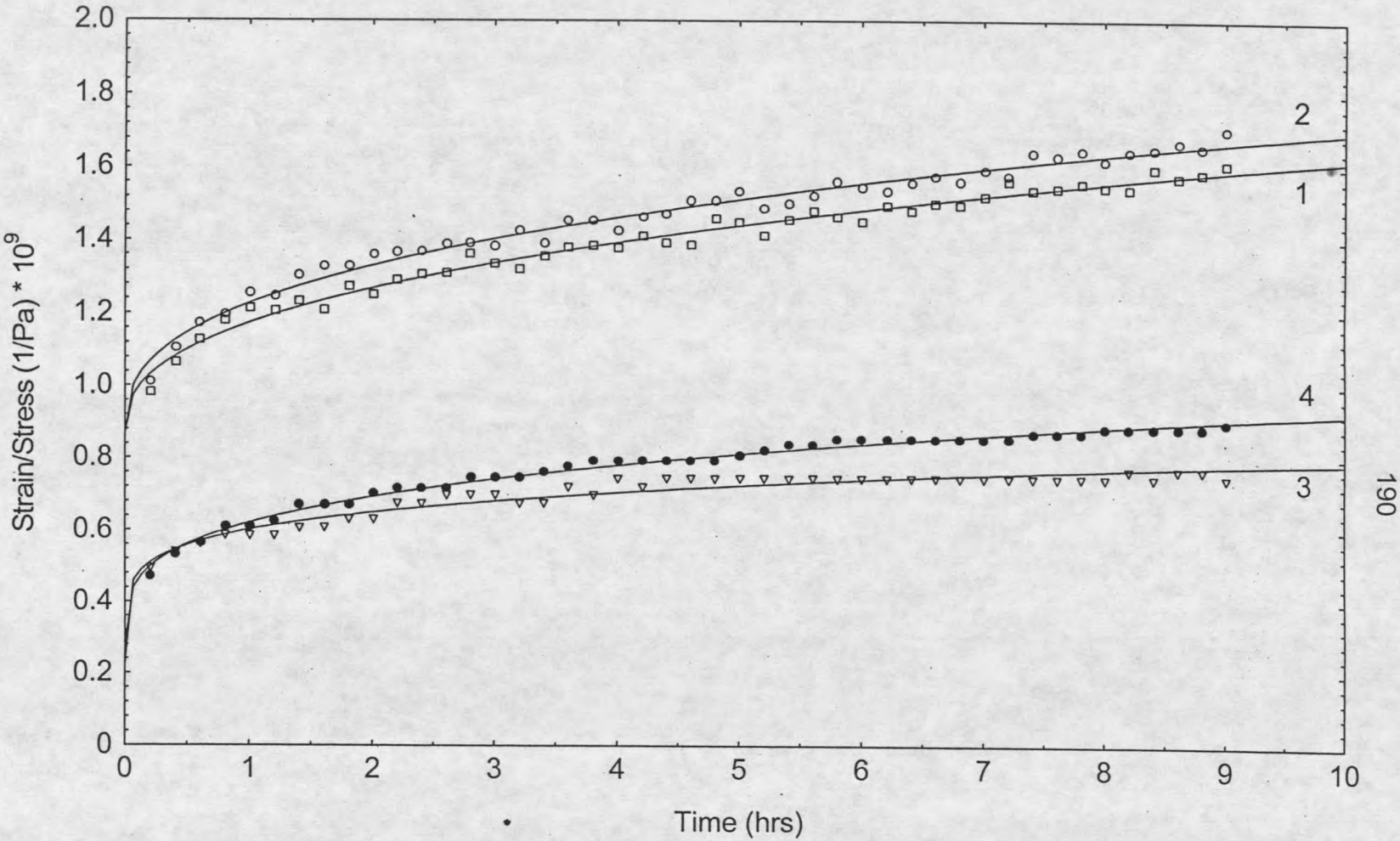


Figure B.II.5 Normalized Vibrocreep Response of Nylon 6/6 at Different Frequencies at 35 °C
1- $(0.16\pm0.10)\sigma_y$, 1 Hz; 2- $(0.16\pm0.10)\sigma_y$, 10 Hz;
3- $(0.16)\sigma_y$, 4- $(0.30)\sigma_y$, Constant Load Creep;
σ_y = 55 MPa at 35 °C

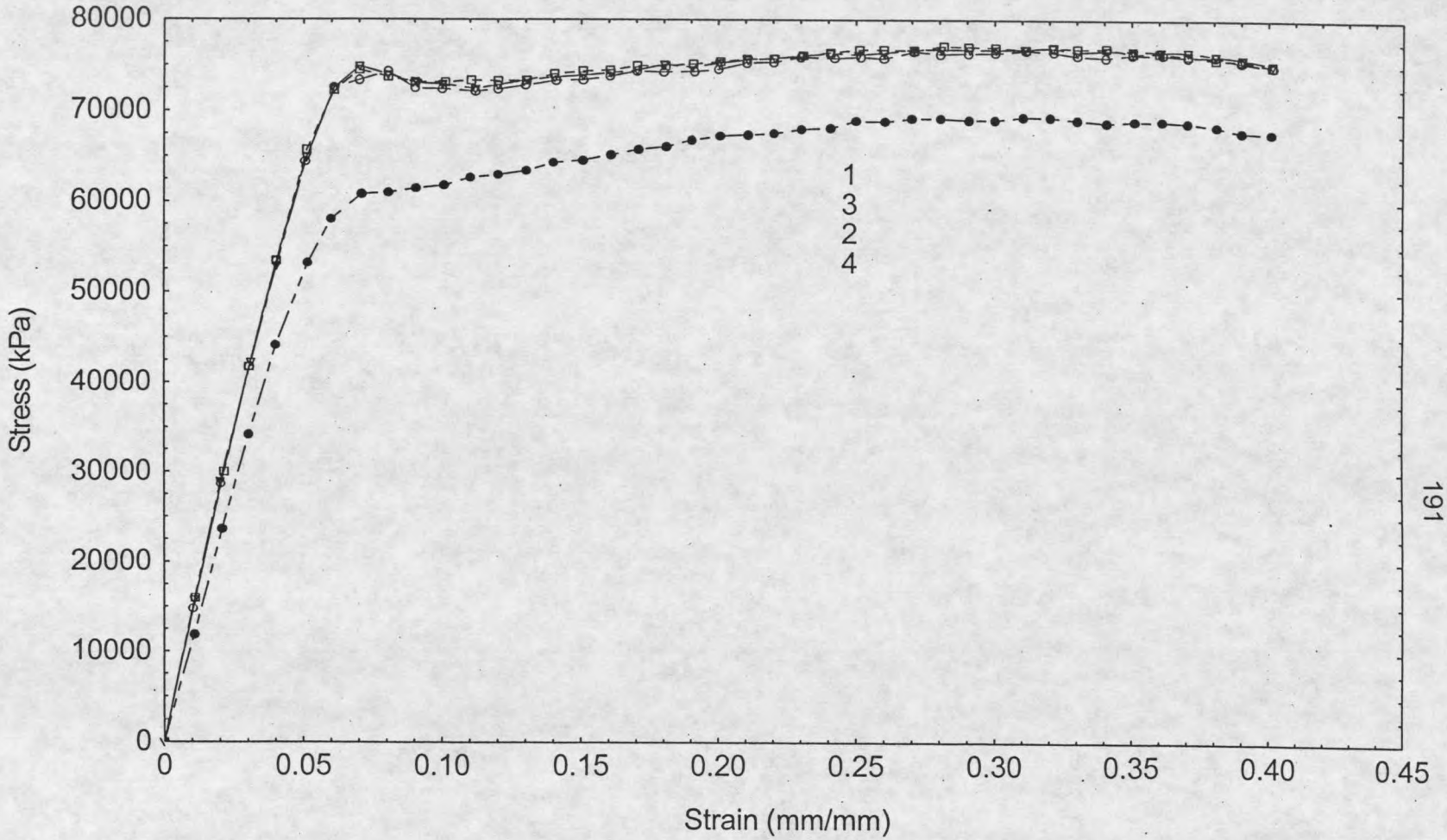


Figure B.II.6 Tensile Testing of Nylon 6/6 Specimens After Cyclic and Constant Loading at 35 °C
1- $(0.16\pm0.10)\sigma_y$, 1 Hz; 2- $(0.16\pm0.10)\sigma_y$, 10 Hz;
3- $(0.16)\sigma_y$, Constant Load Creep; 4- Virgin Specimens;
σ_y = 55 MPa at 35 °C

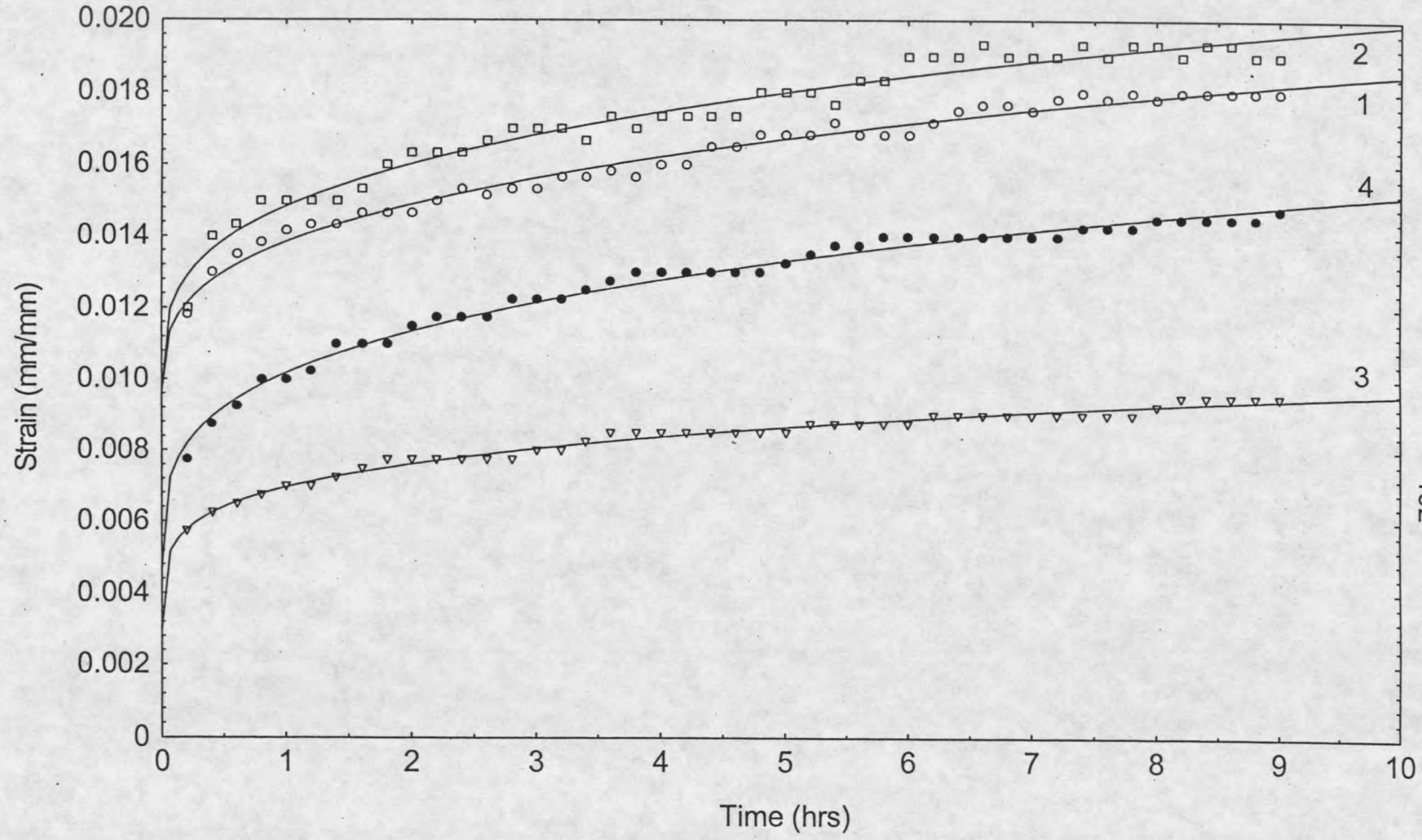


Figure B.II.7 Vibrocreep Response of Nylon 6/6 at Different Frequencies at 35 °C
1- $(0.20\pm0.05)\sigma_y$, 1 Hz; 2- $(0.20\pm0.05)\sigma_y$, 10 Hz;
3- $(0.20)\sigma_y$, 4- $(0.30)\sigma_y$, Constant Load Creep;
σ_y = 55 MPa at 35 °C

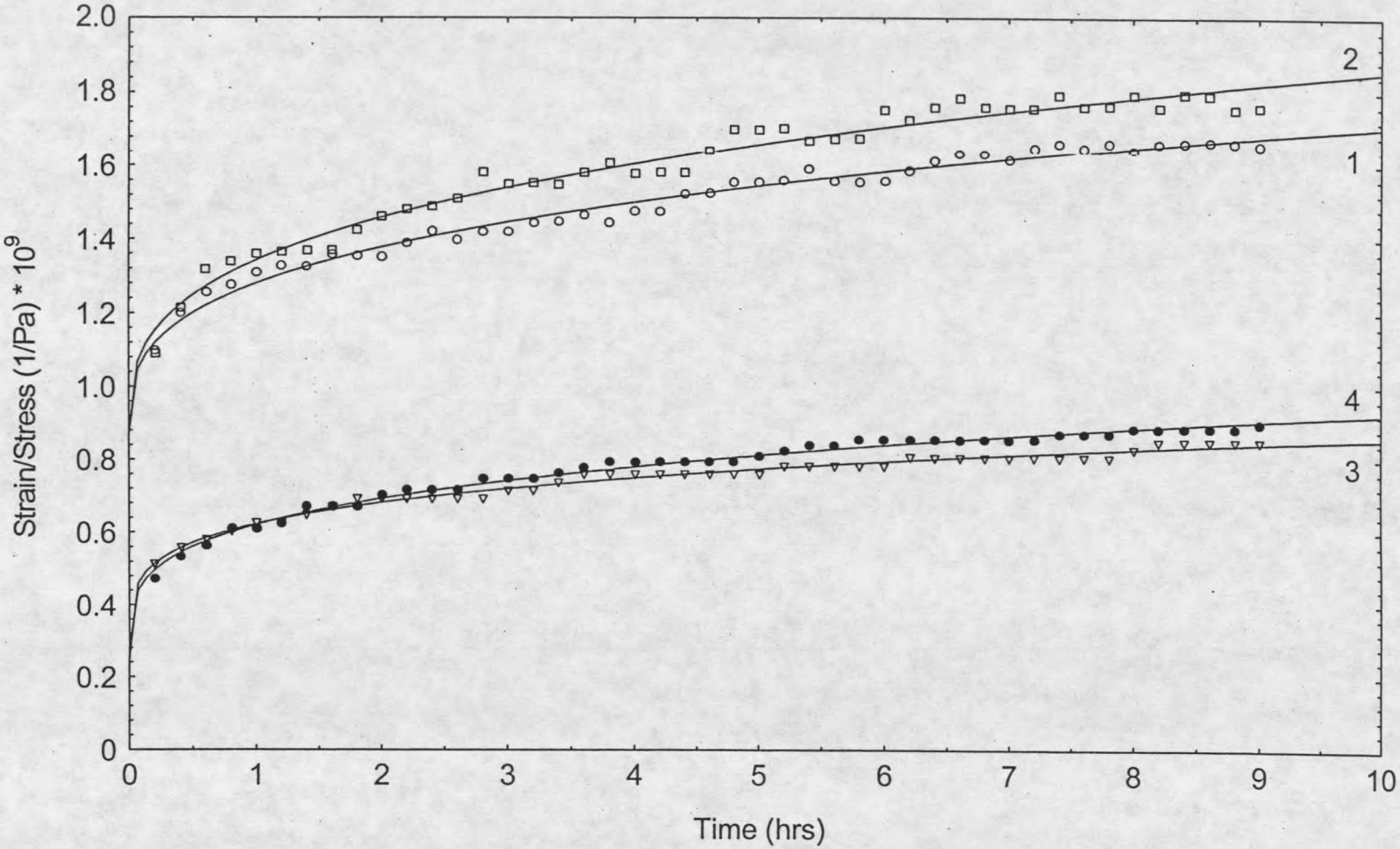


Figure B.II.8 Normalized Vibrocreep Response of Nylon 6/6 at Different Frequencies at 35 °C
1- $(0.20\pm0.05)\sigma_y$, 1 Hz; 2- $(0.20\pm0.05)\sigma_y$, 10 Hz;
3- $(0.20)\sigma_y$, 4- $(0.30)\sigma_y$, Constant Load Creep;
σ_y = 55 MPa at 35 °C

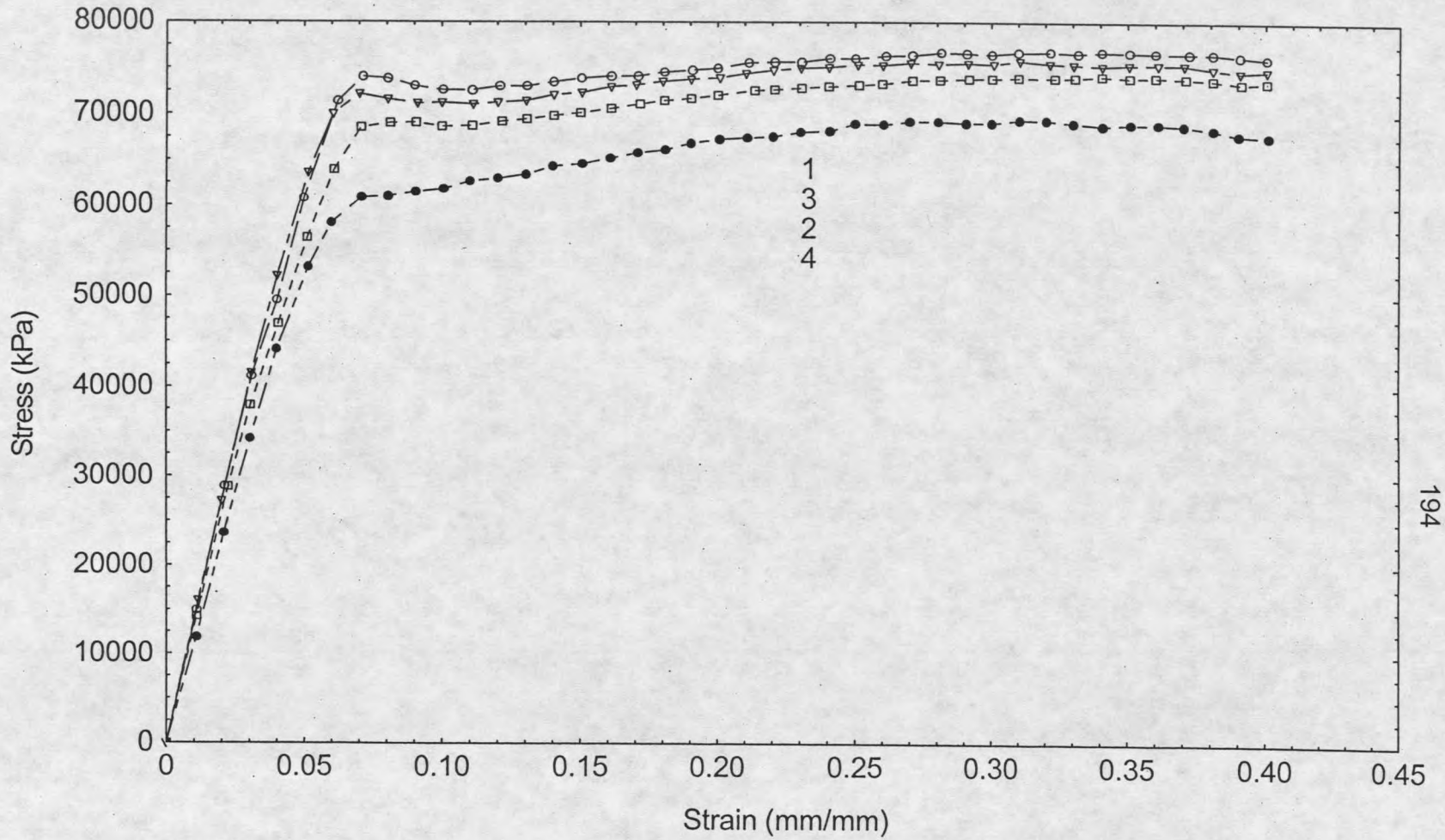


Figure B.II.9 Tensile Testing of Nylon 6/6 Specimens After Cyclic and Constant Loading at 35 °C
1- $(0.20\pm0.05)\sigma_y$, 1 Hz; 2- $(0.20\pm0.05)\sigma_y$, 10 Hz;
3- $(0.20)\sigma$, Constant Load Creep; 4- Virgin Specimens;
σ_y = 55 MPa at 35 °C

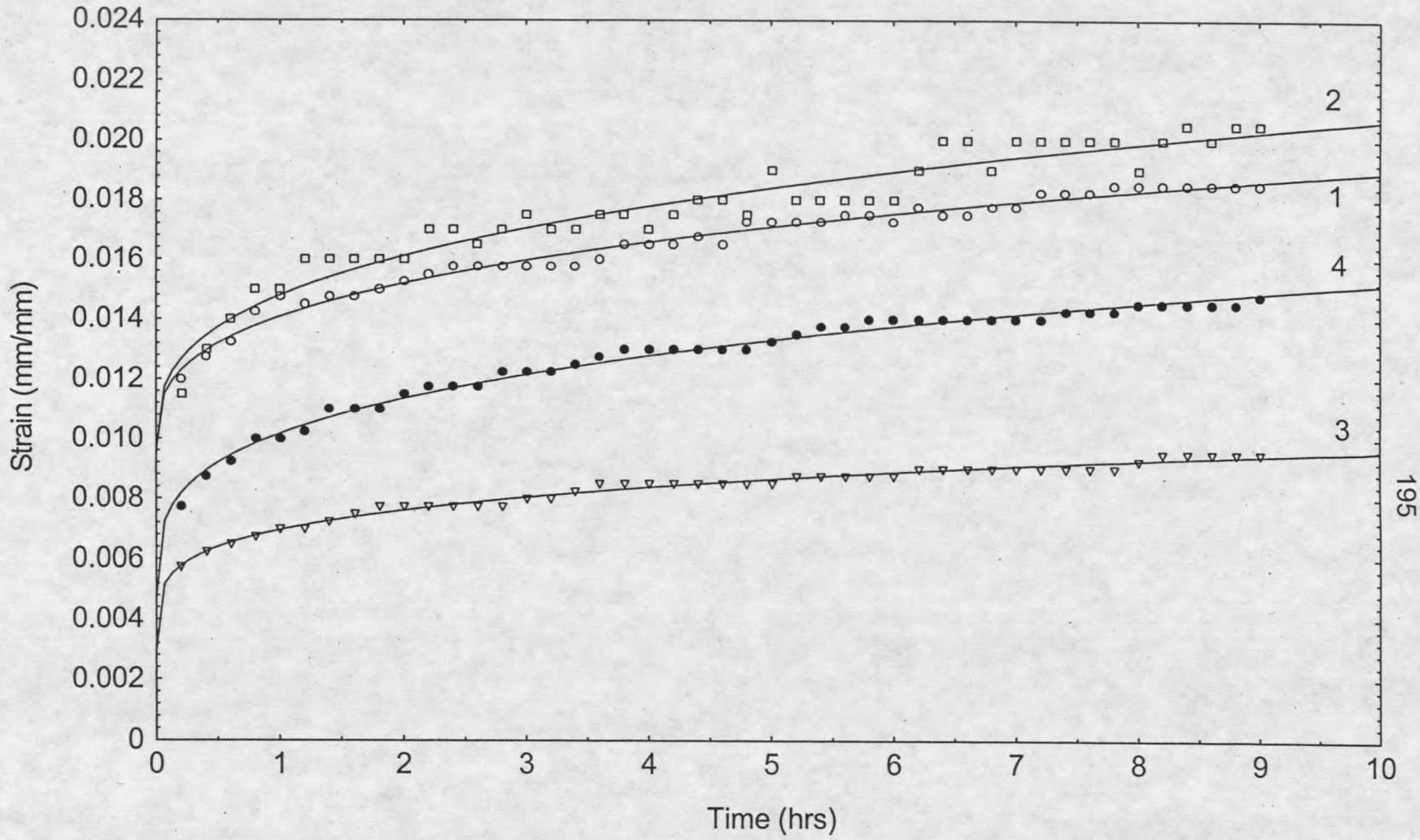


Figure B.II.10 Vibrocreep Response of Nylon 6/6 at Different Frequencies at 35 °C
1- $(0.20\pm0.10)\sigma_y$, 1 Hz; 2- $(0.20\pm0.10)\sigma_y$, 10 Hz;
3- $(0.20)\sigma_y$, 4- $(0.30)\sigma_y$, Constant Load Creep;
σ_y = 55 MPa at 35 °C

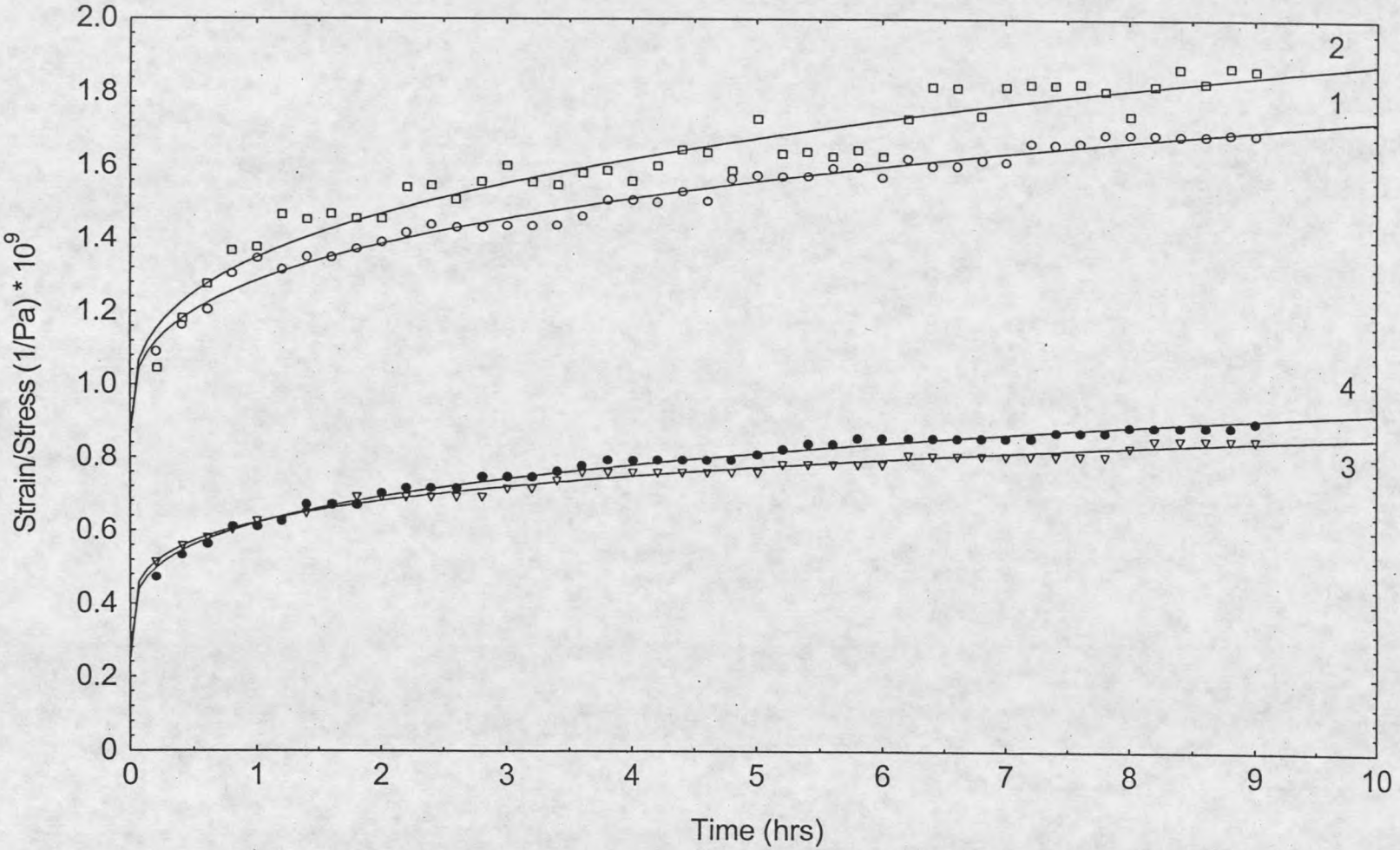


Figure B.II.11 Normalized Vibrocreep Response of Nylon 6/6 at Different Frequencies at 35 °C
1- $(0.20\pm0.10)\sigma_y$, 1 Hz; 2- $(0.20\pm0.10)\sigma_y$, 10 Hz;
3- $(0.20)\sigma_y$, 4- $(0.30)\sigma_y$, Constant Load Creep;
σ_y = 55 MPa at 35 °C

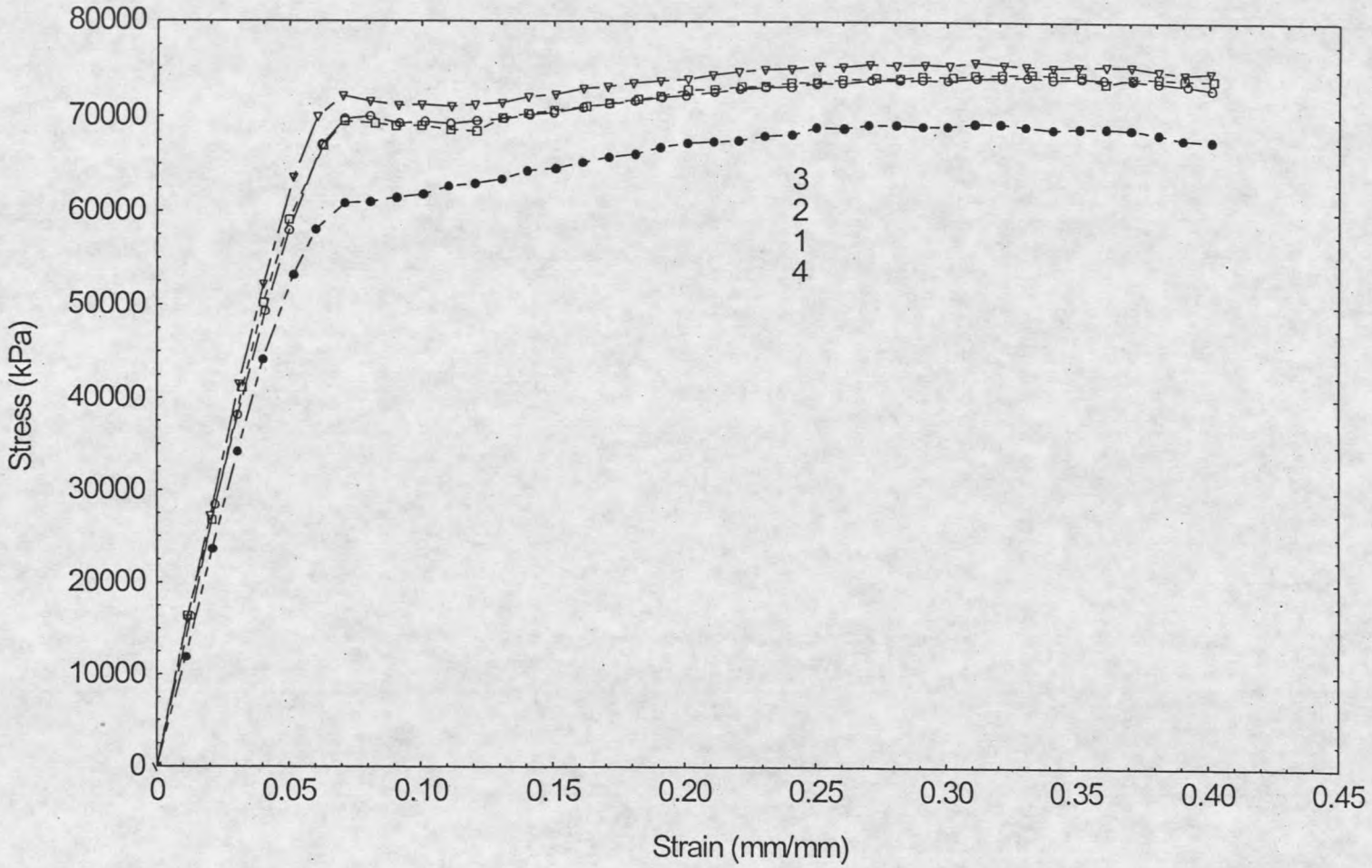


Figure B.II.12 Tensile Testing of Nylon 6/6 Specimens After Cyclic and Constant Loading at 35 °C
1- $(0.20\pm0.10)\sigma_y$, 1 Hz; 2- $(0.20\pm0.10)\sigma_y$, 10 Hz;
3- $(0.20)\sigma_y$, Constant Load Creep; 4- Virgin Specimens;
σ_y = 55 MPa at 35 °C

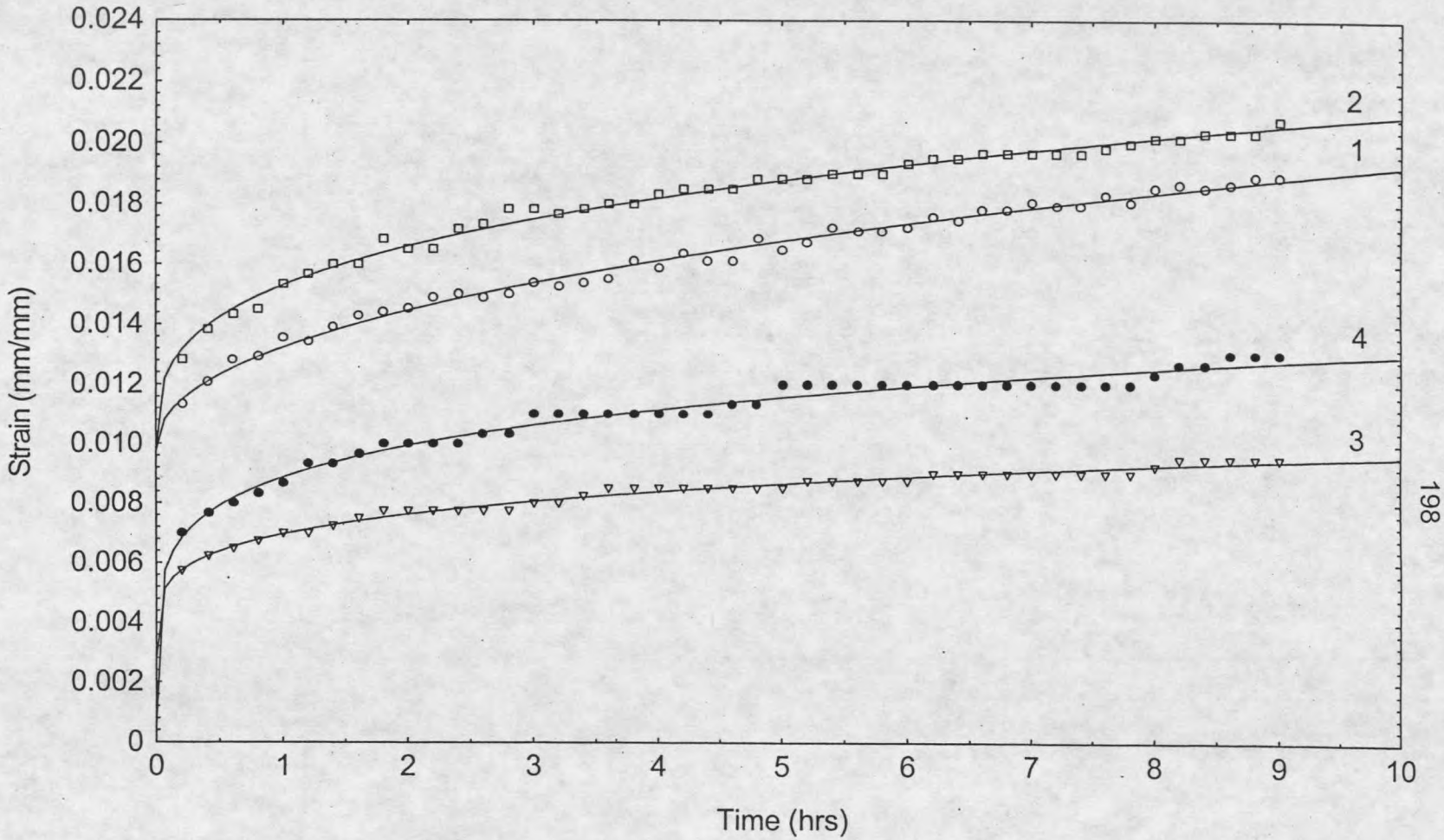


Figure B.II.13 Vibrocreep Response of Nylon 6/6 at Different Frequencies at 35 °C
1- $(0.16\pm0.04)\sigma_y$, 1 Hz; 2- $(0.16\pm0.04)\sigma_y$, 10 Hz;
3- $(0.16)\sigma_y$, 4- $(0.20)\sigma_y$, Constant Load Creep;
σ_y = 70 MPa at 23 °C

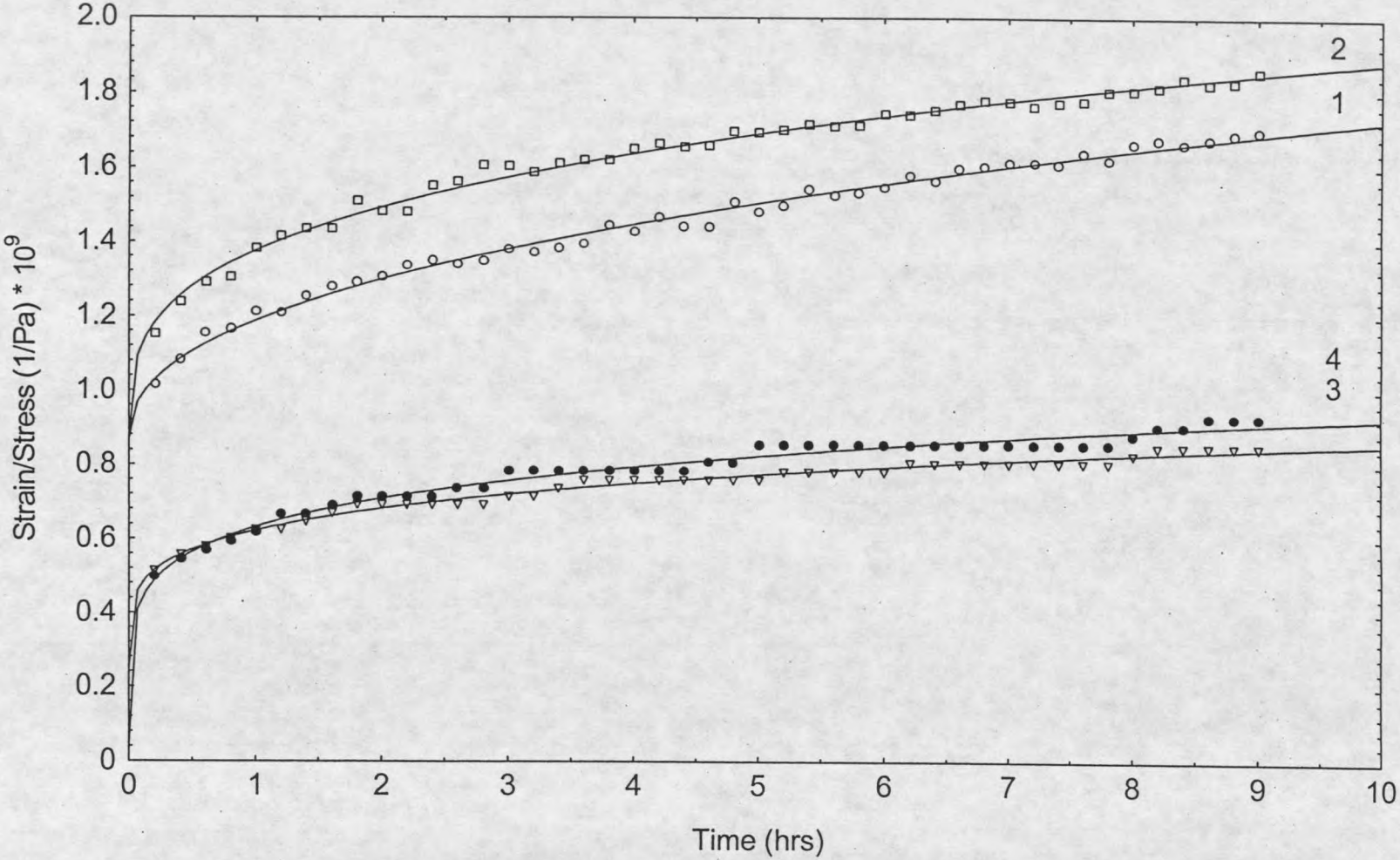


Figure B.II.14 Normalized Vibrocreep Response of Nylon 6/6 at Different Frequencies at 35 °C
1- $(0.16\pm0.04)\sigma_y$, 1 Hz; 2- $(0.16\pm0.04)\sigma_y$, 10 Hz;
3- $(0.16)\sigma_y$, 4- $(0.20)\sigma_y$, Constant Load Creep;
σ_y = 70 MPa at 23 °C

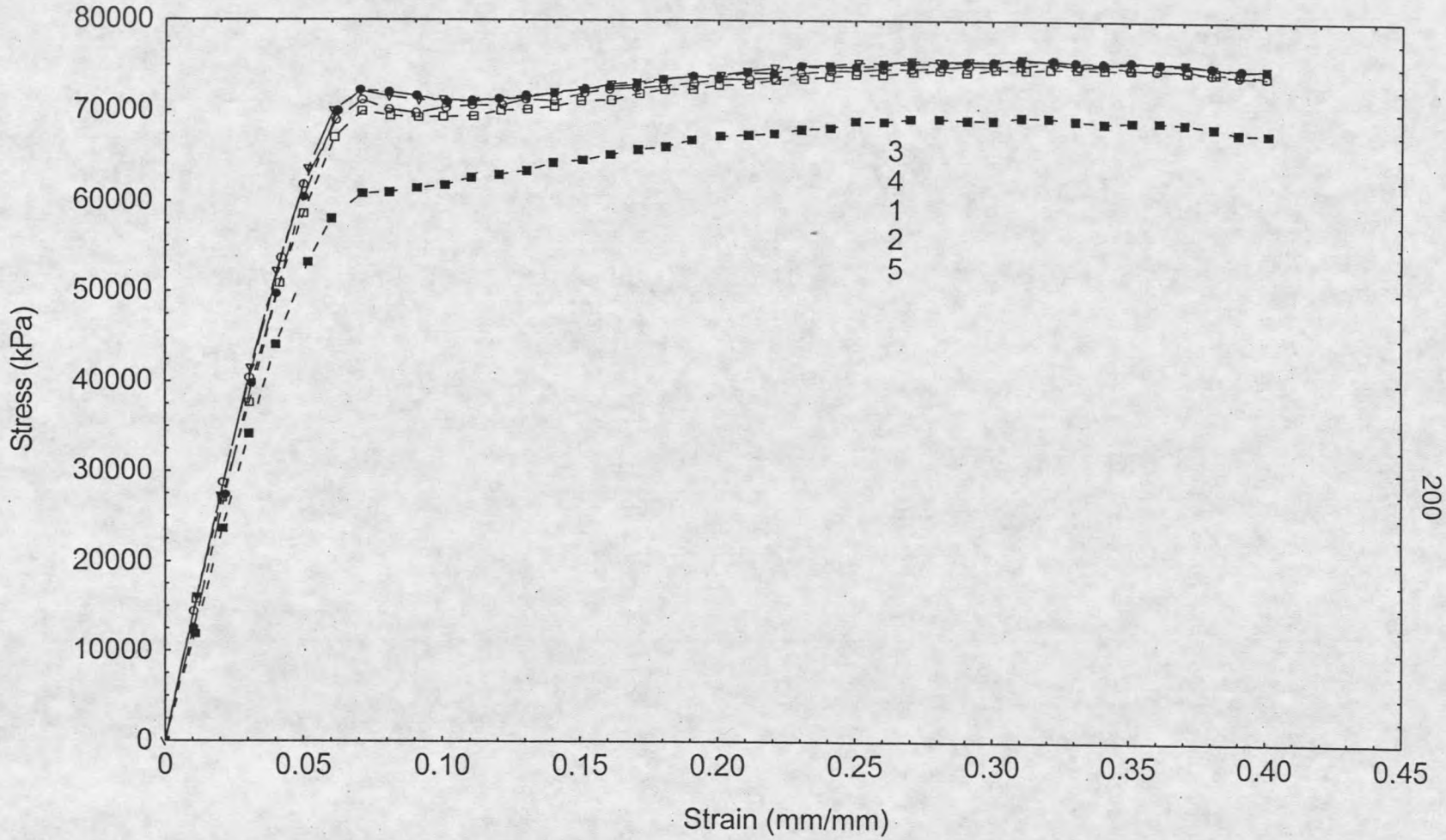


Figure B.II.15 Tensile Testing of Nylon 6/6 Specimens After Cyclic and Constant Loading at 35 °C
1- $(0.16\pm0.04)\sigma_y$, 1 Hz; 2- $(0.16\pm0.04)\sigma_y$, 10 Hz;
3- $(0.16)\sigma_y$, 4- $(0.20)\sigma_y$, Constant Load Creep; 5- Virgin Specimens;
σ_y = 70 MPa at 23 °C

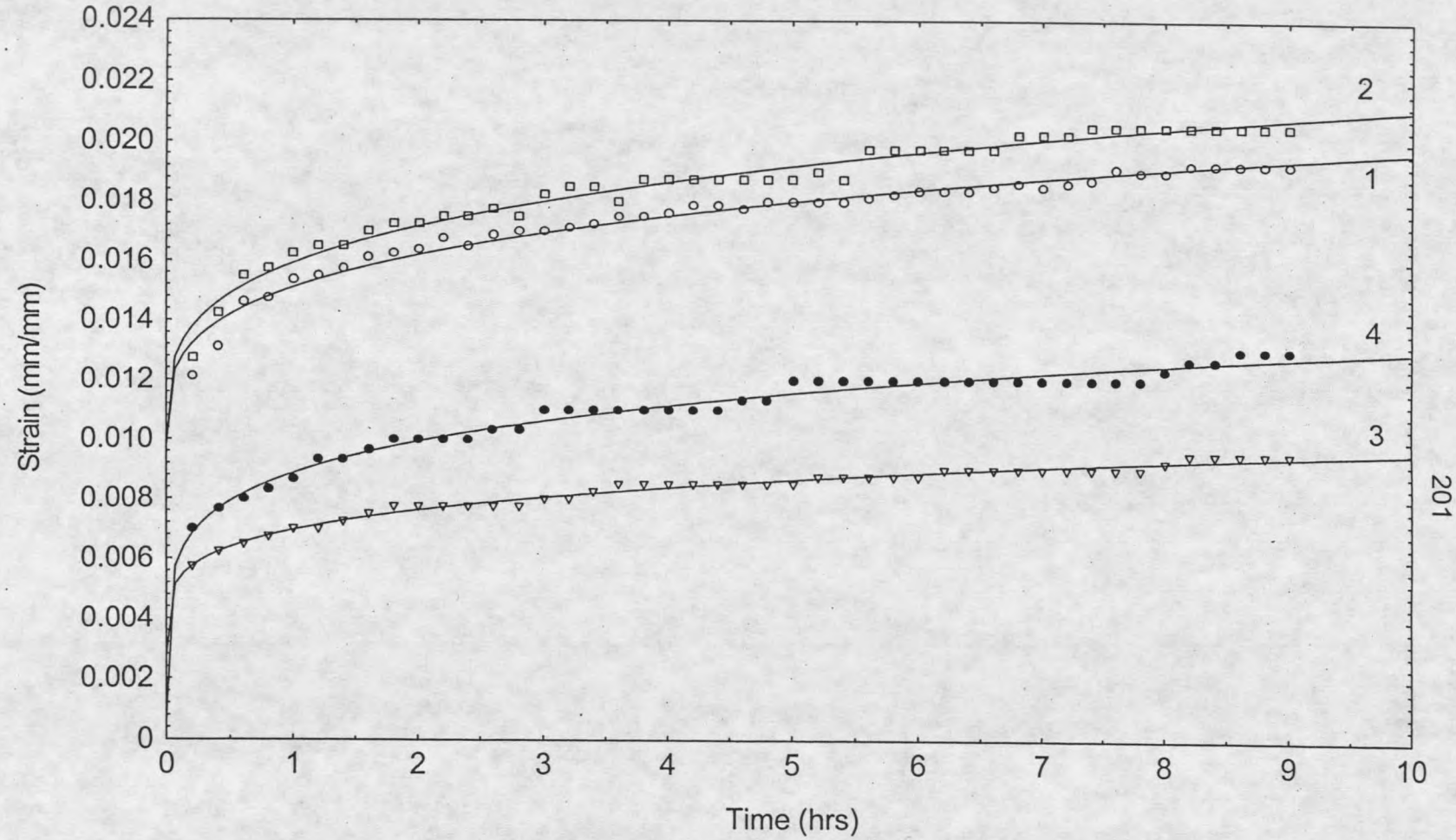


Figure B.II.16 Vibrocreep Response of Nylon 6/6 at Different Frequencies at 35 °C
1- $(0.16\pm0.10)\sigma_y$, 1 Hz; 2- $(0.16\pm0.10)\sigma_y$, 10 Hz;
3- $(0.16)\sigma_y$, 4- $(0.20)\sigma_y$, Constant Load Creep;
σ_y = 70 MPa at 23 °C

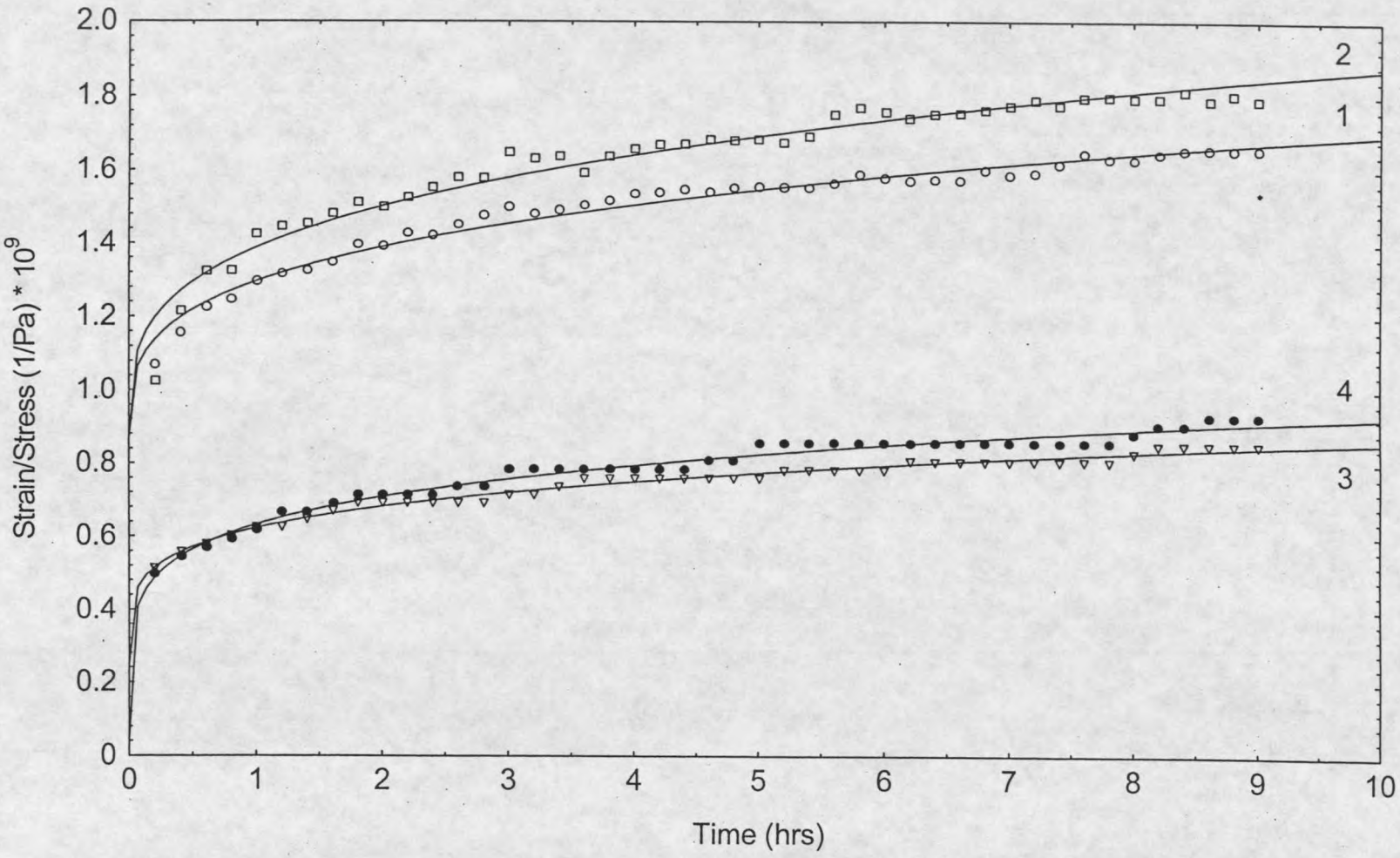


Figure B.II.17 Normalized Vibrocreep Response of Nylon 6/6 at Different Frequencies at 35 °C
1- $(0.16\pm0.10)\sigma_y$, 1 Hz; 2- $(0.16\pm0.10)\sigma_y$, 10 Hz;
3- $(0.16)\sigma_y$, 4- $(0.20)\sigma_y$, Constant Load Creep;
σ_y = 70 MPa at 23 °C

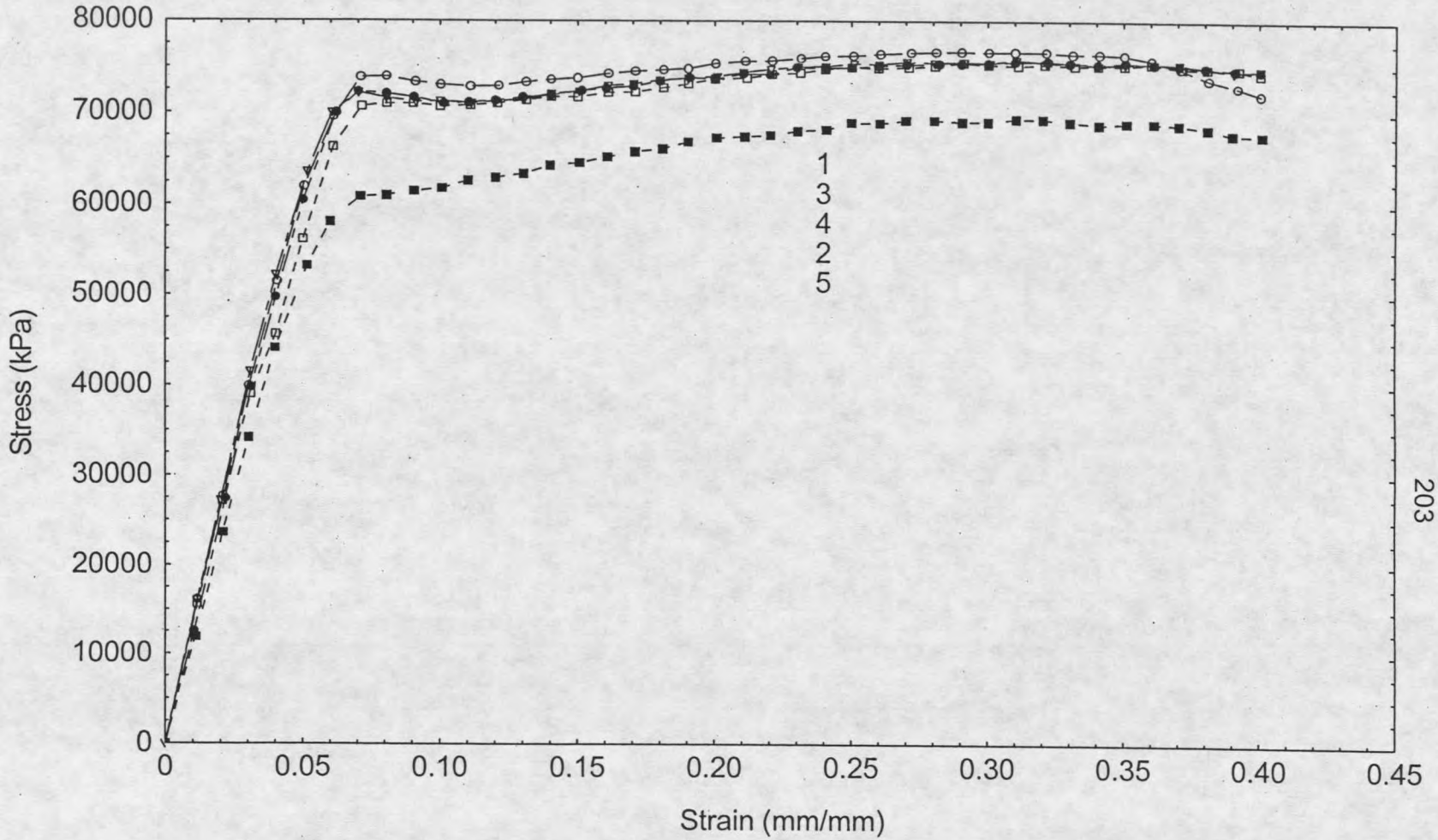


Figure B.II.18 Tensile Testing of Nylon 6/6 Specimens After Cyclic and Constant Loading at 35 °C
1- $(0.16\pm0.10)\sigma_y$, 1 Hz; 2- $(0.16\pm0.10)\sigma_y$, 10 Hz;
3- $(0.16)\sigma_y$, Constant Load Creep; 4- Virgin Specimens;
σ_y = 70 MPa at 23 °C

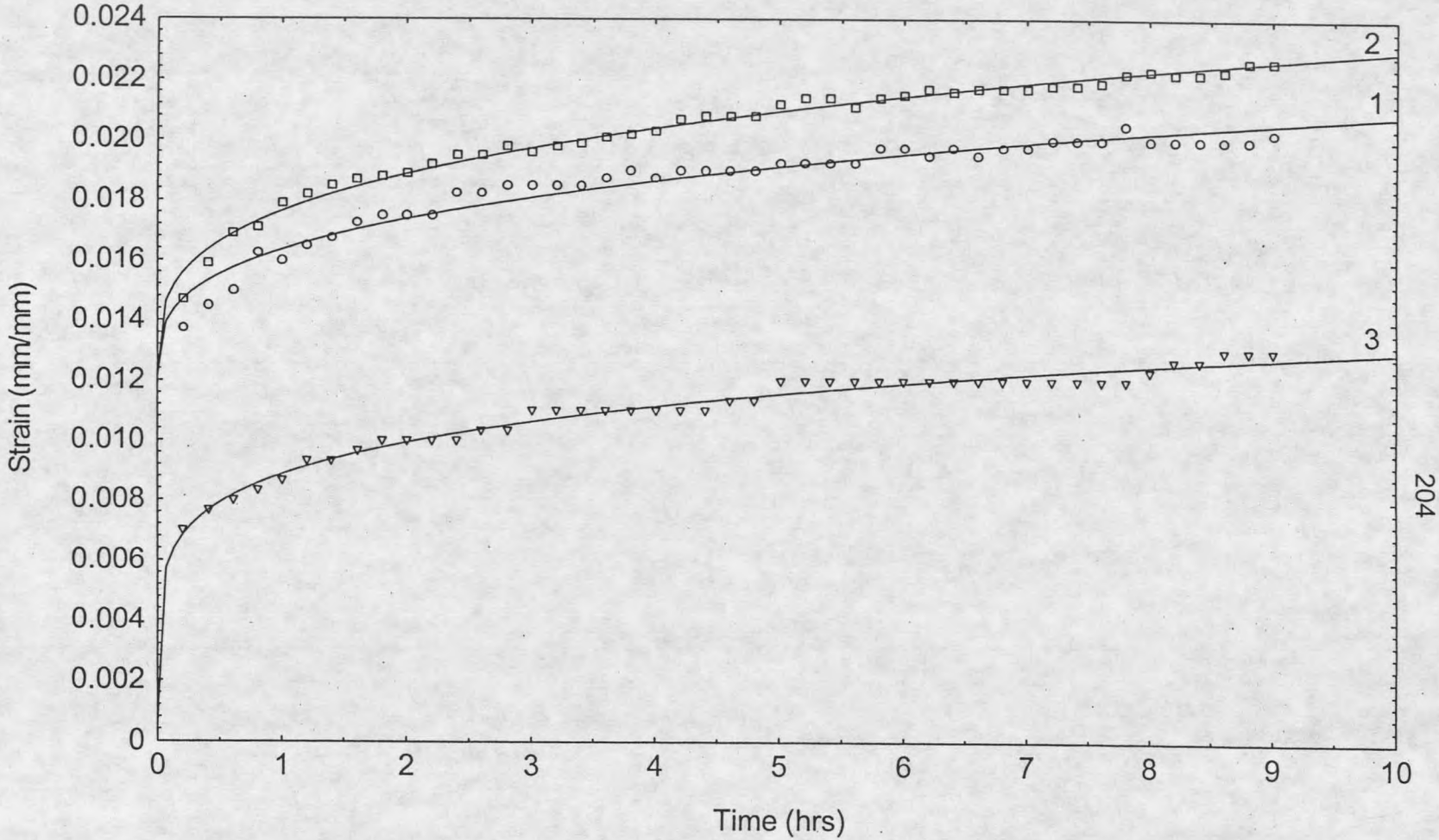


Figure B.II.19 Vibrocreep Response of Nylon 6/6 at Different Frequencies at 35 °C
1- $(0.20\pm0.05)\sigma_y$, 1 Hz; 2- $(0.20\pm0.05)\sigma_y$, 10 Hz;
3- $(0.20)\sigma_y$, Constant Load Creep;
σ_y = 70 MPa at 23 °C

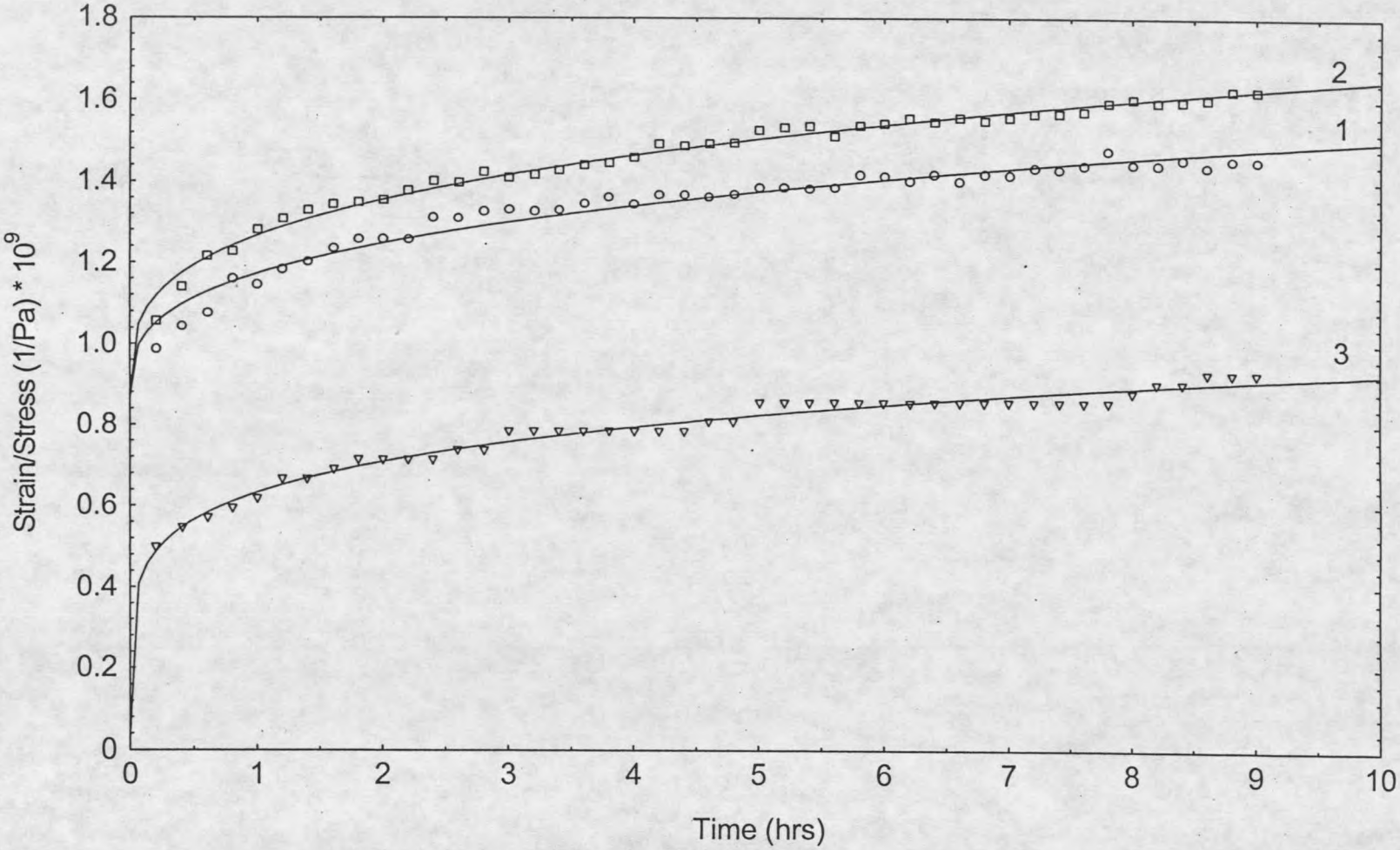


Figure B.II.20 Normalized Vibrocreep Response of Nylon 6/6 at Different Frequencies at 35 °C
1- $(0.20\pm0.05)\sigma_y$, 1 Hz; 2- $(0.20\pm0.05)\sigma_y$, 10 Hz;
3- $(0.20)\sigma_y$, Constant Load Creep;
σ_y = 70 MPa at 23 °C

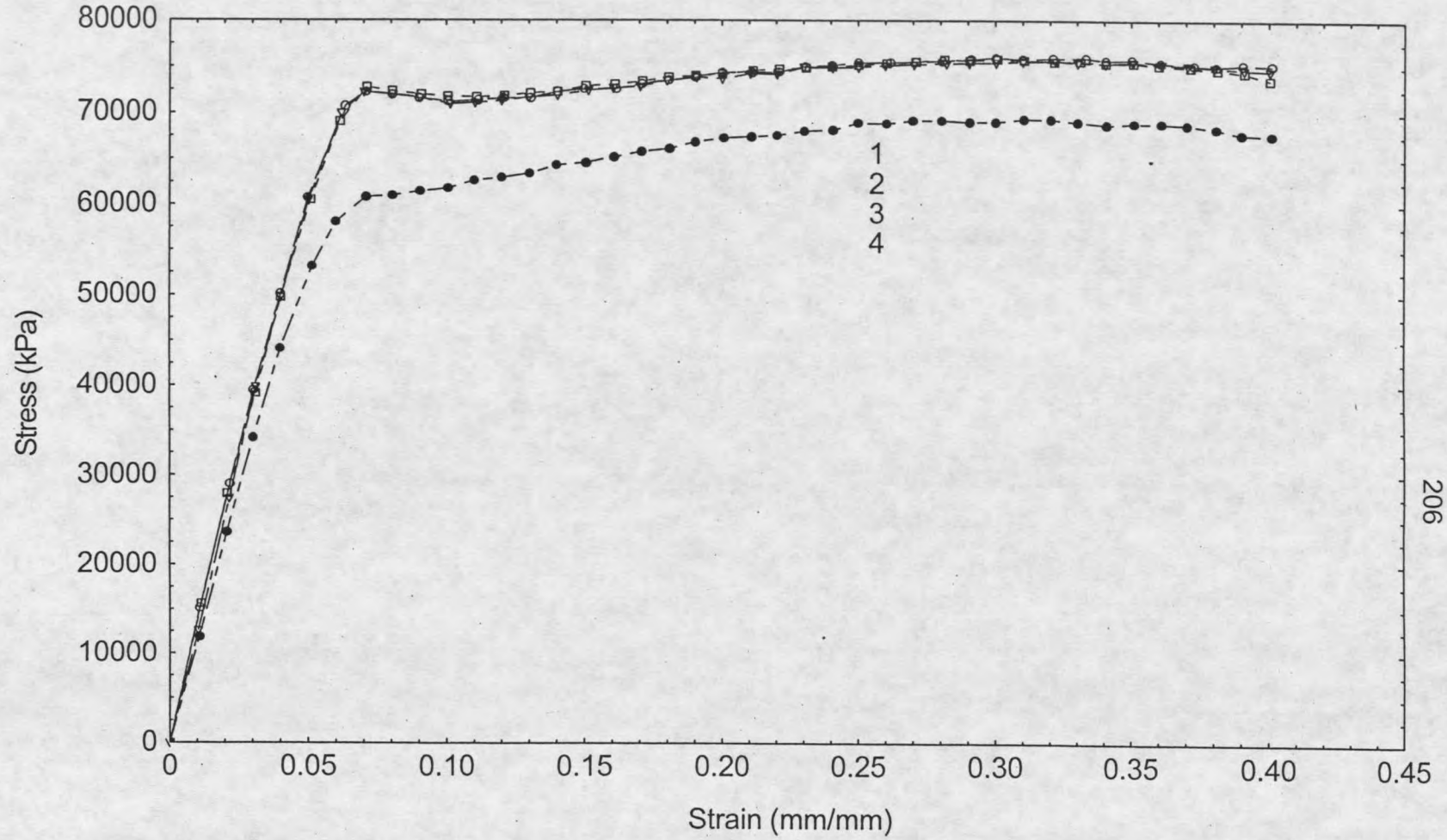


Figure B.II.21 Tensile Testing of Nylon 6/6 Specimens After Cyclic and Constant Loading at 35 °C
1- $(0.20\pm0.05)\sigma_y$, 1 Hz; 2- $(0.20\pm0.05)\sigma_y$, 10 Hz;
3- $(0.20)\sigma$, Constant Load Creep; 4- Virgin Specimens;
σ_y = 70 MPa at 23 °C

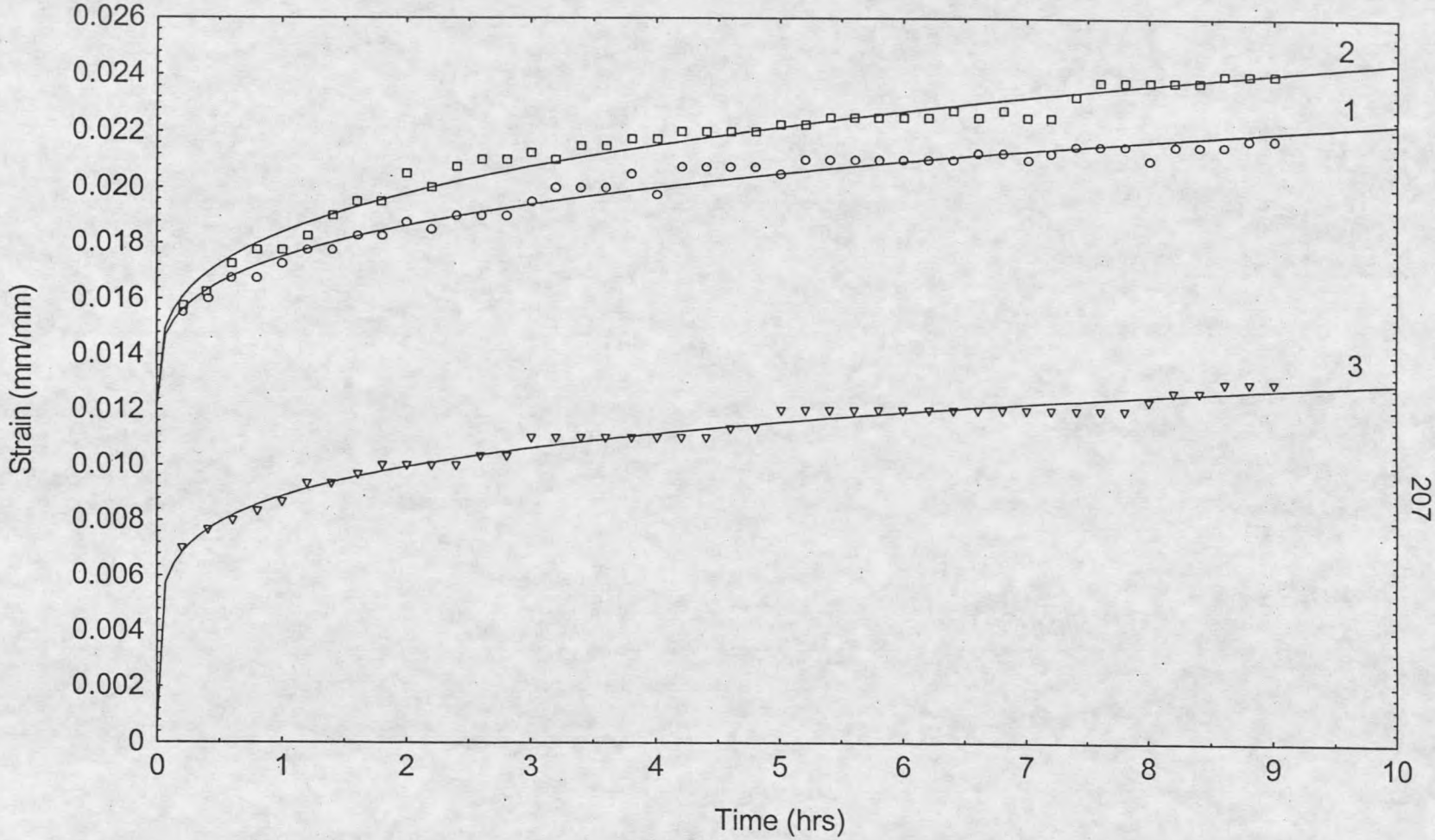


Figure B.II.22 Vibrocreep Response of Nylon 6/6 at Different Frequencies at 35 °C
1- $(0.20\pm0.10)\sigma_y$, 1 Hz; 2- $(0.20\pm0.10)\sigma_y$, 10 Hz;
3- $(0.20)\sigma_y$, Constant Load Creep;
σ_y = 70 MPa at 23 °C

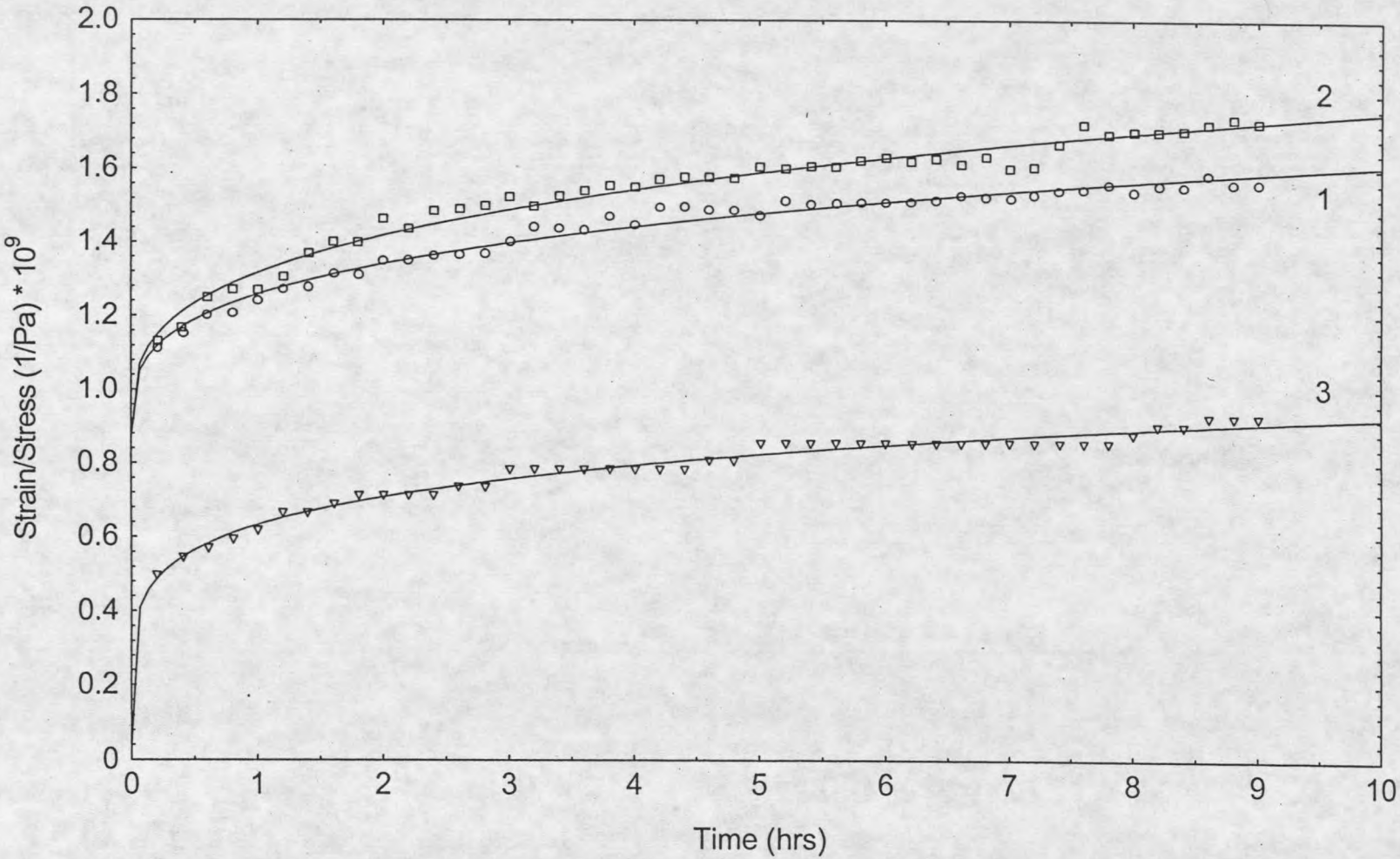


Figure B.II.23 Normalized Vibrocreep Response of Nylon 6/6 at Different Frequencies at 35 °C
1- $(0.20\pm0.10)\sigma_y$, 1 Hz; 2- $(0.20\pm0.10)\sigma_y$, 10 Hz;
3- $(0.20)\sigma_y$, Constant Load Creep;
σ_y = 70 MPa at 23 °C

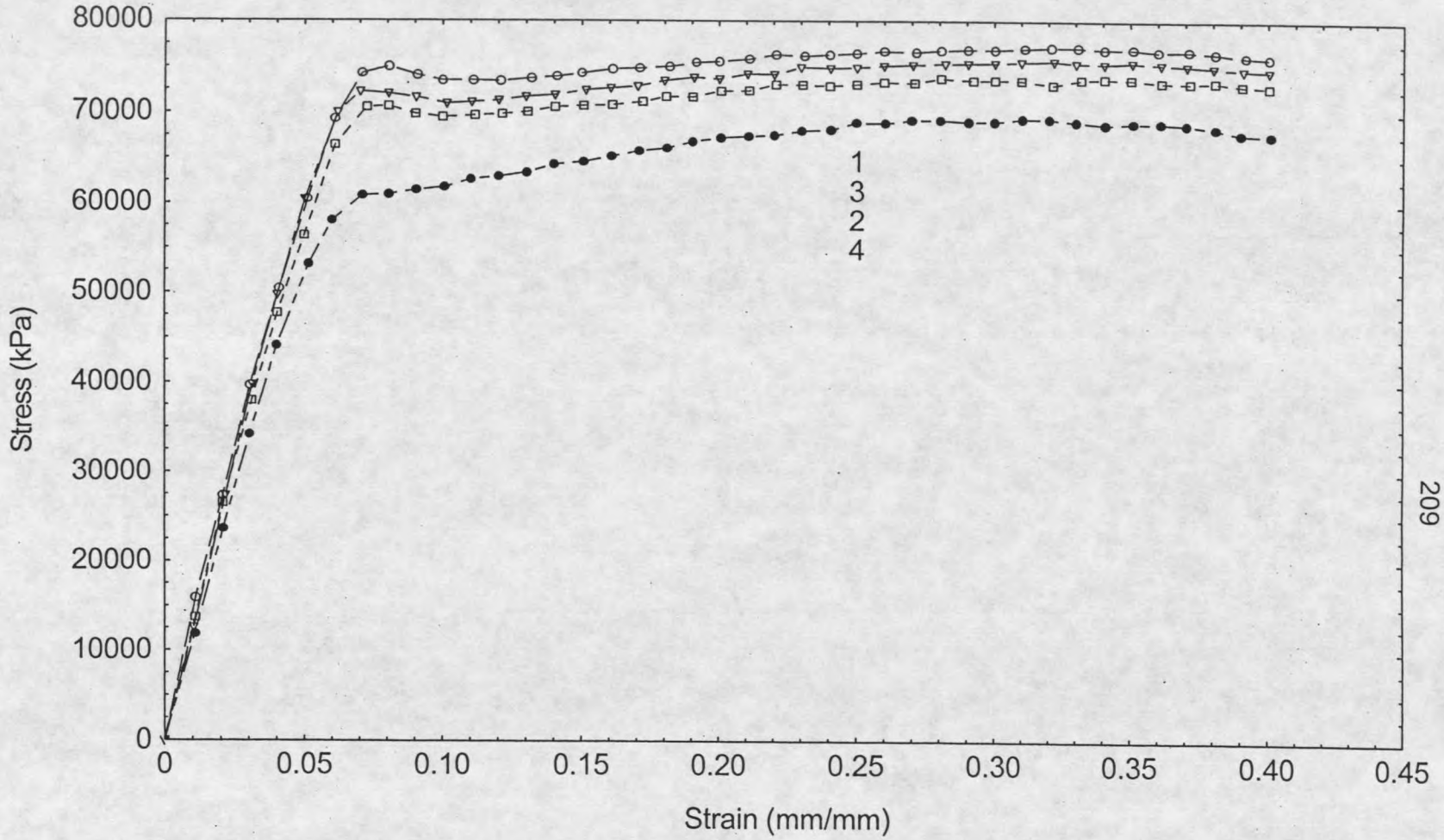


Figure B.II.24 Tensile Testing of Nylon 6/6 Specimens After Cyclic and Constant Loading at 35 °C
1- $(0.20\pm0.10)\sigma_y$, 1 Hz; 2- $(0.20\pm0.10)\sigma_y$, 10 Hz;
3- $(0.20)\sigma_y$, Constant Load Creep; 4- Virgin Specimens;
σ_y = 70 MPa at 23 °C

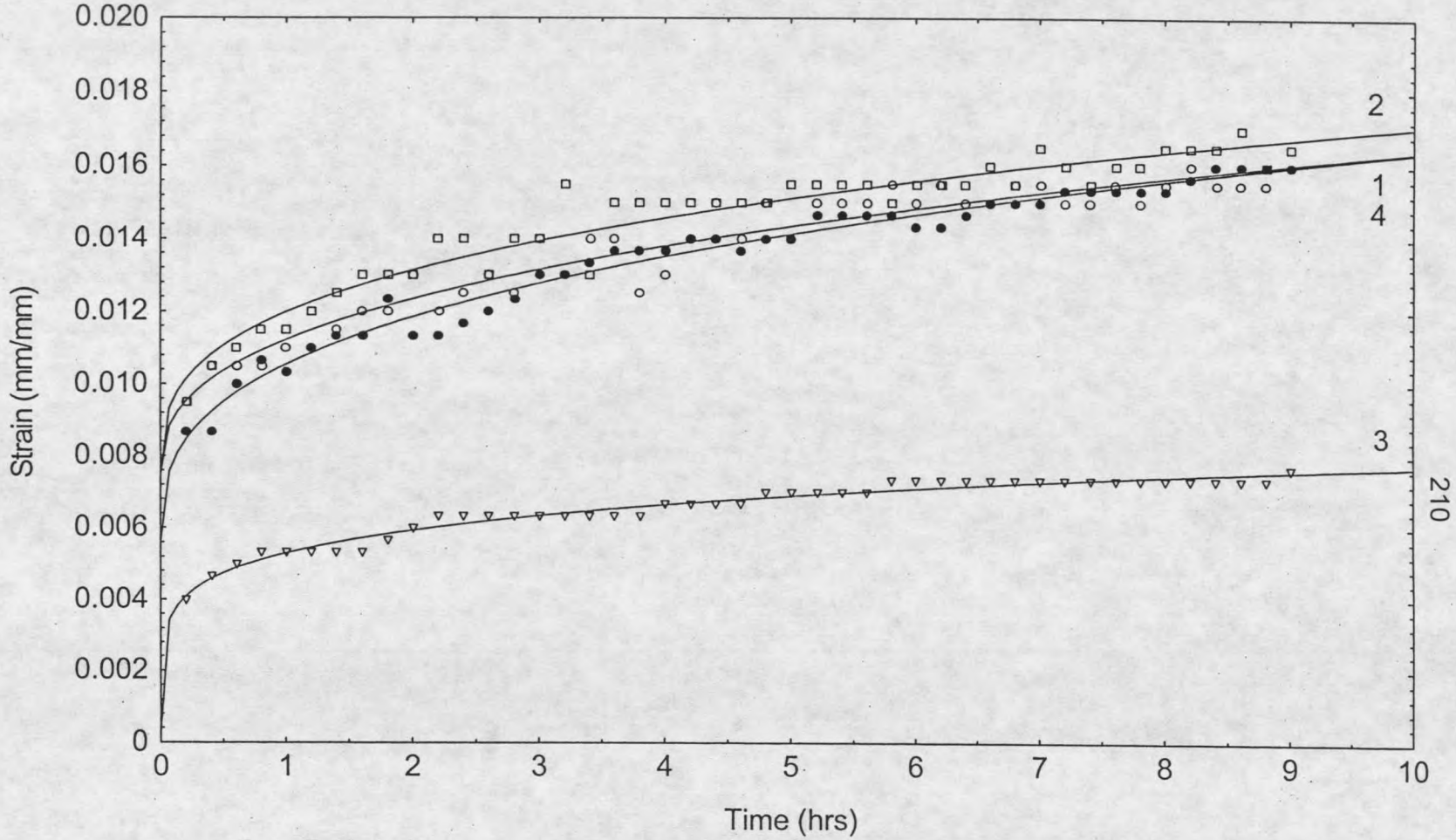


Figure B.III.1 Vibrocreep Response of Nylon 6/6 at Different Frequencies at 41 °C
1- $(0.16\pm0.10)\sigma_y$, 1 Hz; 2- $(0.16\pm0.10)\sigma_y$, 10 Hz;
3- $(0.16)\sigma_y$, 4- $(0.30)\sigma_y$, Constant Load Creep;
σ_y = 45 MPa at 41 °C

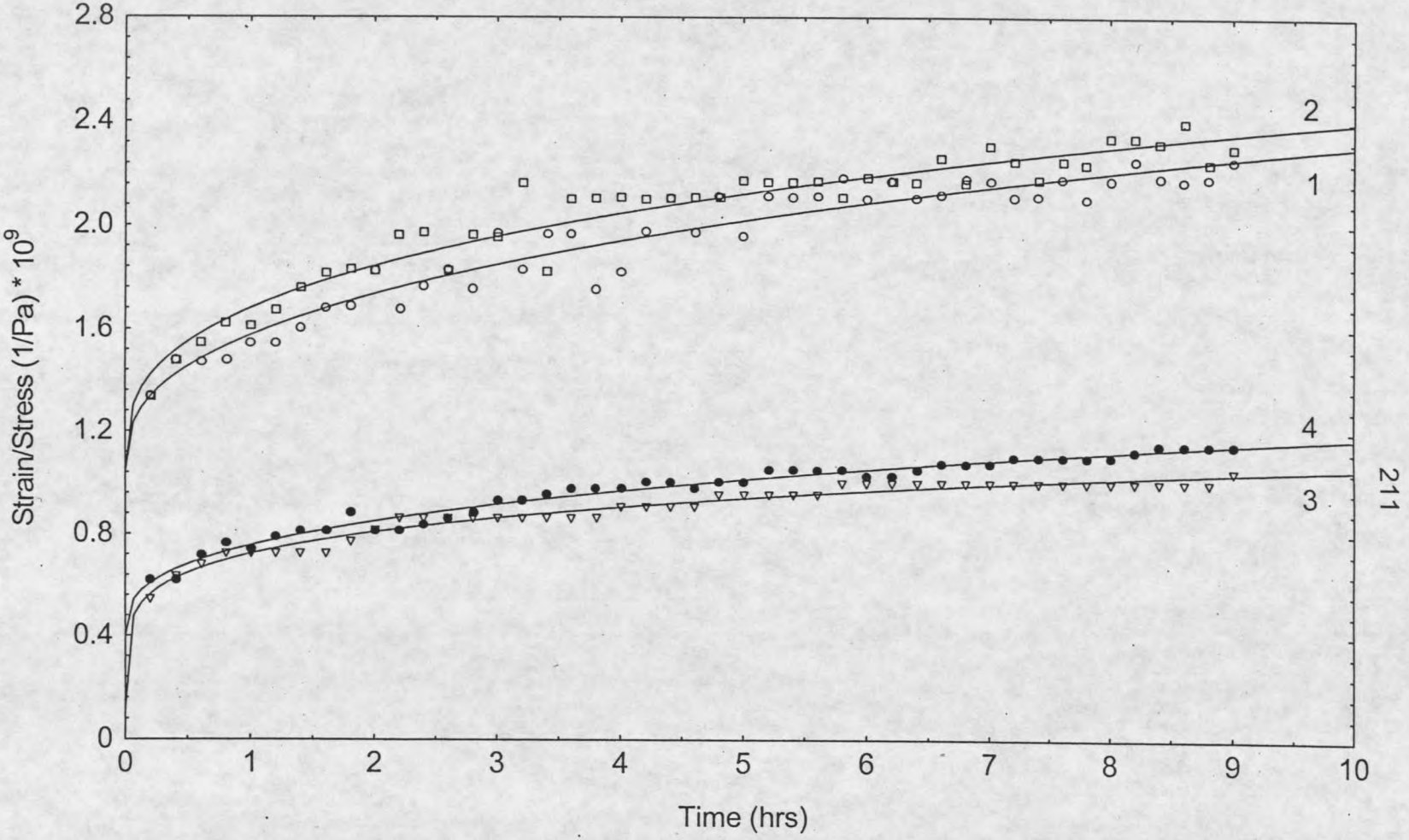


Figure B.III.2 Normalized Vibrocreep Response of Nylon 6/6 at Different Frequencies at 41 °C
1- $(0.16\pm0.10)\sigma_y$, 1 Hz; 2- $(0.16\pm0.10)\sigma_y$, 10 Hz;
3- $(0.16)\sigma_y$, 4- $(0.30)\sigma_y$, Constant Load Creep;
σ_y = 45 MPa at 41 °C

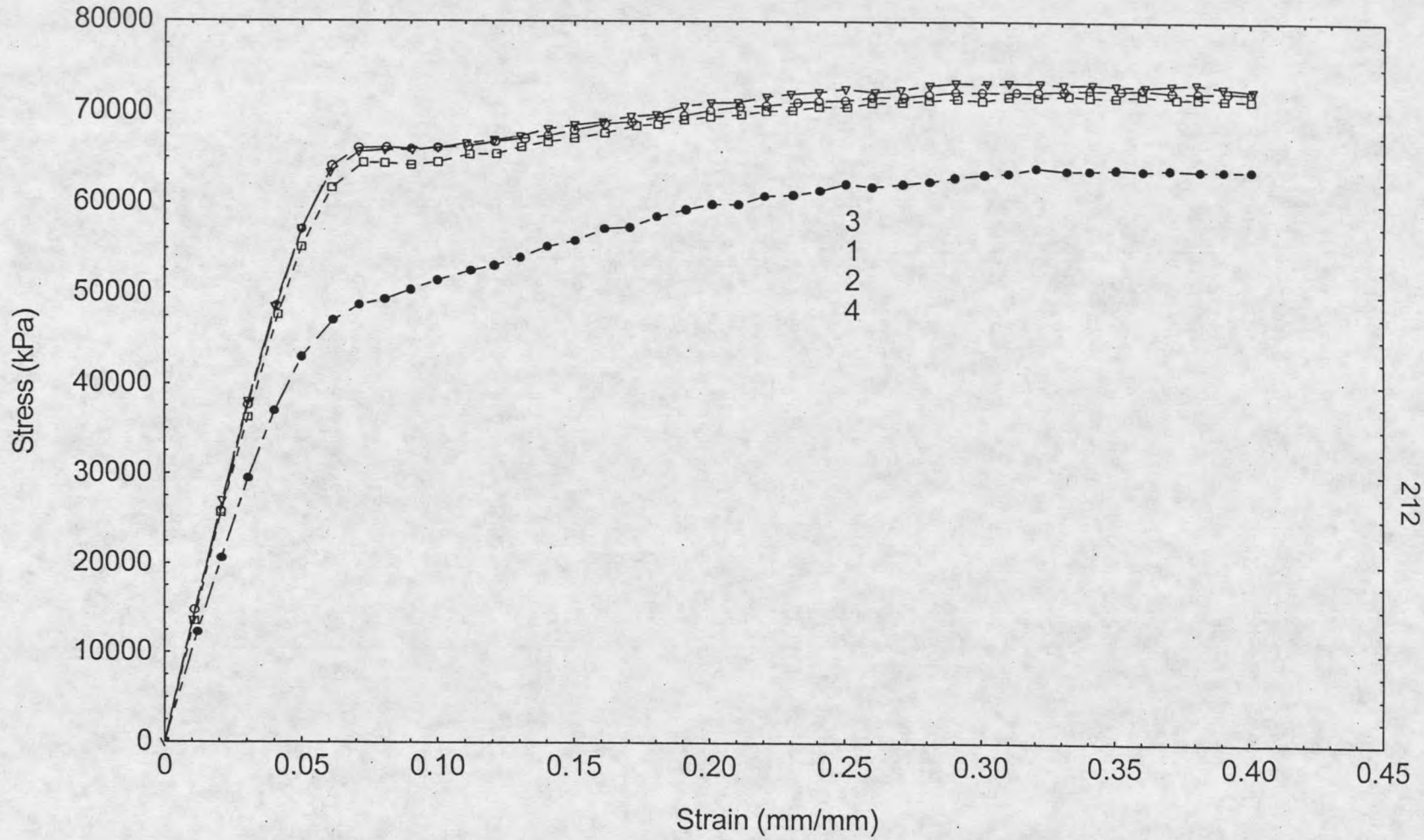


Figure B.III.3 Tensile Testing of Nylon 6/6 Specimens After Cyclic and Constant Loading at 41 °C
1- $(0.16\pm0.10)\sigma_y$, 1 Hz; 2- $(0.16\pm0.10)\sigma_y$, 10 Hz;
3- $(0.16)\sigma_y$, Constant Load Creep; 4- Virgin Specimens;
σ_y = 45 MPa at 41 °C

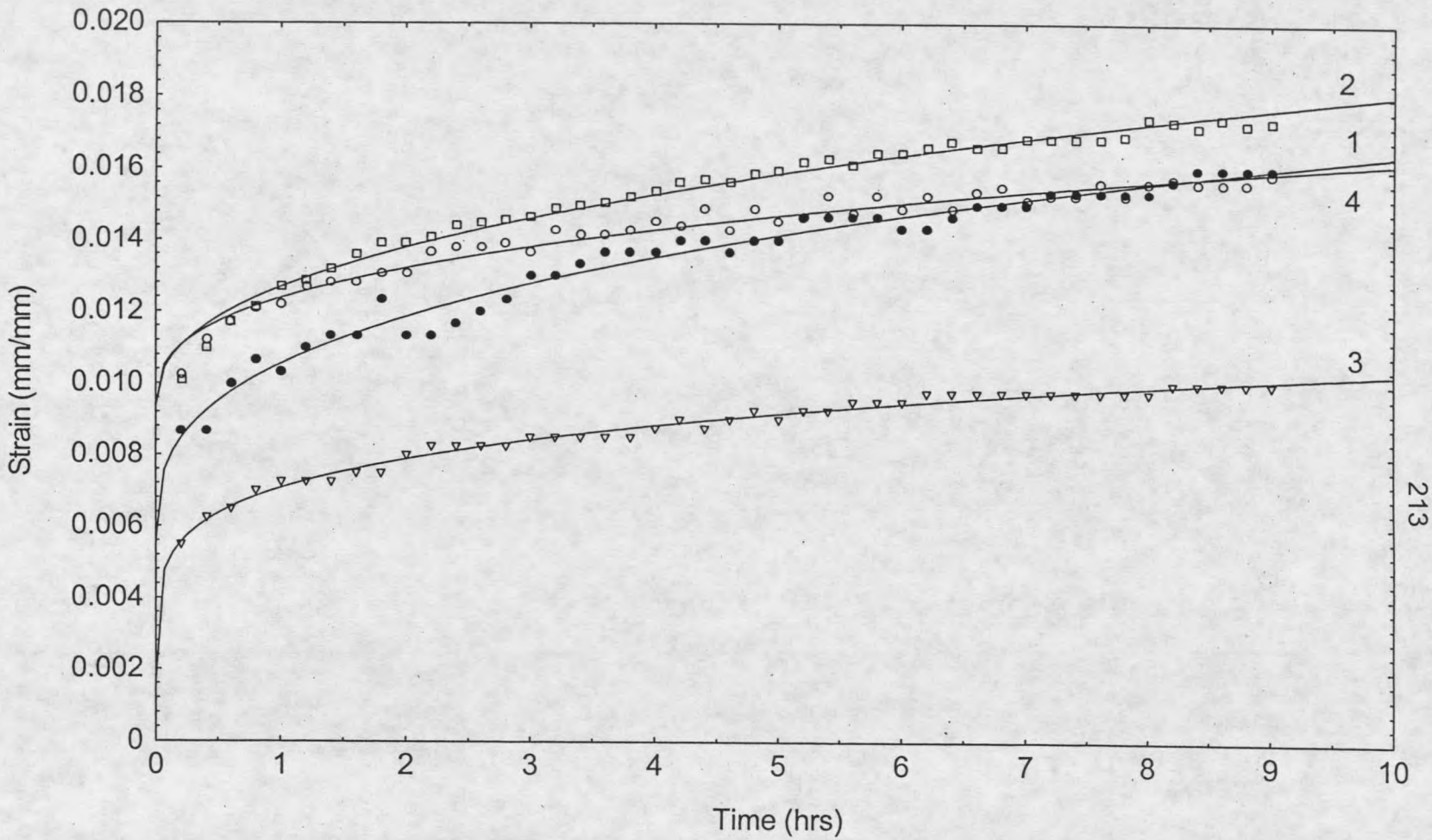


Figure B.III.4 Vibrocreep Response of Nylon 6/6 at Different Frequencies at 41 °C
1- $(0.20\pm0.05)\sigma_y$, 1 Hz; 2- $(0.20\pm0.05)\sigma_y$, 10 Hz;
3- $(0.20)\sigma_y$, 4- $(0.30)\sigma_y$, Constant Load Creep;
σ_y = 45 MPa at 41 °C

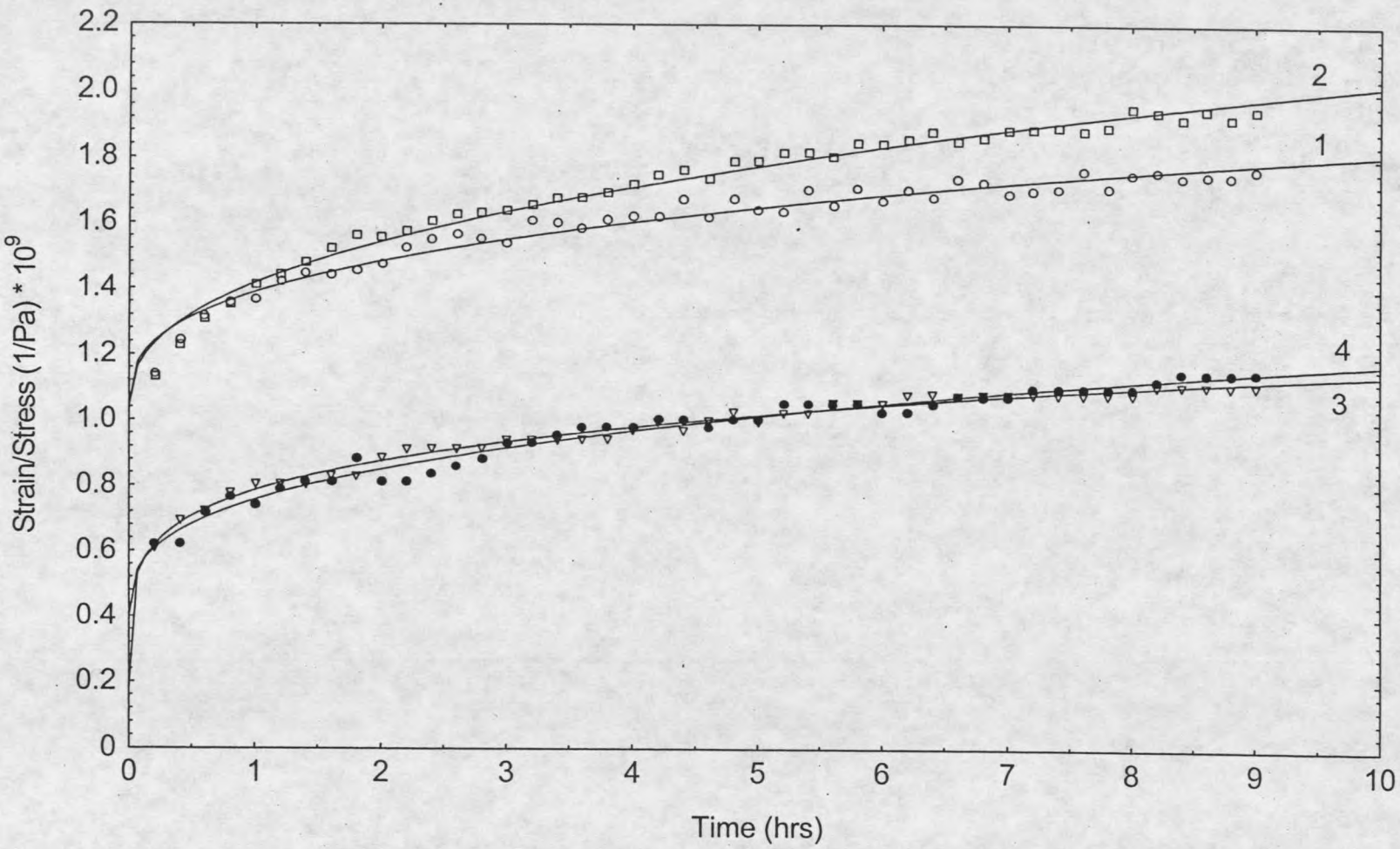


Figure B.III.5 Normalized Vibrocreep Response of Nylon 6/6 at Different Frequencies at 41 °C
1- $(0.20\pm0.05)\sigma_y$, 1 Hz; 2- $(0.20\pm0.05)\sigma_y$, 10 Hz;
3- $(0.20)\sigma_y$, 4- $(0.30)\sigma_y$, Constant Load Creep;
σ_y = 45 MPa at 41 °C

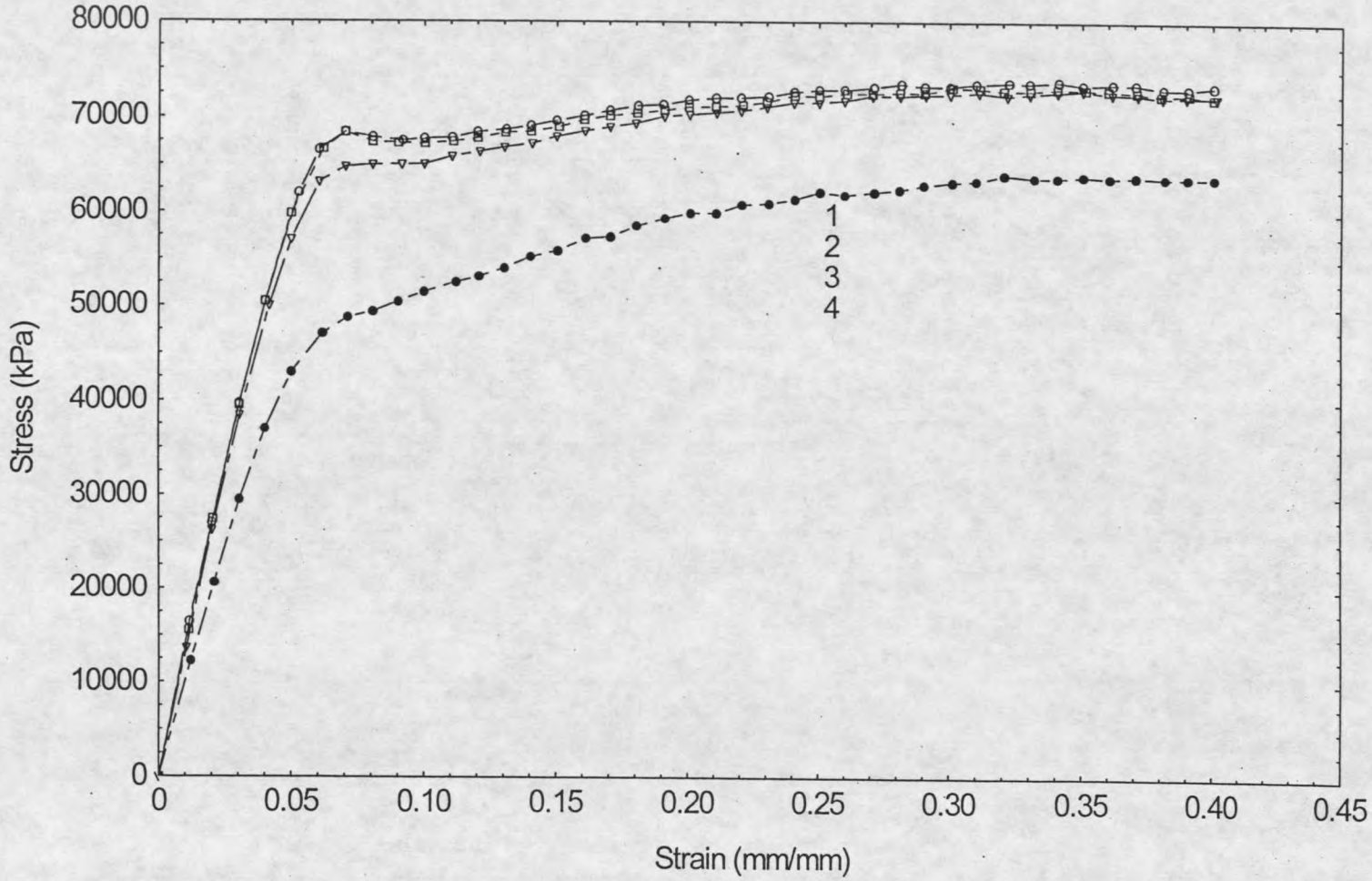


Figure B.III.6 Tensile Testing of Nylon 6/6 Specimens After Cyclic and Constant Loading at 41 °C
1- $(0.20\pm0.05)\sigma_y$, 1 Hz; 2- $(0.20\pm0.05)\sigma_y$, 10 Hz;
3- $(0.20)\sigma$, Constant Load Creep; 4- Virgin Specimens;
σ_y = 45 MPa at 41 °C

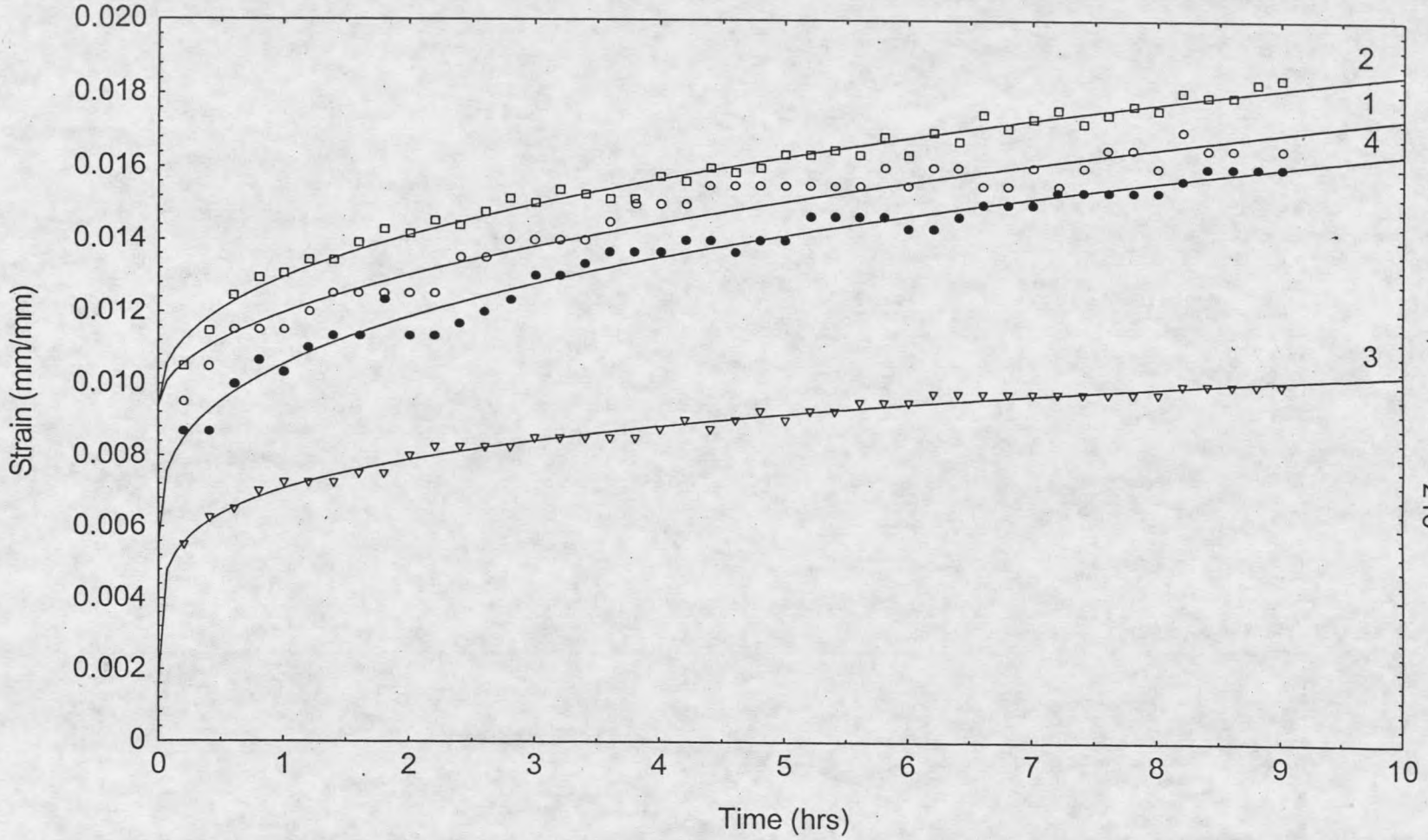


Figure B.III.7 Vibrocreep Response of Nylon 6/6 at Different Frequencies at 41 °C
1- $(0.20\pm0.10)\sigma_y$, 1 Hz; 2- $(0.20\pm0.10)\sigma_y$, 10 Hz;
3- $(0.20)\sigma_y$, 4- $(0.30)\sigma_y$, Constant Load Creep;
σ_y = 45 MPa at 41 °C

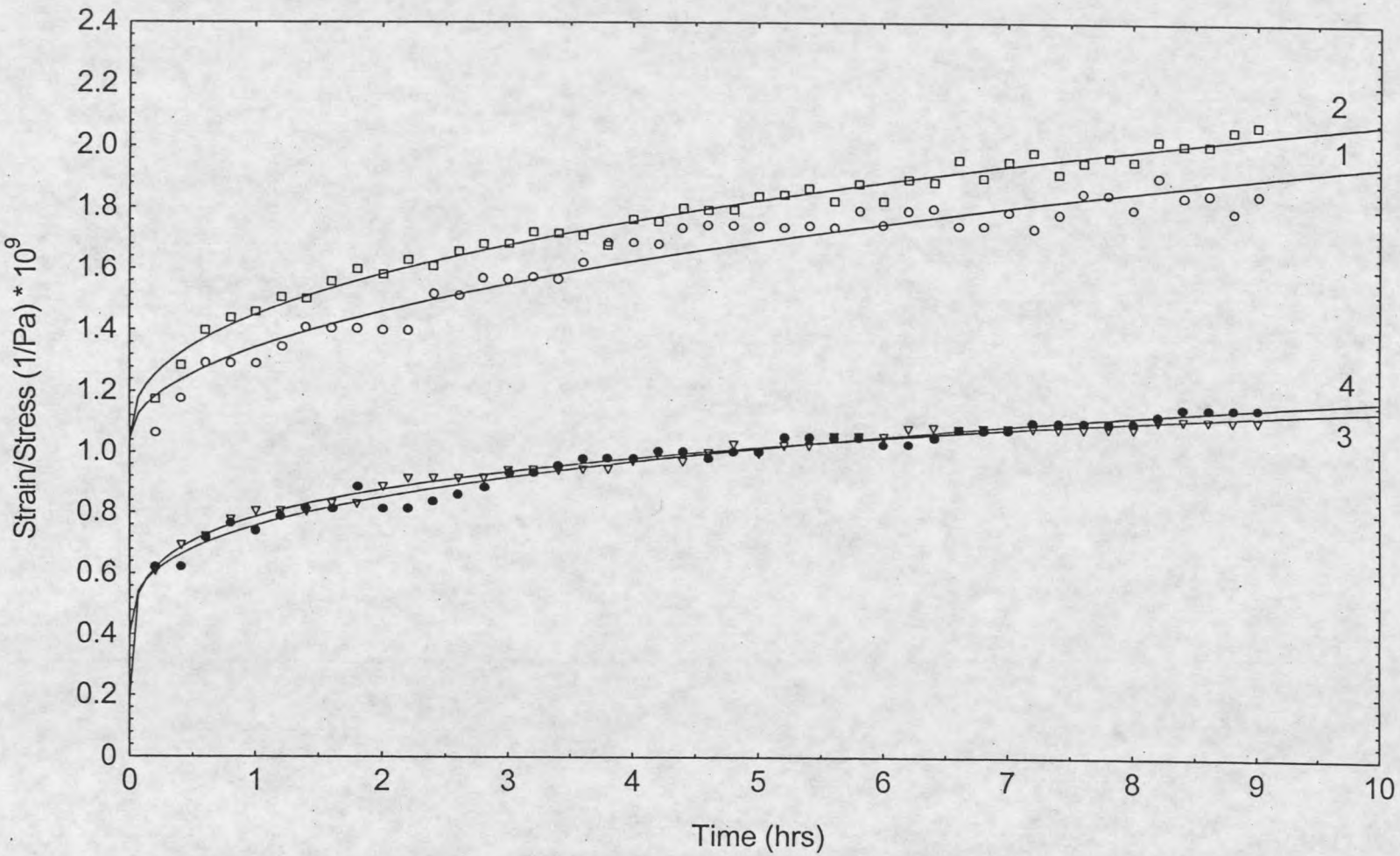


Figure B.III.8 Normalized Vibrocreep Response of Nylon 6/6 at Different Frequencies at 41 °C
1- $(0.20\pm0.10)\sigma_y$, 1 Hz; 2- $(0.20\pm0.10)\sigma_y$, 10 Hz;
3- $(0.20)\sigma_y$, 4- $(0.30)\sigma_y$, Constant Load Creep;
σ_y = 45 MPa at 41 °C

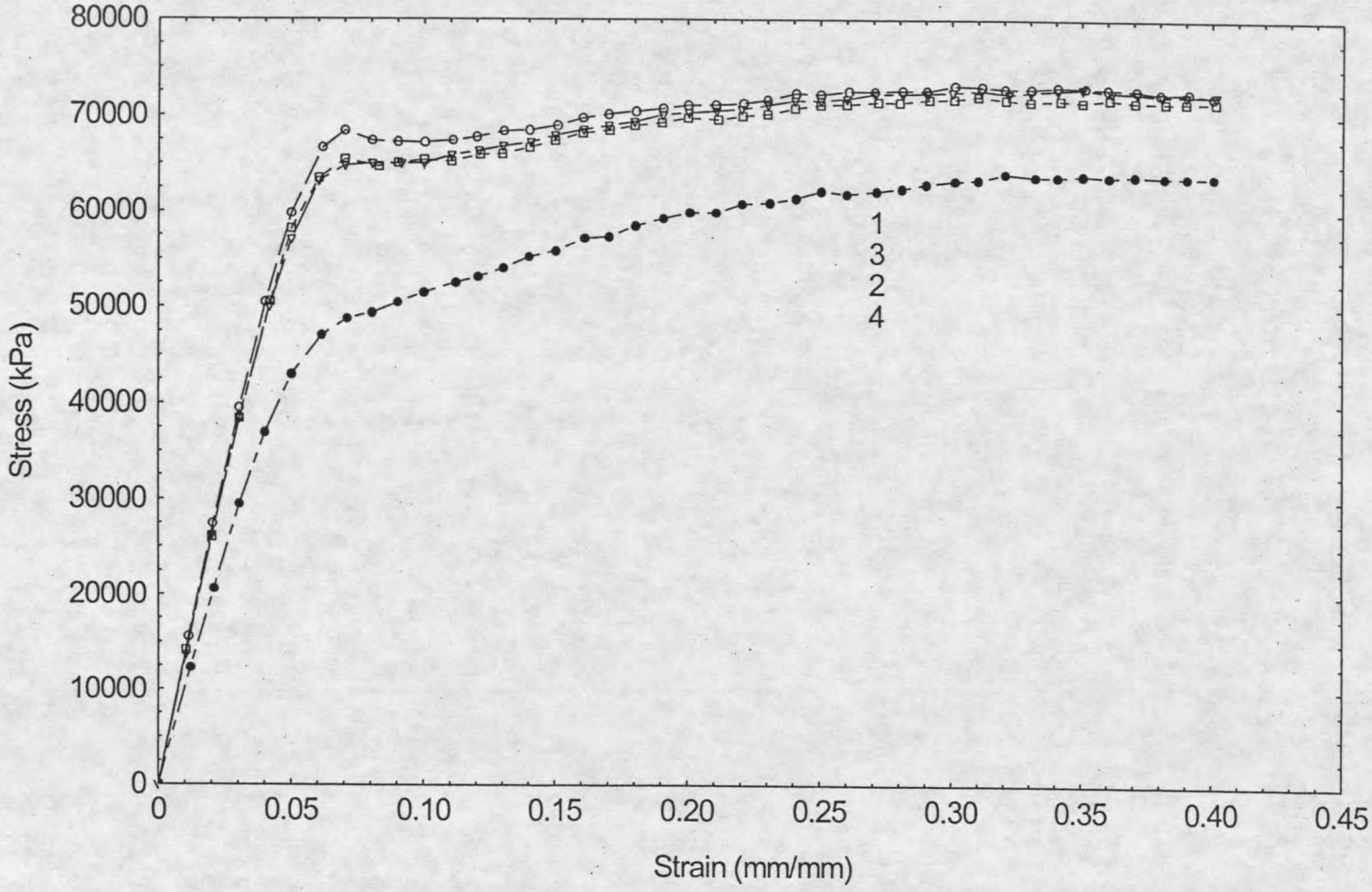


Figure B.III.9 Tensile Testing of Nylon 6/6 Specimens After Cyclic and Constant Loading at 41 °C
1- $(0.20\pm0.10)\sigma_y$, 1 Hz; 2- $(0.20\pm0.10)\sigma_y$, 10 Hz;
3- $(0.20)\sigma_y$, Constant Load Creep; 4- Virgin Specimens;
σ_y = 45 MPa at 41 °C

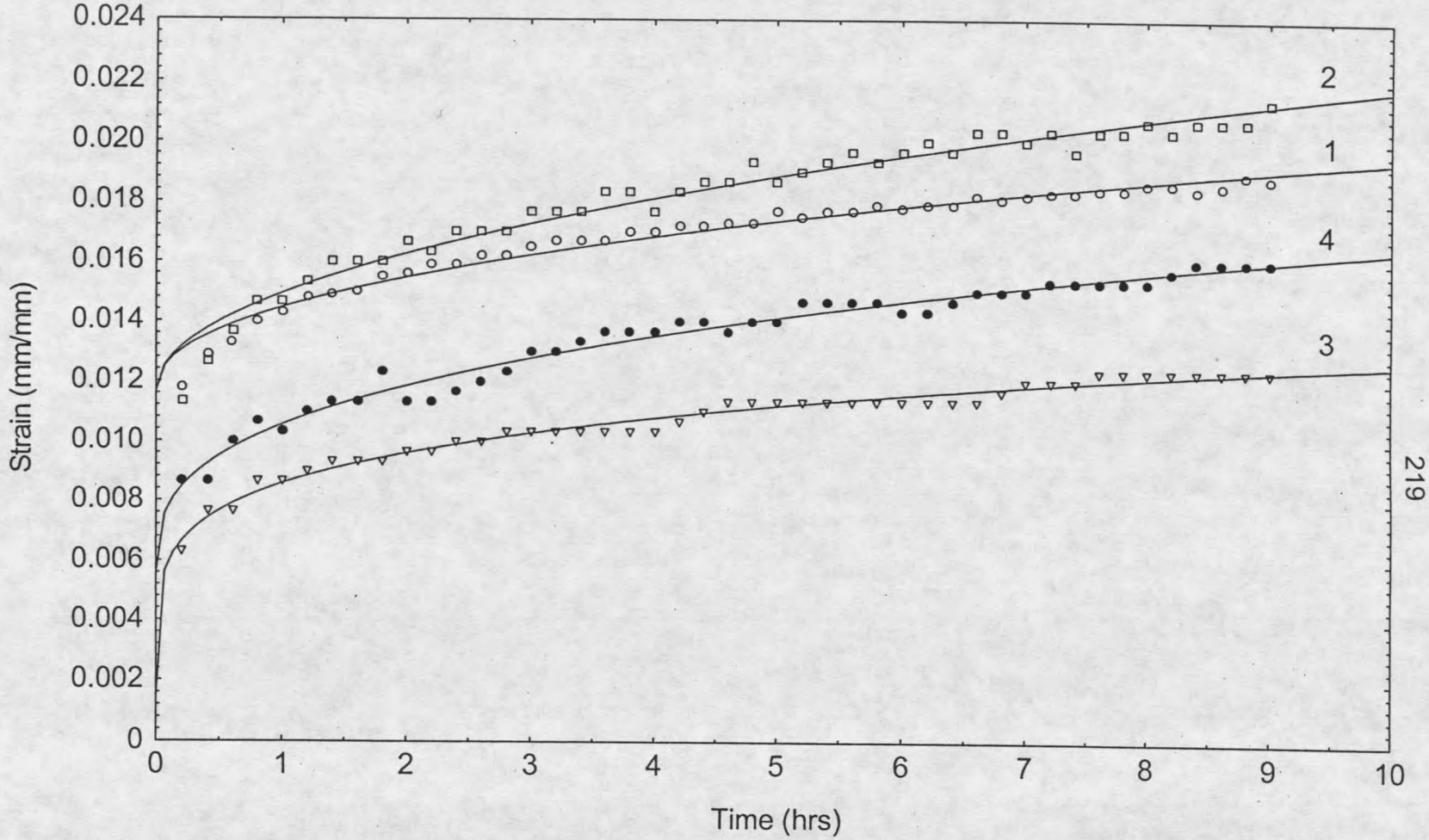


Figure B.III.10 Vibrocreep Response of Nylon 6/6 at Different Frequencies at 41 °C
1- $(0.16\pm0.04)\sigma_y$, 1 Hz; 2- $(0.16\pm0.04)\sigma_y$, 10 Hz;
3- $(0.16)\sigma_y$, 4- $(0.20)\sigma_y$, Constant Load Creep;
σ_y = 70 MPa at 23 °C

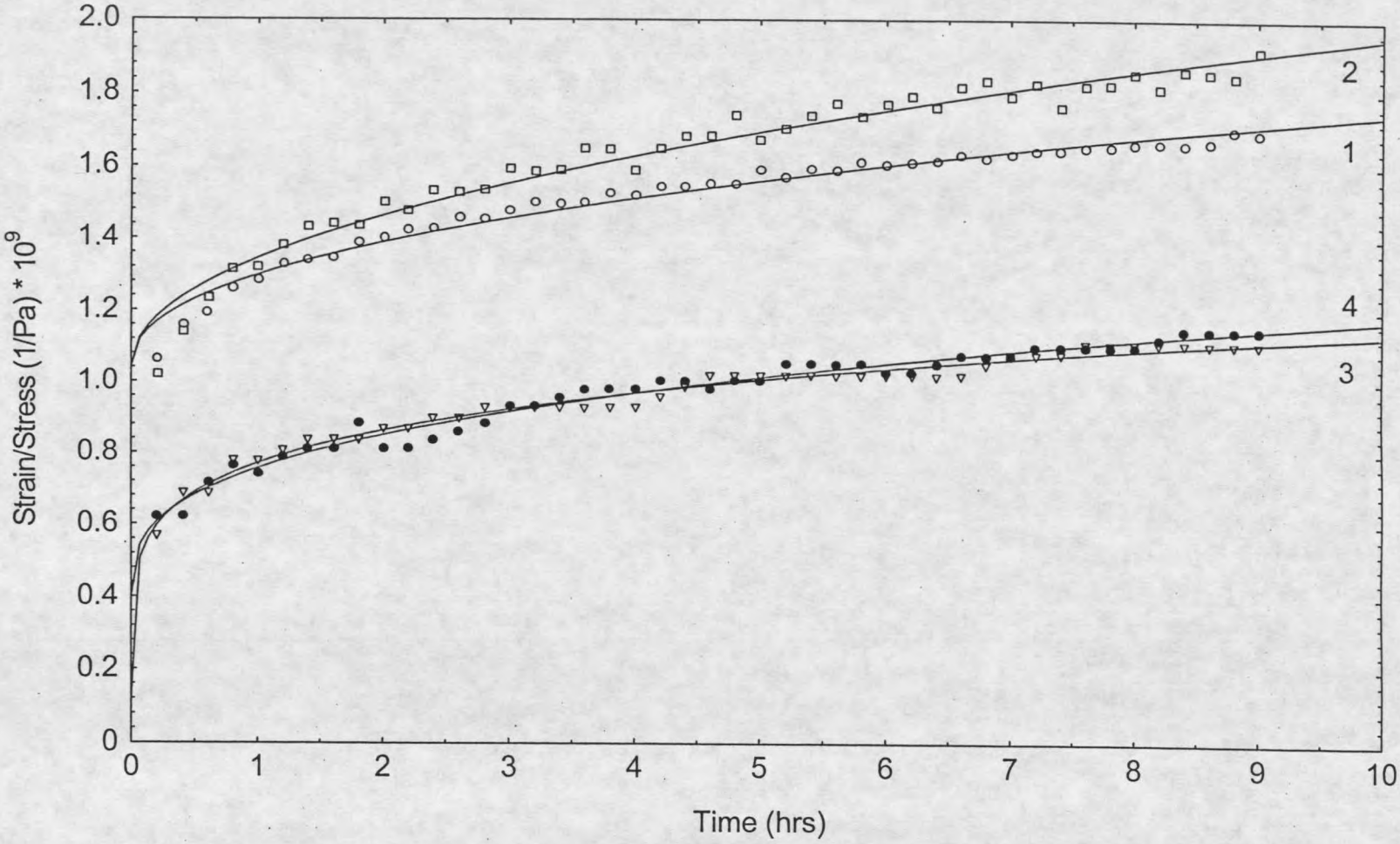


Figure B.III.11 Normalized Vibrocreep Response of Nylon 6/6 at Different Frequencies at 41 °C
1- $(0.16\pm0.04)\sigma_y$, 1 Hz; 2- $(0.16\pm0.04)\sigma_y$, 10 Hz;
3- $(0.16)\sigma_y$, 4- $(0.20)\sigma_y$, Constant Load Creep;
σ_y = 70 MPa at 23 °C

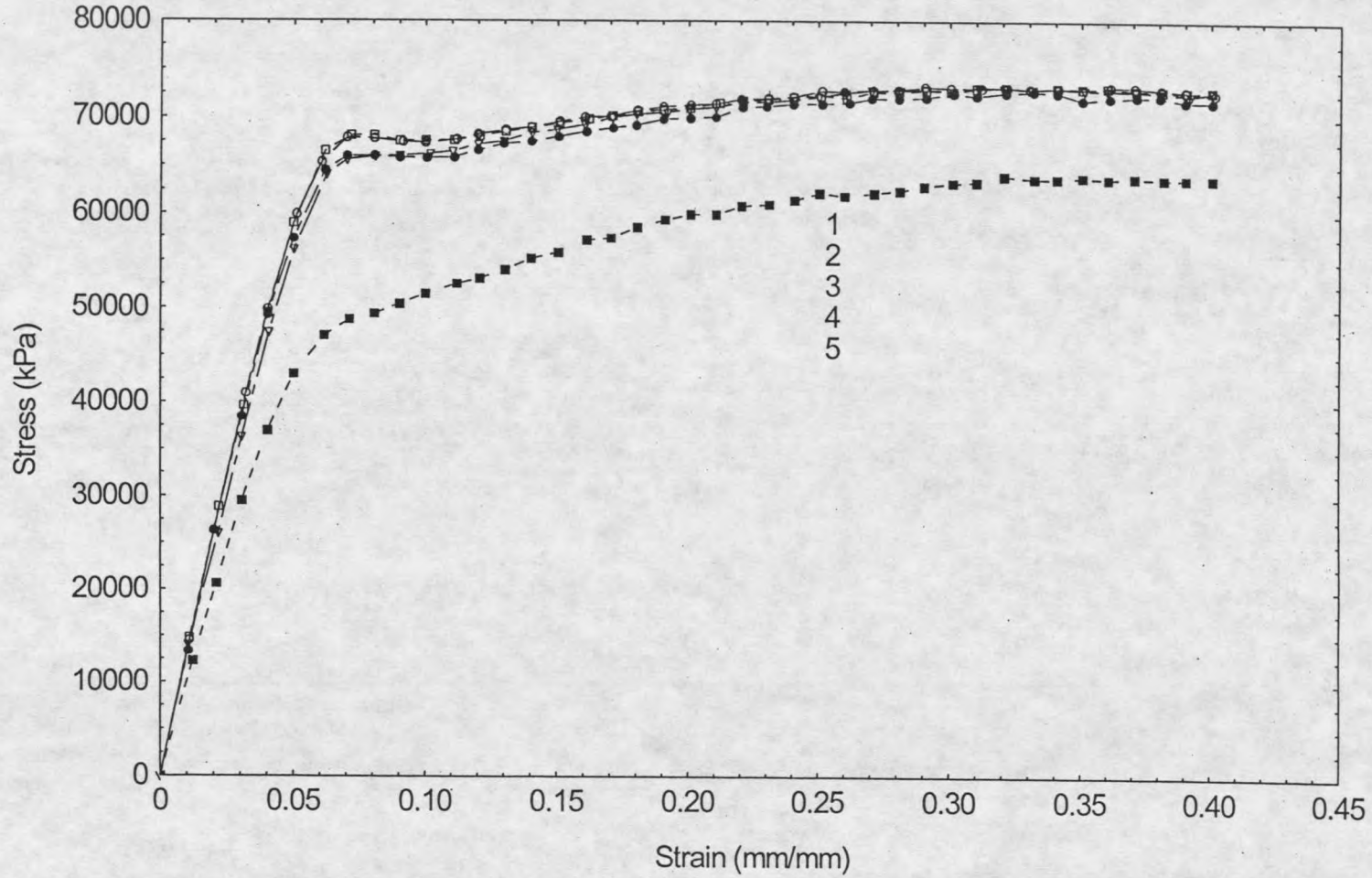


Figure B.III.12 Tensile Testing of Nylon 6/6 Specimens After Cyclic and Constant Loading at 41 °C
1- $(0.16\pm0.04)\sigma_y$, 1 Hz; 2- $(0.16\pm0.04)\sigma_y$, 10 Hz;
3- $(0.16)\sigma_y$, 4- $(0.20)\sigma_y$, Constant Load Creep; 5- Virgin Specimens;
σ_y = 70 MPa at 23 °C

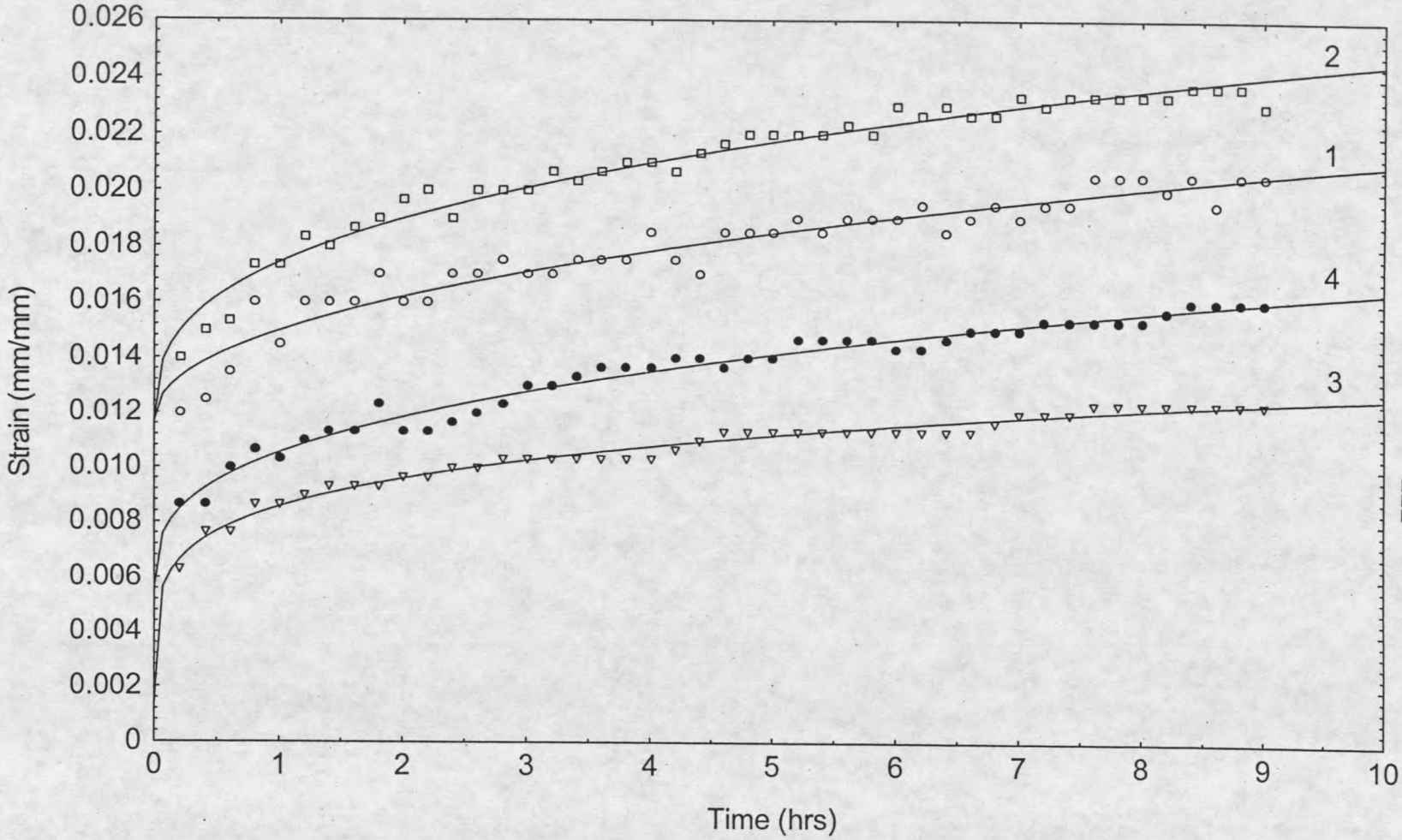


Figure B.III.13 Vibrocreep Response of Nylon 6/6 at Different Frequencies at 41 °C
1- $(0.16\pm0.10)\sigma_y$, 1 Hz; 2- $(0.16\pm0.10)\sigma_y$, 10 Hz;
3- $(0.16)\sigma_y$, 4- $(0.20)\sigma_y$, Constant Load Creep;
σ_y = 70 MPa at 23 °C

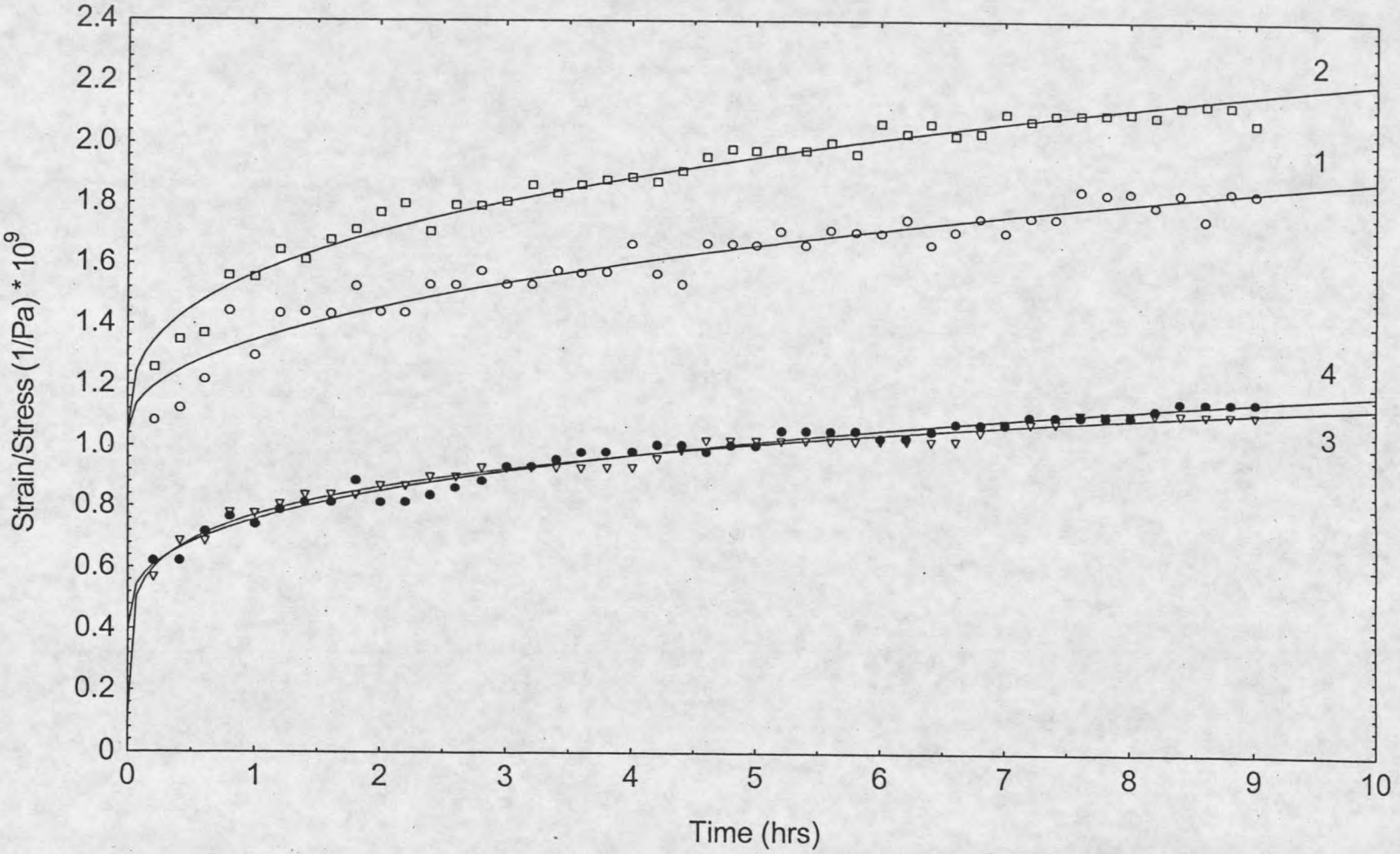


Figure B.III.14 Normalized Vibrocreep Response of Nylon 6/6 at Different Frequencies at 41 °C
1- $(0.16\pm0.10)\sigma_y$, 1 Hz; 2- $(0.16\pm0.10)\sigma_y$, 10 Hz;
3- $(0.16)\sigma_y$, 4- $(0.20)\sigma_y$, Constant Load Creep;
σ_y = 70 MPa at 23 °C

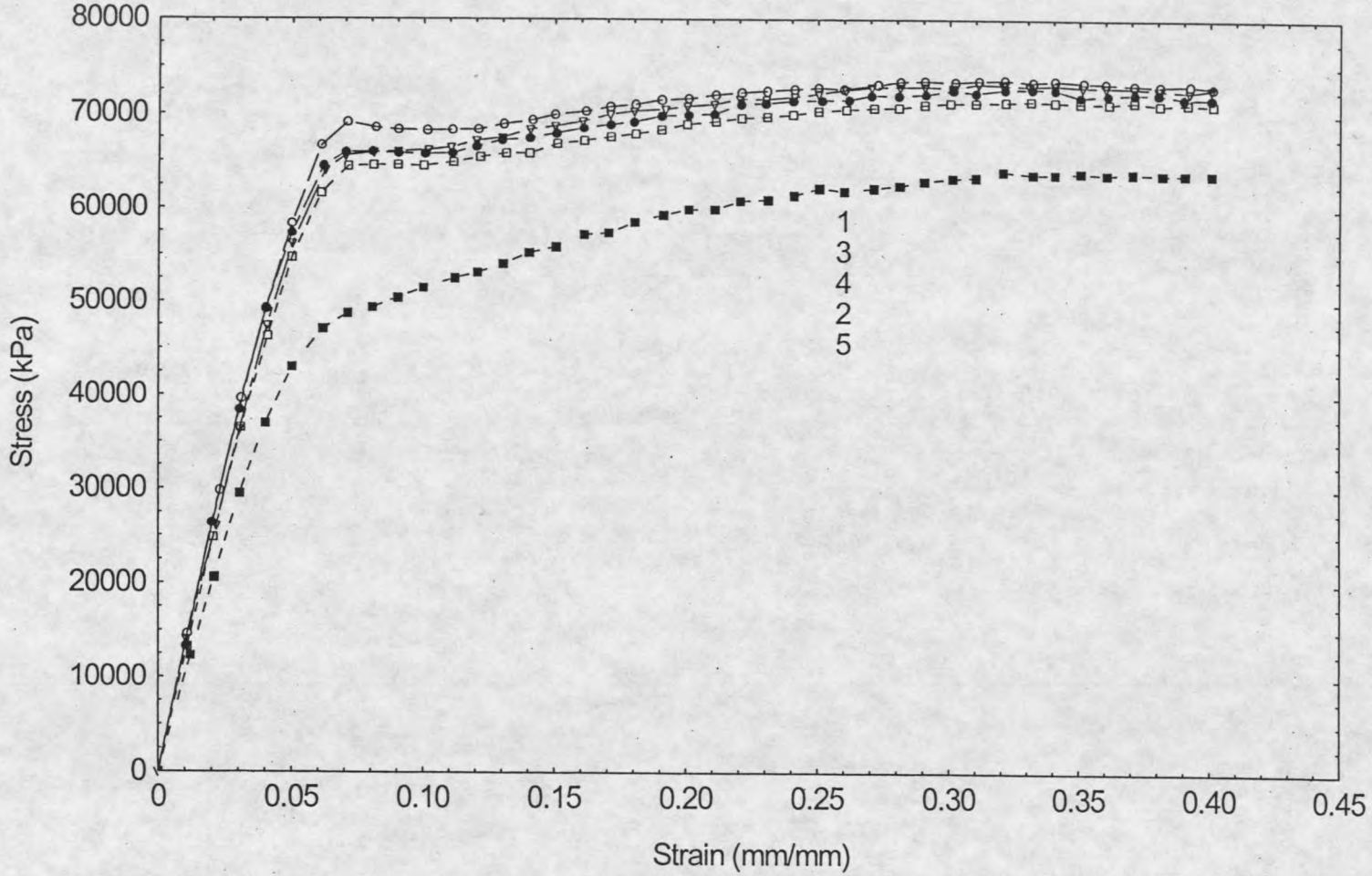


Figure B.III.15 Tensile Testing of Nylon 6/6 Specimens After Cyclic and Constant Loading at 41 °C
1- $(0.16\pm0.10)\sigma_y$, 1 Hz; 2- $(0.16\pm0.10)\sigma_y$, 10 Hz;
3- $(0.16)\sigma_y$, 4- $(0.20)\sigma_y$, Constant Load Creep; 5- Virgin Specimens;
σ_y = 70 MPa at 23 °C

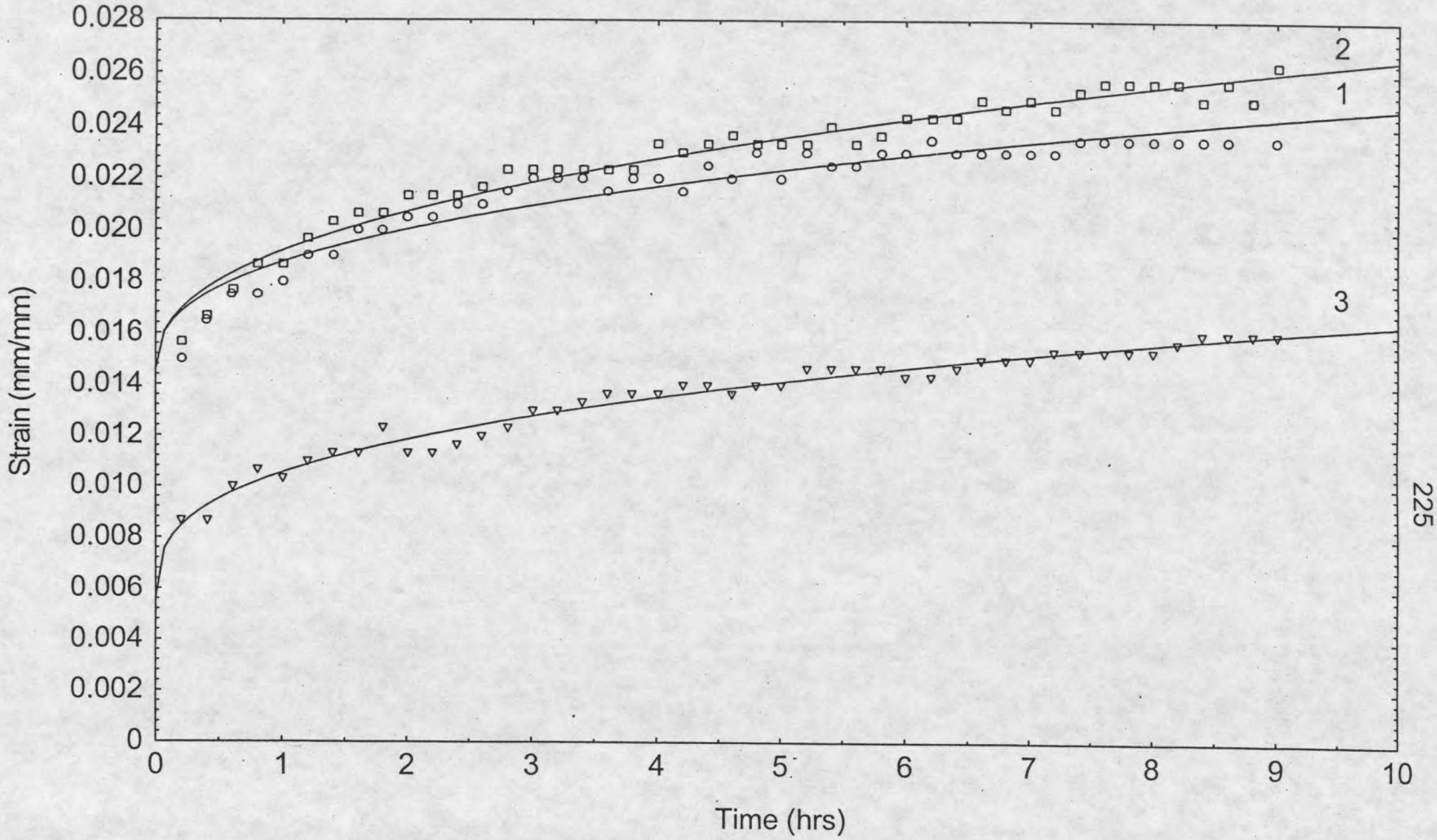


Figure B.III.16 Vibrocreep Response of Nylon 6/6 at Different Frequencies at 41 °C
1- $(0.20\pm0.05)\sigma_y$, 1 Hz; 2- $(0.20\pm0.05)\sigma_y$, 10 Hz;
3- $(0.20)\sigma_y$, Constant Load Creep;
σ_y = 70 MPa at 23 °C

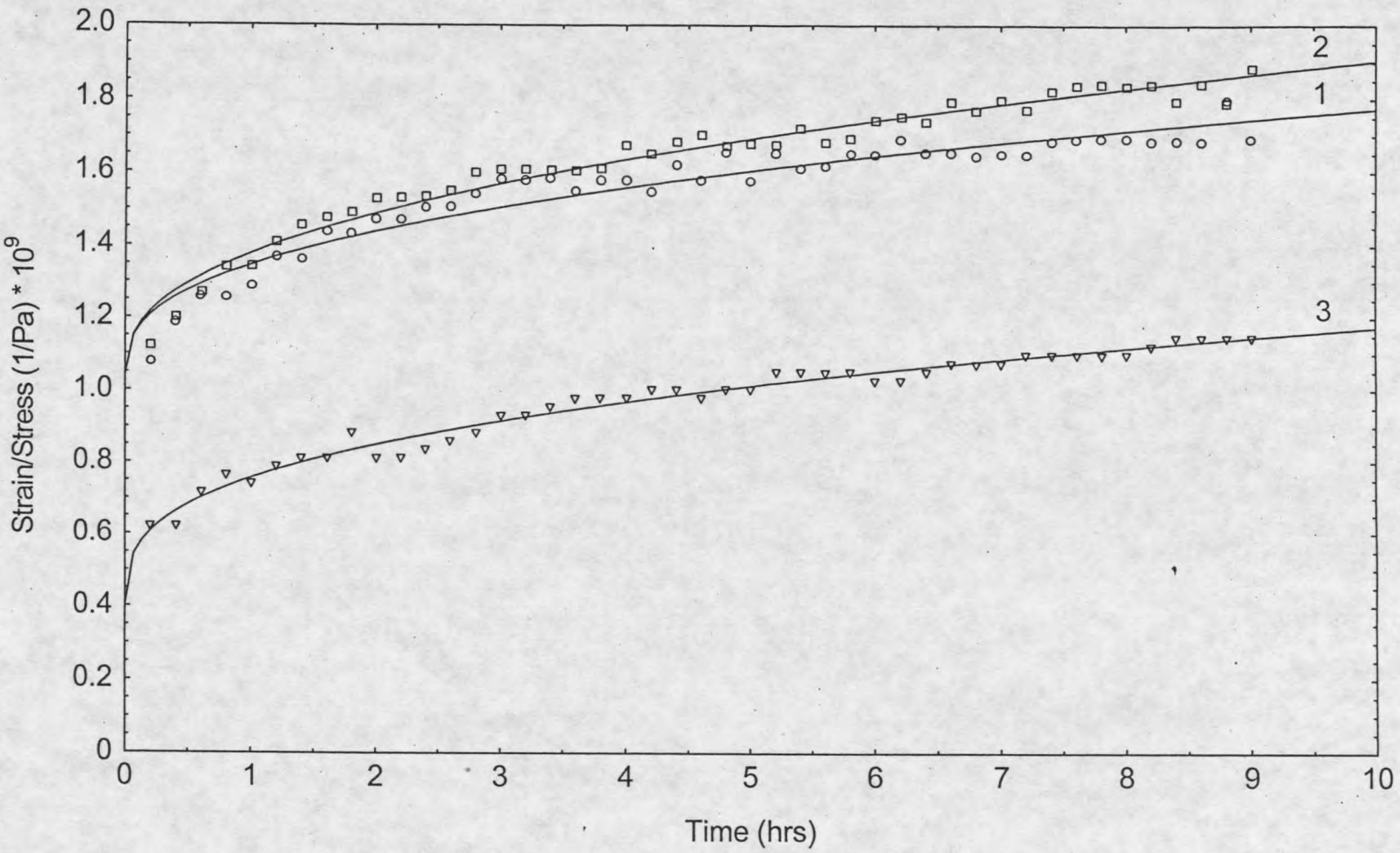


Figure B.III.17 Normalized Vibrocreep Response of Nylon 6/6 at Different Frequencies at 41 °C
1- $(0.20\pm0.05)\sigma_y$, 1 Hz; 2- $(0.20\pm0.05)\sigma_y$, 10 Hz;
3- $(0.20)\sigma_y$, Constant Load Creep;
σ_y = 70 MPa at 23 °C

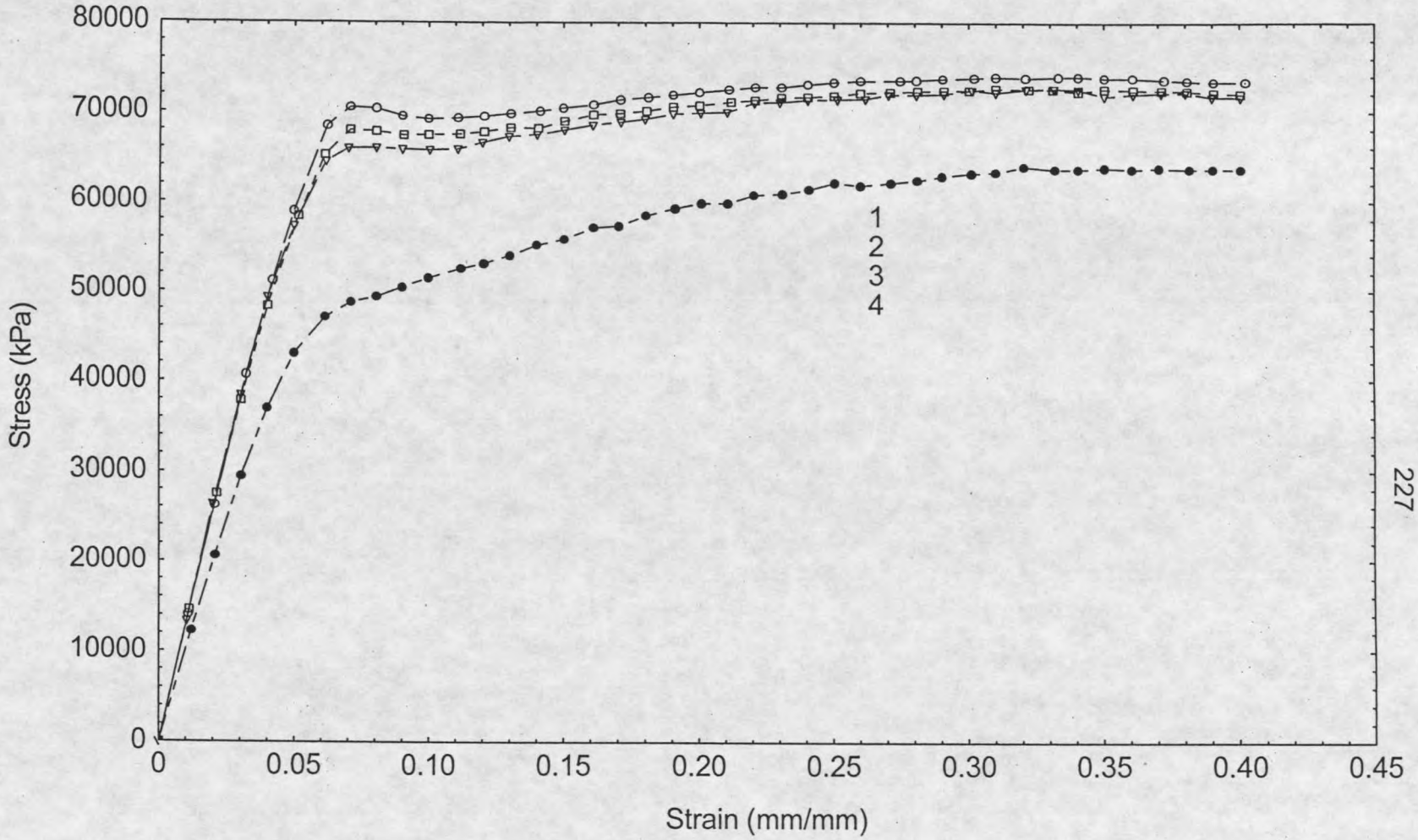


Figure B.III.18 Tensile Testing of Nylon 6/6 Specimens After Cyclic and Constant Loading at 41 °C
1- $(0.20\pm0.05)\sigma_y$, 1 Hz; 2- $(0.20\pm0.05)\sigma_y$, 10 Hz;
3- $(0.20)\sigma$, Constant Load Creep; 4- Virgin Specimens;
σ_y = 70 MPa at 23 °C

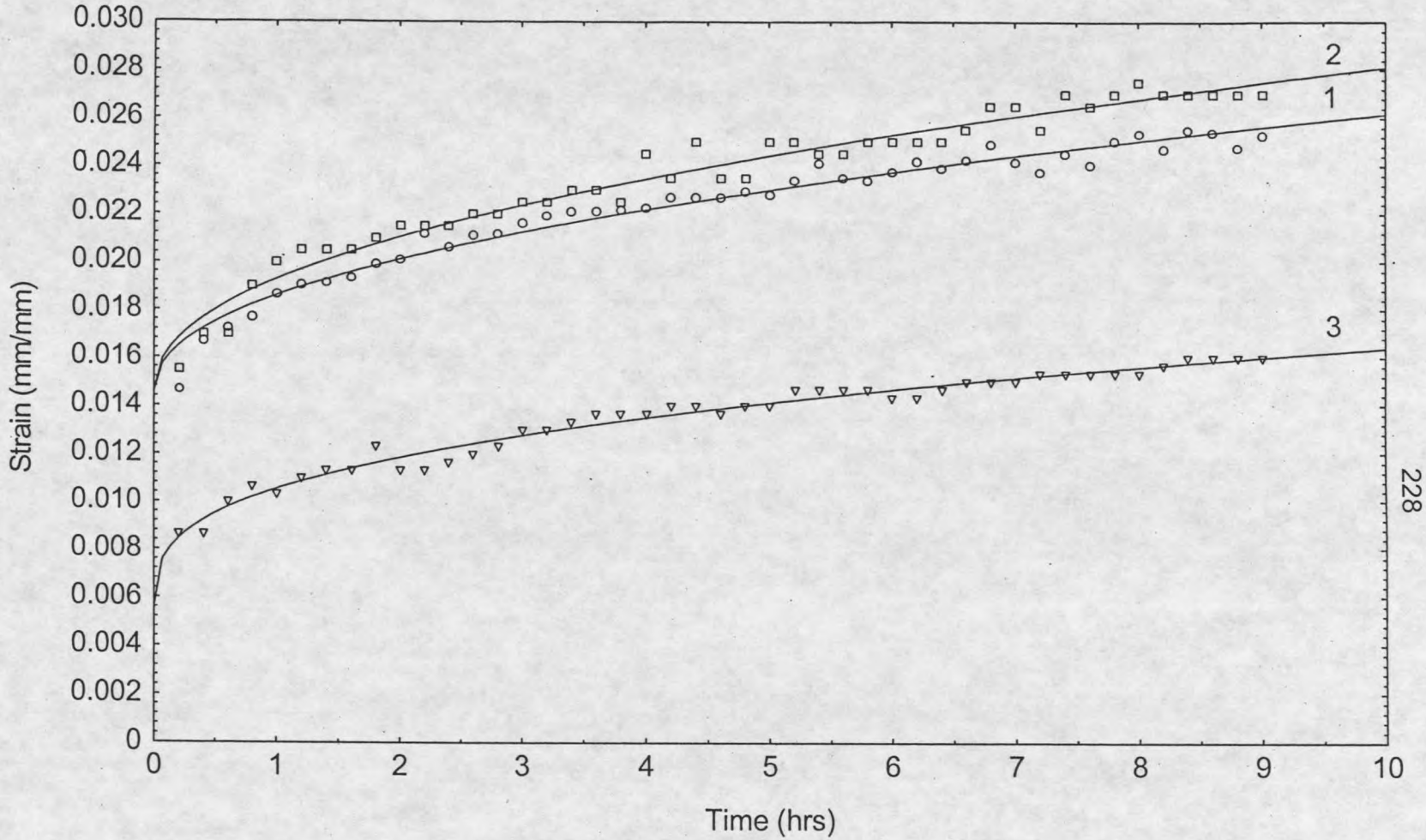


Figure B.III.19 Vibrocreep Response of Nylon 6/6 at Different Frequencies at 41 °C
1- $(0.20\pm0.10)\sigma_y$, 1 Hz; 2- $(0.20\pm0.10)\sigma_y$, 10 Hz;
3- $(0.20)\sigma_y$, Constant Load Creep;
σ_y = 70 MPa at 23 °C

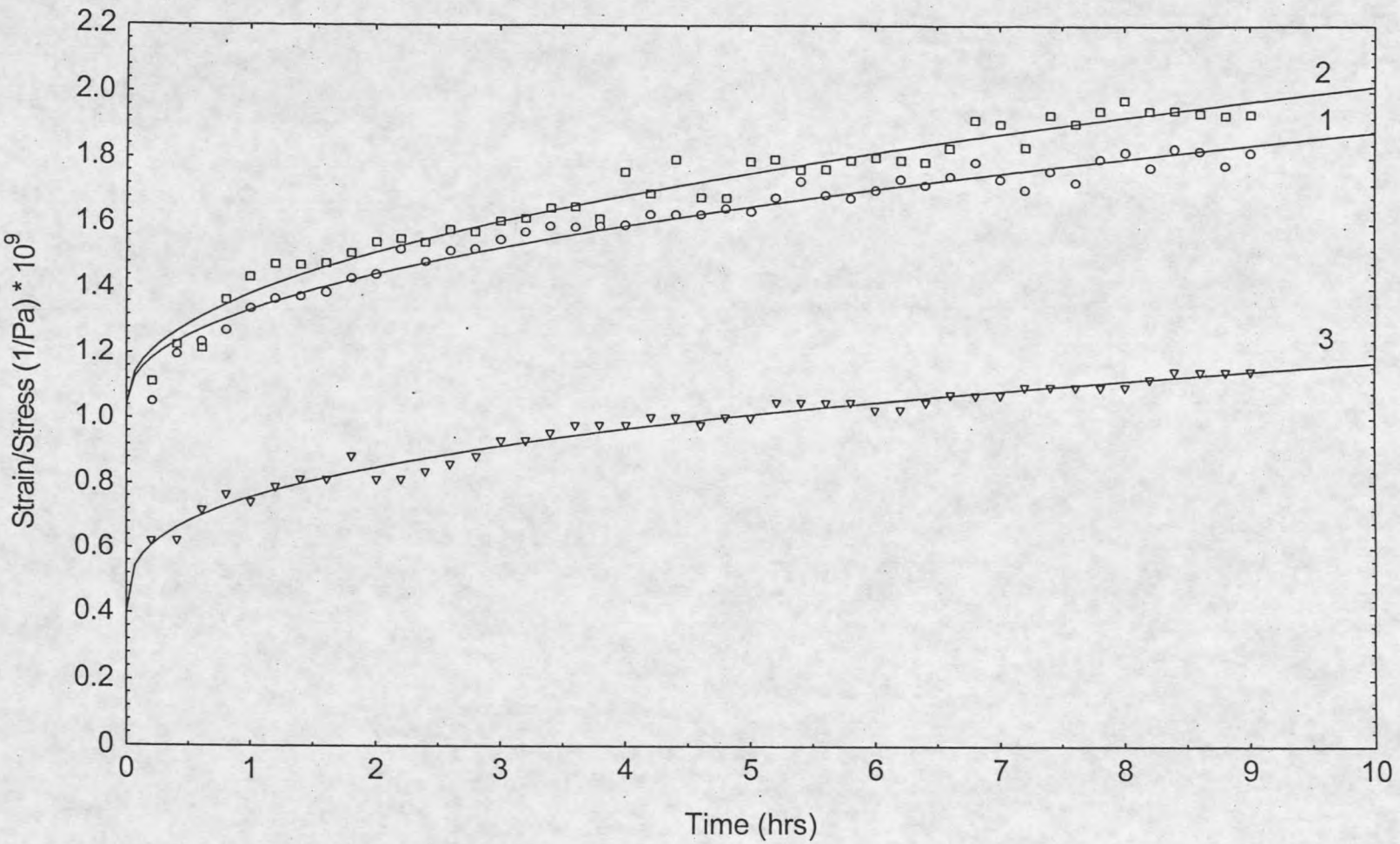


Figure B.III.20 Normalized Vibrocreep Response of Nylon 6/6 at Different Frequencies at 41 °C
1- $(0.20\pm0.10)\sigma_y$, 1 Hz; 2- $(0.20\pm0.10)\sigma_y$, 10 Hz;
3- $(0.20)\sigma_y$, Constant Load Creep;
σ_y = 70 MPa at 23 °C

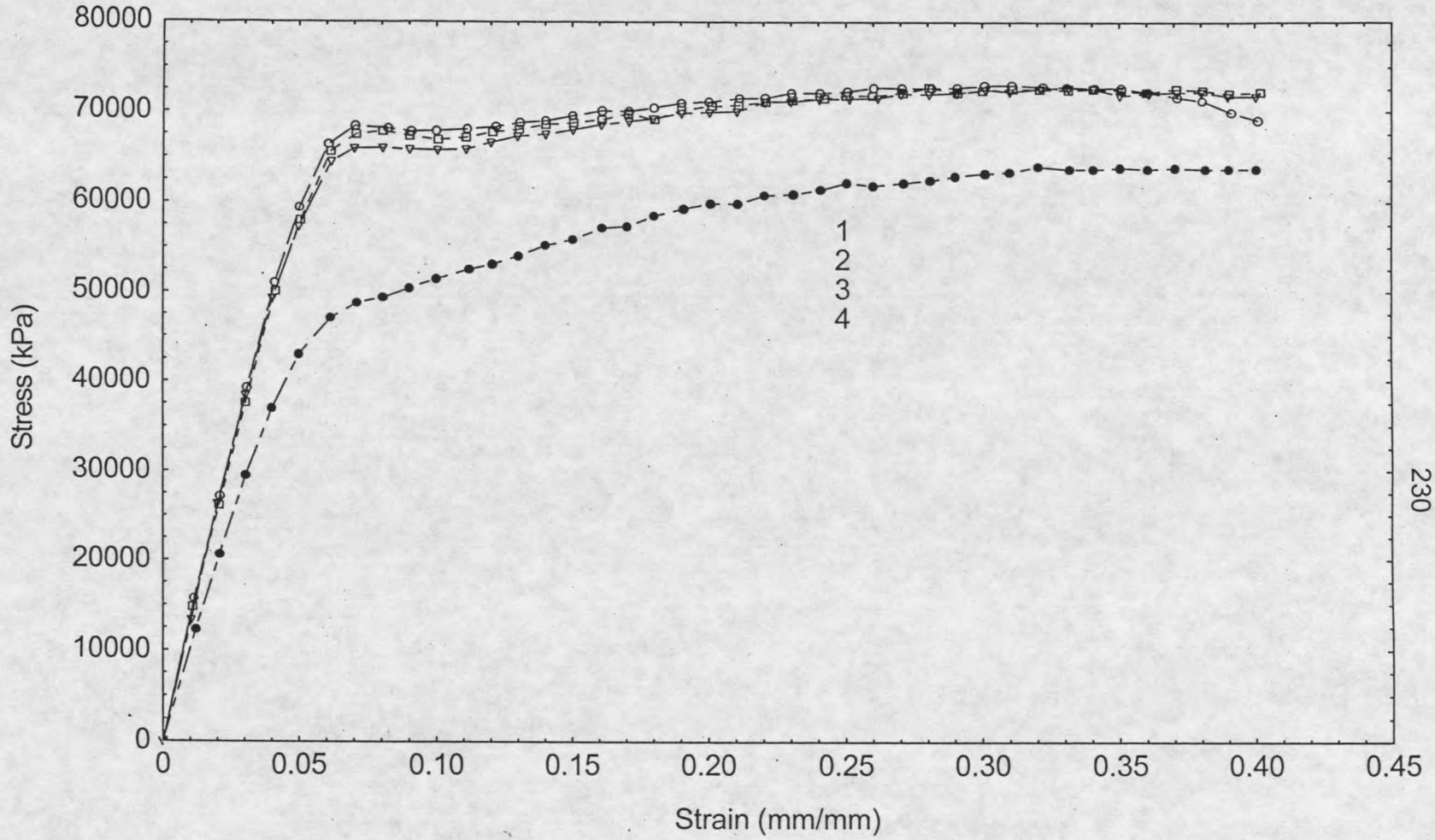


Figure B.III.21 Tensile Testing of Nylon 6/6 Specimens After Cyclic and Constant Loading at 41 °C
1- $(0.20\pm0.10)\sigma_y$, 1 Hz; 2- $(0.20\pm0.10)\sigma_y$, 10 Hz;
3- $(0.20)\sigma_y$, Constant Load Creep; 4- Virgin Specimens;
σ_y = 70 MPa at 23 °C

APPENDIX C

Amplitude Effects from Vibrocreep Testing of Nylon 6/6

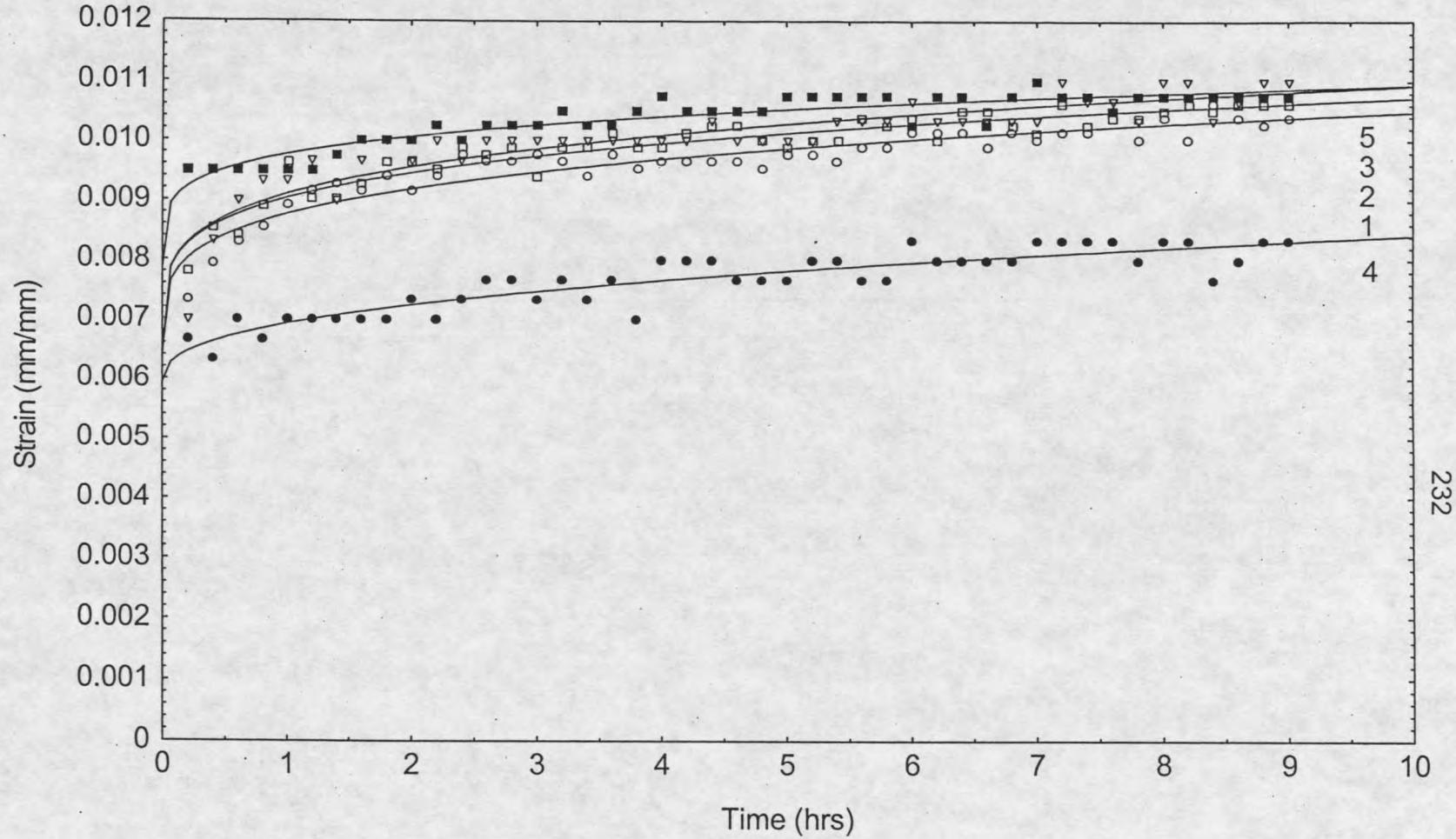


Figure C.I.1 Vibrocreep Response of Nylon 6/6 at Different Amplitudes at 23 °C
1- $(0.12\pm0.04)\sigma_y$, 1 Hz; 2- $(0.12\pm0.075)\sigma_y$, 1 Hz; 3- $(0.12\pm0.10)\sigma_y$, 1 Hz;
4- $(0.16)\sigma_y$, 5- $(0.20)\sigma_y$, Constant Load Creep;
σ_y = 70 MPa at 23 °C

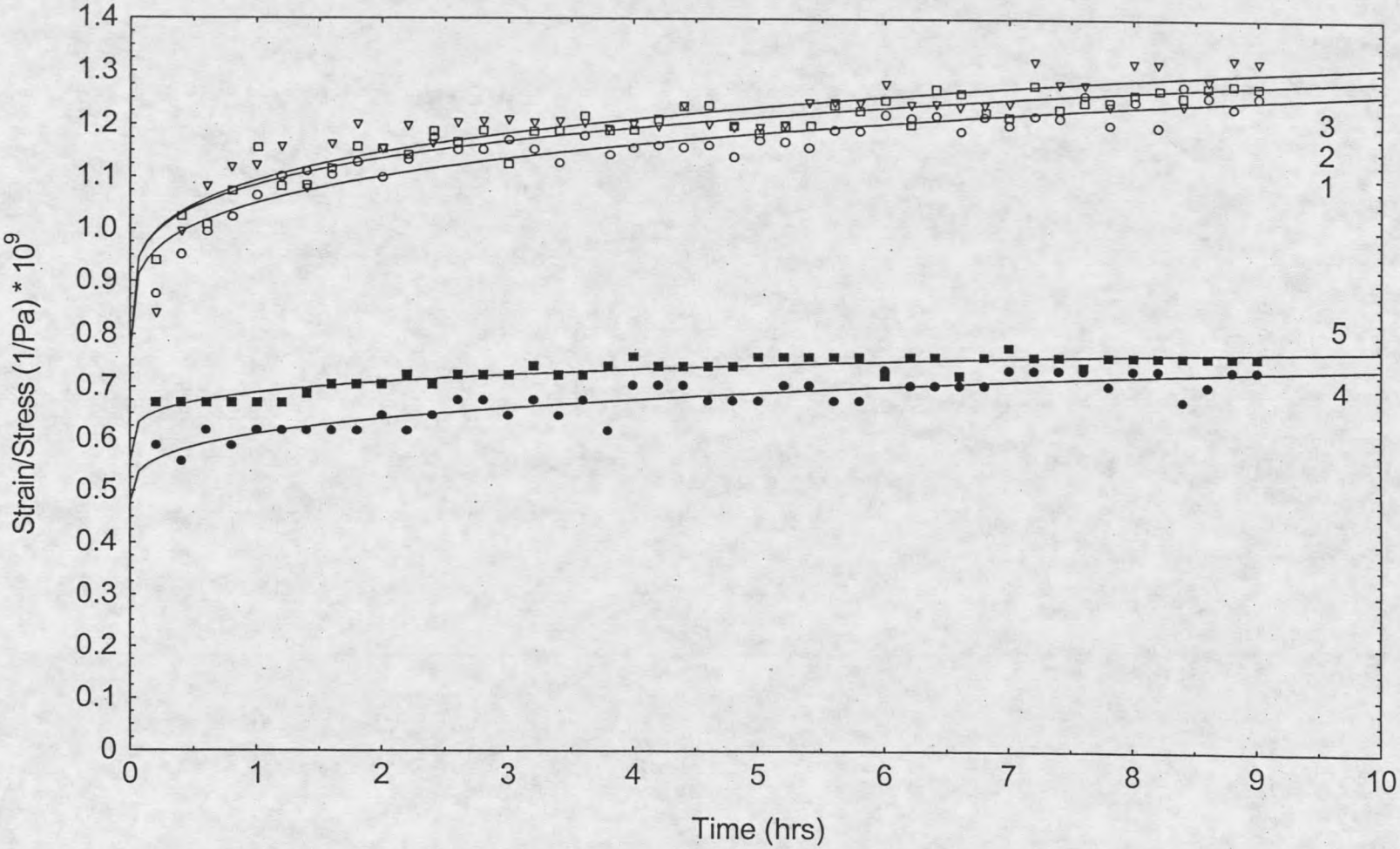


Figure C.I.2 Normalized Vibrocreep Response of Nylon 6/6 at Different Amplitudes at 23 °C
1- $(0.12\pm0.04)\sigma_y$, 1 Hz; 2- $(0.12\pm0.075)\sigma_y$, 1 Hz; 3- $(0.12\pm0.10)\sigma_y$, 1 Hz;
4- $(0.16)\sigma_y$, 5- $(0.20)\sigma_y$, Constant Load Creep;
σ_y = 70 MPa at 23 °C

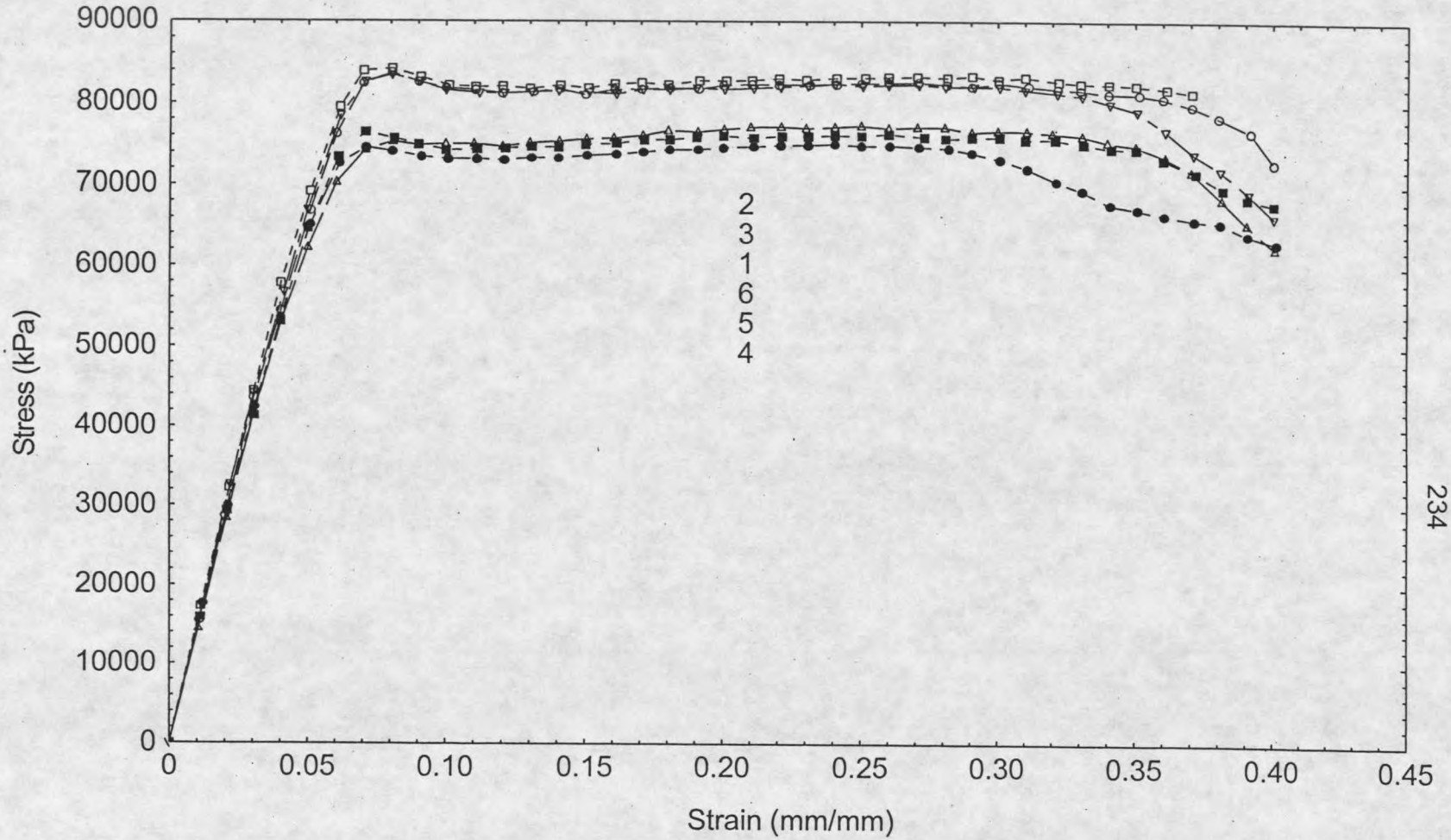


Figure C.I.3 Tensile Testing of Nylon 6/6 Specimens After Cyclic and Constant Loading at 23 °C
1- $(0.12\pm0.04)\sigma_y$, 1 Hz; 2- $(0.12\pm0.075)\sigma_y$, 1 Hz; 3- $(0.12\pm0.10)\sigma_y$, 1 Hz;
4- $(0.16)\sigma_y$, 5- $(0.20)\sigma_y$, Constant Load Creep; 6- Virgin Specimens;
σ_y = 70 MPa at 23 °C

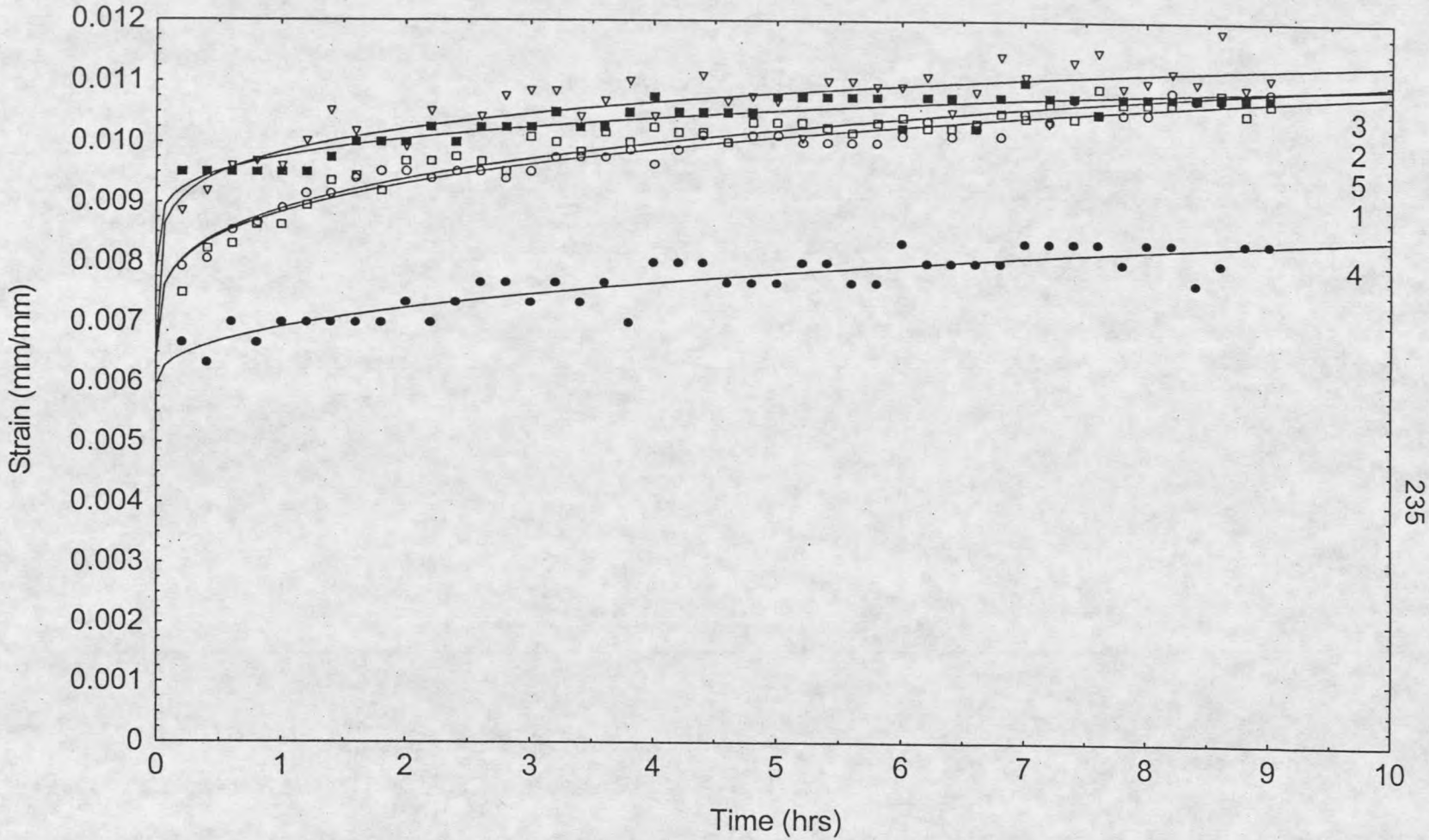


Figure C.I.4 Vibrocreep Response of Nylon 6/6 at Different Amplitudes at 23 °C
1- $(0.12\pm0.04)\sigma_y$, 10 Hz; 2- $(0.12\pm0.075)\sigma_y$, 10 Hz; 3- $(0.12\pm0.10)\sigma_y$, 10 Hz;
4- $(0.16)\sigma_y$, 5- $(0.20)\sigma_y$, Constant Load Creep;
σ_y = 70 MPa at 23 °C

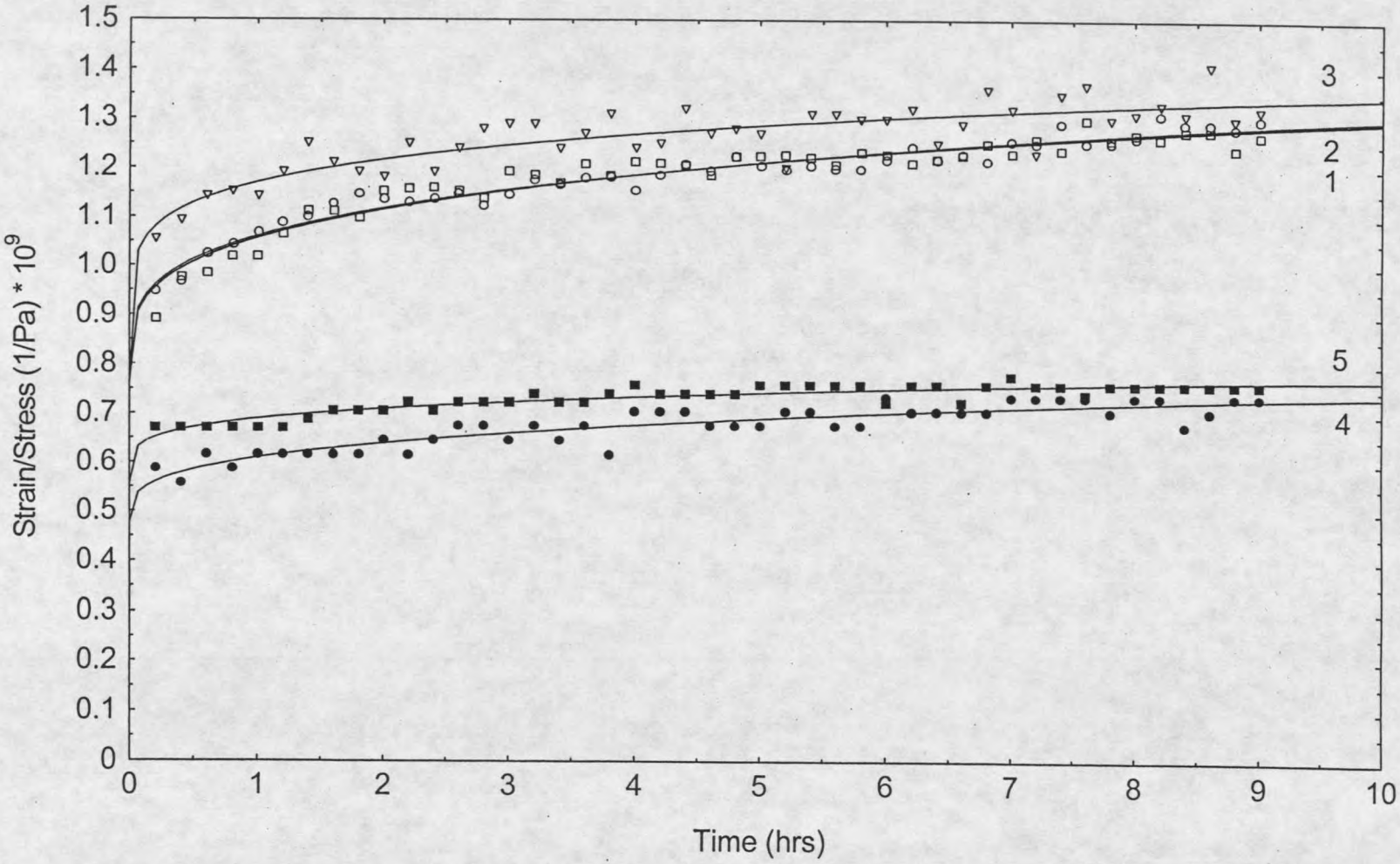


Figure C.I.5 Normalized Vibrocreep Response of Nylon 6/6 at Different Amplitudes at 23 °C
1- $(0.12\pm0.04)\sigma_y$, 10 Hz; 2- $(0.12\pm0.075)\sigma_y$, 10 Hz; 3- $(0.12\pm0.10)\sigma_y$, 10 Hz;
4- $(0.16)\sigma_y$, 5- $(0.20)\sigma_y$, Constant Load Creep;
σ_y = 70 MPa at 23 °C

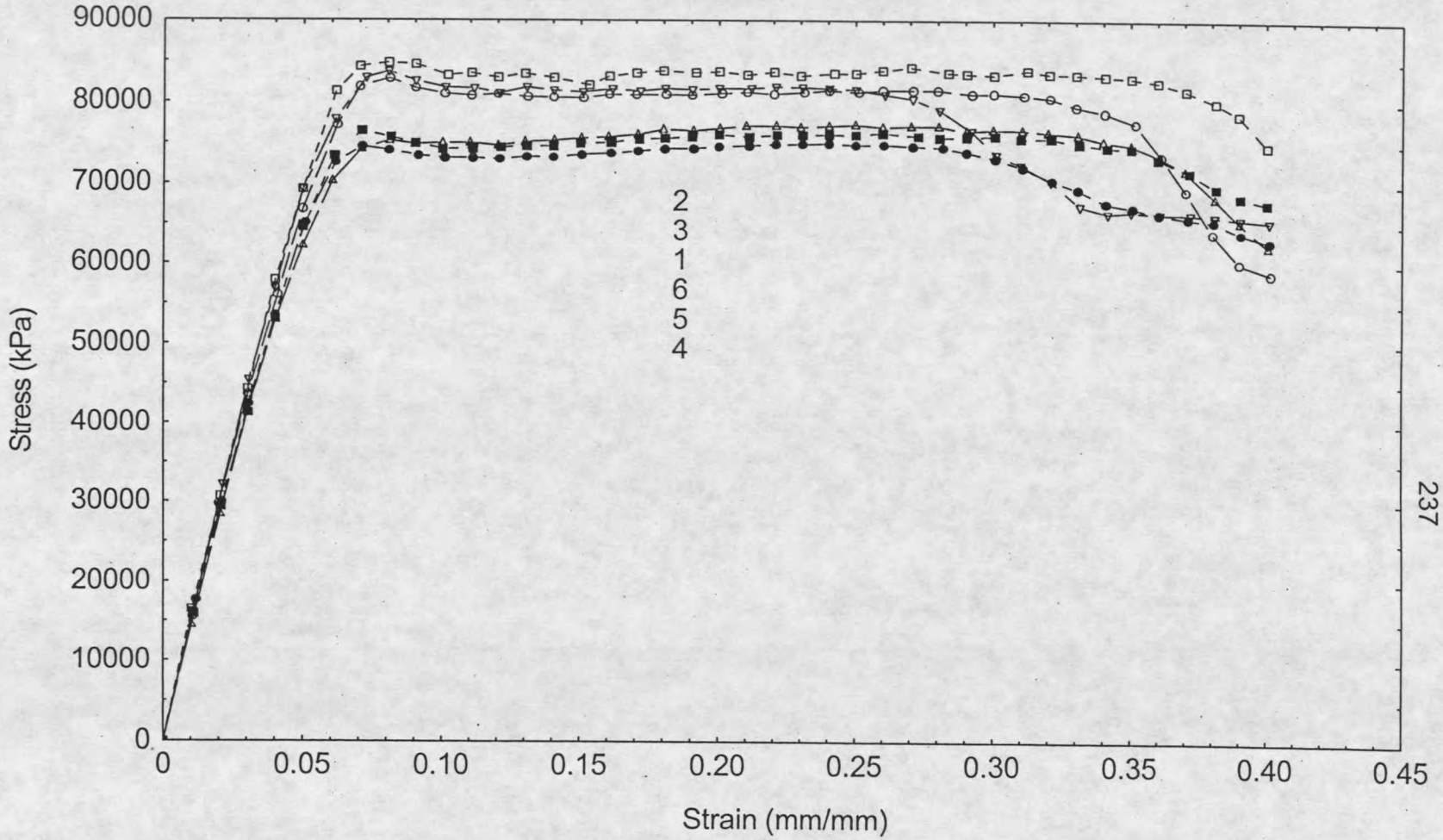


Figure C.I.6 Tensile Testing of Nylon 6/6 Specimens After Cyclic and Constant Loading at 23 °C
1- $(0.12\pm0.04)\sigma_y$, 10 Hz; 2- $(0.12\pm0.075)\sigma_y$, 10 Hz; 3- $(0.12\pm0.10)\sigma_y$, 10 Hz;
4- $(0.16)\sigma_y$, 5- $(0.20)\sigma_y$, Constant Load Creep; 6- Virgin Specimens;
σ_y = 70 MPa at 23 °C

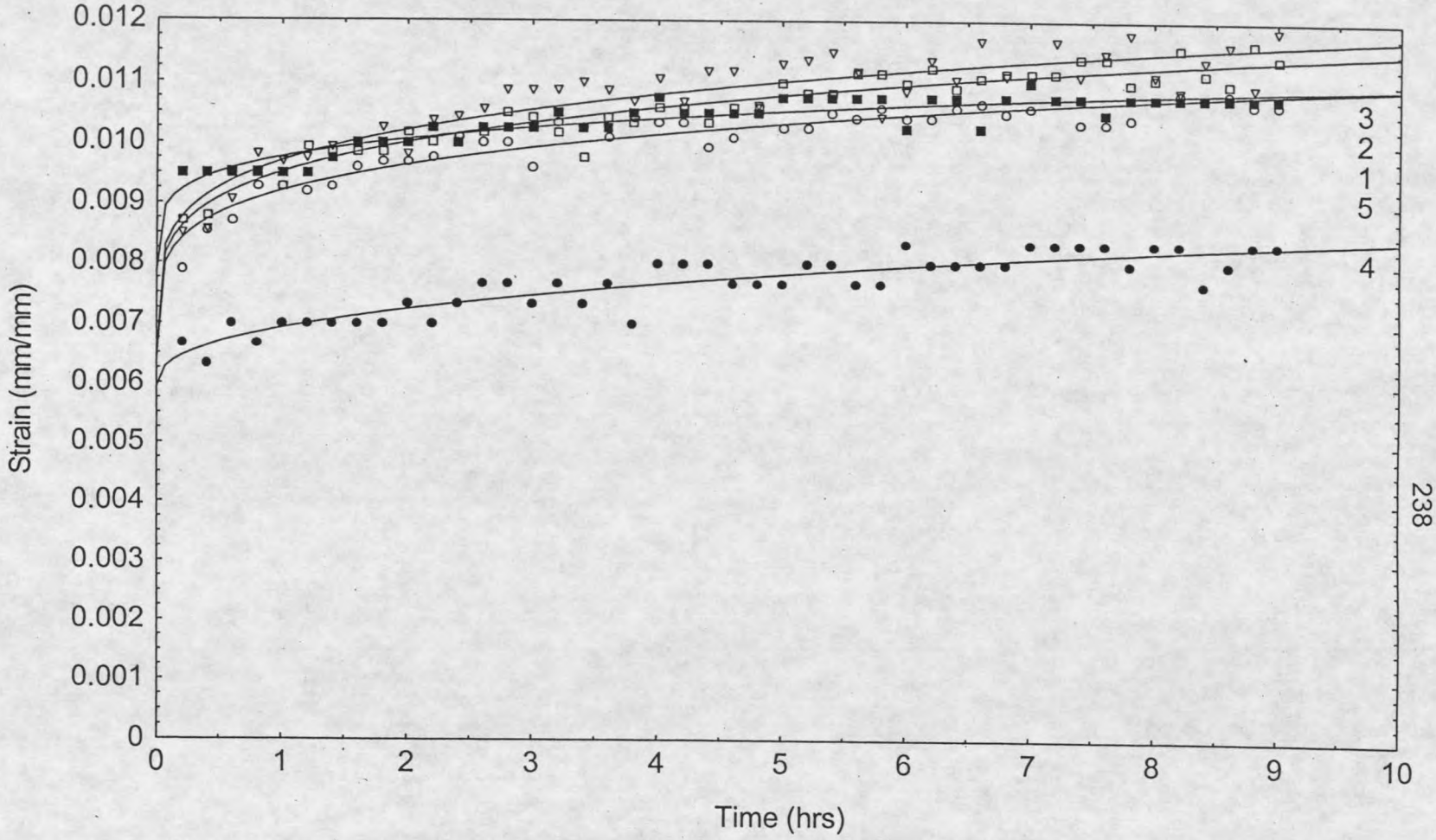


Figure C.I.7 Vibrocreep Response of Nylon 6/6 at Different Amplitudes at 23 °C
1- $(0.12\pm0.04)\sigma_y$, 20 Hz; 2- $(0.12\pm0.075)\sigma_y$, 20 Hz; 3- $(0.12\pm0.10)\sigma_y$, 20 Hz;
4- $(0.16)\sigma_y$, 5- $(0.20)\sigma_y$, Constant Load Creep;
σ_y = 70 MPa at 23 °C

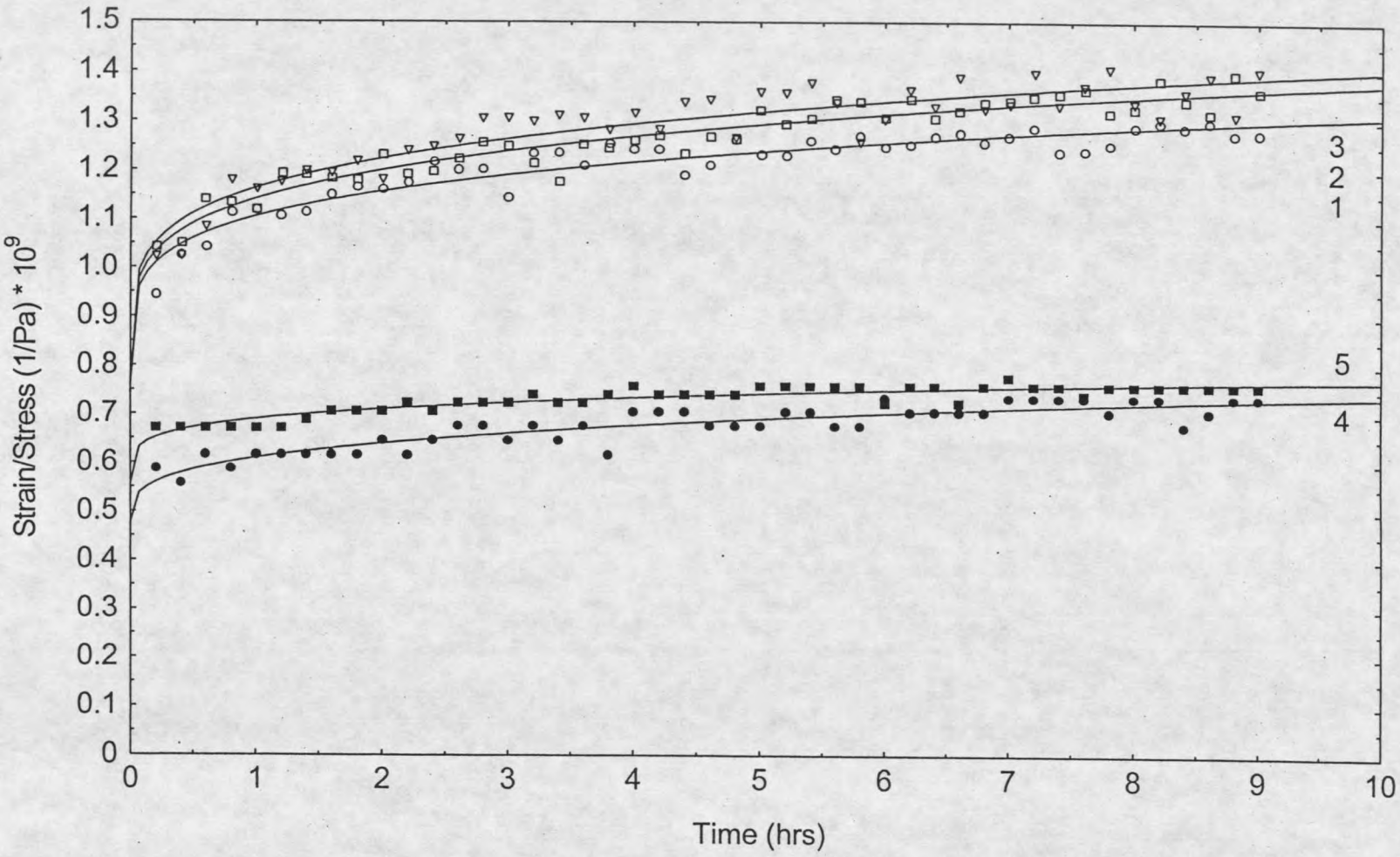


Figure C.I.8 Normalized Vibrocreep Response of Nylon 6/6 at Different Amplitudes at 23 °C
1- $(0.12\pm0.04)\sigma_y$, 20 Hz; 2- $(0.12\pm0.075)\sigma_y$, 20 Hz; 3- $(0.12\pm0.10)\sigma_y$, 20 Hz;
4- $(0.16)\sigma_y$, 5- $(0.20)\sigma_y$, Constant Load Creep;
σ_y = 70 MPa at 23 °C

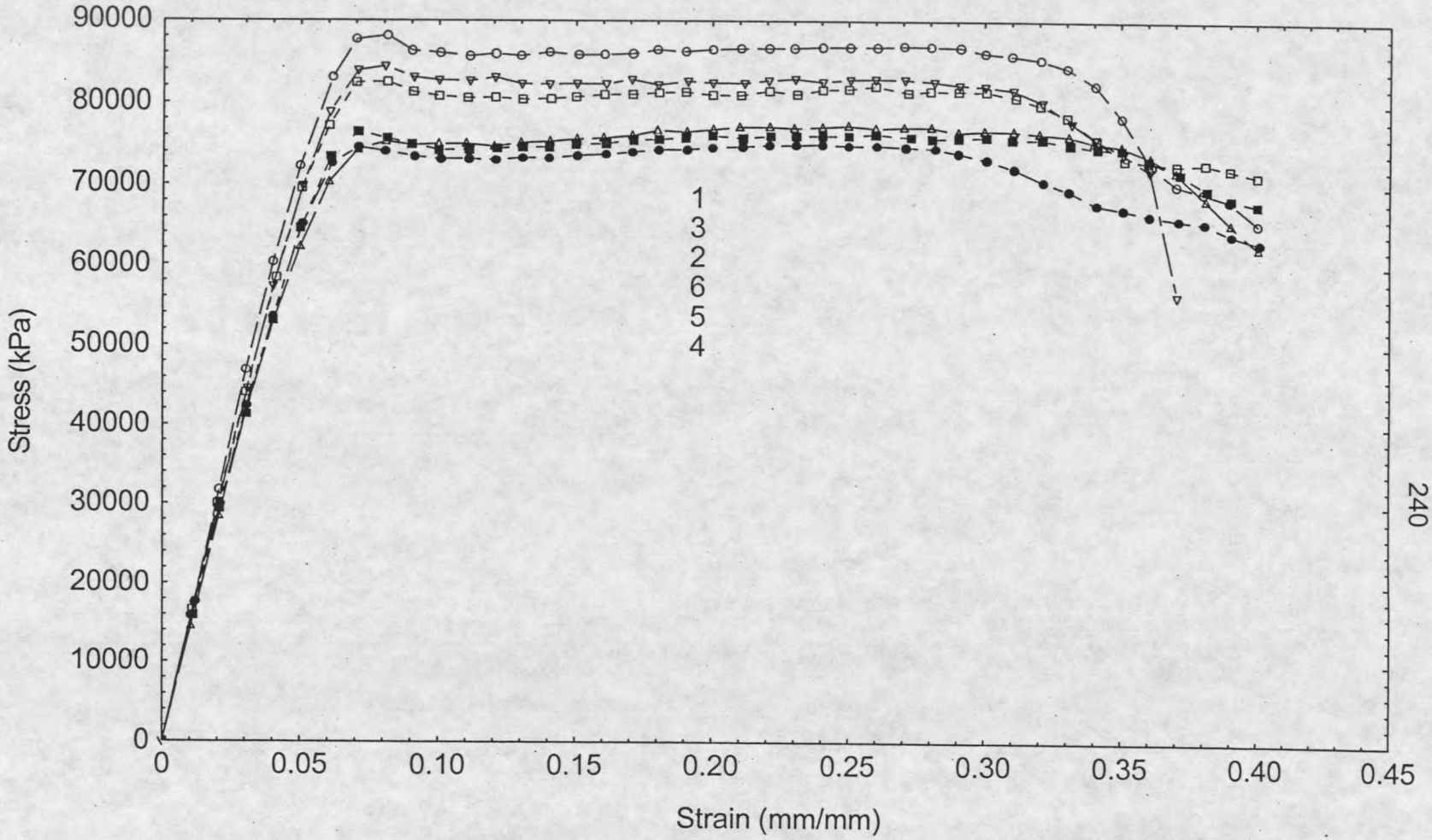


Figure C.I.9 Tensile Testing of Nylon 6/6 Specimens After Cyclic and Constant Loading at 23 °C
1- $(0.12\pm0.04)\sigma_y$, 20 Hz; 2- $(0.12\pm0.075)\sigma_y$, 20 Hz; 3- $(0.12\pm0.10)\sigma_y$, 20 Hz;
4- $(0.16)\sigma_y$, 5- $(0.20)\sigma_y$, Constant Load Creep; 6- Virgin Specimens;
σ_y = 70 MPa at 23 °C

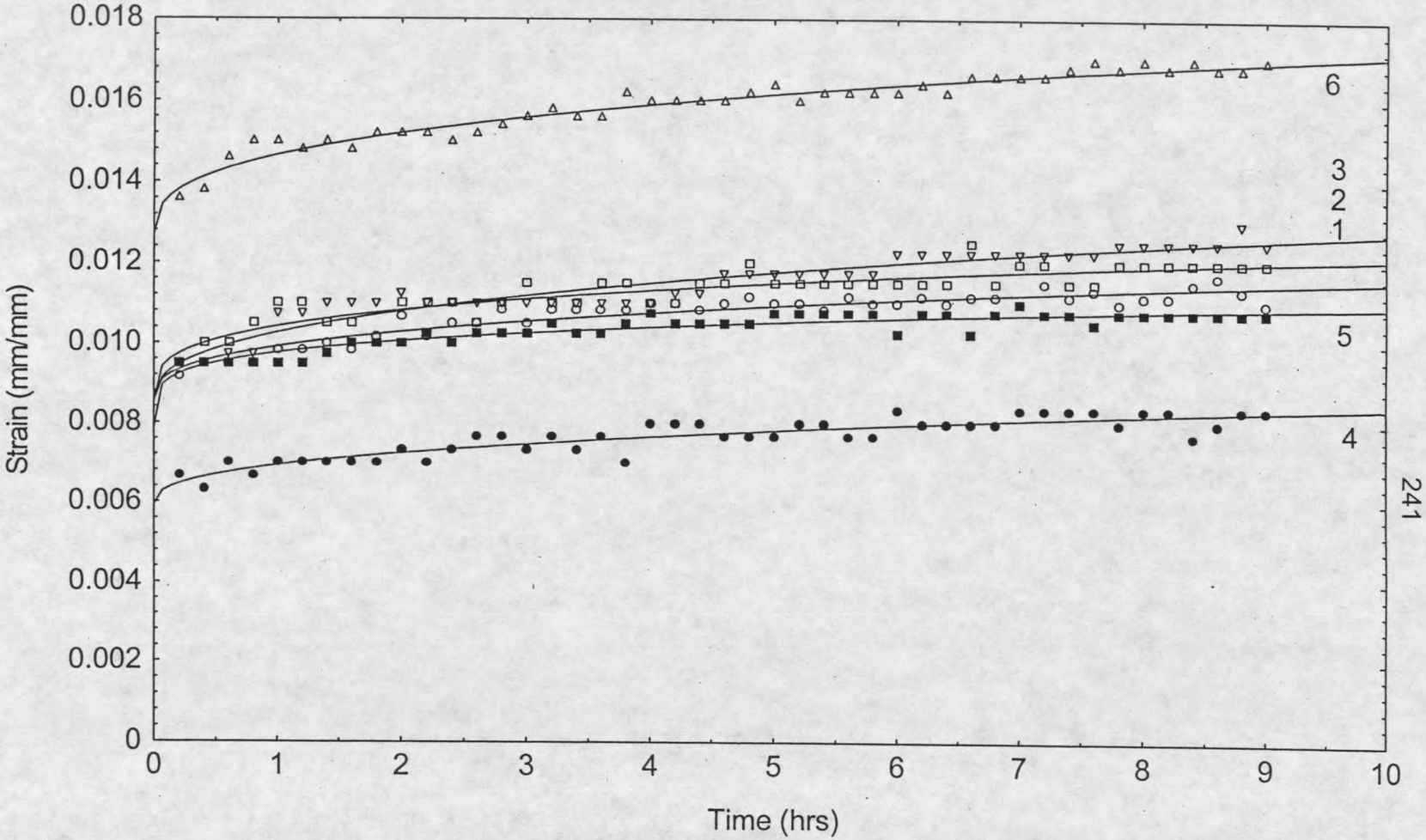


Figure C.I.10 Vibrocreep Response of Nylon 6/6 at Different Amplitudes at 23 °C
1- $(0.16\pm0.04)\sigma_y$, 1 Hz; 2- $(0.16\pm0.075)\sigma_y$, 1 Hz; 3- $(0.16\pm0.10)\sigma_y$, 1 Hz;
4- $(0.16)\sigma_y$, 5- $(0.20)\sigma_y$, 6- $(0.30)\sigma_y$, Constant Load Creep;
σ_y = 70 MPa at 23 °C

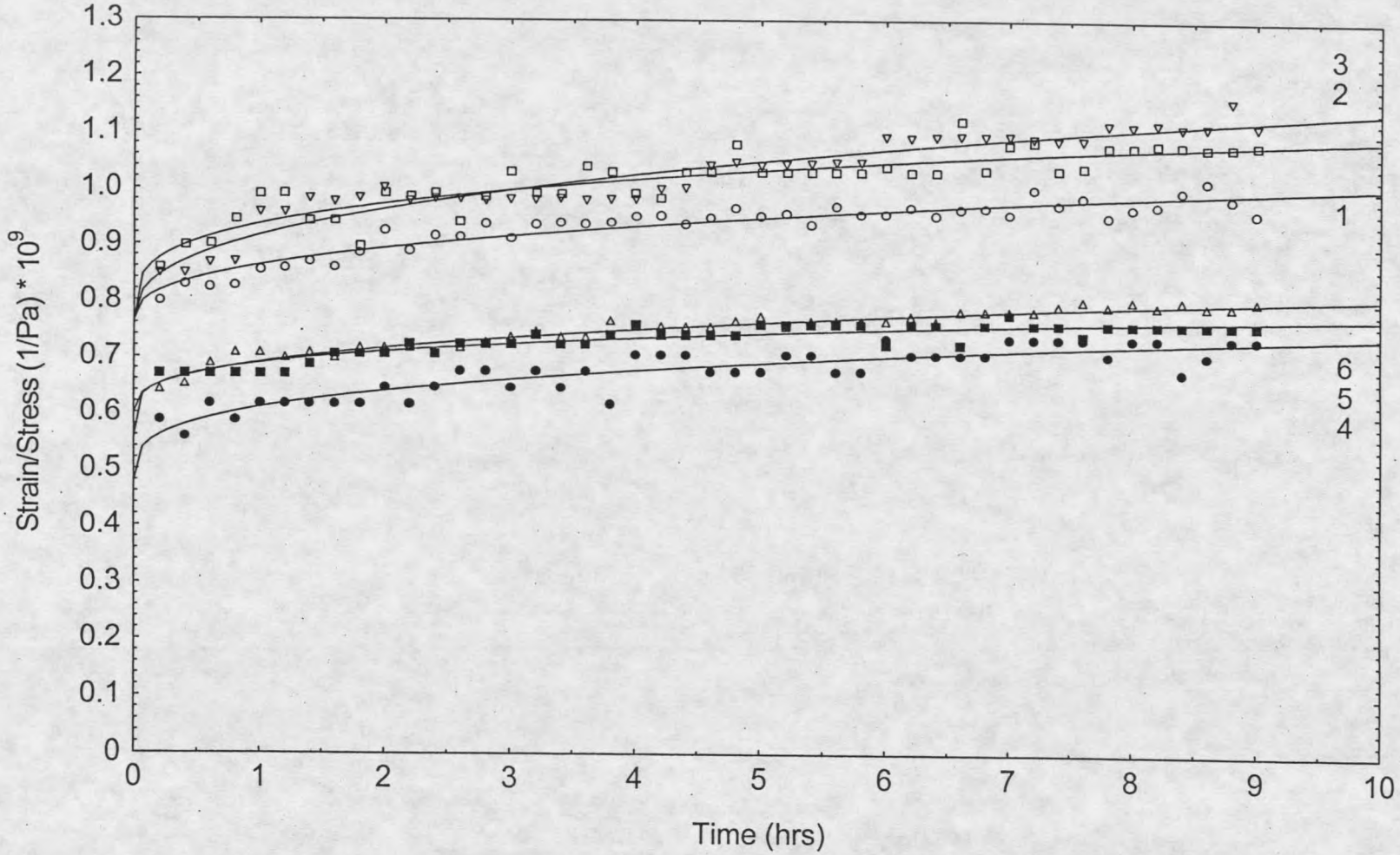


Figure C.I.11 Normalized Vibrocreep Response of Nylon 6/6 at Different Amplitudes at 23 °C
1- $(0.16\pm0.04)\sigma_y$, 1 Hz; 2- $(0.16\pm0.075)\sigma_y$, 1 Hz; 3- $(0.16\pm0.10)\sigma_y$, 1 Hz;
4- $(0.16)\sigma_y$, 5- $(0.20)\sigma_y$, 6- $(0.30)\sigma_y$, Constant Load Creep;
σ_y = 70 MPa at 23 °C

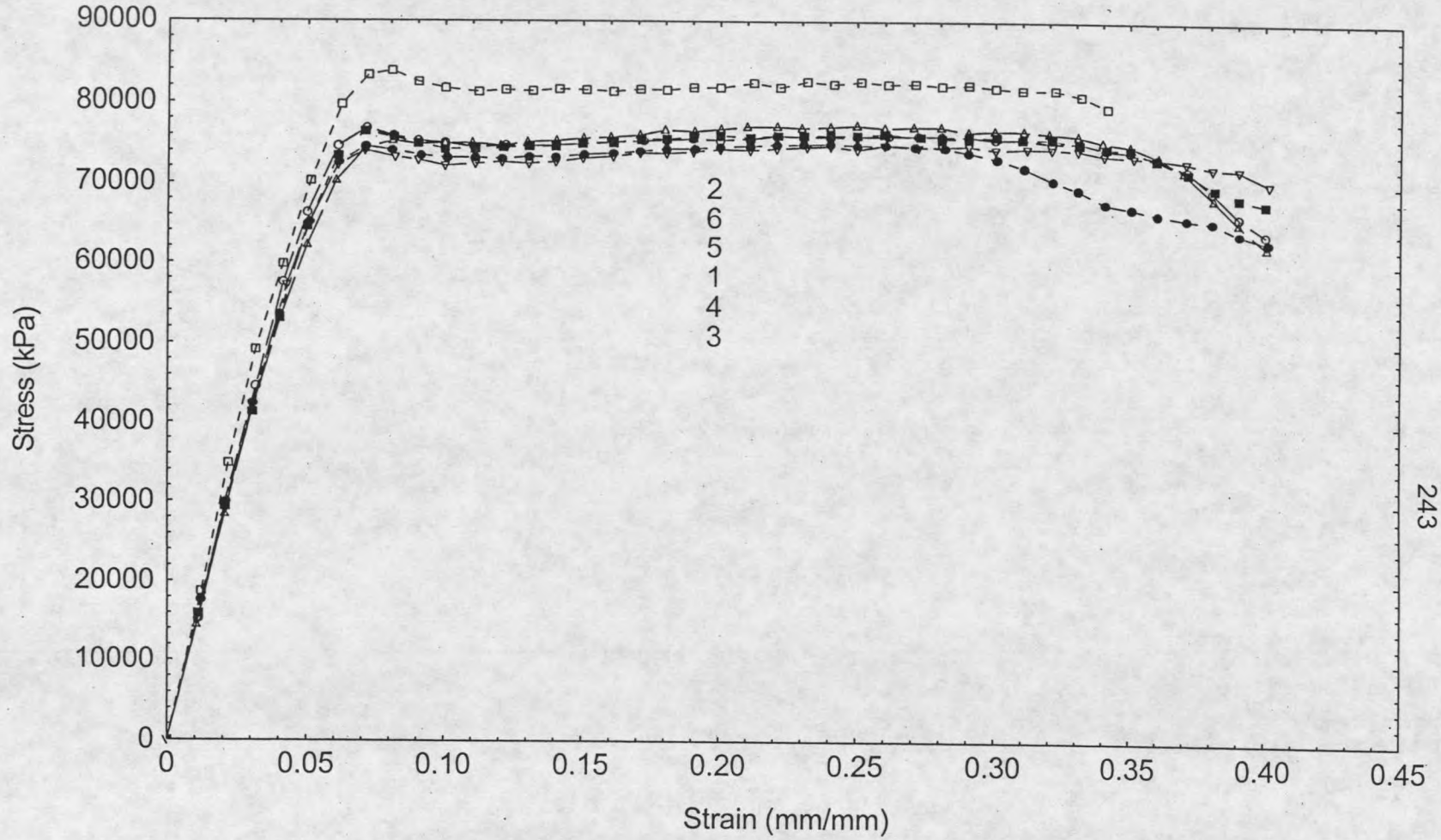


Figure C.I.12 Tensile Testing of Nylon 6/6 Specimens After Cyclic and Constant Loading at 23 °C
1- $(0.16\pm0.04)\sigma_y$, 1 Hz; 2- $(0.16\pm0.075)\sigma_y$, 1 Hz; 3- $(0.16\pm0.10)\sigma_y$, 1 Hz;
4- $(0.16)\sigma_y$, 5- $(0.20)\sigma_y$, Constant Load Creep; 6- Virgin Specimens;
σ_y = 70 MPa at 23 °C

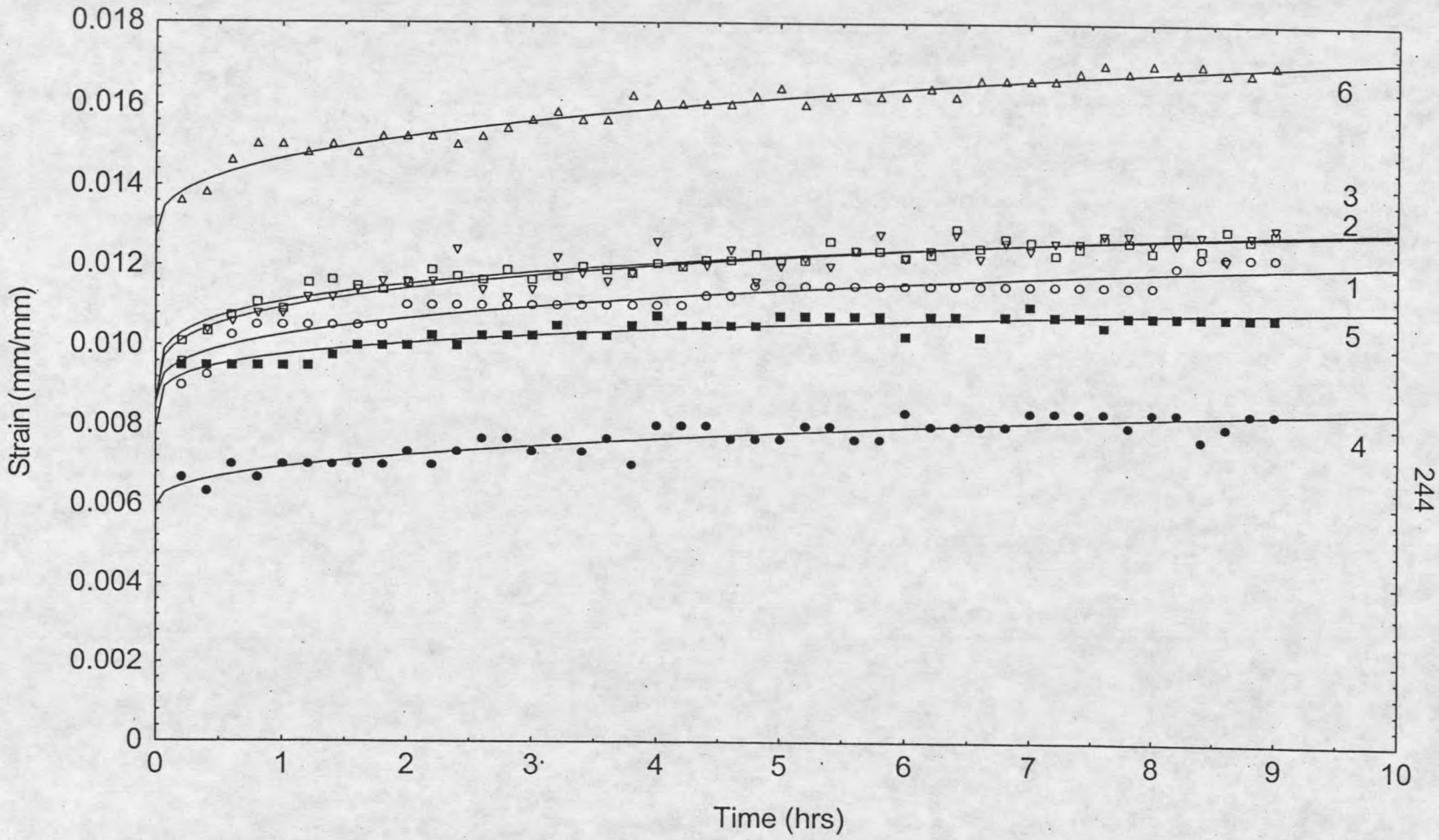


Figure C.I.13 Vibrocreep Response of Nylon 6/6 at Different Amplitudes at 23 °C
1- $(0.16\pm0.04)\sigma_y$, 10 Hz; 2- $(0.16\pm0.075)\sigma_y$, 10 Hz; 3- $(0.16\pm0.10)\sigma_y$, 10 Hz;
4- $(0.16)\sigma_y$, 5- $(0.20)\sigma_y$, 6- $(0.30)\sigma_y$, Constant Load Creep;
σ_y = 70 MPa at 23 °C

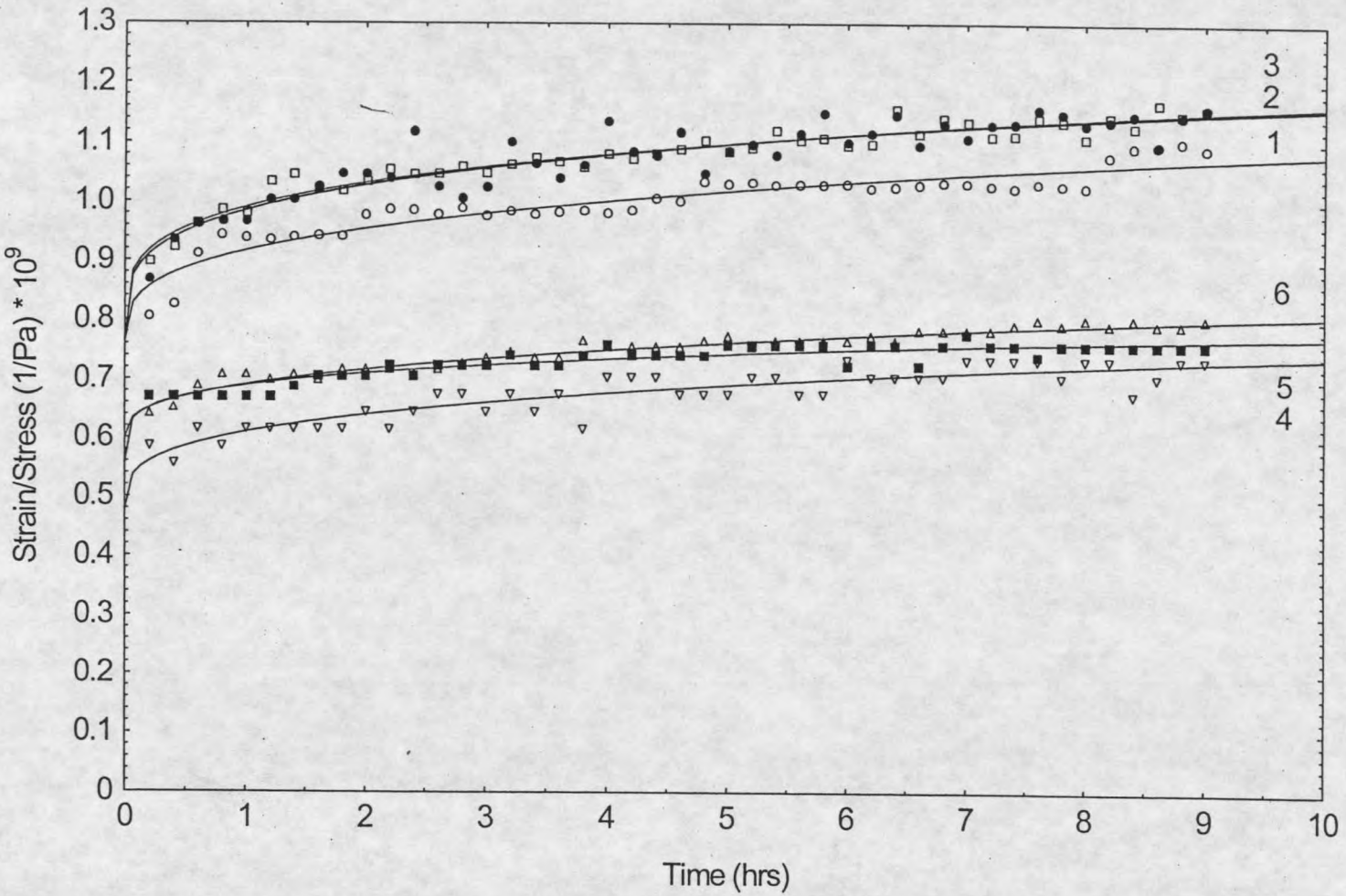


Figure C.I.14 Normalized Vibrocreep Response of Nylon 6/6 at Different Amplitudes at 23 °C
1- $(0.16\pm0.04)\sigma_y$, 10 Hz; 2- $(0.16\pm0.075)\sigma_y$, 10 Hz; 3- $(0.16\pm0.10)\sigma_y$, 10 Hz;
4- $(0.16)\sigma_y$, 5- $(0.20)\sigma_y$, 6- $(0.30)\sigma_y$, Constant Load Creep;
σ_y = 70 MPa at 23 °C

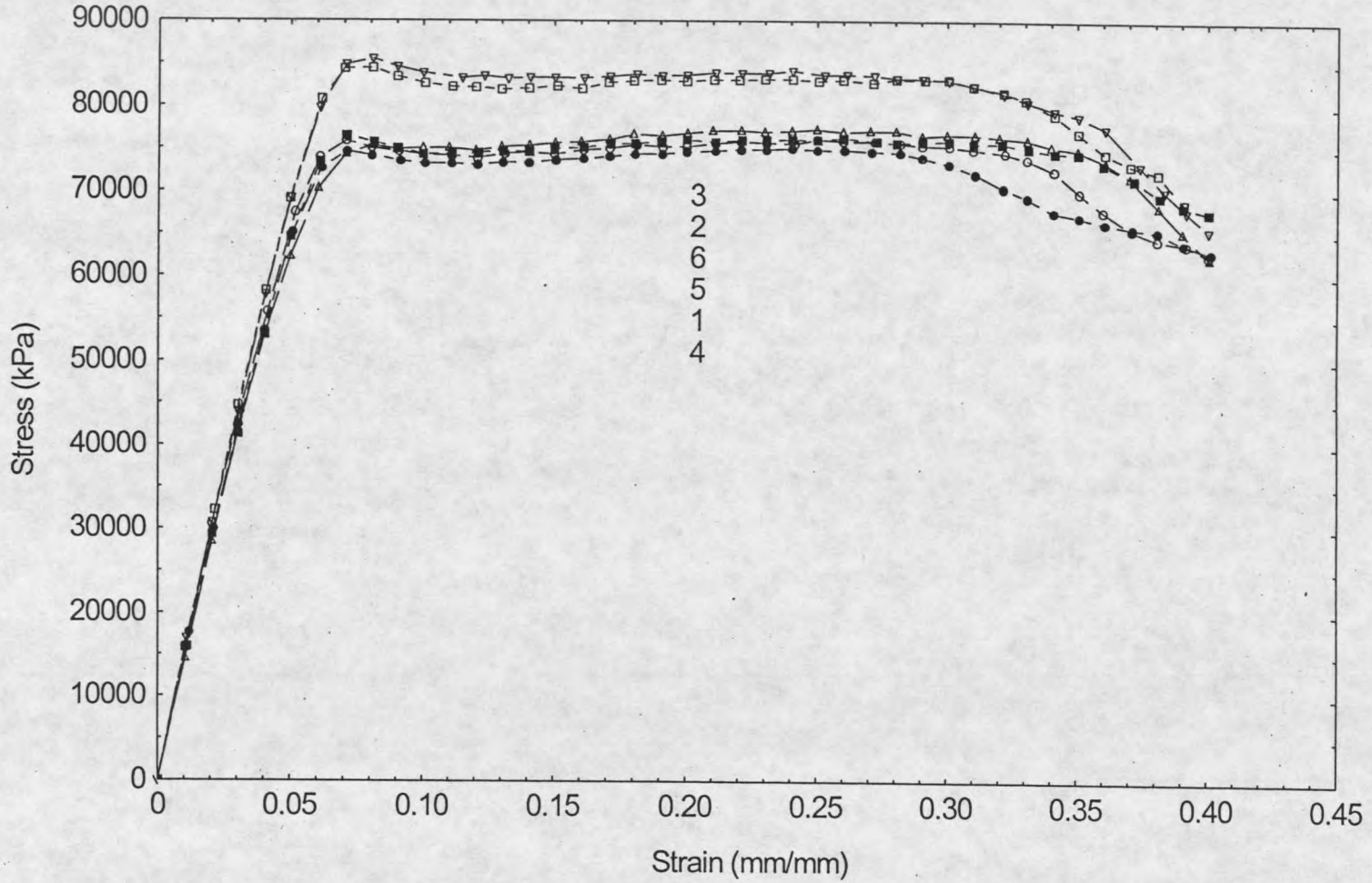


Figure C.I.15 Tensile Testing of Nylon 6/6 Specimens After Cyclic and Constant Loading at 23 °C
1- $(0.16\pm0.04)\sigma_y$, 10 Hz; 2- $(0.16\pm0.075)\sigma_y$, 10 Hz; 3- $(0.16\pm0.10)\sigma_y$, 10 Hz;
4- $(0.16)\sigma_y$, 5- $(0.20)\sigma_y$, Constant Load Creep; 6- Virgin Specimens;
σ_y = 70 MPa at 23 °C

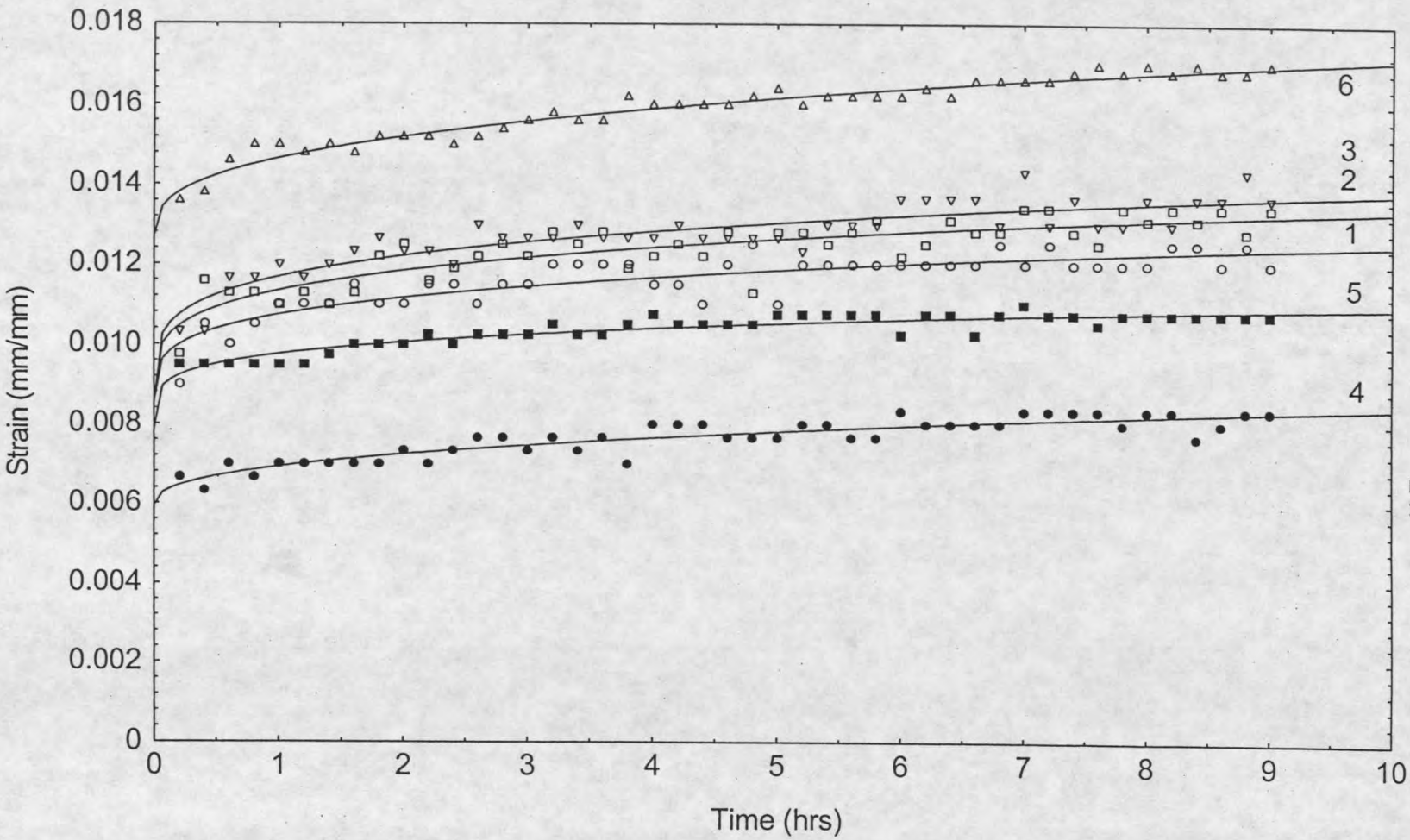


Figure C.I.16 Vibrocreep Response of Nylon 6/6 at Different Amplitudes at 23 °C
1- $(0.16\pm0.04)\sigma_y$, 20 Hz; 2- $(0.16\pm0.075)\sigma_y$, 20 Hz; 3- $(0.16\pm0.10)\sigma_y$, 20 Hz;
4- $(0.16)\sigma_y$, 5- $(0.20)\sigma_y$, 6- $(0.30)\sigma_y$, Constant Load Creep;
σ_y = 70 MPa at 23 °C

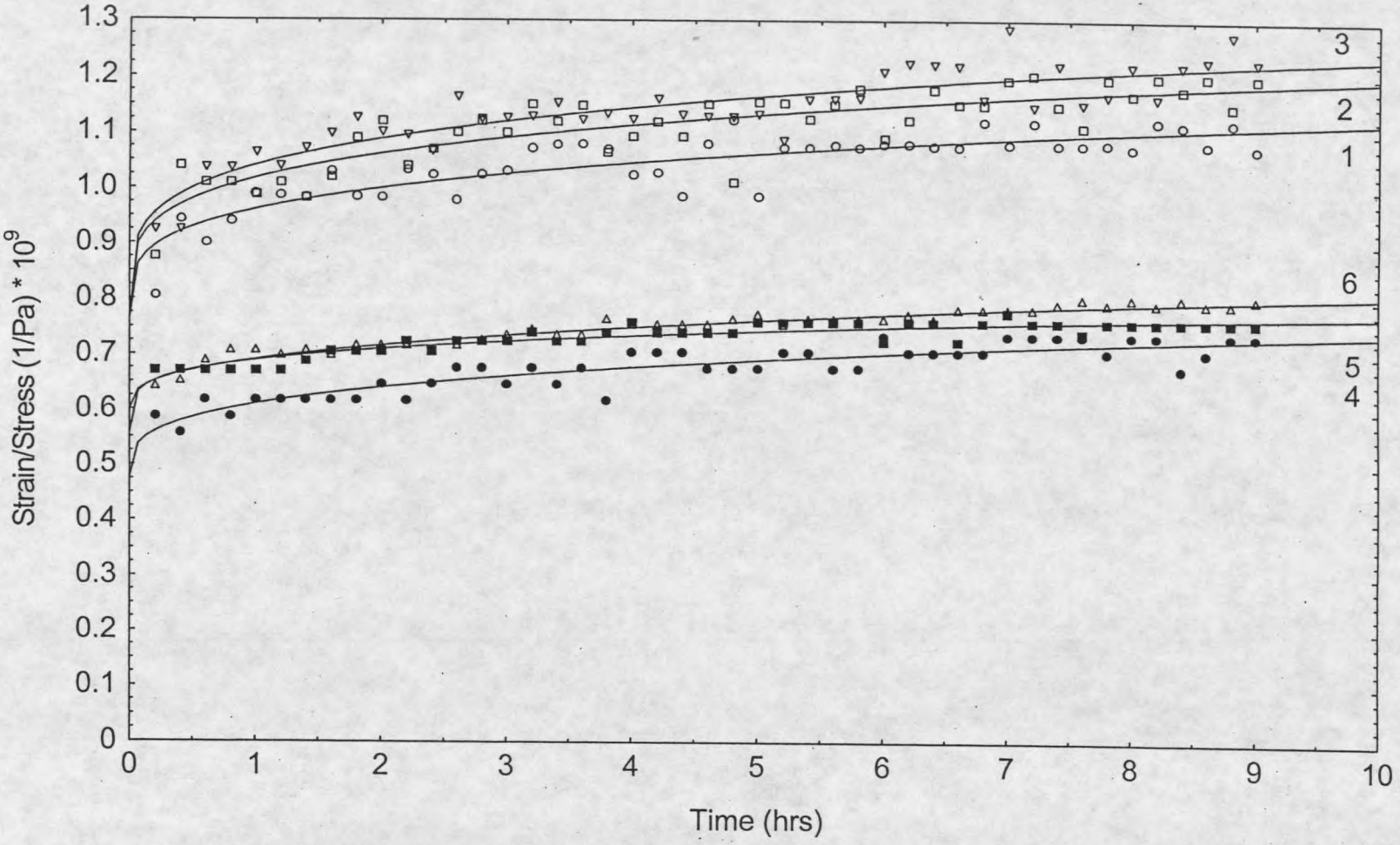


Figure C.I.17 Normalized Vibrocreep Response of Nylon 6/6 at Different Amplitudes at 23 °C
1- $(0.16\pm0.04)\sigma_y$, 20 Hz; 2- $(0.16\pm0.075)\sigma_y$, 20 Hz; 3- $(0.16\pm0.10)\sigma_y$, 20 Hz;
4- $(0.16)\sigma_y$, 5- $(0.20)\sigma_y$, 6- $(0.30)\sigma_y$, Constant Load Creep;
σ_y = 70 MPa at 23 °C

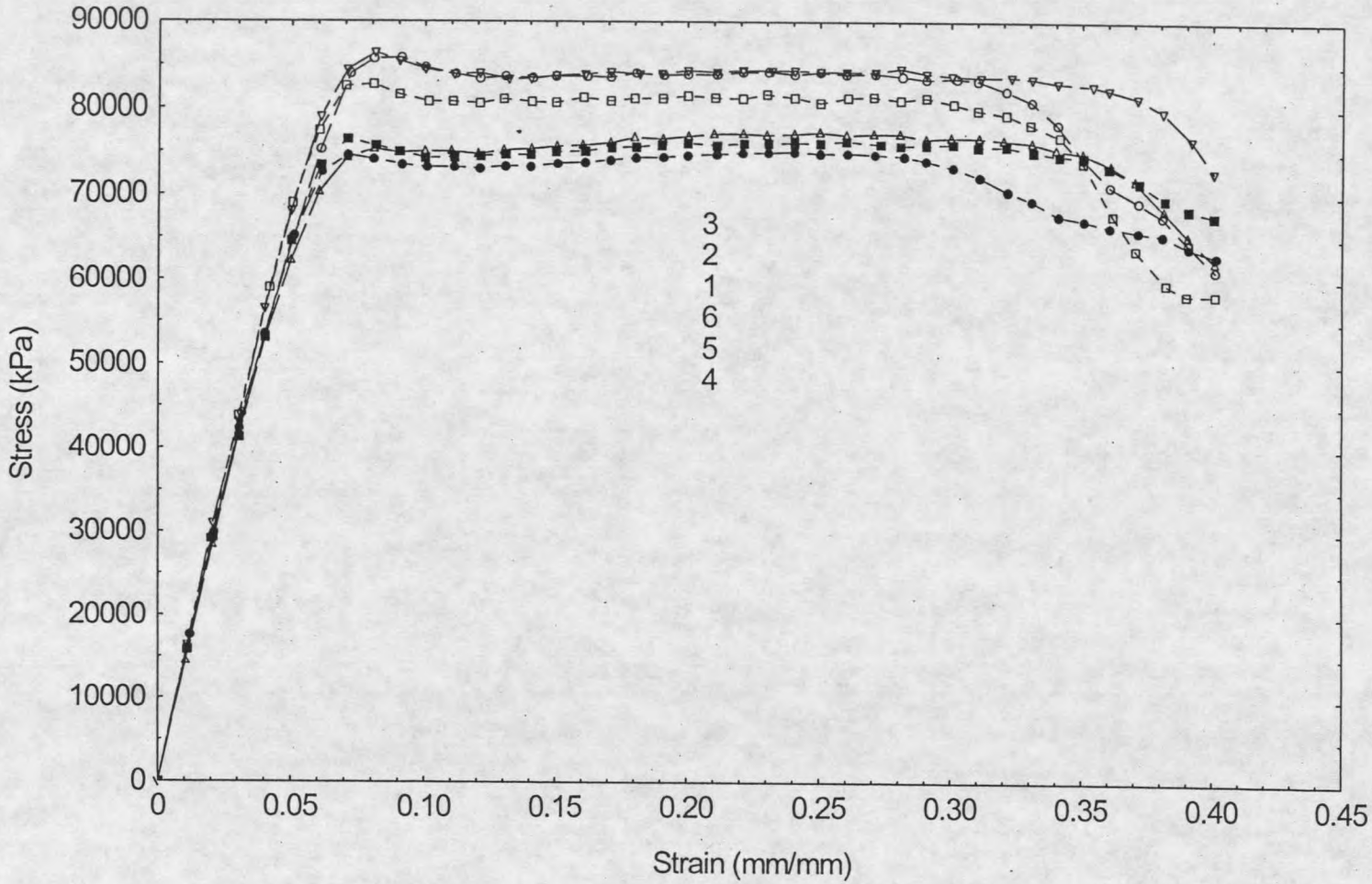


Figure C.I.18 Tensile Testing of Nylon 6/6 Specimens After Cyclic and Constant Loading at 23 °C
1- $(0.16\pm0.04)\sigma_y$, 20 Hz; 2- $(0.16\pm0.075)\sigma_y$, 20 Hz; 3- $(0.16\pm0.10)\sigma_y$, 20 Hz;
4- $(0.16)\sigma_y$, 5- $(0.20)\sigma_y$, Constant Load Creep; 6- Virgin Specimens;
σ_y = 70 MPa at 23 °C

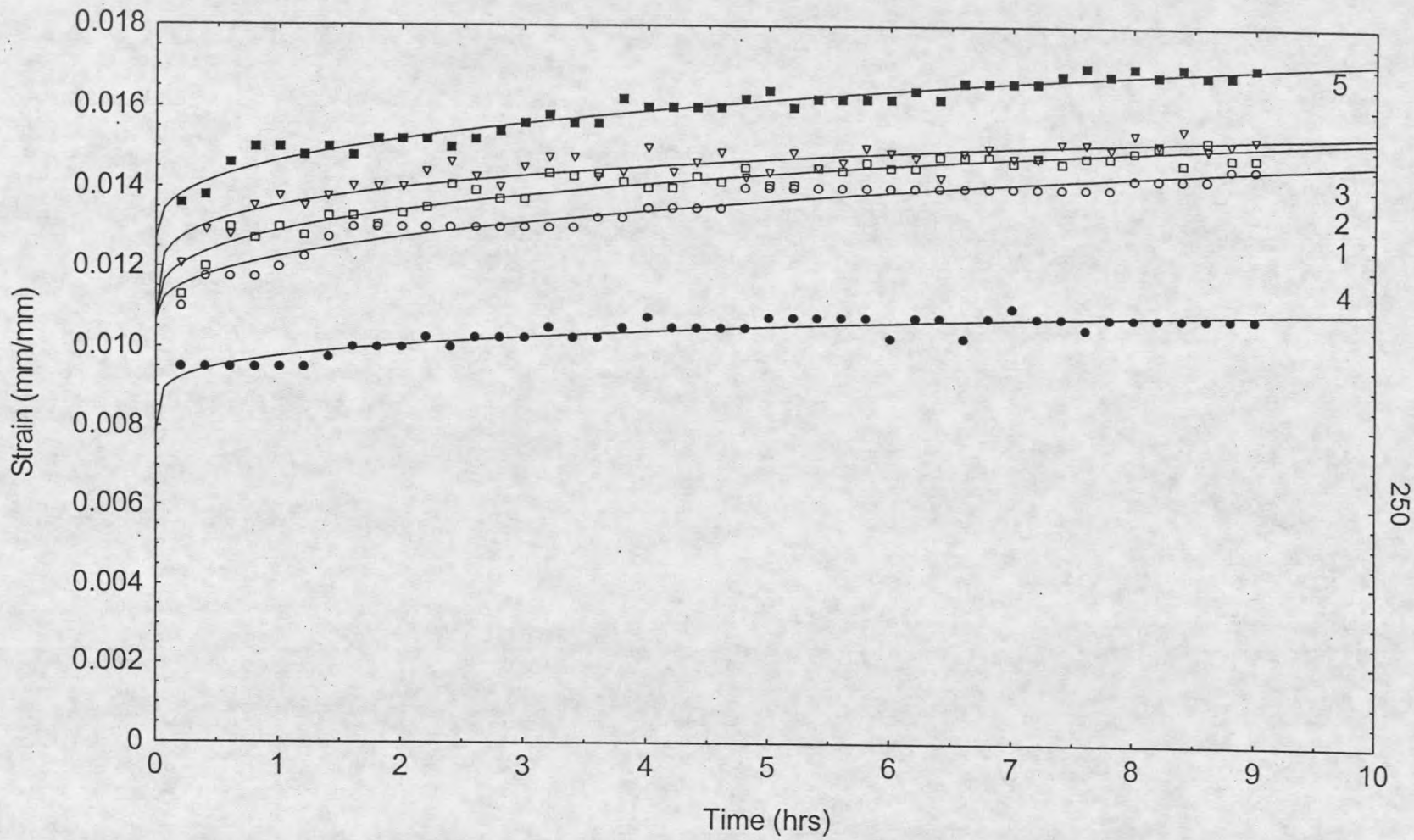


Figure C.I.19 Vibrocreep Response of Nylon 6/6 at Different Amplitudes at 23 °C
1- $(0.20\pm0.05)\sigma_y$, 1 Hz; 2- $(0.20\pm0.075)\sigma_y$, 1 Hz; 3- $(0.20\pm0.10)\sigma_y$, 1 Hz;
4- $(0.20)\sigma_y$, 5- $(0.30)\sigma_y$, Constant Load Creep;
σ_y = 70 MPa at 23 °C

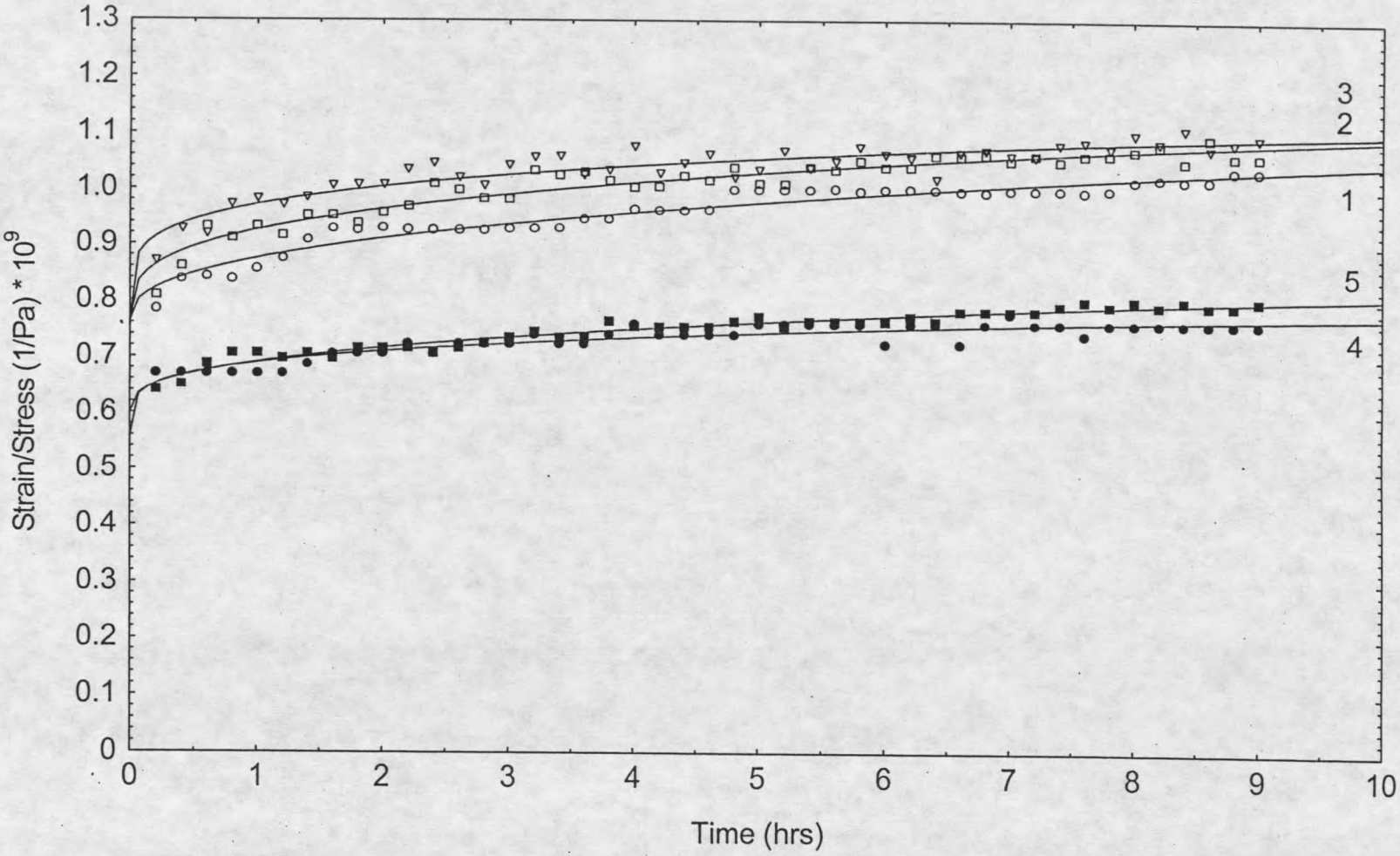


Figure C.I.20 Normalized Vibrocreep Response of Nylon 6/6 at Different Amplitudes at 23 °C
1- $(0.20\pm0.05)\sigma_y$, 1 Hz; 2- $(0.20\pm0.075)\sigma_y$, 1 Hz; 3- $(0.20\pm0.10)\sigma_y$, 1 Hz;
4- $(0.20)\sigma_y$, 5- $(0.30)\sigma_y$, Constant Load Creep;
σ_y = 70 MPa at 23 °C

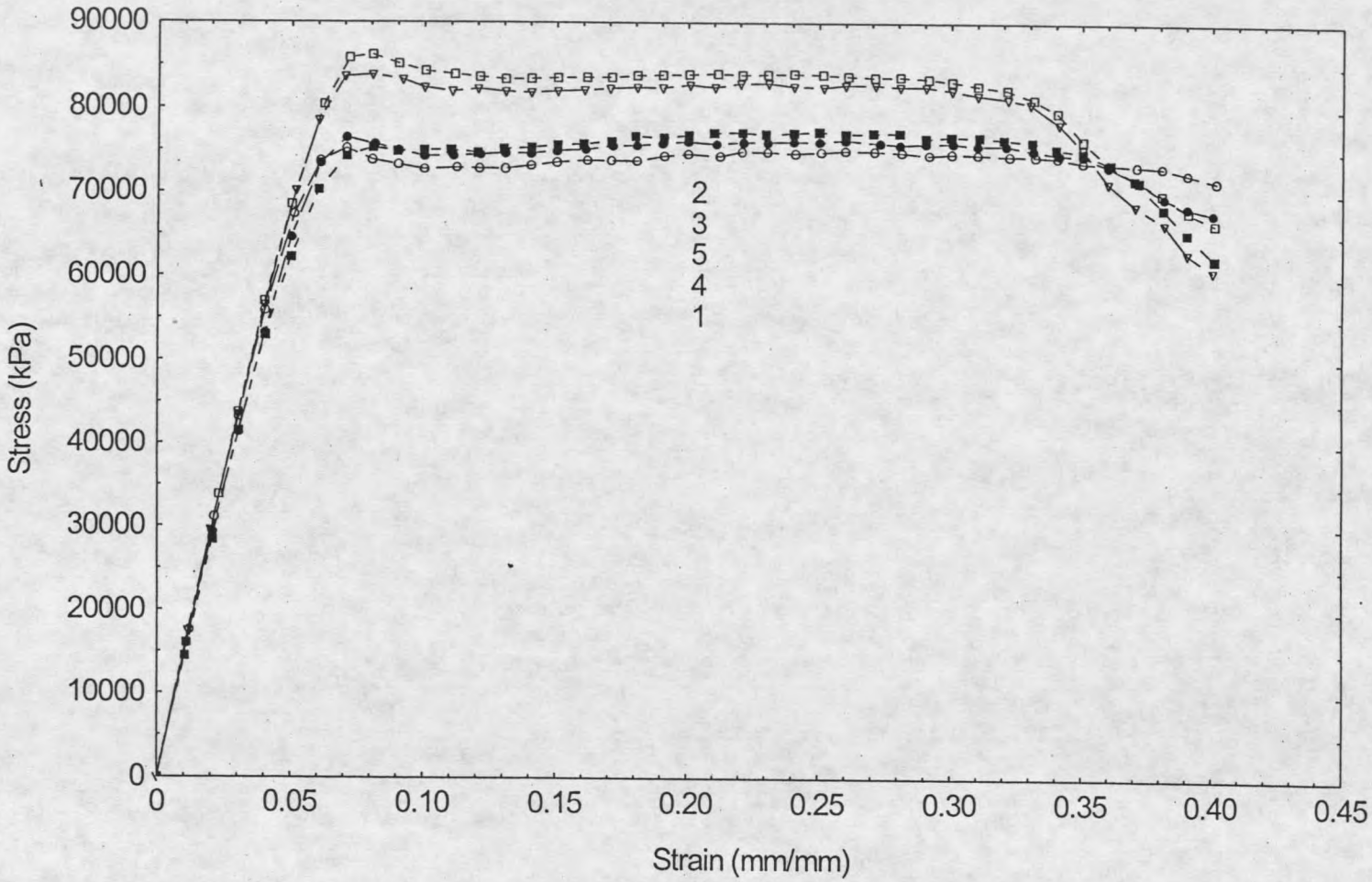


Figure C.I.21 Tensile Testing of Nylon 6/6 Specimens After Cyclic and Constant Loading at 23 °C
1- $(0.20\pm0.05)\sigma_y$, 1 Hz; 2- $(0.20\pm0.075)\sigma_y$, 1 Hz; 3- $(0.20\pm0.10)\sigma_y$, 1 Hz;
4- $(0.20)\sigma_y$, Constant Load Creep; 5- Virgin Specimens;
σ_y = 70 MPa at 23 °C

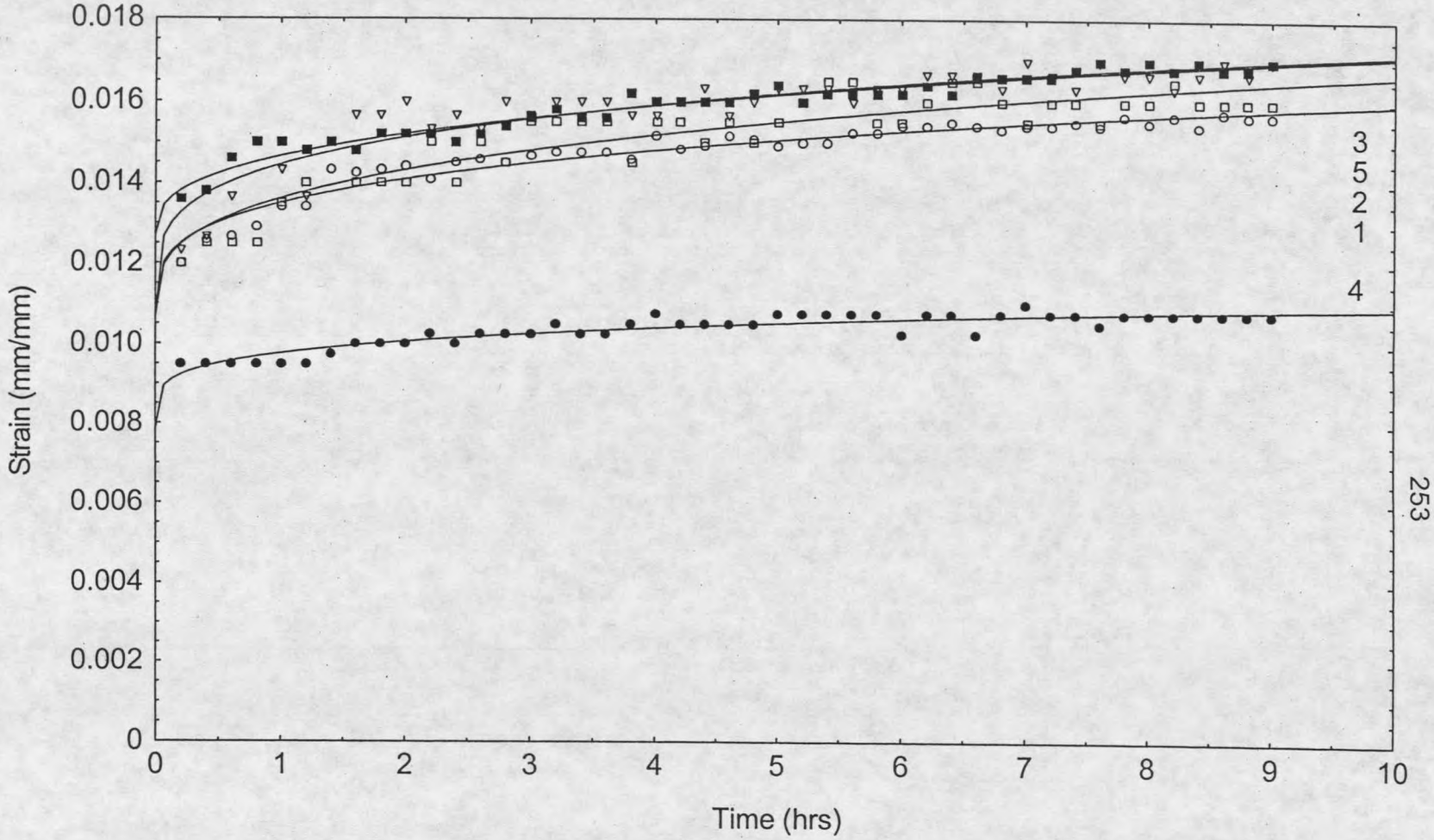


Figure C.I.22 Vibrocreep Response of Nylon 6/6 at Different Amplitudes at 23 °C
1- $(0.20\pm0.05)\sigma_y$, 10 Hz; 2- $(0.20\pm0.075)\sigma_y$, 10 Hz; 3- $(0.20\pm0.10)\sigma_y$, 10 Hz;
4- $(0.20)\sigma_y$, 5- $(0.30)\sigma_y$, Constant Load Creep;
σ_y = 70 MPa at 23 °C

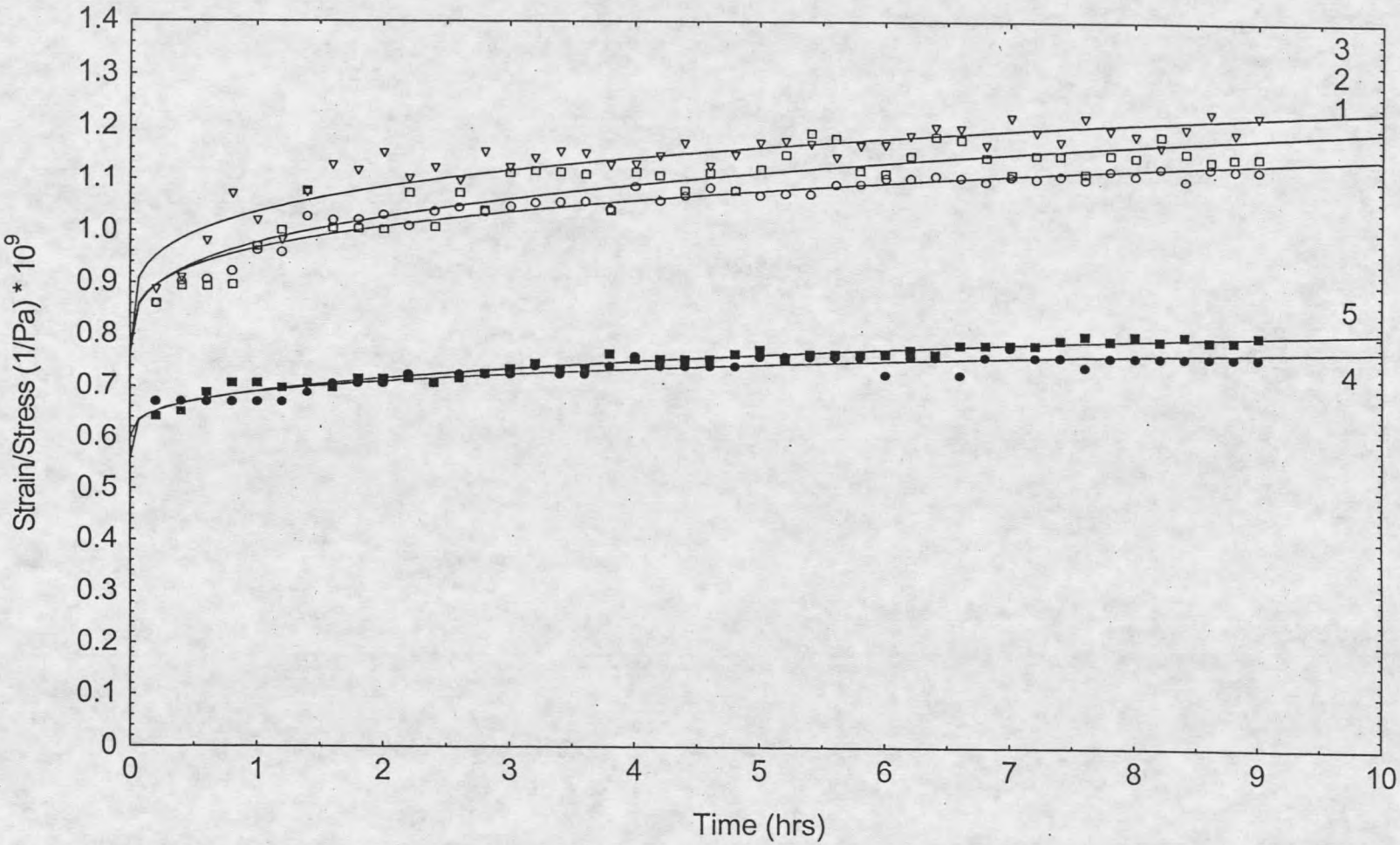


Figure C.I.23 Normalized Vibrocreep Response of Nylon 6/6 at Different Amplitudes at 23 °C
1- $(0.20\pm0.05)\sigma_y$, 10 Hz; 2- $(0.20\pm0.075)\sigma_y$, 10 Hz; 3- $(0.20\pm0.10)\sigma_y$, 10 Hz;
4- $(0.20)\sigma_y$, 5- $(0.30)\sigma_y$, Constant Load Creep;
σ_y = 70 MPa at 23 °C

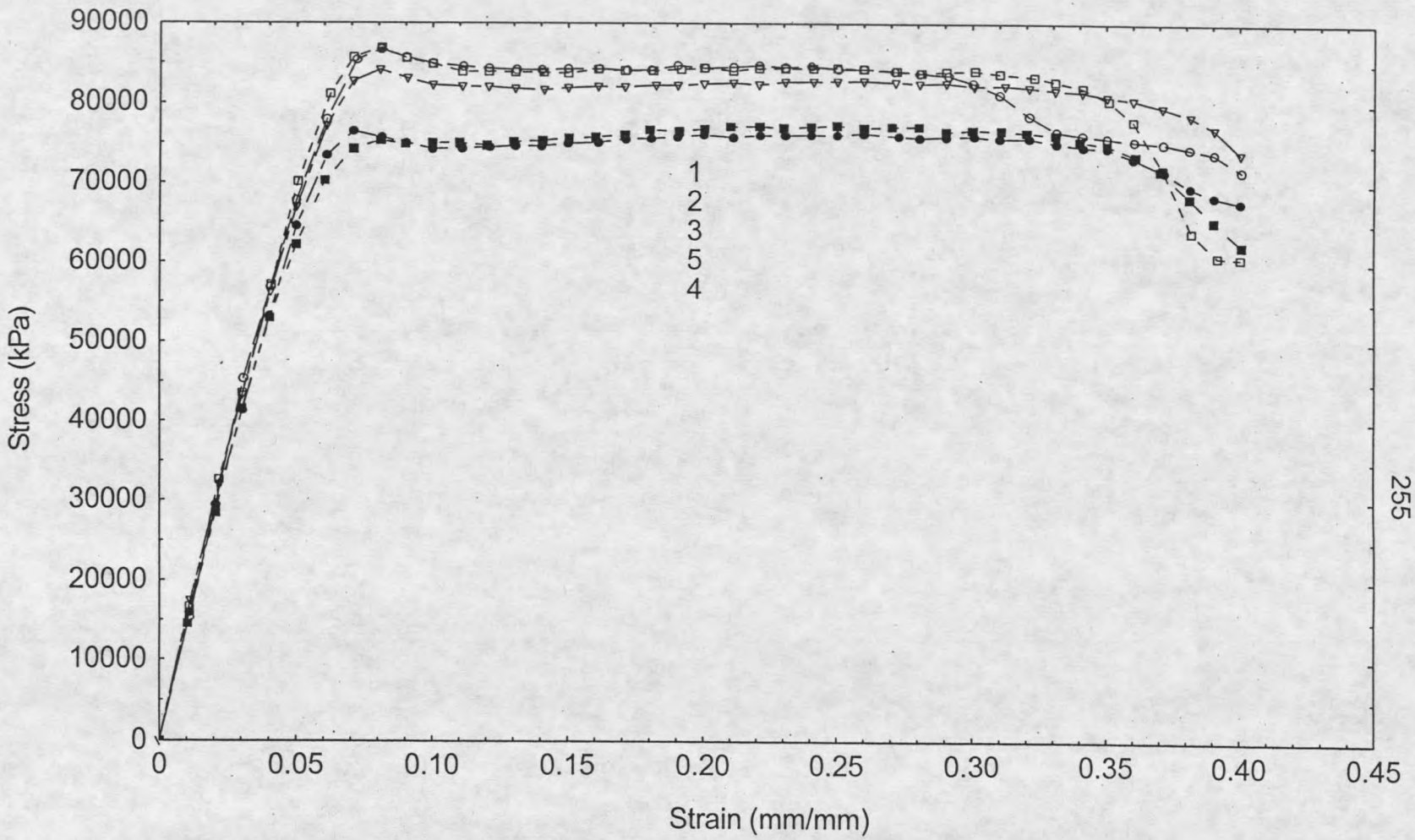


Figure C.I.24 Tensile Testing of Nylon 6/6 Specimens After Cyclic and Constant Loading at 23 °C
1- $(0.20\pm0.05)\sigma_y$, 10 Hz; 2- $(0.20\pm0.075)\sigma_y$, 10 Hz; 3- $(0.20\pm0.10)\sigma_y$, 10 Hz;
4- $(0.20)\sigma_y$, Constant Load Creep; 5- Virgin Specimens;
σ_y = 70 MPa at 23 °C

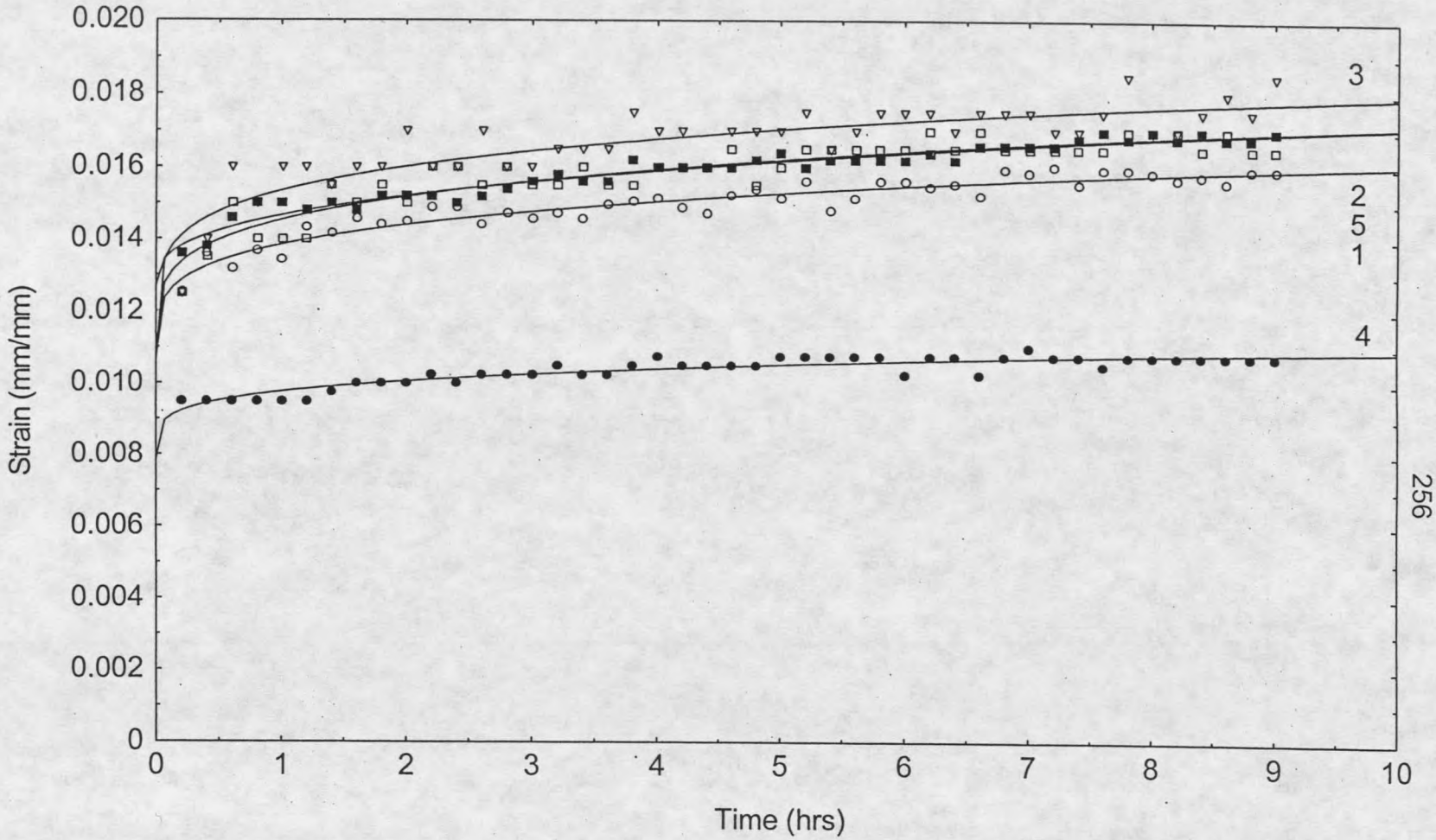


Figure C.I.25 Vibrocreep Response of Nylon 6/6 at Different Amplitudes at 23 °C
1- $(0.20\pm0.05)\sigma_y$, 20 Hz; 2- $(0.20\pm0.075)\sigma_y$, 20 Hz; 3- $(0.20\pm0.10)\sigma_y$, 20 Hz;
4- $(0.20)\sigma_y$, 5- $(0.30)\sigma_y$, Constant Load Creep;
σ_y = 70 MPa at 23 °C

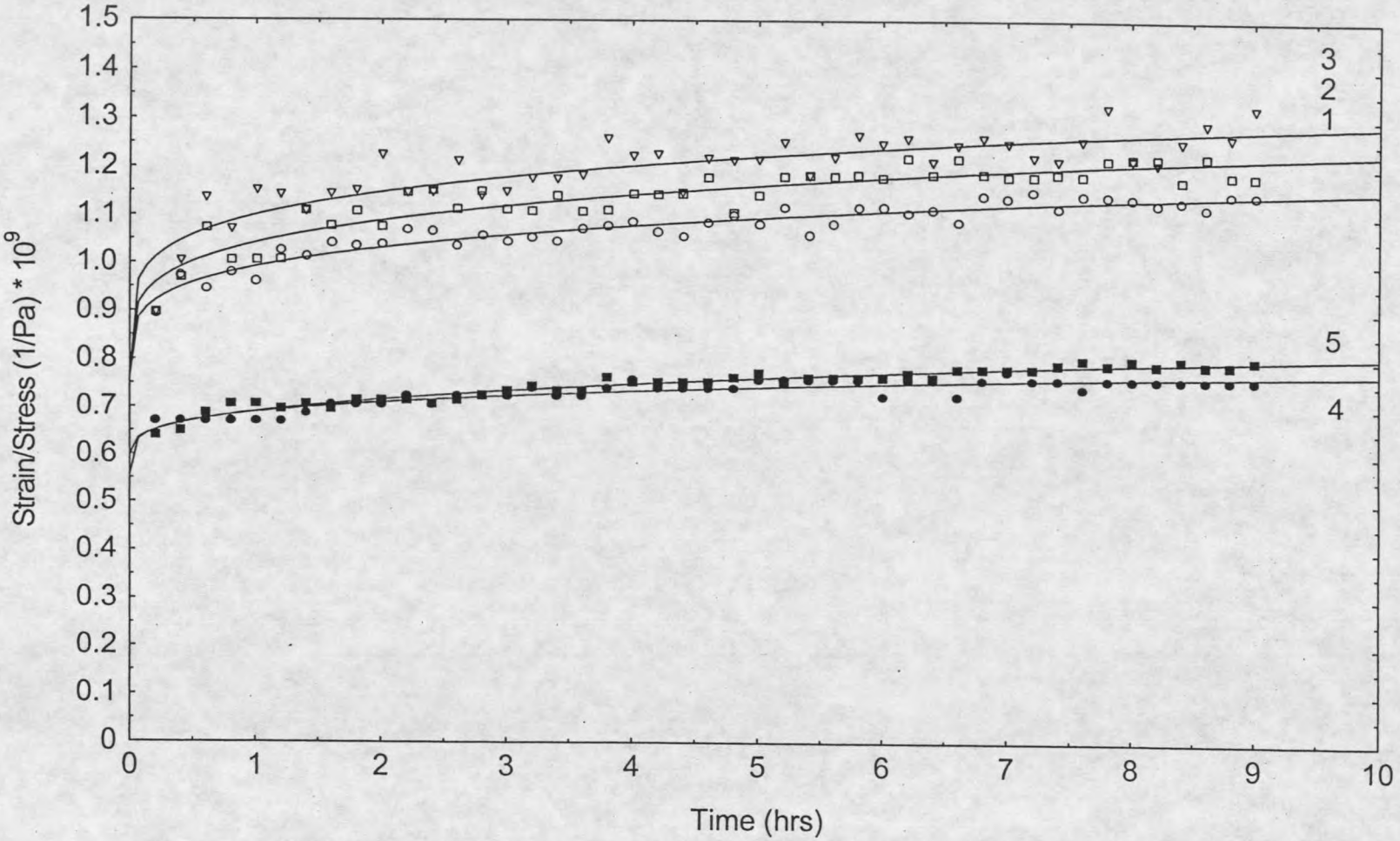


Figure C.I.26 Normalized Vibrocreep Response of Nylon 6/6 at Different Amplitudes at 23 °C
1- $(0.20\pm0.05)\sigma_y$, 20 Hz; 2- $(0.20\pm0.075)\sigma_y$, 20 Hz; 3- $(0.20\pm0.10)\sigma_y$, 20 Hz;
4- $(0.20)\sigma_y$, 5- $(0.30)\sigma_y$, Constant Load Creep;
σ_y = 70 MPa at 23 °C

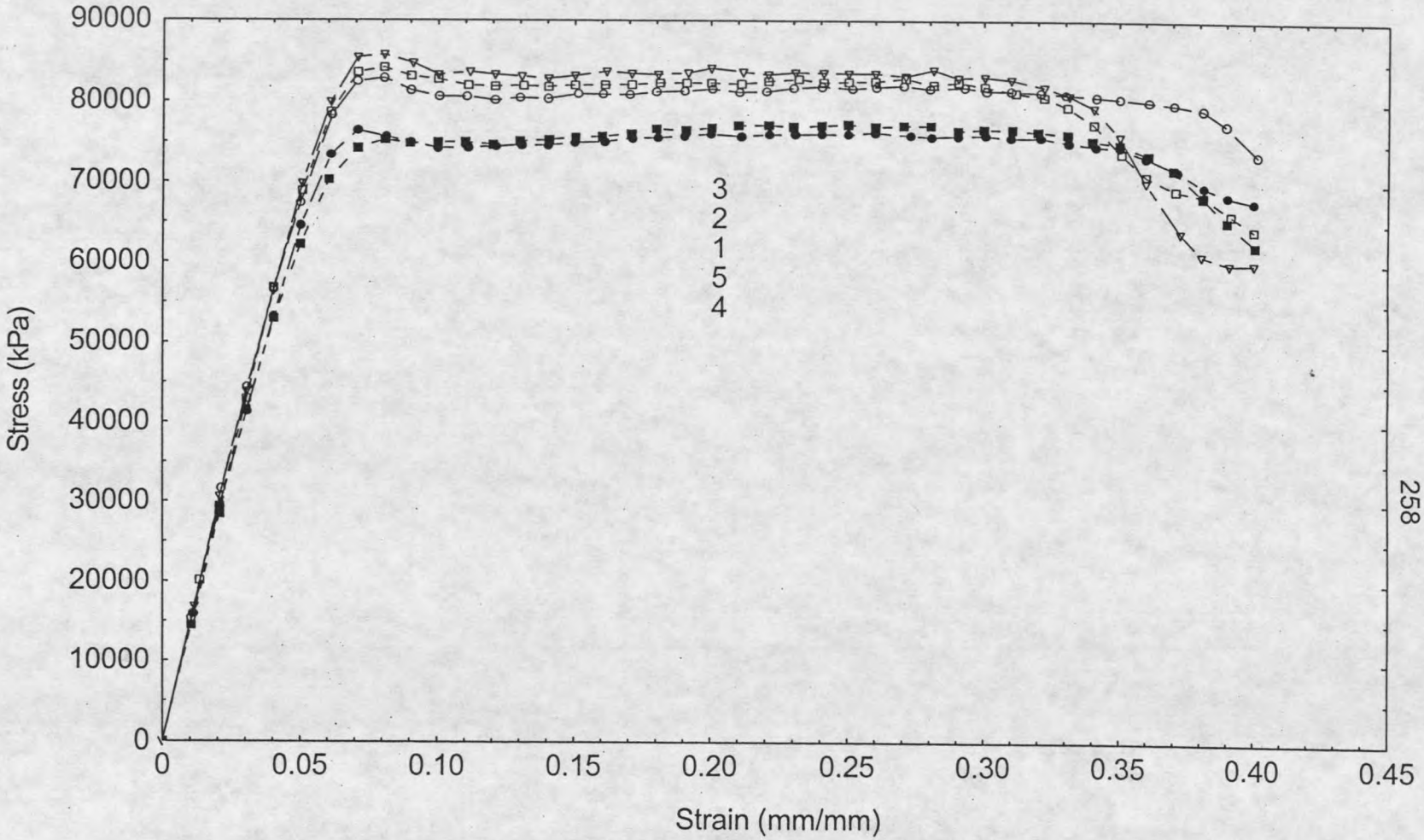


Figure C.I.27 Tensile Testing of Nylon 6/6 Specimens After Cyclic and Constant Loading at 23 °C
1- $(0.20\pm0.05)\sigma_y$, 20 Hz; 2- $(0.20\pm0.075)\sigma_y$, 20 Hz; 3- $(0.20\pm0.10)\sigma_y$, 20 Hz;
4- $(0.20)\sigma_y$, Constant Load Creep; 5- Virgin Specimens;
σ_y = 70 MPa at 23 °C

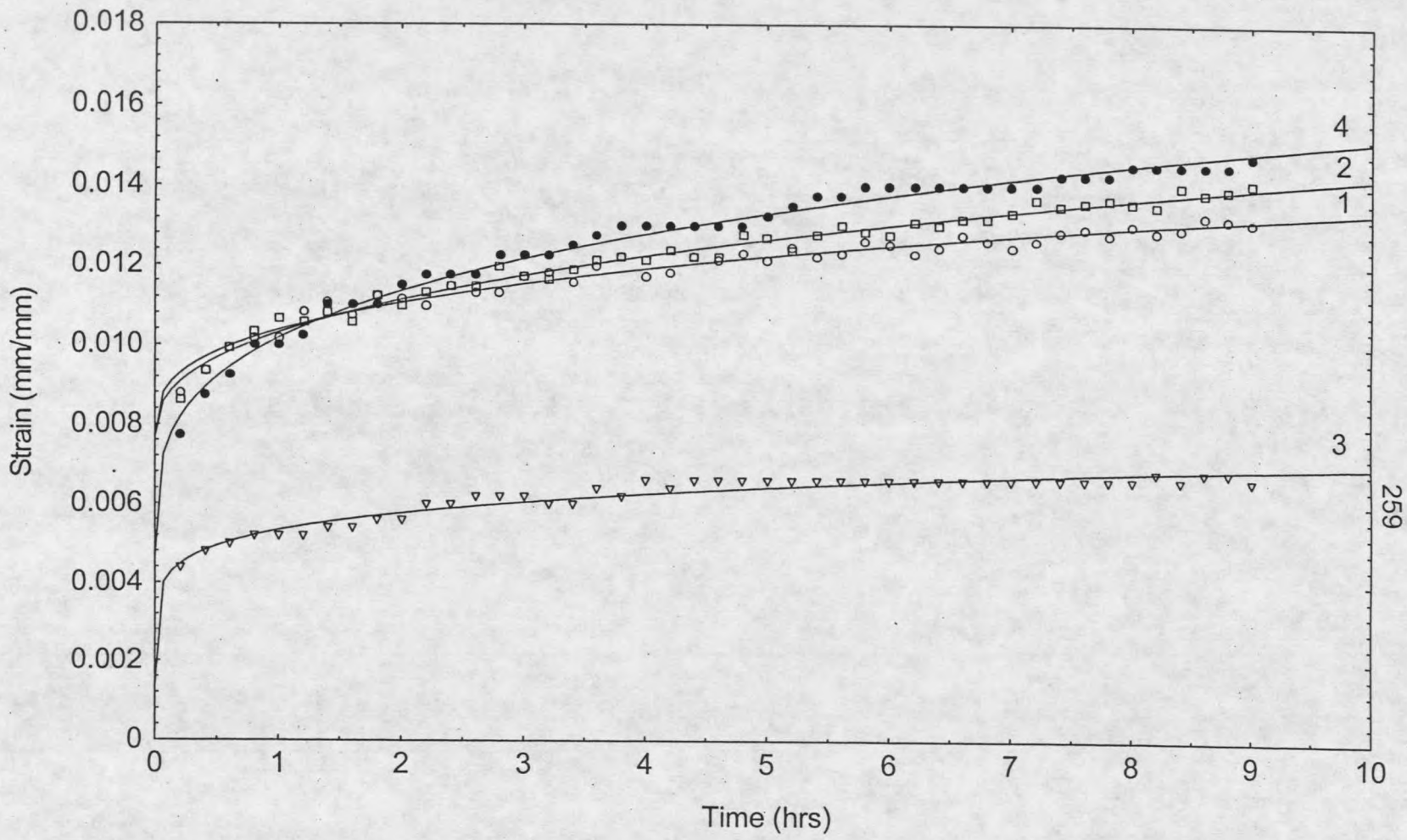


Figure C.II.1 Vibrocreep Response of Nylon 6/6 at Different Amplitudes at 35 °C
1- $(0.16\pm0.04)\sigma_y$, 1 Hz; 2- $(0.16\pm0.10)\sigma_y$, 1 Hz;
3- $(0.16)\sigma_y$, 4- $(0.30)\sigma_y$, Constant Load Creep;
σ_y = 55 MPa at 35 °C

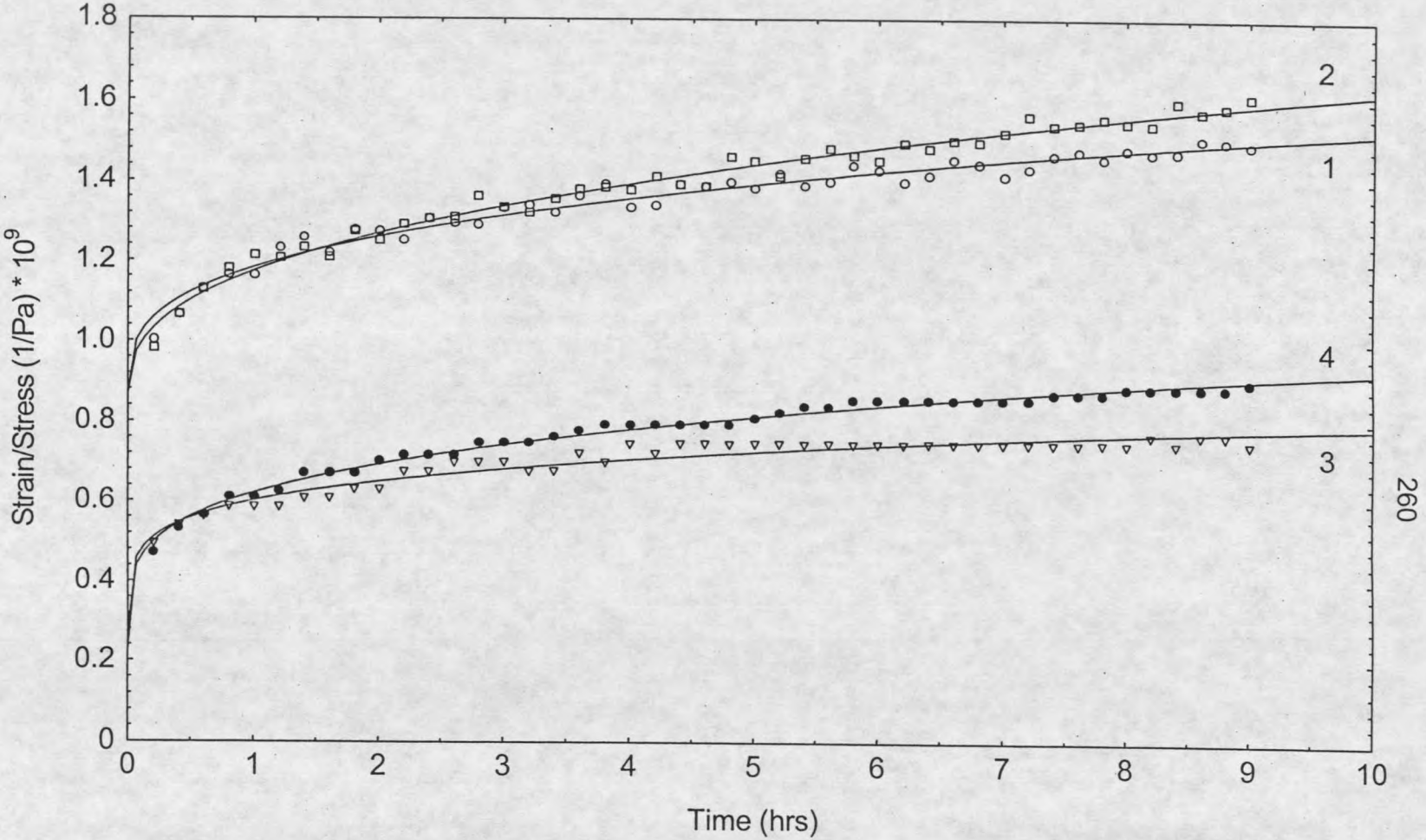


Figure C.II.2 Normalized Vibrocreep Response of Nylon 6/6 at Different Amplitudes at 35 °C
1- $(0.16\pm0.04)\sigma_y$, 1 Hz; 2- $(0.16\pm0.10)\sigma_y$, 1 Hz;
3- $(0.16)\sigma_y$, 4- $(0.30)\sigma_y$, Constant Load Creep;
σ_y = 55 MPa at 35 °C

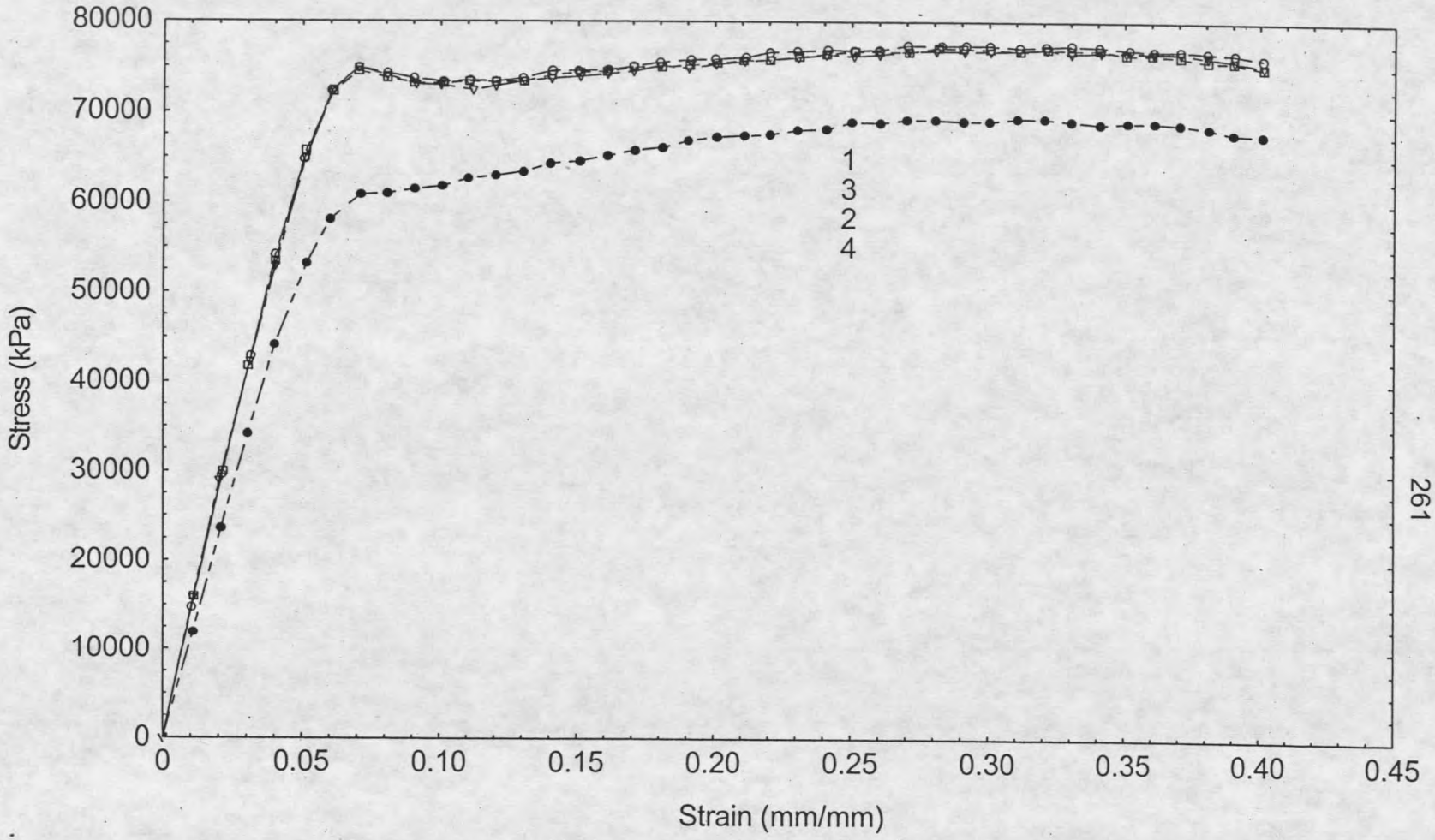


Figure C.II.3 Tensile Testing of Nylon 6/6 Specimens After Cyclic and Constant Loading at 35 °C
1- $(0.16\pm0.04)\sigma_y$, 1 Hz; 2- $(0.16\pm0.10)\sigma_y$, 1 Hz;
3- $(0.16)\sigma_y$, Constant Load Creep; 4- Virgin Specimens;
σ_y = 55 MPa at 35 °C

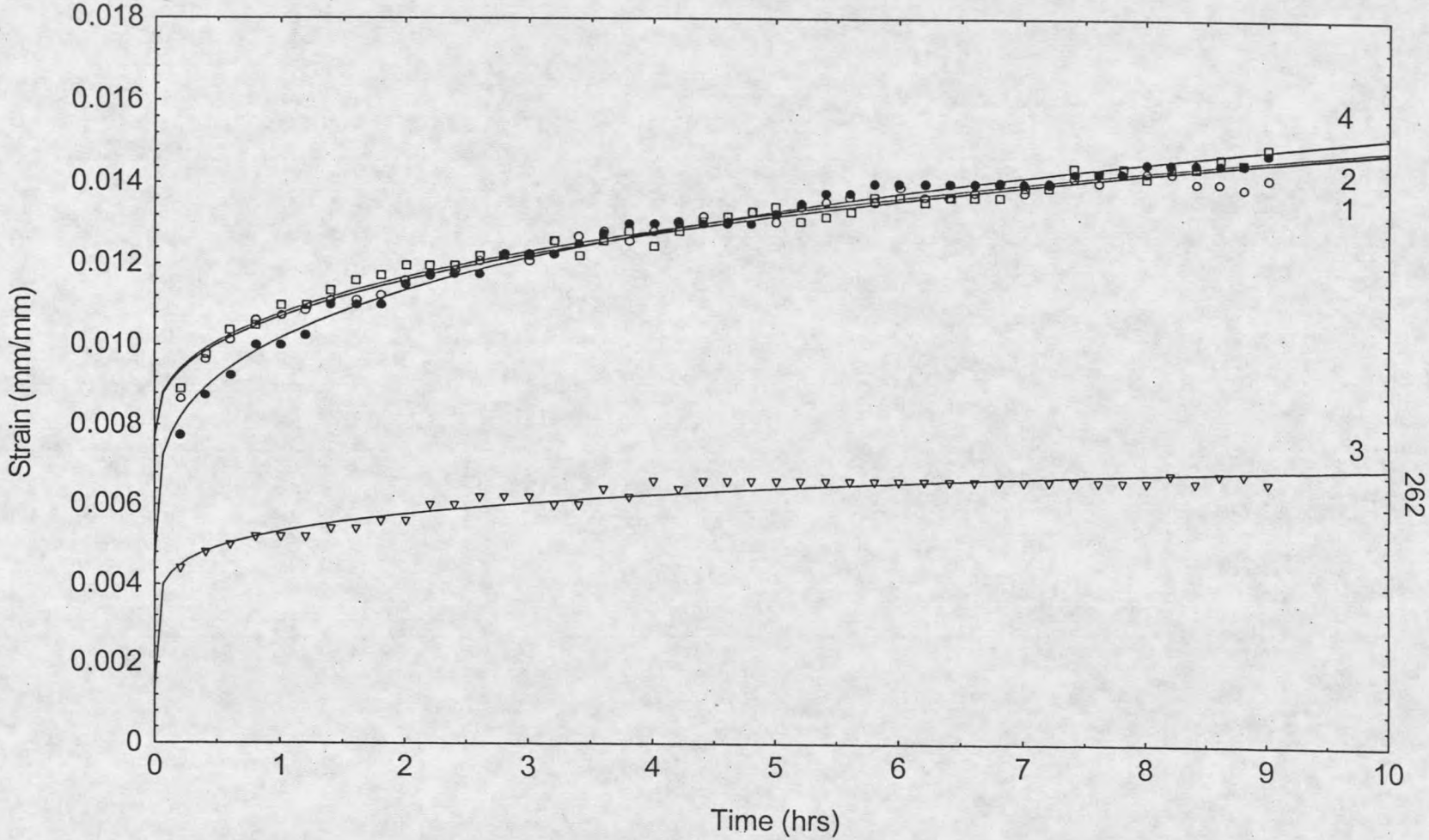


Figure C.II.4 Vibrocreep Response of Nylon 6/6 at Different Amplitudes at 35 °C
1- $(0.16\pm0.04)\sigma_y$, 10 Hz; 2- $(0.16\pm0.10)\sigma_y$, 10 Hz;
3- $(0.16)\sigma_y$, 4- $(0.30)\sigma_y$, Constant Load Creep;
σ_y = 55 MPa at 35 °C

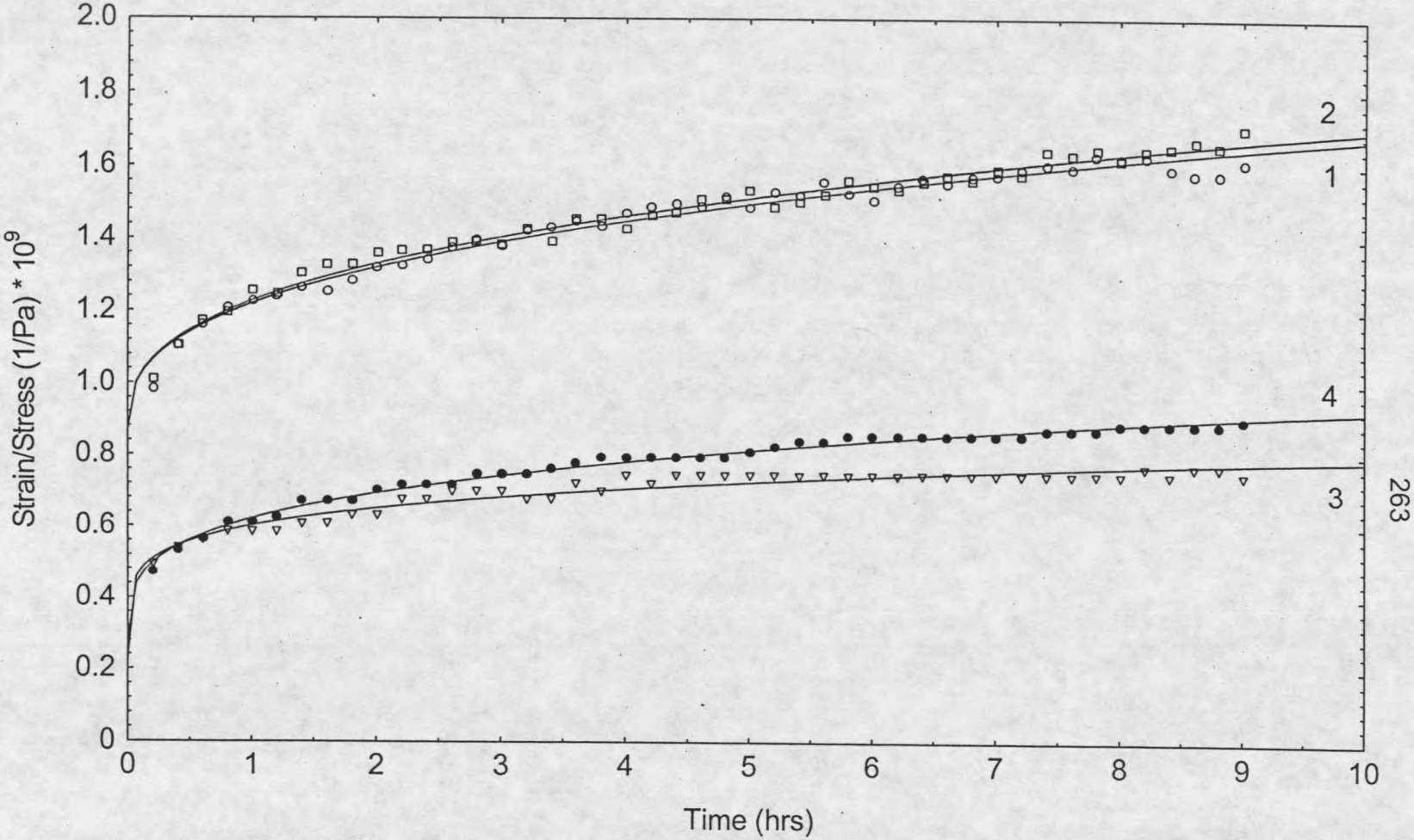


Figure C.II.5 Normalized Vibrocreep Response of Nylon 6/6 at Different Amplitudes at 35 °C
1- $(0.16\pm0.04)\sigma_y$, 10 Hz; 2- $(0.16\pm0.10)\sigma_y$, 10 Hz;
3- $(0.16)\sigma_y$, 4- $(0.30)\sigma_y$, Constant Load Creep;
σ_y = 55 MPa at 35 °C

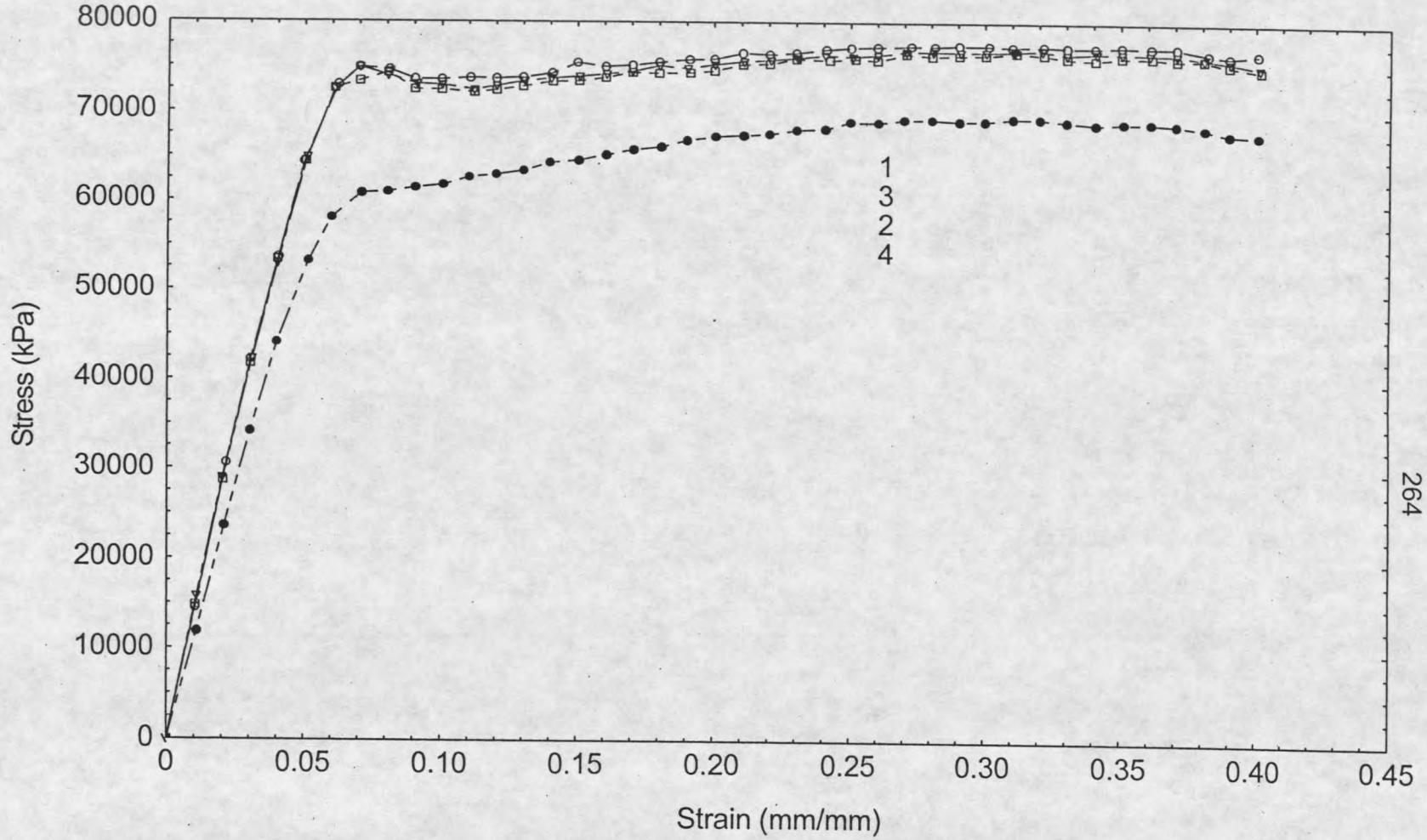


Figure C.II.6 Tensile Testing of Nylon 6/6 Specimens After Cyclic and Constant Loading at 35 °C
1- $(0.16\pm0.04)\sigma_y$, 10 Hz; 2- $(0.16\pm0.10)\sigma_y$, 10 Hz;
3- $(0.16)\sigma_y$, Constant Load Creep; 4- Virgin Specimens;
σ_y = 55 MPa at 35 °C

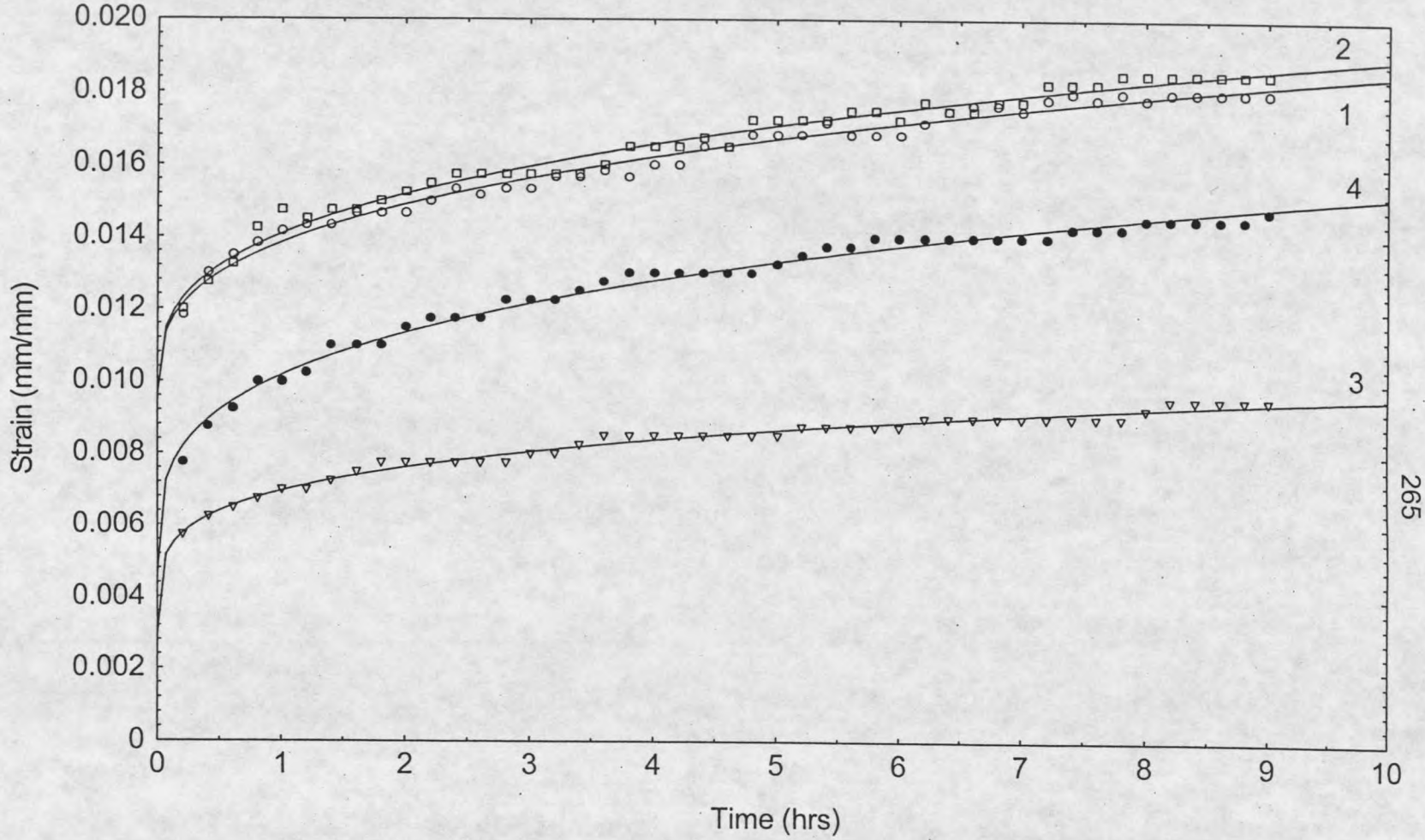


Figure C.II.7 Vibrocreep Response of Nylon 6/6 at Different Amplitudes at 35 °C
1- $(0.20\pm0.05)\sigma_y$, 1 Hz; 2- $(0.20\pm0.10)\sigma_y$, 1 Hz;
3- $(0.20)\sigma_y$, 4- $(0.30)\sigma_y$, Constant Load Creep;
σ_y = 55 MPa at 35 °C

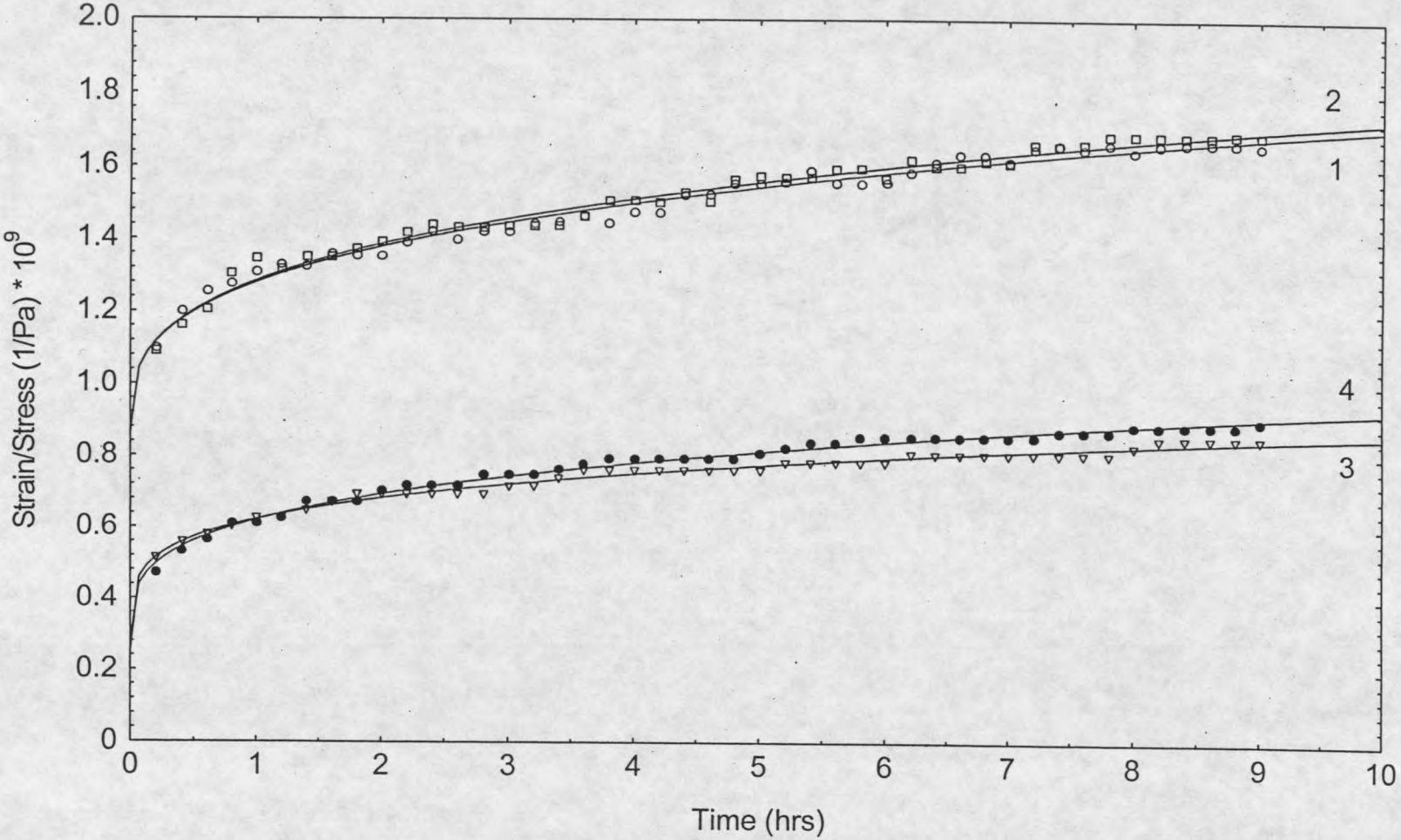


Figure C.II.8 Normalized Vibrocreep Response of Nylon 6/6 at Different Amplitudes at 35 °C
1- $(0.20\pm0.05)\sigma_y$, 1 Hz; 2- $(0.20\pm0.10)\sigma_y$, 1 Hz;
3- $(0.20)\sigma_y$, 4- $(0.30)\sigma_y$, Constant Load Creep;
σ_y = 55 MPa at 35 °C

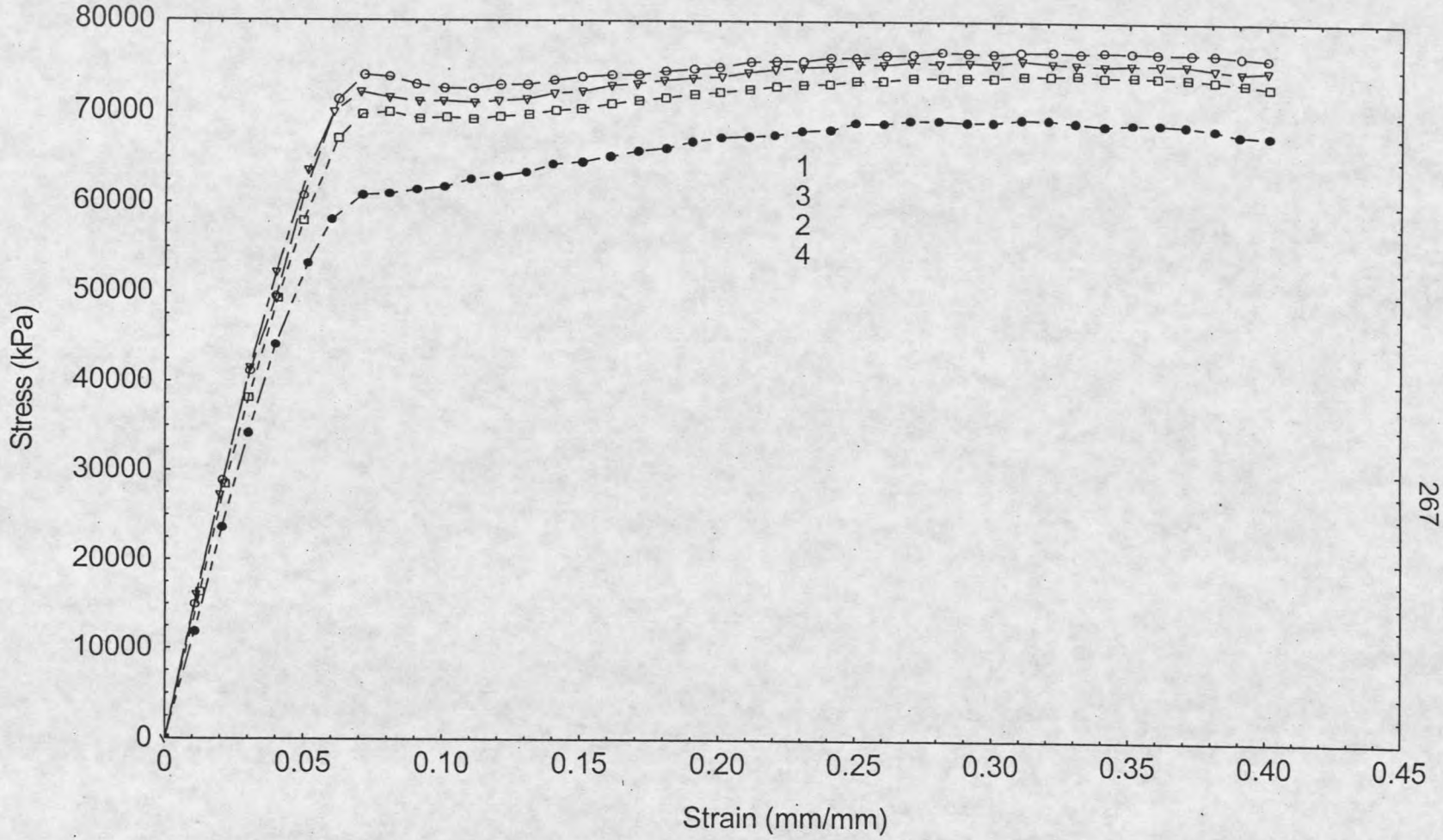


Figure C.II.9 Tensile Testing of Nylon 6/6 Specimens After Cyclic and Constant Loading at 35 °C
1- $(0.20\pm0.05)\sigma_y$, 1 Hz; 2- $(0.20\pm0.10)\sigma_y$, 1 Hz;
3- $(0.20)\sigma_y$, Constant Load Creep; 4- Virgin Specimens;
σ_y = 55 MPa at 35 °C

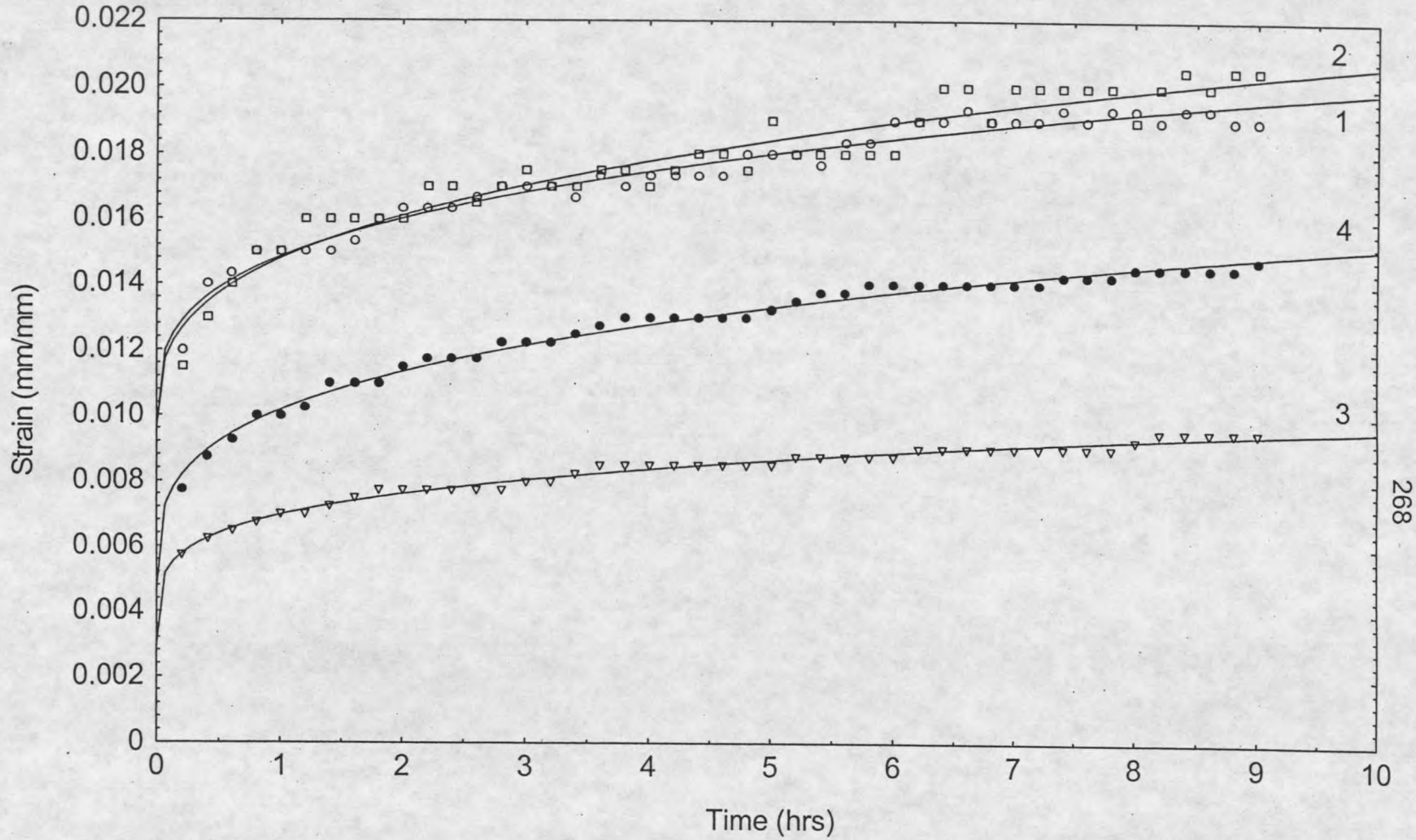


Figure C.II.10 Vibrocreep Response of Nylon 6/6 at Different Amplitudes at 35 °C
1- $(0.20\pm0.05)\sigma_y$, 10 Hz; 2- $(0.20\pm0.10)\sigma_y$, 10 Hz;
3- $(0.20)\sigma_y$, 4- $(0.30)\sigma_y$, Constant Load Creep;
σ_y = 55 MPa at 35 °C

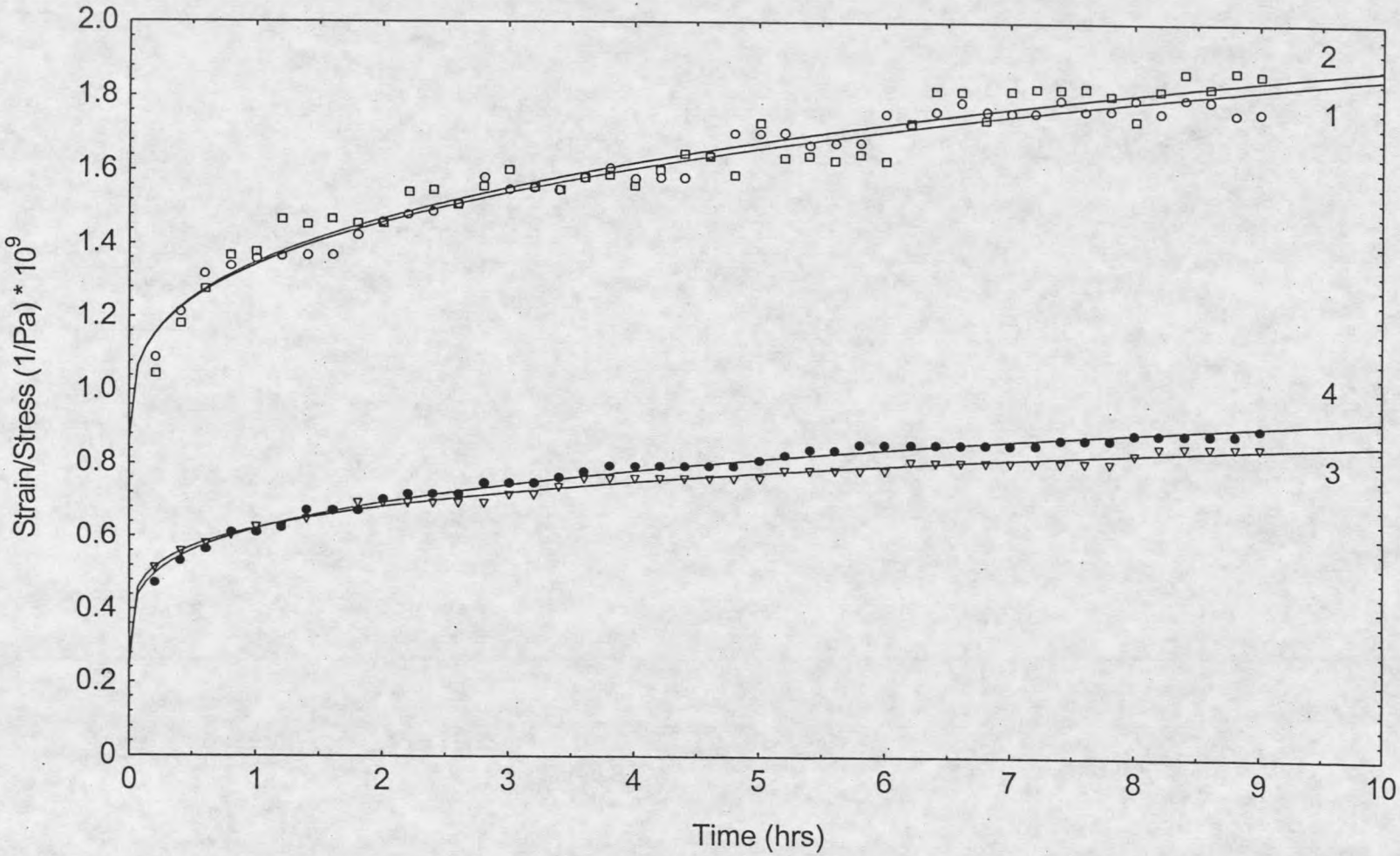


Figure C.II.11 Normalized Vibrocreep Response of Nylon 6/6 at Different Amplitudes at 35 °C
1- $(0.20\pm0.05)\sigma_y$, 10 Hz; 2- $(0.20\pm0.10)\sigma_y$, 10 Hz;
3- $(0.20)\sigma_y$, 4- $(0.30)\sigma_y$, Constant Load Creep;
σ_y = 55 MPa at 35 °C

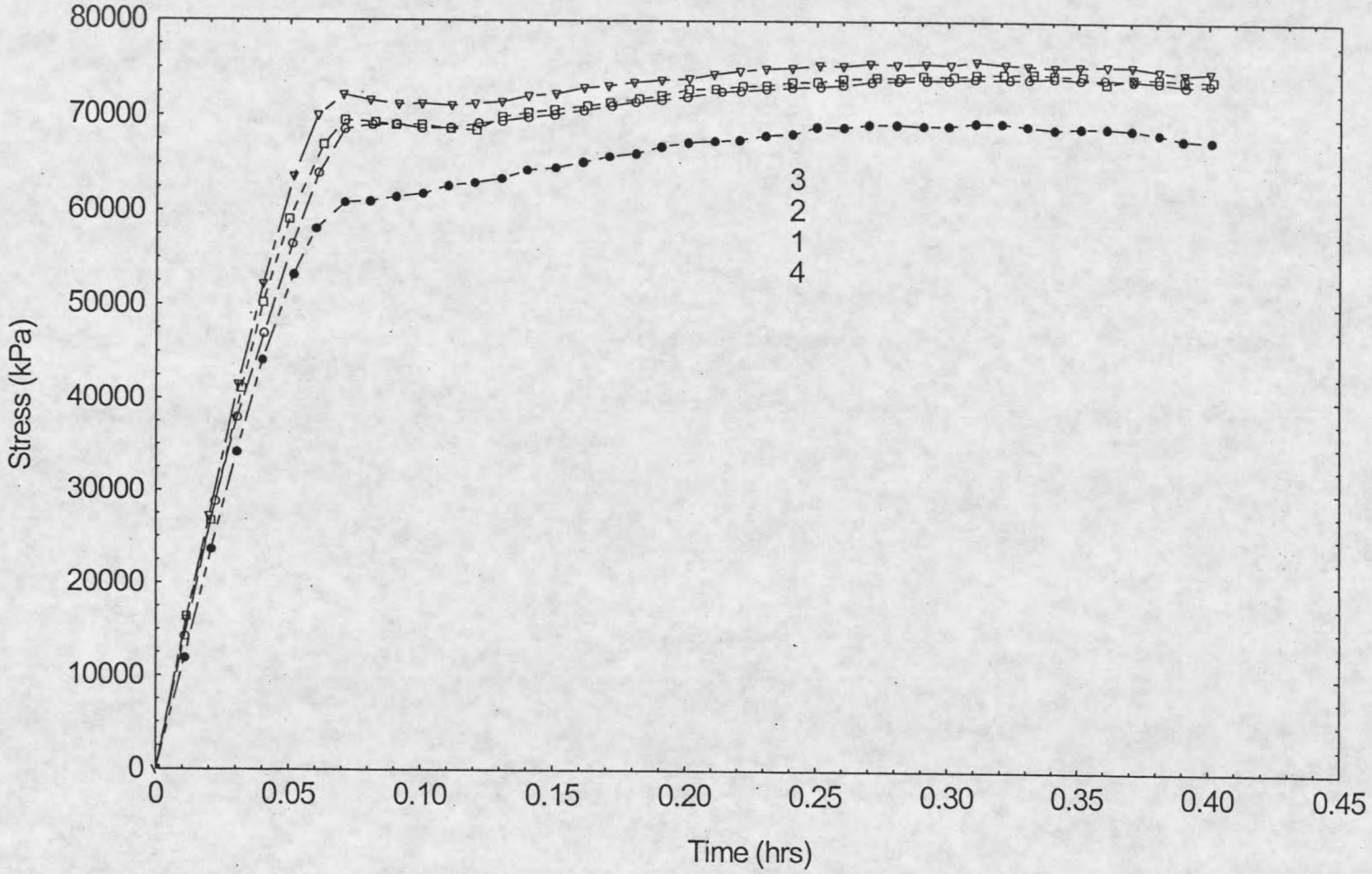


Figure C.II.12 Tensile Testing of Nylon 6/6 Specimens After Cyclic and Constant Loading at 35 °C
1- $(0.20\pm0.05)\sigma_y$, 10 Hz; 2- $(0.20\pm0.10)\sigma_y$, 10 Hz;
3- $(0.20)\sigma_y$, Constant Load Creep; 4- Virgin Specimens;
σ_y = 55 MPa at 35 °C

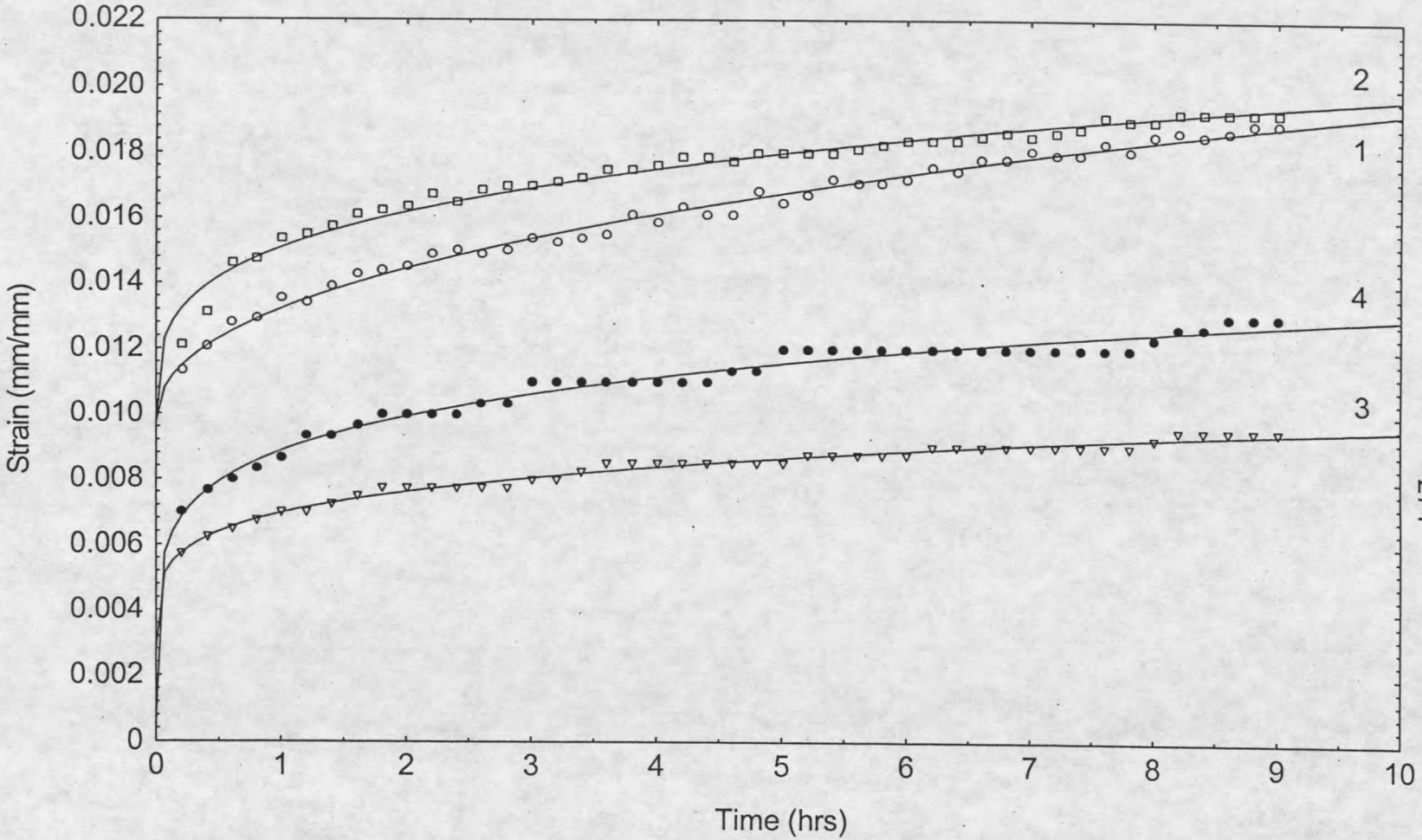


Figure C.II.13 Vibrocreep Response of Nylon 6/6 at Different Amplitudes at 35 °C
1- $(0.16\pm0.04)\sigma_y$, 1 Hz; 2- $(0.16\pm0.10)\sigma_y$, 1 Hz;
3- $(0.16)\sigma_y$, 4- $(0.20)\sigma_y$, Constant Load Creep;
σ_y = 70 MPa at 23 °C

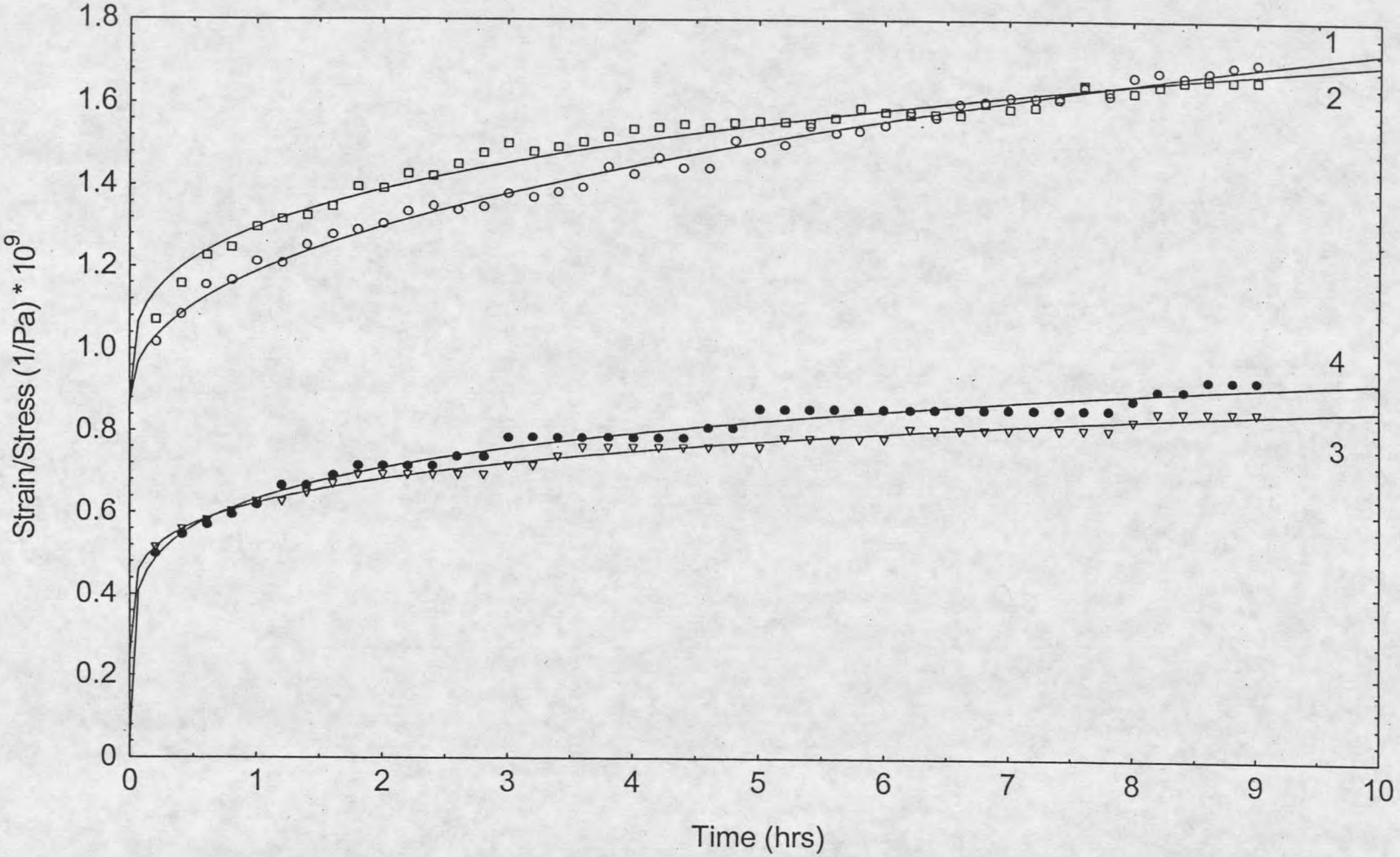


Figure C.II.14 Normalized Vibrocreep Response of Nylon 6/6 at Different Amplitudes at 35 °C
1- $(0.16\pm0.04)\sigma_y$, 1 Hz; 2- $(0.16\pm0.10)\sigma_y$, 1 Hz;
3- $(0.16)\sigma_y$, 4- $(0.20)\sigma_y$, Constant Load Creep;
σ_y = 70 MPa at 23 °C

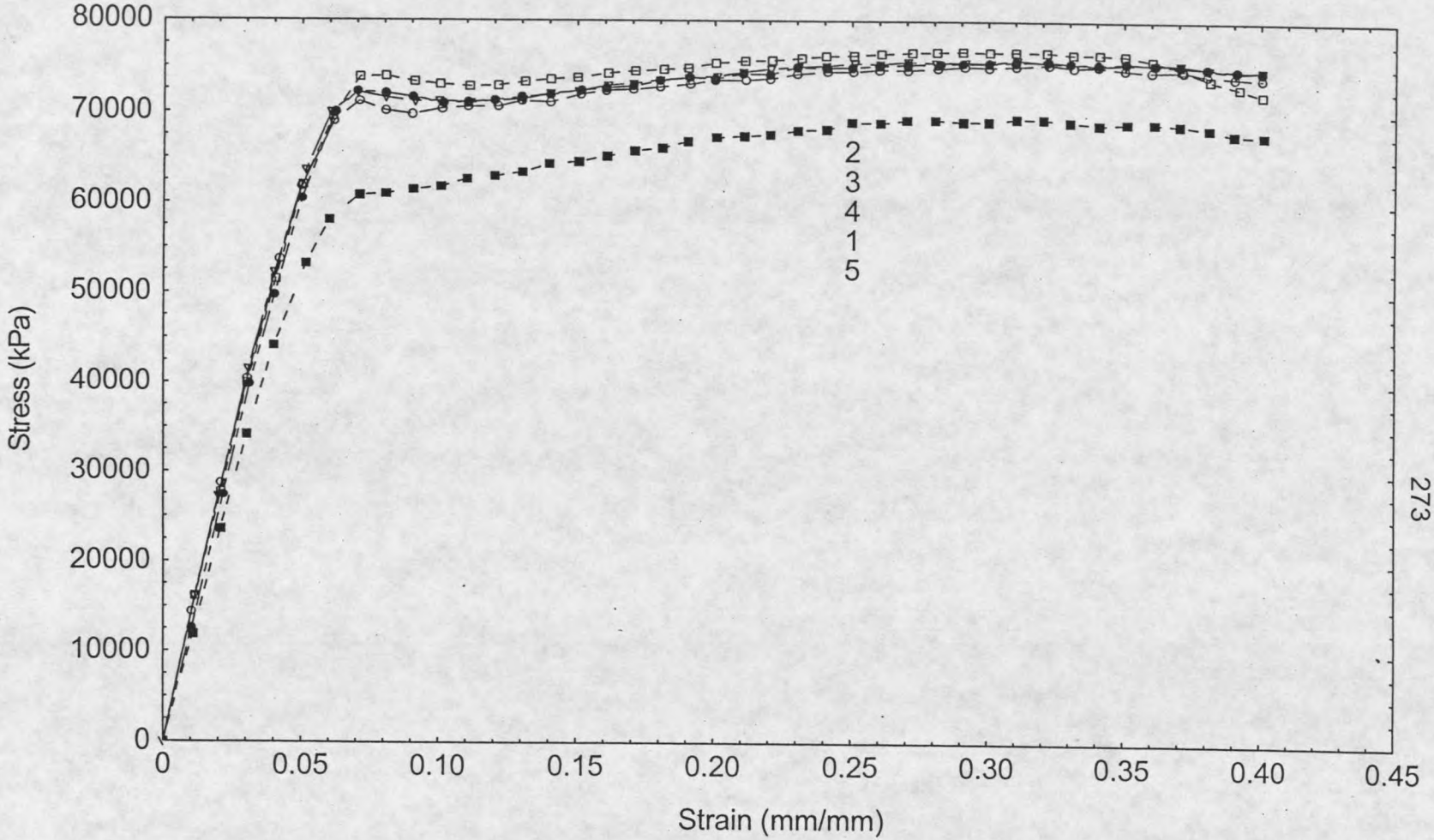


Figure C.II.15 Tensile Testing of Nylon 6/6 Specimens After Cyclic and Constant Loading at 35 °C
1- $(0.16\pm0.04)\sigma_y$, 1 Hz; 2- $(0.16\pm0.10)\sigma_y$, 1 Hz;
3- $(0.16)\sigma_y$, Constant Load Creep; 4- Virgin Specimens;
σ_y = 70 MPa at 23 °C

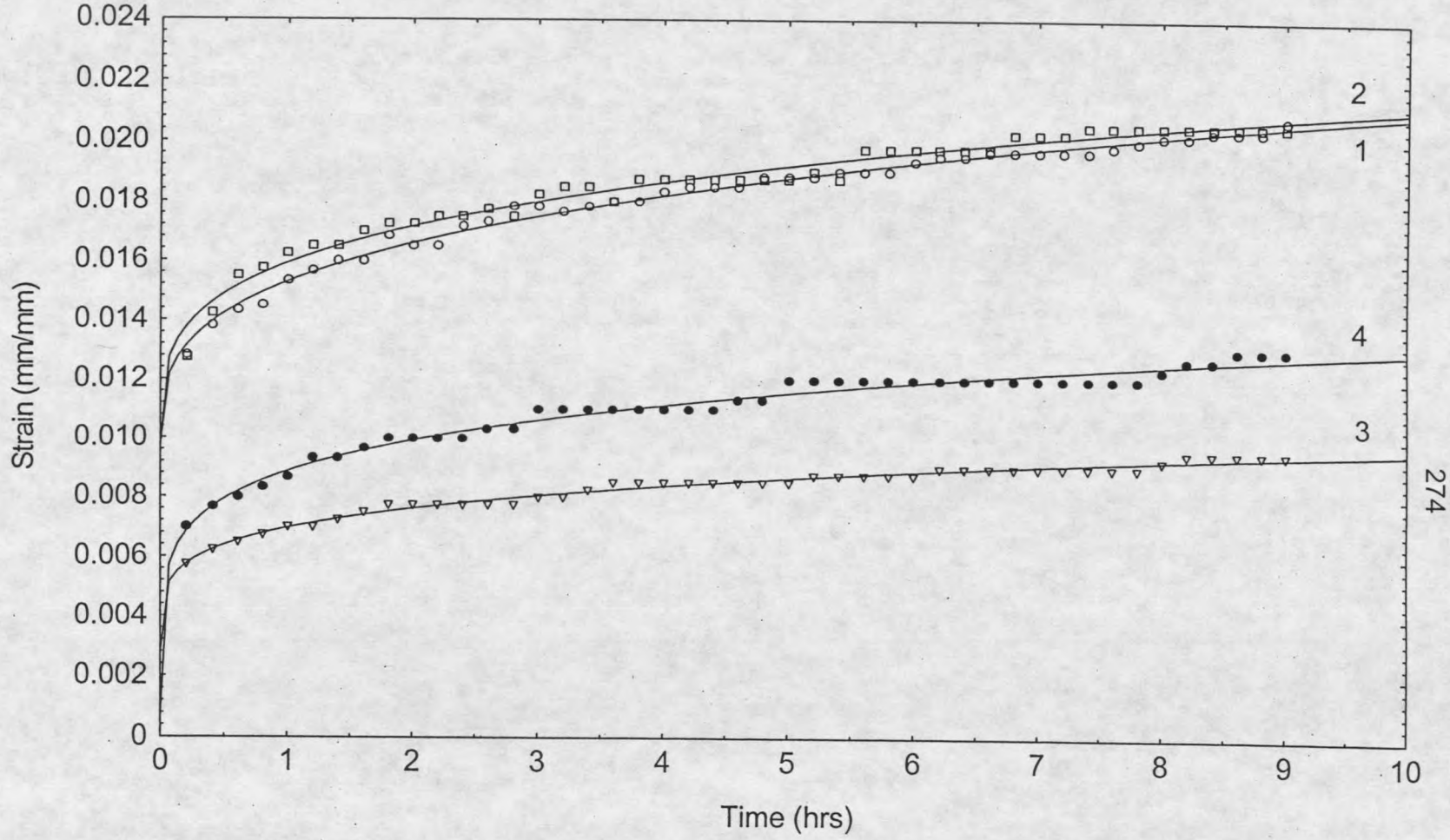


Figure C.II.16 Vibrocreep Response of Nylon 6/6 at Different Amplitudes at 35 °C
1- $(0.16\pm0.04)\sigma_y$, 10 Hz; 2- $(0.16\pm0.10)\sigma_y$, 10 Hz;
3- $(0.16)\sigma_y$, 4- $(0.20)\sigma_y$, Constant Load Creep;
σ_y = 70 MPa at 23 °C

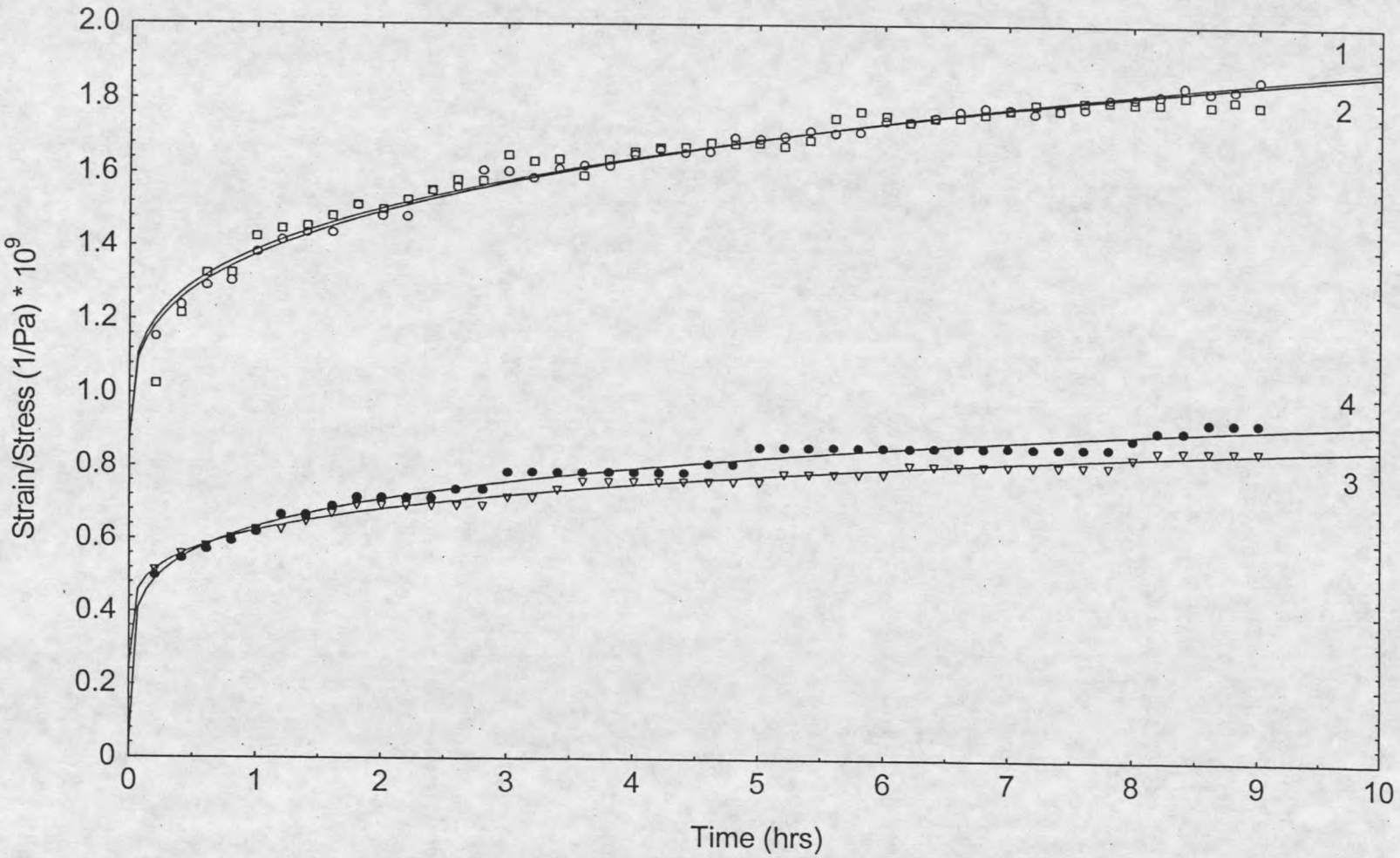


Figure C.II.17 Normalized Vibrocreep Response of Nylon 6/6 at Different Amplitudes at 35 °C
1- $(0.16\pm0.04)\sigma_y$, 10 Hz; 2- $(0.16\pm0.10)\sigma_y$, 10 Hz;
3- $(0.16)\sigma_y$, 4- $(0.20)\sigma_y$, Constant Load Creep;
σ_y = 70 MPa at 23 °C

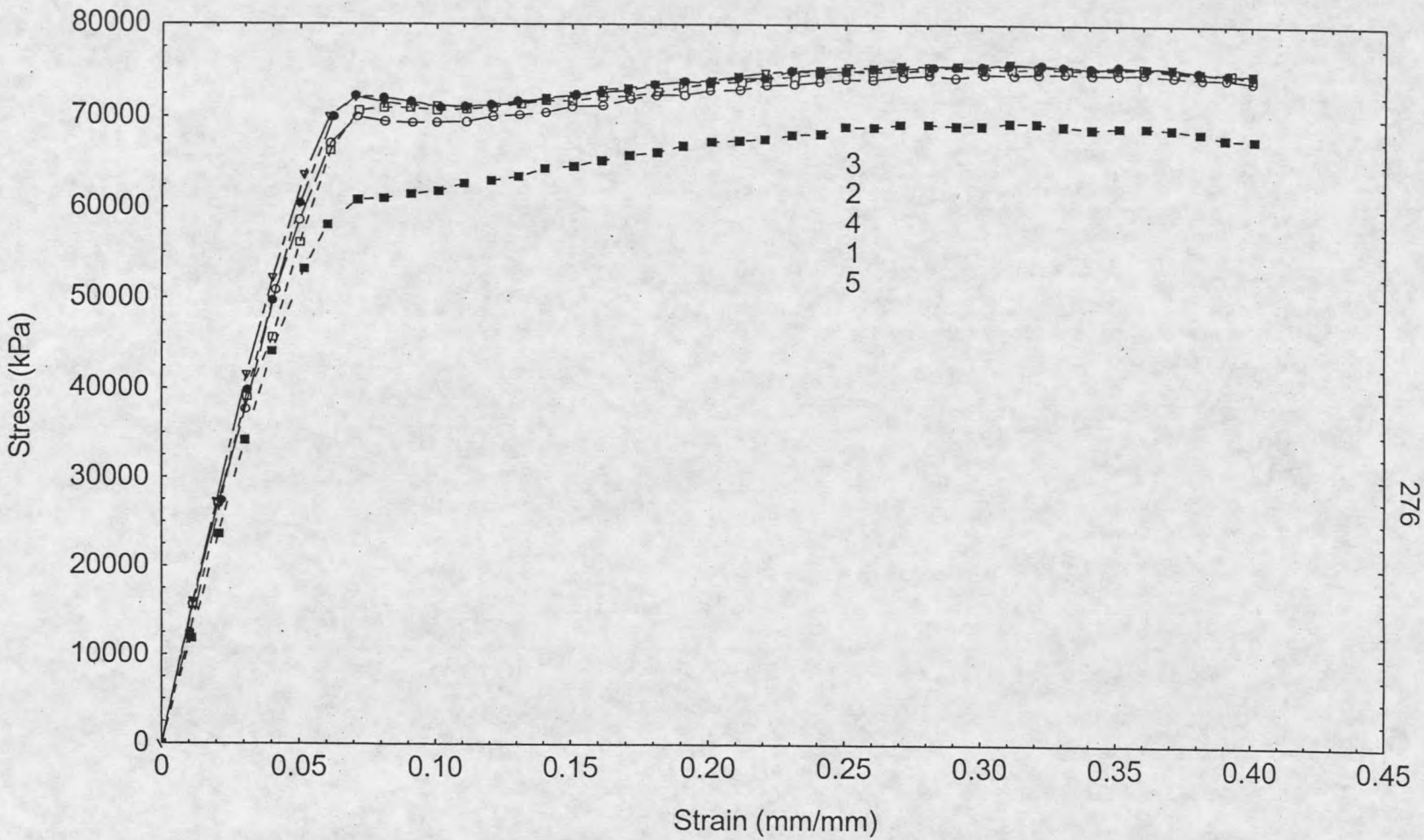


Figure C.II.18 Tensile Testing of Nylon 6/6 Specimens After Cyclic and Constant Loading at 35 °C
1- $(0.16\pm0.04)\sigma_y$, 10 Hz; 2- $(0.16\pm0.10)\sigma_y$, 10 Hz;
3- $(0.16)\sigma_y$, Constant Load Creep; 4- Virgin Specimens;
σ_y = 70 MPa at 23 °C

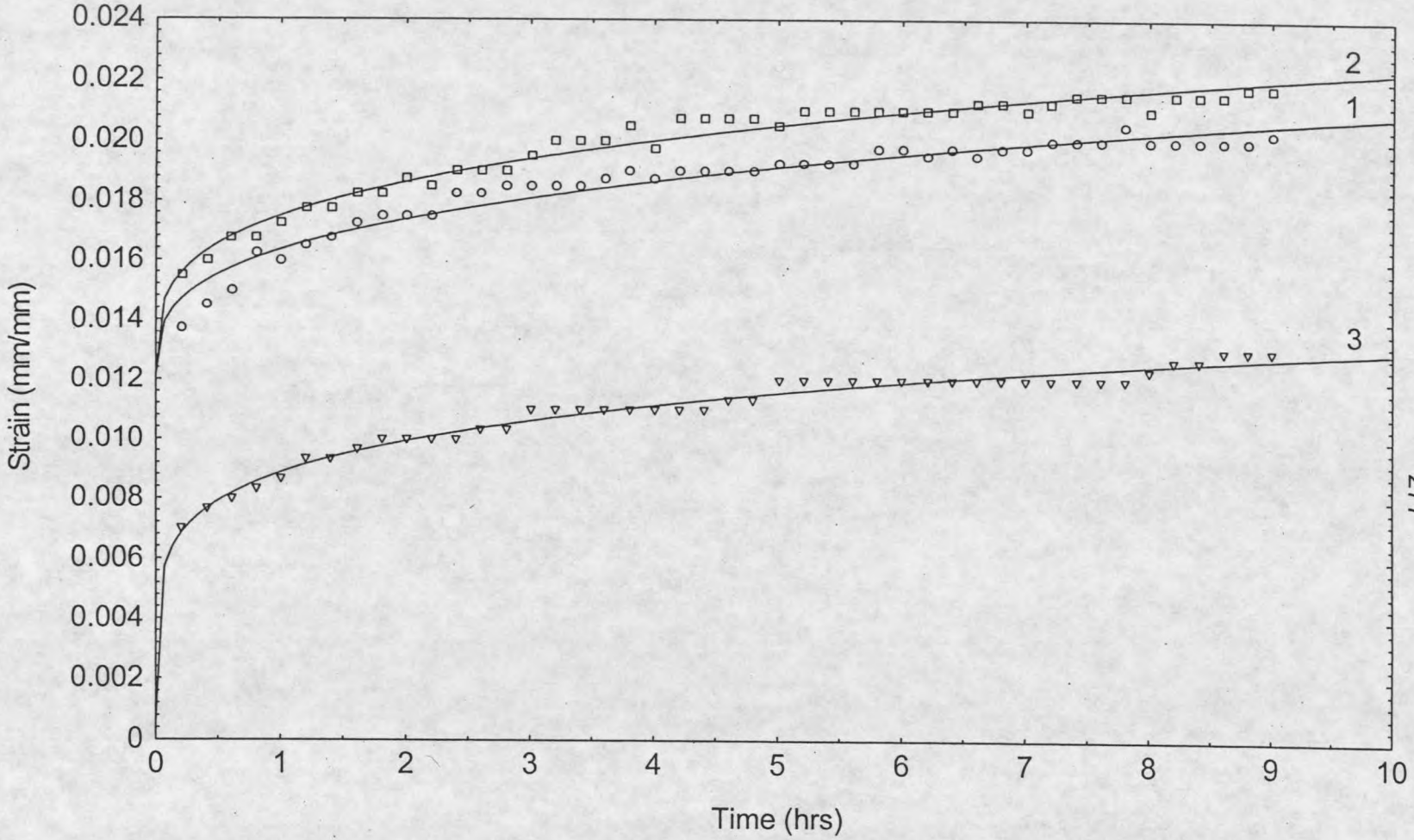


Figure C.II.19 Vibrocreep Response of Nylon 6/6 at Different Amplitudes at 35 °C
1- $(0.20\pm0.05)\sigma_y$, 1 Hz; 2- $(0.20\pm0.10)\sigma_y$, 1 Hz;
3- $(0.20)\sigma_y$, Constant Load Creep;
σ_y = 70 MPa at 23 °C

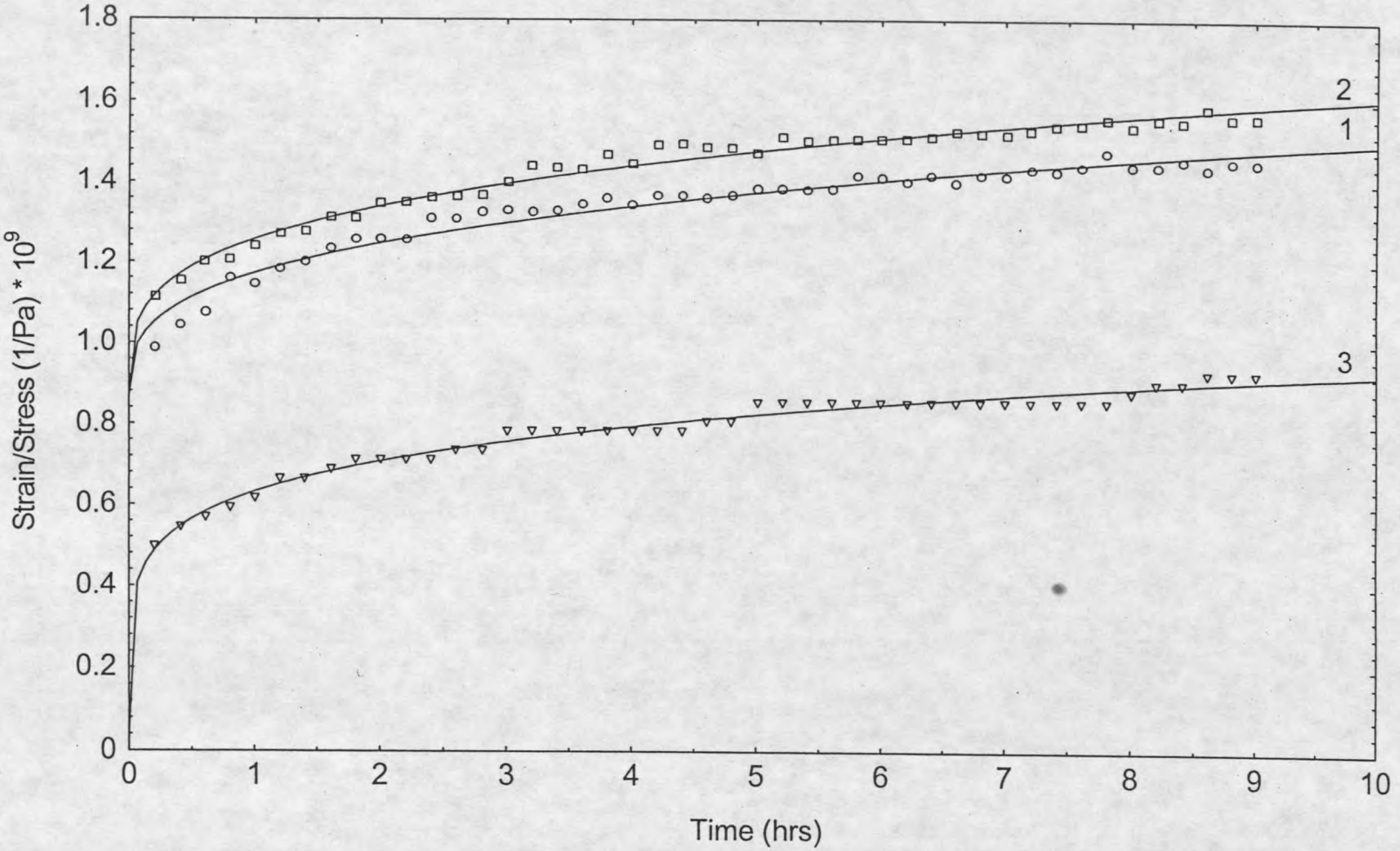


Figure C.II.20 Normalized Vibrocreep Response of Nylon 6/6 at Different Amplitudes at 35 °C
1- $(0.20\pm0.05)\sigma_y$, 1 Hz; 2- $(0.20\pm0.10)\sigma_y$, 1 Hz;
3- $(0.20)\sigma_y$, Constant Load Creep;
σ_y = 70 MPa at 23 °C

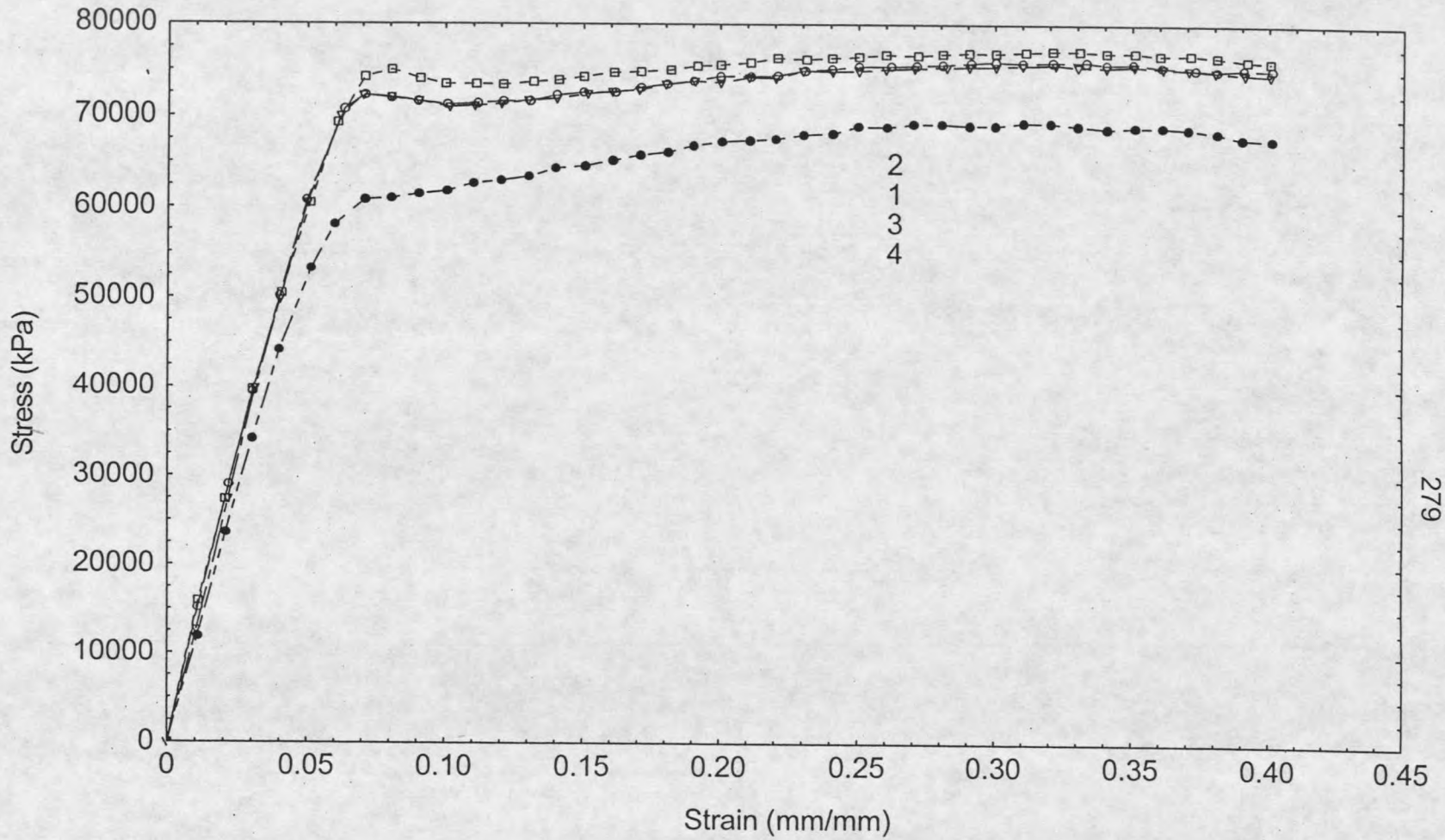


Figure C.II.21 Tensile Testing of Nylon 6/6 Specimens After Cyclic and Constant Loading at 35 °C
1- $(0.20\pm0.05)\sigma_y$, 1 Hz; 2- $(0.20\pm0.10)\sigma_y$, 1 Hz;
3- $(0.20)\sigma_y$, Constant Load Creep; 4- Virgin Specimens;
σ_y = 70 MPa at 23 °C

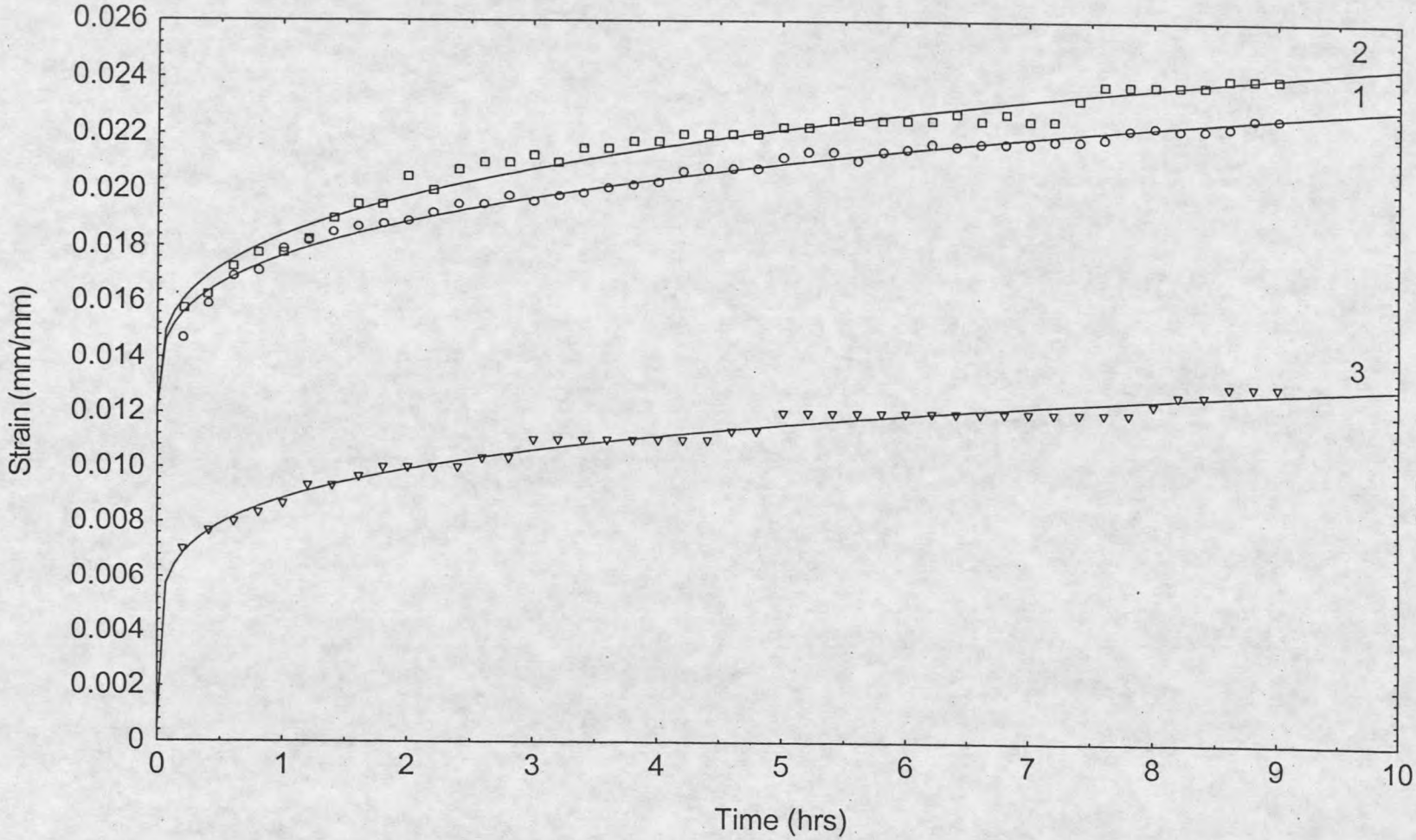


Figure C.II.22 Vibrocreep Response of Nylon 6/6 at Different Amplitudes at 35 °C
1- $(0.20\pm0.05)\sigma_y$, 10 Hz; 2- $(0.20\pm0.10)\sigma_y$, 10 Hz;
3- $(0.20)\sigma_y$, Constant Load Creep;
σ_y = 70 MPa at 23 °C

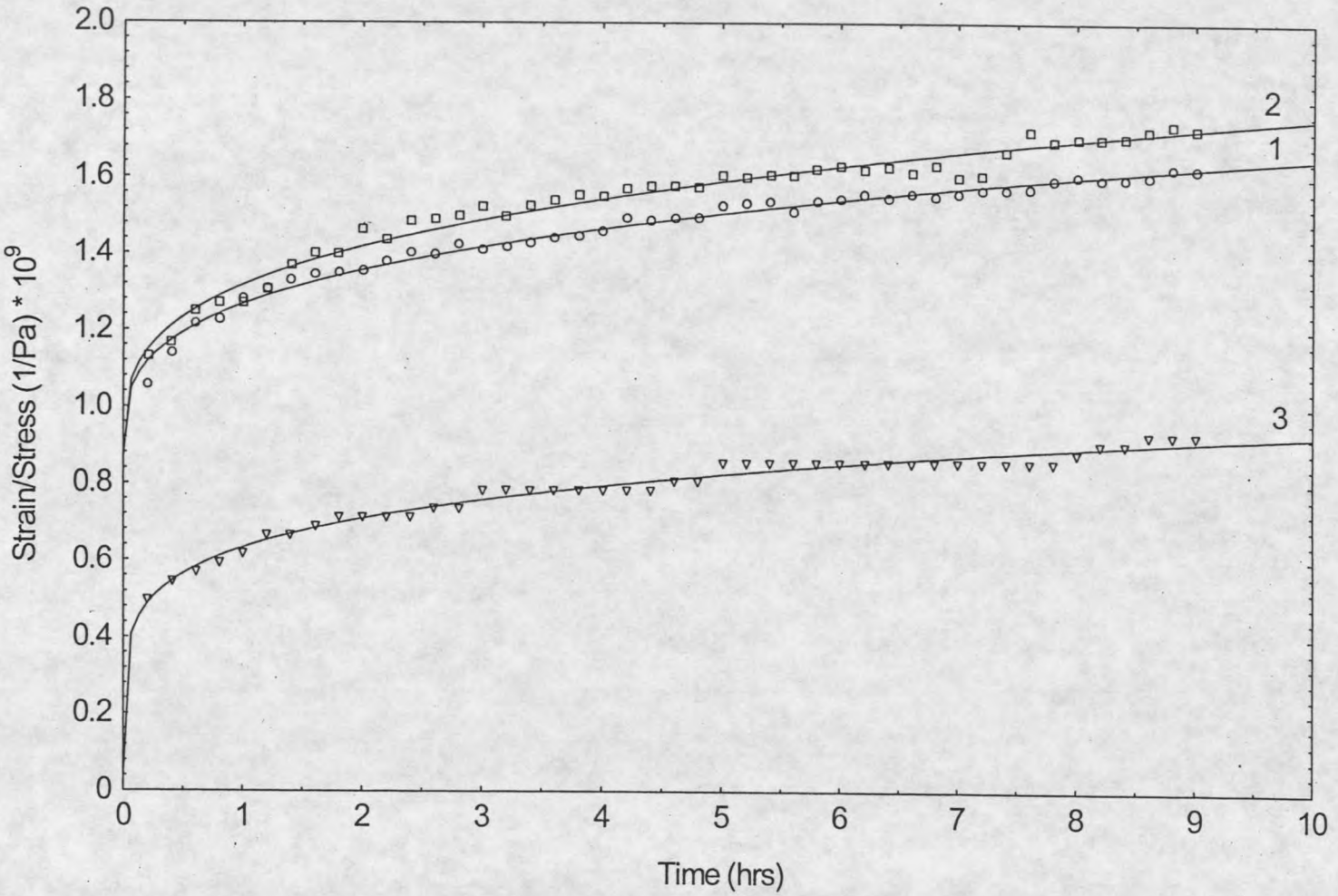


Figure C.II.23 Normalized Vibrocreep Response of Nylon 6/6 at Different Amplitudes at 35 °C
1- $(0.20\pm0.05)\sigma_y$, 10 Hz; 2- $(0.20\pm0.10)\sigma_y$, 10 Hz;
3- $(0.20)\sigma_y$, Constant Load Creep;
σ_y = 70 MPa at 23 °C

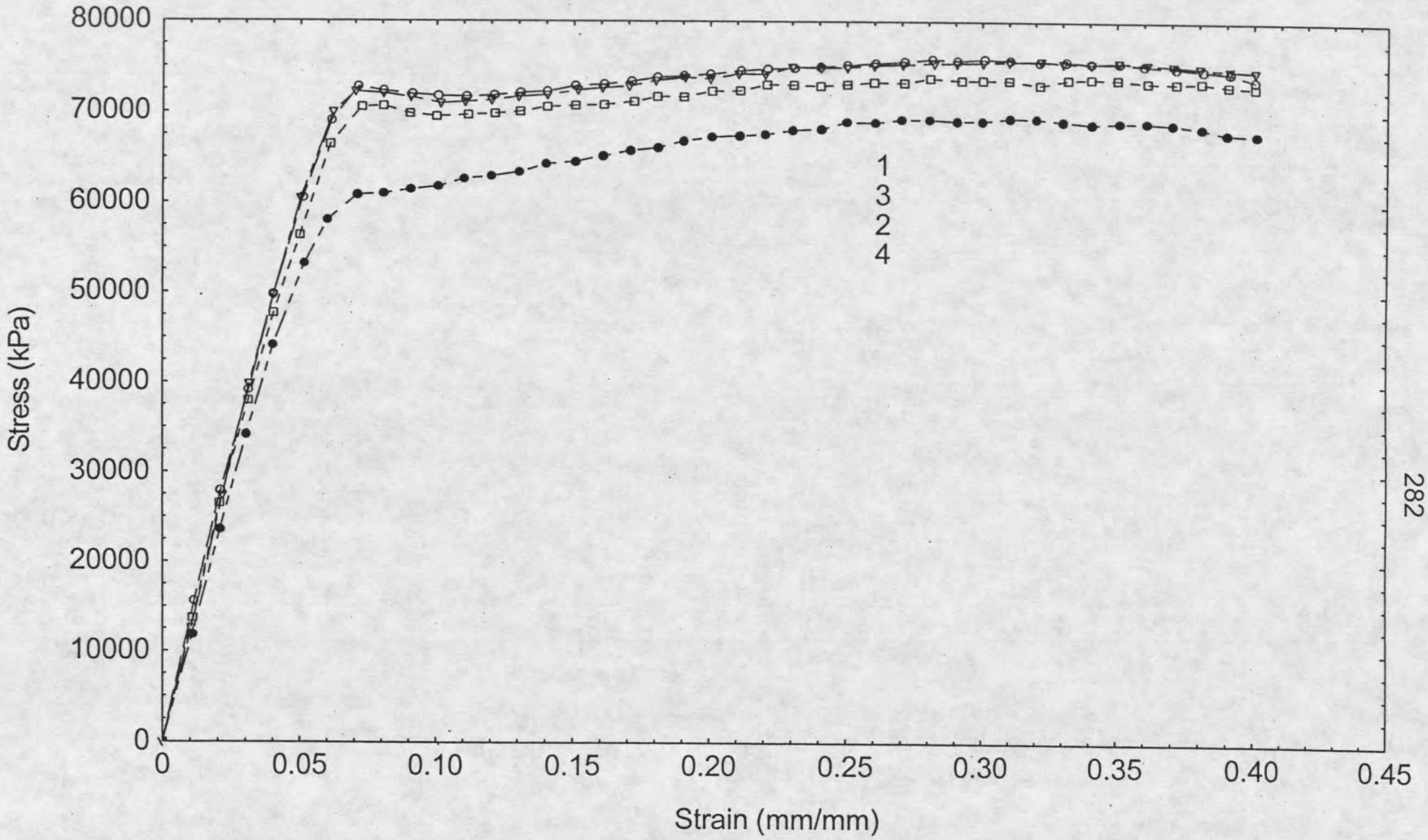


Figure C.II.24 Tensile Testing of Nylon 6/6 Specimens After Cyclic and Constant Loading at 35 °C
1- $(0.20\pm0.05)\sigma_y$, 10 Hz; 2- $(0.20\pm0.10)\sigma_y$, 10 Hz;
3- $(0.20)\sigma_y$, Constant Load Creep; 4- Virgin Specimens;
σ_y = 70 MPa at 23 °C

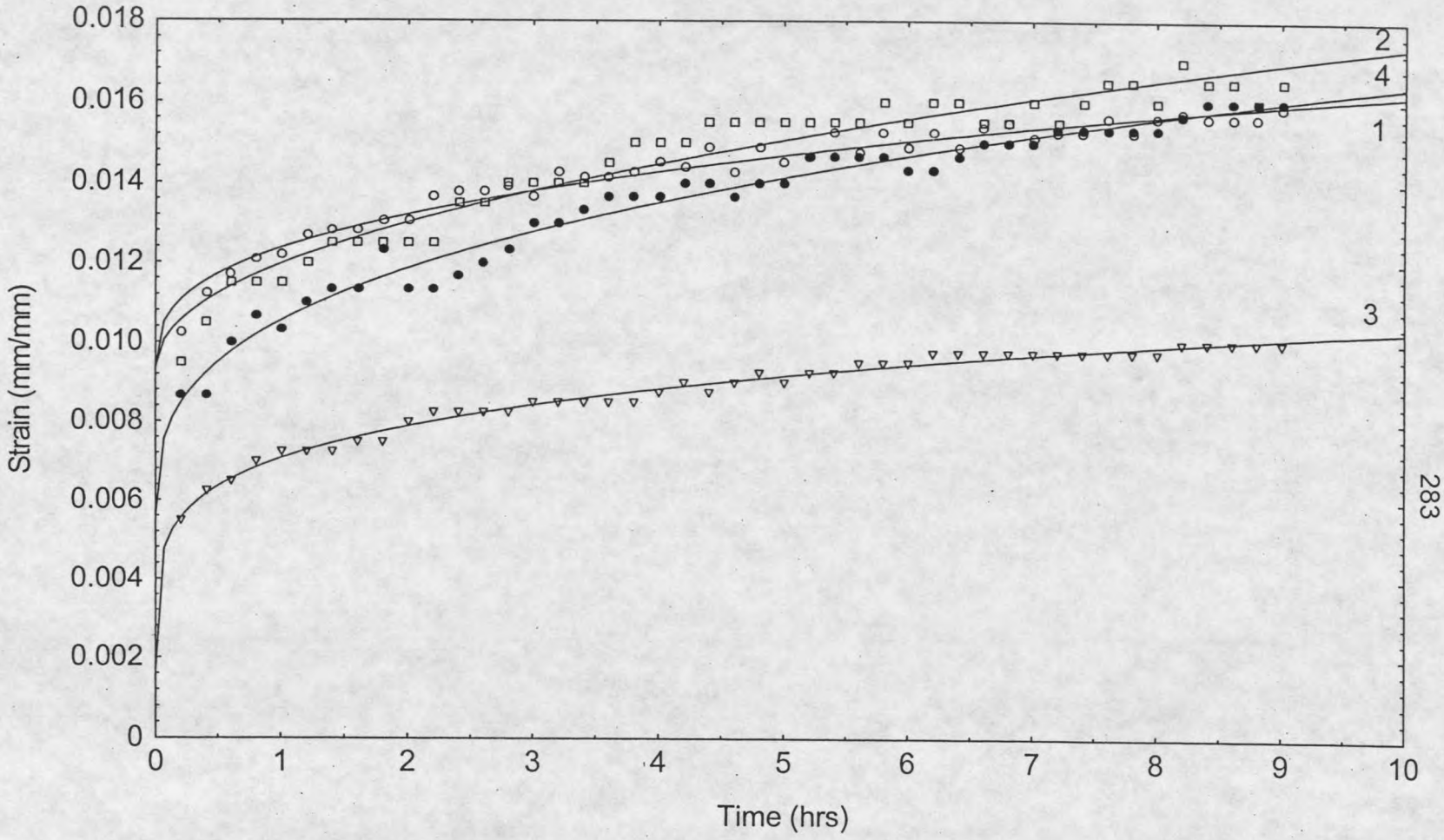


Figure C.III.1 Vibrocreep Response of Nylon 6/6 at Different Amplitudes at 41 °C
1- $(0.20\pm0.05)\sigma_y$, 1 Hz; 2- $(0.20\pm0.10)\sigma_y$, 1 Hz;
3- $(0.20)\sigma_y$, 4- $(0.30)\sigma_y$, Constant Load Creep;
σ_y = 45 MPa at 41 °C

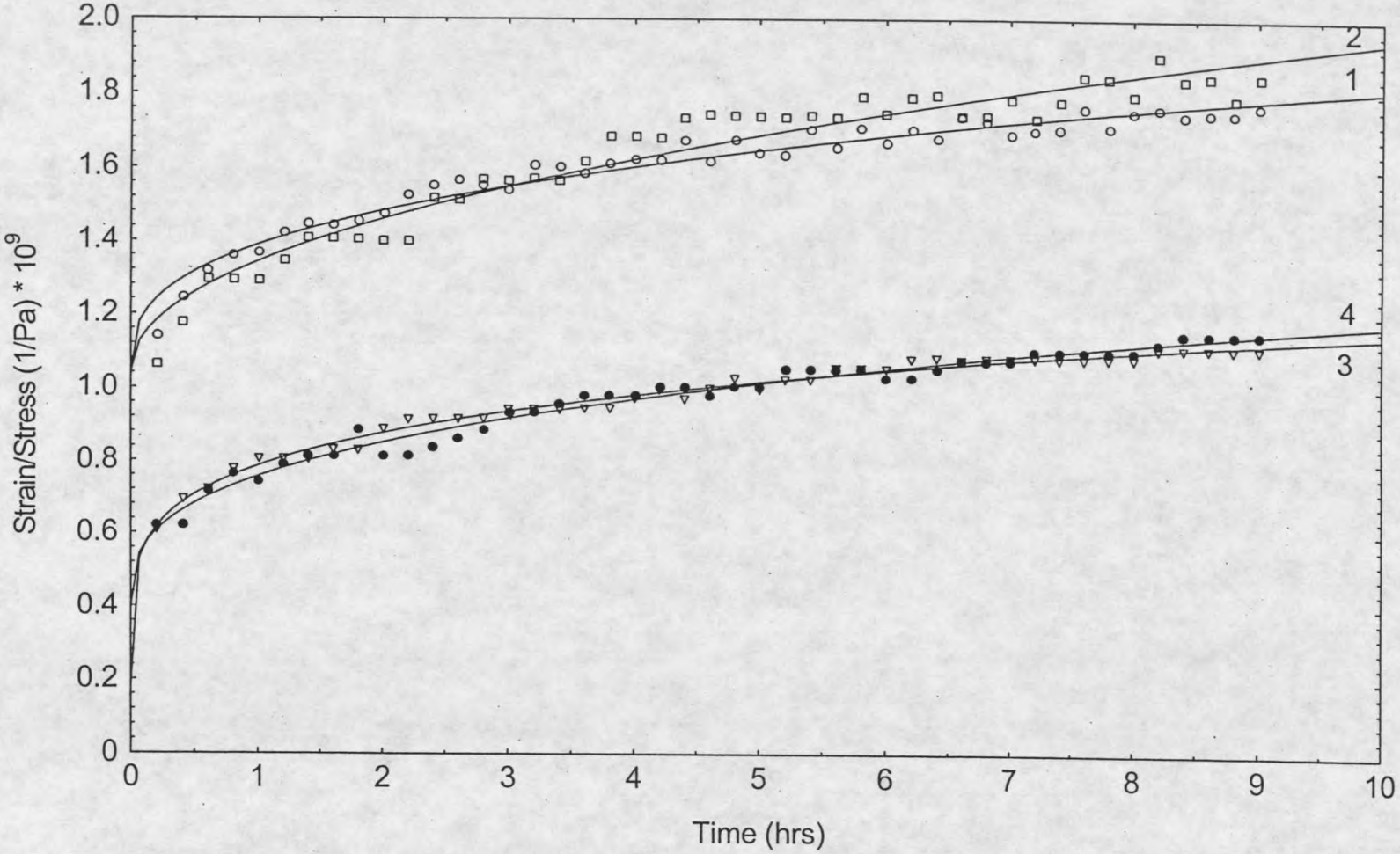


Figure C.III.2 Normalized Vibrocreep Response of Nylon 6/6 at Different Amplitudes at 41 °C
1- $(0.20\pm0.05)\sigma_y$, 1 Hz; 2- $(0.20\pm0.10)\sigma_y$, 1 Hz;
3- $(0.20)\sigma_y$, 4- $(0.30)\sigma_y$, Constant Load Creep;
σ_y = 45 MPa at 41 °C

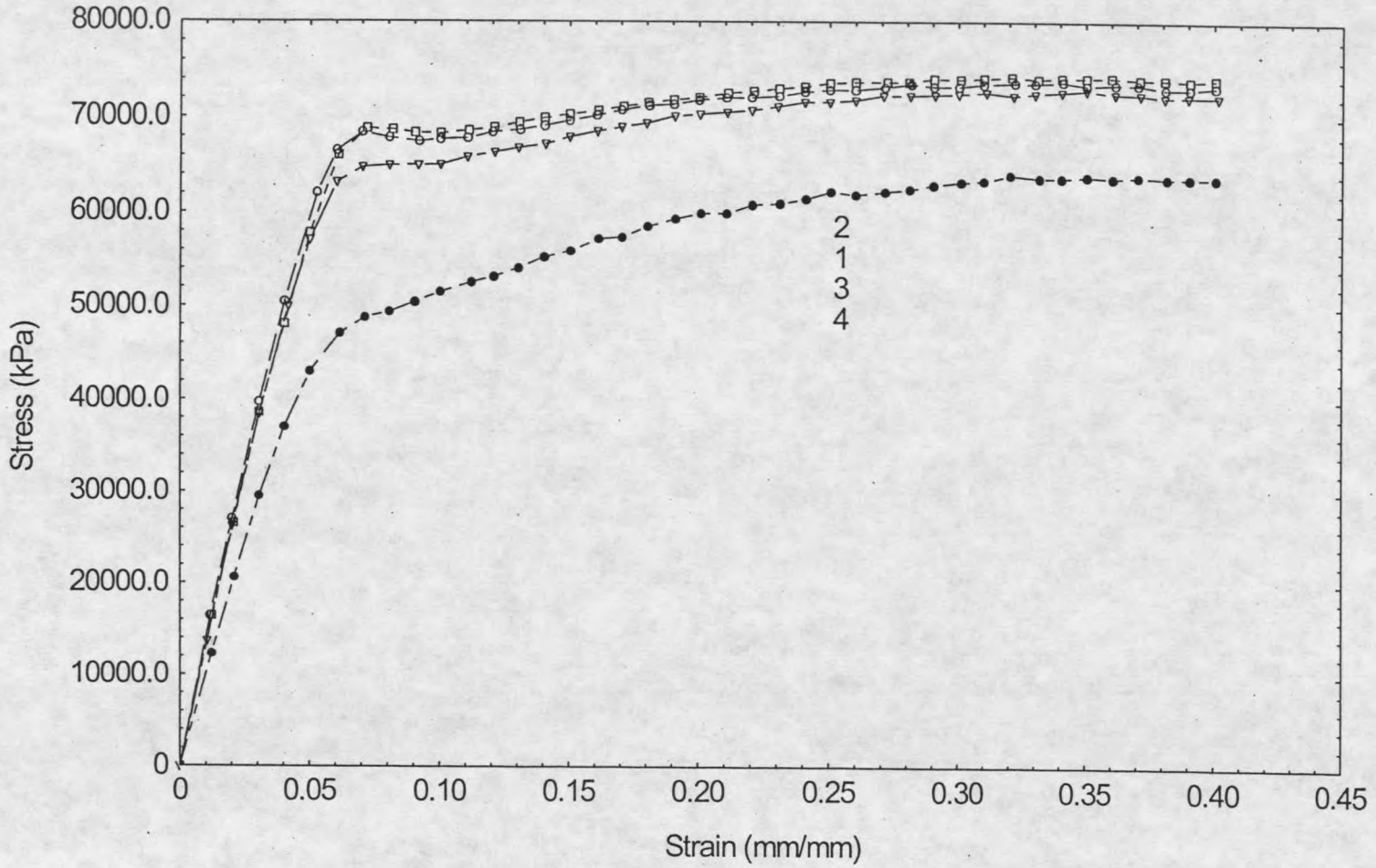


Figure C.III.3 Tensile Testing of Nylon 6/6 Specimens After Cyclic and Constant Loading at 41 °C
1- $(0.20\pm0.05)\sigma_y$, 1 Hz; 2- $(0.20\pm0.10)\sigma_y$, 1 Hz;
3- $(0.20)\sigma_y$, Constant Load Creep; 4- Virgin Specimens;
σ_y = 45 MPa at 41 °C

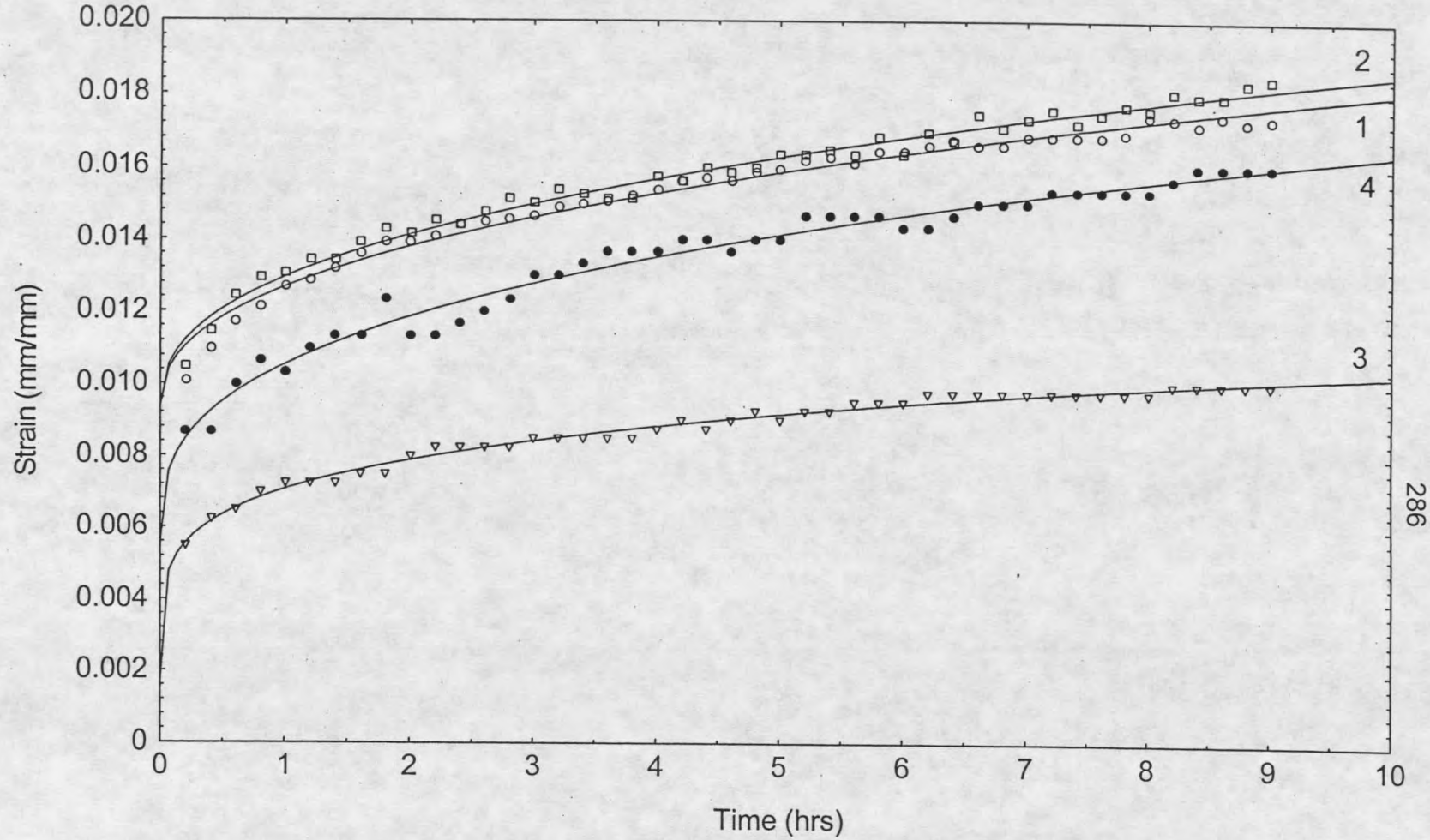


Figure C.III.4 Vibrocreep Response of Nylon 6/6 at Different Amplitudes at 41 °C
1- $(0.20\pm0.05)\sigma_y$, 10 Hz; 2- $(0.20\pm0.10)\sigma_y$, 10 Hz;
3- $(0.20)\sigma_y$, 4- $(0.30)\sigma_y$, Constant Load Creep;
σ_y = 45 MPa at 41 °C

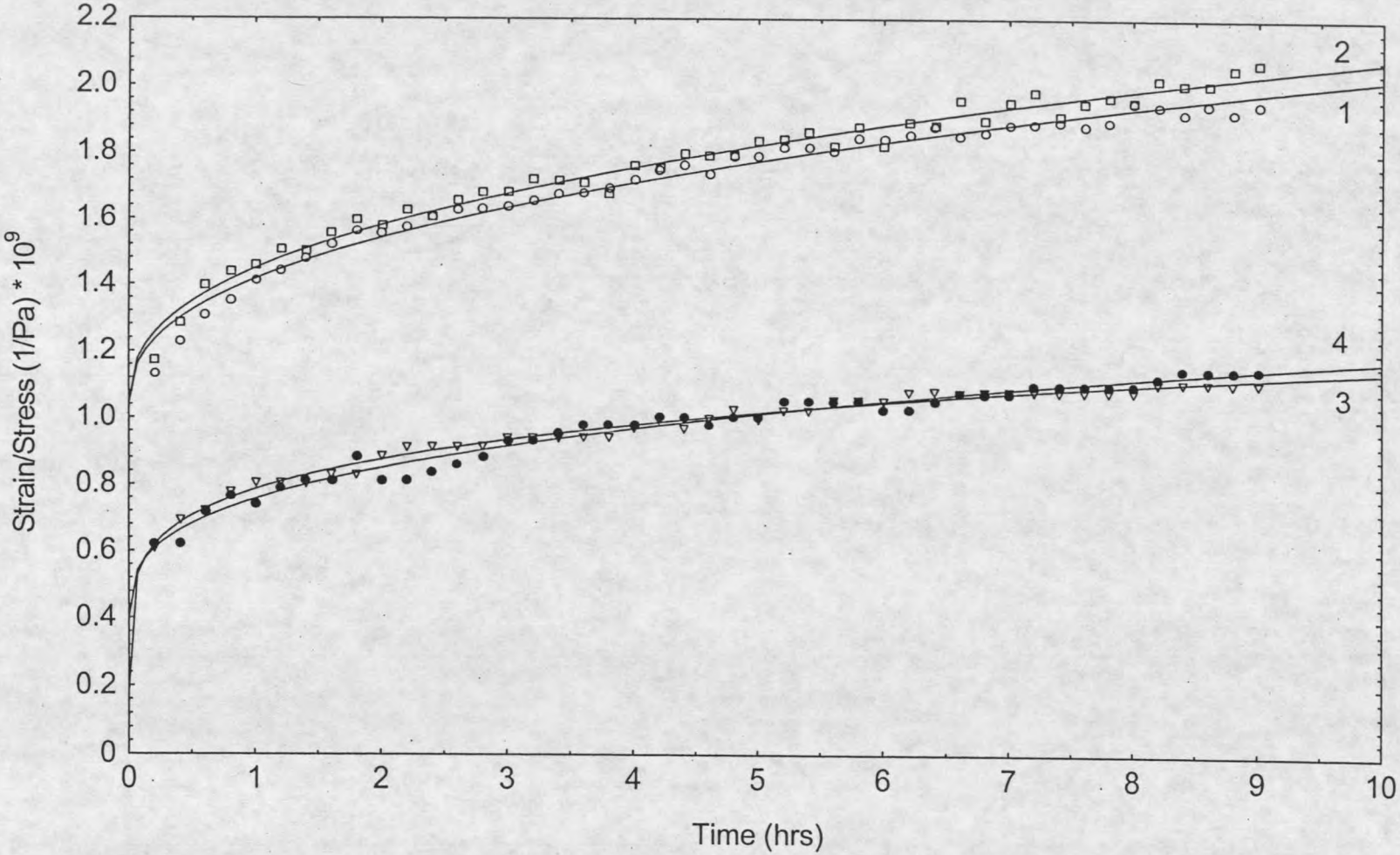


Figure C.III.5 Normalized Vibrocreep Response of Nylon 6/6 at Different Amplitudes at 41 °C
1- $(0.20\pm0.05)\sigma_y$, 10 Hz; 2- $(0.20\pm0.10)\sigma_y$, 10 Hz;
3- $(0.20)\sigma_y$, 4- $(0.30)\sigma_y$, Constant Load Creep;
σ_y = 45 MPa at 41 °C

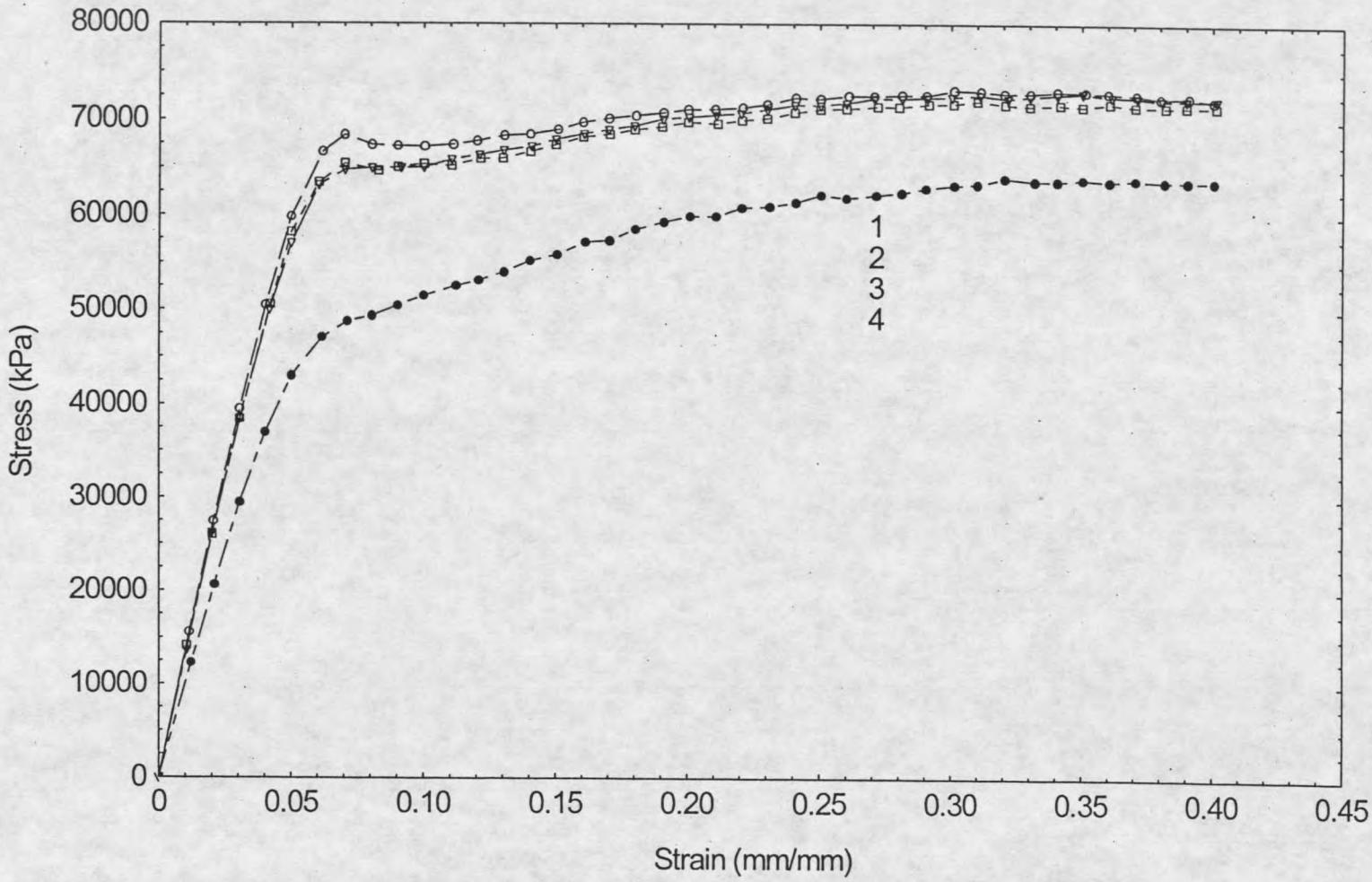


Figure C.III.6 Tensile Testing of Nylon 6/6 Specimens After Cyclic and Constant Loading at 41 °C
1- $(0.20\pm0.05)\sigma_y$, 10 Hz; 2- $(0.20\pm0.10)\sigma_y$, 10 Hz;
3- $(0.20)\sigma_y$, Constant Load Creep; 4- Virgin Specimens;
σ_y = 45 MPa at 41 °C

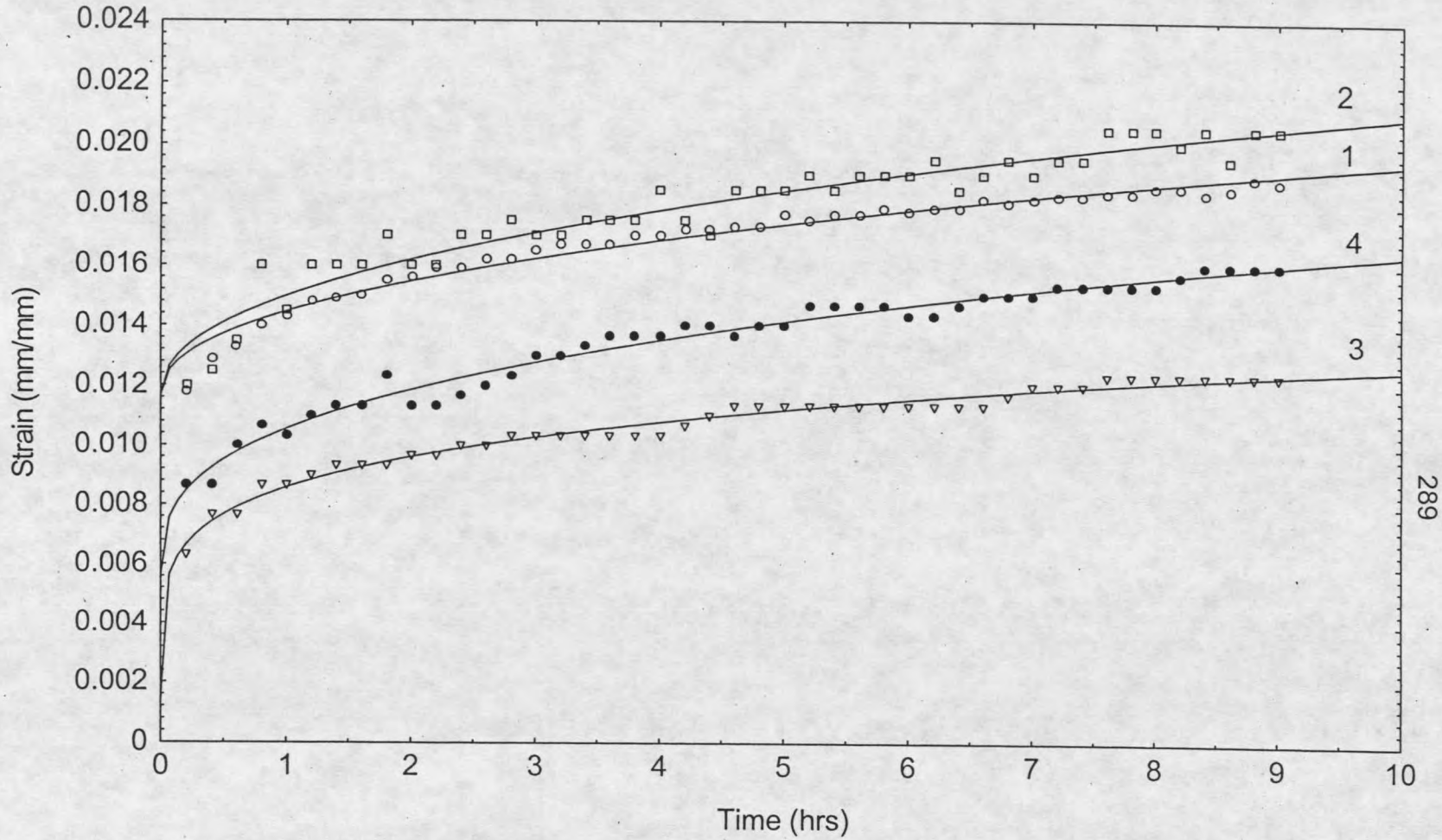


Figure C.III.7 Vibrocreep Response of Nylon 6/6 at Different Amplitudes at 41 °C
1- $(0.16\pm0.04)\sigma_y$, 1 Hz; 2- $(0.16\pm0.10)\sigma_y$, 1 Hz;
3- $(0.16)\sigma_y$, 4- $(0.20)\sigma_y$, Constant Load Creep;
σ_y = 70 MPa at 23 °C

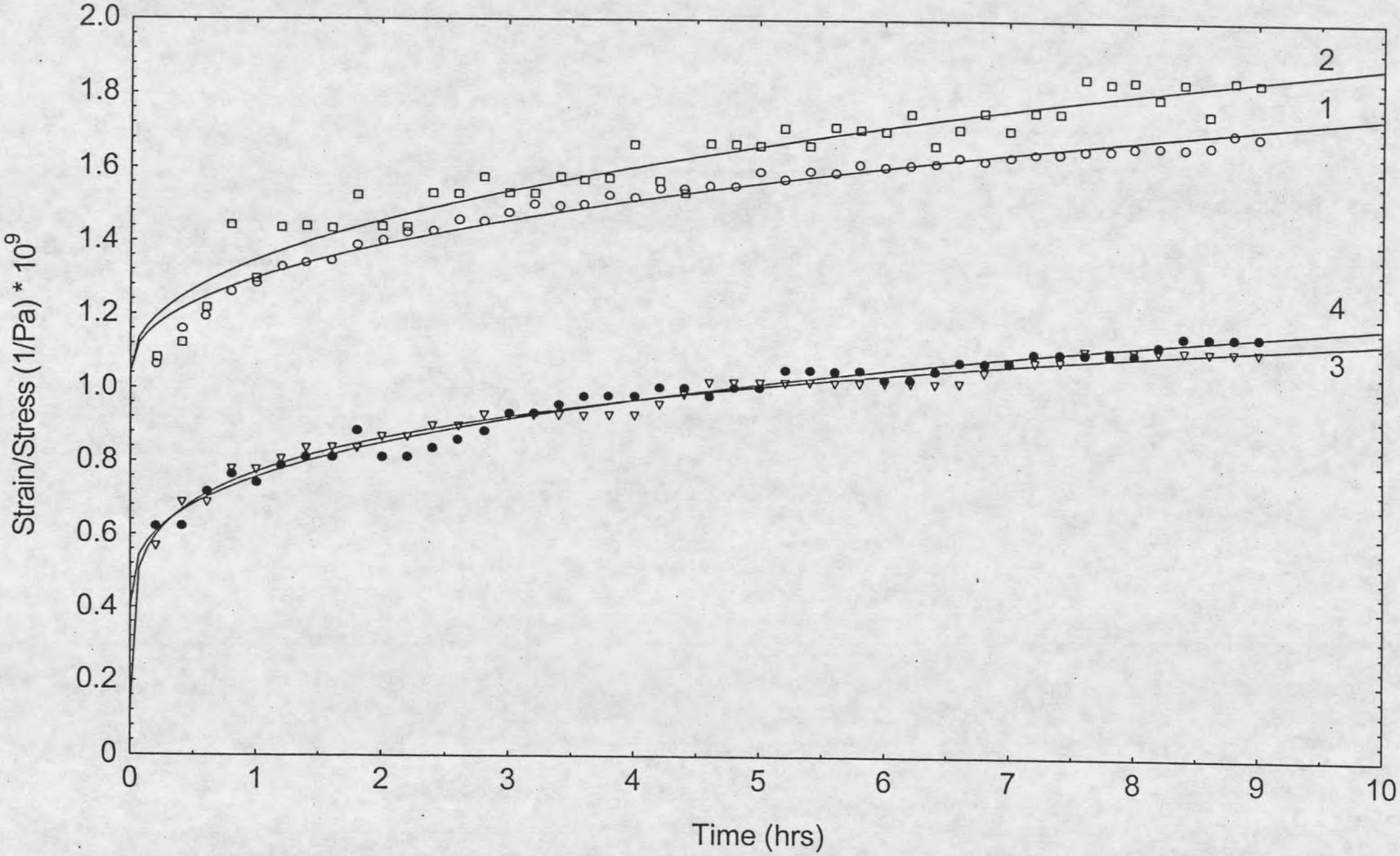


Figure C.III.8 Normalized Vibrocreep Response of Nylon 6/6 at Different Amplitudes at 41 °C
1- $(0.16\pm0.04)\sigma_y$, 1 Hz; 2- $(0.16\pm0.10)\sigma_y$, 1 Hz;
3- $(0.16)\sigma_y$, 4- $(0.20)\sigma_y$, Constant Load Creep;
σ_y = 70 MPa at 23 °C

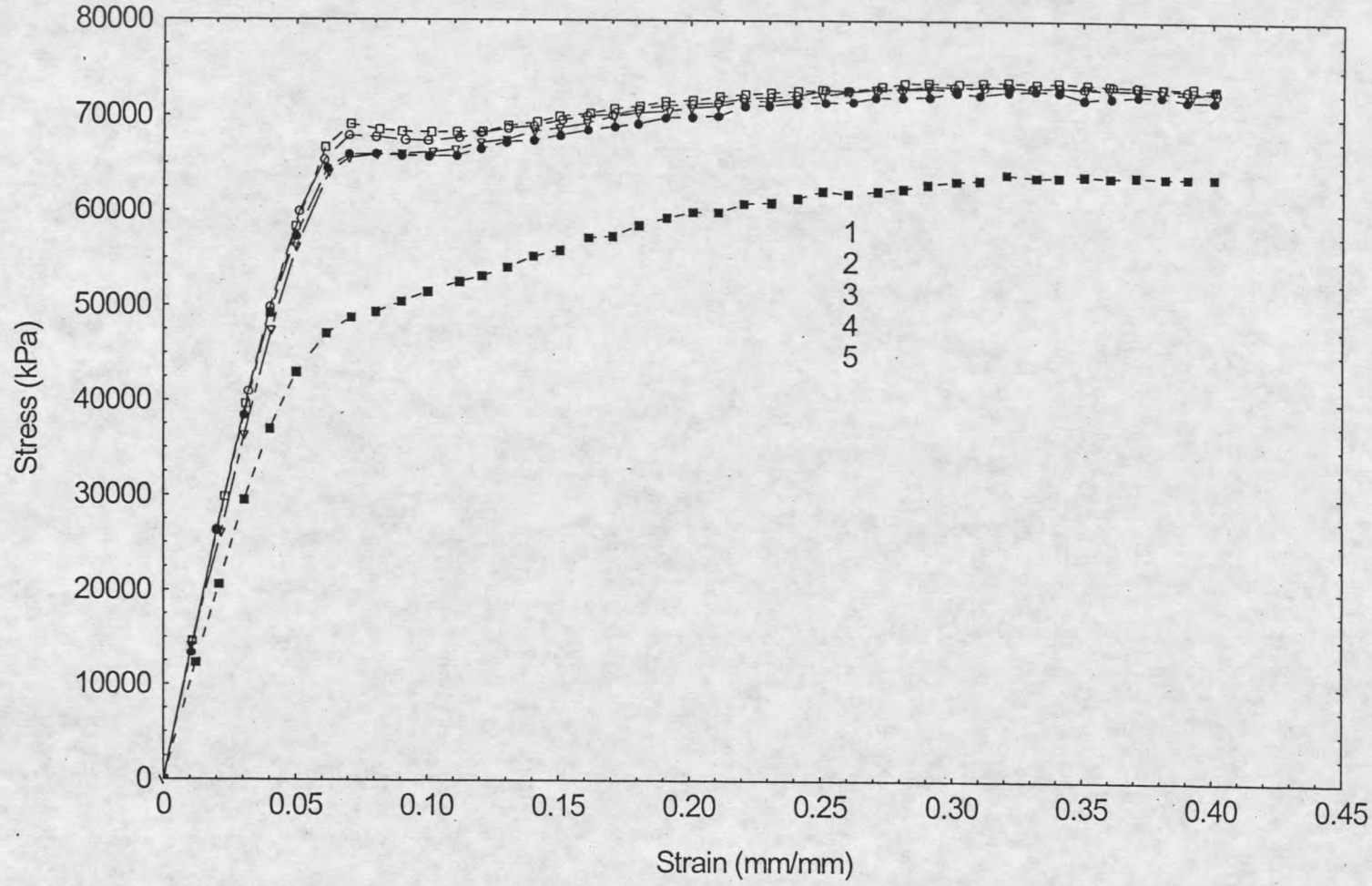


Figure C.III.9 Tensile Testing of Nylon 6/6 Specimens After Cyclic and Constant Loading at 41 °C
1- $(0.16\pm0.04)\sigma_y$, 1 Hz; 2- $(0.16\pm0.10)\sigma_y$, 1 Hz;
3- $(0.16)\sigma_y$, 4- $(0.20)\sigma_y$, Constant Load Creep; 5- Virgin Specimens;
σ_y = 70 MPa at 23 °C

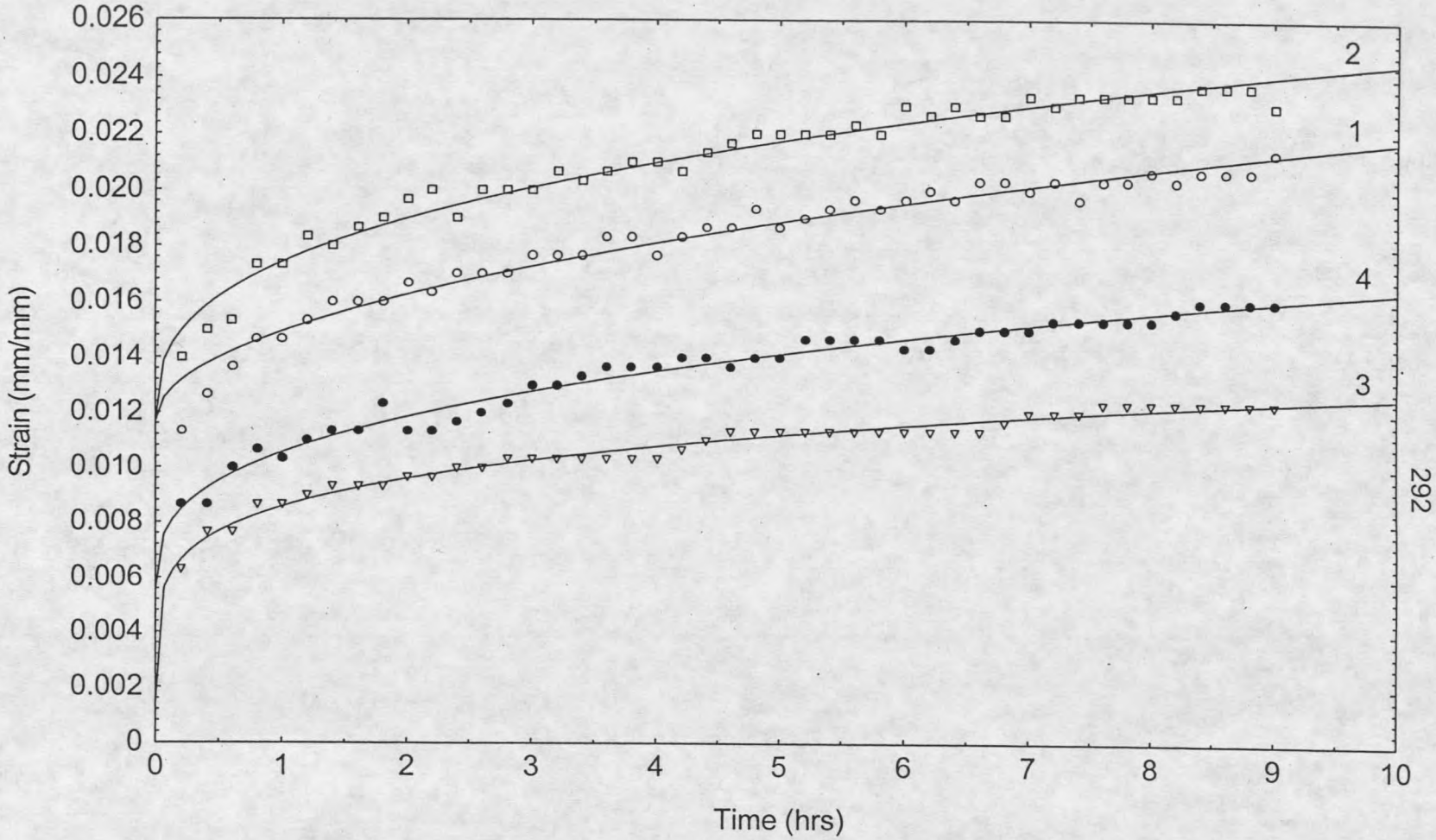


Figure C.III.10 Vibrocreep Response of Nylon 6/6 at Different Amplitudes at 41 °C
1- $(0.16\pm0.04)\sigma_y$, 10 Hz; 2- $(0.16\pm0.10)\sigma_y$, 10 Hz;
3- $(0.16)\sigma_y$, 4- $(0.20)\sigma_y$, Constant Load Creep;
σ_y = 70 MPa at 23 °C

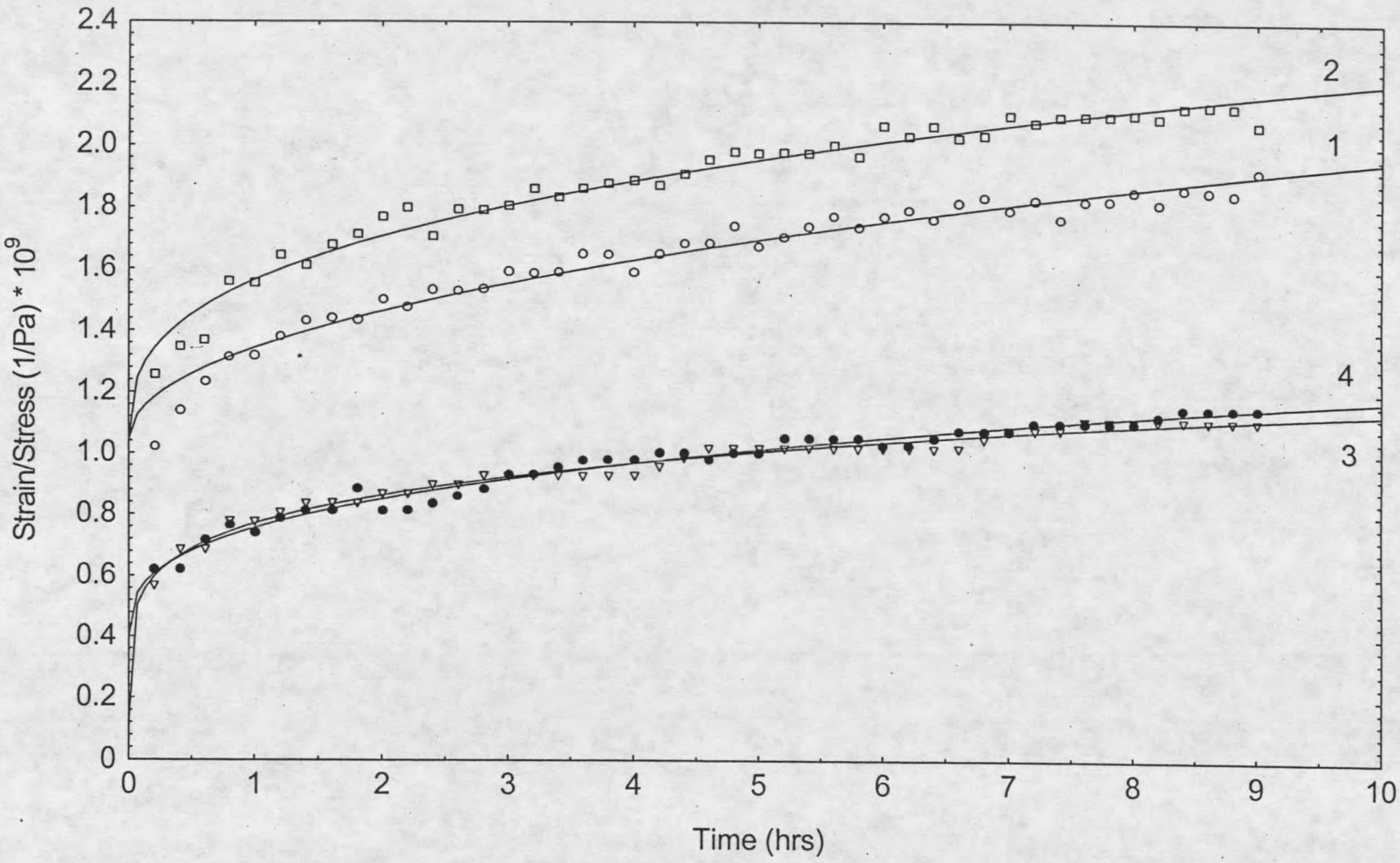


Figure C.III.11 Normalized Vibrocreep Response of Nylon 6/6 at Different Amplitudes at 41 °C
1- $(0.16\pm0.04)\sigma_y$, 10 Hz; 2- $(0.16\pm0.10)\sigma_y$, 10 Hz;
3- $(0.16)\sigma_y$, 4- $(0.20)\sigma_y$, Constant Load Creep;
σ_y = 70 MPa at 23 °C

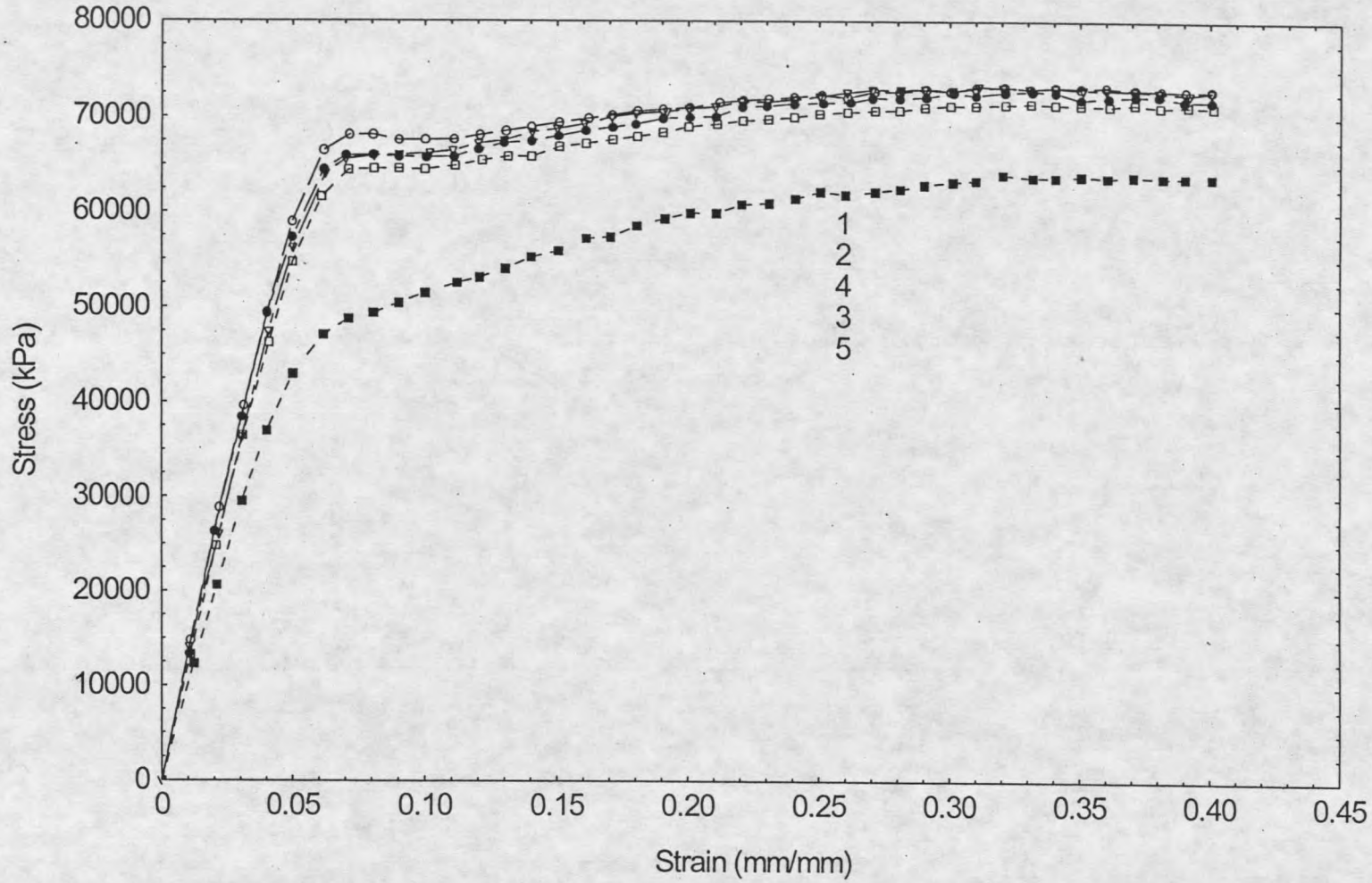


Figure C.III.12 Tensile Testing of Nylon 6/6 Specimens After Cyclic and Constant Loading at 41 °C
1- $(0.16\pm0.04)\sigma_y$, 10 Hz; 2- $(0.16\pm0.10)\sigma_y$, 10 Hz;
3- $(0.16)\sigma_y$, 4- $(0.20)\sigma_y$ Constant Load Creep; 5- Virgin Specimens;
σ_y = 70 MPa at 23 °C

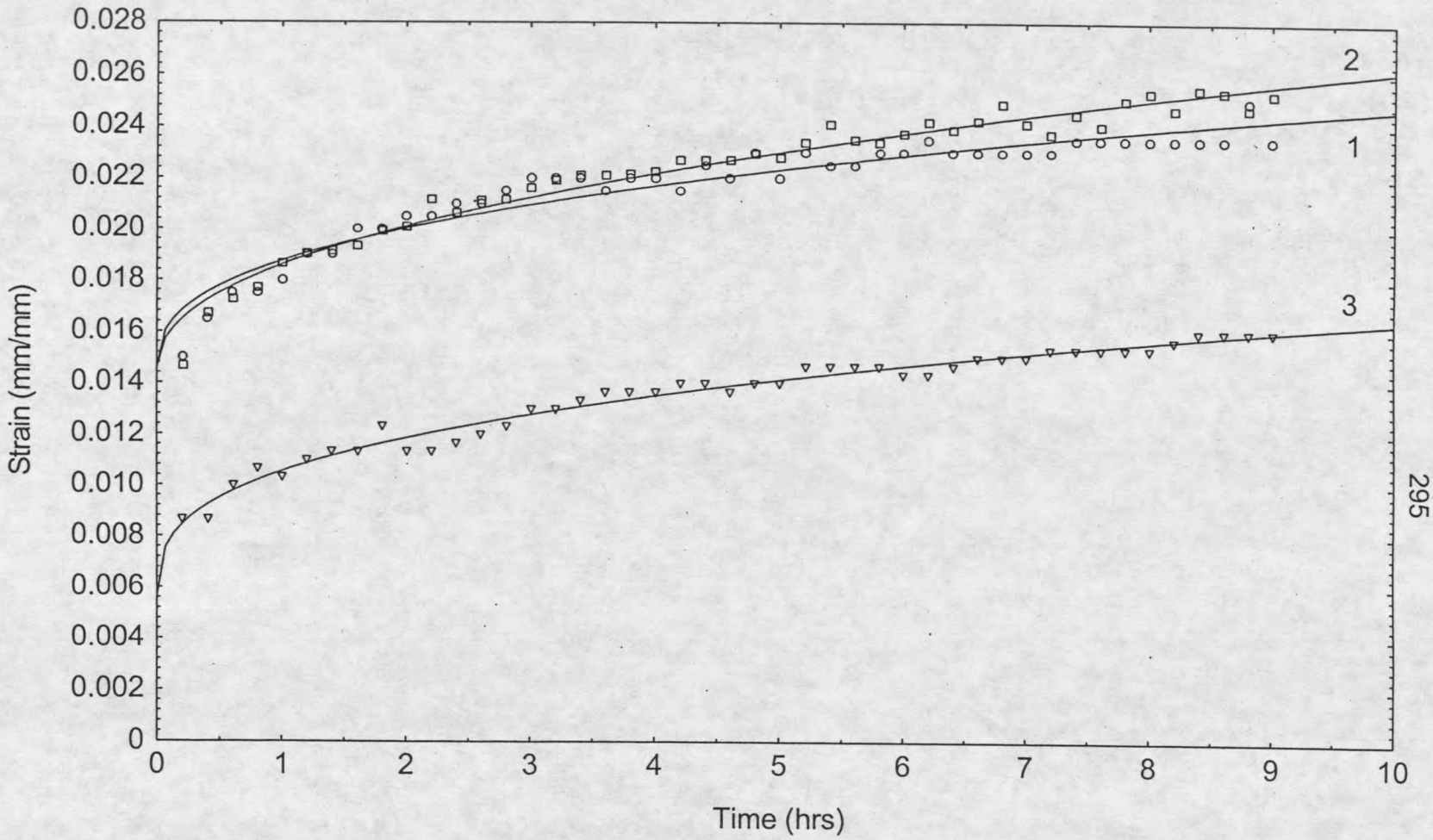


Figure C.III.13 Vibrocreep Response of Nylon 6/6 at Different Amplitudes at 41 °C
1- $(0.20\pm0.05)\sigma_y$, 1 Hz; 2- $(0.20\pm0.10)\sigma_y$, 1 Hz;
3- $(0.20)\sigma_y$, Constant Load Creep;
σ_y = 70 MPa at 23 °C

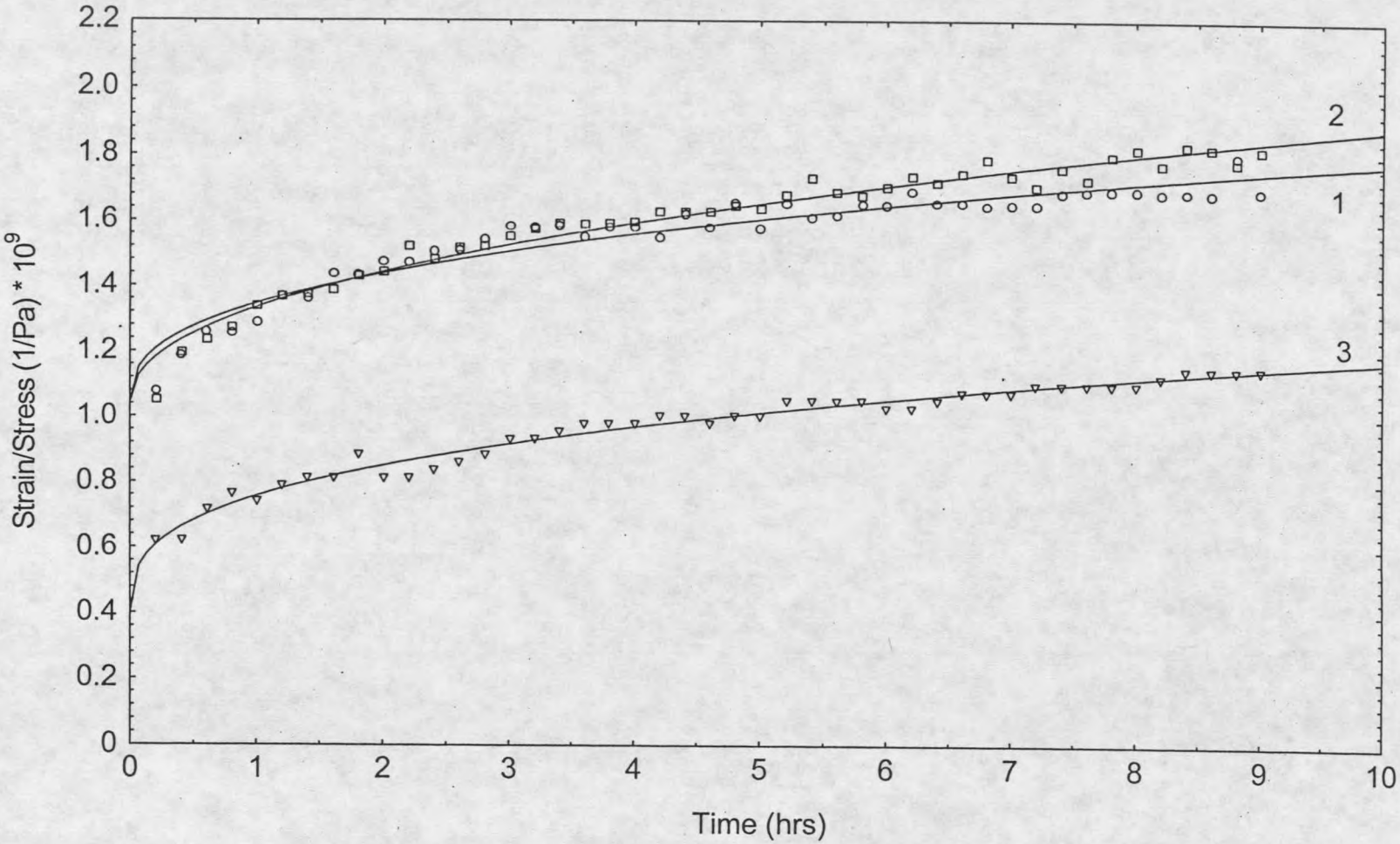


Figure C.III.14 Normalized Vibrocreep Response of Nylon 6/6 at Different Amplitudes at 41 °C
1- $(0.20\pm0.05)\sigma_y$, 1 Hz; 2- $(0.20\pm0.10)\sigma_y$, 1 Hz;
3- $(0.20)\sigma_y$, Constant Load Creep;
σ_y = 70 MPa at 23 °C

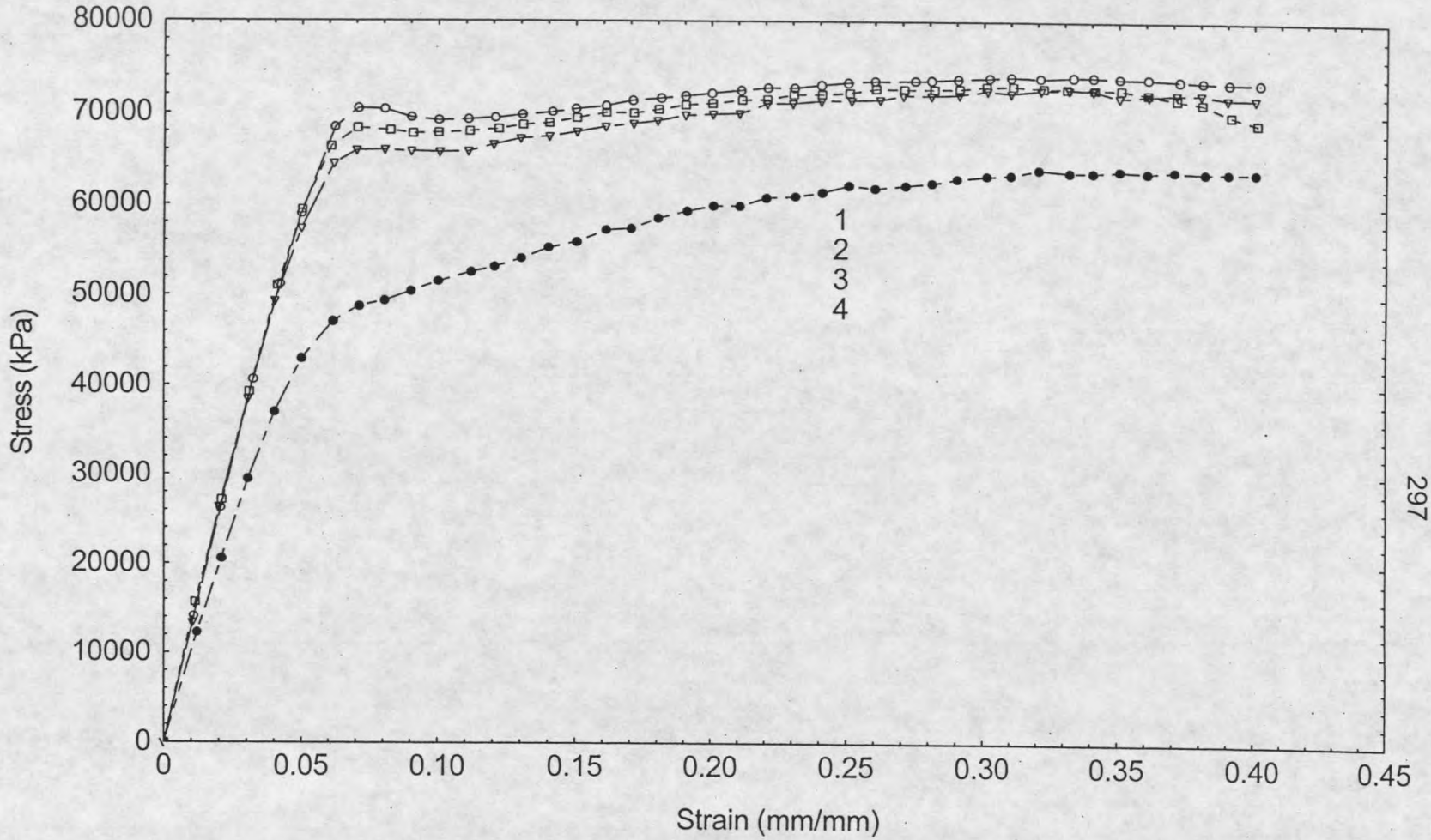


Figure C.III.15 Tensile Testing of Nylon 6/6 Specimens After Cyclic and Constant Loading at 41 °C
1- $(0.20\pm0.05)\sigma_y$, 1 Hz; 2- $(0.20\pm0.10)\sigma_y$, 1 Hz;
3- $(0.20)\sigma_y$, Constant Load Creep; 4- Virgin Specimens;
σ_y = 70 MPa at 23 °C

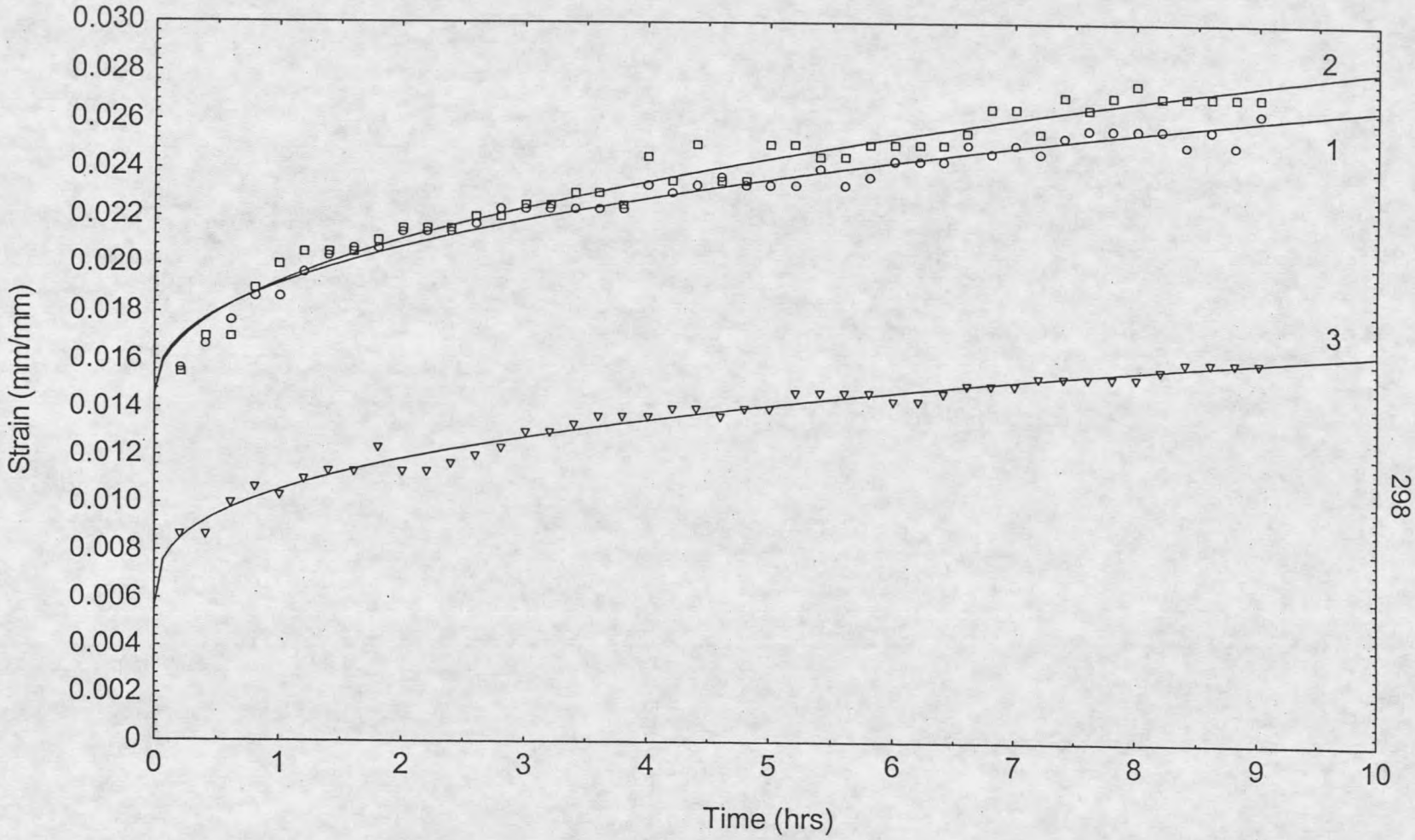


Figure C.III.16 Vibrocreep Response of Nylon 6/6 at Different Amplitudes at 41 °C
1- $(0.20\pm0.05)\sigma_y$, 10 Hz; 2- $(0.20\pm0.10)\sigma_y$, 10 Hz;
3- $(0.20)\sigma_y$, Constant Load Creep;
σ_y = 70 MPa at 23 °C

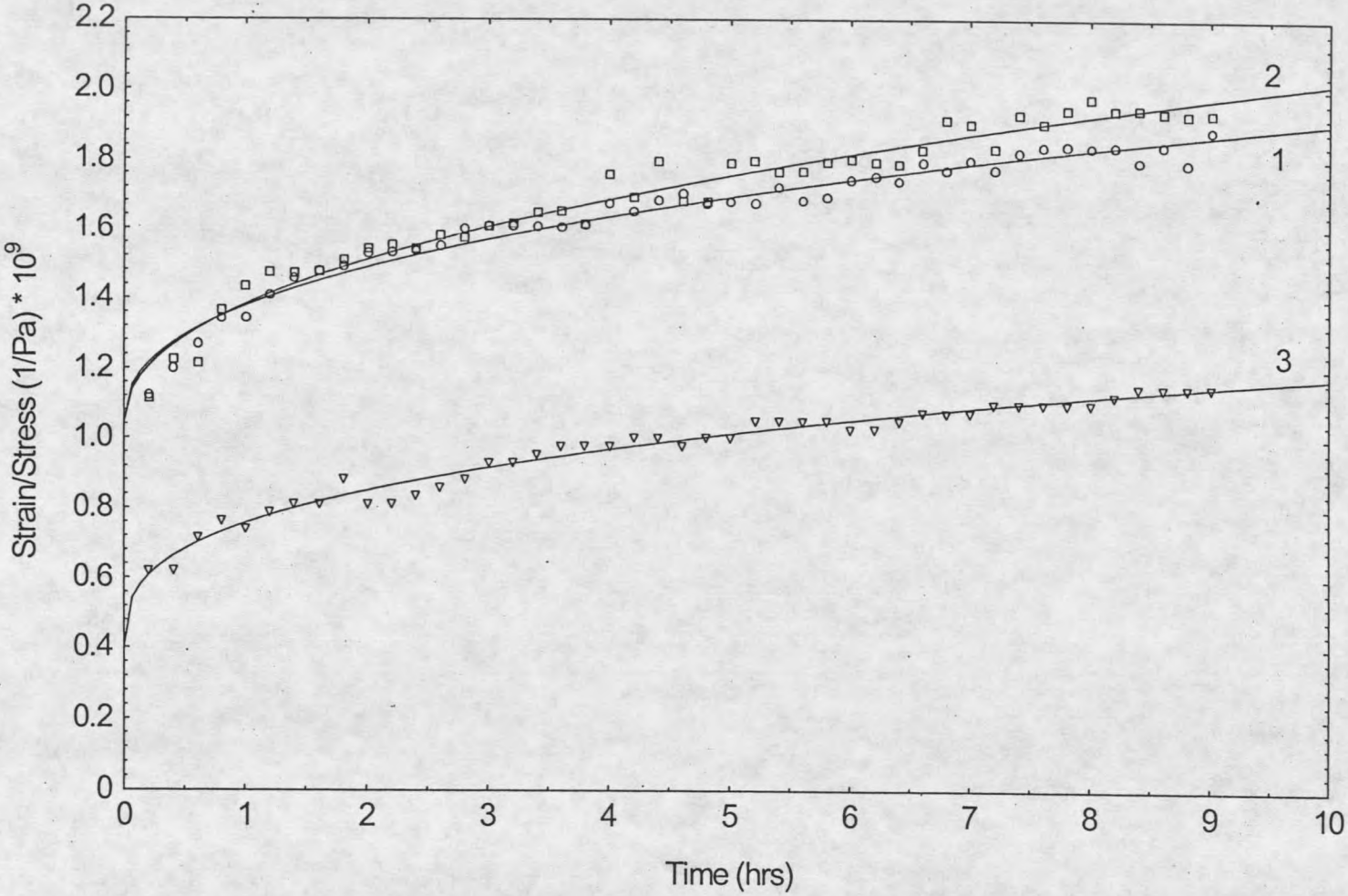


Figure C.III.17 Normalized Vibrocreep Response of Nylon 6/6 at Different Amplitudes at 41 °C
1- $(0.20\pm0.05)\sigma_y$, 10 Hz; 2- $(0.20\pm0.10)\sigma_y$, 10 Hz;
3- $(0.20)\sigma_y$, Constant Load Creep;
σ_y = 70 MPa at 23 °C

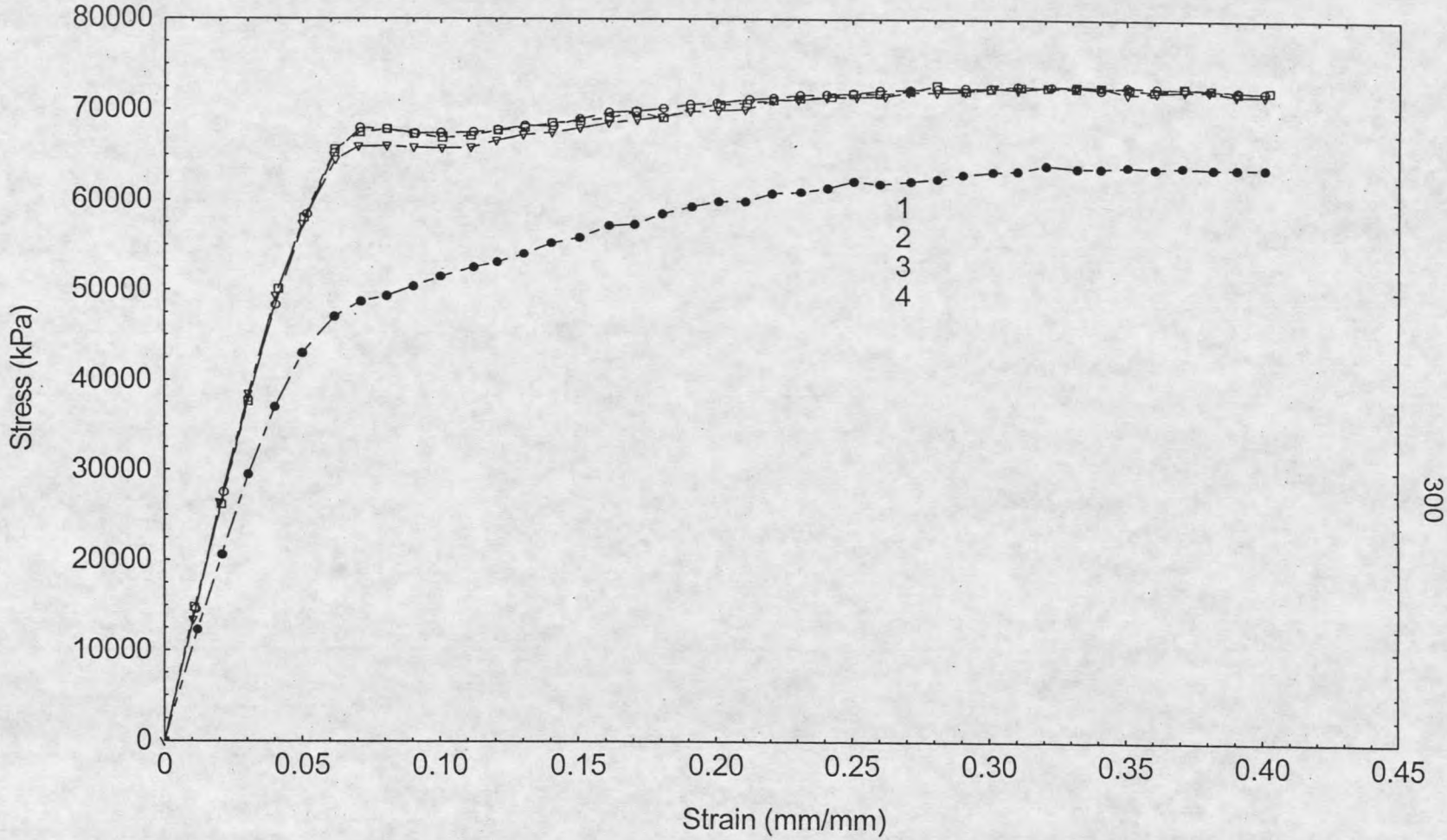


Figure C.III.18 Tensile Testing of Nylon 6/6 Specimens After Cyclic and Constant Loading at 41 °C
1- $(0.20\pm0.05)\sigma_y$, 10 Hz; 2- $(0.20\pm0.10)\sigma_y$, 10 Hz;
3- $(0.20)\sigma_y$, Constant Load Creep; 4- Virgin Specimens;
σ_y = 70 MPa at 23 °C

APPENDIX D

The Influence of the Parameter μ from Vibrocreep Testing of Nylon 6/6

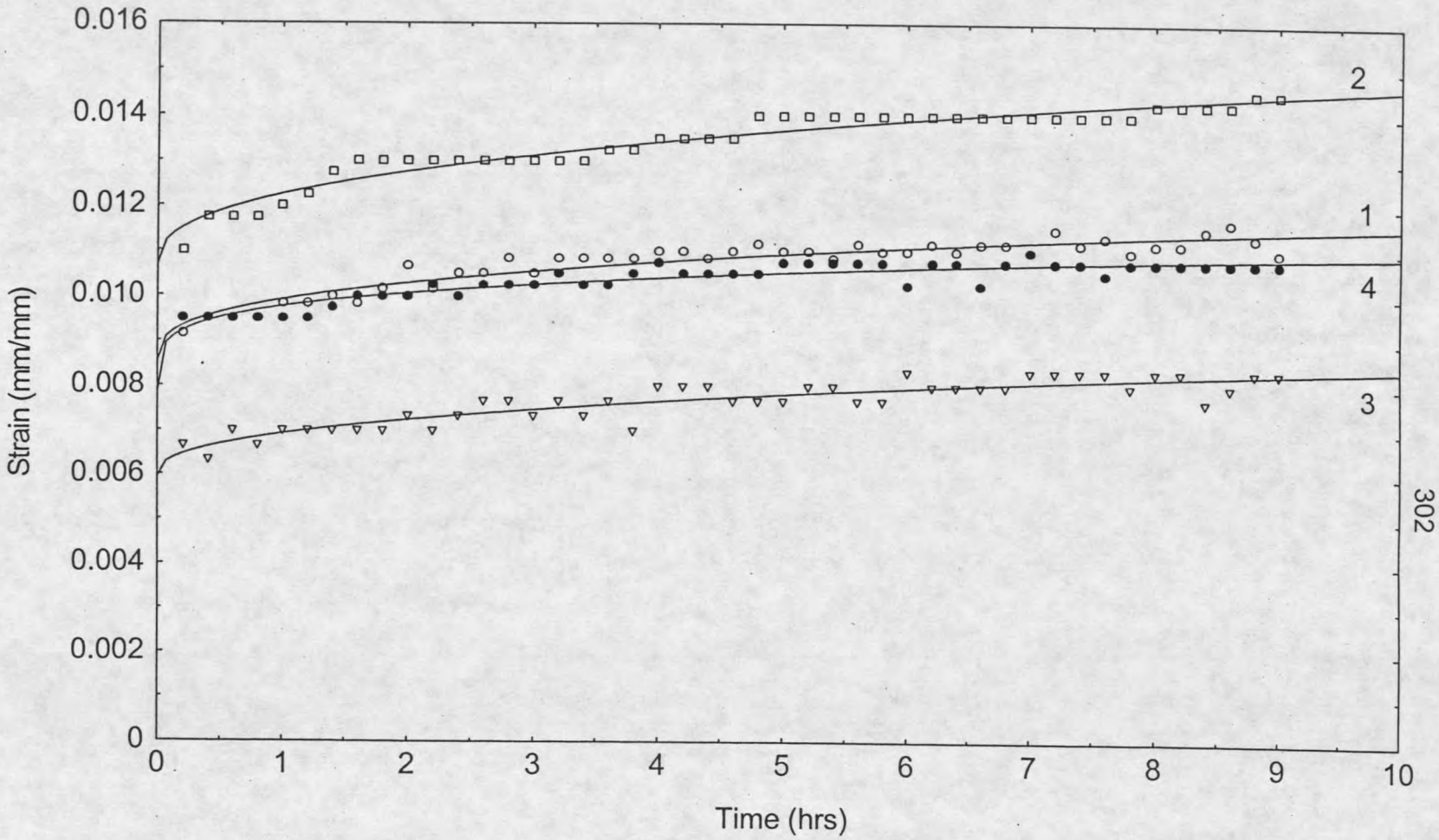


Figure D.I.1 Vibrocreep Response of Nylon 6/6 with μ=4 at 23 °C
1- $(0.16\pm0.04)\sigma_y$, 1 Hz; 2- $(0.20\pm0.05)\sigma_y$, 1 Hz;
3- $(0.16)\sigma_y$, 4- $(0.20)\sigma_y$ Constant Load Creep;
σ_y = 70 MPa at 23 °C

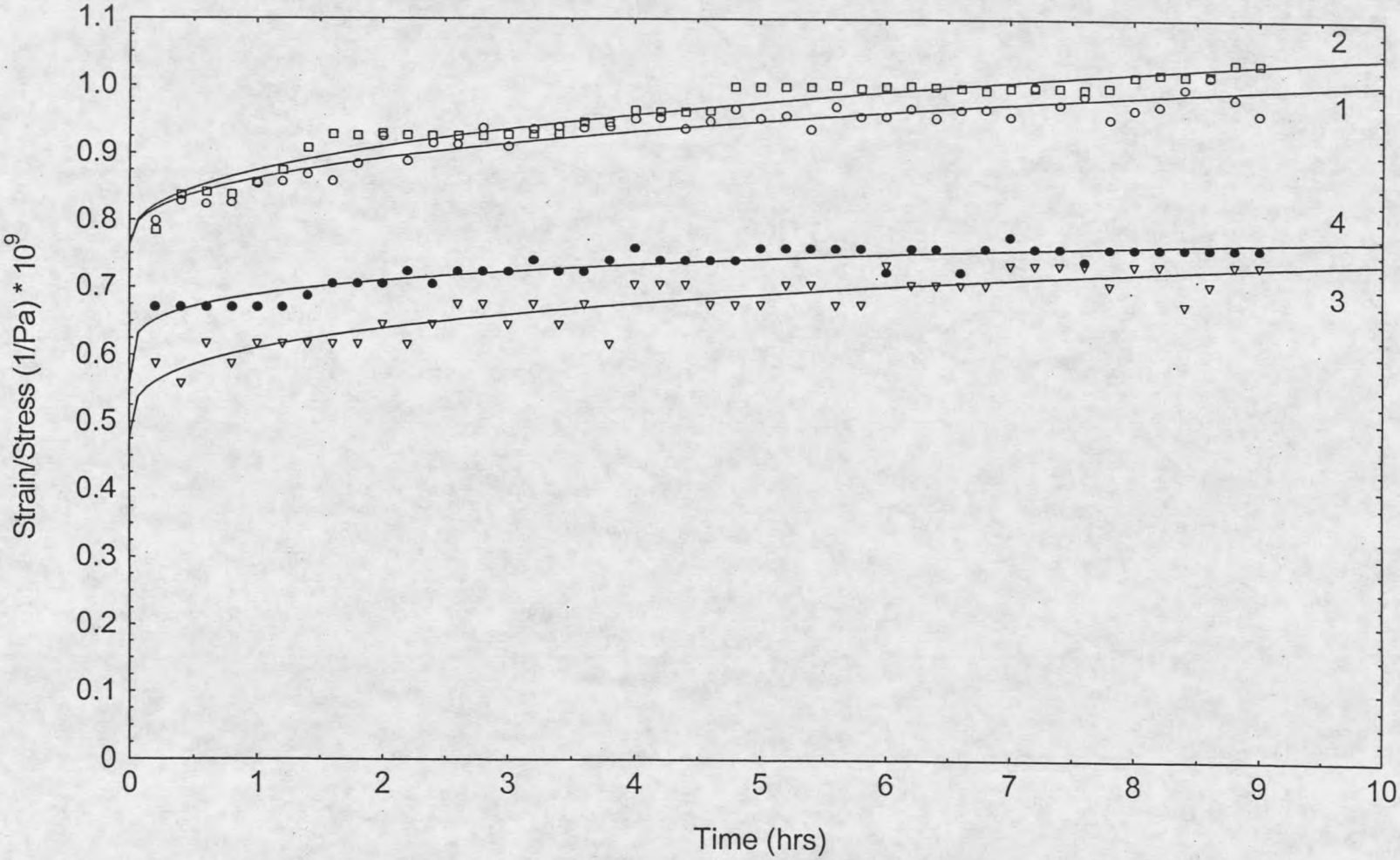


Figure D.I.2 Normalized Vibrocreep Response of Nylon 6/6 with μ=4 at 23 °C
1- $(0.16\pm0.04)\sigma_y$, 1 Hz; 2- $(0.20\pm0.05)\sigma_y$, 1 Hz;
3- $(0.16)\sigma_y$, 4- $(0.20)\sigma_y$ Constant Load Creep;
σ_y = 70 MPa at 23 °C

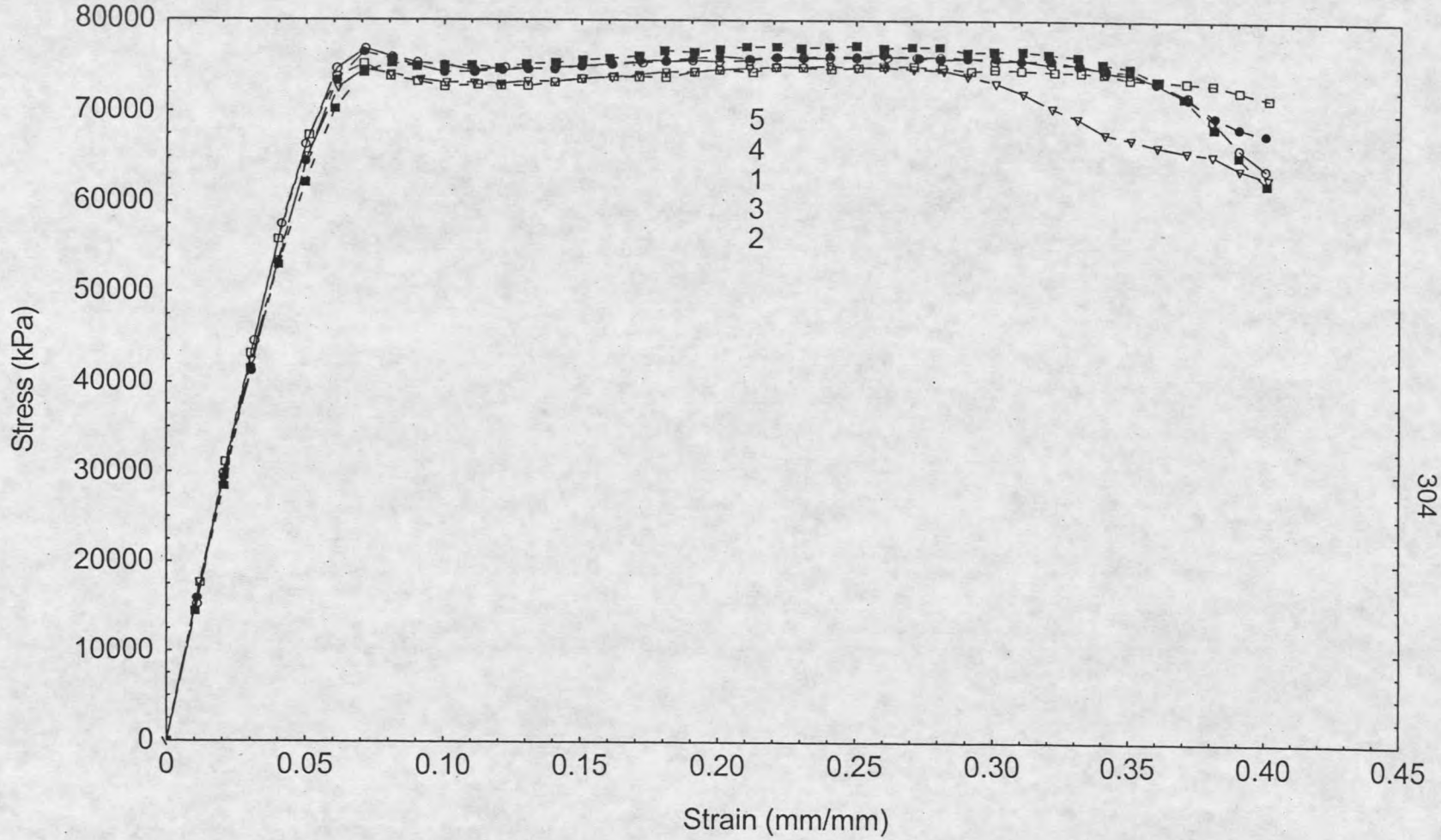


Figure D.I.3 Tensile Testing of Nylon 6/6 Specimens After Cyclic and Constant Loading at 23 °C
1- $(0.16\pm0.04)\sigma_y$, 1 Hz; 2- $(0.20\pm0.05)\sigma_y$, 1 Hz;
3- $(0.16)\sigma_y$, 4- $(0.20)\sigma_y$ Constant Load Creep; 5- Virgin Specimens;
σ_y = 70 MPa at 23 °C

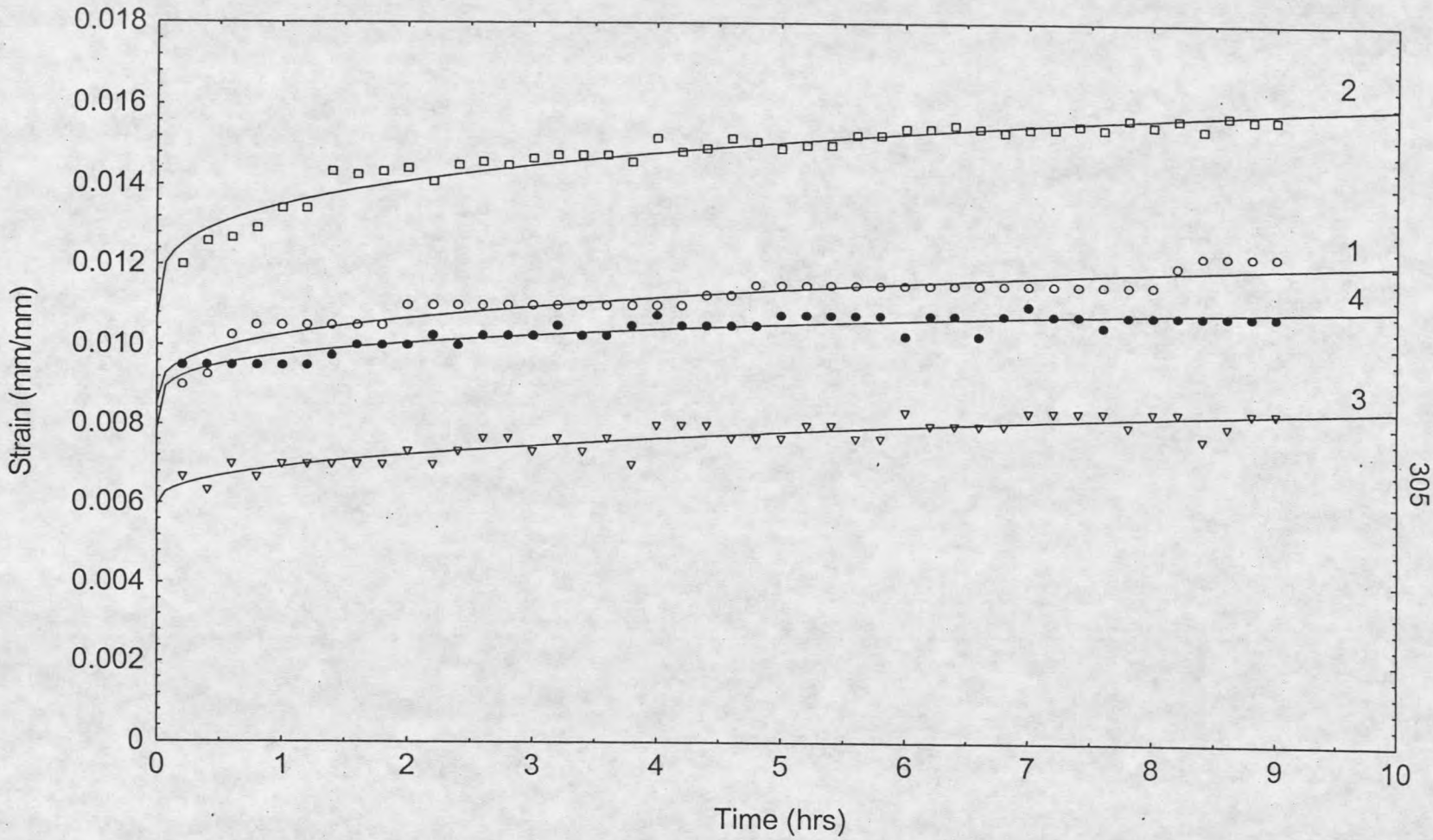


Figure D.I.4 Vibrocreep Response of Nylon 6/6 with μ=4 at 23 °C
1- 0.16±0.04)σ_y, 10 Hz; 2- (0.20±0.05)σ_y, 10 Hz;
3- (0.16)σ_y, 4- (0.20)σ_y Constant Load Creep;
σ_y = 70 MPa at 23 °C

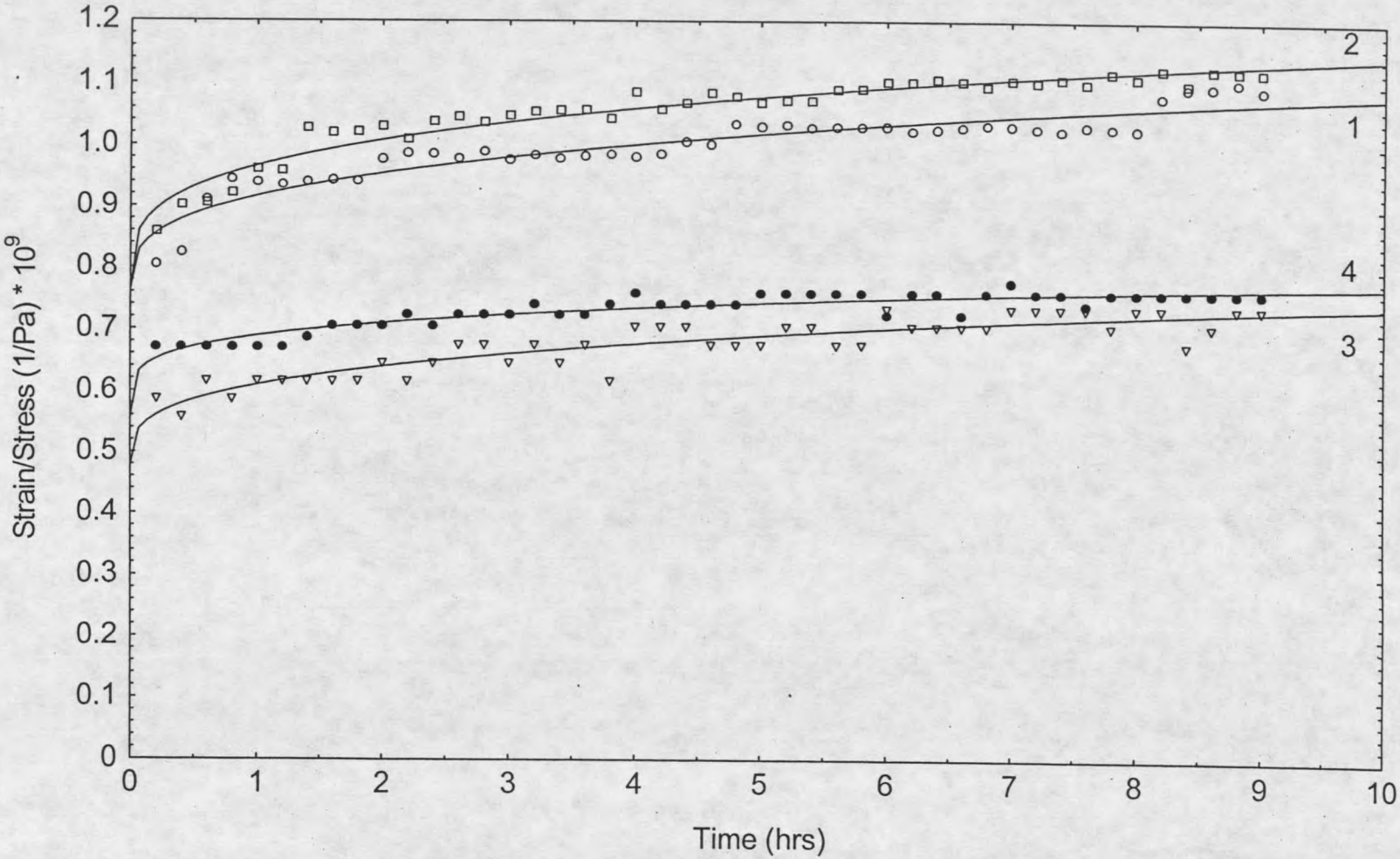


Figure D.I.5 Normalized Vibrocreep Response of Nylon 6/6 with μ=4 at 23 °C
1- $(0.16\pm0.04)\sigma_y$, 10 Hz; 2- $(0.20\pm0.05)\sigma_y$, 10 Hz;
3- $(0.16)\sigma_y$, 4- $(0.20)\sigma_y$ Constant Load Creep;
σ_y = 70 MPa at 23 °C

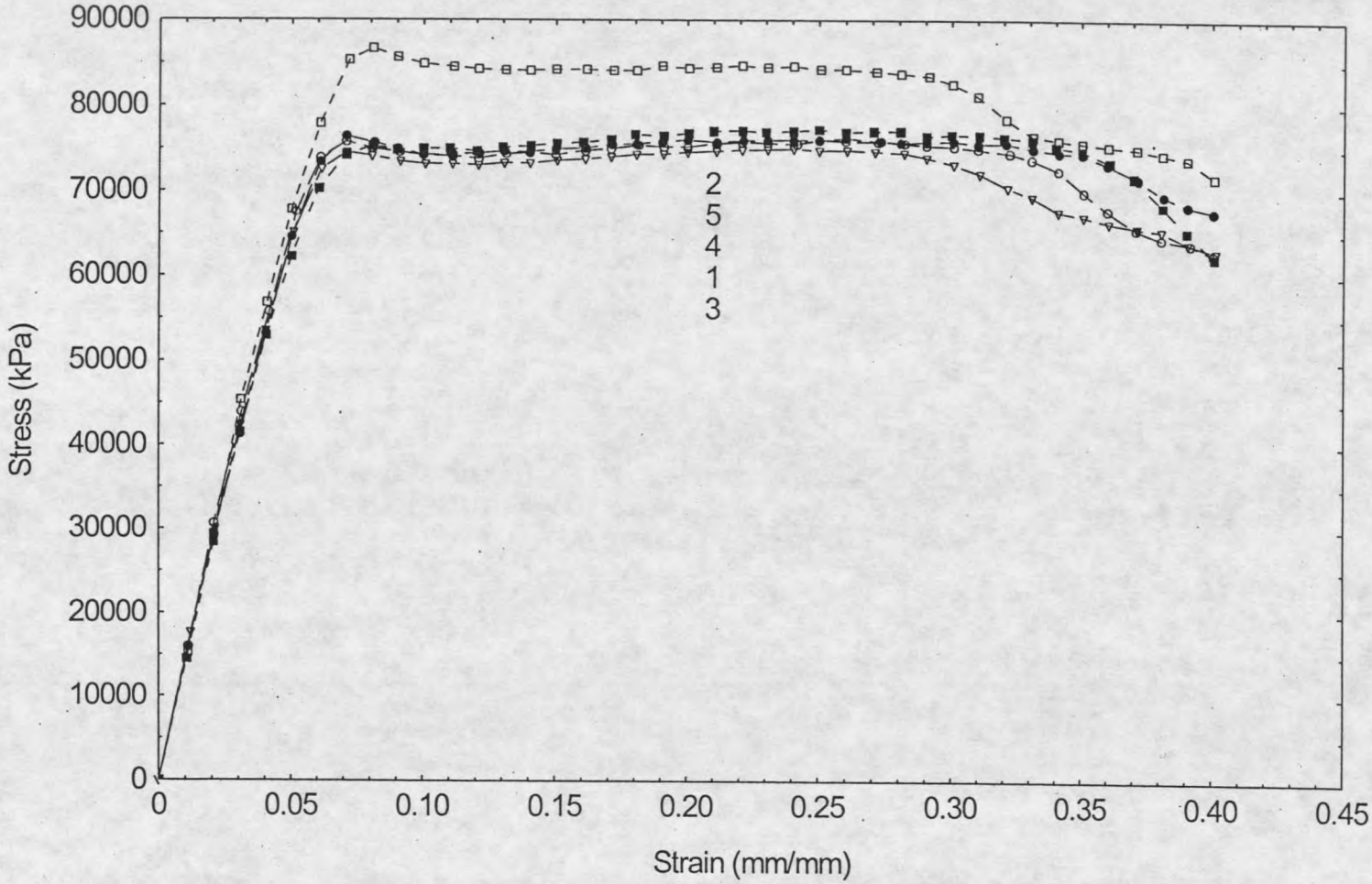


Figure D.I.6 Tensile Testing of Nylon 6/6 Specimens After Cyclic and Constant Loading at 23 °C
1- $(0.16\pm0.04)\sigma_y$, 10 Hz; 2- $(0.20\pm0.05)\sigma_y$, 10 Hz;
3- $(0.16)\sigma_y$, 4- $(0.20)\sigma_y$ Constant Load Creep; 5- Virgin Specimens;
σ_y = 70 MPa at 23 °C

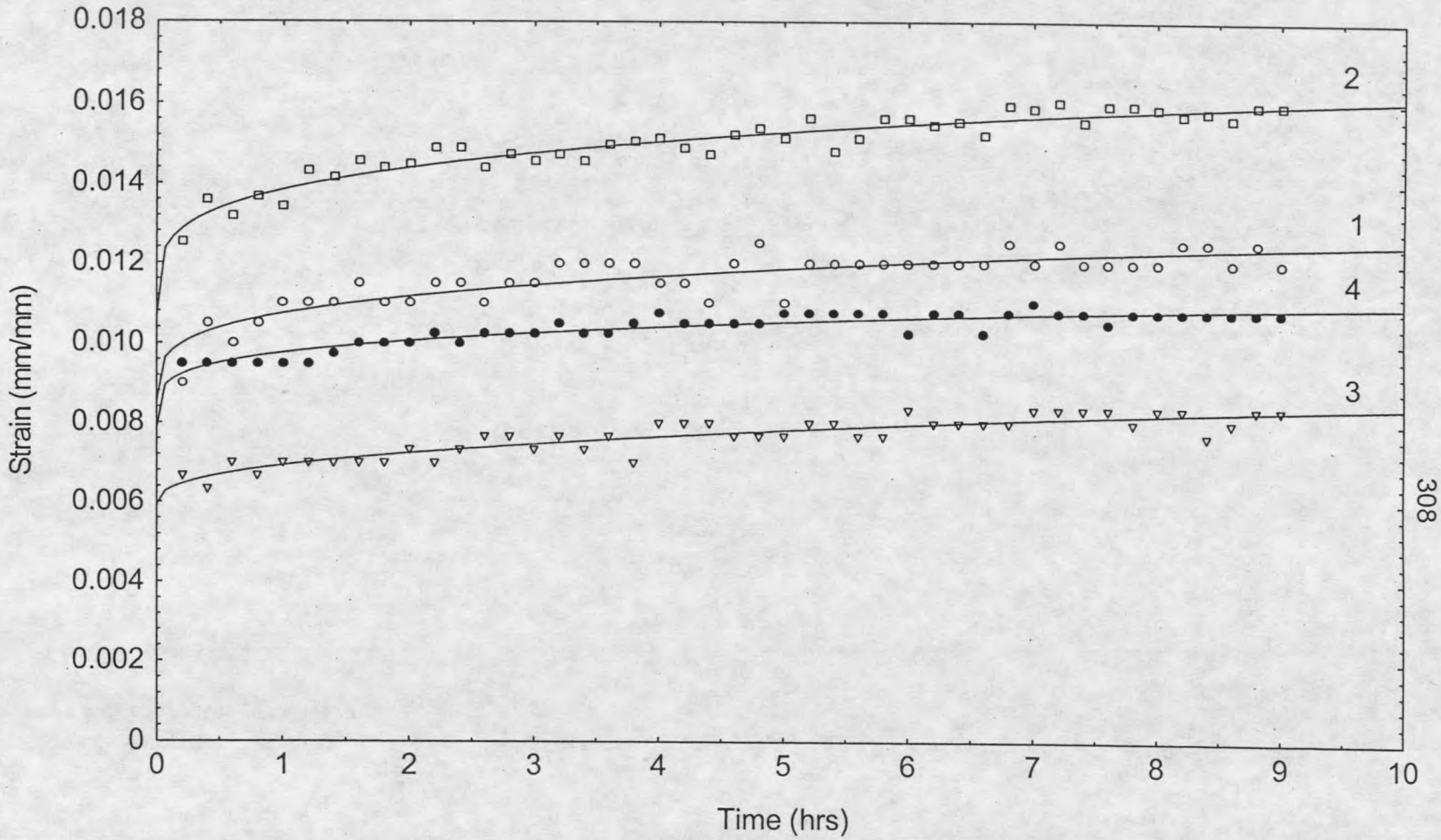


Figure D.I.7 Vibrocreep Response of Nylon 6/6 with μ=4 at 23 °C
1- $(0.16\pm0.04)\sigma_y$, 20 Hz; 2- $(0.20\pm0.05)\sigma_y$, 20 Hz;
3- $(0.16)\sigma_y$, 4- $(0.20)\sigma_y$ Constant Load Creep;
σ_y = 70 MPa at 23 °C

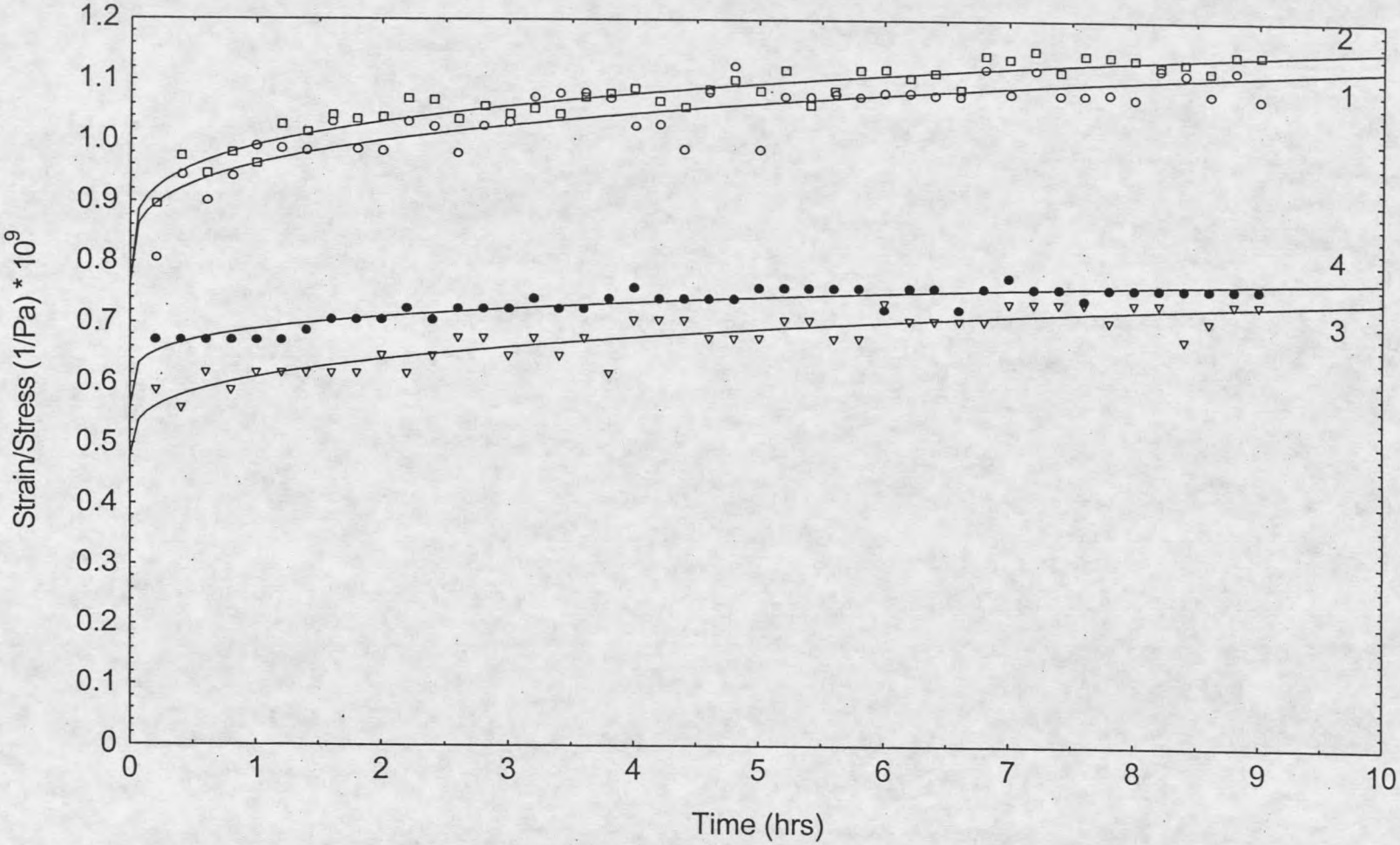


Figure D.I.8 Normalized Vibrocreep Response of Nylon 6/6 with μ=4 at 23 °C
1- $(0.16\pm0.04)\sigma_y$, 20 Hz; 2- $(0.20\pm0.05)\sigma_y$, 20 Hz;
3- $(0.16)\sigma_y$, 4- $(0.20)\sigma_y$ Constant Load Creep;
σ_y = 70 MPa at 23 °C

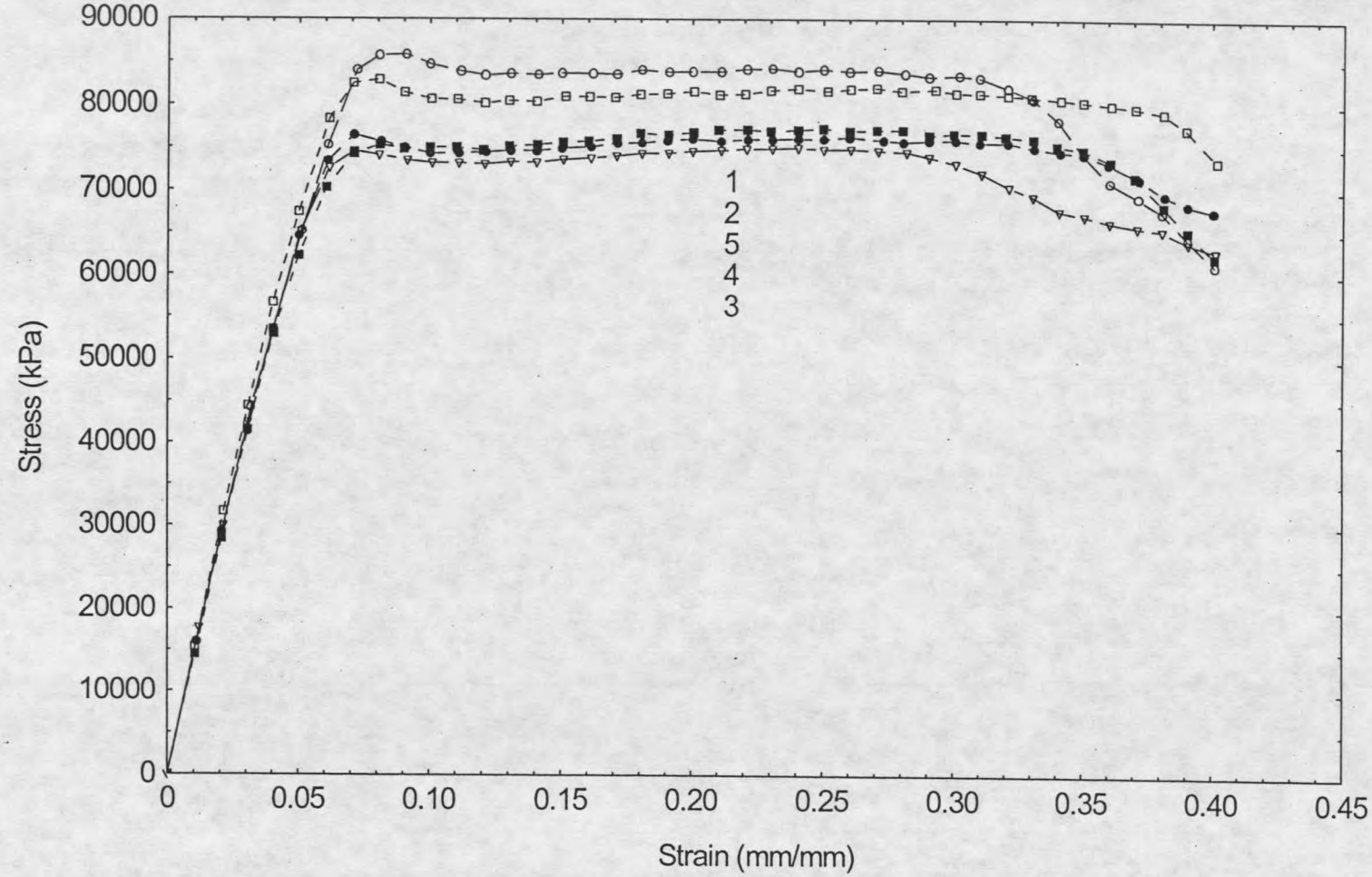


Figure D.I.9 Tensile Testing of Nylon 6/6 Specimens After Cyclic and Constant Loading at 23 °C
1- $(0.16\pm0.04)\sigma_y$, 20 Hz; 2- $(0.20\pm0.05)\sigma_y$, 20 Hz;
3- $(0.16)\sigma_y$, 4- $(0.20)\sigma_y$ Constant Load Creep; 5- Virgin Specimens;
σ_y = 70 MPa at 23 °C

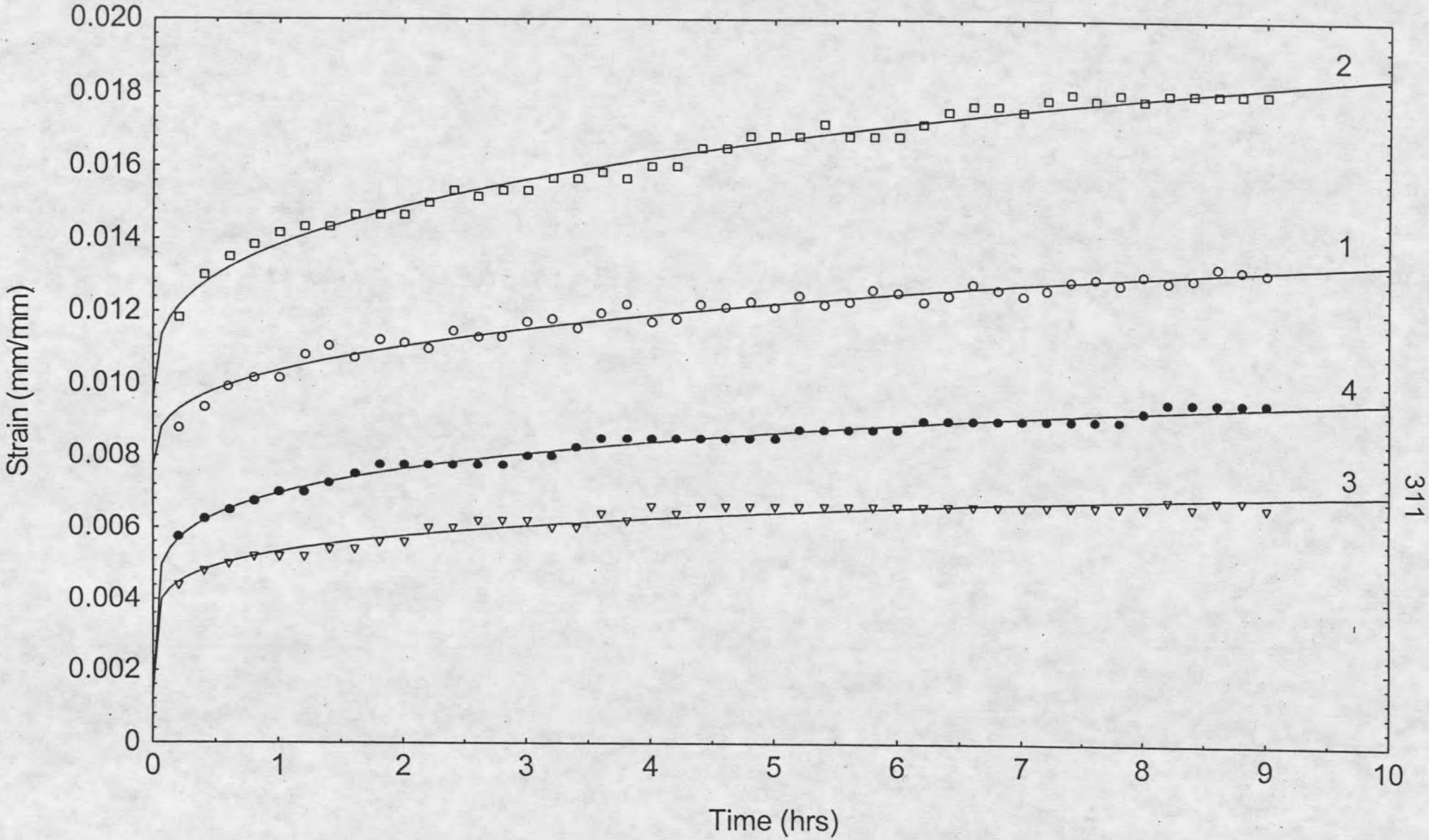


Figure D.II.1 Vibrocreep Response of Nylon 6/6 with μ=4 at 35 °C
1- $(0.16\pm0.04)\sigma_y$, 1 Hz; 2- $(0.20\pm0.05)\sigma_y$, 1 Hz;
3- $(0.16)\sigma_y$, 4- $(0.20)\sigma_y$, Constant Load Creep;
σ_y = 55 MPa at 35 °C

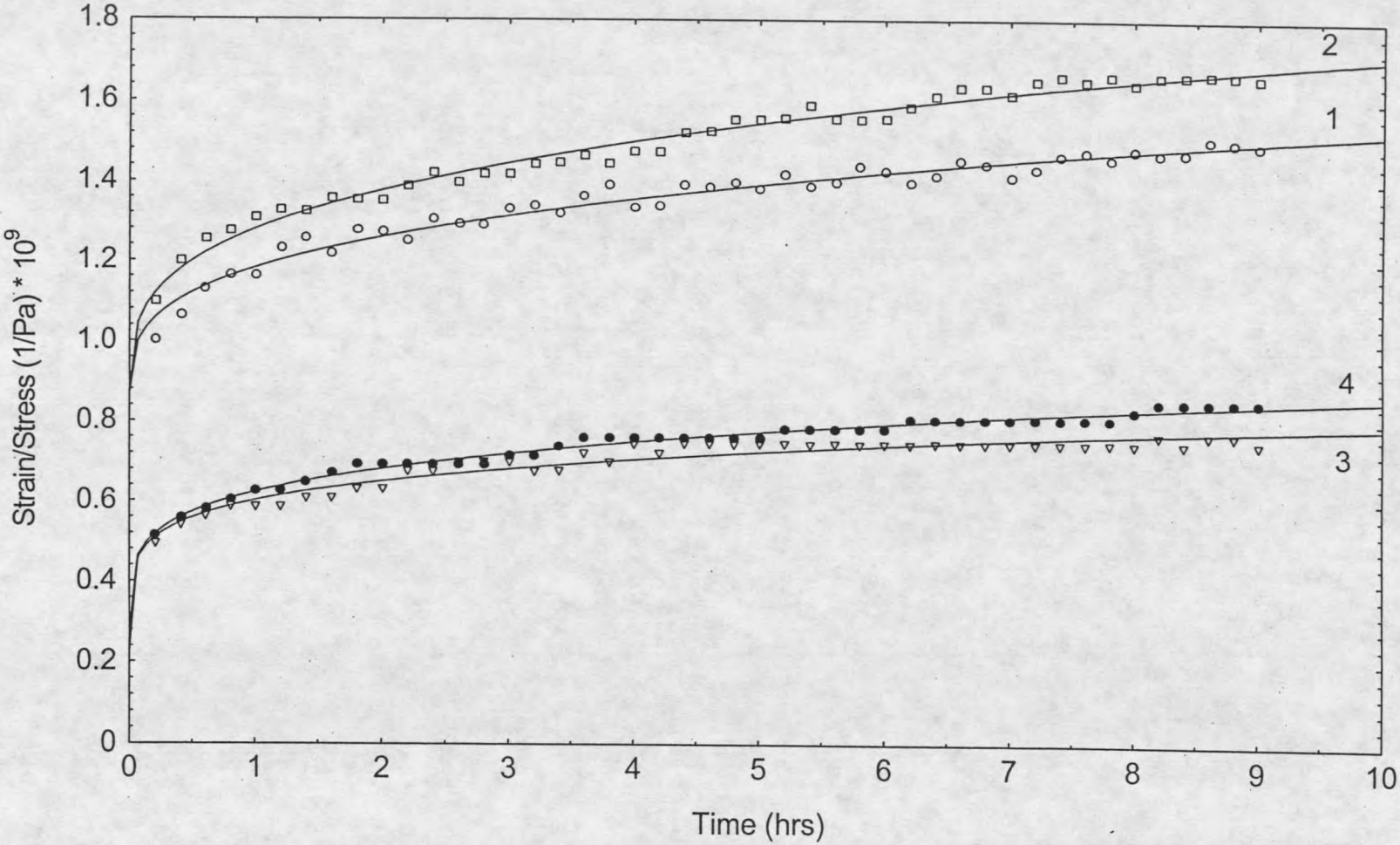


Figure D.II.2 Normalized Vibrocreep Response of Nylon 6/6 with μ=4 at 35 °C
1- $(0.16\pm0.04)\sigma_y$, 1 Hz; 2- $(0.20\pm0.05)\sigma_y$, 1 Hz;
3- $(0.16)\sigma_y$, 4- $(0.20)\sigma_y$, Constant Load Creep;
σ_y = 55 MPa at 35 °C

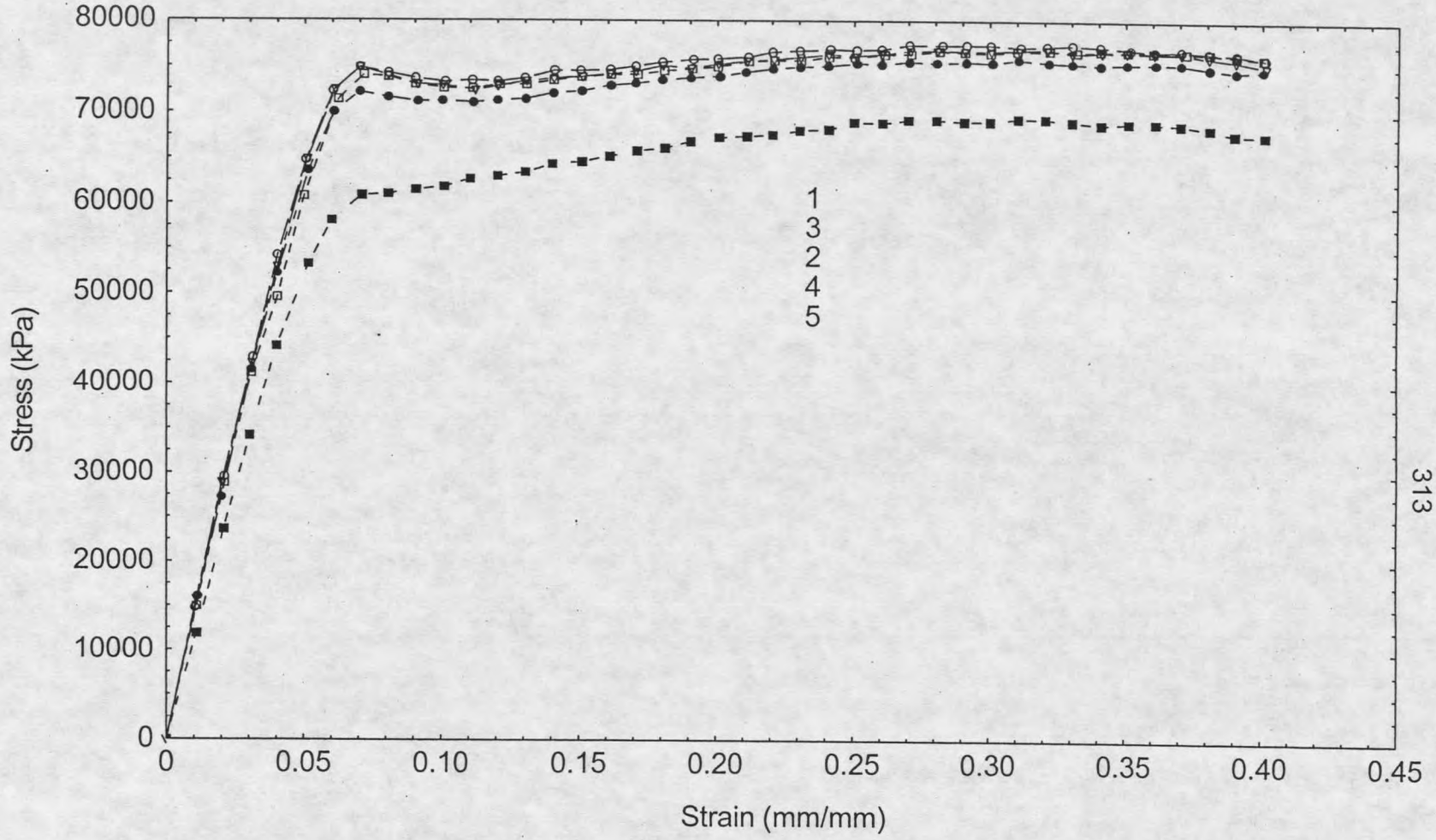


Figure D.II.3 Tensile Testing of Nylon 6/6 Specimens After Cyclic and Constant Loading at 35 °C
1- $(0.16\pm0.04)\sigma_y$, 1 Hz; 2- $(0.20\pm0.05)\sigma_y$, 1 Hz;
3- $(0.16)\sigma_y$, 4- $(0.20)\sigma_y$, Constant Load Creep; 5- Virgin Specimens;
σ_y = 55 MPa at 35 °C

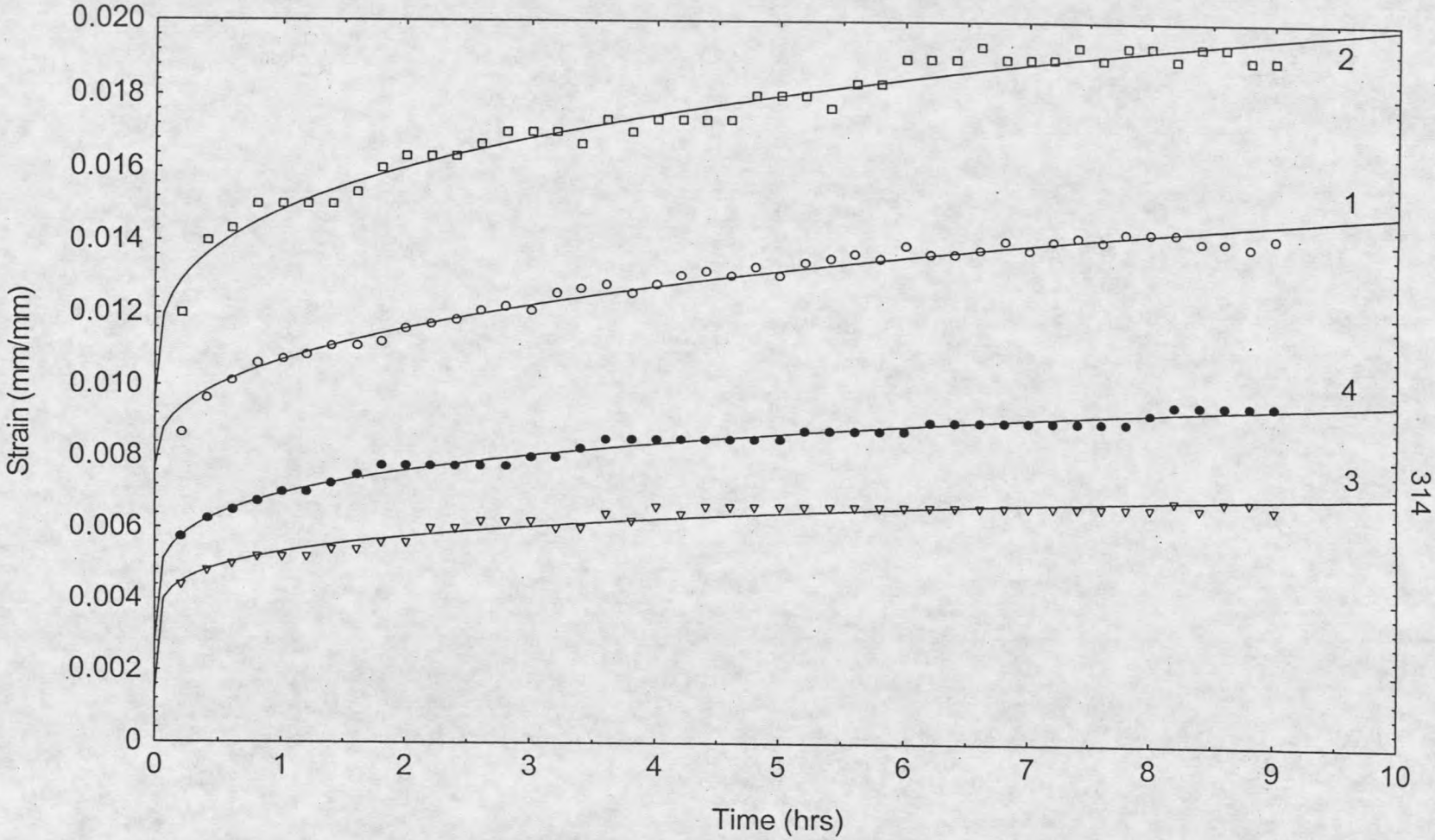


Figure D.II.4 Vibrocreep Response of Nylon 6/6 with μ=4 at 35 °C
1- $(0.16\pm0.04)\sigma_y$, 10 Hz; 2- $(0.20\pm0.05)\sigma_y$, 10 Hz;
3- $(0.16)\sigma_y$, 4- $(0.20)\sigma_y$, Constant Load Creep;
σ_y = 55 MPa at 35 °C

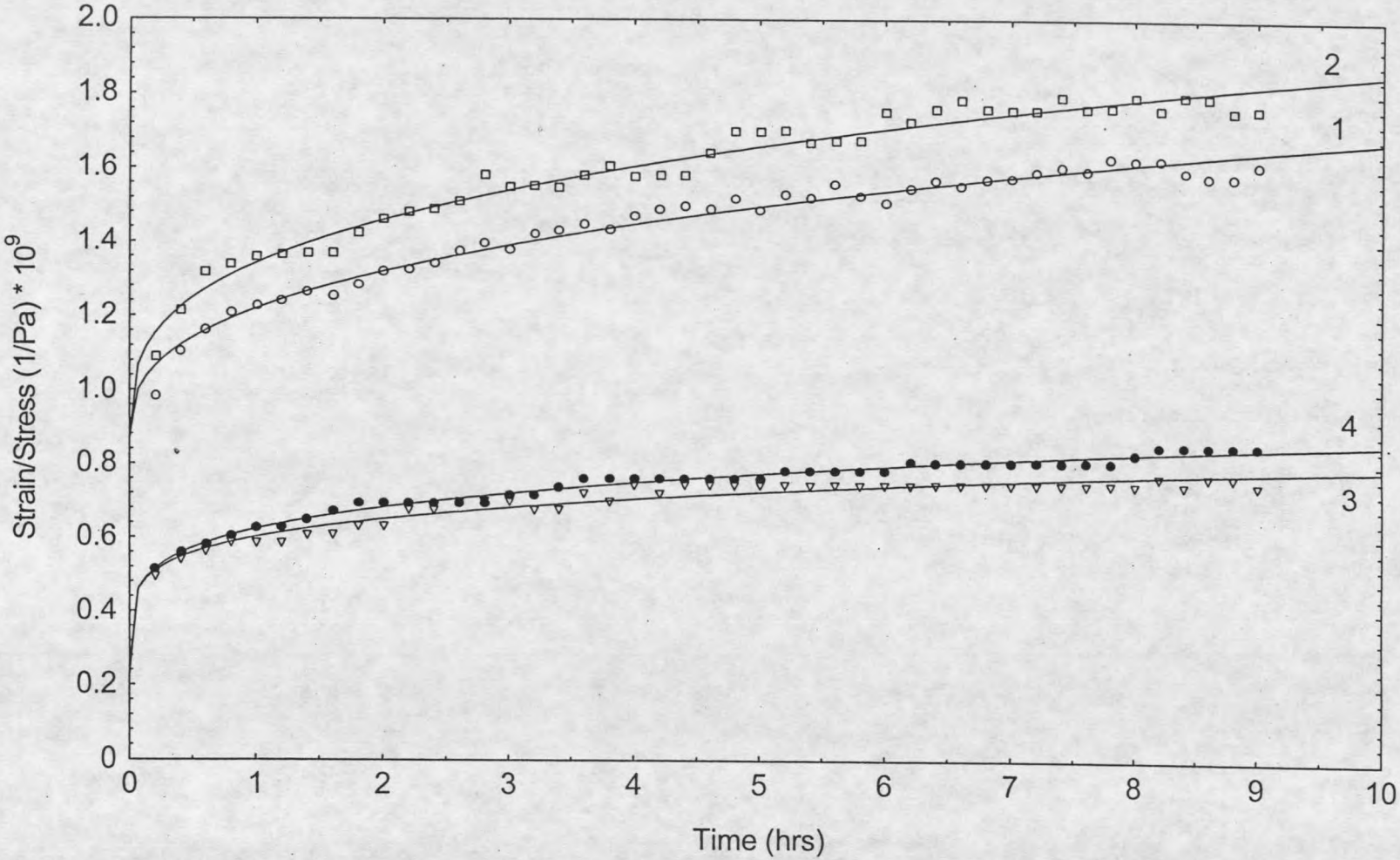


Figure D.II.5 Normalized Vibrocreep Response of Nylon 6/6 with μ=4 at 35 °C
1- $(0.16\pm0.04)\sigma_y$, 10 Hz; 2- $(0.20\pm0.05)\sigma_y$, 10 Hz;
3- $(0.16)\sigma_y$, 4- $(0.20)\sigma_y$, Constant Load Creep;
σ_y = 55 MPa at 35 °C

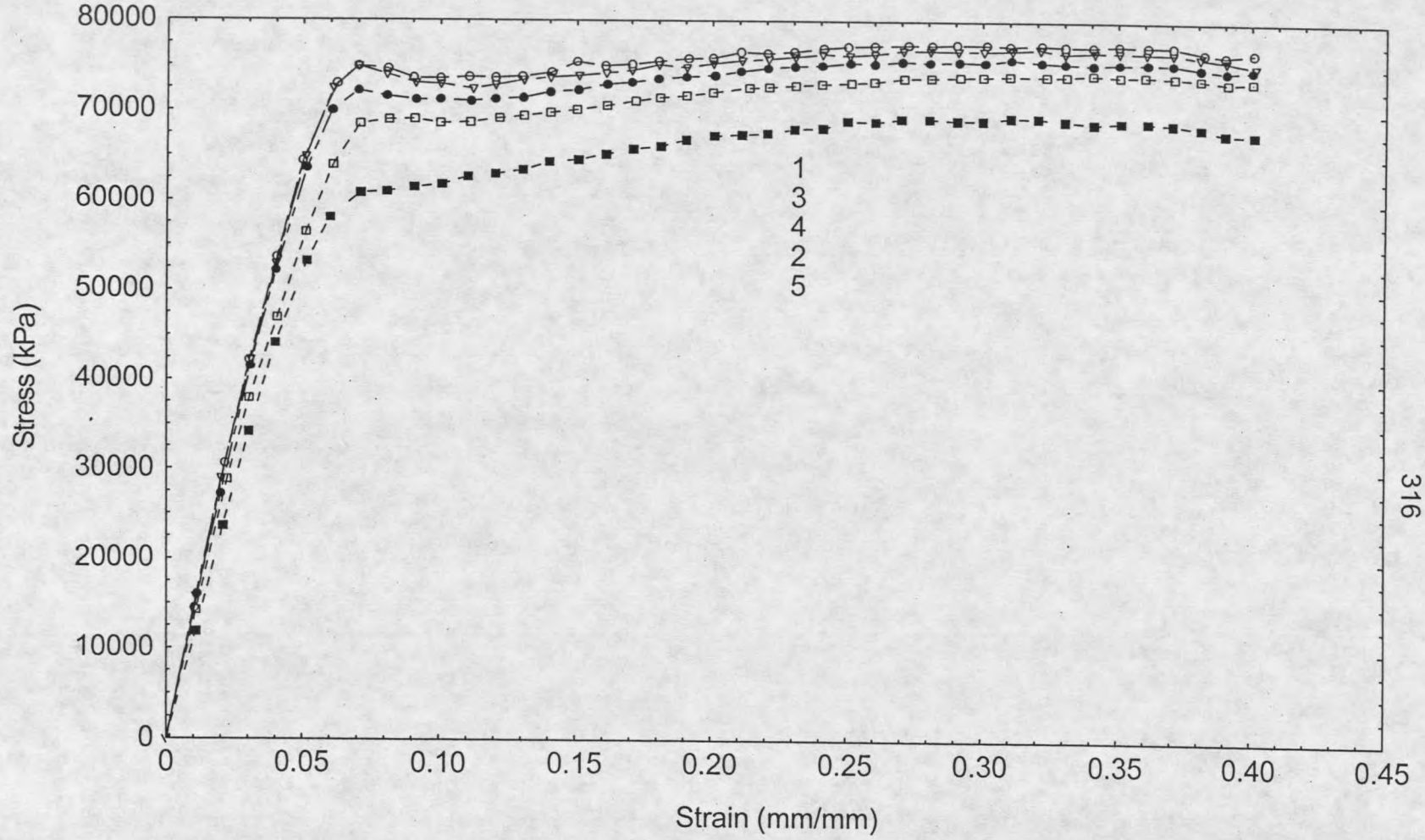


Figure D.II.6 Tensile Testing of Nylon 6/6 Specimens After Cyclic and Constant Loading at 35 °C
1- $(0.16\pm0.04)\sigma_y$, 10 Hz; 2- $(0.20\pm0.05)\sigma_y$, 10 Hz;
3- $(0.16)\sigma_y$, 4- $(0.20)\sigma_y$, Constant Load Creep; 5- Virgin Specimens;
σ_y = 55 MPa at 35 °C

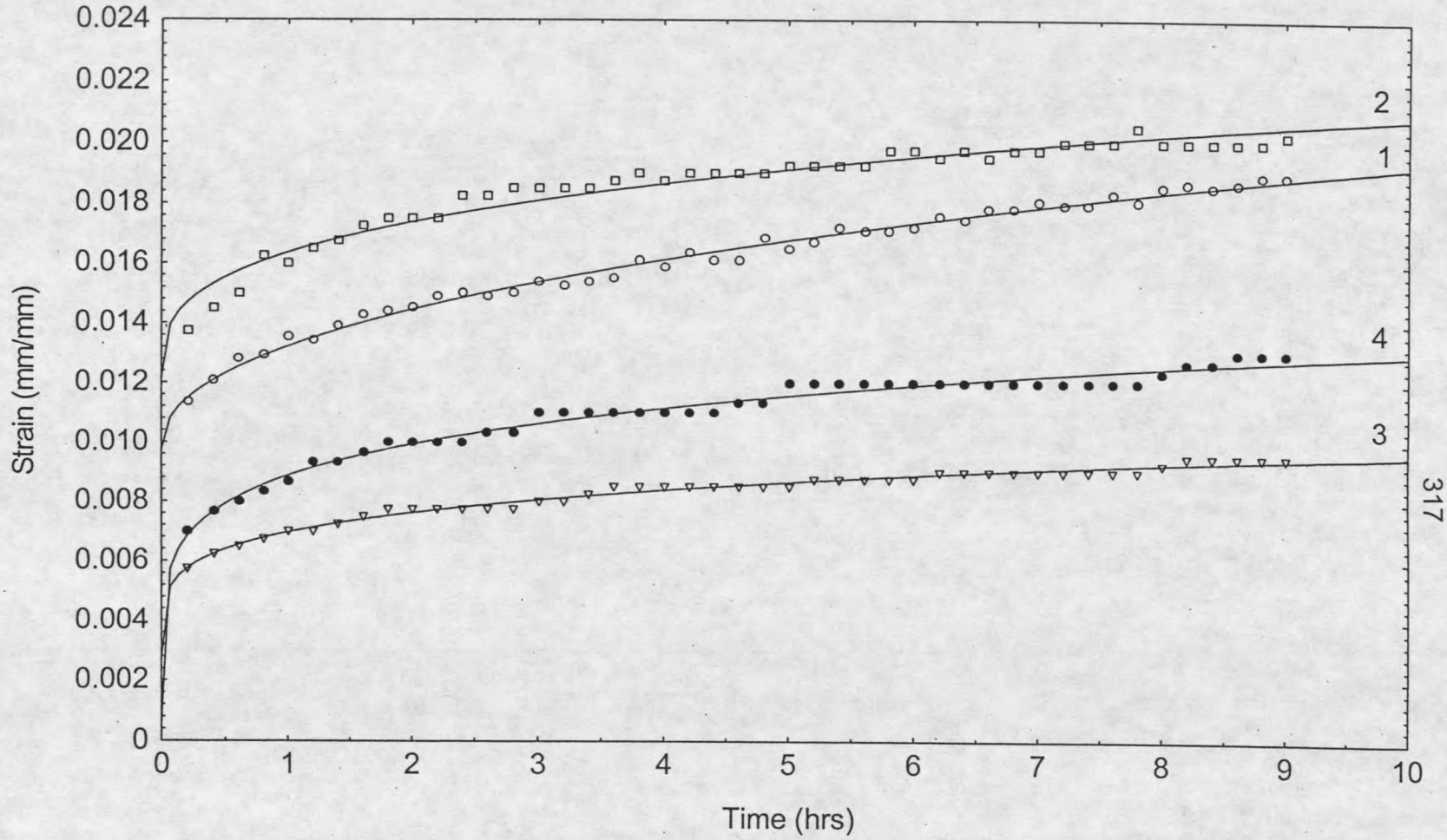


Figure D.II.7 Vibrocreep Response of Nylon 6/6 with μ=4 at 35 °C
1- $(0.16\pm0.04)\sigma_y$, 1 Hz; 2- $(0.20\pm0.05)\sigma_y$, 1 Hz;
3- $(0.16)\sigma_y$, 4- $(0.20)\sigma_y$, Constant Load Creep;
σ_y = 70 MPa at 23 °C

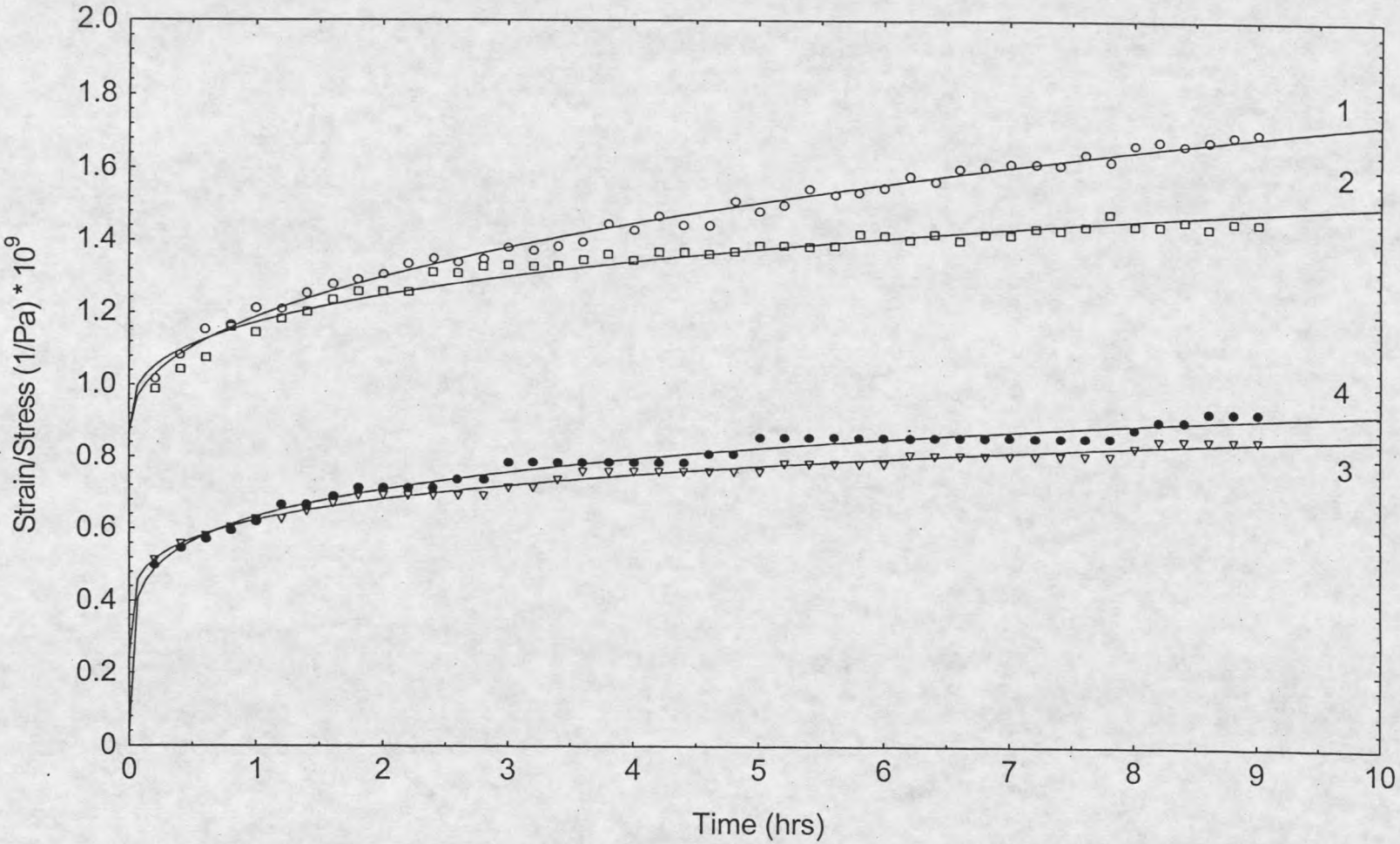


Figure D.II.8 Normalized Vibrocreep Response of Nylon 6/6 with μ=4 at 35 °C
1- $(0.16\pm0.04)\sigma_y$, 1 Hz; 2- $(0.20\pm0.05)\sigma_y$, 1 Hz;
3- $(0.16)\sigma_y$, 4- $(0.20)\sigma_y$, Constant Load Creep;
σ_y = 70 MPa at 23 °C

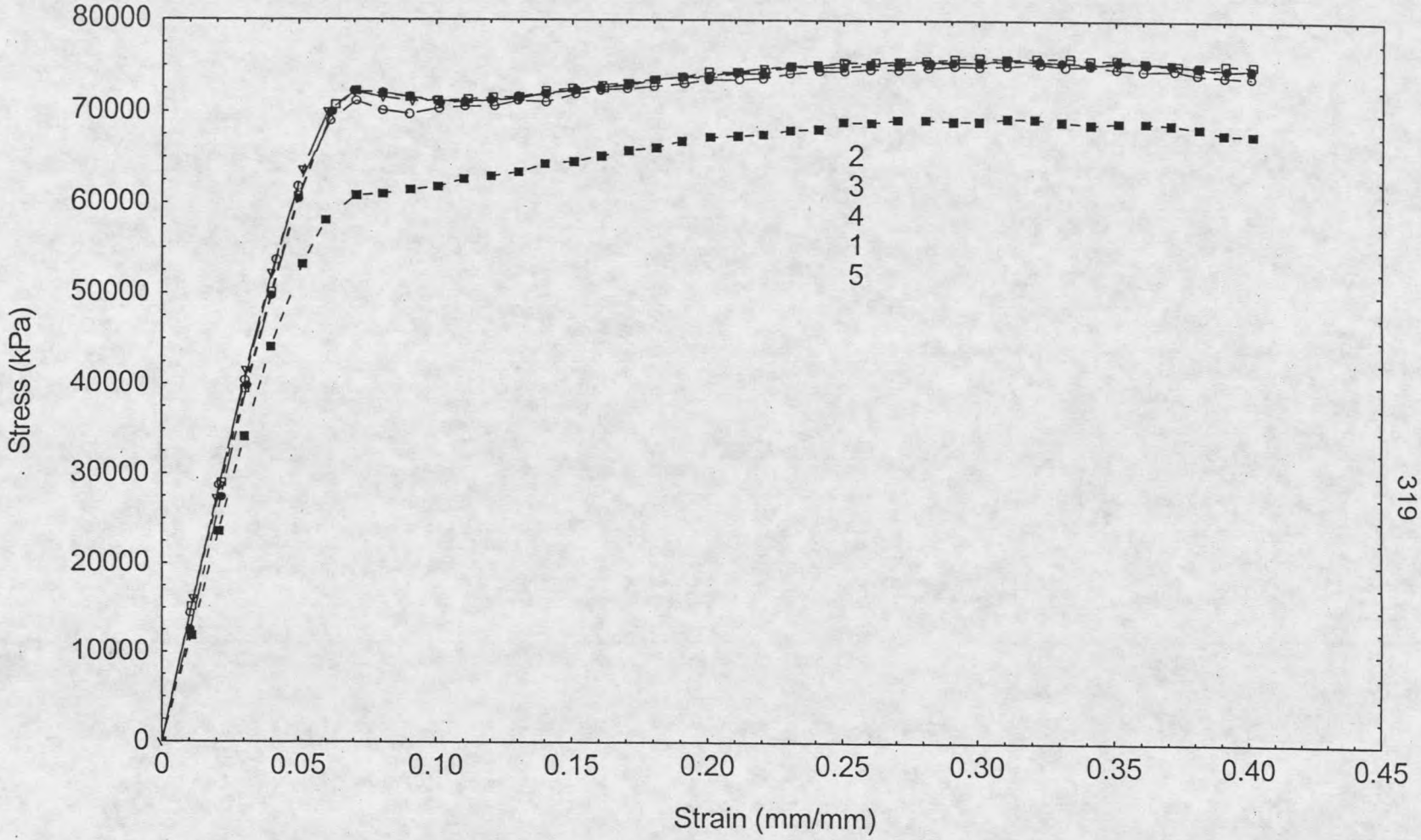


Figure D.II.9 Tensile Testing of Nylon 6/6 Specimens After Cyclic and Constant Loading μ=4 at 35 °C
1- $(0.16\pm0.04)\sigma_y$, 1 Hz; 2- $(0.20\pm0.05)\sigma_y$, 1 Hz;
3- $(0.16)\sigma_y$, 4- $(0.20)\sigma_y$, Constant Load Creep; 5- Virgin Specimens;
σ_y = 70 MPa at 23 °C

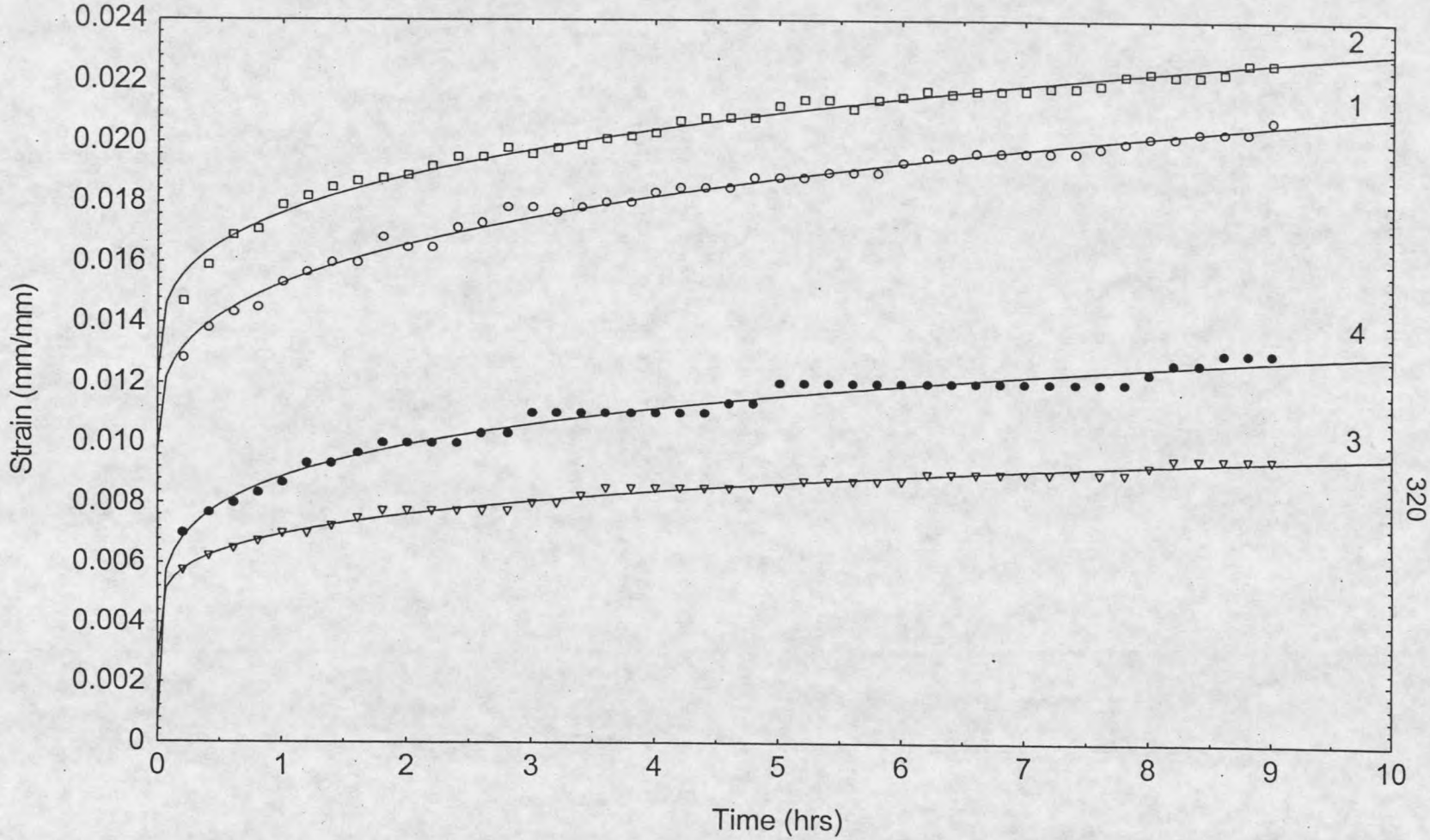


Figure D.II.10 Vibrocreep Response of Nylon 6/6 with μ=4 at 35 °C
1- $(0.16\pm0.04)\sigma_y$, 10 Hz; 2- $(0.20\pm0.05)\sigma_y$, 10 Hz;
3- $(0.16)\sigma_y$, 4- $(0.20)\sigma_y$, Constant Load Creep;
σ_y = 70 MPa at 23 °C

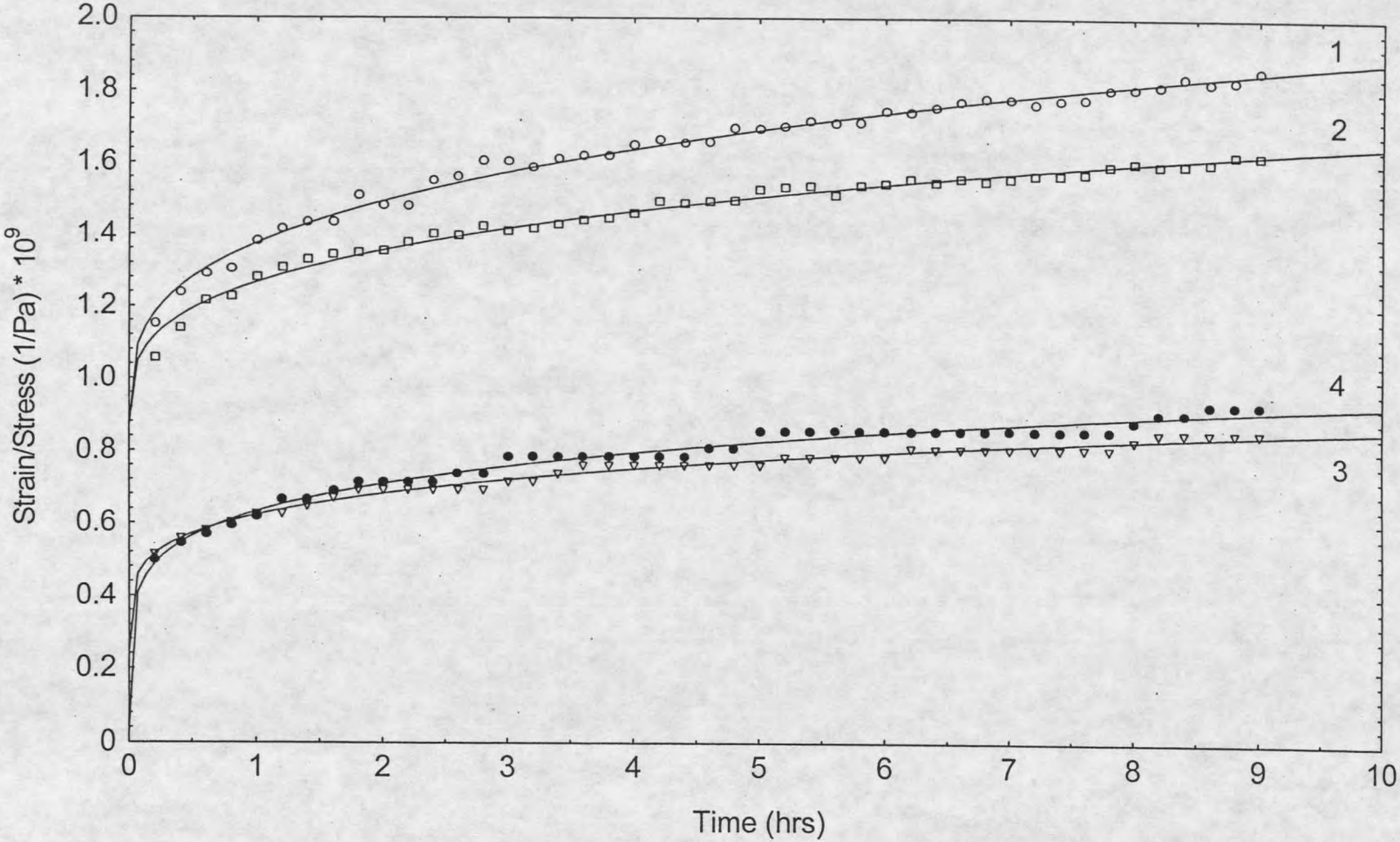


Figure D.II.11 Normalized Vibrocreep Response of Nylon 6/6 with μ=4 at 35 °C
1- $(0.16\pm0.04)\sigma_y$, 10 Hz; 2- $(0.20\pm0.05)\sigma_y$, 10 Hz;
3- $(0.16)\sigma_y$, 4- $(0.20)\sigma_y$, Constant Load Creep;
σ_y = 70 MPa at 23 °C

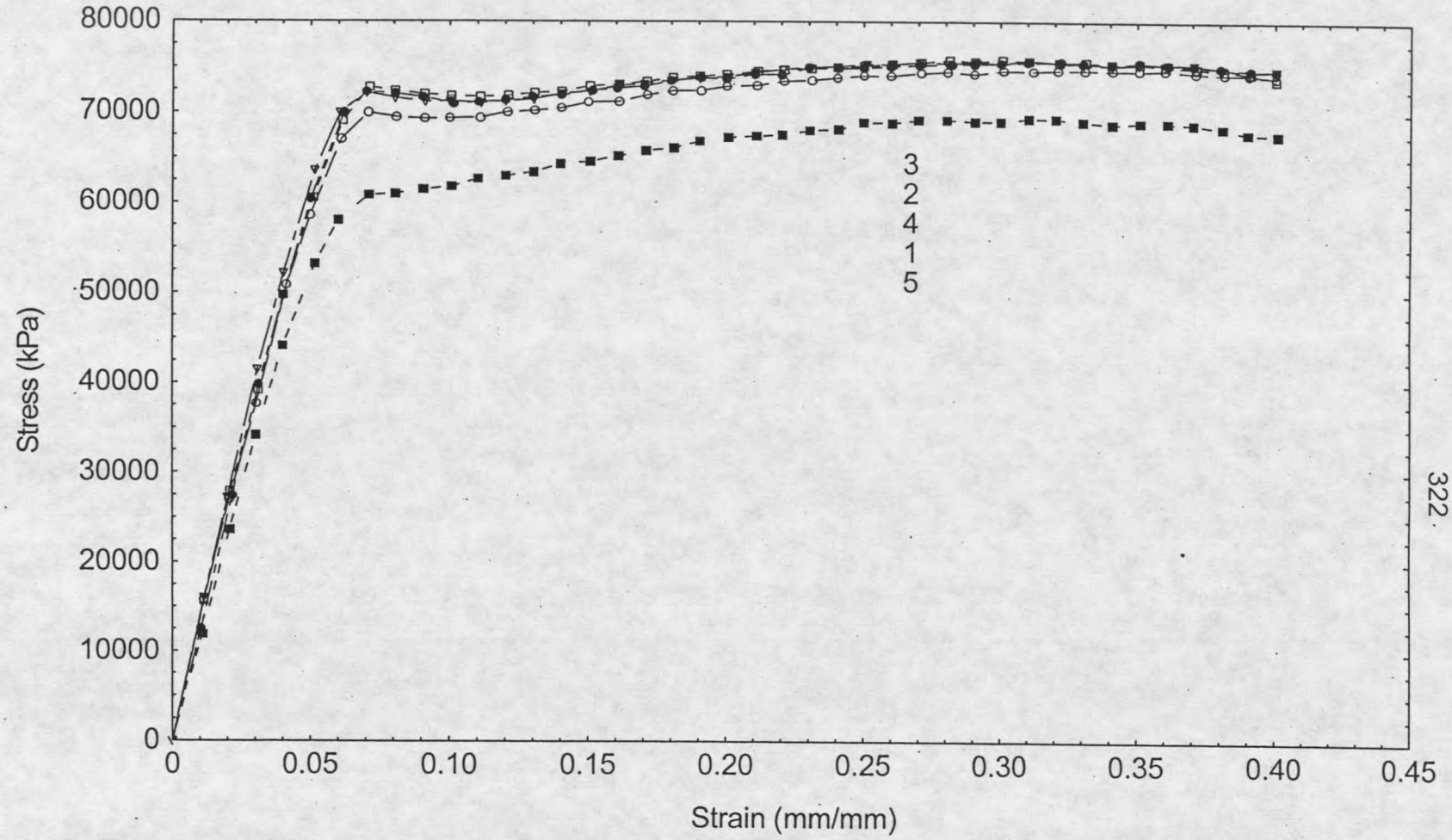


Figure D.II.12 Tensile Testing of Nylon 6/6 Specimens After Cyclic and Constant Loading μ=4 at 35 °C
1- $(0.16\pm0.04)\sigma_y$, 10 Hz; 2- $(0.20\pm0.05)\sigma_y$, 10 Hz;
3- $(0.16)\sigma_y$, 4- $(0.20)\sigma_y$, Constant Load Creep; 5- Virgin Specimens;
σ_y = 70 MPa at 23 °C

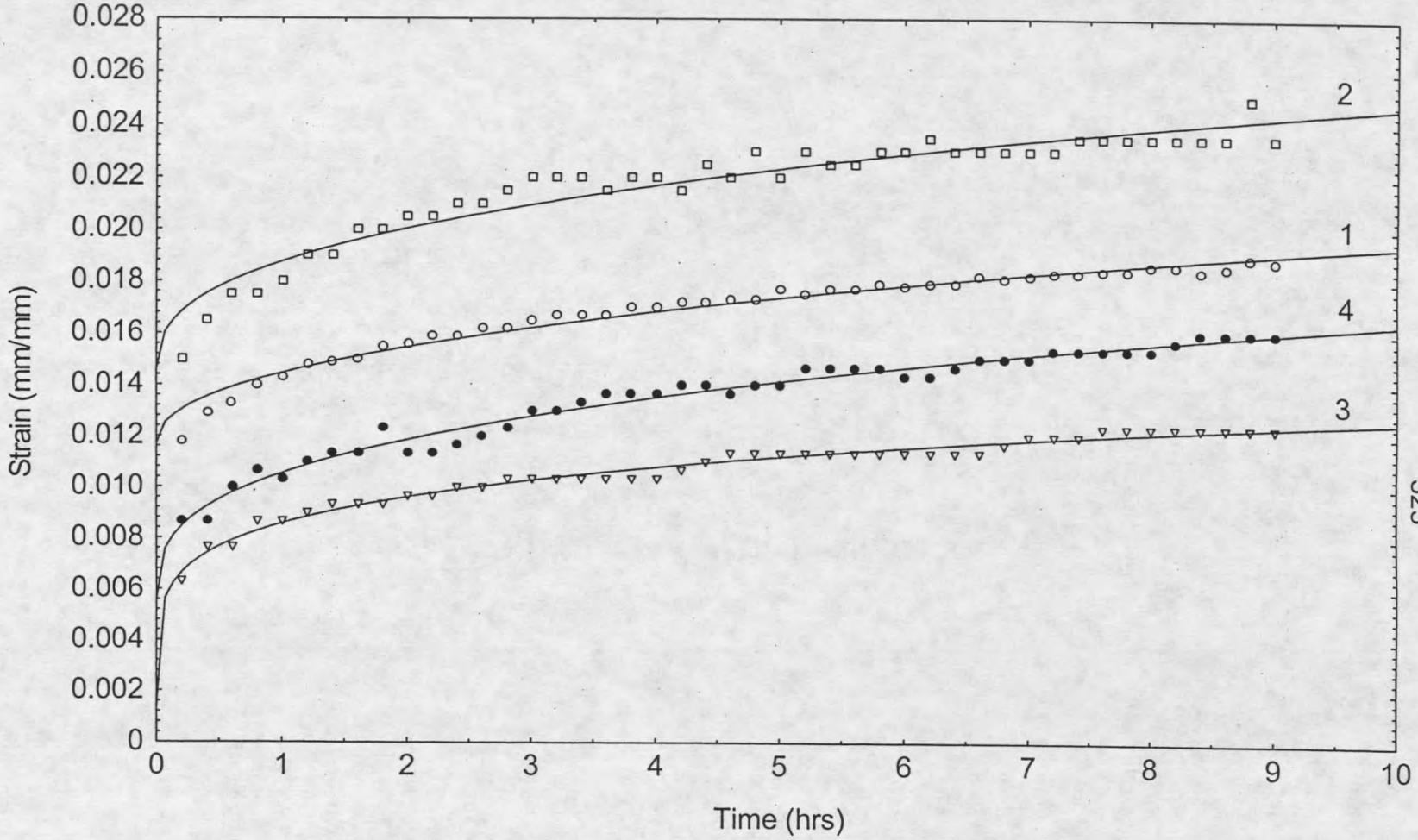


Figure D.III.1 Vibrocreep Response of Nylon 6/6 with μ=4 at 41 °C
1- $(0.16\pm0.04)\sigma_y$, 1 Hz; 2- $(0.20\pm0.05)\sigma_y$, 1 Hz;
3- $(0.16)\sigma_y$, 4- $(0.20)\sigma_y$, Constant Load Creep;
σ_y = 70 MPa at 23 °C

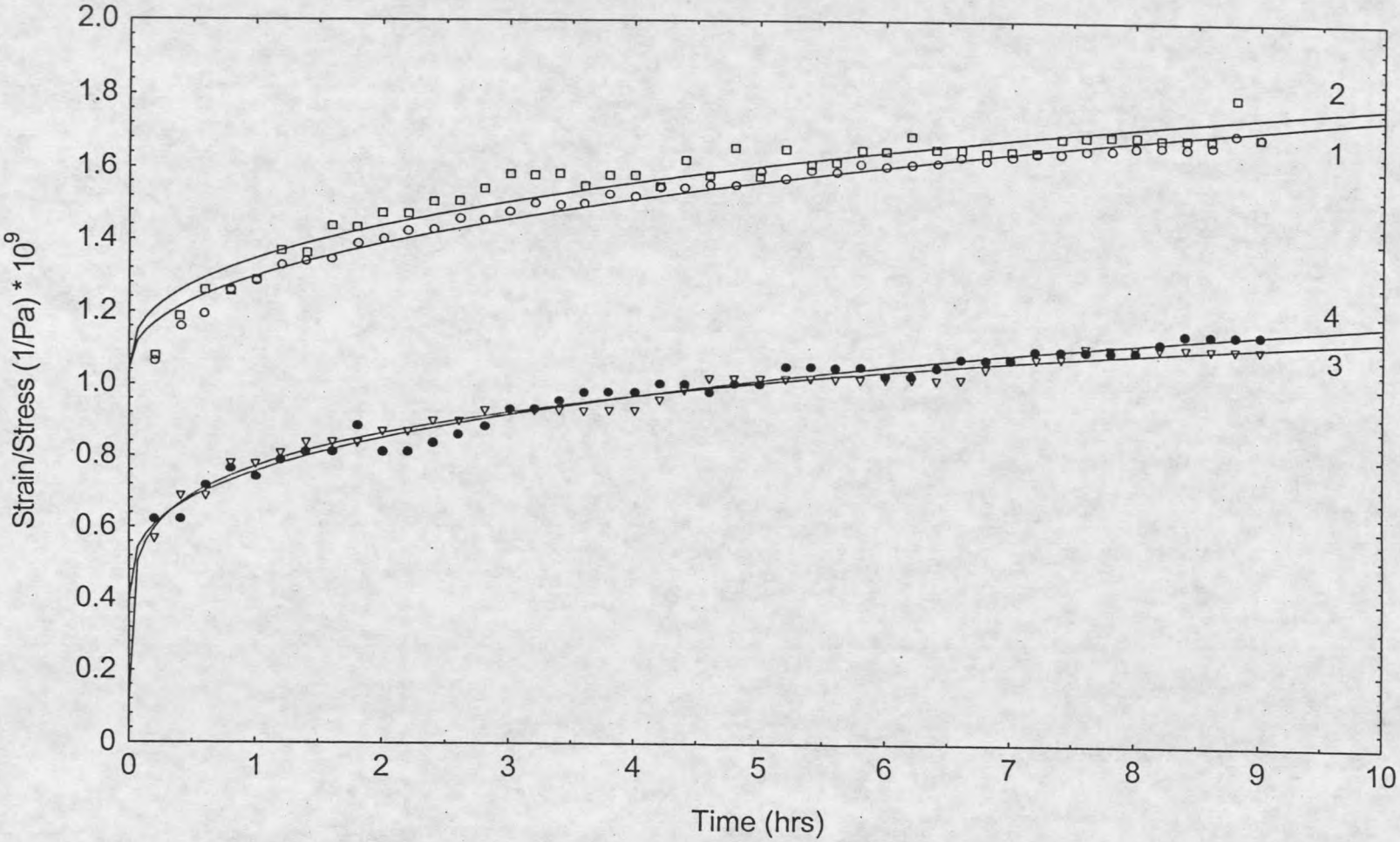


Figure D.III.2 Normalized Vibrocreep Response of Nylon 6/6 with μ=4 at 41 °C
1- $(0.16\pm0.04)\sigma_y$, 1 Hz; 2- $(0.20\pm0.05)\sigma_y$, 1 Hz;
3- $(0.16)\sigma_y$, 4- $(0.20)\sigma_y$, Constant Load Creep;
σ_y = 70 MPa at 23 °C

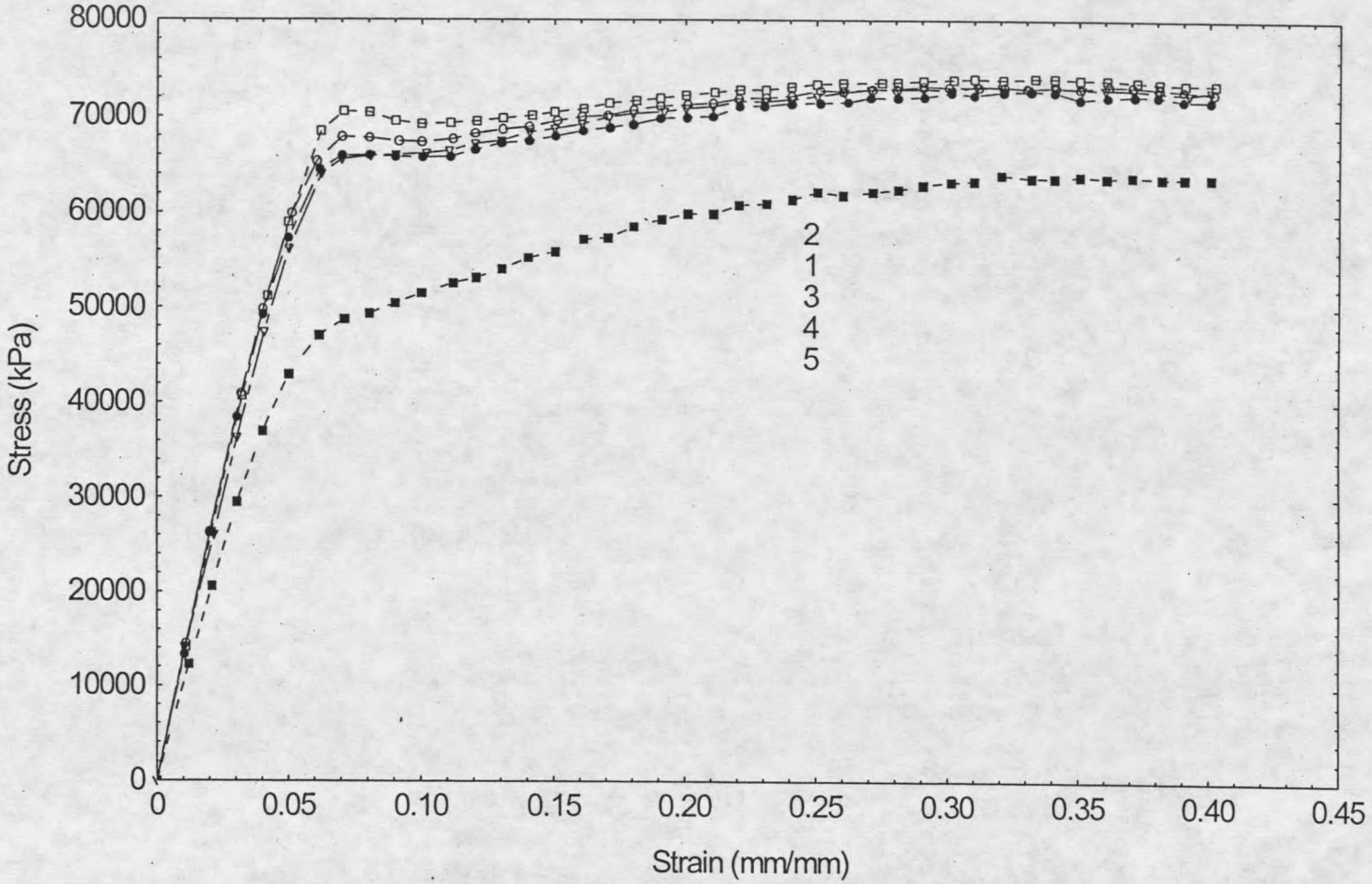


Figure D.III.3 Tensile Testing of Nylon 6/6 Specimens After Cyclic and Constant at 41 °C
1- $(0.16\pm0.04)\sigma_y$, 1 Hz; 2- $(0.20\pm0.05)\sigma_y$, 1 Hz;
3- $(0.16)\sigma_y$, 4- $(0.20)\sigma_y$, Constant Load Creep; 5- Virgin Specimens;
σ_y = 70 MPa at 23 °C

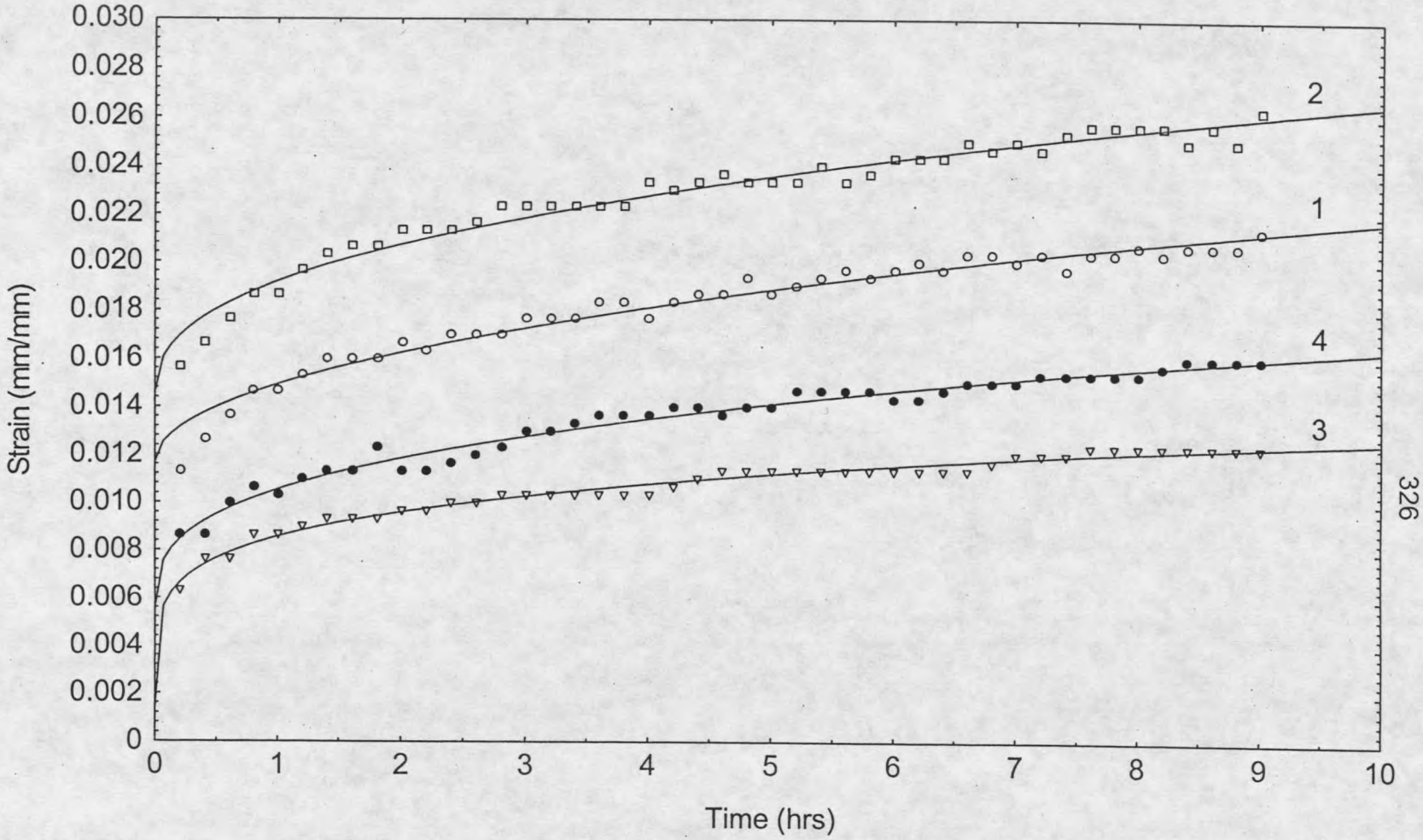


Figure D.III.4 Vibrocreep Response of Nylon 6/6 with μ=4 at 41 °C
1- $(0.16\pm0.04)\sigma_y$, 10 Hz; 2- $(0.20\pm0.05)\sigma_y$, 10 Hz;
3- $(0.16)\sigma_y$, 4- $(0.20)\sigma_y$, Constant Load Creep;
σ_y = 70 MPa at 23 °C

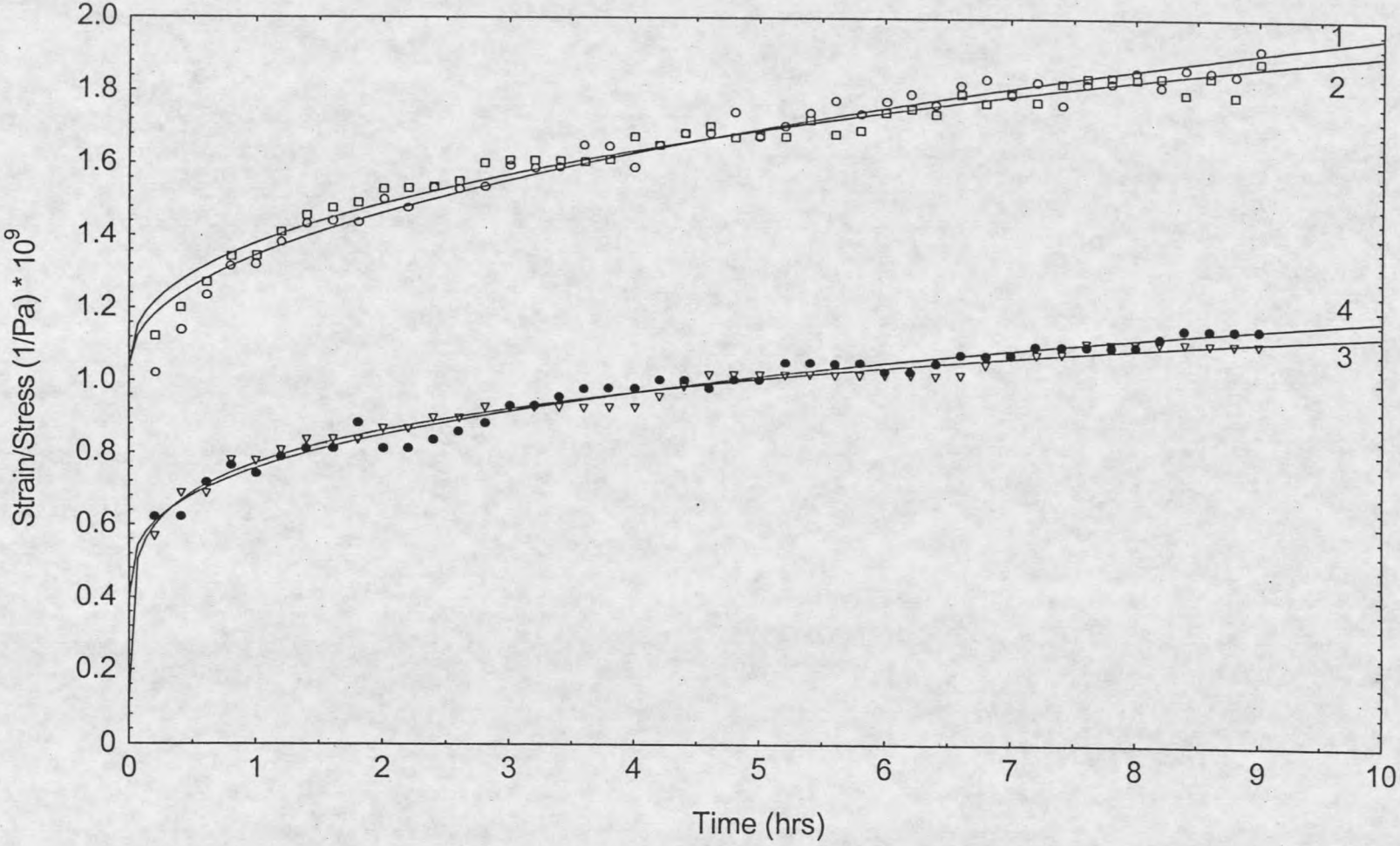


Figure D.III.5 Normalized Vibrocreep Response of Nylon 6/6 with μ=4 at 41 °C
1- $(0.16\pm0.04)\sigma_y$, 10 Hz; 2- $(0.20\pm0.05)\sigma_y$, 10 Hz;
3- $(0.16)\sigma_y$, 4- $(0.20)\sigma_y$, Constant Load Creep;
σ_y = 70 MPa at 23 °C

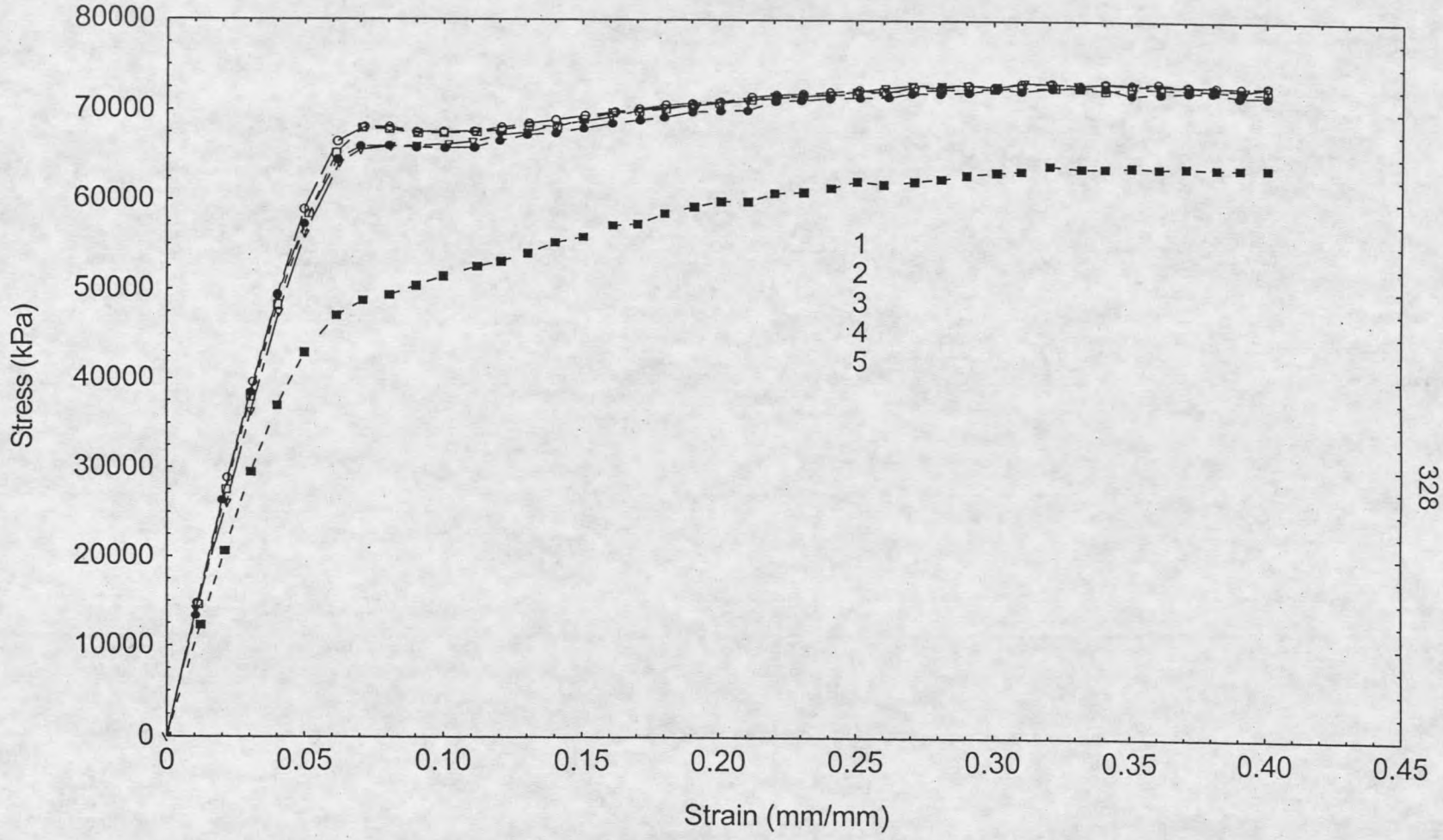


Figure D.III.6 Tensile Testing of Nylon 6/6 Specimens After Cyclic and Constant Loading at 41 °C
1- $(0.16\pm0.04)\sigma_y$, 10 Hz; 2- $(0.20\pm0.05)\sigma_y$, 10 Hz;
3- $(0.16)\sigma_y$, 4- $(0.20)\sigma_y$, Constant Load Creep; 5- Virgin Specimens;
σ_y = 70 MPa at 23 °C

APPENDIX E

Mean Stress Effects from Vibrocreep Testing of Nylon 6/6

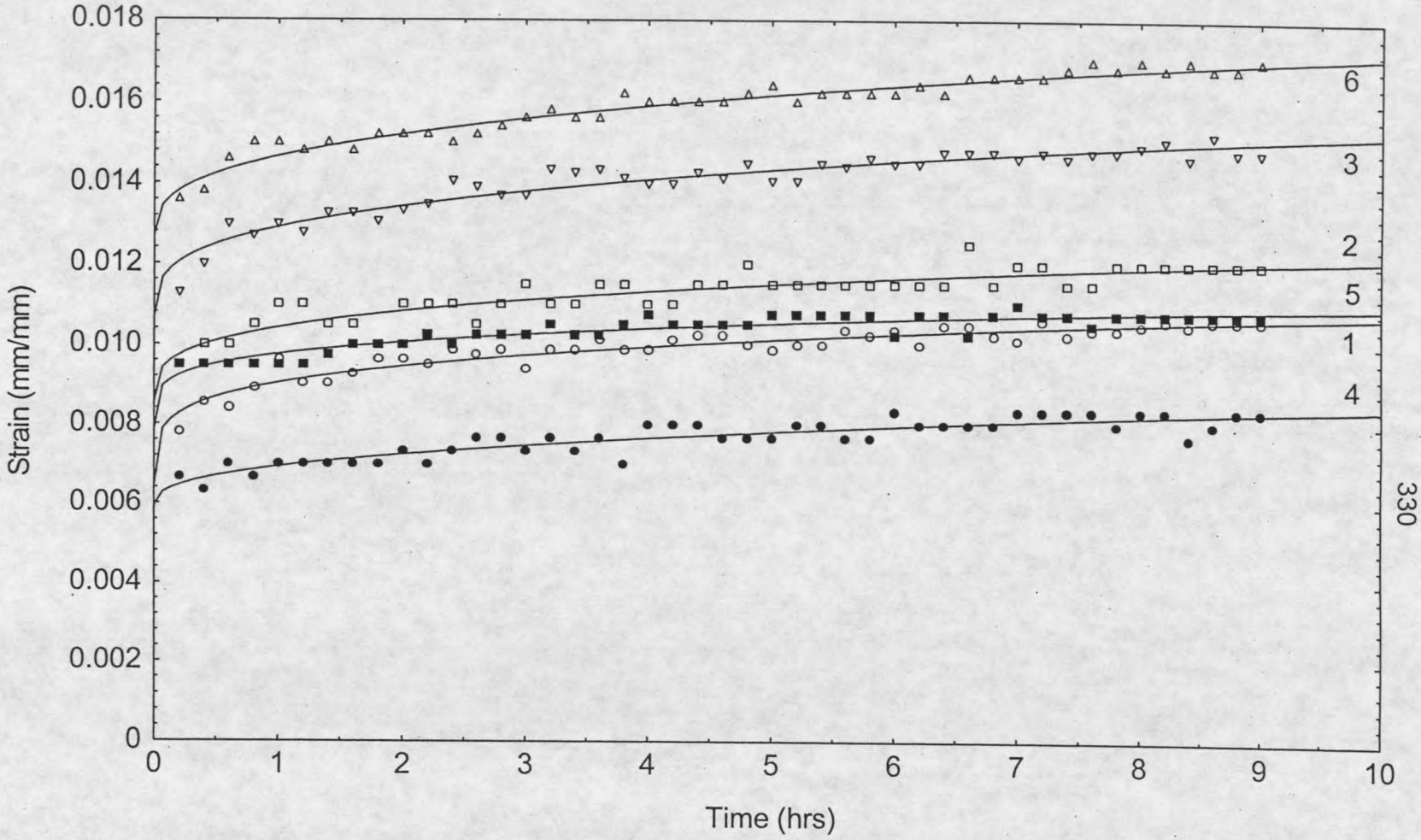


Figure E.I.1 Vibrocreep Response of Nylon 6/6 at Different Mean Stresses at 23 °C
1- $(0.12\pm0.075)\sigma_y$, 1 Hz; 2- $(0.16\pm0.075)\sigma_y$, 1 Hz; 3- $(0.20\pm0.075)\sigma_y$, 1 Hz;
4- $(0.16)\sigma_y$, 5- $(0.20)\sigma_y$, 6- $(0.30)\sigma_y$ Constant Load Creep;
σ_y = 70 MPa at 23 °C

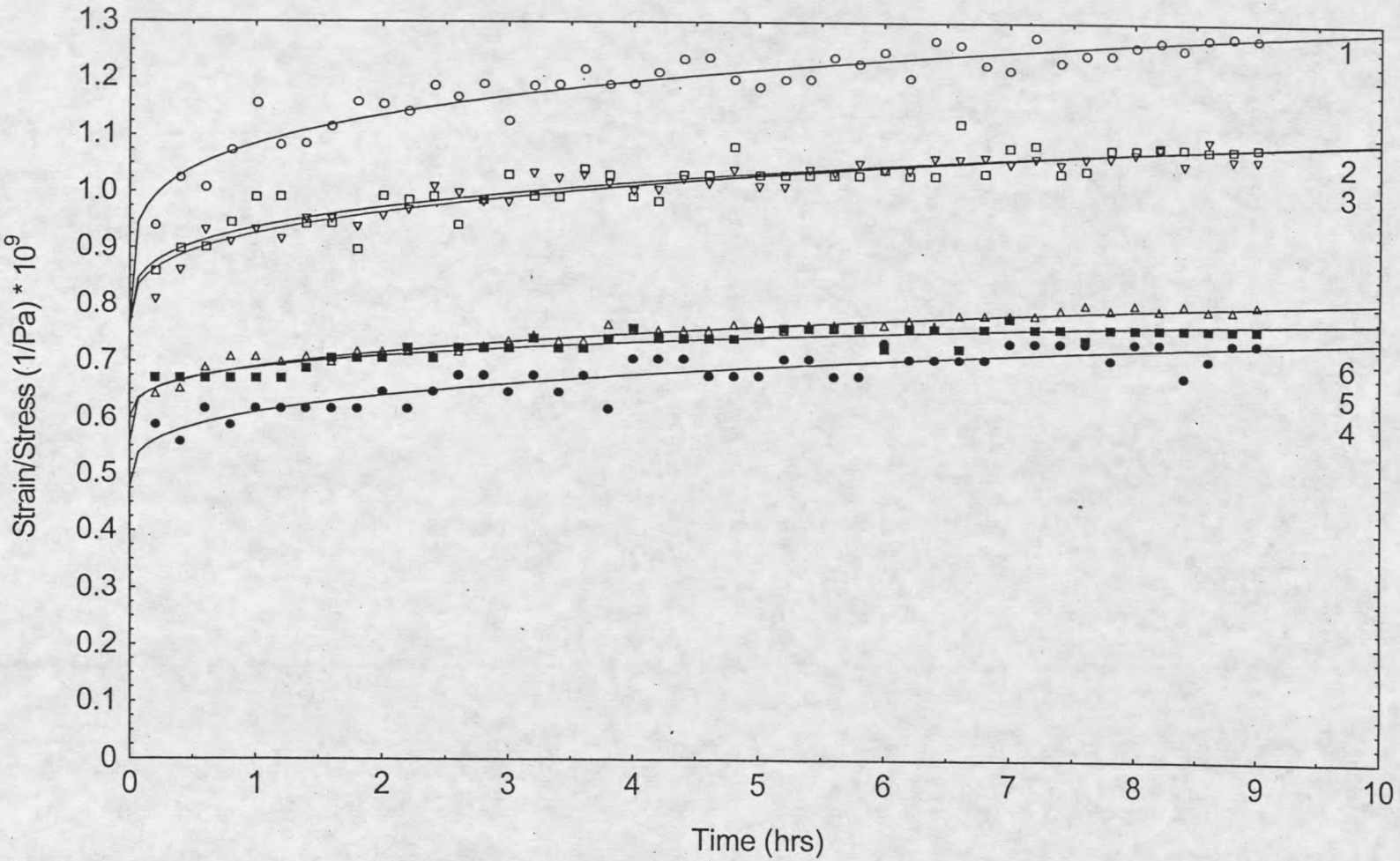


Figure E.I.2 Normalized Vibrocreep Response of Nylon 6/6 at Different Mean Stresses at 23 °C
1- $(0.12\pm0.075)\sigma_y$, 1 Hz; 2- $(0.16\pm0.075)\sigma_y$, 1 Hz; 3- $(0.20\pm0.075)\sigma_y$, 1 Hz;
4- $(0.16)\sigma_y$, 5- $(0.20)\sigma_y$, 6- $(0.30)\sigma_y$ Constant Load Creep;
σ_y = 70 MPa at 23 °C

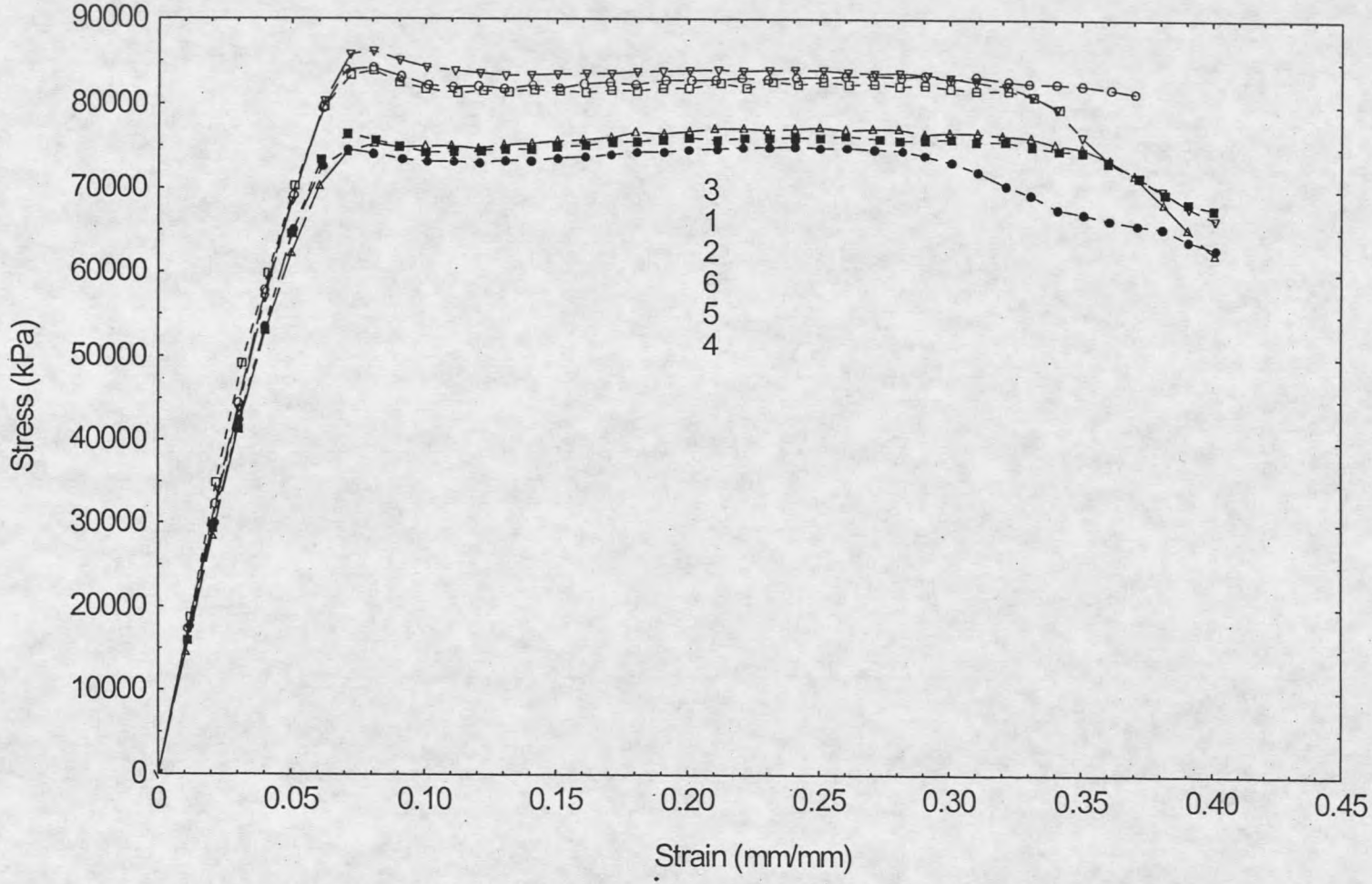


Figure E.I.3 Tensile Testing of Nylon 6/6 Specimens After Cyclic and Constant Loading at 23 °C
1- $(0.12\pm0.075)\sigma_y$, 1 Hz; 2- $(0.16\pm0.075)\sigma_y$, 1 Hz; 3- $(0.20\pm0.075)\sigma_y$, 1 Hz;
4- $(0.16)\sigma_y$, 5- $(0.20)\sigma_y$, Constant Load Creep; 6- Virgin Specimens;
σ_y = 70 MPa at 23 °C

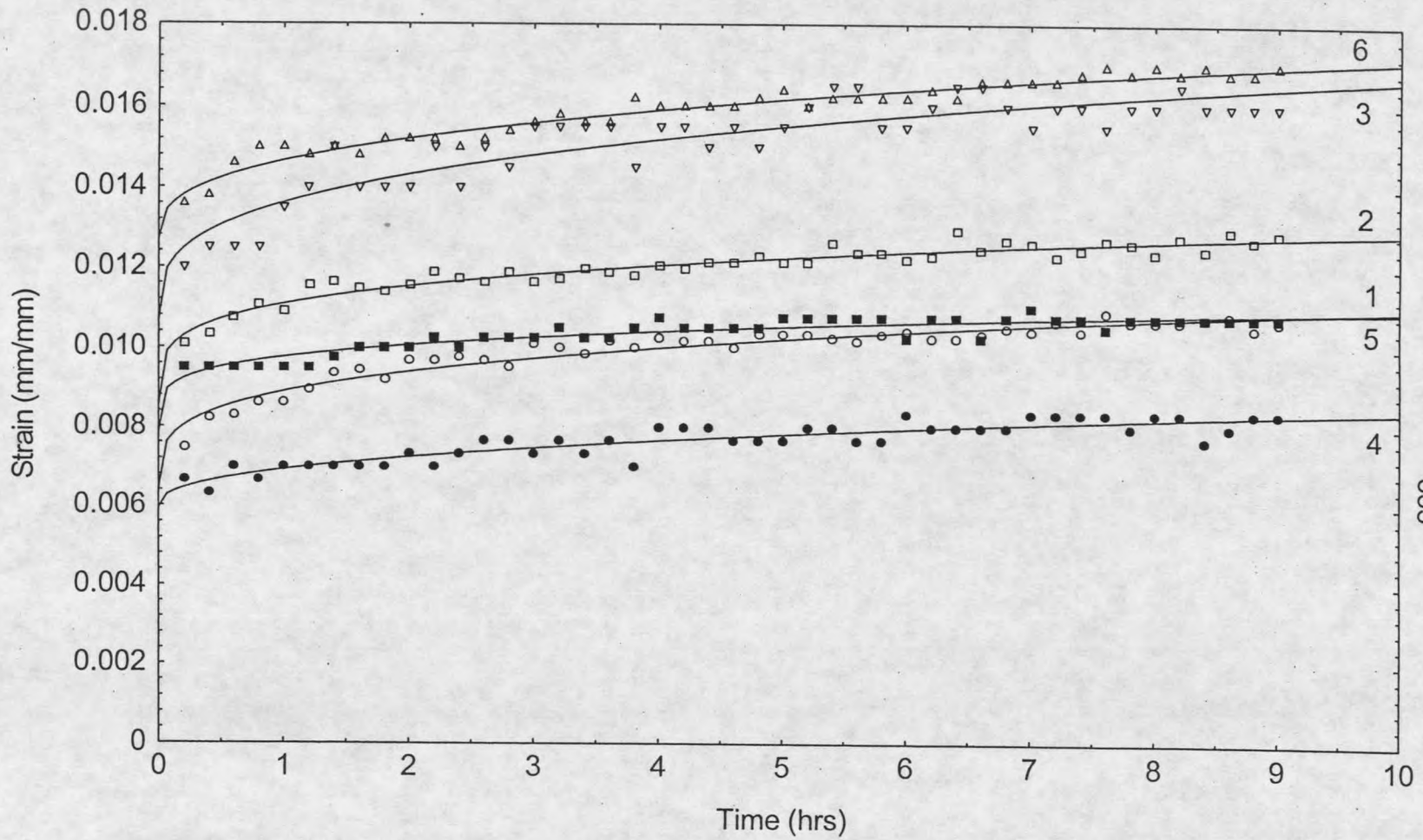


Figure E.I.4 Vibrocreep Response of Nylon 6/6 at Different Mean Stresses at 23 °C
1- $(0.12\pm0.075)\sigma_y$, 10 Hz; 2- $(0.16\pm0.075)\sigma_y$, 10 Hz; 3- $(0.20\pm0.075)\sigma_y$, 10 Hz;
4- $(0.16)\sigma_y$, 5- $(0.20)\sigma_y$, 6- $(0.30)\sigma_y$ Constant Load Creep;
σ_y = 70 MPa at 23 °C

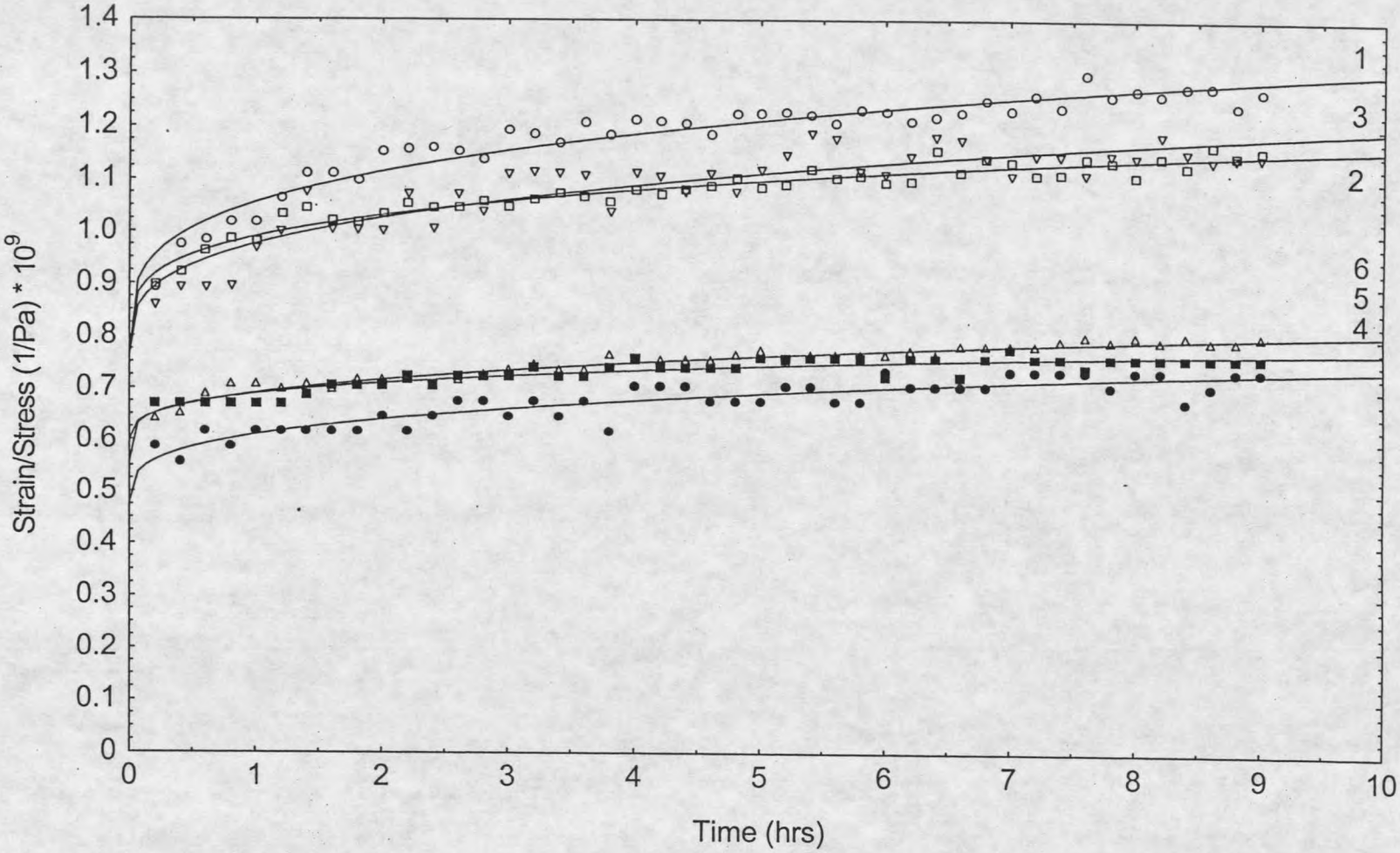


Figure E.I.5 Normalized Vibrocreep Response of Nylon 6/6 at Different Mean Stresses at 23 °C
1- $(0.12\pm0.075)\sigma_y$, 10 Hz; 2- $(0.16\pm0.075)\sigma_y$, 10 Hz; 3- $(0.20\pm0.075)\sigma_y$, 10 Hz;
4- $(0.16)\sigma_y$, 5- $(0.20)\sigma_y$, 6- $(0.30)\sigma_y$ Constant Load Creep;
σ_y = 70 MPa at 23 °C

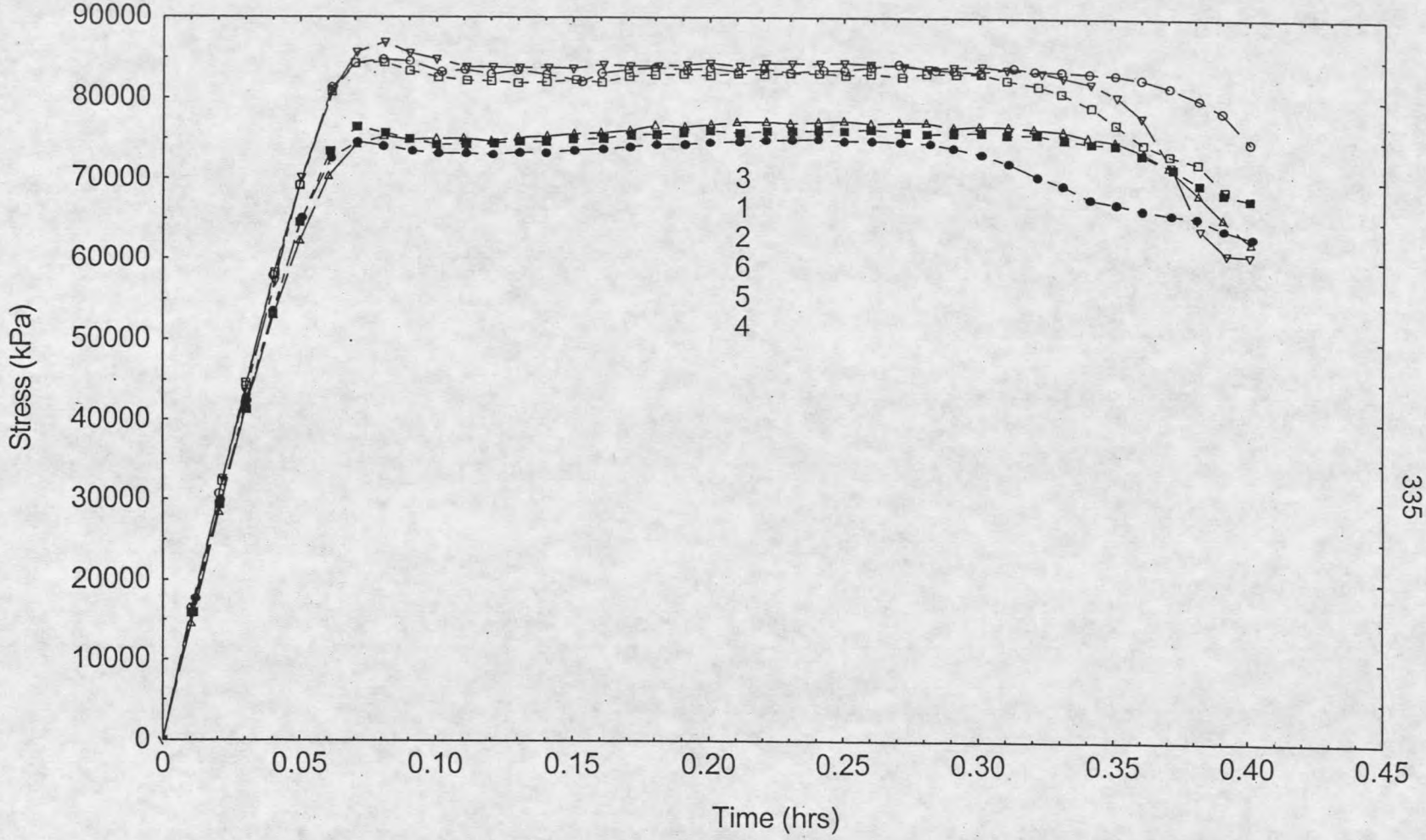


Figure E.I.6 Tensile Testing of Nylon 6/6 Specimens After Cyclic and Constant Loading at 23 °C
1- $(0.12\pm0.075)\sigma_y$, 10 Hz; 2- $(0.16\pm0.075)\sigma_y$, 10 Hz; 3- $(0.20\pm0.075)\sigma_y$, 10 Hz;
4- $(0.16)\sigma_y$, 5- $(0.20)\sigma_y$, Constant Load Creep; 6- Virgin Specimens;
σ_y = 70 MPa at 23 °C

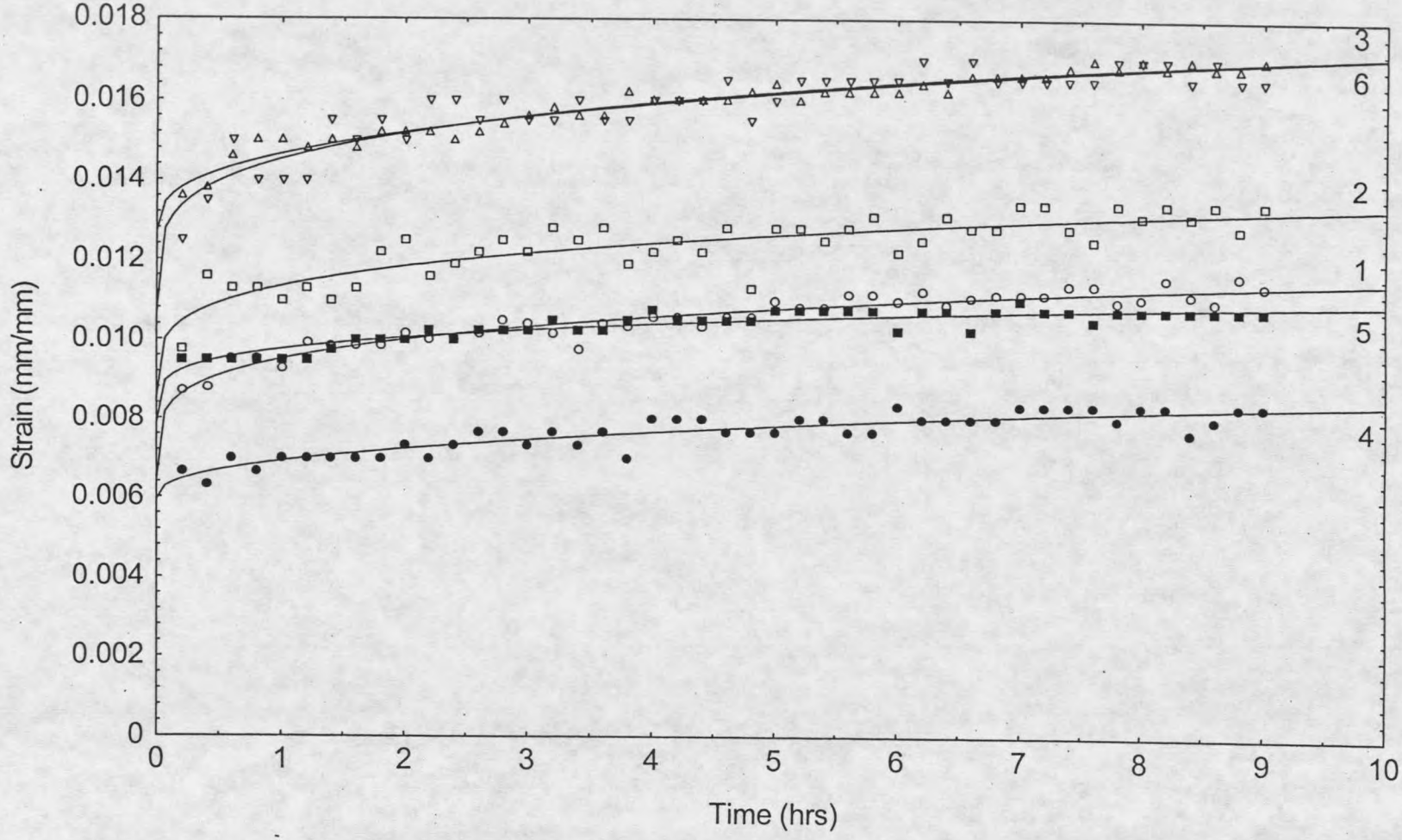


Figure E.I.7 Vibrocreep Response of Nylon 6/6 at Different Mean Stresses at 23 °C
1- $(0.12\pm0.075)\sigma_y$, 20 Hz; 2- $(0.16\pm0.075)\sigma_y$, 20 Hz; 3- $(0.20\pm0.075)\sigma_y$, 20 Hz;
4- $(0.16)\sigma_y$, 5- $(0.20)\sigma_y$, 6- $(0.30)\sigma_y$ Constant Load Creep;
σ_y = 70 MPa at 23 °C

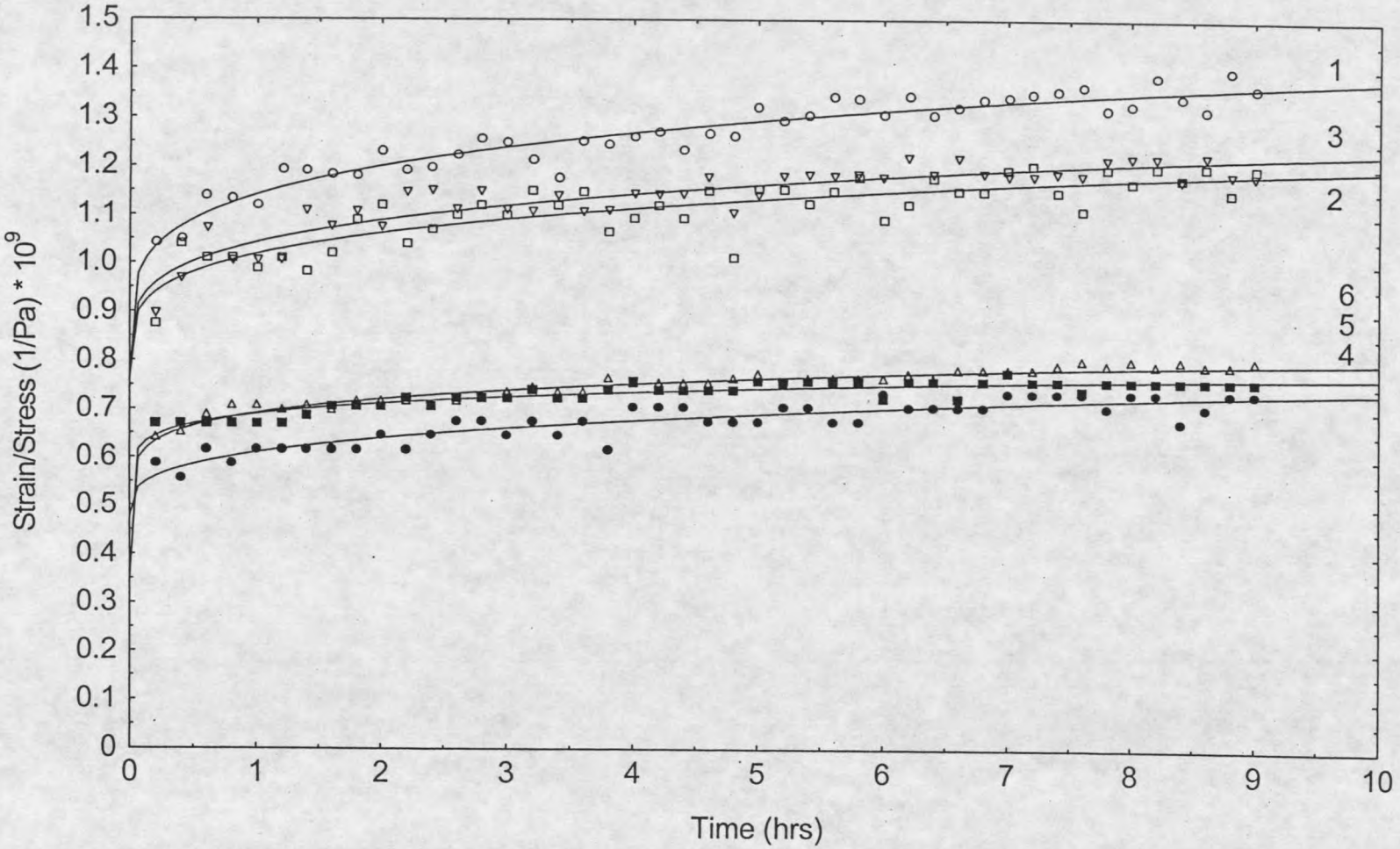


Figure E.I.8 Normalized Vibrocreep Response of Nylon 6/6 at Different Mean Stresses at 23 °C
1- $(0.12\pm0.075)\sigma_y$, 20 Hz; 2- $(0.16\pm0.075)\sigma_y$, 20 Hz; 3- $(0.20\pm0.075)\sigma_y$, 20 Hz;
4- $(0.16)\sigma_y$, 5- $(0.20)\sigma_y$, 6- $(0.30)\sigma_y$ Constant Load Creep;
σ_y = 70 MPa at 23 °C

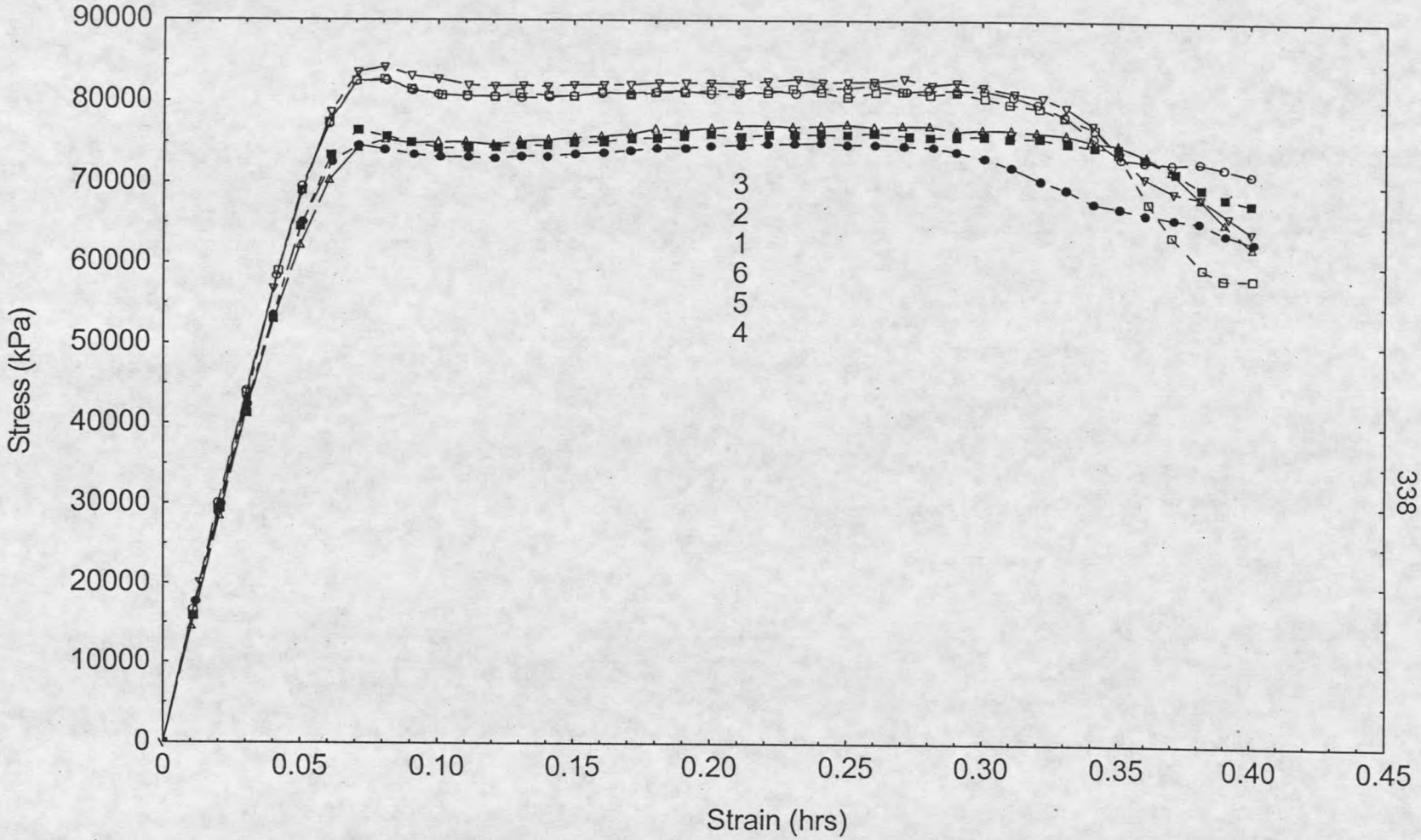


Figure E.I.9 Tensile Testing of Nylon 6/6 Specimens After Cyclic and Constant Loading at 23 °C
1- $(0.12\pm0.075)\sigma_y$, 20 Hz; 2- $(0.16\pm0.075)\sigma_y$, 20 Hz; 3- $(0.20\pm0.075)\sigma_y$, 20 Hz;
4- $(0.16)\sigma_y$, 5- $(0.20)\sigma_y$, Constant Load Creep; 6- Virgin Specimens;
σ_y = 70 MPa at 23 °C

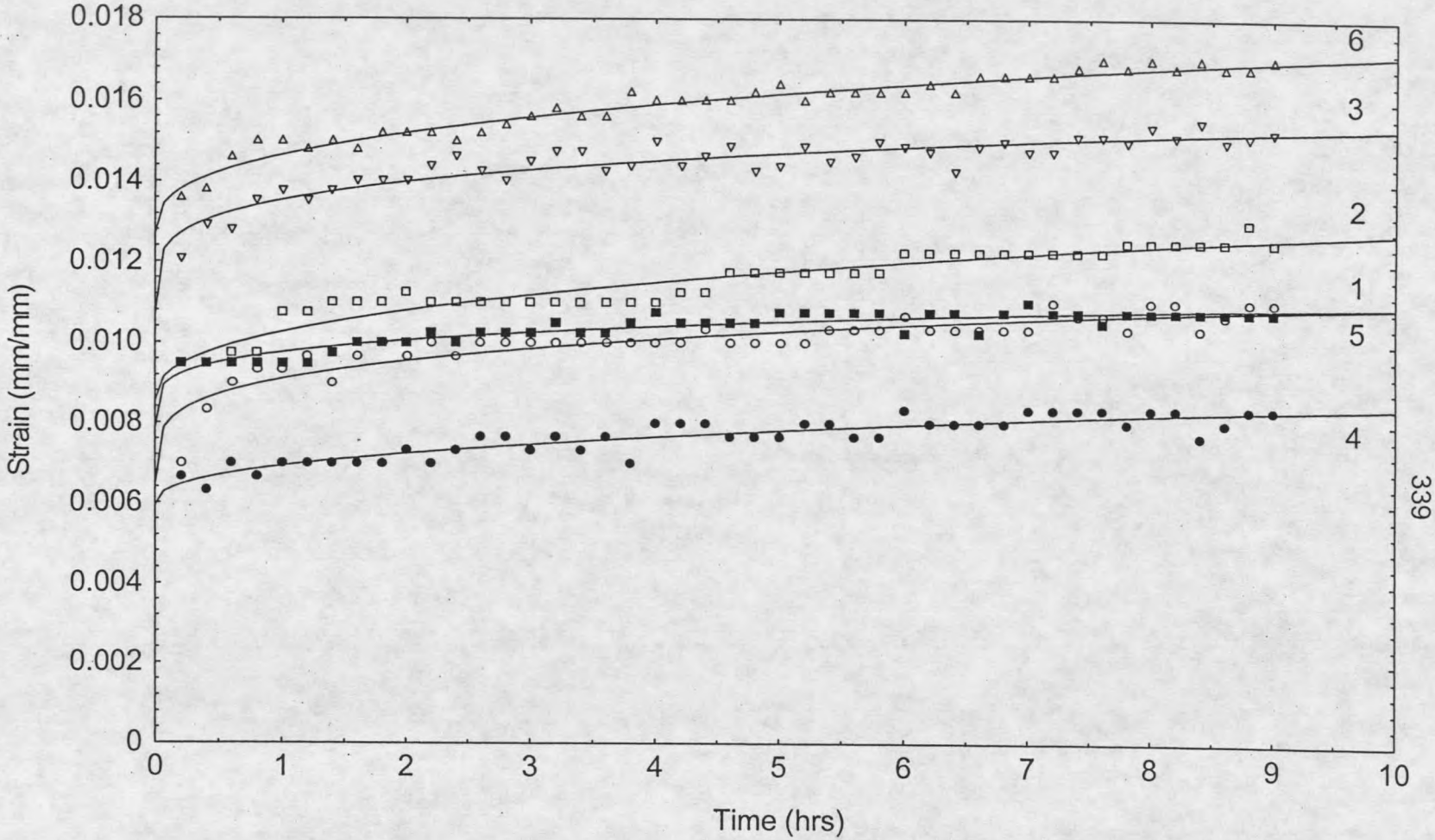


Figure E.I.10 Vibrocreep Response of Nylon 6/6 at Different Mean Stresses at 23 °C
1- $(0.12\pm0.10)\sigma_y$, 1 Hz; 2- $(0.16\pm0.10)\sigma_y$, 1 Hz; 3- $(0.20\pm0.10)\sigma_y$, 1 Hz;
4- $(0.16)\sigma_y$, 5- $(0.20)\sigma_y$, 6- $(0.30)\sigma_y$ Constant Load Creep;
σ_y = 70 MPa at 23 °C

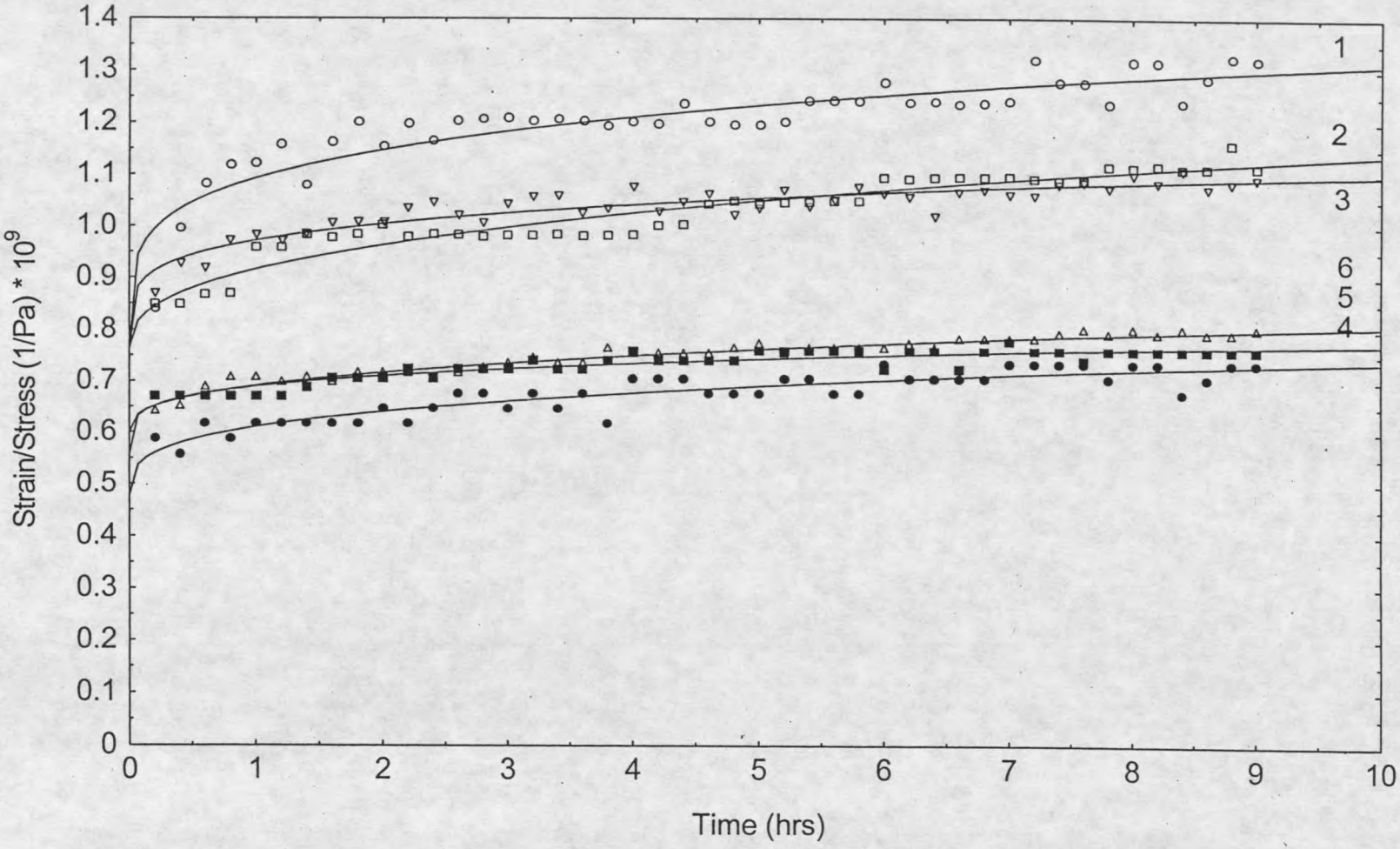


Figure E.I.11 Normalized Vibrocreep Response of Nylon 6/6 at Different Mean Stresses at 23 °C
1- $(0.12\pm0.10)\sigma_y$, 1 Hz; 2- $(0.16\pm0.10)\sigma_y$, 1 Hz; 3- $(0.20\pm0.10)\sigma_y$, 1 Hz;
4- $(0.16)\sigma_y$, 5- $(0.20)\sigma_y$, 6- $(0.30)\sigma_y$ Constant Load Creep;
σ_y = 70 MPa at 23 °C

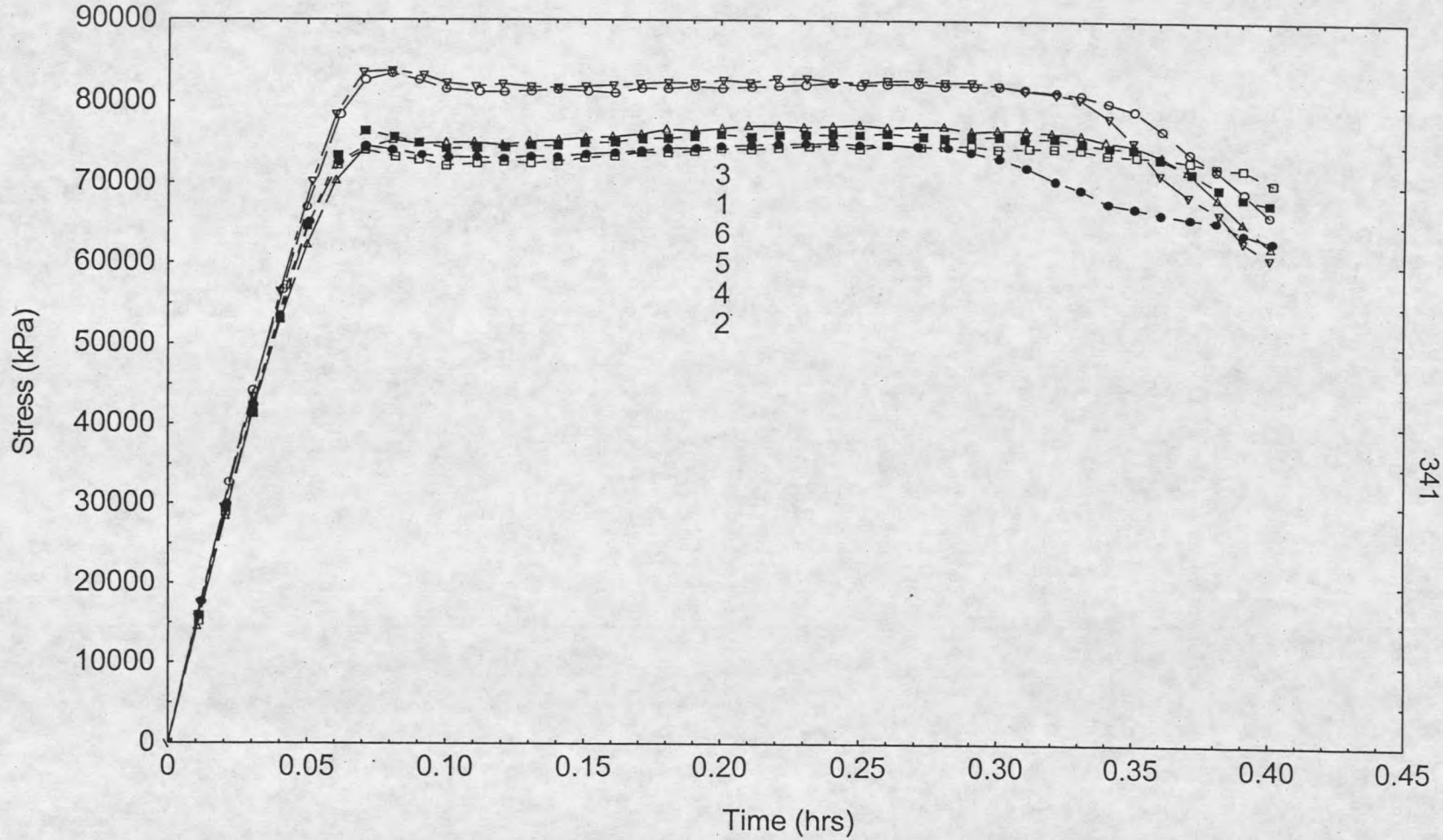


Figure E.I.12 Tensile Testing of Nylon 6/6 Specimens After Cyclic and Constant Loading at 23 °C
1- $(0.12\pm0.10)\sigma_y$, 1 Hz; 2- $(0.16\pm0.10)\sigma_y$, 1 Hz; 3- $(0.20\pm0.10)\sigma_y$, 1 Hz;
4- $(0.16)\sigma_y$, 5- $(0.20)\sigma_y$, Constant Load Creep; 6- Virgin Specimens;
σ_y = 70 MPa at 23 °C

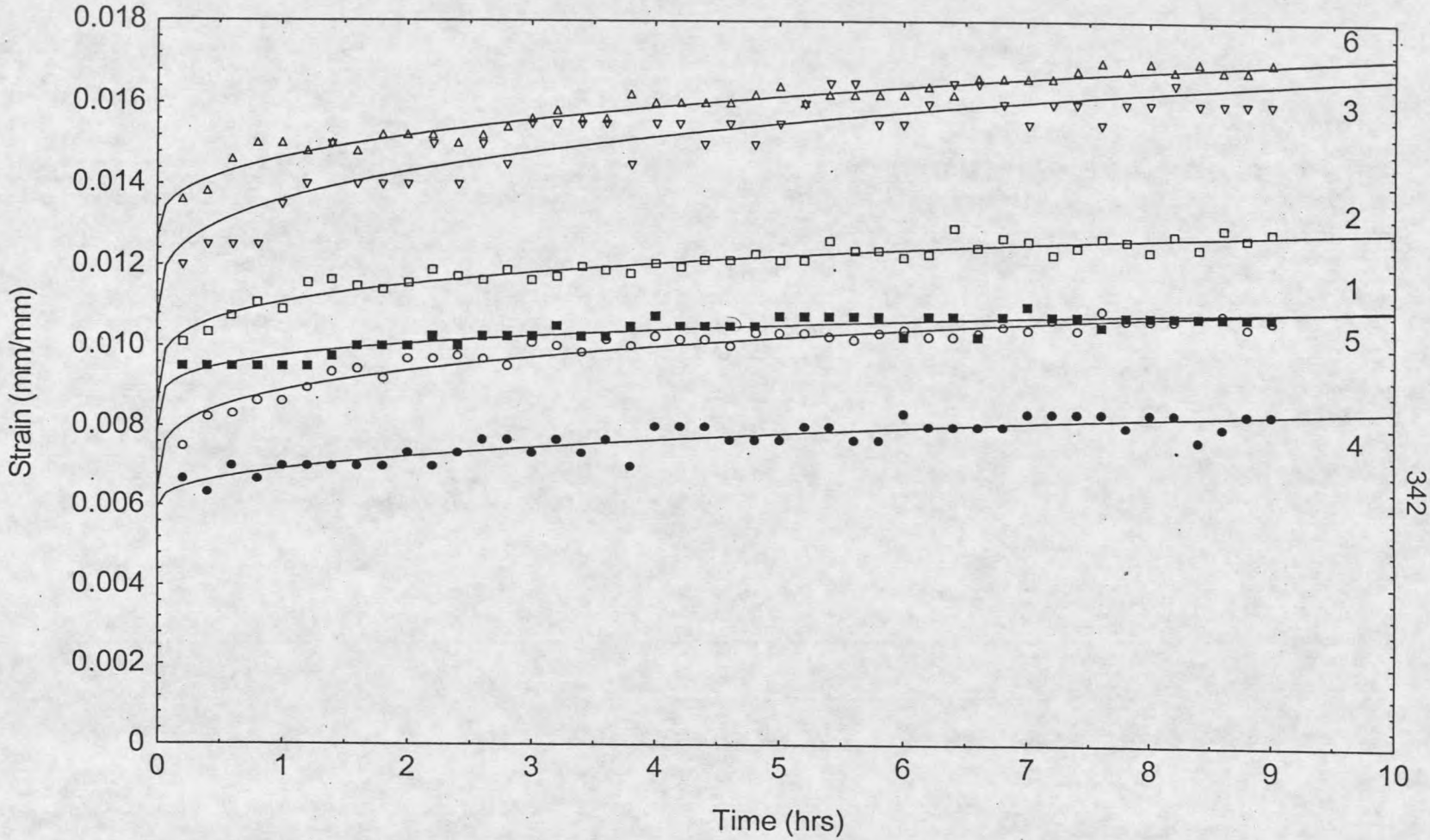


Figure E.I.13 Vibrocreep Response of Nylon 6/6 at Different Mean Stresses at 23 °C
1- $(0.12\pm0.10)\sigma_y$, 10 Hz; 2- $(0.16\pm0.10)\sigma_y$, 10 Hz; 3- $(0.20\pm0.10)\sigma_y$, 10 Hz;
4- $(0.16)\sigma_y$, 5- $(0.20)\sigma_y$, 6- $(0.30)\sigma_y$ Constant Load Creep;
σ_y = 70 MPa at 23 °C

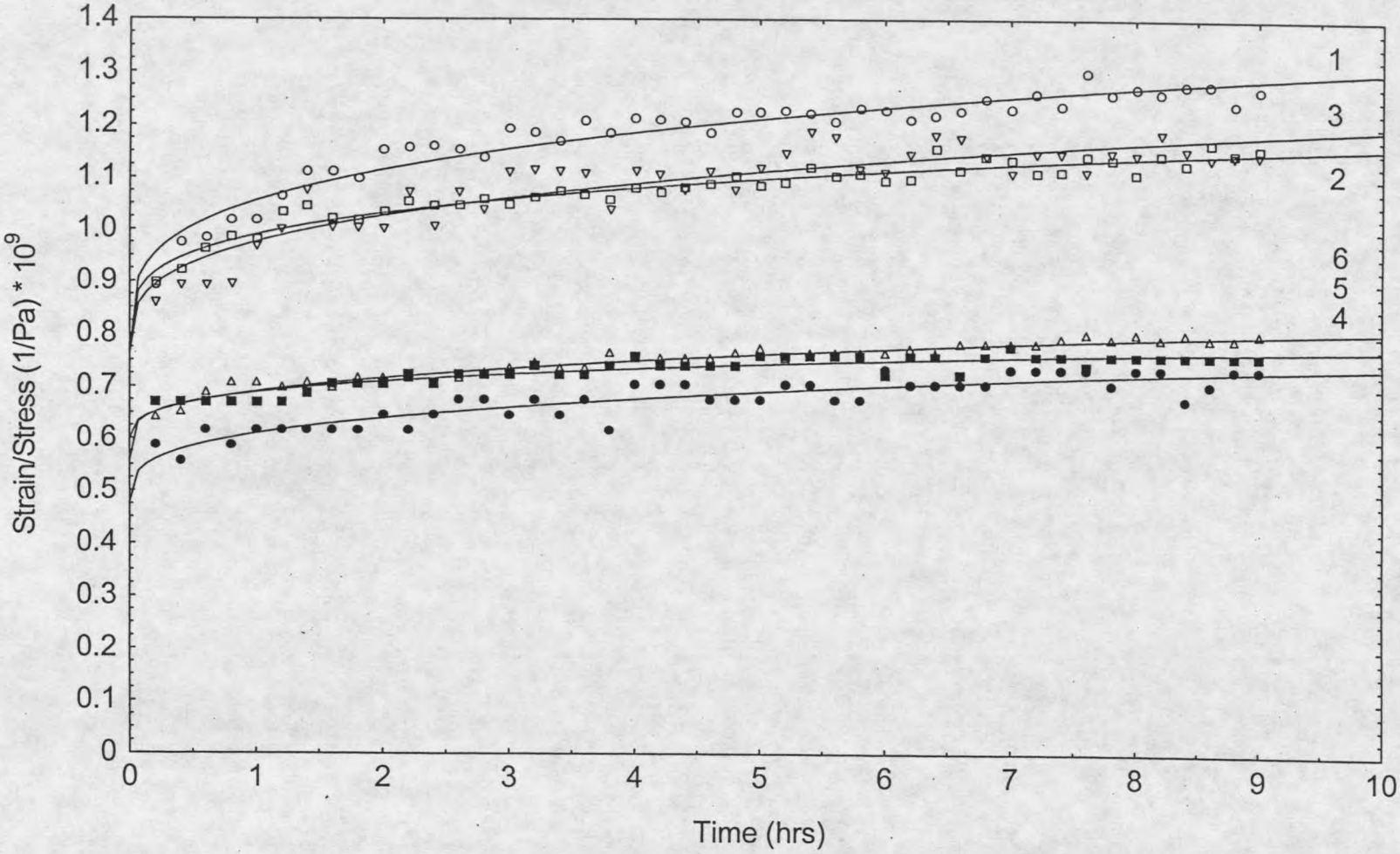


Figure E.I.14 Normalized Vibrocreep Response of Nylon 6/6 at Different Mean Stresses at 23 °C
1- $(0.12\pm0.10)\sigma_y$, 10 Hz; 2- $(0.16\pm0.10)\sigma_y$, 10 Hz; 3- $(0.20\pm0.10)\sigma_y$, 10 Hz;
4- $(0.16)\sigma_y$, 5- $(0.20)\sigma_y$, 6- $(0.30)\sigma_y$ Constant Load Creep;
σ_y = 70 MPa at 23 °C

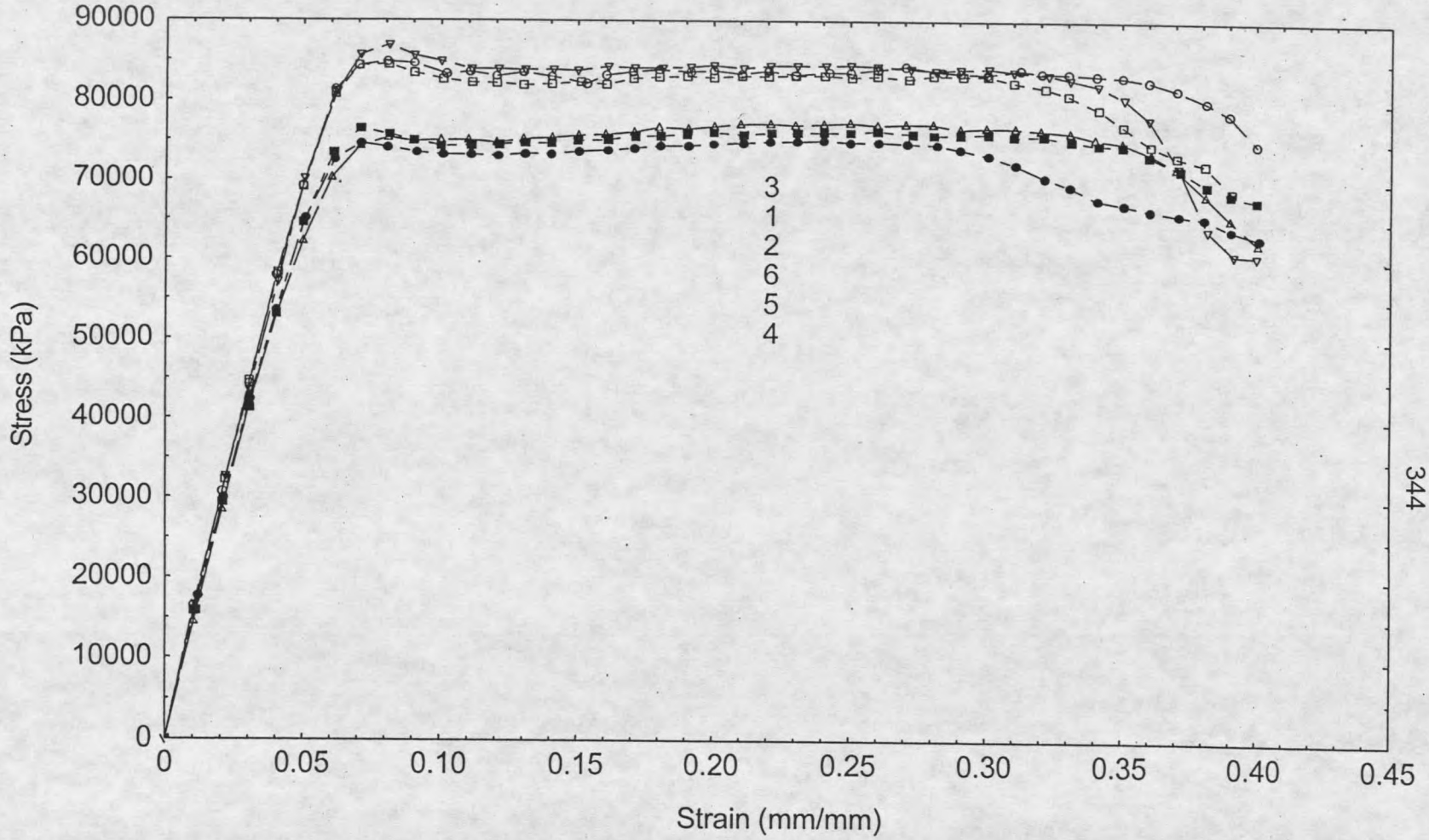


Figure E.I.15 Tensile Testing of Nylon 6/6 Specimens After Cyclic and Constant Loading at 23 °C
1- $(0.12\pm0.10)\sigma_y$, 10 Hz; 2- $(0.16\pm0.10)\sigma_y$, 10 Hz; 3- $(0.20\pm0.10)\sigma_y$, 10 Hz;
4- $(0.16)\sigma_y$, 5- $(0.20)\sigma_y$, Constant Load Creep; 6- Virgin Specimens;
σ_y = 70 MPa at 23 °C

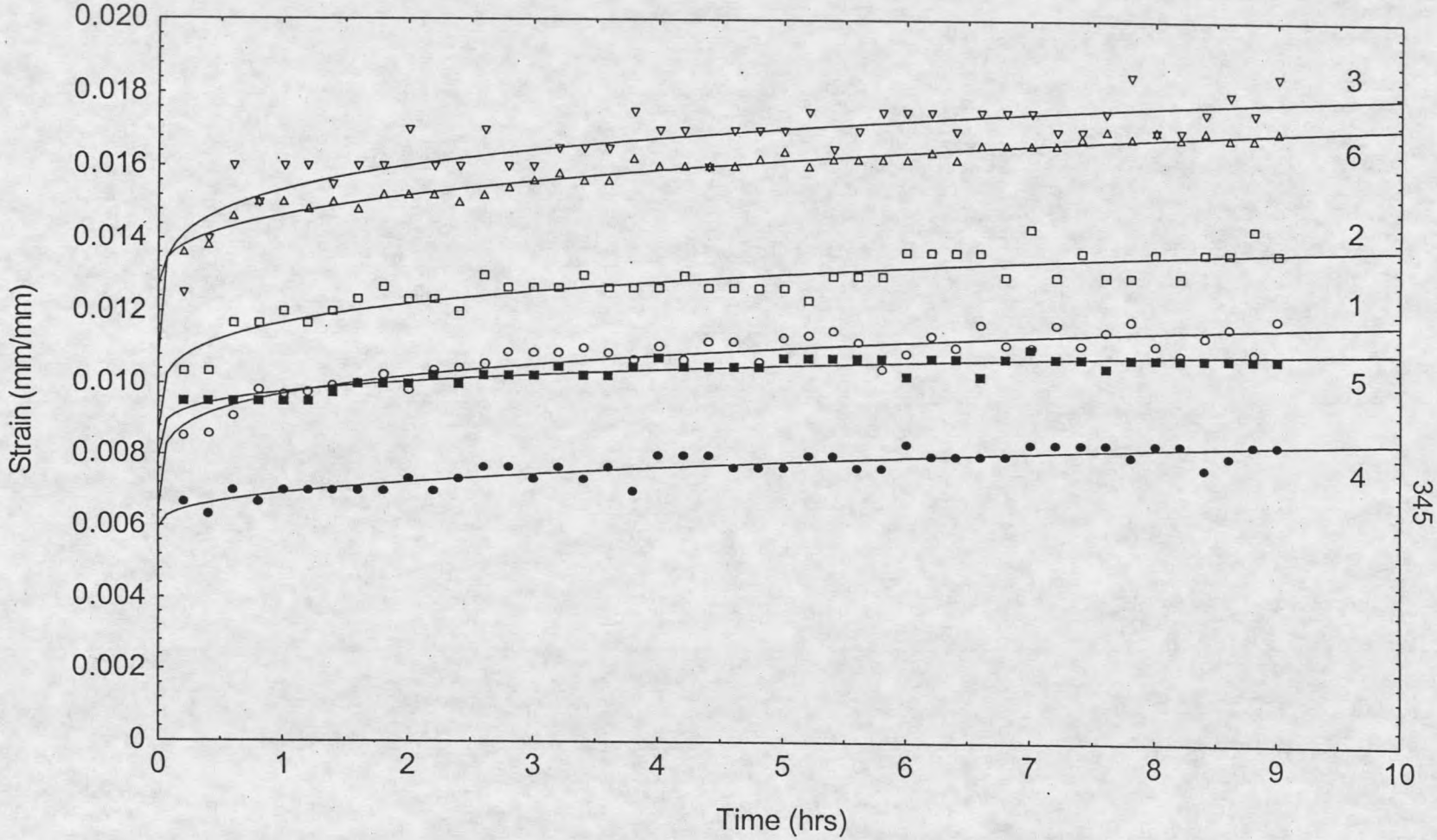


Figure E.I.16 Vibrocreep Response of Nylon 6/6 at Different Mean Stresses at 23 °C
1- $(0.12\pm0.10)\sigma_y$, 20 Hz; 2- $(0.16\pm0.10)\sigma_y$, 20 Hz; 3- $(0.20\pm0.10)\sigma_y$, 20 Hz;
4- $(0.16)\sigma_y$, 5- $(0.20)\sigma_y$, 6- $(0.30)\sigma_y$ Constant Load Creep;
σ_y = 70 MPa at 23 °C

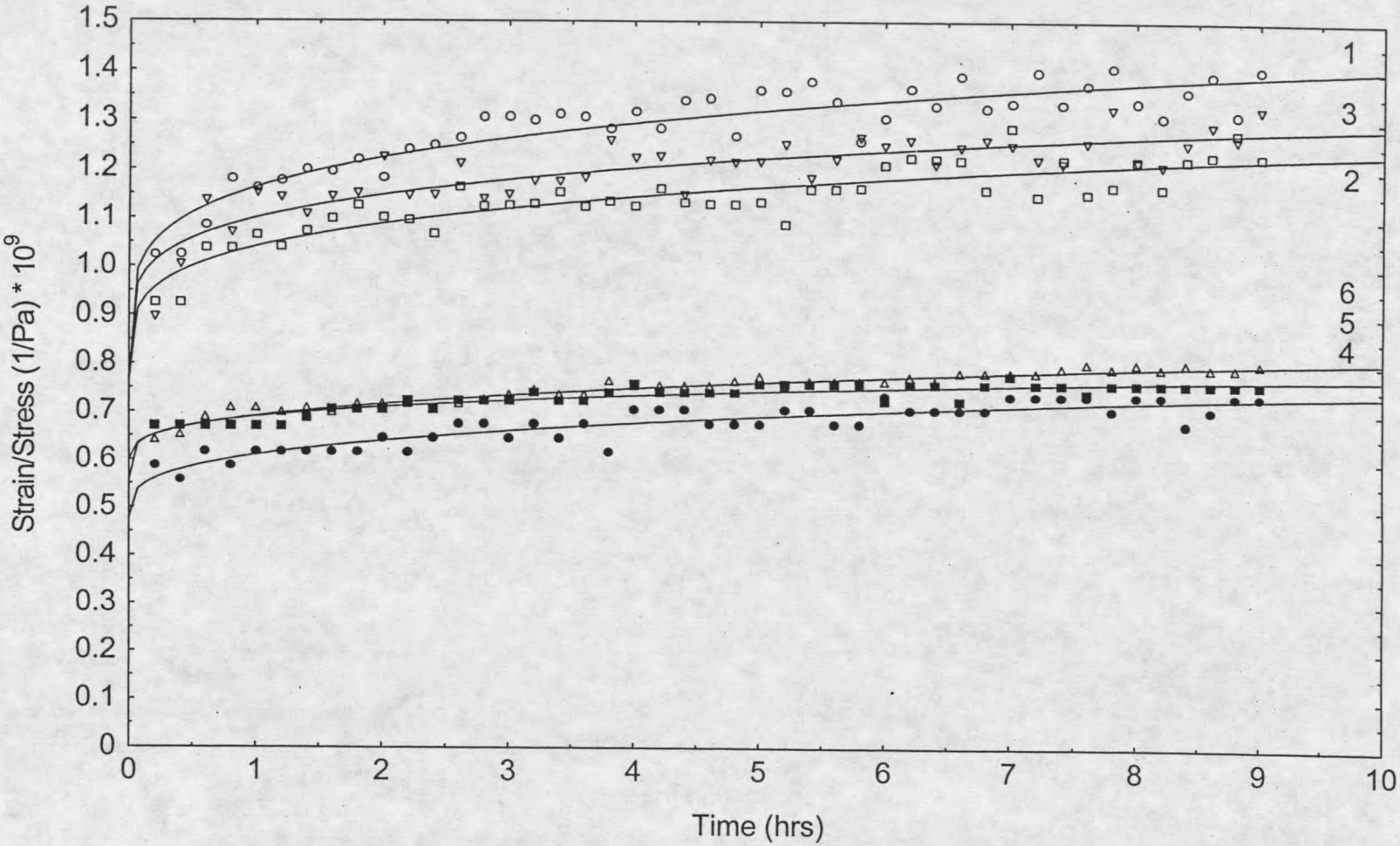


Figure E.I.17 Normalized Vibrocreep Response of Nylon 6/6 at Different Mean Stresses at 23 °C
1- $(0.12\pm0.10)\sigma_y$, 20 Hz; 2- $(0.16\pm0.10)\sigma_y$, 20 Hz; 3- $(0.20\pm0.10)\sigma_y$, 20 Hz;
4- $(0.16)\sigma_y$, 5- $(0.20)\sigma_y$, 6- $(0.30)\sigma_y$ Constant Load Creep;
σ_y = 70 MPa at 23 °C

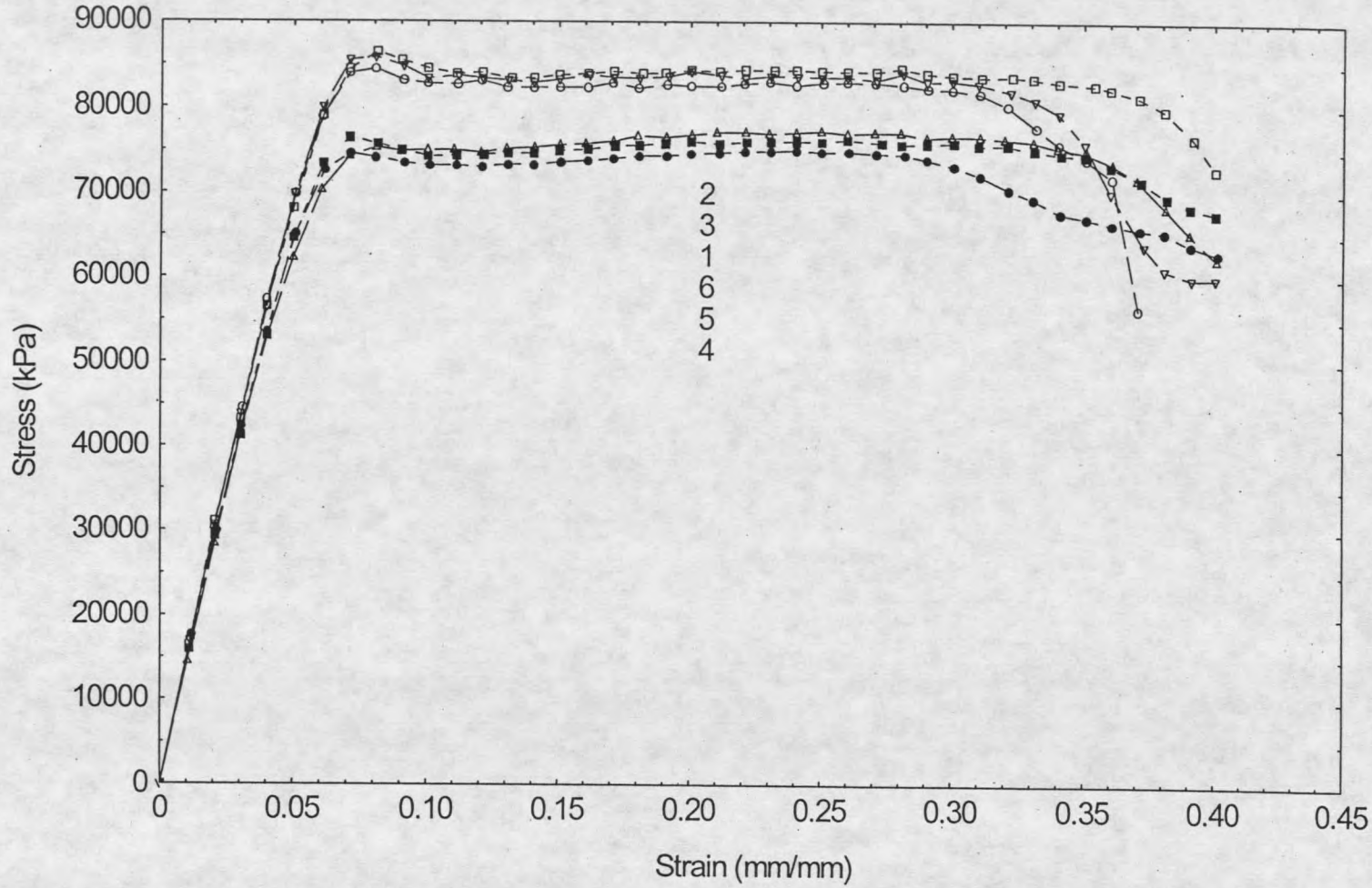


Figure E.I.18 Tensile Testing of Nylon 6/6 Specimens After Cyclic and Constant Loading at 23 °C
1- $(0.12\pm0.10)\sigma_y$, 20 Hz; 2- $(0.16\pm0.10)\sigma_y$, 20 Hz; 3- $(0.20\pm0.10)\sigma_y$, 20 Hz;
4- $(0.16)\sigma_y$, 5- $(0.20)\sigma_y$, Constant Load Creep; 6- Virgin Specimens;
σ_y = 70 MPa at 23 °C

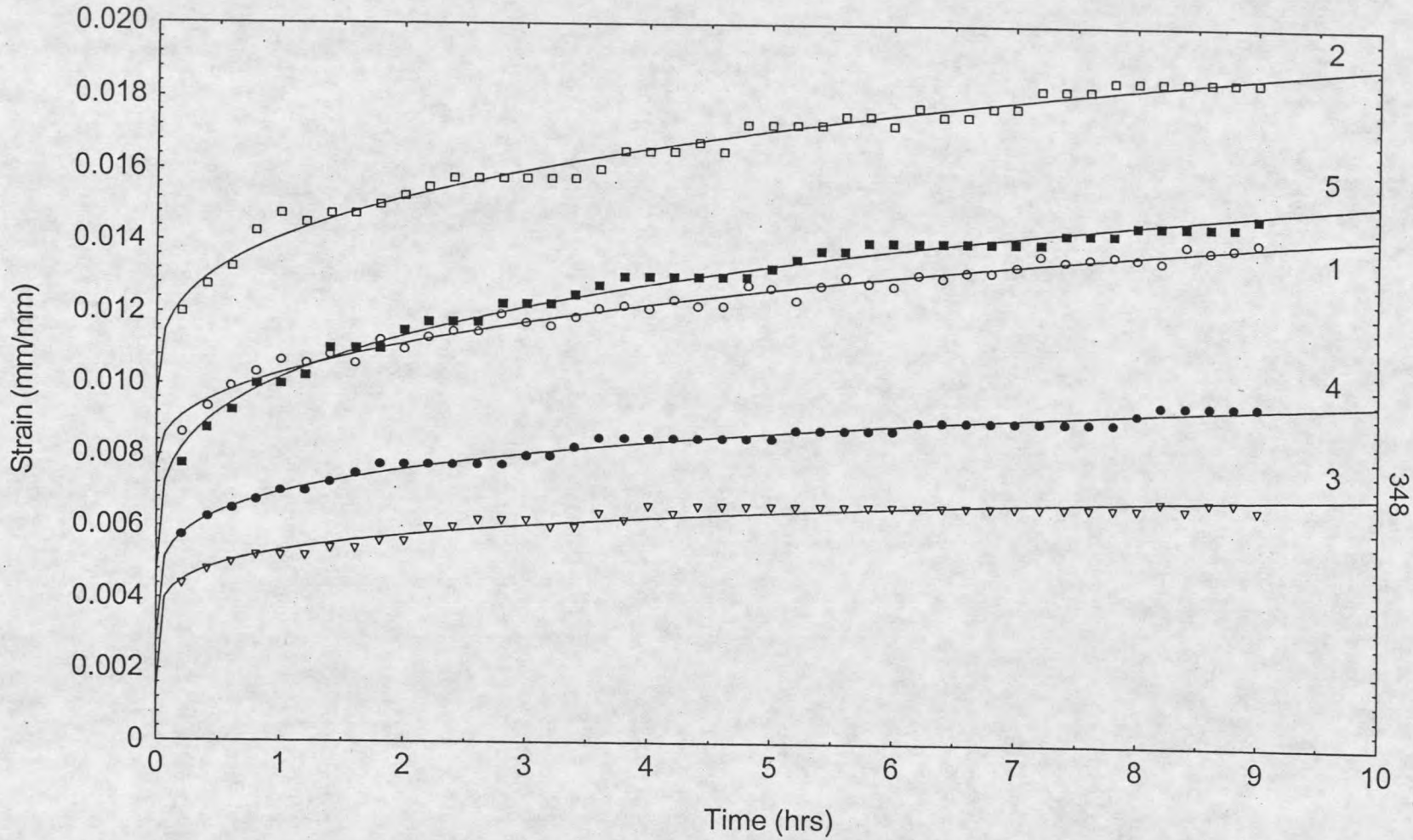


Figure E.II.1 Vibrocreep Response of Nylon 6/6 at Different Mean Stresses at 35 °C
1- $(0.16\pm0.10)\sigma_y$, 1 Hz; 2- $(0.20\pm0.10)\sigma_y$, 1 Hz;
3- $(0.16)\sigma_y$, 4- $(0.20)\sigma_y$, 5- $(0.30)\sigma_y$, Constant Load Creep;
σ_y = 55 MPa at 35 °C

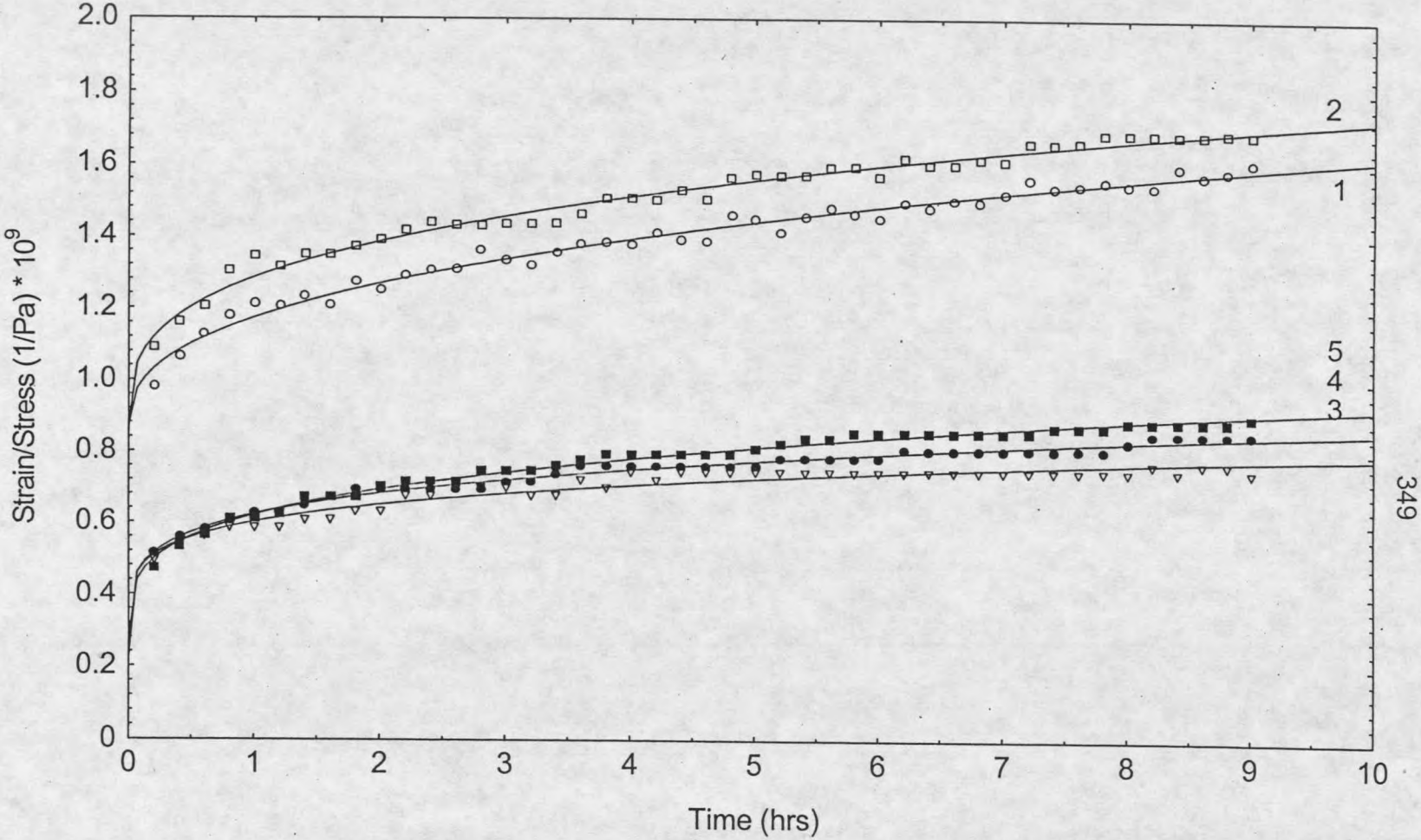


Figure E.II.2 Normalized Vibrocreep Response of Nylon 6/6 at Different Mean Stresses at 35 °C
1- $(0.16\pm0.10)\sigma_y$, 1 Hz; 2- $(0.20\pm0.10)\sigma_y$, 1 Hz;
3- $(0.16)\sigma_y$, 4- $(0.20)\sigma_y$, 5- $(0.30)\sigma_y$, Constant Load Creep;
σ_y = 55 MPa at 35 °C

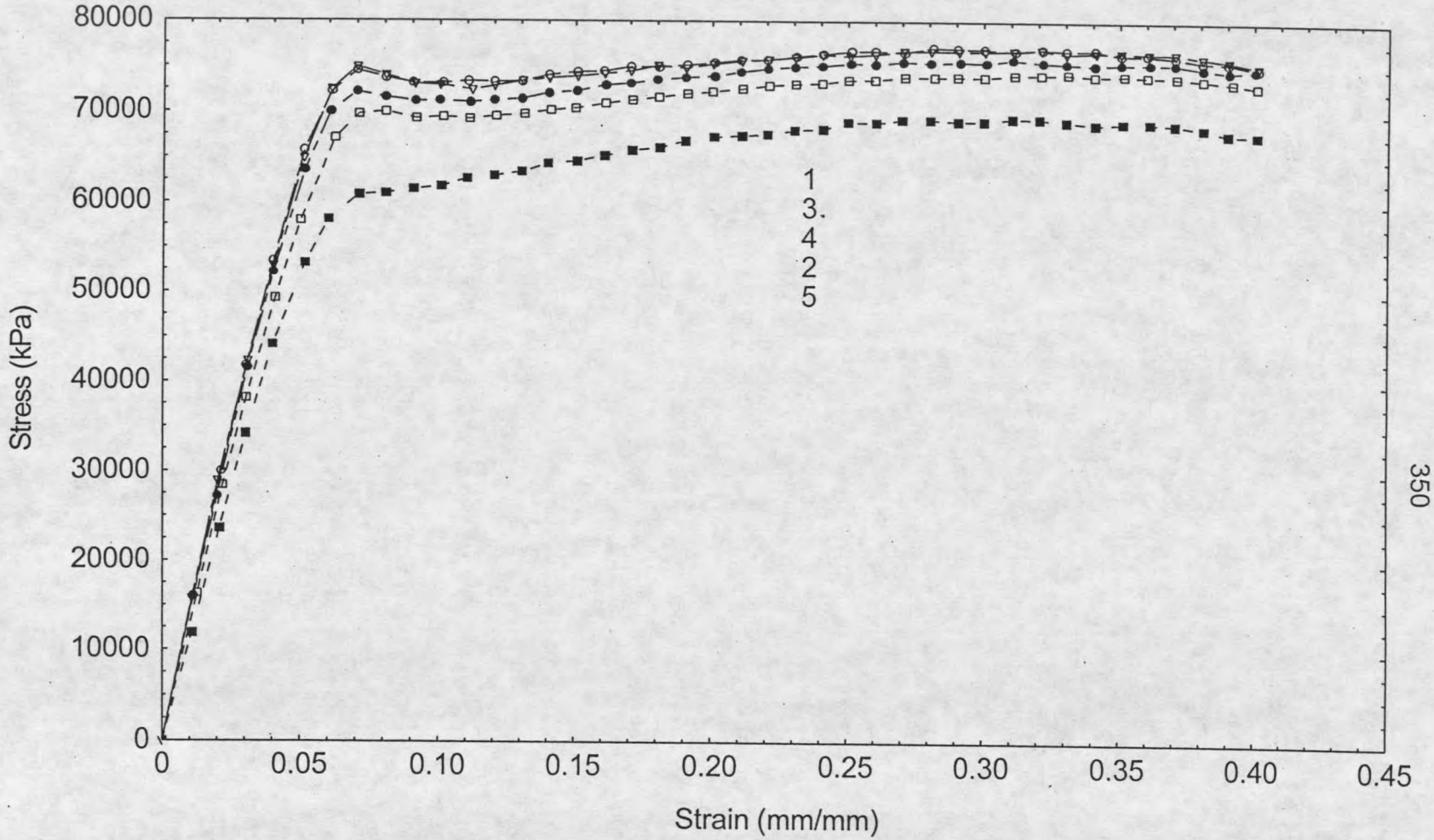


Figure E.II.3 Tensile Testing of Nylon 6/6 Specimens After Cyclic and Constant Loading at 35 °C
1- $(0.16\pm0.10)\sigma_y$, 1 Hz; 2- $(0.20\pm0.10)\sigma_y$, 1 Hz;
3- $(0.16)\sigma_y$, 4- $(0.20)\sigma_y$, Constant Load Creep; 5- Virgin Specimens;
σ_y = 55 MPa at 35 °C

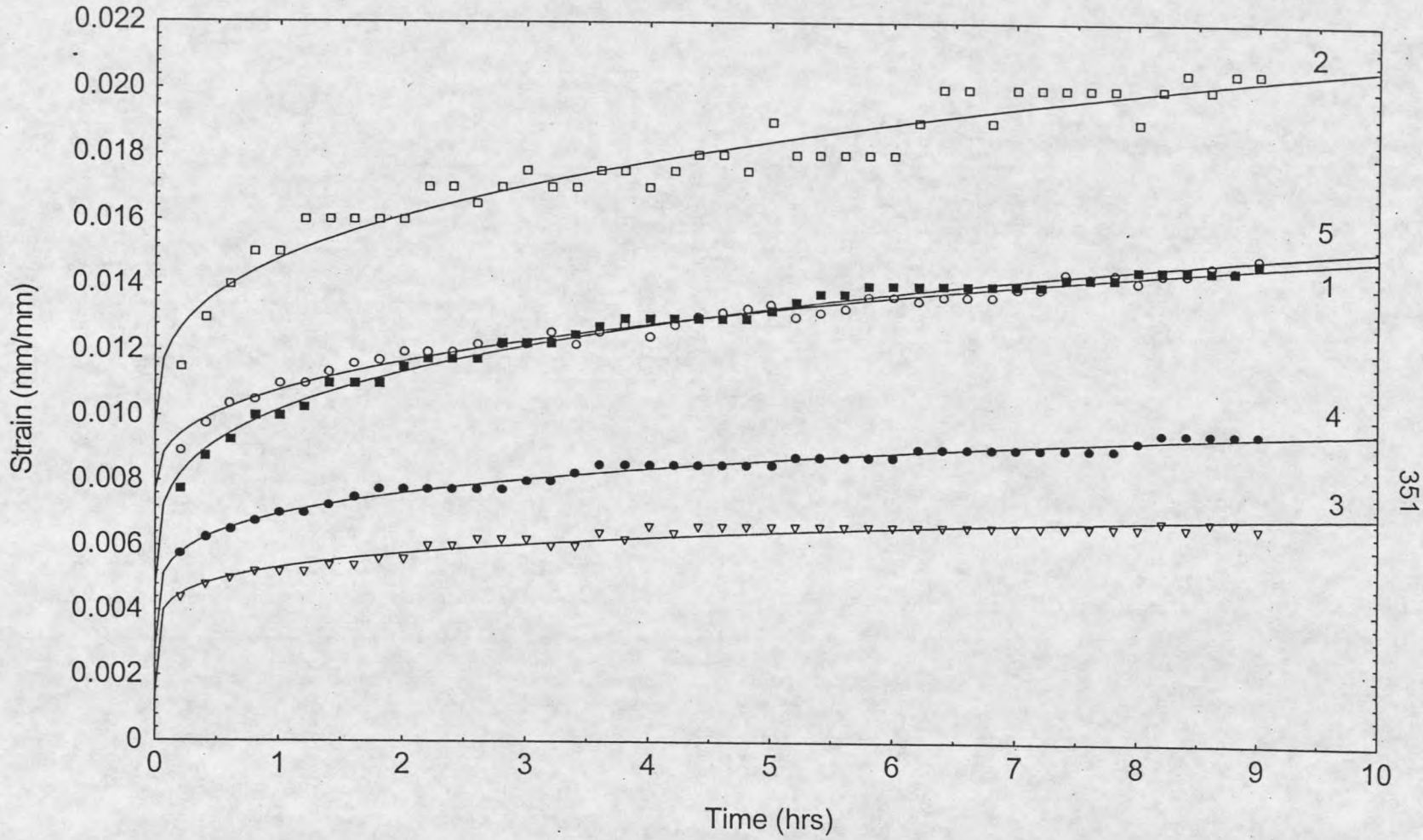


Figure E.II.4 Vibrocreep Response of Nylon 6/6 at Different Mean Stresses at 35 °C
1- $(0.16\pm0.10)\sigma_y$, 10 Hz; 2- $(0.20\pm0.10)\sigma_y$, 10 Hz;
3- $(0.16)\sigma_y$, 4- $(0.20)\sigma_y$, 5- $(0.30)\sigma_y$, Constant Load Creep;
σ_y = 55 MPa at 35 °C

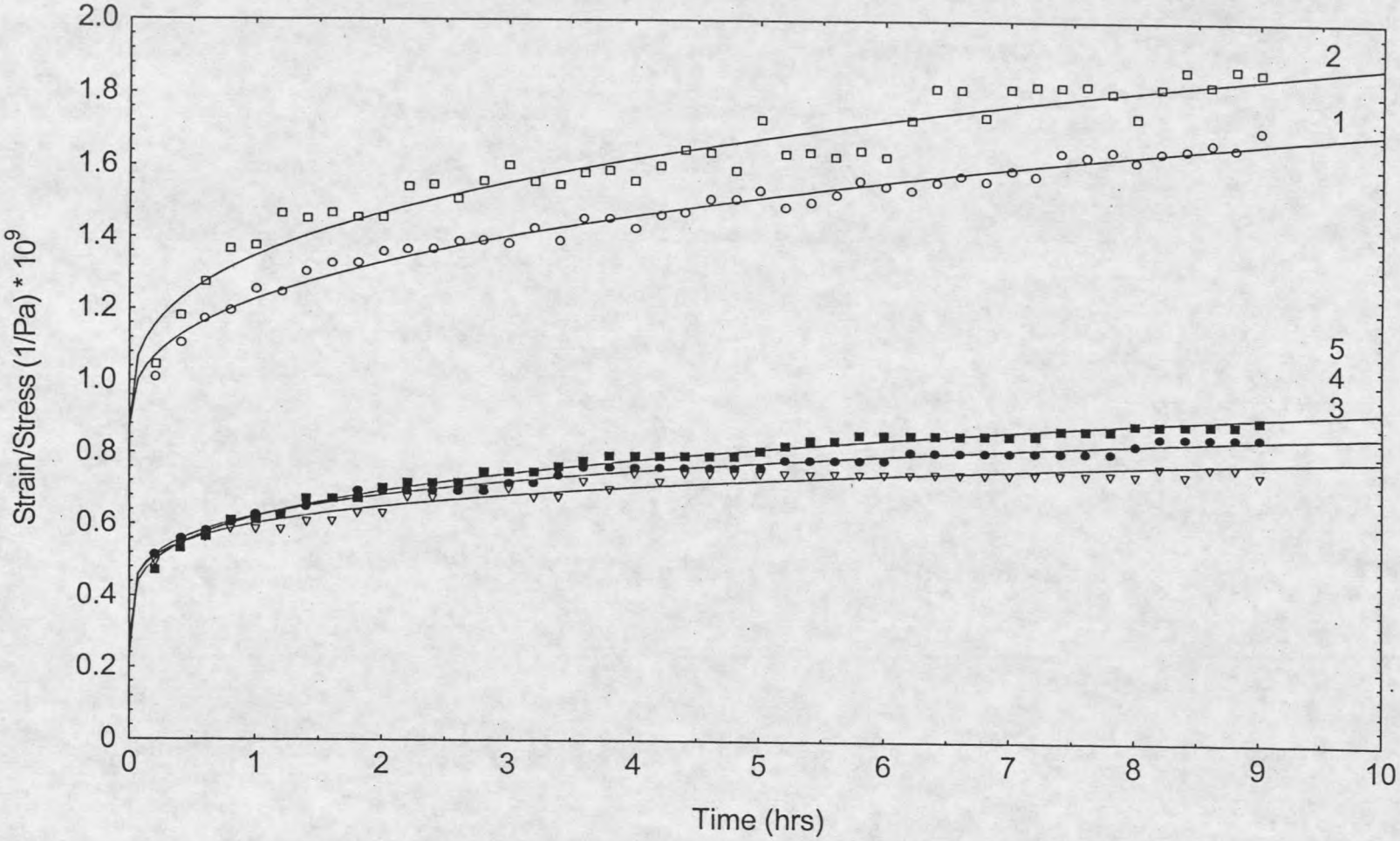


Figure E.II.5 Normalized Vibrocreep Response of Nylon 6/6 at Different Mean Stresses at 35 °C
1- $(0.16\pm0.10)\sigma_y$, 10 Hz; 2- $(0.20\pm0.10)\sigma_y$, 10 Hz;
3- $(0.16)\sigma_y$, 4- $(0.20)\sigma_y$, 5- $(0.30)\sigma_y$, Constant Load Creep;
σ_y = 55 MPa at 35 °C

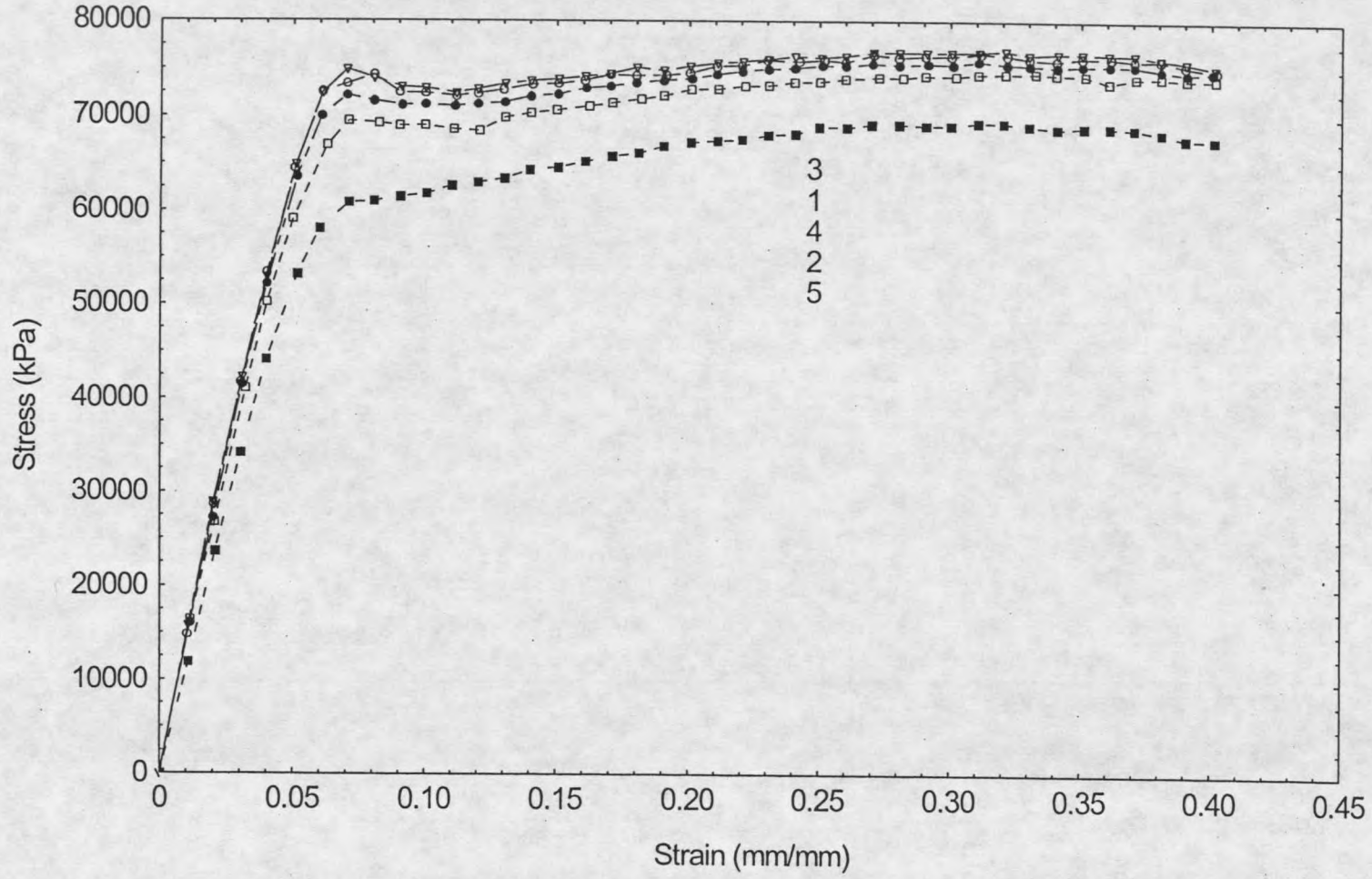


Figure E.II:6 Tensile Testing of Nylon 6/6 Specimens After Cyclic and Constant Loading at 35 °C
(1- $(0.16\pm0.10)\sigma_y$, 10 Hz; 2- $(0.20\pm0.10)\sigma_y$, 10 Hz;
3- $(0.16)\sigma_y$, 4- $(0.20)\sigma_y$, Constant Load Creep; 5- Virgin Specimens;
σ_y = 55 MPa at 35 °C

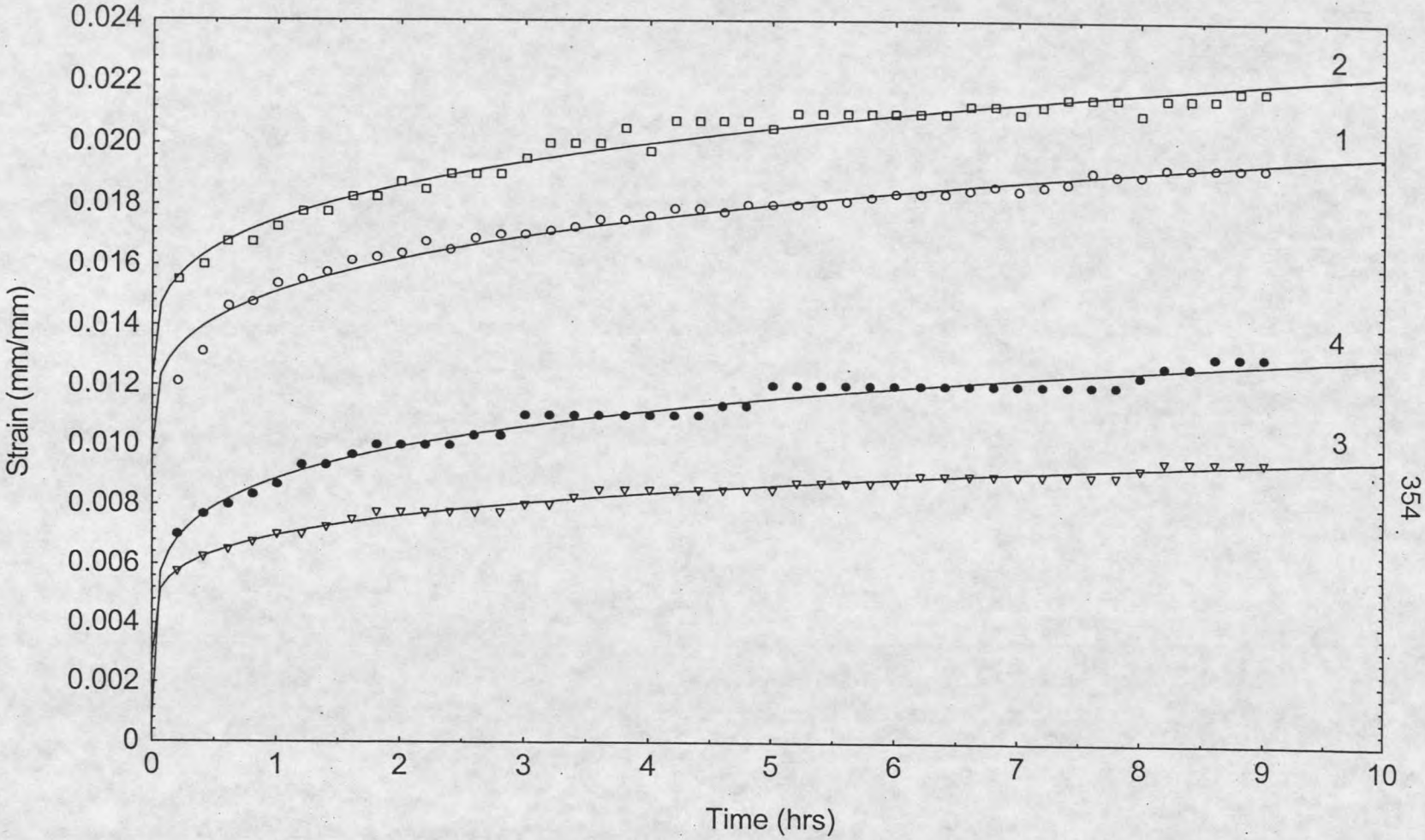


Figure E.II.7 Vibrocreep Response of Nylon 6/6 at Different Mean Stresses at 35 °C
1- $(0.16\pm0.10)\sigma_y$, 1 Hz; 2- $(0.20\pm0.10)\sigma_y$, 1 Hz;
3- $(0.16)\sigma_y$, 4- $(0.20)\sigma_y$, Constant Load Creep;
σ_y = 70 MPa at 23 °C

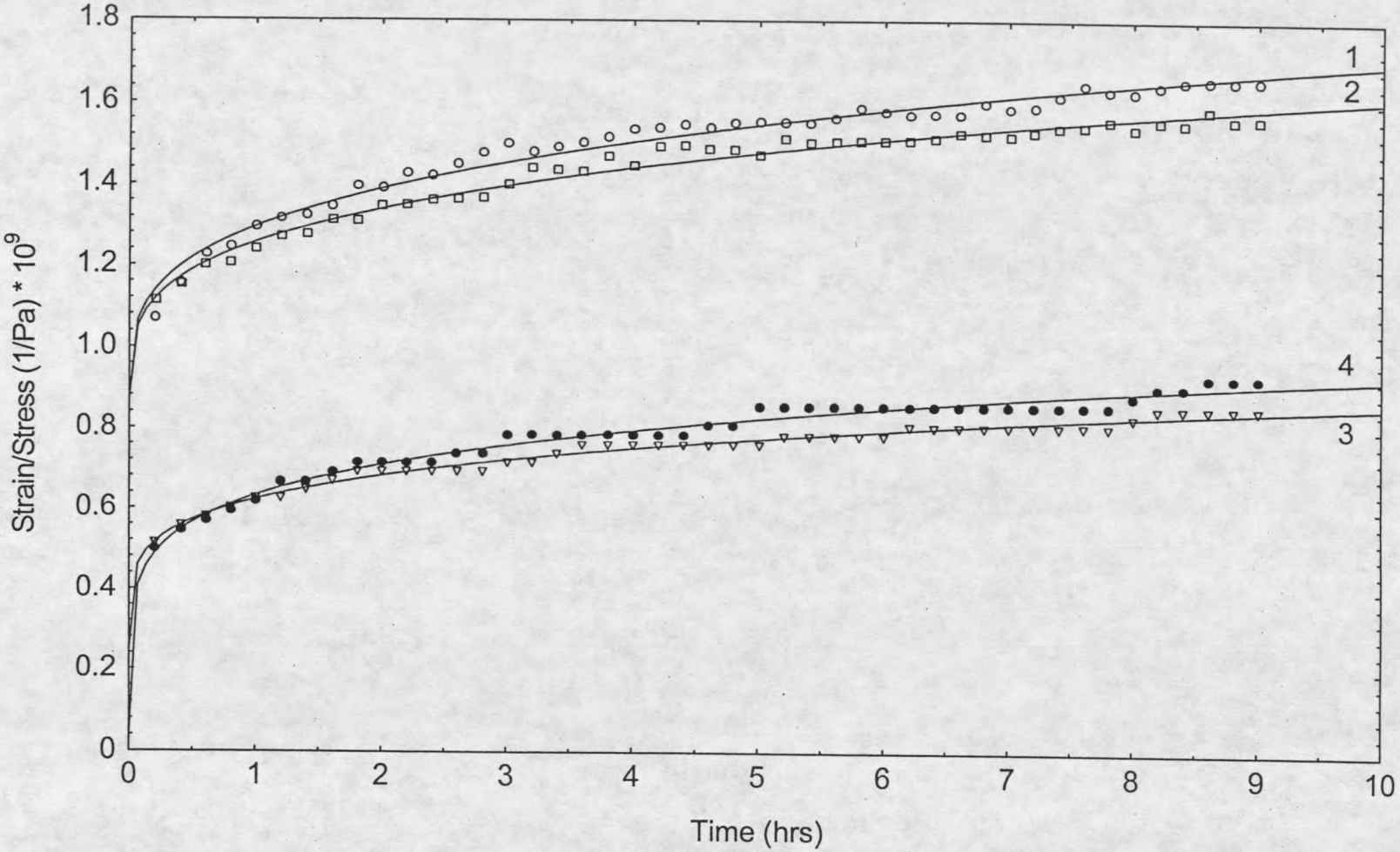


Figure E.II.8 Normalized Vibrocreep Response of Nylon 6/6 at Different Mean Stresses at 35 °C
1- $(0.16\pm0.10)\sigma_y$, 1 Hz; 2- $(0.20\pm0.10)\sigma_y$, 1 Hz;
3- $(0.16)\sigma_y$, 4- $(0.20)\sigma_y$, Constant Load Creep;
σ_y = 70 MPa at 23 °C

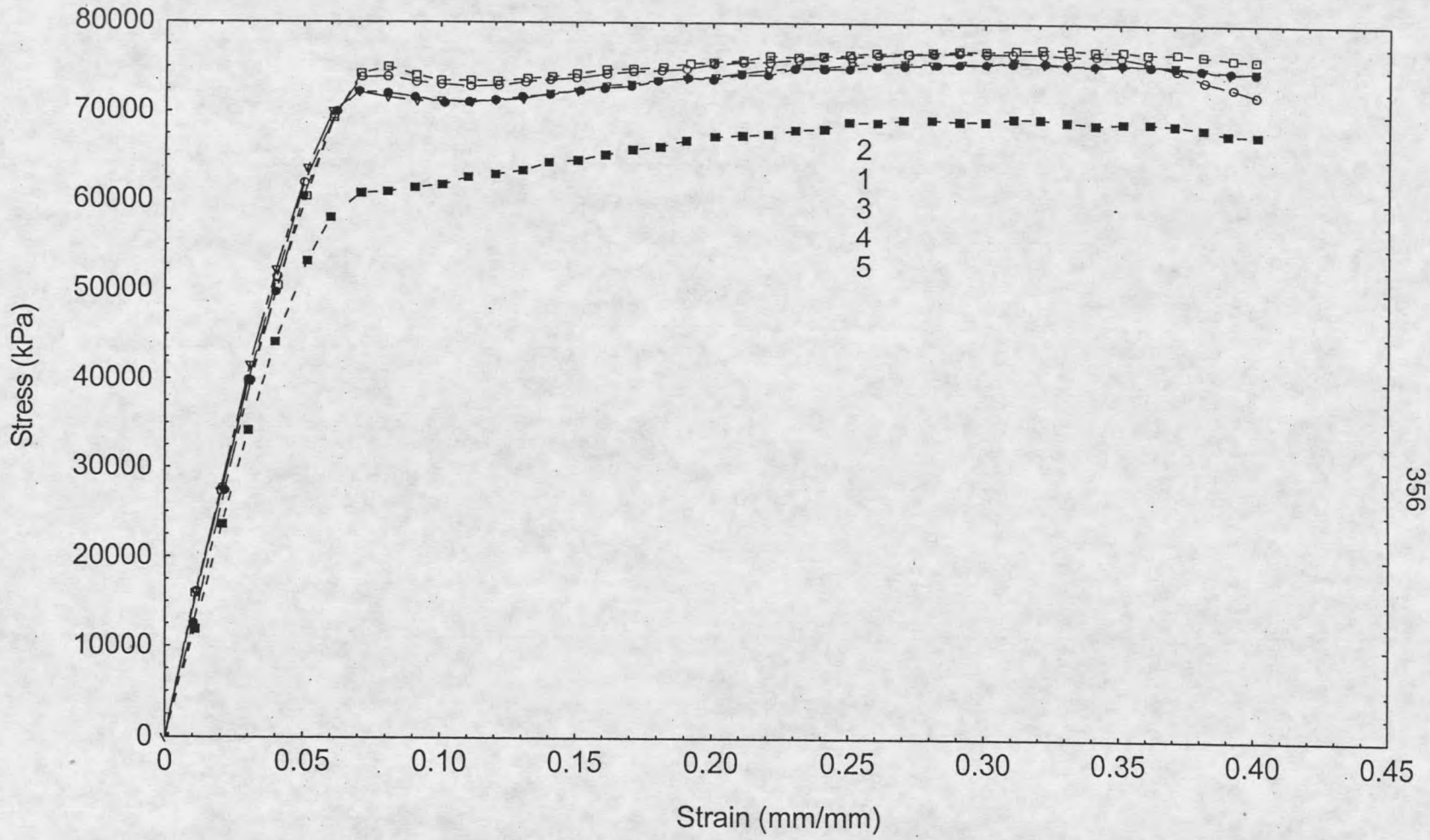


Figure E.II.9 Tensile Testing of Nylon 6/6 Specimens After Cyclic and Constant Loading at 35 °C
1- $(0.16\pm0.10)\sigma_y$, 1 Hz; 2- $(0.20\pm0.10)\sigma_y$, 1 Hz;
3- $(0.16)\sigma_y$, 4- $(0.20)\sigma_y$, Constant Load Creep; 5- Virgin Specimens;
σ_y = 70 MPa at 23 °C

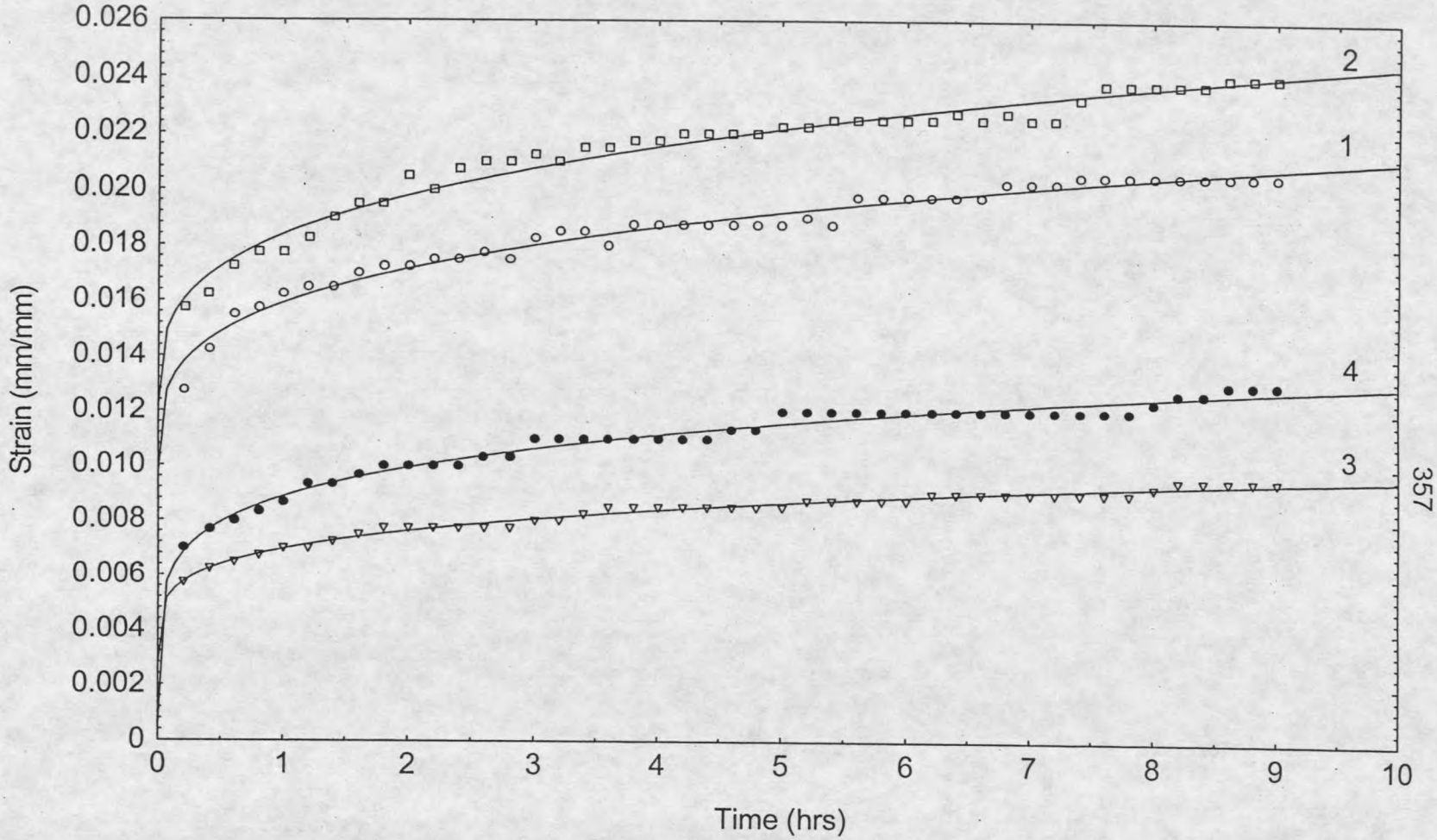


Figure E.II.10 Vibrocreep Response of Nylon 6/6 at Different Mean Stresses at 35 °C
1- $(0.16\pm0.10)\sigma_y$, 10 Hz; 2- $(0.20\pm0.10)\sigma_y$, 10 Hz;
3- $(0.16)\sigma_y$, 4- $(0.20)\sigma_y$, Constant Load Creep;
σ_y = 70 MPa at 23 °C

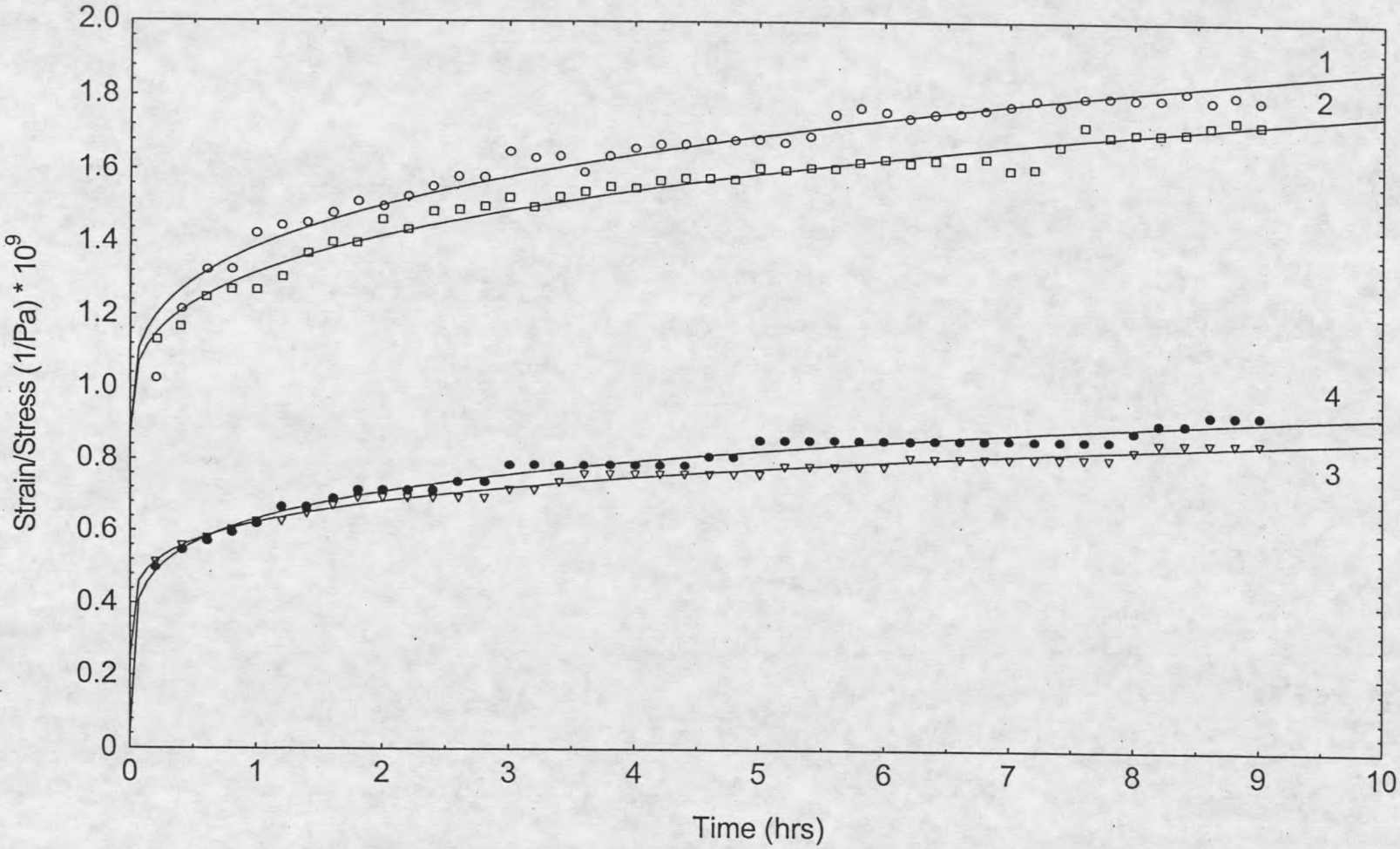


Figure E.II.11 Normalized Vibrocreep Response of Nylon 6/6 at Different Mean Stresses at 35 °C
1- $(0.16\pm0.10)\sigma_y$, 10 Hz; 2- $(0.20\pm0.10)\sigma_y$, 10 Hz;
3- $(0.16)\sigma_y$, 4- $(0.20)\sigma_y$, Constant Load Creep;
σ_y = 70 MPa at 23 °C

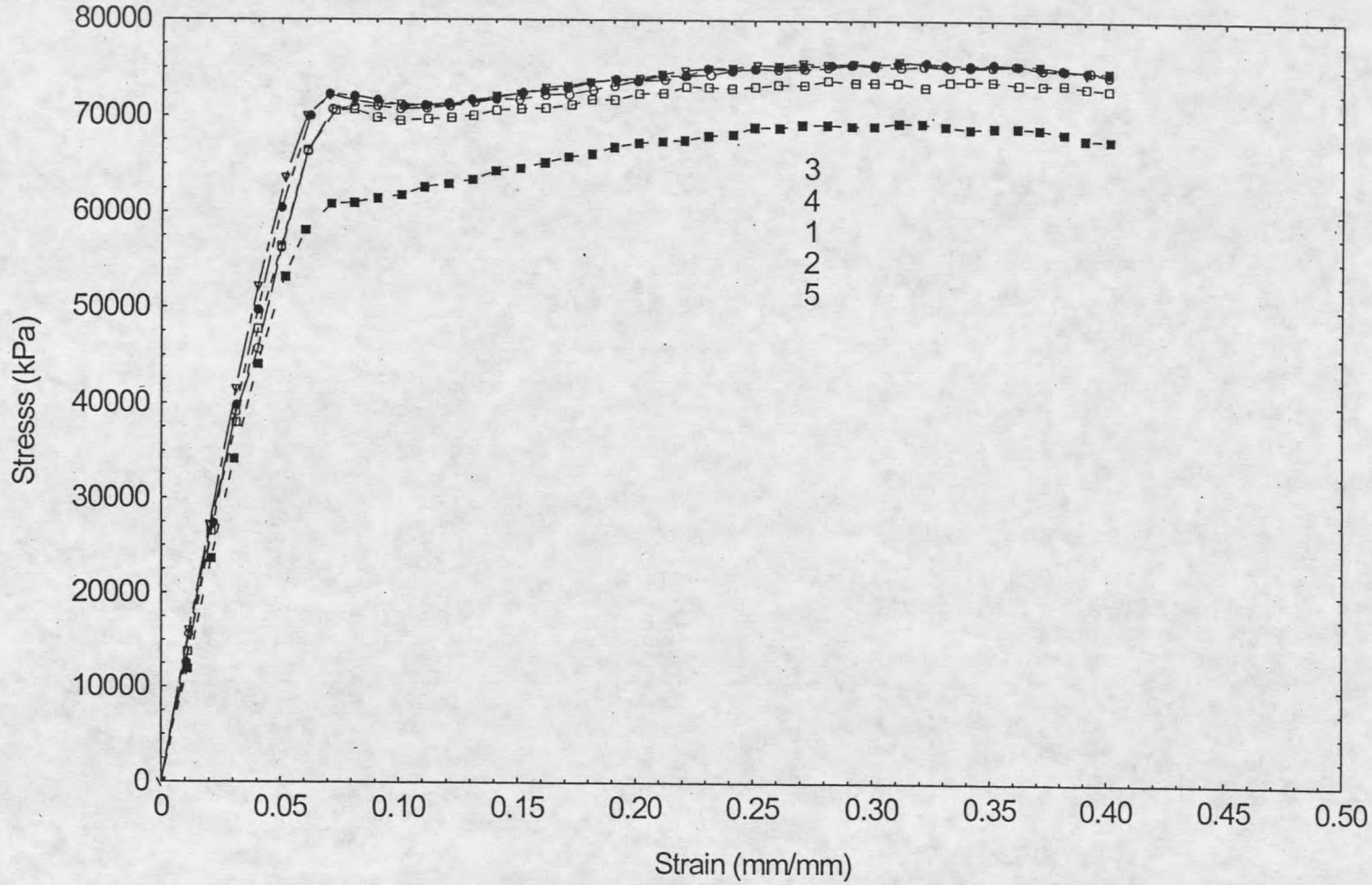


Figure E.II.12 Tensile Testing of Nylon 6/6 Specimens After Cyclic and Constant Loading at 35 °C
1- $(0.16\pm0.10)\sigma_y$, 10 Hz; 2- $(0.20\pm0.10)\sigma_y$, 10 Hz;
3- $(0.16)\sigma_y$, 4- $(0.20)\sigma_y$, Constant Load Creep; 5- Virgin Specimens;
σ_y = 70 MPa at 23 °C

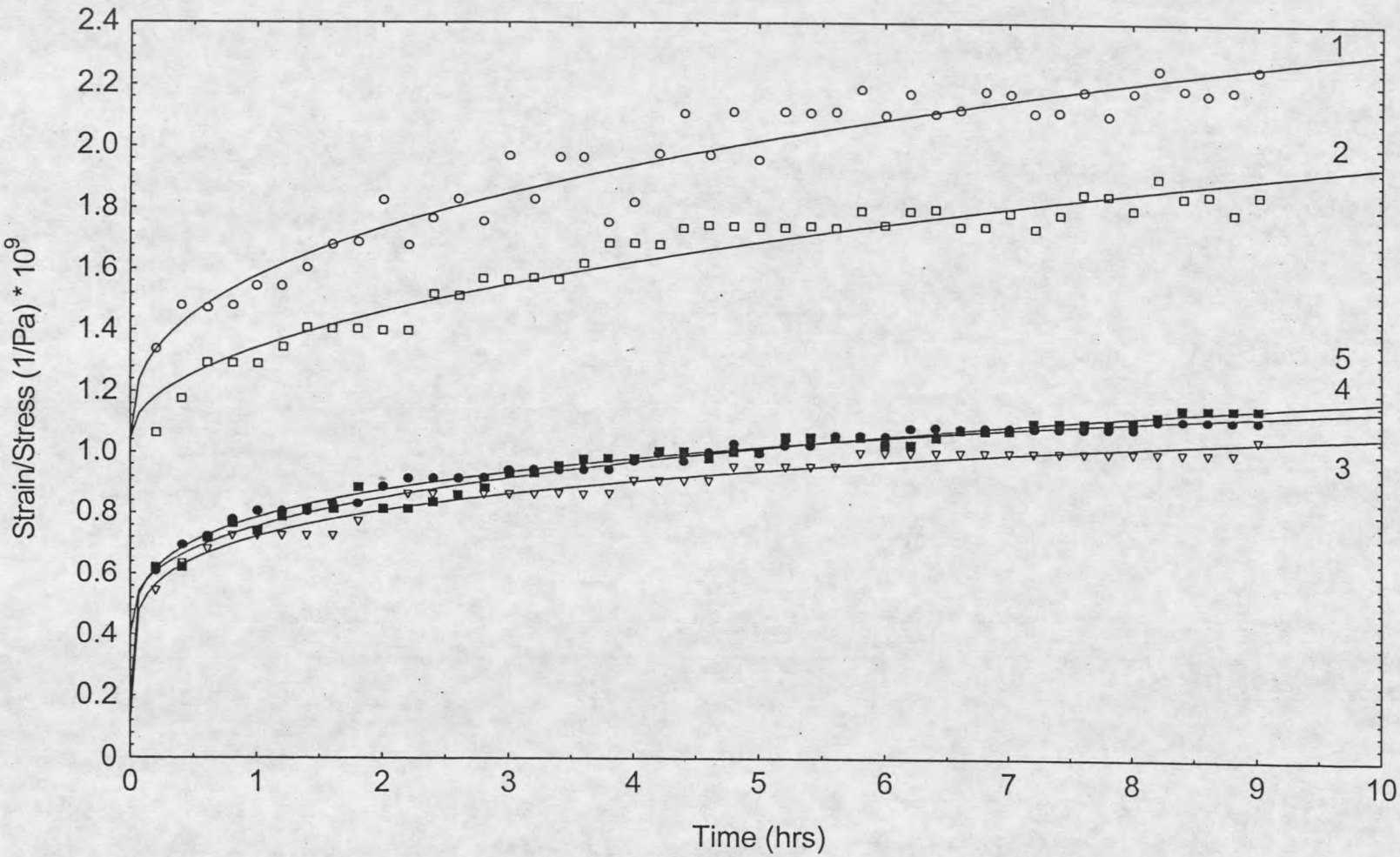


Figure E.III.2 Normalized Vibrocreep Response of Nylon 6/6 at Different Mean Stresses at 41 °C
(1- $(0.16\pm0.10)\sigma_y$, 1 Hz; 2- $(0.20\pm0.10)\sigma_y$, 1 Hz;
3- $(0.16)\sigma_y$, 4- $(0.20)\sigma_y$, 5- $(0.30)\sigma_y$, Constant Load Creep;
σ_y = 45 MPa at 41 °C

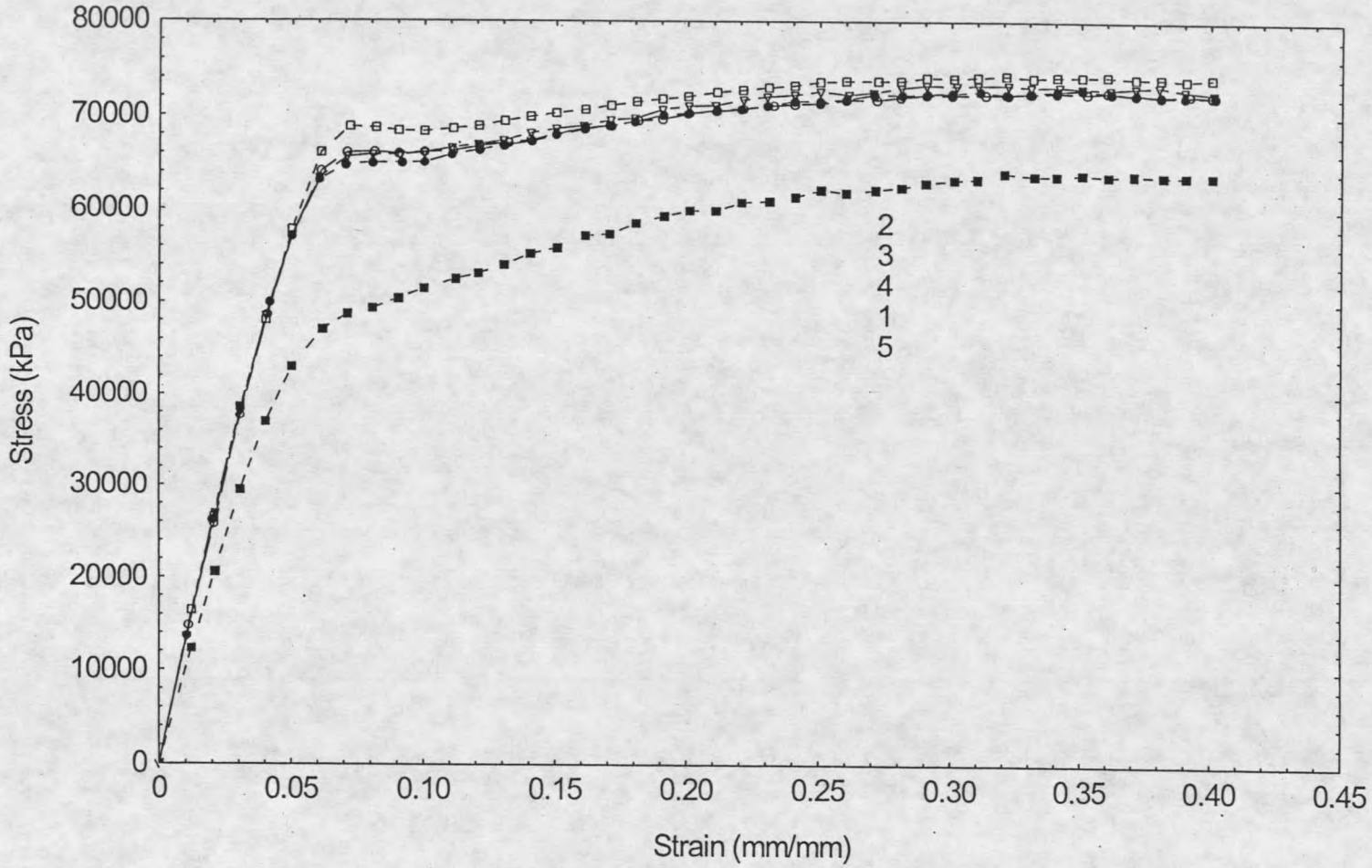


Figure E.III.3 Tensile Testing of Nylon 6/6 Specimens After Cyclic and Constant Loading at 41 °C
1- $(0.16\pm0.10)\sigma_y$, 1 Hz; 2- $(0.20\pm0.10)\sigma_y$, 1 Hz;
3- $(0.16)\sigma_y$, 4- $(0.20)\sigma_y$, Constant Load Creep; 5- Virgin Specimens;
σ_y = 45 MPa at 41 °C

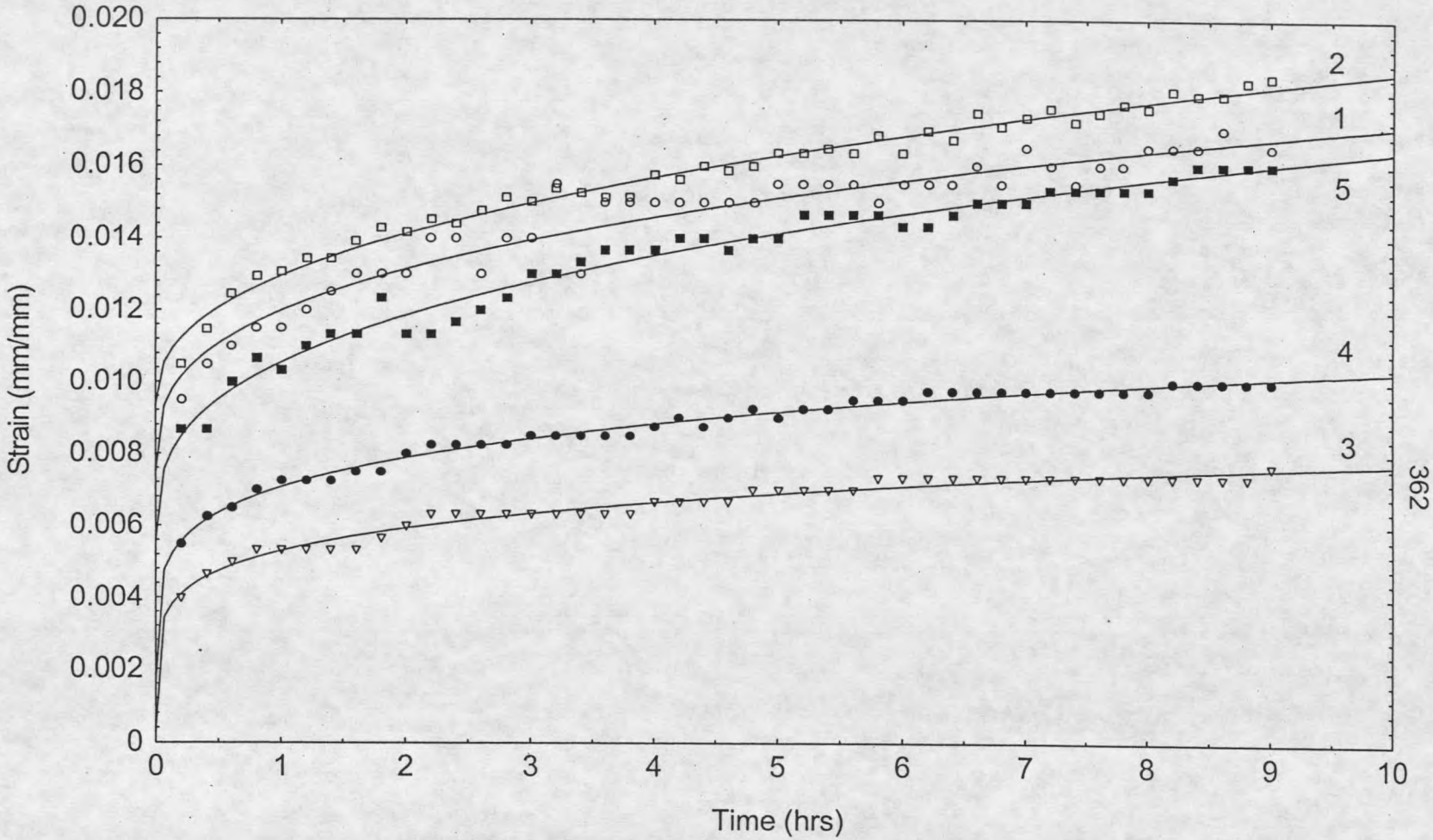


Figure E.III.4 Vibrocreep Response of Nylon 6/6 at Different Mean Stresses at 41 °C
1- $(0.16\pm0.10)\sigma_y$, 10 Hz; 2- $(0.20\pm0.10)\sigma_y$, 10 Hz;
3- $(0.16)\sigma_y$, 4- $(0.20)\sigma_y$, 5- $(0.30)\sigma_y$, Constant Load Creep;
σ_y = 45 MPa at 41 °C

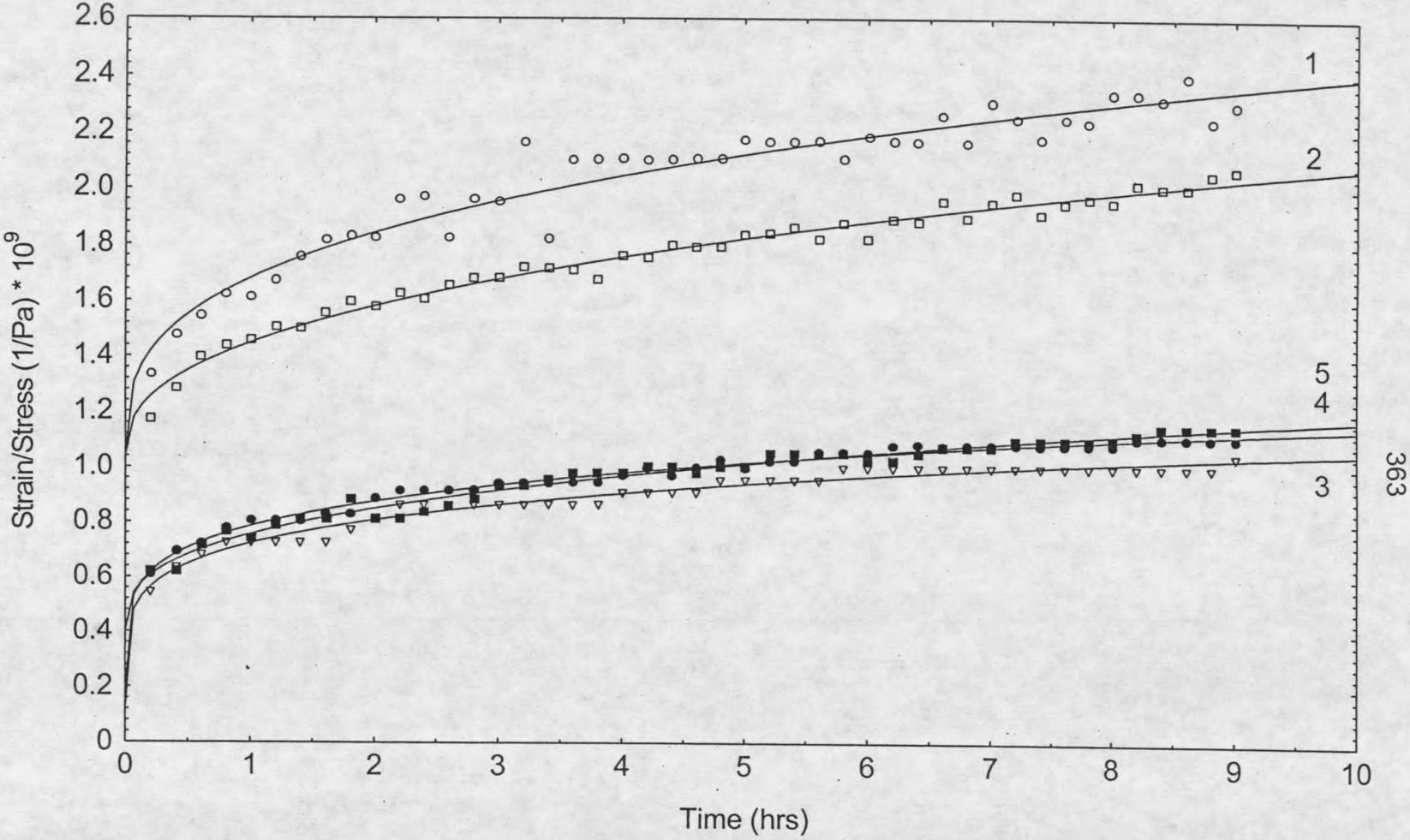


Figure E.III.5 Normalized Vibrocreep Response of Nylon 6/6 at Different Mean Stresses at 41 °C
1- $(0.16\pm0.10)\sigma_y$, 10 Hz; 2- $(0.20\pm0.10)\sigma_y$, 10 Hz;
3- $(0.16)\sigma_y$, 4- $(0.20)\sigma_y$, 5- $(0.30)\sigma_y$, Constant Load Creep;
σ_y = 45 MPa at 41 °C

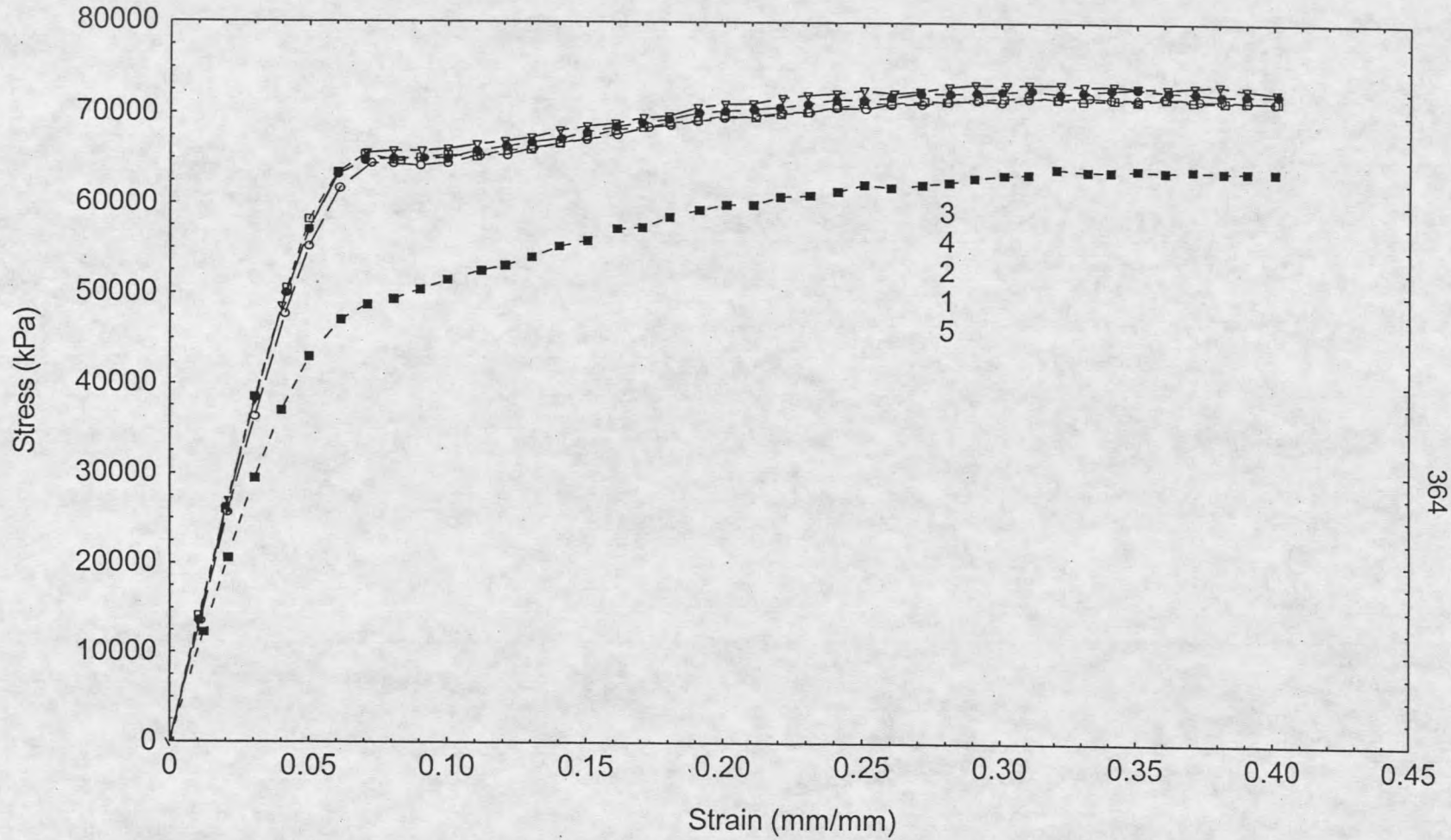


Figure E.III.6 Tensile Testing of Nylon 6/6 Specimens After Cyclic and Constant Loading at 41 °C
1- $(0.16\pm0.10)\sigma_y$, 10 Hz; 2- $(0.20\pm0.10)\sigma_y$, 10 Hz;
3- $(0.16)\sigma_y$, 4- $(0.20)\sigma_y$, Constant Load Creep; 5- Virgin Specimens;
σ_y = 45 MPa at 41 °C

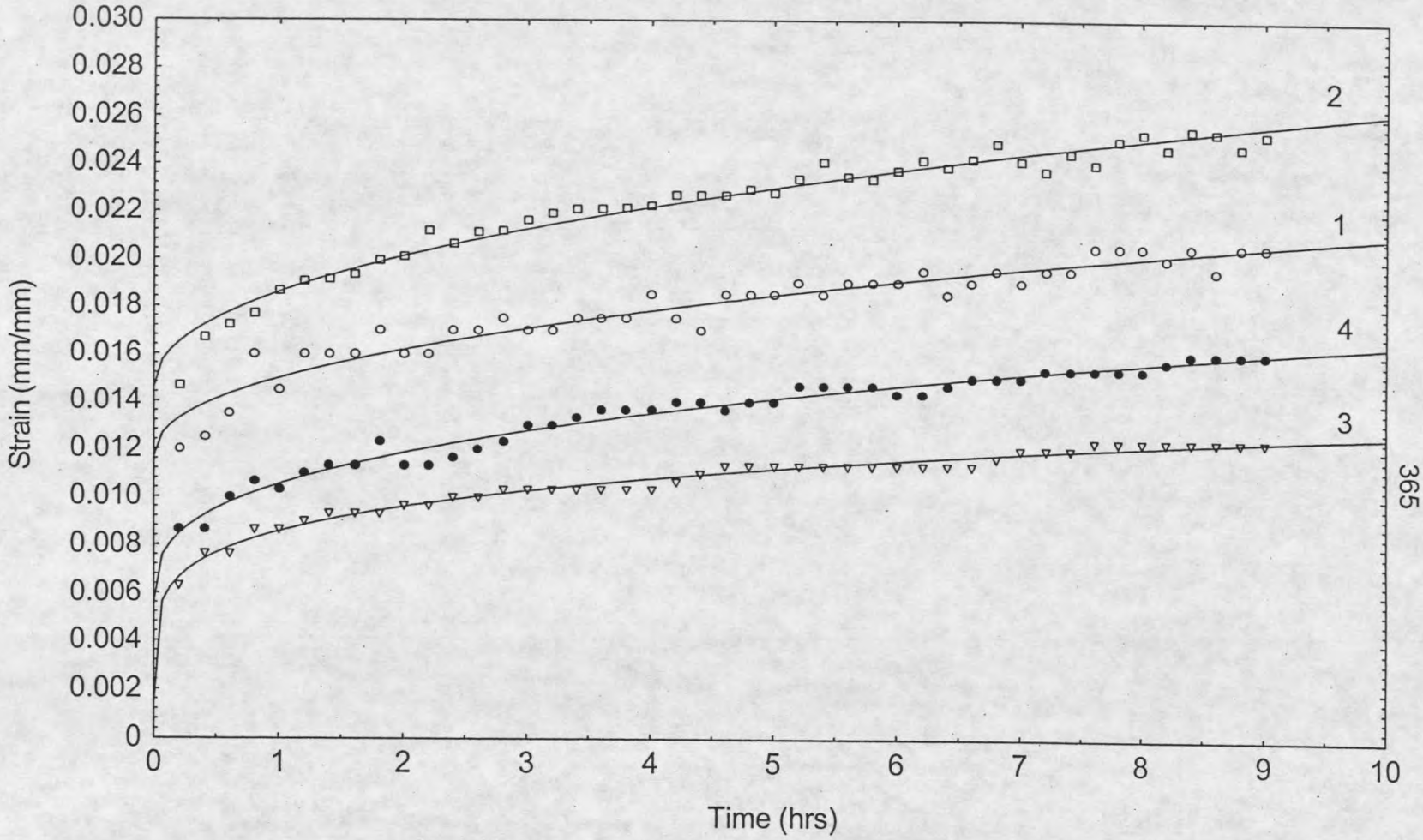


Figure E.III.7 Vibrocreep Response of Nylon 6/6 at Different Mean Stresses at 41 °C
1- $(0.16\pm0.10)\sigma_y$, 1 Hz; 2- $(0.20\pm0.10)\sigma_y$, 1 Hz;
3- $(0.16)\sigma_y$, 4- $(0.20)\sigma_y$, Constant Load Creep;
σ_y = 70 MPa at 23 °C

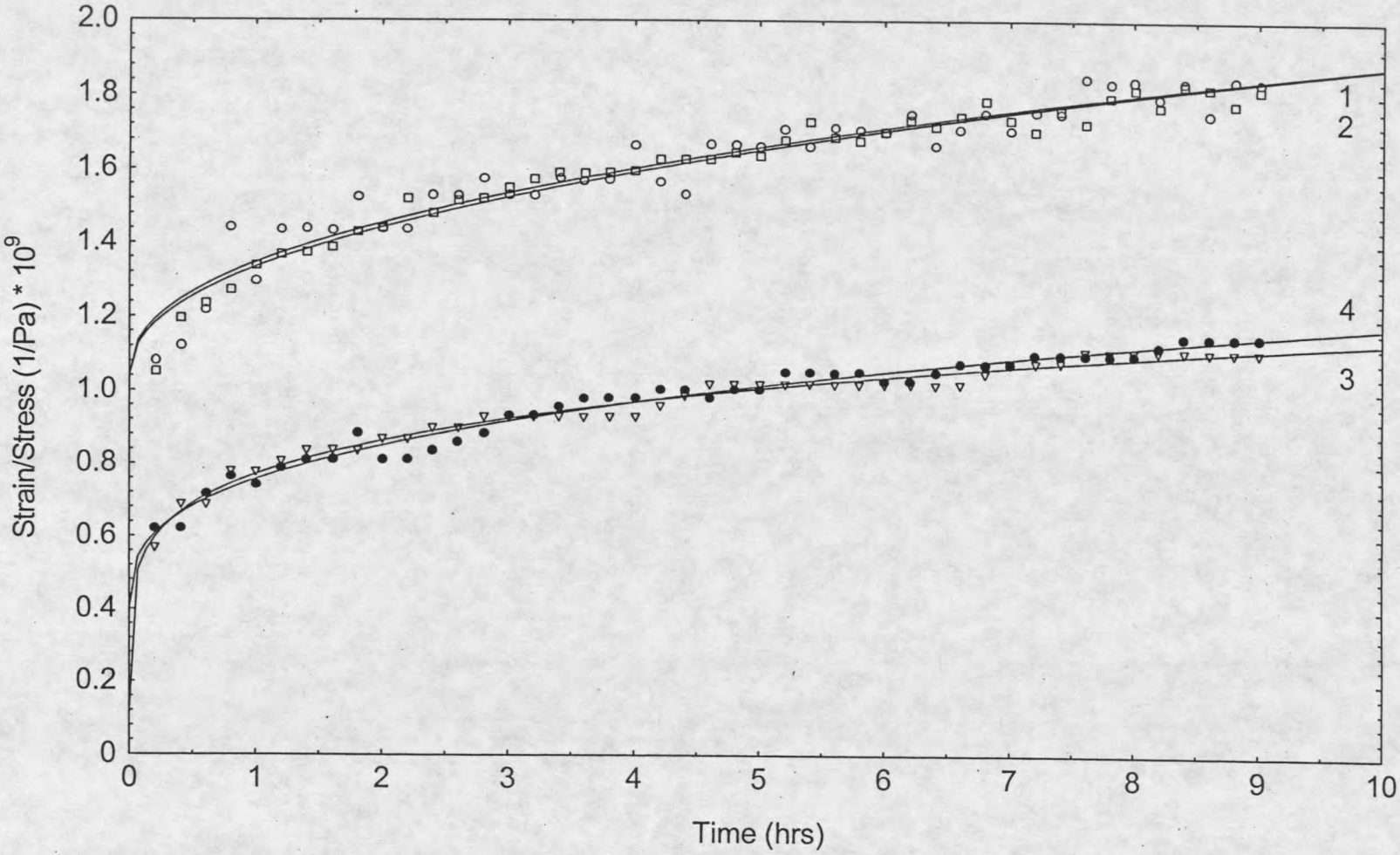


Figure E.III.8 Normalized Vibrocreep Response of Nylon 6/6 at Different Mean Stresses at 41 °C
1- $(0.16\pm0.10)\sigma_y$, 1 Hz; 2- $(0.20\pm0.10)\sigma_y$, 1 Hz;
3- $(0.16)\sigma_y$, 4- $(0.20)\sigma_y$, Constant Load Creep;
σ_y = 70 MPa at 23 °C

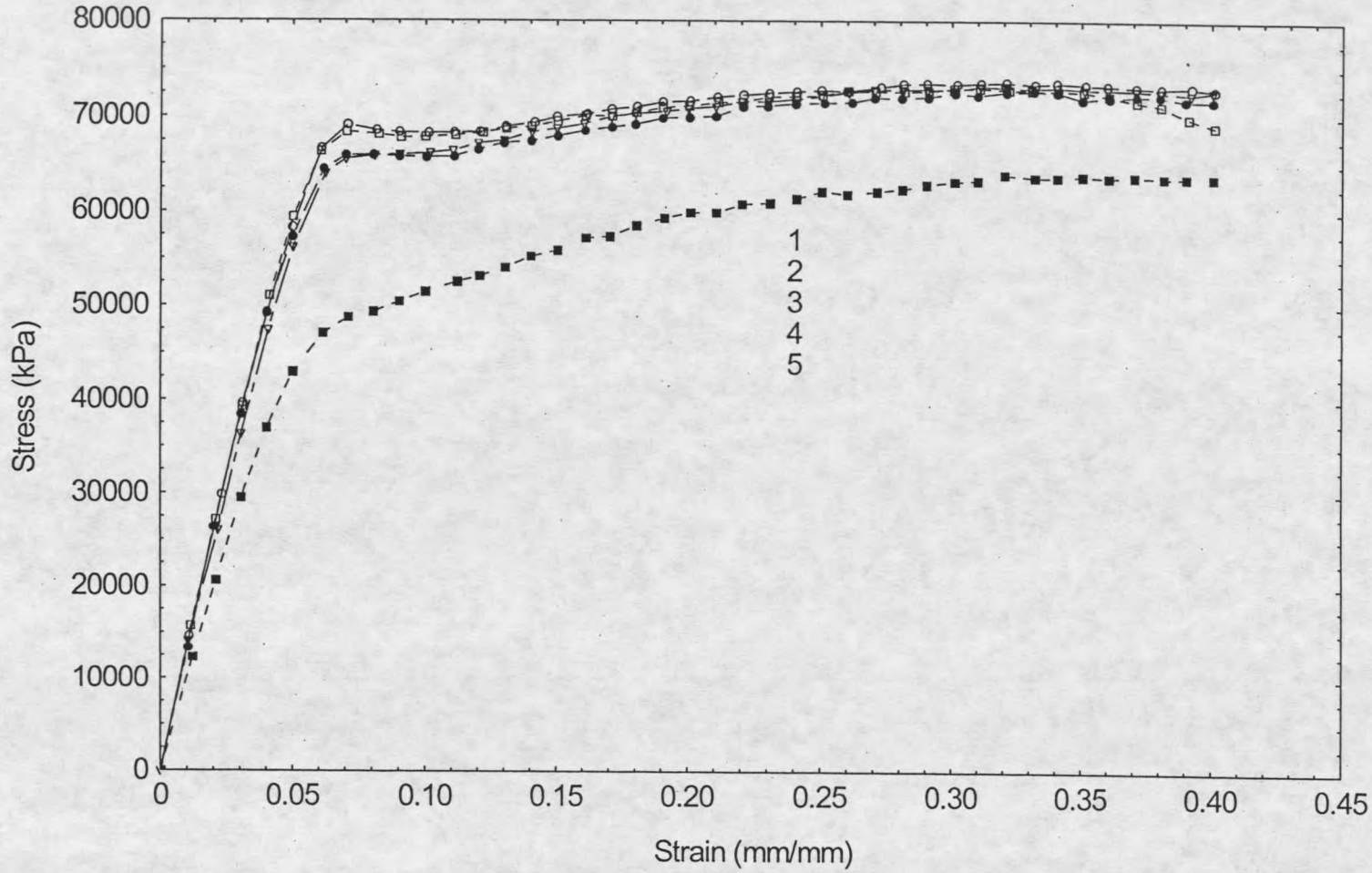


Figure E.III.9 Tensile Testing of Nylon 6/6 Specimens After Cyclic and Constant Loading at 41 °C
1- $(0.16\pm0.10)\sigma_y$, 1 Hz; 2- $(0.20\pm0.10)\sigma_y$, 1 Hz;
3- $(0.16)\sigma_y$, 4- $(0.20)\sigma_y$, Constant Load Creep; 5- Virgin Specimens;
σ_y = 70 MPa at 23 °C

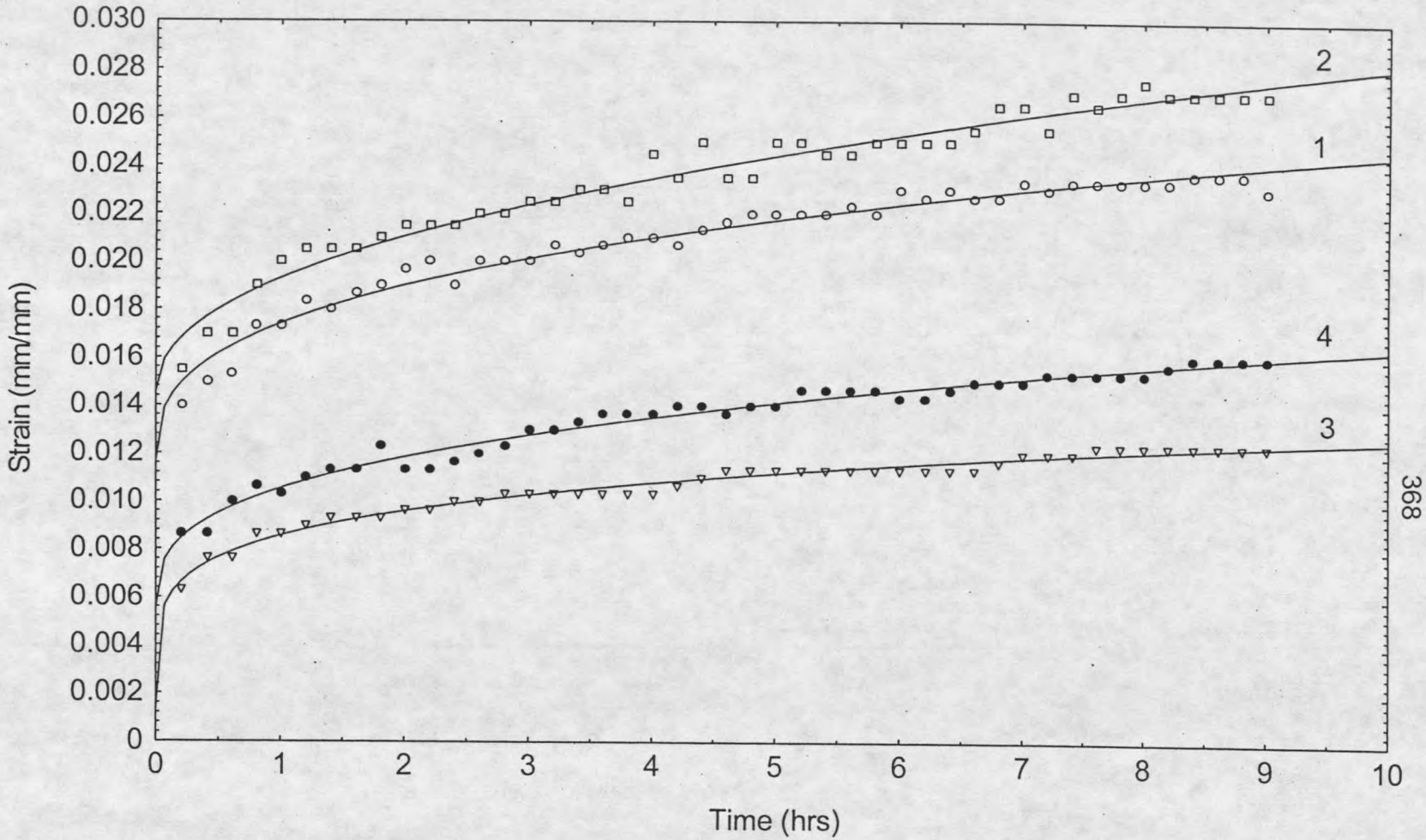


Figure E.III.10 Vibrocreep Response of Nylon 6/6 at Different Mean Stresses at 41 °C
1- $(0.16\pm0.10)\sigma_y$, 10 Hz; 2- $(0.20\pm0.10)\sigma_y$, 10 Hz;
3- $(0.16)\sigma_y$, 4- $(0.20)\sigma_y$, Constant Load Creep;
σ_y = 70 MPa at 23 °C

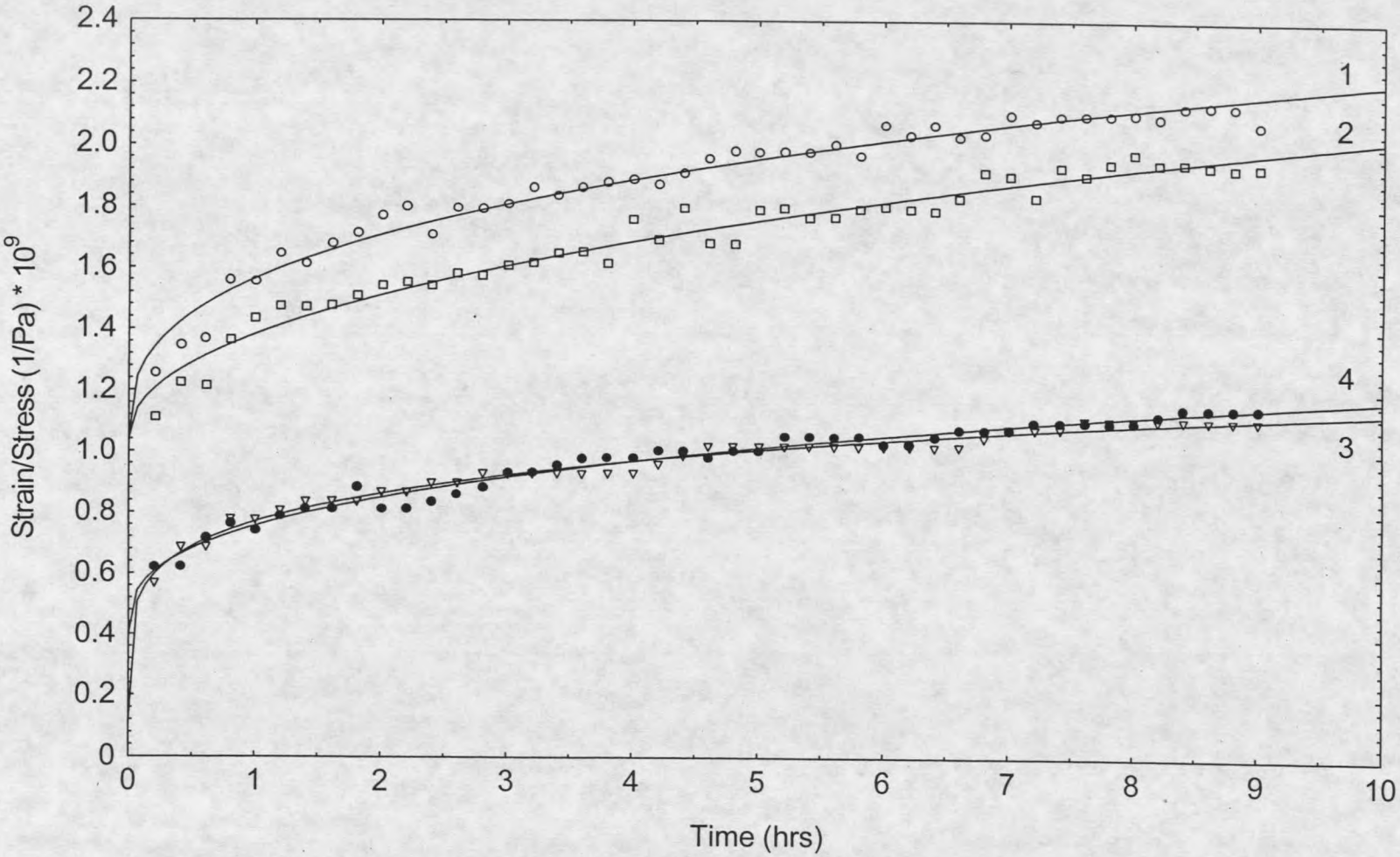


Figure E.III.11 Normalized Vibrocreep Response of Nylon 6/6 at Different Mean Stresses at 41 °C
1- $(0.16\pm0.10)\sigma_y$, 10 Hz; 2- $(0.20\pm0.10)\sigma_y$, 10 Hz;
3- $(0.16)\sigma_y$, 4- $(0.20)\sigma_y$, Constant Load Creep;
σ_y = 70 MPa at 23 °C

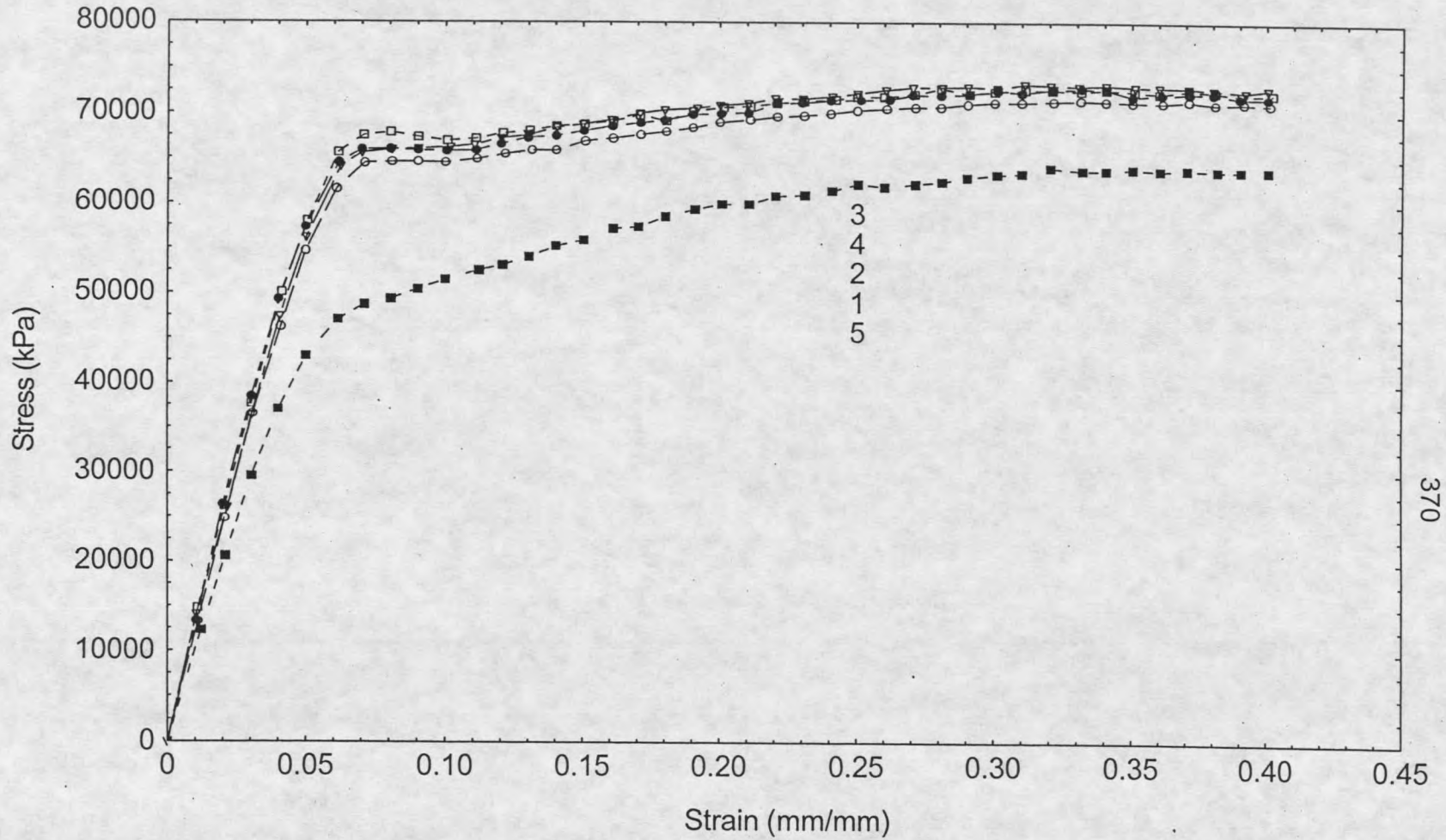


Figure E.III.12 Tensile Testing of Nylon 6/6 Specimens After Cyclic and Constant Loading at 41 °C
1- $(0.16\pm0.10)\sigma_y$, 10 Hz; 2- $(0.20\pm0.10)\sigma_y$, 10 Hz;
3- $(0.16)\sigma_y$, 4- $(0.20)\sigma_y$, Constant Load Creep; 5- Virgin Specimens;
σ_y = 70 MPa at 23 °C

APPENDIX F

Temperature Effects from Tensile, Constant Load Creep, and Vibrocreep Testing of Nylon 6/6

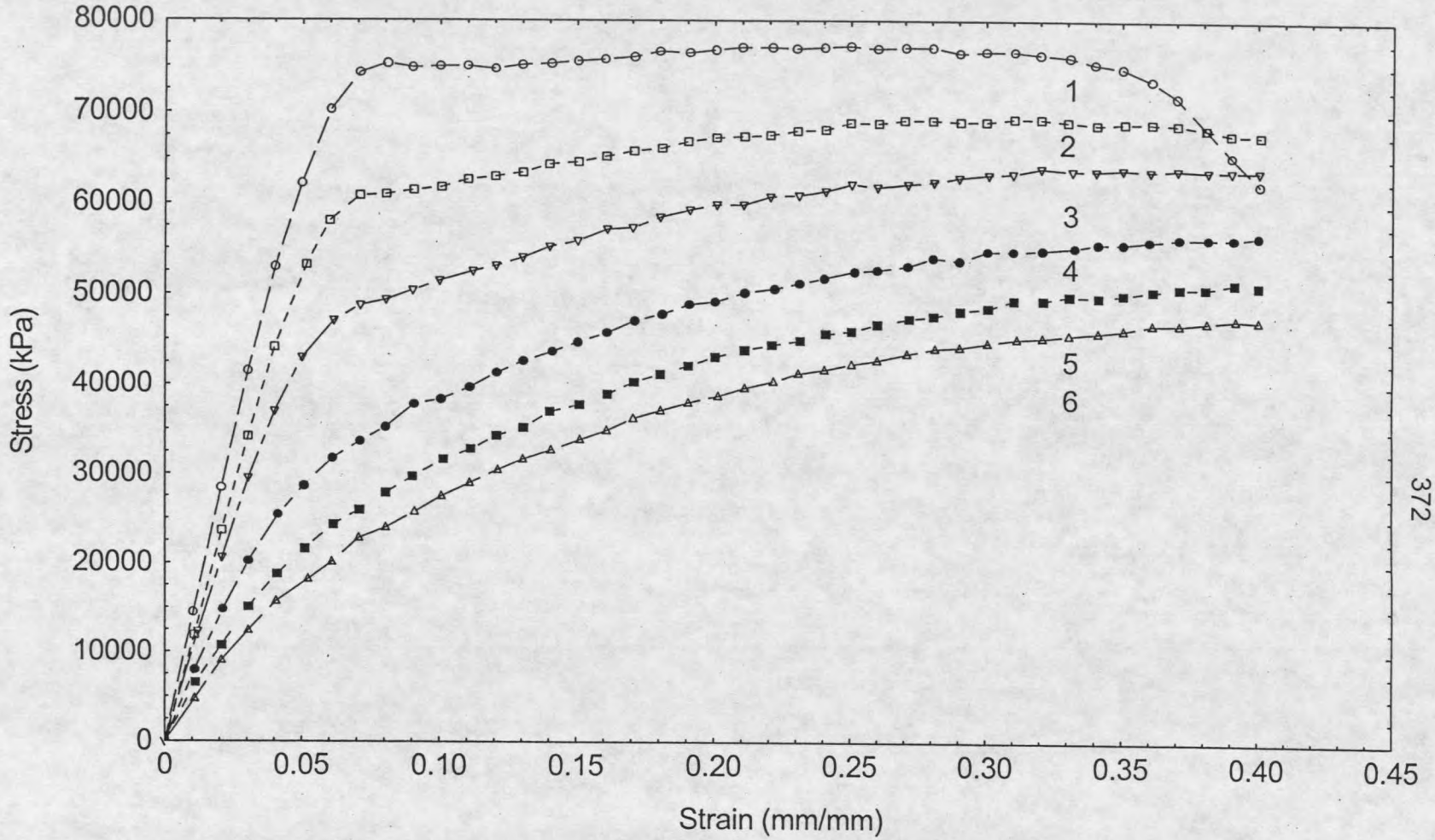


Figure F.1 Tensile Testing of Nylon 6/6 at Different Temperatures
1- 23 °C; 2- 35 °C; 3- 41 °C; 4- 50 °C; 5- 59 °C; 6- 68 °C;
σ_y = 70 MPa at 23 °C

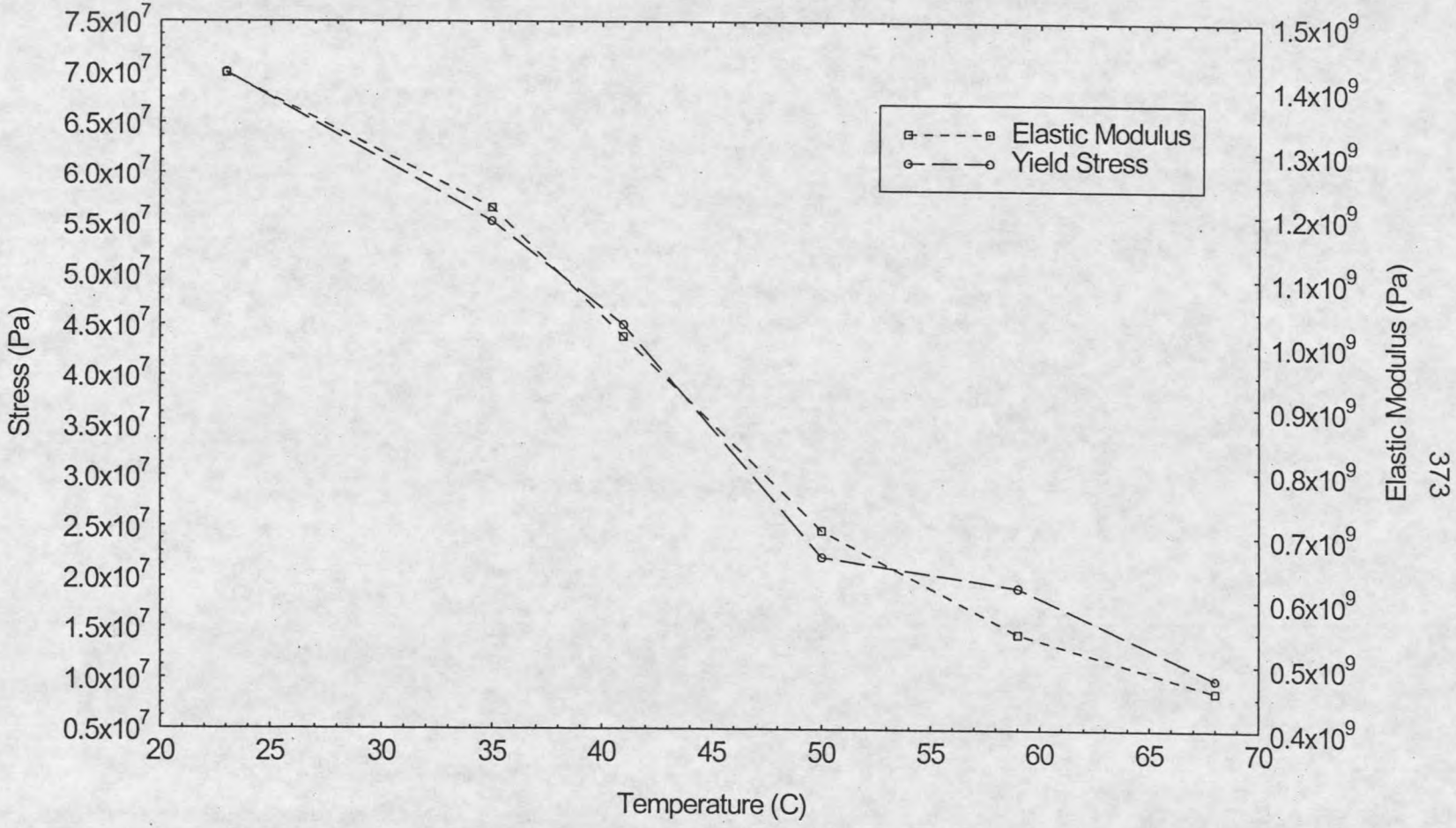


Figure F.2 Yield Stress and Elastic Modulus vs. Temperature

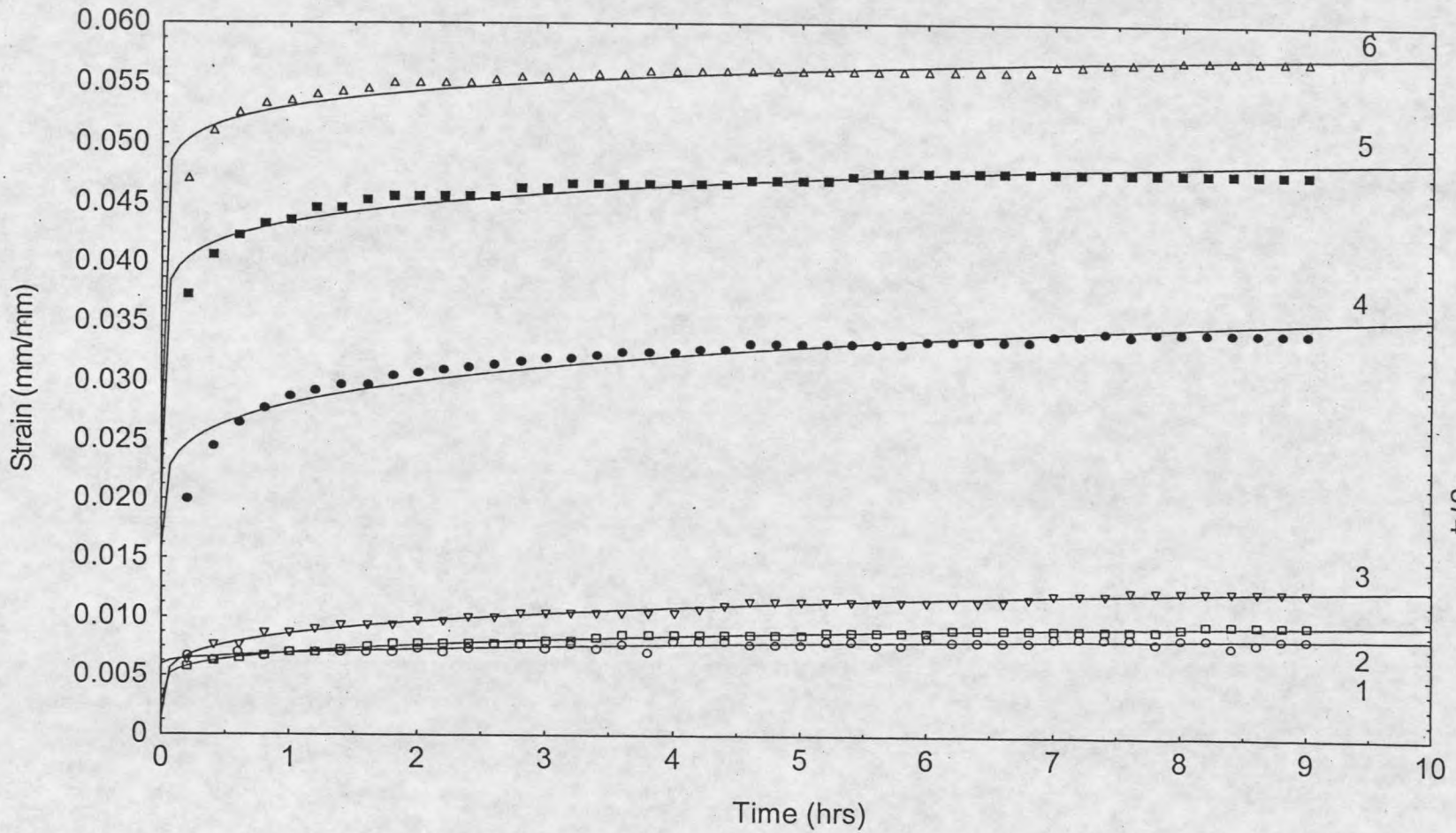


Figure F.3 Constant Load Creep of Nylon 6/6 at Different Temperatures
1- $(0.16)\sigma_y$ at 23 °C; 2- $(0.16)\sigma_y$ at 35 °C; 3- $(0.16)\sigma_y$ at 41 °C;
4- $(0.16)\sigma_y$ at 50 °C; 5- $(0.16)\sigma_y$ at 59 °C; 6- $(0.16)\sigma_y$ at 68 °C;
σ_y = 70 MPa at 23 °C

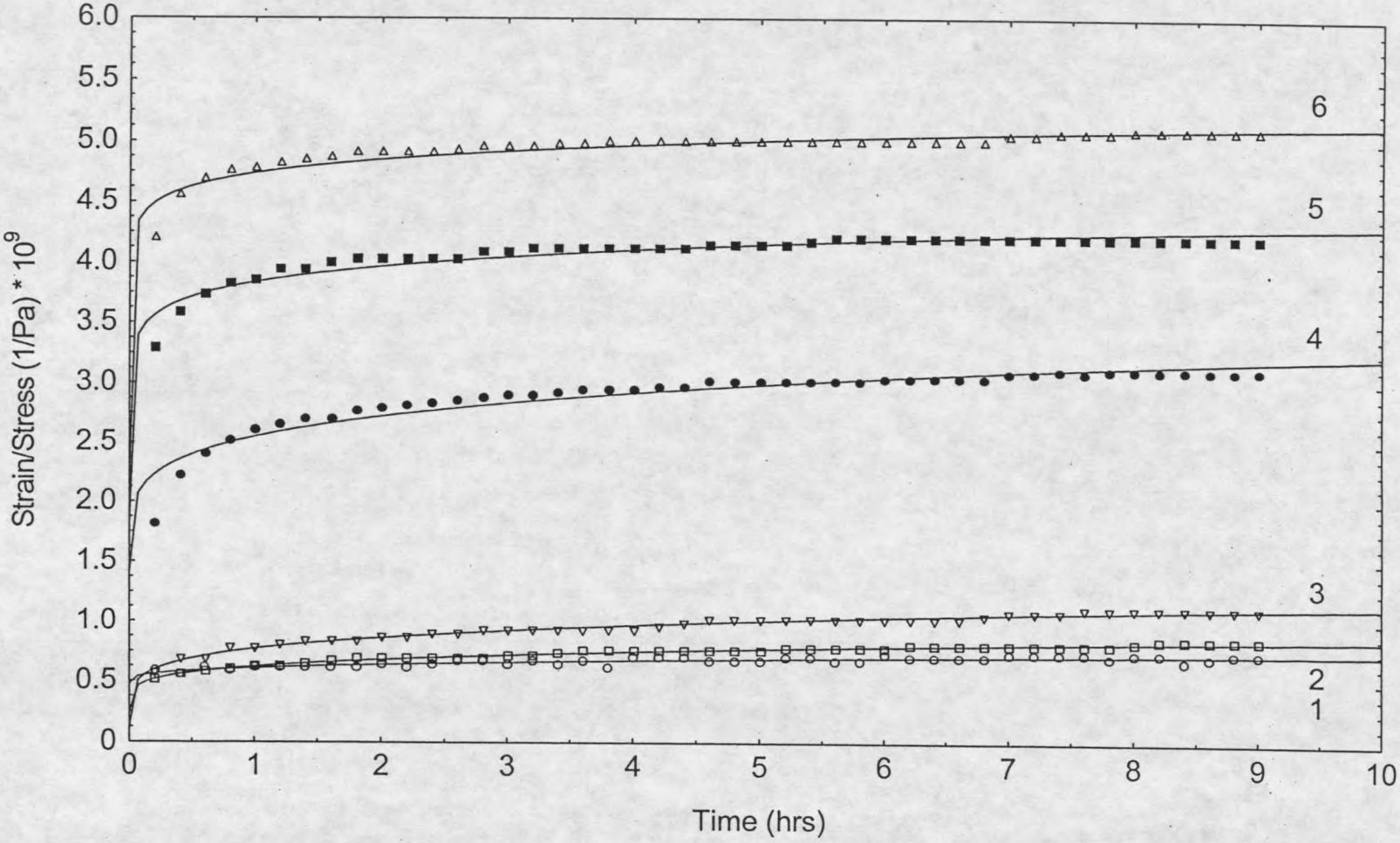


Figure F.4 Normalized Constant Load Creep of Nylon 6/6 at Different Temperatures
1- $(10.16)\sigma_y$ at 23 °C; 2- $(0.16)\sigma_y$ at 35 °C; 3- $(0.16)\sigma_y$ at 41 °C;
4- $(0.16)\sigma_y$ at 50 °C; 5- $(0.16)\sigma_y$ at 59 °C; 6- $(0.16)\sigma_y$ at 68 °C;
σ_y = 70 MPa at 23 °C

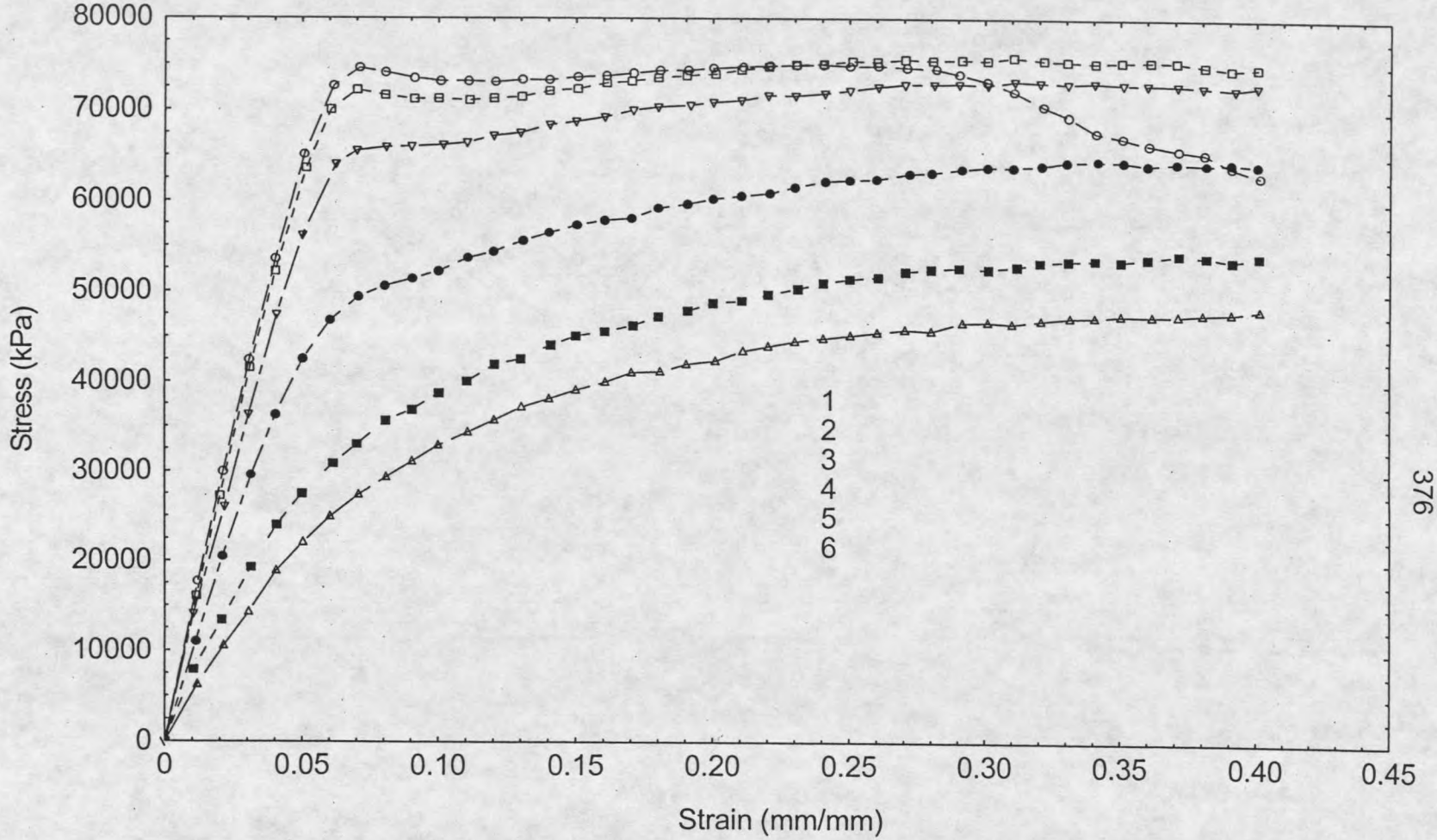


Figure F.5 Tensile Testing of Nylon 6/6 Specimens After Constant Loading
1- $(0.16)\sigma_y$ at 23 °C; 2- $(0.16)\sigma_y$ at 35 °C; 3- $(0.16)\sigma_y$ at 41 °C;
4- $(0.16)\sigma_y$ at 50 °C; 5- $(0.16)\sigma_y$ at 59 °C; 6- $(0.16)\sigma_y$ at 68 °C;
σ_y = 70 MPa at 23 °C

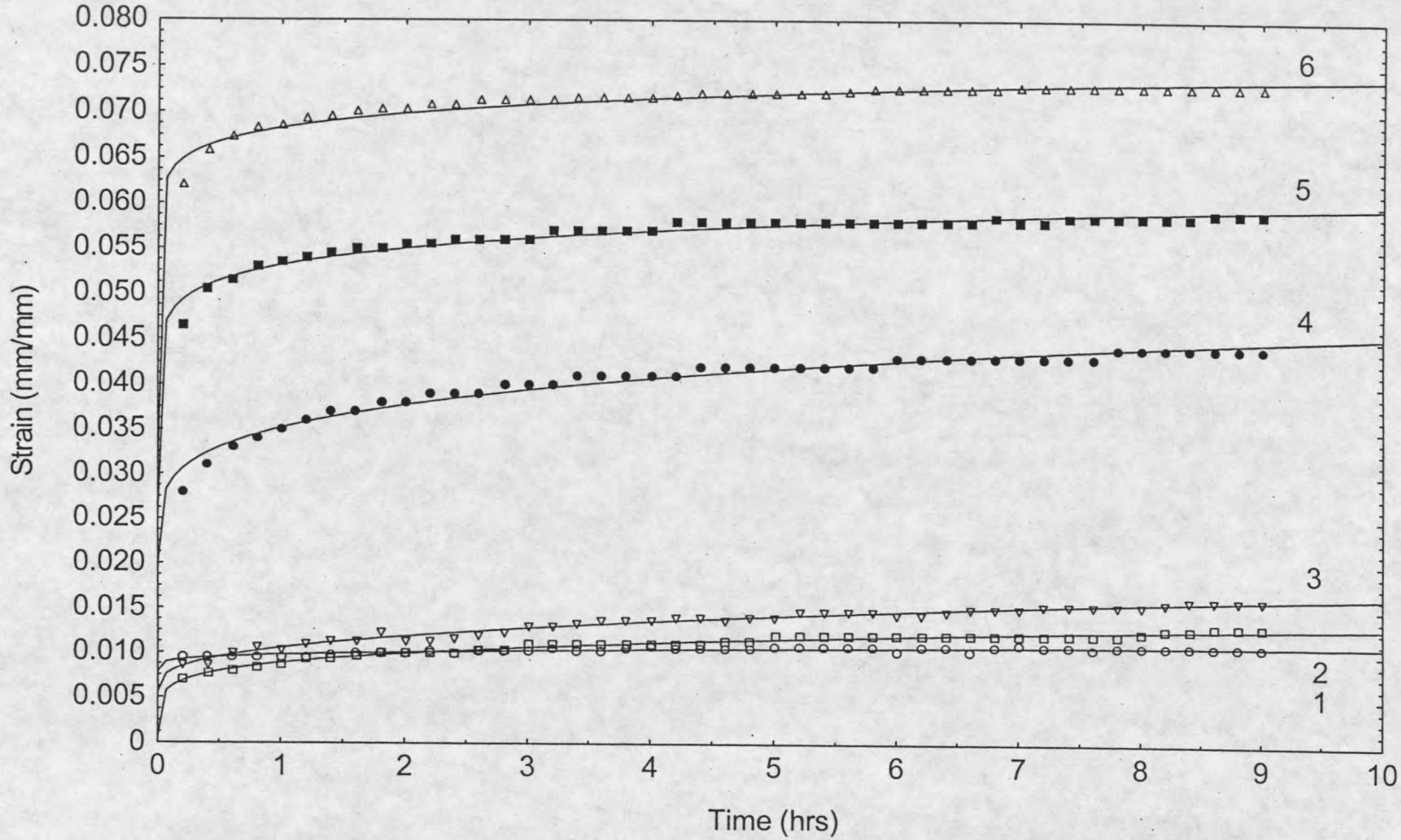


Figure F.6 Constant Load Creep of Nylon 6/6 at Different Temperatures
1- $(0.20)\sigma_y$ at 23 °C; 2- $(0.20)\sigma_y$ at 35 °C; 3- $(0.20)\sigma_y$ at 41 °C;
4- $(0.20)\sigma_y$ at 50 °C; 5- $(0.20)\sigma_y$ at 59 °C; 6- $(0.20)\sigma_y$ at 68 °C;
σ_y = 70 MPa at 23 °C

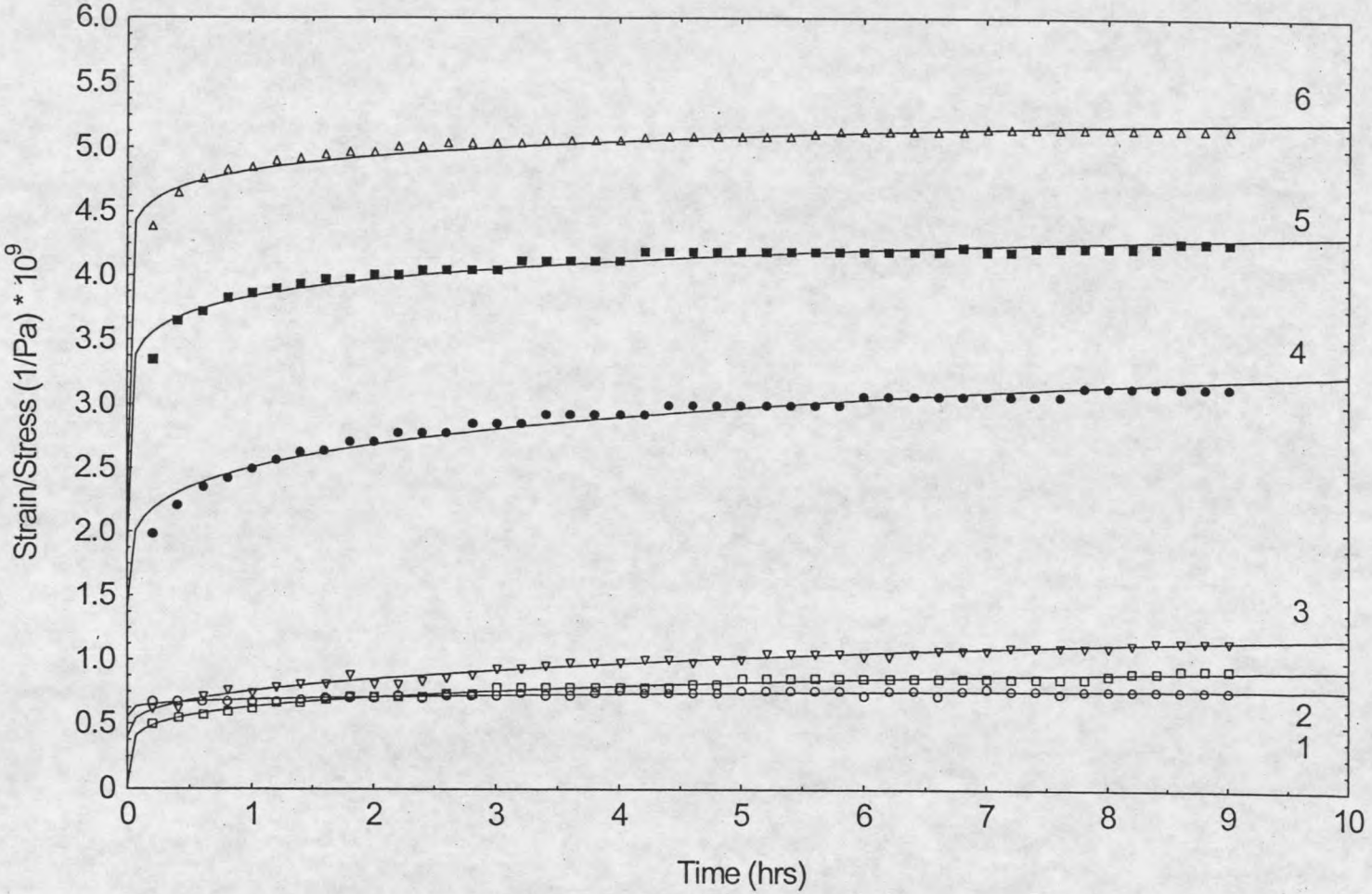


Figure F.7 Normalized Constant Load Creep of Nylon 6/6 at Different Temperatures
1- $(0.20)\sigma_y$ at 23 °C; 2- $(0.20)\sigma_y$ at 35 °C; 3- $(0.20)\sigma_y$ at 41 °C;
4- $(0.20)\sigma_y$ at 50 °C; 5- $(0.20)\sigma_y$ at 59 °C; 6- $(0.20)\sigma_y$ at 68 °C;
σ_y = 70 MPa at 23 °C

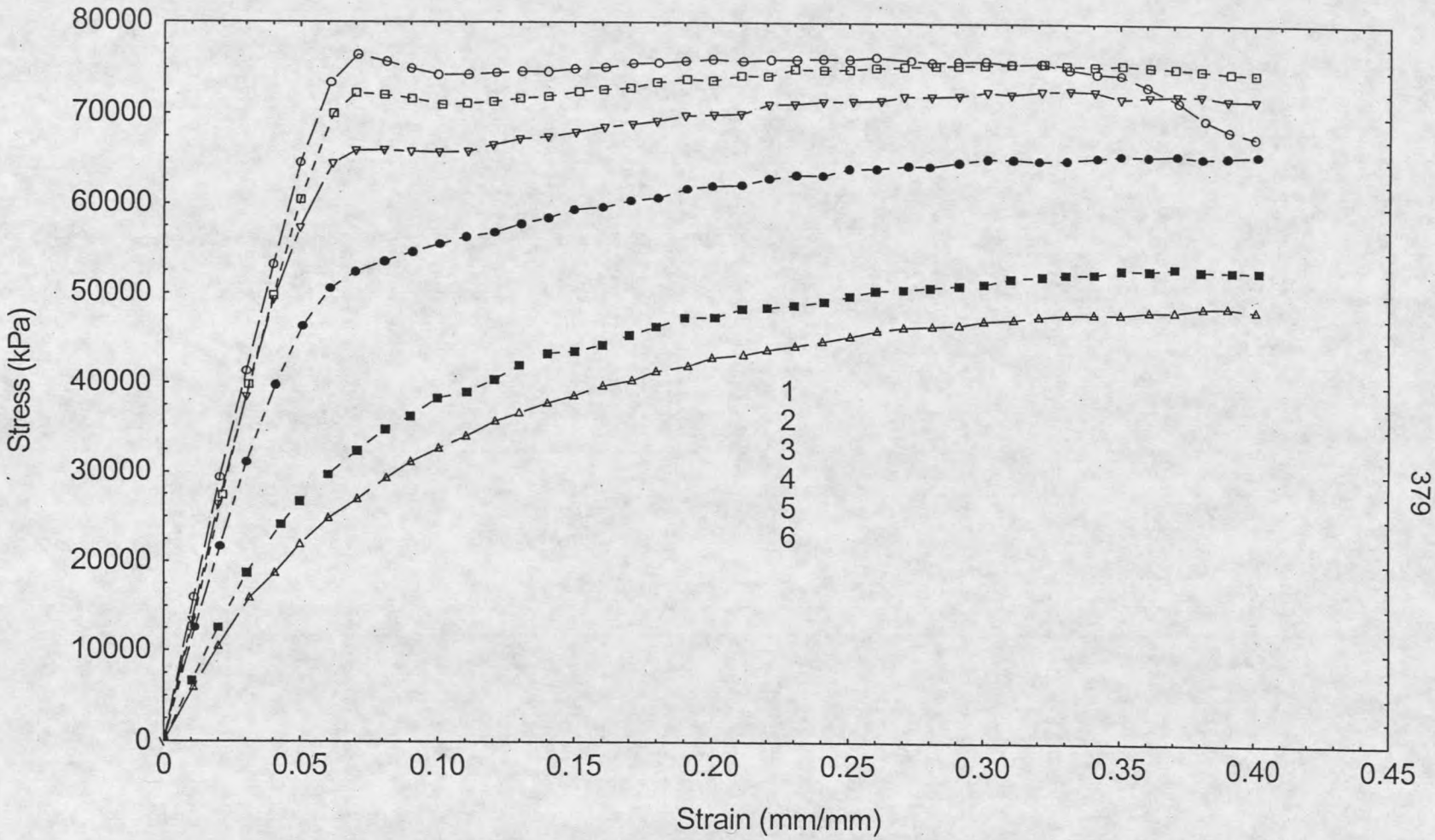


Figure F.8 Tensile Testing of Nylon 6/6 Specimens After Cyclic and Constant Loading
1- $(0.20)\sigma_y$ at 23 °C; 2- $(0.20)\sigma_y$ at 35 °C; 3- $(0.20)\sigma_y$ at 41 °C;
4- $(0.20)\sigma_y$ at 50 °C; 5- $(0.20)\sigma_y$ at 59 °C; 6- $(0.20)\sigma_y$ at 68 °C;
σ_y = 70 MPa at 23 °C

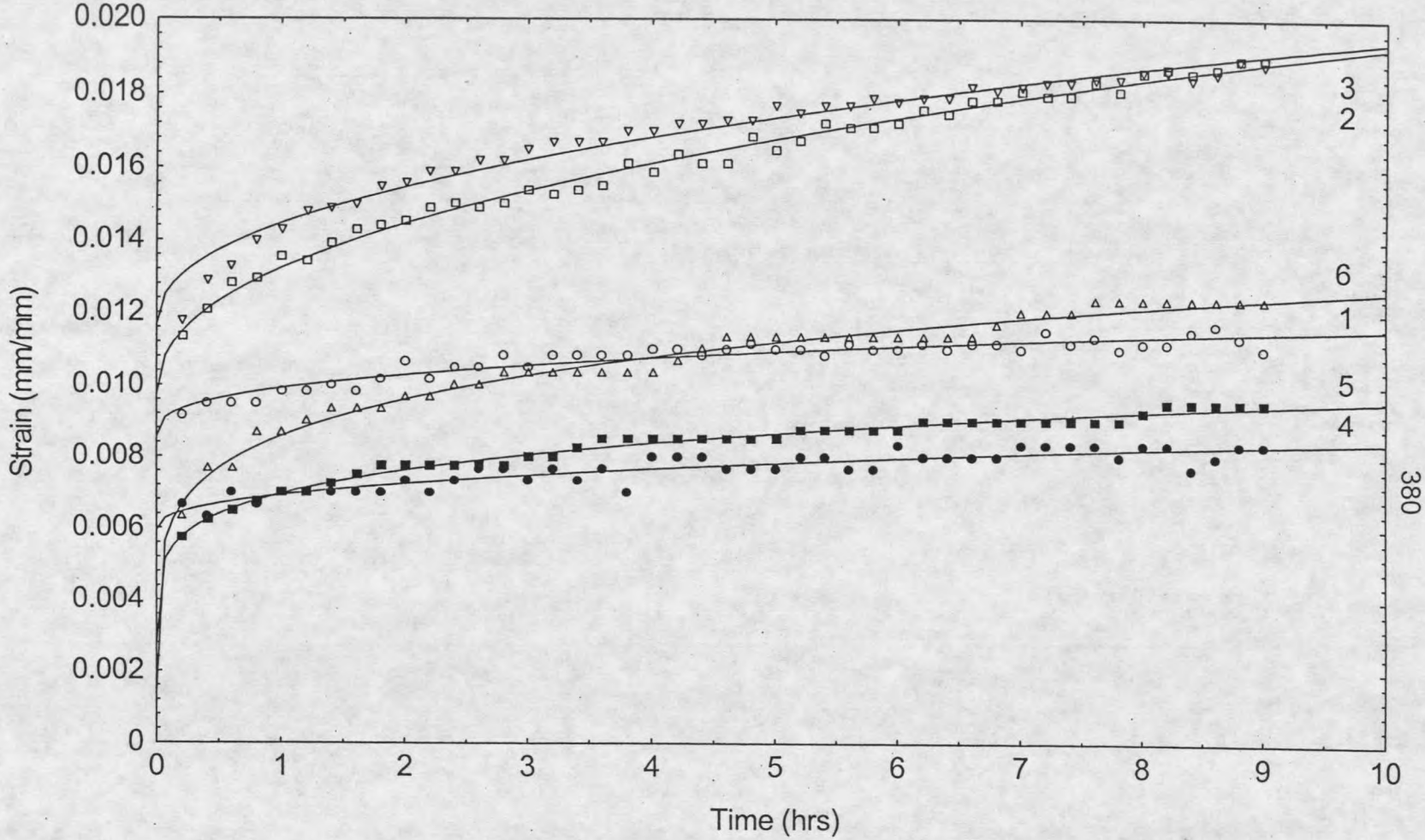


Figure F.9 Vibrocreep Response of Nylon 6/6 at Different Temperatures
1- $(0.16\pm0.04)\sigma_y$, 1 Hz at 23 °C; 2- $(0.16\pm0.04)\sigma_y$, 1 Hz at 35 °C; 3- $(0.16\pm0.04)\sigma_y$, 1 Hz at 41 °C;
4- $(0.16)\sigma_y$ at 23 °C, 5- $(0.16)\sigma_y$ at 35 °C, 6- $(0.16)\sigma_y$ at 41 °C, Constant Load Creep;
σ_y = 70 MPa at 23 °C

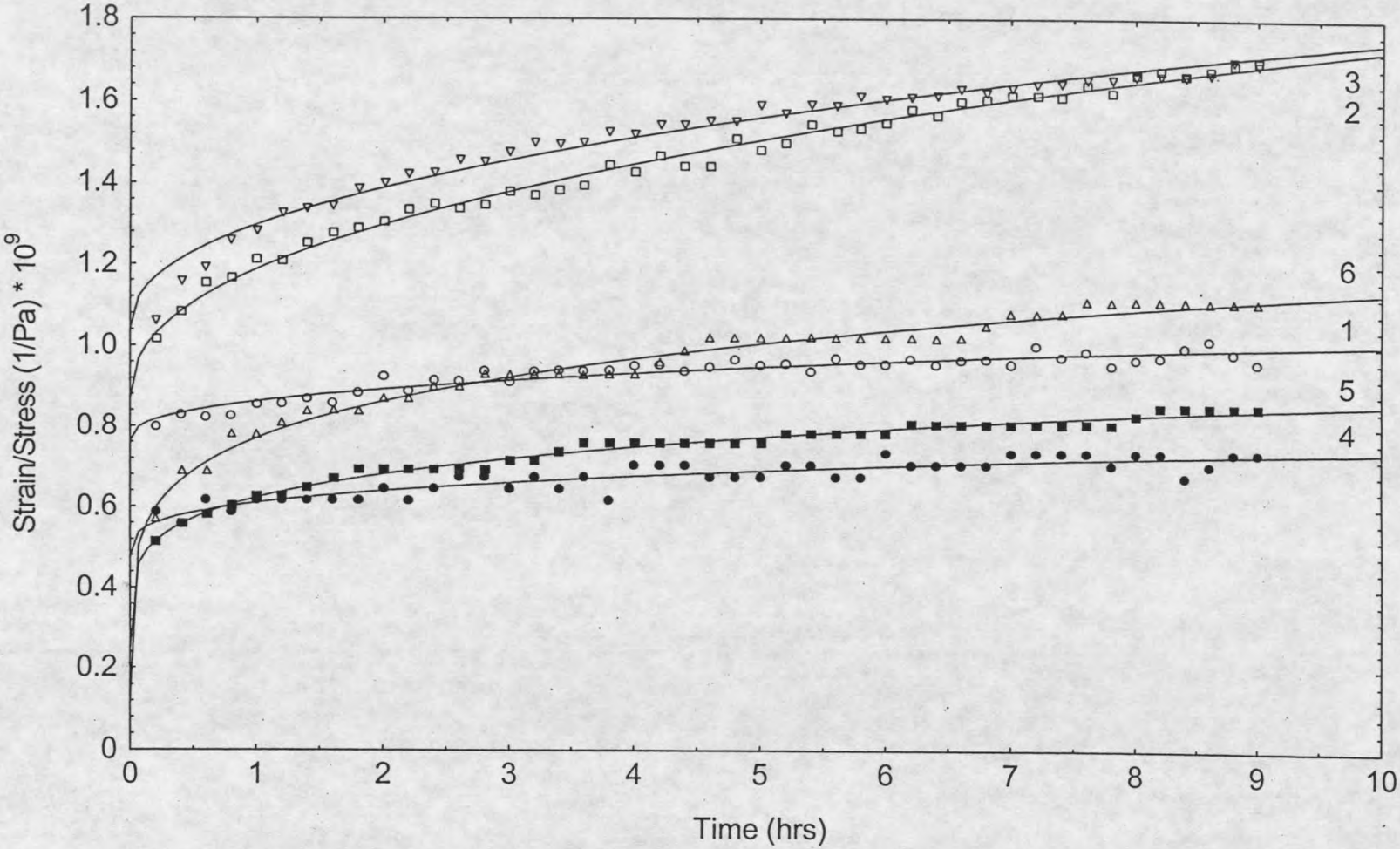


Figure F.10 Normalized Vibrocreep Response of Nylon 6/6 at Different Temperatures
1- $(0.16\pm0.04)\sigma_y$, 1 Hz at 23 °C; 2- $(0.16\pm0.04)\sigma_y$, 1 Hz at 35 °C; 3- $(0.16\pm0.04)\sigma_y$, 1 Hz at 41 °C;
4- $(0.16)\sigma_y$ at 23 °C, 5- $(0.16)\sigma_y$ at 35 °C, 6- $(0.16)\sigma_y$ at 41 °C, Constant Load Creep;
σ_y = 70 MPa at 23 °C

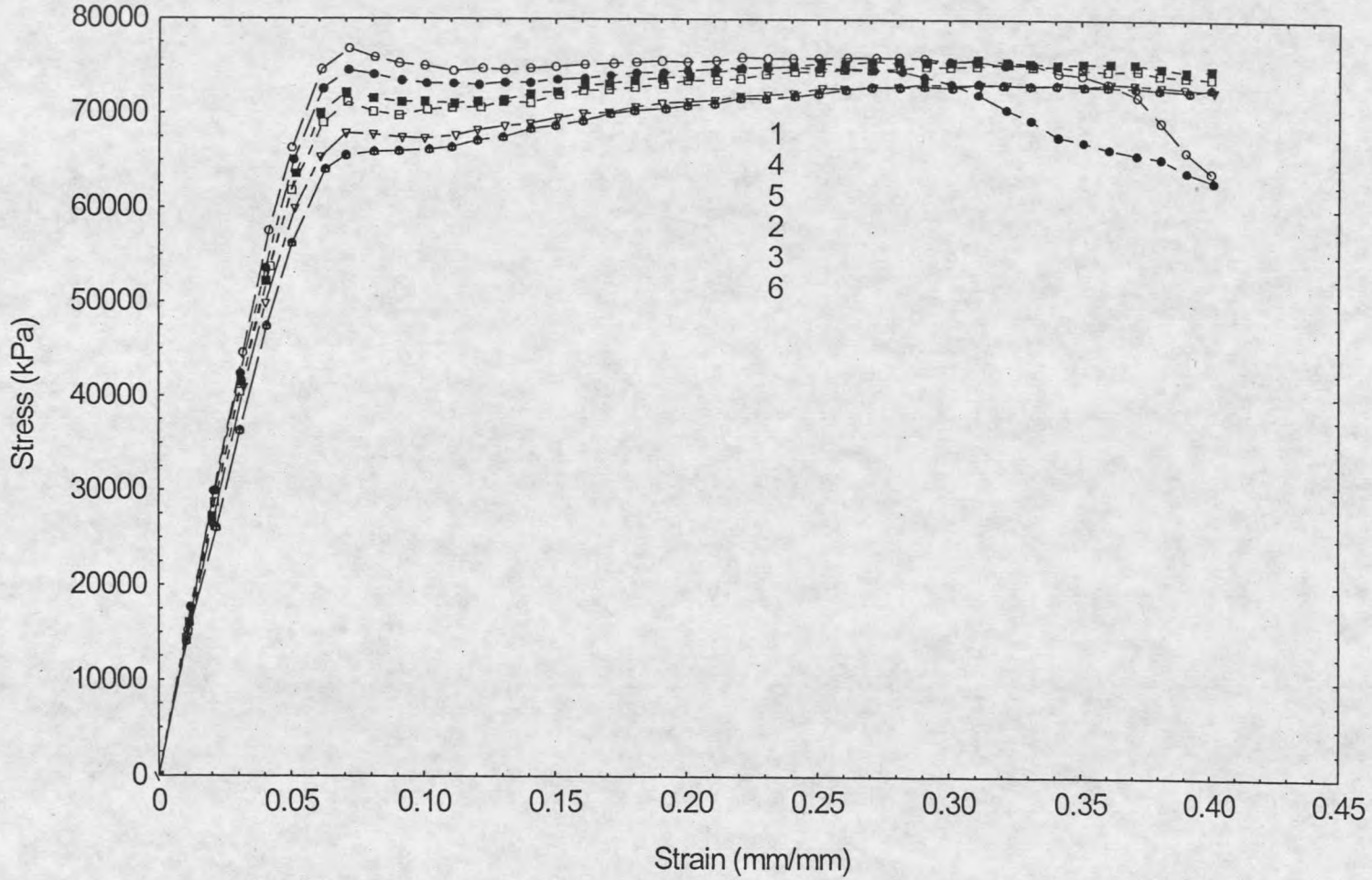


Figure F.11 Tensile Testing of Nylon 6/6 Specimens After Cyclic and Constant Loading
1- $(0.16\pm0.04)\sigma_y$, 1 Hz at 23 °C; 2- $(0.16\pm0.04)\sigma_y$, 1 Hz at 35 °C; 3- $(0.16\pm0.04)\sigma_y$, 1 Hz at 41 °C;
4- $(0.16)\sigma_y$ at 23 °C, 5- $(0.16)\sigma_y$ at 35 °C, 6- $(0.16)\sigma_y$ at 41 °C, Constant Load Creep;
σ_y = 70 MPa at 23 °C

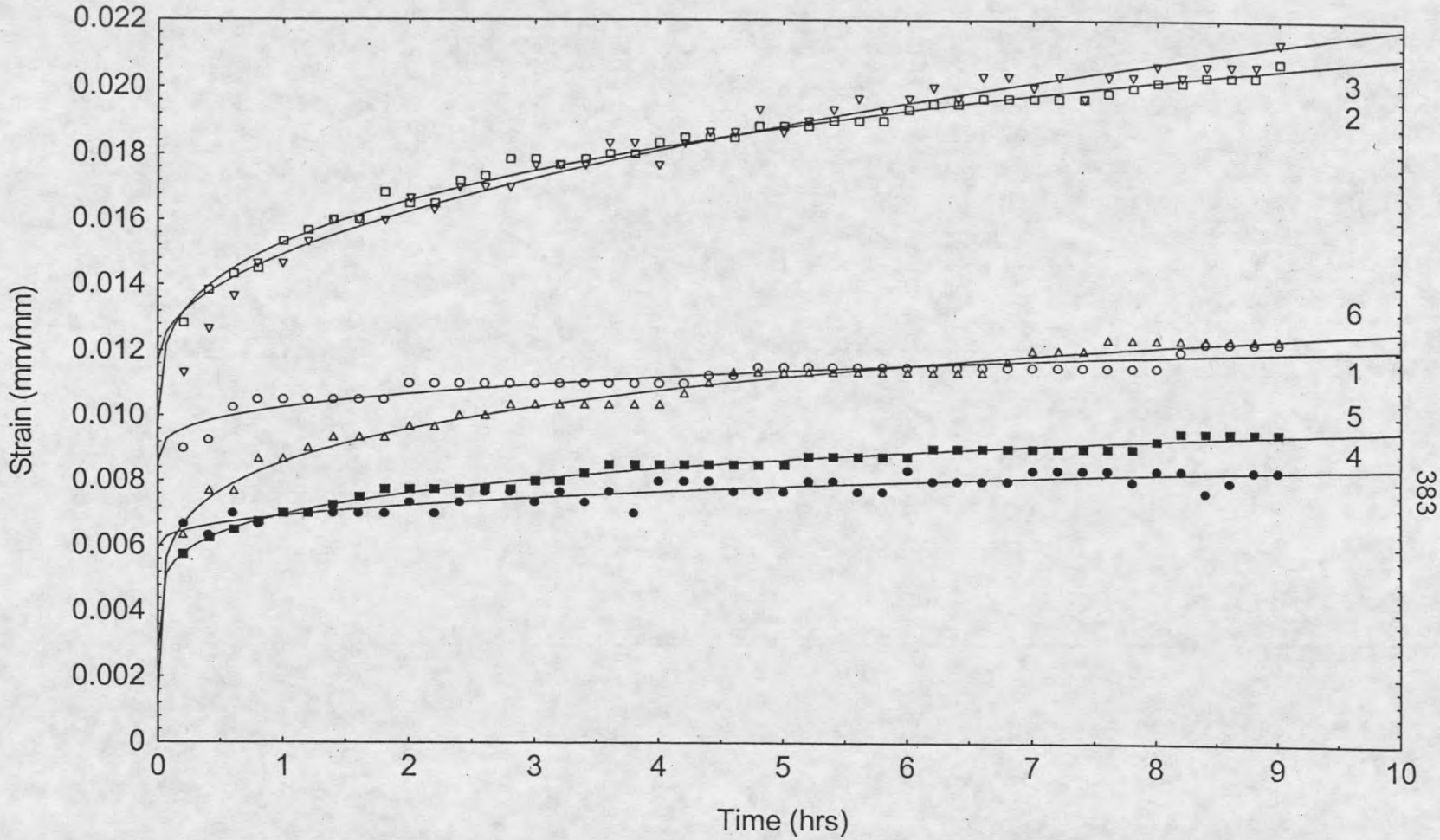


Figure F.12 Vibrocreep Response of Nylon 6/6 at Different Temperatures
1- $(0.16\pm0.04)\sigma_y$, 10 Hz at 23 °C; 2- $(0.16\pm0.04)\sigma_y$, 10 Hz at 35 °C; 3- $(0.16\pm0.04)\sigma_y$, 10 Hz at 41 °C;
4- $(0.16)\sigma_y$ at 23 °C, 5- $(0.16)\sigma_y$ at 35 °C, 6- $(0.16)\sigma_y$ at 41 °C, Constant Load Creep;
σ_y = 70 MPa at 23 °C

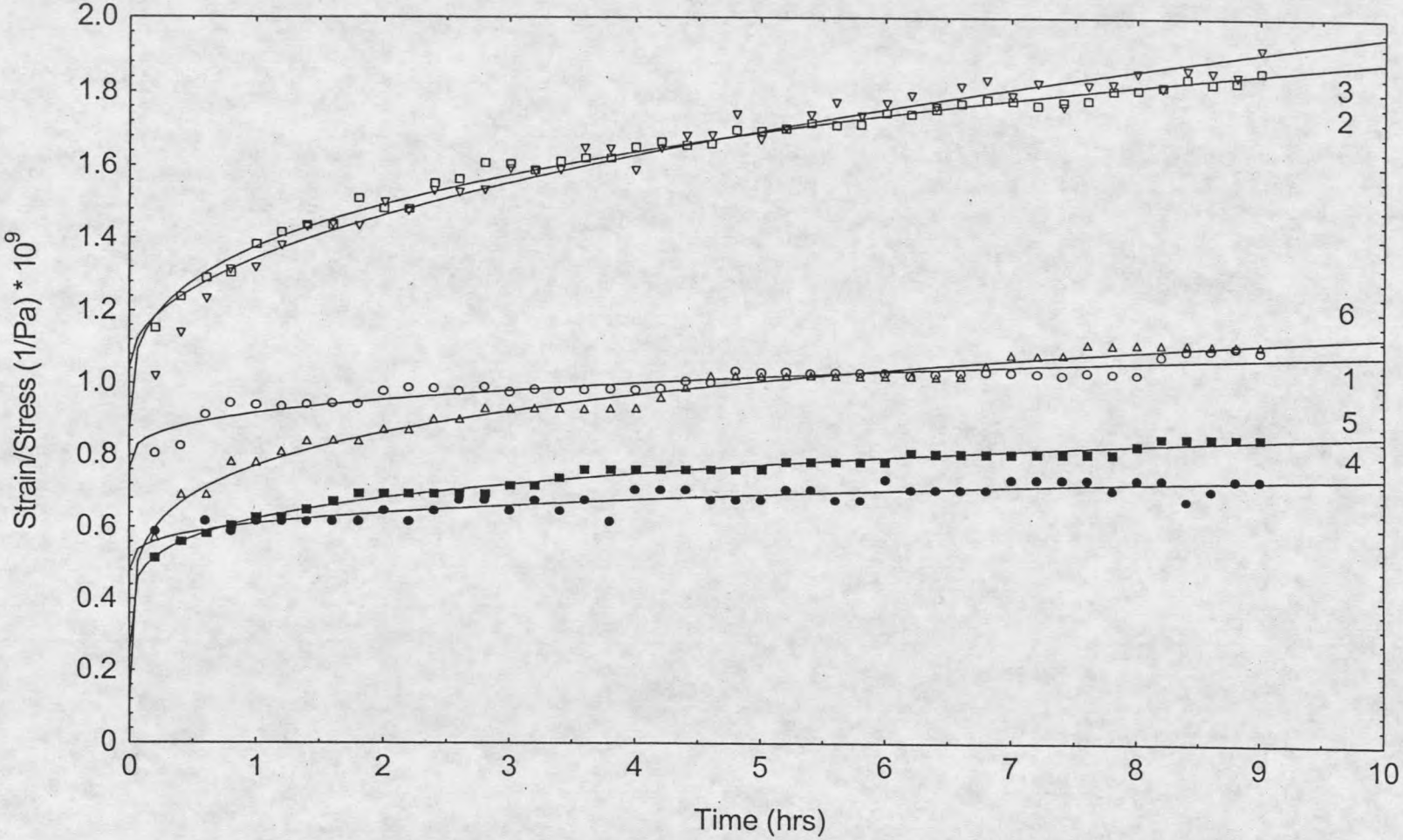


Figure F.13 Normalized Vibrocreep Response of Nylon 6/6 at Different Temperatures
1- $(0.16\pm0.04)\sigma_y$, 10 Hz at 23 °C; 2- $(0.16\pm0.04)\sigma_y$, 10 Hz at 35 °C; 3- $(0.16\pm0.04)\sigma_y$, 10 Hz at 41 °C;
4- $(0.16)\sigma_y$ at 23 °C, 5- $(0.16)\sigma_y$ at 35 °C, 6- $(0.16)\sigma_y$ at 41 °C, Constant Load Creep;
σ_y = 70 MPa at 23 °C

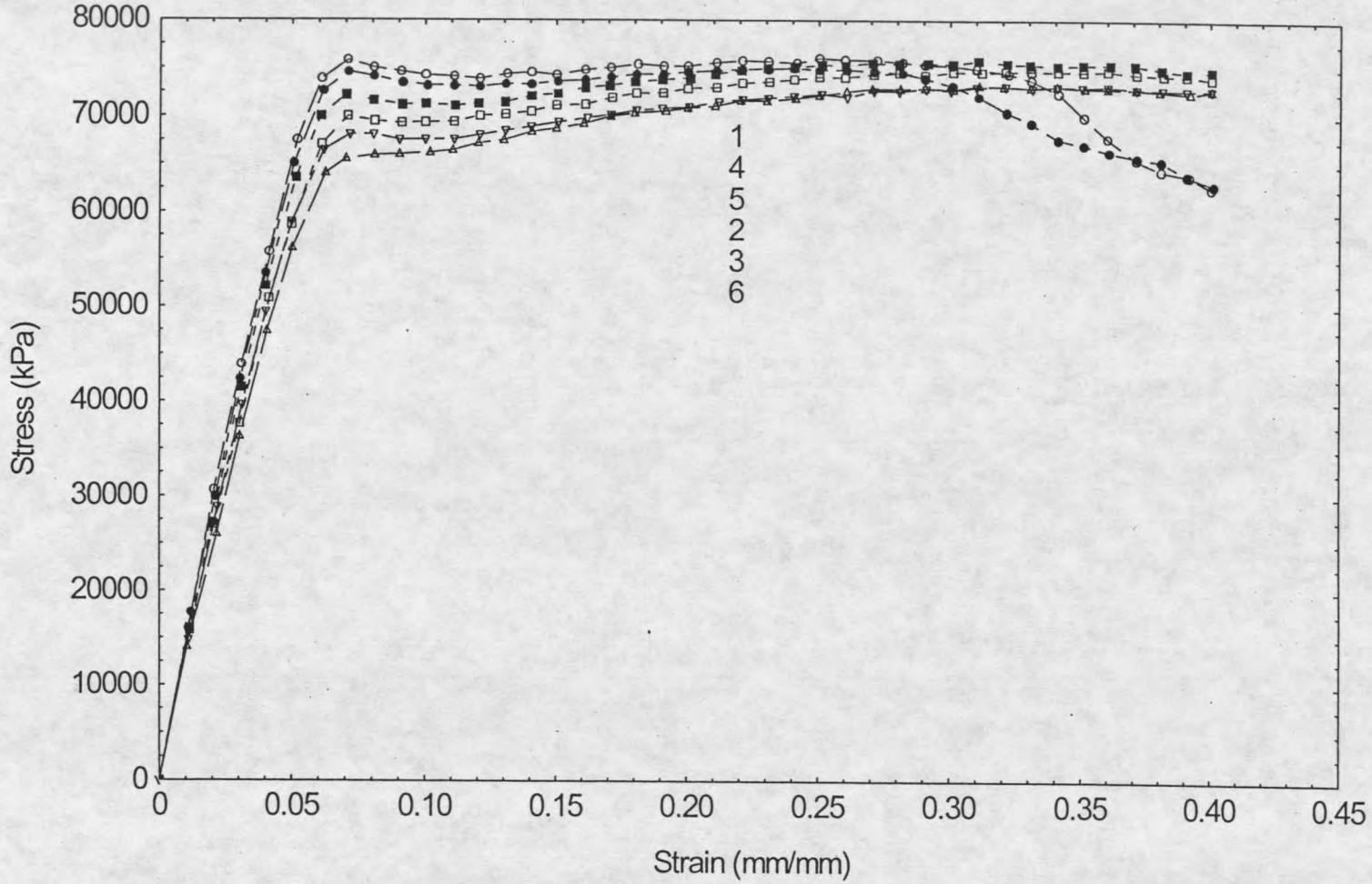


Figure F.14 Tensile Testing of Nylon 6/6 Specimens After Cyclic and Constant Loading
1- $(0.16\pm0.04)\sigma_y$, 10 Hz at 23 °C; 2- $(0.16\pm0.04)\sigma_y$, 10 Hz at 35 °C; 3- $(0.16\pm0.04)\sigma_y$, 10 Hz at 41 °C;
4- $(0.16)\sigma_y$ at 23 °C, 5- $(0.16)\sigma_y$ at 35 °C, 6- $(0.16)\sigma_y$ at 41 °C, Constant Load Creep;
σ_y = 70 MPa at 23 °C

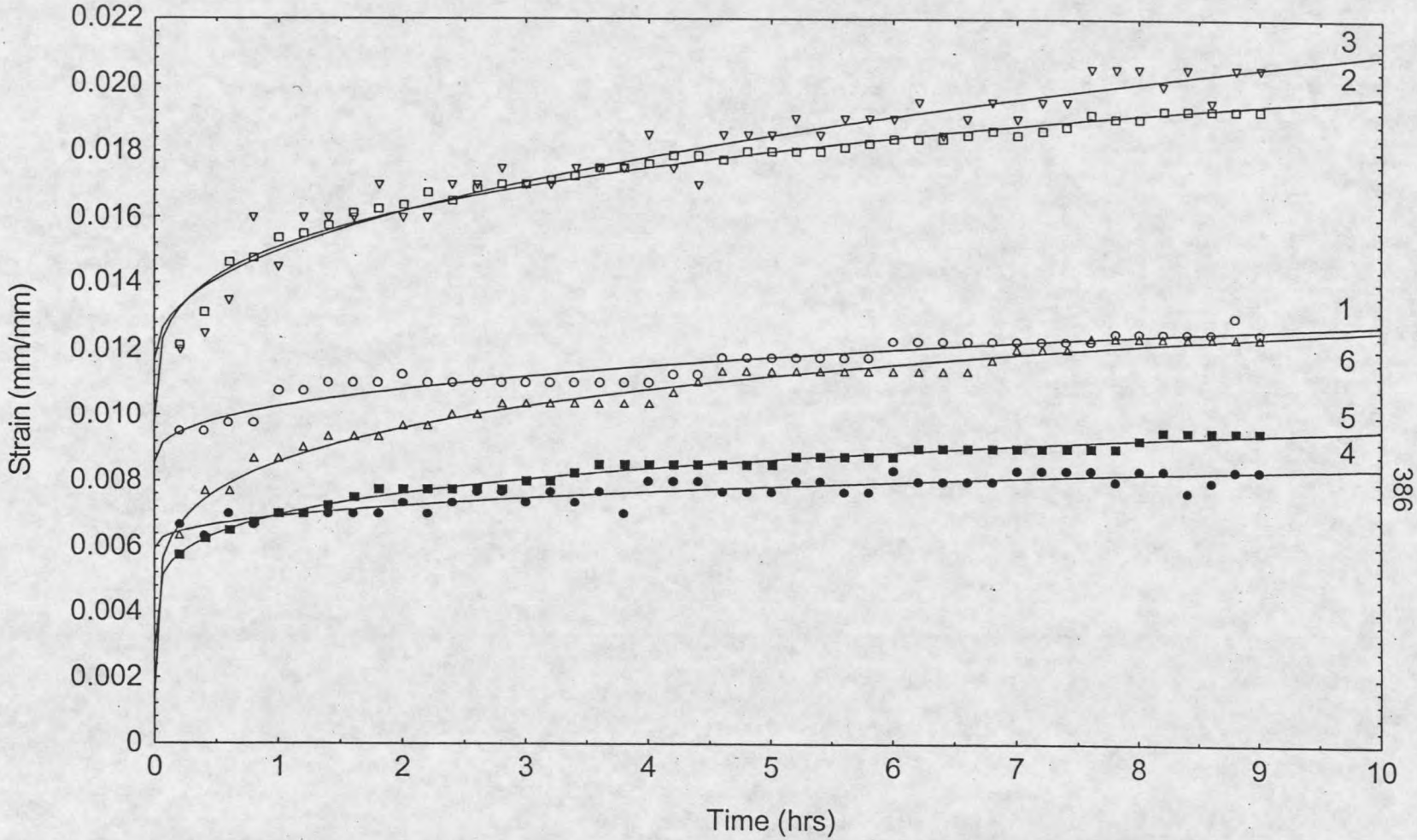


Figure F.15 Vibrocreep Response of Nylon 6/6 at Different Temperatures
1- $(0.16\pm0.10)\sigma_y$, 1 Hz at 23 °C; 2- $(0.16\pm0.10)\sigma_y$, 1 Hz at 35 °C; 3- $(0.16\pm0.10)\sigma_y$, 1 Hz at 41 °C;
4- $(0.16)\sigma_y$ at 23 °C, 5- $(0.16)\sigma_y$ at 35 °C, 6- $(0.16)\sigma_y$ at 41 °C, Constant Load Creep;
σ_y = 70 MPa at 23 °C

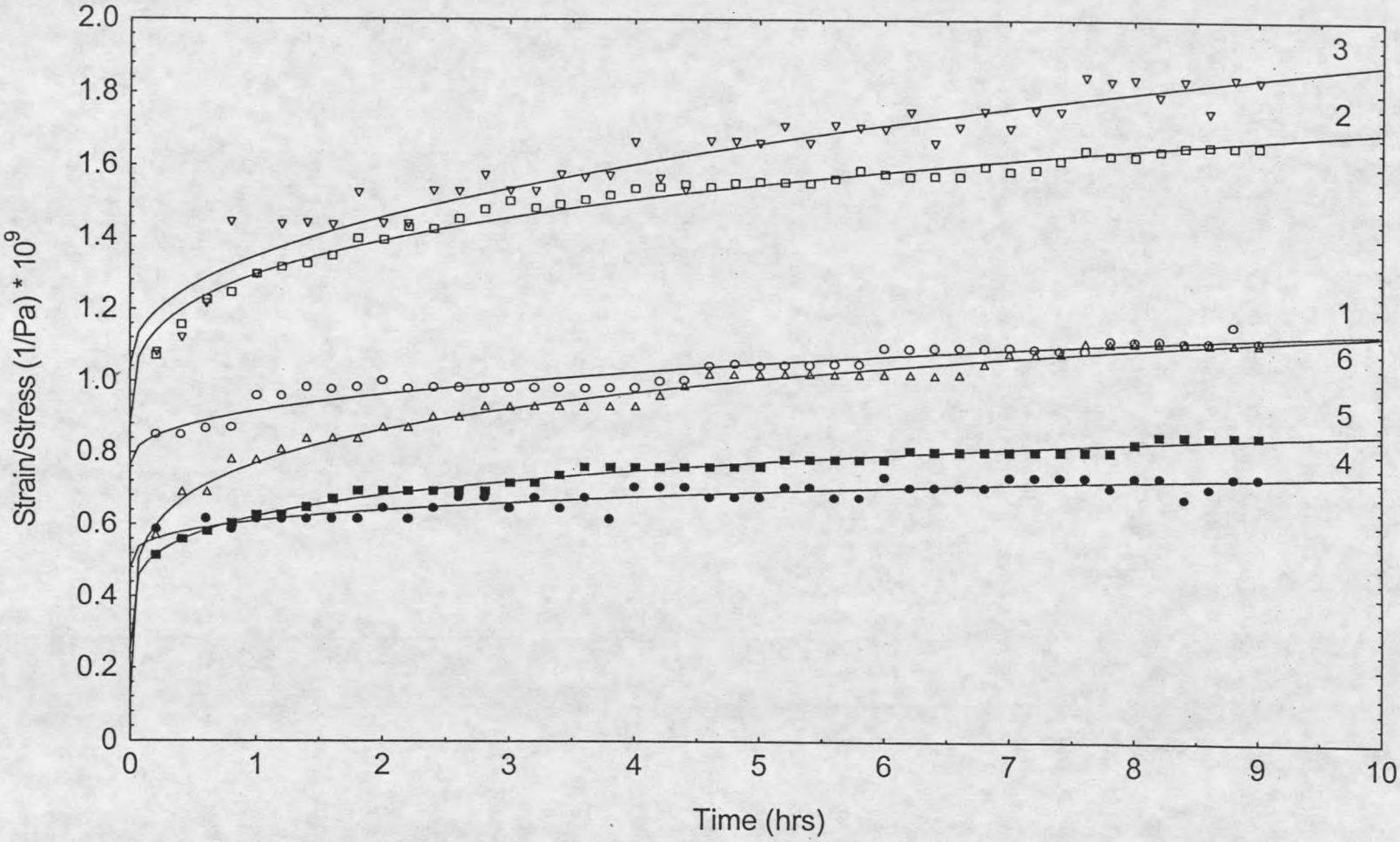


Figure F.16 Normalized Vibrocreep Response of Nylon 6/6 at Different Temperatures
1- $(0.16\pm0.10)\sigma_y$, 1 Hz at 23 °C; 2- $(0.16\pm0.10)\sigma_y$, 1 Hz at 35 °C; 3- $(0.16\pm0.10)\sigma_y$, 1 Hz at 41 °C;
4- $(0.16)\sigma_y$ at 23 °C, 5- $(0.16)\sigma_y$ at 35 °C, 6- $(0.16)\sigma_y$ at 41 °C, Constant Load Creep;
σ_y = 70 MPa at 23 °C

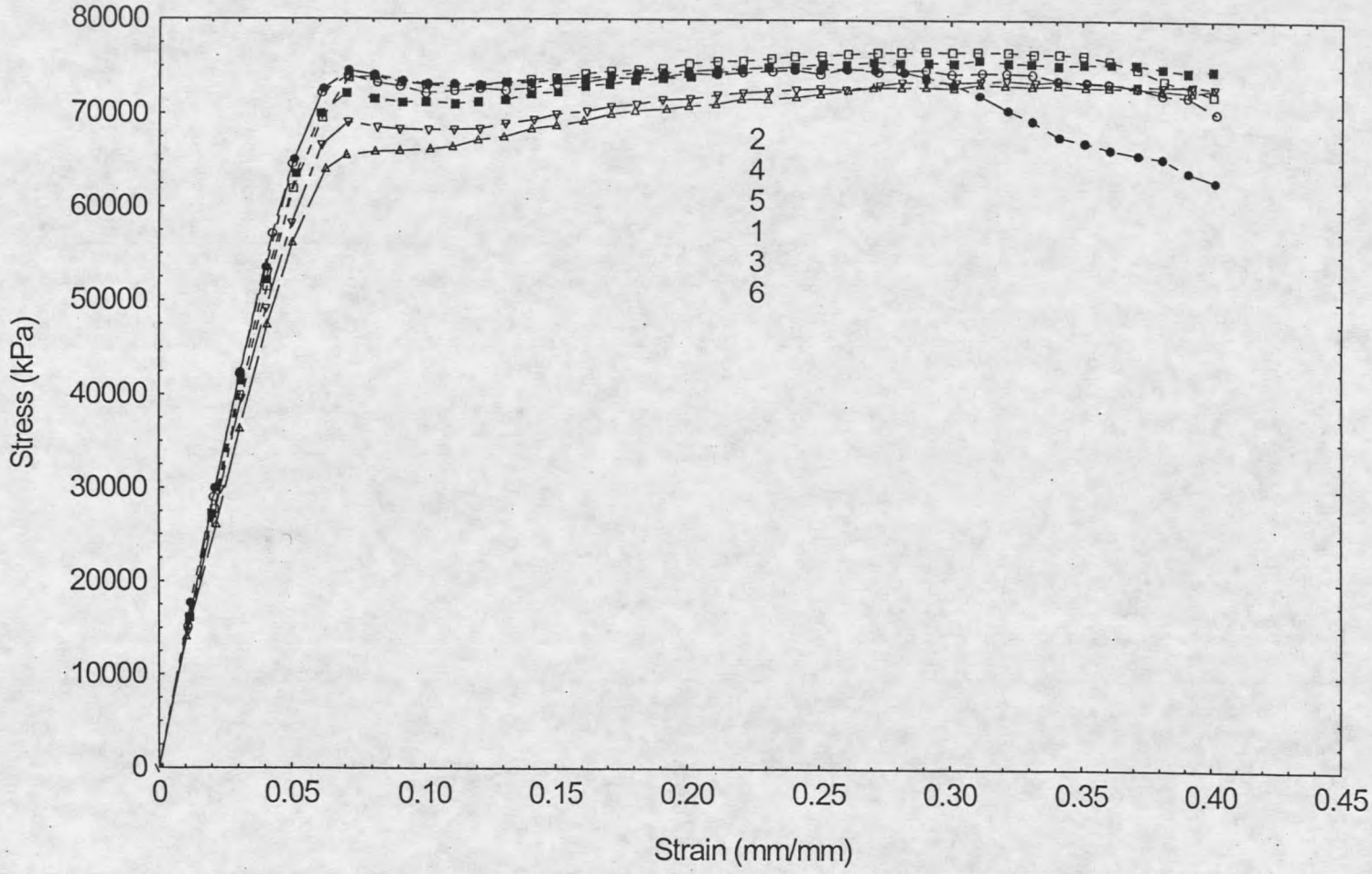


Figure F.17 Tensile Testing of Nylon 6/6 Specimens After Cyclic and Constant Loading
1- $(0.16\pm0.10)\sigma_y$, 1 Hz at 23 °C; 2- $(0.16\pm0.10)\sigma_y$, 1 Hz at 35 °C; 3- $(0.16\pm0.10)\sigma_y$, 1 Hz at 41 °C;
4- $(0.16)\sigma_y$ at 23 °C, 5- $(0.16)\sigma_y$ at 35 °C, 6- $(0.16)\sigma_y$ at 41 °C, Constant Load Creep;
σ_y = 70 MPa at 23 °C

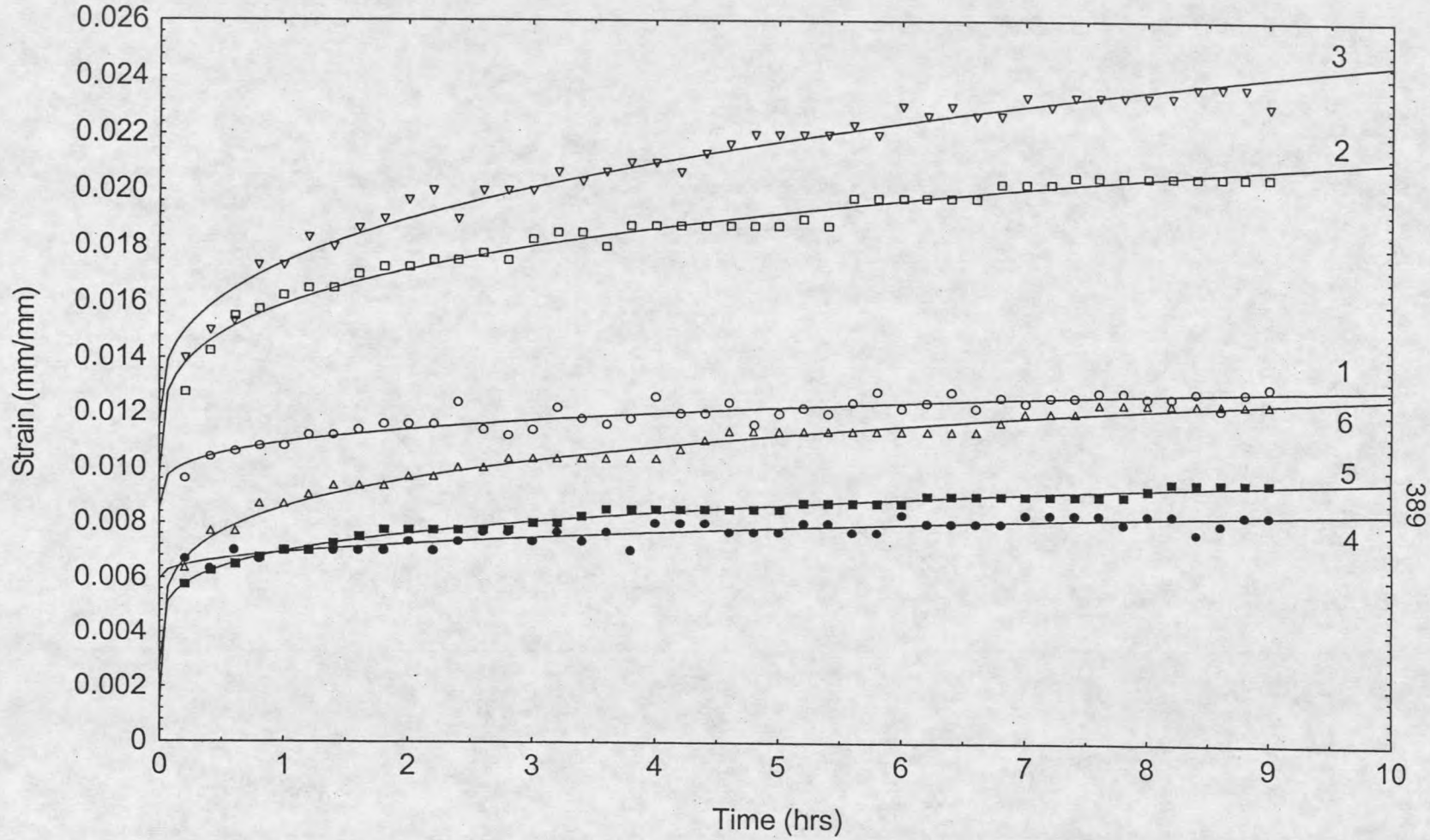


Figure F.18 Vibrocreep Response of Nylon 6/6 at Different Temperatures
1- $(0.16\pm0.10)\sigma_y$, 10 Hz at 23 °C; 2- $(0.16\pm0.10)\sigma_y$, 10 Hz at 35 °C; 3- $(0.16\pm0.10)\sigma_y$, 10 Hz at 41 °C;
4- $(0.16)\sigma_y$ at 23 °C, 5- $(0.16)\sigma_y$ at 35 °C, 6- $(0.16)\sigma_y$ at 41 °C, Constant Load Creep;
σ_y = 70 MPa at 23 °C

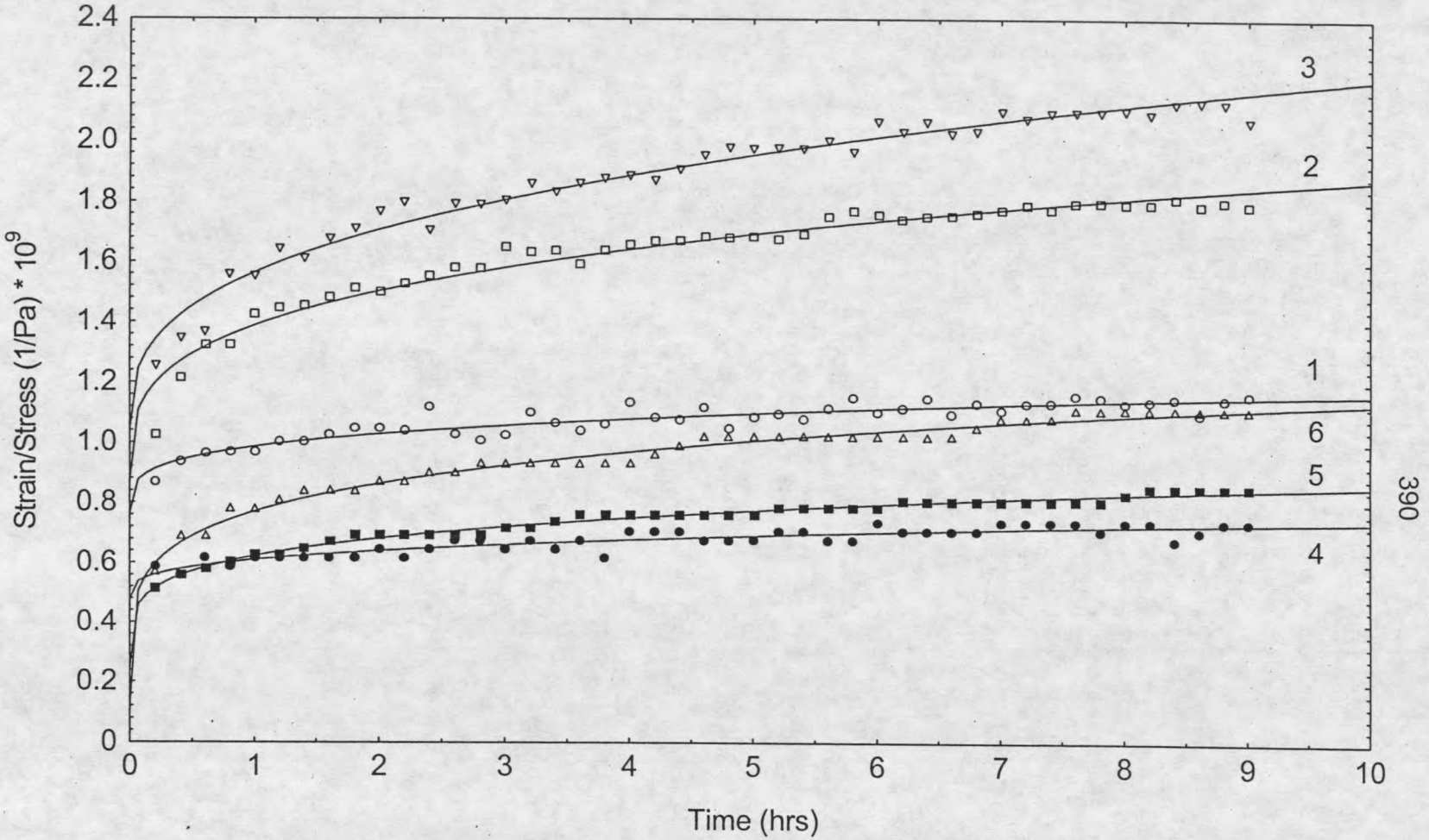


Figure F.19 Normalized Vibrocreep Response of Nylon 6/6 at Different Temperatures
1- $(0.16\pm0.10)\sigma_y$, 10 Hz at 23 °C; 2- $(0.16\pm0.10)\sigma_y$, 10 Hz at 35 °C; 3- $(0.16\pm0.10)\sigma_y$, 10 Hz at 41 °C;
4- $(0.16)\sigma_y$ at 23 °C, 5- $(0.16)\sigma_y$ at 35 °C, 6- $(0.16)\sigma_y$ at 41 °C, Constant Load Creep;
σ_y = 70 MPa at 23 °C

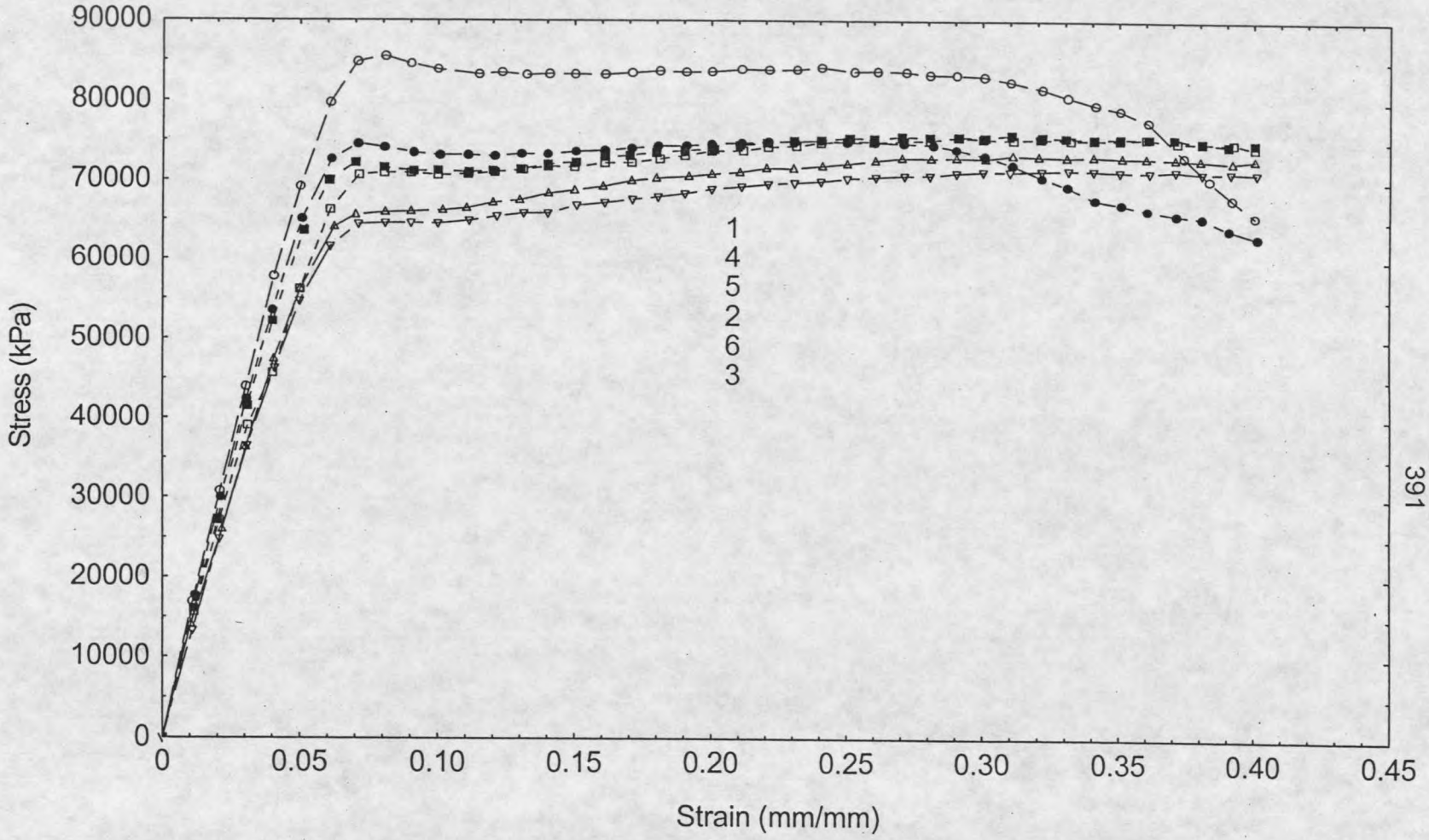


Figure F.20 Tensile Testing of Nylon 6/6 Specimens After Cyclic and Constant Loading
1- $(0.16\pm0.10)\sigma_y$, 10 Hz at 23 °C; 2- $(0.16\pm0.10)\sigma_y$, 10 Hz at 35 °C; 3- $(0.16\pm0.10)\sigma_y$, 10 Hz at 41 °C;
4- $(0.16)\sigma_y$ at 23 °C, 5- $(0.16)\sigma_y$ at 35 °C, 6- $(0.16)\sigma_y$ at 41 °C, Constant Load Creep;
σ_y = 70 MPa at 23 °C

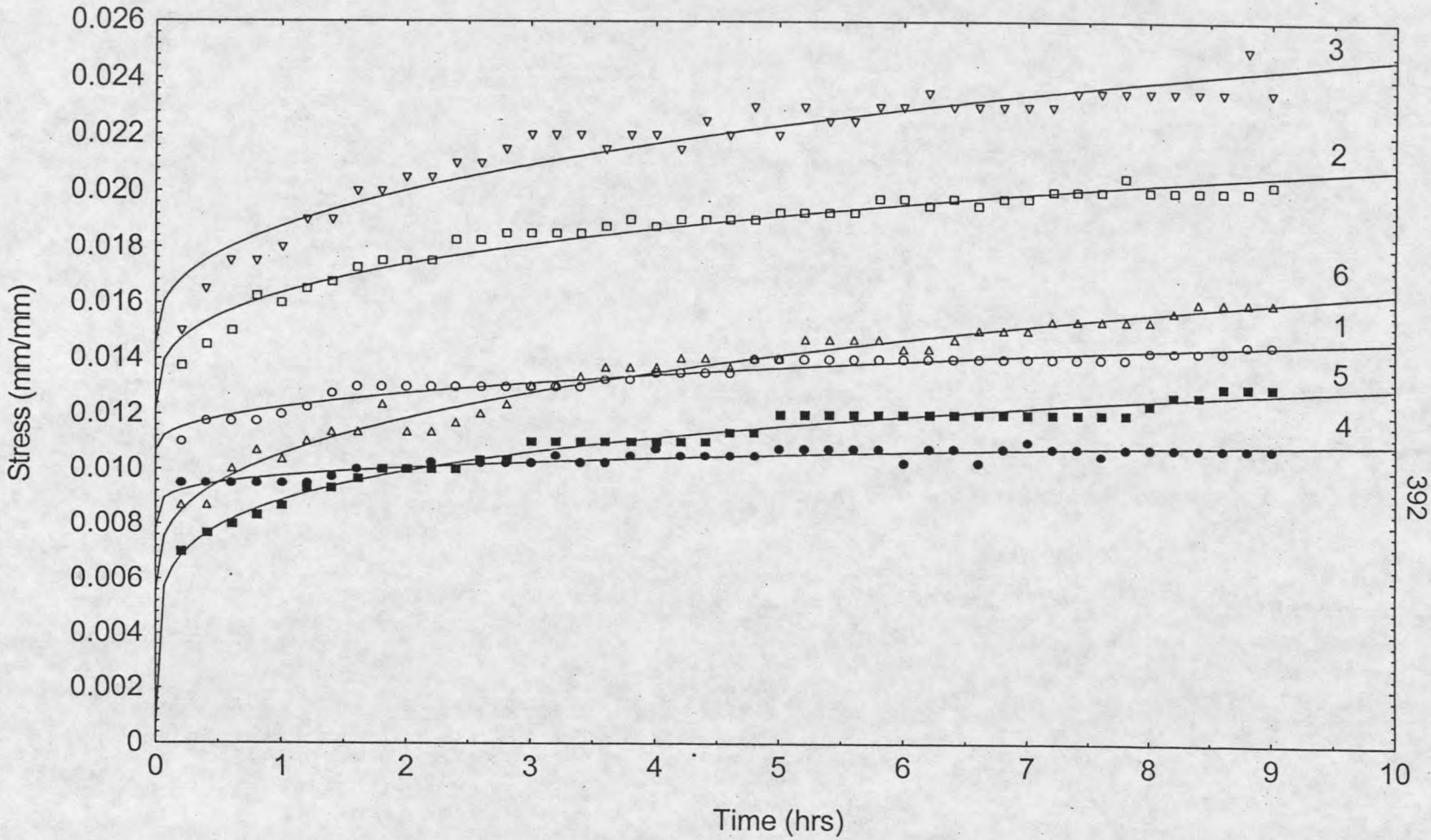


Figure F.21 Vibrocreep Response of Nylon 6/6 at Different Temperatures
1- $(0.20\pm0.05)\sigma_y$, 1 Hz at 23 °C; 2- $(0.20\pm0.05)\sigma_y$, 1 Hz at 35 °C; 3- $(0.20\pm0.05)\sigma_y$, 1 Hz at 41 °C;
4- $(0.20)\sigma_y$ at 23 °C, 5- $(0.20)\sigma_y$ at 35 °C, 6- $(0.20)\sigma_y$ at 41 °C, Constant Load Creep;
σ_y = 70 MPa at 23 °C

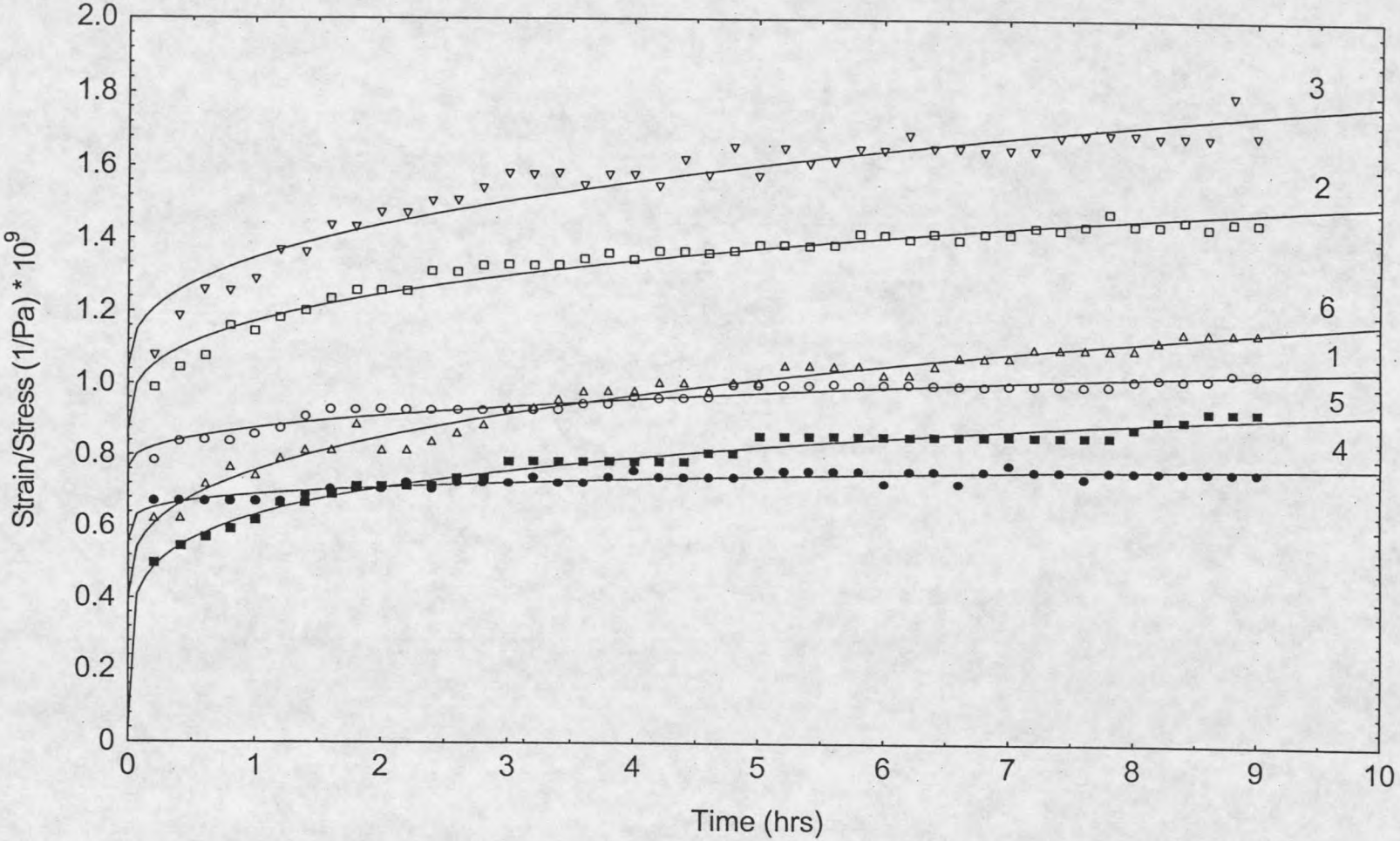


Figure F.22 Normalized Vibrocreep Response of Nylon 6/6 at Different Temperatures
1- $(0.20\pm0.05)\sigma_y$, 1 Hz at 23 °C; 2- $(0.20\pm0.05)\sigma_y$, 1 Hz at 35 °C; 3- $(0.20\pm0.05)\sigma_y$, 1 Hz at 41 °C;
4- $(0.20)\sigma_y$ at 23 °C, 5- $(0.20)\sigma_y$ at 35 °C, 6- $(0.20)\sigma_y$ at 41 °C, Constant Load Creep;
σ_y = 70 MPa at 23 °C

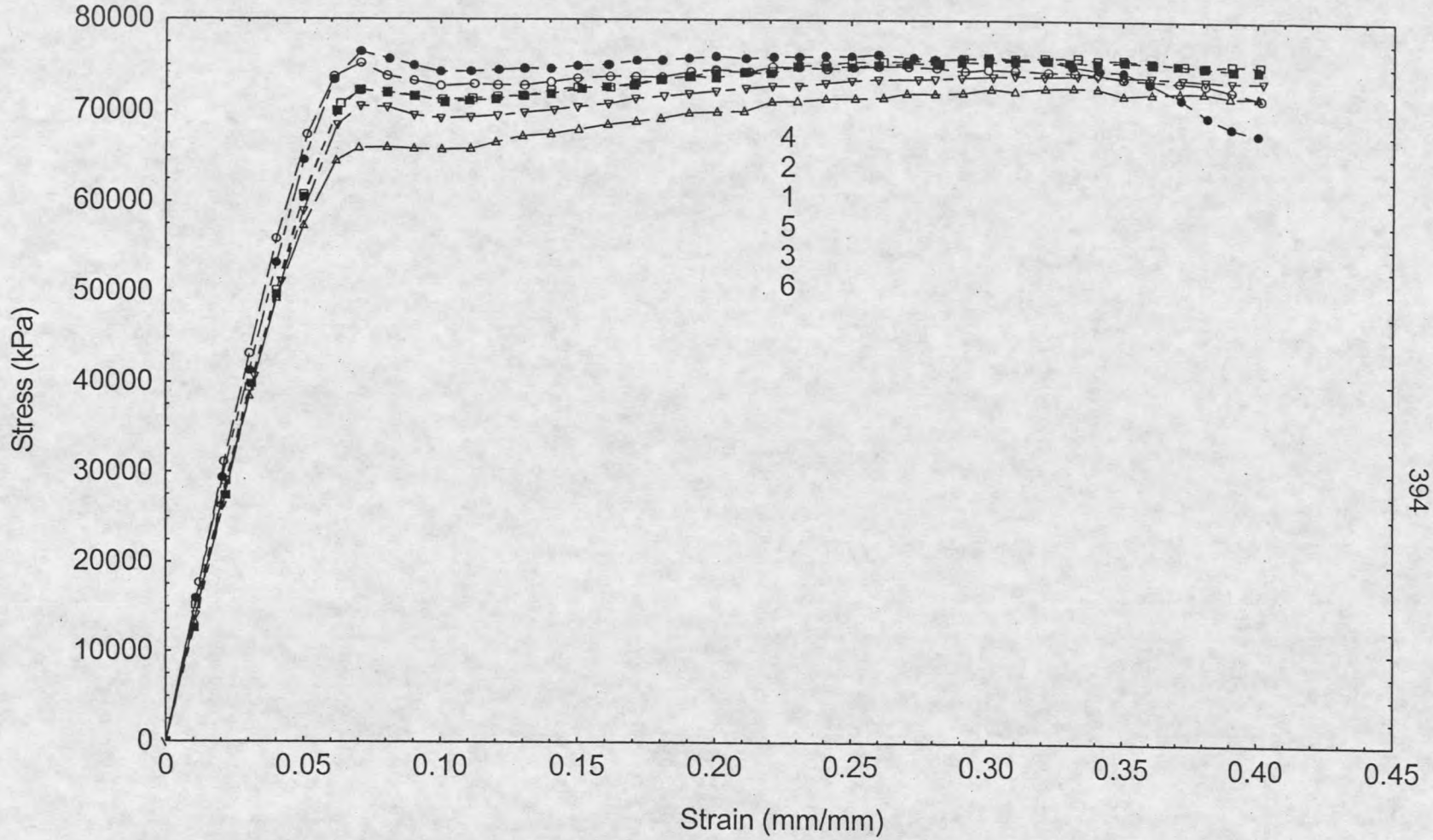


Figure F.23 Tensile Testing of Nylon 6/6 Specimens After Cyclic and Constant Loading
1- $(0.20\pm0.05)\sigma_y$, 1 Hz at 23 °C; 2- $(0.20\pm0.05)\sigma_y$, 1 Hz at 35 °C; 3- $(0.20\pm0.05)\sigma_y$, 1 Hz at 41 °C;
4- $(0.20)\sigma_y$ at 23 °C, 5- $(0.20)\sigma_y$ at 35 °C, 6- $(0.20)\sigma_y$ at 41 °C, Constant Load Creep;
σ_y = 70 MPa at 23 °C

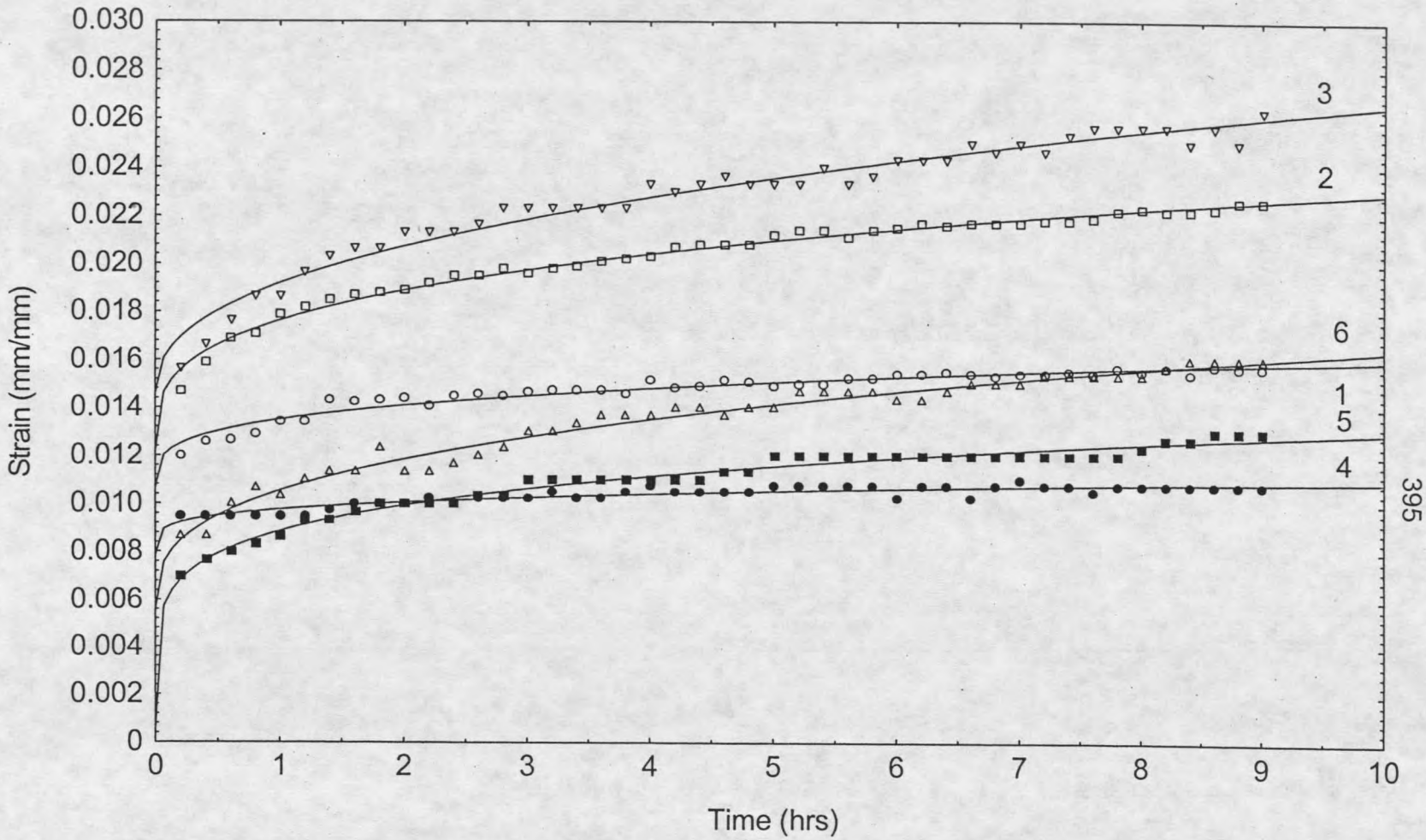


Figure F.24 Vibrocreep Response of Nylon 6/6 at Different Temperatures
1- $(0.20\pm0.05)\sigma_y$, 10 Hz at 23 °C; 2- $(0.20\pm0.05)\sigma_y$, 10 Hz at 35 °C; 3- $(0.20\pm0.05)\sigma_y$, 10 Hz at 41 °C;
4- $(0.20)\sigma_y$ at 23 °C, 5- $(0.20)\sigma_y$ at 35 °C, 6- $(0.20)\sigma_y$ at 41 °C, Constant Load Creep;
σ_y = 70 MPa at 23 °C

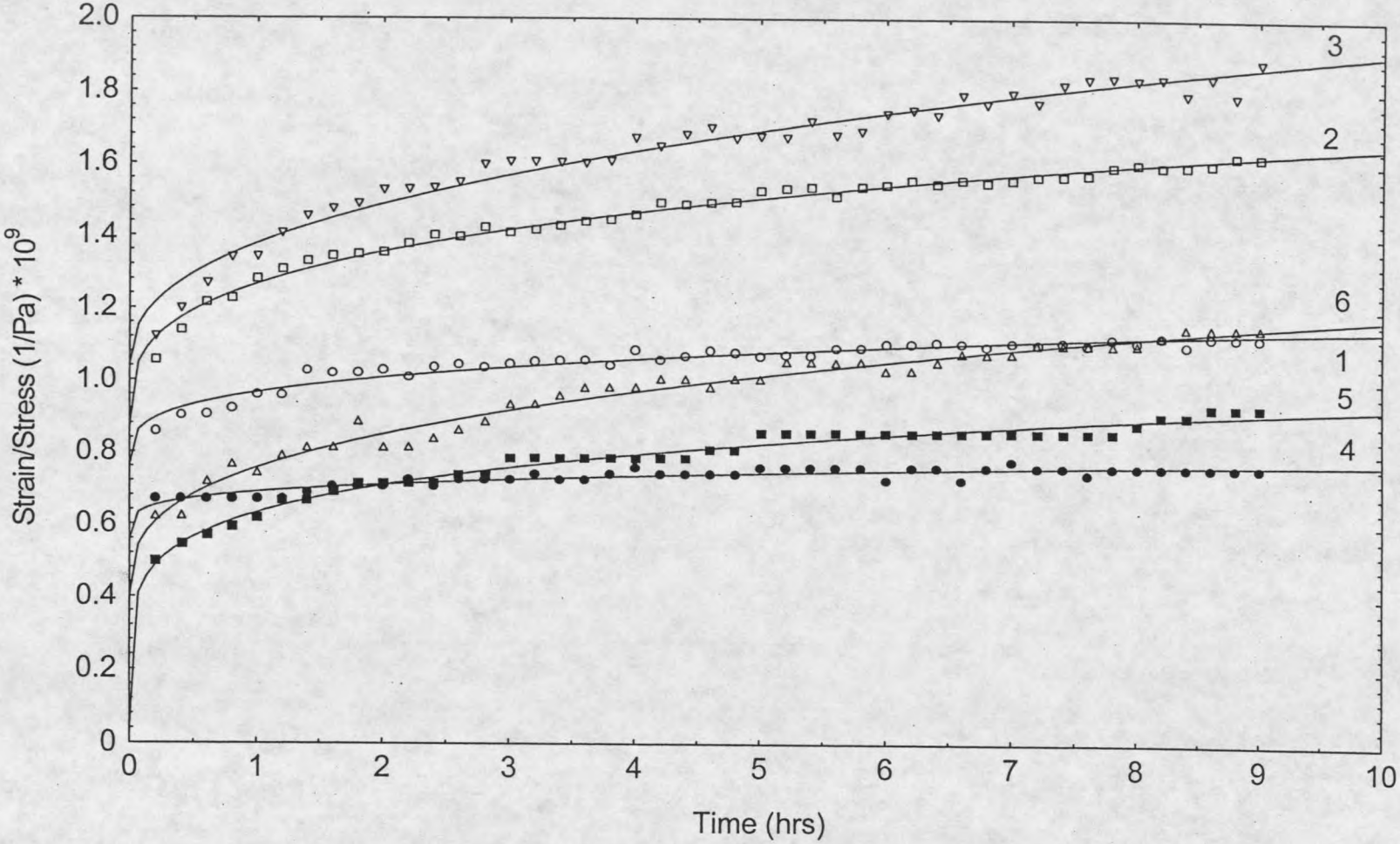


Figure F.25 Normalized Vibrocreep Response of Nylon 6/6 at Different Temperatures
1- $(0.20\pm0.05)\sigma_y$, 10 Hz at 23 °C; 2- $(0.20\pm0.05)\sigma_y$, 10 Hz at 35 °C; 3- $(0.20\pm0.05)\sigma_y$, 10 Hz at 41 °C;
4- $(0.20)\sigma_y$ at 23 °C, 5- $(0.20)\sigma_y$ at 35 °C, 6- $(0.20)\sigma_y$ at 41 °C, Constant Load Creep;
σ_y = 70 MPa at 23 °C

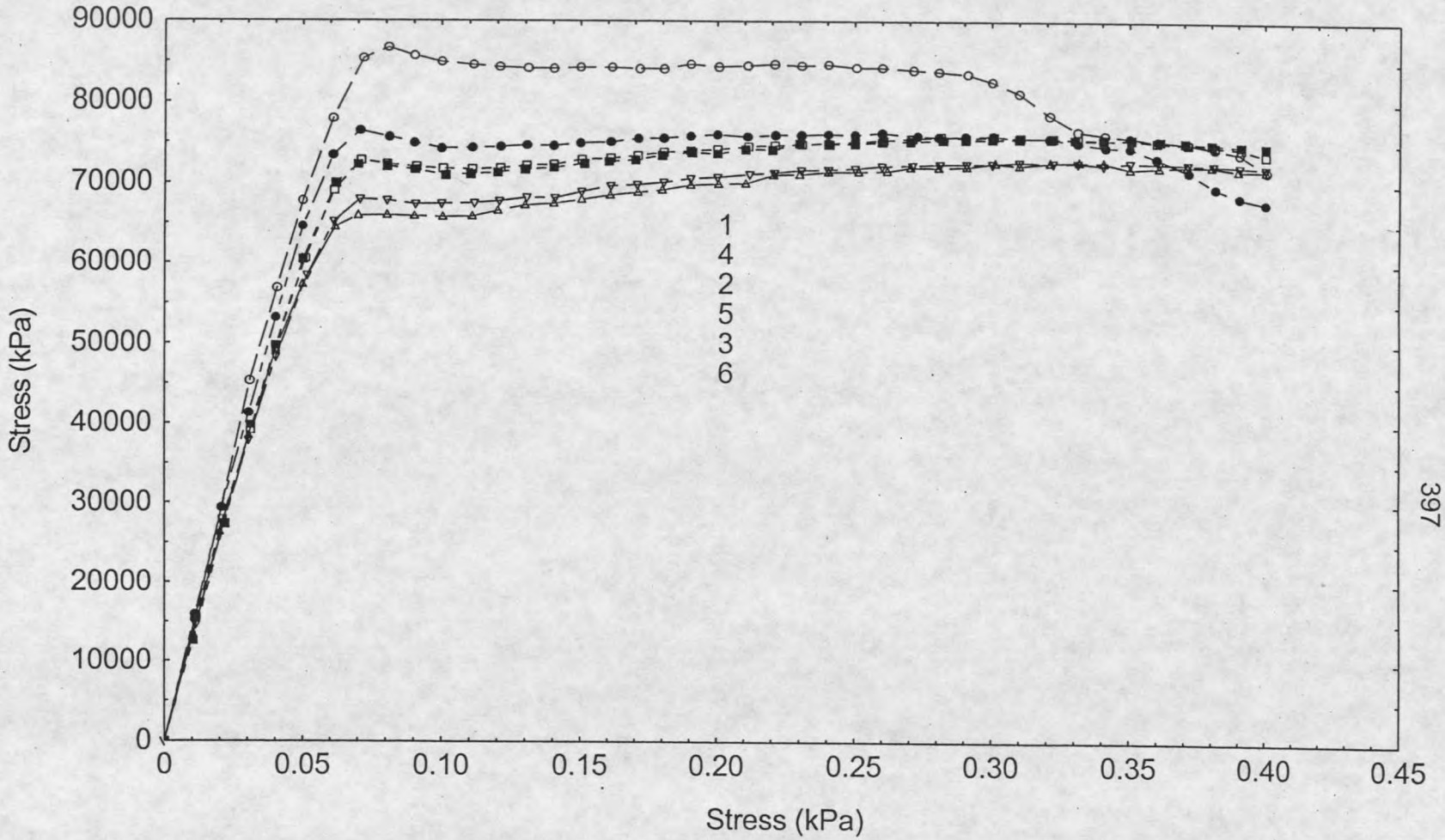


Figure F.26 Tensile Testing of Nylon 6/6 Specimens After Cyclic and Constant Loading
1- $(0.20\pm0.05)\sigma_y$, 10 Hz at 23 °C; 2- $(0.20\pm0.05)\sigma_y$, 10 Hz at 35 °C; 3- $(0.20\pm0.05)\sigma_y$, 10 Hz at 41 °C;
4- $(0.20)\sigma_y$ at 23 °C, 5- $(0.20)\sigma_y$ at 35 °C, 6- $(0.20)\sigma_y$ at 41 °C, Constant Load Creep;
σ_y = 70 MPa at 23 °C

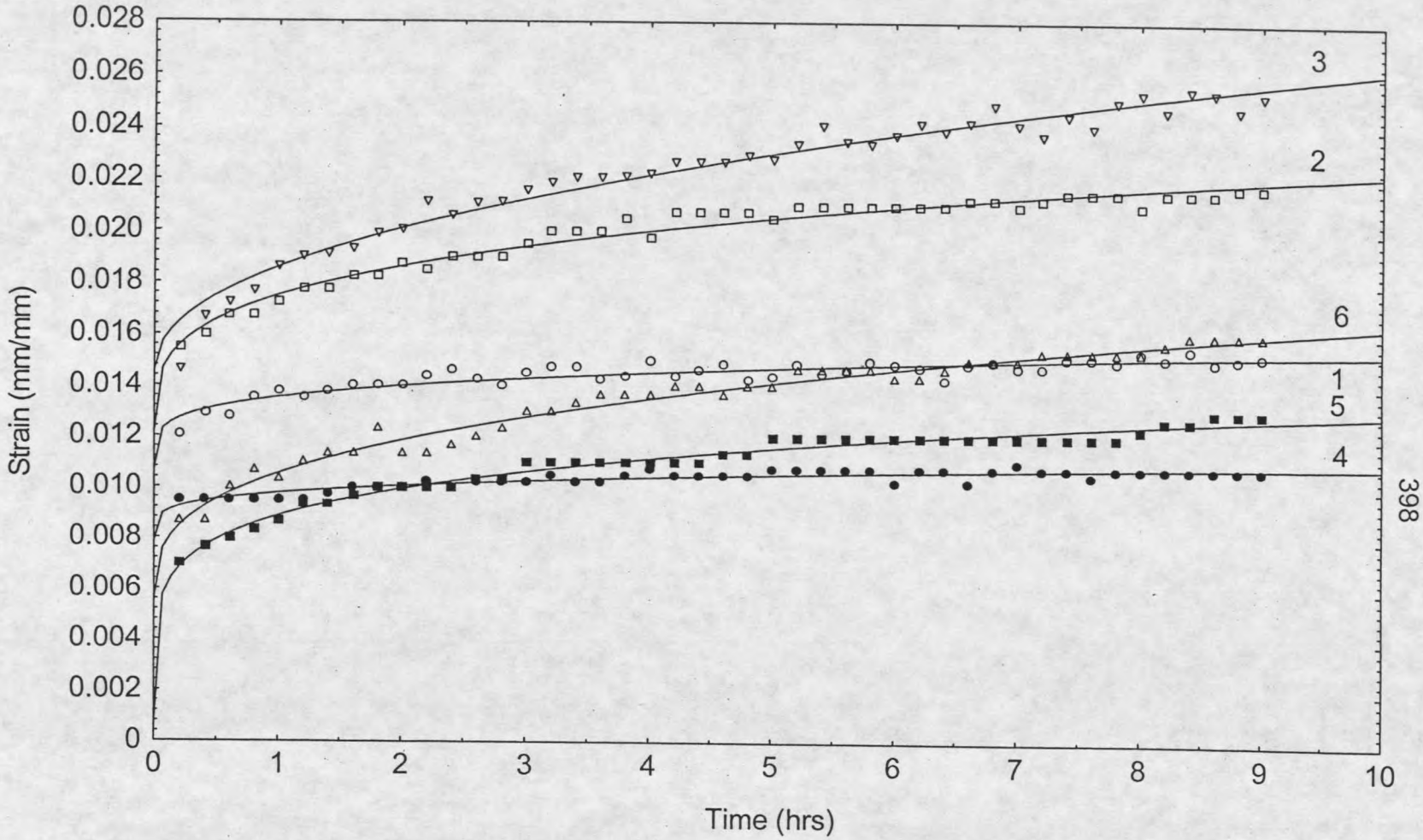


Figure F.27 Vibrocreep Response of Nylon 6/6 at Different Temperatures
1- $(0.20\pm0.10)\sigma_y$, 1 Hz at 23 °C; 2- $(0.20\pm0.10)\sigma_y$, 1 Hz at 35 °C; 3- $(0.20\pm0.10)\sigma_y$, 1 Hz at 41 °C;
4- $(0.20)\sigma_y$ at 23 °C, 5- $(0.20)\sigma_y$ at 35 °C, 6- $(0.20)\sigma_y$ at 41 °C, Constant Load Creep;
σ_y = 70 MPa at 23 °C

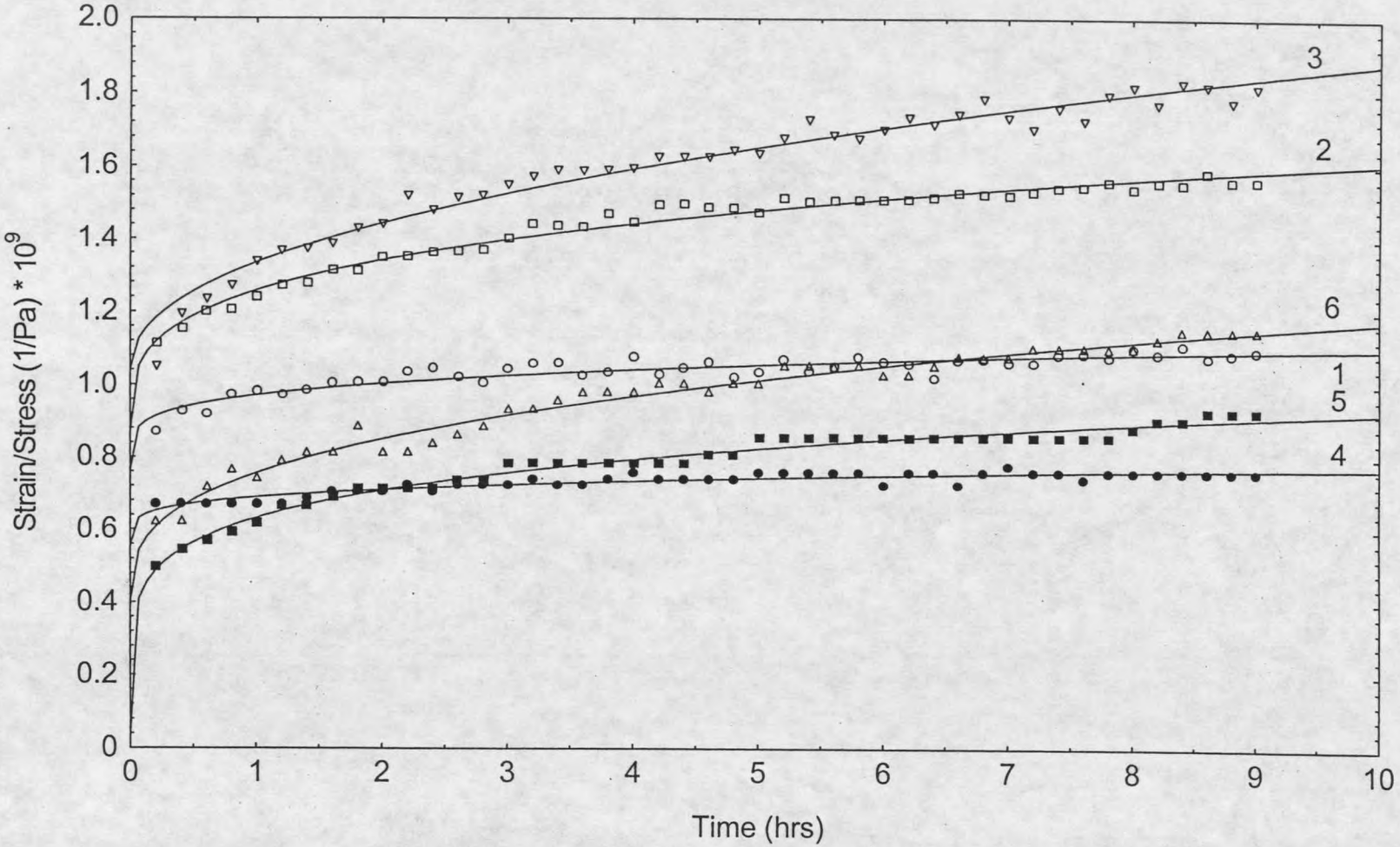


Figure F.28 Normalized Vibrocreep Response of Nylon 6/6 at Different Temperatures
1- $(0.20\pm0.10)\sigma_y$, 1 Hz at 23 °C; 2- $(0.20\pm0.10)\sigma_y$, 1 Hz at 35 °C; 3- $(0.20\pm0.10)\sigma_y$, 1 Hz at 41 °C;
4- $(0.20)\sigma_y$ at 23 °C, 5- $(0.20)\sigma_y$ at 35 °C, 6- $(0.20)\sigma_y$ at 41 °C, Constant Load Creep;
σ_y = 70 MPa at 23 °C

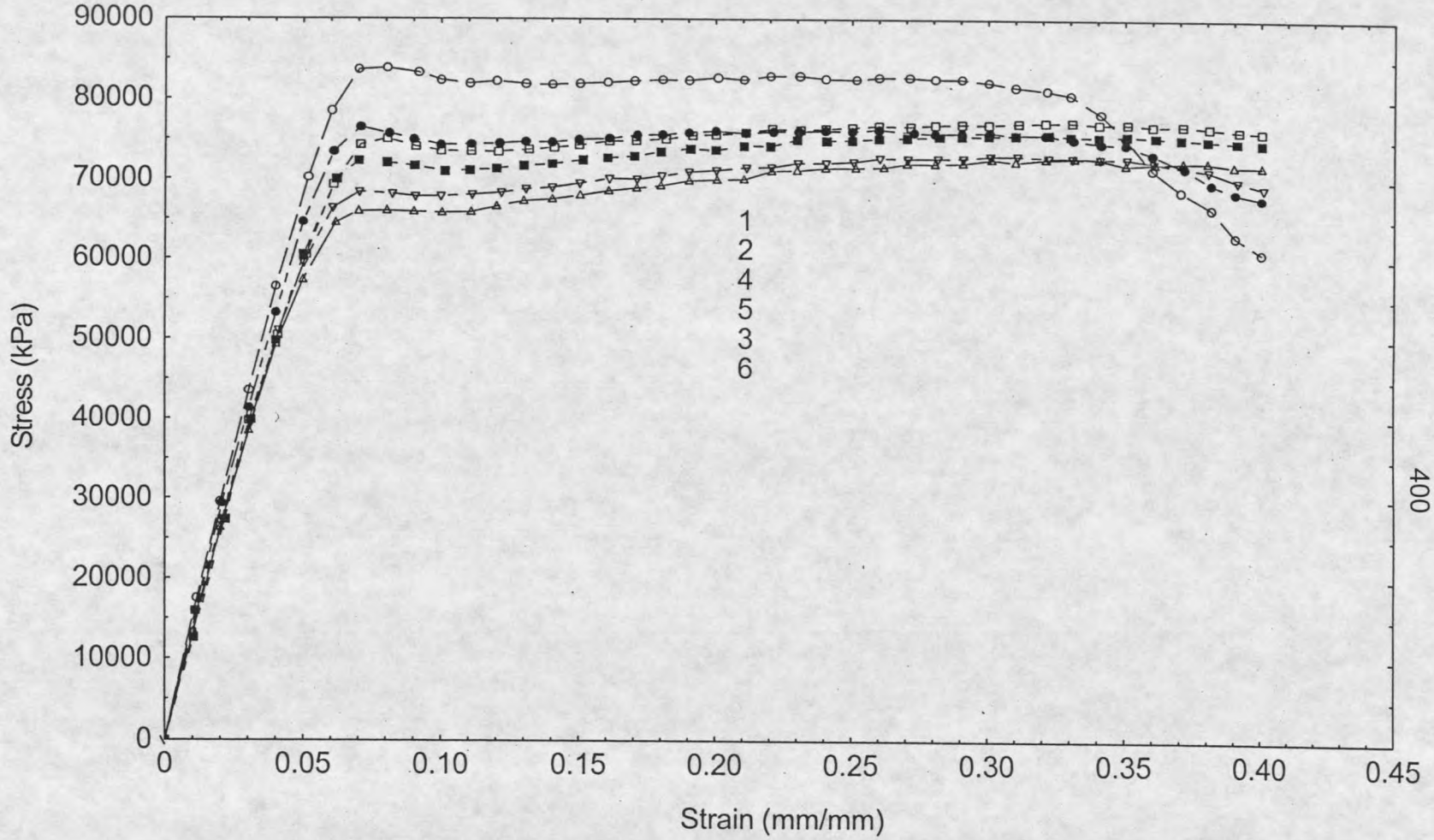


Figure F.29 Tensile Testing of Nylon 6/6 Specimens After Cyclic and Constant Loading
1- $(0.20\pm0.10)\sigma_y$, 1 Hz at 23 °C; 2- $(0.20\pm0.10)\sigma_y$, 1 Hz at 35 °C; 3- $(0.20\pm0.10)\sigma_y$, 1 Hz at 41 °C;
4- $(0.20)\sigma_y$ at 23 °C, 5- $(0.20)\sigma_y$ at 35 °C, 6- $(0.20)\sigma_y$ at 41 °C, Constant Load Creep;
σ_y = 70 MPa at 23 °C

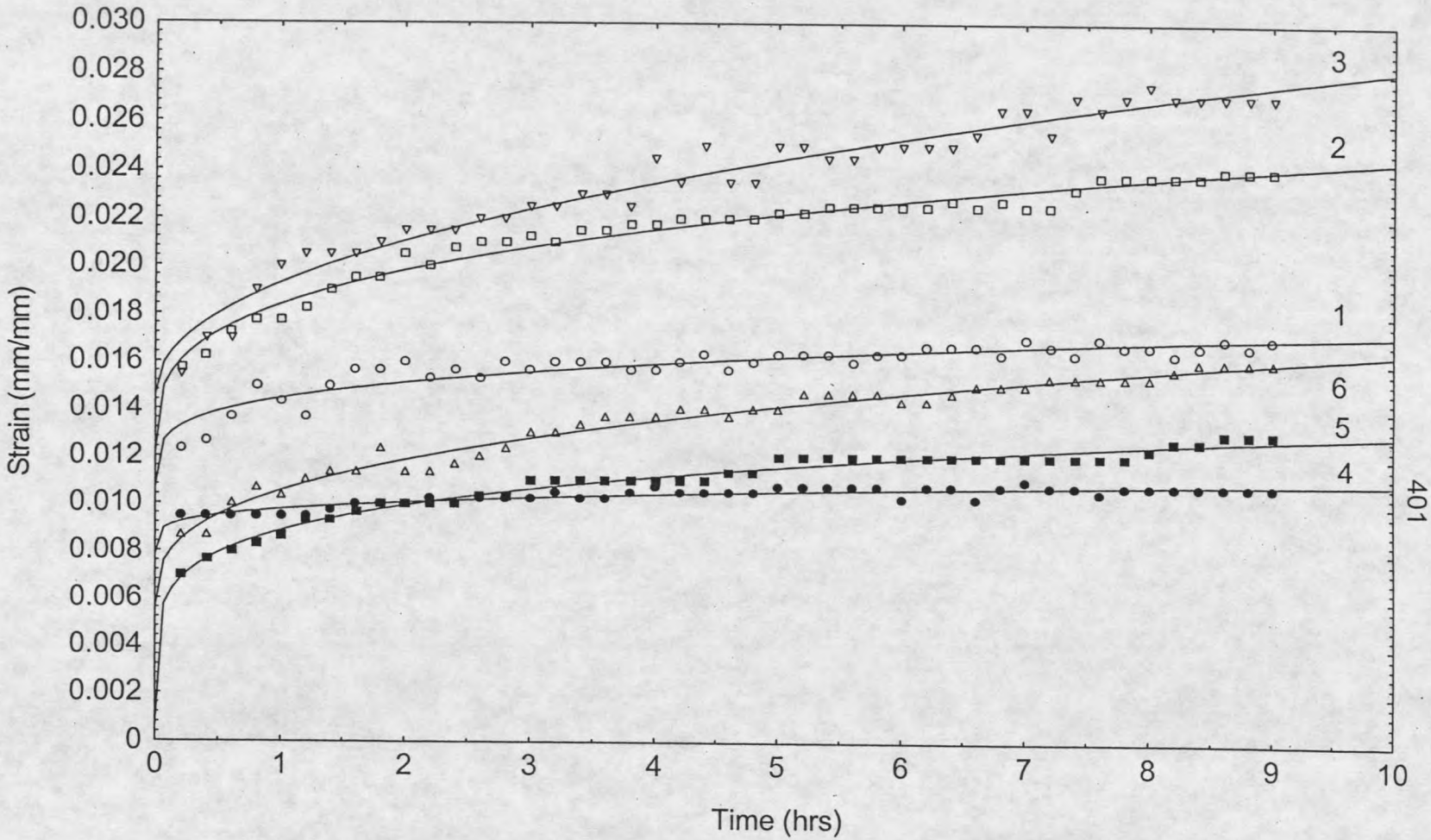


Figure F.30 Vibrocreep Response of Nylon 6/6 at Different Temperatures
1- $(0.20\pm0.10)\sigma_y$, 10 Hz at 23 °C; 2- $(0.20\pm0.10)\sigma_y$, 10 Hz at 35 °C; 3- $(0.20\pm0.10)\sigma_y$, 10 Hz at 41 °C;
4- $(0.20)\sigma_y$ at 23 °C, 5- $(0.20)\sigma_y$ at 35 °C, 6- $(0.20)\sigma_y$ at 41 °C, Constant Load Creep;
σ_y = 70 MPa at 23 °C

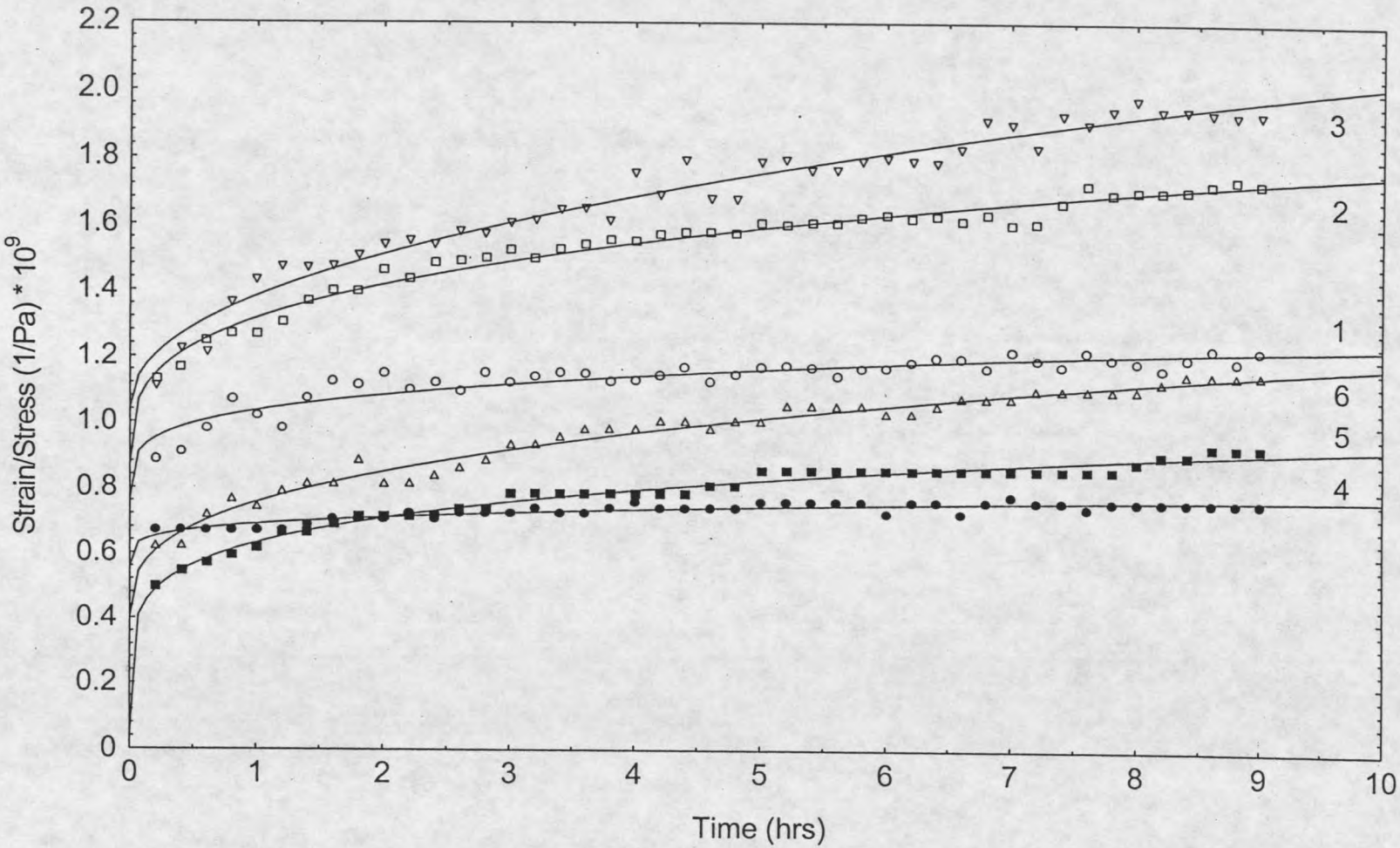


Figure F.31 Normalized Vibrocreep Response of Nylon 6/6 at Different Temperatures
1- $(0.20\pm0.10)\sigma_y$, 10 Hz at 23 °C; 2- $(0.20\pm0.10)\sigma_y$, 10 Hz at 35 °C; 3- $(0.20\pm0.10)\sigma_y$, 10 Hz at 41 °C;
4- $(0.20)\sigma_y$ at 23 °C, 5- $(0.20)\sigma_y$ at 35 °C, 6- $(0.20)\sigma_y$ at 41 °C, Constant Load Creep;
σ_y = 70 MPa at 23 °C

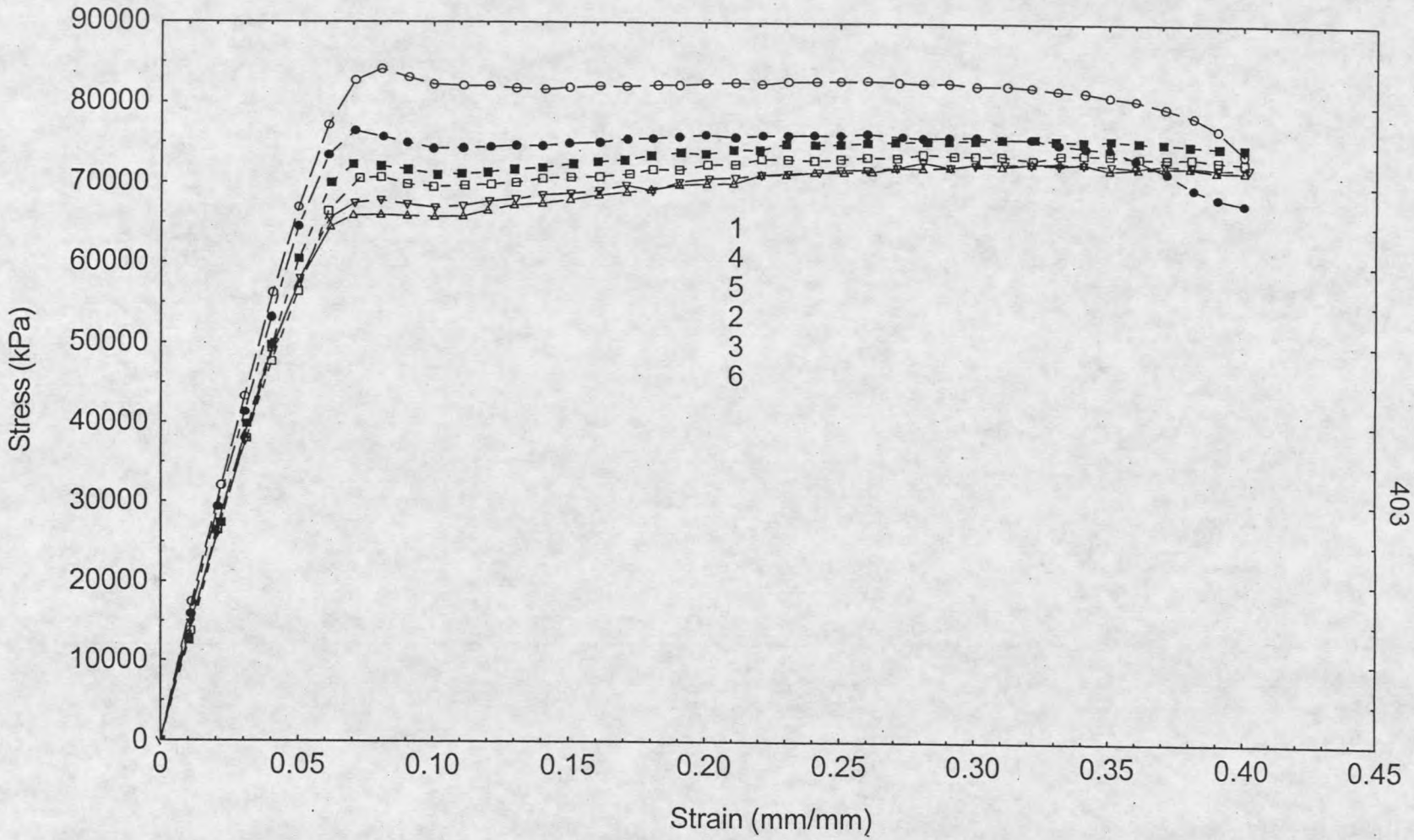


Figure F.32 Tensile Testing of Nylon 6/6 Specimens After Cyclic and Constant Loading
1- $(0.20\pm0.10)\sigma_y$, 10 Hz at 23 °C; 2- $(0.20\pm0.10)\sigma_y$, 10 Hz at 35 °C; 3- $(0.20\pm0.10)\sigma_y$, 10 Hz at 41 °C;
4- $(0.20)\sigma_y$ at 23 °C, 5- $(0.20)\sigma_y$ at 35 °C, 6- $(0.20)\sigma_y$ at 41 °C, Constant Load Creep;
σ_y = 70 MPa at 23 °C

APPENDIX G

Post Cyclic Testing Results

Data	Yield Stress (MPa)	Strain at Yield (mm/mm)	Maximum Stress (MPa)	Elastic Modulus (GPa)
23 C				
Virgin	70.000	0.06420	78.000	1.42000
16%	65.567	0.06515	74.543	1.32600
20%	63.171	0.06885	76.427	1.34830
12%+-4% 1 Hz	78.651	0.06500	83.520	1.42910
12%+-4% 10 Hz	77.109	0.06195	82.834	1.44470
12%+-4% 20 Hz	83.037	0.06164	88.133	1.53480
12%+-7.5% 1 Hz	79.231	0.06100	84.082	1.47310
12%+-7.5% 10 Hz	81.291	0.06164	84.754	1.46910
12%+-7.5% 20 Hz	77.193	0.06042	82.531	1.46360
12%+-10% 1 Hz	78.463	0.06185	83.458	1.37910
12%+-10% 10 Hz	77.847	0.06144	83.708	1.47940
12%+-10% 20Hz	78.841	0.06074	84.413	1.44710
16%+-4% 1 Hz	74.631	0.06104	76.818	1.39820
16%+-4% 10 Hz	73.864	0.06104	75.788	1.43330
16%+-4% 20 Hz	81.647	0.06854	85.785	1.39980
16%+-7.5% 1 Hz	79.697	0.06225	83.877	1.55970
16%+-7.5% 10 Hz	80.754	0.06164	84.414	1.47250
16%+-7.5% 20 Hz	77.394	0.06042	82.676	1.43950
16%+-10% 1 Hz	72.209	0.06105	74.053	1.38680
16%+-10% 10 Hz	82.397	0.06593	85.779	1.48580
16%+-10% 20 Hz	79.005	0.06104	86.405	1.44550
20%+-5% 1 Hz	75.509	0.05939	75.166	1.43060
20%+-5% 10 Hz	82.022	0.06723	86.672	1.44620
20%+-5% 20 Hz	78.298	0.06144	82.871	1.45920
20%+-7.5% 1 Hz	80.341	0.06226	86.134	1.44350
20%+-7.5% 10 Hz	81.095	0.06226	86.876	1.45060
20%+-7.5% 20 Hz	78.677	0.06104	84.209	1.42060
20%+-10% 1 Hz	78.473	0.08056	83.813	1.44510
20%+-10% 10 Hz	77.147	0.06104	84.097	1.43960
20%+-10% 20 Hz	79.923	0.06104	85.789	1.44980
35				
Virgin	55.200	0.05440	70.200	1.21000
16%	65.425	0.05189	74.866	1.31140
20%	57.391	0.04800	72.165	1.32130
16% R 23	57.391	0.04800	72.165	1.32130
20% R 23	57.600	0.04759	72.232	1.26340
16%+-4% 1 Hz	72.260	0.06042	74.845	1.37550
16%+-4% 10 Hz	72.930	0.06255	74.872	1.39290
16%+-10% 1 Hz	72.203	0.06103	74.458	1.38010
16%+-10% 10 Hz	71.011	0.05939	74.276	0.13814
20%+-5% 1 Hz	71.363	0.06225	74.018	0.13424
20%+-5% 10 Hz	67.275	0.06723	69.049	0.12617
20%+-10% 1 Hz	67.073	0.06226	69.995	1.26610
20%+-10% 10 Hz	66.935	0.06286	69.484	1.28740
16%+-4% 1 Hz R 23	68.987	0.06165	71.168	1.34050

16%+-4% 10 Hz R 23	67.044	0.06104	69.947	1.26650
16%+-10% 1 Hz R 23	69.507	0.06128	73.902	1.31870
16%+-10% 10 Hz R 23	66.262	0.06105	70.941	1.27690
20%+-5% 1 Hz R 23	70.743	0.06348	72.275	1.30780
20%+-5% 10 Hz R 23	69.073	0.06153	72.763	1.28400
20%+-10% 1 Hz R 23	72.359	0.06593	75.002	1.31740
20%+-10% 10 Hz R 23	66.445	0.06104	70.654	1.23870

41

Virgin	44.600	0.05510	65.000	0.96000
16%	52.006	0.04425	65.787	1.23080
20%	57.034	0.05005	64.950	1.27170
16% R 23	50.075	0.04360	65.543	1.20360
20% R 23	57.299	0.05005	65.906	1.27550
16%+-10% 1 Hz	64.080	0.06104	66.076	1.24610
16%+-10% 10 Hz	61.670	0.06104	64.419	1.20550
20%+-5% 1 Hz	66.541	0.06424	68.399	1.32250
20%+-5% 10 Hz	65.318	0.05940	68.372	1.31220
20%+-10% 1 Hz	66.019	0.06104	68.789	1.27600
20%+-10% 10 Hz	63.411	0.06042	65.374	1.27680
16%+-4% 1 Hz R 23	65.360	0.06073	67.891	1.28810
16%+-4% 10 Hz R 23	66.485	0.06185	68.080	1.28540
16%+-10% 1 Hz R 23	66.634	0.06103	69.085	1.28310
16%+-10% 10 Hz R 23	64.535	0.08096	64.582	1.18680
20%+-5% 1 Hz R 23	66.574	0.06940	70.503	1.26090
20%+-5% 10 Hz R 23	65.190	0.06145	67.819	1.25540
20%+-10% 1 Hz R 23	66.353	0.06145	68.365	1.28300
20%+-10% 10 Hz R 23	65.594	0.06079	67.817	1.24950

50

Virgin	22.000	0.03320	57.500	0.70800
16% R 23	35.383	0.03900	64.538	0.95370
20% R 23	37.456	0.03829	65.667	1.03200

59

Virgin	19.000	0.03680	52.400	0.54800
16% R 23	21.911	0.03654	54.136	0.63420
20% R 23	21.266	0.03642	53.030	0.31289

68

Virgin	10.000	0.02380	48.900	0.45900
16% R 23	19.718	0.04300	48.110	0.47995
20% R 23	17.094	0.03550	48.663	0.50969

APPENDIX H

Tensile and Constant Load Creep Testing Results for PVDF

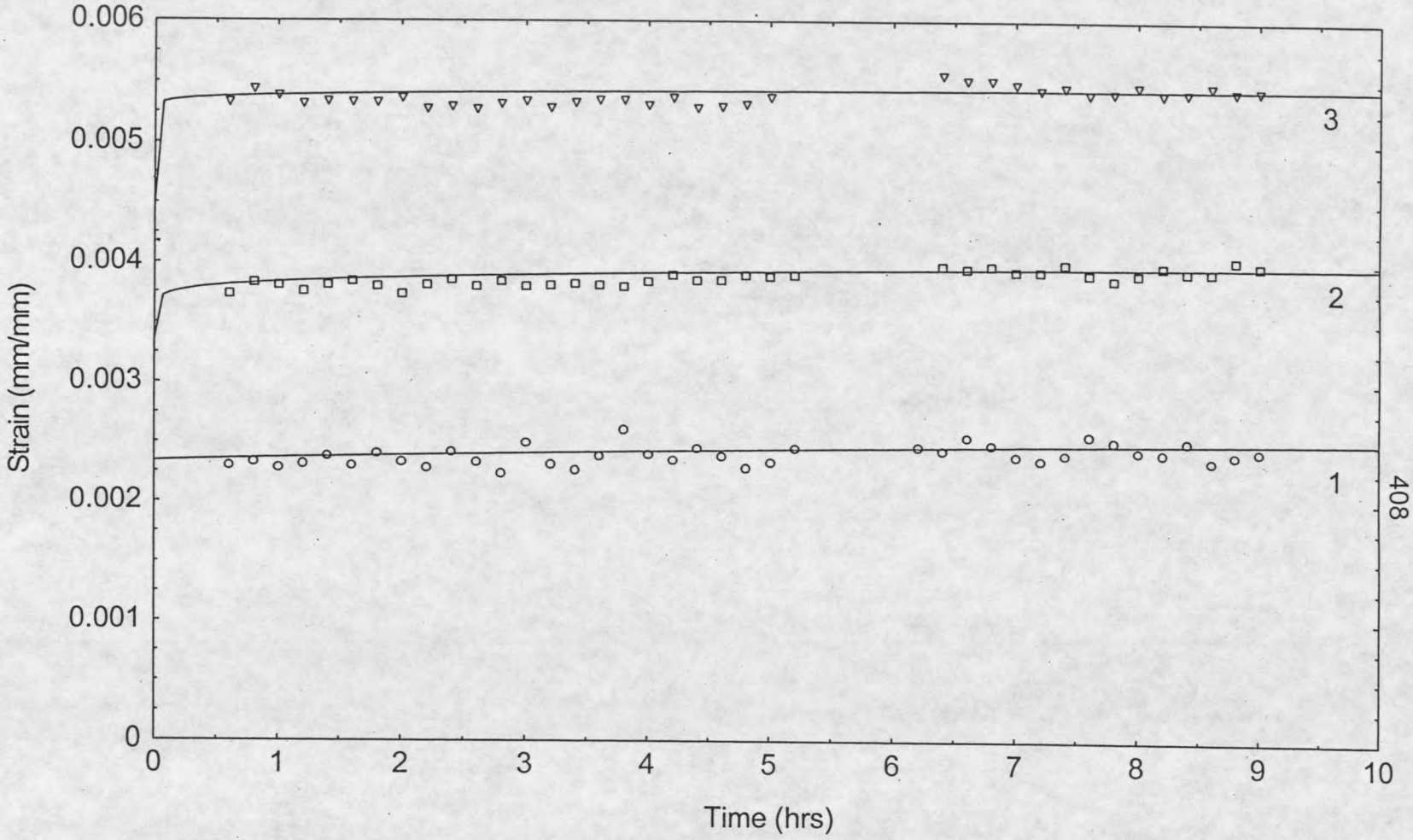


Figure H.I.1 Constant Load Creep of PVDF at -25 °C
1- $(0.30)\sigma_y$; 2- $(0.45)\sigma_y$; 3- $(0.60)\sigma_y$;
σ_y = 30.428 MPa at 23 °C

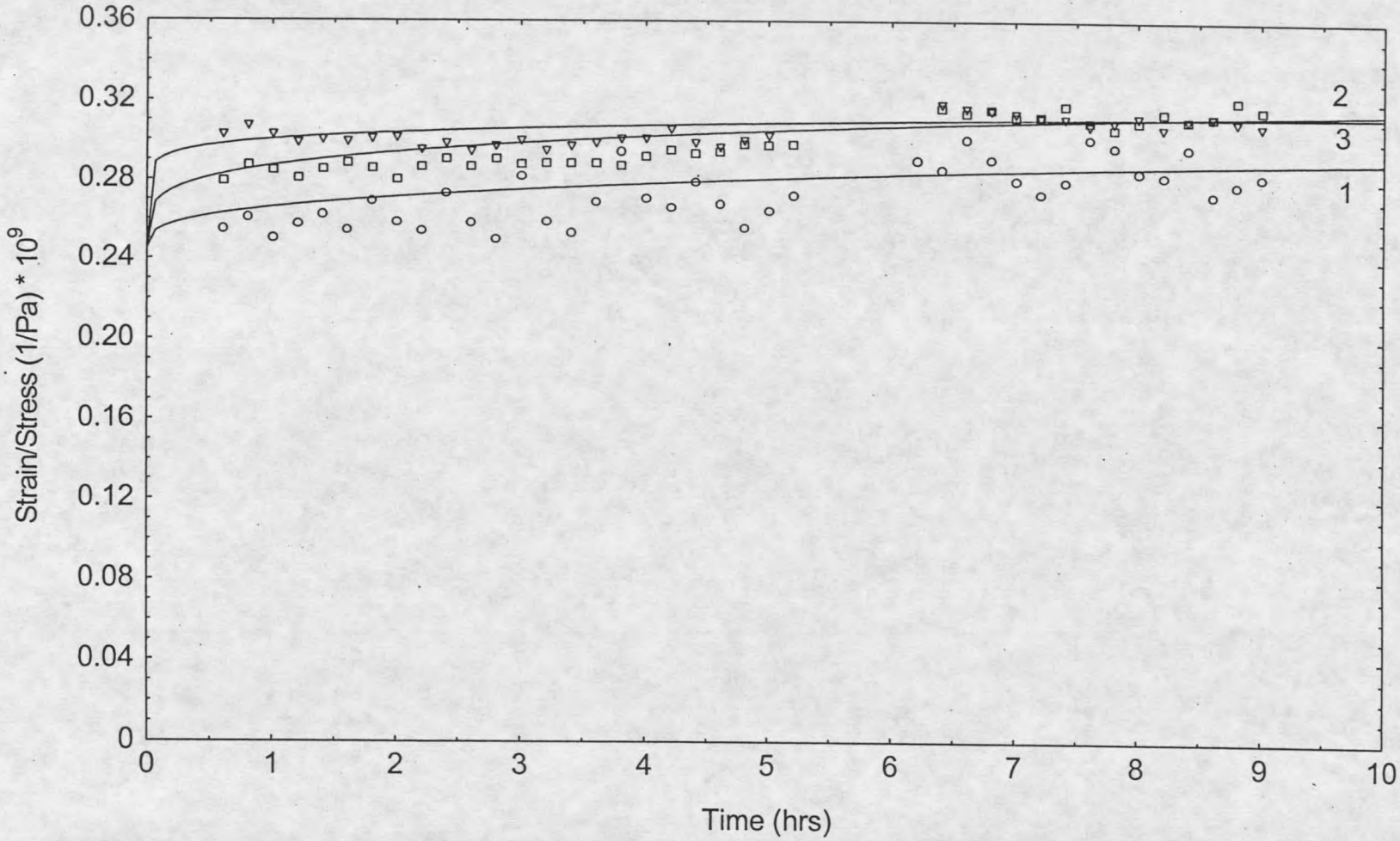


Figure H.I.2 Normalized Constant Load Creep of PVDF at -25 °C
1- $(0.30)\sigma_y$; 2- $(0.45)\sigma_y$; 3- $(0.60)\sigma_y$;
σ_y = 30.428 MPa at 23 °C

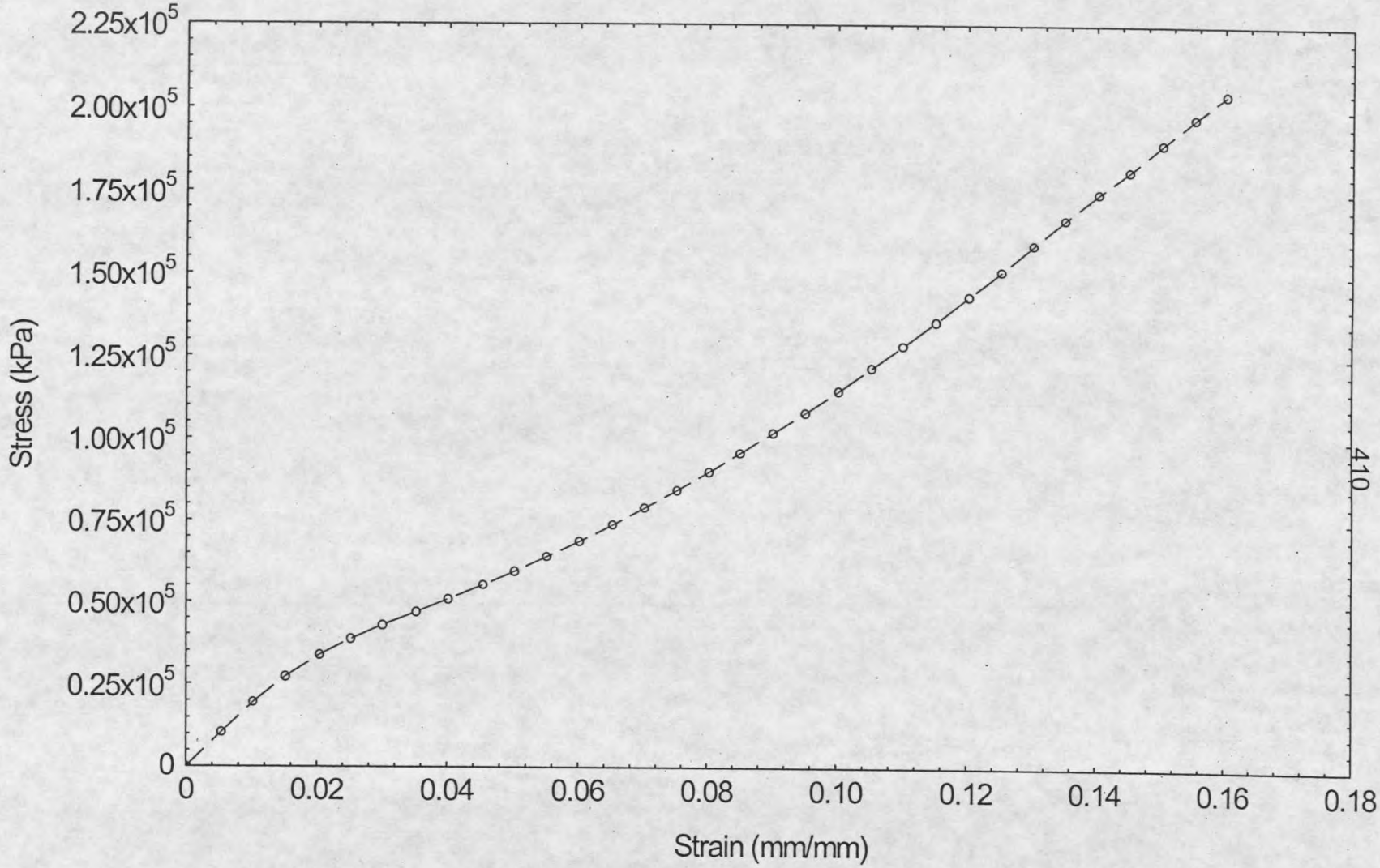


Figure H.II.1 Tensile Test of PVDF Direction 1 at 23 °C

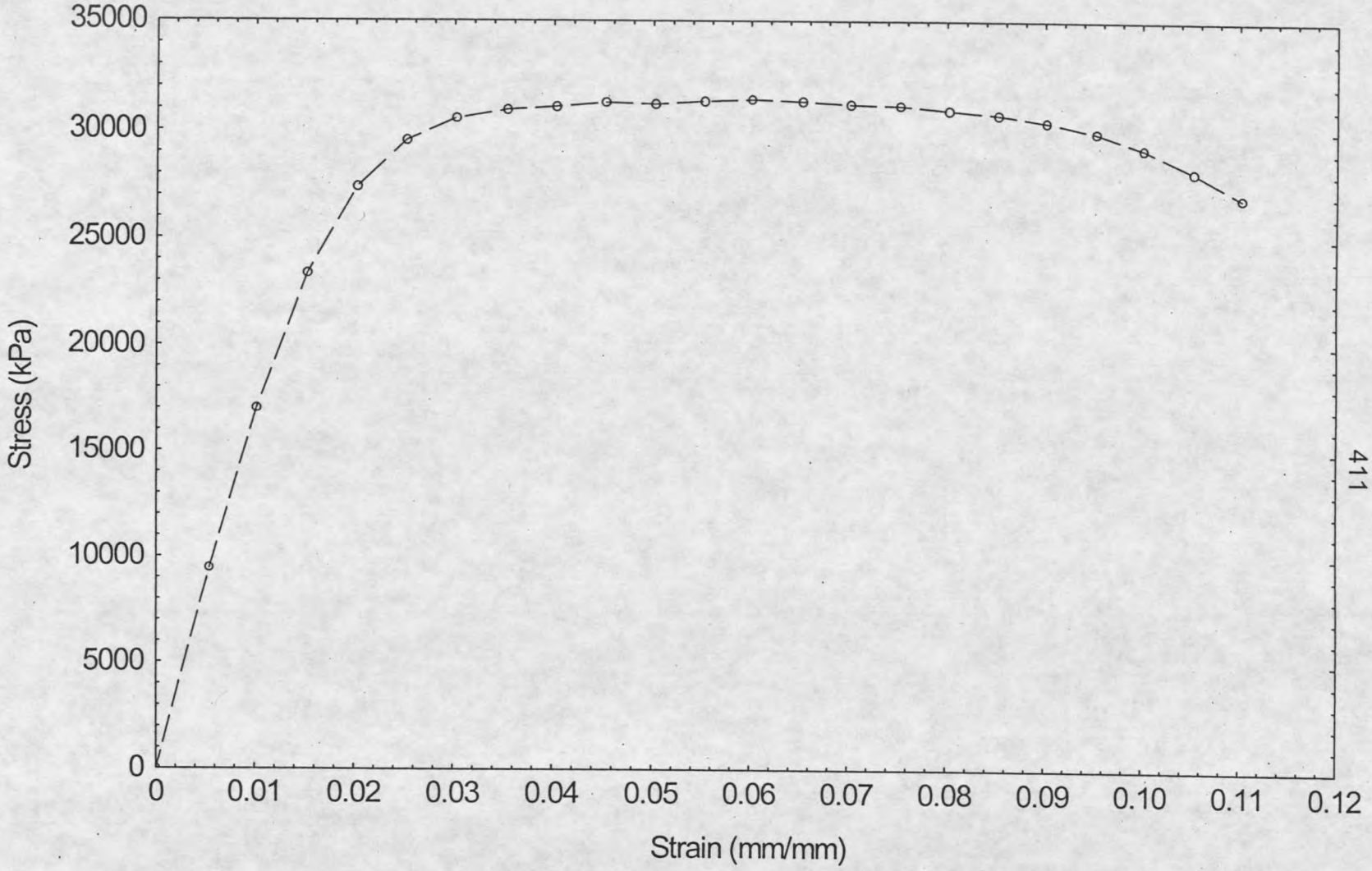


Figure H.II.2 Tensile Test of PVDF Direction 2 at 23 °C

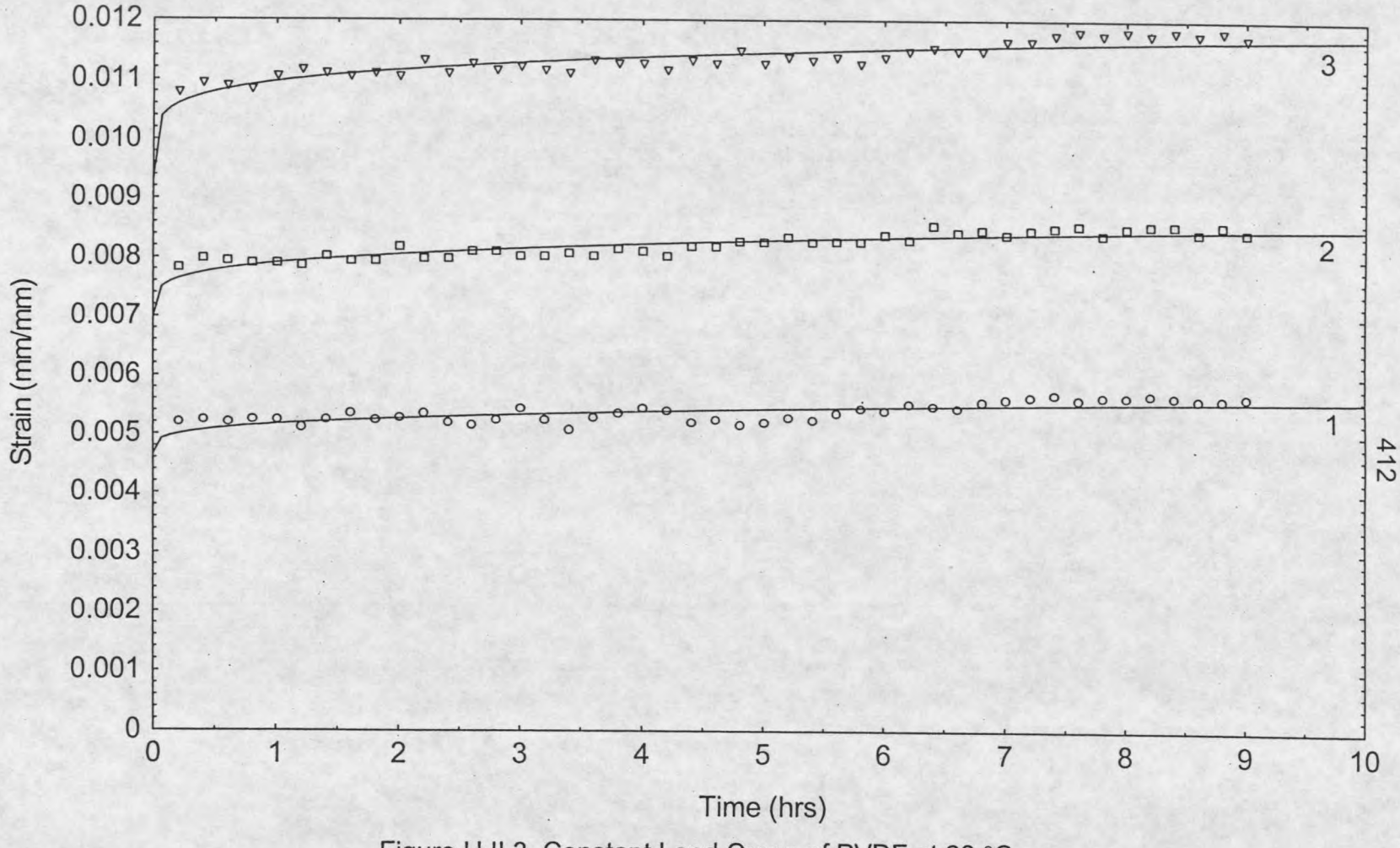


Figure H.II.3 Constant Load Creep of PVDF at 23 °C
1- $(0.30)\sigma_y$; 2- $(0.45)\sigma_y$; 3- $(0.60)\sigma_y$;
σ_y = 30.428 MPa at 23 °C

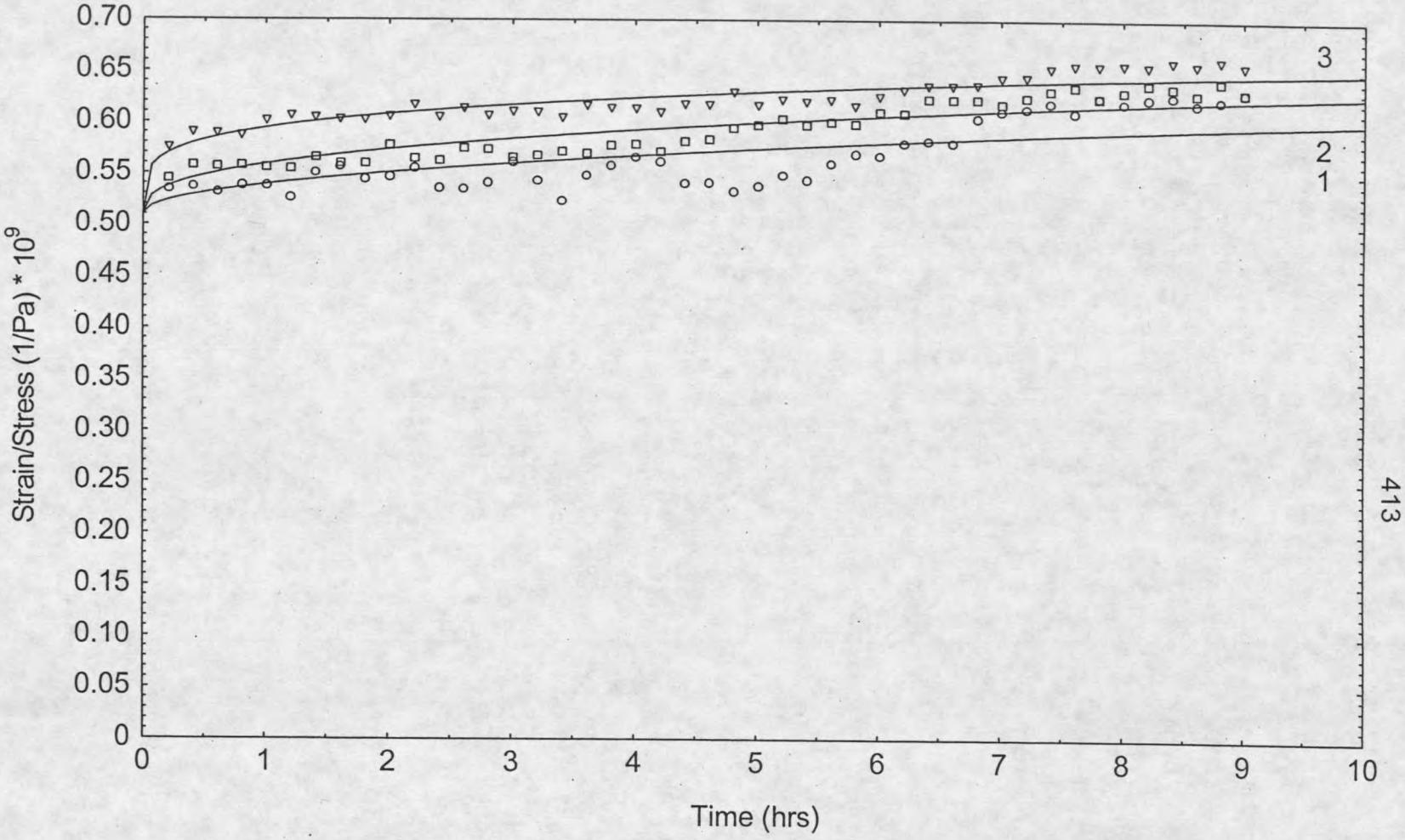


Figure H.II.4 Normalized Constant Load Creep of PVDF at 23 °C
1- $(0.30)\sigma_y$; 2- $(0.45)\sigma_y$; 3- $(0.60)\sigma_y$;
σ_y = 30.428 MPa at 23 °C

APPENDIX I

Frequency Effects from Vibrocreep Testing of PVDF

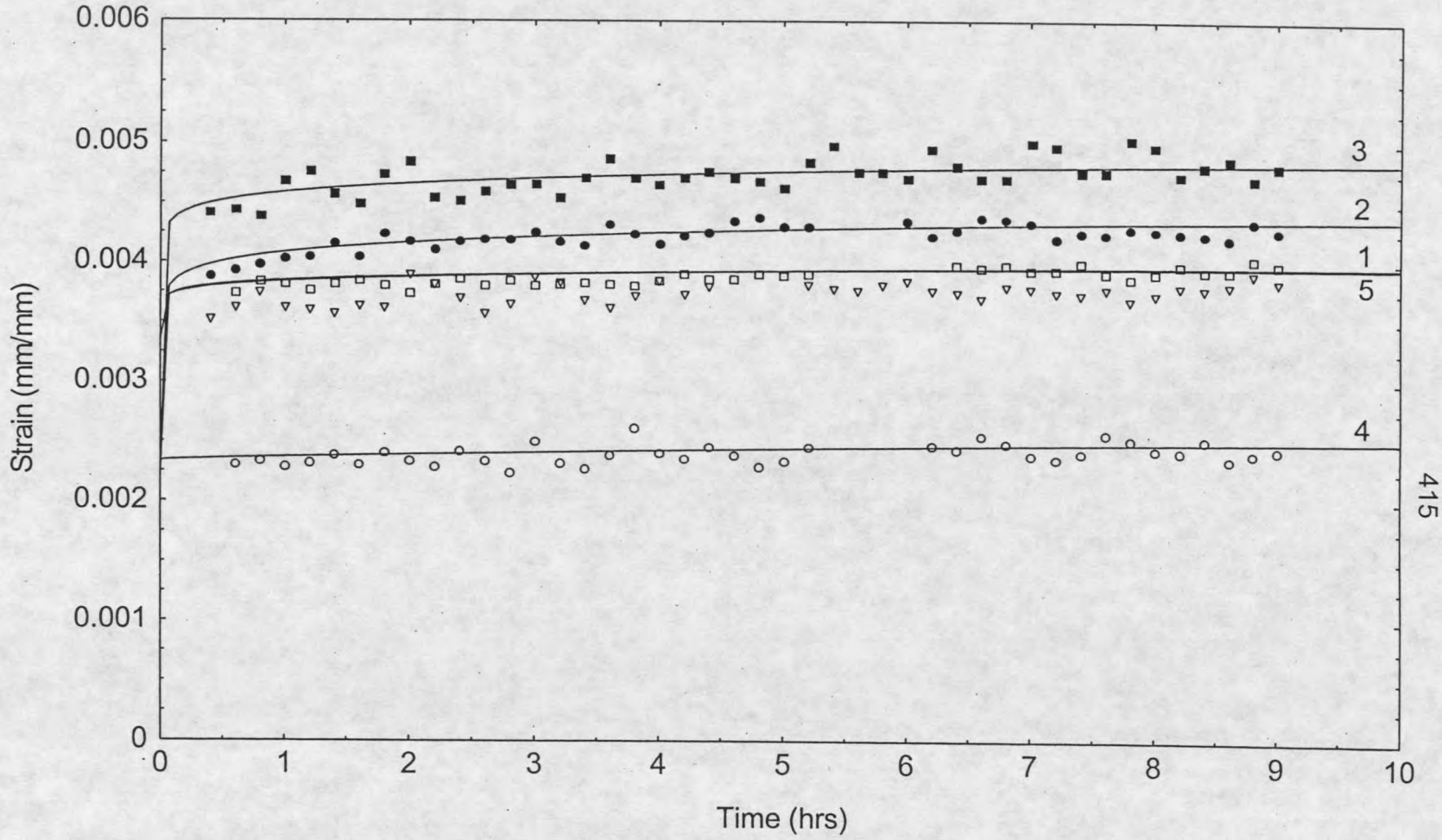


Figure I.I.1 Vibrocreep Response of PVDF at Different Frequencies at -25 °C
1- $(0.30\pm0.20)\sigma_y$, 5 Hz; 2- $(0.30\pm0.20)\sigma_y$, 10 Hz; 3- $(0.30\pm0.020)\sigma_y$, 20 Hz;
4- $(0.30)\sigma_y$, 5- $(0.45)\sigma_y$, Constant Load Creep;
σ_y = 30.428 MPa at 23 °C

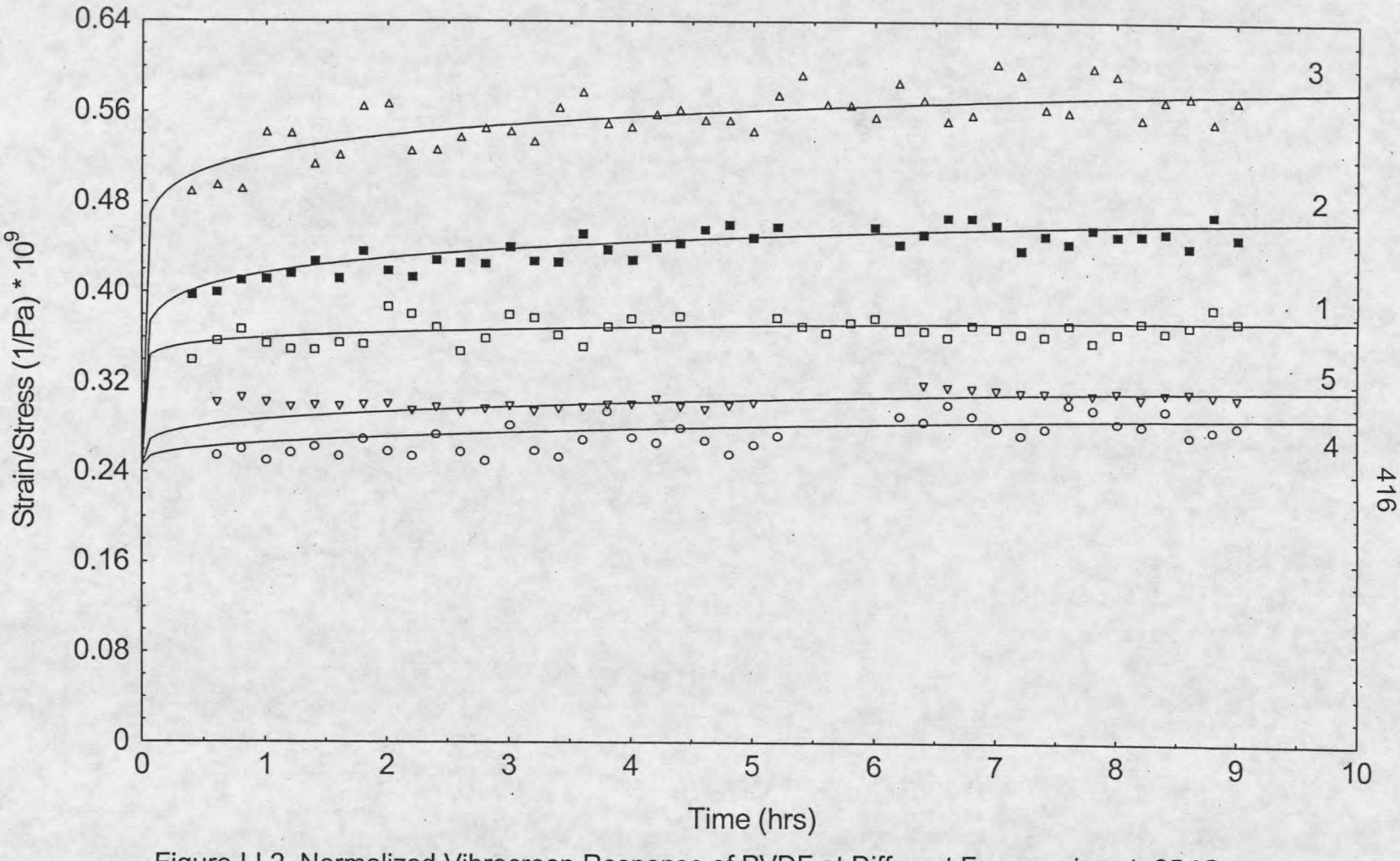


Figure I.I.2 Normalized Vibrocreep Response of PVDF at Different Frequencies at -25 °C
1- $(0.30\pm0.20)\sigma_y$, 5 Hz; 2- $(0.30\pm0.20)\sigma_y$, 10 Hz; 3- $(0.30\pm0.020)\sigma_y$, 20 Hz;
4- $(0.30)\sigma_y$, 5- $(0.45)\sigma_y$, Constant Load Creep;
σ_y = 30.428 MPa at 23 °C

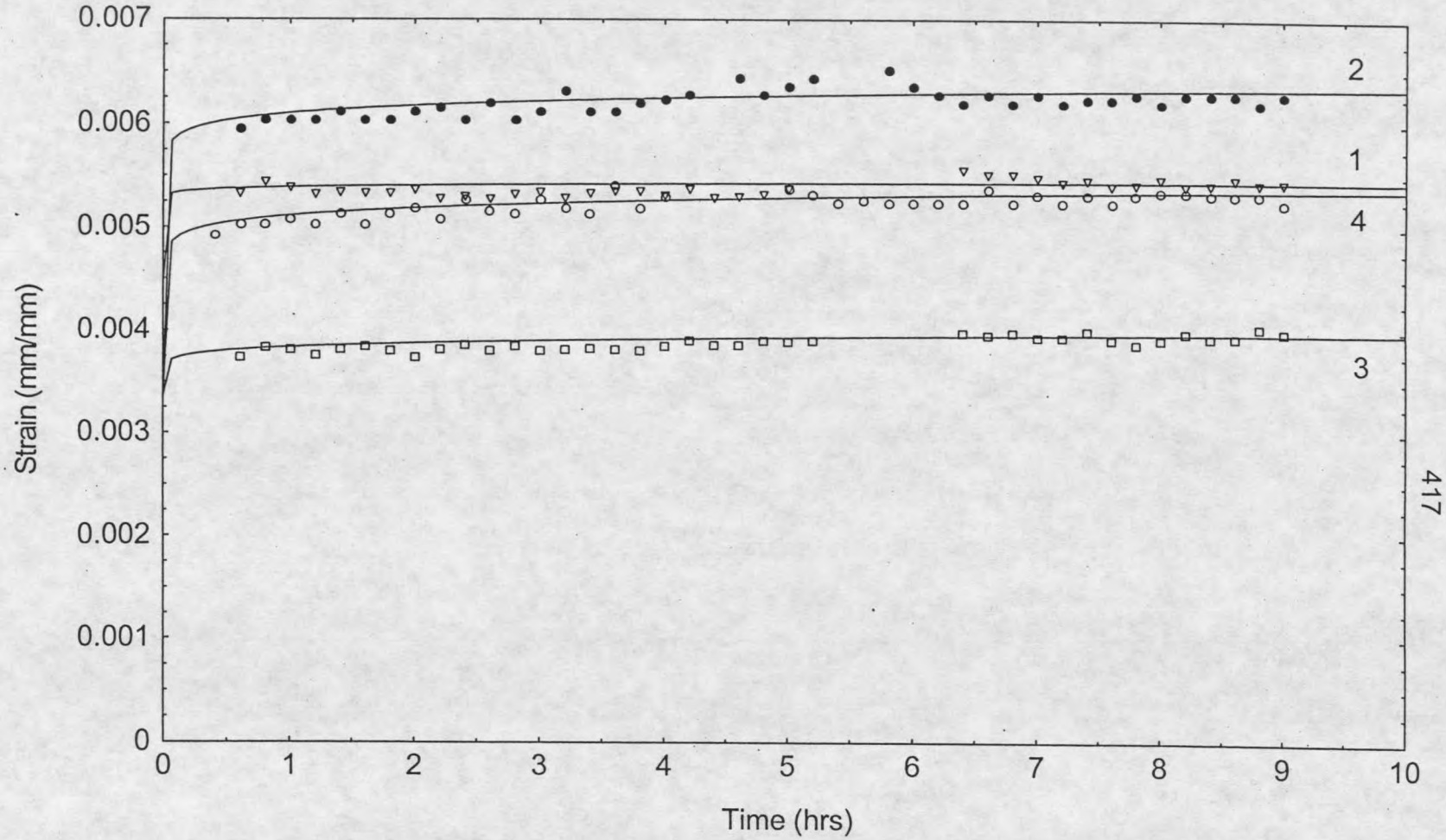


Figure I.I.3 Vibrocreep Response of PVDF at Different Frequencies at -25 °C
1- $(0.45\pm0.20)\sigma_y$, 5 Hz; 2- $(0.45\pm0.20)\sigma_y$, 10 Hz;
3- $(0.45)\sigma_y$, 4- $(0.60)\sigma_y$, Constant Load Creep;
σ_y = 30.428 MPa at 23 °C

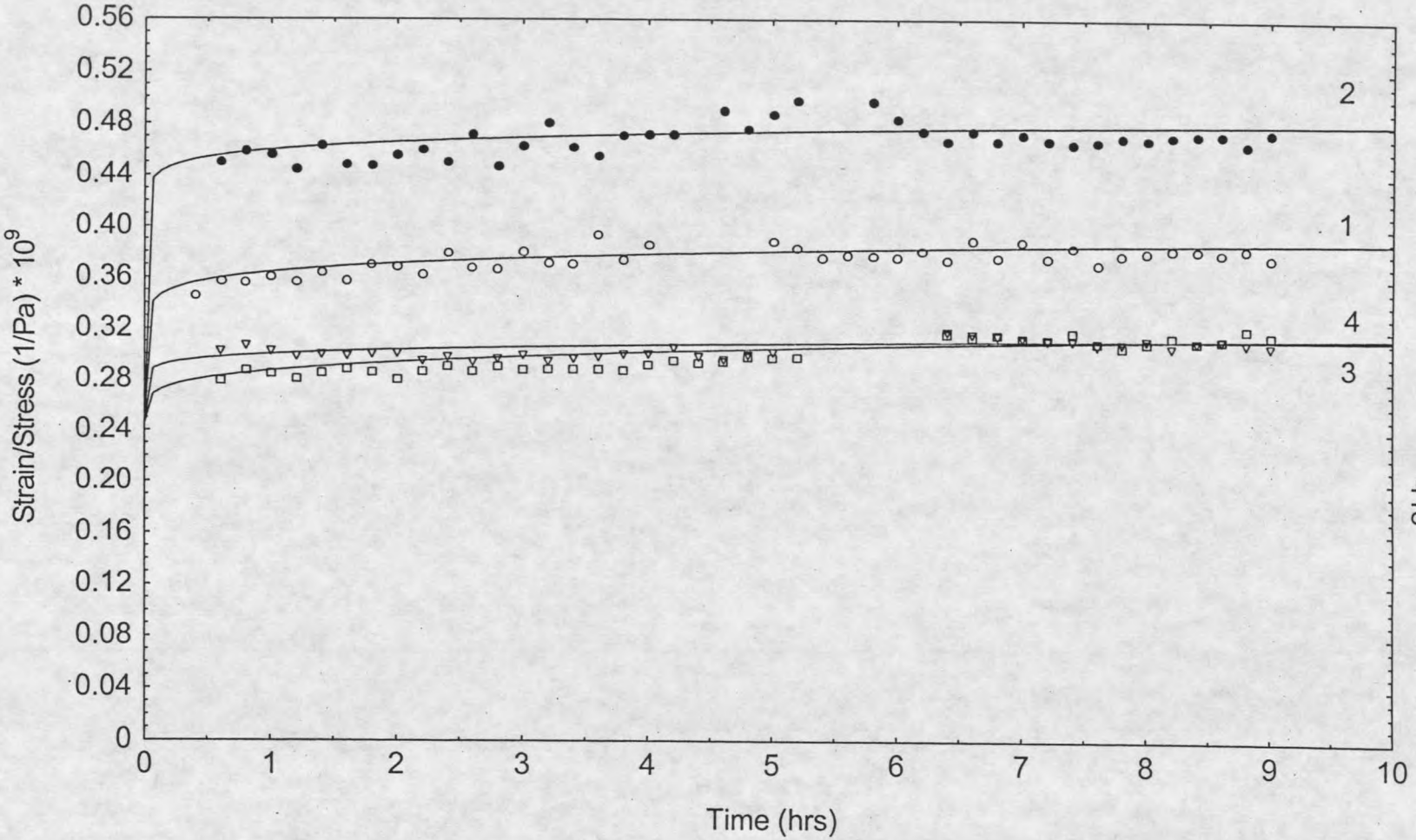


Figure I.I.4 Normalized Vibrocreep Response of PVDF at Different Frequencies at -25 °C
1- $(0.45\pm0.20)\sigma_y$, 5 Hz; 2- $(0.45\pm0.20)\sigma_y$, 10 Hz;
3- $(0.45)\sigma_y$, 4- $(0.60)\sigma_y$, Constant Load Creep;
σ_y = 30.428 MPa at 23 °C

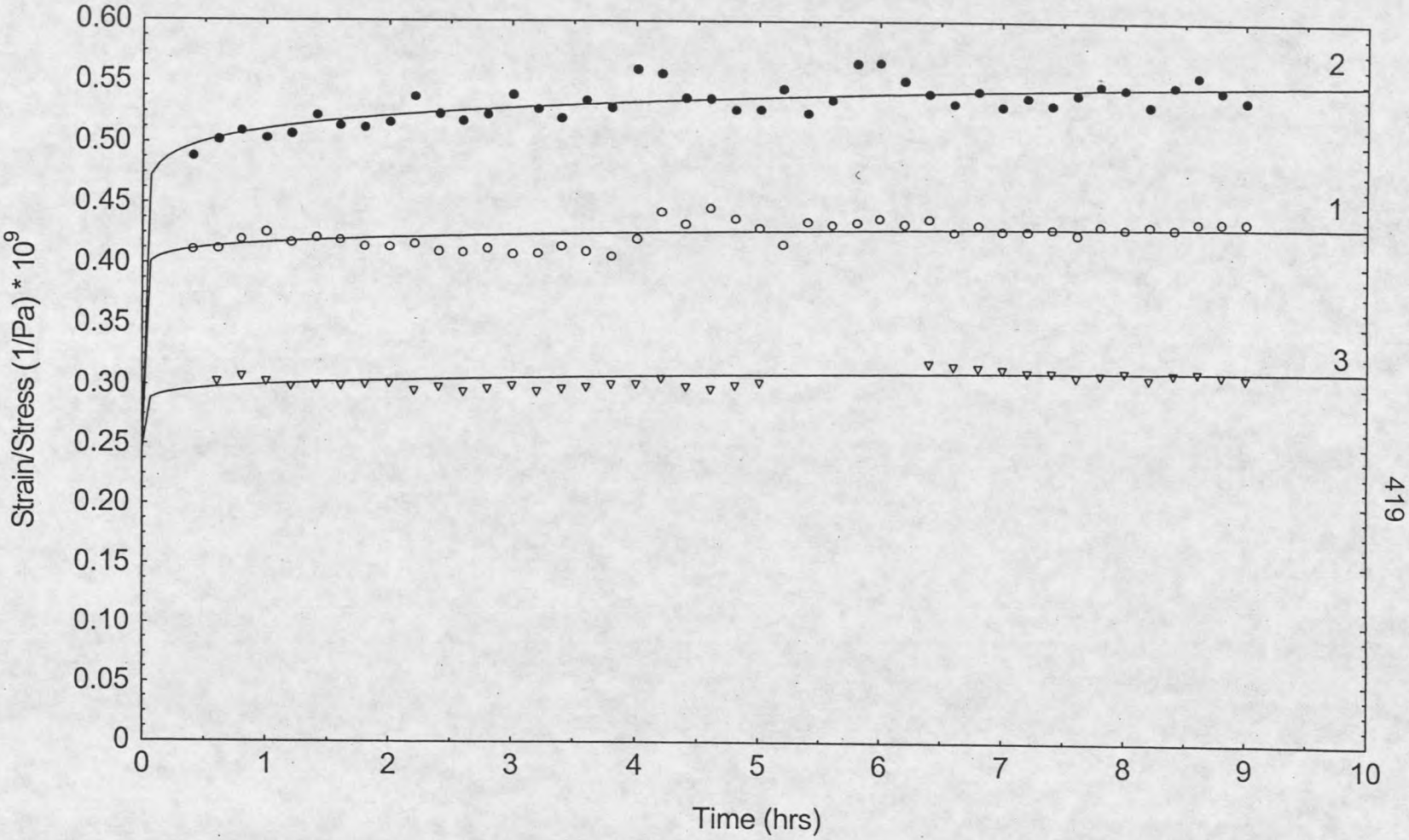


Figure I.I.5 Vibrocreep Response of PVDF at Different Frequencies at -25 °C
1- $(0.60\pm0.20)\sigma_y$, 5 Hz; 2- $(0.60\pm0.20)\sigma_y$, 10 Hz;
3- $(0.60)\sigma_y$, Constant Load Creep;
σ_y = 30.428 MPa at 23 °C

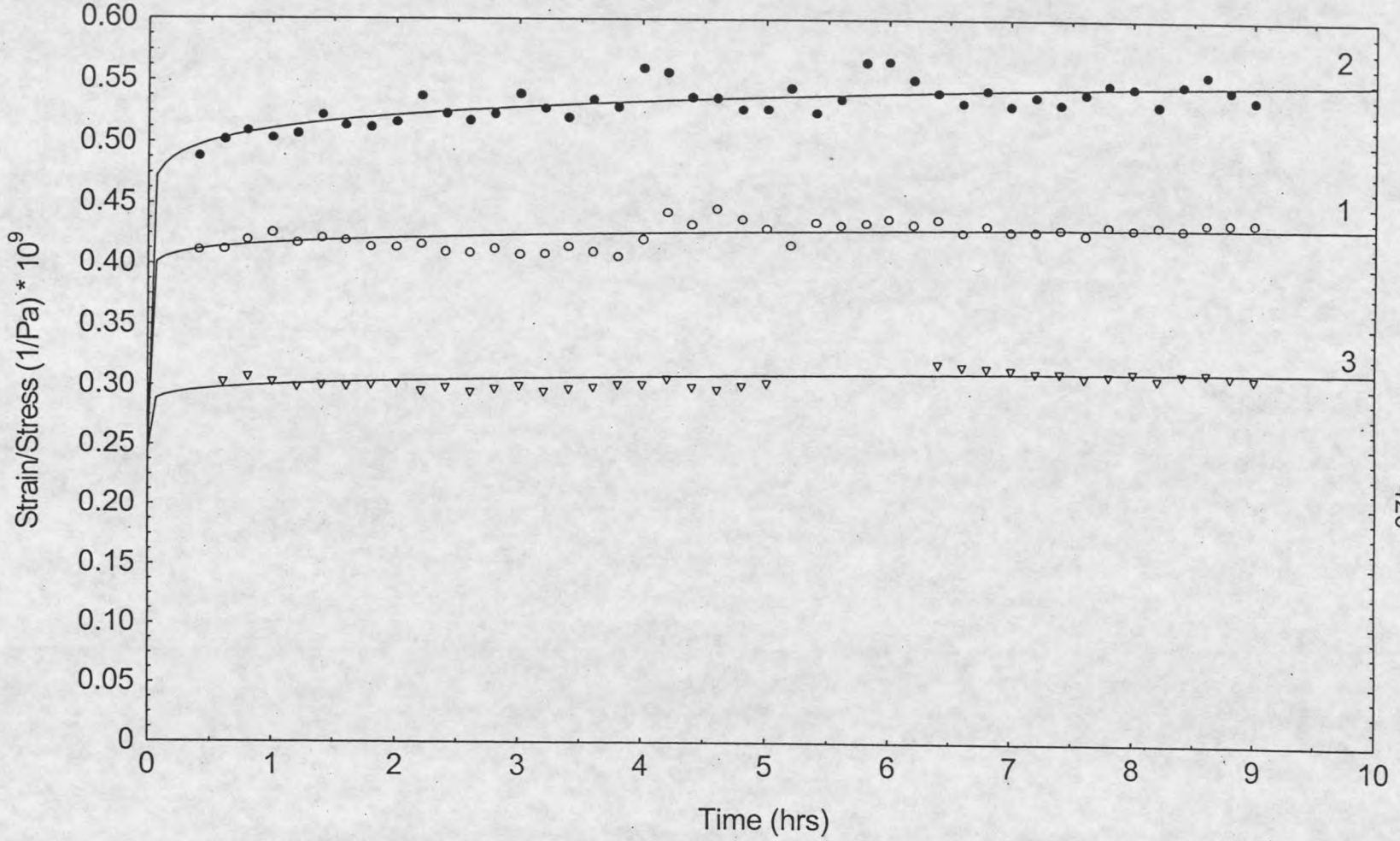


Figure I.I.6 Normalized Vibrocreep Response of PVDF at Different Frequencies at -25 °C
1- $(0.60\pm0.20)\sigma_y$, 5 Hz; 2- $(0.60\pm0.20)\sigma_y$, 10 Hz;
3- $(0.60)\sigma_y$, Constant Load Creep;
σ_y = 30.428 MPa at 23 °C

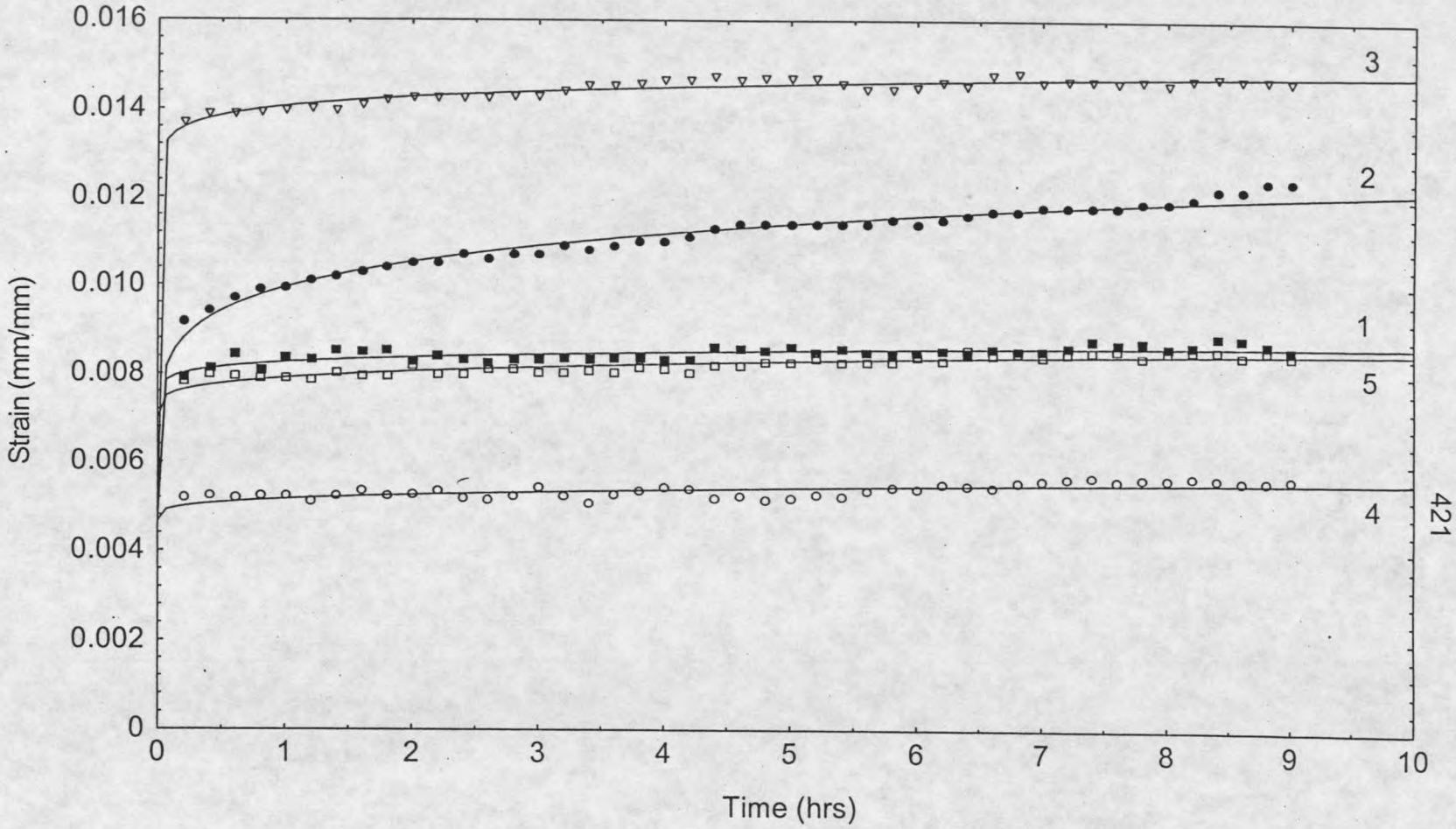


Figure I.II.1 Vibrocreep Response of PVDF at Different Frequencies at 23 °C
1- $(0.30\pm0.10)\sigma_y$, 5 Hz; 2- $(0.30\pm0.10)\sigma_y$, 10 Hz; 3- $(0.30\pm0.10)\sigma_y$, 20 Hz;
4- $(0.30)\sigma_y$, 5- $(0.45)\sigma_y$, Constant Load Creep;
σ_y = 30.428 MPa at 23 °C .

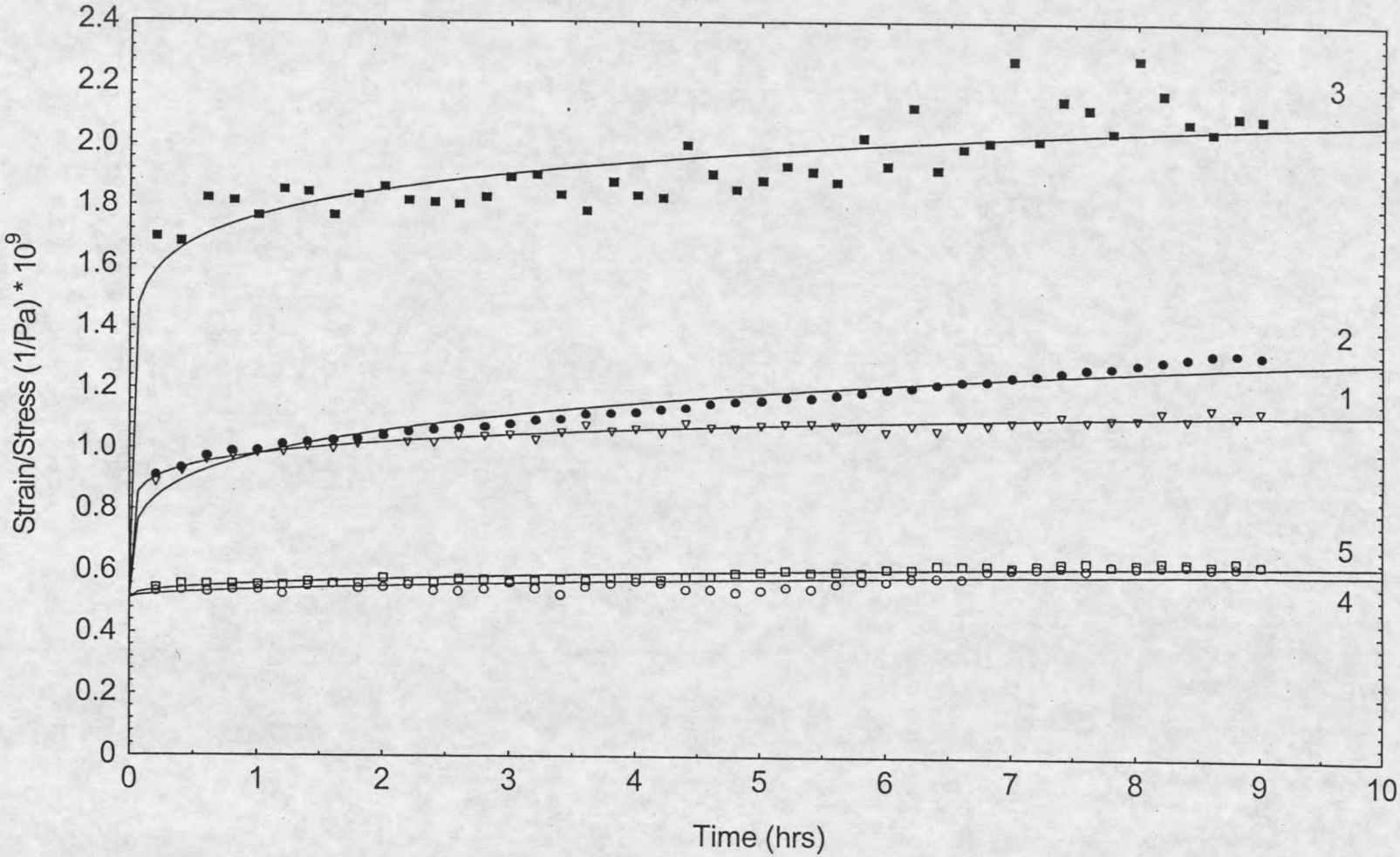


Figure I.II.2 Normalized Vibrocreep Response of PVDF at Different Frequencies at 23 °C
1- $(0.30\pm0.10)\sigma_y$, 5 Hz; 2- $(0.30\pm0.10)\sigma_y$, 10 Hz; 3- $(0.30\pm0.10)\sigma_y$, 20 Hz;
4- $(0.30)\sigma_y$, 5- $(0.45)\sigma_y$, Constant Load Creep;
σ_y = 30.428 MPa at 23 °C

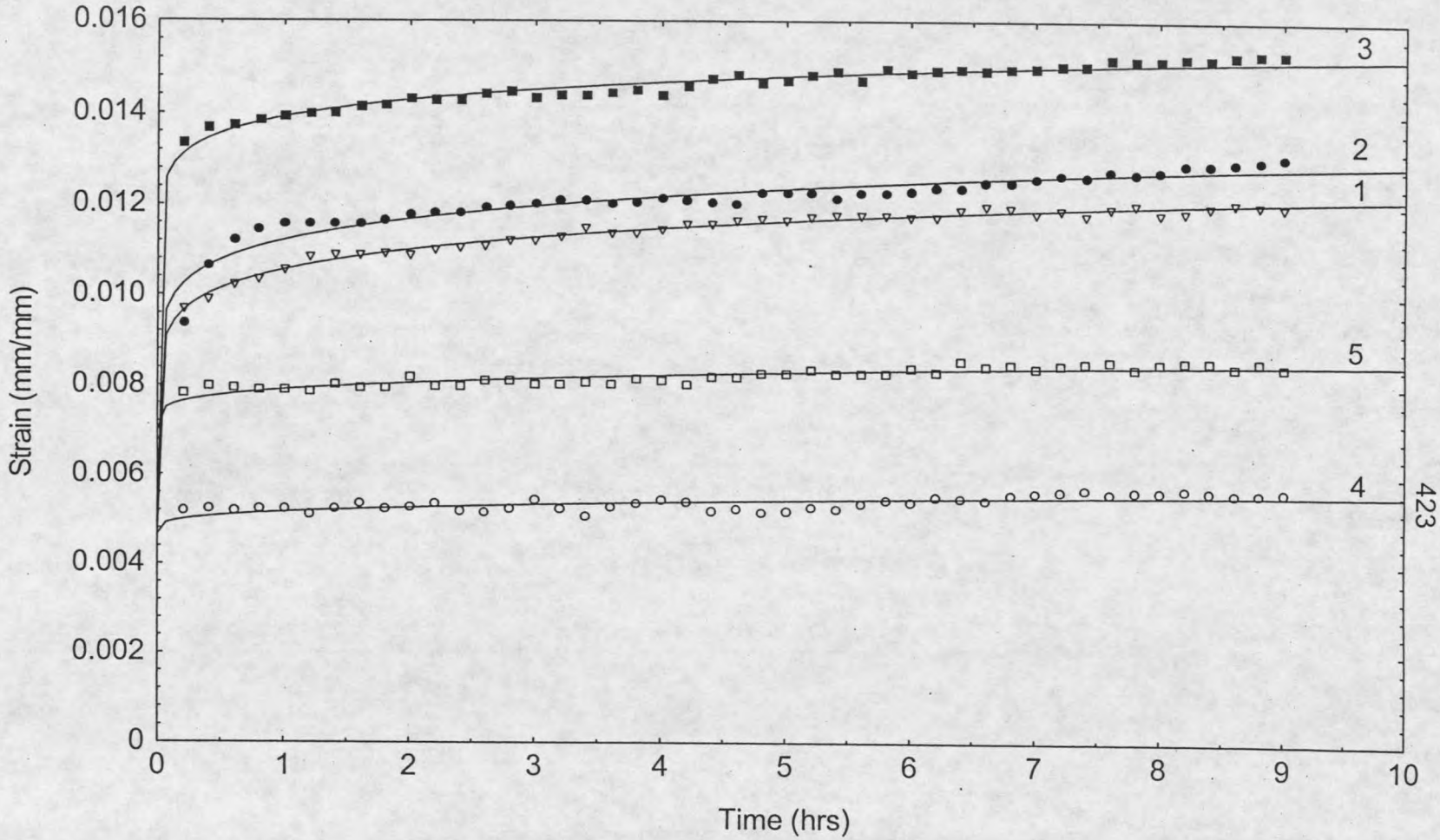


Figure I.II.3 Vibrocreep Response of PVDF at Different Frequencies at 23 °C
1- $(0.30\pm0.20)\sigma_y$, 5 Hz; 2- $(0.30\pm0.20)\sigma_y$, 10 Hz; 3- $(0.30\pm0.20)\sigma_y$, 20 Hz;
4- $(0.30)\sigma_y$, 5- $(0.45)\sigma_y$, Constant Load Creep;
σ_y = 30.428 MPa at 23 °C

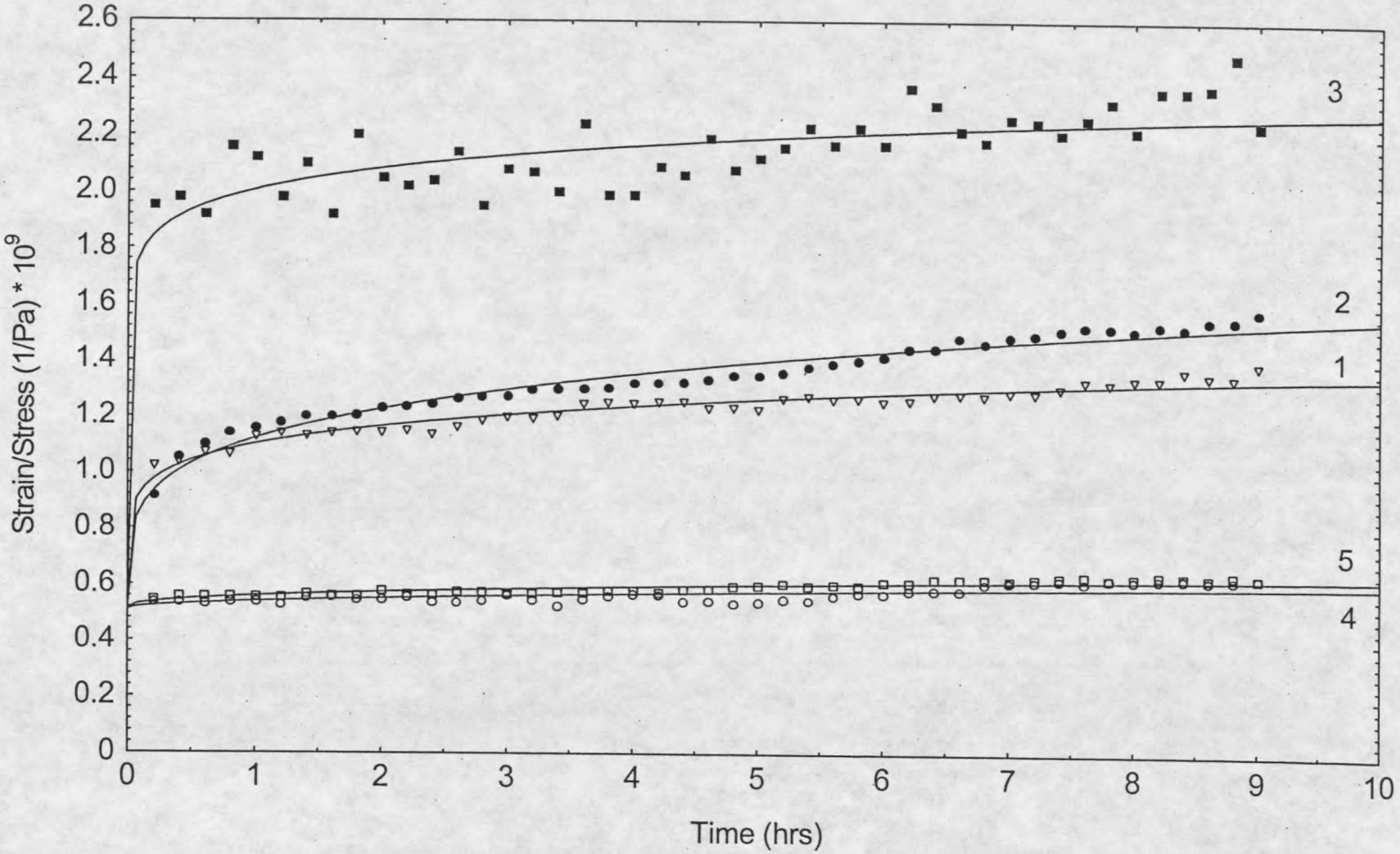


Figure I.II.4 Normalized Vibrocreep Response of PVDF at Different Frequencies at 23 °C
1- $(0.30\pm0.20)\sigma_y$, 5 Hz; 2- $(0.30\pm0.20)\sigma_y$, 10 Hz; 3- $(0.30\pm0.20)\sigma_y$, 20 Hz;
4- $(0.30)\sigma_y$, 5- $(0.45)\sigma_y$, Constant Load Creep;
σ_y = 30.428 MPa at 23 °C

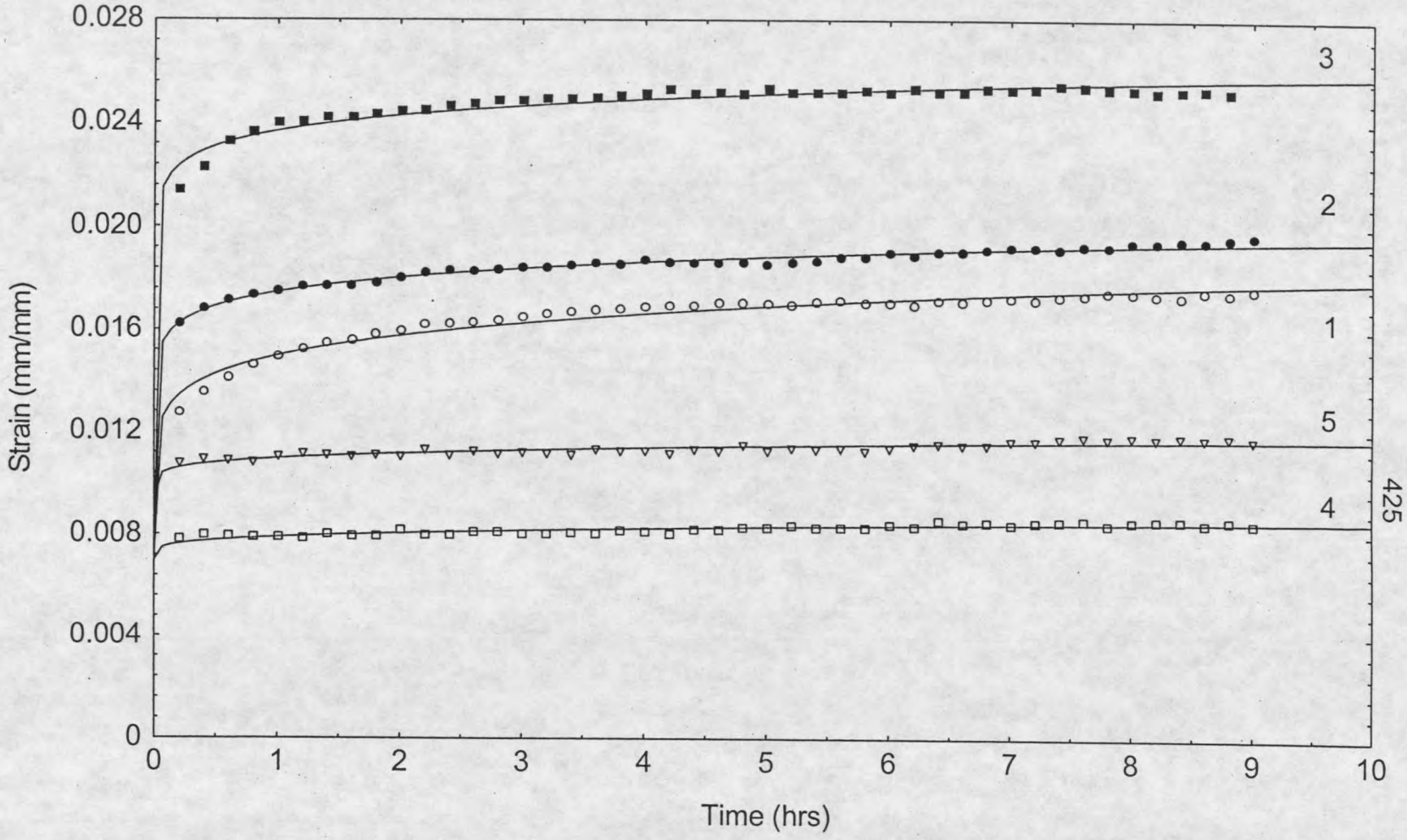


Figure I.II.5 Vibrocreep Response of PVDF at Different Frequencies at 23 °C
1- $(0.45\pm0.10)\sigma_y$, 5 Hz; 2- $(0.45\pm0.10)\sigma_y$, 10 Hz; 3- $(0.45\pm0.10)\sigma_y$, 20 Hz;
4- $(0.45)\sigma_y$, 5- $(0.60)\sigma_y$, Constant Load Creep;
σ_y = 30.428 MPa at 23 °C

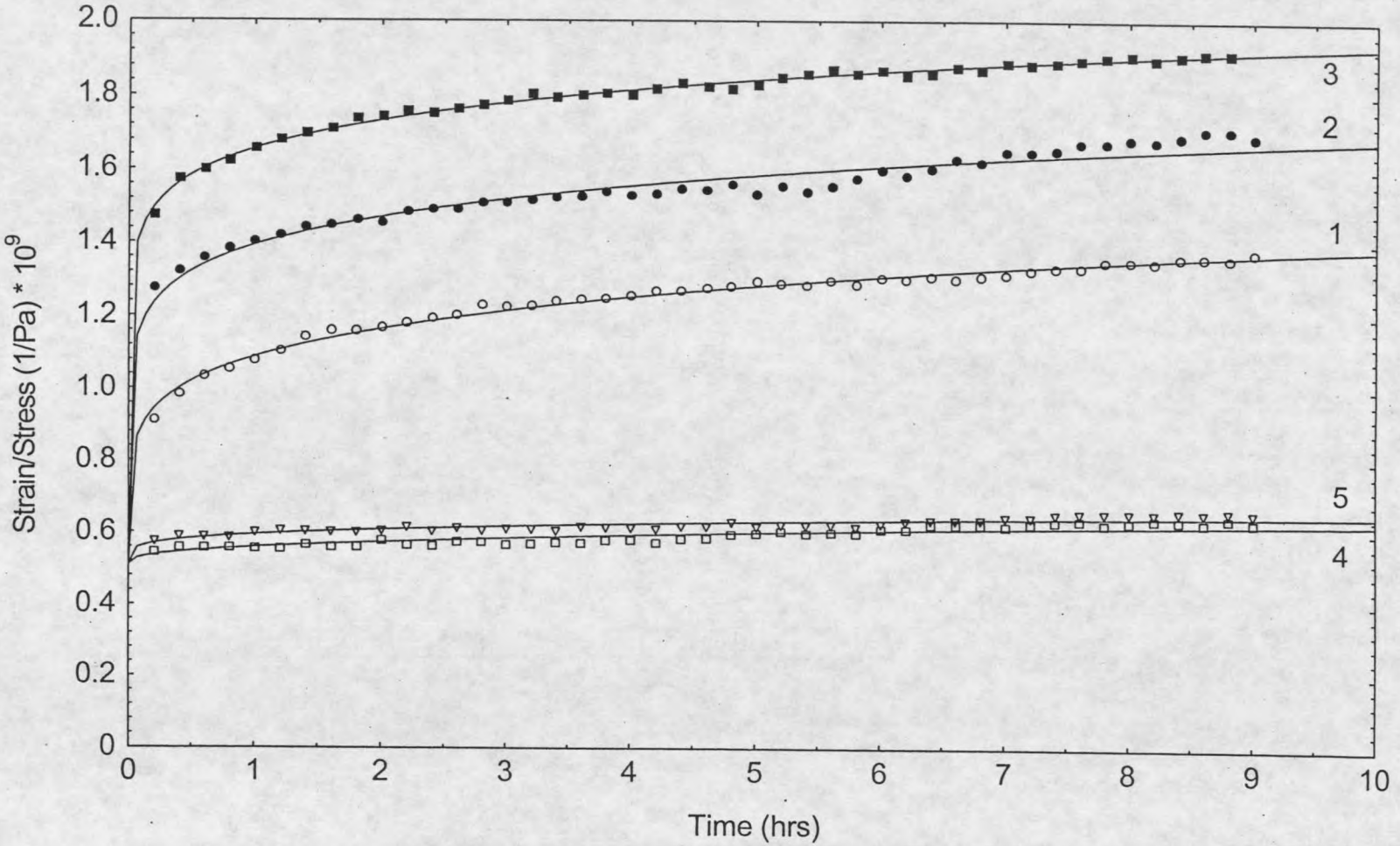


Figure I.II.6 Normalized Vibrocreep Response of PVDF at Different Frequencies at 23 °C
1- $(0.45\pm0.10)\sigma_y$, 5Hz; 2- $(0.45\pm0.10)\sigma_y$, 10 Hz; 3- $(0.45\pm0.10)\sigma_y$, 20 Hz;
4- $(0\ .45)\sigma_y$, 5- $(0.60)\sigma_y$, Constant Load Creep;
σ_y = 30.428 MPa at 23 °C

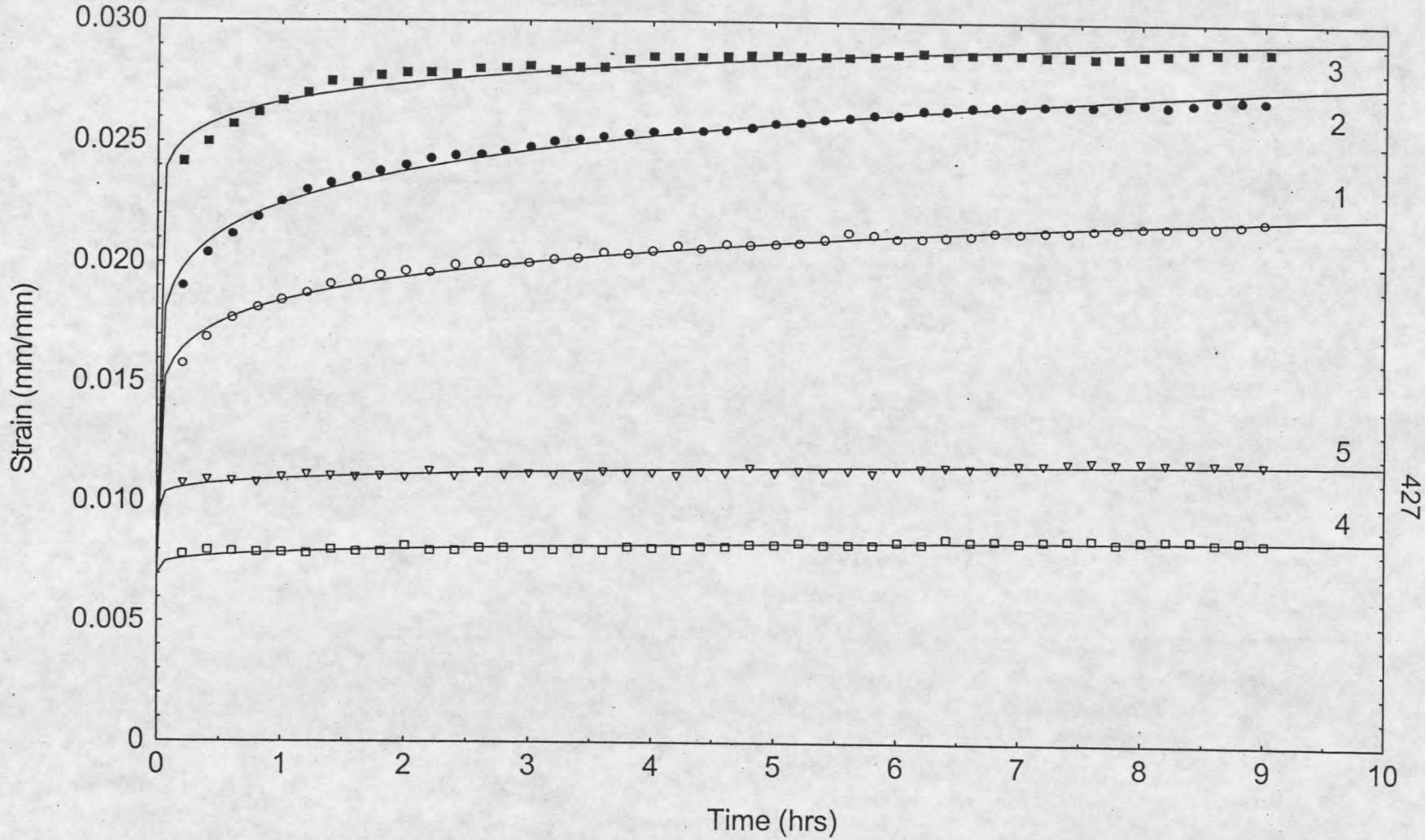


Figure I.II.7 Vibrocreep Response of PVDF at Different Frequencies at 23 °C
1- $(0.45\pm0.20)\sigma_y$, 5 Hz; 2- $(0.45\pm0.20)\sigma_y$, 10 Hz; 3- $(0.45\pm0.20)\sigma_y$, 20 Hz;
4- $(0.45)\sigma_y$, 5- $(0.60)\sigma_y$, Constant Load Creep;
σ_y = 30.428 MPa at 23 °C

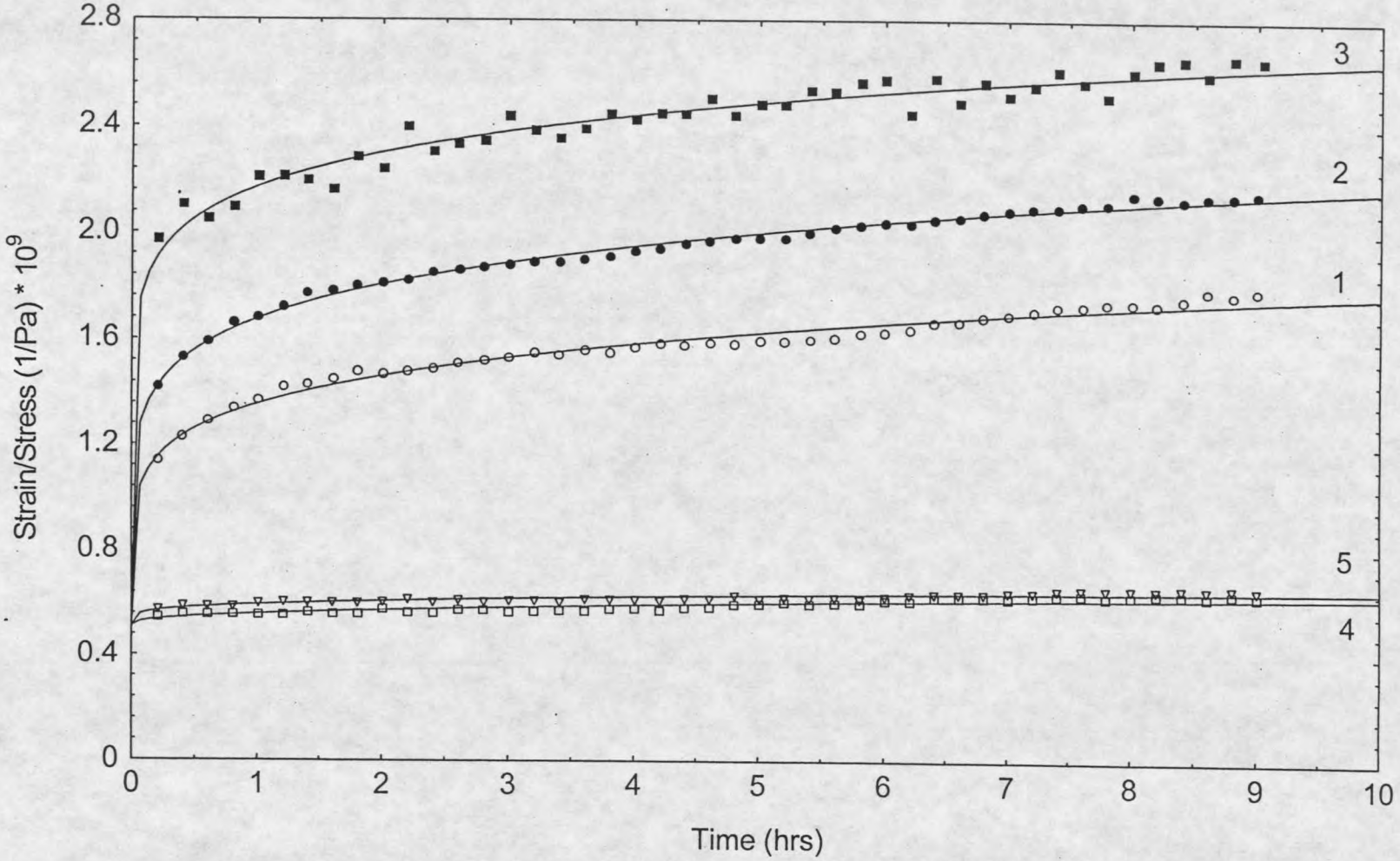


Figure I.II.8 Normalized Vibrocreep Response of PVDF at Different Frequencies at 23 °C
1- $(0.45\pm0.20)\sigma_y$, 5 Hz; 2- $(0.45\pm0.20)\sigma_y$, 10 Hz; 3- $(0.45\pm0.20)\sigma_y$, 20 Hz;
4- $(0.45)\sigma_y$, 5- $(0.60)\sigma_y$, Constant Load Creep;
σ_y = 30.428 MPa at 23 °C

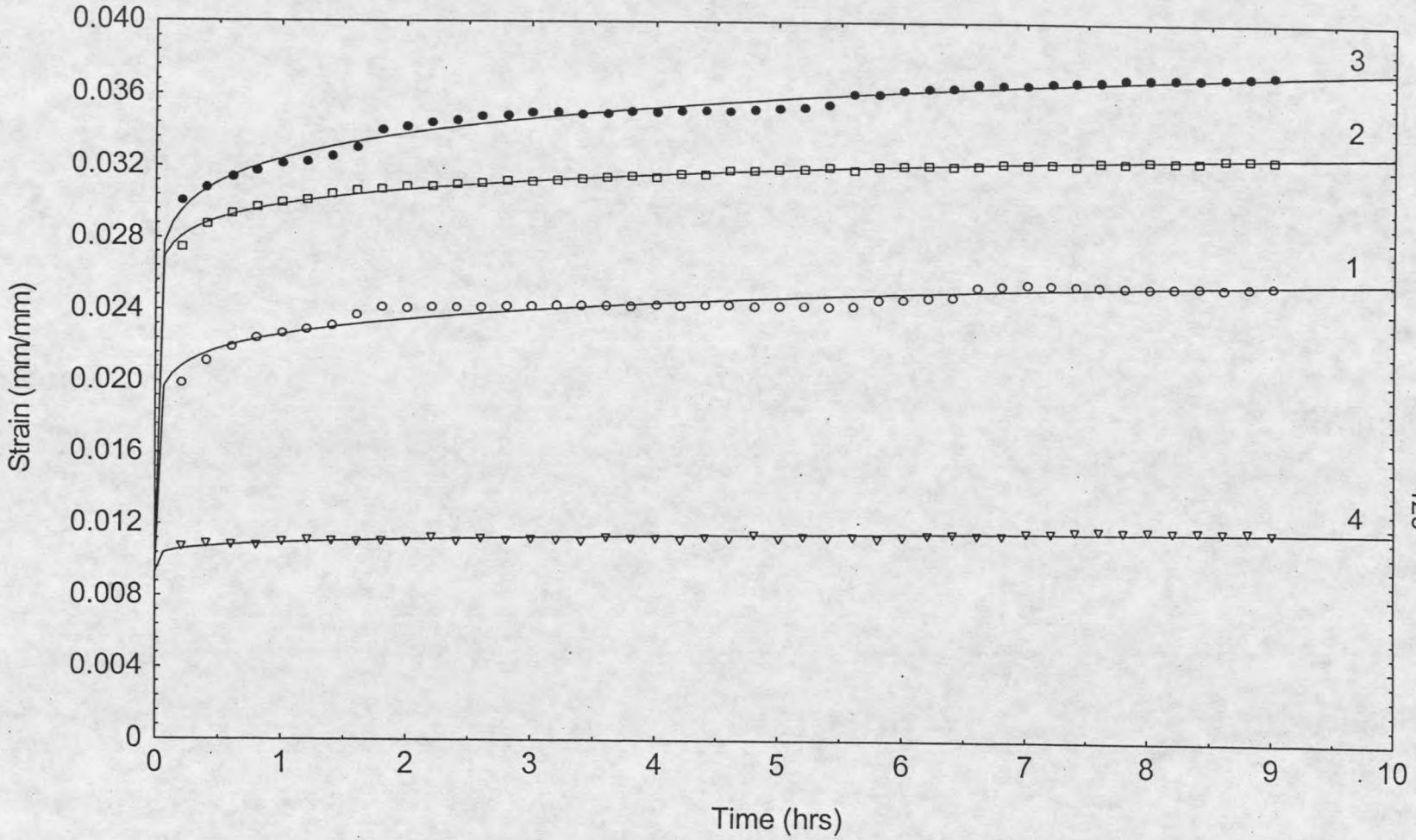


Figure I.II.9 Vibrocreep Response of PVDF at Different Frequencies at 23 °C
1- $(0.60\pm0.10)\sigma_y$, 5 Hz; 2- $(0.60\pm0.10)\sigma_y$, 10 Hz; 3- $(0.60\pm0.10)\sigma_y$, 20 Hz;
4- $(0.60)\sigma_y$, Constant Load Creep;
σ_y = 30.428 MPa at 23 °C

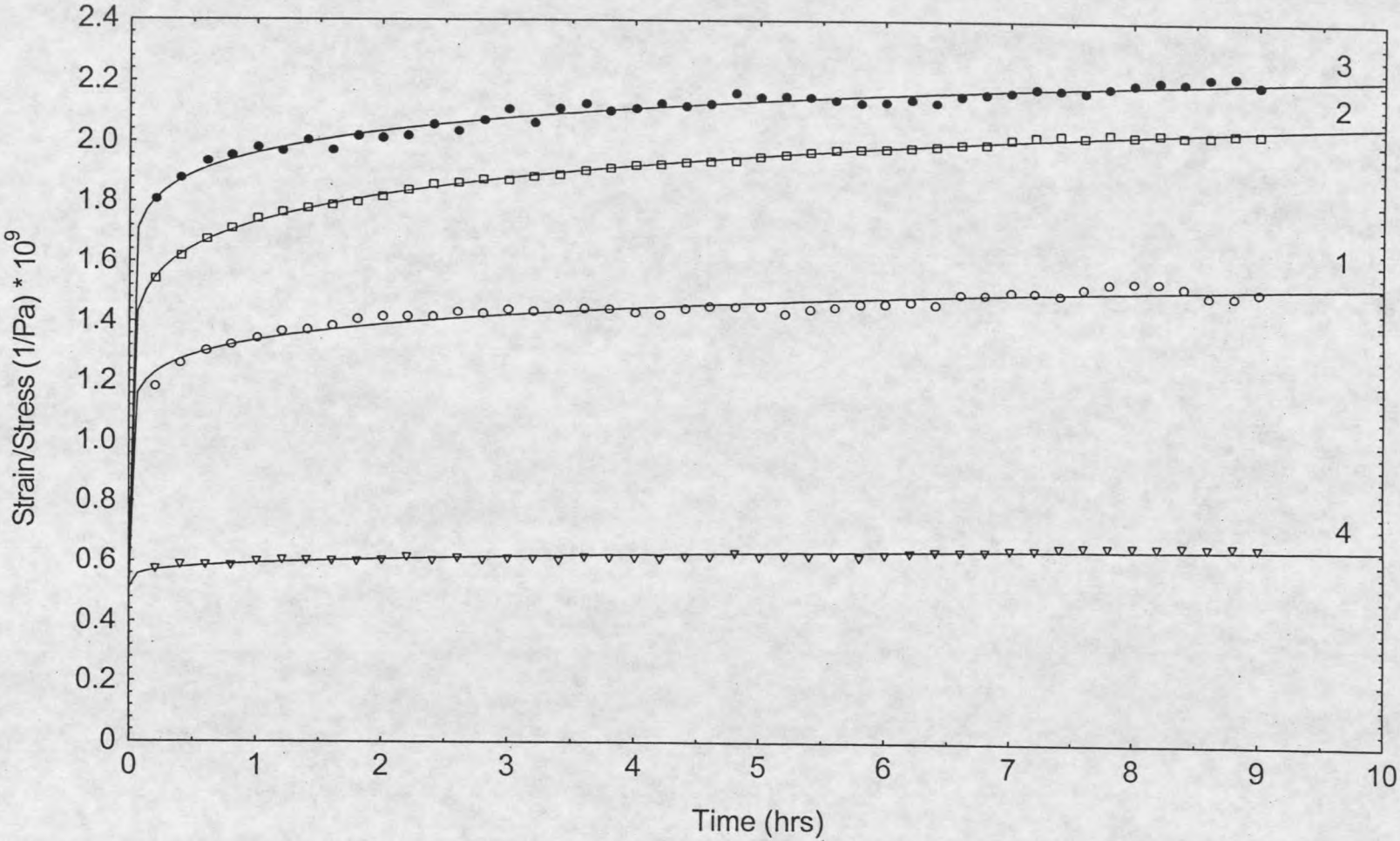


Figure I.II.10 Normalized Vibrocreep Response of PVDF at Different Frequencies at 23 °C
1- $(0.60\pm0.10)\sigma_y$, 5 Hz; 2- $(0.60\pm0.10)\sigma_y$, 10 Hz; 3- $(0.60\pm0.10)\sigma_y$, 20 Hz;
4- $(0.60)\sigma_y$, Constant Load Creep;
σ_y = 30.428 MPa at 23 °C

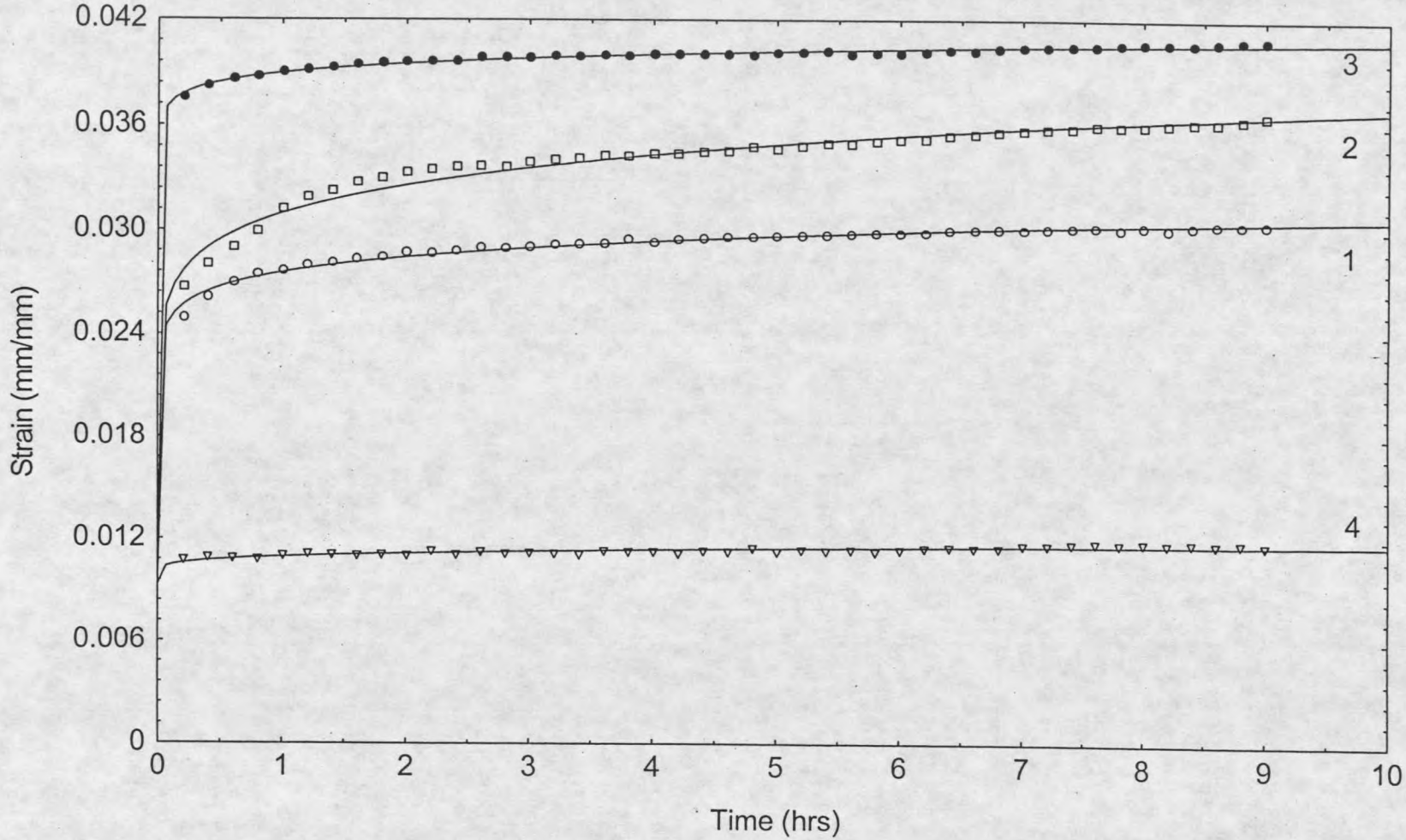


Figure I.II.11 Vibrocreep Response of PVDF at Different Frequencies at 23 °C
1- $(0.60\pm0.20)\sigma_y$, 5 Hz; 2- $(0.60\pm0.20)\sigma_y$, 10 Hz; 3- $(0.60\pm0.20)\sigma_y$, 20 Hz;
4- $(0.60)\sigma_y$, Constant Load Creep;
σ_y = 30.428 MPa at 23 °C

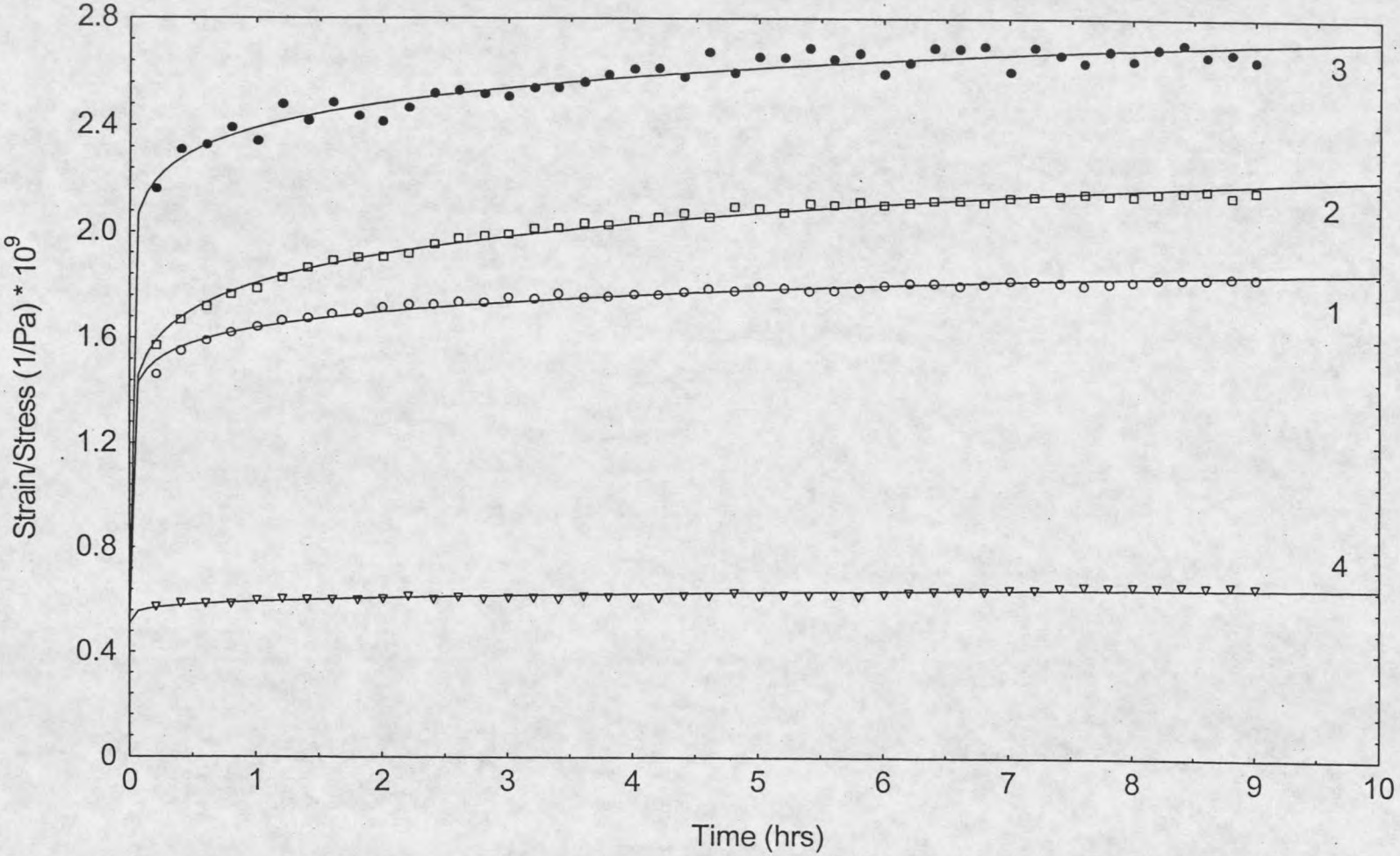


Figure I.II.12 Normalized Vibrocreep Response of PVDF at Different Frequencies at 23 °C
1- $(0.60\pm0.20)\sigma_y$, 5 Hz; 2- $(0.60\pm0.20)\sigma_y$, 10 Hz; 3- $(0.60\pm0.20)\sigma_y$, 20 Hz;
4- $(0.60)\sigma_y$, Constant Load Creep;
σ_y = 30.428 MPa at 23 °C

APPENDIX J

Amplitude Effects from Vibrocreep Testing of PVDF

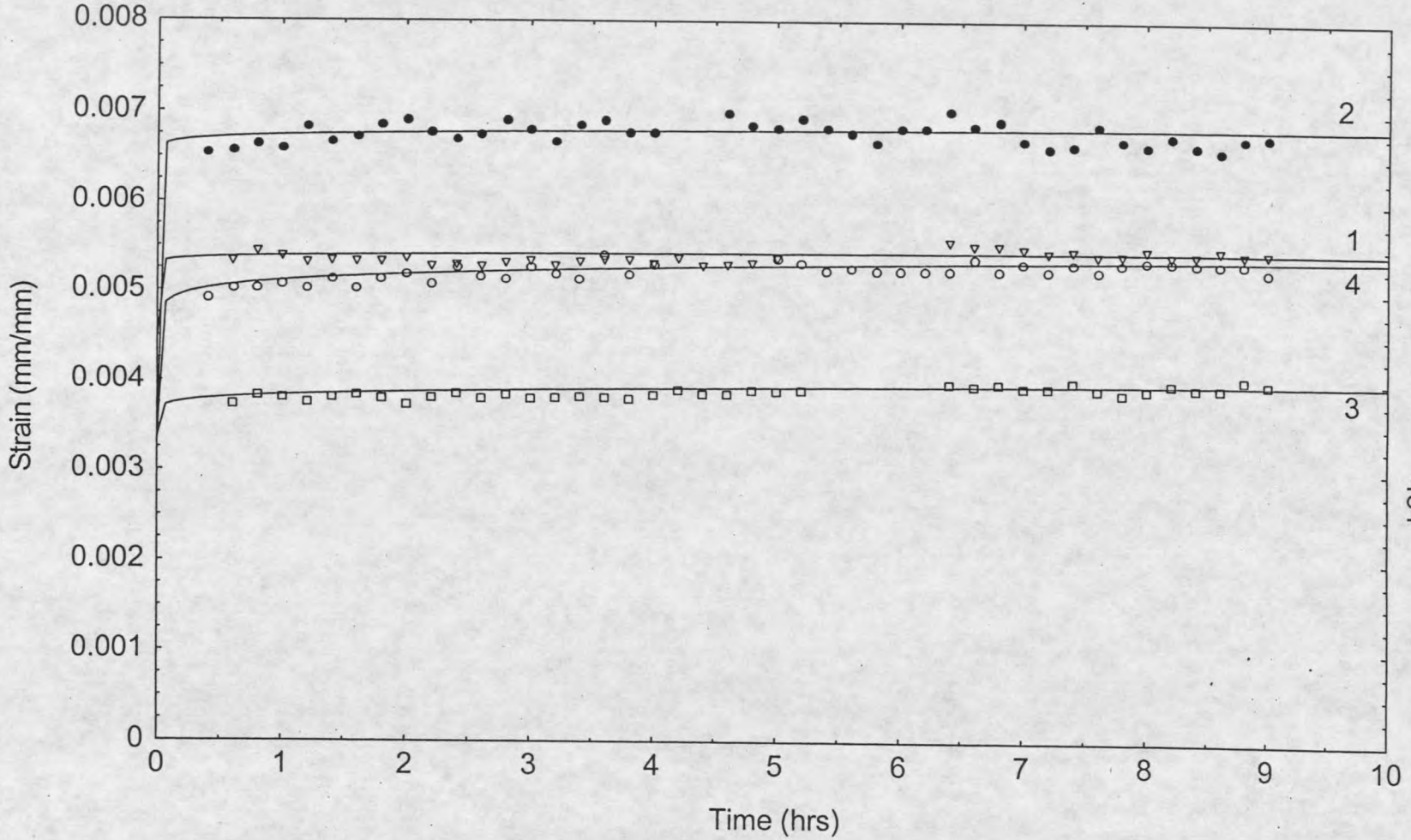


Figure J.I.1 Vibrocreep Response of PVDF at Different Amplitudes at -25 °C
1- $(0.45\pm0.20)\sigma_y$, 5 Hz; 2- $(0.45\pm0.35)\sigma_y$, 5 Hz;
3- $(0.45)\sigma_y$, 4- $(0.60)\sigma_y$, Constant Load Creep;
σ_y = 30.428 MPa at 23 °C

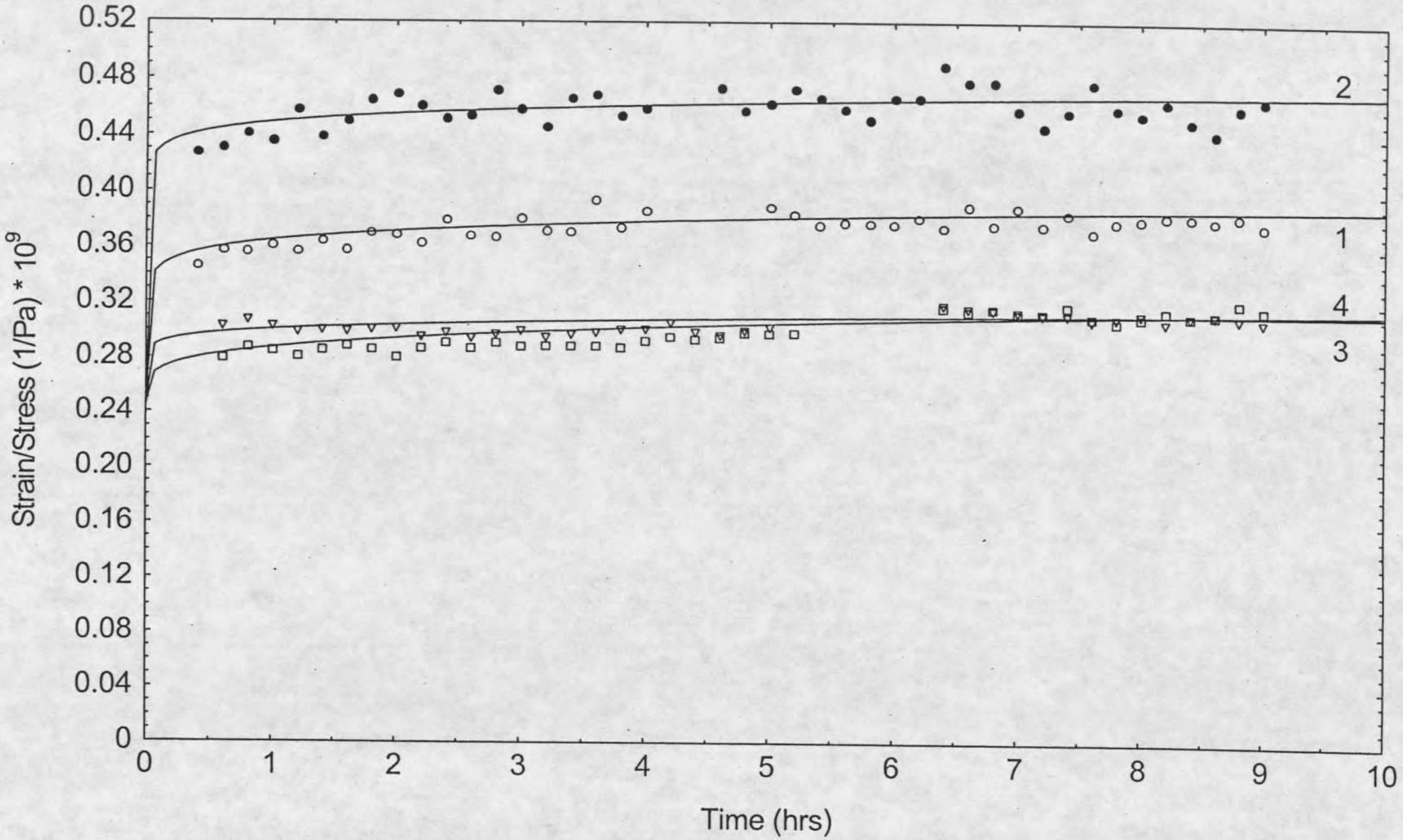


Figure J.I.2 Normalized Vibrocreep Response of PVDF at Amplitudes at -25 °C
1- $(0.45\pm0.20)\sigma_y$, 5 Hz; 2- $(0.45\pm0.35)\sigma_y$, 5 Hz;
3- $(0.45)\sigma_y$, 4- $(0.60)\sigma_y$, Constant Load Creep;
σ_y = 30.428 MPa at 23 °C

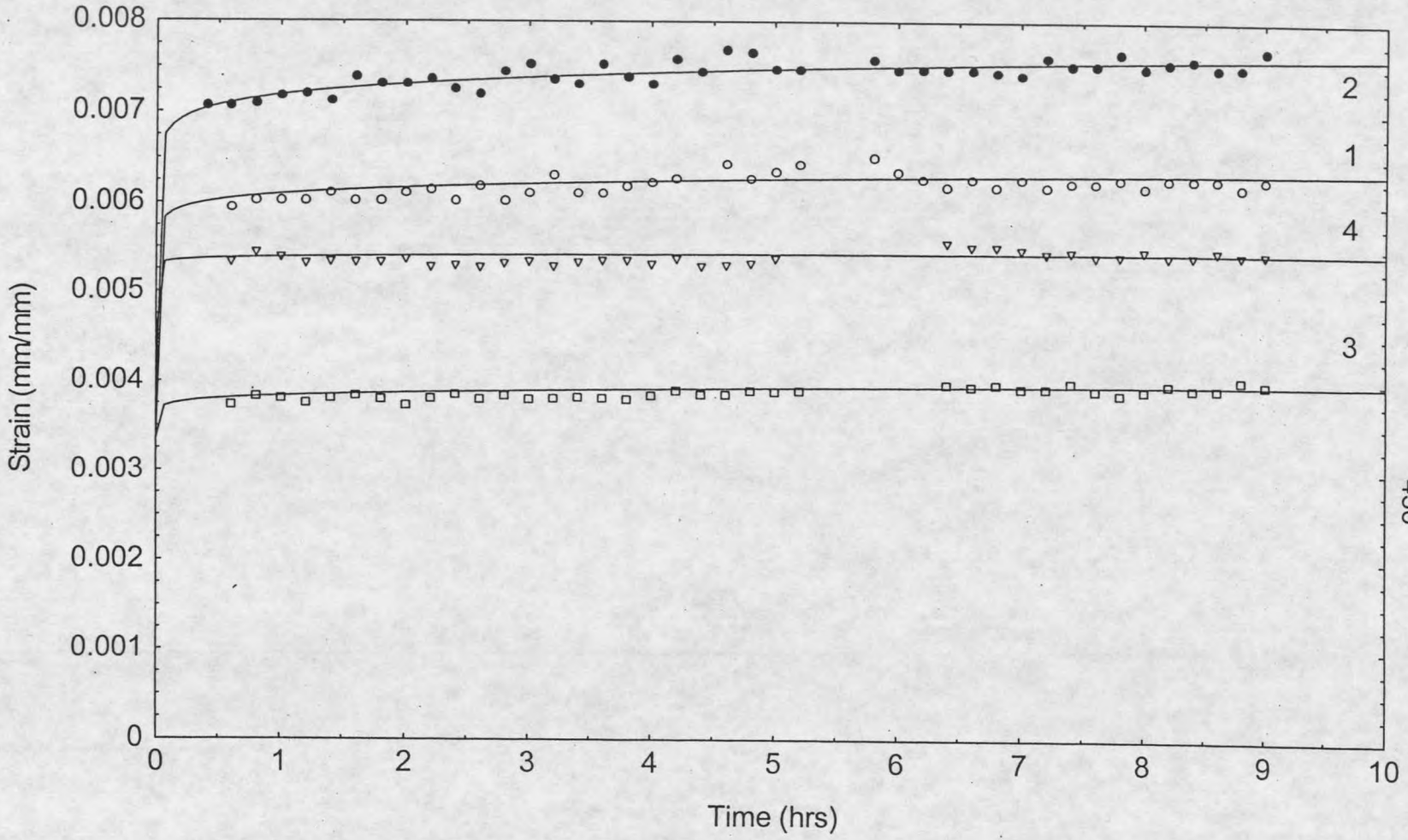


Figure J.I.3 Vibrocreep Response of PVDF at Different Amplitudes at -25 °C
1- $(0.45\pm0.20)\sigma_y$, 10 Hz; 2- $(0.45\pm0.40)\sigma_y$, 10 Hz;
3- $(0.45)\sigma_y$, 4- $(0.60)\sigma_y$, Constant Load Creep;
σ_y = 30.428 MPa at 23 °C

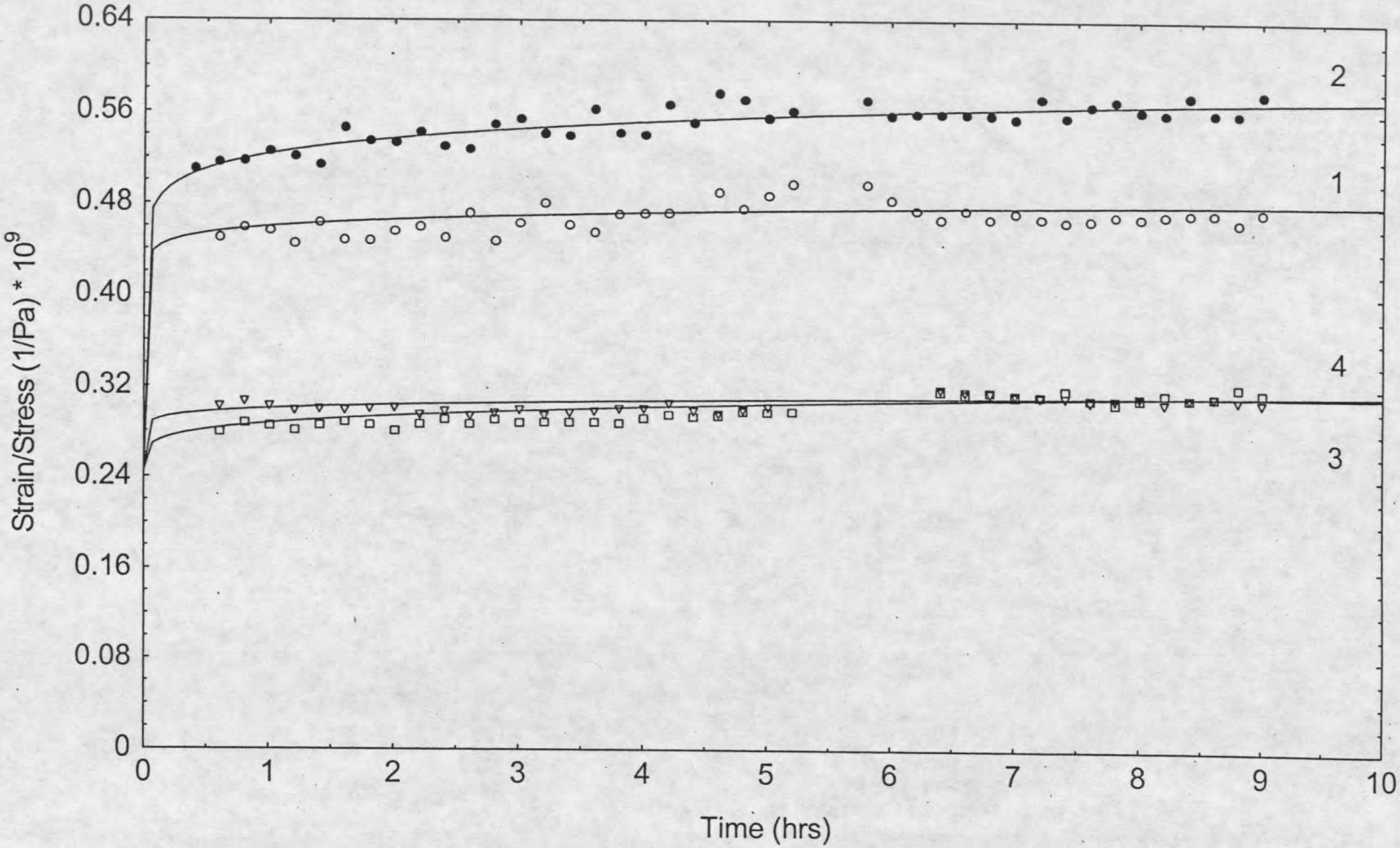


Figure J.I.4 Normalized Vibrocreep Response of PVDF at Amplitudes at -25 °C
1- $(0.45\pm0.20)\sigma_y$, 10 Hz; 2- $(0.45\pm0.40)\sigma_y$, 10 Hz;
3- $(0.45)\sigma_y$, 4- $(0.60)\sigma_y$, Constant Load Creep;
σ_y = 30.428 MPa at 23 °C

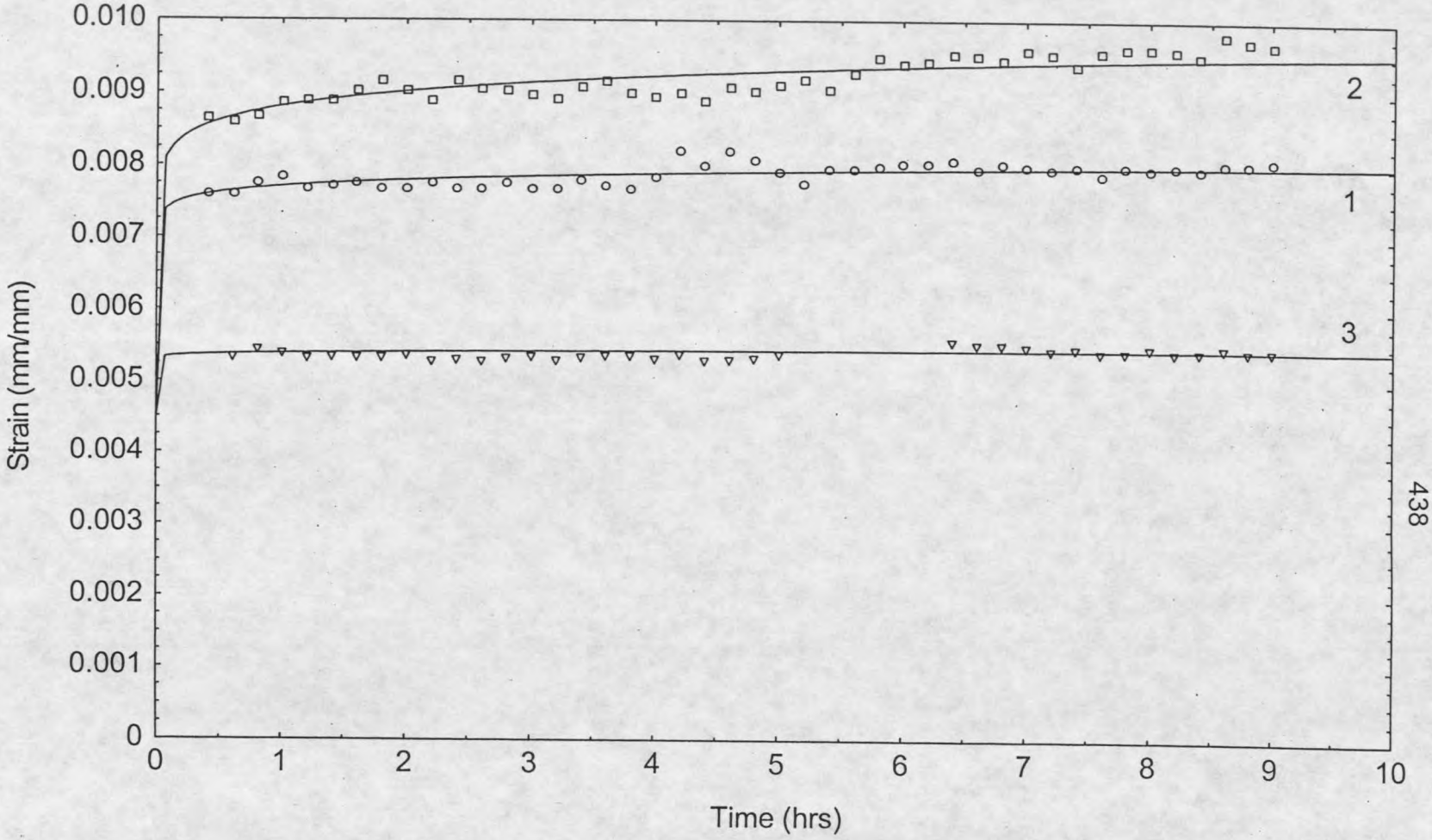


Figure J.I.5 Vibrocreep Response of PVDF at Different Amplitudes at -25 °C
1- $(0.60\pm0.20)\sigma_y$, 5 Hz; 2- $(0.60\pm0.40)\sigma_y$, 5 Hz;
3- $(0.60)\sigma_y$, Constant Load Creep;
σ_y = 30.428 MPa at 23 °C

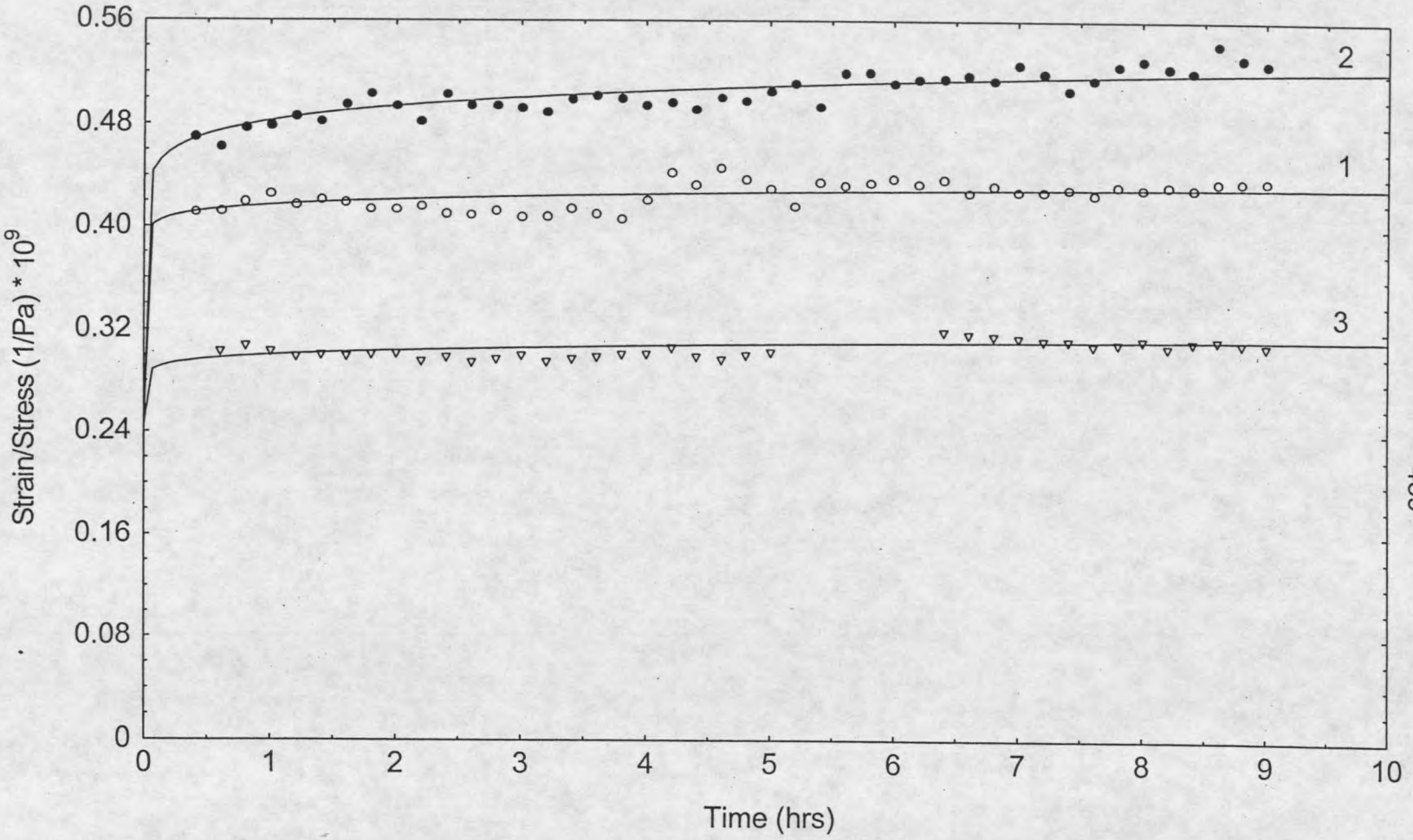


Figure J.I.6 Normalized Vibrocreep Response of PVDF at Different Amplitudes at -25 °C
1- $(0.60\pm0.20)\sigma_y$, 5 Hz; 2- $(0.60\pm0.40)\sigma_y$, 5 Hz;
3- $(0.60)\sigma_y$, Constant Load Creep;
σ_y = 30.428 MPa at 23 °C

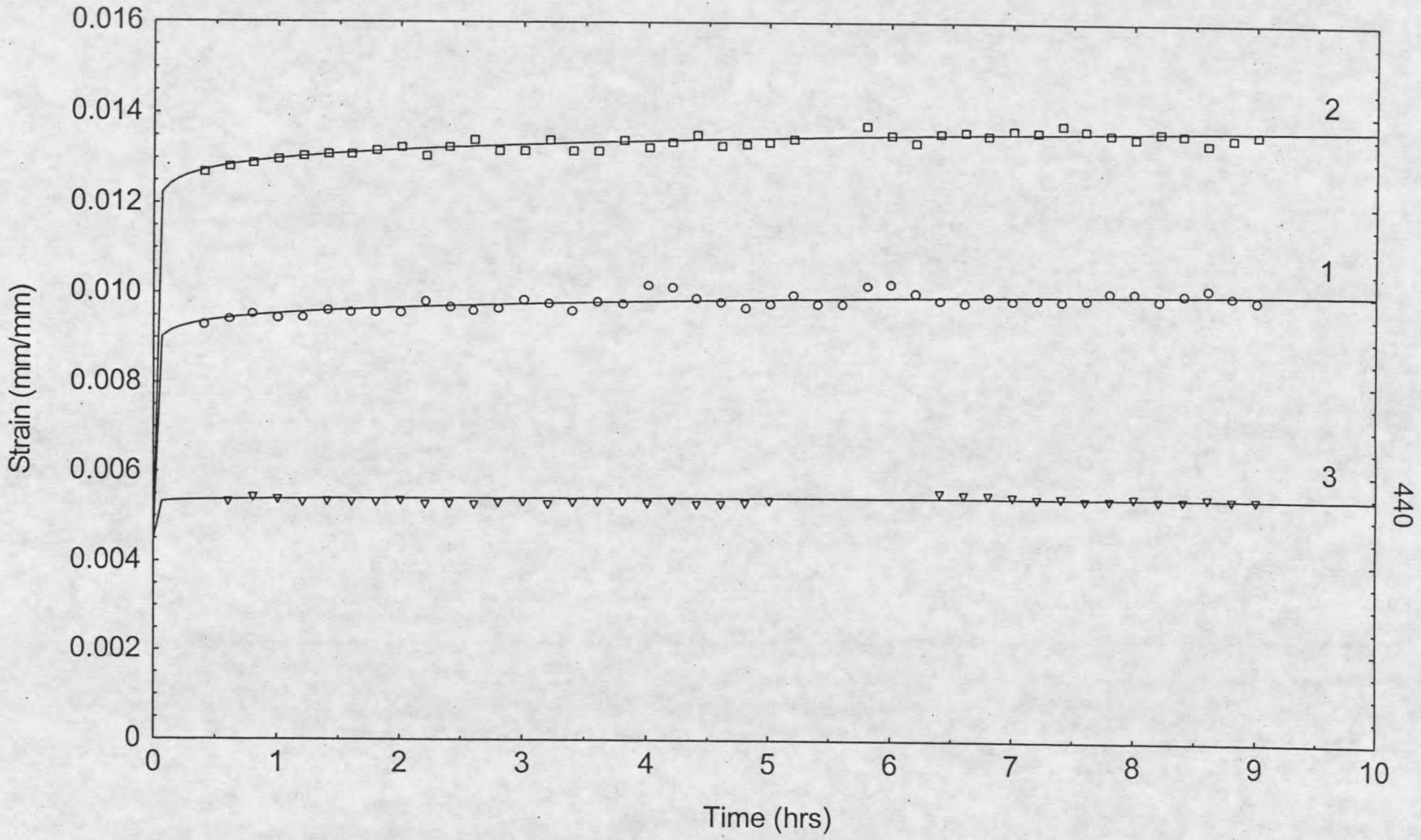


Figure J.I.7 Vibrocreep Response of PVDF at Different Amplitudes at -25 °C
1- $(0.60\pm0.20)\sigma_y$, 10 Hz; 2- $(0.60\pm0.50)\sigma_y$, 10 Hz;
3- $(0.60)\sigma_y$, Constant Load Creep;
σ_y = 30.428 MPa at 23 °C

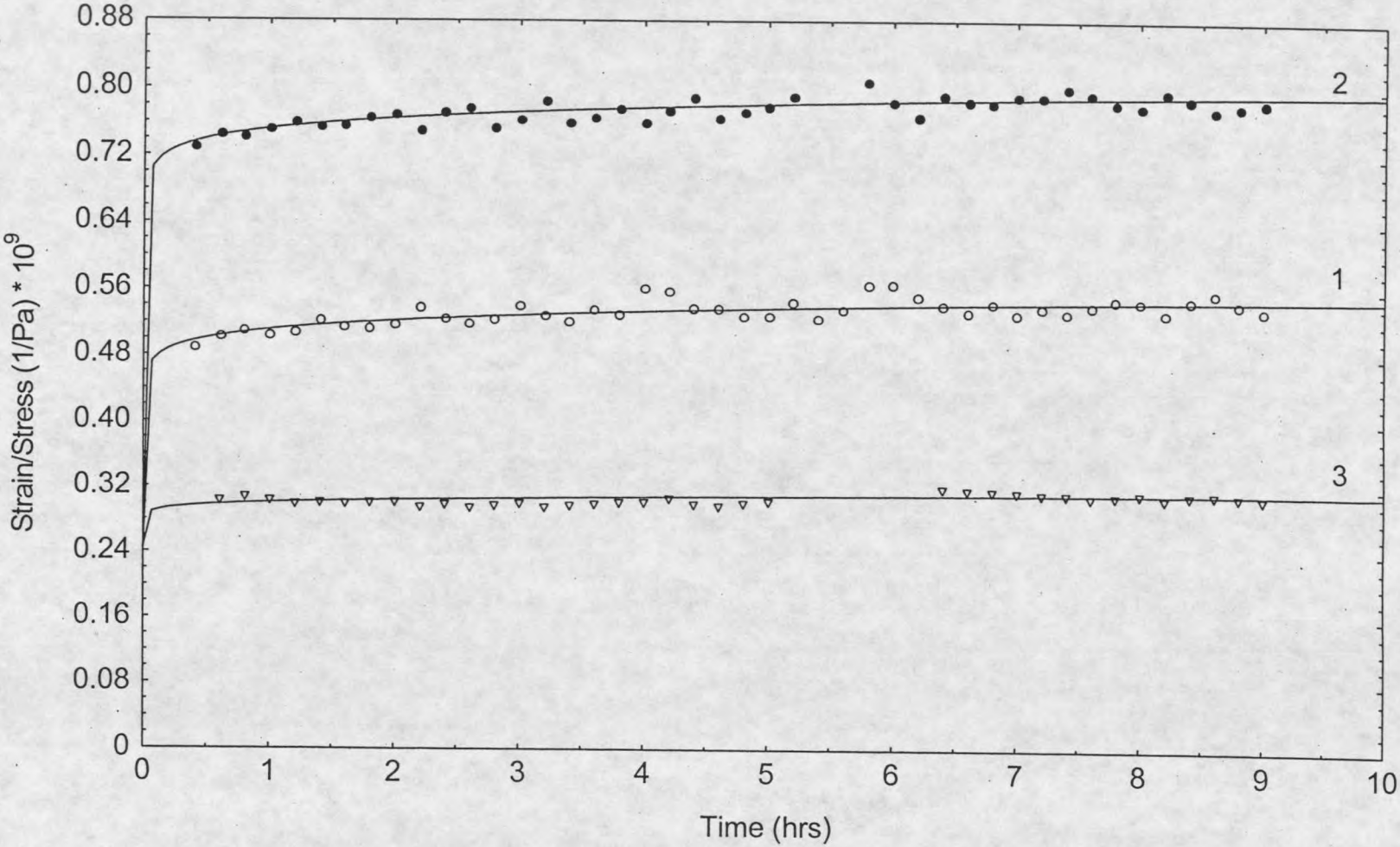


Figure J.I.8 Normalized Vibrocreep Response of PVDF at Different Amplitudes at -25 °C
1- $(0.60\pm0.20)\sigma_y$, 10 Hz; 2- $(0.60\pm0.50)\sigma_y$, 10 Hz;
3- $(0.60)\sigma_y$, Constant Load Creep;
σ_y = 30.428 MPa at 23 °C

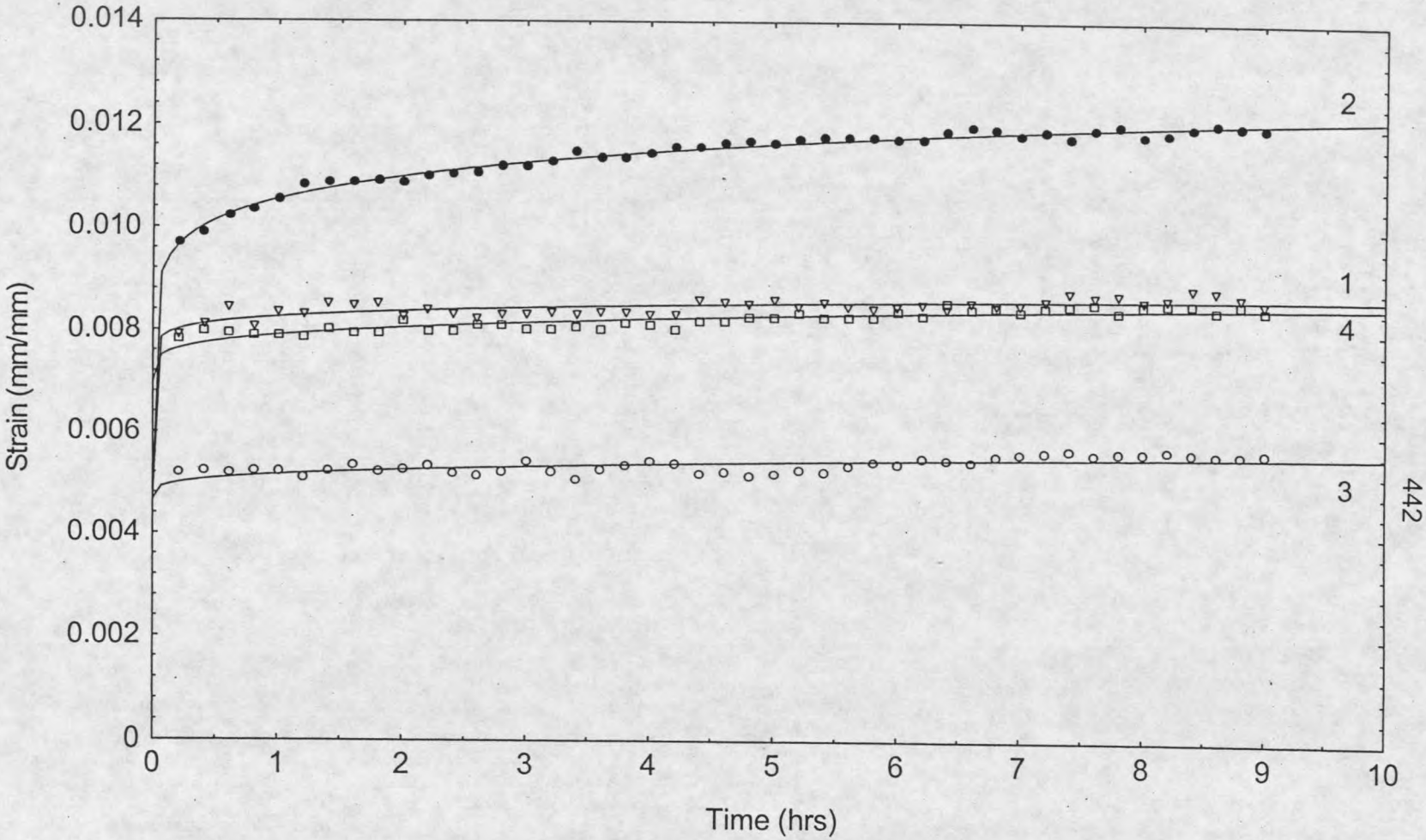


Figure J.II.1 Vibrocreep Response of PVDF at Different Amplitudes at 23 °C
1- $(0.30\pm0.10)\sigma_y$, 5 Hz; 2- $(0.30\pm0.20)\sigma_y$, 5 Hz;
3- $(0.30)\sigma_y$, 4- $(0.45)\sigma_y$, Constant Load Creep;
σ_y = 30.428 MPa at 23 °C

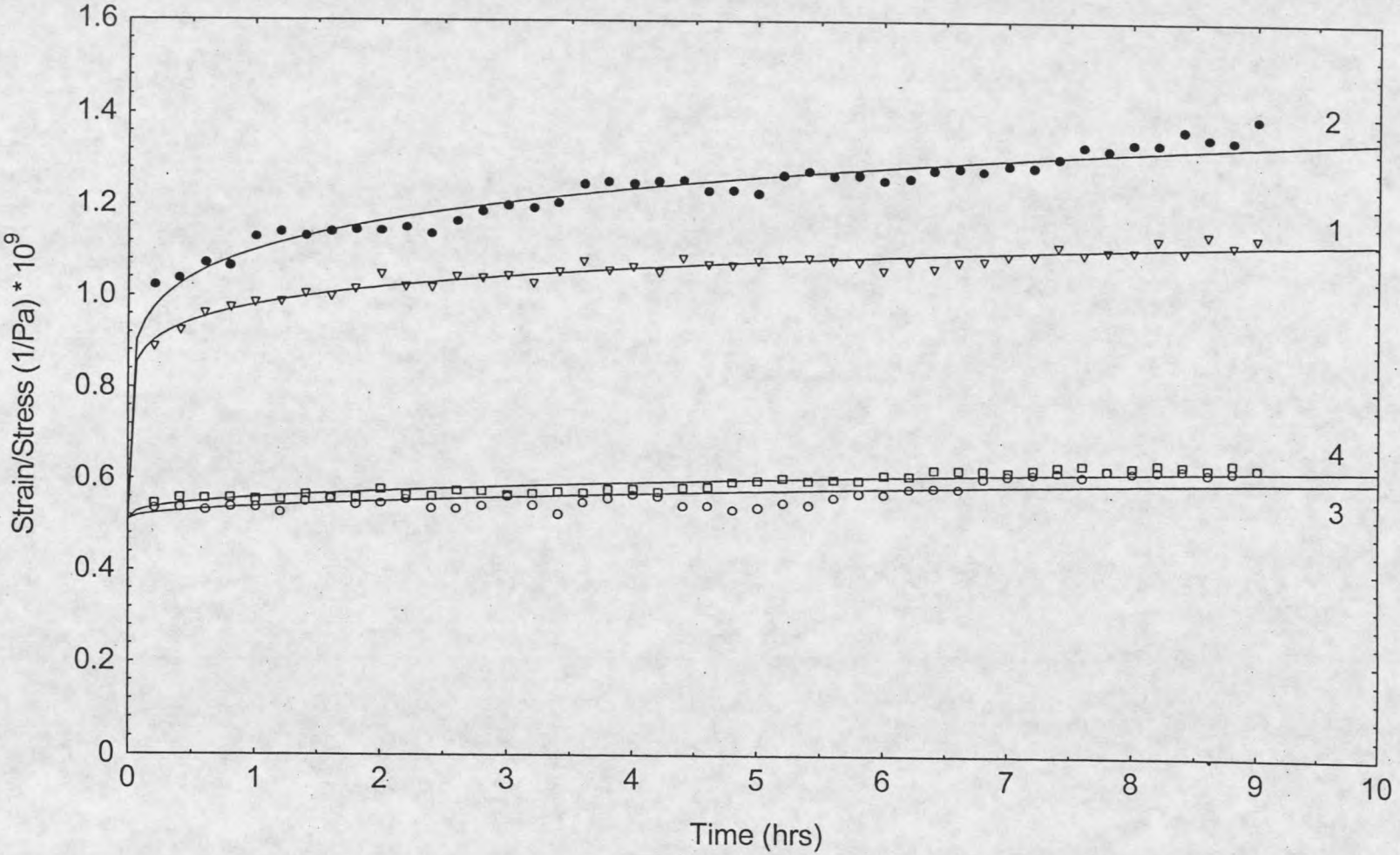


Figure J.II.2 Normalized Vibrocreep Response of PVDF at Different Amplitudes at 23 °C
1- $(0.30\pm0.10)\sigma_y$, 5 Hz; 2- $(0.30\pm0.20)\sigma_y$, 5 Hz;
3- $(0.30)\sigma_y$, 4- $(0.45)\sigma_y$, Constant Load Creep;
σ_y = 30.428 MPa at 23 °C

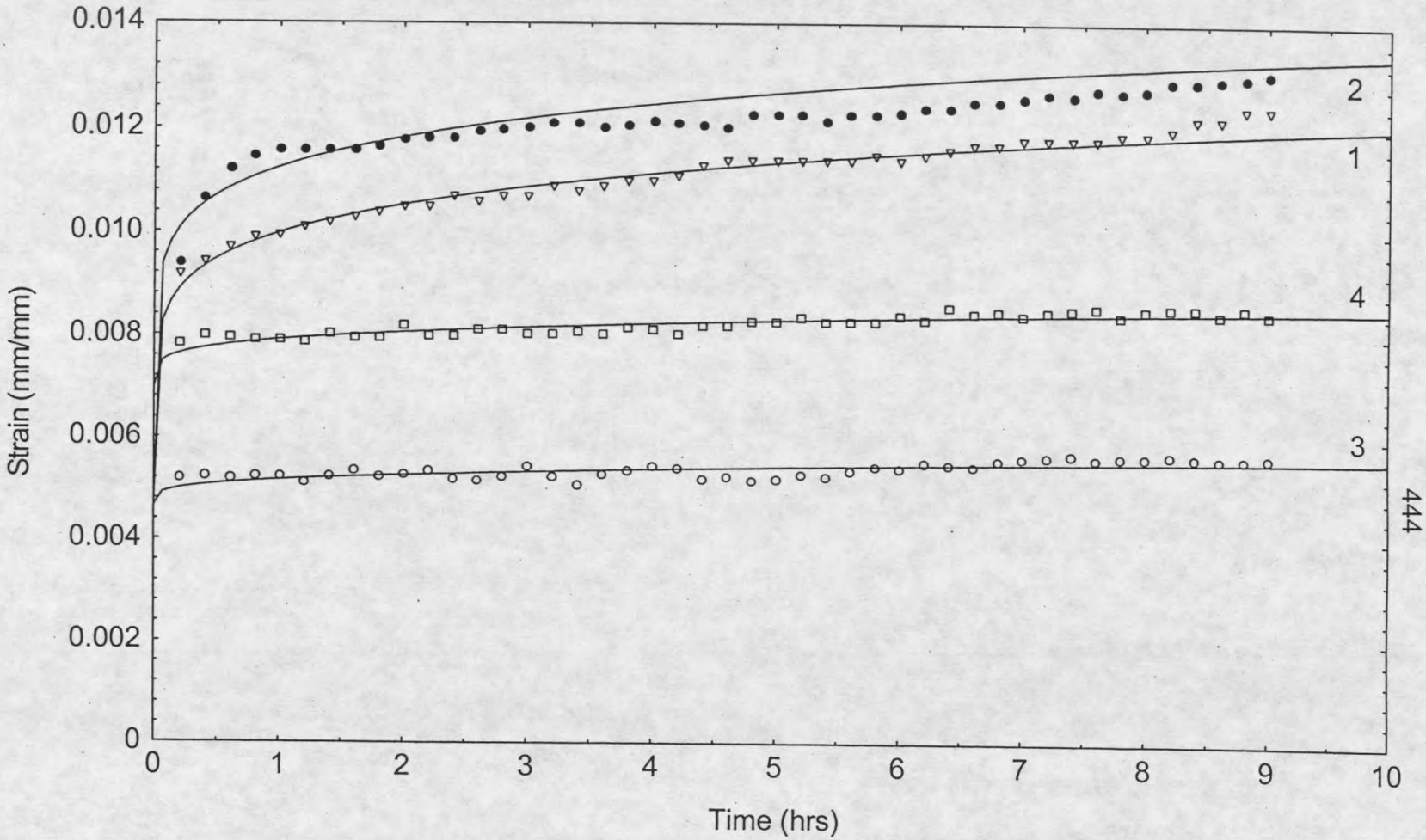


Figure J.II.3 Vibrocreep Response of PVDF at Different Amplitudes at 23 °C
1- $(0.30\pm0.10)\sigma_y$, 10 Hz; 2- $(0.30\pm0.20)\sigma_y$, 10 Hz;
3- $(0.30)\sigma_y$, 4- $(0.45)\sigma_y$, Constant Load Creep;
σ_y = 30.428 MPa at 23 °C

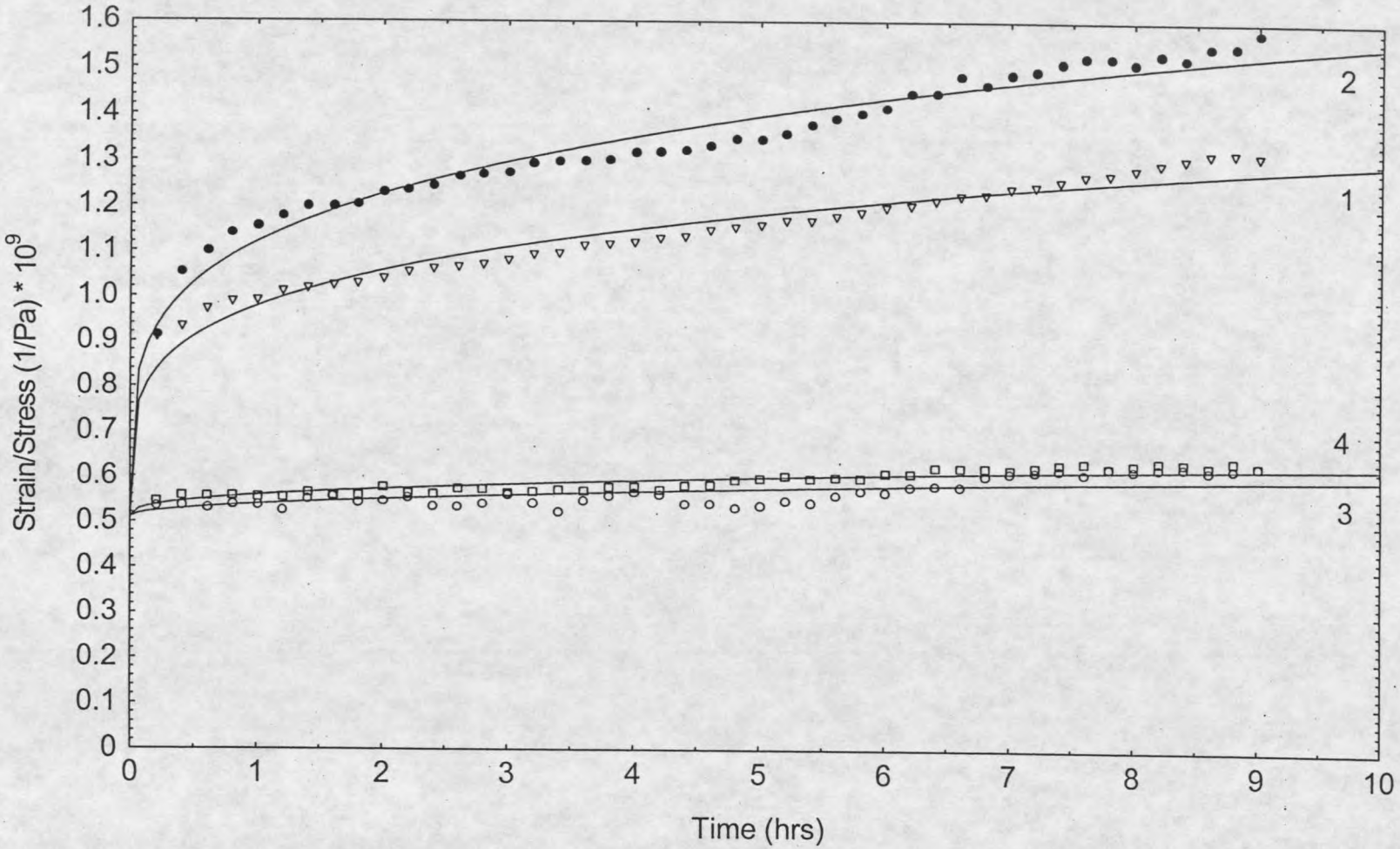


Figure J.II.4 Normalized Vibrocreep Response of PVDF at Different Amplitudes at 23 °C
1- $(0.30\pm0.10)\sigma_y$, 10 Hz; 2- $(0.30\pm0.20)\sigma_y$, 10 Hz;
4- $(0.30)\sigma_y$, 5- $(0.45)\sigma_y$, Constant Load Creep;
σ_y = 30.428 MPa at 23 °C

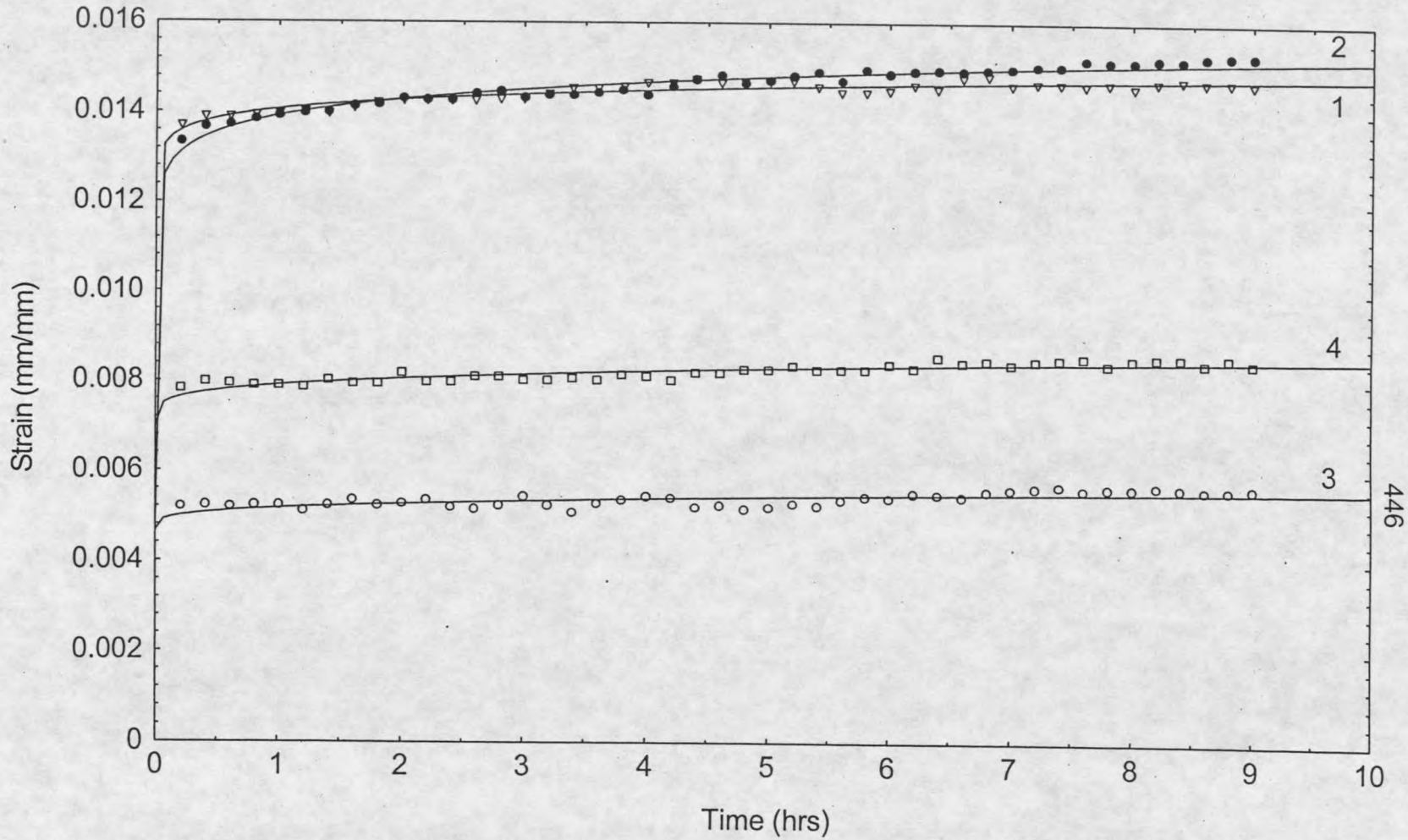


Figure J.II.5 Vibrocreep Response of PVDF at Different Amplitudes at 23 °C
1- $(0.30\pm0.10)\sigma_y$, 20 Hz; 2- $(0.30\pm0.20)\sigma_y$, 20 Hz;
3- $(0.30)\sigma_y$, 4- $(0.45)\sigma_y$, Constant Load Creep;
σ_y = 30.428 MPa at 23 °C

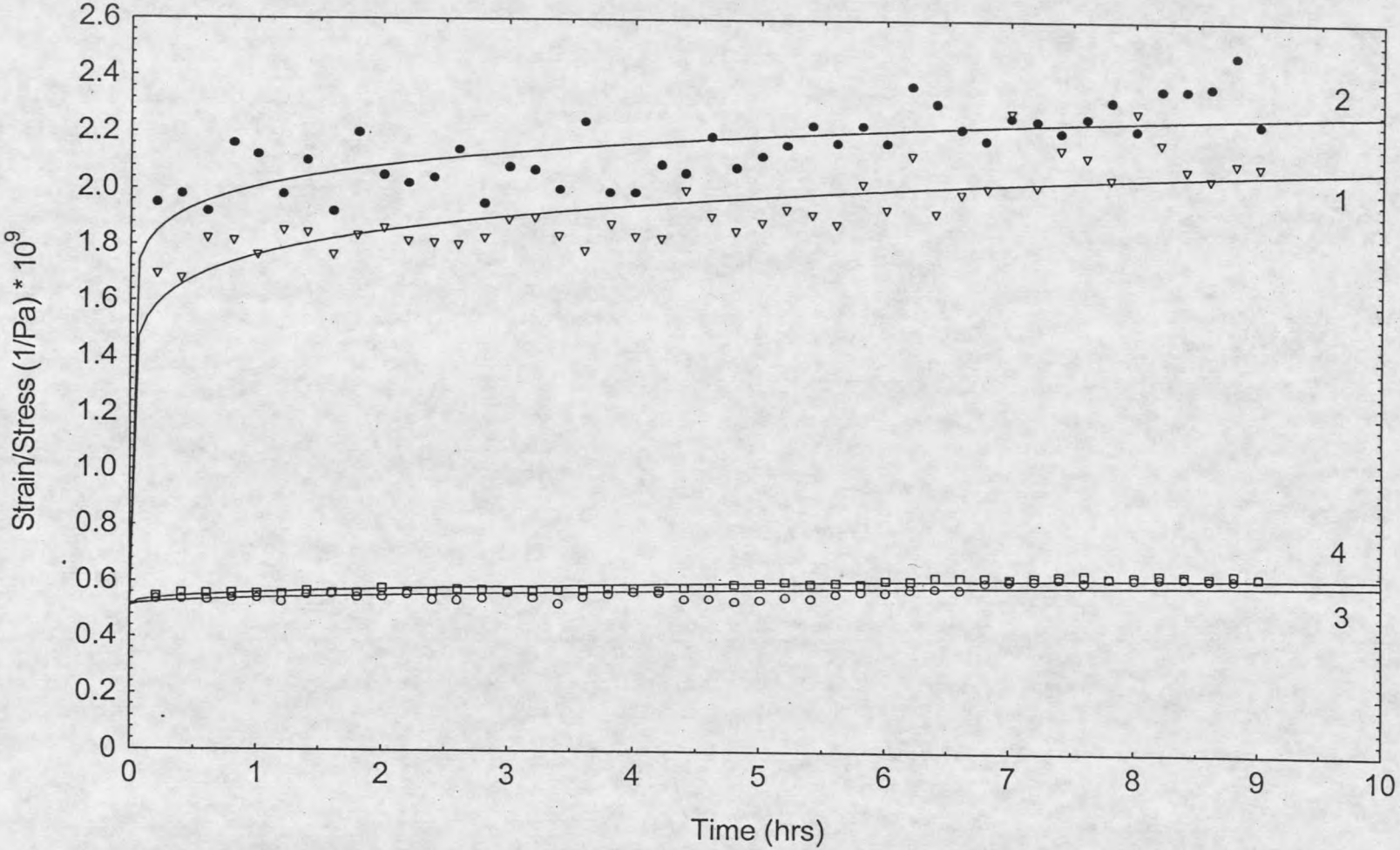


Figure J.II.6 Normalized Vibrocreep Response of PVDF at Different Amplitudes at 23 °C
1- $(0.30\pm0.10)\sigma_y$, 20 Hz; 2- $(0.30\pm0.20)\sigma_y$, 20 Hz;
4- $(0.30)\sigma_y$, 5- $(0.45)\sigma_y$, Constant Load Creep;
σ_y = 30.428 MPa at 23 °C

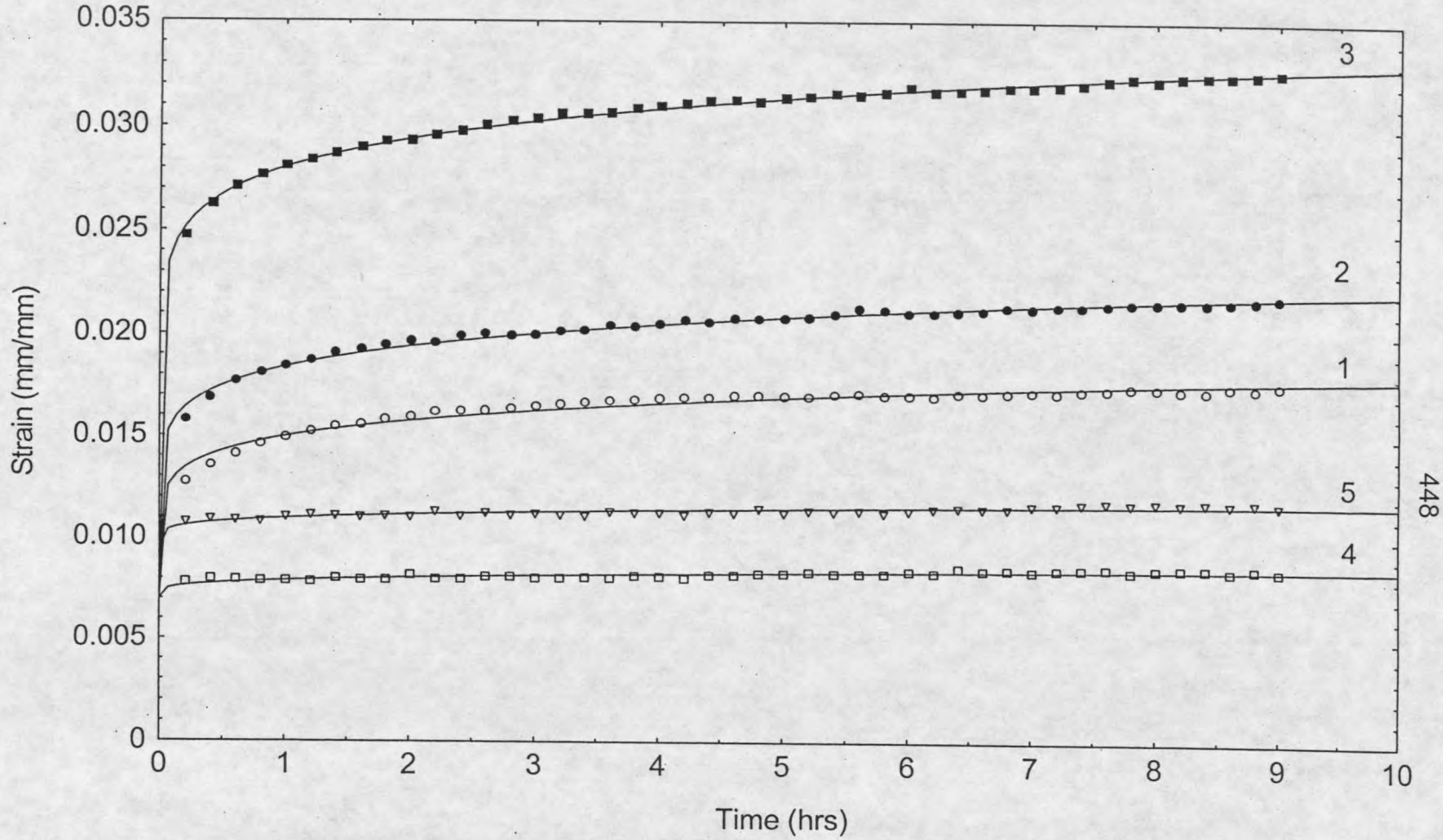


Figure J.II.7 Vibrocreep Response of PVDF at Different Amplitudes at 23 °C
1- $(0.45\pm0.10)\sigma_y$, 5 Hz; 2- $(0.45\pm0.20)\sigma_y$, 5 Hz; 3- $(0.45\pm0.35)\sigma_y$, 5 Hz;
4- $(0.45)\sigma_y$, 5- $(0.60)\sigma_y$, Constant Load Creep;
σ_y = 30.428 MPa at 23 °C

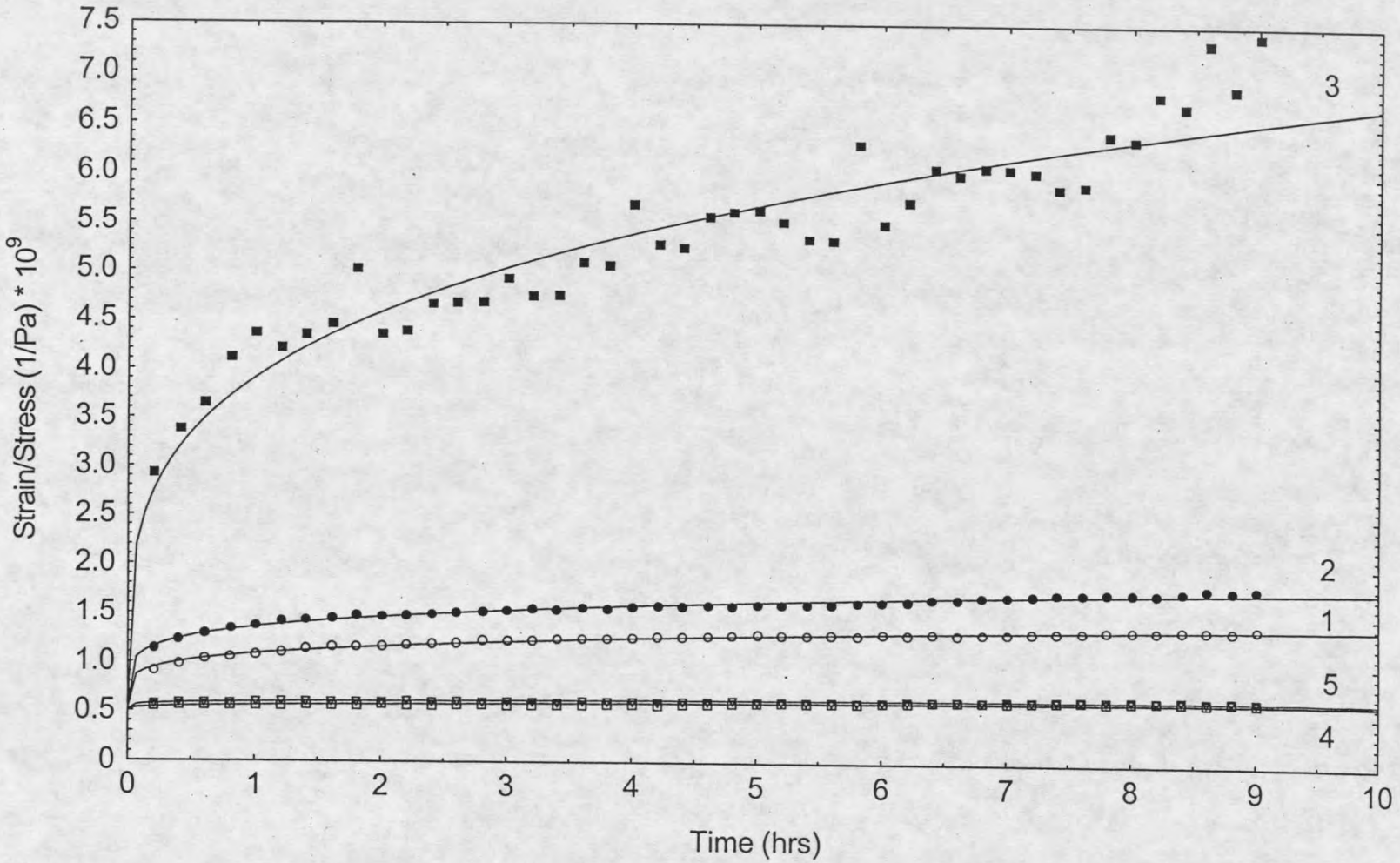


Figure J.II.8 Normalized Vibrocreep Response of PVDF at Amplitudes at 23 °C
1- $(0.45\pm0.10)\sigma_y$, 5 Hz; 2- $(0.45\pm0.20)\sigma_y$, 5 Hz; 3- $(0.45\pm0.35)\sigma_y$, 5 Hz;
4- $(0.45)\sigma_y$, 5- $(0.60)\sigma_y$, Constant Load Creep;
σ_y = 30.428 MPa at 23 °C

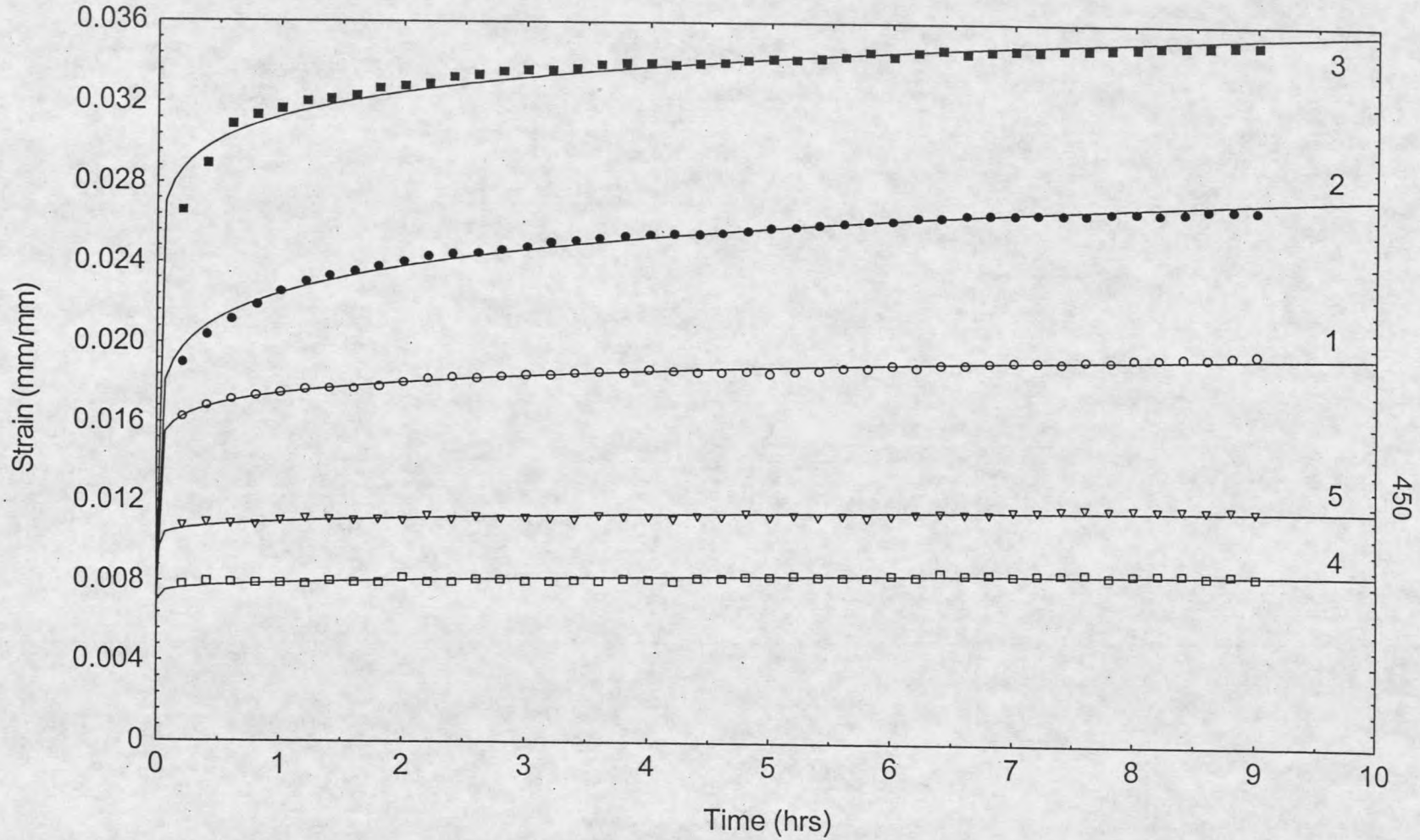


Figure J.II.9 Vibrocreep Response of PVDF at Different Amplitudes at 23 °C
1- $(0.45\pm0.10)\sigma_y$, 10 Hz; 2- $(0.45\pm0.20)\sigma_y$, 10 Hz; 3- $(0.45\pm0.35)\sigma_y$, 10 Hz;
4- $(0.45)\sigma_y$, 5- $(0.60)\sigma_y$, Constant Load Creep;
σ_y = 30.428 MPa at 23 °C

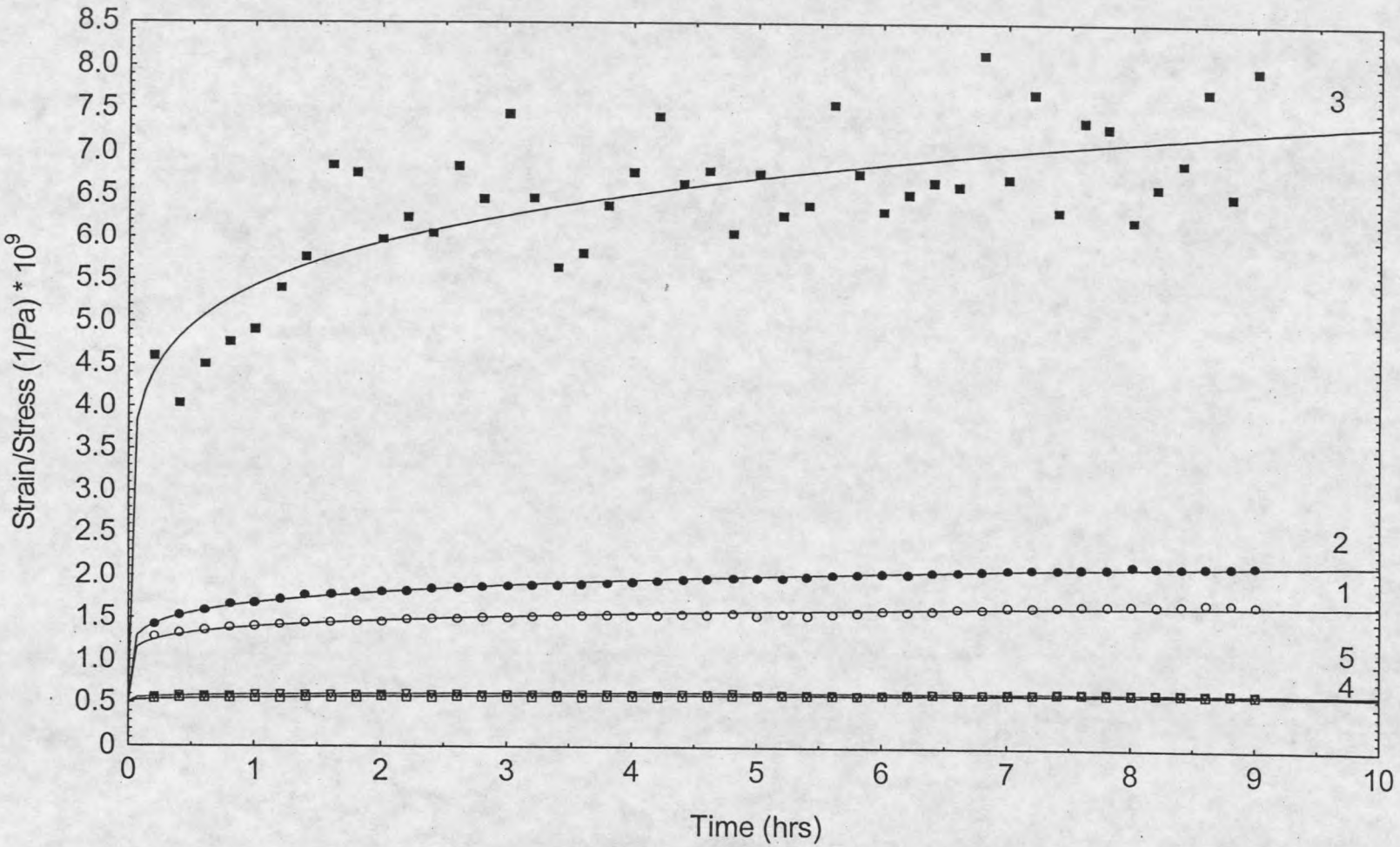


Figure J.II.10 Normalized Vibrocreep Response of PVDF at Amplitudes at 23 °C
1- $(0.45\pm0.10)\sigma_y$, 10 Hz; 2- $(0.45\pm0.20)\sigma_y$, 10 Hz; 3- $(0.45\pm0.35)\sigma_y$, 10 Hz;
4- $(0.45)\sigma_y$, 5- $(0.60)\sigma_y$, Constant Load Creep;
σ_y = 30.428 MPa at 23 °C

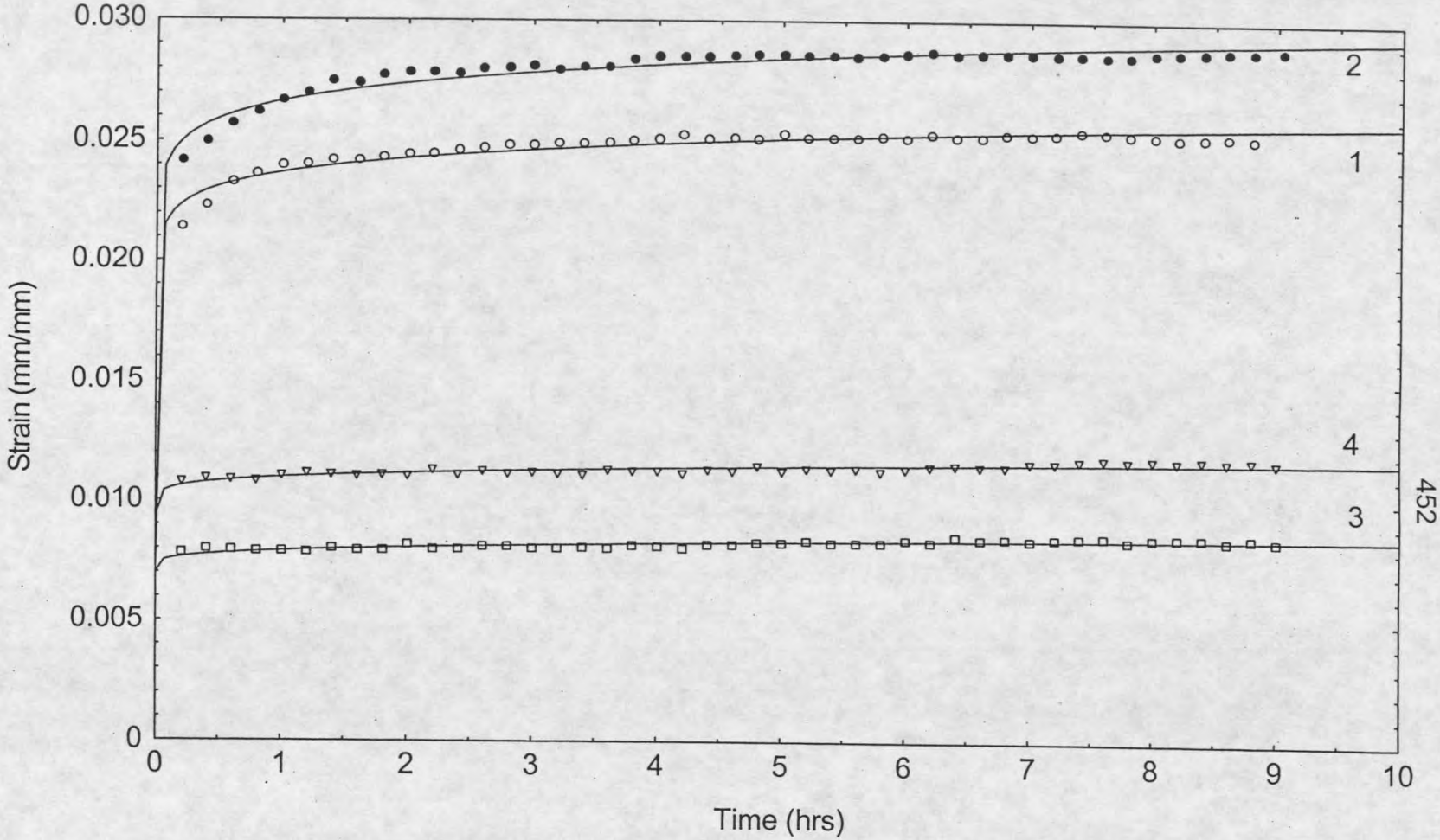


Figure J.II.11 Vibrocreep Response of PVDF at Different Amplitudes at 23 °C
1- $(0.45\pm0.10)\sigma_y$, 20 Hz; 2- $(0.45\pm0.20)\sigma_y$, 20 Hz;
3- $(0.45)\sigma_y$, 4- $(0.60)\sigma_y$, Constant Load Creep;
σ_y = 30.428 MPa at 23 °C

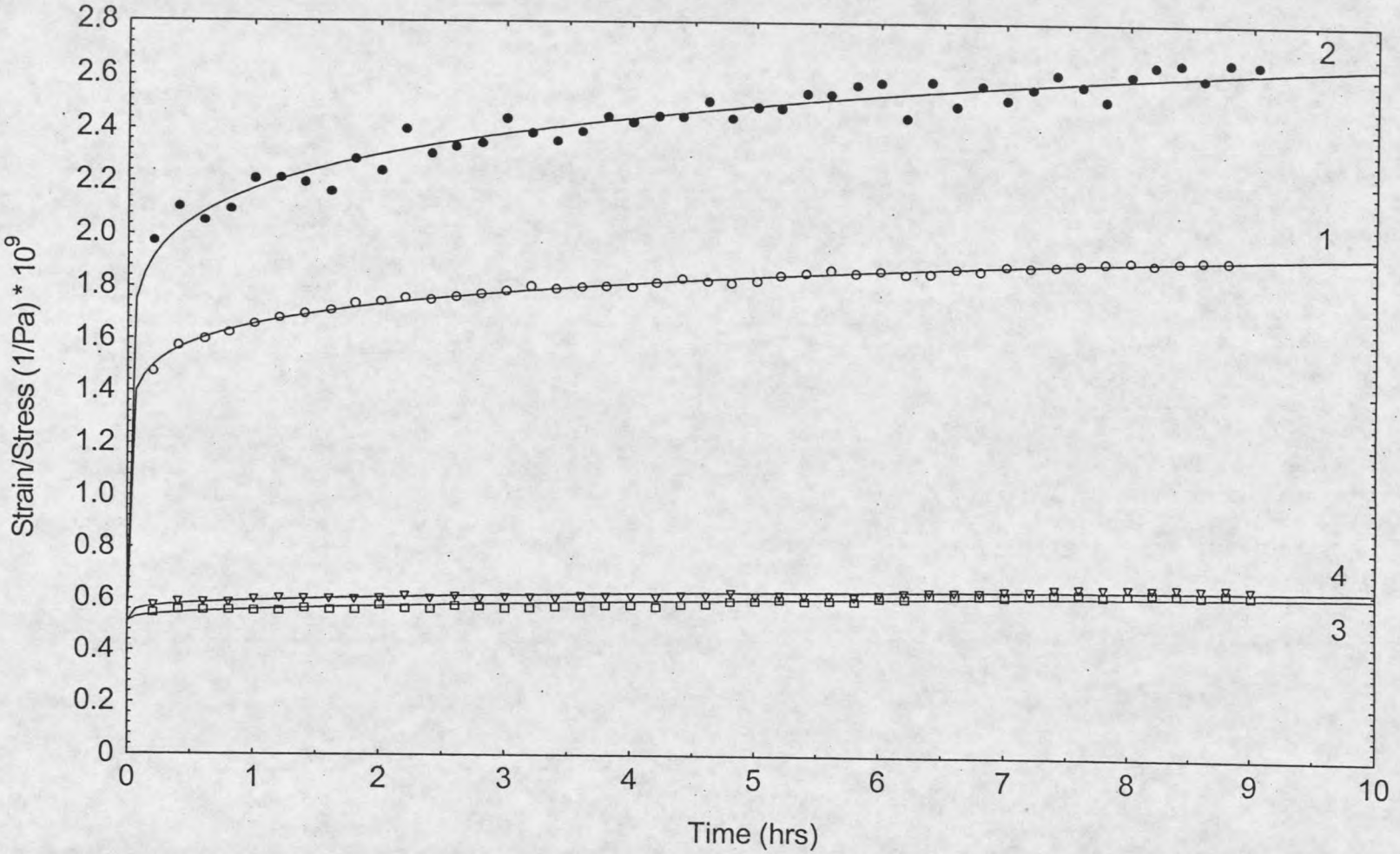


Figure J.II.12 Normalized Vibrocreep Response of PVDF at Amplitudes at 23 °C
1- $(0.45\pm0.10)\sigma_y$, 20 Hz; 2- $(0.45\pm0.20)\sigma_y$, 20 Hz;
3- $(0.45)\sigma_y$, 4- $(0.60)\sigma_y$, Constant Load Creep;
σ_y = 30.428 MPa at 23 °C

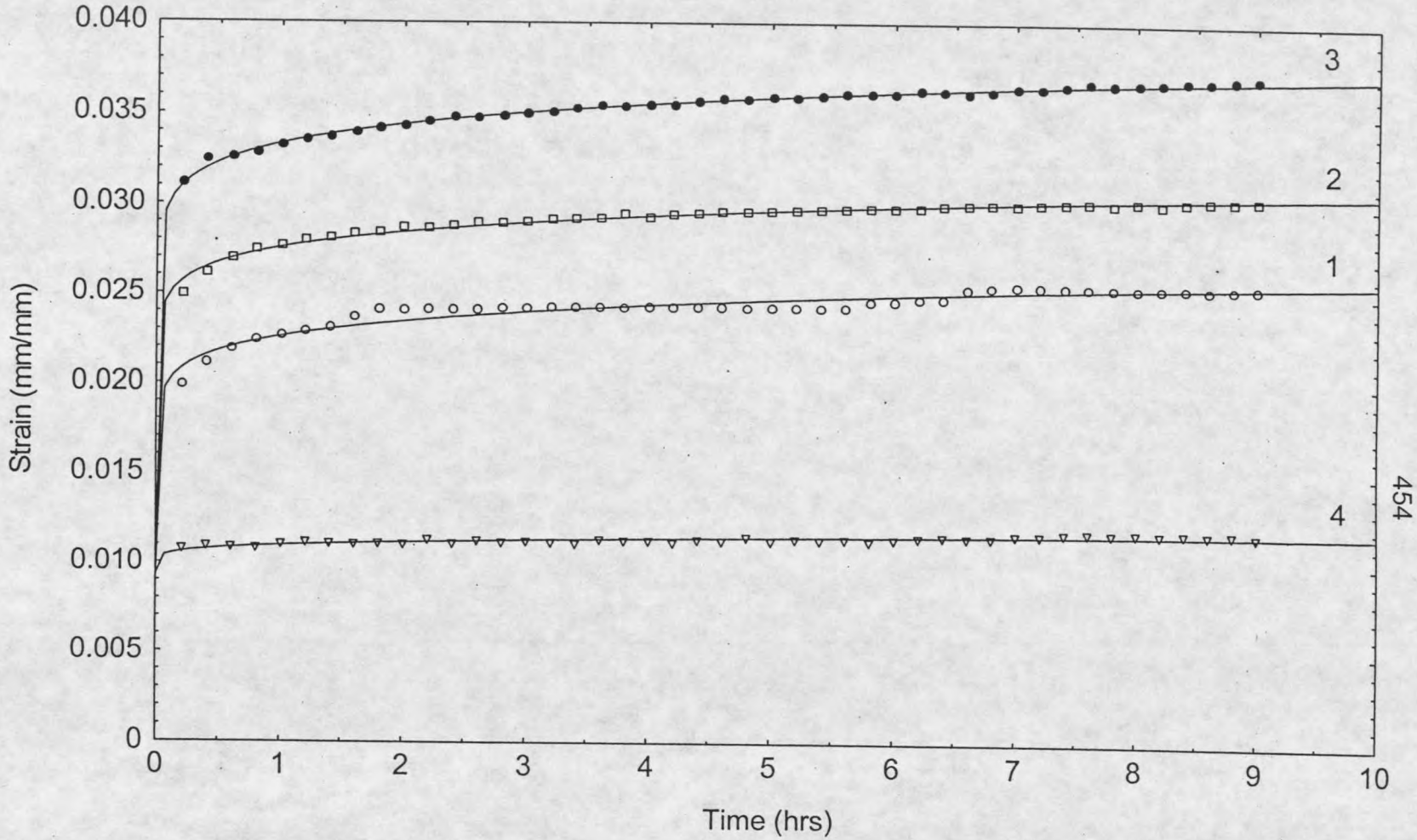


Figure J.II.13 Vibrocreep Response of PVDF at Different Amplitudes at 23 °C
1- $(0.60\pm0.10)\sigma_y$, 5 Hz; 2- $(0.60\pm0.20)\sigma_y$, 5 Hz; 3- $(0.60\pm0.45)\sigma_y$, 5 Hz;
4- $(0.60)\sigma_y$, Constant Load Creep;
σ_y = 30.428 MPa at 23 °C

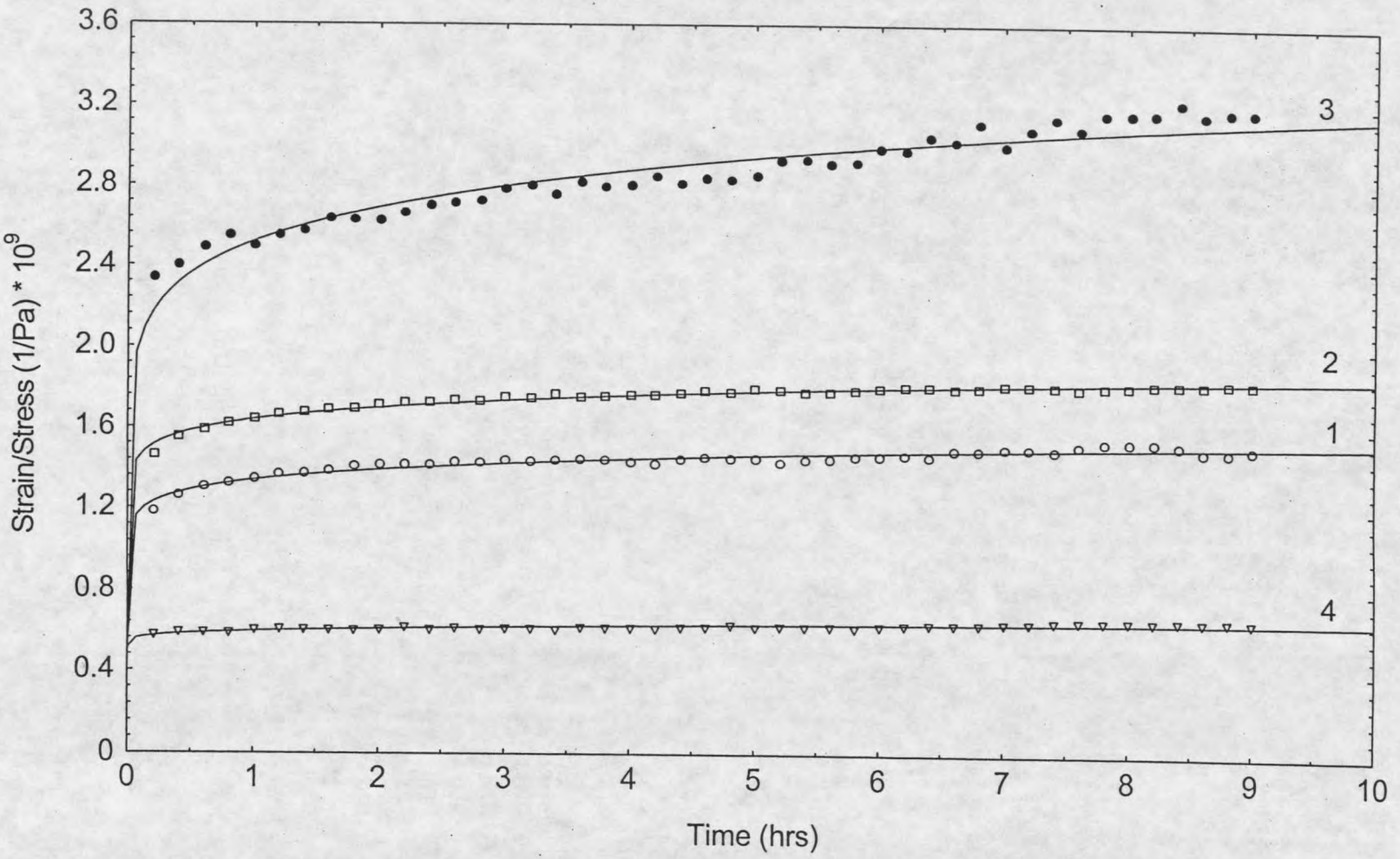


Figure J.II.14 Normalized Vibrocreep Response of PVDF at Different Amplitudes at 23 °C
1- $(0.60\pm0.10)\sigma_y$, 5 Hz; 2- $(0.60\pm0.20)\sigma_y$, 5 Hz; 3- $(0.60\pm0.45)\sigma_y$, 5 Hz;
3- $(0.60)\sigma_y$, Constant Load Creep;
σ_y = 30.428 MPa at 23 °C

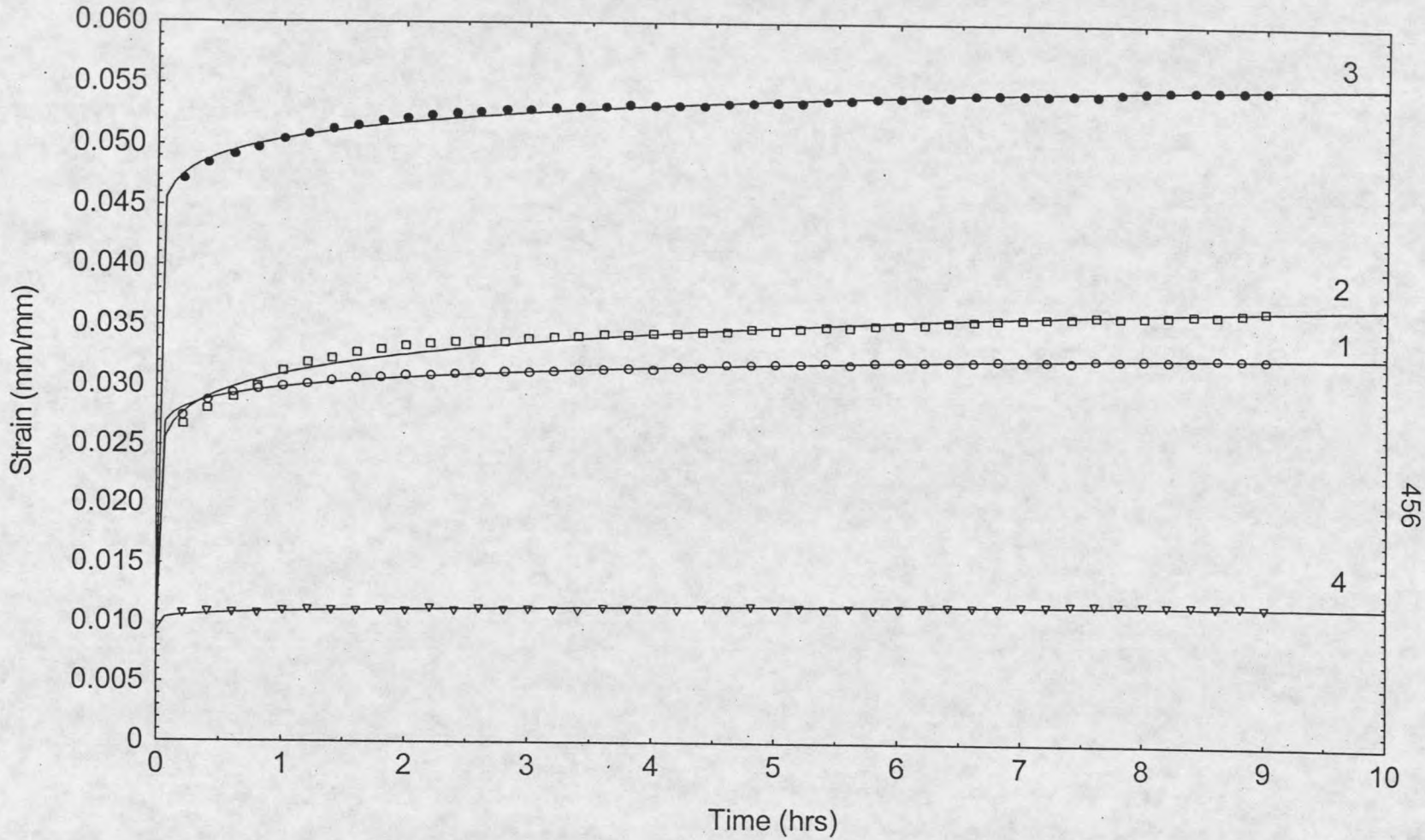


Figure J.II.15 Vibrocreep Response of PVDF at Different Amplitudes at 23 °C
1- $(0.60\pm0.10)\sigma_y$, 10 Hz; 2- $(0.60\pm0.20)\sigma_y$, 10 Hz; 3- $(0.60\pm0.50)\sigma_y$, 10 Hz;
4- $(0.60)\sigma_y$, Constant Load Creep;
σ_y = 30.428 MPa at 23 °C

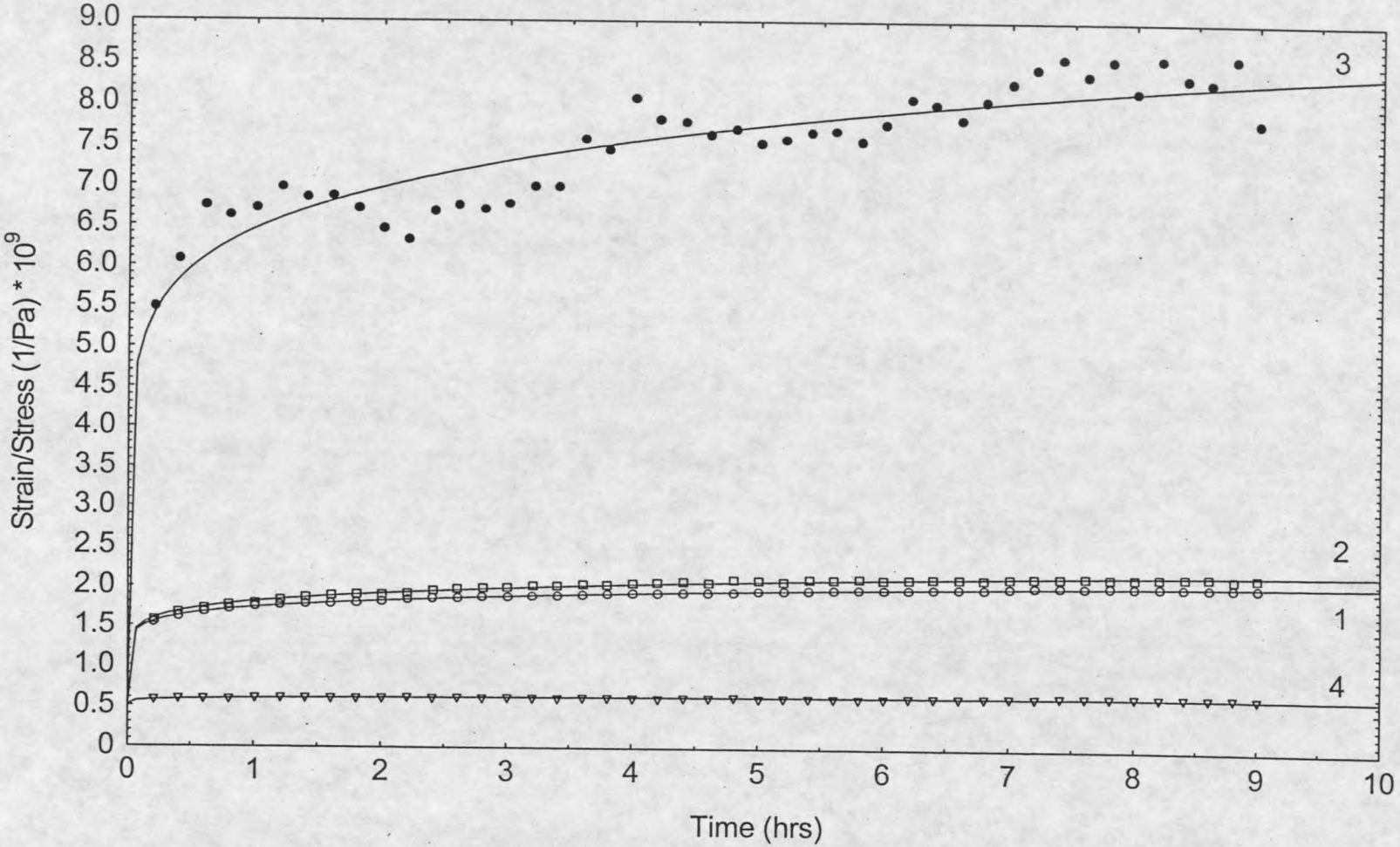


Figure J.II.16 Normalized Vibrocreep Response of PVDF at Different Amplitudes at 23 °C
1- $(0.60\pm0.10)\sigma_y$, 10 Hz; 2- $(0.60\pm0.20)\sigma_y$, 10 Hz; 3- $(0.60\pm0.50)\sigma_y$, 10 Hz;
4- $(0.60)\sigma_y$, Constant Load Creep;
σ_y = 30.428 MPa at 23 °C

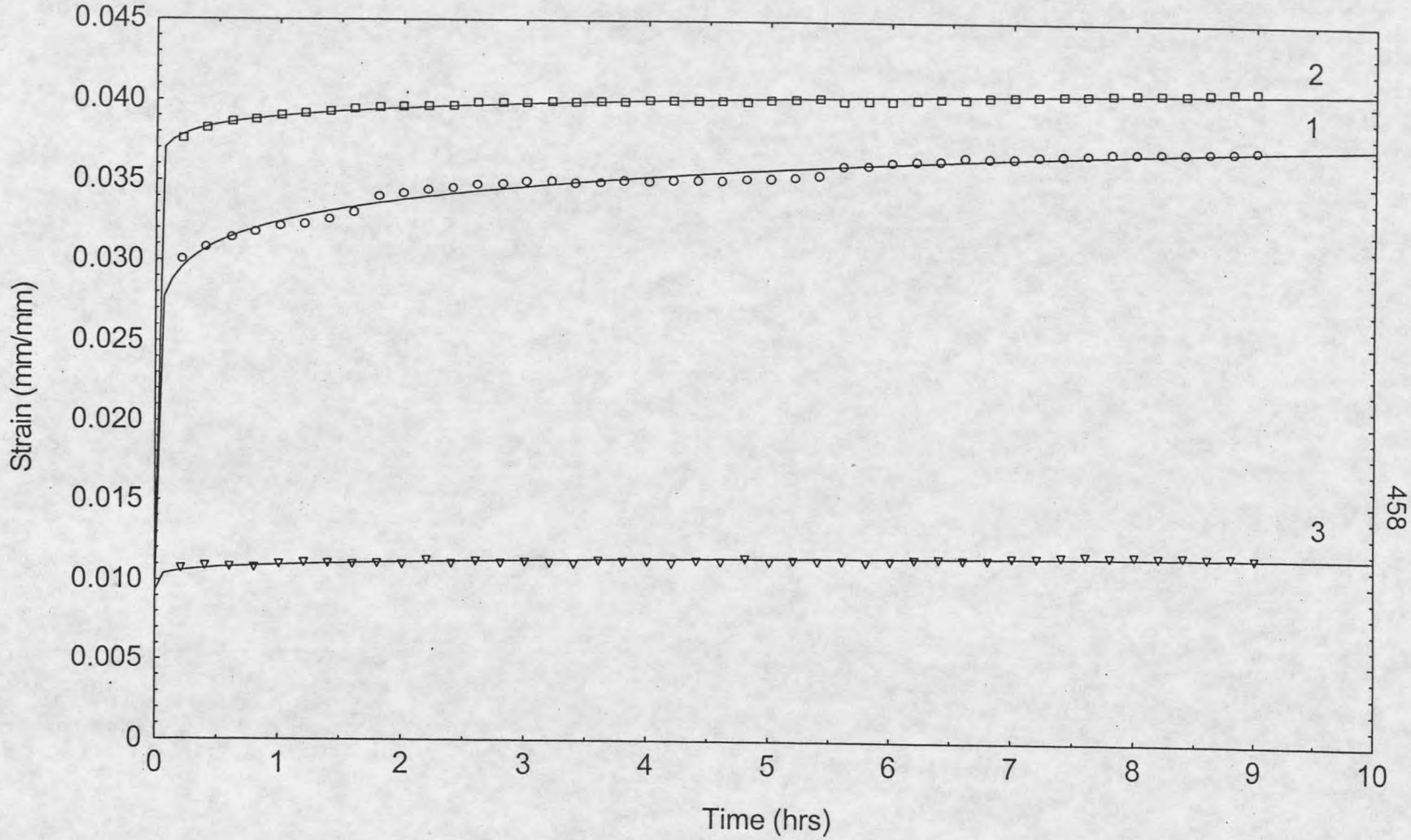


Figure J.II.17 Vibrocreep Response of PVDF at Different Amplitudes at 23 °C
1- $(0.60\pm0.10)\sigma_y$, 20 Hz; 2- $(0.60\pm0.20)\sigma_y$, 20 Hz;
3- $(0.60)\sigma_y$, Constant Load Creep;
σ_y = 30.428 MPa at 23 °C

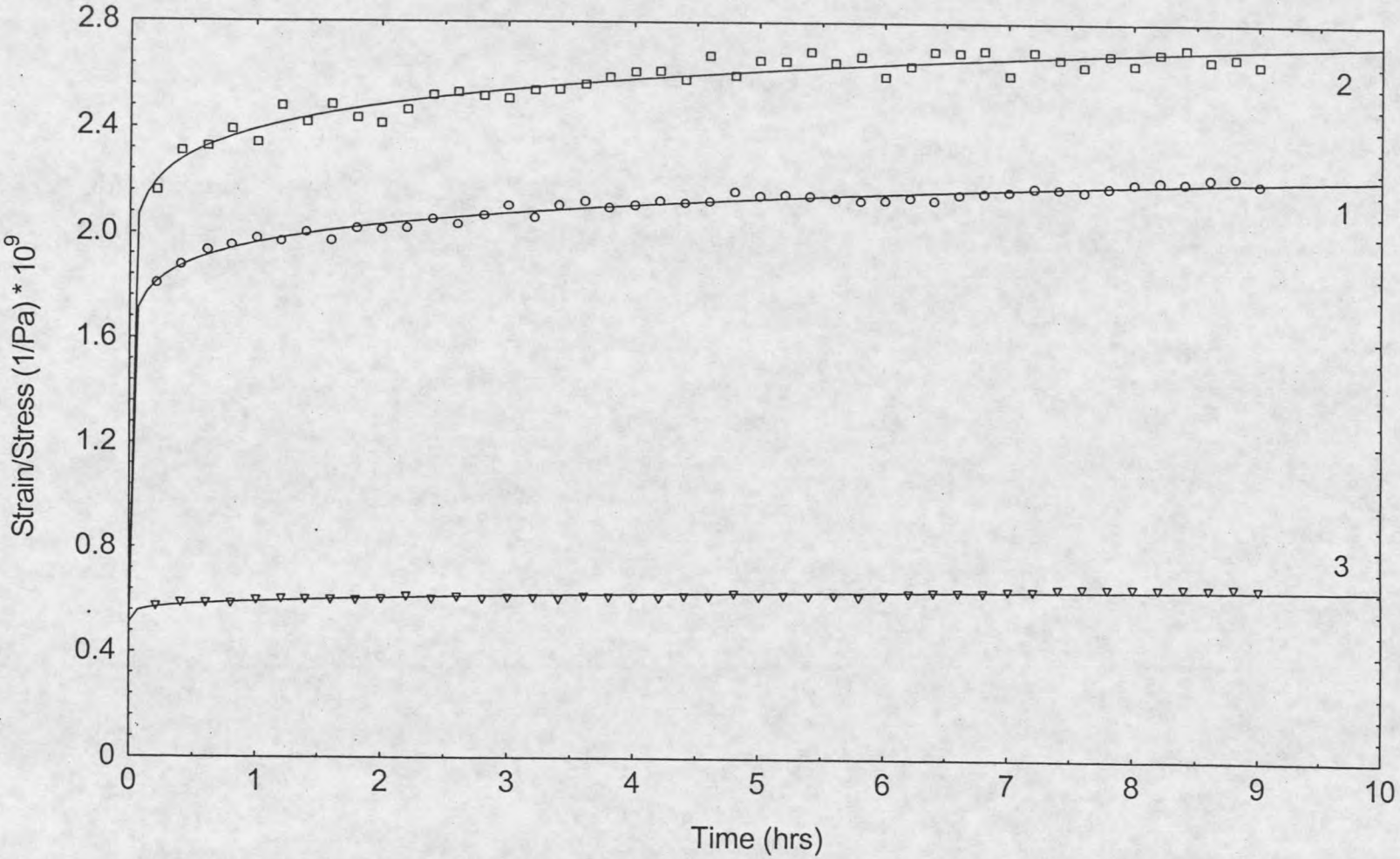


Figure J.II.18 Normalized Vibrocreep Response of PVDF at Different Amplitudes at 23 °C
1- $(0.60\pm0.10)\sigma_y$, 20 Hz; 2- $(0.60\pm0.20)\sigma_y$, 20 Hz;
3- $(0.60)\sigma_y$, Constant Load Creep;
σ_y = 30.428 MPa at 23 °C

APPENDIX K

Mean Stress Effects from Vibrocreep Testing of PVDF

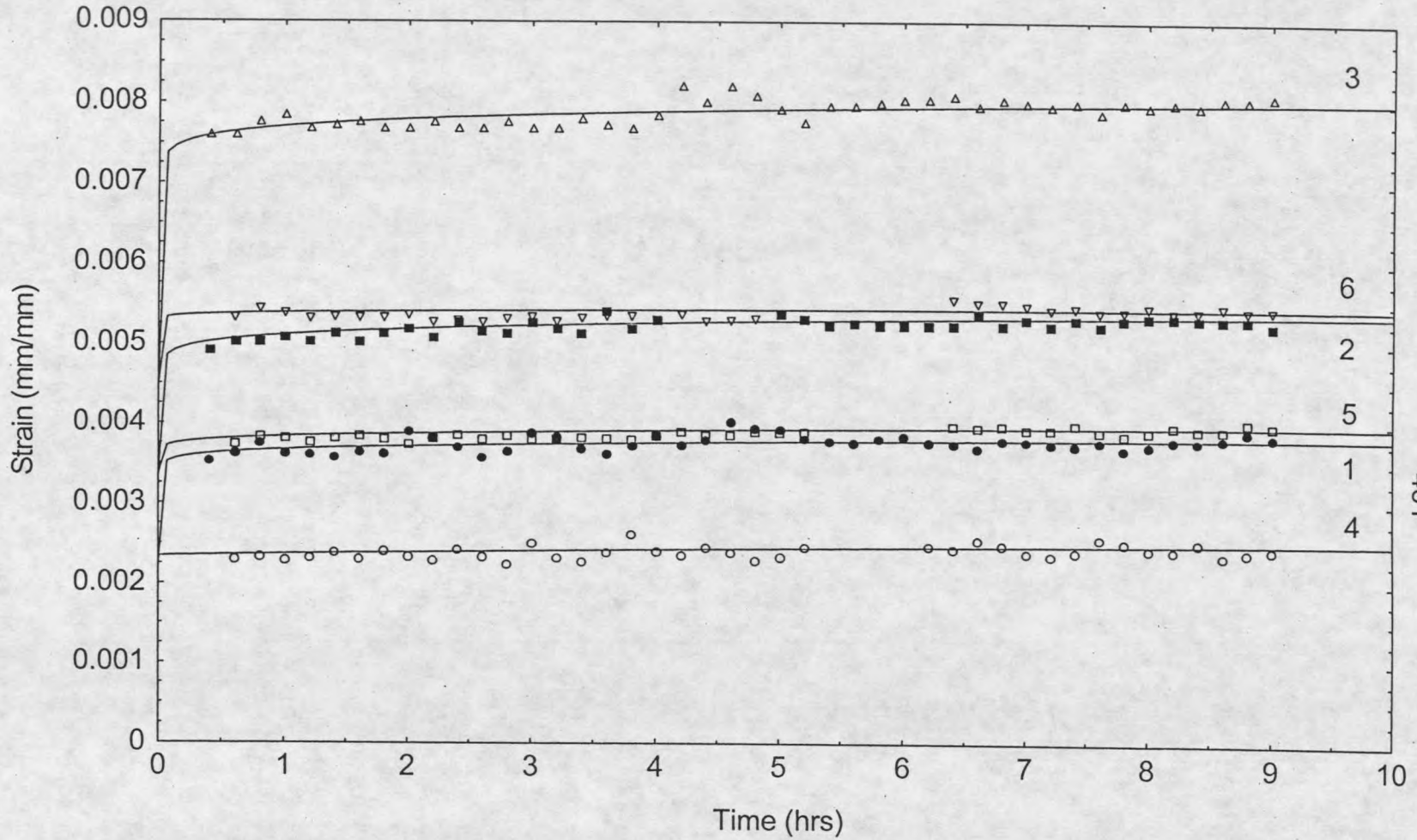


Figure K.I.1 Vibrocreep Response of PVDF at Different Mean Stresses at -25 °C
1- $(0.30\pm0.20)\sigma_y$, 5 Hz; 2- $(0.45\pm0.20)\sigma_y$, 5 Hz; 3- $(0.60\pm0.20)\sigma_y$, 5 Hz;
4- $(0.30)\sigma_y$, 5- $(0.45)\sigma_y$, 6- $(0.60)\sigma_y$, Constant Load Creep;
σ_y = 30.428 MPa at 23 °C

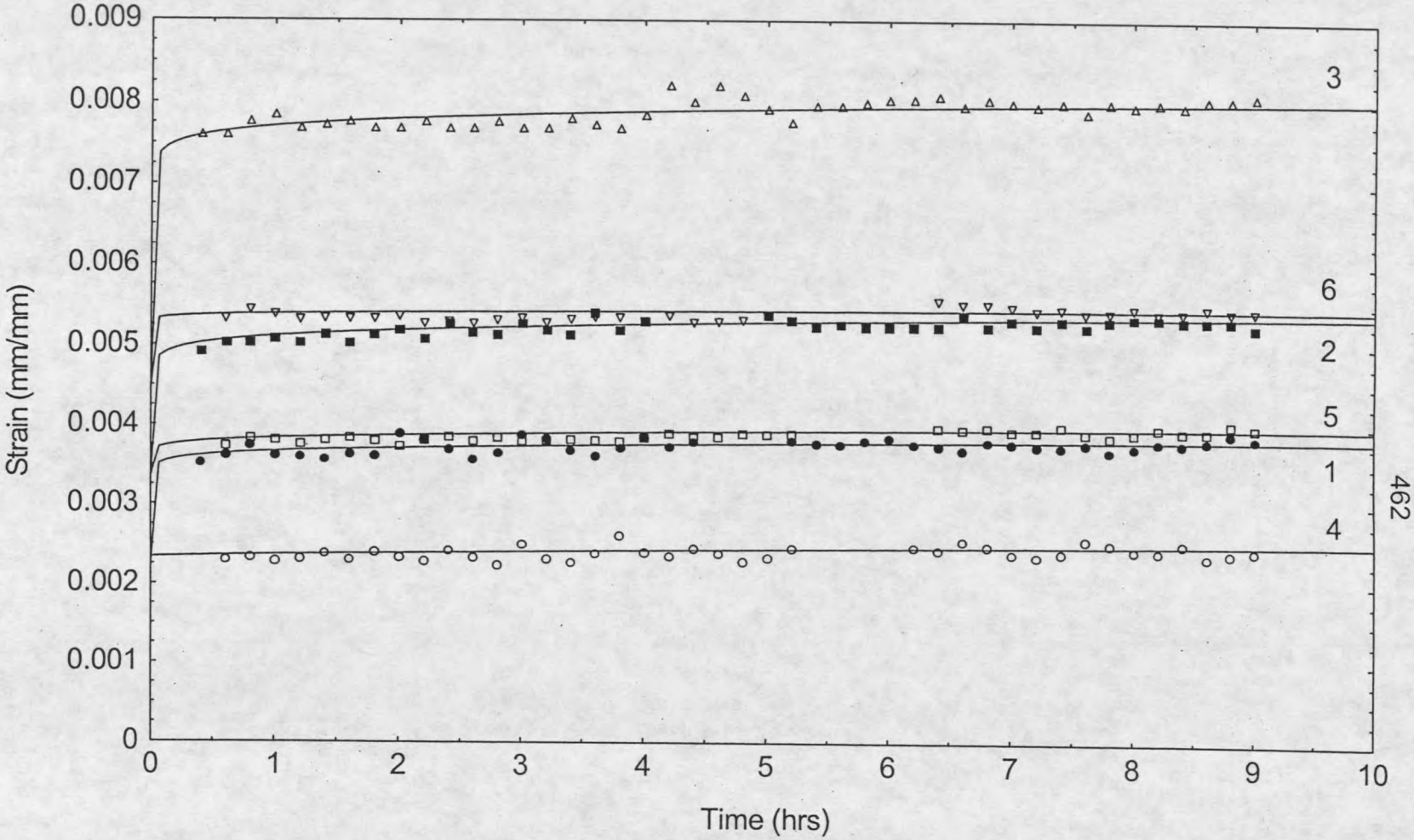


Figure K.I.2 Normalized Vibrocreep Response of PVDF at Different Mean Stresses at -25 °C
1- $(0.30\pm0.20)\sigma_y$, 5 Hz; 2- $(0.45\pm0.20)\sigma_y$, 5 Hz; 3- $(0.60\pm0.20)\sigma_y$, 5 Hz;
4- $(0.30)\sigma_y$, 5- $(0.45)\sigma_y$, 6- $(0.60)\sigma_y$, Constant Load Creep;
σ_y = 30.428 MPa at 23 °C

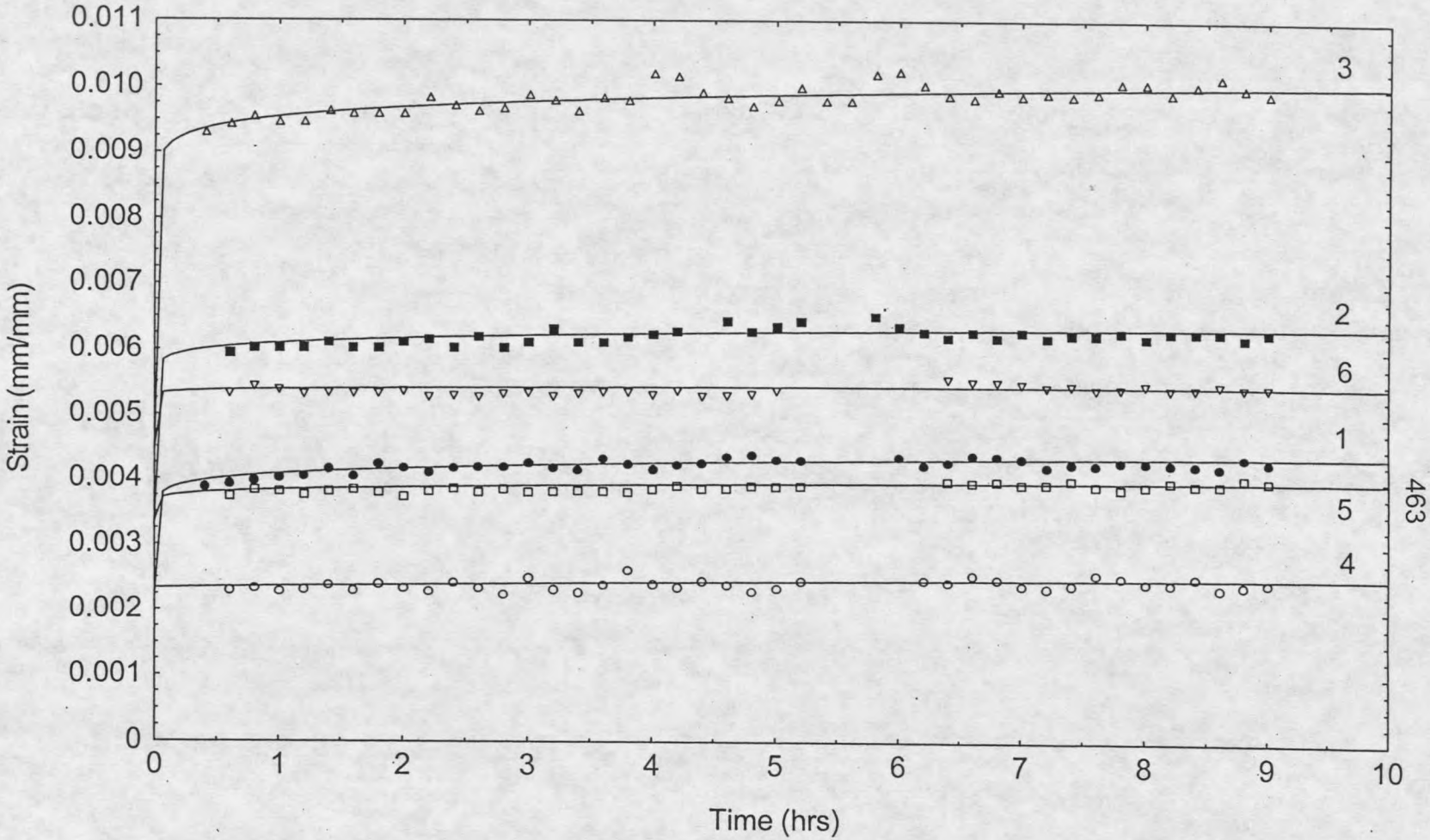


Figure K.I.3 Vibrocreep Response of PVDF at Different Mean Stresses at -25 °C
1- $(0.30\pm0.20)\sigma_y$, 10 Hz; 2- $(0.45\pm0.20)\sigma_y$, 10 Hz; 3- $(0.60\pm0.20)\sigma_y$, 10 Hz;
4- $(0.30)\sigma_y$, 5- $(0.45)\sigma_y$, 6- $(0.60)\sigma_y$, Constant Load Creep;
σ_y = 30.428 MPa at 23 °C

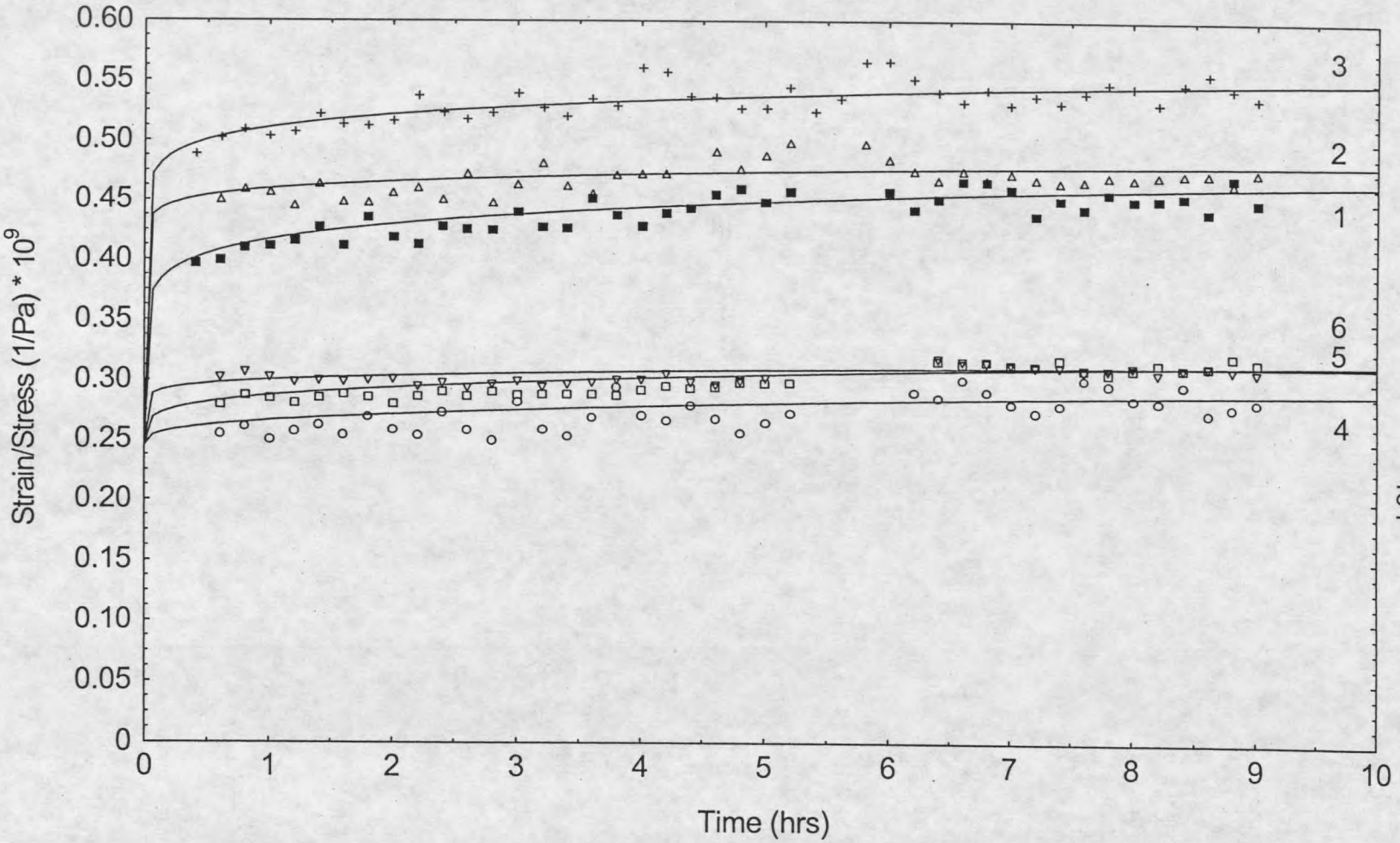


Figure K.I.4 Normalized Vibrocreep Response of PVDF at Different Mean Stresses at -25 °C
1- $(0.30\pm0.20)\sigma_y$, 10 Hz; 2- $(0.45\pm0.20)\sigma_y$, 10 Hz; 3- $(0.60\pm0.20)\sigma_y$, 10 Hz;
4- $(0.30)\sigma_y$, 5- $(0.45)\sigma_y$, 6- $(0.60)\sigma_y$, Constant Load Creep;
σ_y = 30.428 MPa at 23 °C

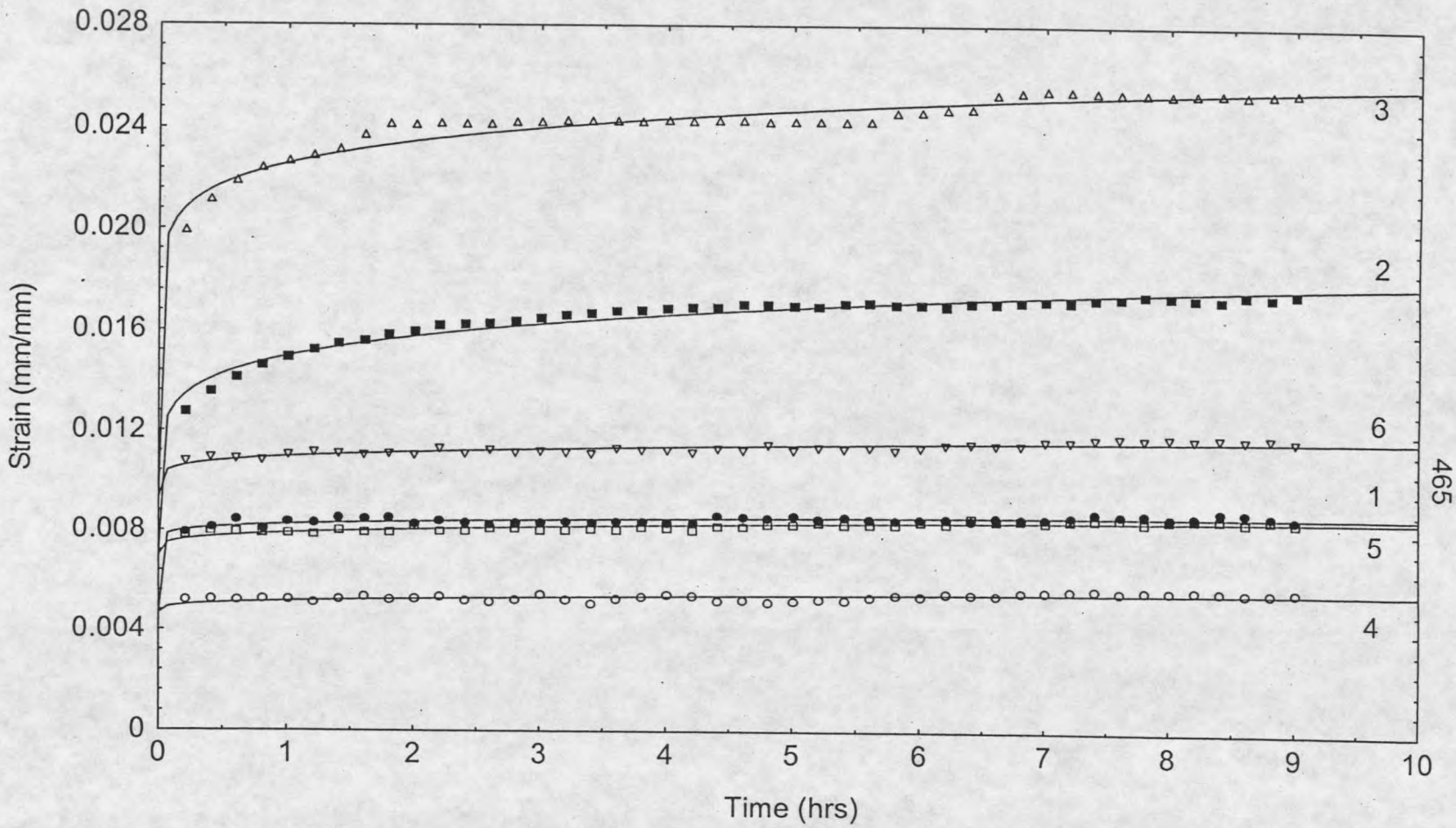


Figure K.II.1 Vibrocreep Response of PVDF at Different Mean Stresses at 23 °C
1- $(0.30\pm0.10)\sigma_y$, 5 Hz; 2- $(0.45\pm0.10)\sigma_y$, 5 Hz; 3- $(0.60\pm0.10)\sigma_y$, 5 Hz;
4- $(0.30)\sigma_y$, 5- $(0.45)\sigma_y$, 6- $(0.60)\sigma_y$, Constant Load Creep;
σ_y = 30.428 MPa at 23 °C

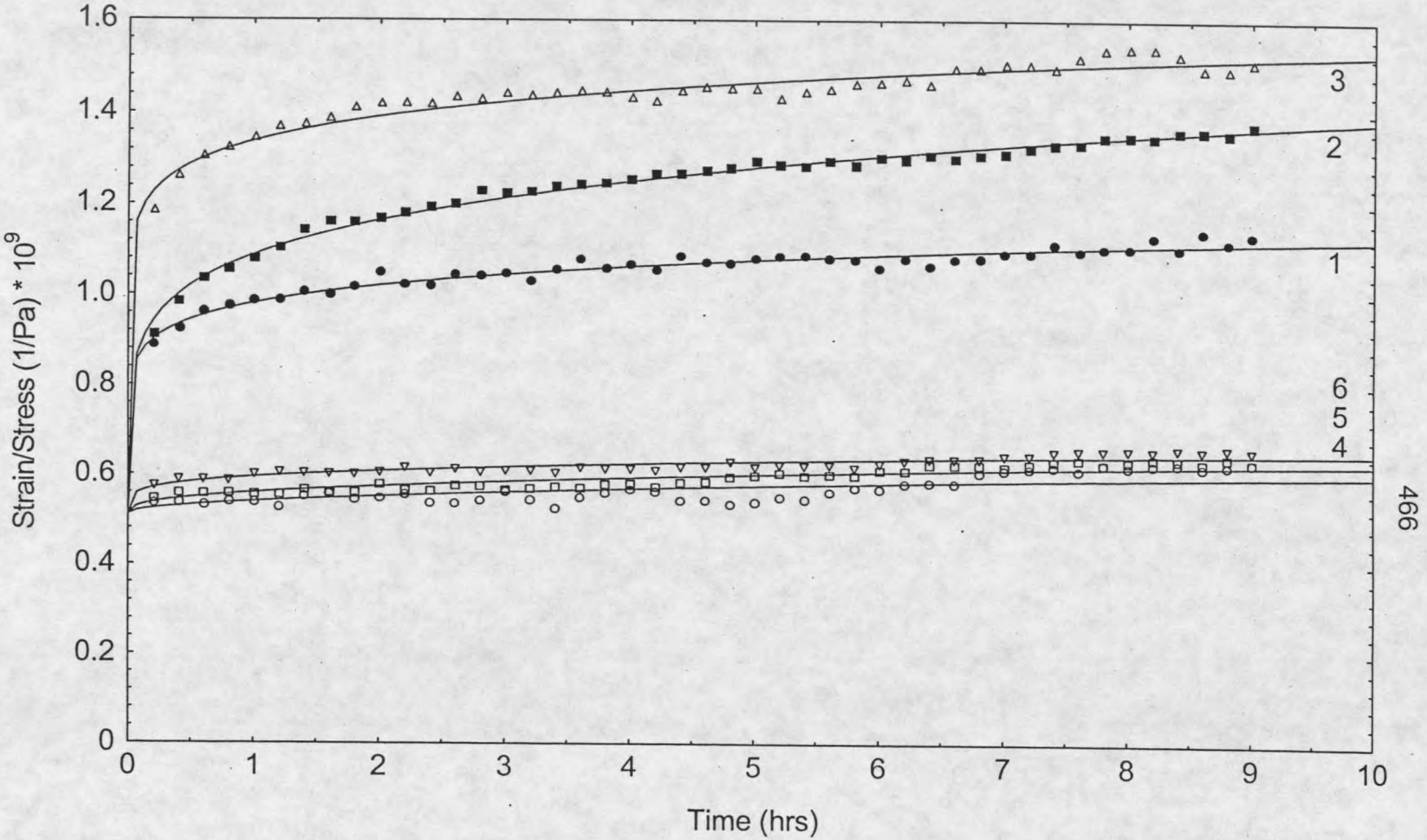


Figure K.II.2 Normalized Vibrocreep Response of PVDF at Different Mean Stresses at 23 °C
1- $(0.30\pm0.10)\sigma_y$, 5 Hz; 2- $(0.45\pm0.10)\sigma_y$, 5 Hz; 3- $(0.60\pm0.10)\sigma_y$, 5 Hz;
4- $(0.30)\sigma_y$, 5- $(0.45)\sigma_y$, 6- $(0.60)\sigma_y$, Constant Load Creep;
σ_y = 30.428 MPa at 23 °C

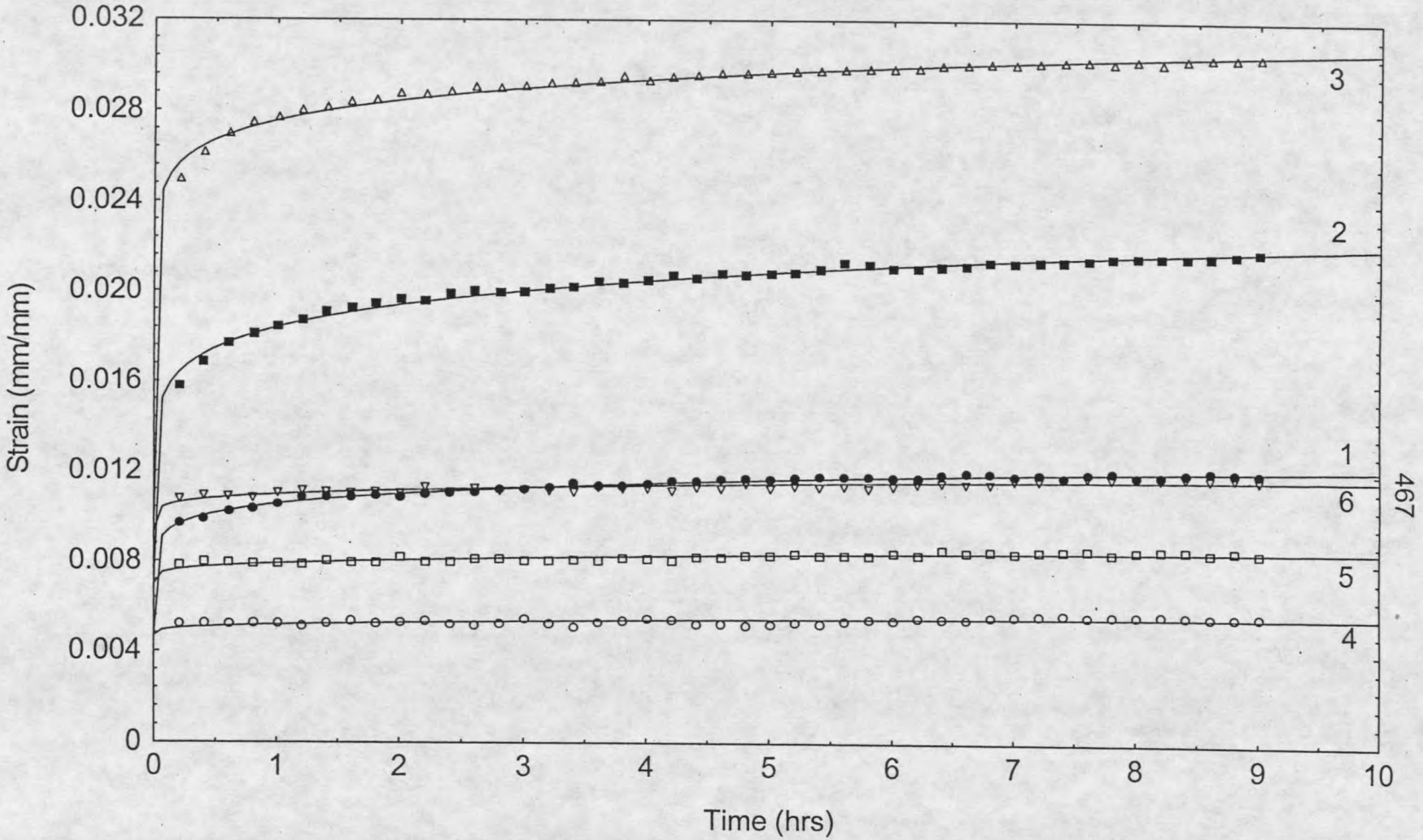


Figure K.II.3 Vibrocreep Response of PVDF at Different Mean Stresses at 23 °C
1- $(0.30\pm0.20)\sigma_y$, 5 Hz; 2- $(0.45\pm0.20)\sigma_y$, 5 Hz; 3- $(0.60\pm0.20)\sigma_y$, 5 Hz;
4- $(0.30)\sigma_y$, 5- $(0.45)\sigma_y$, 6- $(0.60)\sigma_y$, Constant Load Creep;
σ_y = 30.428 MPa at 23 °C

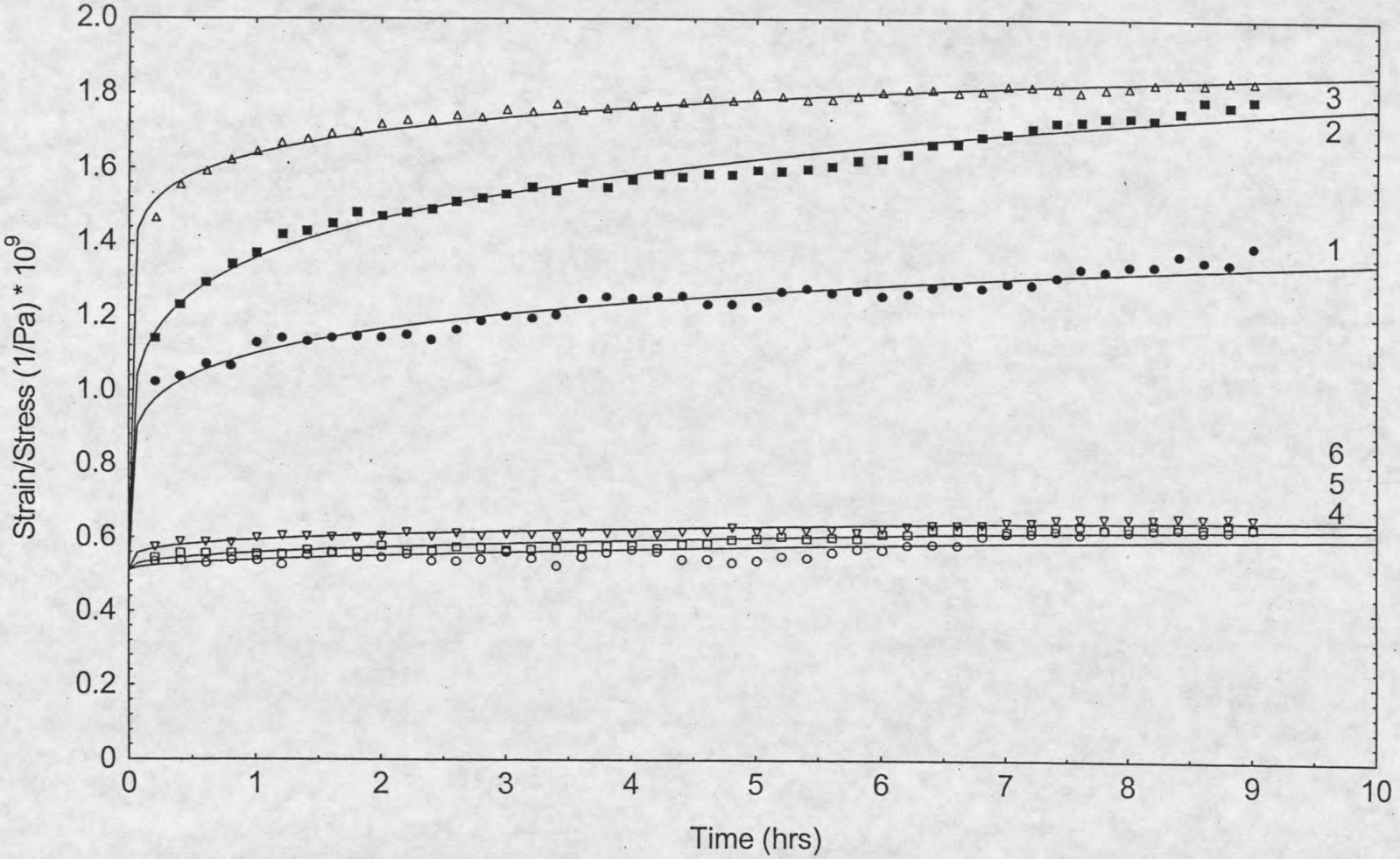


Figure K.II.4 Normalized Vibrocreep Response of PVDF at Different Mean Stresses at 23 °C
1- $(0.30\pm0.20)\sigma_y$, 5 Hz; 2- $(0.45\pm0.20)\sigma_y$, 5 Hz; 3- $(0.60\pm0.20)\sigma_y$, 5 Hz;
4- $(0.30)\sigma_y$, 5- $(0.45)\sigma_y$, 6- $(0.60)\sigma_y$, Constant Load Creep;
σ_y = 30.428 MPa at 23 °C

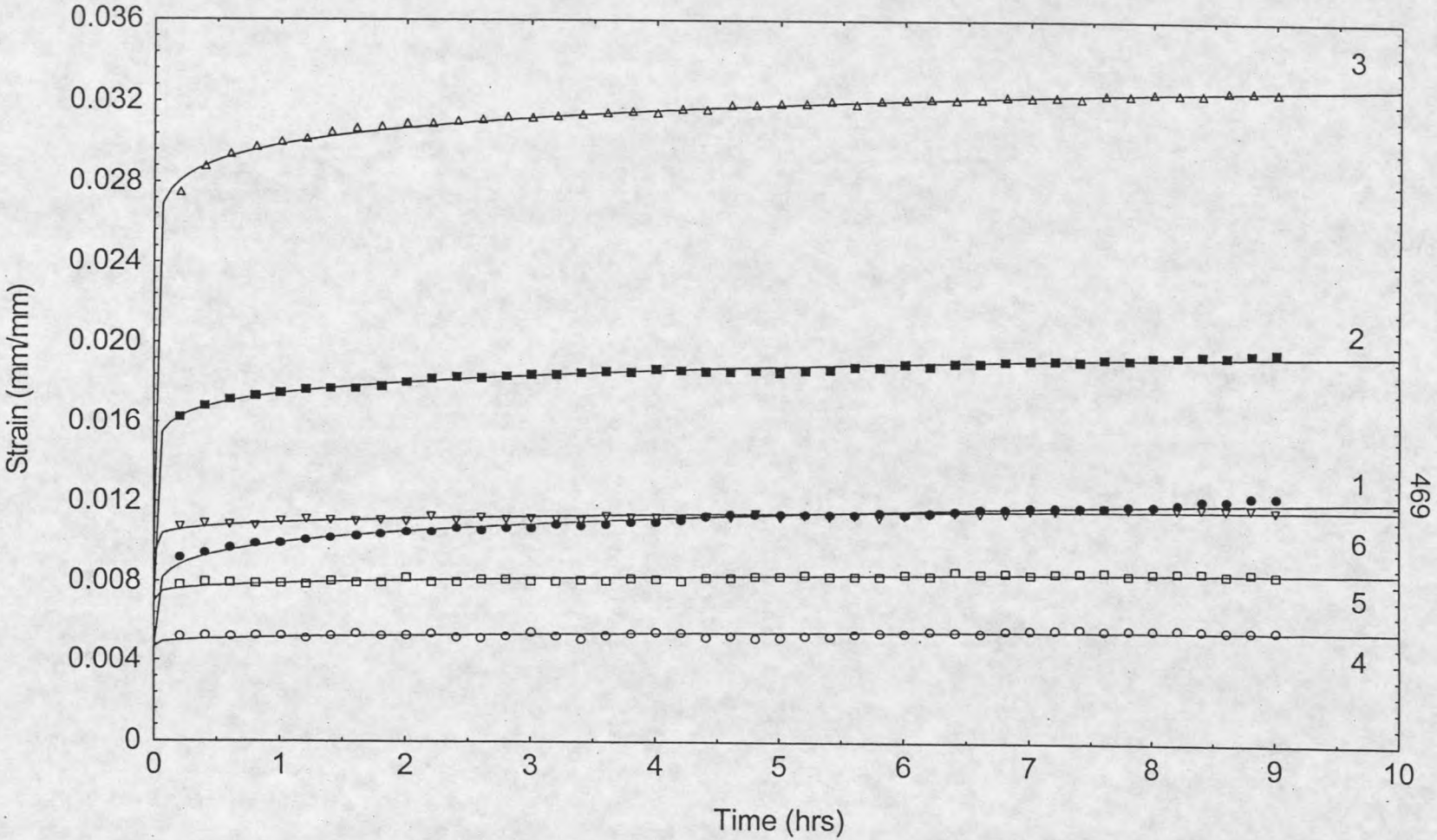


Figure K.II.5 Vibrocreep Response of PVDF at Different Mean Stresses at 23 °C
1- $(0.30\pm0.10)\sigma_y$, 10 Hz; 2- $(0.45\pm0.10)\sigma_y$, 10 Hz; 3- $(0.60\pm0.10)\sigma_y$, 10 Hz;
4- $(0.30)\sigma_y$, 5- $(0.45)\sigma_y$, 6- $(0.60)\sigma_y$, Constant Load Creep;
σ_y = 30.428 MPa at 23 °C

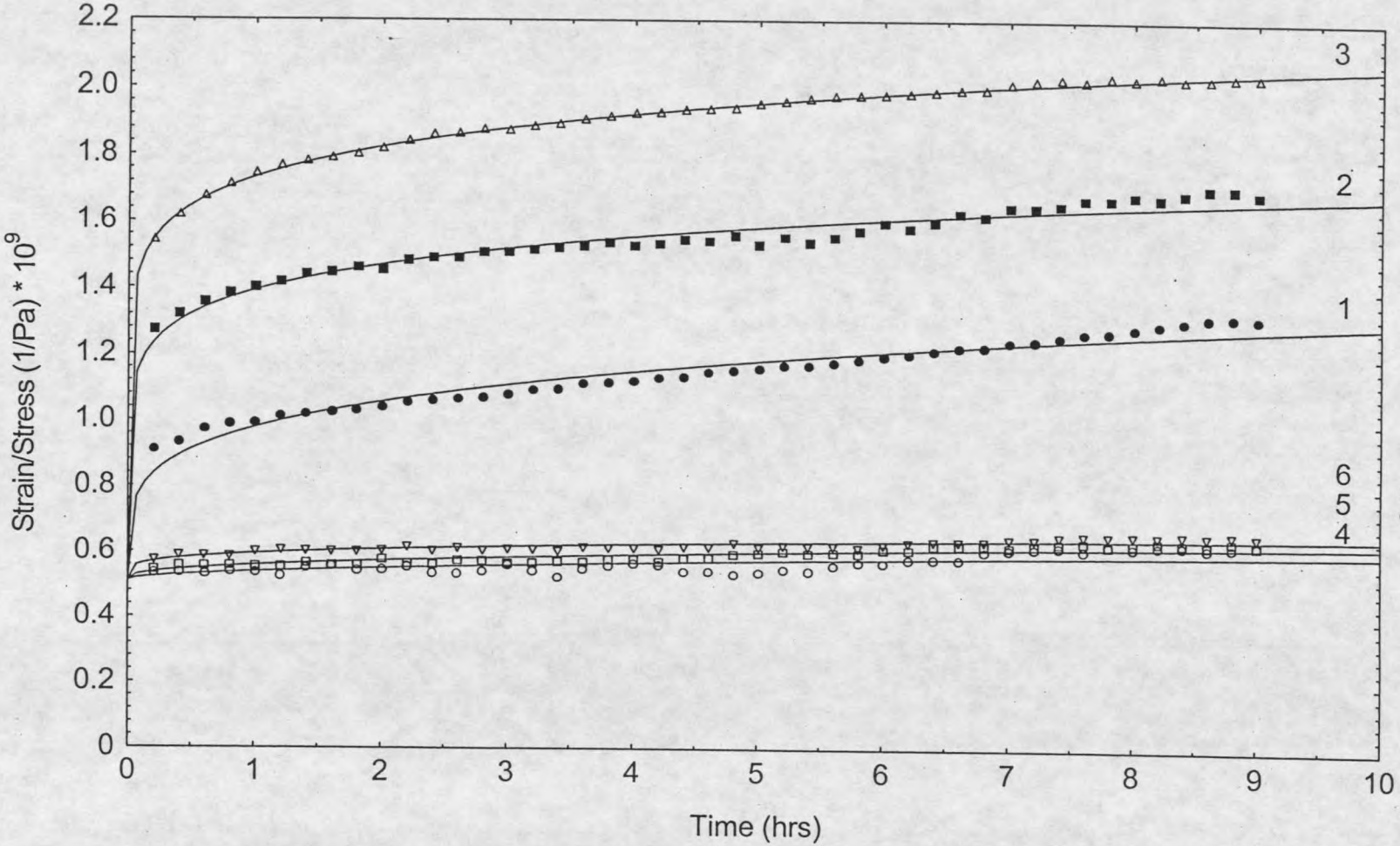


Figure K.II.6 Normalized Vibrocreep Response of PVDF at Different Mean Stresses at 23 °C
1- $(0.30\pm0.10)\sigma_y$, 10 Hz; 2- $(0.45\pm0.10)\sigma_y$, 10 Hz; 3- $(0.60\pm0.10)\sigma_y$, 10 Hz;
4- $(0.30)\sigma_y$, 5- $(0.45)\sigma_y$, 6- $(0.60)\sigma_y$, Constant Load Creep;
σ_y = 30.428 MPa at 23 °C

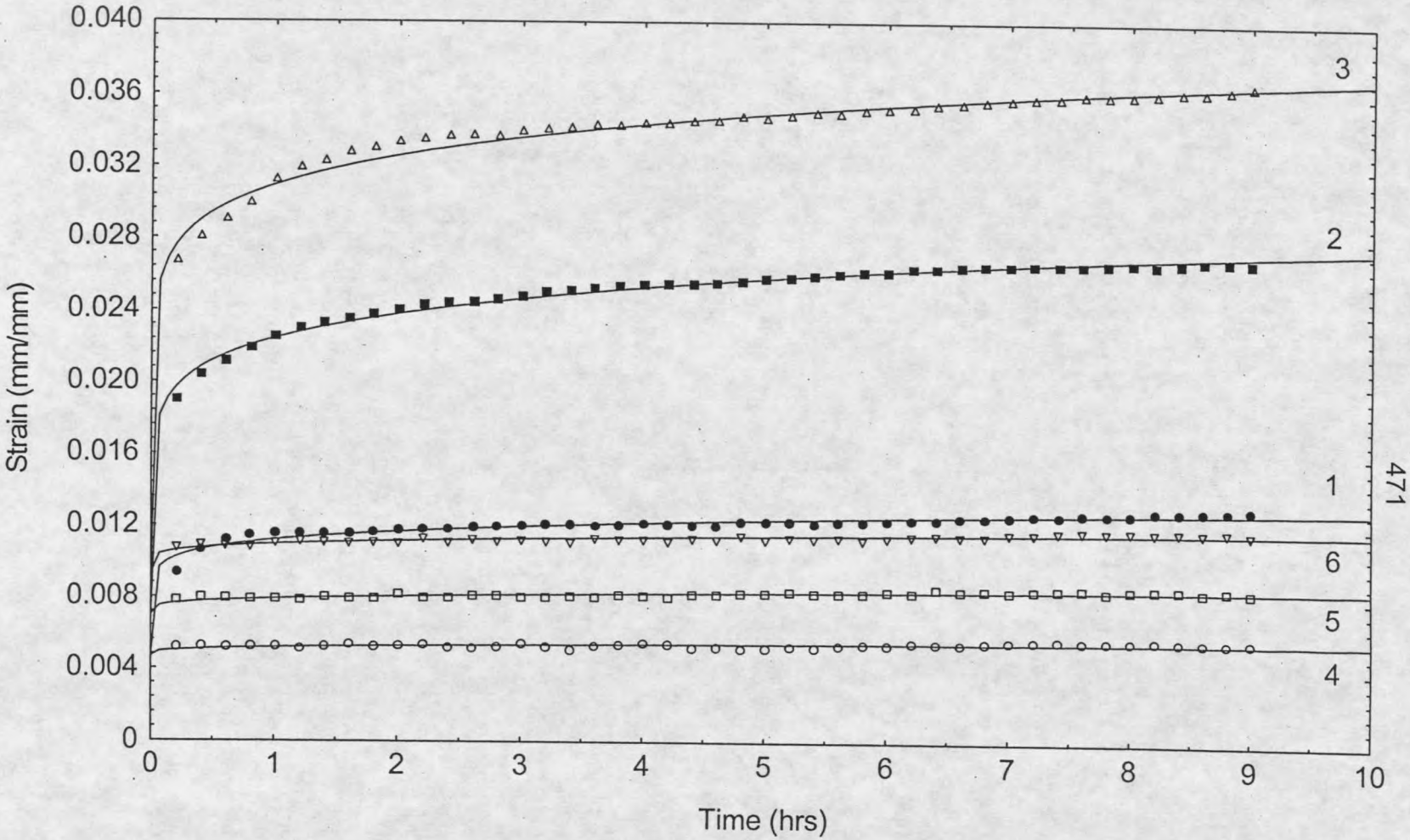


Figure K.II.7 Vibrocreep Response of PVDF at Different Mean Stresses at 23 °C
1- $(0.30\pm0.20)\sigma_y$, 10 Hz; 2- $(0.45\pm0.20)\sigma_y$, 10 Hz; 3- $(0.60\pm0.20)\sigma_y$, 10 Hz;
4- $(0.30)\sigma_y$, 5- $(0.45)\sigma_y$, 6- $(0.60)\sigma_y$, Constant Load Creep;
σ_y = 30.428 MPa at 23 °C

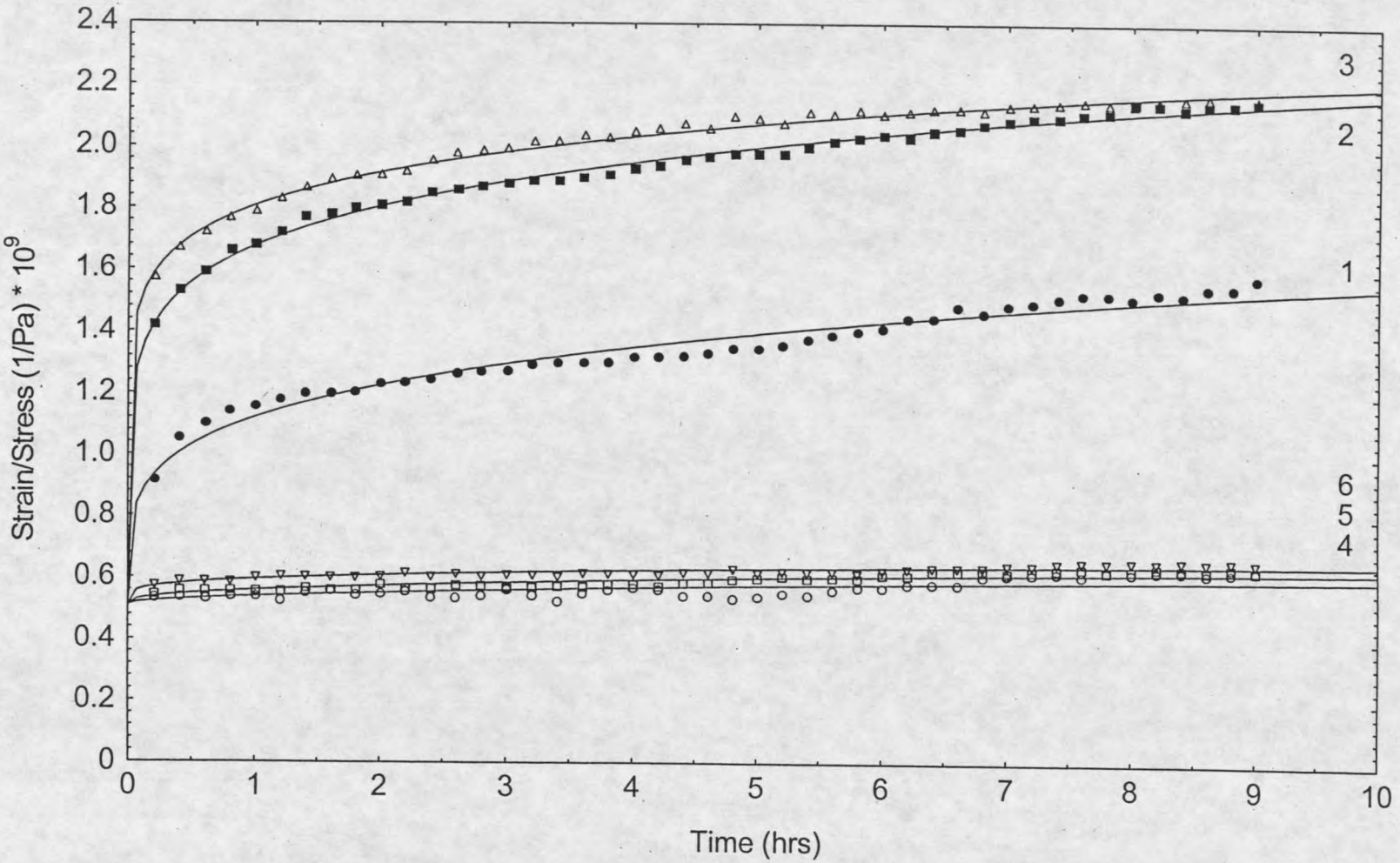


Figure K.II.8 Normalized Vibrocreep Response of PVDF at Different Mean Stresses at 23 °C
1- $(0.30\pm0.20)\sigma_y$, 10 Hz; 2- $(0.45\pm0.20)\sigma_y$, 10 Hz; 3- $(0.60\pm0.20)\sigma_y$, 10 Hz;
4- $(0.30)\sigma_y$, 5- $(0.45)\sigma_y$, 6- $(0.60)\sigma_y$, Constant Load Creep;
σ_y = 30.428 MPa at 23 °C

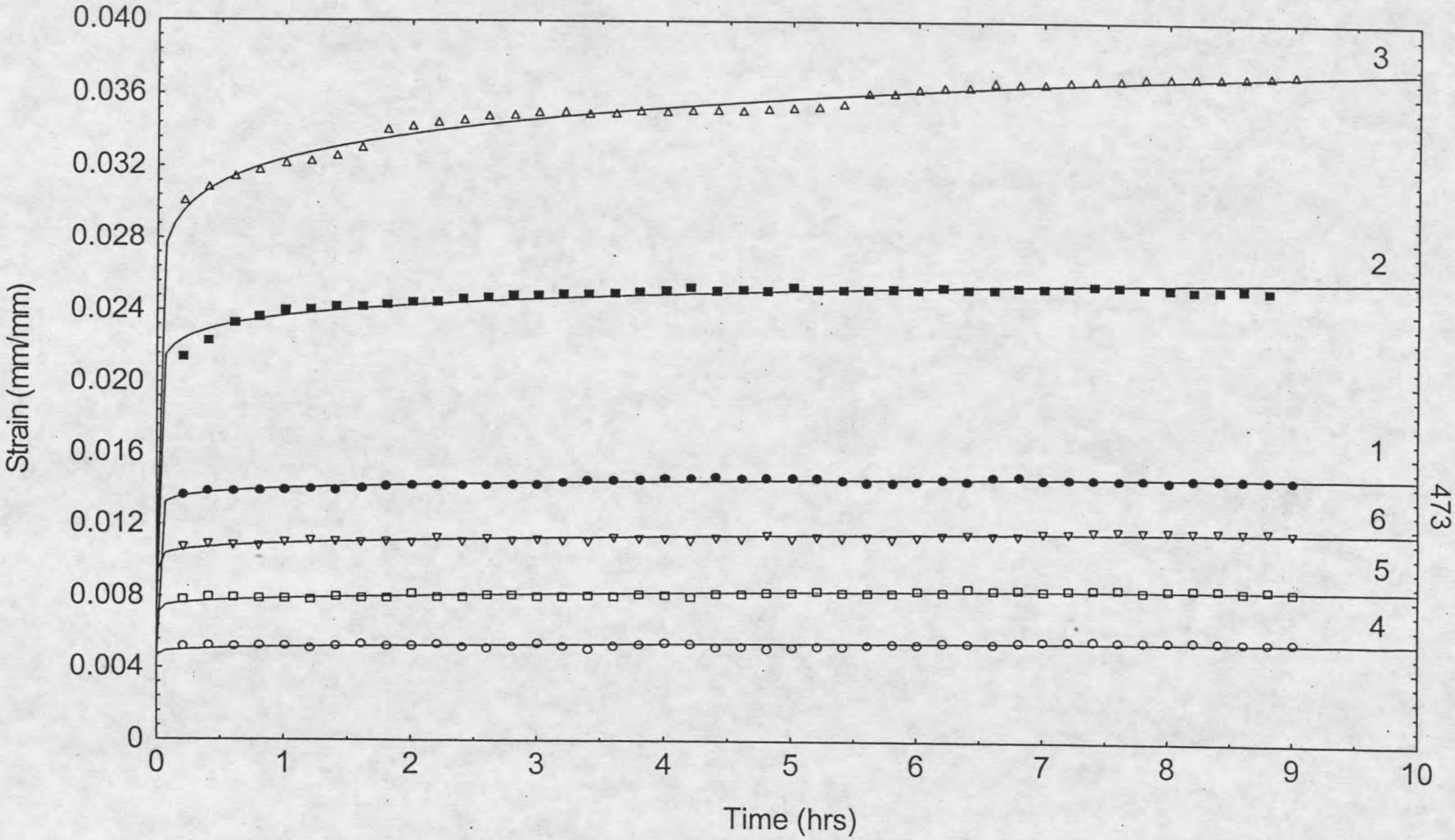


Figure K.II.9 Vibrocreep Response of PVDF at Different Mean Stresses at 23 °C
1- $(0.30\pm0.10)\sigma_y$, 20 Hz; 2- $(0.45\pm0.10)\sigma_y$, 20 Hz; 3- $(0.60\pm0.10)\sigma_y$, 20 Hz;
4- $(0.30)\sigma_y$, 5- $(0.45)\sigma_y$, 6- $(0.60)\sigma_y$, Constant Load Creep;
σ_y = 30.428 MPa at 23 °C

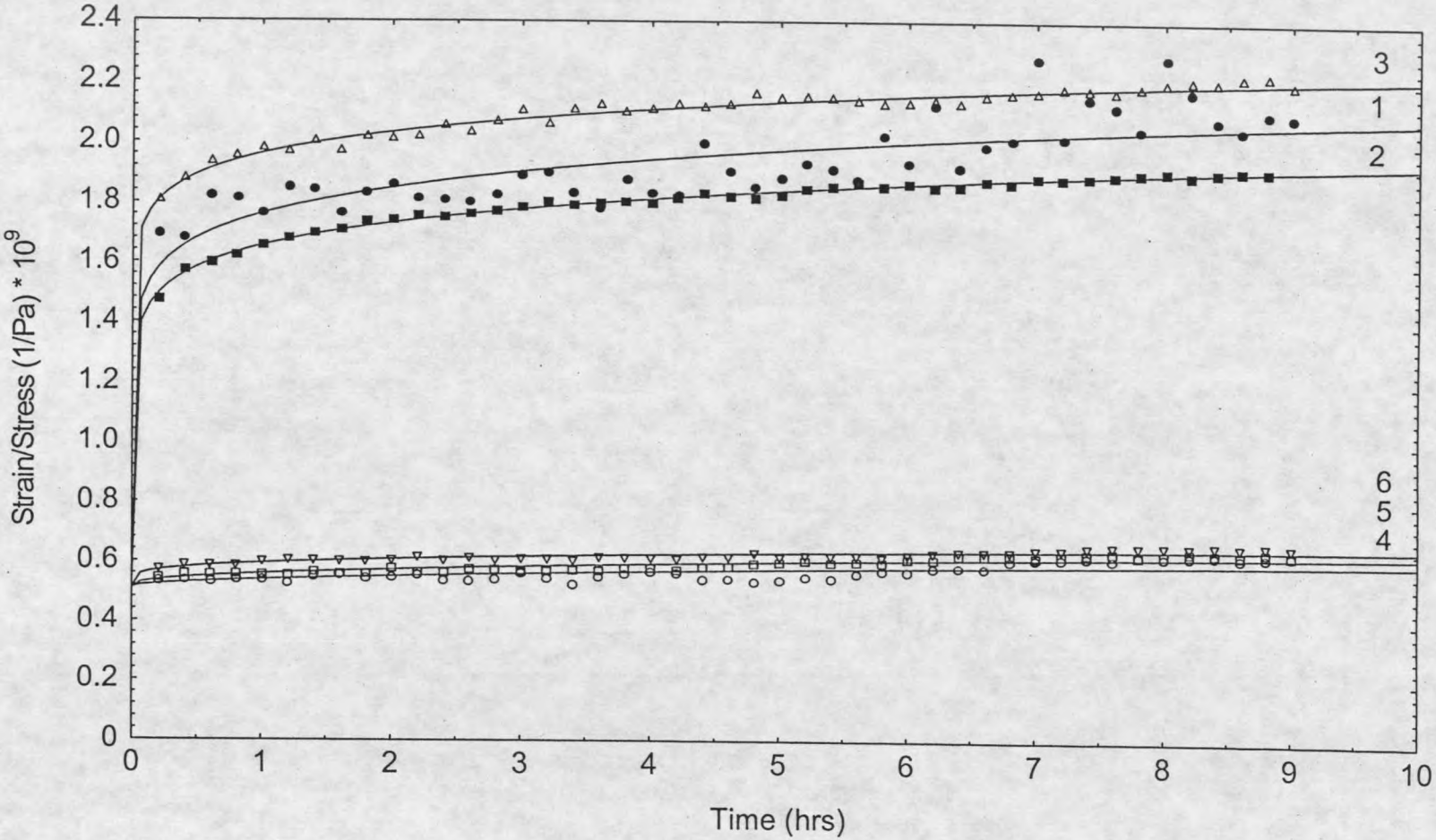


Figure K.II.10 Normalized Vibrocreep Response of PVDF at Different Mean Stresses at 23 °C
1- $(0.30\pm0.10)\sigma_y$, 20 Hz; 2- $(0.45\pm0.10)\sigma_y$, 20 Hz; 3- $(0.60\pm0.10)\sigma_y$, 20 Hz;
4- $(0.30)\sigma_y$, 5- $(0.45)\sigma_y$, 6- $(0.60)\sigma_y$, Constant Load Creep;
σ_y = 30.428 MPa at 23 °C

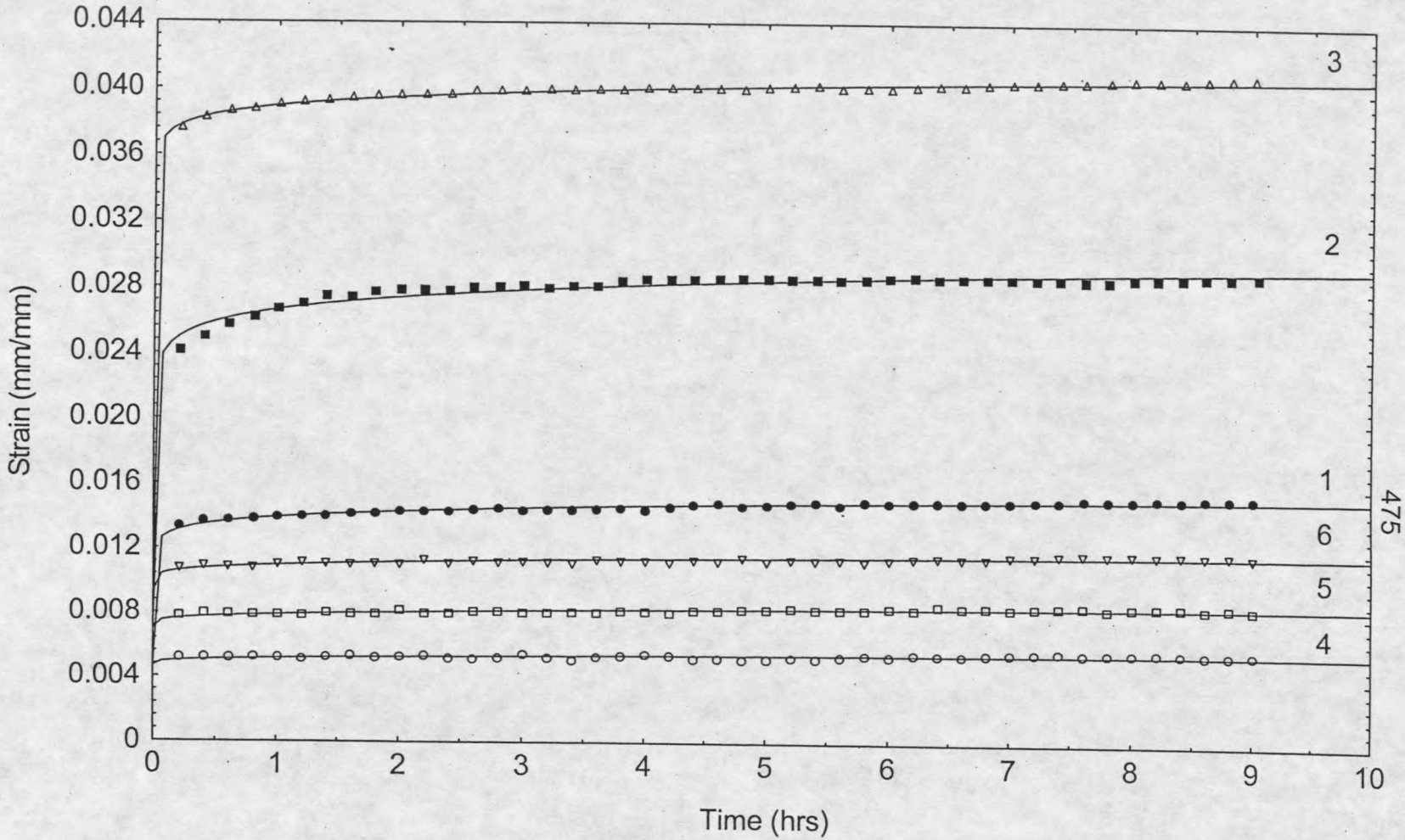


Figure K.II.11 Vibrocreep Response of PVDF at Different Mean Stresses at 23 °C
1- $(0.30\pm0.20)\sigma_y$, 20 Hz; 2- $(0.45\pm0.20)\sigma_y$, 20 Hz; 3- $(0.60\pm0.20)\sigma_y$, 20 Hz;
4- $(0.30)\sigma_y$, 5- $(0.45)\sigma_y$, 6- $(0.60)\sigma_y$, Constant Load Creep;
σ_y = 30.428 MPa at 23 °C

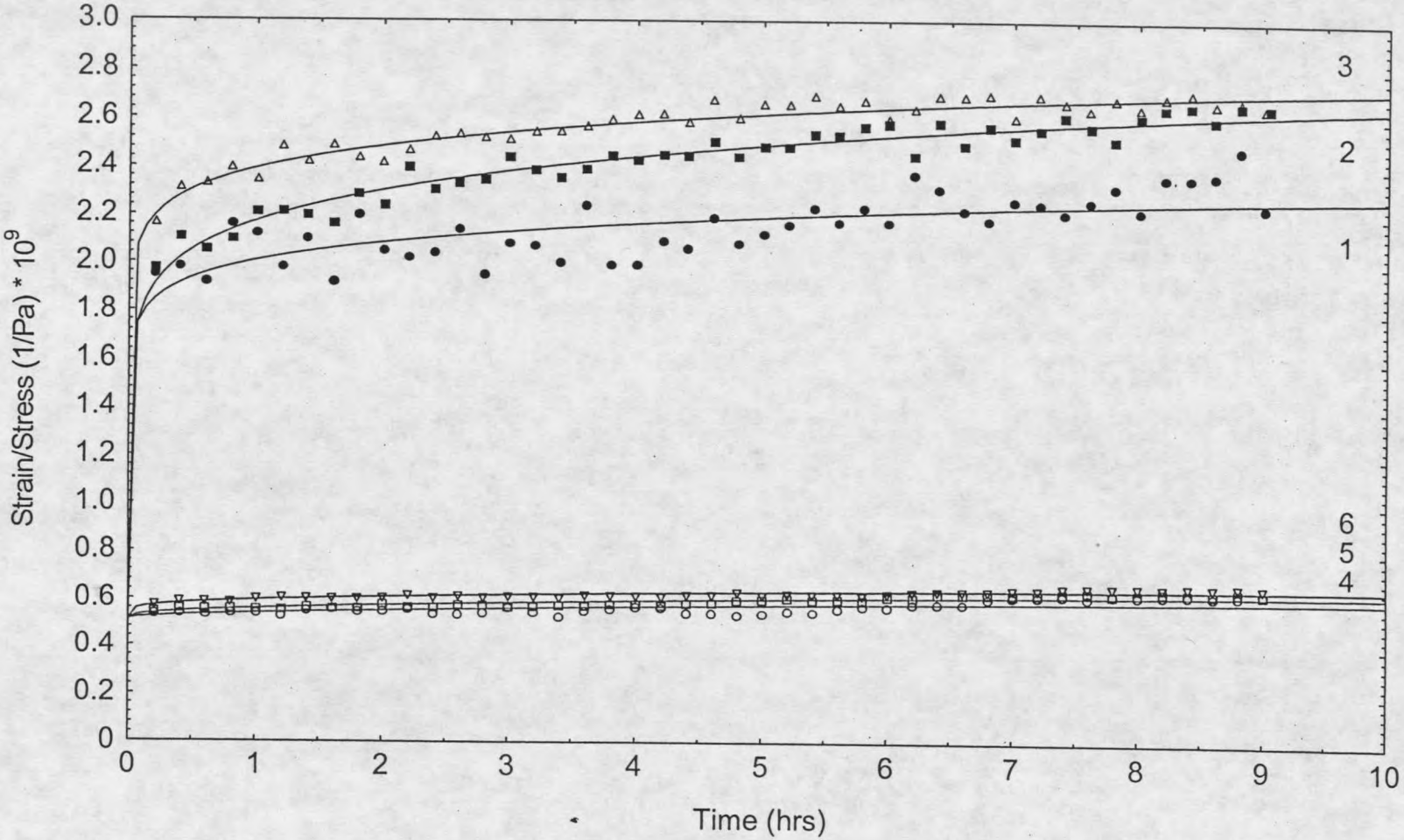


Figure K.II.12 Normalized Vibrocreep Response of PVDF at Different Mean Stresses at 23 °C
1- $(0.30\pm0.20)\sigma_y$, 20 Hz; 2- $(0.45\pm0.20)\sigma_y$, 20 Hz; 3- $(0.60\pm0.20)\sigma_y$, 20 Hz;
4- $(0.30)\sigma_y$, 5- $(0.45)\sigma_y$, 6- $(0.60)\sigma_y$, Constant Load Creep;
σ_y = 30.428 MPa at 23 °C

APPENDIX L

Temperature Effects from Tensile, Constant Load Creep, and Vibrocreep of PVDF

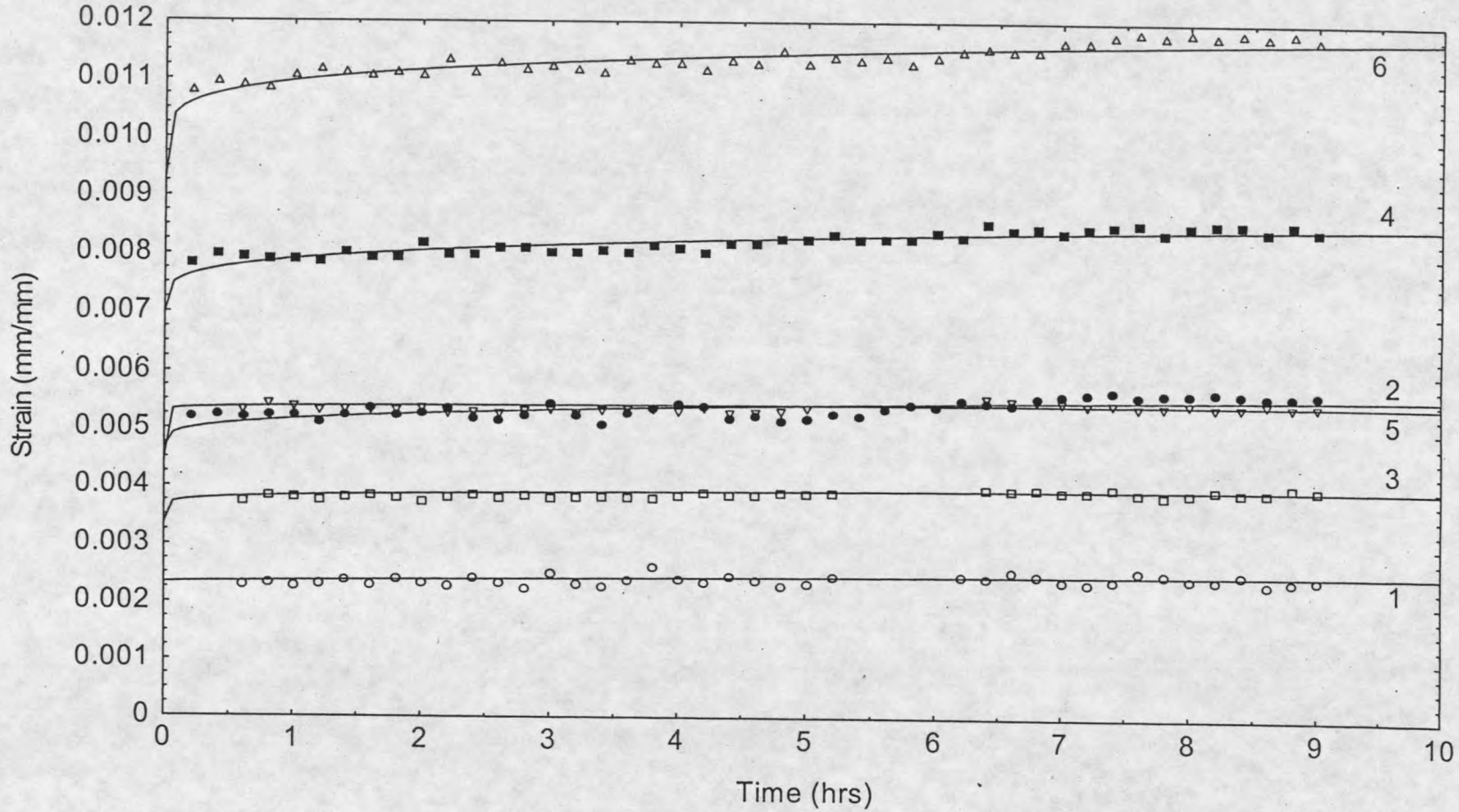


Figure L.1 Constant Load Creep of PVDF at Different Temperatures
1- $(0.30)\sigma_y$ at -25 °C; 2- $(0.30)\sigma_y$ at 23 °C;
3- $(0.45)\sigma_y$ at -25 °C; 4- $(0.45)\sigma_y$ at 23 °C;
5- $(0.60)\sigma_y$ at -25 °C; 6- $(0.60)\sigma_y$ at 23 °C;
σ_y = 30.428 MPa at 23 °C

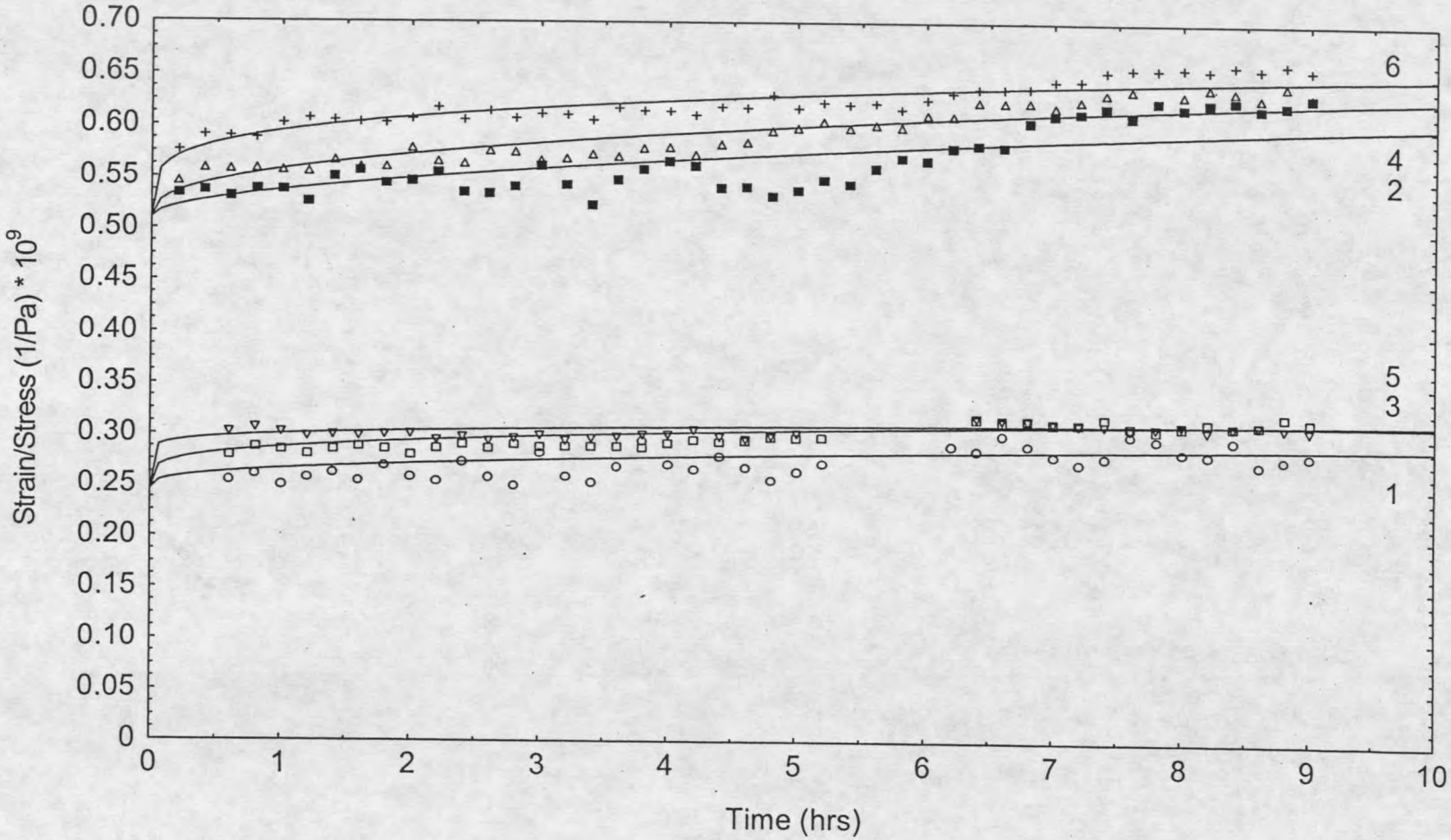


Figure L.2 Normalized Constant Load Creep of PVDF at Different Temperatures

1- $(0.30)\sigma_y$ at -25 °C; 2- $(0.30)\sigma_y$ at 23 °C;

3- $(0.45)\sigma_y$ at -25 °C; 4- $(0.45)\sigma_y$ at 23 °C;

5- $(0.60)\sigma_y$ at -25 °C; 6- $(0.60)\sigma_y$ at 23 °C;

σ_y = 30.428 MPa at 23 °C

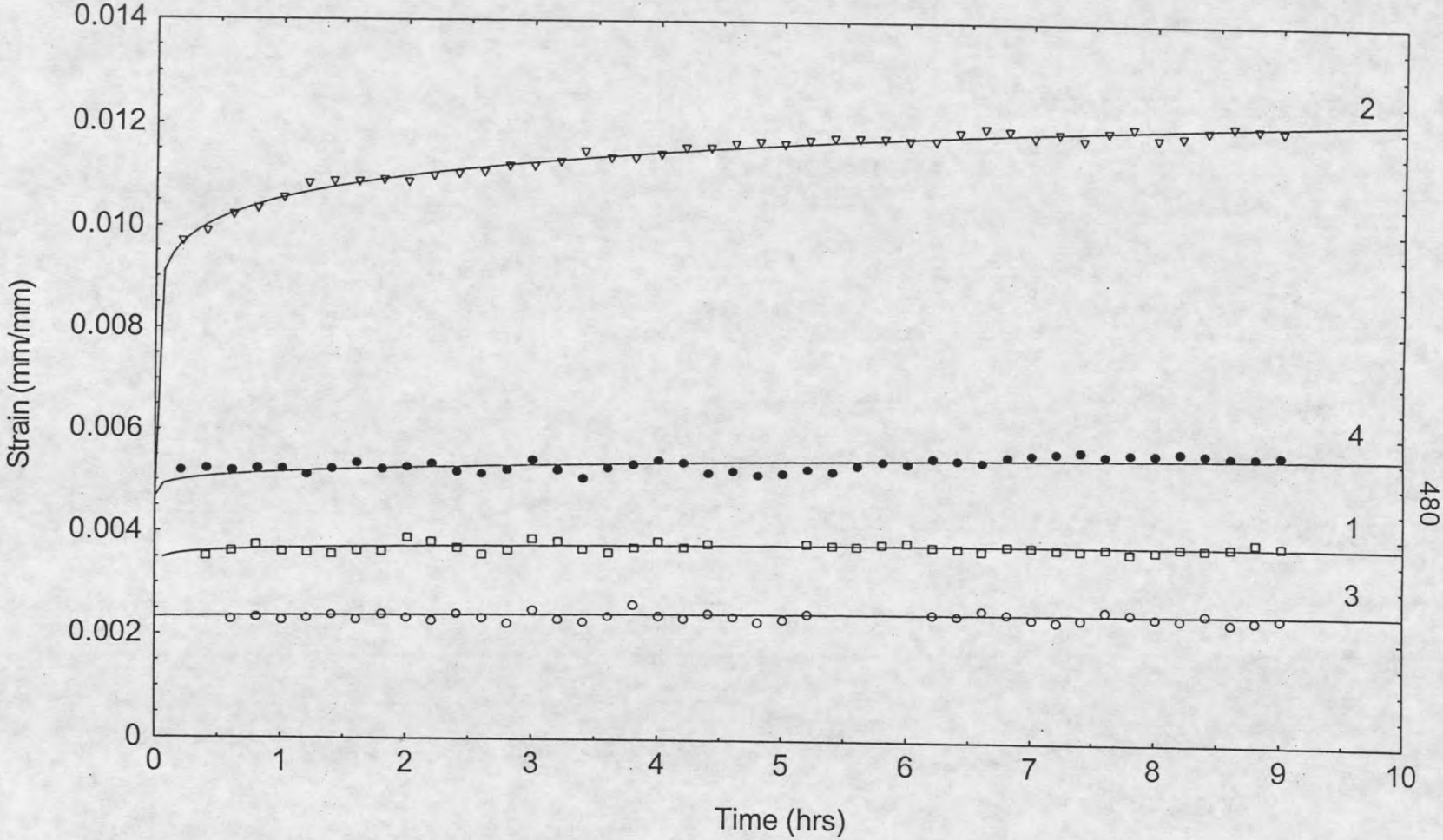


Figure L.3 Vibrocreep Response of PVDF at Different Temperatures
1- $(0.30\pm0.20)\sigma_y$, 5 Hz at -25 °C; 2- $(0.30\pm0.20)\sigma_y$, 5 Hz at 23 °C;
3- $(0.30)\sigma_y$ at -25 °C, 4- $(0.30)\sigma_y$ at 23 °C, Constant Load Creep;
σ_y = 30.428 MPa at 23 °C

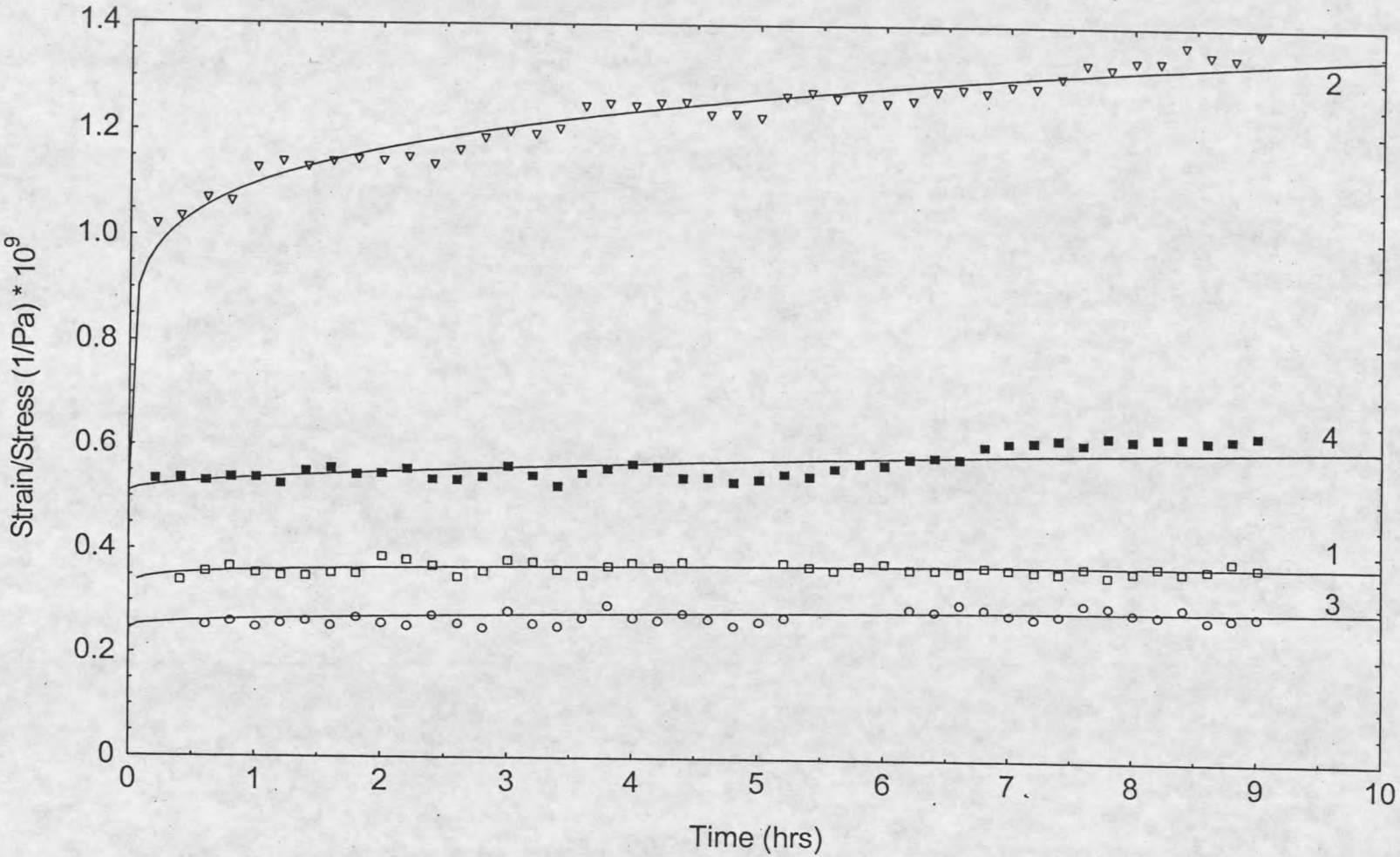


Figure L.4 Normalized Vibrocreep Response of PVDF at Different Temperatures
1- $(0.30\pm0.20)\sigma_y$, 5 Hz at -25 °C; 2- $(0.30\pm0.20)\sigma_y$, 5 Hz at 23 °C;
3- $(0.30)\sigma_y$ at -25 °C, 4- $(0.30)\sigma_y$ at 23 °C, Constant Load Creep;
σ_y = 30.428 MPa at 23 °C

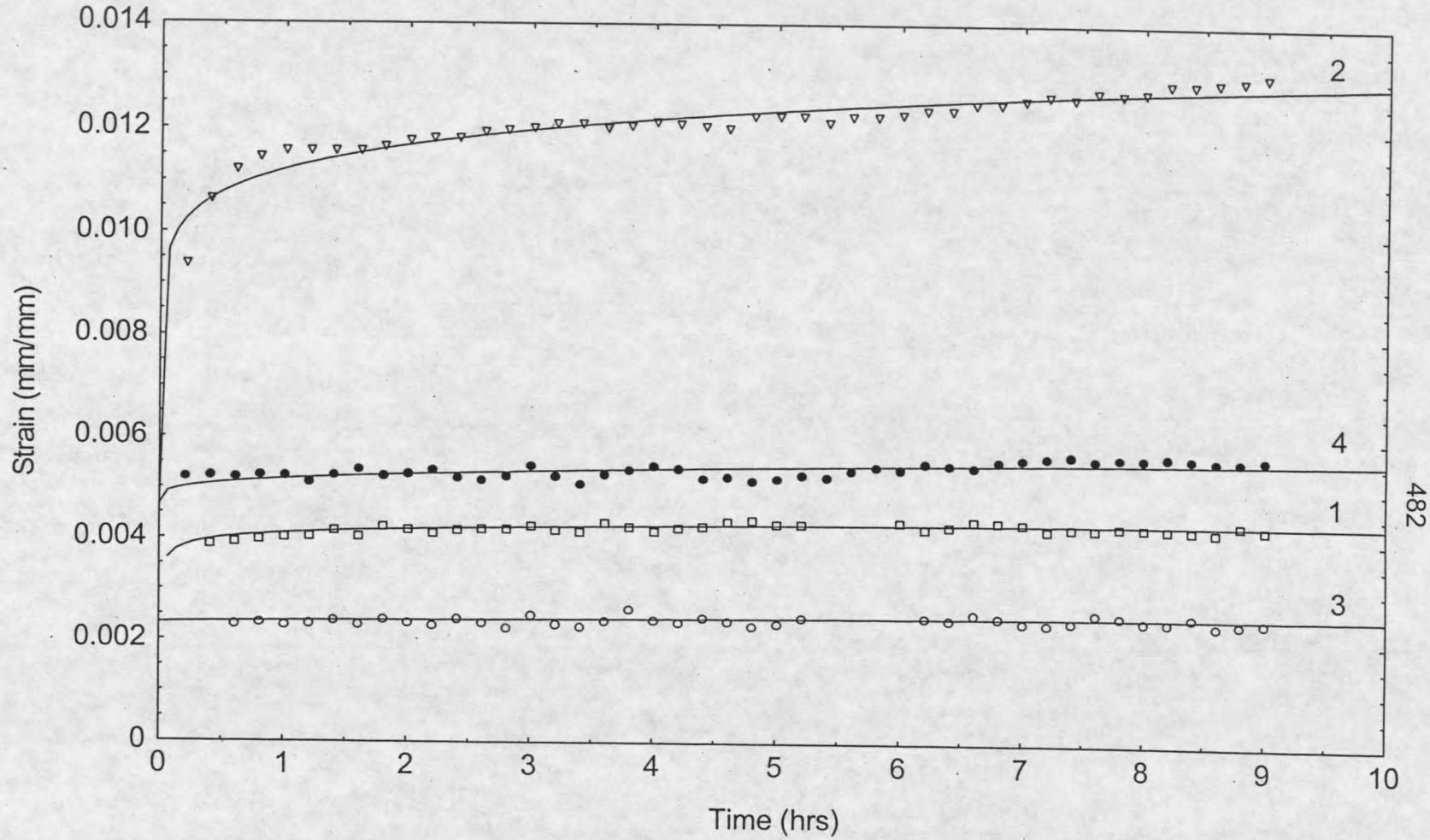


Figure L.5 Vibrocreep Response of PVDF at Different Temperatures
1- $(0.30\pm0.20)\sigma_y$, 10 Hz at -25 °C; 2- $(0.30\pm0.20)\sigma_y$, 10 Hz at 23 °C;
3- $(0.30)\sigma_y$ at -25 °C, 4- $(0.30)\sigma_y$ at 23 °C, Constant Load Creep;
σ_y = 30.428 MPa at 23 °C

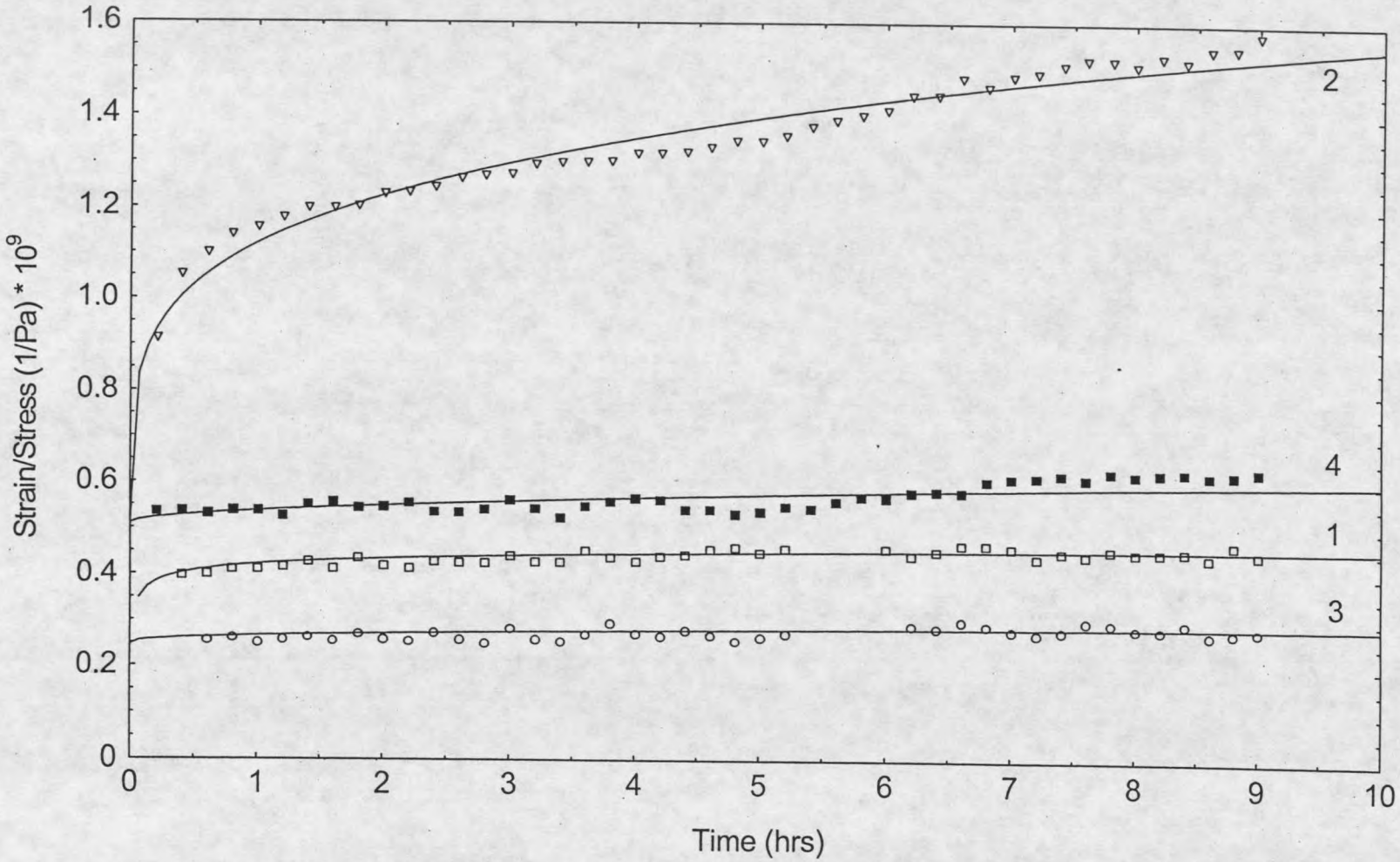


Figure L.6 Normalized Vibrocreep Response of PVDF at Different Temperatures
1- $(0.30\pm0.20)\sigma_y$, 10 Hz at -25 °C; 2- $(0.30\pm0.20)\sigma_y$, 10 Hz at 23 °C;
3- $(0.30)\sigma_y$ at -25 °C, 4- $(0.30)\sigma_y$ at 23 °C, Constant Load Creep;
σ_y = 30.428 MPa at 23 °C

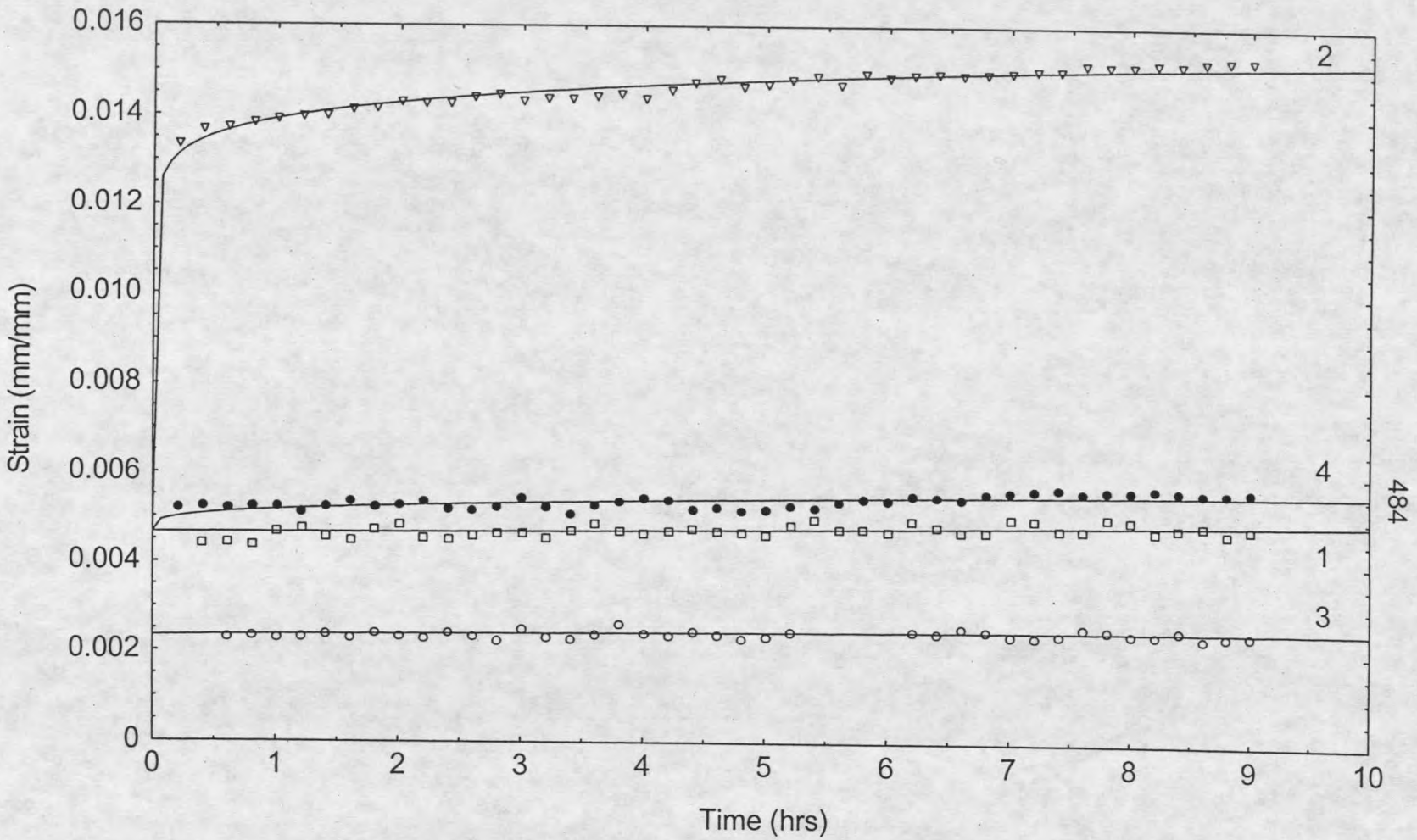


Figure L.7 Vibrocreep Response of PVDF at Different Temperatures
1- $(0.30\pm0.20)\sigma_y$, 20 Hz at -25 °C; 2- $(0.30\pm0.20)\sigma_y$, 20 Hz at 23 °C;
3- $(0.30)\sigma_y$ at -25 °C, 4- $(0.30)\sigma_y$ at 23 °C, Constant Load Creep;
σ_y = 30.428 MPa at 23 °C

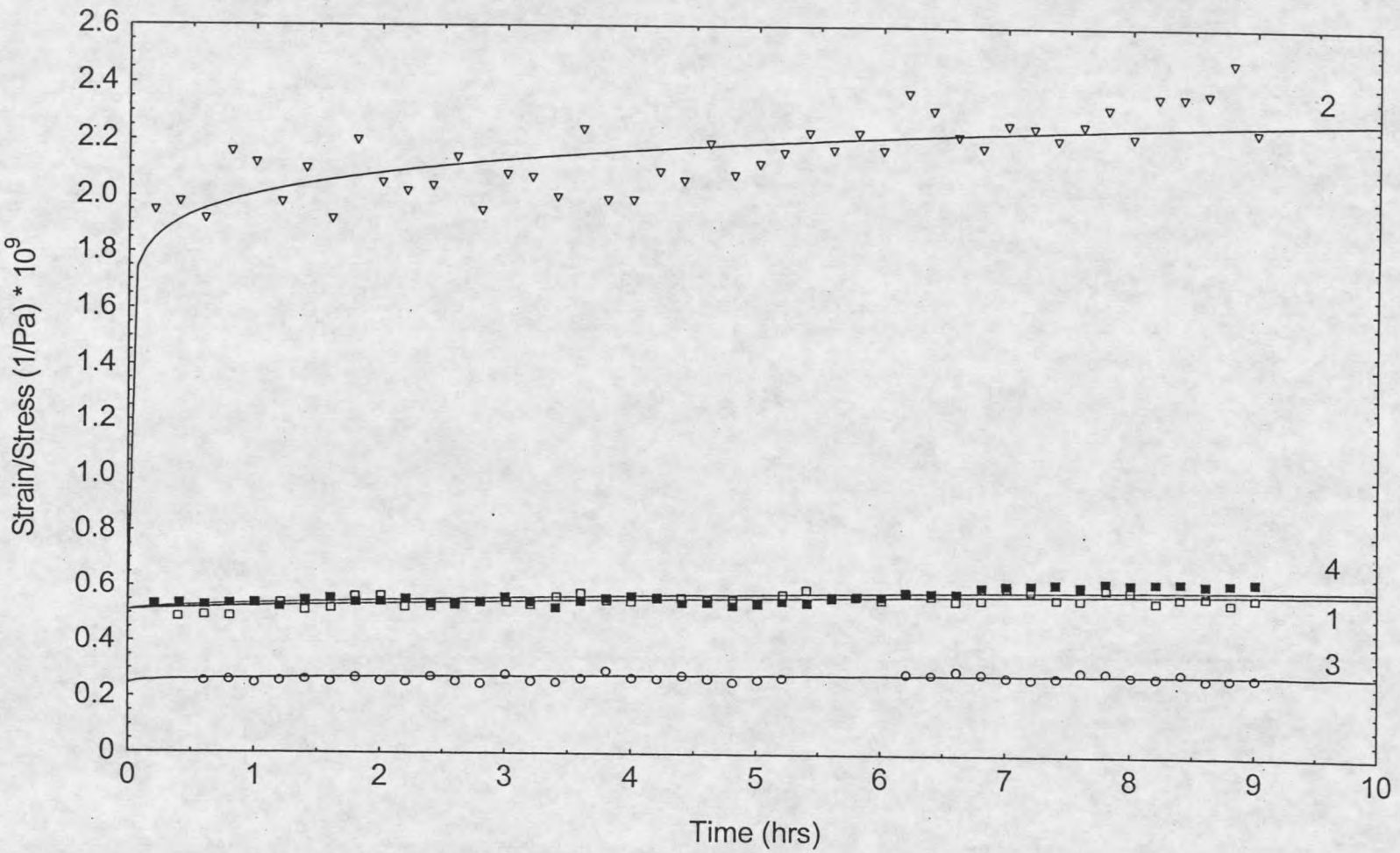


Figure L.8 Normalized Vibrocreep Response of PVDF at Different Temperatures
1- $(0.30\pm0.20)\sigma_y$, 20 Hz at -25 °C; 2- $(0.30\pm0.20)\sigma_y$, 20 Hz at 23 °C;
3- $(0.30)\sigma_y$ at -25 °C, 4- $(0.30)\sigma_y$ at 23 °C, Constant Load Creep;
σ_y = 30.428 MPa at 23 °C

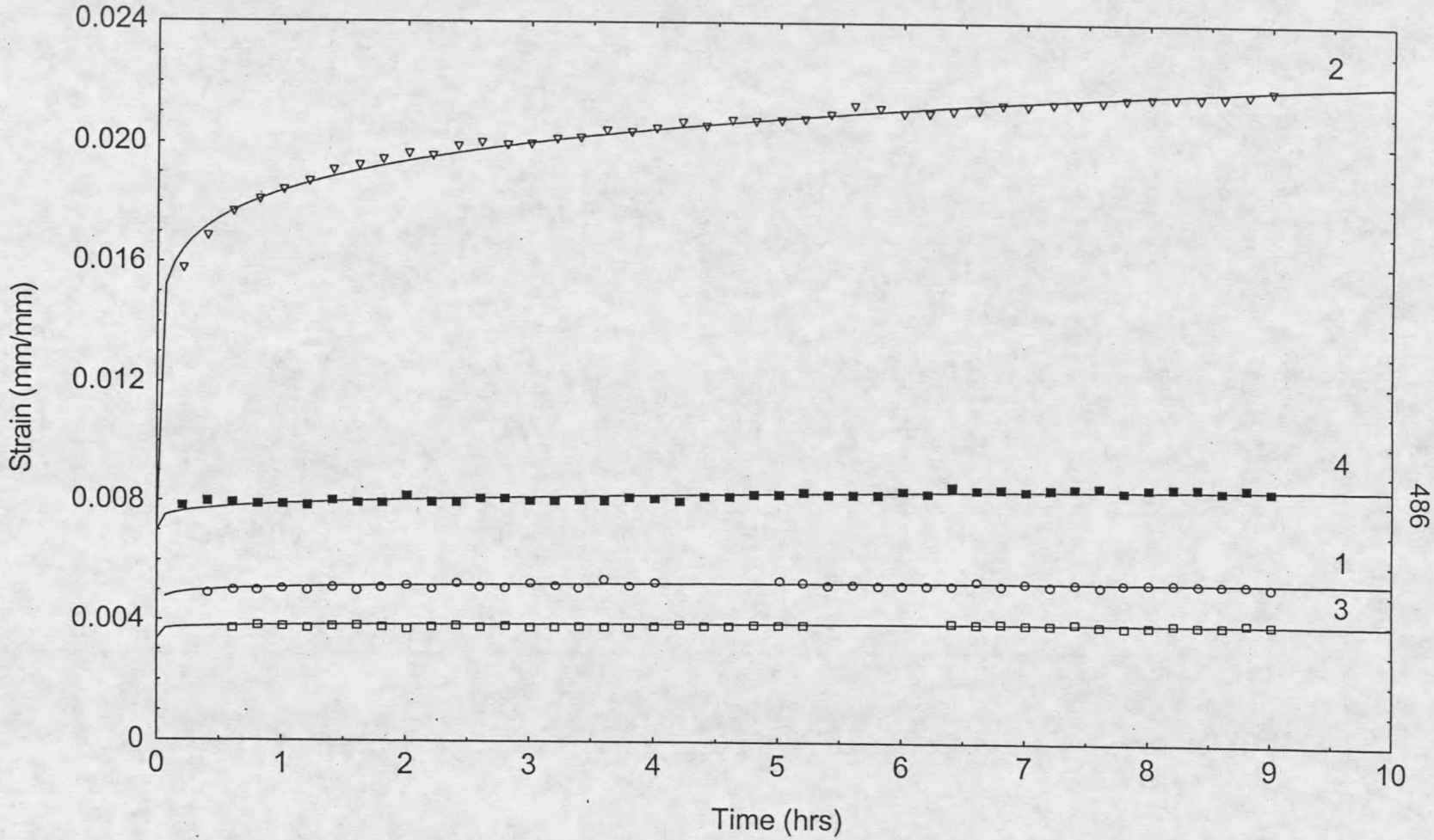


Figure L.9 Vibrocreep Response of PVDF at Different Temperatures
1- $(0.45\pm0.20)\sigma_y$, 5 Hz at -25 °C; 2- $(0.45\pm0.20)\sigma_y$, 5 Hz at 23 °C;
3- $(0.45)\sigma_y$ at -25 °C, 4- $(0.45)\sigma_y$ at 23 °C, Constant Load Creep;
σ_y = 30.428 MPa at 23 °C

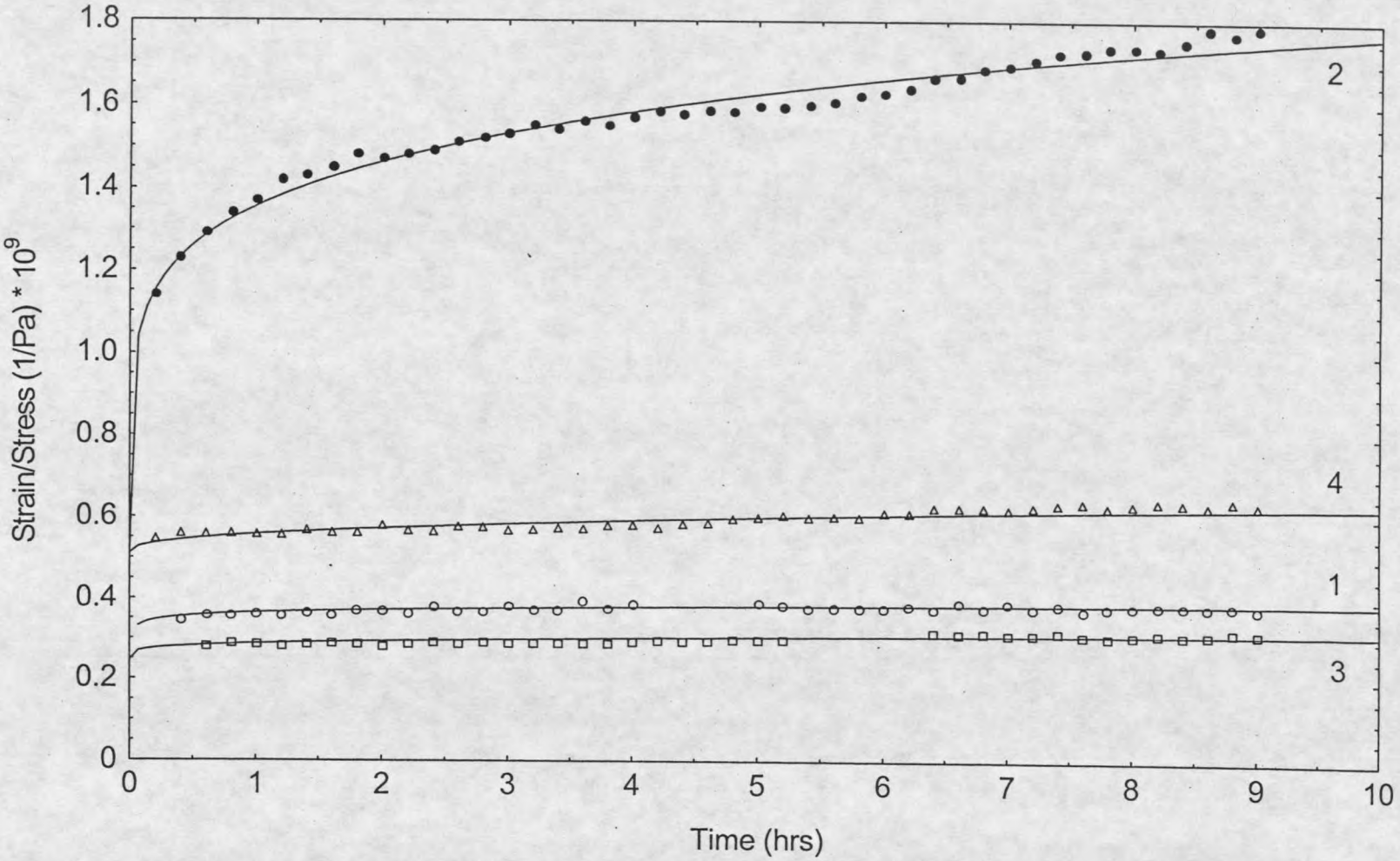


Figure L.10 Normalized Vibrocreep Response of PVDF at Different Temperatures
1- $(0.45\pm0.20)\sigma_y$, 5 Hz at -25 °C; 2- $(0.45\pm0.20)\sigma_y$, 5 Hz at 23 °C;
3- $(0.45)\sigma_y$ at -25 °C, 4- $(0.45)\sigma_y$ at 23 °C, Constant Load Creep;
σ_y = 30.428 MPa at 23 °C

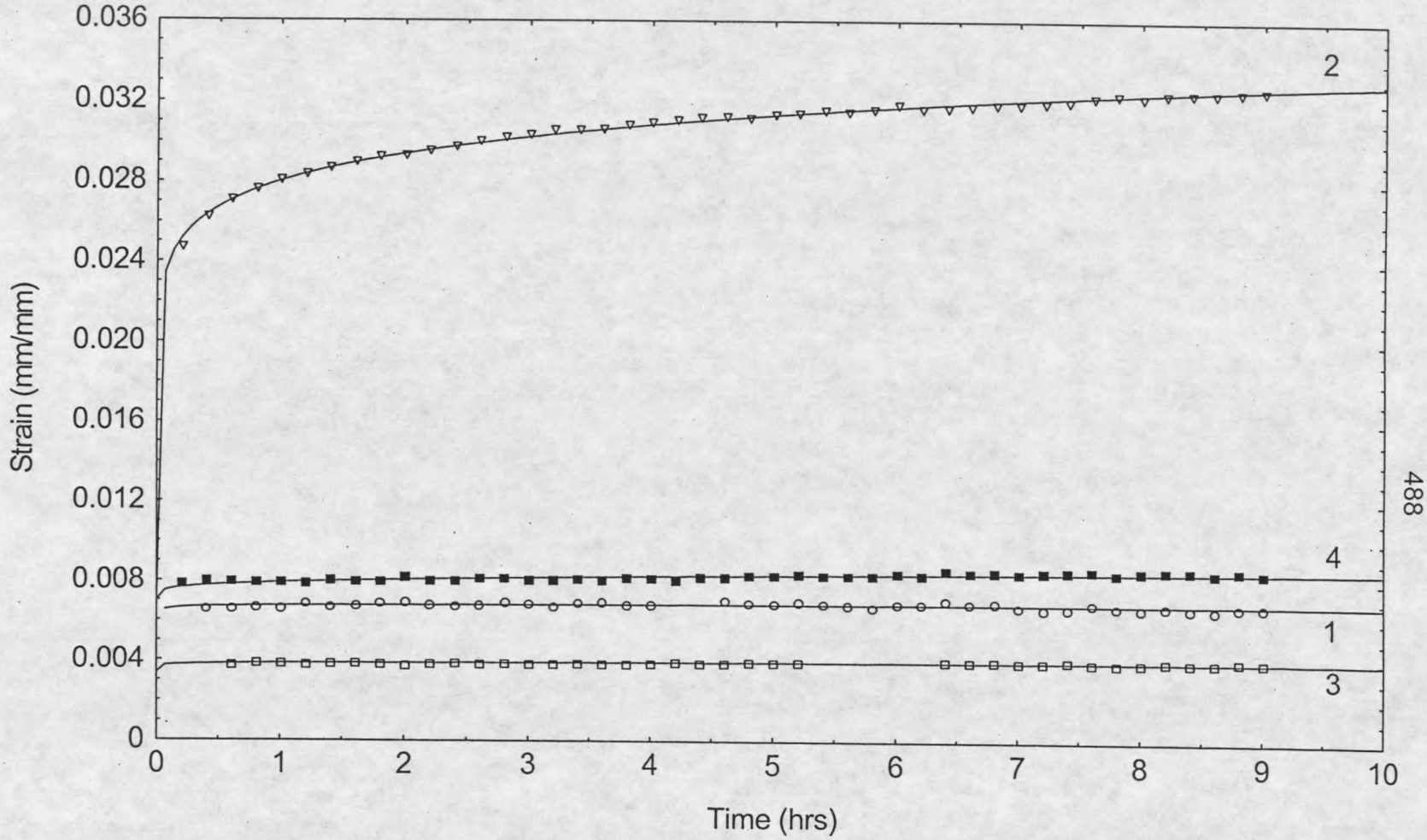


Figure L.11 Vibrocreep Response of PVDF at Different Temperatures
1- $(0.45\pm0.35)\sigma_y$, 5 Hz at -25 °C; 2- $(0.45\pm0.35)\sigma_y$, 5 Hz at 23 °C;
3- $(0.45)\sigma_y$ at -25 °C, 4- $(0.45)\sigma_y$ at 23 °C, Constant Load Creep;
σ_y = 30.428 MPa at 23 °C

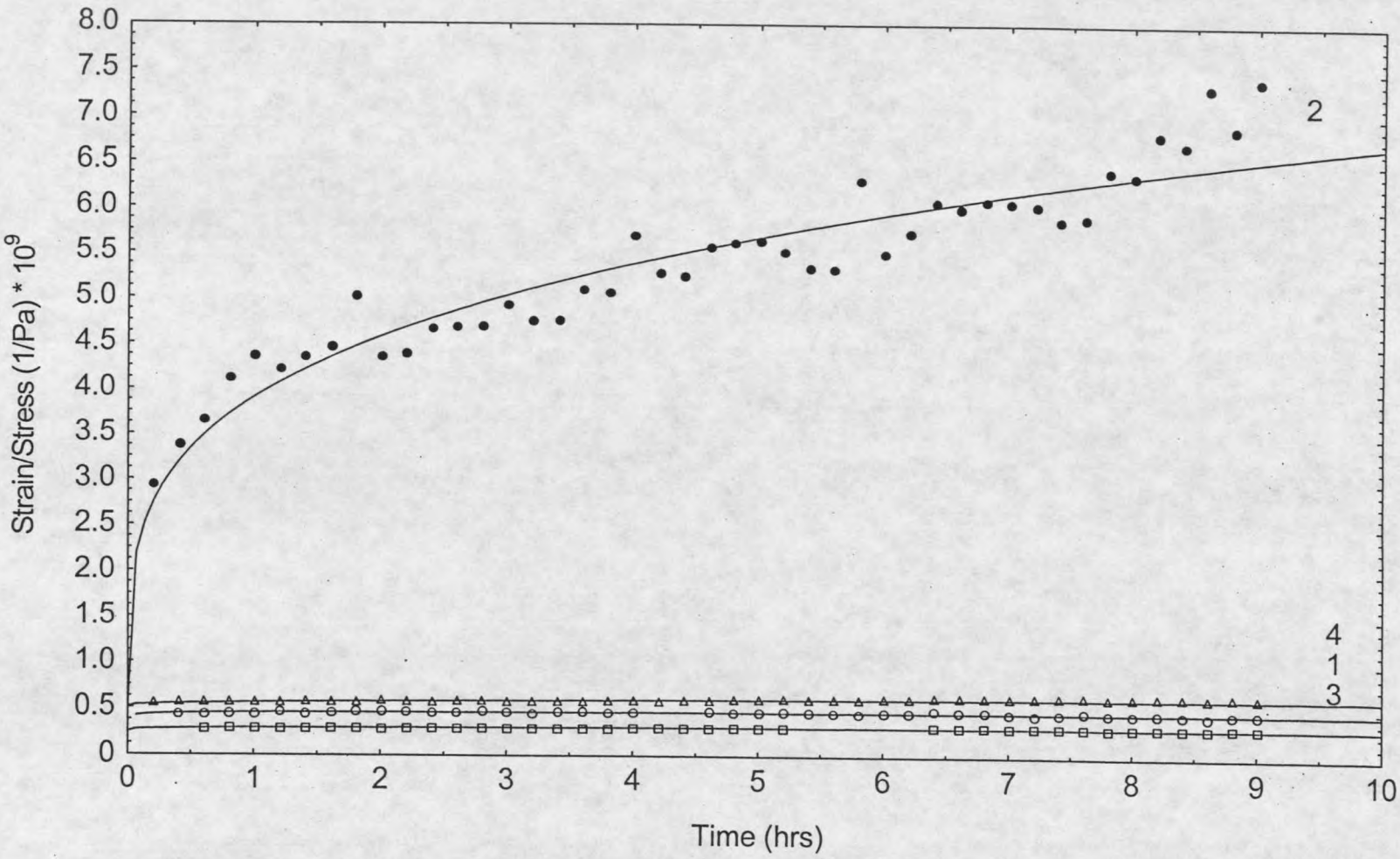


Figure L.12 Normalized Vibrocreep Response of PVDF at Different Temperatures
1- $(0.45\pm0.35)\sigma_y$, 5 Hz at -25 °C; 2- $(0.45\pm0.35)\sigma_y$, 5 Hz at 23 °C;
3- $(0.45)\sigma_y$ at -25 °C, 4- $(0.45)\sigma_y$ at 23 °C, Constant Load Creep;
σ_y = 30.428 MPa at 23 °C

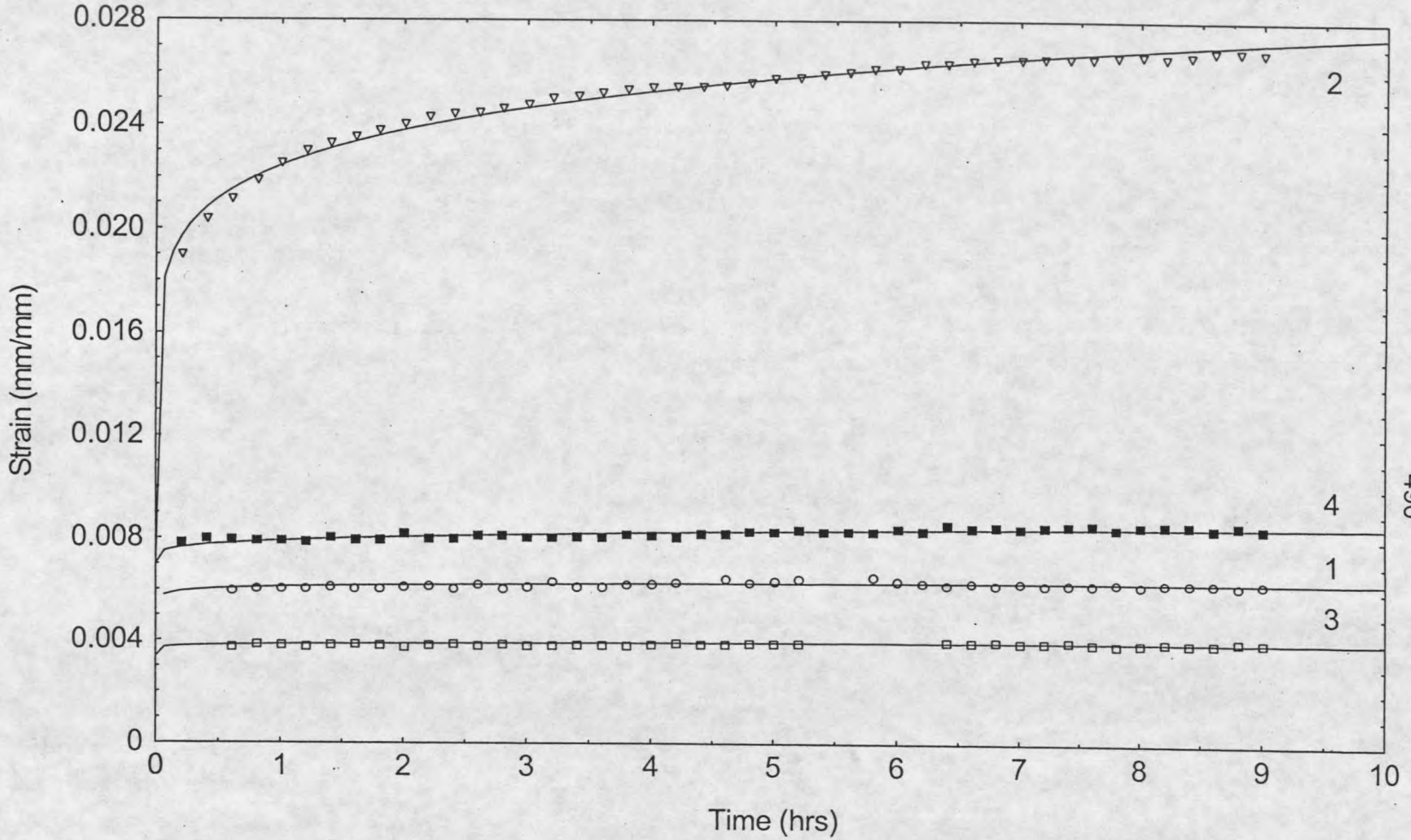


Figure L.13 Vibrocreep Response of PVDF at Different Temperatures
1- $(0.45\pm0.20)\sigma_y$, 10 Hz at -25 °C; 2- $(0.45\pm0.20)\sigma_y$, 10 Hz at 23 °C;
3- $(0.45)\sigma_y$ at -25 °C, 4- $(0.45)\sigma_y$ at 23 °C, Constant Load Creep;
σ_y = 30.428 MPa at 23 °C

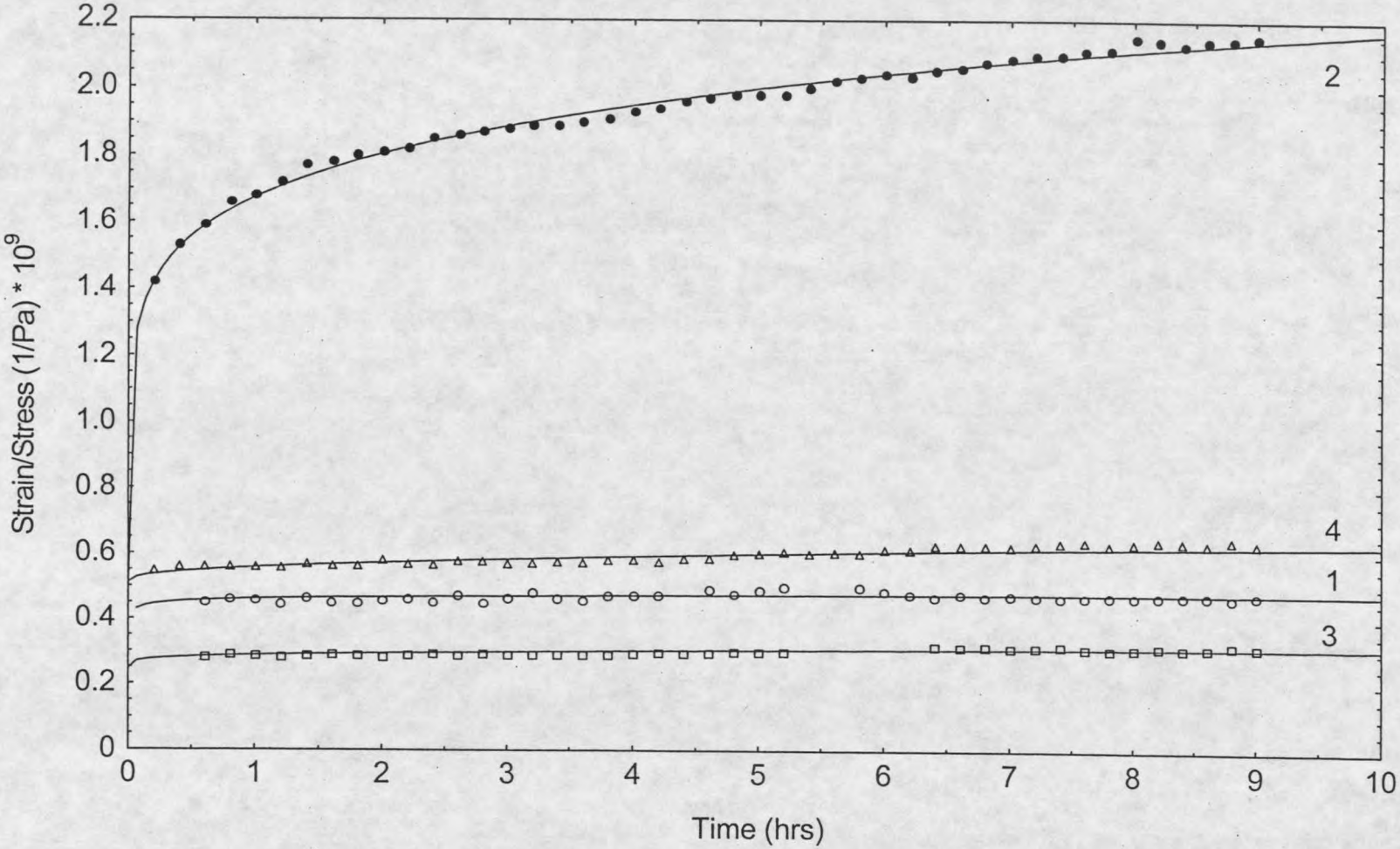


Figure L.14 Normalized Vibrocreep Response of PVDF at Different Temperatures
1- $(0.45\pm0.20)\sigma_y$, 10 Hz at -25 °C; 2- $(0.45\pm0.20)\sigma_y$, 10 Hz at 23 °C;
3- $(0.45)\sigma_y$ at -25 °C, 4- $(0.45)\sigma_y$ at 23 °C, Constant Load Creep;
σ_y = 30.428 MPa at 23 °C

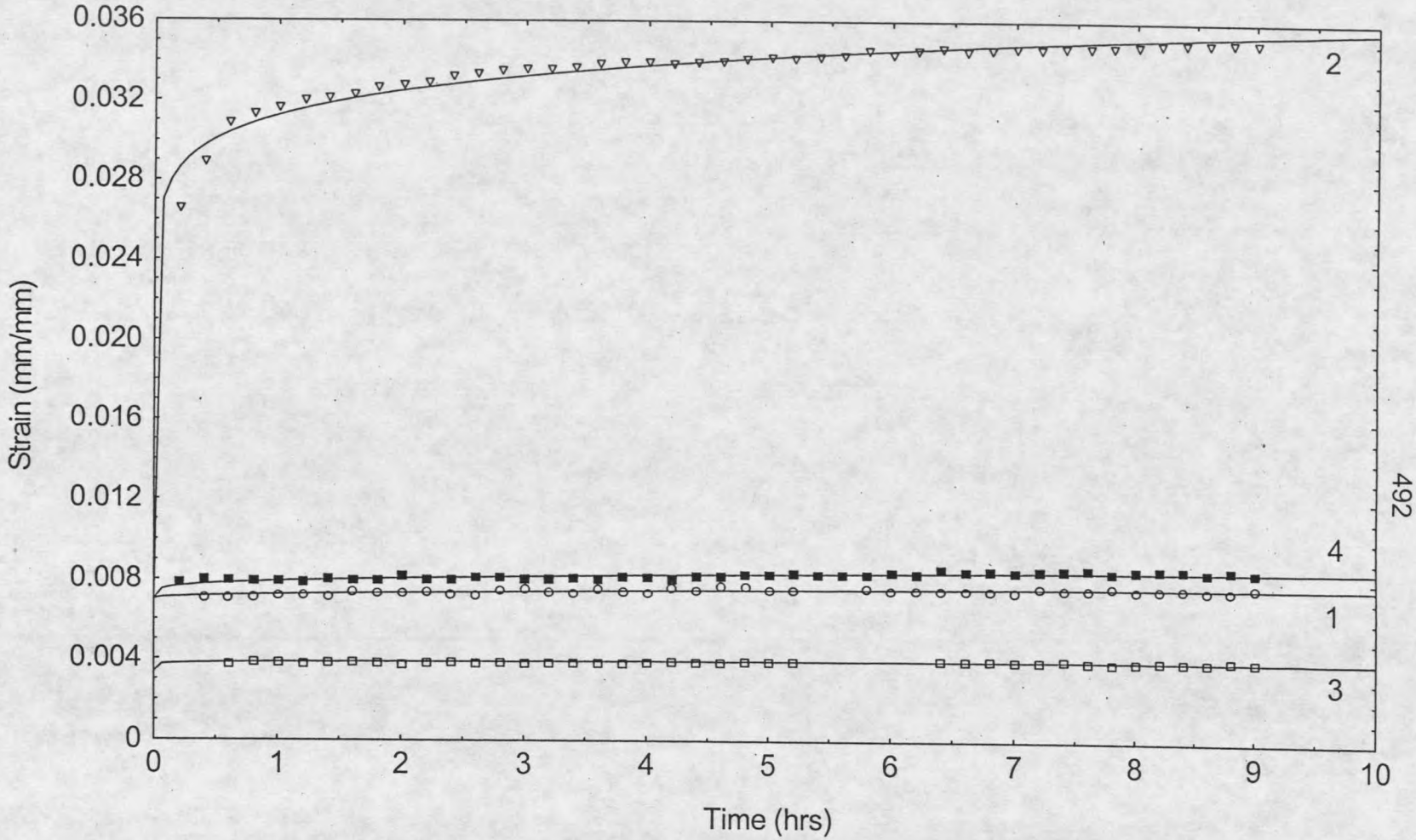


Figure L.15 Vibrocreep Response of PVDF at Different Temperatures
1- $(0.45\pm0.40)\sigma_y$, 10 Hz at -25 °C; 2- $(0.45\pm0.40)\sigma_y$, 10 Hz at 23 °C;
3- $(0.45)\sigma_y$ at -25 °C, 4- $(0.45)\sigma_y$ at 23 °C, Constant Load Creep;
σ_y = 30.428 MPa at 23 °C

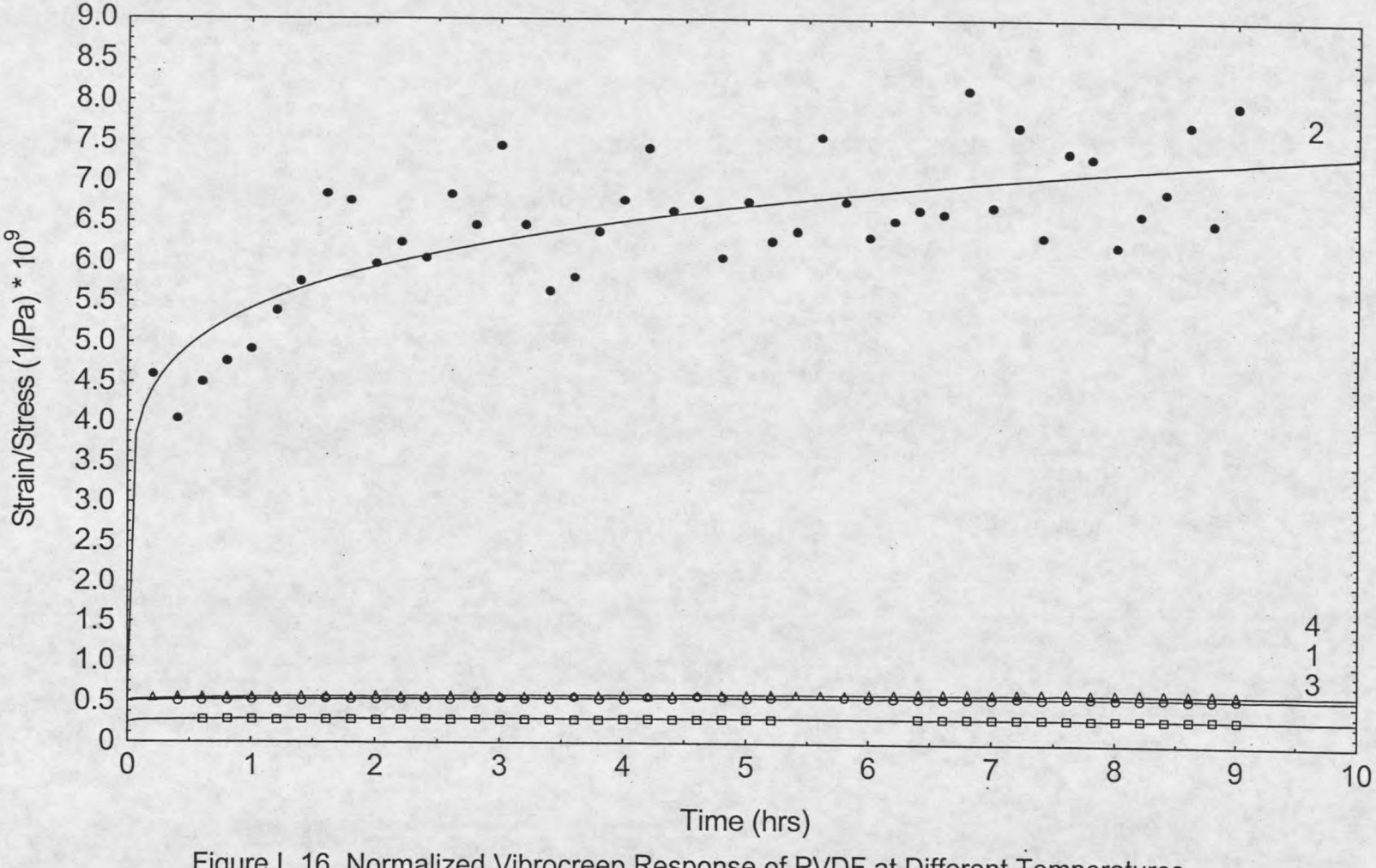


Figure L.16 Normalized Vibrocreep Response of PVDF at Different Temperatures
1- $(0.45\pm0.40)\sigma_y$, 10 Hz at -25 °C; 2- $(0.45\pm0.40)\sigma_y$, 10 Hz at 23 °C;
3- $(0.45)\sigma_y$ at -25 °C, 4- $(0.45)\sigma_y$ at 23 °C, Constant Load Creep;
σ_y = 30.428 MPa at 23 °C

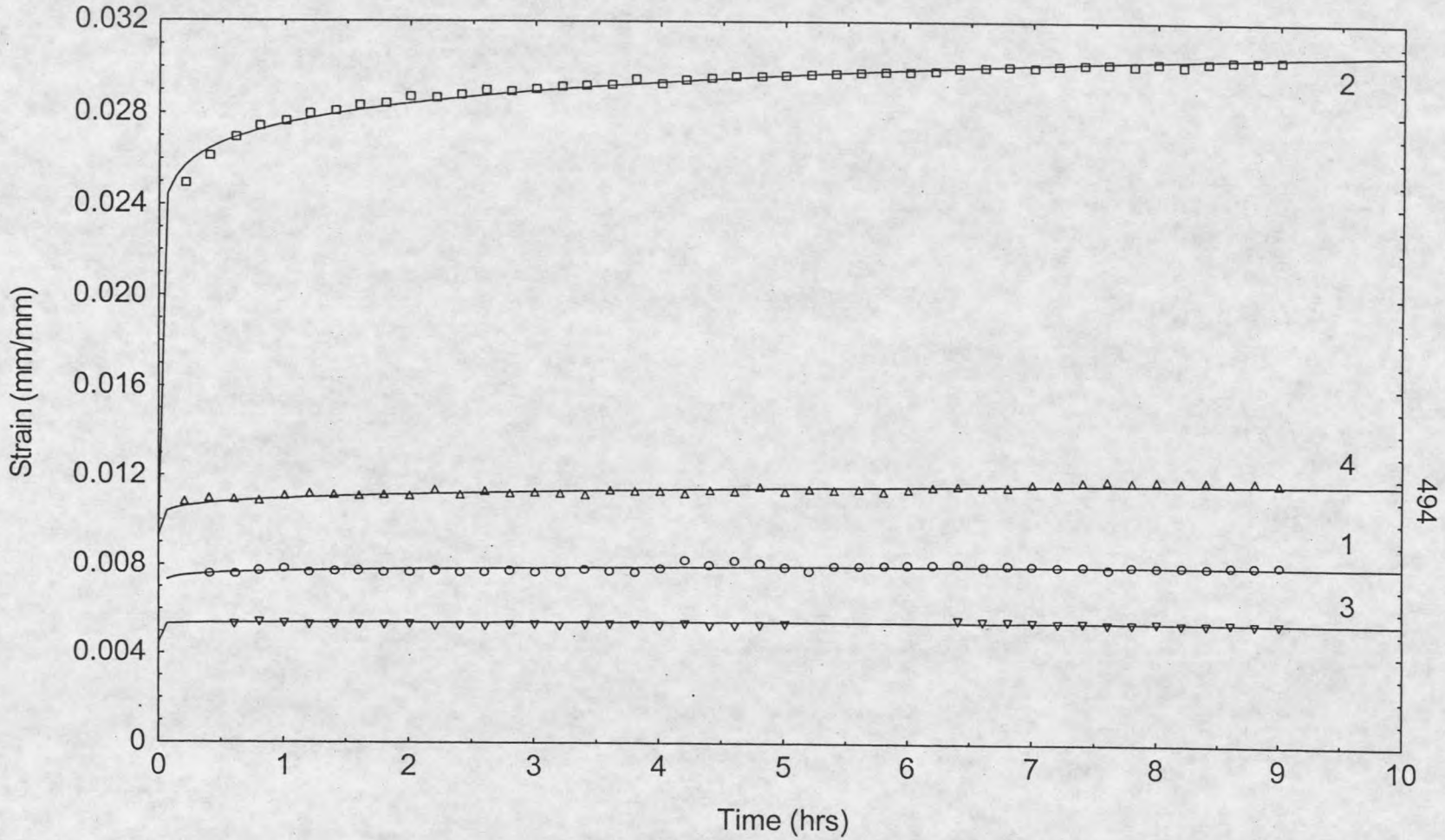


Figure L.17 Vibrocreep Response of PVDF at Different Temperatures
1- $(0.60\pm0.20)\sigma_y$, 5 Hz at -25 °C; 2- $(0.60\pm0.20)\sigma_y$, 5 Hz at 23 °C;
3- $(0.60)\sigma_y$ at -25 °C, 4- $(0.60)\sigma_y$ at 23 °C, Constant Load Creep;
σ_y = 30.428 MPa at 23 °C

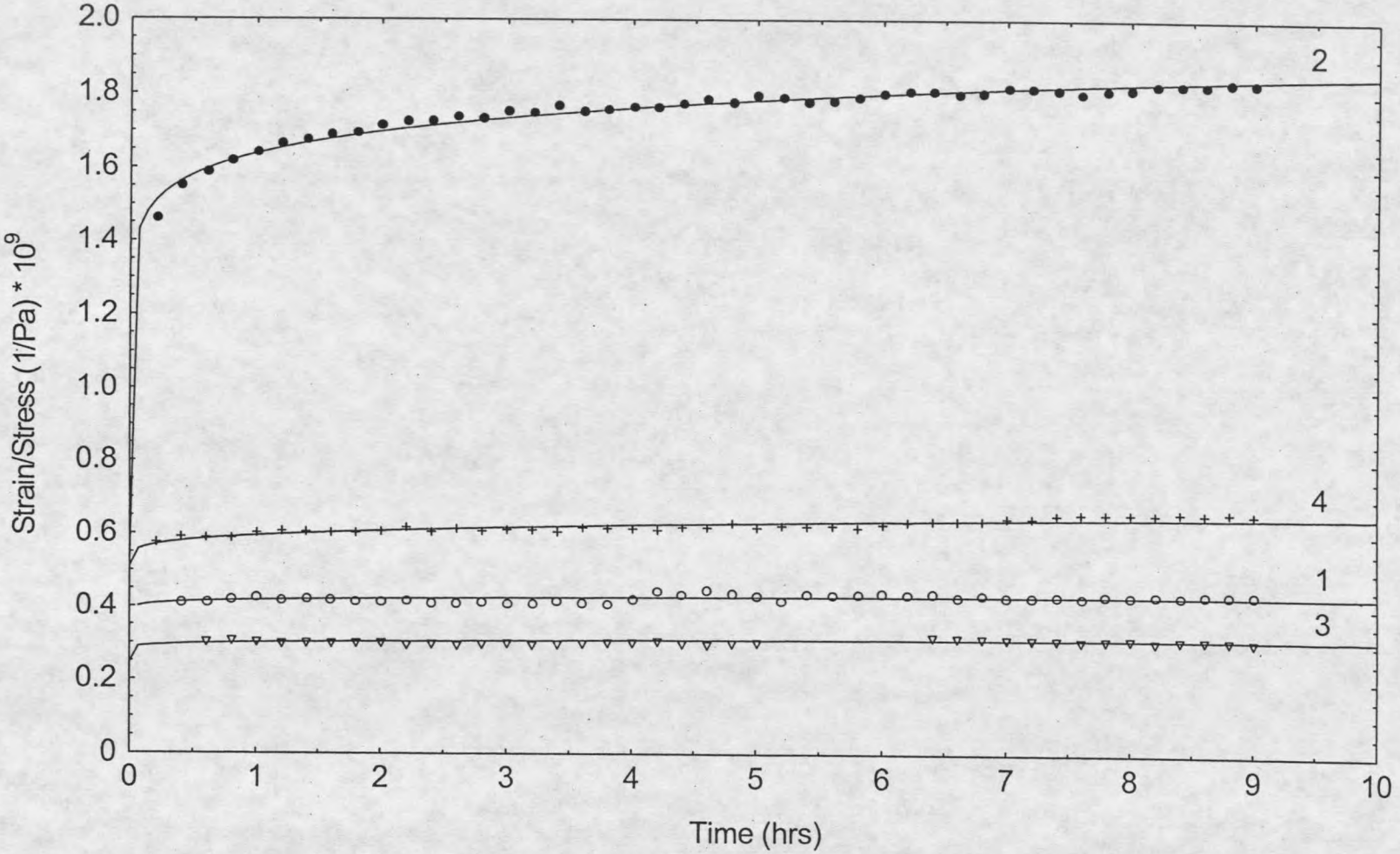


Figure L.18 Normalized Vibrocreep Response of PVDF at Different Temperatures
1- $(0.60\pm0.20)\sigma_y$, 5 Hz at -25 °C; 2- $(0.60\pm0.20)\sigma_y$, 5 Hz at 23 °C;
3- $(0.60)\sigma_y$ at -25 °C, 4- $(0.60)\sigma_y$ at 23 °C, Constant Load Creep;
σ_y = 30.428 MPa at 23 °C

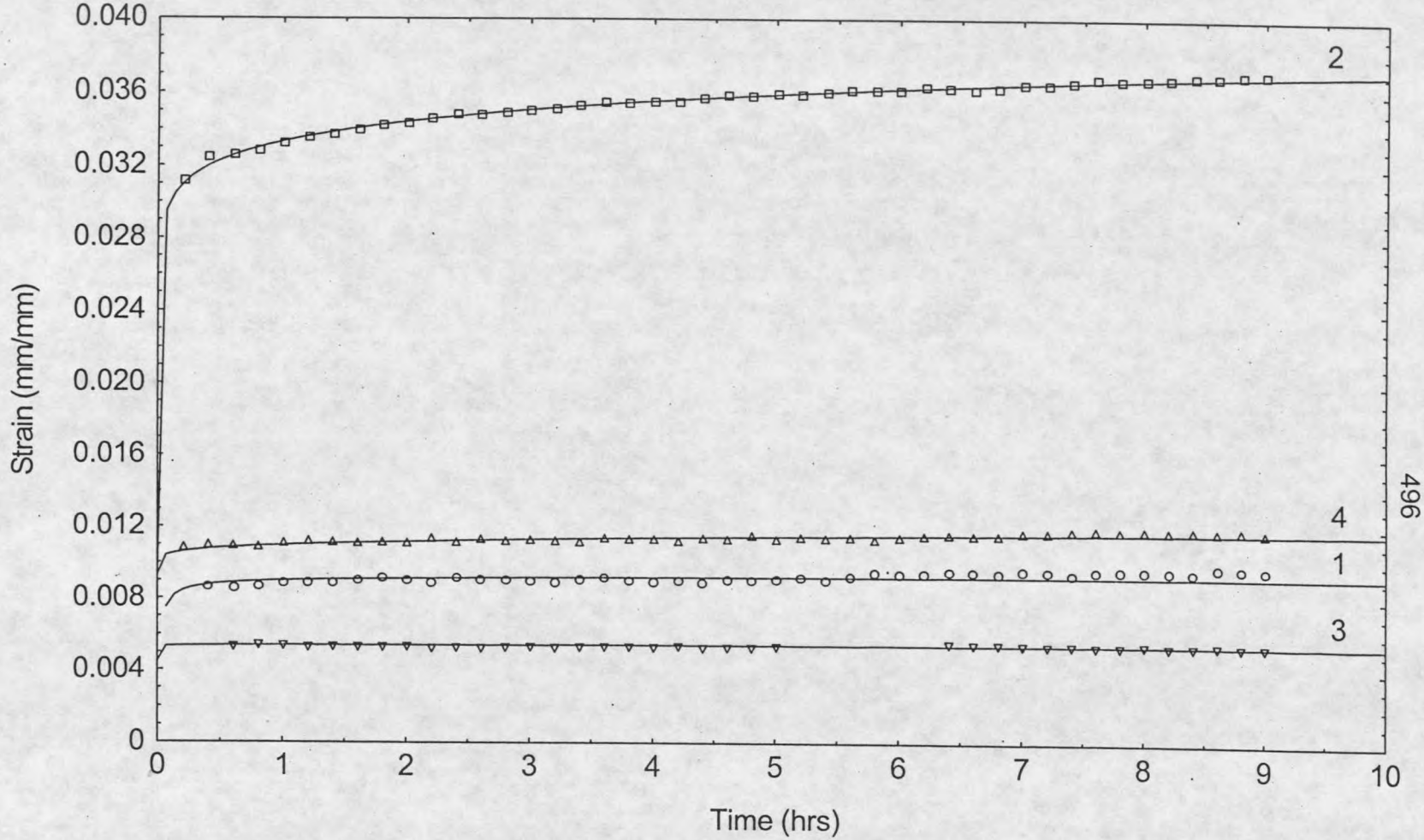


Figure L.19 Vibrocreep Response of PVDF at Different Temperatures
1- $(0.60\pm0.45)\sigma_y$, 5 Hz at -25 °C; 2- $(0.60\pm0.45)\sigma_y$, 5 Hz at 23 °C;
3- $(0.60)\sigma_y$ at -25 °C, 4- $(0.60)\sigma_y$ at 23 °C, Constant Load Creep;
σ_y = 30.428 MPa at 23 °C

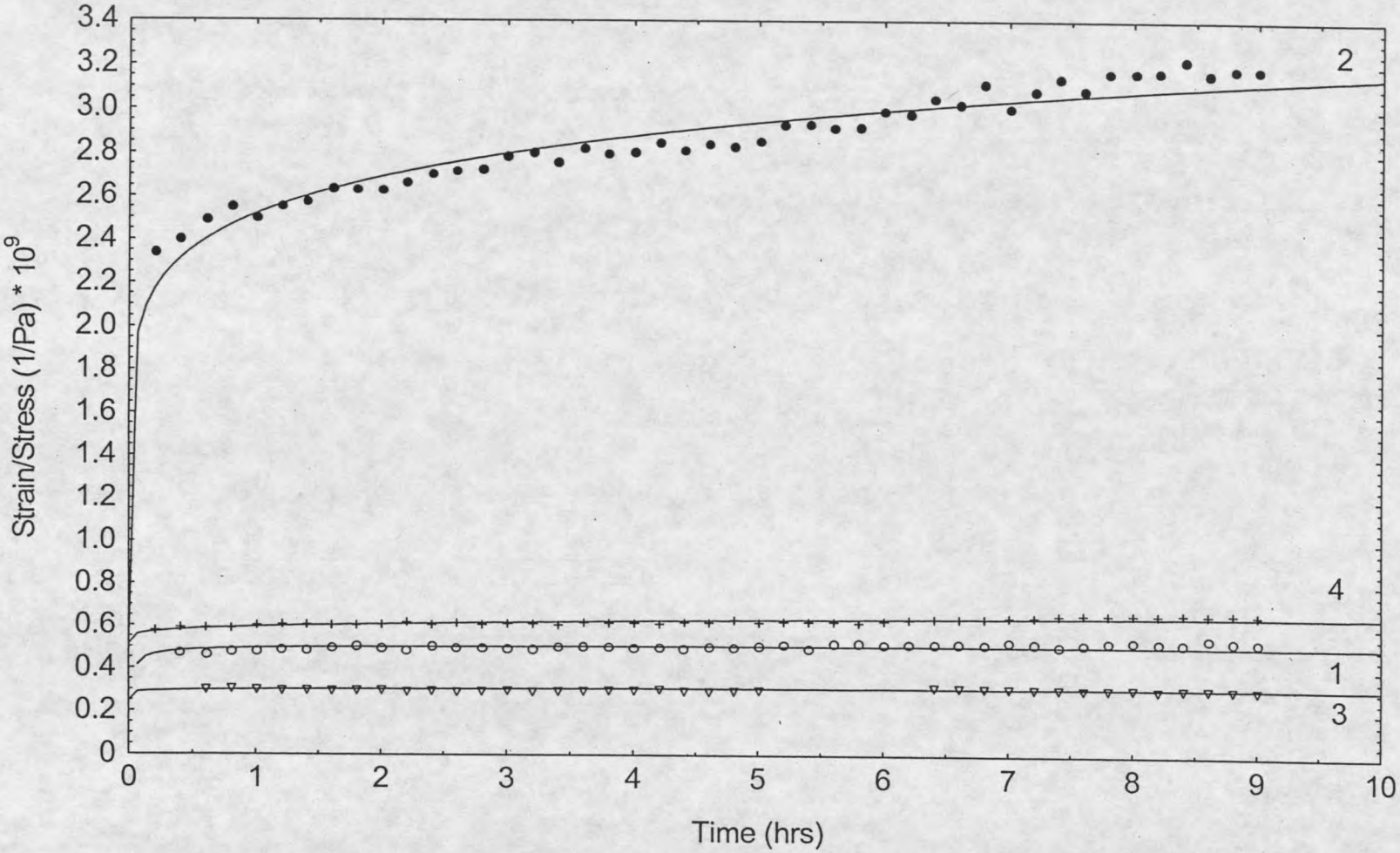


Figure L.20 Normalized Vibrocreep Response of PVDF at Different Temperatures
1- $(0.60\pm0.45)\sigma_y$, 5 Hz at -25 °C; 2- $(0.60\pm0.45)\sigma_y$, 5 Hz at 23 °C;
3- $(0.60)\sigma_y$ at -25 °C, 4- $(0.60)\sigma_y$ at 23 °C, Constant Load Creep;
σ_y = 30.428 MPa at 23 °C

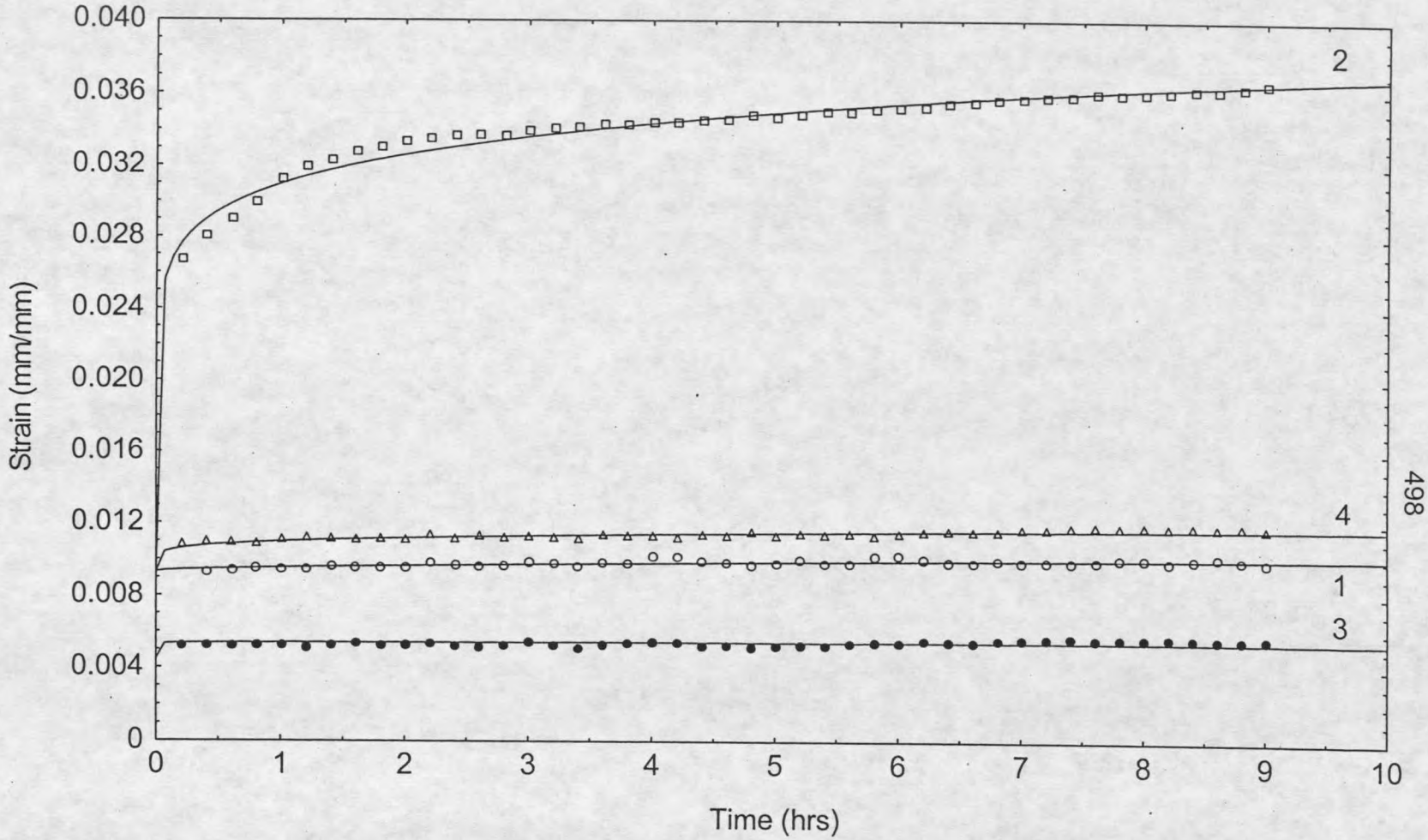


Figure L.21 Vibrocreep Response of PVDF at Different Temperatures
1- $(0.60\pm0.20)\sigma_y$, 10 Hz at -25 °C; 2- $(0.60\pm0.20)\sigma_y$, 10 Hz at 23 °C;
3- $(0.60)\sigma_y$ at -25 °C, 4- $(0.60)\sigma_y$ at 23 °C, Constant Load Creep;
σ_y = 30.428 MPa at 23 °C

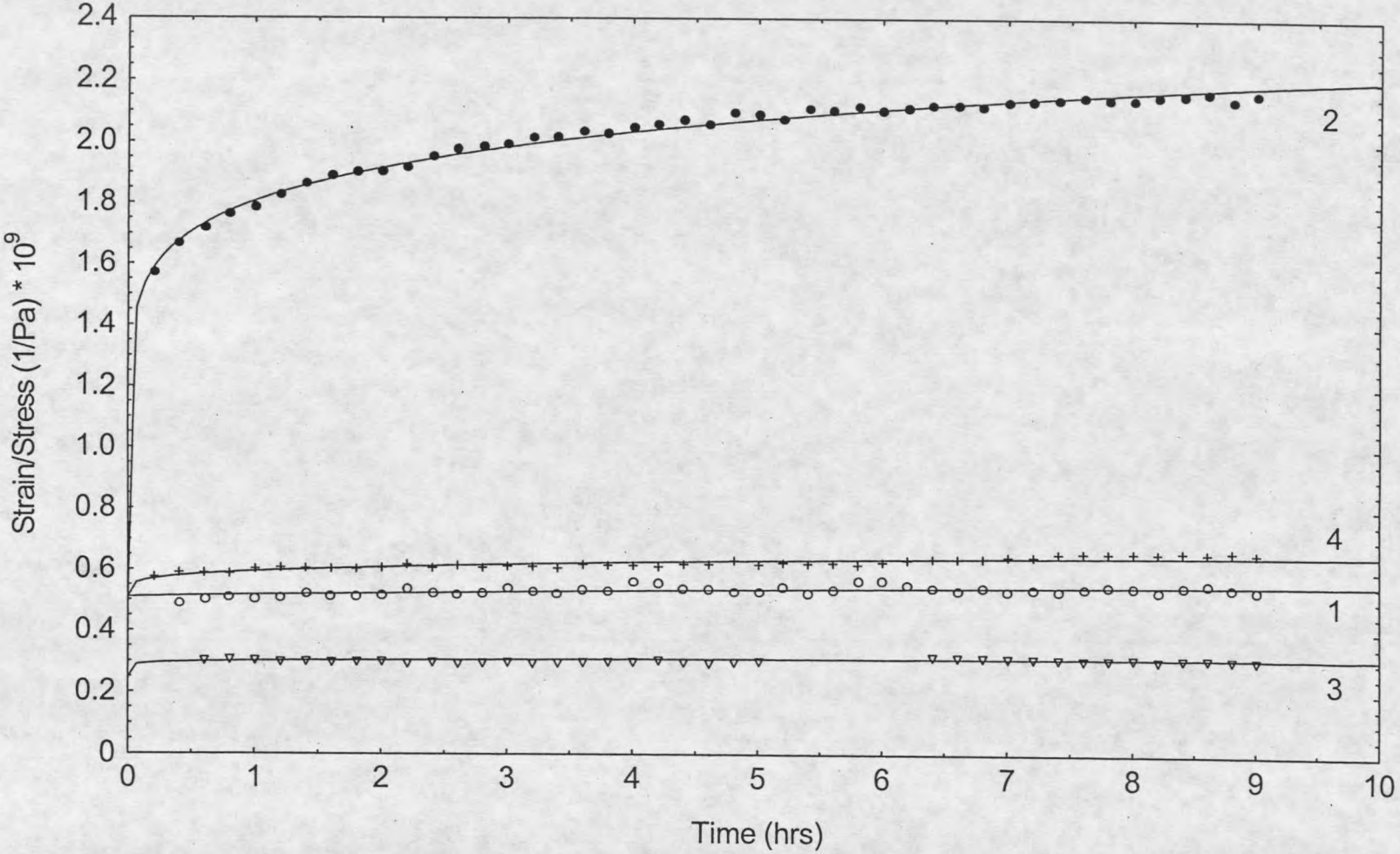


Figure L.22 Normalized Vibrocreep Response of PVDF at Different Temperatures
1- $(0.60\pm0.20)\sigma_y$, 10 Hz at -25 °C; 2- $(0.60\pm0.20)\sigma_y$, 10 Hz at 23 °C;
3- $(0.60)\sigma_y$ at -25 °C, 4- $(0.60)\sigma_y$ at 23 °C, Constant Load Creep;
σ_y = 30.428 MPa at 23 °C

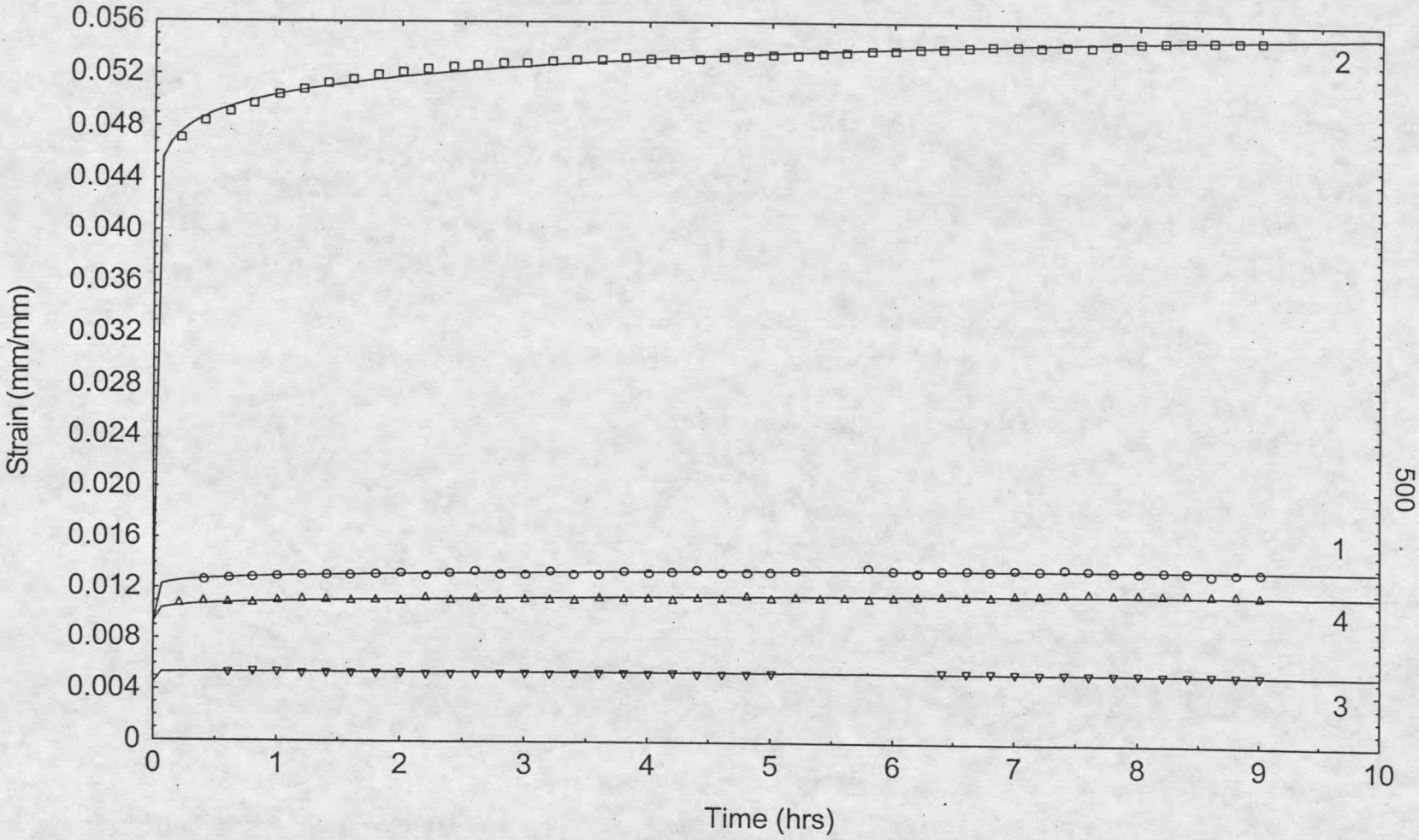


Figure L.23 Vibrocreep Response of PVDF at Different Temperatures
1- $(0.60\pm0.50)\sigma_y$, 10 Hz at -25 °C; 2- $(0.60\pm0.50)\sigma_y$, 10 Hz at 23 °C;
3- $(0.60)\sigma_y$ at -25 °C, 4- $(0.60)\sigma_y$ at 23 °C, Constant Load Creep;
σ_y = 30.428 MPa at 23 °C

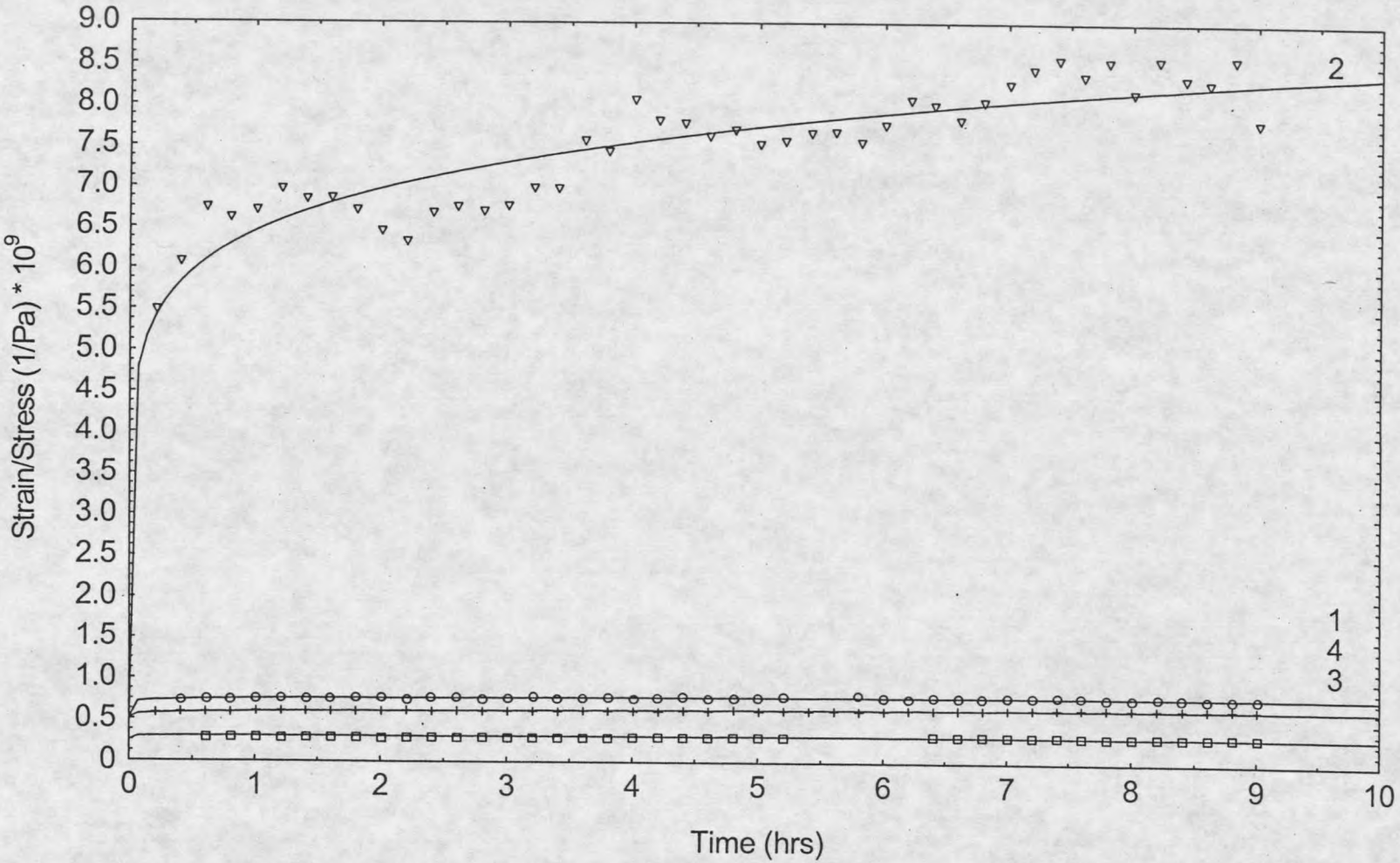


Figure L.24 Normalized Vibrocreep Response of PVDF at Different Temperatures
1- $(0.60\pm0.50)\sigma_y$, 10 Hz at -25 °C; 2- $(0.60\pm0.50)\sigma_y$, 10 Hz at 23 °C;
3- $(0.60)\sigma_y$ at -25 °C, 4- $(0.60)\sigma_y$ at 23 °C, Constant Load Creep;
σ_y = 30.428 MPa at 23 °C

APPENDIX M

Statistical Results

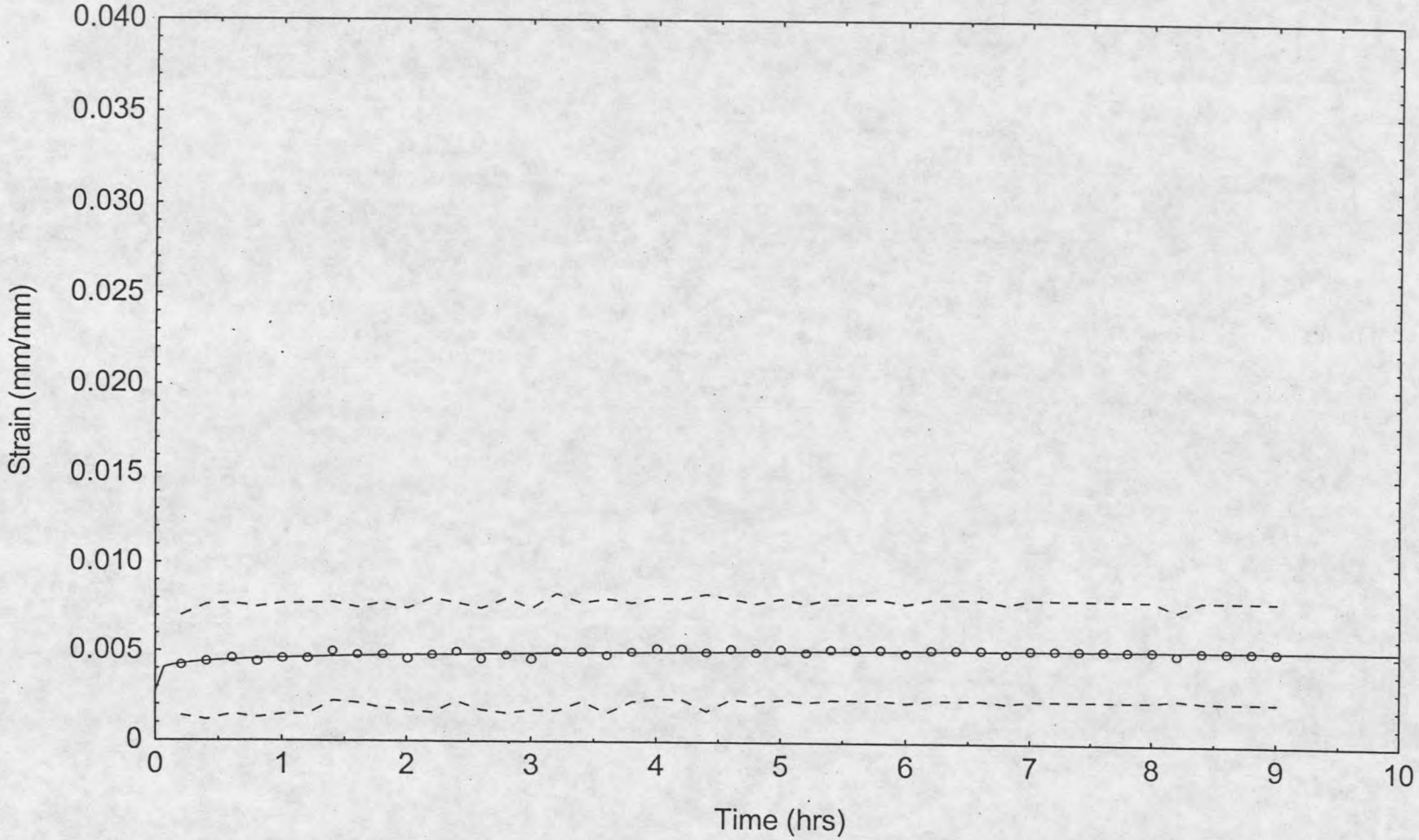


Figure M.I.1 Statistical Analysis of Nylon 6/6 Quasi Static Creep with 95% Confidence
$(0.10)\sigma_y$ at 23 °C;
σ_y = 70 MPa at 23 °C

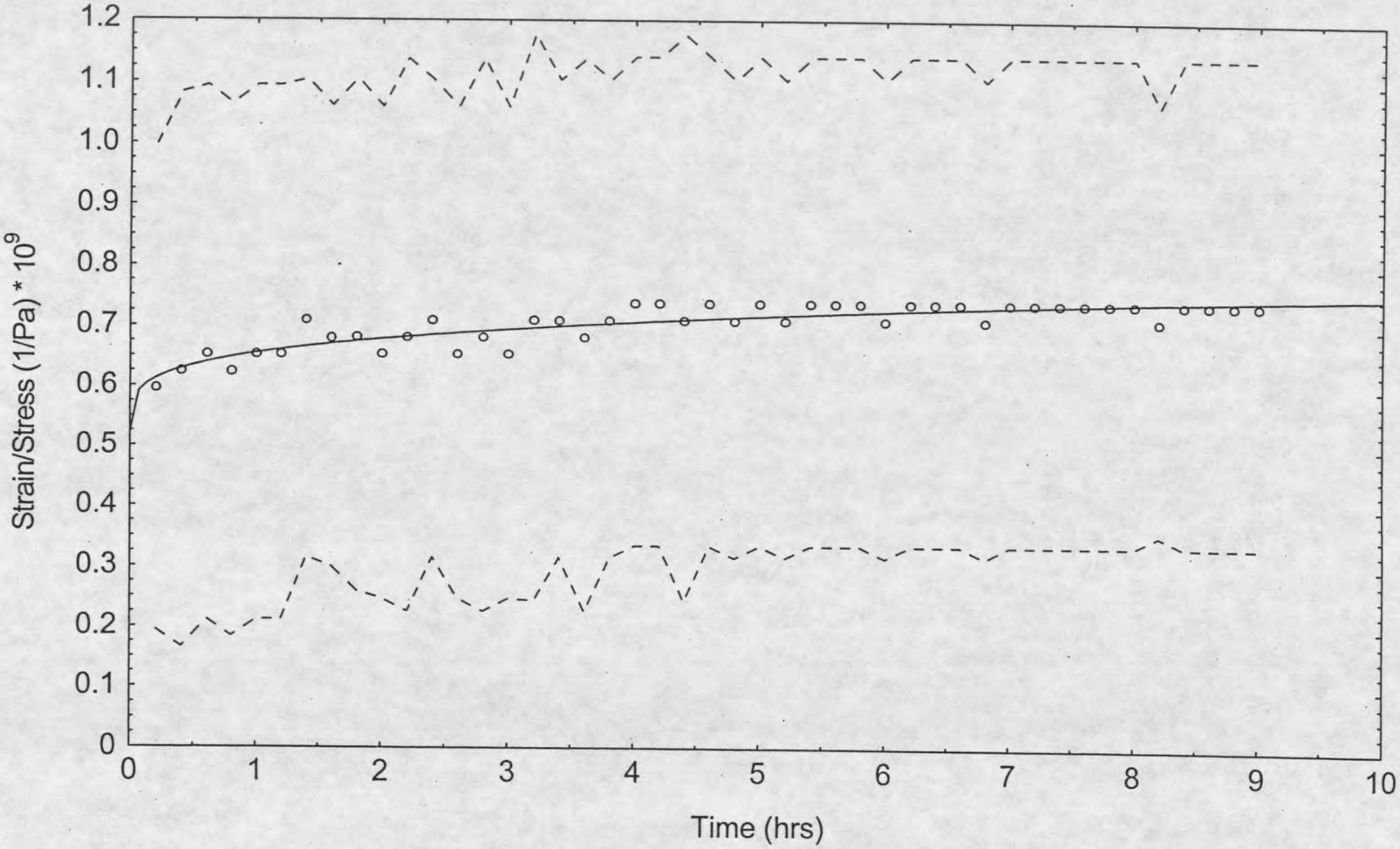


Figure M.I.2 Normalized Statistical Analysis of Nylon 6/6 Quasi Static Creep with 95% Confidence
$(0.10)\sigma_y$ at 23 °C;
σ_y = 70 MPa at 23 °C

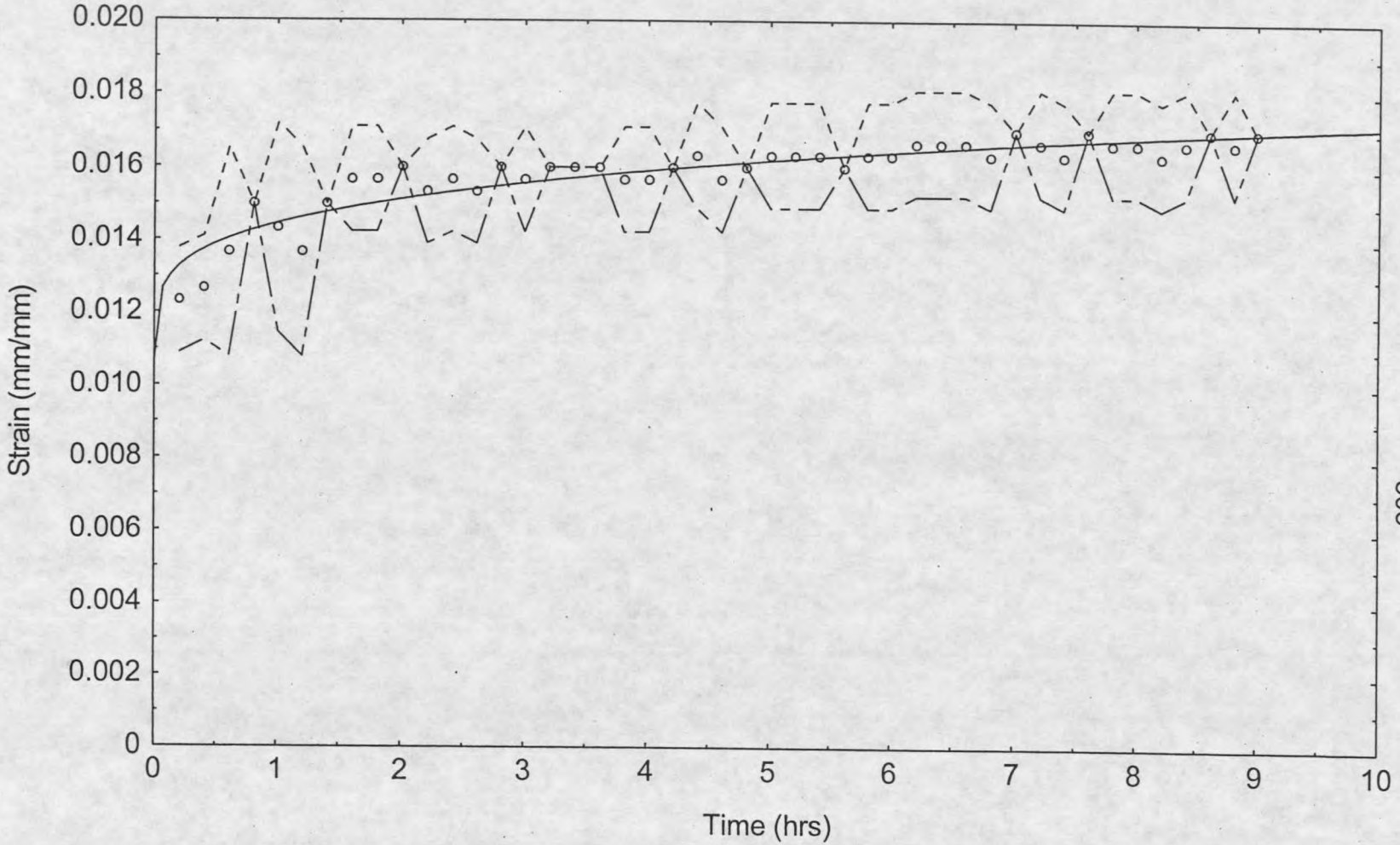


Figure M.I.3 Statistical Analysis of Nylon 6/6 Vibrocreep Response with 95% Confidence
$(0.20\pm0.10)\sigma_y$, 10 Hz at 23 °C;
σ_y = 70 MPa at 23 °C

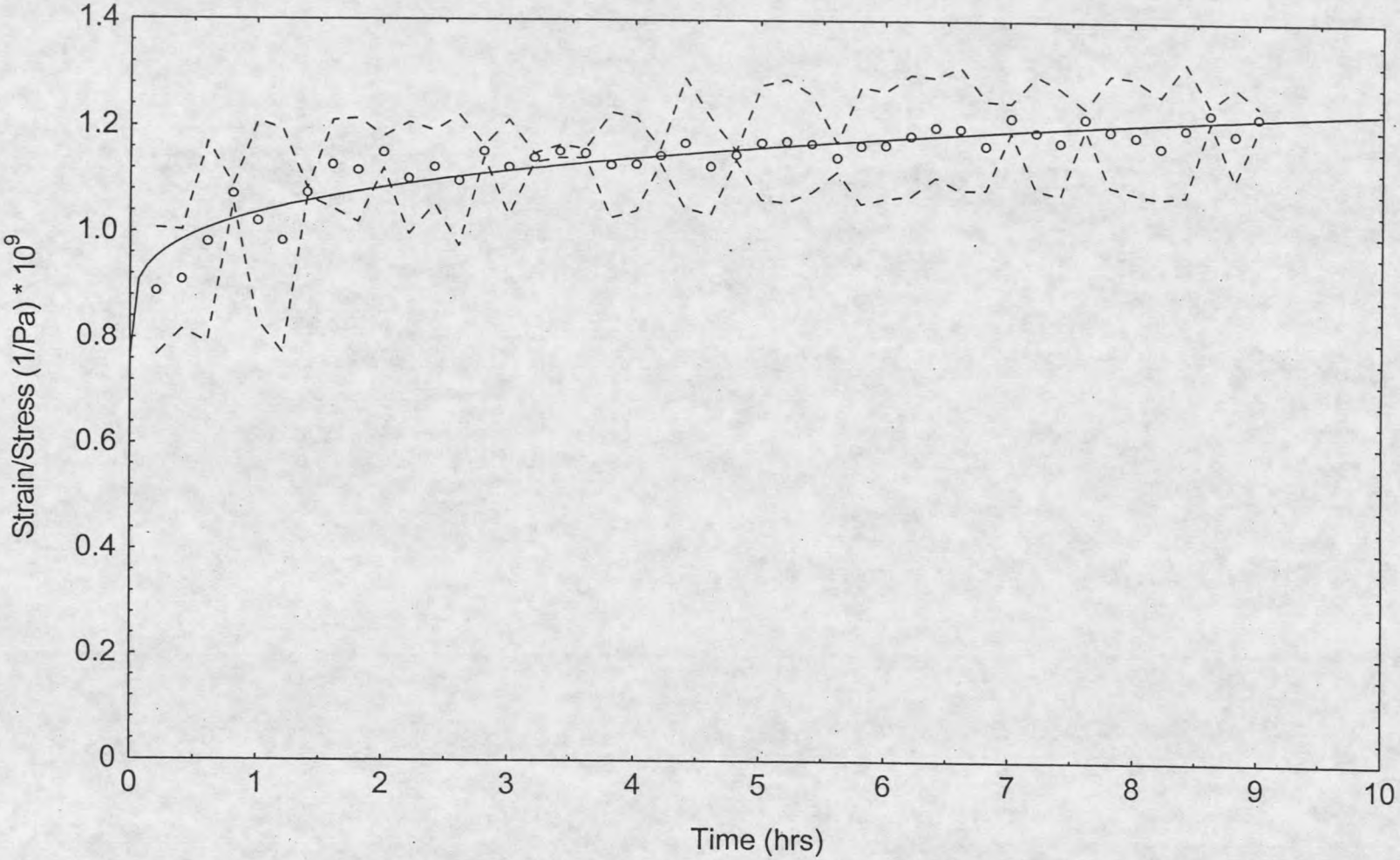


Figure M.I.4 Normalized Statistical Analysis of Nylon 6/6 Vibrocreep Response with 95% Confidence
$(0.20\pm0.10)\sigma_y$, 10 Hz at 23 °C;
σ_y = 70 MPa at 23 °C

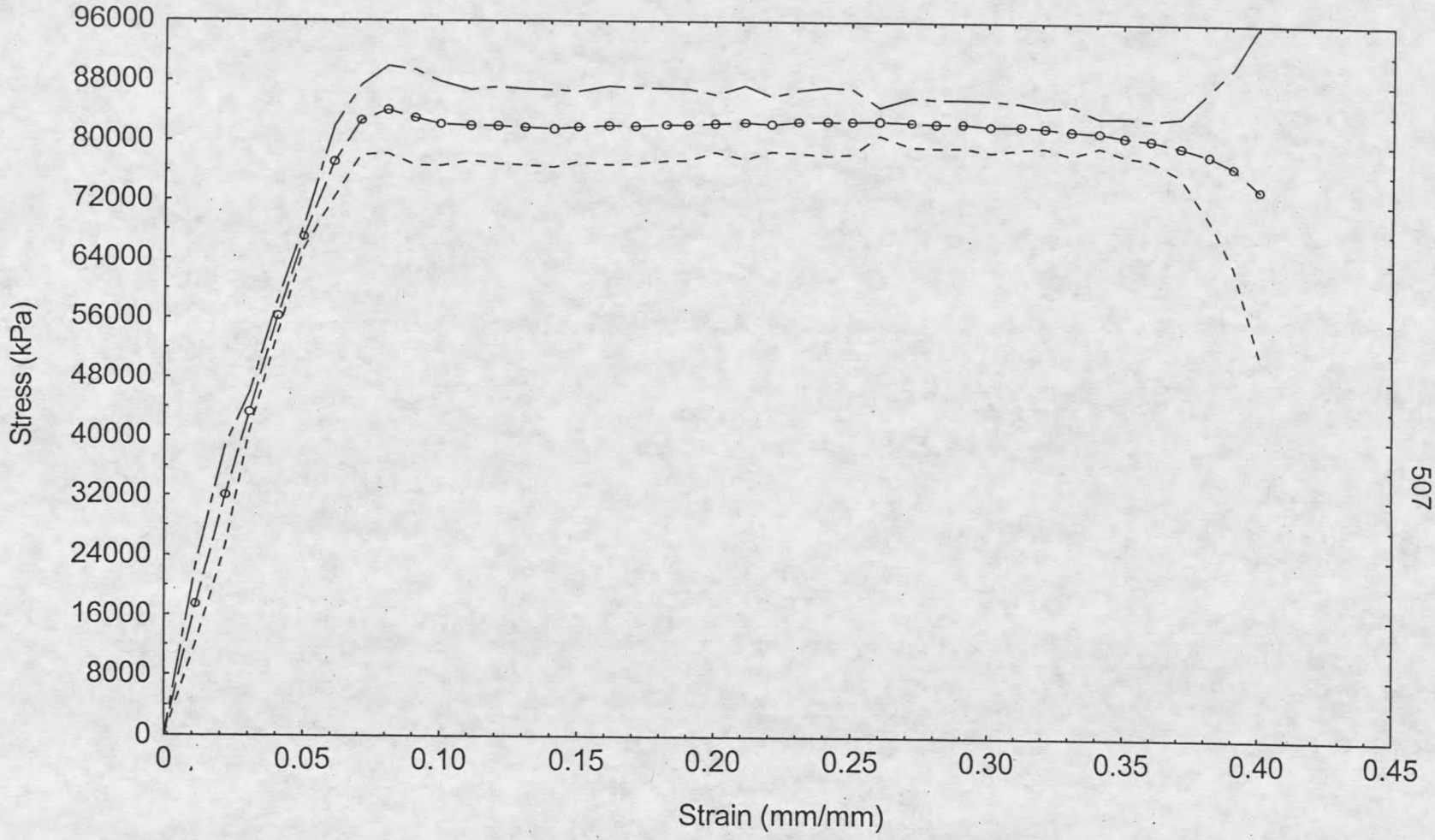


Figure M.I.5 Statistical Analysis of Nylon 6/6 Vibrocreep Response Post Tensile Testing with 95% Confidence
$(0.20\pm0.10)\sigma_y$, 10 Hz at 23 °C;
σ_y = 70 MPa at 23 °C

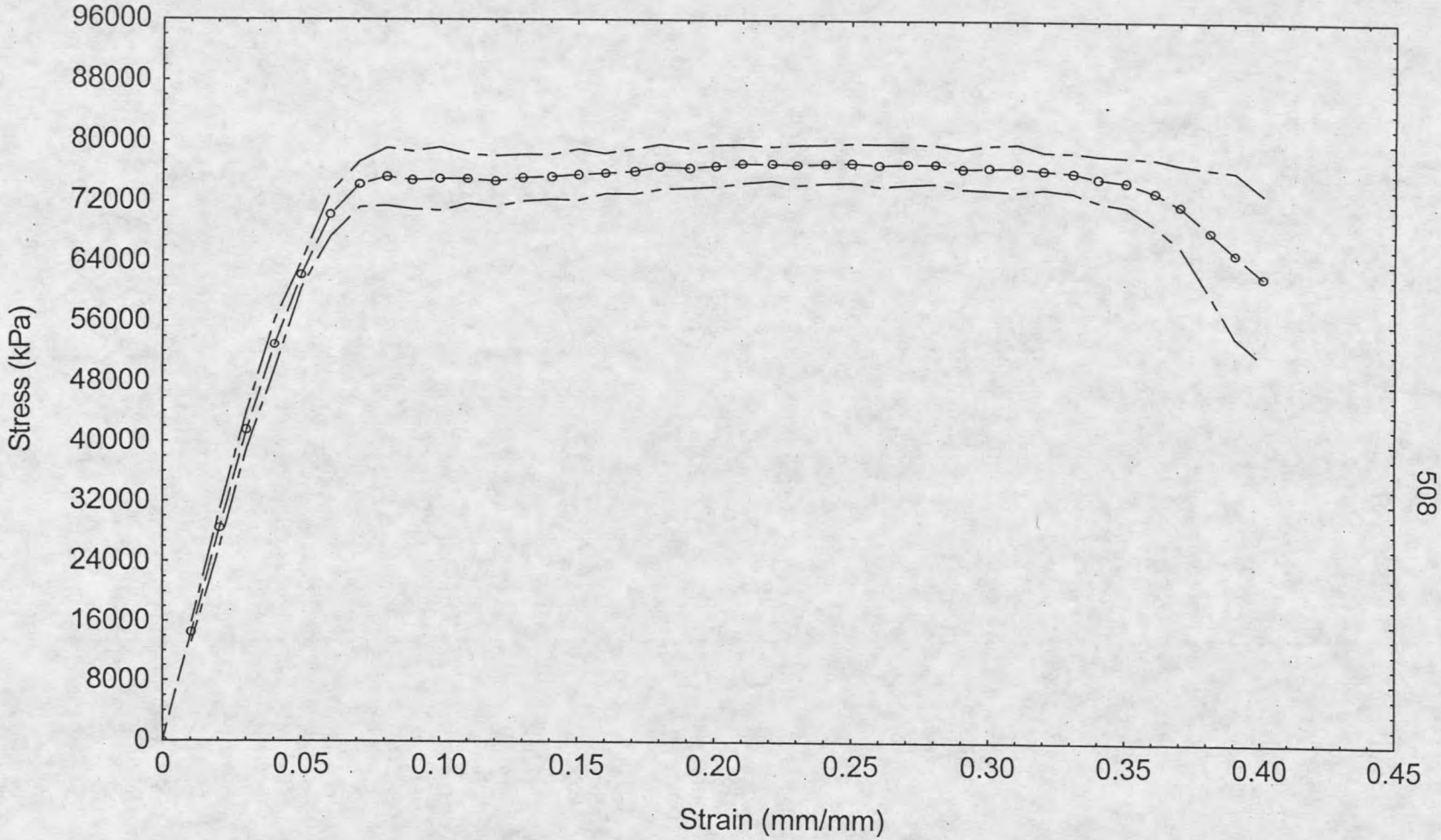


Figure M.I.6 Statistical Analysis of Nylon 6/6 Tensile Testing with 95% Confidence at 23 °C

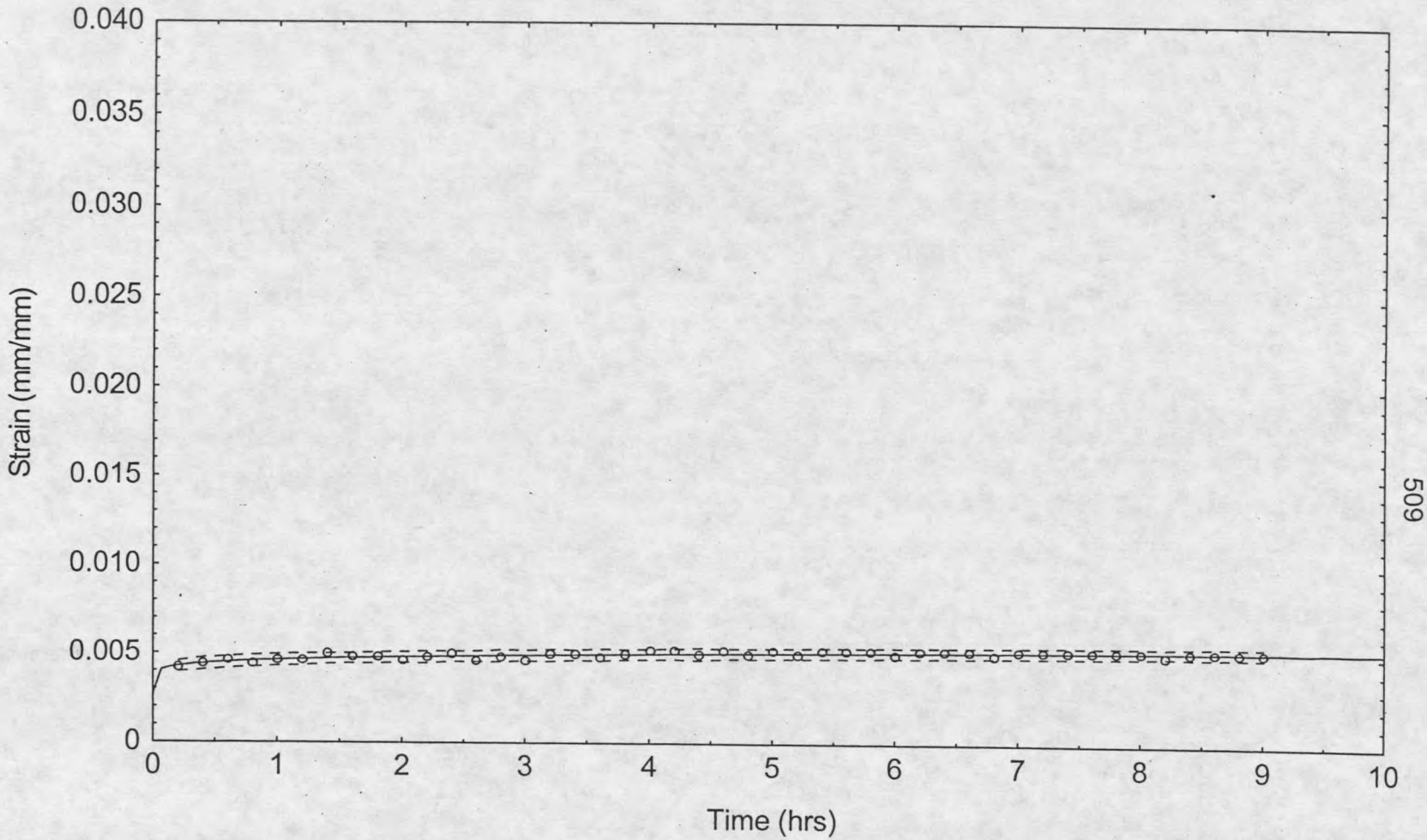


Figure M.I.7 Statistical Curve Fit Analysis of Nylon 6/6 Quasi Static Creep with 95% Confidence
$(0.10)\sigma_y$ at 23 °C;
σ_y = 70 MPa at 23 °C

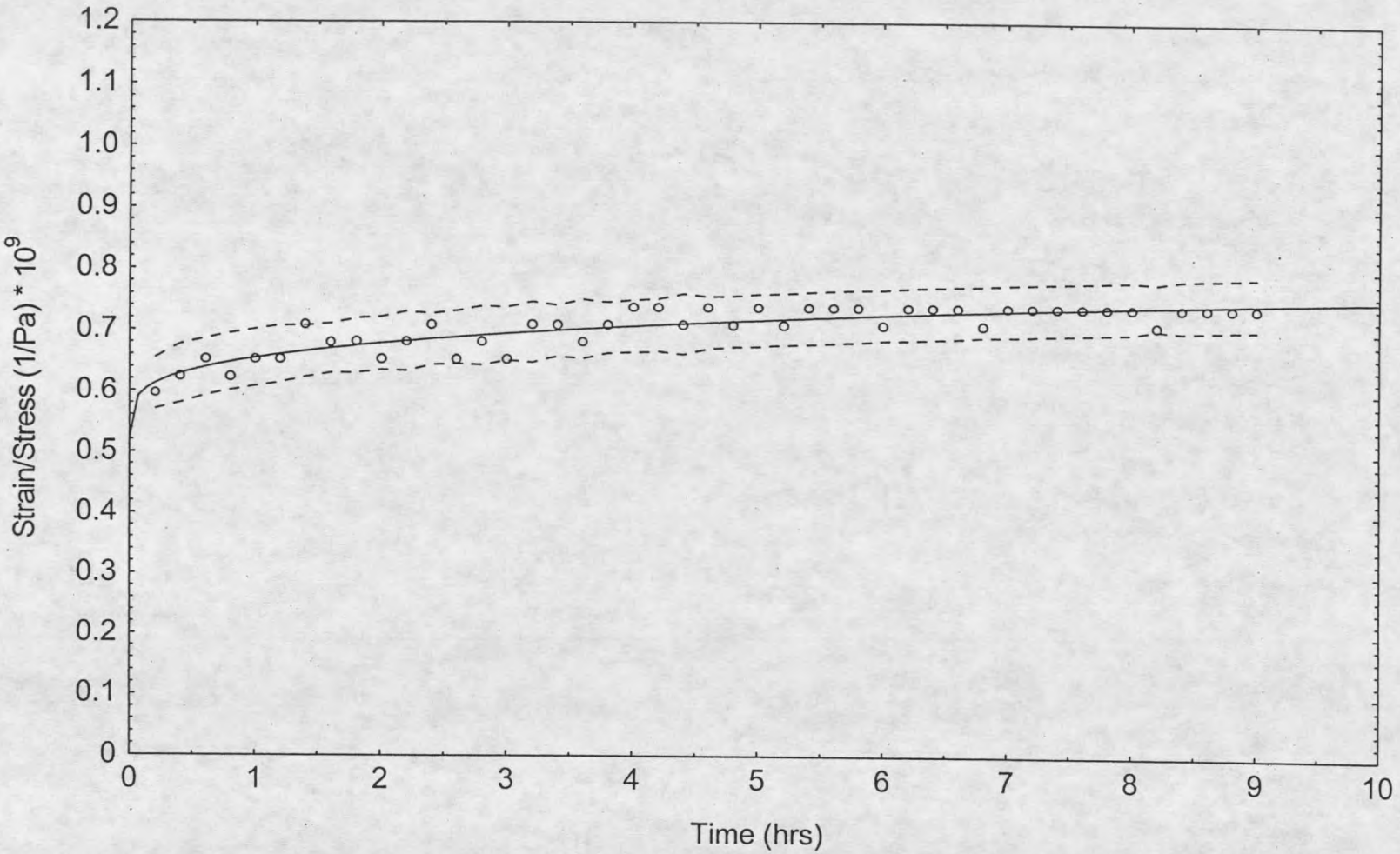


Figure M.I.8 Normalized Statistical Curve Fit Analysis of Nylon 6/6 Quasi Static Creep with 95% Confidence
$(0.10)\sigma_y$ at 23 °C;
σ_y = 70 MPa at 23 °C

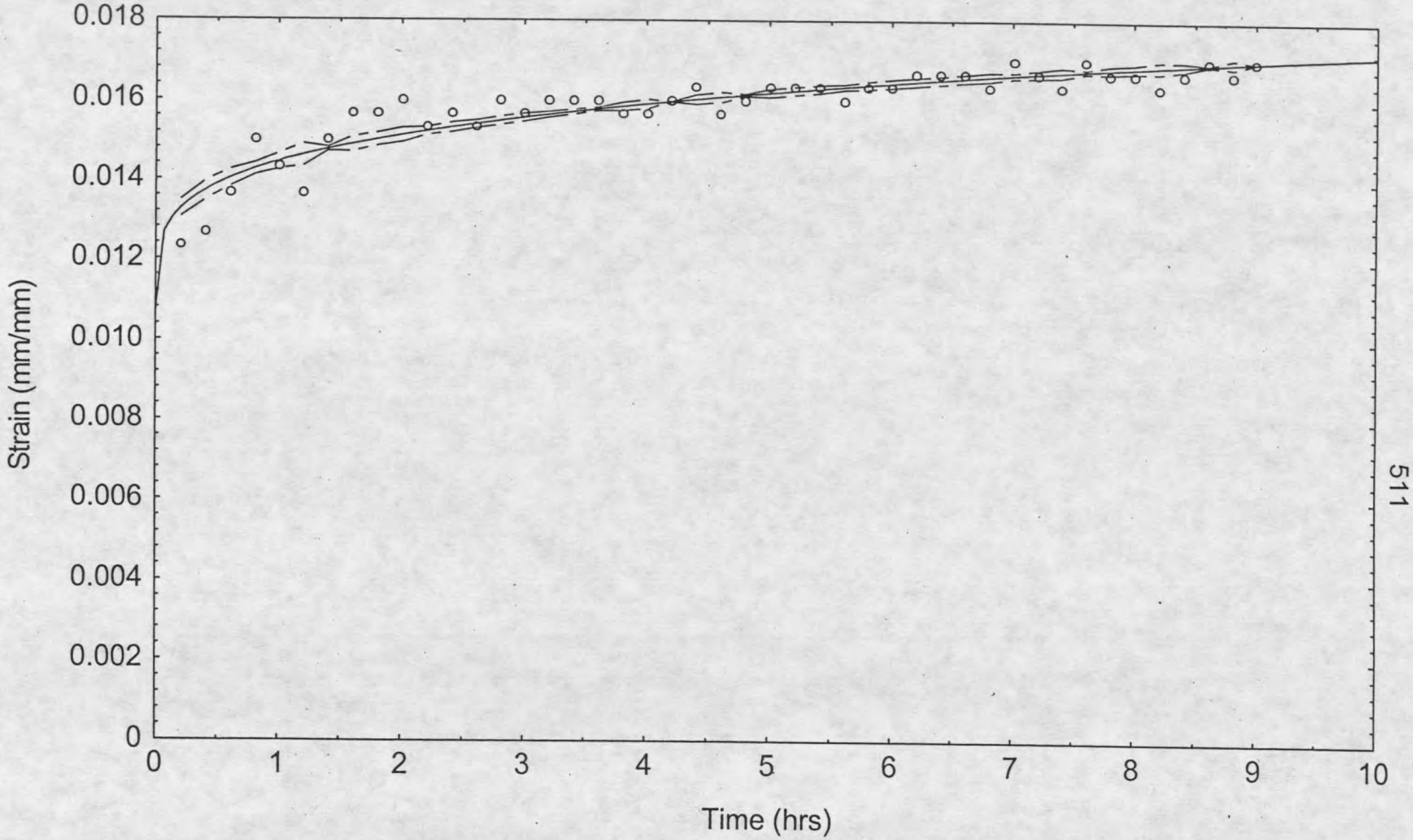


Figure M.I.9 Statistical Curve Fit Analysis of Nylon 6/6 Vibrocreep Response with 95% Confidence
$(0.20 \pm 0.10)\sigma_y$, 10 Hz at 23 °C;
σ_y = 70 MPa at 23 °C

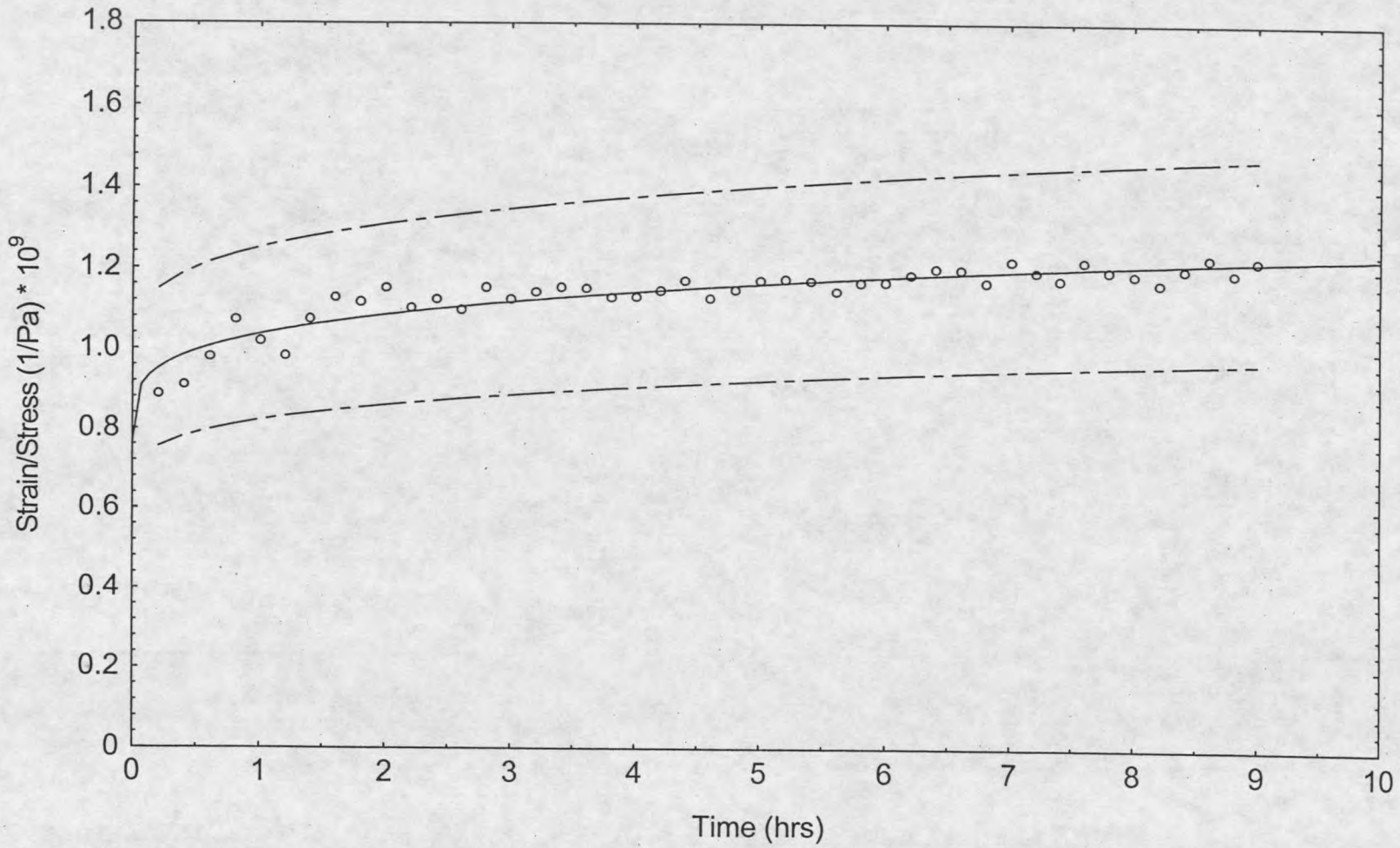


Figure M.I.10 Normalized Statistical Curve Fit Analysis of Nylon 6/6 Vibrocreep Response with 95% Confidence
$(0.20\pm0.10)\sigma_y$, 10 Hz at 23 °C;
σ_y = 70 MPa at 23 °C

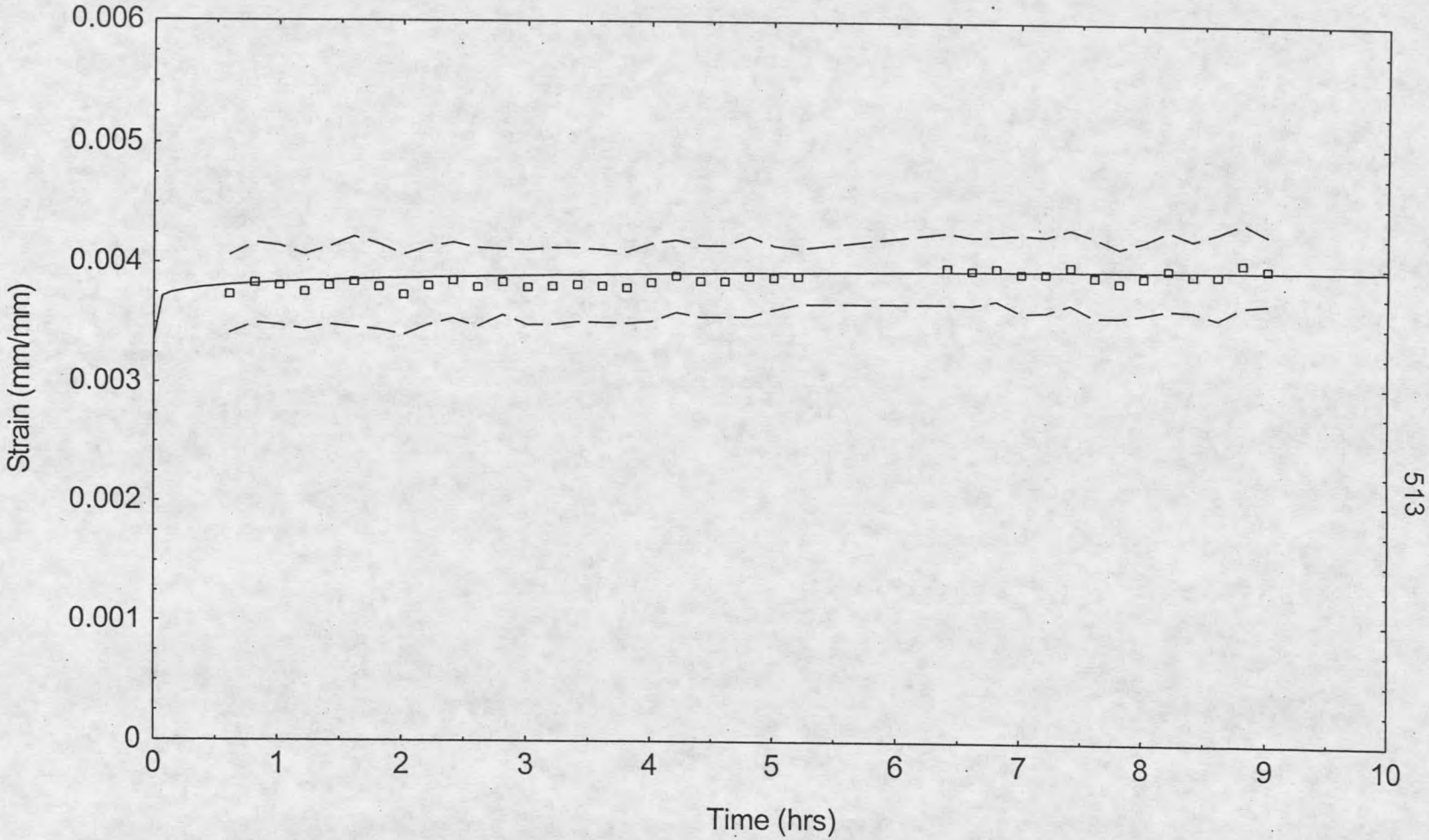


Figure M.II.1 Statistical Analysis of PVDF Quasi Static Creep with 95% Confidence
$(0.45)\sigma_y$ at -25 °C;
σ_y = 30.428 MPa at 23 °C

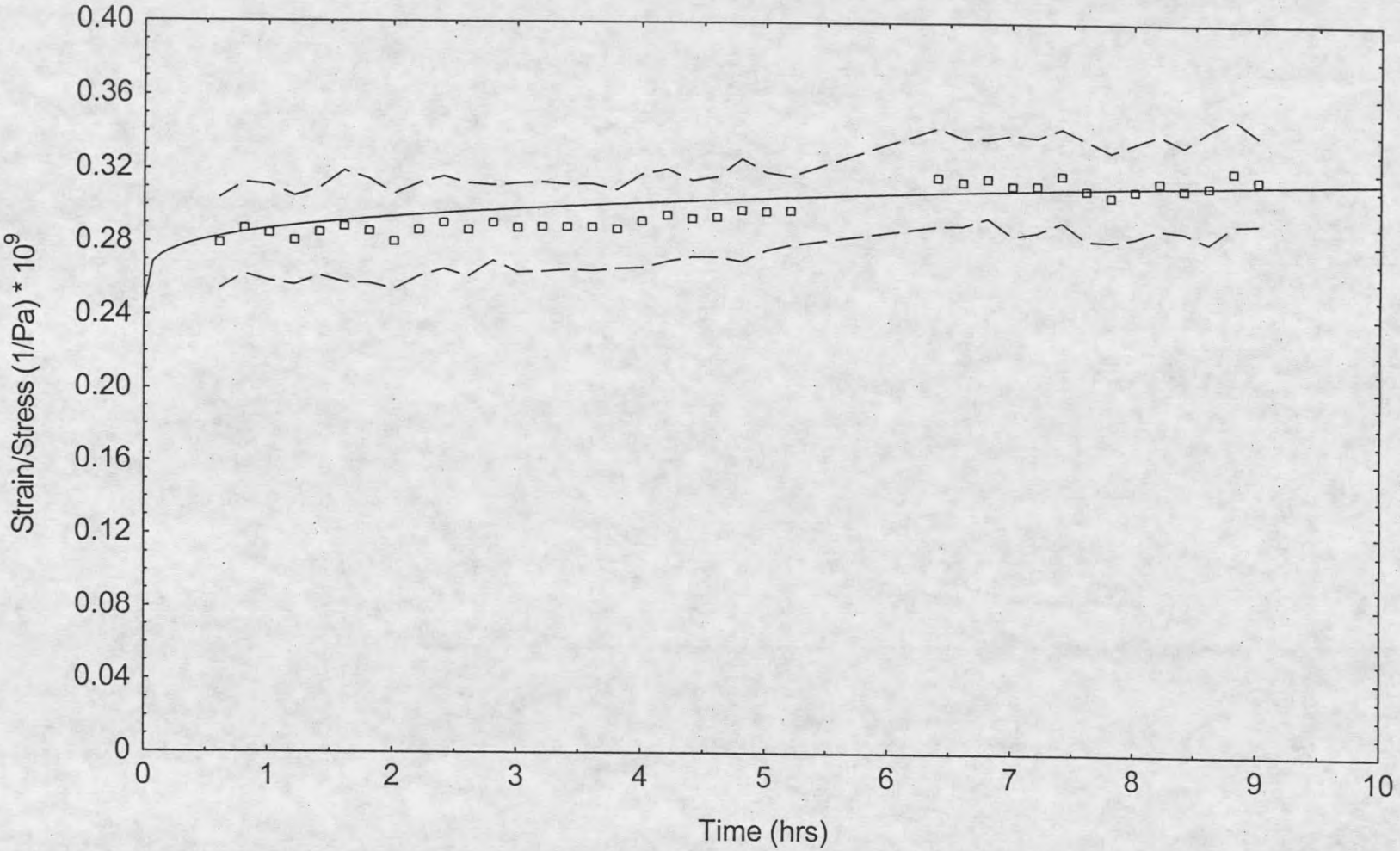


Figure M.II.2 Normalized Statistical Analysis of PVDF Quasi Static Creep with 95% Confidence
$(0.45)\sigma_y$ at -25 °C;
σ_y = 30.428 MPa at 23 °C

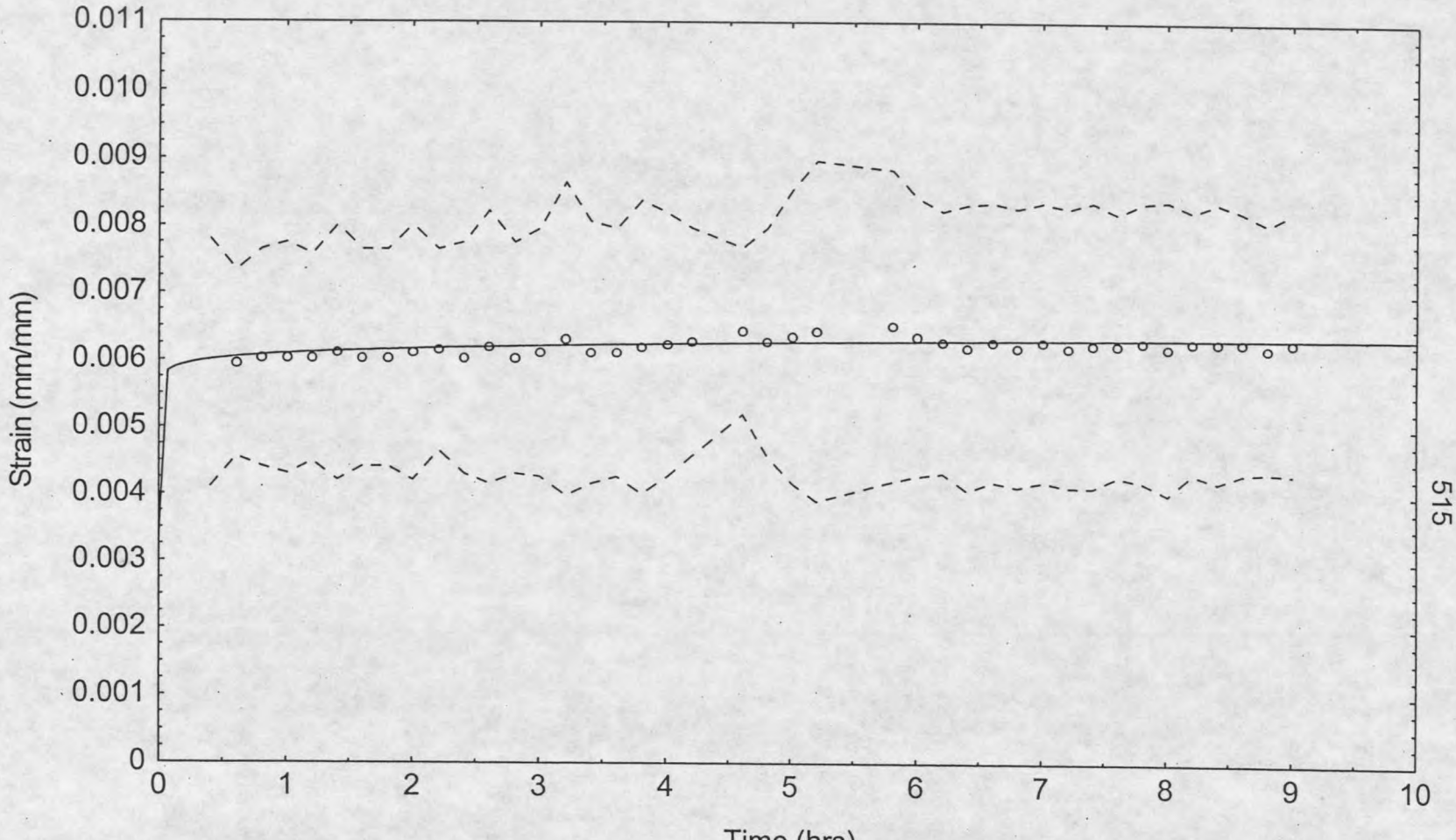


Figure M.II.3 Statistical Analysis of PVDF Vibrocreep Response with 95% Confidence
$(0.45\pm0.20)\sigma_y$, 10 Hz at -25 °C;
σ_y = 30.428 MPa at 23 °C

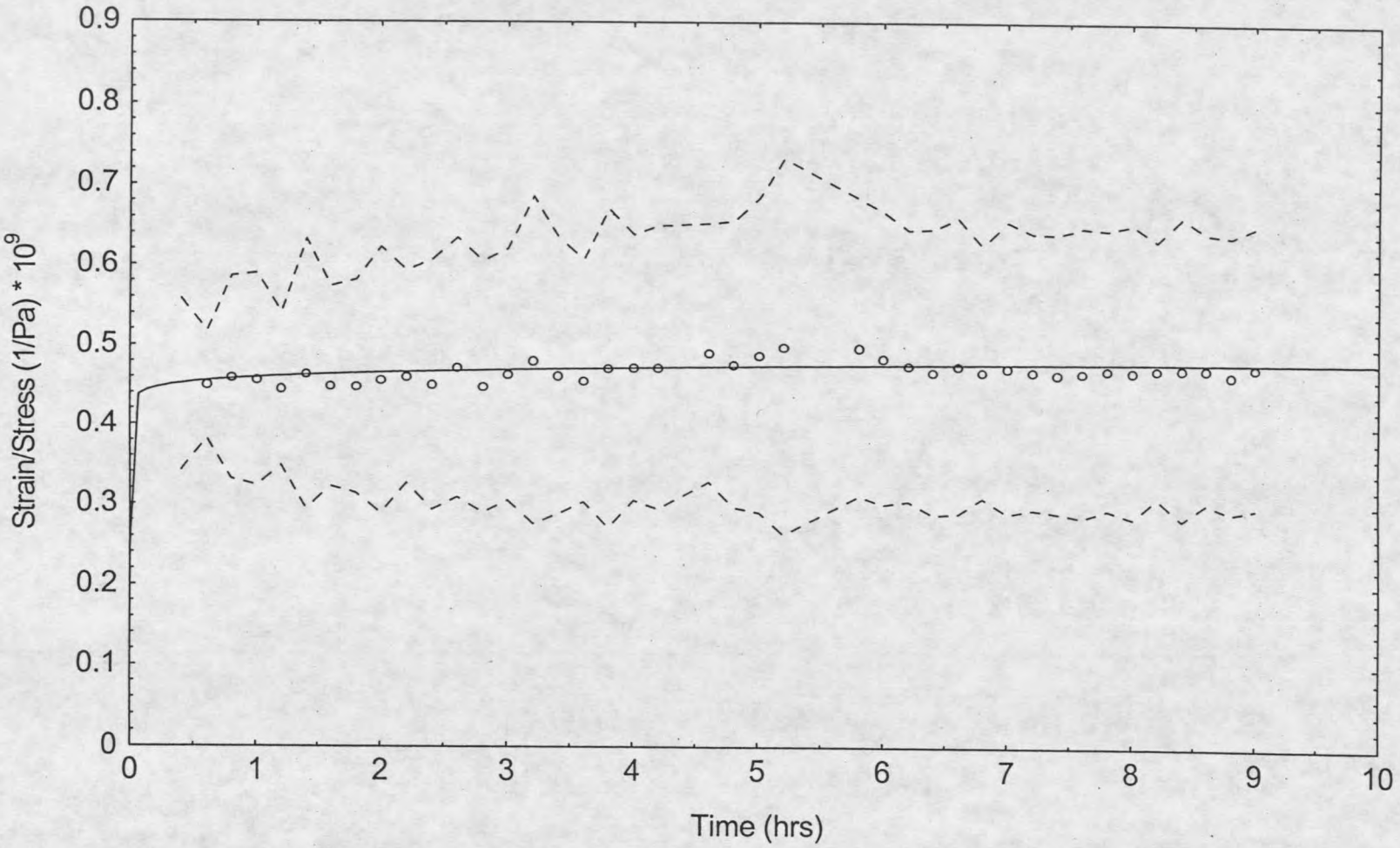


Figure M.II.4 Normalized Statistical Analysis of PVDF Vibrocreep Response with 95% Confidence
$(0.45\pm0.20)\sigma_y$, 10 Hz at -25 °C;
σ_y = 30.428 MPa at 23 °C

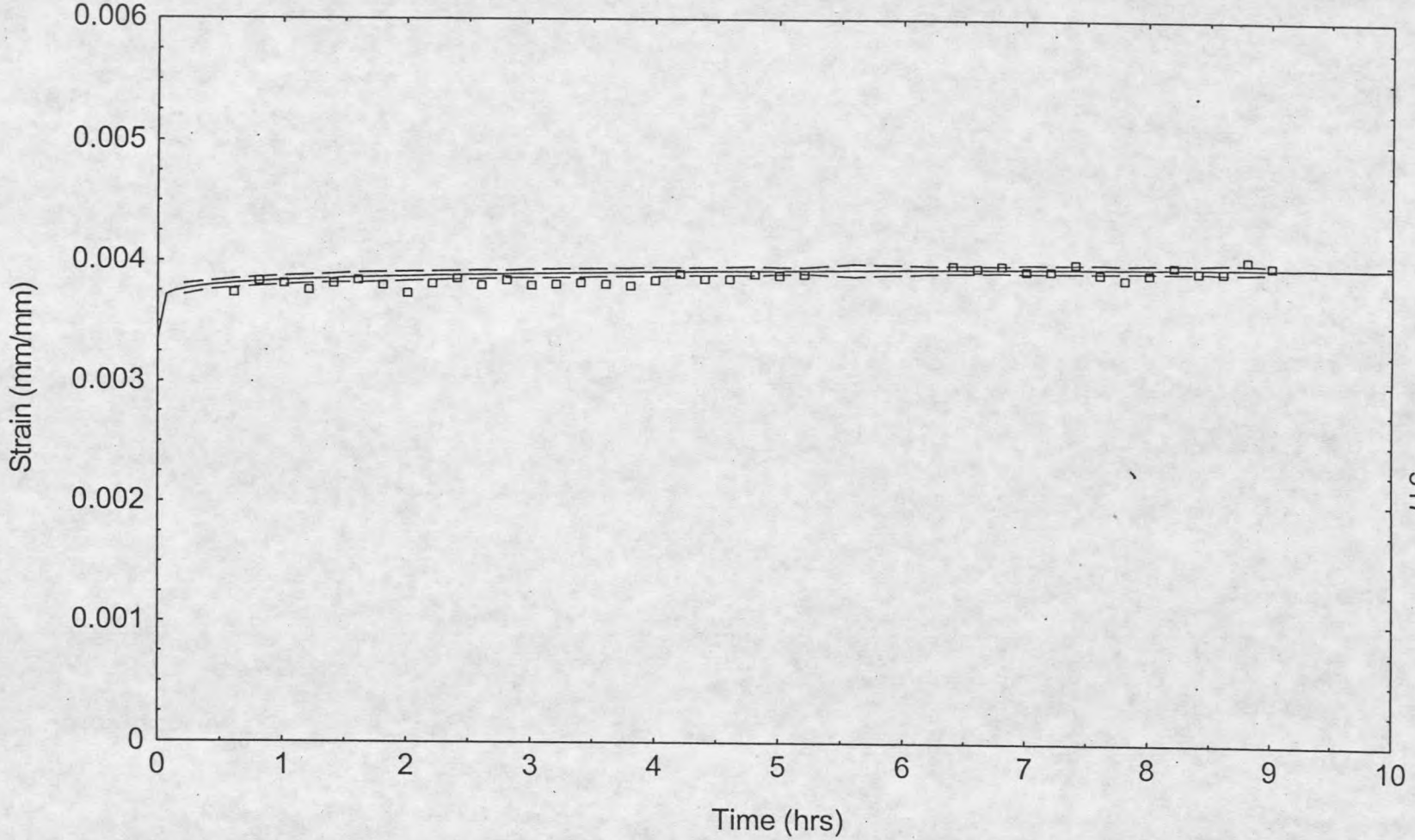


Figure M.II.5 Statistical Curve Fit Analysis of PVDF Quasi Static Creep with 95% Confidence
$(0.45)\sigma_y$ at -25 °C;
σ_y = 30.428 MPa at 23 °C

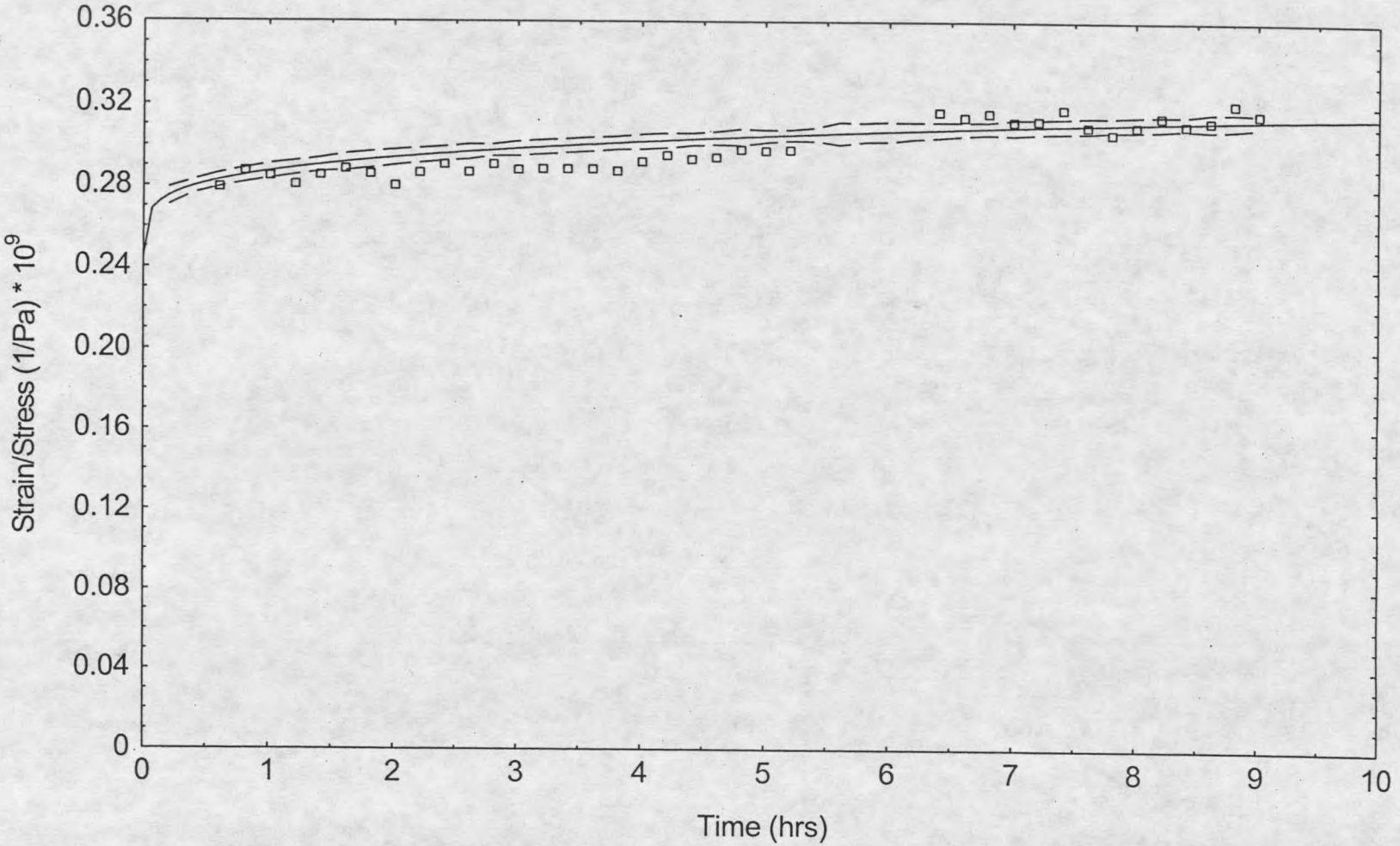


Figure M.II.6 Normalized Statistical Curve Fit Analysis of PVDF Quasi Static Creep with 95% Confidence
$(0.45)\sigma_y$ at -25 °C;
σ_y = 30.428 MPa at 23 °C

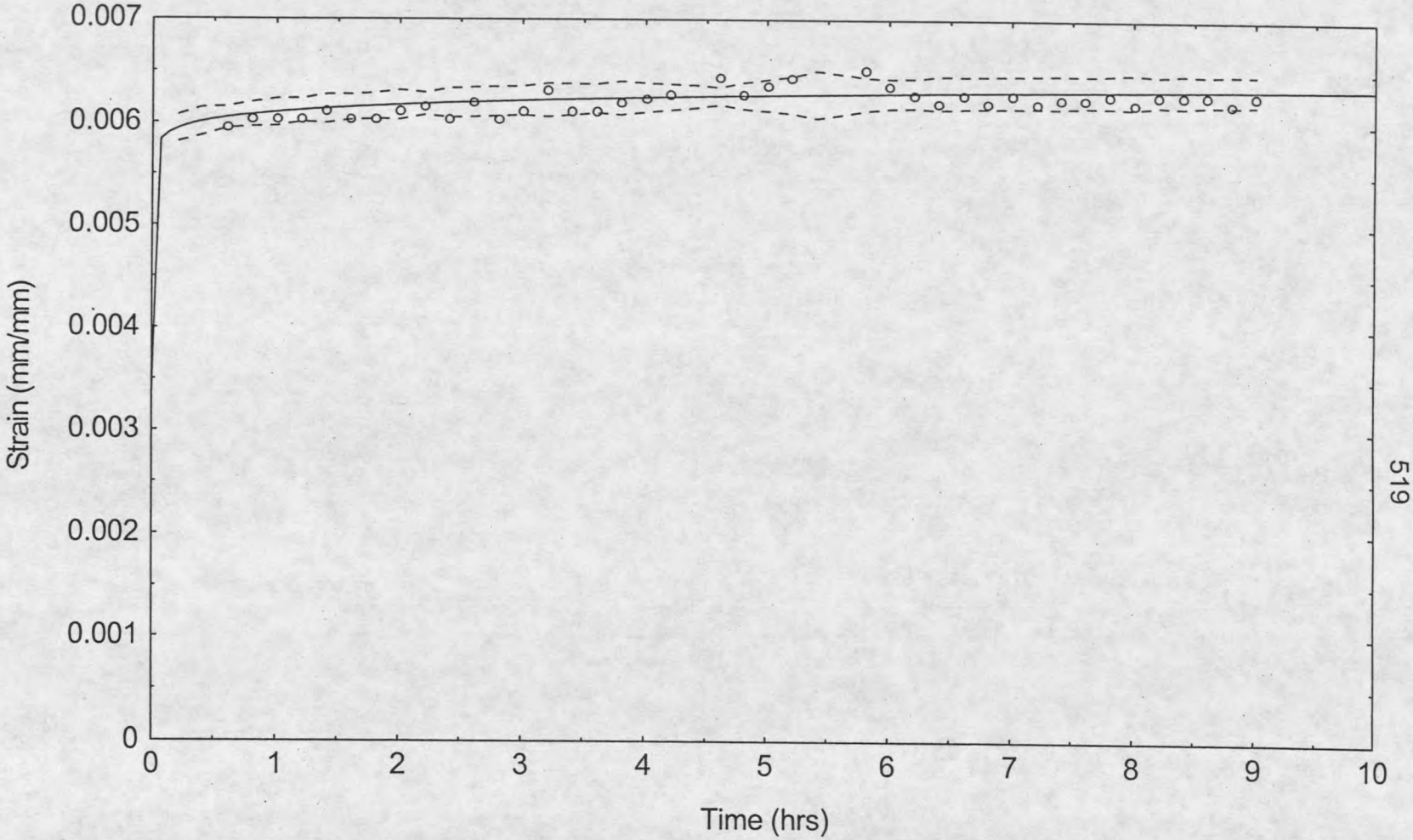


Figure M.II.7 Statistical Curve Fit Analysis of PVDF Vibrocreep Response with 95% Confidence
$(0.45\pm0.20)\sigma_y$, 10 Hz at -25 °C;
σ_y = 30.428 MPa at 23 °C

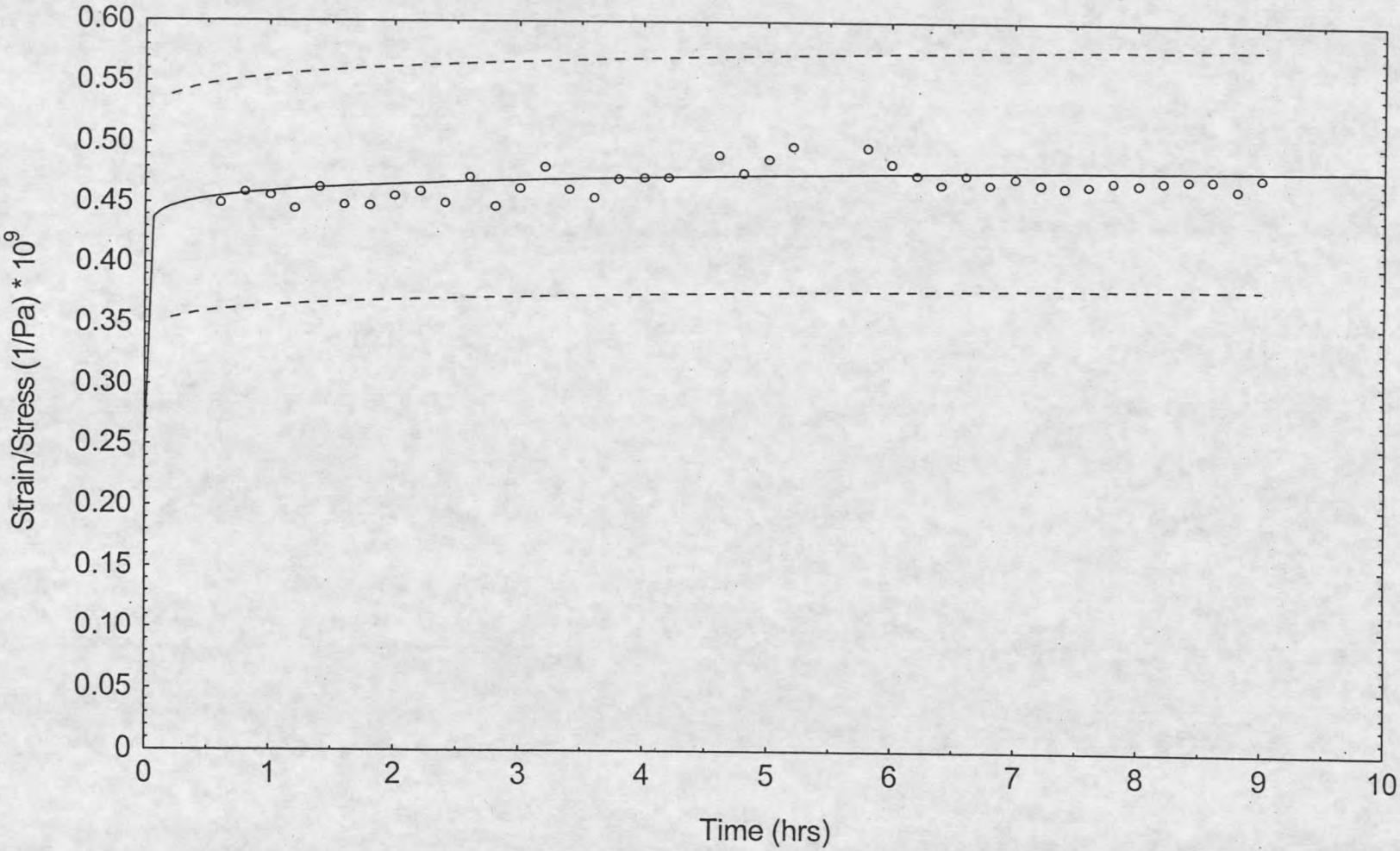


Figure M.II.8 Normalized Statistical Curve Fit Analysis of PVDF Vibrocreep Response with 95% Confidence
$(0.45 \pm 0.20)\sigma_y$, 10 Hz at -25 °C;
σ_y = 30.428 MPa at 23 °C

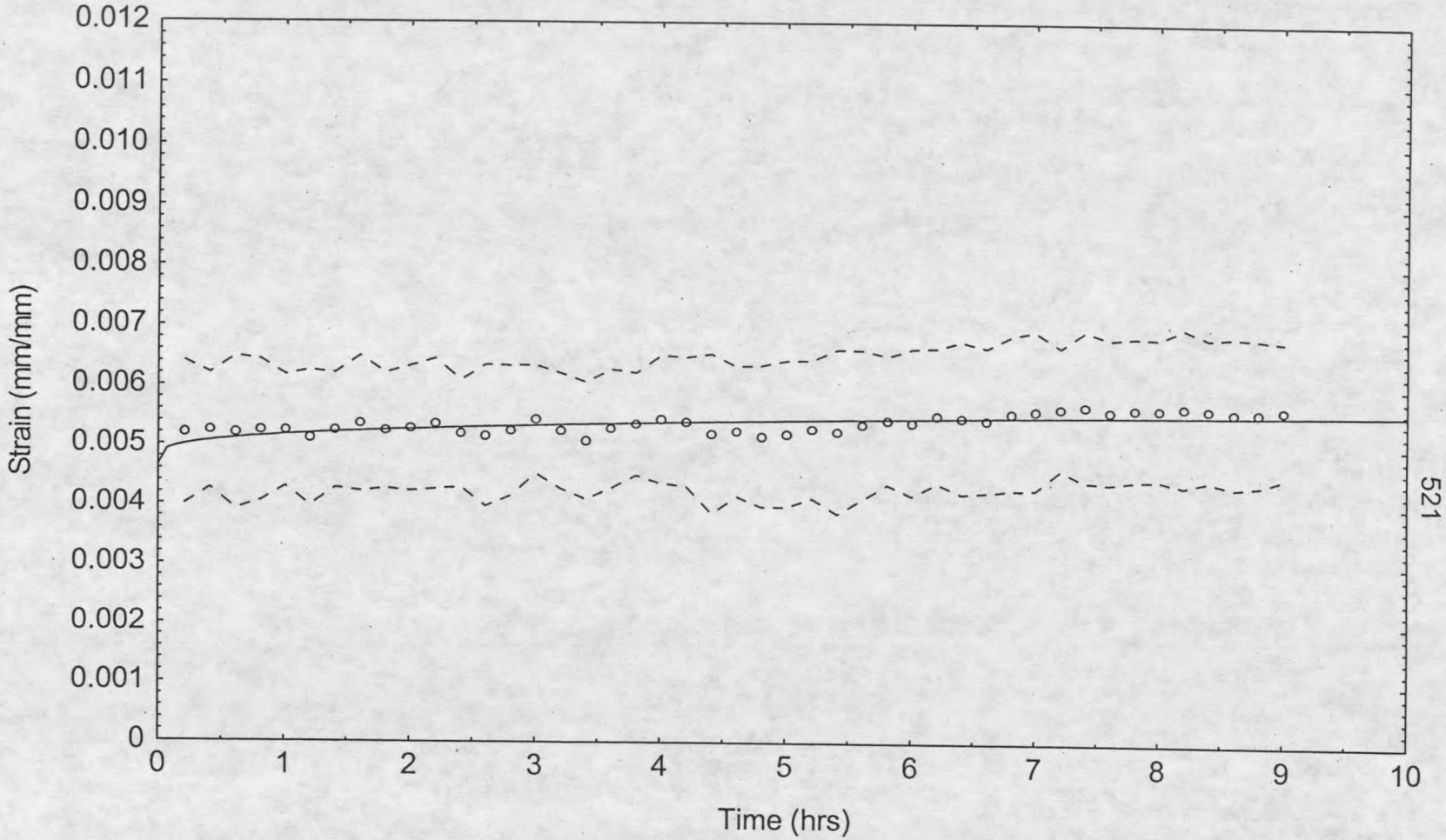


Figure M.II.9 Statistical Analysis of PVDF Quasi Static Creep with 95% Confidence
$(0.30)\sigma_y$ at 23 °C;
σ_y = 30.428 MPa at 23 °C

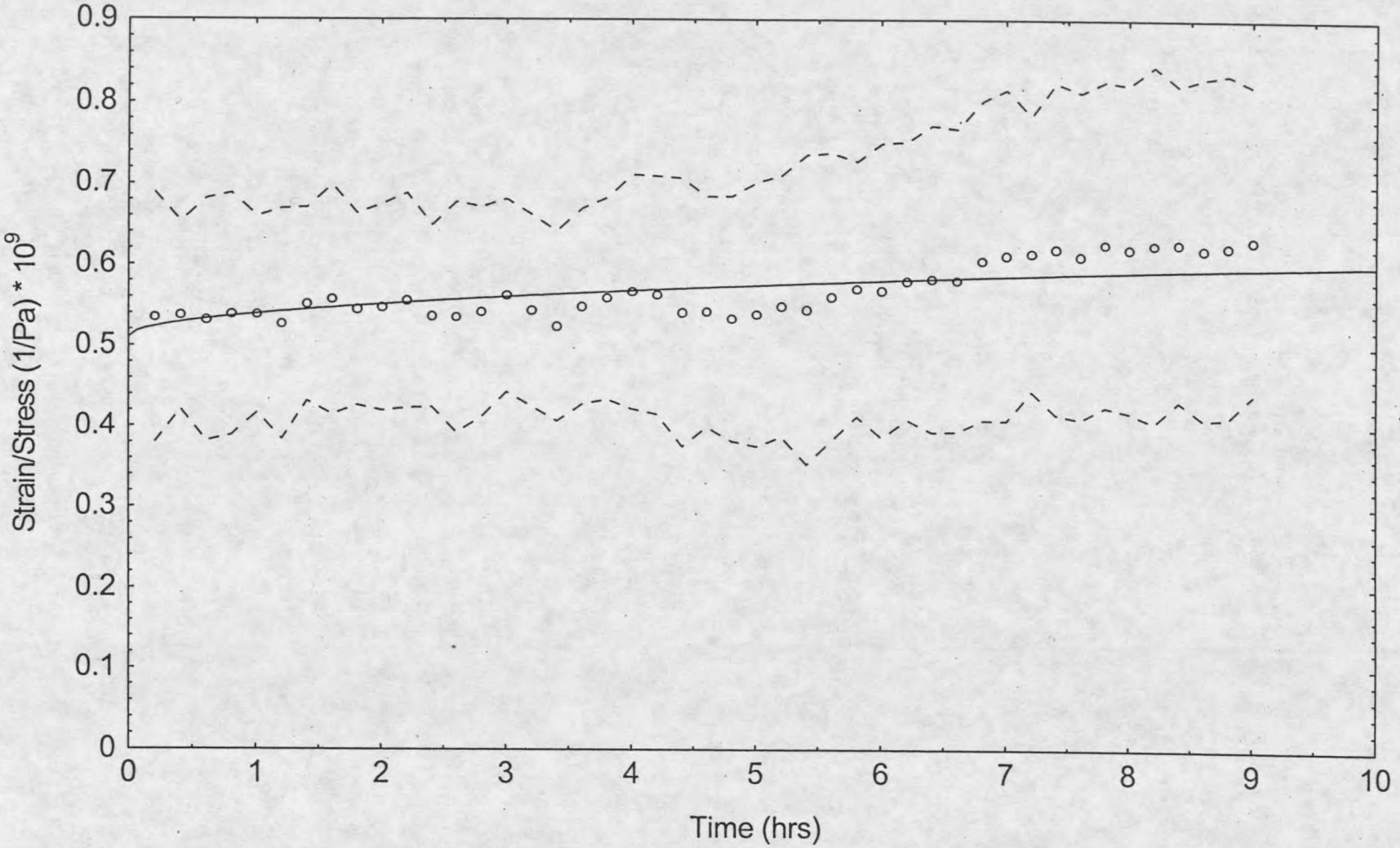


Figure M.II.10 Normalized Statistical Analysis of PVDF Quasi Static Creep with 95% Confidence
$(0.30)\sigma_y$ at 23 °C;
σ_y = 30.428 MPa at 23 °C

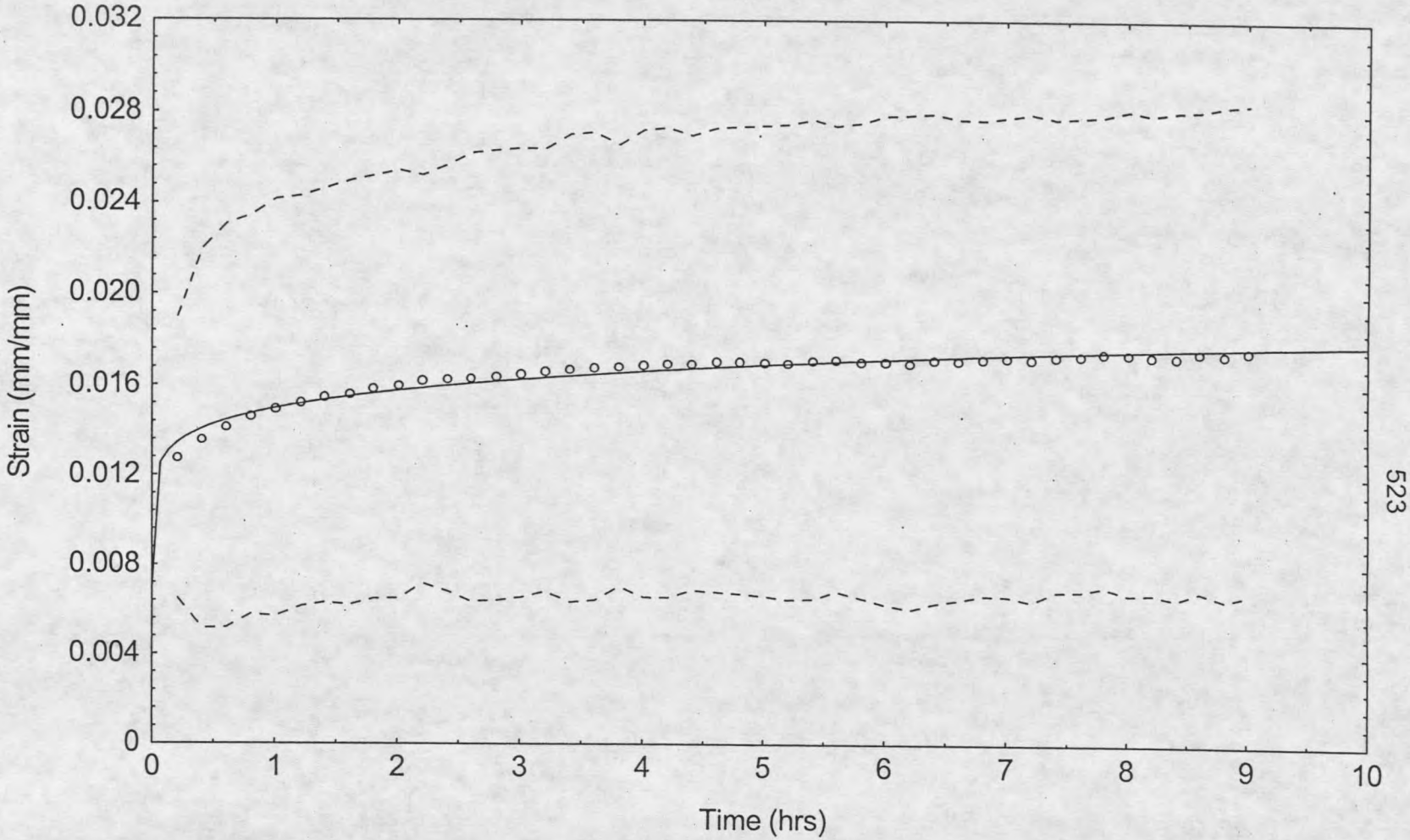


Figure M.II.11 Statistical Analysis of PVDF Vibrocreep Response with 95% Confidence
$(0.45\pm0.10)\sigma_y$, 5 Hz at 23 °C;
σ_y = 30.428 MPa at 23 °C

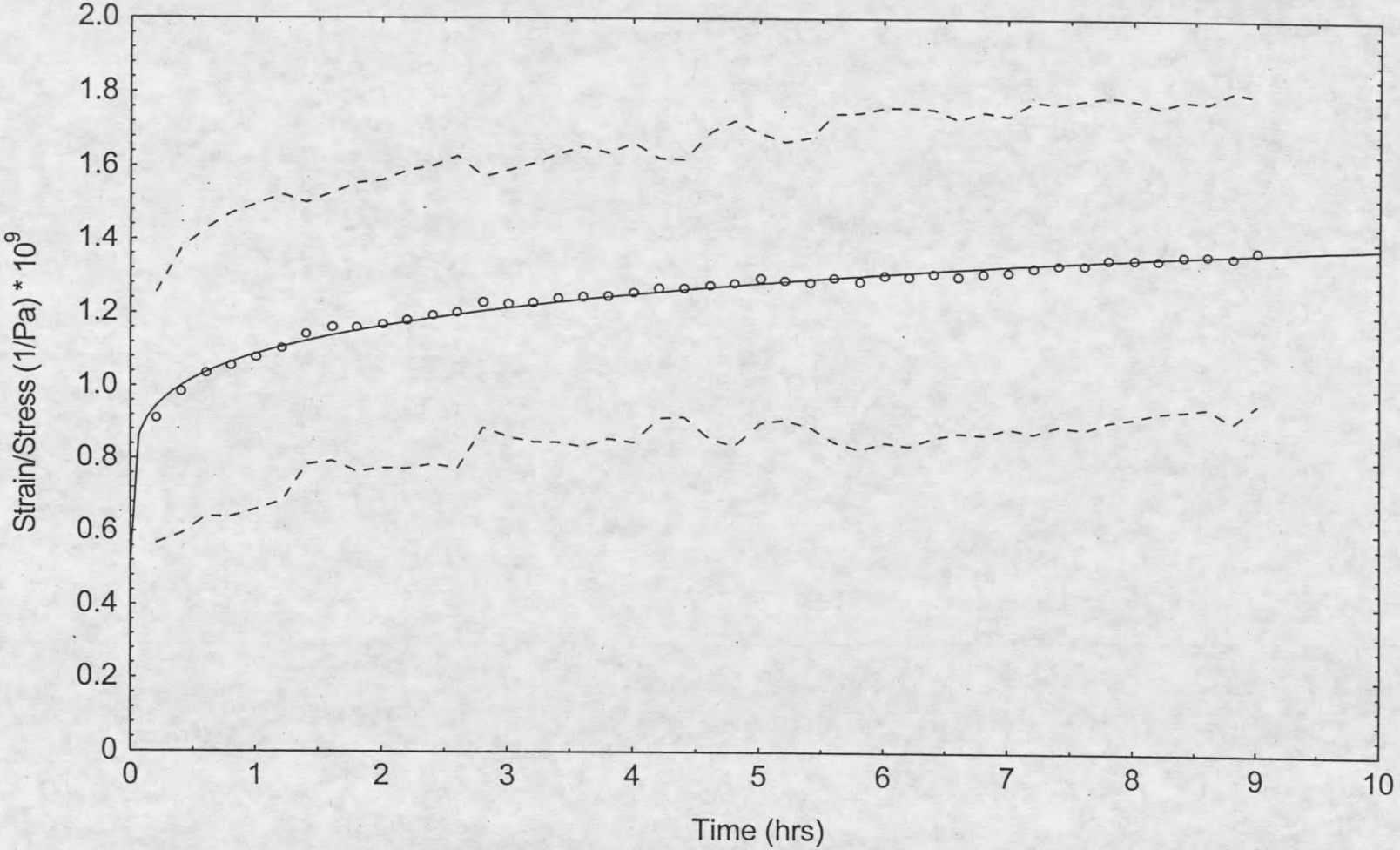


Figure M.II.12 Normalized Statistical Analysis of PVDF Vibrocreep Response with 95% Confidence
$(0.45\pm0.10)\sigma_y$, 5 Hz at 23 °C;
σ_y = 30.428 MPa at 23 °C

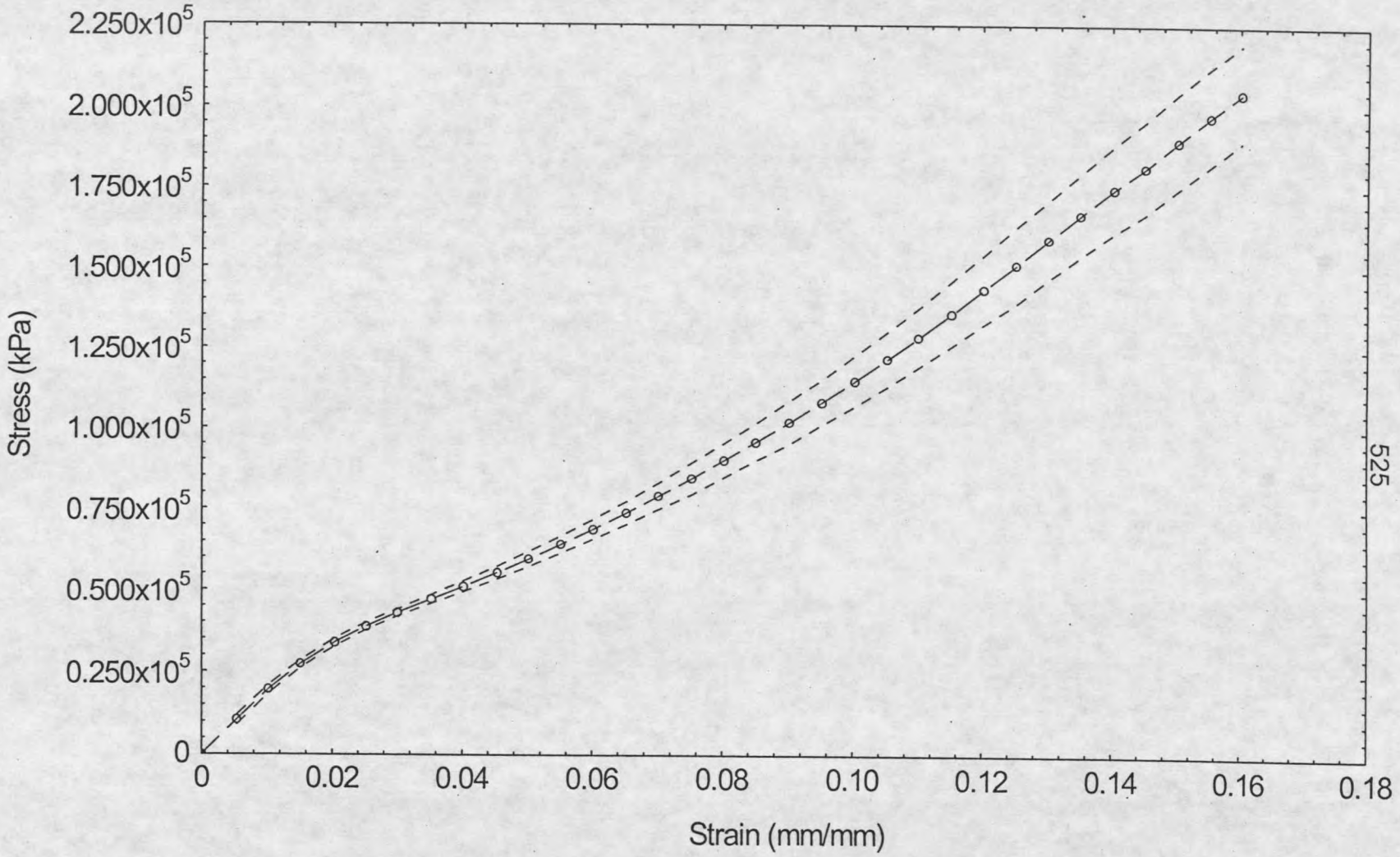


Figure M.II.13 Statistical Analysis of PVDF Direction 1 Tensile Testing with 95% Confidence at 23 °C

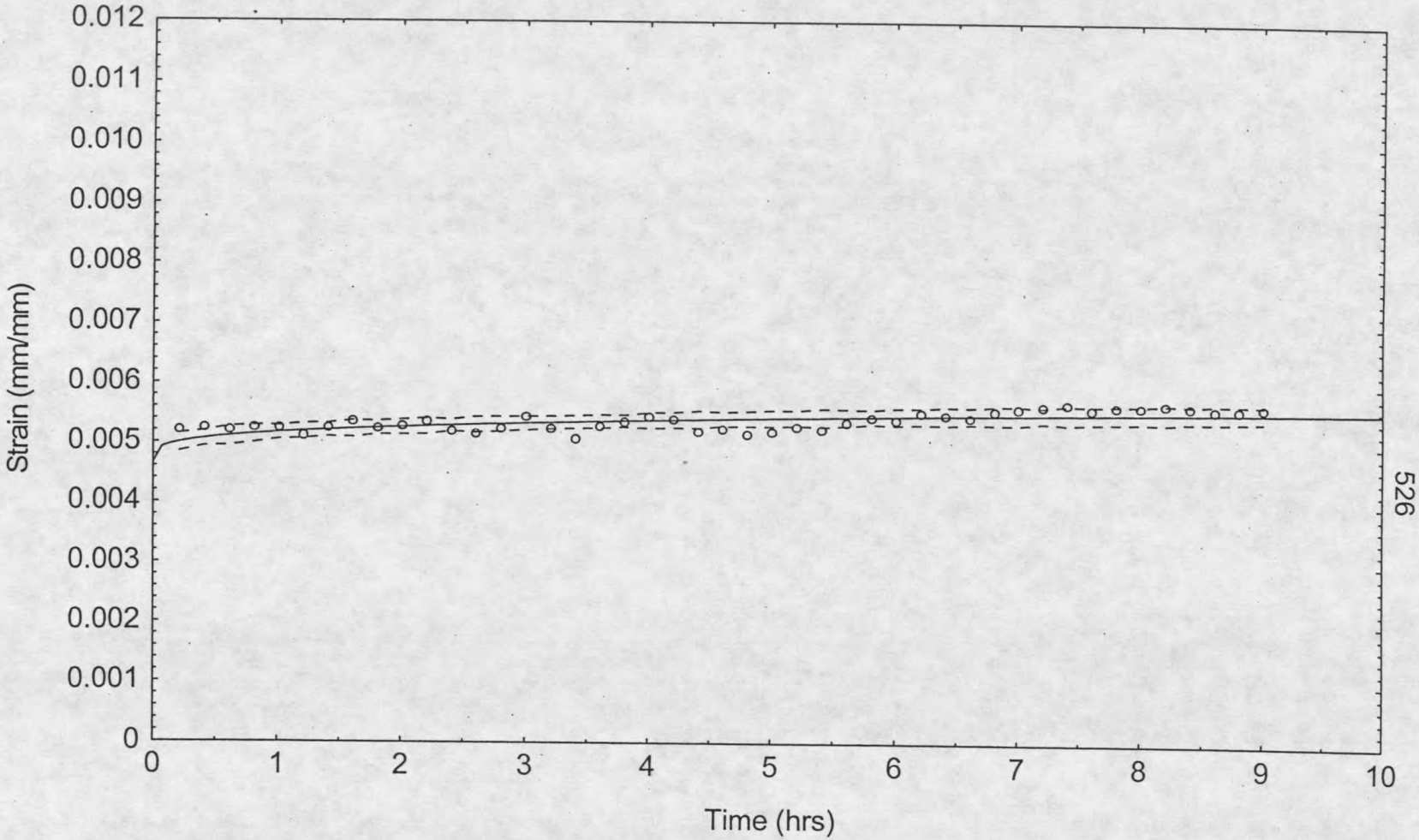


Figure M.II.14 Statistical Curve Fit Analysis of PVDF Quasi Static Creep with 95% Confidence
$(0.30)\sigma_y$ at 23 °C;
σ_y = 30.428 MPa at 23 °C

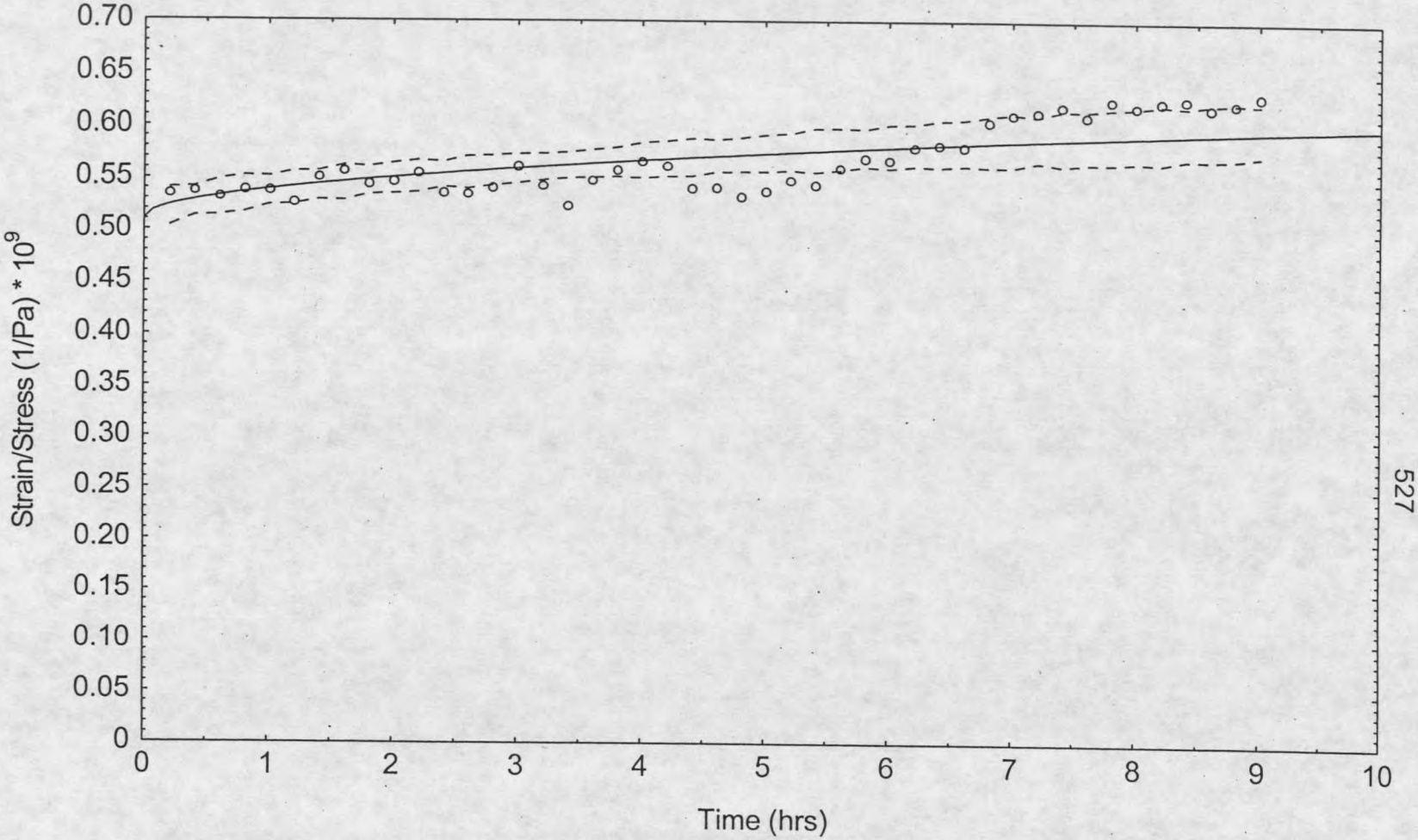


Figure M.II.15 Normalized Statistical Curve Fit Analysis of PVDF Quasi Static Creep with 95% Confidence
$(0.30)\sigma_y$ at 23 °C;
σ_y = 30.428 MPa at 23 °C

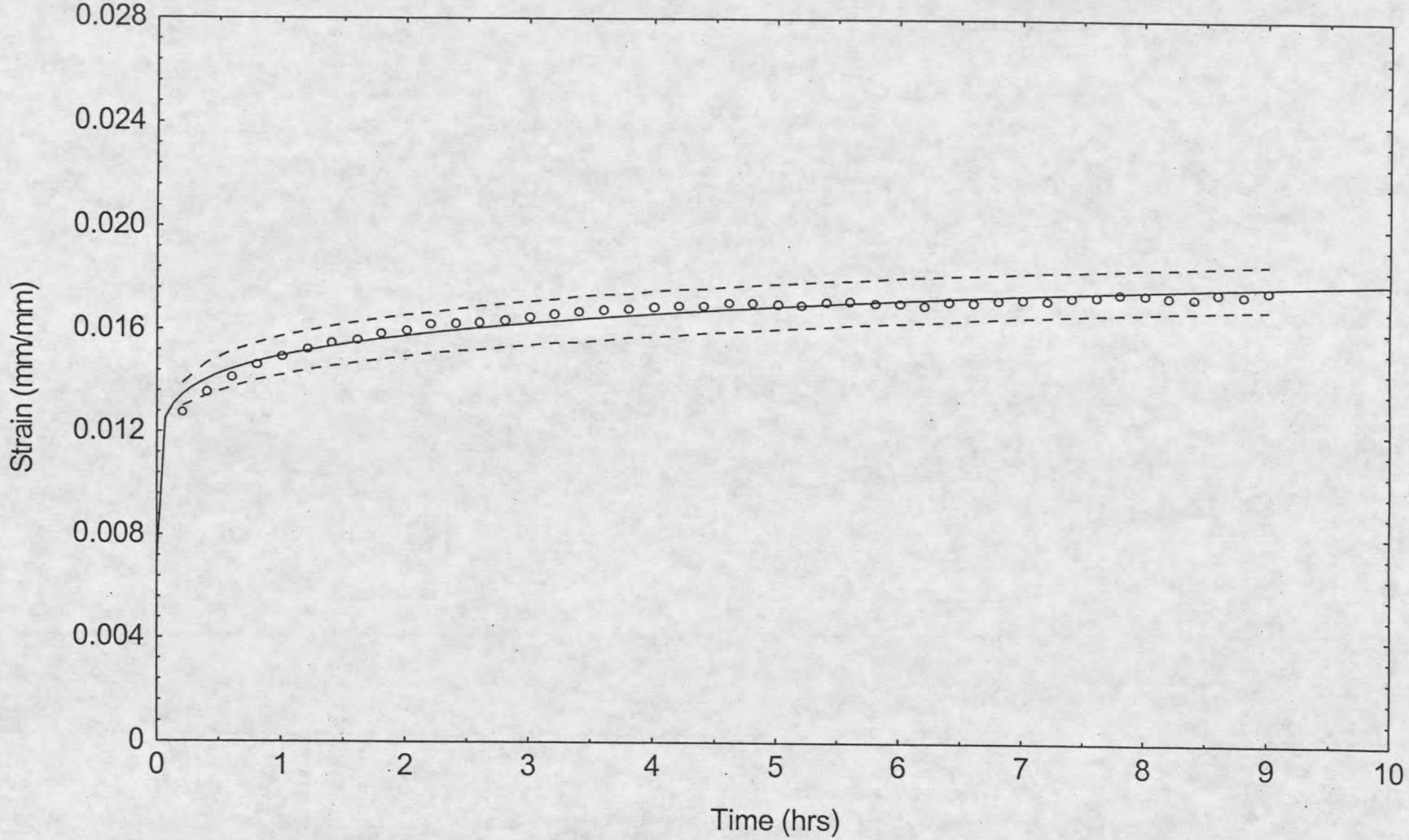


Figure M.II.16 Statistical Curve Fit Analysis of PVDF Vibrocreep Response with 95% Confidence
$(0.45\pm0.10)\sigma_y$, 5 Hz at 23 °C;
σ_y = 30.428 MPa at 23 °C

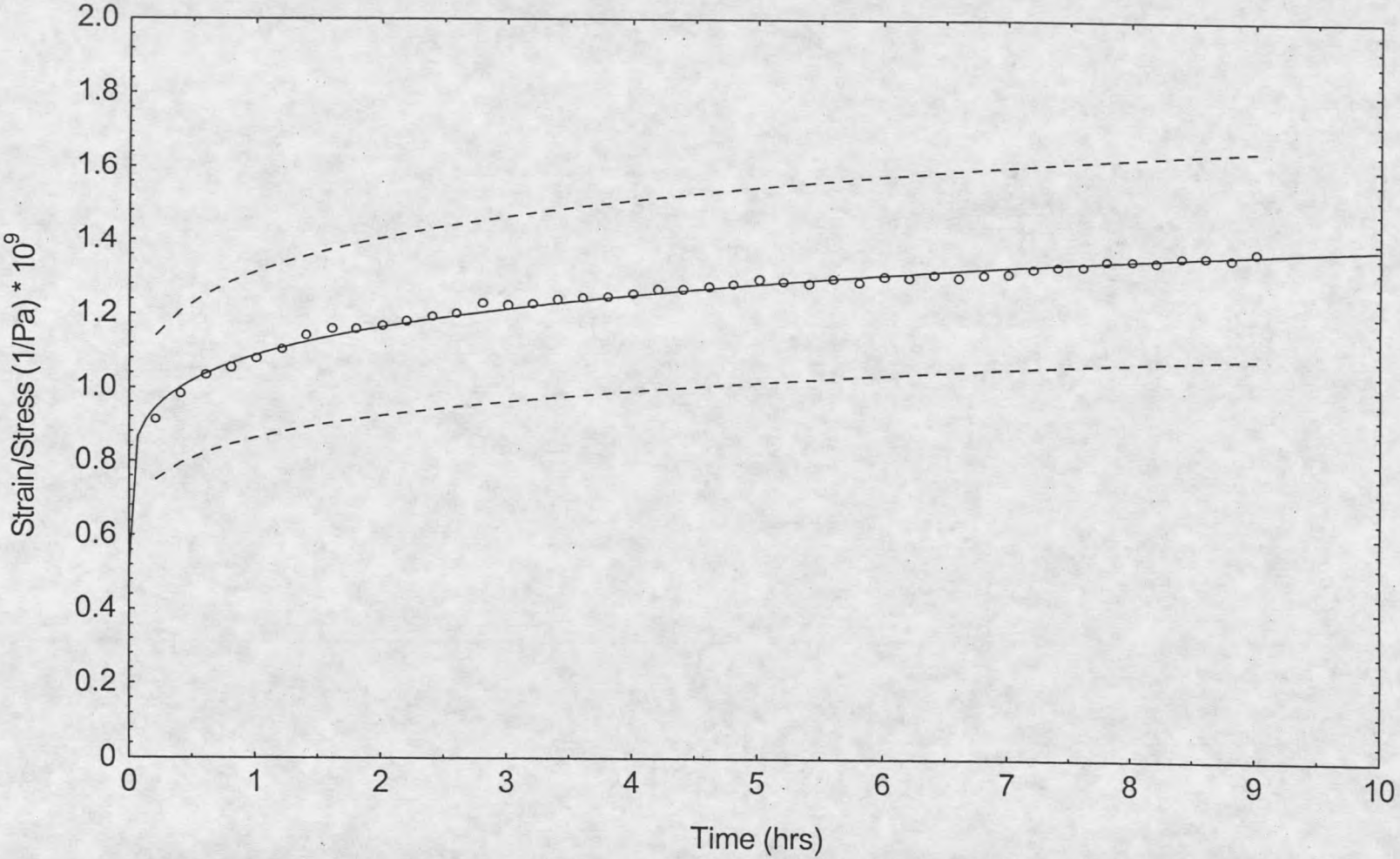


Figure M.II.17 Normalized Statistical Curve Fit Analysis of PVDF Vibrocreep Response with 95% Confidence
$(0.45\pm0.10)\sigma_y$, 5 Hz at 23 °C;
σ_y = 30.428 MPa at 23 °C

Curve Fit Results For Nylon 6/6

Data	a	b	c	a*b
23 C				
10%	**0.00190**	0.13139	0.00270	0.00025
N	**0.13300**	0.23952	0.52159	0.03186
16%	0.00989	0.39972	0.00590	0.00395
N	**0.13300**	0.29299	0.47702	0.03897
20%	0.00190	0.20700	0.00780	0.00039
N	0.13314	0.20914	0.55634	0.02784
30%	0.00196	0.35488	0.01277	0.00069
N	0.09125	0.35740	0.59949	0.03261
40%	0.00313	0.44499	0.01978	0.00139
N	0.10900	0.44800	0.69800	0.04883
50%	0.00200	0.33600	0.02400	0.00067
N	0.20000	0.33800	0.69000	0.06760
12%+-4% 1 Hz	0.00235	0.23835	**0.00641**	0.00056
N	0.28658	0.23854	**0.76300**	0.06836
12%+-4% 10 Hz	0.00243	0.25789	**0.00641**	0.00063
N	0.29733	0.25422	**0.76300**	0.07559
12%+-4% 20 Hz	0.00279	0.20846	**0.00641**	0.00058
N	0.34176	0.20397	**0.76300**	0.06971
12%+-7.5% 1 Hz	0.00260	0.21660	**0.00641**	0.00056
N	0.32158	0.21123	**0.76300**	0.06793
12%+-7.5% 10 Hz	0.00248	0.26447	**0.00641**	0.00066
N	0.29296	0.26464	**0.76300**	0.07753
12%+-7.5% 20 Hz	0.00310	0.21316	**0.00641**	0.00066
N	0.37786	0.20994	**0.76300**	0.07933
12%+-10% 1 Hz	0.00269	0.22510	**0.00641**	0.00061
N	0.32951	0.22093	**0.76300**	0.07280
12%+-10% 10 Hz	0.00341	0.15613	**0.00641**	0.00053
N	0.40171	0.15609	**0.76300**	0.06270
12%+-10% 20Hz	0.00329	0.20762	**0.00641**	0.00068
N	0.40013	0.20762	**0.76300**	0.08307
16%+-4% 1 Hz	0.00137	0.03429	**0.00854**	0.00005
N	0.09948	0.38547	**0.76300**	0.03835
16%+-4% 10 Hz	0.00171	0.31288	**0.00854**	0.00054
N	0.15361	0.31472	**0.76300**	0.04834
16%+-4% 20 Hz	0.00219	0.25570	**0.00854**	0.00056
N	0.19867	0.25440	**0.76300**	0.05054
16%+-7.5% 1 Hz	0.00187	0.28193	**0.00854**	0.00053
N	0.17323	0.27503	**0.76300**	0.04764
16%+-7.5% 10 Hz	0.00254	0.23206	**0.00854**	0.00059
N	0.22744	0.23981	**0.76300**	0.05454
16%+-7.5% 20 Hz	0.00280	0.23614	**0.00854**	0.00066
N	0.25474	0.22950	**0.76300**	0.05846
16%+-10% 1 Hz	0.00172	0.38946	**0.00854**	0.00067
N	0.15250	0.39067	**0.76300**	0.05958
16%+-10% 10 Hz	0.00239	0.26372	**0.00854**	0.00063
N	0.22184	0.25440	**0.76300**	0.05644

16%+-10% 20 Hz	0.00314	0.22428	**0.00854**	0.00070
N	0.27759	0.22849	**0.76300**	0.06343
20%+-5% 1 Hz	0.00157	0.40008	**0.01068**	0.00063
N	0.11530	0.40154	**0.76300**	0.04630
20%+-5% 10 Hz	0.00282	0.27346	**0.01068**	0.00077
N	0.20310	0.22120	**0.76300**	0.04493
20%+-5% 20 Hz	0.00316	0.23276	**0.01068**	0.00074
N	0.22876	0.23051	**0.76300**	0.05273
20%+-7.5% 1 Hz	0.00222	0.30845	**0.01068**	0.00069
N	0.16425	0.30539	**0.76300**	0.05016
20%+-7.5% 10 Hz	0.00293	0.30835	**0.01068**	0.00090
N	0.21345	0.30509	**0.76300**	0.06512
20%+-7.5% 20 Hz	0.00342	0.26743	**0.01068**	0.00092
N	0.27876	0.22274	**0.76300**	0.06209
20%+-10% 1 Hz	0.00286	0.21198	**0.01068**	0.00061
N	0.20863	0.20730	**0.76300**	0.04325
20%+-10% 10 Hz	0.00377	0.23614	**0.01068**	0.00089
N	0.27335	0.23368	**0.76300**	0.06388
20%+-10% 20 Hz	0.00466	0.19267	**0.01068**	0.00090
N	0.33684	0.19215	**0.76300**	0.06472

35

16%	**0.00400**	0.14927	0.00133	0.00060
N	**0.37600**	0.17510	0.22510	0.06584
20%	0.00400	0.20900	0.00270	0.00084
N	0.37600	0.20900	0.24600	0.07858
30%	**0.00550**	0.27990	0.00468	0.00154
N	**0.34460**	0.27400	0.27580	0.09442
40%	0.00620	0.36300	0.00780	0.00225
N	0.27400	0.37100	0.36600	0.10165
50%	0.00780	0.30900	0.01500	0.00241
N	0.28200	0.31290	0.56800	0.08824
16% R 23	0.00421	0.20956	0.00276	0.00088
N	0.37615	0.20969	0.24634	0.07887
20% R 23	0.00826	0.17522	0.00060	0.00145
N	0.59611	0.17319	0.03604	0.10324
16%+-4% 1 Hz	0.00269	0.32367	**0.00768**	0.00087
N	0.31317	0.31770	**0.86900**	0.09949
16%+-4% 10 Hz	0.00302	0.37201	**0.00768**	0.00112
N	0.34974	0.36707	**0.86900**	0.12838
16%+-10% 1 Hz	0.00262	0.39597	**0.00768**	0.00104
N	0.30408	0.39174	**0.86900**	0.11912
16%+-10% 10 Hz	0.00309	0.36537	**0.00768**	0.00113
N	0.35750	0.36467	**0.86900**	0.13037
20%+-5% 1 Hz	0.00422	0.32210	**0.00160**	0.00136
N	0.40972	0.31009	**0.86900**	0.12705
20%+-5% 10 Hz	0.00523	0.29300	**0.00160**	0.00153
N	0.47220	0.31907	**0.86900**	0.15066
20%+-10% 1 Hz	0.00517	0.32942	**0.00160**	0.00170

N	0.42092	0.31135	**0.86900**	0.13105
20%+-10% 10 Hz	0.00468	0.31911	**0.00160**	0.00149
N	0.48471	0.32094	**0.86900**	0.15556
16%+-4% 1 Hz R 23	0.00348	0.43579	**0.00974**	0.00152
N	0.31822	0.42962	**0.86900**	0.13671
16%+-4% 10 Hz R 23	0.00555	0.30367	**0.00974**	0.00168
N	0.50599	0.30110	**0.86900**	0.15235
16%+-10% 1 Hz R 23	0.00535	0.26861	**0.00974**	0.00144
N	0.51865	0.28648	**0.86900**	0.14858
16%+-10% 10 Hz R 23	0.00617	0.26437	**0.00974**	0.00163
N	0.42641	0.28747	**0.86900**	0.12258
20%+-5% 1 Hz R 23	0.00418	0.31573	**0.01217**	0.00132
N	0.30329	0.31763	**0.86900**	0.09633
20%+-5% 10 Hz R 23	0.00546	0.29500	**0.01217**	0.00161
N	0.39663	0.29308	**0.86900**	0.11624
20%+-10% 1 Hz R 23	0.00532	0.27856	**0.01217**	0.00148
N	0.00789	0.78008	**0.86900**	0.00615
20%+-10% 10 Hz R 23	0.00620	0.29556	**0.01217**	0.00183
N	0.44659	0.29614	**0.86900**	0.13225

41

16%	**0.00500**	0.17110	0.00030	0.00086
N	**0.60600**	0.18953	0.11661	0.11486
20%	0.00500	0.20282	0.00160	0.00101
N	0.60600	0.20060	0.17790	0.12156
30%	0.00400	0.33800	0.00560	0.00135
N	0.35657	0.33684	0.39937	0.12011
40%	0.01100	0.23671	0.00300	0.00260
N	0.60789	0.24492	0.20700	0.14888
50%	0.01400	0.26100	0.00600	0.00365
N	0.63052	0.26145	0.28461	0.16485
16% R 23	0.00719	0.19284	0.00137	0.00139
N	0.65540	0.19070	0.11439	0.12498
20% R 23	0.00495	0.33831	0.00559	0.00168
N	0.35654	0.33686	0.39940	0.12010
16%+-10% 1 Hz	0.00117	0.37763	**0.00749**	0.00044
N	0.53398	0.37413	**1.04170**	0.19978
16%+-10% 10 Hz	0.00449	0.32912	**0.00749**	0.00148
N	0.63776	0.32727	**1.04170**	0.20872
20%+-5% 1 Hz	0.00299	0.35602	**0.00937**	0.00107
N	0.34654	0.34642	**1.04170**	0.12005
20%+-5% 10 Hz	0.00330	0.41977	**0.00937**	0.00138
N	0.37452	0.41647	**1.04170**	0.15598
20%+-10% 1 Hz	0.00259	0.48771	**0.00937**	0.00127
N	0.30019	0.47592	**1.04170**	0.14287
20%+-10% 10 Hz	0.00357	0.20968	**0.00937**	0.00075
N	0.40661	0.40497	**1.04170**	0.16466
16%+-4% 1 Hz R 23	0.00279	0.44276	**0.01167**	0.00123
N	0.25584	0.43833	**1.04170**	0.11214

16%+-4% 10 Hz R 23	0.00326	0.49079	**0.01167**	0.00160
N	0.30199	0.47852	**1.04170**	0.14451
16%+-10% 1 Hz R 23	0.00330	0.44849	**0.01167**	0.00148
N	0.30454	0.43961	**1.04170**	0.13388
16%+-10% 10 Hz R 23	0.00573	0.34960	**0.01167**	0.00200
N	0.52158	0.34699	**1.04170**	0.18098
20%+-5% 1 Hz R 23	0.00417	0.38542	**0.01458**	0.00161
N	0.30429	0.38098	**1.04170**	0.11593
20%+-5% 10 Hz R 23	0.00460	0.41573	**0.01458**	0.00191
N	0.33592	0.40909	**1.04170**	0.13742
20%+-10% 1 Hz R 23	0.00401	0.46118	**0.01458**	0.00185
N	0.29187	0.45731	**1.04170**	0.13348
20%+-10% 10 Hz R 23	0.00469	0.46054	**0.01458**	0.00216
N	0.34091	0.45654	**1.04170**	0.15564

50

20%	0.00215	0.44368	**0.00622**	0.00095
N	0.46900	0.45110	**1.41243**	0.21157
30%	0.00524	0.23553	**0.00933**	0.00123
N	0.79200	0.23670	**1.41243**	0.18747
40%	0.00938	0.20495	**0.01244**	0.00192
N	1.05540	0.20500	**1.41243**	0.21636
50%	0.01254	0.20250	**0.01555**	0.00254
N	1.34900	0.20318	**1.41243**	0.27409
16% R 23	0.01223	0.20596	**0.01582**	0.00252
N	1.13500	0.20318	**1.41243**	0.23061
20% R 23	0.01539	0.22080	**0.01977**	0.00340
N	1.08960	0.22320	**1.41243**	0.24320

59

20%	0.00353	0.17740	**0.00694**	0.00063
N	0.92900	0.17500	**1.82482**	0.16258
30%	0.00563	0.19537	**0.01041**	0.00110
N	1.04000	0.18900	**1.82482**	0.19656
40%	0.00761	0.18441	**0.01387**	0.00140
N	1.05500	0.17900	**1.82482**	0.18885
50%	0.02333	0.06915	**0.01734**	0.00161
N	2.64000	0.07150	**1.82482**	0.18876
16% R 23	0.02301	0.08972	**0.02044**	0.00206
N	2.00980	0.09058	**1.82482**	0.18205
20% R 23	0.02757	0.09330	**0.02555**	0.00257
N	2.00870	0.09294	**1.82482**	0.18669

68

20%	0.00318	0.02516	**0.00436**	0.00008
N	1.60350	0.02502	**2.17864**	0.04012
30%	0.00469	0.06342	**0.00654**	0.00030
N	1.51270	0.06278	**2.17864**	0.09497
40%	0.00608	0.08287	**0.00872**	0.00050
N	1.45760	0.08479	**2.17864**	0.12358
50%	0.00958	0.06223	**0.01090**	0.00060

N	1.74940	0.06509	**2.17864**	0.11388
16% R 23	0.02865	0.06254	**0.02440**	0.00179
N	2.55910	0.06224	**2.17864**	0.15927
20% R 23	0.03777	0.05845	**0.03050**	0.00221
N	2.64230	0.05910	**2.17864**	0.15617

Curve Fit Results For PVDF

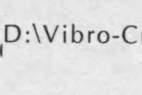
Data	a	b	c	a*b
-25 C				
30%	0.00003	0.72455	**0.00224**	0.00002
N	0.02110	0.32694	**0.24500**	0.00690
45%	0.00048	0.10763	**0.00336**	0.00005
N	0.04216	0.21634	**0.24500**	0.00912
60%	0.00091	0.02611	**0.00447**	0.00002
N	0.05526	0.08844	**0.24500**	0.00489
30%+-20% 5 Hz	0.00161	0.03064	**0.00224**	0.00005
N	0.11492	0.05517	**0.24500**	0.00634
30%+-20% 10 Hz	0.00184	0.06285	**0.00224**	0.00012
N	0.17191	0.10589	**0.24500**	0.01820
30%+-20% 20 Hz	0.00235	0.04410	**0.00224**	0.00010
N	0.27819	0.07974	**0.24500**	0.02218
45%+-20% 5 Hz	0.00176	0.05881	**0.00336**	0.00010
N	0.11940	0.08065	**0.24500**	0.00963
45%+-20% 10 Hz	0.00274	0.03748	**0.00336**	0.00010
N	0.21474	0.04057	**0.24500**	0.00871
45%+-35% 5 Hz	0.00338	0.01159	**0.00336**	0.00004
N	0.20388	0.04246	**0.24500**	0.00866
45%+-40% 10 Hz	0.00963	0.03027	**0.00336**	0.00029
N	0.05069	0.03541	**0.24500**	0.00180
60%+-20% 5 Hz	0.00323	0.03980	**0.00447**	0.00013
N	0.17203	0.03565	**0.24500**	0.00613
60%+-20% 10 Hz	0.00852	0.03411	**0.00447**	0.00029
N	0.26591	0.05831	**0.24500**	0.01551
60%+-40% 5 Hz	0.00434	0.06650	**0.00447**	0.00029
N	0.23758	0.06681	**0.24500**	0.01587
60%+-50% 10 Hz	0.00507	0.03998	**0.00447**	0.00020
N	0.50693	0.03541	**0.24500**	0.01795
23 C				
30%	0.00051	0.25511	**0.00466**	0.00013
N	0.02772	0.52603	**0.51020**	0.01458
45%	0.00092	0.21741	**0.00699**	0.00020
N	0.04769	0.38593	**0.51020**	0.01840
60%	0.00166	0.15950	**0.00931**	0.00026
N	0.08680	0.15497	**0.51020**	0.01345
30%+-10% 5 Hz	0.00361	0.04498	**0.00466**	0.00016
N	0.46993	0.11483	**0.51020**	0.05396
30%+-10% 10 Hz	0.00532	0.14302	**0.00466**	0.00076
N	0.46778	0.22464	**0.51020**	0.10508
30%+-10% 20 Hz	0.00940	0.03247	**0.00466**	0.00031
N	1.25190	0.09726	**0.51020**	0.12175
30%+-20% 5 Hz	0.00588	0.10434	**0.00466**	0.00061
N	0.58930	0.15102	**0.51020**	0.08900
30%+-20% 10 Hz	0.00658	0.12256	**0.00466**	0.00081
N	0.60962	0.23152	**0.51020**	0.14114
30%+-20% 20 Hz	0.00926	0.05649	**0.00466**	0.00052

N	1.49640	0.07155	**0.51020**	0.10706
45%+-10% 5 Hz	0.00799	0.13452	**0.00699**	0.00107
N	0.57686	0.17992	**0.51020**	0.10379
45%+-10% 10 Hz	0.01046	0.07706	**0.00699**	0.00081
N	4.91040	0.14397	**0.51020**	0.70695
45%+-10% 20 Hz	0.01670	0.05129	**0.00699**	0.00086
N	1.14510	0.09335	**0.51020**	0.10690
45%+-20% 5 Hz	0.01141	0.12024	**0.00699**	0.00137
N	0.84524	0.17164	**0.51020**	0.14508
45%+-20% 10 Hz	0.01545	0.12163	**0.00699**	0.00188
N	0.88145	0.12220	**0.51020**	0.10771
45%+-20% 20 Hz	0.01965	0.05465	**0.00699**	0.00107
N	1.66200	0.10827	**0.51020**	0.17994
45%+-35% 5 Hz	0.02105	0.09062	**0.00699**	0.00191
N	3.39370	0.26051	**0.51020**	0.88409
45%+-40% 10 Hz	0.02427	0.07090	**0.00699**	0.00172
N	1.64500	0.15269	**0.51020**	0.25118
60%+-10% 5 Hz	0.01329	0.09068	**0.00931**	0.00121
N	0.82770	0.08898	**0.51020**	0.07365
60%+-10% 10 Hz	0.02054	0.05736	**0.00931**	0.00118
N	1.77210	0.10382	**0.51020**	0.18398
60%+-10% 20 Hz	0.02309	0.08427	**0.00931**	0.00195
N	1.45140	0.06991	**0.51020**	0.10147
60%+-20% 5 Hz	0.01823	0.06827	**0.00931**	0.00124
N	1.12790	0.07497	**0.51020**	0.08456
60%+-20% 10 Hz	0.02164	0.10463	**0.00931**	0.00226
N	1.29630	0.11618	**0.51020**	0.15060
60%+-20% 20 Hz	0.02965	0.02535	**0.00931**	0.00075
N	1.88160	0.06955	**0.51020**	0.13086
60%+-40% 5 Hz	0.02619	0.03665	**0.00931**	0.00096
N	2.24500	0.08780	**0.51020**	0.19711
60%+-50% 10 Hz	0.04114	0.04651	**0.00931**	0.00191
N	5.94080	0.12160	**0.51020**	0.72240

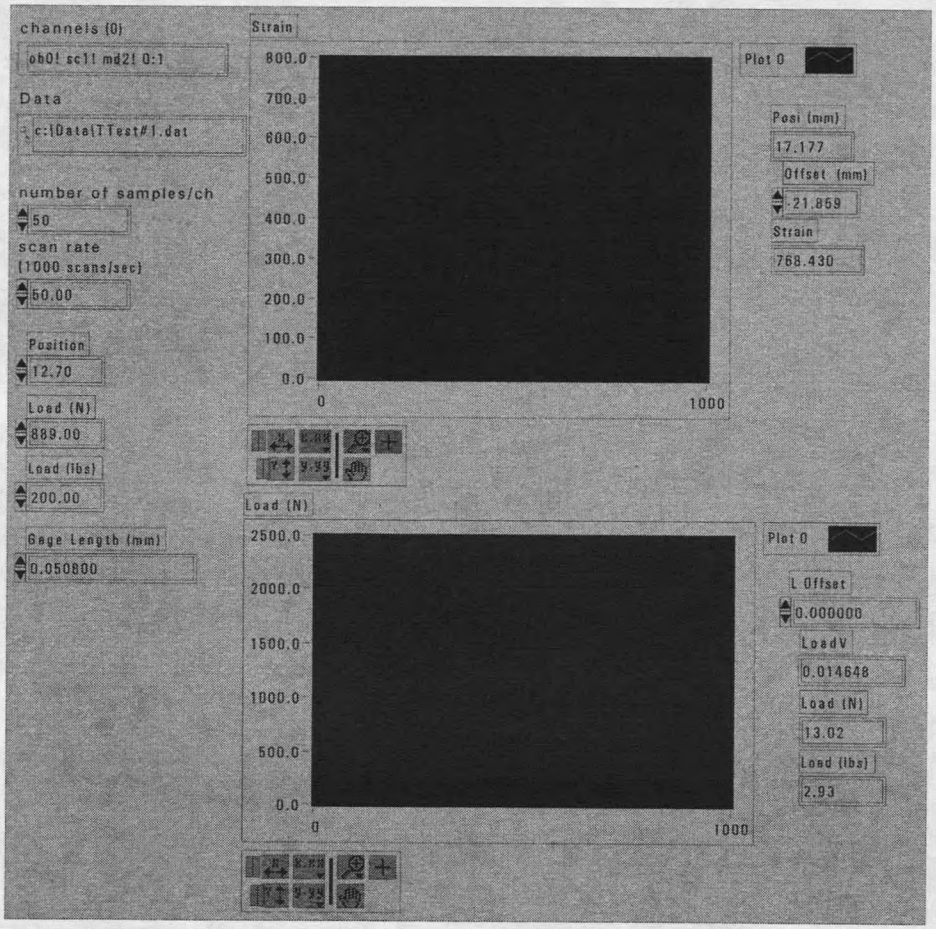
APPENDIX N

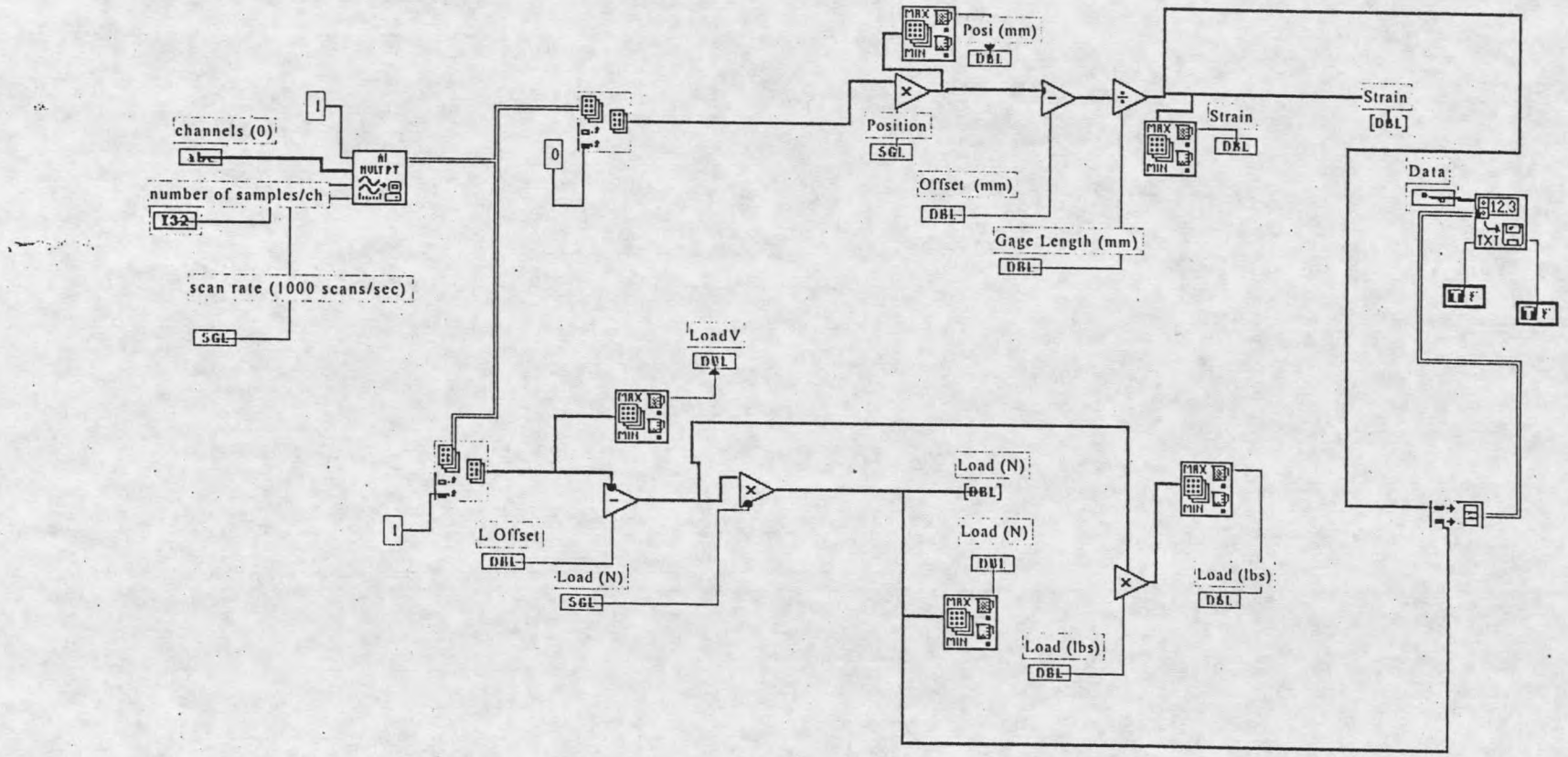
Data Acquisition Programs

Data Acquisition Program for Tensile Testing



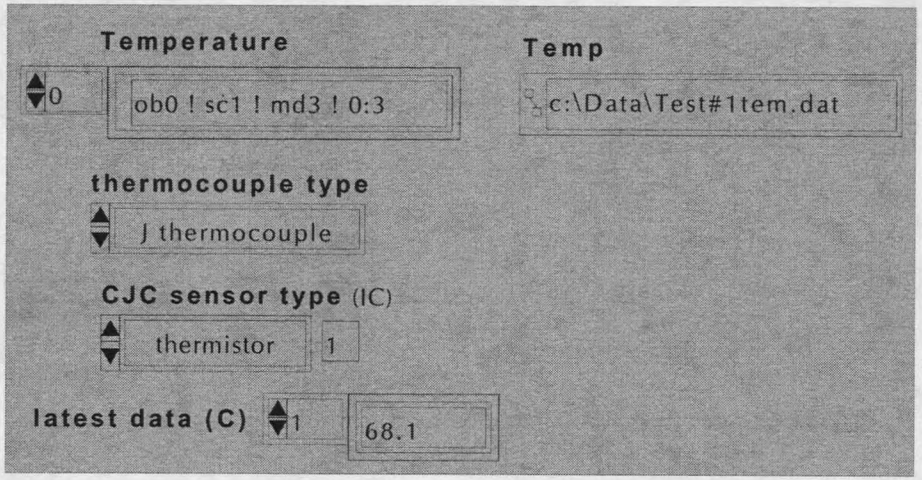
Last modified on 6/1/2000 at 2:42 PM
Printed on 7/18/2000 at 5:38 PM

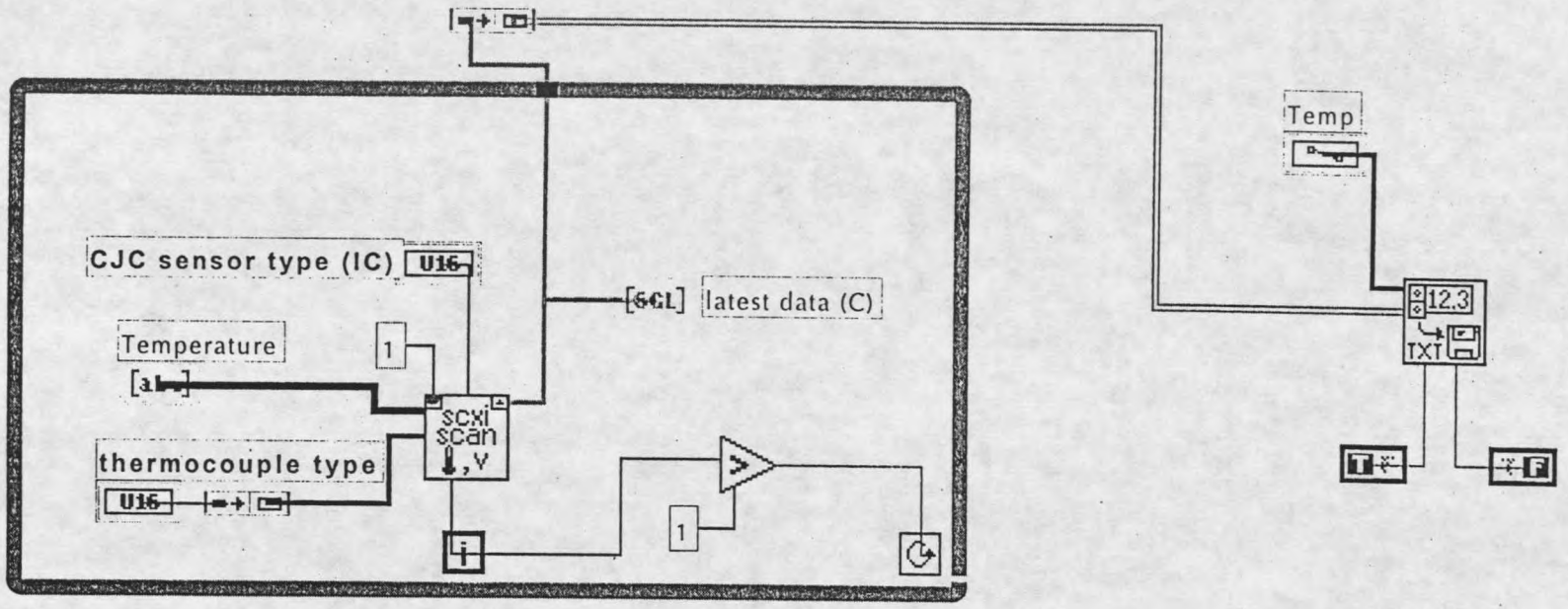



channels (0)
abc
number of samples/ch
I32
scan rate (1000 scans/sec)
SGL
1
AI MULTPT
0
Posi (mm)
DBL
Position
SGL
Offset (mm)
DBL
Gage Length (mm)
DBL
Strain
DBL
Strain
DBL
Data
12.3
TXT
TF
TF
LoadV
DBL
1
L Offset
DBL
Load (N)
SGL
Load (N)
DBL
Load (N)
DBL
Load (lbs)
DBL
Load (lbs)
DBL

Data Acquisition Program for Temperature Measurement During Tensile Testing

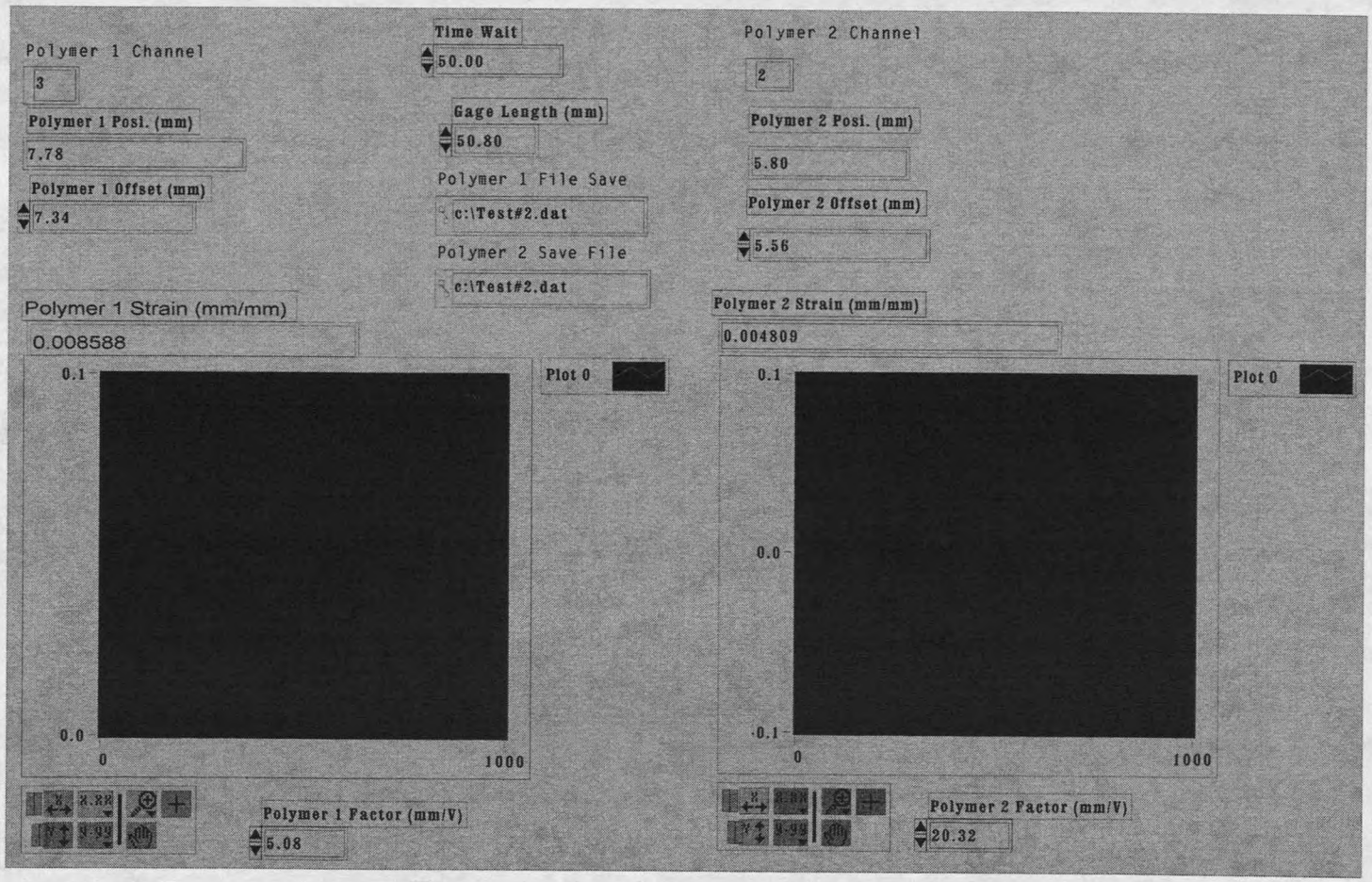
Last modified on 6/1/2000 at 4:17 PM
Printed on 7/18/2000 at 5:48 PM

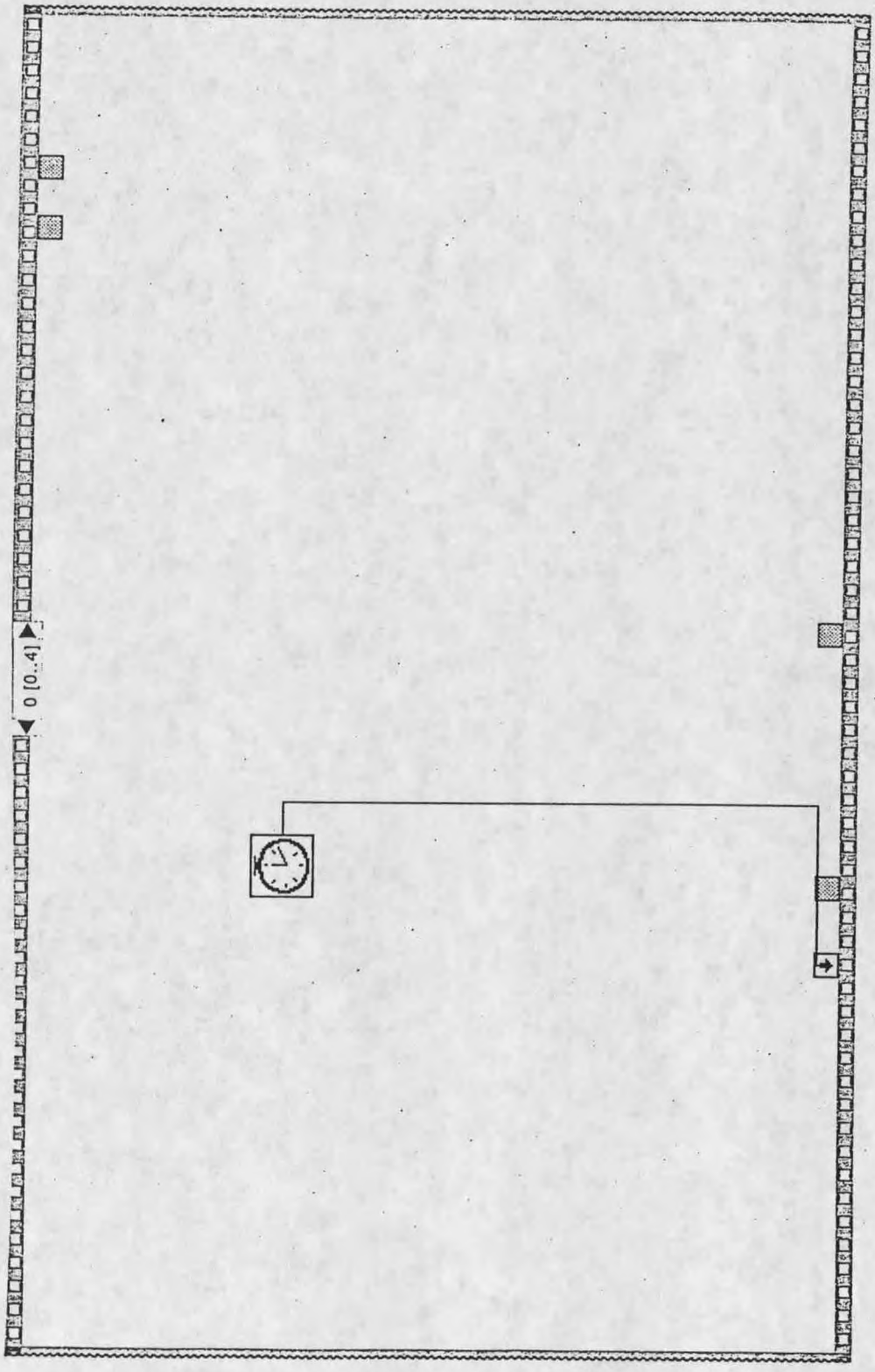


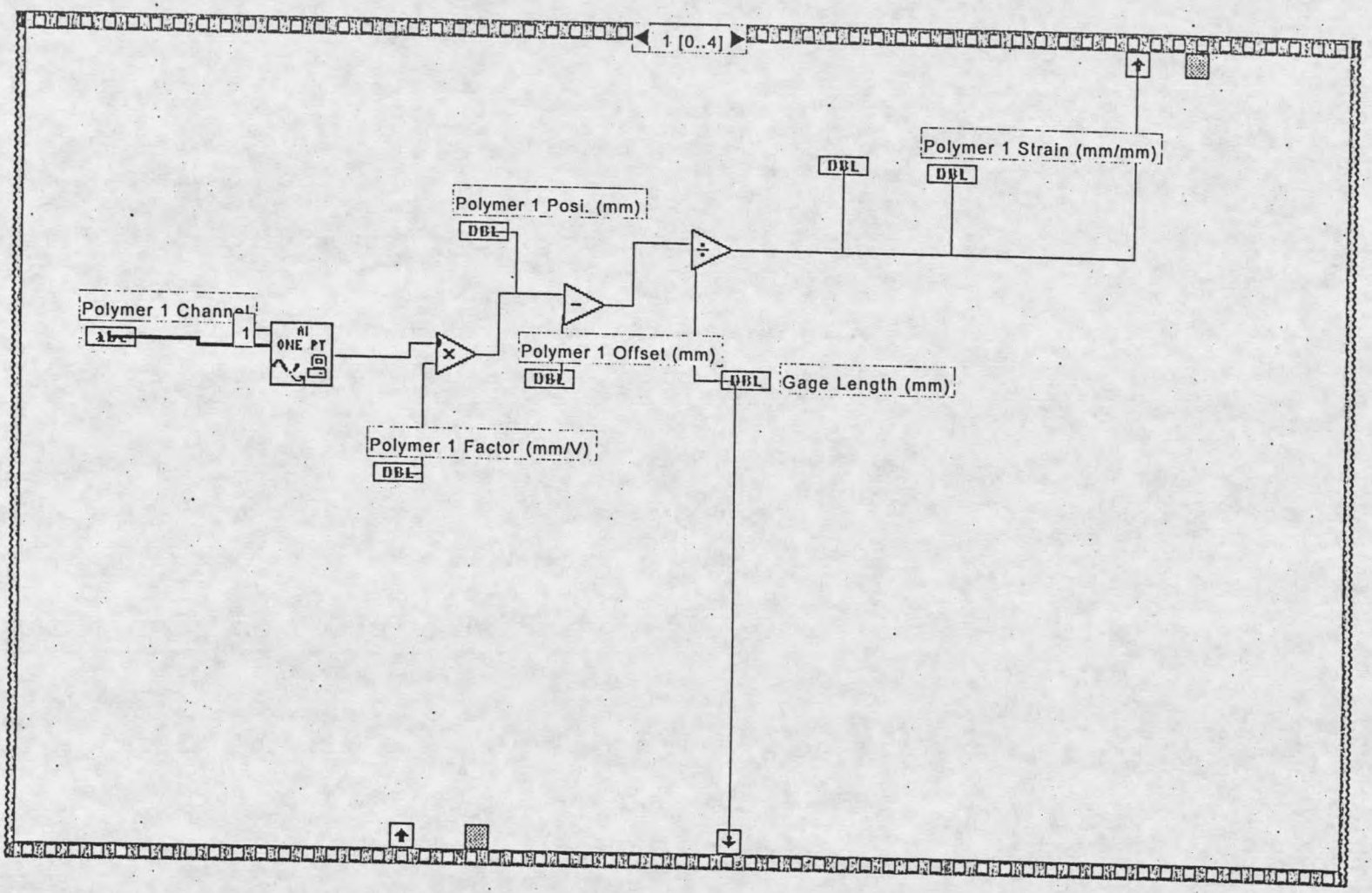

CJC sensor type (IC)
U16
Temperature
thermocouple type
U16
1
scxi
scan
,V
[SGL]
latest data (C)
1
Temp
12.3
TXT
T
F

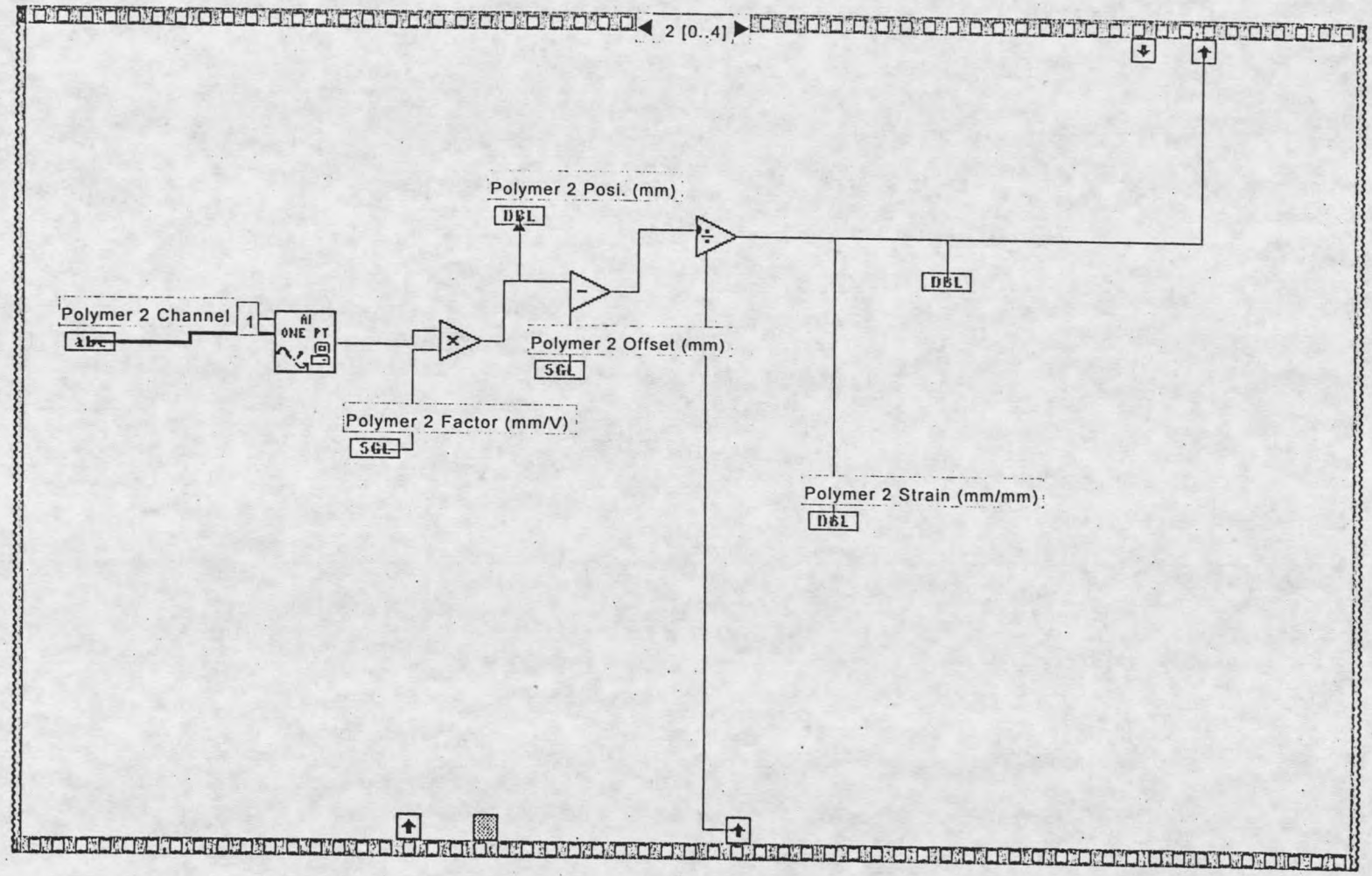
Data Acquisition Program for Constant Load Creep Testing of Solid Polymers

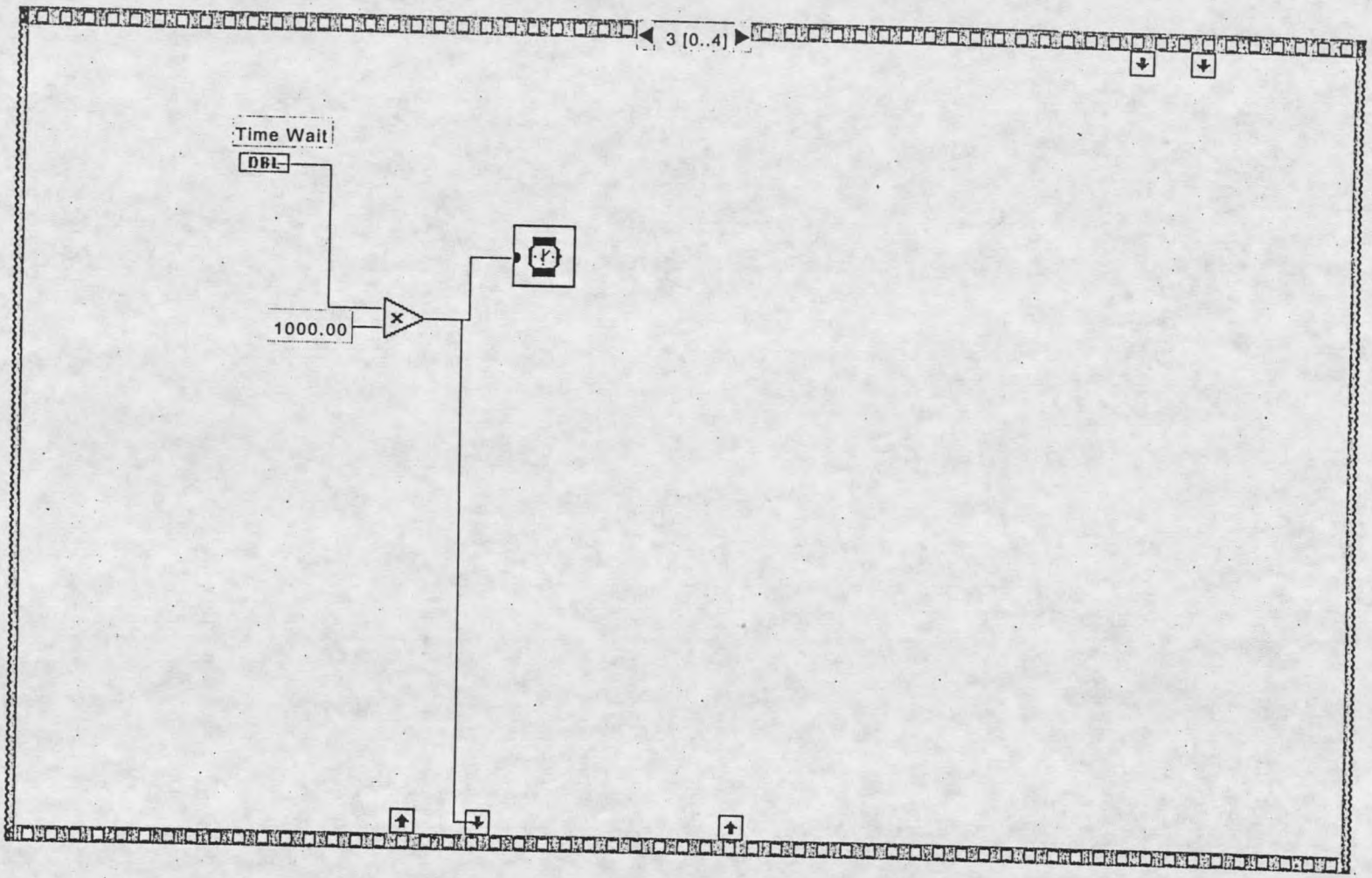
Last modified on 6/1/2000 at 1:47 PM
Printed on 7/18/2000 at 5:51 PM

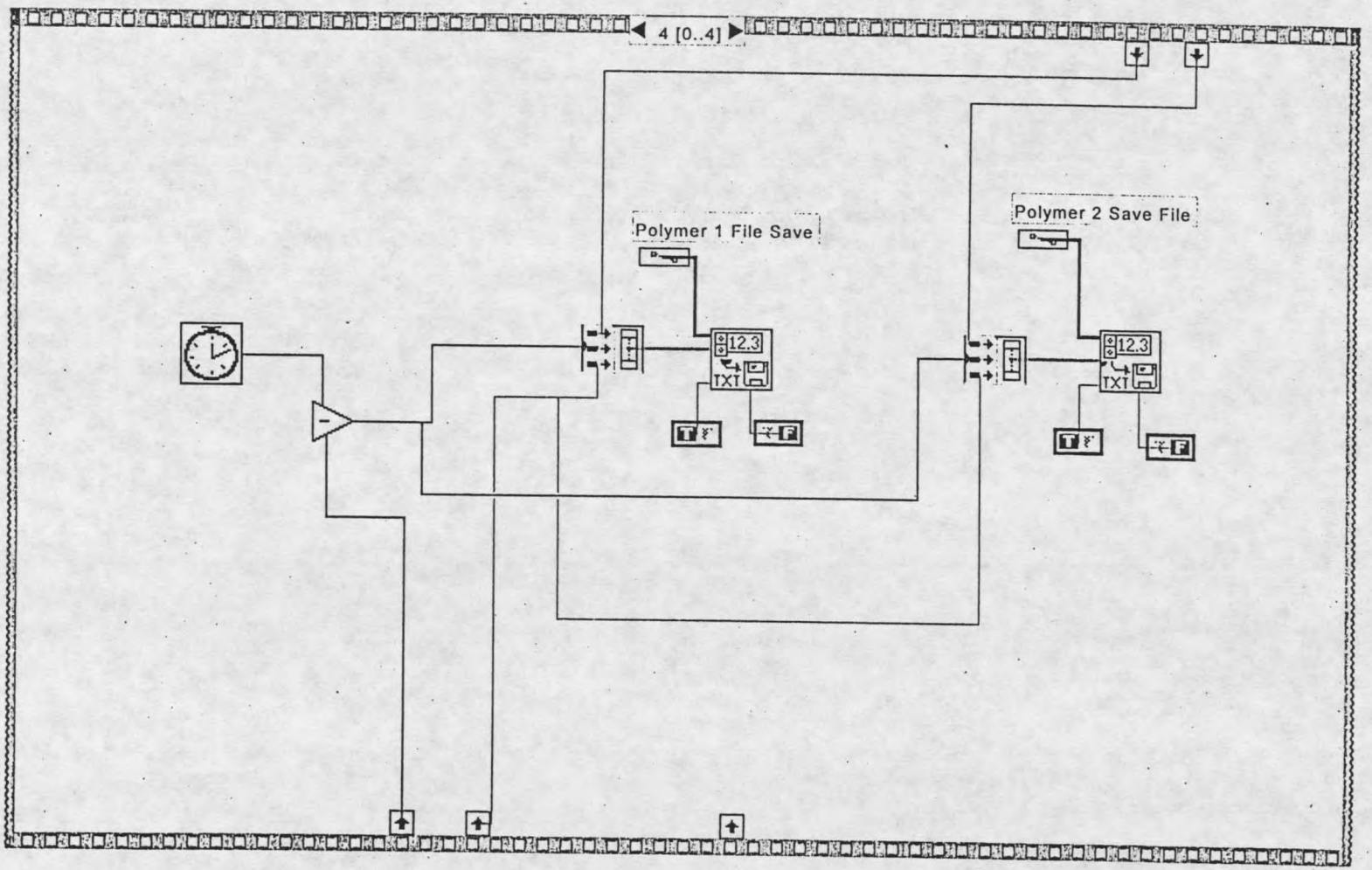



0 [0..4]


1 [0..4]
Polymer 1 Strain (mm/mm)
DBL
DBL
Polymer 1 Posi. (mm)
DBL
Polymer 1 Channel
abc
1
AI
ONE PT
Polymer 1 Offset (mm)
DBL
DBL
Gage Length (mm)
Polymer 1 Factor (mm/V)
DBL

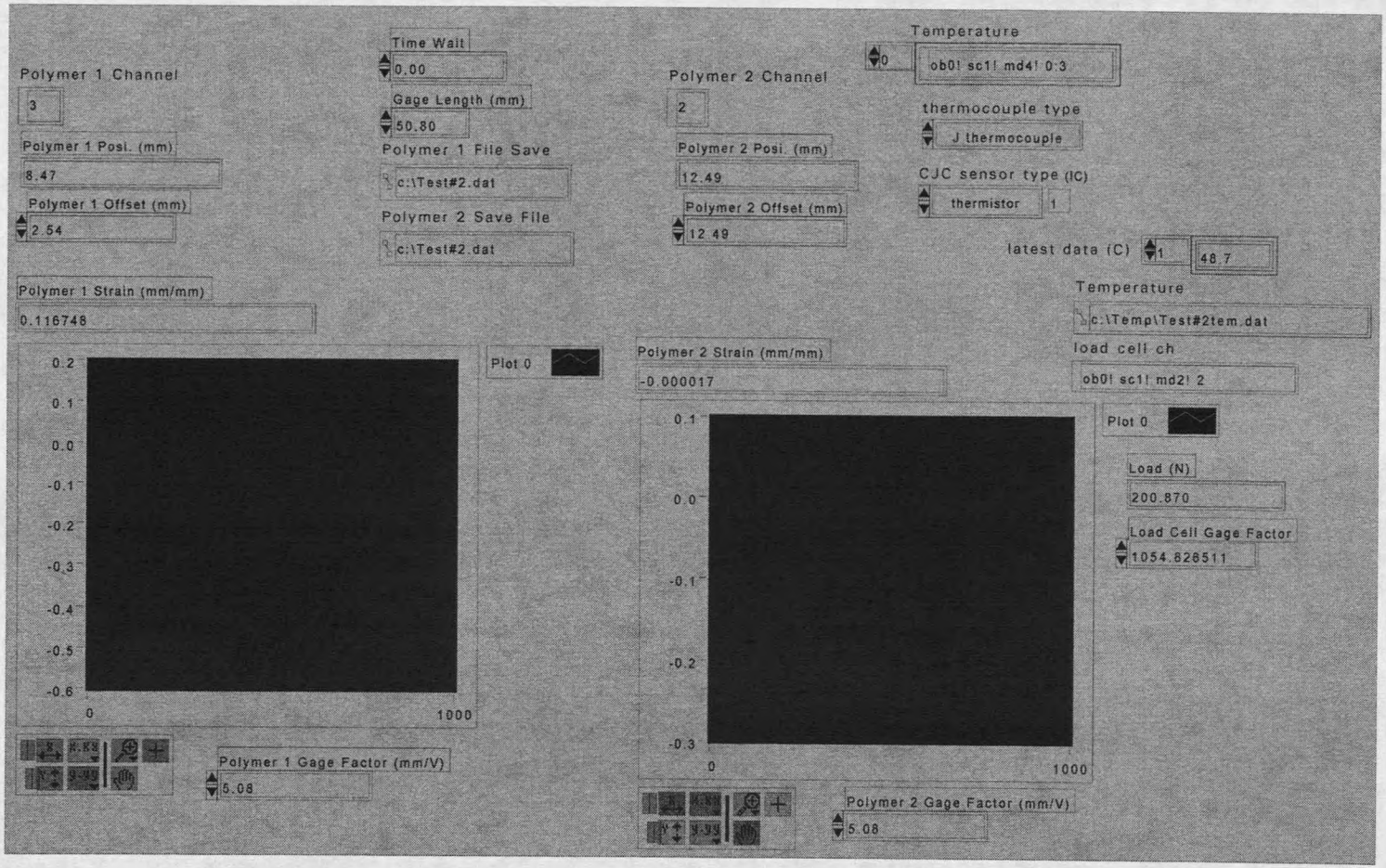

2 [0..4]
Polymer 2 Posi. (mm)
DBL
Polymer 2 Channel
1
abc
AI
ONE PT
Polymer 2 Offset (mm)
SGL
Polymer 2 Factor (mm/V)
SGL
DBL
Polymer 2 Strain (mm/mm)
DBL

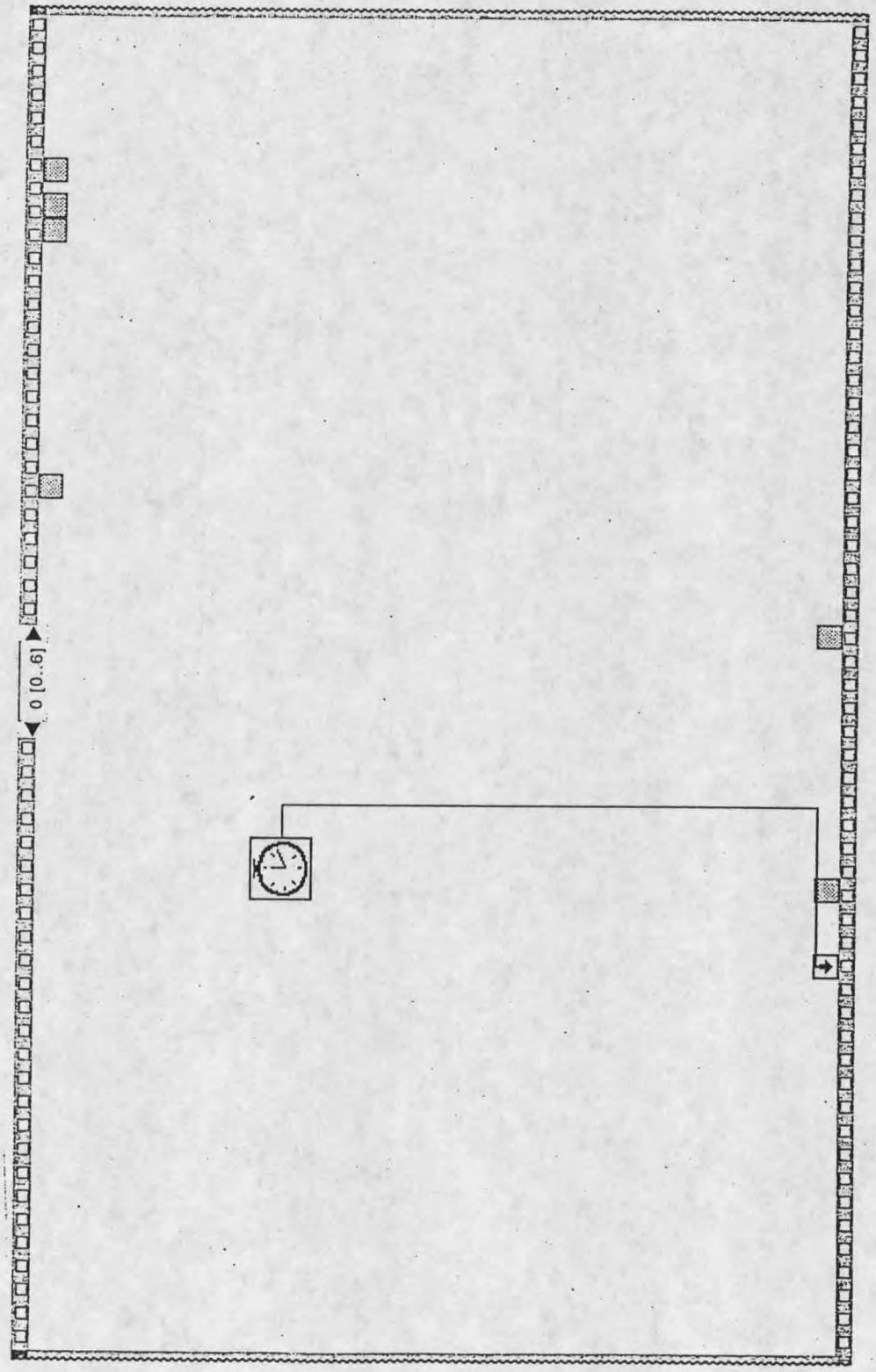

3 [0..4]
Time Wait
DBL
1000.00

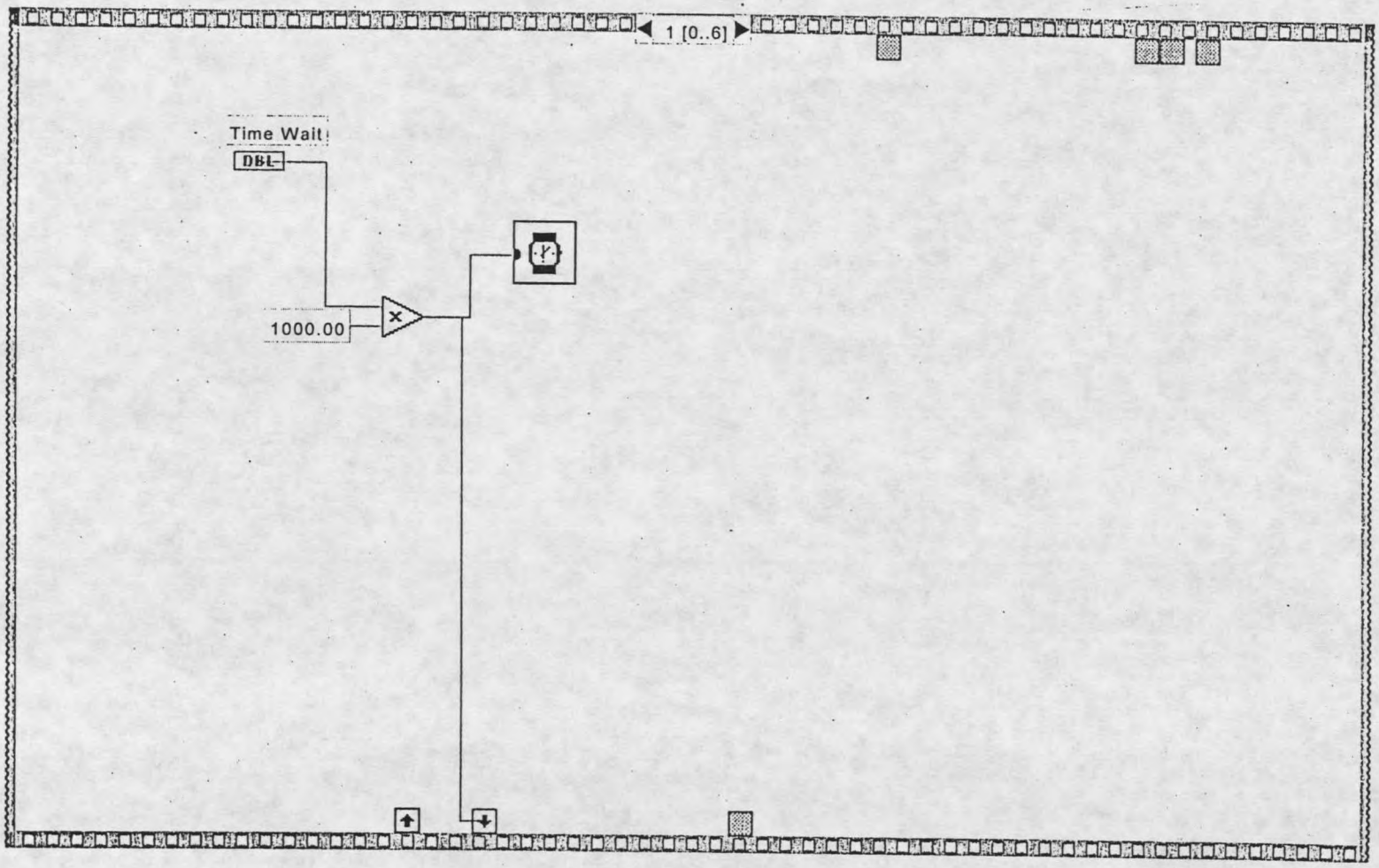

4 [0..4]
Polymer 1 File Save
Polymer 2 Save File
12.3
TXT
12.3
TXT

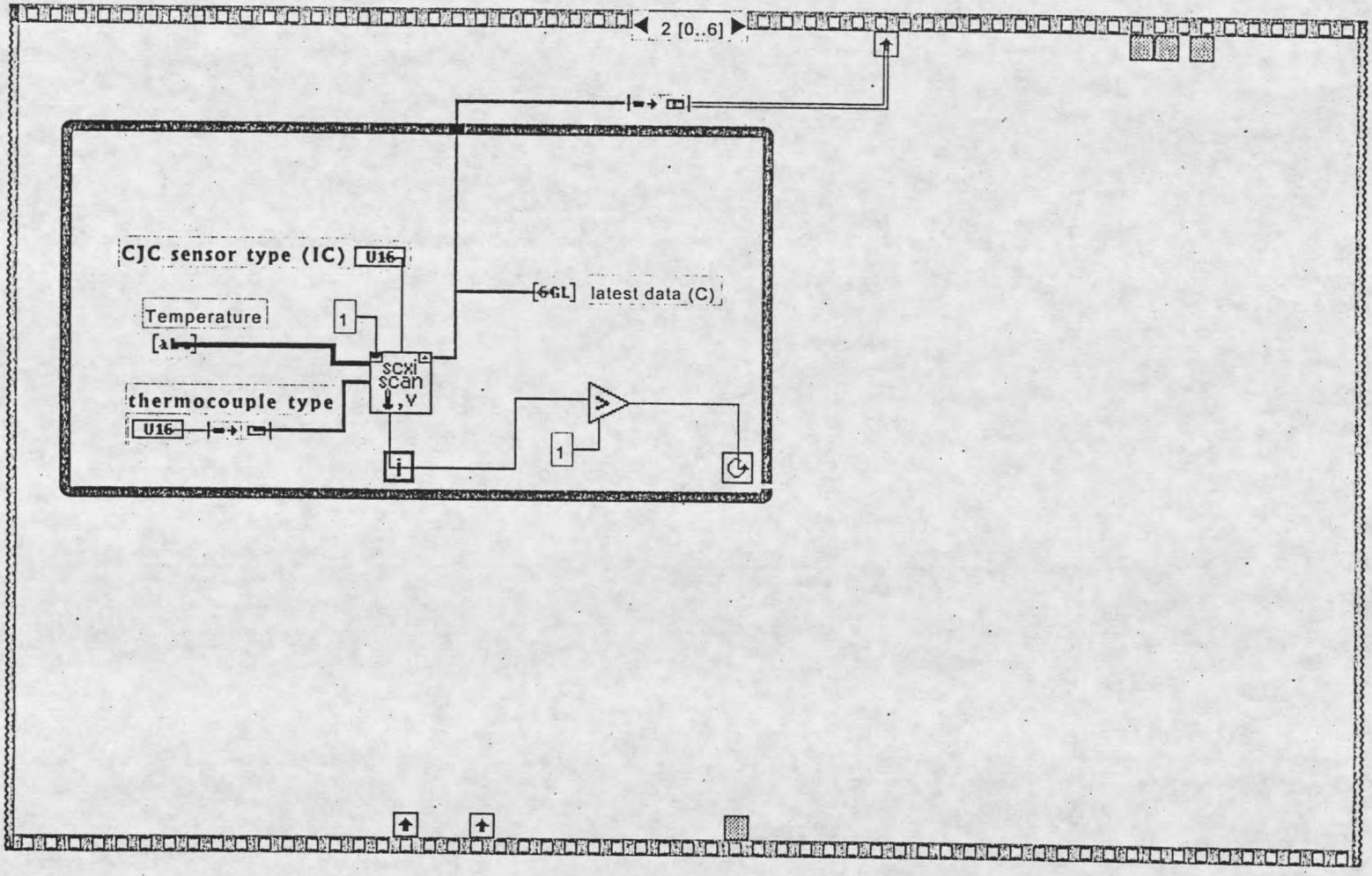
Data Acquisition Program for Constant Load Creep Testing of Solid Polymers with a Load Cell

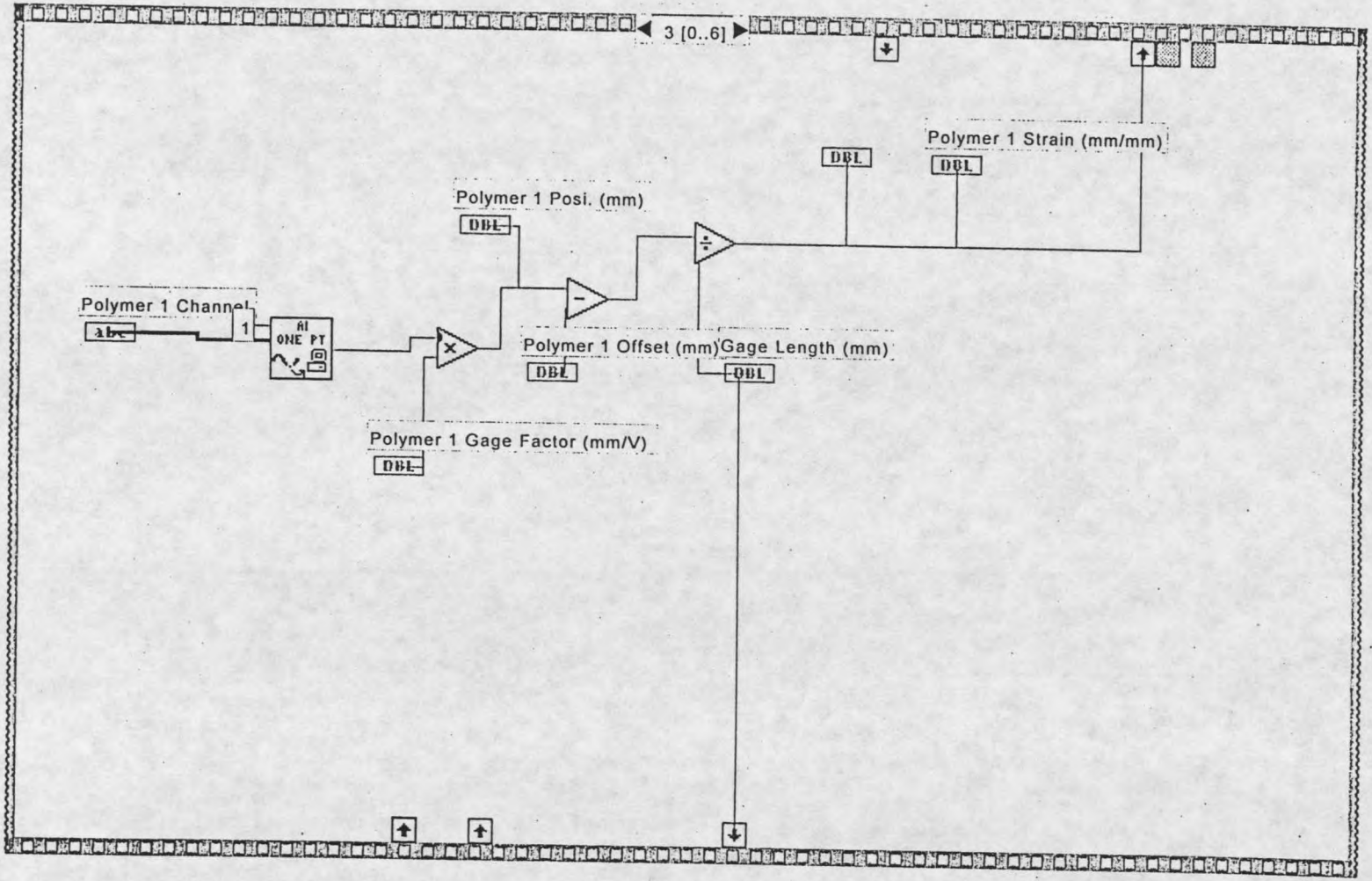
Last modified on 6/1/2000 at 2:43 PM
Printed on 7/18/2000 at 5:50 PM

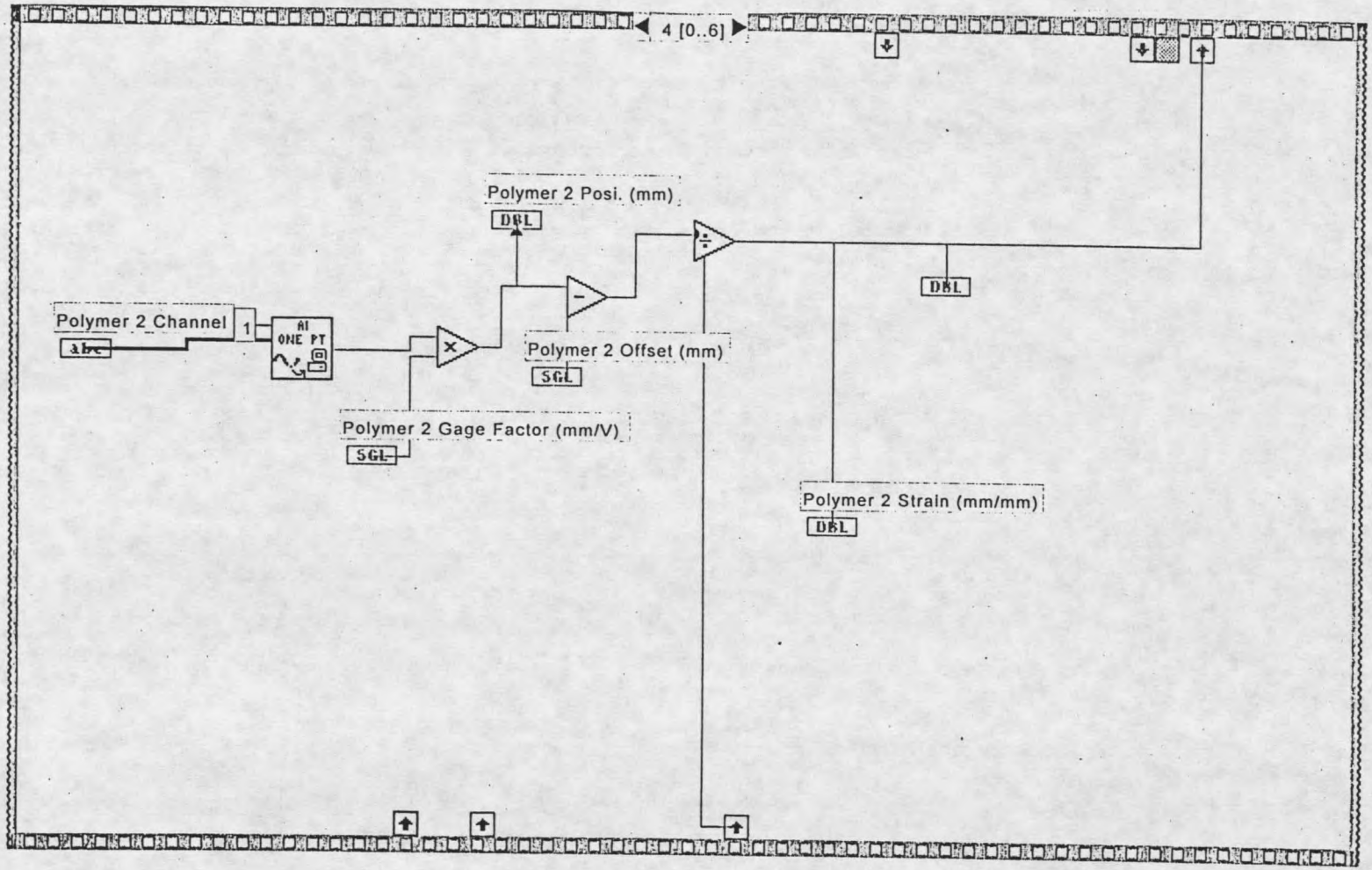


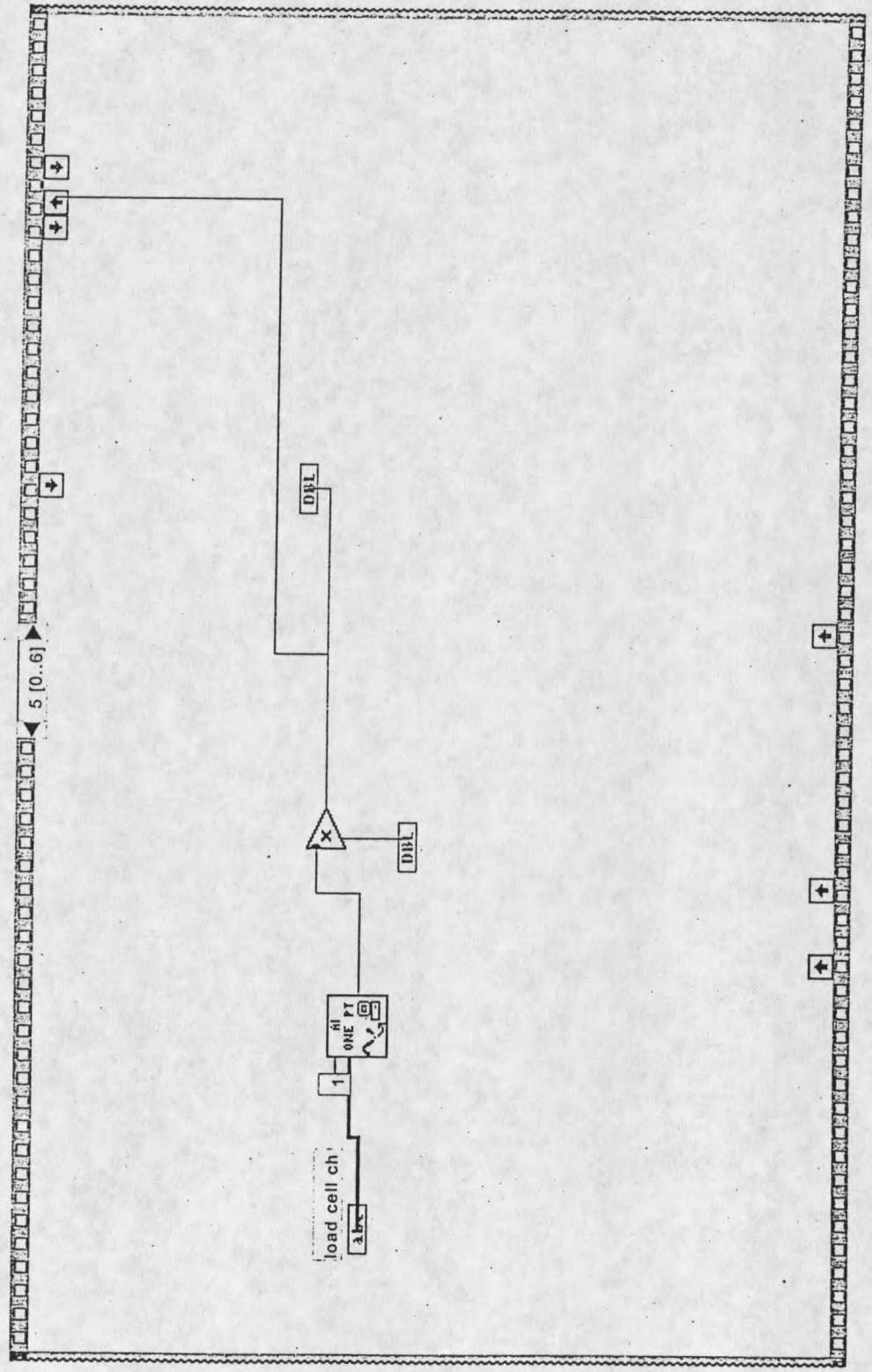

0 [0..6]

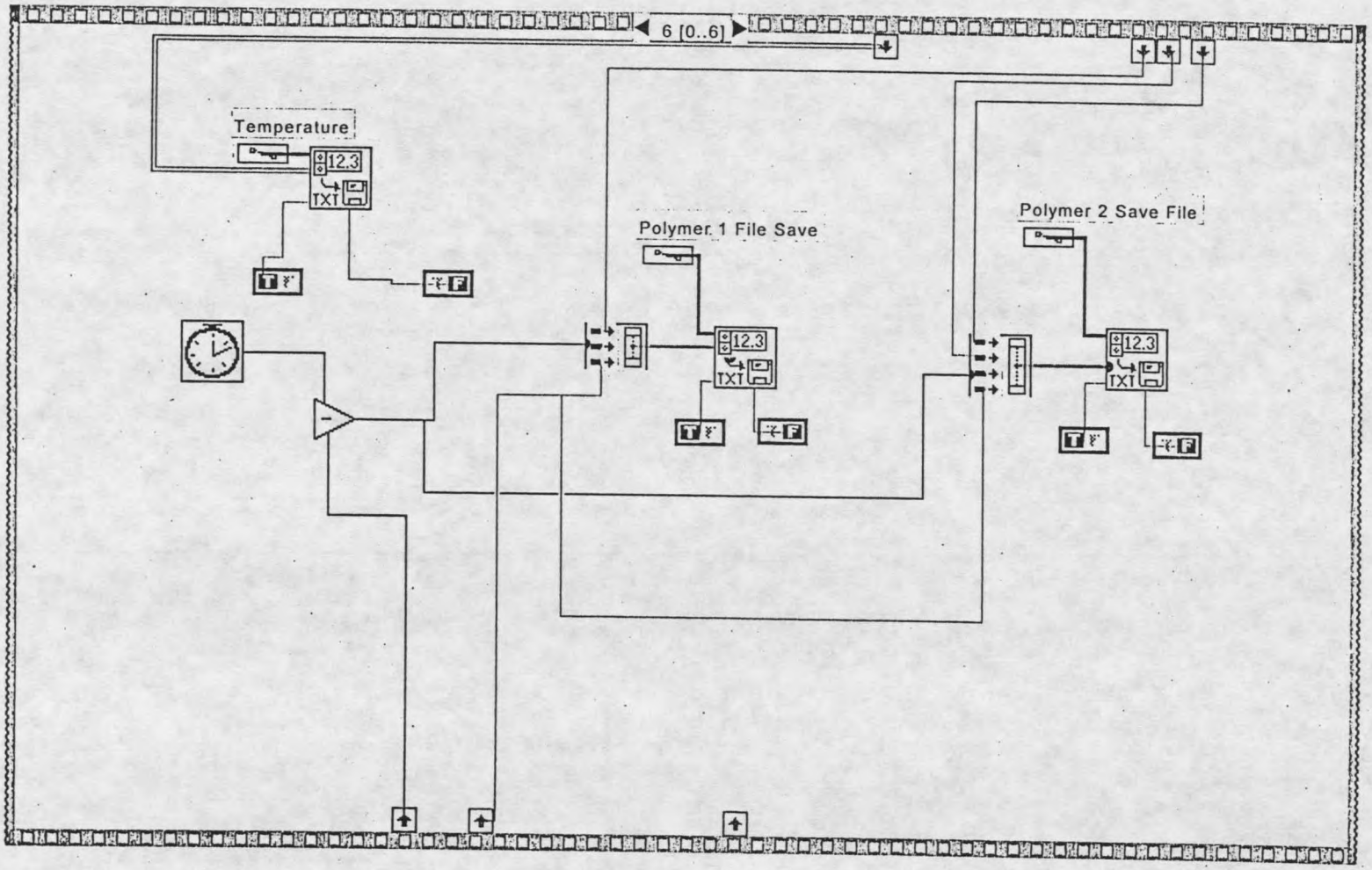

1 [0..6]
Time Wait
DBL
1000.00


2 [0..6]
CJC sensor type (IC)
U16
Temperature
1
[6GL] latest data (C)
scxi
scan
,V
thermocouple type
U16
i
1


3 [0..6]
Polymer 1 Strain (mm/mm)
DBL
DBL
Polymer 1 Posi. (mm)
DBL
Polymer 1 Channel
abc
1
AI
ONE PT
Polymer 1 Offset (mm)
DBL
Gage Length (mm)
DBL
Polymer 1 Gage Factor (mm/V)
DBL

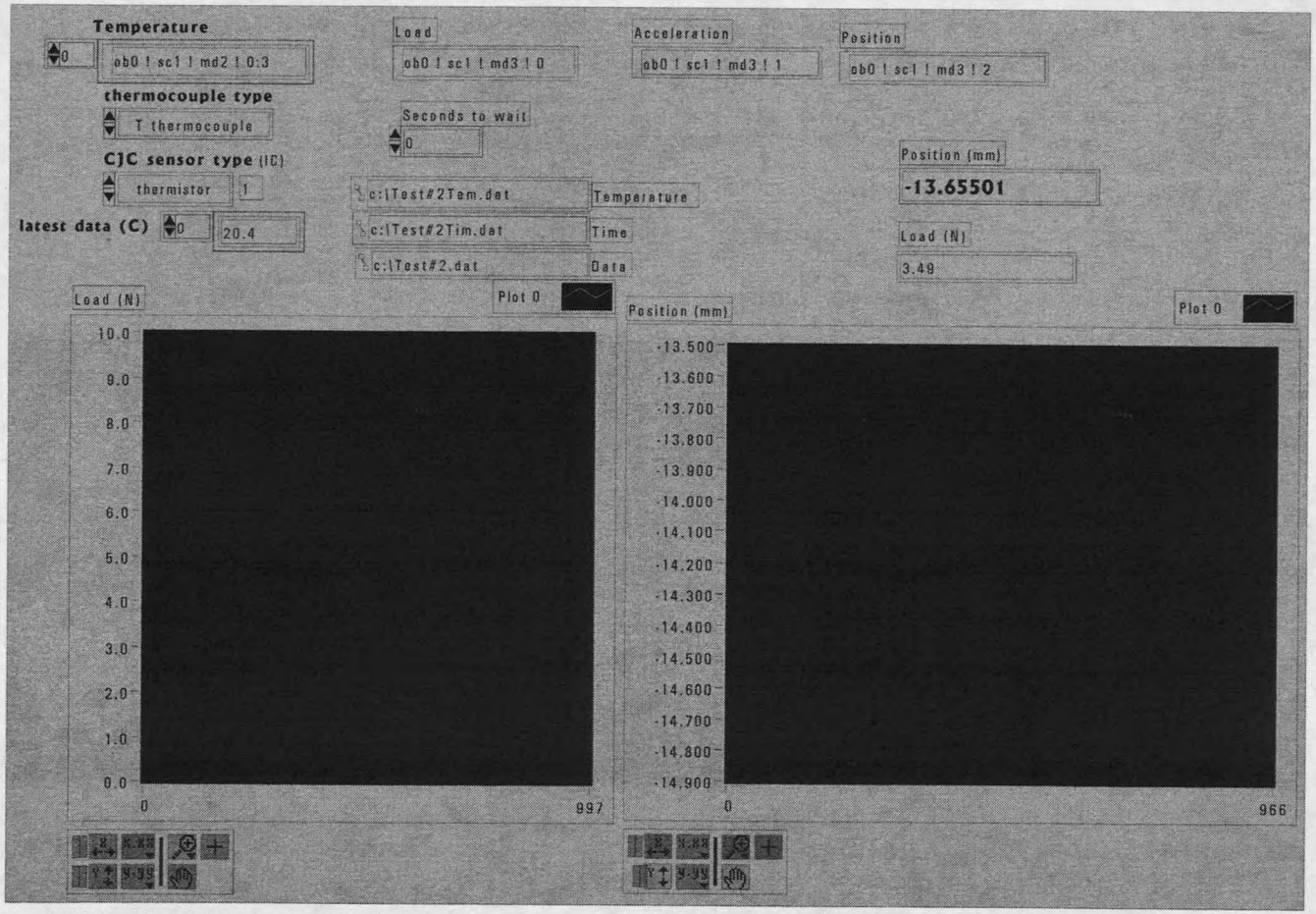

4 [0..6]
Polymer 2 Posi. (mm)
DBL
Polymer 2 Channel
abc
1
AI
ONE PT
Polymer 2 Offset (mm)
SGL
Polymer 2 Gage Factor (mm/V)
SGL
DBL
Polymer 2 Strain (mm/mm)
DBL

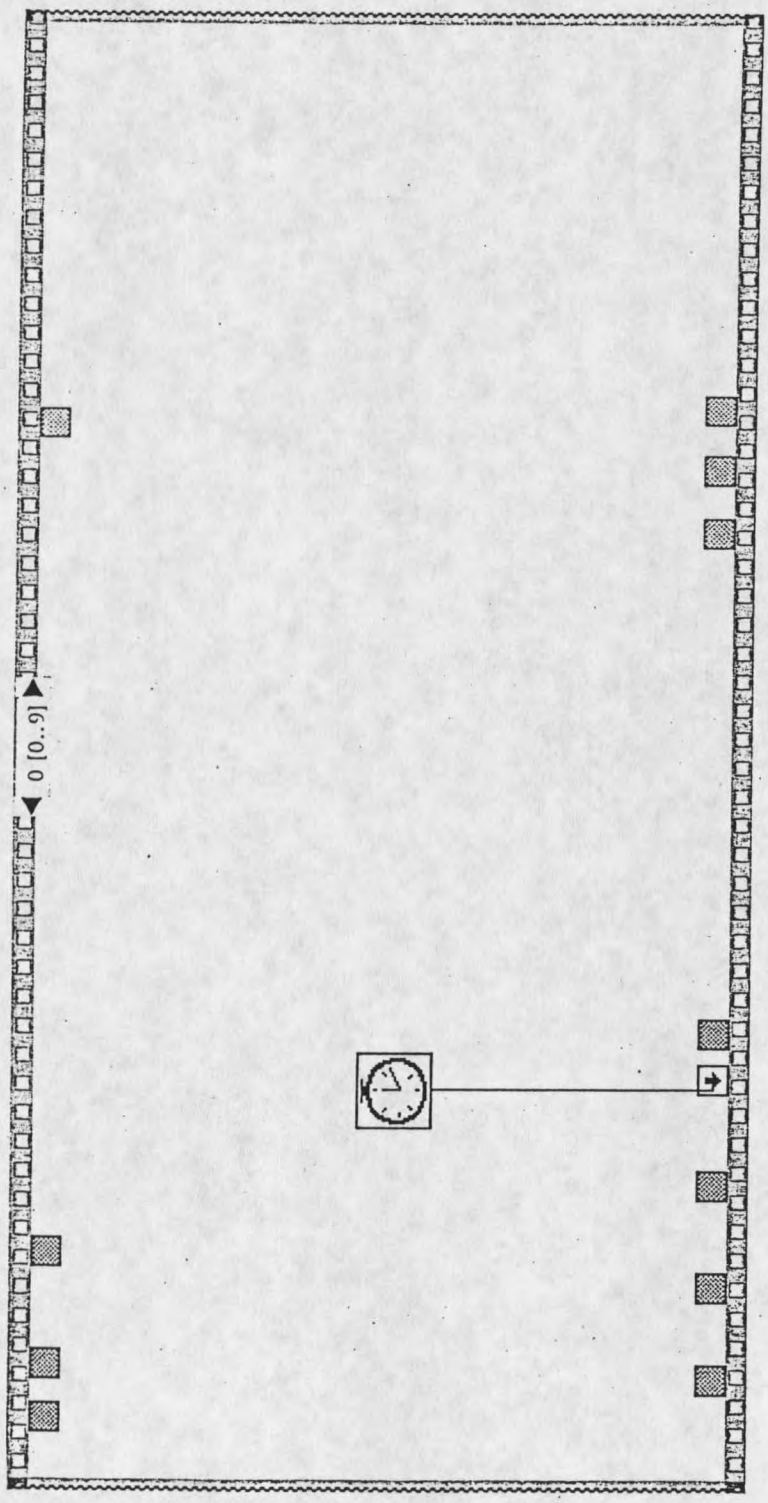

5 [0..6]
DBL
DBL
AI
ONE PT
1
load cell ch
abc

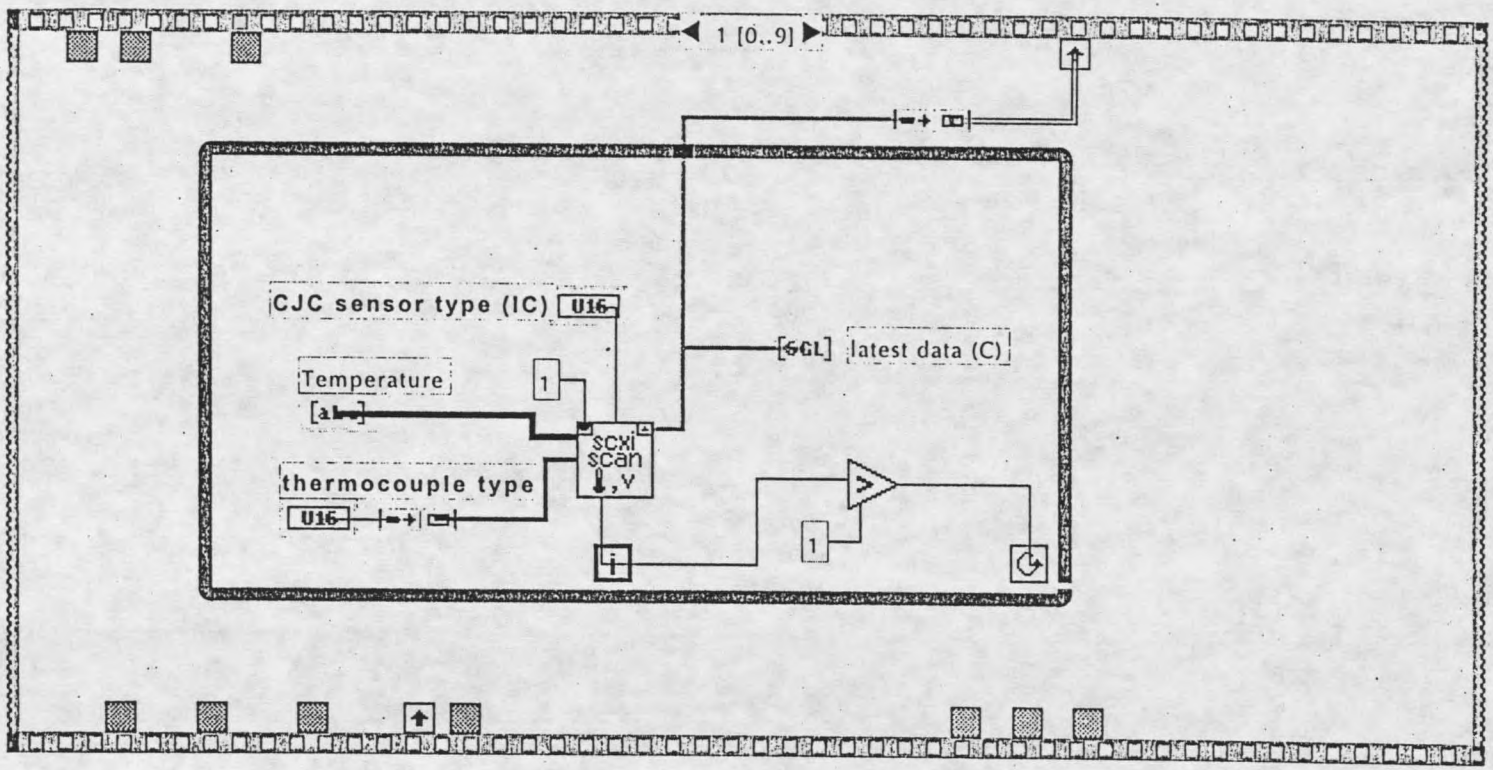

6 [0..6]
Temperature
12.3
TXT
Polymer 1 File Save
Polymer 2 Save File

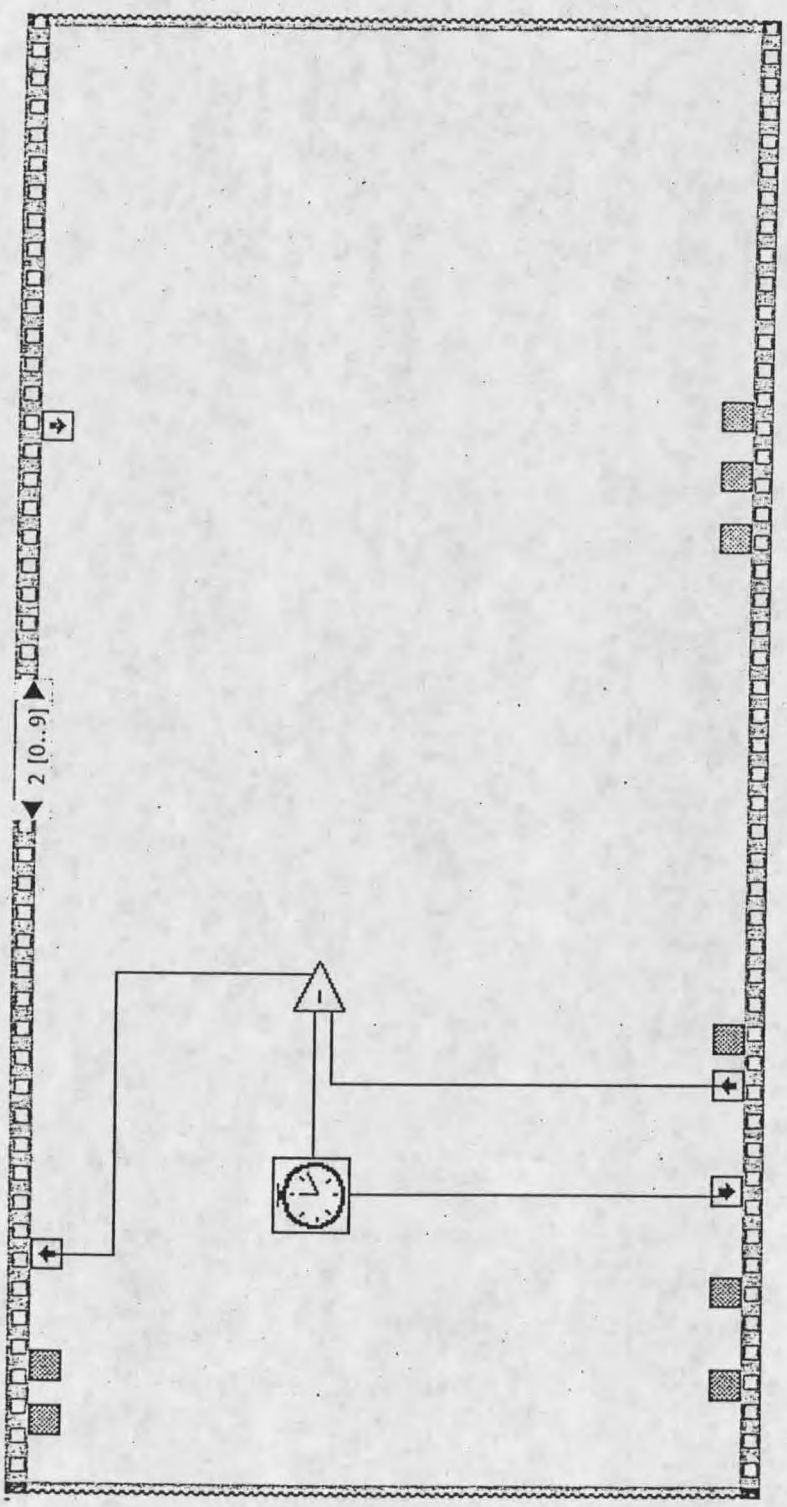
Data Acquisition Program for Constant Load Creep Testing of Thin Films

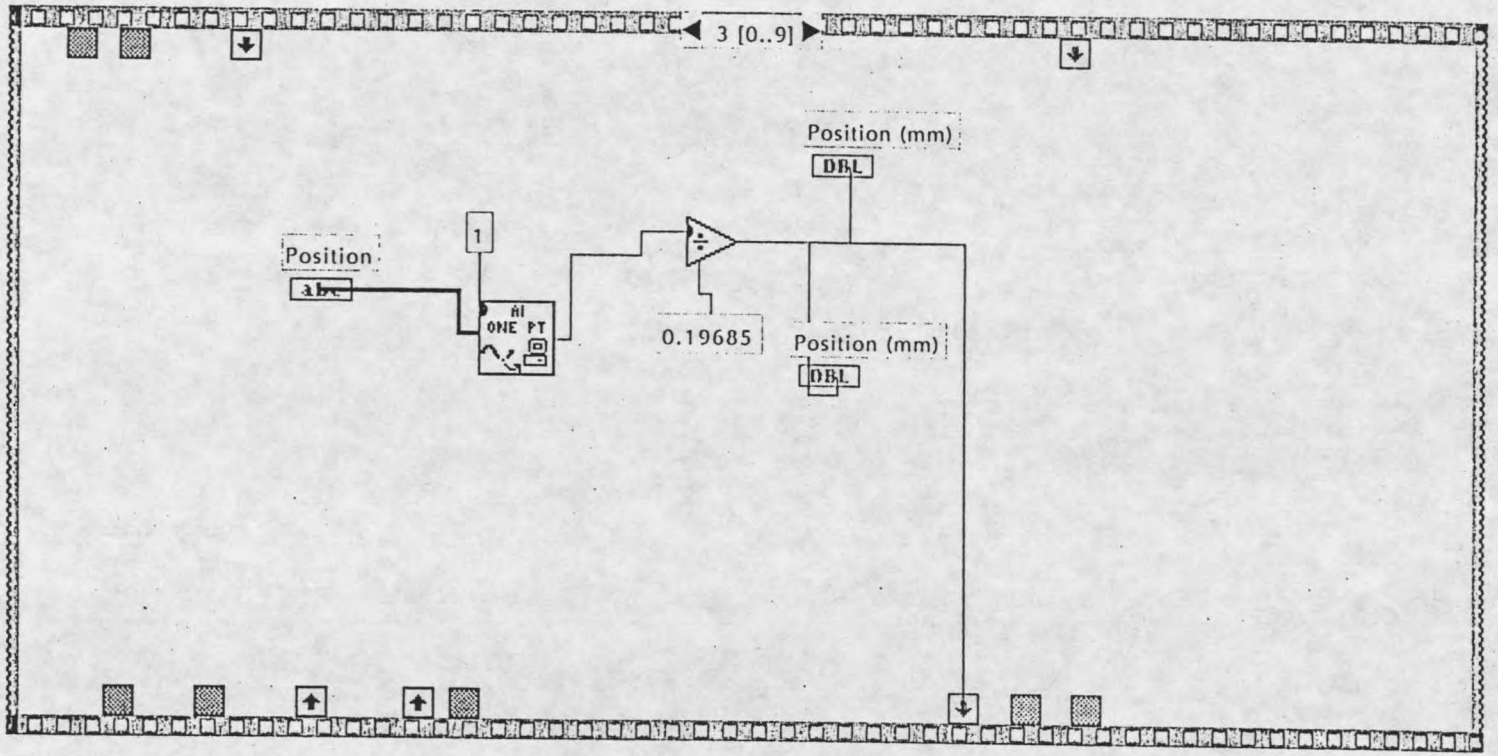
Last modified on 6/1/2000 at 2:45 PM
Printed on 7/18/2000 at 5:51 PM

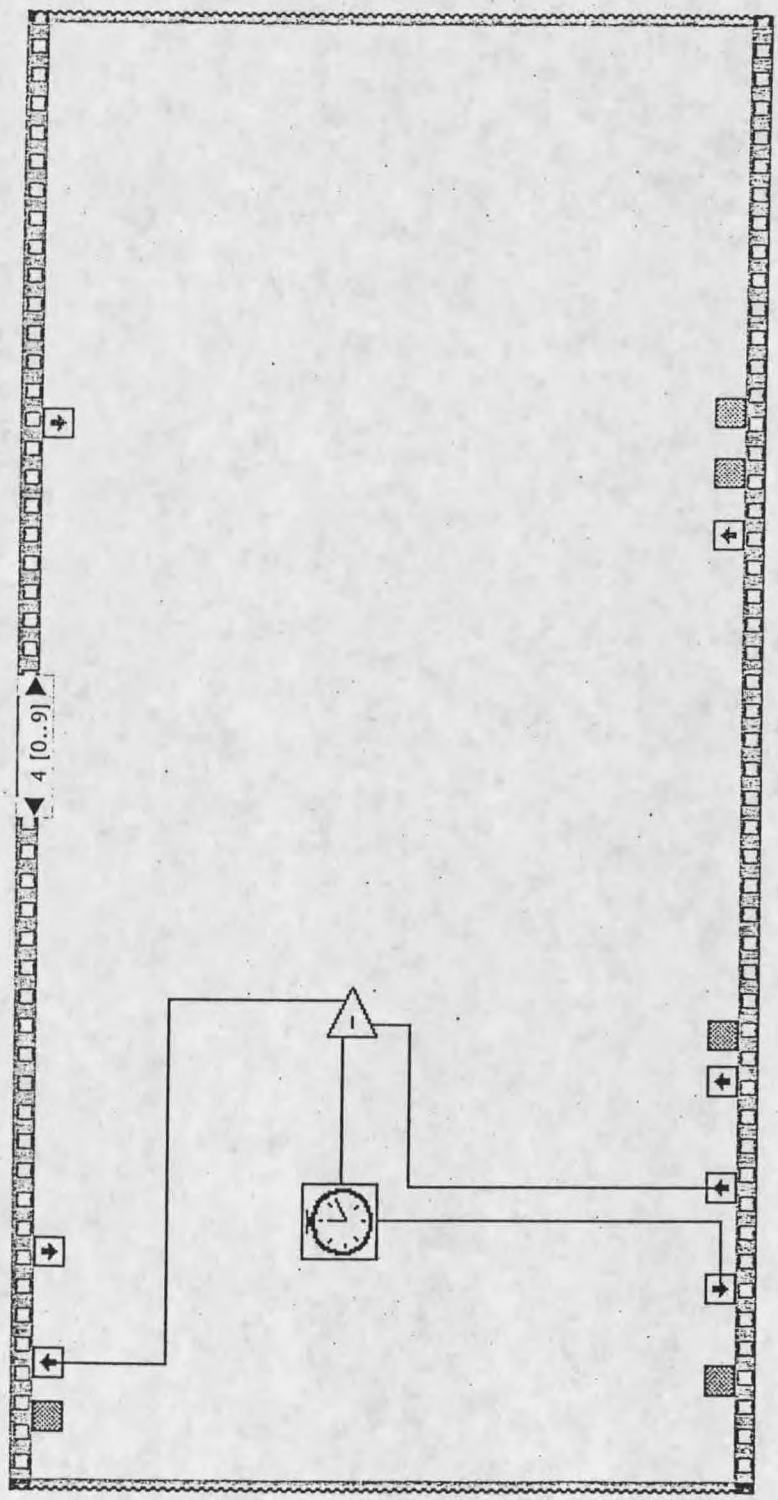


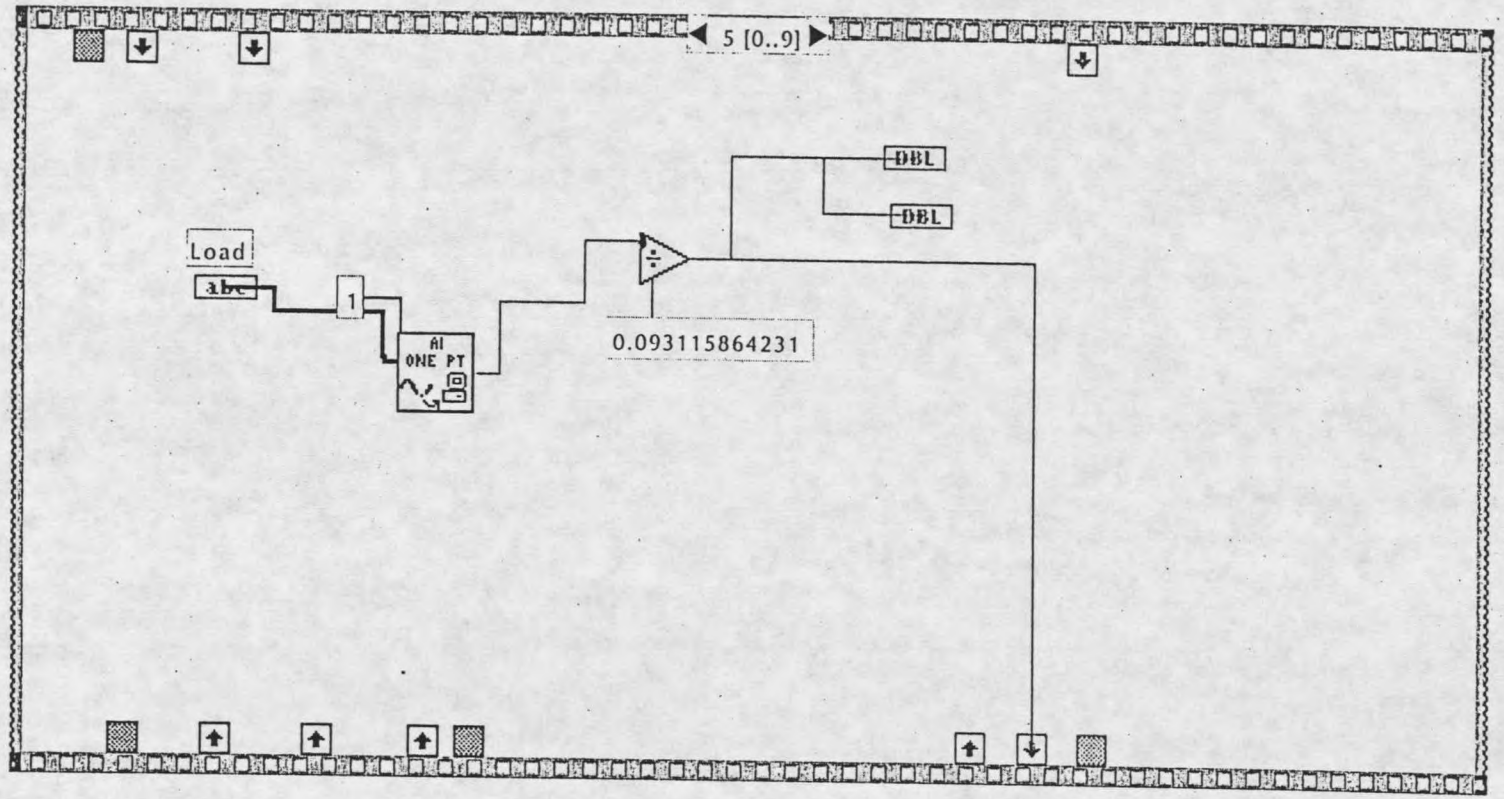

0 [0..9]

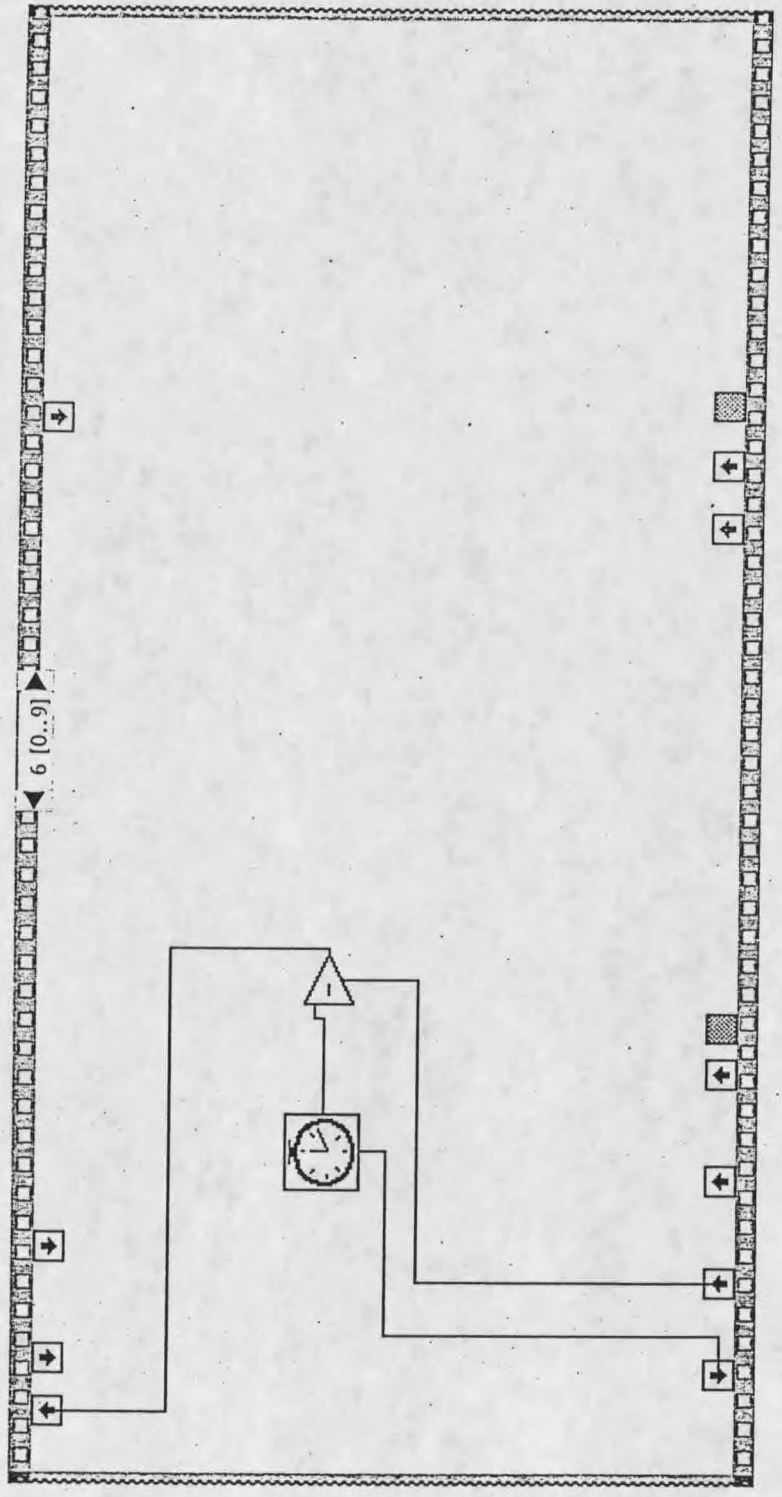

1 [0..9]
CJC sensor type (IC)
U16
Temperature
1
[a
thermocouple type
U16
SCXI
scan
,V
i
[SGL]
latest data (C)
1

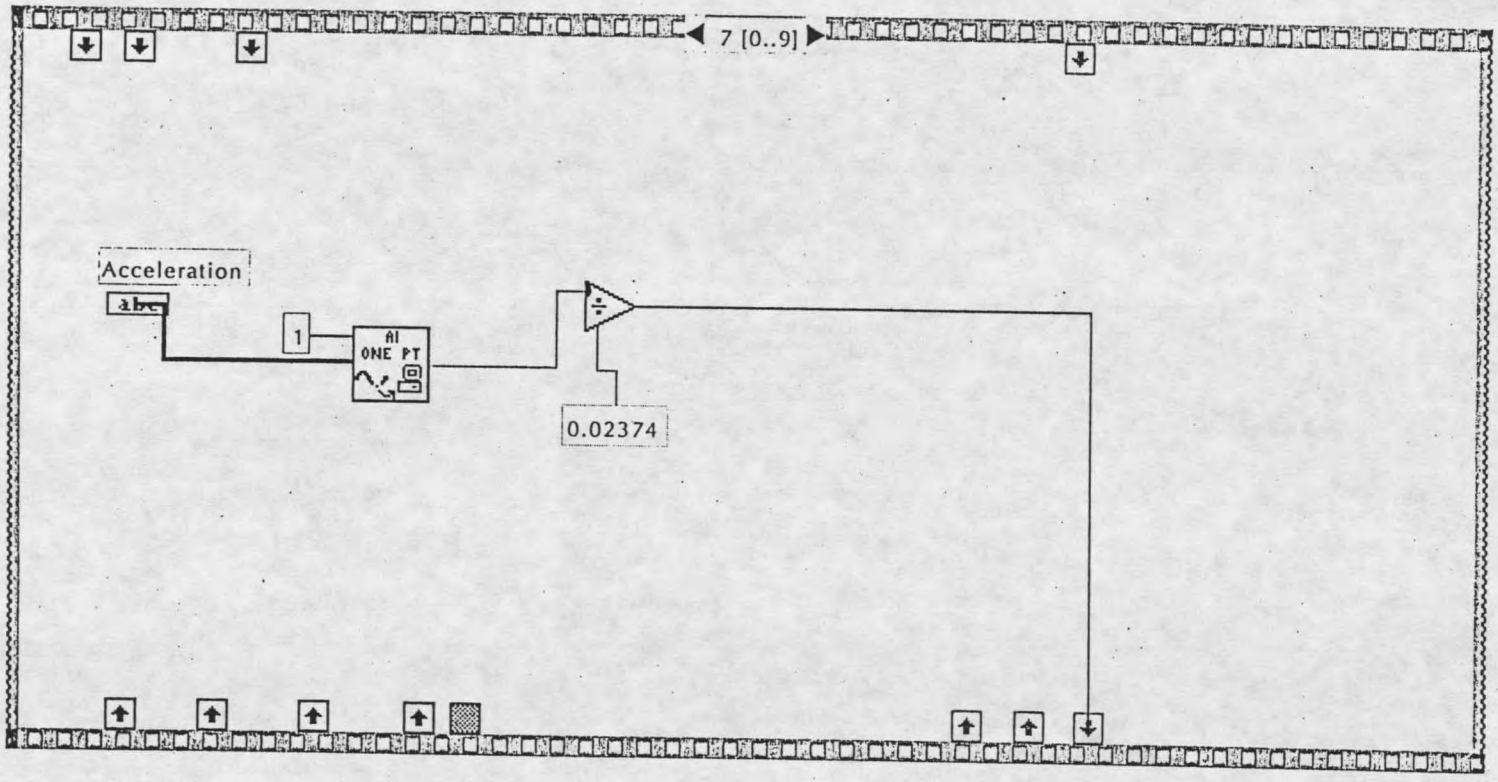

2 [0..9]
1

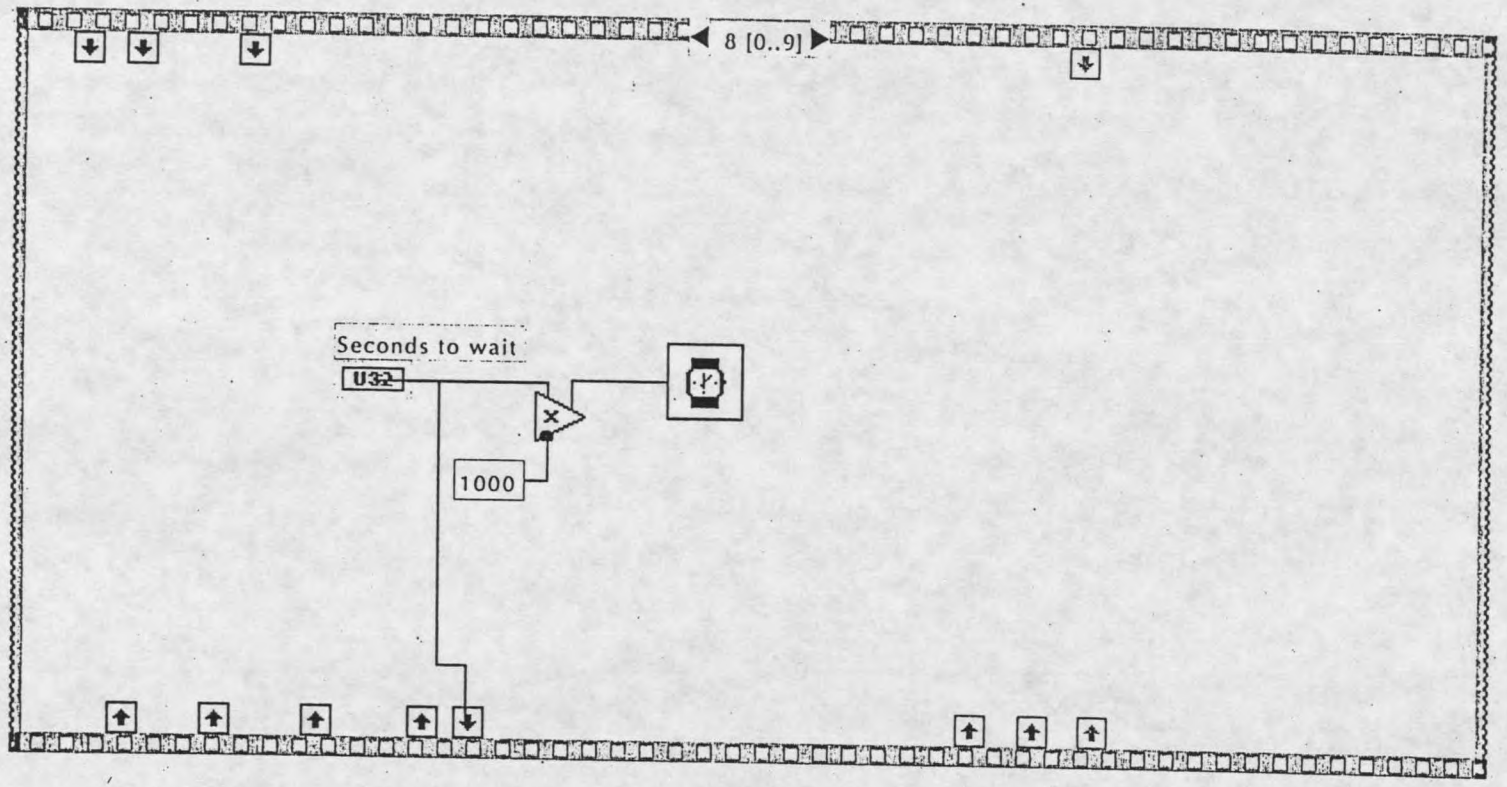

3 [0..9]
Position (mm)
DBL
Position
abc
1
AI
ONE PT
0.19685
Position (mm)
DBL

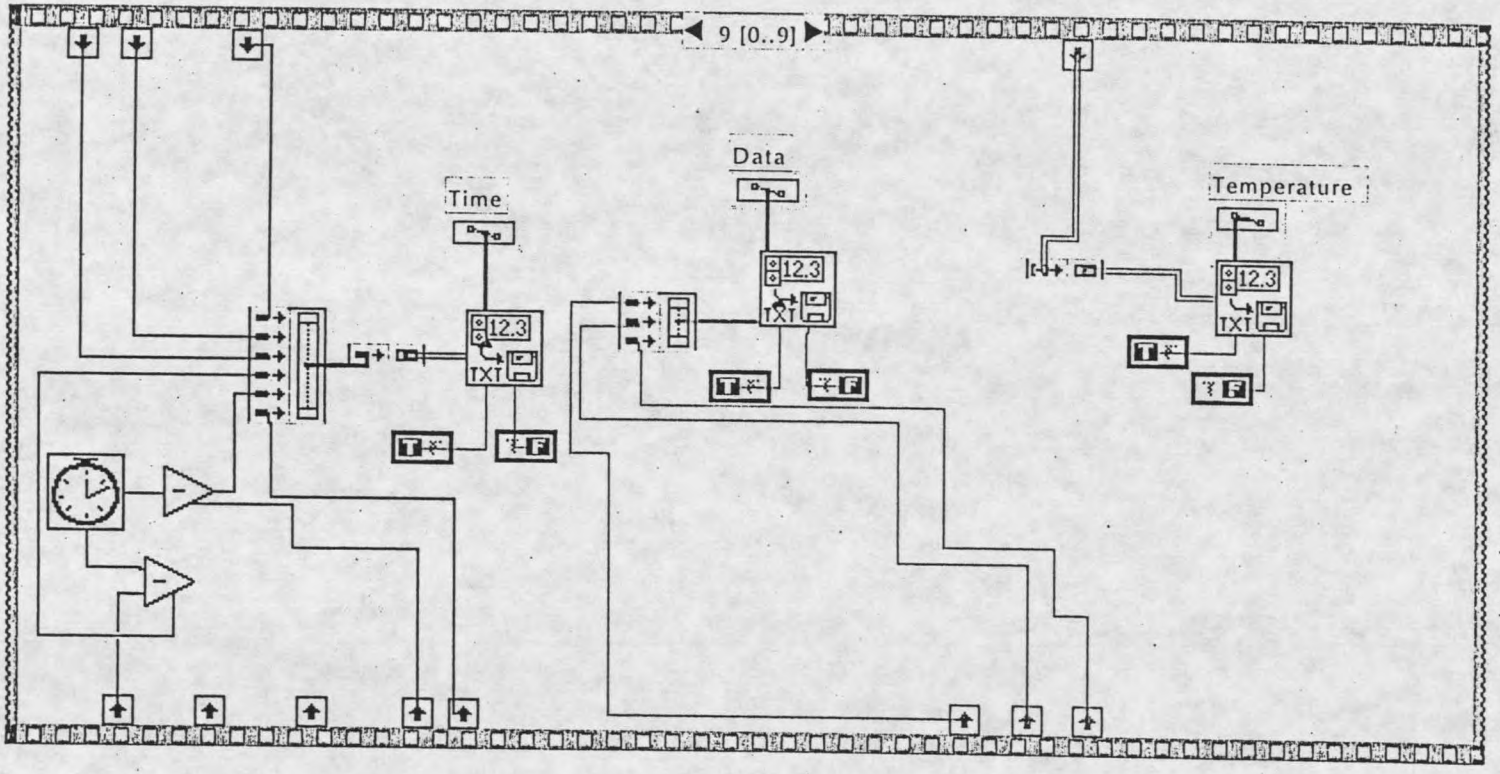

4 [0..9]
1


5 [0..9]
DBL
DBL
Load
abc
1
AI
ONE PT
0.093115864231


6 [0..9]

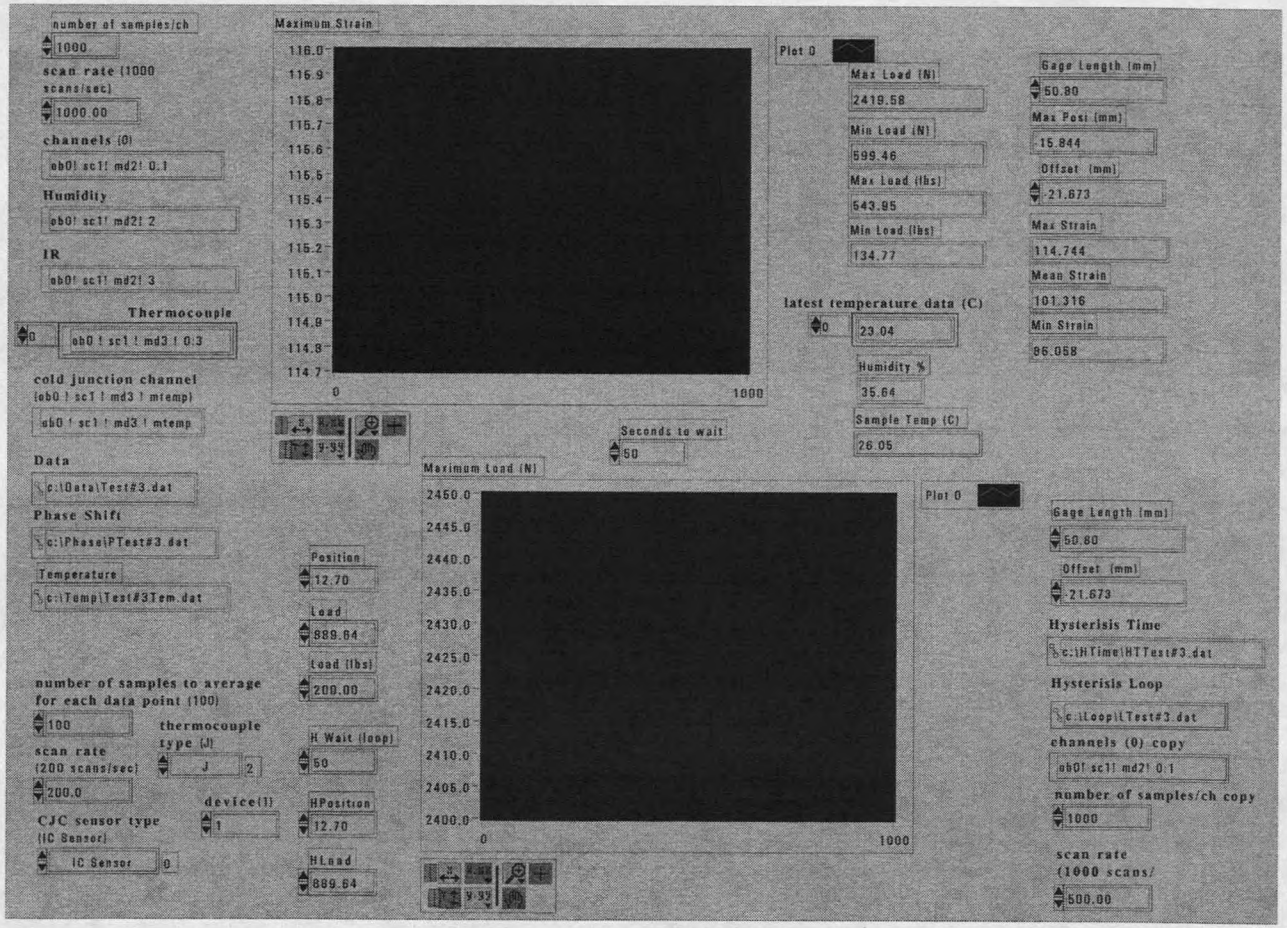

7 [0..9]
Acceleration
abc
1
AI
ONE PT
0.02374

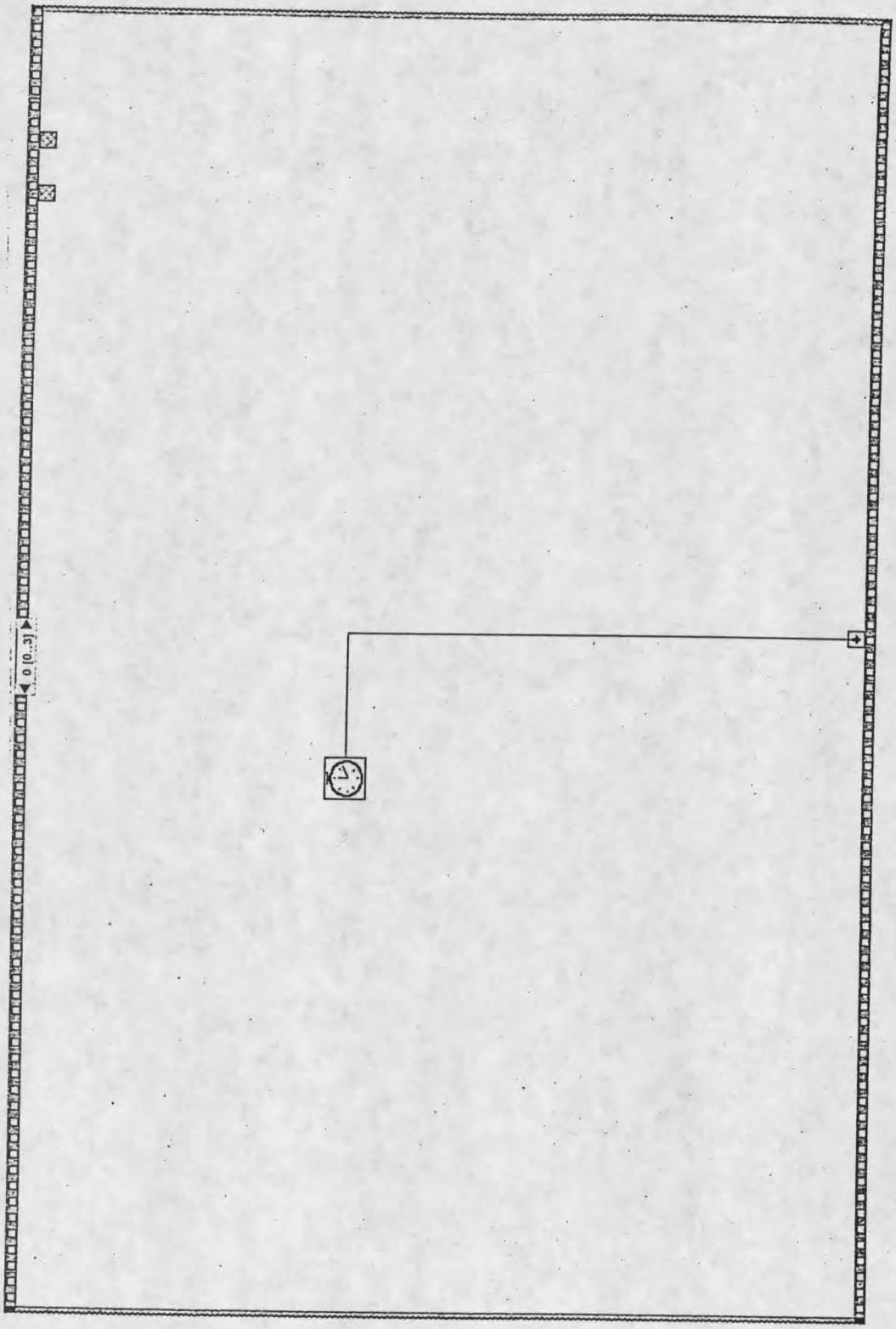

8 [0..9]
Seconds to wait
U32
1000

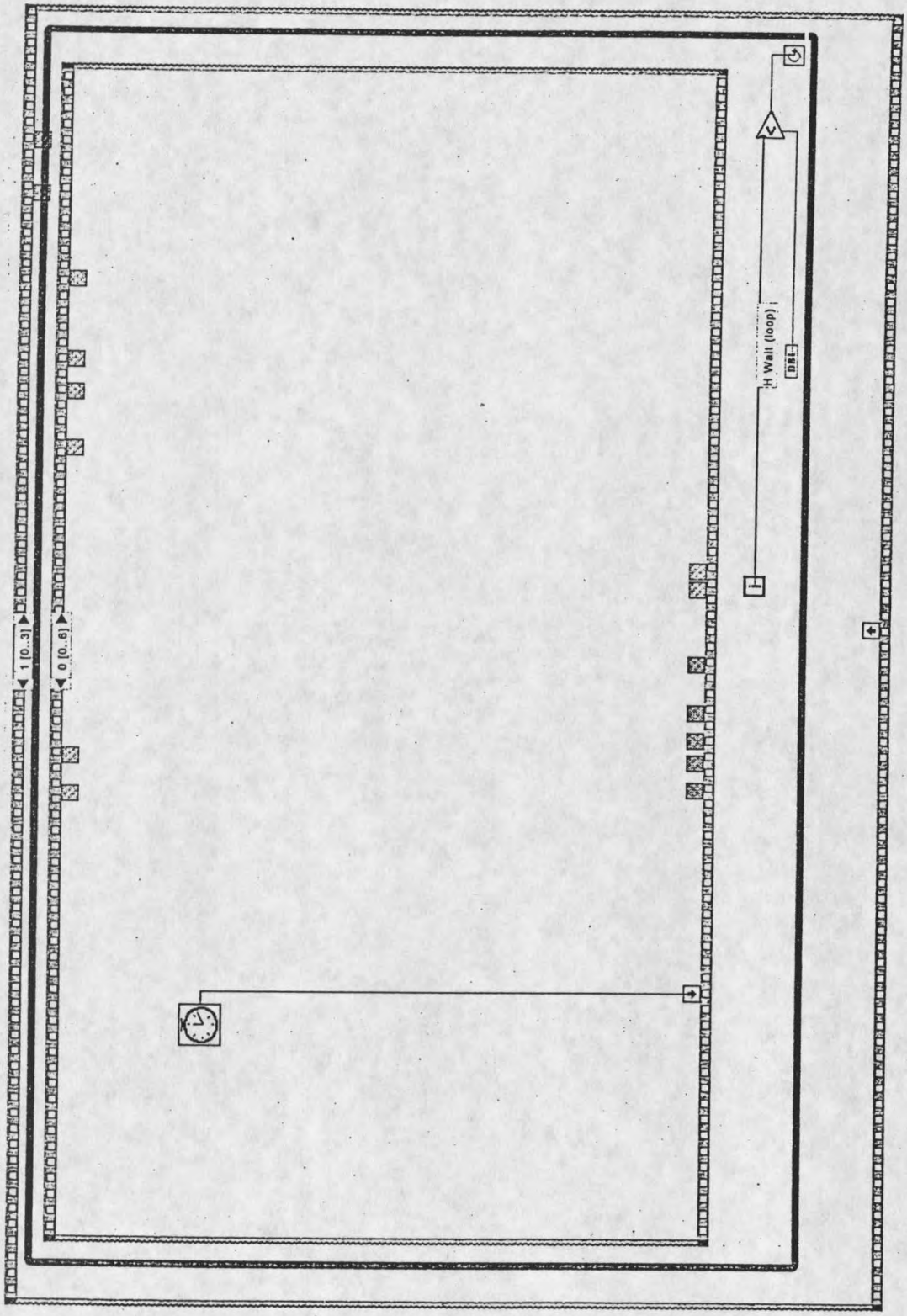

9 [0..9]
Time
Data
Temperature
12.3
TXT
T
F

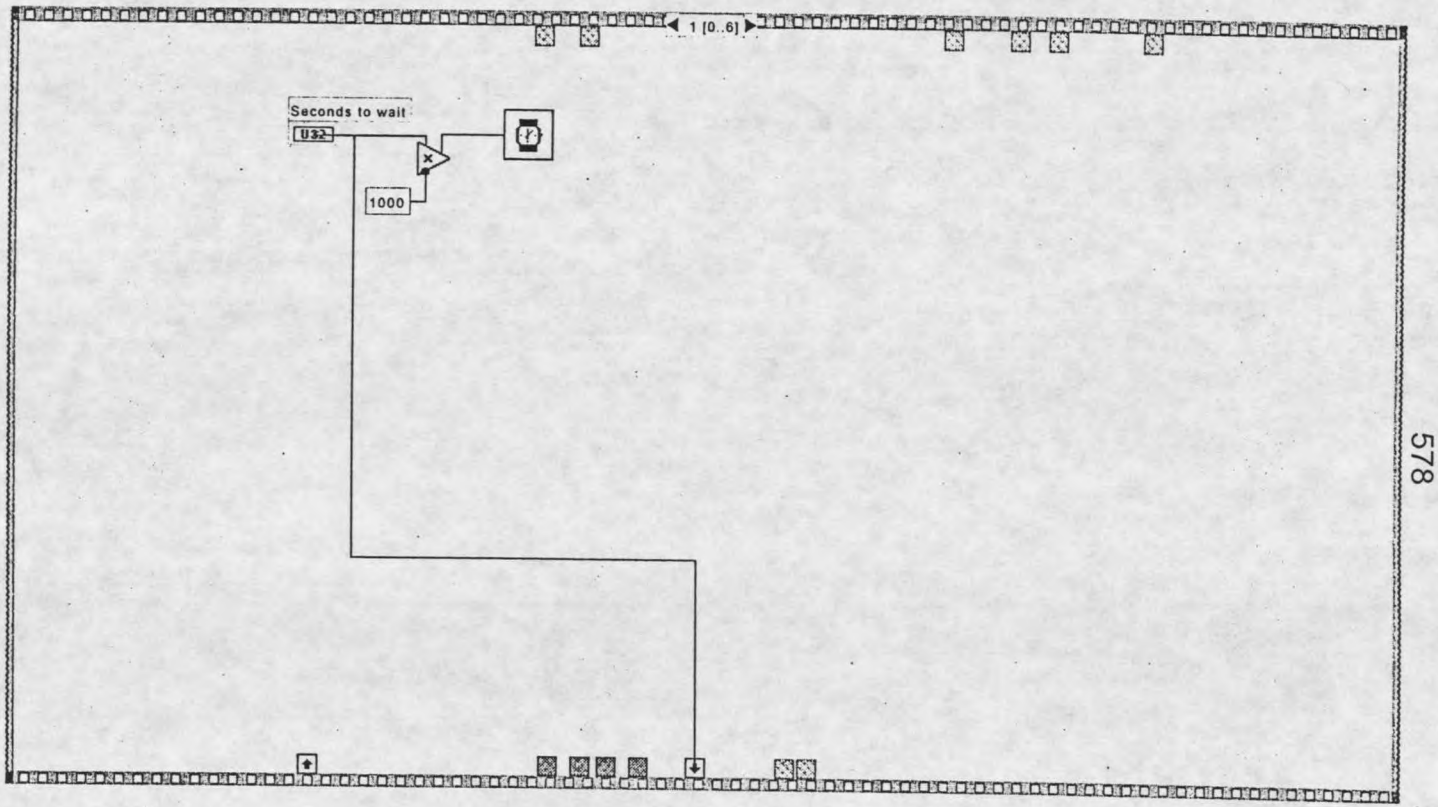
Data Acquisition Program for Vibrocreep of Solid Polymers

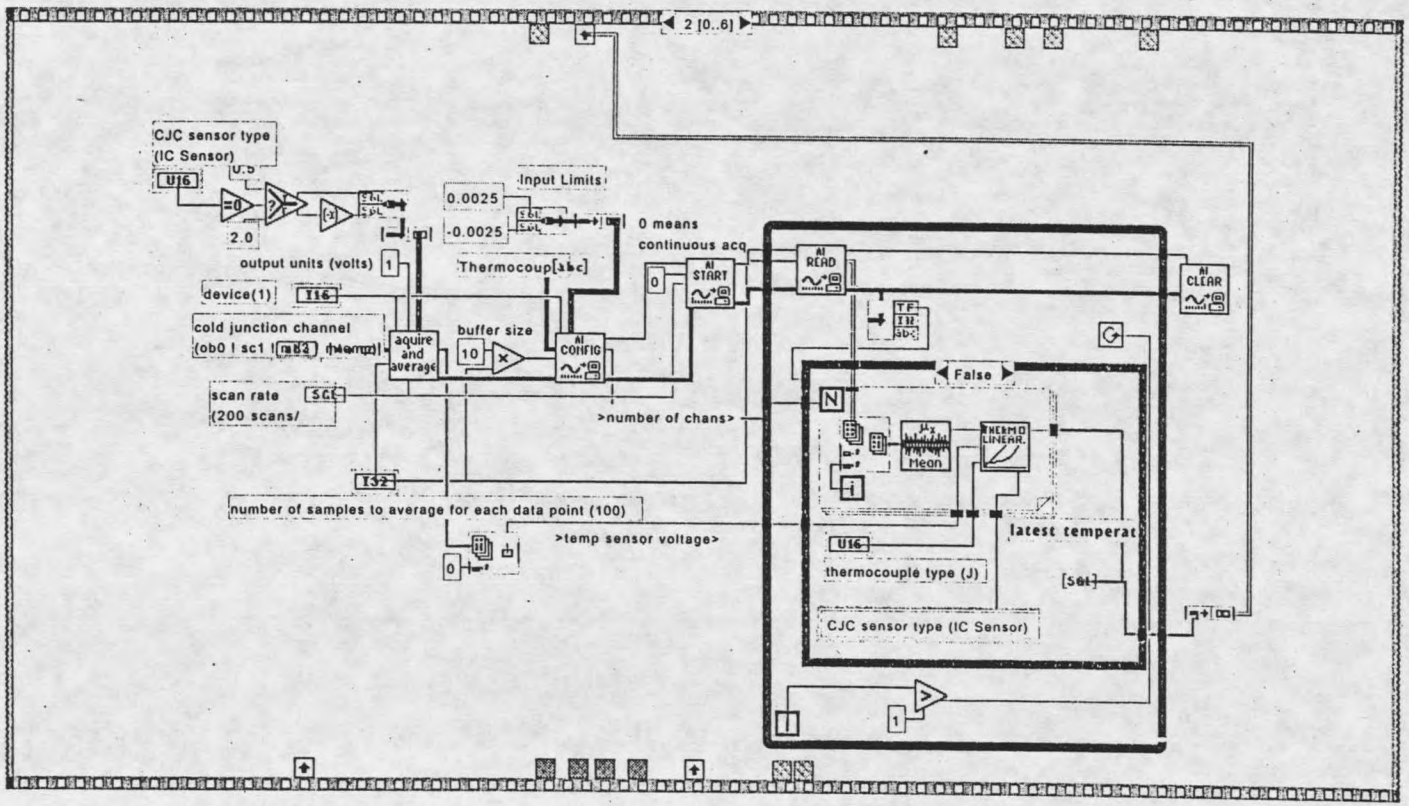
Last modified on 6/1/2000 at 2:51 PM
Printed on 7/18/2000 at 5:49 PM

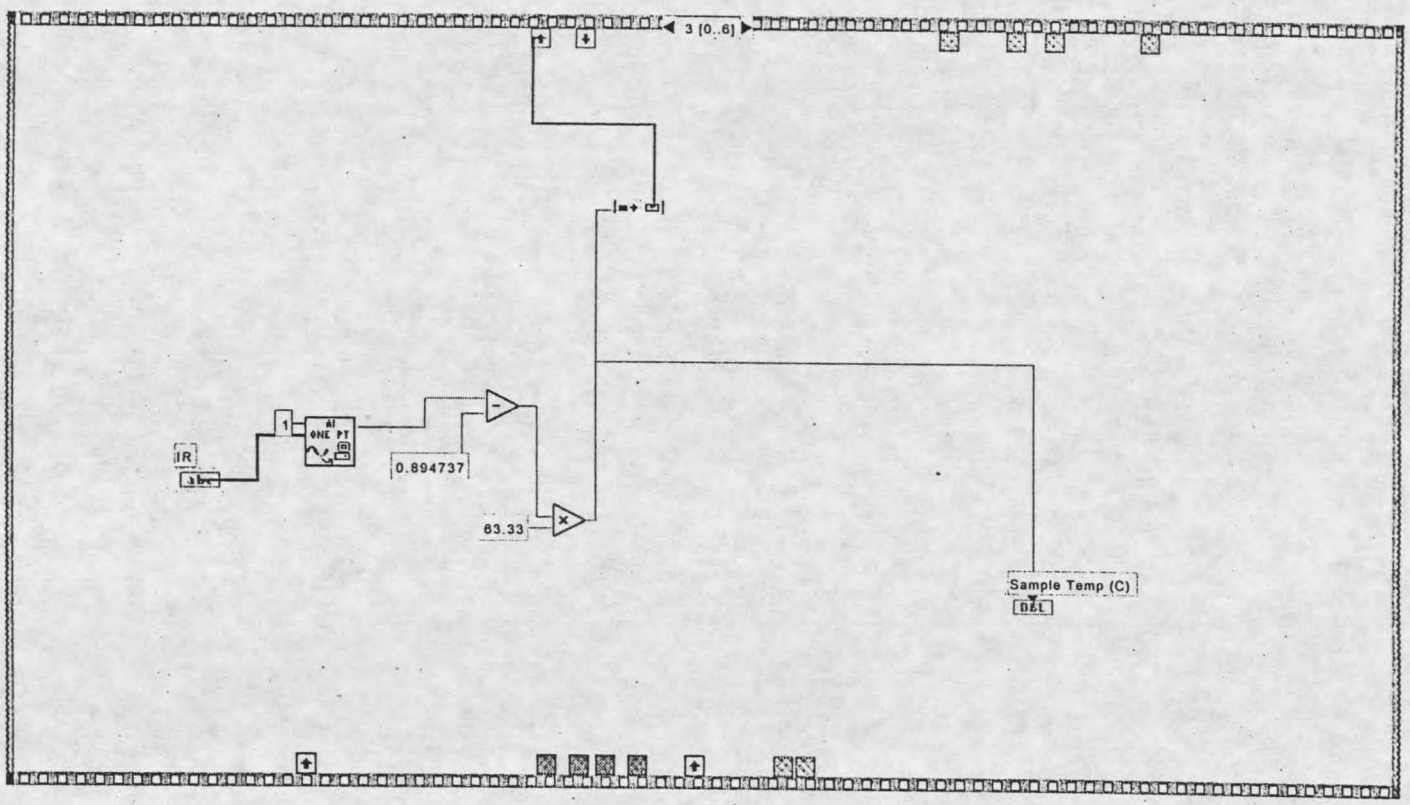


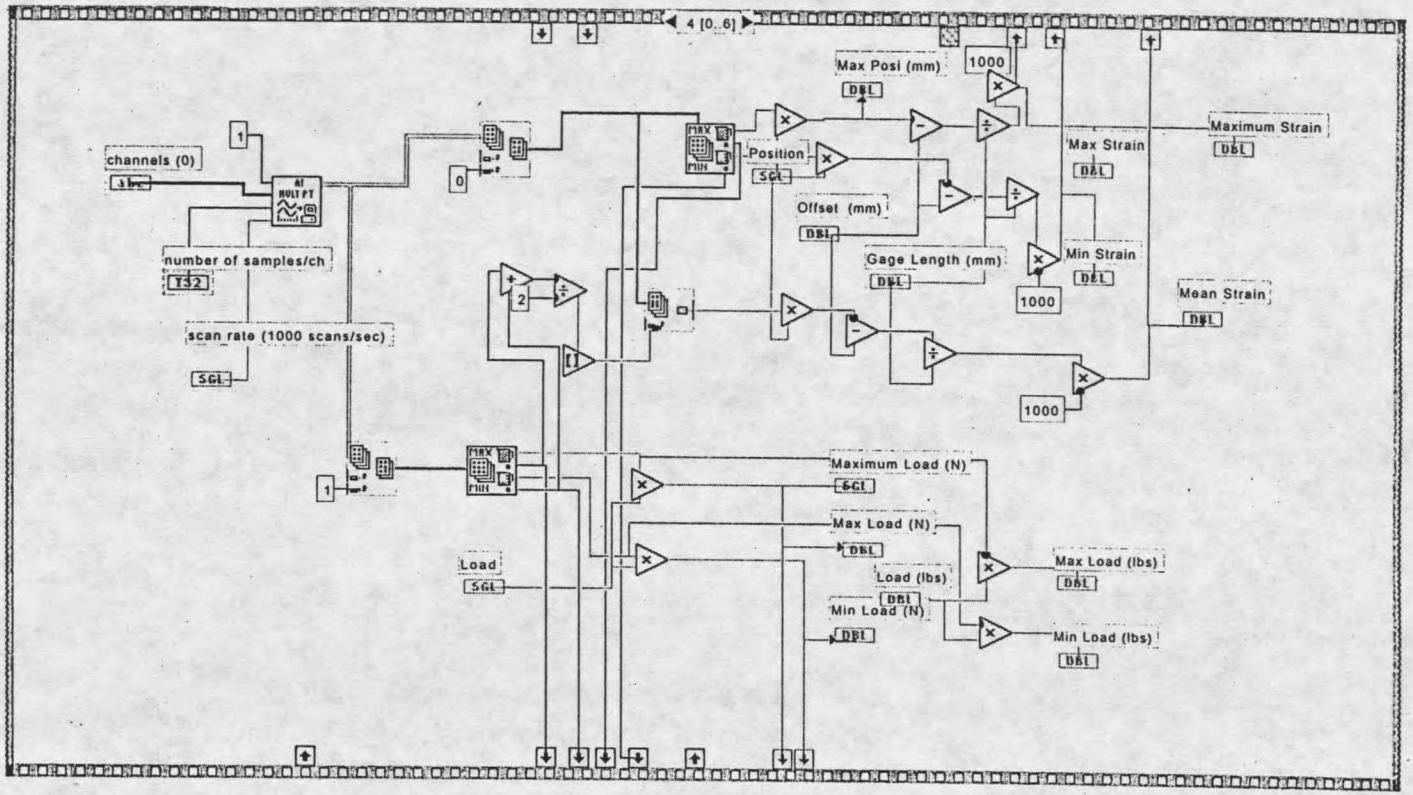

0 [0..3]

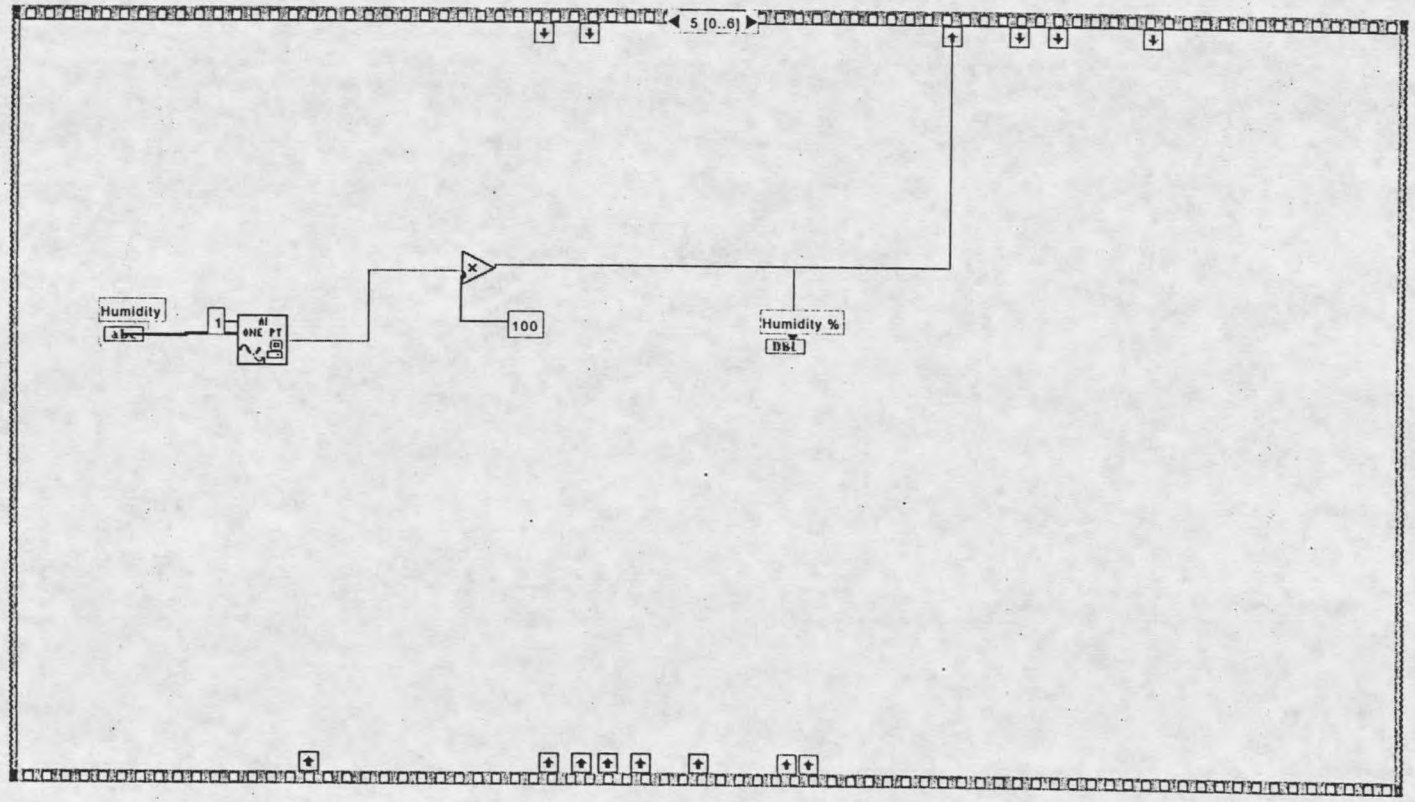

1 [0..3]
0 [0..6]
Wait (loop)
ms

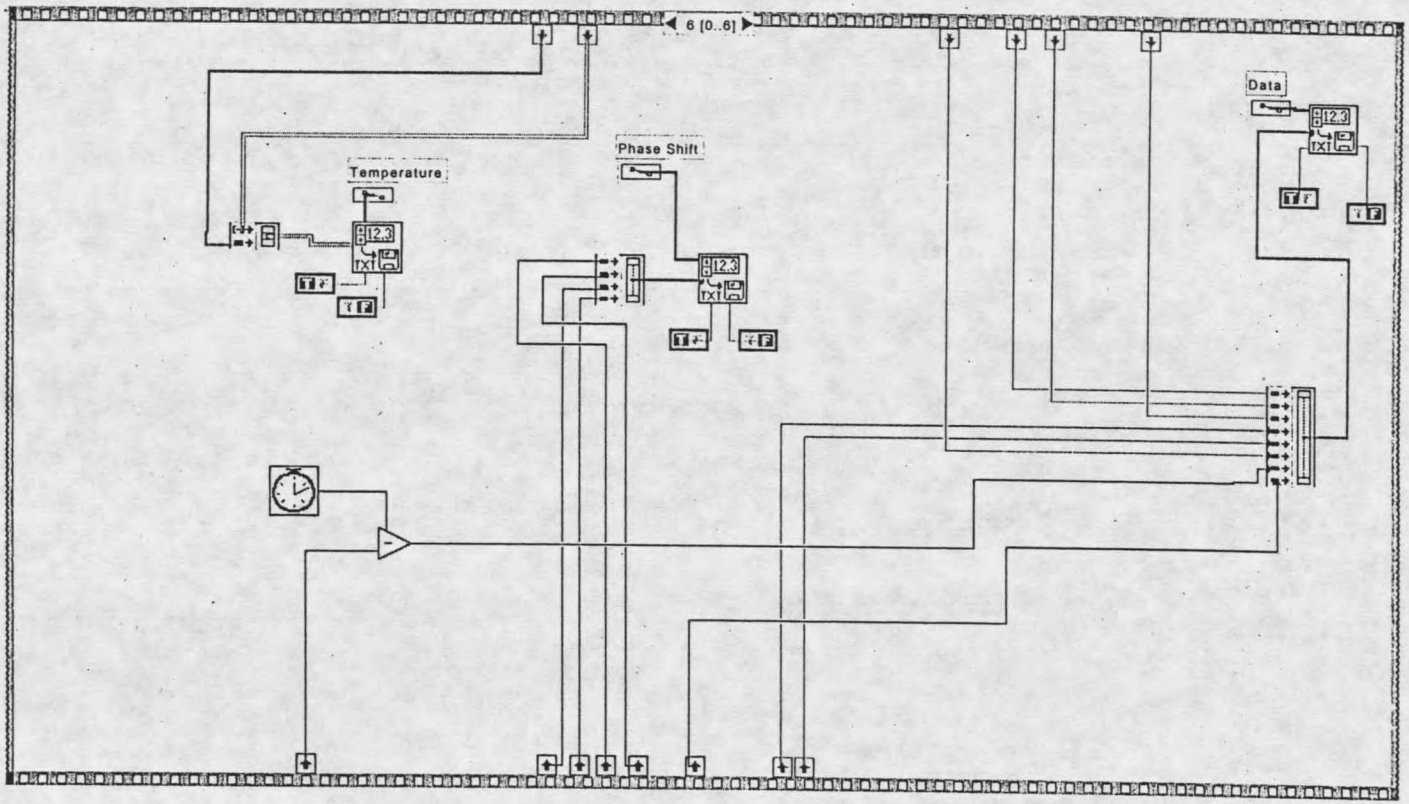

1 [0..6]
Seconds to wait
U32
1000

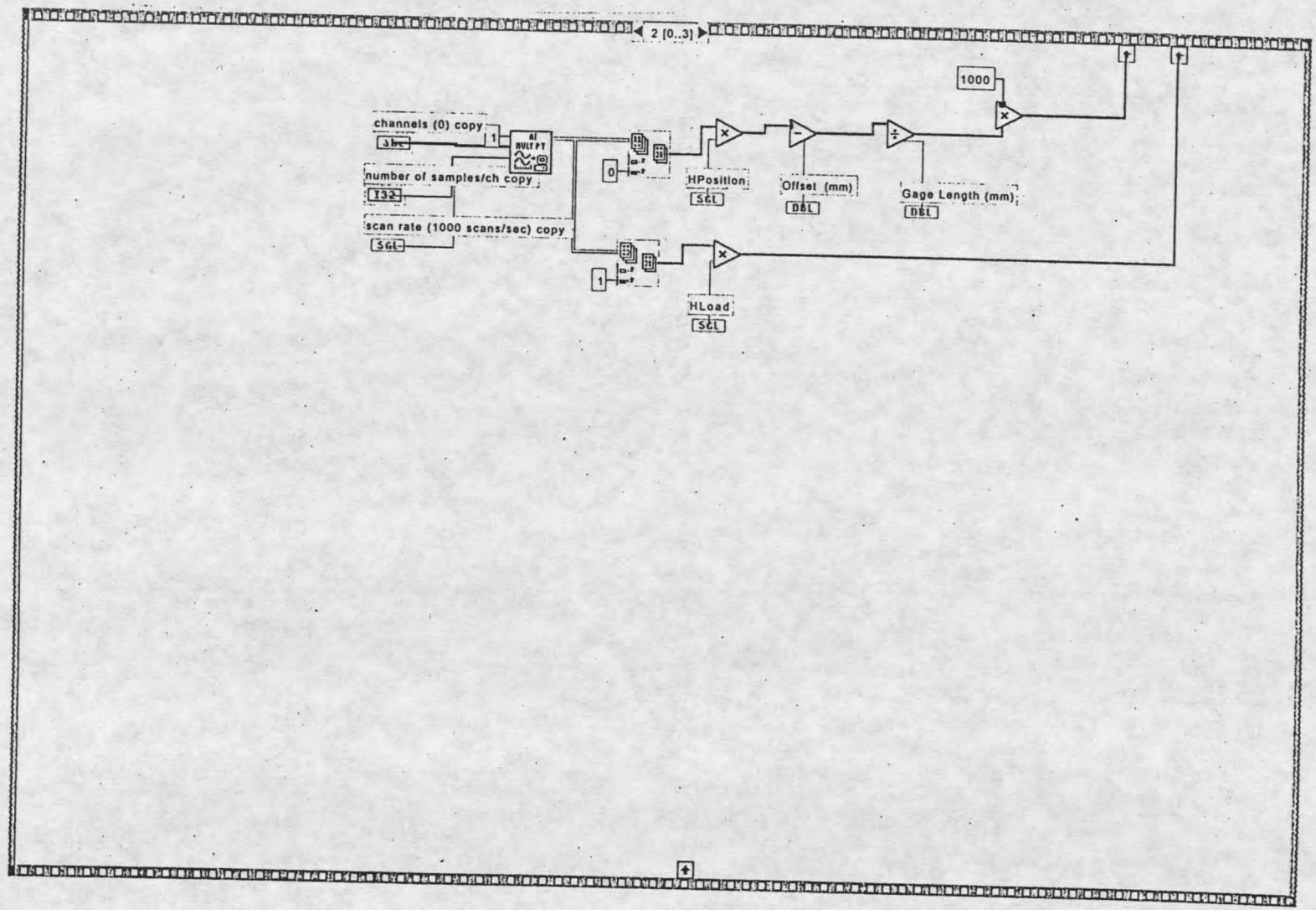

2 [0..6]
CJC sensor type
(IC Sensor)
U16
0.5
=0
2.0
Input Limits
0.0025
-0.0025
0 means
continuous acq
output units (volts)
1
Thermocoup[a b c]
device(1)
I16
cold junction channel
(ob0 ! sc1 !
aquire
and
average
buffer size
10
AI
CONFIG
AI
START
0
AI
READ
AI
CLEAR
scan rate
(200 scans/
SGL
>number of chans>
I32
number of samples to average for each data point (100)
>temp sensor voltage>
0
False
N
i
Mean
THERMO
LINEAR
latest temperat
U16
thermocouple type (J)
[set]
CJC sensor type (IC Sensor)
1

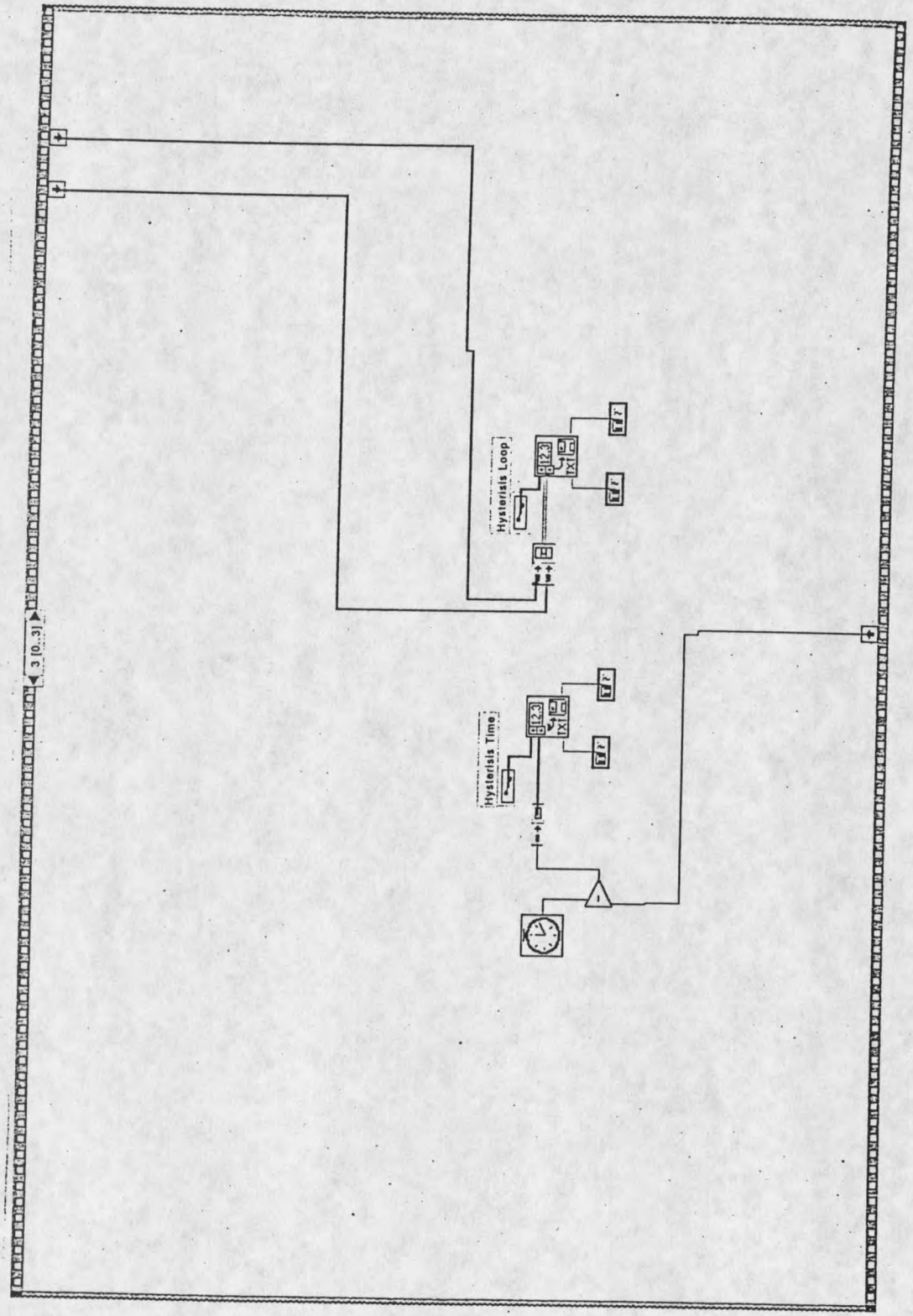

3 [0..6]
IR
1
AI
ONE PT
0.894737
63.33
Sample Temp (C)
DBL


4 [0..6]
channels (0)
number of samples/ch
scan rate (1000 scans/sec)
SGL
Max Posi (mm)
DBL
1000
Position
SGL
Offset (mm)
DBL
Gage Length (mm)
DBL
Max Strain
DBL
Maximum Strain
DBL
Min Strain
DBL
Mean Strain
DBL
Maximum Load (N)
SGL
Max Load (N)
DBL
Load
SGL
Load (lbs)
DBL
Min Load (N)
DBL
Max Load (lbs)
DBL
Min Load (lbs)
DBL


5 [0..6]
Humidity
abc
1
AI
ONE PT
100
Humidity %
DBL

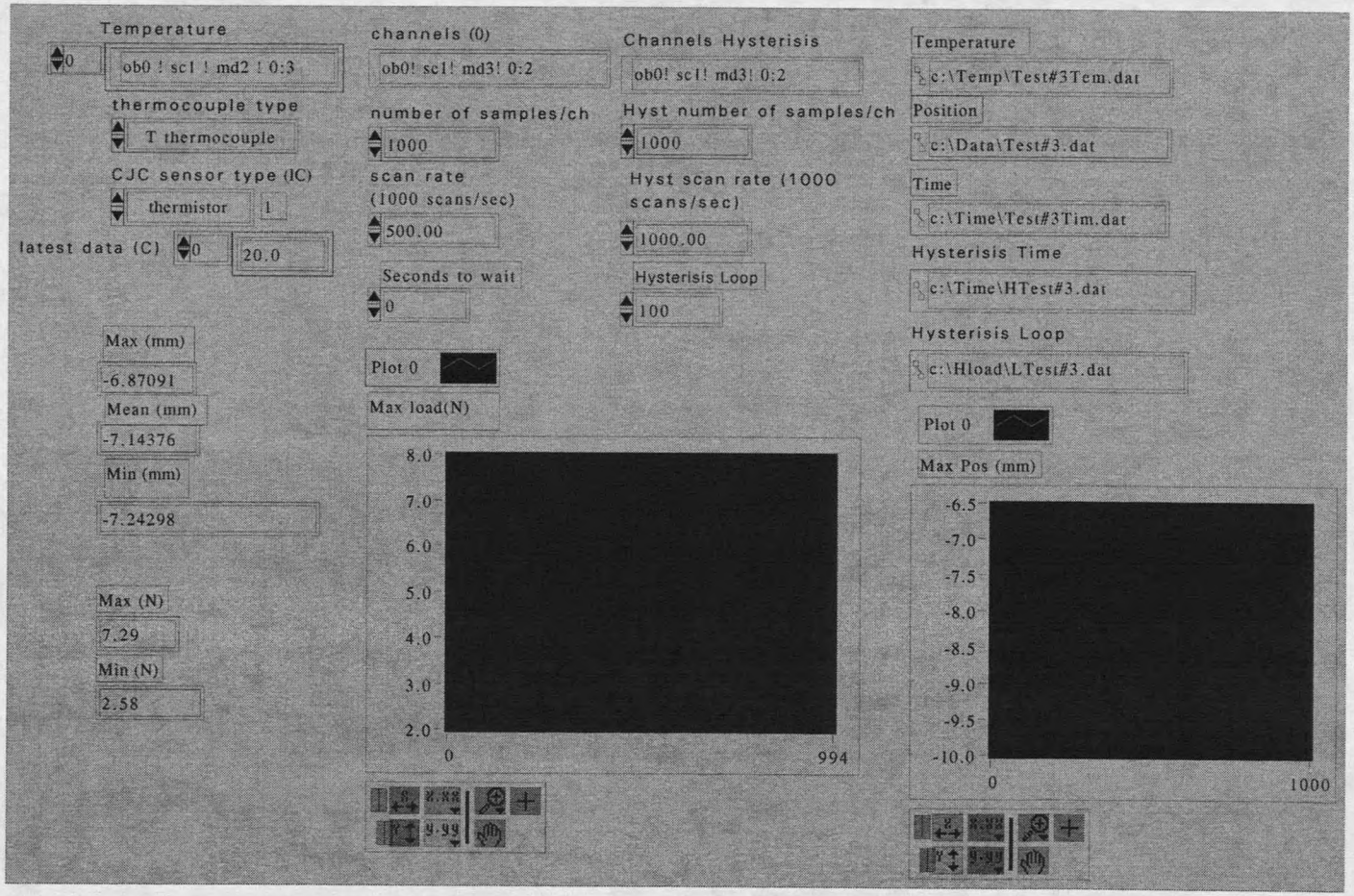

6 [0..6]
Temperature
Phase Shift
Data

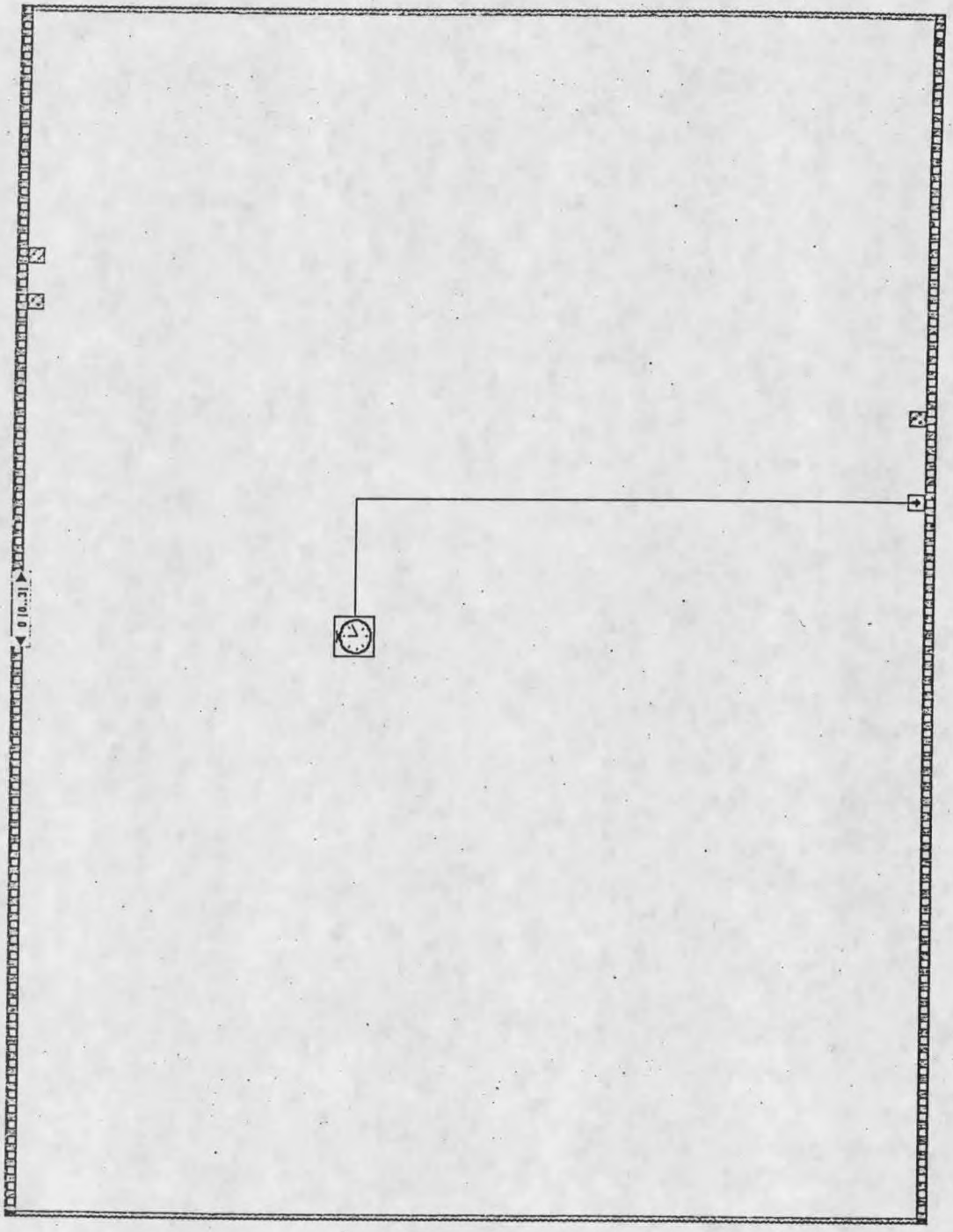

2 [0..3]
channels (0) copy
abc
number of samples/ch copy
I32
scan rate (1000 scans/sec) copy
SGL
AI MULTPT
0
1
HPosition
SGL
Offset (mm)
DBL
Gage Length (mm)
DBL
1000
HLoad
SGL

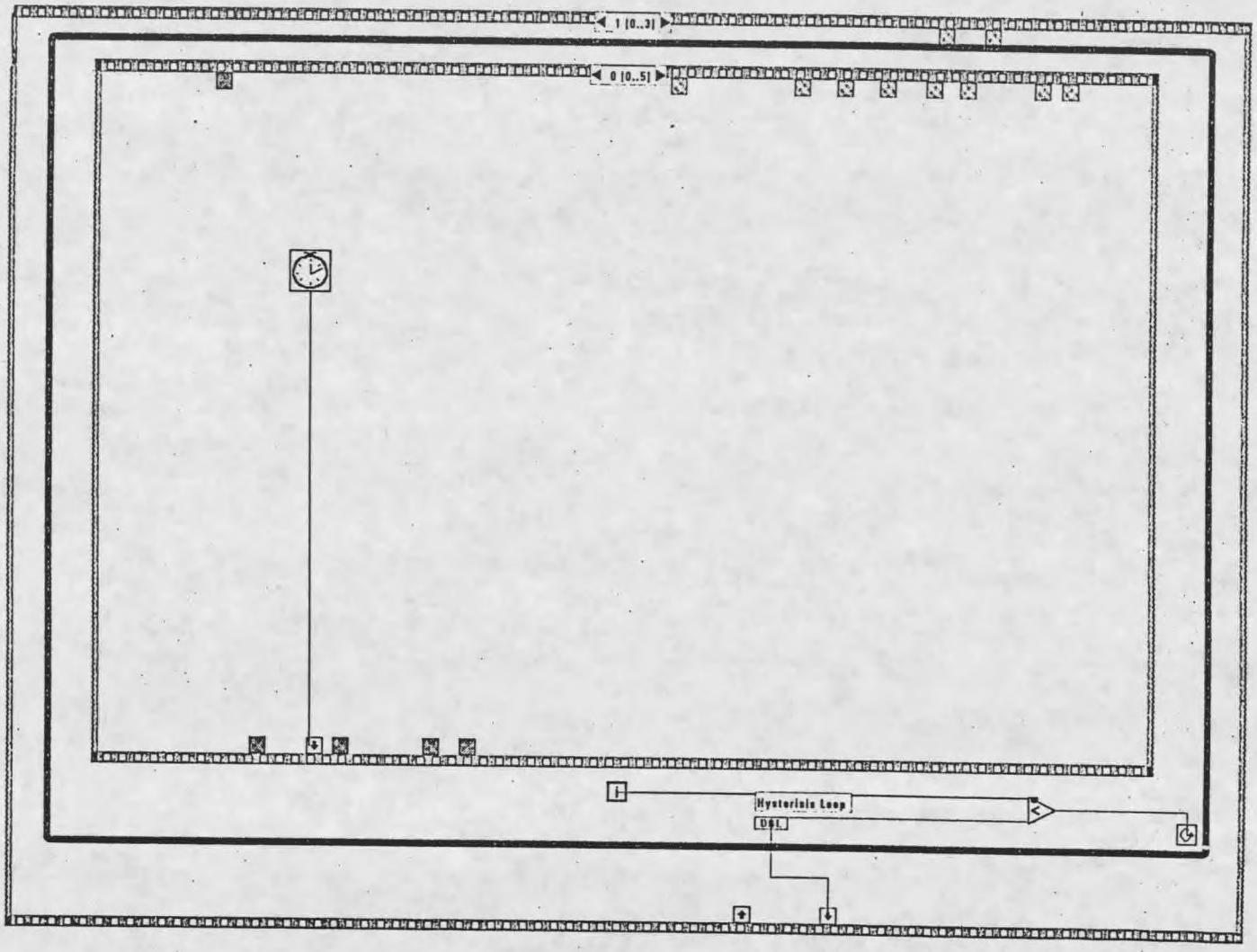

3 [0..3]
Hysterisis Loop
Hysterisis Time
-1

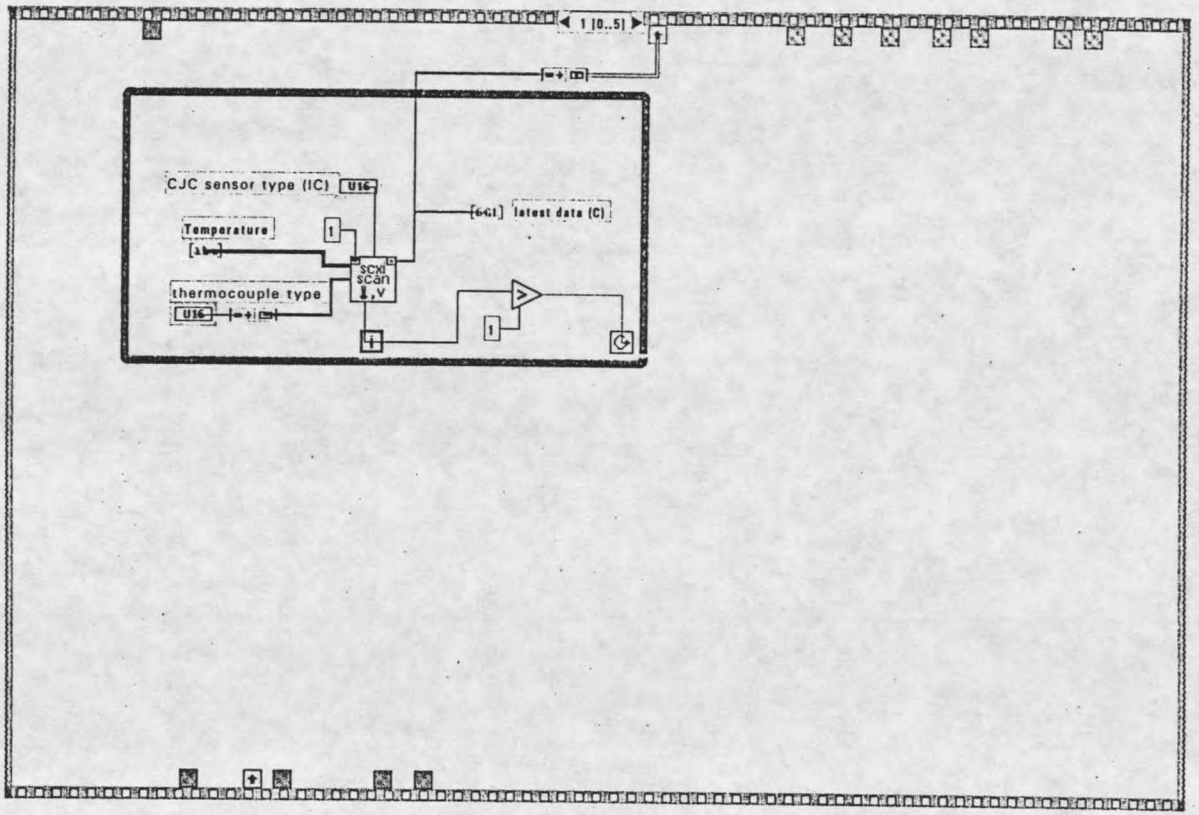
Data Acquisition Program for Vibrocreep of Thin Films

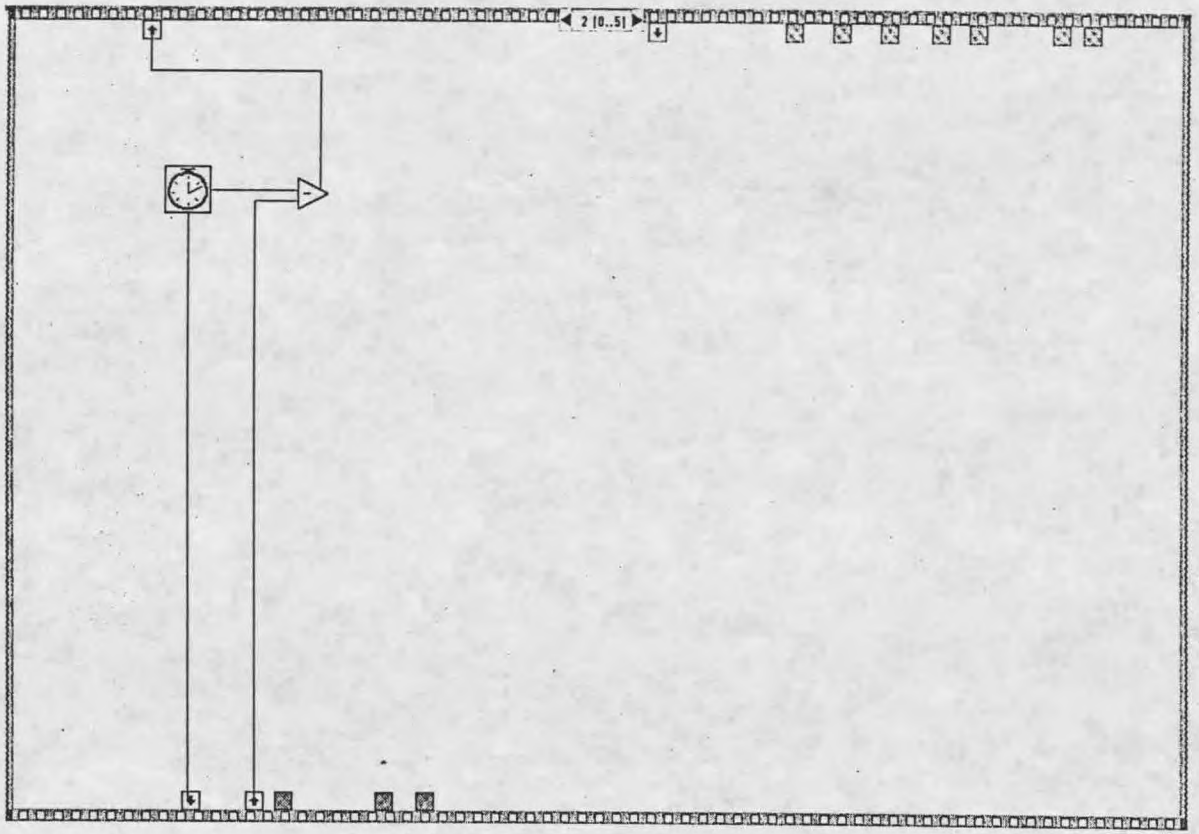
Last modified on 6/1/2000 at 4:22 PM
Printed on 7/18/2000 at 5:51 PM

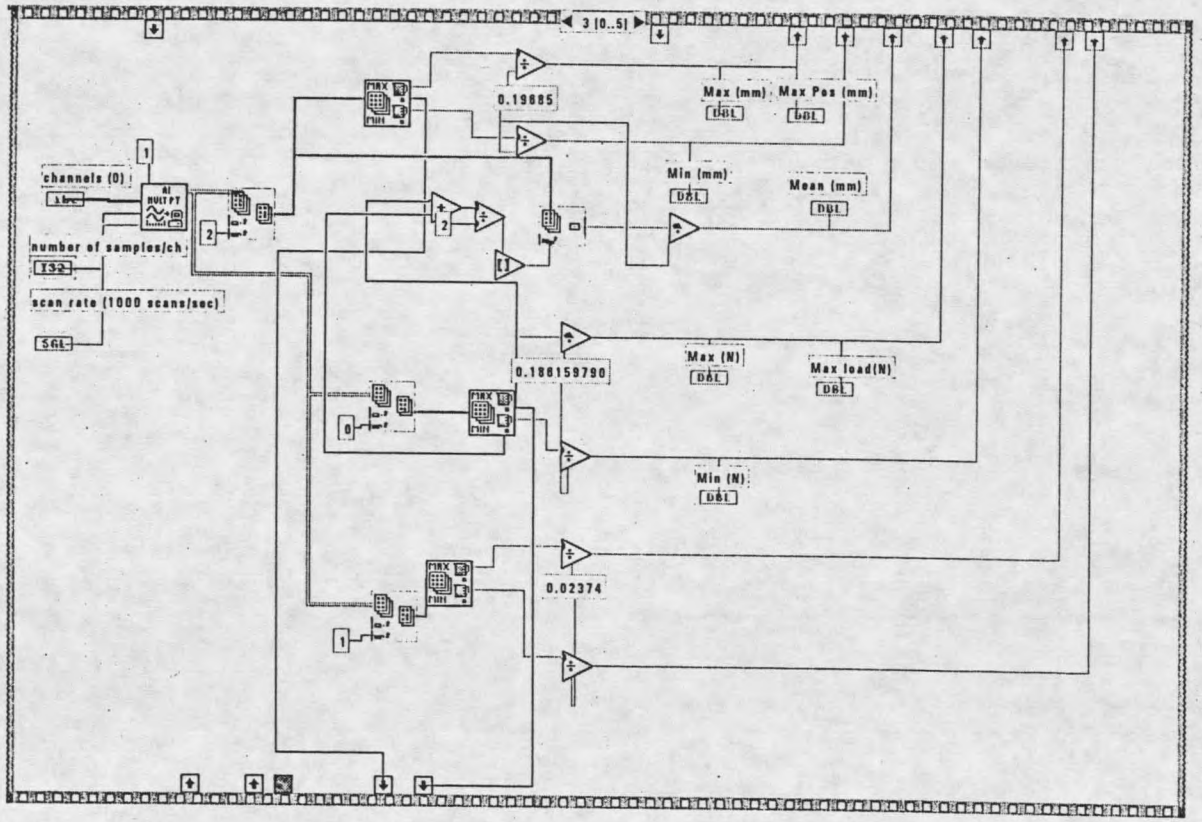


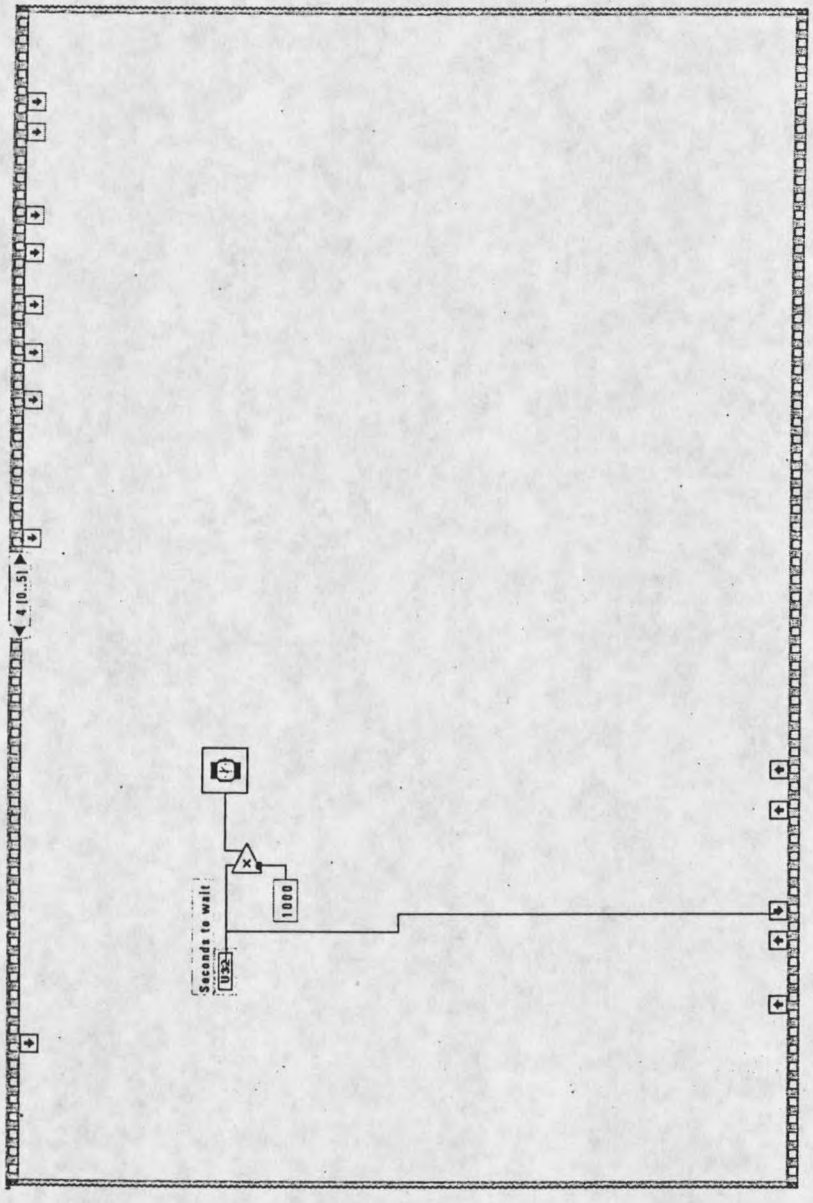

31..0

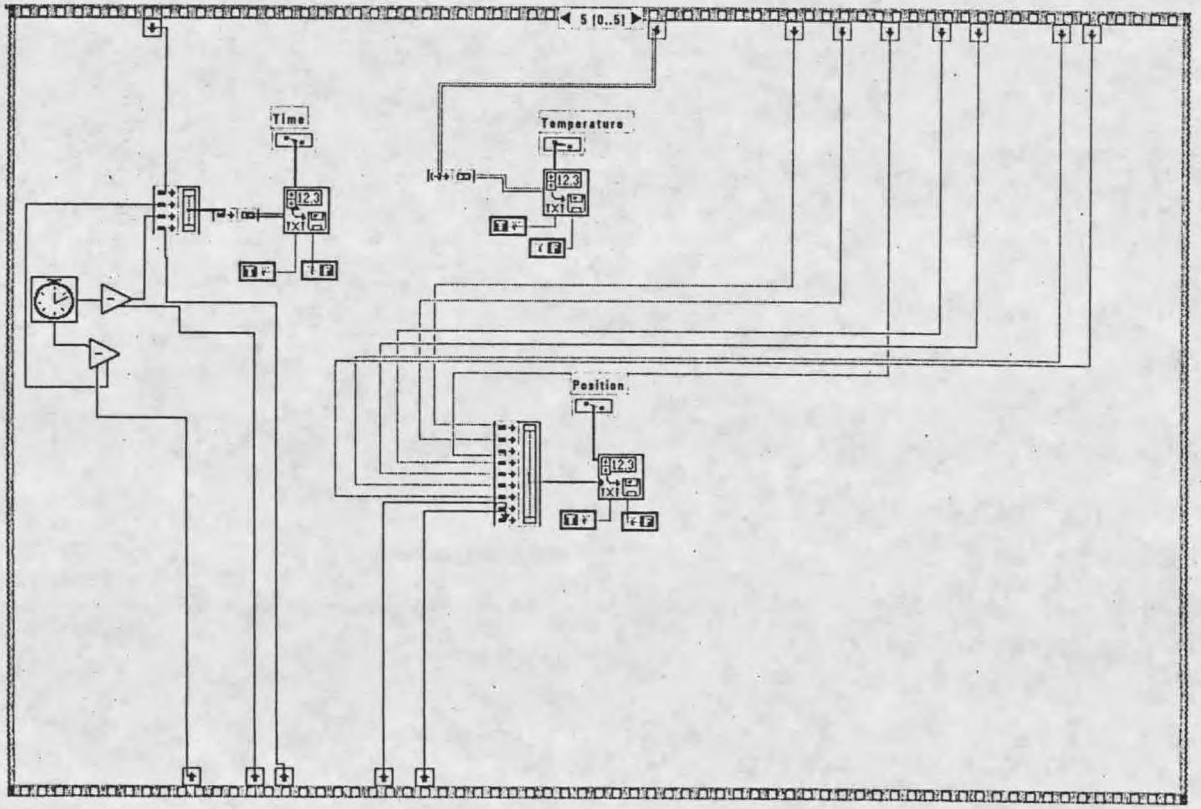

i [0..3]
0 [0..5]
Hysterisis Loop
DBL

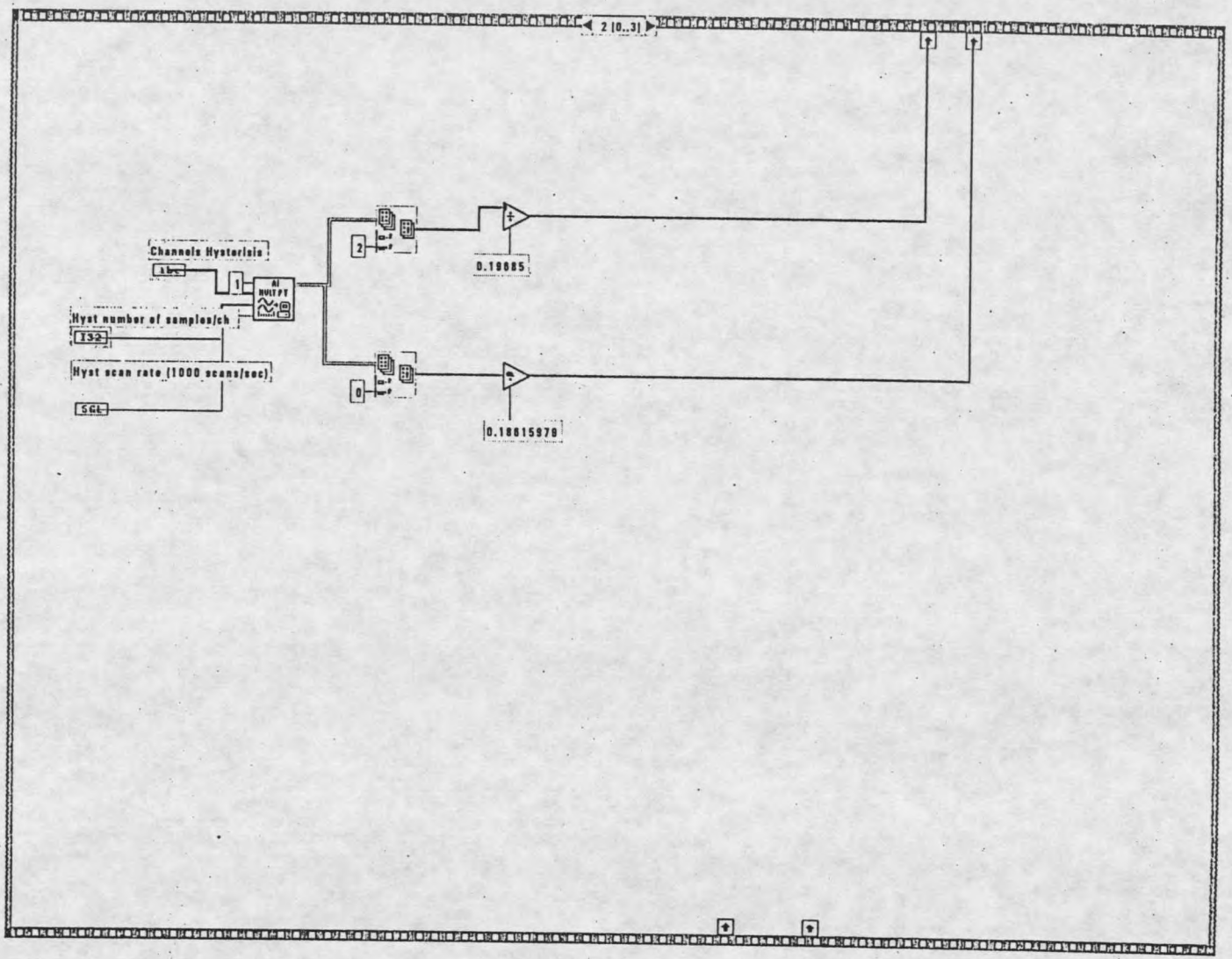

1 [0..5]
CJC sensor type (IC)
U16
Temperature
thermocouple type
U16
scxi
scan
[6G]
latest data (C)
1
1

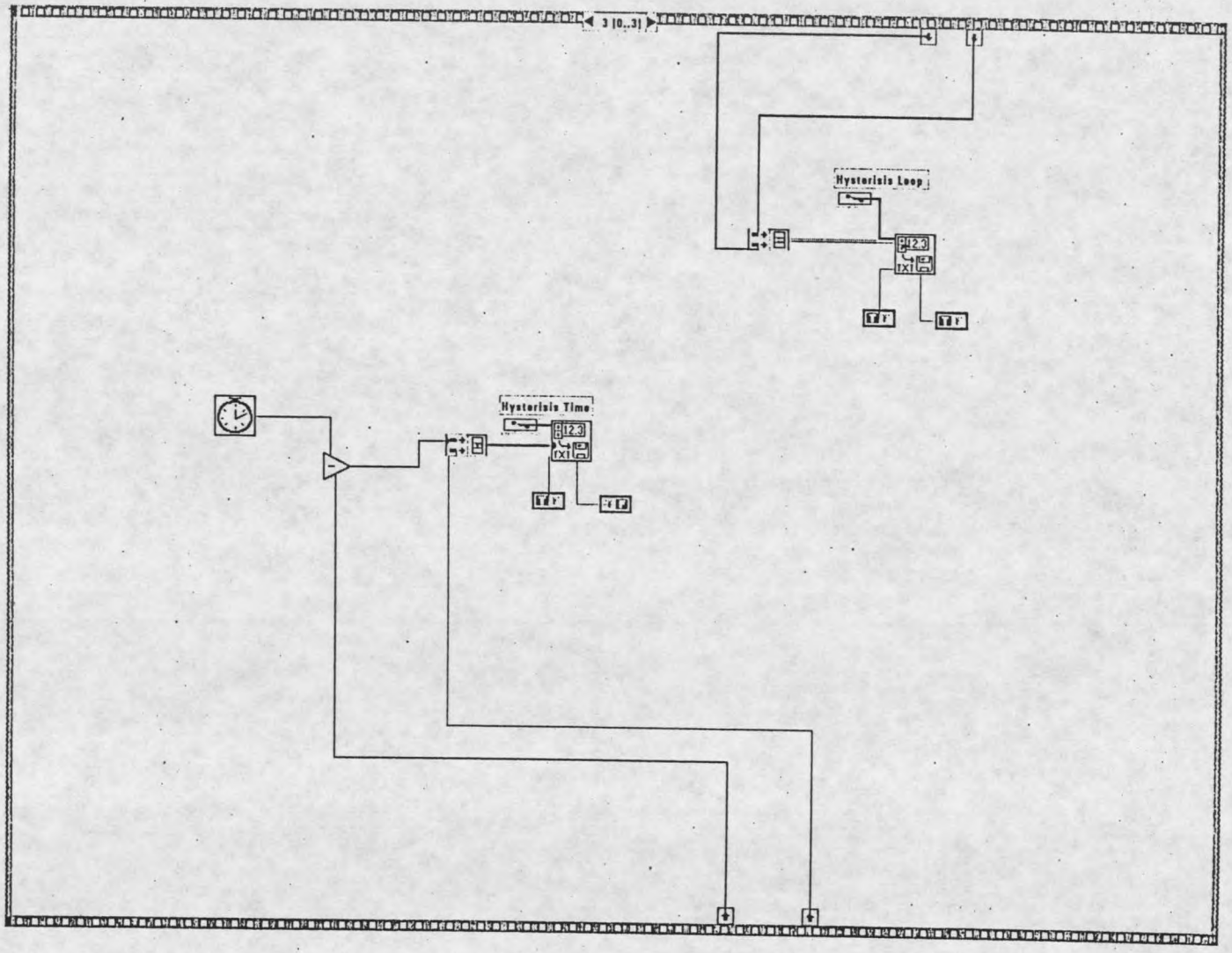

2 [0..5]


channels (0)
number of samples/ch
scan rate (1000 scans/sec)
SGL
0.19885
Max (mm)
Max Pos (mm)
Min (mm)
Mean (mm)
0.186159790
Max (N)
Max load(N)
Min (N)
0.02374


i
1000
Seconds to wait
U32


5 [0..5]
Time
Temperature
Position


2 [0..3]
Channels Hysterisis
1
AI
MULTPT
Hyst number of samples/ch
132
Hyst scan rate (1000 scans/sec)
SGL
2
0
0.19885
0.18615979


3 [0..3]
Hysterisis Loop
Hysterisis Time

APPENDIX O

Macros for Data Management

```
'
' Sample5 Macro
' Macro recorded 8/10/99 by Shane Schumacher
'
'
Sub Sample5()
    Tim = 45
    Column = 1
    Columncounter = 0
    SaveColumn = 16
    comp2 = 3
    Do Until Columncounter > 12
        Row = 1
        SaveRow = 1
        Rowcounter = 1
        Mynum = Sheets("Sheet1").Cells(Row, Column)
        Do Until Rowcounter > Tim
            comp = Rowcounter / 5
            Do Until Mynum > comp Or Mynum = comp
              Mynum = Sheets("Sheet1").Cells(Row, Column)
               Row = Row + 1
             Loop
            MinusColumn = Column
            MinusRow = Row - 1
            Do Until MinusColumn > comp2
                Sheets("Sheet1").Cells(SaveRow, SaveColumn) = Sheets("Sh
eet1").Cells(MinusRow, MinusColumn)
                MinusColumn = MinusColumn + 1
                SaveColumn = SaveColumn + 1
            Loop
            SaveColumn = SaveColumn - 3
            SaveRow = SaveRow + 1
            Rowcounter = Rowcounter + 1
        Loop
        Columncounter = Columncounter + 3
        Column = Column + 3
        SaveColumn = SaveColumn + 3
        comp2 = comp2 + 3
    Loop
End Sub
```

```
'
' Ave5 Macro
' Macro recorded 8/10/99 by Shane Schumacher
'
'
Sub Ave5()
Tim = 45
Column1 = 16
Column2 = 19
Column3 = 22
Column4 = 25
Column5 = 28
Column = 1
SaveColumn = 31
Do Until Column > 3
    Row = 1
    Do Until Row > Tim
        myNum1 = Sheets("Sheet1").Cells(Row, Column1)
        myNum2 = Sheets("Sheet1").Cells(Row, Column2)
        myNum3 = Sheets("Sheet1").Cells(Row, Column3)
        myNum4 = Sheets("Sheet1").Cells(Row, Column4)
        myNum5 = Sheets("Sheet1").Cells(Row, Column5)
        total = (myNum1 + myNum2 + myNum3 + myNum4 + myNum5) / 5
        Sheets("Sheet1").Cells(Row, SaveColumn) = total
        Row = Row + 1
    Loop
    SaveColumn = SaveColumn + 1
    Column1 = Column1 + 1
    Column2 = Column2 + 1
    Column3 = Column3 + 1
    Column4 = Column4 + 1
    Column5 = Column5 + 1
    Column = Column + 1
    Loop
End Sub
```

```
'
' DynSamAve Macro
' Macro recorded 8/10/99 by Shane Schumacher
'
'
Sub DynSamAve()
    Tim = 45
    Column = 1
    Columncounter = 0
    SaveColumn = 22
    comp2 = 7
    Do Until Columncounter > 14
        Row = 1
        SaveRow = 1
        Rowcounter = 1
        Mynum = Sheets("Sheet1").Cells(Row, Column)
        Do Until Rowcounter > Tim
            comp = Rowcounter / 5
            Do Until Mynum > comp Or Mynum = comp
              Mynum = Sheets("Sheet1").Cells(Row, Column)
               Row = Row + 1
             Loop
            MinusColumn = Column
            MinusRow = Row - 1
            Do Until MinusColumn > comp2
                Sheets("Sheet1").Cells(SaveRow, SaveColumn) = Sheets("Sh
eet1").Cells(MinusRow, MinusColumn)
                MinusColumn = MinusColumn + 1
                SaveColumn = SaveColumn + 1
            Loop
            SaveColumn = SaveColumn - 7
            SaveRow = SaveRow + 1
            Rowcounter = Rowcounter + 1
        Loop
        Columncounter = Columncounter + 7
        Column = Column + 7
        SaveColumn = SaveColumn + 7
        comp2 = comp2 + 7
    Loop
End Sub
```

```
'
' AveDyn3 Macro
' Macro recorded 8/10/99 by Shane Schumacher
'
'
Sub AveDyn3()
Tim = 45
Column1 = 22
Column2 = 29
Column3 = 36
Column = 1
SaveColumn = 43
Do Until Column > 7
    Row = 1
    Do Until Row > Tim
        myNum1 = Sheets("Sheet1").Cells(Row, Column1)
        myNum2 = Sheets("Sheet1").Cells(Row, Column2)
        myNum3 = Sheets("Sheet1").Cells(Row, Column3)
        total = (myNum1 + myNum2 + myNum3) / 3
        Sheets("Sheet1").Cells(Row, SaveColumn) = total
        Row = Row + 1
    Loop
    SaveColumn = SaveColumn + 1
    Column1 = Column1 + 1
    Column2 = Column2 + 1
    Column3 = Column3 + 1
    Column = Column + 1
    Loop
End Sub
```

```
'
' 3Tensile Macro
' Macro recorded 8/10/99 by Shane Schumacher
'
'
Sub Tensile3()
    Strain = 40
    Column = 1
    Columncounter = 0
    SaveColumn = 7
    comp2 = 2
    Do Until Columncounter > 4
        Row = 1
        SaveRow = 1
        Rowcounter = 1
        Mynum = Sheets("Sheet1").Cells(Row, Column)
        Do Until Rowcounter > Strain
            comp = Rowcounter / 100
            Do Until Mynum > comp Or Mynum = comp
              Mynum = Sheets("Sheet1").Cells(Row, Column)
               Row = Row + 1
             Loop
            MinusColumn = Column
            MinusRow = Row - 1
            Do Until MinusColumn > comp2
                Sheets("Sheet1").Cells(SaveRow, SaveColumn) = Sheets("Sh
eet1").Cells(MinusRow, MinusColumn)
                MinusColumn = MinusColumn + 1
                SaveColumn = SaveColumn + 1
            Loop
            SaveColumn = SaveColumn - 2
            SaveRow = SaveRow + 1
            Rowcounter = Rowcounter + 1
        Loop
        Columncounter = Columncounter + 2
        Column = Column + 2
        SaveColumn = SaveColumn + 2
        comp2 = comp2 + 2
    Loop
End Sub
```

```
'
' 3TensileAve Macro
' Macro recorded 8/10/99 by Shane Schumacher
'
'
Sub TensileAve3()
Tim = 40
Column1 = 7
Column2 = 9
Column3 = 11
Column = 1
SaveColumn = 13
Do Until Column > 2
    Row = 1
    Do Until Row > Tim
        myNum1 = Sheets("Sheet1").Cells(Row, Column1)
        myNum2 = Sheets("Sheet1").Cells(Row, Column2)
        myNum3 = Sheets("Sheet1").Cells(Row, Column3)
        total = (myNum1 + myNum2 + myNum3) / 3
        Sheets("Sheet1").Cells(Row, SaveColumn) = total
        Row = Row + 1
    Loop
    SaveColumn = SaveColumn + 1
    Column1 = Column1 + 1
    Column2 = Column2 + 1
    Column3 = Column3 + 1
    Column = Column + 1
    Loop
End Sub
```

```
'
' 5Tensile Macro
' Macro recorded 8/10/99 by Shane Schumacher
'
'
Sub Tensile5()
    Strain = 40
    Column = 1
    Columncounter = 0
    SaveColumn = 11
    comp2 = 2
    Do Until Columncounter > 8
        Row = 1
        SaveRow = 1
        Rowcounter = 1
        Mynum = Sheets("Sheet1").Cells(Row, Column)
        Do Until Rowcounter > Strain
            comp = Rowcounter / 100
            Do Until Mynum > comp Or Mynum = comp
              Mynum = Sheets("Sheet1").Cells(Row, Column)
                Row = Row + 1
             Loop
            MinusColumn = Column
            MinusRow = Row - 1
            Do Until MinusColumn > comp2
                Sheets("Sheet1").Cells(SaveRow, SaveColumn) = Sheets("Sh
eet1").Cells(MinusRow, MinusColumn)
                MinusColumn = MinusColumn + 1
                SaveColumn = SaveColumn + 1
            Loop
            SaveColumn = SaveColumn - 2
            SaveRow = SaveRow + 1
            Rowcounter = Rowcounter + 1
        Loop
        Columncounter = Columncounter + 2
        Column = Column + 2
        SaveColumn = SaveColumn + 2
        comp2 = comp2 + 2
    Loop
End Sub
```

```
'
' 5TenAve Macro
' Macro recorded 8/10/99 by Shane Schumacher
'
'
Sub TenAve5()
Tim = 40
Column1 = 11
Column2 = 13
Column3 = 15
Column4 = 17
Column5 = 19
Column = 1
SaveColumn = 21
Do Until Column > 2
    Row = 1
    Do Until Row > Tim
        myNum1 = Sheets("Sheet1").Cells(Row, Column1)
        myNum2 = Sheets("Sheet1").Cells(Row, Column2)
        myNum3 = Sheets("Sheet1").Cells(Row, Column3)
        myNum4 = Sheets("Sheet1").Cells(Row, Column4)
        myNum5 = Sheets("Sheet1").Cells(Row, Column5)
        total = (myNum1 + myNum2 + myNum3 + myNum4 + myNum5) / 5
        Sheets("Sheet1").Cells(Row, SaveColumn) = total
        Row = Row + 1
    Loop
    SaveColumn = SaveColumn + 1
    Column1 = Column1 + 1
    Column2 = Column2 + 1
    Column3 = Column3 + 1
    Column4 = Column4 + 1
    Column5 = Column5 + 1
    Column = Column + 1
    Loop
End Sub
```

APPENDIX P

Manufacture Material Data for Nylon 6/6 and PVDF

DUPONT

Zytel®

nylon resin

Zytel® 42A NC010

Nylon Resin

Zytel® 42A NC010 is a high viscosity molding and extrusion grade PA 66 resin, suitable for film and tubing applications.

Property	Test Method	Units	Value	
			DAM	50% RH
Mechanical				
Tensile Strength	ASTM D 638	MPa (kpsi)		
-40C (-40F)			117.2 (17.0)	111 (16.1)
23C (73F)			85.5 (12.4)	77.2 (11.2)
77C (170F)			58.6 (8.5)	40.7 (5.9)
121C (250F)			43.4 (6.3)	32.4 (4.7)
Tensile Strength at Yield	ASTM D 638	MPa (kpsi)		
-40C (-40F)			117.2 (17.0)	111 (16.1)
23C (73F)			85.5 (12.4)	59.3 (8.6)
77C (170F)			58.6 (8.5)	40.7 (5.9)
121C (250F)			35.1 (5.1)	32.4 (4.7)
Elongation at Yield	ASTM D 638	%		
-40C (-40F)				5
23C (73F)			5	30
77C (170F)			30	30
121C (250F)			30	30
Elongation at Break	ASTM D 638	%		
-40C (-40F)			15	35
23C (73F)			90	>300
77C (170F)			155	>300
121C (250F)			200	>300
Shear Strength	ASTM D 732	MPa (kpsi)	66.2 (9.6)	63.4 (9.1)
Flexural Modulus	ASTM D 790	MPa (kpsi)		
-40C (-40F)			3241 (470)	3447 (500)
23C (73F)			2827 (410)	1207 (175)
77C (170F)			690 (100)	565 (82)
121C (250F)			538 (78)	414 (60)

Contact DuPont for Material Safety Data Sheet, general guides and/or additional information about ventilation, handling, purging, drying, etc.
Mechanical properties measured at 23°C (73°F) unless otherwise noted.

Zytel® is a DuPont registered trademark.

9/6/03/1/99/1/0/1/4

The information provided in this data sheet corresponds to our knowledge on the subject at the date of its publication. This information may be subject to revision as new knowledge and experience become available. The data provided fall within the normal range of product properties and relate only to the specific material designated; these data may not be valid for such material used in combination with any other materials or additives or in any process, unless expressly indicated otherwise. The data provided should not be used to establish specification limits or used alone as the basis of design; they are not intended to substitute for any testing you may need to conduct to determine for yourself the suitability of a specific material for your particular purposes. Since DuPont cannot anticipate all variations in actual end-use conditions DuPont makes no warranties and assumes no liability in connection with any use of this information. Nothing in this publication is to be considered as a license to operate under or a recommendation to infringe any patent rights. Caution: Do not use this product in medical applications involving permanent implantation in the human body. For other medical applications see "DuPont Medical Caution Statement", H-51459 or H-50102.

Zytel® 42A NC010

Property	Test Method	Units	Value	
			DAM	50% RH
Mechanical				
Tensile Impact Strength	ASTM D 1822	kJ/m2 (ft lb/in2)		
Long specimen			535 (255)	
Izod Impact	ASTM D 256	J/m (ft lb/in)		
-40C (-40F)			32 (0.6)	27 (0.5)
23C (73F)			64 (1.2)	133 (2.5)
Thermal				
Heat Deflection Temperature	ASTM D 648	°C (°F)		
0.45MPa (66psi)			210 (410)	
1.8MPa (264psi)			65 (149)	
CLTE, Parallel	ASTM D 696	E-4/C (E-4/F)	0.7 (0.39)	
Melting Point	ASTM D 3418	°C (°F)	263 (505)	
Thermal Conductivity	ASTM C 177	W/m K (Btu in/h ft2 F)		
Conco-Fitch apparatus			0.25 (1.7)	
Electrical				
Volume Resistivity	ASTM D 257	ohm cm	1 E15	1 E13
Dielectric Constant	ASTM D 150			
1E2 Hz			4.0	8.0
1E3 Hz			3.9	7.0
1E6 Hz			3.6	4.6
Dissipation Factor	ASTM D 150			
1E2 Hz			0.01	0.20
1E3 Hz			0.02	0.20
1E6 Hz			0.02	0.10
Arc Resistance	ASTM D 495	s	116	
CTI	UL 746A	V	>600	
Flammability				
Flammability Classification	UL94			
0.71mm (0.028in)			HB	
1.5mm			HB	
3.0mm			V-2	
6.0mm			V-2	
Rating @ Thickness	UL94		HB	
Thickness Tested	UL94	mm	0.71	
High Amperage Arc Ignition Resistance	UL 746A	arcs	182	
High Voltage Arc Tracking Rate	UL 746A	mm/min (in/min)	25.9 (1.02)	
Hot Wire Ignition	UL 746A	s	35	
Temperature Index				
RTI Electrical	UL 746B	°C		
0.71mm			125	
1.5mm			125	
3.0mm			125	
6.0mm			125	

Contact DuPont for Material Safety Data Sheet, general guides and/or additional information about ventilation, handling, purging, drying, etc.
Mechanical properties measured at 23°C (73°F) unless otherwise stated.

Zytel® is a DuPont registered trademark. 980531/991014

The information provided in this data sheet corresponds to our knowledge on the subject at the time of its publication. This information may be subject to revision as new knowledge and experience becomes available. The data provided fall within the normal range of product properties and relate only to the specific material designated; these data may not be valid for such material used in combination with any other materials or additives or in any process, unless expressly indicated otherwise. The data provided should not be used to establish specification limits or used alone as the basis of design; they are not intended to substitute for any testing you may need to conduct to determine for yourself the suitability of a specific material for your particular purposes. Since DuPont cannot anticipate all variations in actual end-use conditions DuPont makes no warranties and assumes no liability in connection with any use of this information. Nothing in this publication is to be considered as a license to operate under or a recommendation to infringe any patent rights. Caution: Do not use this product in medical applications involving permanent implantation in the human body. For other medical applications see "DuPont Medical Caution Statement", H-51459 or H-50102.

Zytel® 42A NC010

Property	Test Method	Units	Value	
			DAM	50% RH
Temperature Index				
RTI, Mechanical with Impact	UL 746B	°C		
0.71mm			65	
1.5mm			75	
3.0mm			75	
6.0mm			75	
RTI, Mechanical without Impact	UL 746B	°C		
0.71mm			65	
1.5mm			85	
3.0mm			85	
6.0mm			85	
Other				
Specific Gravity	ASTM D 792		1.14	
Hardness, Rockwell	ASTM D 785			
Scale M			80	60
Scale R			121	108
Taber Abrasion	ASTM D 1044	mg		
CS-17 Wheel, 1kg, 1000 cycles				4
Water Absorption	ASTM D 570	%		
Immersion 24h			1.2	
Saturation			8.5	
Mold Shrinkage		%		
Flow, 3.2mm (0.126in)			1.5	
Brittleness Temperature	ASTM D 746	°C (°F)	-100 (-148)	-85 (-121)
Processing				
Melt Temperature Range		°C (°F)	280-305 (530-550)	
Drying Time, Dehumidified Dryer		h	2-4	
Drying Temperature		°C (°F)	80 (175)	
Processing Moisture Content		%	<0.05	

Contact DuPont for Material Safety Data Sheet, general guides and/or additional information about ventilation, handling, purging, drying, etc.
Mechanical properties measured at 23°C (73°F) unless otherwise stated.

Zytel® is a DuPont registered trademark.

9-05531/991014

The information provided in this data sheet corresponds to our knowledge on the subject at the date of its publication. This information may be subject to revision as new knowledge and experience become available. The data provided fall within the normal range of product properties and relate only to the specific material designated; these data may not be valid for such material used in combination with any other materials or additives or in any process, unless expressly indicated otherwise. The data provided should not be used to establish specification limits or used alone as the basis of design; they are not intended to substitute for any testing you may need to conduct to determine for yourself the suitability of a specific material for your particular purposes. Since DuPont cannot anticipate all variations in actual end-use conditions DuPont makes no warranties and assumes no liability in connection with any use of this information. Nothing in this publication is to be considered as a license to operate under or a recommendation to infringe any patent rights. Caution: Do not use this product in medical applications involving permanent implantation in the human body. For other medical applications see "DuPont Medical Caution Statement", H-51459 or H-50102.

Table 2. Comparison of piezoelectric materials

Property	Units	PVDF Film	PZT	$BaTi0_3$
Density	10^3kg/m3	1.78	7.5	5.7
Relative Permittivity	$\varepsilon/\varepsilon_0$	12	1,200	1,700
d_{31} Constant	(10^{-12})C/N	23	110	78
g_{31} Constant	(10^{-3})Vm/N	216	10	5
k_{31} Constant	% at 1 kHz	12	30	21
Acoustic Impedance	(10^6)kg/m^2-sec.	2.7	30	30

OPERATING PROPERTIES FOR A TYPICAL PIEZO FILM ELEMENT

The DT1 element is a standard MSI piezo film configuration consisting of a 12x30 mm active area printed with silver ink electrodes on both surfaces of a 15x40 mm die-cut piezo polymer substrate.

1. Electro-Mechanical Conversion
   (1 direction) 25 x 10^{-12}m/V, 700 x 10^{-6}N/V
   (3 direction) 33 x 10^{-12}m/V

2. Mechano-Electrical Conversion
   (1 direction) 12 x 10^{-3}Vμ/ε, 400 x 10^{-3}V/μm 14.4V/N
   (3 direction) 13 x 10^{-3}V/N

3. Pyro-Electrical Conversion
   8V/°K (@ 25°C)

4. Capacitance
   1.36 x 10^{-9}F; Dissipation Factor 0.018 @ 10 KHz Impedance @ 10 KHz 12 KΩ

5. Maximum Operating Voltage
   DC: 280 V (yields 7 µm displacement in 1 direction)
   AC: 840 V (yields 21 µm displacement in 1 direction)

6. Maximum Applied Force (at break, 1 direction)
   6-9 kgF (yields voltage output of 830 to 1275 V)

Electrical to Mechanical Conversion

Large displacements or forces are not generally available from Piezo Film. This becomes apparent when designing loudspeaker elements for instance, as low frequency performance (below 500Hz) tends to be very limited. Even a large sheet of film is unable to create high amplitude pressure pulses as low audio frequencies. This does not apply, however, to low to high frequency ultrasonic frequencies, as seen in current designs for ultrasound air ranging transducers (40-50 kHz) and in medical ultrasonic imaging applications.

Figure 4. DT1 Element

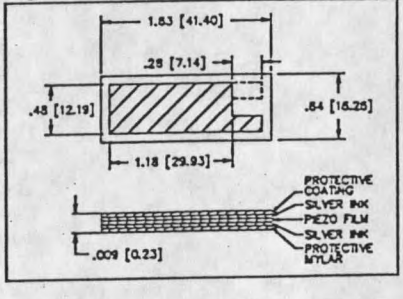


Table 2. Comparison of piezoelectric materials

Property	Units	PVDF Film	PZT	$BaTi0_3$
Density	10^3kg/m3	1.78	7.5	5.7
Relative Permittivity	$\varepsilon/\varepsilon_0$	12	1,200	1,700
d_{31} Constant	(10^{-12})C/N	23	110	78
g_{31} Constant	(10^{-3})Vm/N	216	10	5
k_{31} Constant	% at 1 kHz	12	30	21
Acoustic Impedance	(10^6)kg/m^2-sec.	2.7	30	30

OPERATING PROPERTIES FOR A TYPICAL PIEZO FILM ELEMENT

The DT1 element is a standard MSI piezo film configuration consisting of a 12x30 mm active area printed with silver ink electrodes on both surfaces of a 15x40 mm die-cut piezo polymer substrate.

1. Electro-Mechanical Conversion
   (1 direction) 25 x 10^{-12}m/V, 700 x 10^{-6}N/V
   (3 direction) 33 x 10^{-12}m/V

2. Mechano-Electrical Conversion
   (1 direction) 12 x 10^{-3}Vμ/ε, 400 x 10^{-3}V/μm 14.4V/N
   (3 direction) 13 x 10^{-3}V/N

3. Pyro-Electrical Conversion
   8V/°K (@ 25°C)

4. Capacitance
   1.36 x 10^{-9}F; Dissipation Factor 0.018 @ 10 KHz Impedance @ 10 KHz 12 KΩ

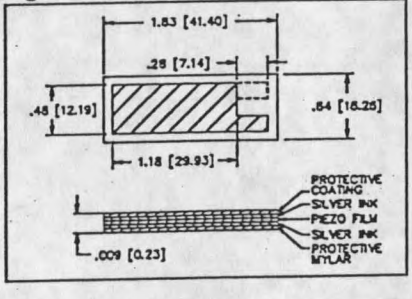
5. Maximum Operating Voltage
   DC: 280 V (yields 7 μm displacement in 1 direction)
   AC: 840 V (yields 21 μm displacement in 1 direction)

6. Maximum Applied Force (at break, 1 direction)
   6-9 kgF (yields voltage output of 830 to 1275 V)

Electrical to Mechanical Conversion

Large displacements or forces are not generally available from Piezo Film. This becomes apparent when designing loudspeaker elements for instance, as low frequency performance (below 500Hz) tends to be very limited. Even a large sheet of film is unable to create high amplitude pressure pulses as low audio frequencies. This does not apply, however, to low to high frequency ultrasonic frequencies, as seen in current designs for ultrasound air ranging transducers (40-50 kHz) and in medical ultrasonic imaging applications.

Figure 4. DT1 Element



APPENDIX Q

Instron 1350 Environmental Chamber Design

Instron 1350 Environmental Chamber Design

Q = Heat in the inslulated volume approximately $= m_{st} \cdot C_{pst} \cdot (T_{in} - T_{inf})$

Qdot = Heat loss by conduction through the insulation $- k_{ins} \cdot \frac{A_{box}}{\delta_{ins}} \cdot (T_{in} - T_{inf})$

$m_{st} := 14.166 \quad kg$ Mass of Steel Environmental Chamber

$C_{pst} := 447 \quad \frac{J}{kg \cdot K}$ Specific Heat Coefficient for Steel

$k_{ins} := .035594 \quad \frac{W}{m \cdot K}$ Thermal Conductivity of the Insulation

$A_{box} := .5723 \quad m^2$ Surface Area of the Environmental Chamber

$\delta_{ins} := .1016 \quad m$ Thickness of the Insulation

$T_{in} := 573 \quad K$ Temperature Inside the Environmental Chamb

$T_{inf} := 300 \quad K$ Temperature of the Surroundings

t Time in seconds

Derivation

$$Q = m_{st} \cdot C_{pst} \cdot (T_{in} - T_{inf})$$

$$Qdot = m_{st} \cdot C_{pst} \cdot \left[\frac{d}{dt} (T_{in} - T_{inf}) \right]$$

$$\frac{d}{dt} (T_{in} - T_{inf}) = \frac{1}{m_{st} \cdot C_{pst}} \cdot \left(-k_{ins} \cdot \frac{A_{box}}{\delta_{ins}} \right) \cdot (T_{in} - T_{inf})$$

$$p := \frac{k_{ins}}{m_{st} \cdot C_{pst}} \cdot \frac{A_{box}}{\delta_{ins}}$$

$$\frac{d(T_{in} - T_{inf})}{(T_{in} - T_{inf})} = -p \cdot dt$$

$$\ln\left(T_{in} - T_{inf}\right) = C - \frac{t}{\tau} \qquad \tau = \frac{1}{p}$$

$$T_{in} - T_{inf} = e^{C} \cdot e^{\frac{-t}{\tau}}$$

At $t = 0$, $\quad T_{in} - T_{inf} = \Delta T_o$

$$\Delta T = \Delta T_o \cdot e^{\frac{-t}{\tau}}$$

$$\tau := \frac{1}{p} \cdot .05$$ 5 % Fluctuation in the temperature

Cycle Time $\quad \tau = 1.579 \cdot 10^{3}$ sec

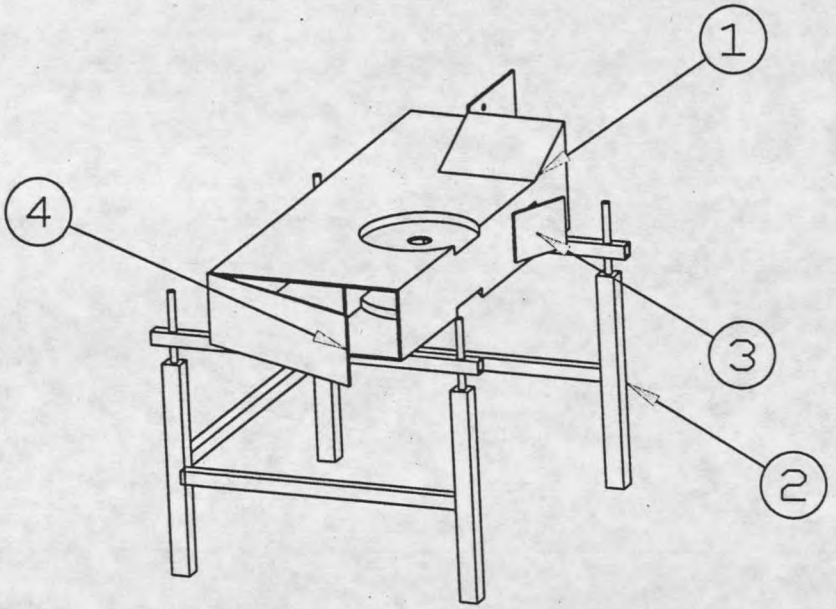
26.3 min

Heater Sizing where Steady State Conditions Are Used

$$\frac{dQ}{dt} = W_{dot} - k_{ins} \cdot \frac{A_{box}}{\delta_{ins}} \cdot \left(T_{in} - T_{inf}\right)$$

W_{dot} Heat Generation by the Heater

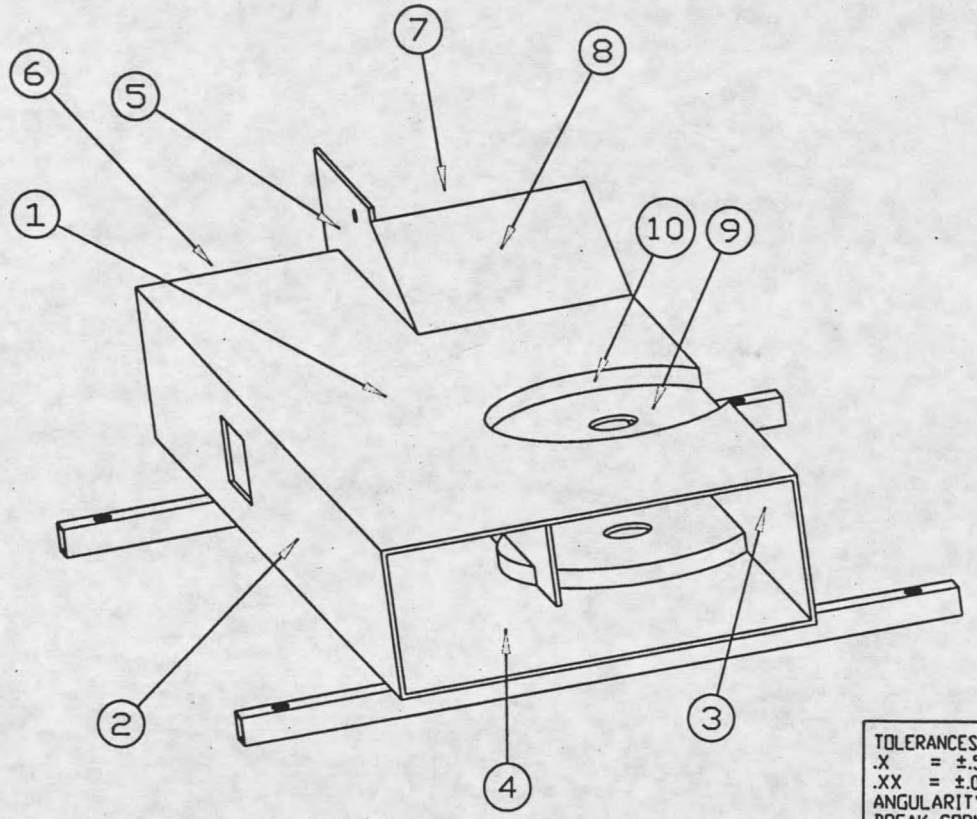
$$k_{ins} \cdot \frac{A_{box}}{\delta_{ins}} \cdot \left(T_{in} - T_{inf}\right) = 54.73\epsilon W$$



1	Enviromental Chamber
2	Support Stand
3	Enviro Chamber Door
4	Heater Access Door

TOLERANCES UNLESS NOTED .X = ±.50 .XX = ±.025 ANGULARITY = ±.5° BREAK CORNERS - .010 MAX FILLET RADII - .015 MAX DIMENSIONS ARE IN MM UNLESS NOTED	MATERIAL	Steel
	FINISH	As Delivered
	Montana State University	
	Enviro Chamber & Stand	
DRAWN Carl Thrasher	SIZE A	DWG NO. ENVIRONCHAM
ENGINEER Shane Schumacher		
CREATION DATE 20-Jun-00	SCALE: NTS	SHEET 1 of 1

615



1	Top
2	Left Side
3	Right Side
4	Bottom
5	Center Piece
6	Back No Hole
7	Back Fan Hole
8	Slanted Top
9	Grip Cut Out Plates
10	Grip Cut Out Ring

TOLERANCES UNLESS NOTED
.X = ±.50
.XX = ±.025
ANGULARITY = ±.5°
BREAK CORNERS - .010 MAX
FILLET RADII - .015 MAX
DIMENSIONS ARE IN MM
UNLESS NOTED

MATERIAL	Steel
FINISH	As Delivered

Montana State University

Environmental Chamber

DRAWN Carl Thrasher

ENGINEER Shane Schumacher

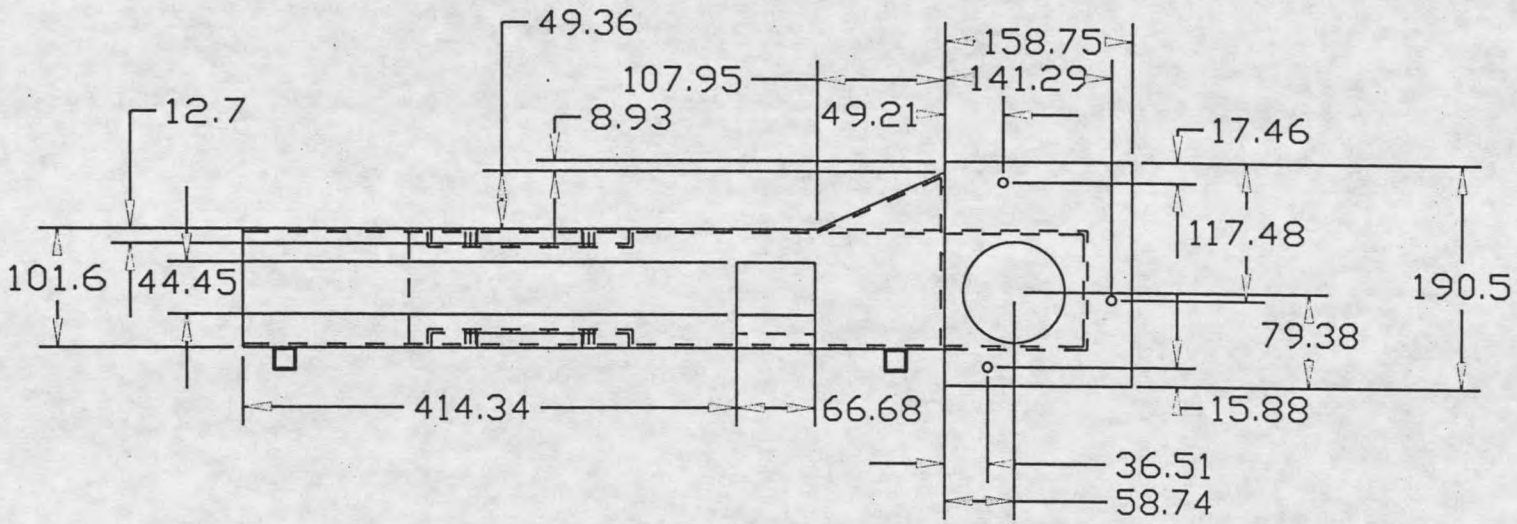
CREATION DATE 20-Jun-00

SIZE A

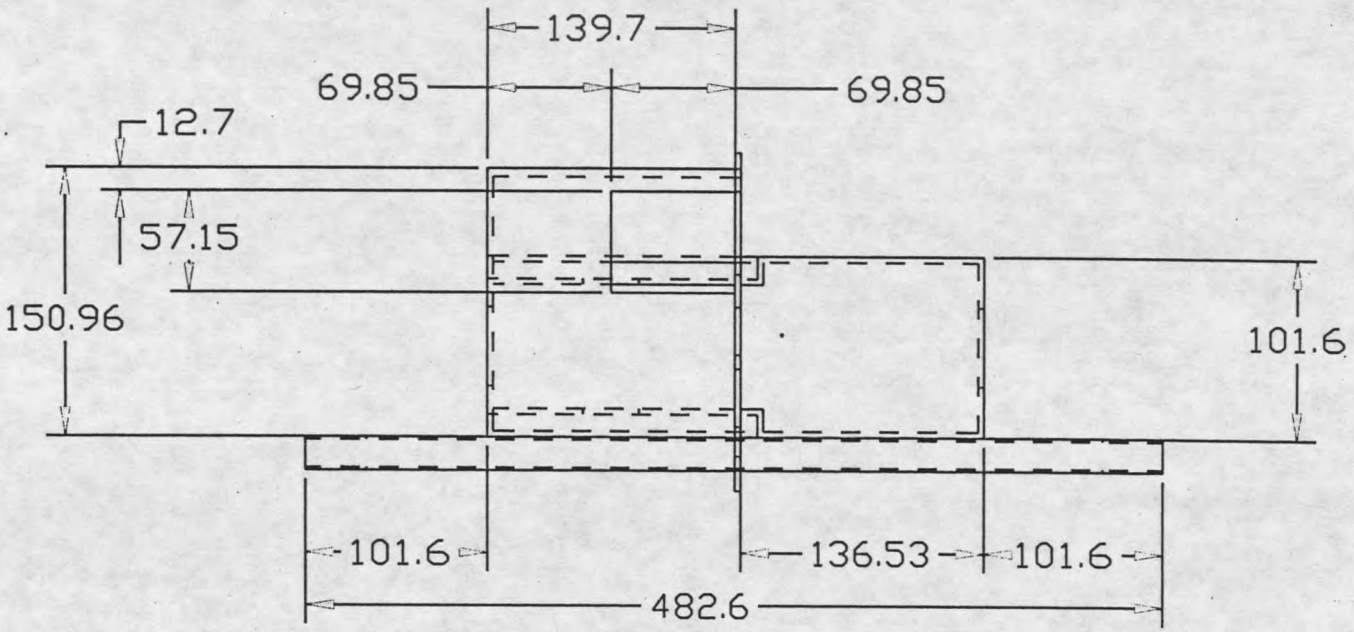
DWG NO. CHAMBER

SCALE: NTS

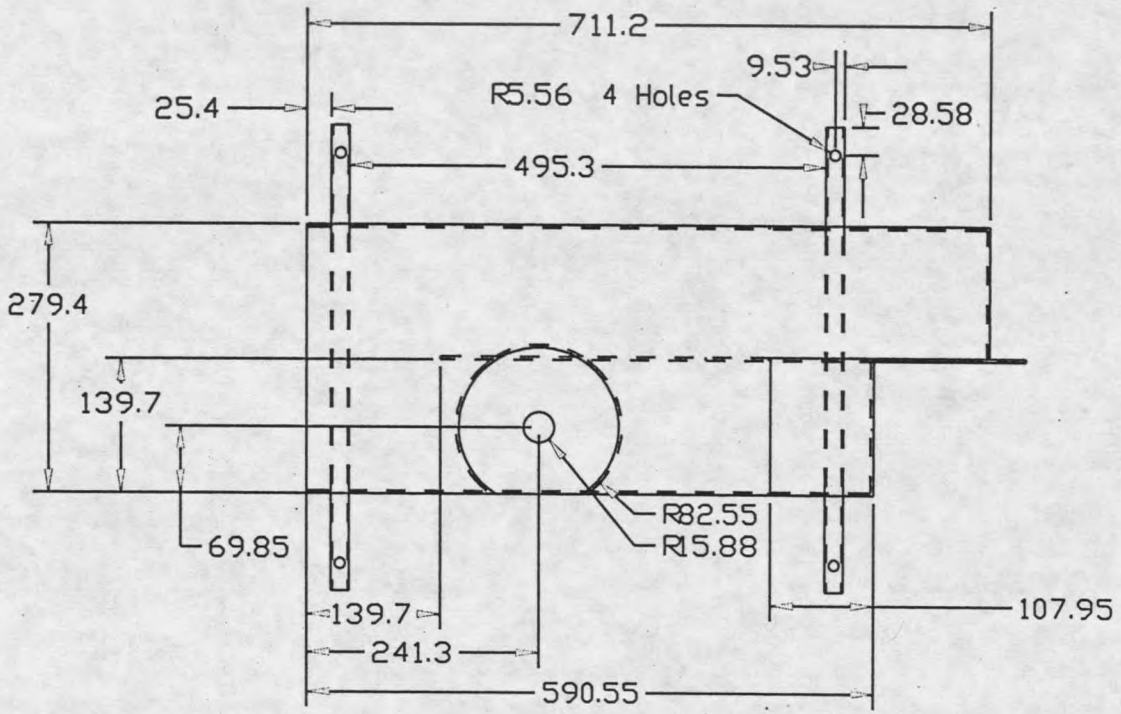
SHEET 1 of 4



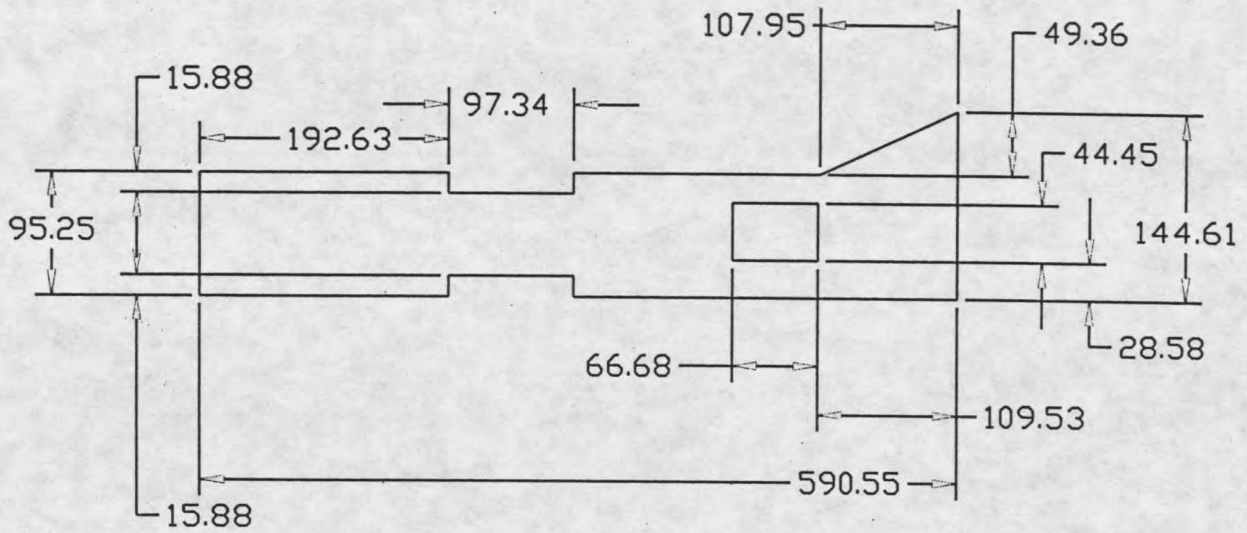
TOLERANCES UNLESS NOTED .X = ±.50 .XX = ±.025 ANGULARITY = ±.5° BREAK CORNERS - .010 MAX FILLET RADII - .015 MAX DIMENSIONS ARE IN MM UNLESS NOTED	MATERIAL	Steel
	FINISH	As Delivered
	Montana State University	
	SIDE VIEW - ENVIRO CHAMBER	
DRAWN Carl Thrasher	SIZE A	DWG NO. CHAMBER
ENGINEER Shane Schumacher		
CREATION DATE 20-Jun-00	SCALE: NTS	SHEET 2 of 4



TOLERANCES UNLESS NOTED .X = ±.50 .XX = ±.025 ANGULARITY = ±.5° BREAK CORNERS - .010 MAX FILLET RADII - .015 MAX DIMENSIONS ARE IN MM UNLESS NOTED	MATERIAL	Steel
	FINISH	As Delivered
	Montana State University	
	BACK VIEW - TEMP CHAMBER	
DRAWN Carl Thrasher	SIZE A	DWG NO. CHAMBER
ENGINEER Shane Schumacher		
CREATION DATE 20-Jun-00	SCALE: NTS	SHEET 3 of 4

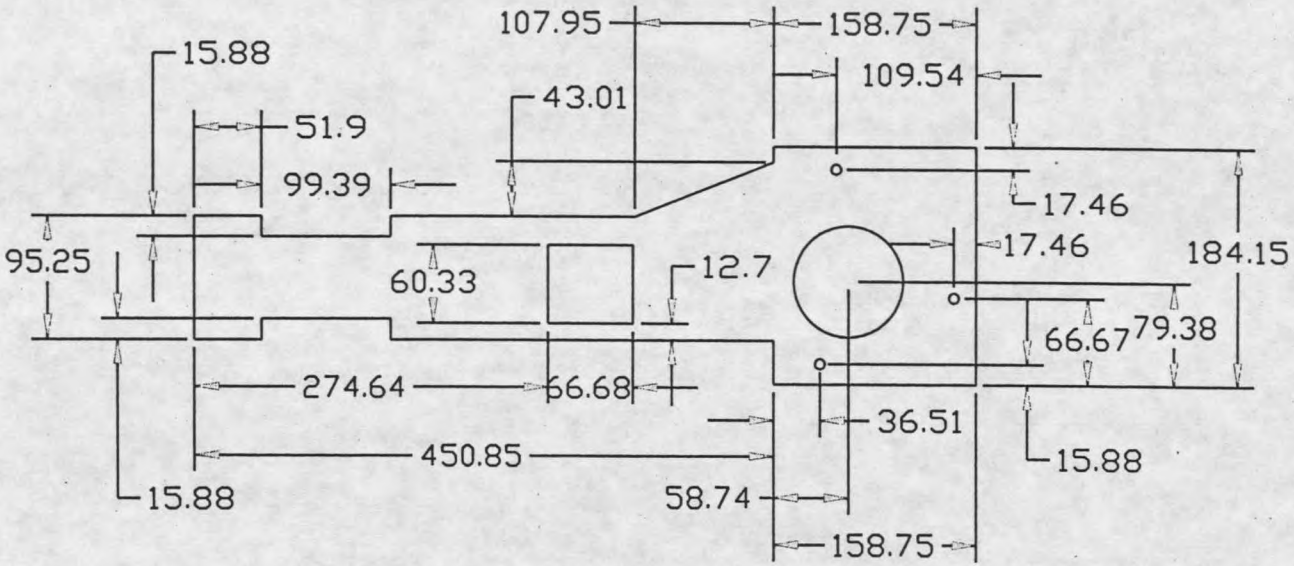


TOLERANCES UNLESS NOTED .X = ±.50 .XX = ±.025 ANGULARITY = ±.5° BREAK CORNERS - .010 MAX FILLET RADII - .015 MAX DIMENSIONS ARE IN MM UNLESS NOTED	MATERIAL	Steel
	FINISH	As Delivered
	Montana State University	
	TOP VIEW - TEMP CHAMBER	
DRAWN Carl Thrasher	SIZE A	DWG NO. CHAMBER
ENGINEER Shane Schumacher		
CREATION DATE 20-Jun-00	SCALE: NTS	SHEET 4 of 4



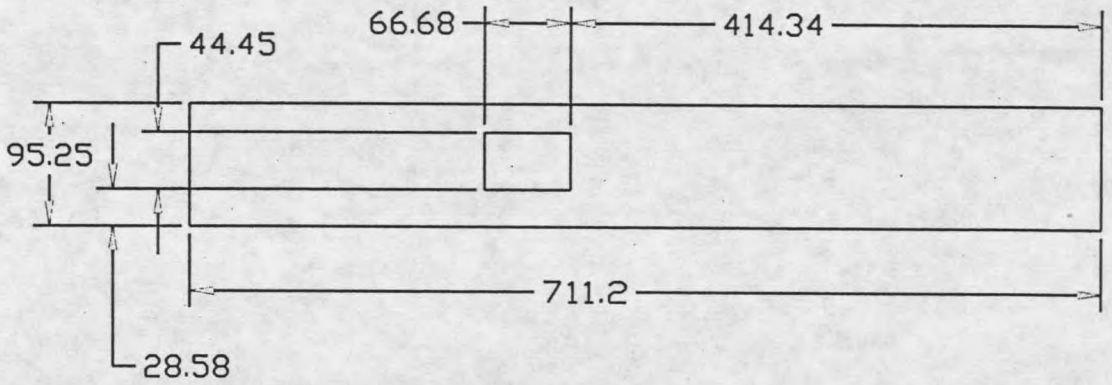
TOLERANCES UNLESS NOTED .X = ±.50 .XX = ±.025 ANGULARITY = ±.5° BREAK CORNERS - .010 MAX FILLET RADII - .015 MAX DIMENSIONS ARE IN MM UNLESS NOTED	MATERIAL	Steel
	FINISH	As Delivered
	Montana State University	
	Right Side - Enviro Chamber	
DRAWN Carl Thrasher	SIZE A	DWG NO. RIGHT
ENGINEER Shane Schumacher		
CREATION DATE 20-Jun-00	SCALE NTS	SHEET 1 of 1

620

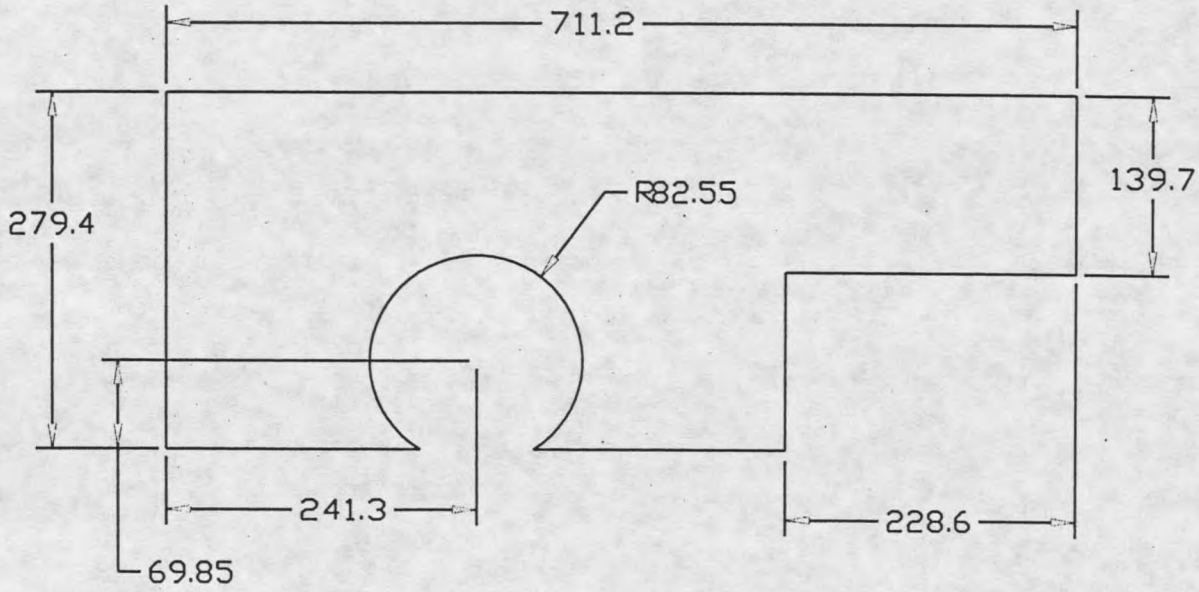


TOLERANCES UNLESS NOTED .X = ±.50 .XX = ±.025 ANGULARITY = ±.5° BREAK CORNERS - .010 MAX FILLET RADII - .015 MAX DIMENSIONS ARE IN MM UNLESS NOTED	MATERIAL	Steel
	FINISH	As Delivered
	Montana State University	
	Center Environ Chamber	
DRAWN Carl Thrasher	SIZE A	DWG NO. CENTER
ENGINEER Shane Schumacher		
CREATION DATE 20-Jun-00	SCALE NTS	SHEET 1 of 1

621

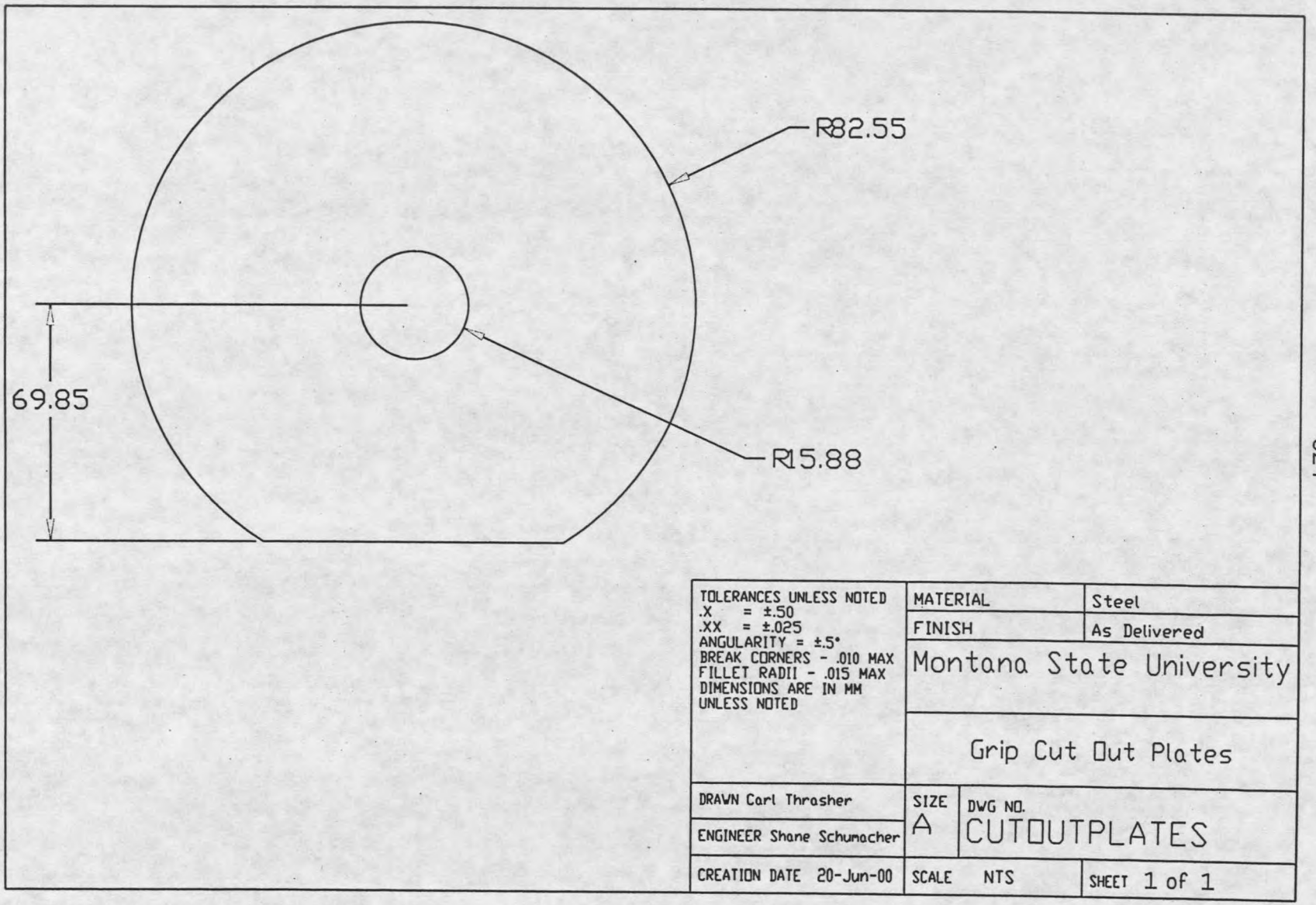


TOLERANCES UNLESS NOTED .X = ±.50 .XX = ±.025 ANGULARITY = ±.5° BREAK CORNERS - .010 MAX FILLET RADII - .015 MAX DIMENSIONS ARE IN MM UNLESS NOTED	MATERIAL	Steel
	FINISH	As Delivered
	Montana State University	
	Left Side - Enviro Chamber	
DRAWN Carl Thrasher	SIZE A	DWG NO. LEFT
ENGINEER Shane Schumacher		
CREATION DATE 20-Jun-00	SCALE NTS	SHEET 1 of 1

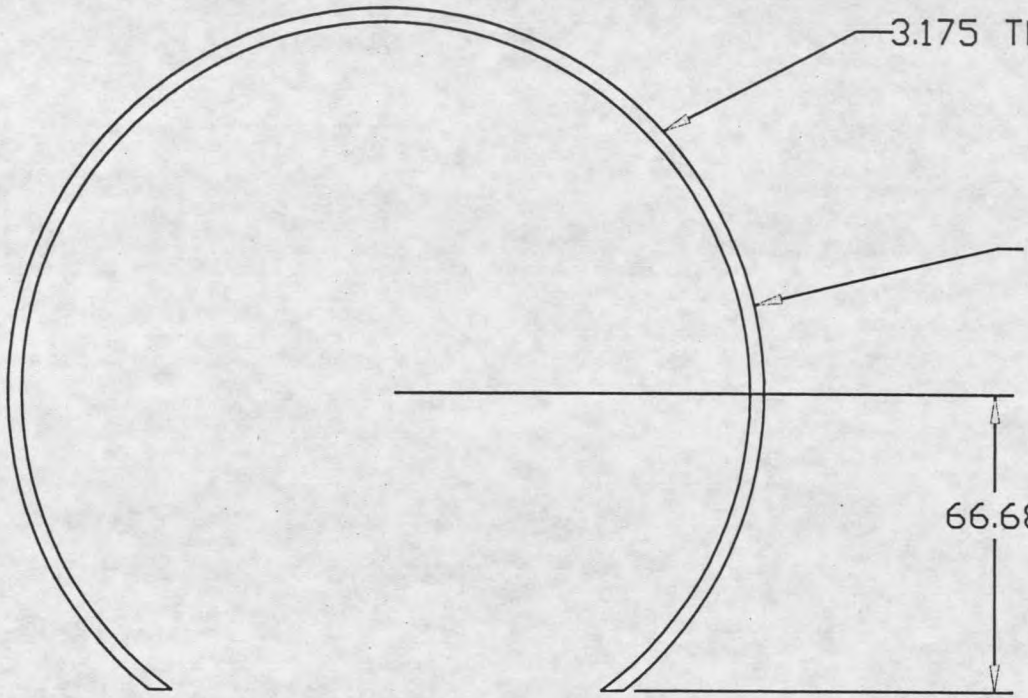


TOLERANCES UNLESS NOTED .X = ±.50 .XX = ±.025 ANGULARITY = ±.5° BREAK CORNERS - .010 MAX FILLET RADII - .015 MAX DIMENSIONS ARE IN MM UNLESS NOTED	MATERIAL	Steel
	FINISH	As Delivered
	Montana State University	
	Top - Enviro Chamber	
DRAWN Carl Thrasher	SIZE A	DWG NO. TOP
ENGINEER Shane Schumacher		
CREATION DATE 20-Jun-00	SCALE NTS	SHEET 1 of 1

623

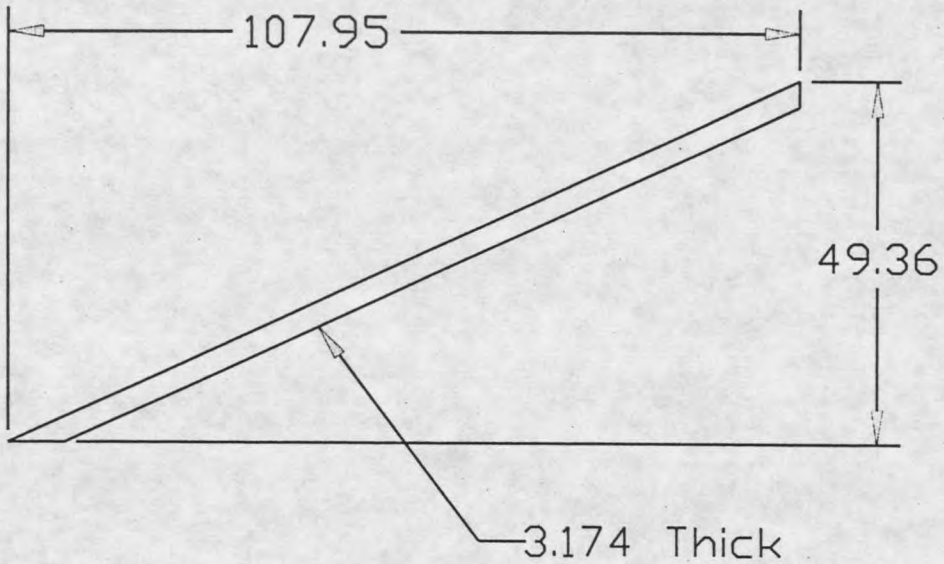


TOLERANCES UNLESS NOTED .X = ±.50 .XX = ±.025 ANGULARITY = ±.5° BREAK CORNERS - .010 MAX FILLET RADII - .015 MAX DIMENSIONS ARE IN MM UNLESS NOTED	MATERIAL	Steel
	FINISH	As Delivered
	Montana State University	
	Grip Cut Out Plates	
DRAWN Carl Thrasher	SIZE A	DWG NO. CUTOUTPLATES
ENGINEER Shane Schumacher		
CREATION DATE 20-Jun-00	SCALE NTS	SHEET 1 of 1



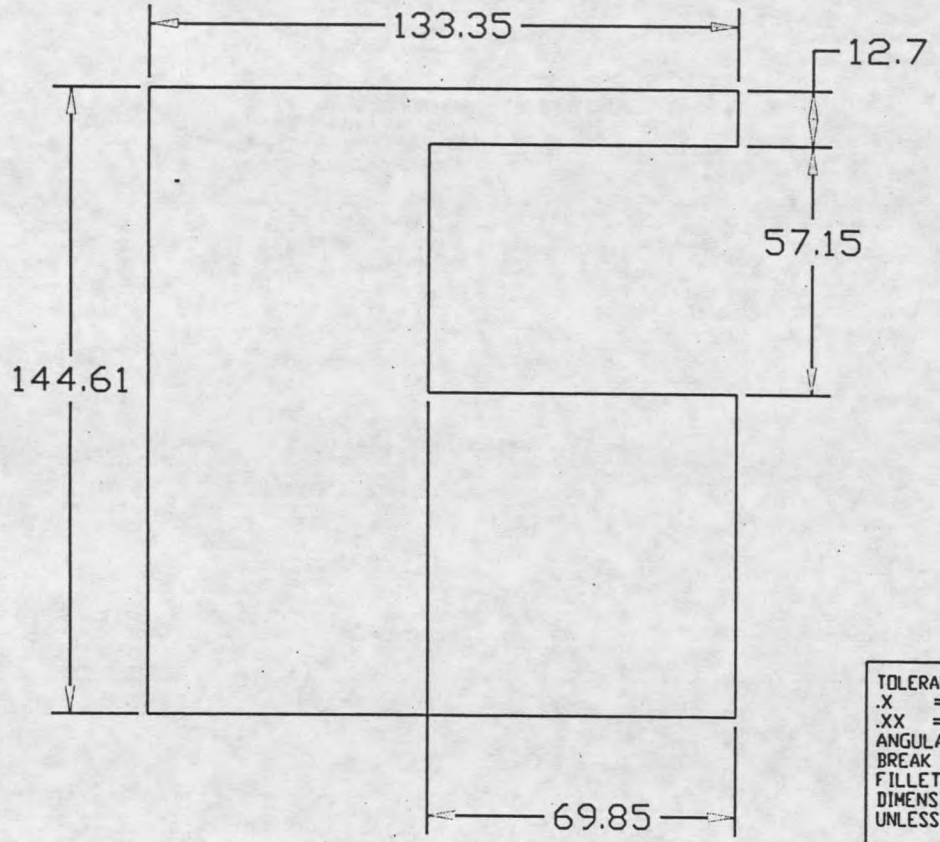
TOLERANCES UNLESS NOTED .X = ±.50 .XX = ±.025 ANGULARITY = ±.5° BREAK CORNERS - .010 MAX FILLET RADII - .015 MAX DIMENSIONS ARE IN MM UNLESS NOTED	MATERIAL	Steel
	FINISH	As Delivered
	Montana State University	
	Grip Cut Out Rings	
DRAWN Carl Thrasher	SIZE A	DWG NO. GRIPCUTOUTRINGS
ENGINEER Shane Schumacher		
CREATION DATE 20-Jun-00	SCALE NTS	SHEET 1 of 1

625



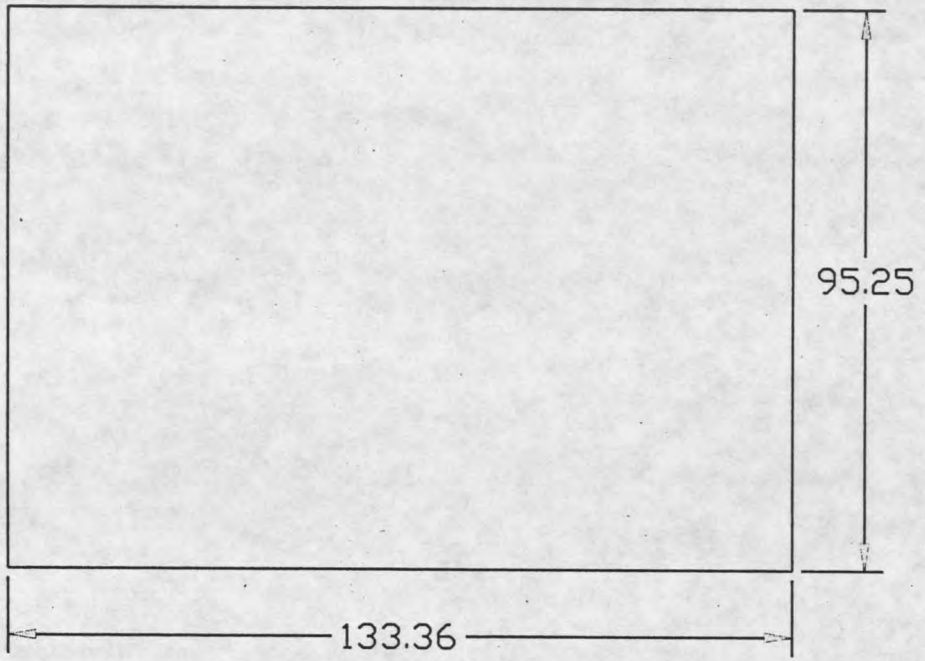
626

TOLERANCES UNLESS NOTED .X = ±.50 .XX = ±.025 ANGULARITY = ±.5° BREAK CORNERS - .010 MAX FILLET RADII - .015 MAX DIMENSIONS ARE IN MM UNLESS NOTED	MATERIAL	Steel
	FINISH	As Delivered
	Montana State University	
	Slanted Top	
DRAWN Carl Thrasher	SIZE A	DWG NO. SLANTEDTOP
ENGINEER Shane Schumacher		
CREATION DATE 20-Jun-00	SCALE NTS	SHEET 1 of 1



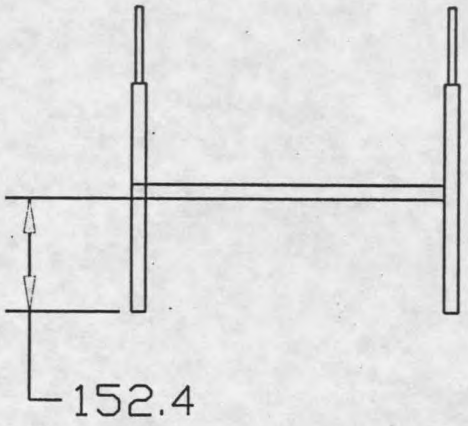
TOLERANCES UNLESS NOTED .X = ±.50 .XX = ±.025 ANGULARITY = ±.5° BREAK CORNERS - .010 MAX FILLET RADII - .015 MAX DIMENSIONS ARE IN MM UNLESS NOTED	MATERIAL	Steel
	FINISH	As Delivered
	Montana State University	
	Back Plate With Fan Hole	
DRAWN Carl Thrasher	SIZE A	DWG NO. BACKFANHOLE
ENGINEER Shane Schumacher		
CREATION DATE 20-Jun-00	SCALE NTS	SHEET 1 of 1

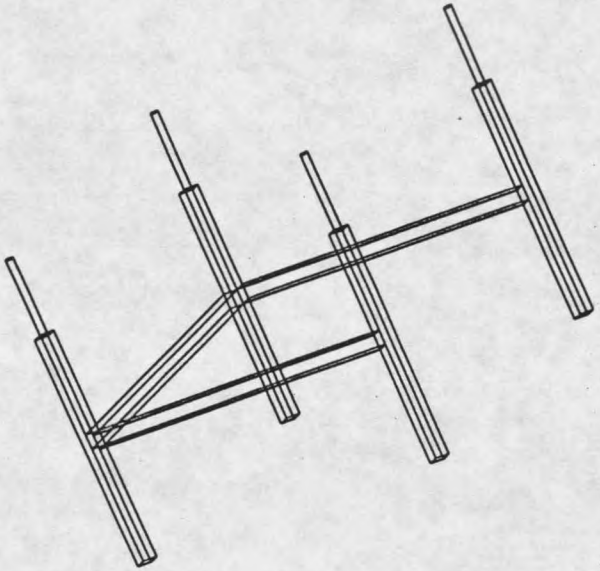
627

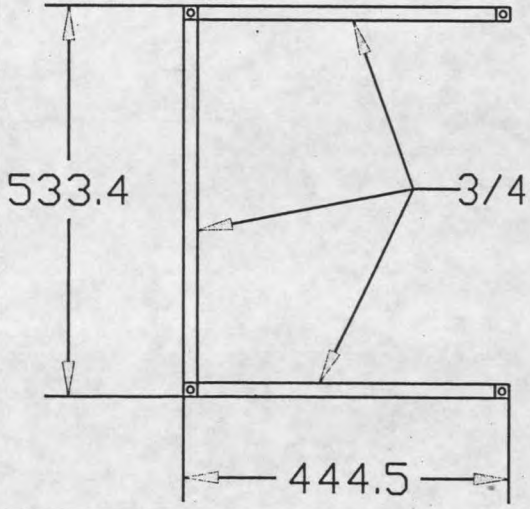


628

TOLERANCES UNLESS NOTED .X = ±.50 .XX = ±.0250 ANGULARITY = ±.5° BREAK CORNERS - .010 MAX FILLET RADII - .015 MAX DIMENSIONS ARE IN MM UNLESS NOTED	MATERIAL	Steel
	FINISH	As Delivered
	Montana State University	
	Back Plate	
DRAWN Carl Thrasher	SIZE A	DWG NO. BACKNOHOLE
ENGINEER Shane Schumacher		
CREATION DATE 20-Jun-00	SCALE NTS	SHEET 1 of 1

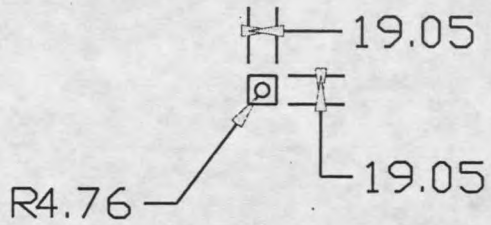


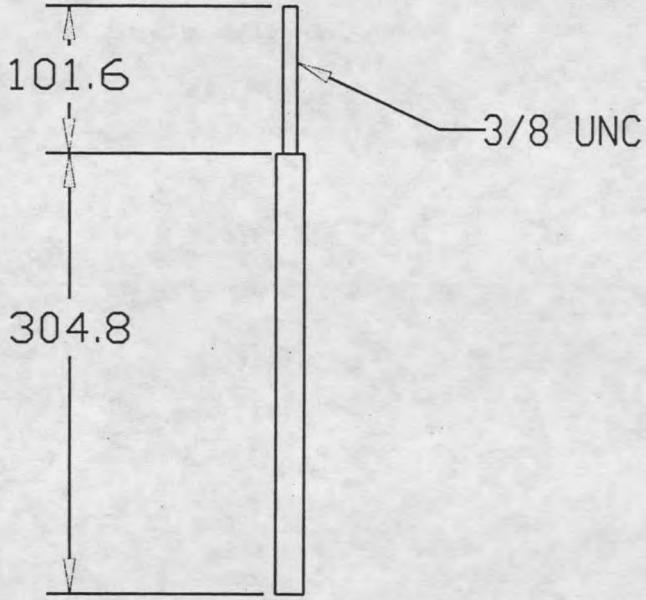




TOLERANCES UNLESS NOTED .X = ±.50 .XX = ±.025 ANGULARITY = ±.5° BREAK CORNERS - .010 MAX FILLET RADII - .015 MAX DIMENSIONS ARE IN MM UNLESS NOTED	MATERIAL	Steel
	FINISH	As Delivered
	Montana State University	
	Enviro Chamber Support Rack	
DRAWN Carl Thrasher	SIZE A	DWG NO. SUPPORTRACK
ENGINEER Shane Schumacher		
CREATION DATE 20-Jun-00	SCALE NTS	SHEET 1 of 1

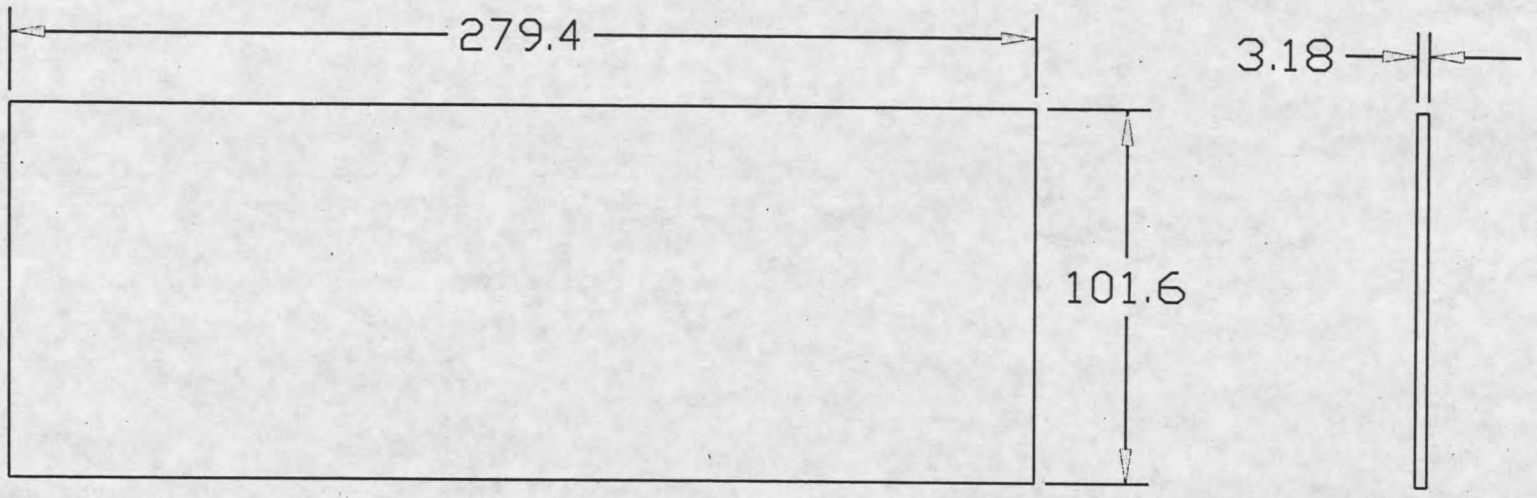
629





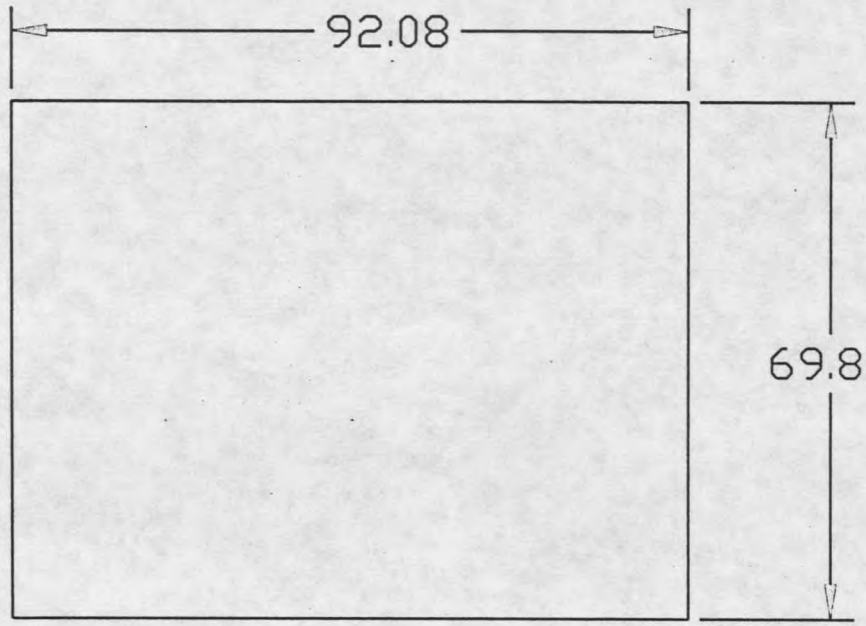
TOLERANCES UNLESS NOTED .X = ±.50 .XX = ±.025 ANGULARITY = ±.5° BREAK CORNERS - .010 MAX FILLET RADII - .015 MAX DIMENSIONS ARE IN MM UNLESS NOTED	MATERIAL	Steel
	FINISH	As Delivered
	Montana State University	
	Support Columns	
DRAWN Carl Thrasher	SIZE A	DWG NO. COLUMNS
ENGINEER Shane Schumacher		
CREATION DATE 20-Jun-00	SCALE NTS	SHEET 1 of 1

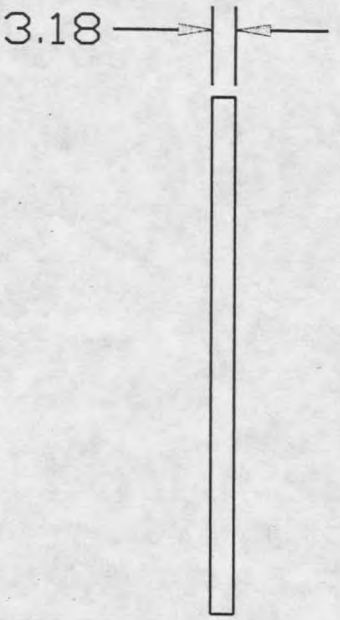
630



631

TOLERANCES UNLESS NOTED .X = ±.50 .XX = ±.025 ANGULARITY = ±.5° BREAK CORNERS - .010 MAX FILLET RADII - .015 MAX DIMENSIONS ARE IN MM UNLESS NOTED	MATERIAL	Steel
	FINISH	As Delivered
	Montana State University	
	Enviro Chamber Front Door	
DRAWN Carl Thrasher	SIZE A	DWG NO. FRONTDOOR
ENGINEER Shane Schumacher		
CREATION DATE 20-Jun-00	SCALE NTS	SHEET 1 of 1





632

TOLERANCES UNLESS NOTED .X = ±.50 .XX = ±.025 ANGULARITY = ±.5° BREAK CORNERS - .010 MAX FILLET RADII - .015 MAX DIMENSIONS ARE IN MM UNLESS NOTED	MATERIAL	Steel
	FINISH	As Delivered
	Montana State University	
	Heater Access Door	
DRAWN Carl Thrasher	SIZE A	DWG NO. HEATERDOOR
ENGINEER Shane Schumacher		
CREATION DATE 20-Jun-00	SCALE NTS	SHEET 1 of 1

APPENDIX R

Tensile and Creep Environmental Chamber Design

Tensile and Creep Environmental Chamber Design

Q = Heat in the inslulated volume approximately $= m_{st} \cdot C_{pst} \cdot (T_{in} - T_{inf})$

Qdot = Heat loss by conduction through the insulation $- k_{ins} \cdot \frac{A_{box}}{\delta_{ins}} \cdot (T_{in} - T_{inf})$

$m_{st} := 20.89 \quad kg$ Mass of Steel Environmental Chamber

$C_{pst} := 447 \quad \frac{J}{kg \cdot K}$ Specific Heat Coefficient for Steel

$k_{ins} := .035594 \quad \frac{W}{m \cdot K}$ Thermal Conductivity of the Insulation

$A_{box} := 1.672 \quad m^2$ Surface Area of the Environmental Chamber

$\delta_{ins} := .1016 \quad m$ Thickness of the Insulation

$T_{in} := 573 \quad K$ Temperature Inside the Environmental Chamb

$T_{inf} := 300 \quad K$ Temperature of the Surroundings

t Time in seconds

Derivation

$$Q = m_{st} \cdot C_{pst} \cdot (T_{in} - T_{inf})$$

$$Qdot = m_{st} \cdot C_{pst} \cdot \left[\frac{d}{dt} (T_{in} - T_{inf}) \right]$$

$$\frac{d}{dt} (T_{in} - T_{inf}) = \frac{1}{m_{st} \cdot C_{pst}} \cdot \left(- k_{ins} \cdot \frac{A_{box}}{\delta_{ins}} \right) \cdot (T_{in} - T_{inf})$$

$$p := \frac{k_{ins}}{m_{st} \cdot C_{pst}} \cdot \frac{A_{box}}{\delta_{ins}}$$

$$\frac{d(T_{in} - T_{inf})}{(T_{in} - T_{inf})} = -p \cdot dt$$

$$\ln(T_{in} - T_{inf}) = C - \frac{t}{\tau} \qquad \tau = \frac{1}{p}$$

$$T_{in} - T_{inf} = e^{C} \cdot e^{\frac{-t}{\tau}}$$

At t = 0, $T_{in} - T_{inf} = \Delta T_o$

$$\Delta T = \Delta T_o \cdot e^{\frac{-t}{\tau}}$$

$\tau := \frac{1}{p} \cdot .05$ 5 % Fluctuation in the temperature

Cycle Time $\tau = 797.07$ sec

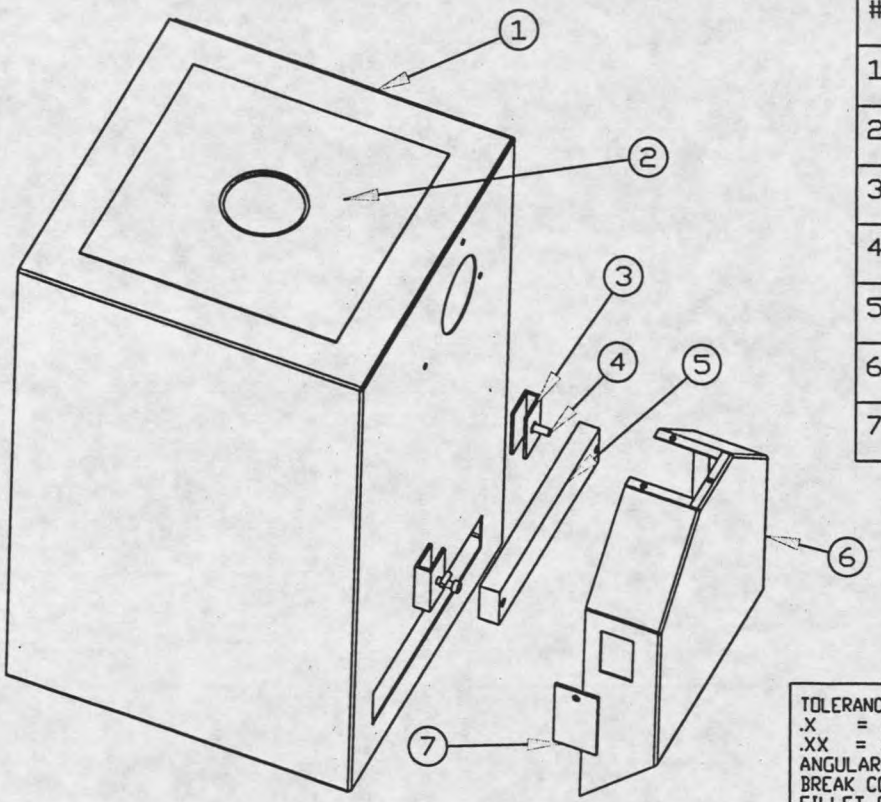
13.28 min

Heater Sizing where Steady State Conditions Are Used

$$\frac{dQ}{dt} = W_{dot} - k_{ins} \cdot \frac{A_{box}}{\delta_{ins}} \cdot (T_{in} - T_{inf})$$

W_{dot} Heat Generation by the Heater

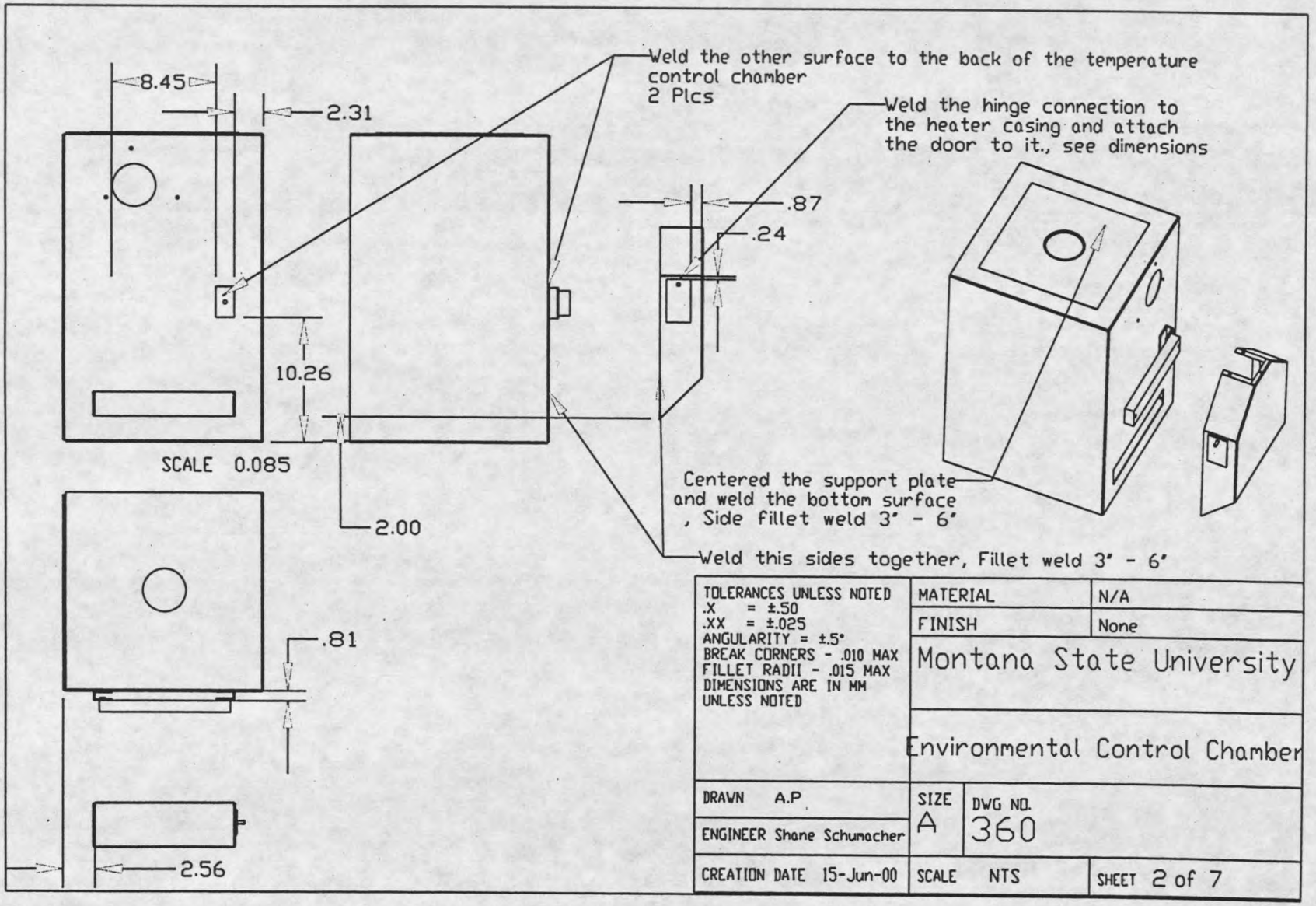
$k_{ins} \cdot \frac{A_{box}}{\delta_{ins}} \cdot (T_{in} - T_{inf}) = 159.912$ W



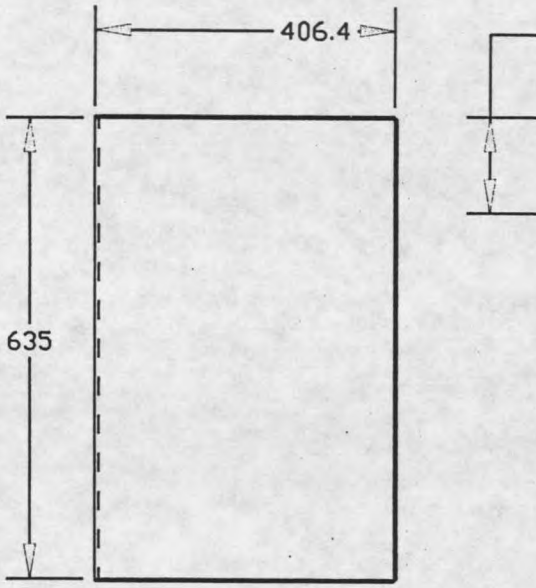
#	DESCRIPTION	PART #	QTY
1	Environmental Control Chamber	370	1
2	Plate Support	380	1
3	C_Channel_Heater_Bracket	390	2
4	1/4" X 3/4" UNC Bolt	400	2
5	Heater	410	1
6	Heater Casing	420	1
7	Opening Door	430	2

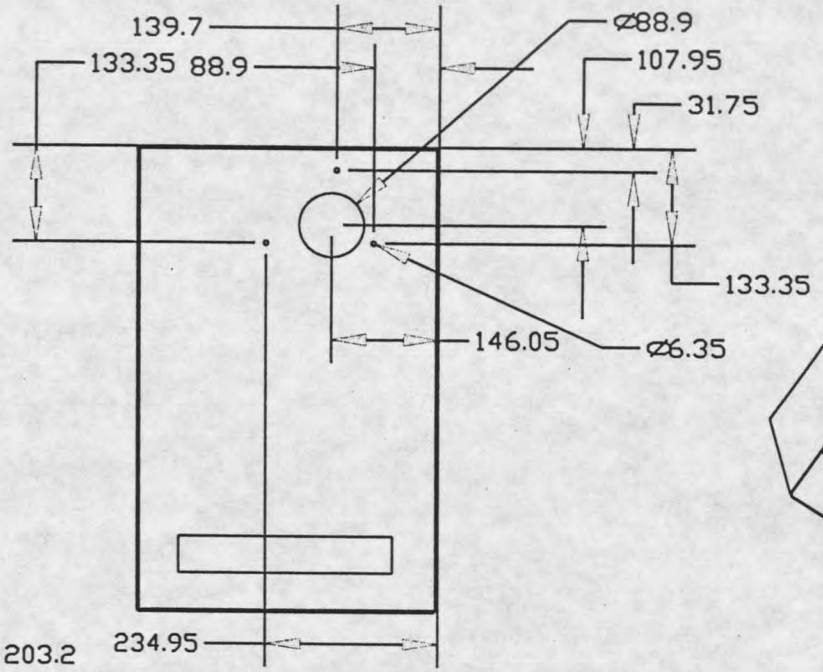
636

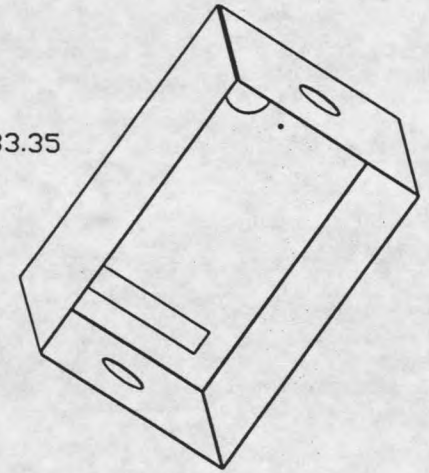
TOLERANCES UNLESS NOTED .X = ±.50 .XX = ±.025 ANGULARITY = ±.5° BREAK CORNERS - .010 MAX FILLET RADII - .015 MAX DIMENSIONS ARE IN MM UNLESS NOTED	MATERIAL	See BOM
	FINISH	None
	Montana State University	
	Assembly Environmental Chamber	
DRAWN A.P	SIZE A	DWG NO. 360
ENGINEER Shane Schumacher		
CREATION DATE 15-Jun-00	SCALE NTS	SHEET 1 of 7

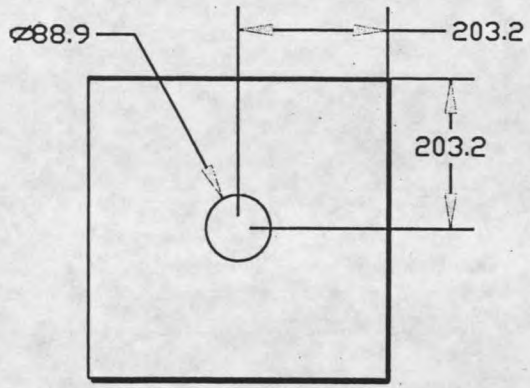


TOLERANCES UNLESS NOTED .X = ±.50 .XX = ±.025 ANGULARITY = ±.5° BREAK CORNERS - .010 MAX FILLET RADII - .015 MAX DIMENSIONS ARE IN MM UNLESS NOTED	MATERIAL	N/A
	FINISH	None
	Montana State University	
	Environmental Control Chamber	
DRAWN A.P	SIZE A	DWG NO. 360
ENGINEER Shane Schumacher		
CREATION DATE 15-Jun-00	SCALE NTS	SHEET 2 of 7



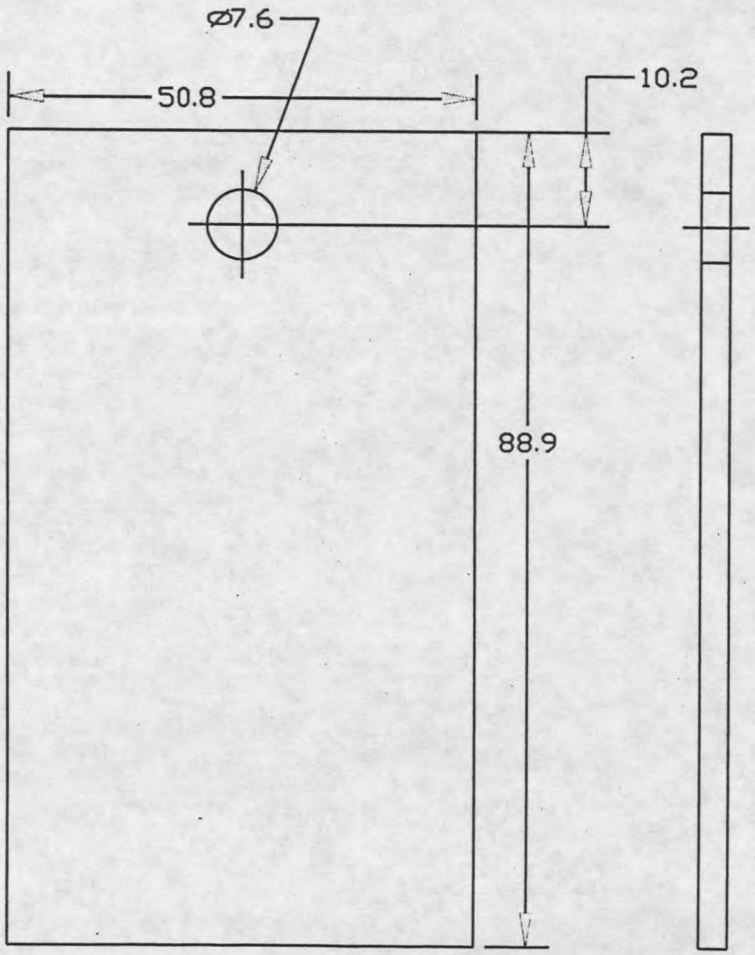




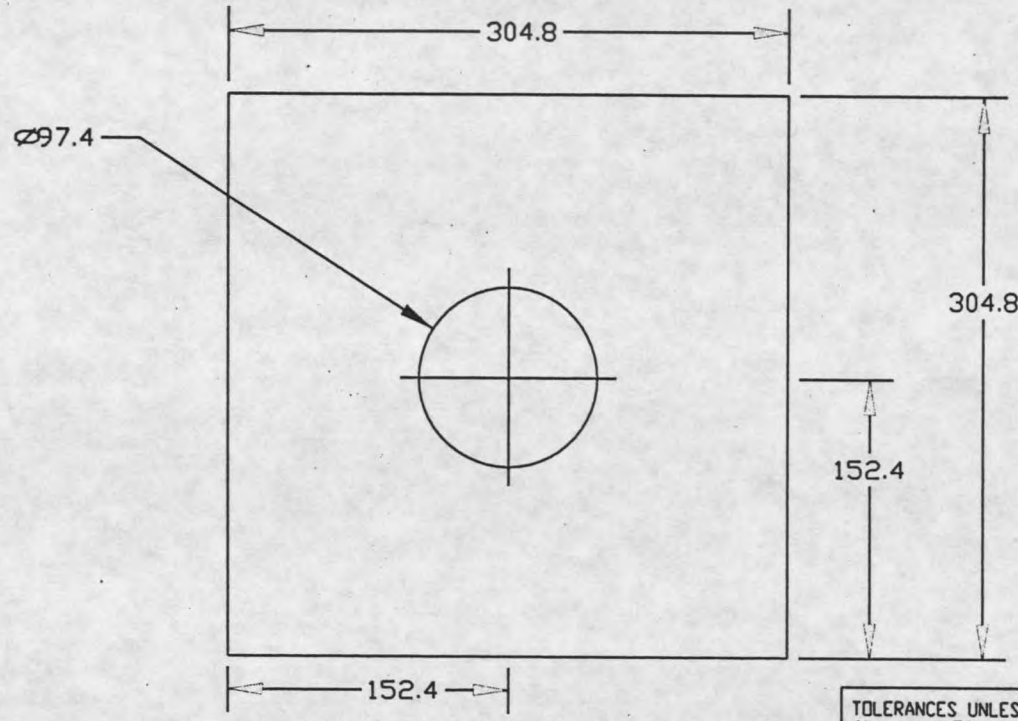


638

TOLERANCES UNLESS NOTED .X = ±.50 .XX = ±.025 ANGULARITY = ±.5° BREAK CORNERS - .010 MAX FILLET RADII - .015 MAX DIMENSIONS ARE IN MM UNLESS NOTED	MATERIAL	1/16" Sheet Metal
	FINISH	None
	Montana State University	
	Environmental Control Chamber	
DRAWN A.P	SIZE A	DWG NO. 370
ENGINEER Shane Schumacher		
CREATION DATE 15-Jun-00	SCALE NTS	SHEET 3 of 7

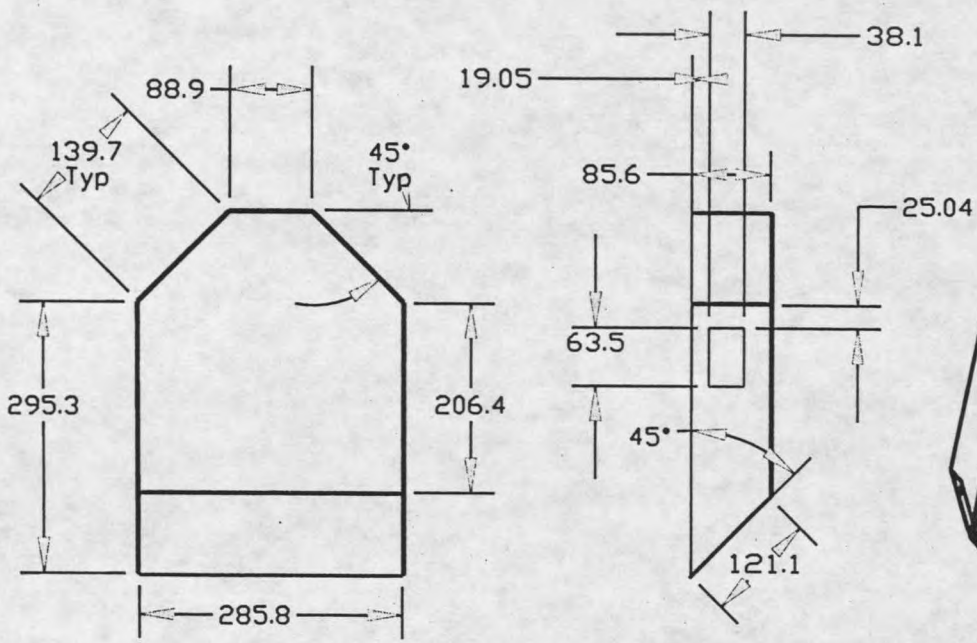


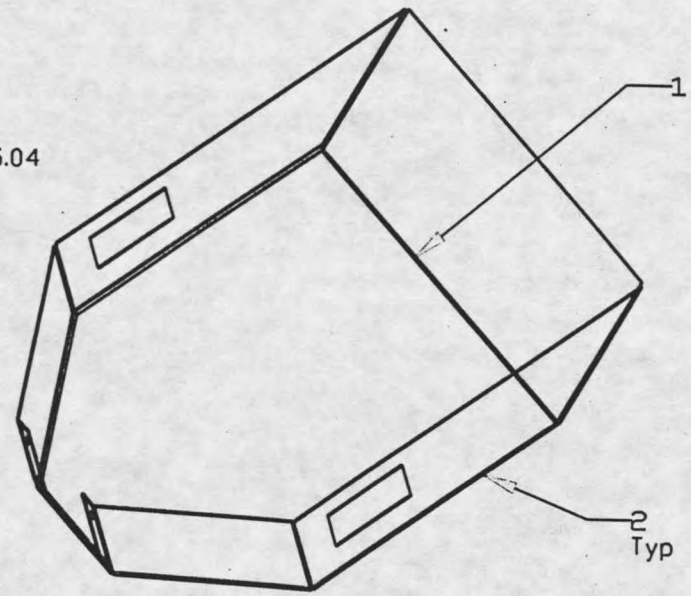
TOLERANCES UNLESS NOTED .X = ±.50 .XX = ±.025 ANGULARITY = ±.5° BREAK CORNERS - .010 MAX FILLET RADII - .015 MAX DIMENSIONS ARE IN MM UNLESS NOTED	MATERIAL	1/16" Sheet Metal
	FINISH	None
	Montana State University	
	Opening Door	
DRAWN A.P	SIZE A	DWG NO. 430
ENGINEER Shane Schumacher		
CREATION DATE 15-Jun-00	SCALE NTS	SHEET 4 of 7

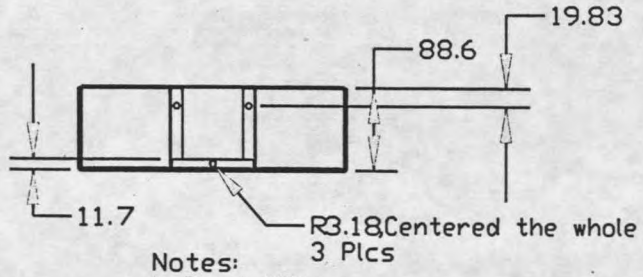


TOLERANCES UNLESS NOTED .X = ±.50 .XX = ±.025 ANGULARITY = ±.5° BREAK CORNERS - .010 MAX FILLET RADII - .015 MAX DIMENSIONS ARE IN MM UNLESS NOTED	MATERIAL	1/16" Sheet Metal	
	FINISH	None	
	Montana State University		
	Plate Support		
DRAWN A.P	SIZE A	DWG NO. 380	
ENGINEER Shane Schumacher			
CREATION DATE 15-Jun-00	SCALE NTS		SHEET 5 of 7

640



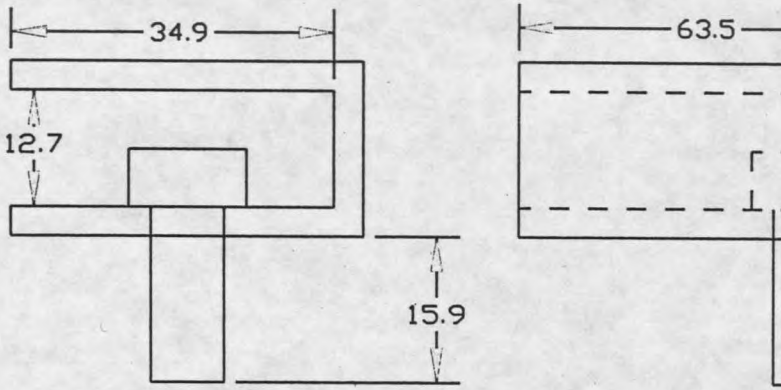


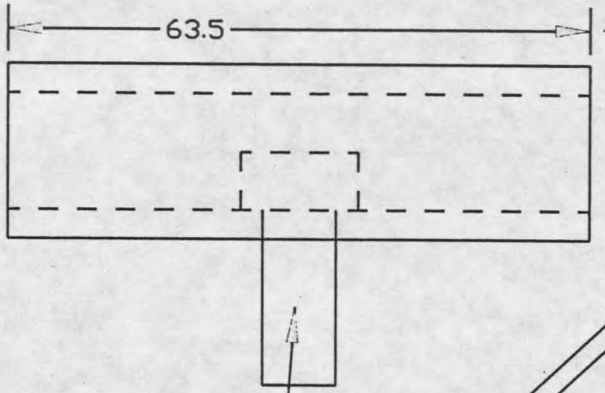


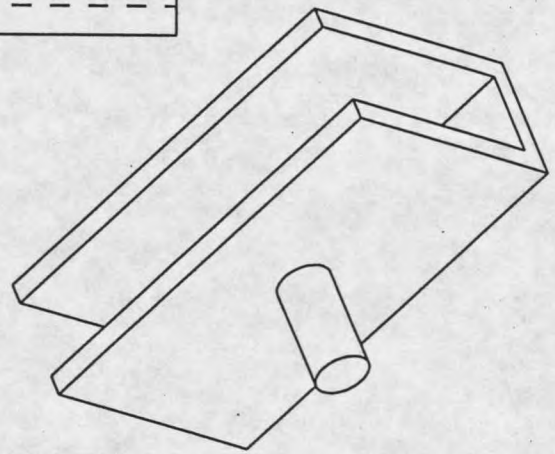
Notes:
1. Bend 45°
2. Bend 90°
3. Bend radii is Mat'l thickness
4. Material: 16 gage Steel
6. All Features Thru

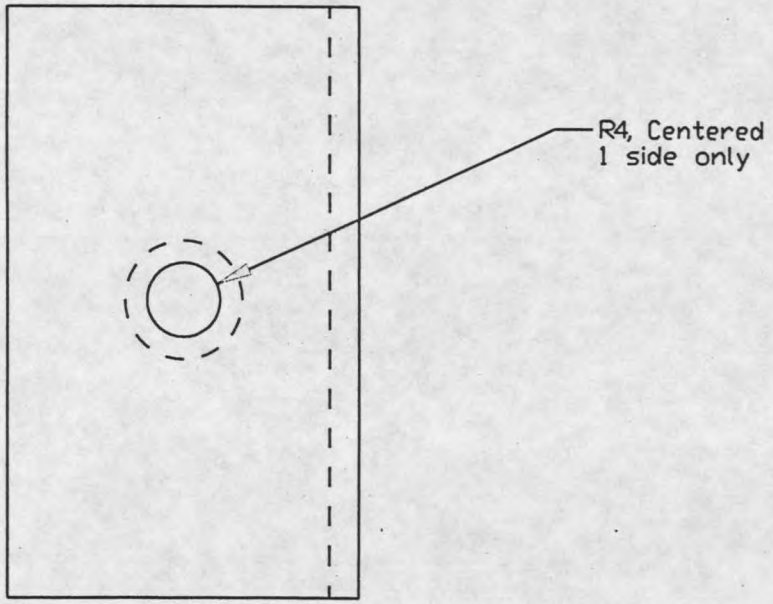
TOLERANCES UNLESS NOTED .X = ±.50 .XX = ±.025 ANGULARITY = ±.5° BREAK CORNERS - .010 MAX FILLET RADII - .015 MAX DIMENSIONS ARE IN MM UNLESS NOTED	MATERIAL	1/16" Sheet Metal
	FINISH	None
	Montana State University	
	Heater Casing	
DRAWN A.P.	SIZE A	DWG NO. 420
ENGINEER Shane Schumacher		
CREATION DATE 15-Jun-00	SCALE NTS	SHEET 6 of 7

641









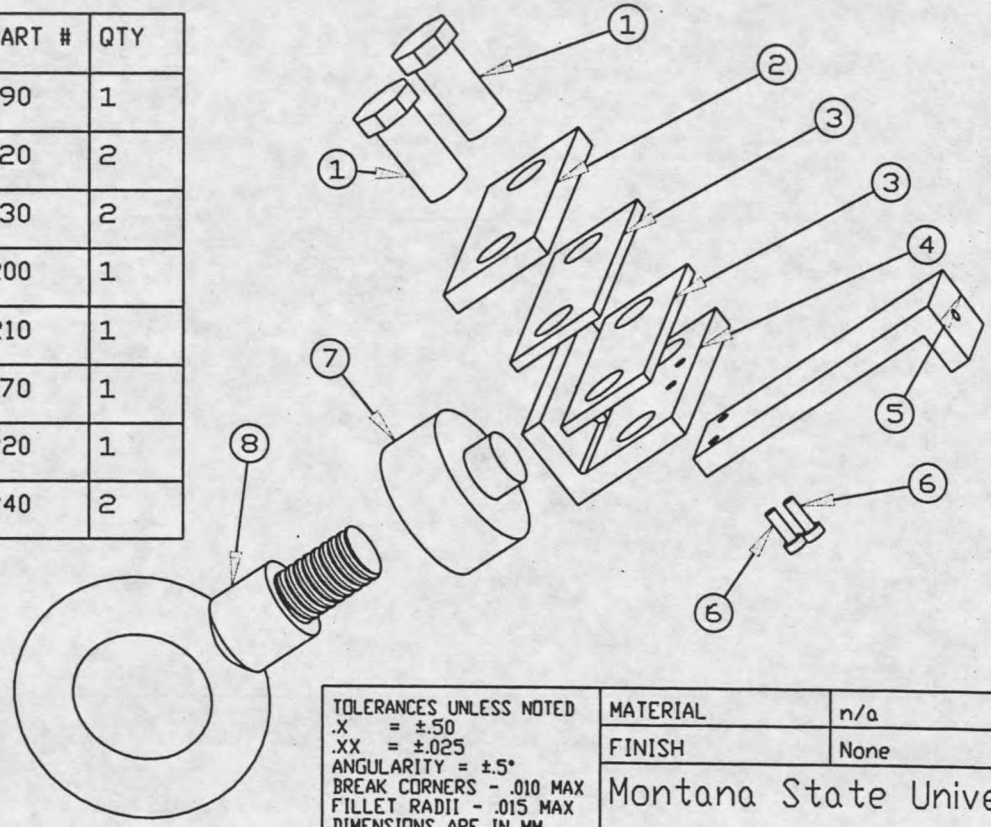
TOLERANCES UNLESS NOTED .X = ±.50 .XX = ±.025 ANGULARITY = ±.5° BREAK CORNERS - .010 MAX FILLET RADII - .015 MAX DIMENSIONS ARE IN MM UNLESS NOTED	MATERIAL	Steel
	FINISH	None
	Montana State University	
	Assembly_C_Heater_Bracket	
DRAWN A.P	SIZE A	DWG NO. 390
ENGINEER Shane Schumacher		
CREATION DATE 15-Jun-00	SCALE NTS	SHEET 7 of 7

642

APPENDIX S

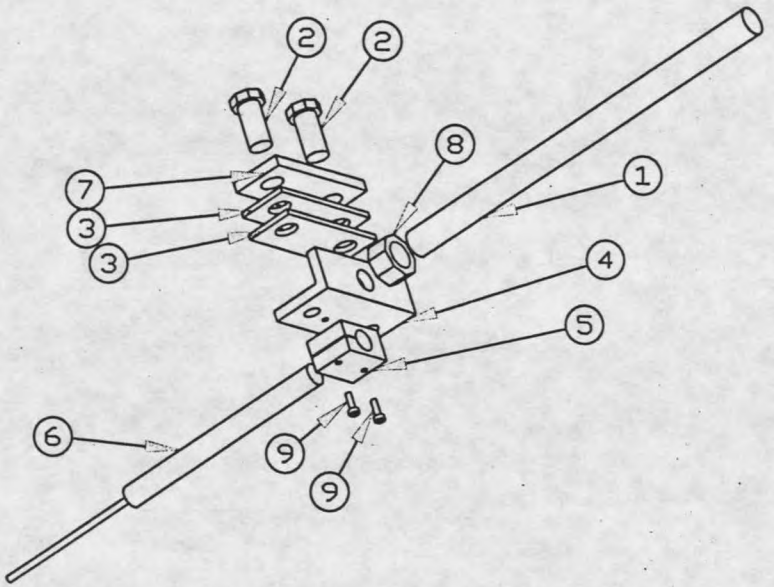
Creep Testing Equipment Design

#	DESCRIPTION	PART #	QTY
8	HOOK ROD 5/8" DIA. 24 UNC	190	1
1	CLAMPING BOLTS	120	2
3	INTERCHANGEABLE GRIP PLATES	130	2
5	SECOND L BRACKET	200	1
4	REAR GRIP JAW B	210	1
2	FRONT GRIP JAW	170	1
7	Adapter - 5/8" - UNC -> UNF	220	1
6	SHCS_1/8	240	2



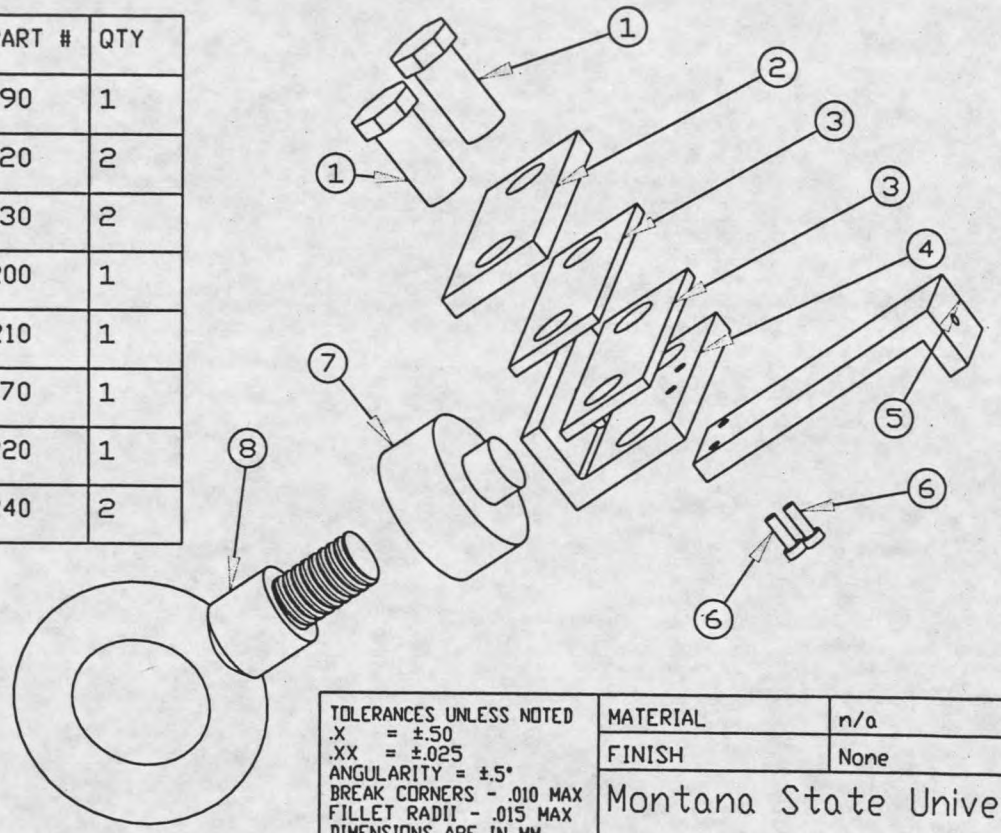
TOLERANCES UNLESS NOTED .X = ±.50 .XX = ±.025 ANGULARITY = ±.5° BREAK CORNERS - .010 MAX FILLET RADII - .015 MAX DIMENSIONS ARE IN MM UNLESS NOTED	MATERIAL	n/a
	FINISH	None
	Montana State University	
	Lower Assembly Fixture	
DRAWN A.P	SIZE A	DWG NO. 180
ENGINEER Shane Schumacher		
CREATION DATE 15-Jun-00	SCALE NTS	SHEET 1 of 9

#	DESCRIPTION	PART #	QTY
1	SUPPORT ROD 5/8" DIA. 24 UNF	160	1
2	CLAMPING BOLTS	2	2
3	INTERCHANGEABLE GRIP PLATES	130	2
4	REAR GRIP JAW	140	1
5	LVDT MOUNTING BLOCK	150	1
6	LVDT DATA INSTRUMENT	6	1
7	FRONT GRIP JAW	170	1
8	NUT 5/8"	8	1
9	SHCS 1/8"	9	2

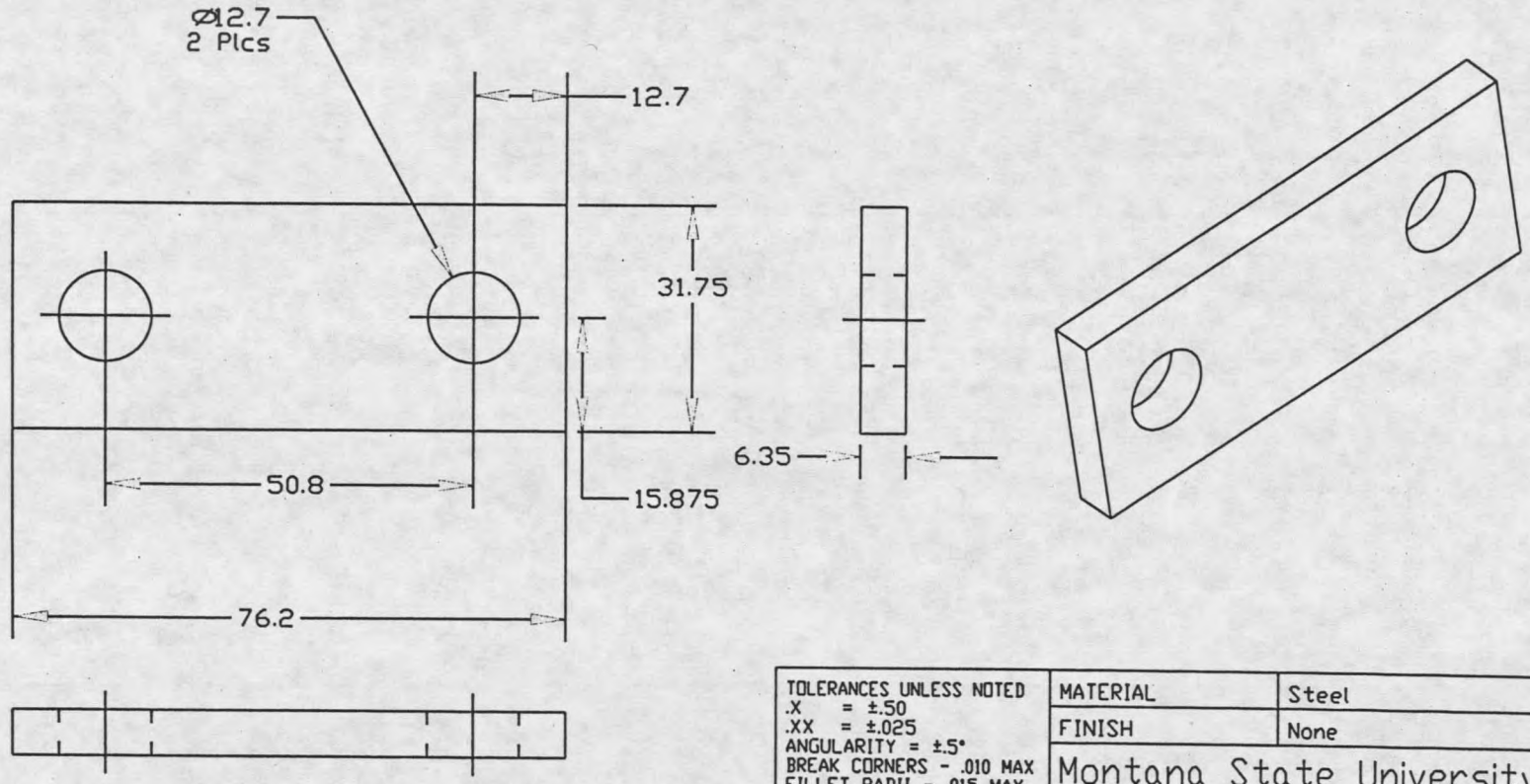


TOLERANCES UNLESS NOTED .X = ±.50 .XX = ±.025 ANGULARITY = ±.5° BREAK CORNERS - .010 MAX FILLET RADII - .015 MAX DIMENSIONS ARE IN MM UNLESS NOTED	MATERIAL	See BOM
	FINISH	None
	Montana State University	
	Upper Assembly Fixture	
DRAWN A.P	SIZE A	DWG NO. 100
ENGINEER Shane Schumacher		
CREATION DATE 15-Jun-00	SCALE NTS	SHEET 2 of 9

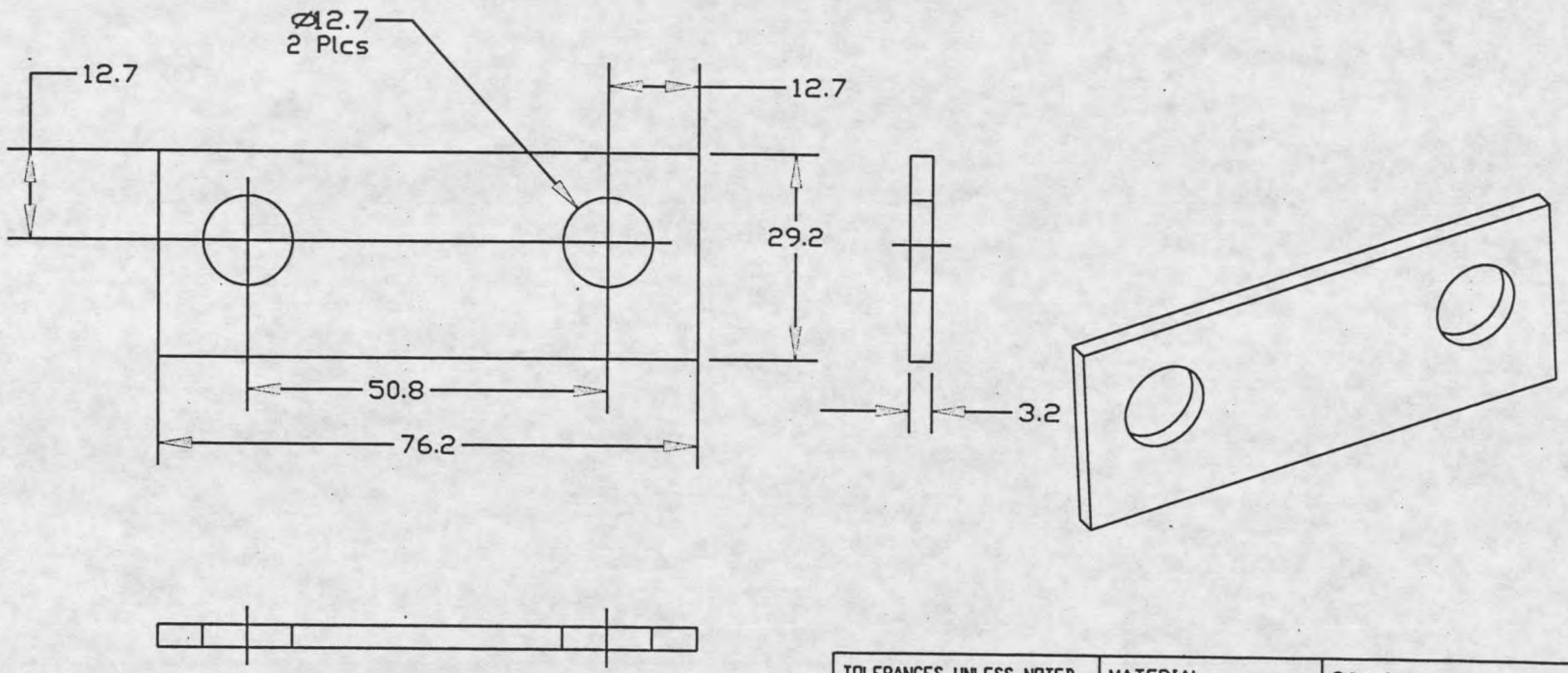
#	DESCRIPTION	PART #	QTY
8	HOOK ROD 5/8" DIA. 24 UNC	190	1
1	CLAMPING BOLTS	120	2
3	INTERCHANGEABLE GRIP PLATES	130	2
5	SECOND L BRACKET	200	1
4	REAR GRIP JAW B	210	1
2	FRONT GRIP JAW	170	1
7	Adapter - 5/8" - UNC -> UNF	220	1
6	SHCS_1/8	240	2



TOLERANCES UNLESS NOTED .X = ±.50 .XX = ±.025 ANGULARITY = ±.5° BREAK CORNERS - .010 MAX FILLET RADII - .015 MAX DIMENSIONS ARE IN MM UNLESS NOTED	MATERIAL	n/a
	FINISH	None
	Montana State University	
	Lower Assembly Fixture	
DRAWN A.P	SIZE A	DWG NO. 180
ENGINEER Shane Schumacher		
CREATION DATE 15-Jun-00	SCALE NTS	SHEET 1 of 9

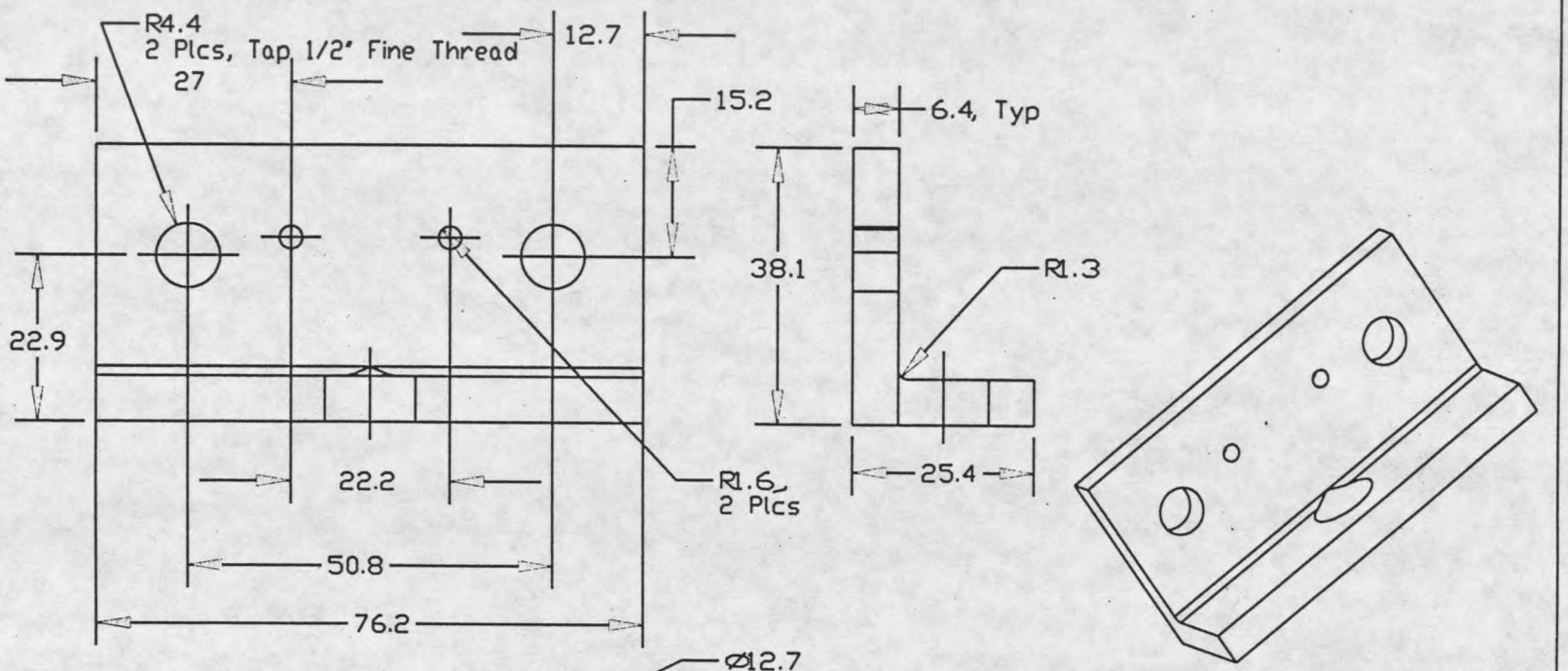


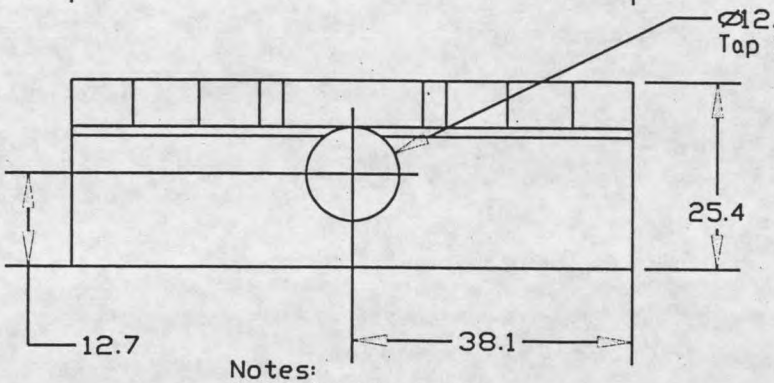
TOLERANCES UNLESS NOTED .X = ±.50 .XX = ±.025 ANGULARITY = ±.5° BREAK CORNERS - .010 MAX FILLET RADII - .015 MAX DIMENSIONS ARE IN MM UNLESS NOTED	MATERIAL	Steel
	FINISH	None
	Montana State University	
	Front Grip Jaw	
DRAWN A.P	SIZE A	DWG NO. 170
ENGINEER Shane Schumacher		
CREATION DATE 15-Jun-00	SCALE NTS	SHEET 3 of 9



Notes:
1. All features trhu
2. Deburr edges

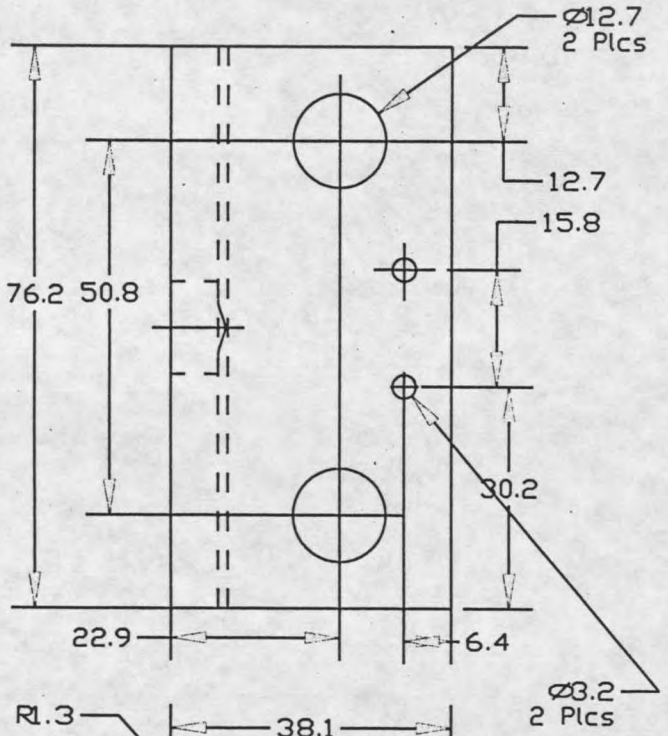
TOLERANCES UNLESS NOTED .X = ±.50 .XX = ±.025 ANGULARITY = ±.5° BREAK CORNERS - .010 MAX FILLET RADII - .015 MAX DIMENSIONS ARE IN MM UNLESS NOTED	MATERIAL	Steel
	FINISH	None
	Montana State University	
	Interchangeable Grip Plate	
DRAWN A.P	SIZE A	DWG NO. 130
ENGINEER Shane Schumacher		
CREATION DATE 15-Jun-00	SCALE NTS	SHEET 4 of 9

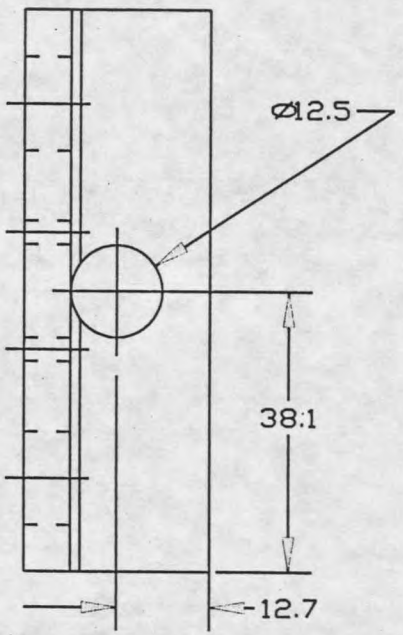


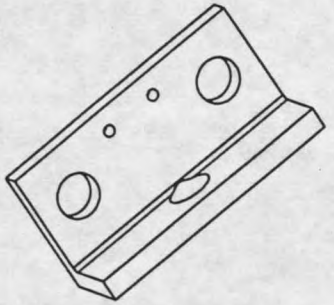


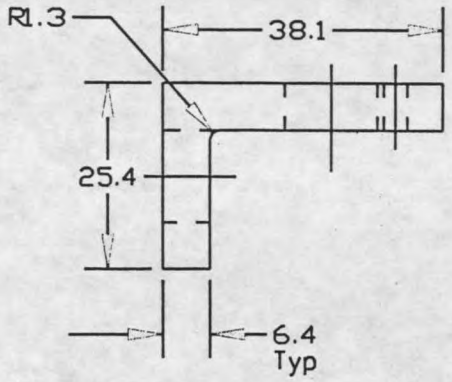
Notes:
1. All features thru
2. Deburr edges

TOLERANCES UNLESS NOTED .X = ±.50 .XX = ±.025 ANGULARITY = ±.5° BREAK CORNERS - .010 MAX FILLET RADII - .015 MAX DIMENSIONS ARE IN MM UNLESS NOTED	MATERIAL	Aluminum
	FINISH	None
	Montana State University	
	Rear Grip Jaw	
DRAWN A.P	SIZE A	DWG NO. 140
ENGINEER Shane Schumacher		
CREATION DATE 15-Jun-00	SCALE NTS	SHEET 5 of 9





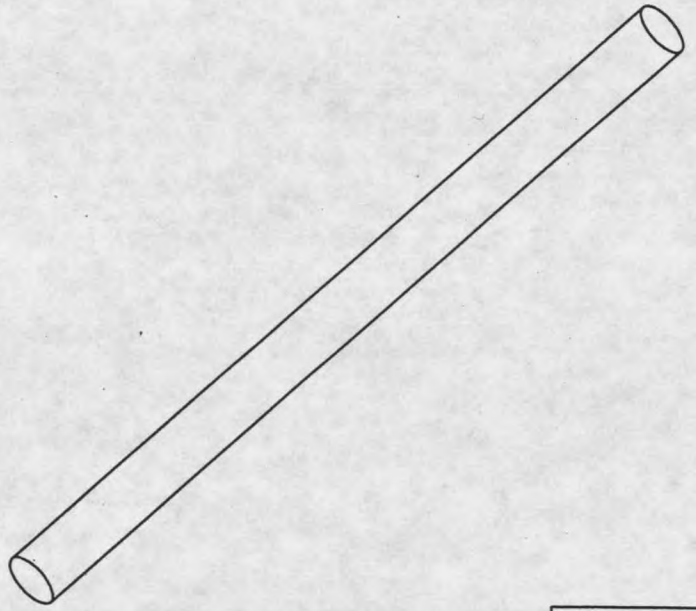




Notes:
1. All features thru
2. deburr edges

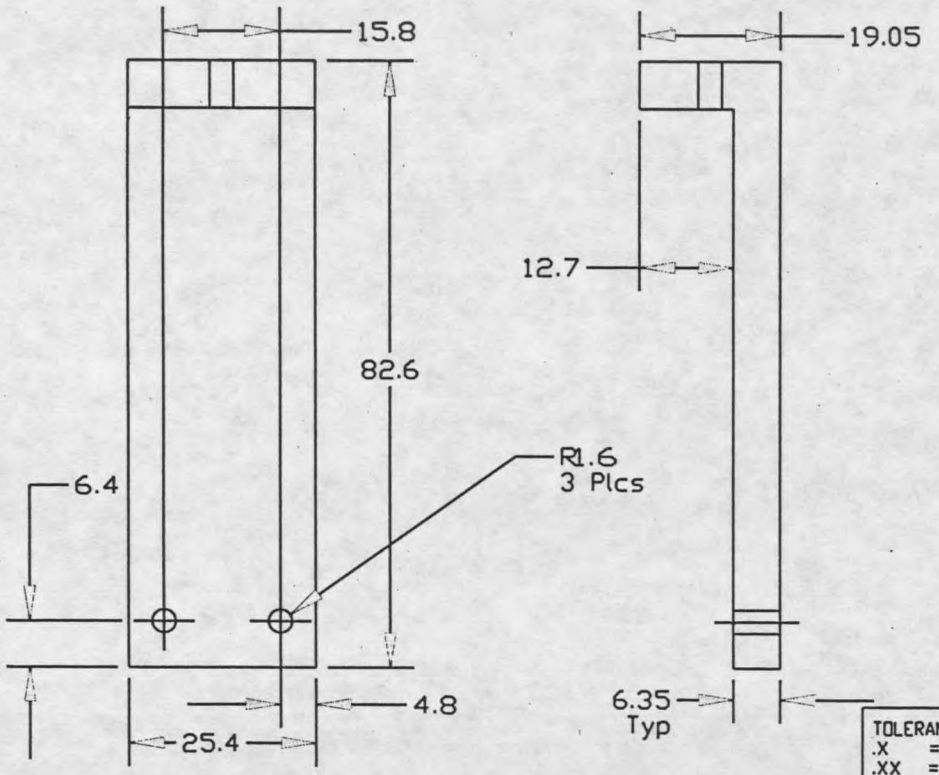
TOLERANCES UNLESS NOTED .X = ±.50 .XX = ±.025 ANGULARITY = ±.5° BREAK CORNERS - .010 MAX FILLET RADII - .015 MAX DIMENSIONS ARE IN MM UNLESS NOTED	MATERIAL	Steel
	FINISH	None
	Montana State University	
	Rear Grip Jaw B	
DRAWN A.P	SIZE A	DWG NO. 210
ENGINEER Shane Schumacher		
CREATION DATE 15-Jun-00	SCALE NTS	SHEET 6 of 9

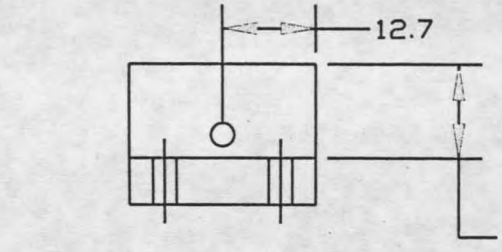
650



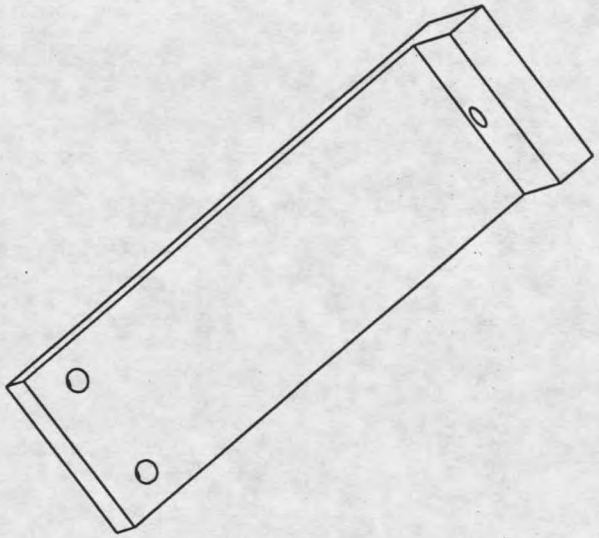
TOLERANCES UNLESS NOTED .X = ±.50 .XX = ±.025 ANGULARITY = ±.5° BREAK CORNERS - .010 MAX FILLET RADII - .015 MAX DIMENSIONS ARE IN MM UNLESS NOTED	MATERIAL	See notes
	FINISH	None
	Montana State University	
	Support Rod ø 5/8" x 24 UNF	
DRAWN A.P	SIZE A	DWG NO. 160
ENGINEER Shane Schumacher		
CREATION DATE 15-Jun-00	SCALE NTS	SHEET 7 of 9

651



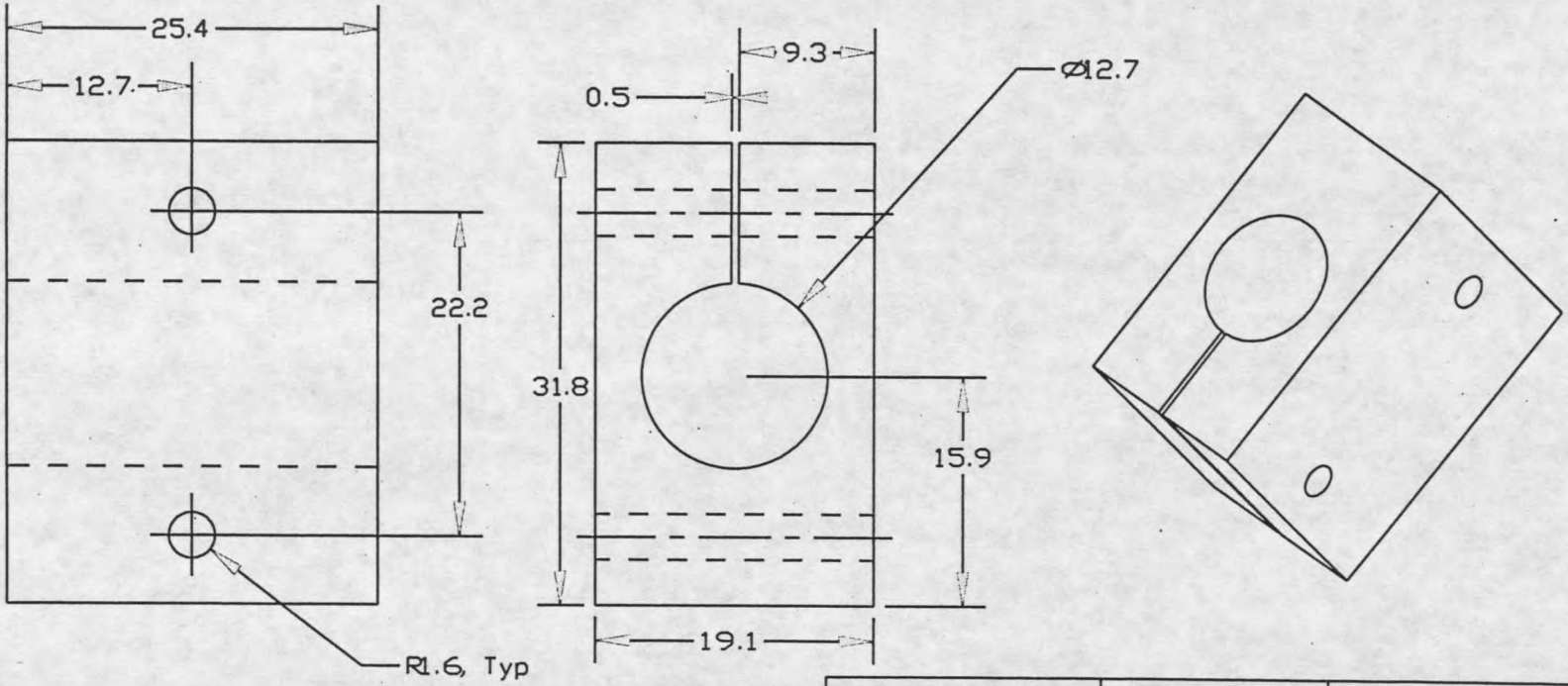


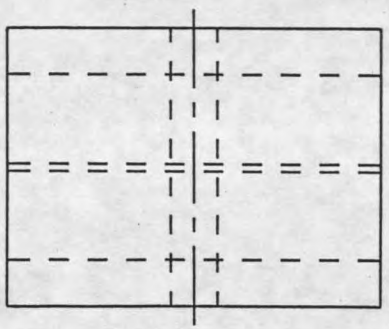
Notes:
1. All features thru
2. Deburr edges



TOLERANCES UNLESS NOTED .X = ±.50 .XX = ±.025 ANGULARITY = ±.5° BREAK CORNERS - .010 MAX FILLET RADII - .015 MAX DIMENSIONS ARE IN MM UNLESS NOTED	MATERIAL	Aluminum
	FINISH	None
	Montana State University	
	Second L Bracket	
DRAWN A.P	SIZE A	DWG NO. 200
ENGINEER Shane Schumacher		
CREATION DATE 15-Jun-00	SCALE NTS	SHEET 8 of 9

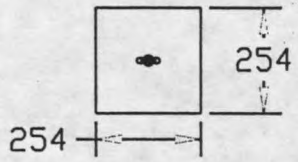
652

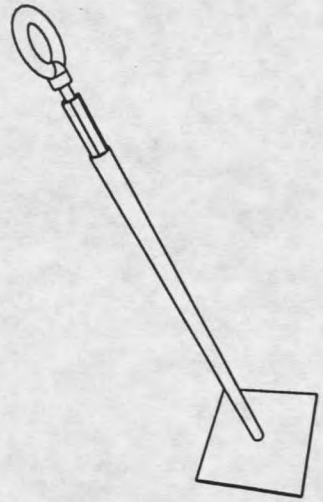


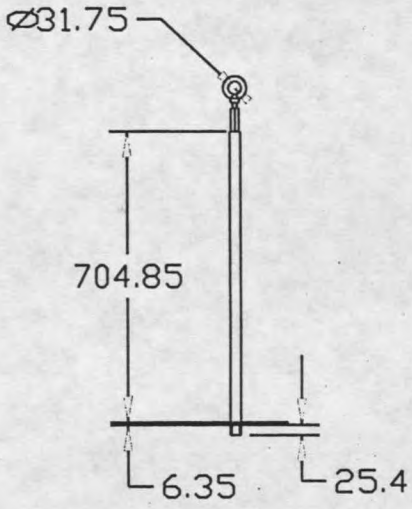


Notes:
1. All Features Thru.
2. Deburr edges

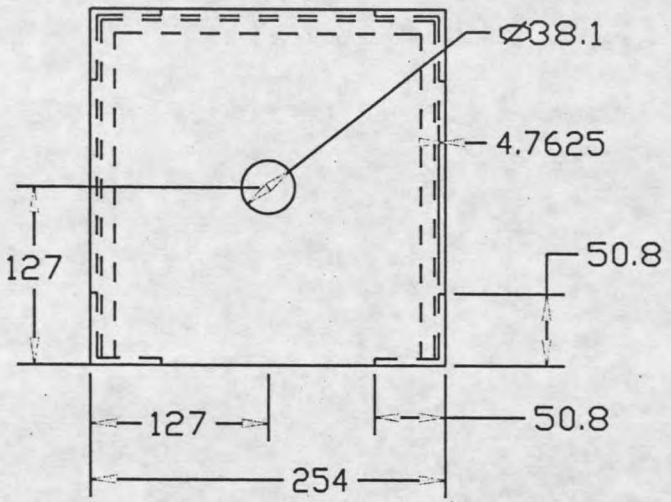
TOLERANCES UNLESS NOTED .X = ±.50 .XX = ±.025 ANGULARITY = ±.5° BREAK CORNERS - .010 MAX FILLET RADII - .015 MAX DIMENSIONS ARE IN MM UNLESS NOTED	MATERIAL	Aluminum	
	FINISH	None	
	Montana State University		
	LVDT Mounting Block		
DRAWN A.P	SIZE A	DWG NO. 150	
ENGINEER Shane Schumacher			
CREATION DATE 15-Jun-00	SCALE NTS		SHEET 9 of 9

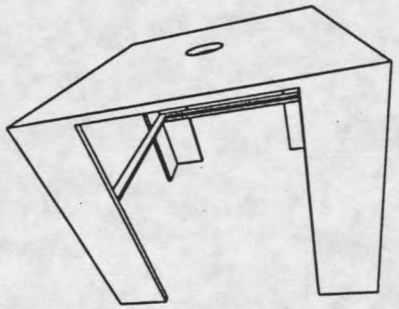


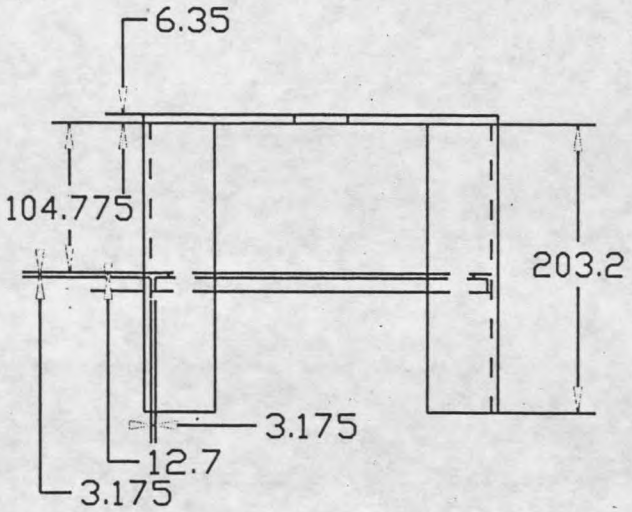




TOLERANCES UNLESS NOTED .X = ±.50 .XX = ±.025 ANGULARITY = ±.5° BREAK CORNERS - .010 MAX FILLET RADII - .015 MAX DIMENSIONS ARE IN MM UNLESS NOTED	MATERIAL	Steel
	FINISH	As Delivered
	Montana State University	
	Load Tray	
DRAWN Carl Thrasher	SIZE A	DWG NO. DRW0002
ENGINEER Shane Schumacher		
CREATION DATE 19-Jun-00	SCALE: NTS	SHEET 1 of 1





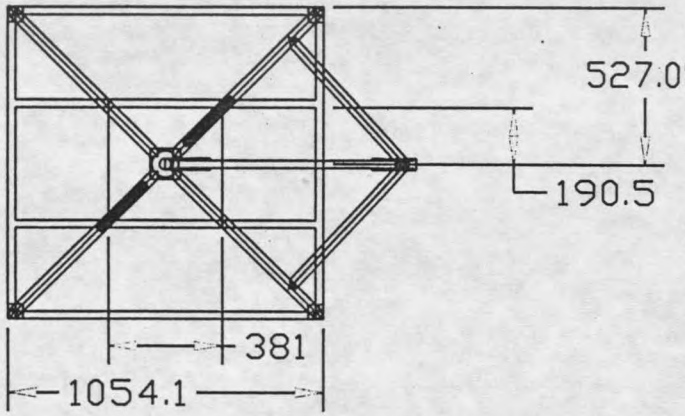


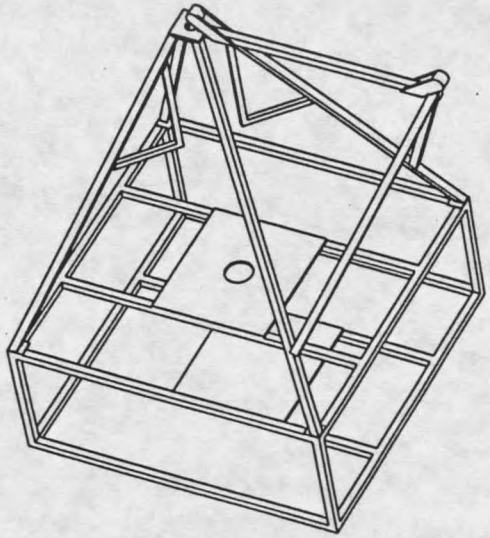
TOLERANCES UNLESS NOTED .X = ±.50 .XX = ±.025 ANGULARITY = ±.5° BREAK CORNERS - .010 MAX FILLET RADII - .015 MAX DIMENSIONS ARE IN MM UNLESS NOTED	MATERIAL	Steel
	FINISH	As Delivered
	Montana State University	
	Load Tray Support	
DRAWN Carl Thrasher	SIZE A	DWG NO. LOADTRAYSUPPORT
ENGINEER Shane Schumacher		
CREATION DATE 19-Jun-00	SCALE: NTS	SHEET 1 of 1

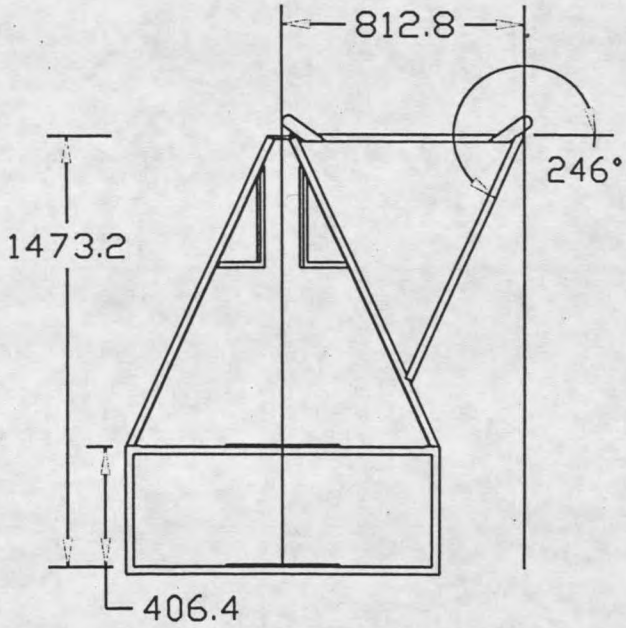
655

APPENDIX T

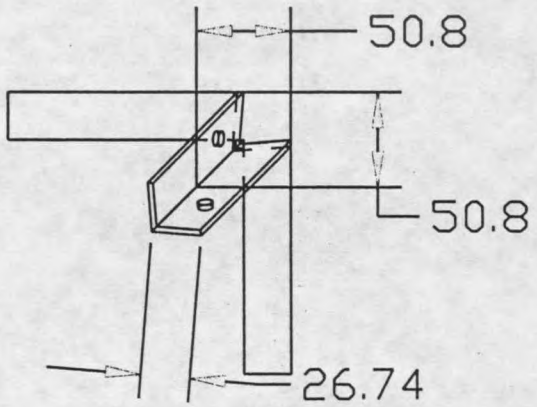
Creep and Vibrocreep Test Fixture for Thin Film Testing

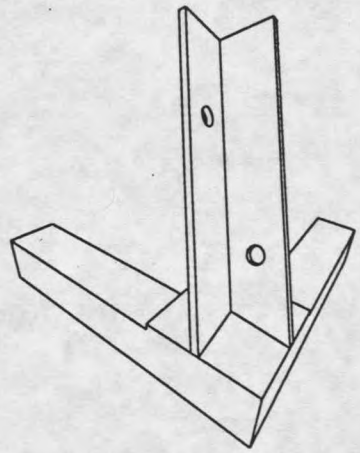


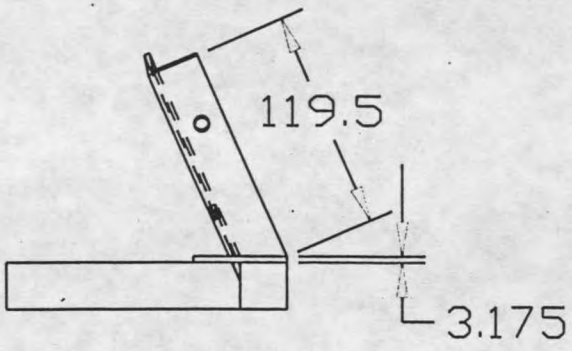




TOLERANCES UNLESS NOTED .X = ±.50 .XX = ±.0250 ANGULARITY = ±.5° BREAK CORNERS - .010 MAX FILLET RADII - .015 MAX DIMENSIONS ARE IN MM UNLESS NOTED	MATERIAL	Steel
	FINISH	As Delivered
	Montana State University	
	PVDF TEST FIXTURE	
DRAWN Carl Thrasher	SIZE A	DWG NO. DRW0001
ENGINEER Shane Schumacher		
CREATION DATE 19-Jun-00	SCALE: NTS	SHEET 1 of 1



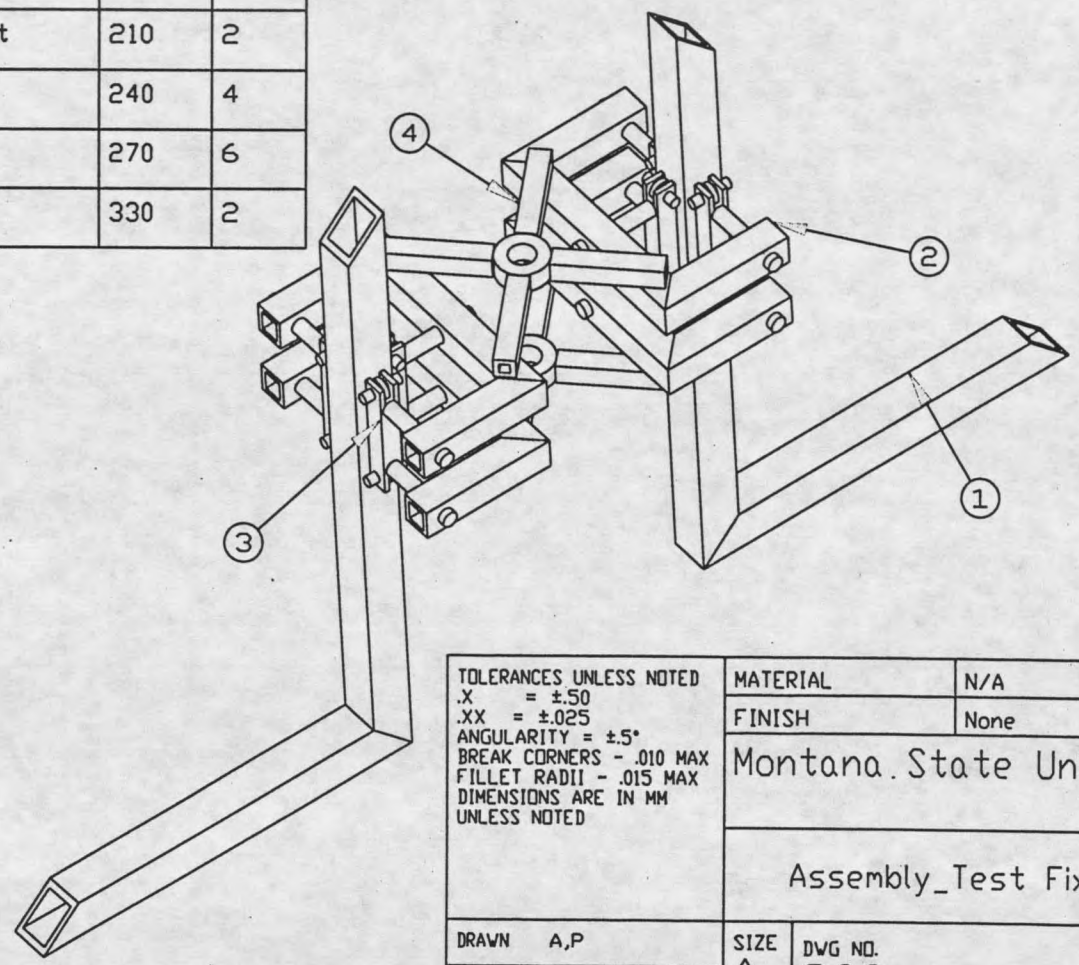




TOLERANCES UNLESS NOTED .X = ±.50 .XX = ±.025 ANGULARITY = ±.5° BREAK CORNERS - .010 MAX FILLET RADII - .015 MAX DIMENSIONS ARE IN MM UNLESS NOTED	MATERIAL	Steel
	FINISH	As Delivered
	Montana State University	
	Attachment Detail	
DRAWN Carl Thrasher	SIZE A	DWG NO. DETAIL
ENGINEER Shane Schumacher		
CREATION DATE 19-Jun-00	SCALE: NTS	SHEET 1 of 1

658

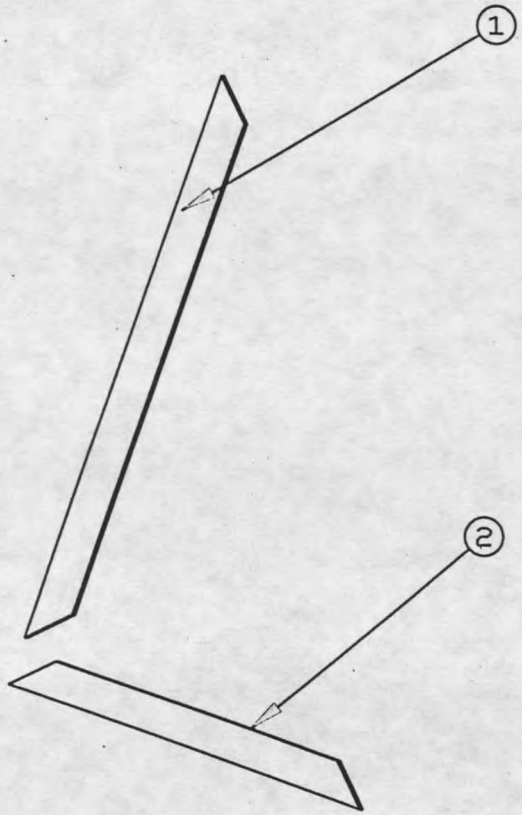
#	DESCRIPTION	PART #	QTY
1	Assembly Triangular Support	210	2
2	Assembly C Bracket	240	4
3	Assembly Roller Bearing	270	6
4	Assembly Cross Member	330	2

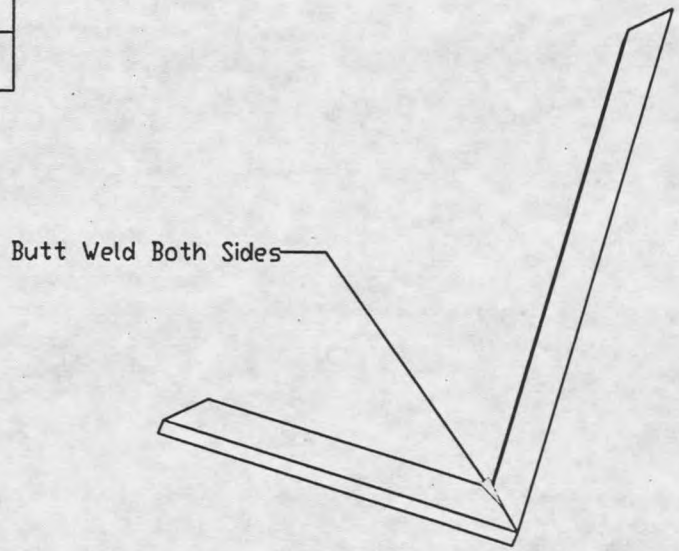


659

TOLERANCES UNLESS NOTED .X = ±.50 .XX = ±.025 ANGULARITY = ±.5° BREAK CORNERS - .010 MAX FILLET RADII - .015 MAX DIMENSIONS ARE IN MM UNLESS NOTED	MATERIAL	N/A
	FINISH	None
	Montana. State University	
	Assembly_Test Fixture	
DRAWN A,P	SIZE A	DWG NO. 200
ENGINEER Shane Schumacher		
CREATION DATE 15-Jun-00	SCALE NTS	SHEET 1 of 11

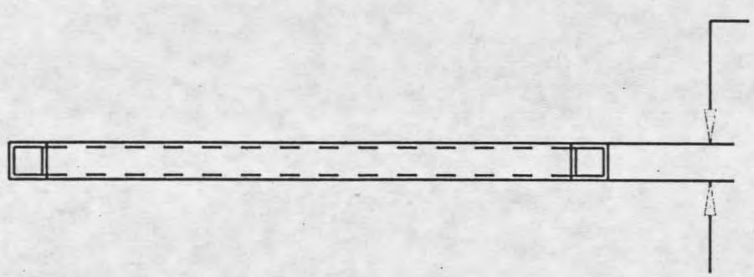
#	DESCRIPTION	PART #	QTY
1	25.4 Square Tubing	220	1
2	25.4 Square Tubing	230	1

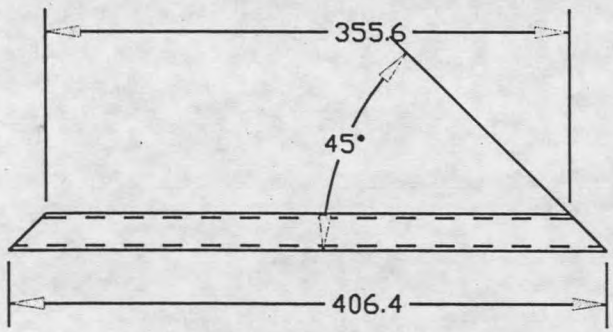


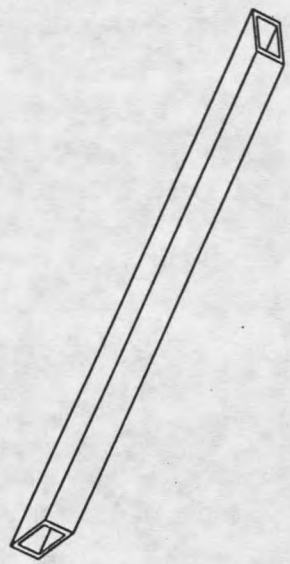


TOLERANCES UNLESS NOTED .X = ±.50 .XX = ±.025 ANGULARITY = ±.5° BREAK CORNERS - .010 MAX FILLET RADII - .015 MAX DIMENSIONS ARE IN MM UNLESS NOTED	MATERIAL	See BOM
	FINISH	None
	Montana State University	
	Assembly_Triangular_Support	
DRAWN A.P	SIZE A	DWG NO. 210
ENGINEER Shane Schumacher		
CREATION DATE 15-Jun-00	SCALE NTS	SHEET 2 of 11

660

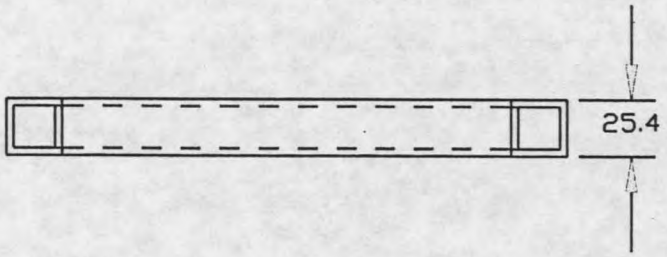


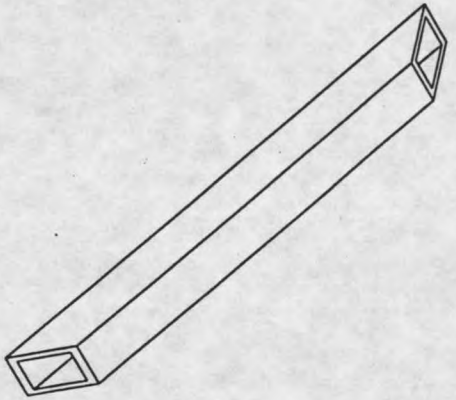


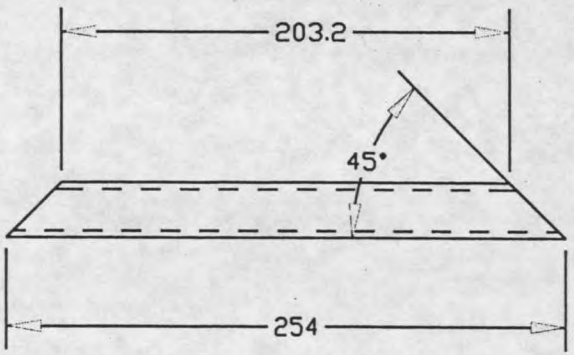


661

TOLERANCES UNLESS NOTED .X = ±.50 .XX = ±.025 ANGULARITY = ±.5° BREAK CORNERS - .010 MAX FILLET RADII - .015 MAX DIMENSIONS ARE IN MM UNLESS NOTED	MATERIAL	25.4 Square tube
	FINISH	None
	Montana State University	
	25.4 square tube	
DRAWN A.P	SIZE A	DWG NO. 220
ENGINEER Shane Schumacher		
CREATION DATE 15-Jun-00	SCALE NTS	SHEET 3 of 11

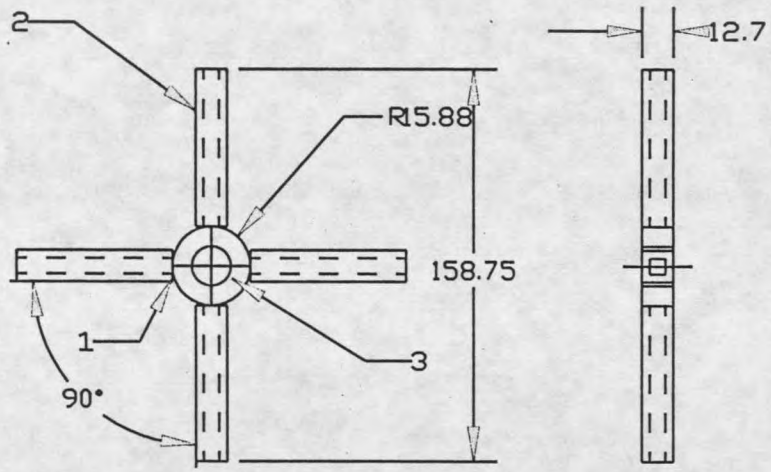


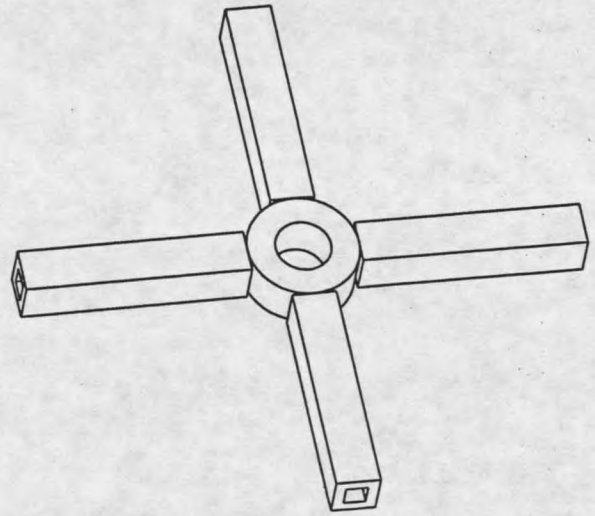




662

TOLERANCES UNLESS NOTED .X = ±.50 .XX = ±.025 ANGULARITY = ±.5° BREAK CORNERS - .010 MAX FILLET RADII - .015 MAX DIMENSIONS ARE IN MM UNLESS NOTED	MATERIAL	25.4 Square Tube
	FINISH	None
	Montana State University	
	25.4 Square tube	
DRAWN A.P	SIZE A	DWG NO. 230
ENGINEER Shane Schumacher		
CREATION DATE 15-Jun-00	SCALE NTS	SHEET 4 of 11

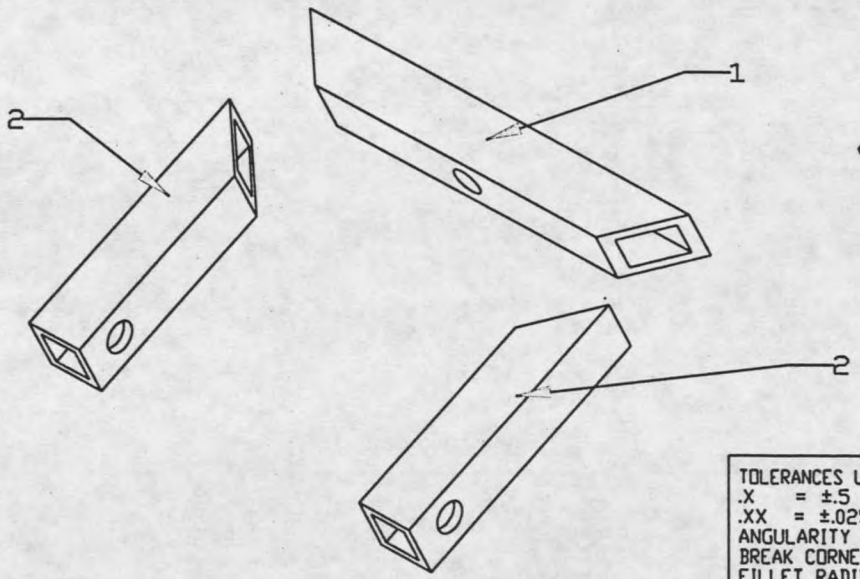


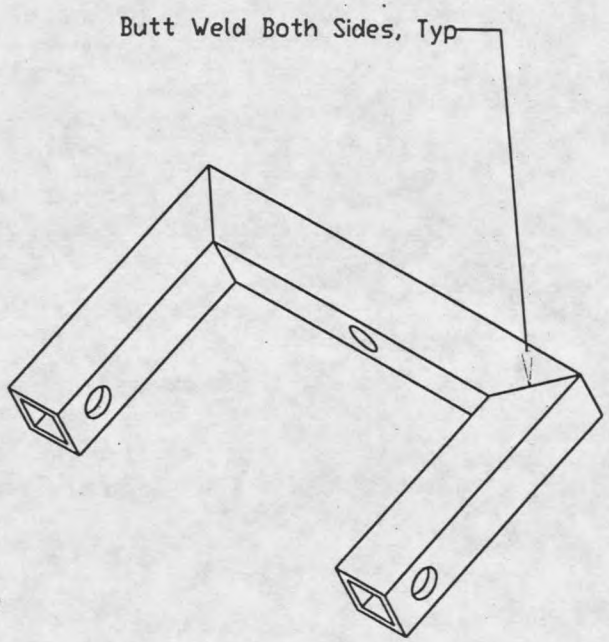


Notes:
1. 1/4"-1/2" Fillet Weld Both Sides.
2. Mat'l: 12.7 Square tubing.
3. Round Bushing, 5/8 threaded UNF

TOLERANCES UNLESS NOTED .X = ±.5 .XX = ±.025 ANGULARITY = ±.5° BREAK CORNERS - .010 MAX FILLET RADII - .015 MAX DIMENSIONS ARE IN MM UNLESS NOTED	MATERIAL	See notes
	FINISH	None
	Montana State University	
	ASSEMBLY_CROSS_MEMBER	
DRAWN A.P.	SIZE A	DWG NO. 330
ENGINEER Shane Schumacher		
CREATION DATE 15-Jun-00	SCALE NTS	SHEET 5 of 11

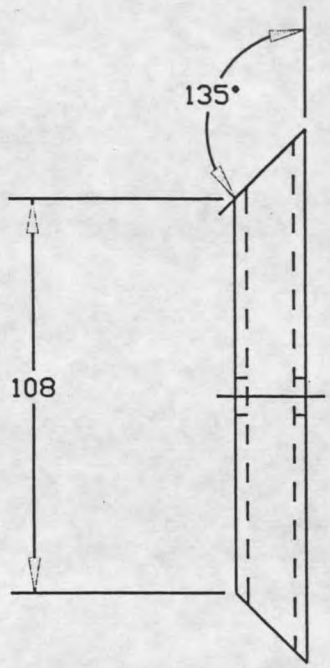
#	DESCRIPTION	PART #	QTY
1	.75 Square Tubing	250	1
2	.75 Square Tubing	260	2

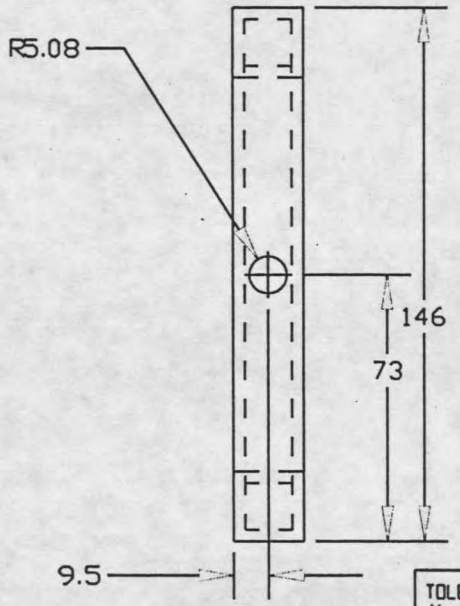


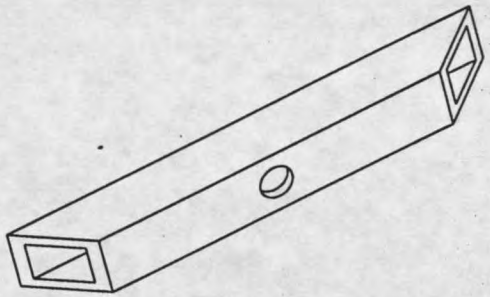


TOLERANCES UNLESS NOTED .X = ±.5 .XX = ±.025 ANGULARITY = ±.5° BREAK CORNERS - .010 MAX FILLET RADII - .015 MAX DIMENSIONS ARE IN MM UNLESS NOTED	MATERIAL	See BOM
	FINISH	None
	Montana State University	
	Assembly_C_Bracket	
DRAWN A.P	SIZE A	DWG NO. 240
ENGINEER Shane Schumacher		
CREATION DATE 15-Jun-00	SCALE NTS	SHEET 6 of 11

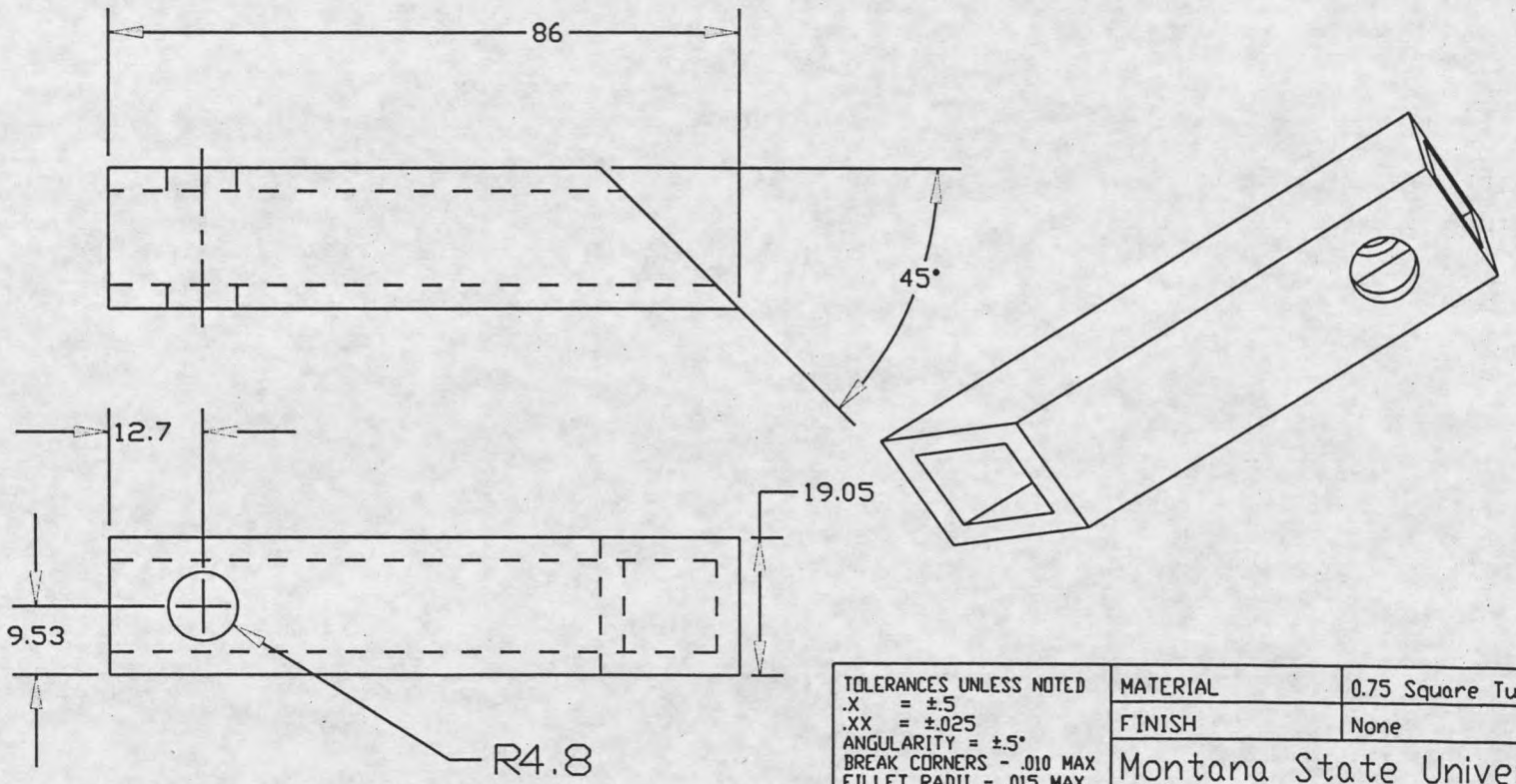
664







TOLERANCES UNLESS NOTED .X = ±.5 .XX = ±.025 ANGULARITY = ±.5° BREAK CORNERS - .010 MAX FILLET RADII - .015 MAX DIMENSIONS ARE IN MM UNLESS NOTED	MATERIAL	.75 Square Tube
	FINISH	None
	Montana State University	
	.75 Square Tube	
DRAWN A.P	SIZE A	DWG NO. 250
ENGINEER Shane Schumacher		
CREATION DATE 15-Jun-00	SCALE NTS	SHEET 7 of 11

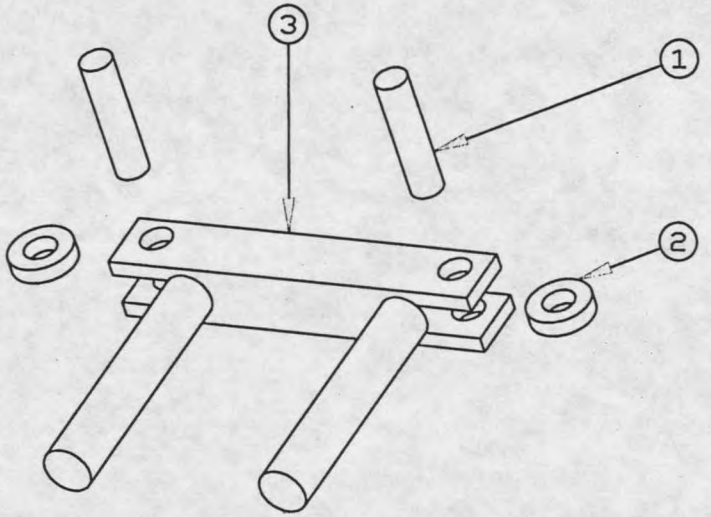


Notes:
1. All features thru

TOLERANCES UNLESS NOTED .X = ±.5 .XX = ±.025 ANGULARITY = ±.5° BREAK CORNERS - .010 MAX FILLET RADII - .015 MAX DIMENSIONS ARE IN MM UNLESS NOTED	MATERIAL	0.75 Square Tube
	FINISH	None
	Montana State University	
	.75 Square Tube	
DRAWN A.P	SIZE A	DWG NO. 260
ENGINEER Shane Schumacher		
CREATION DATE 15-Jun-00	SCALE NTS	SHEET 8 of 11

699

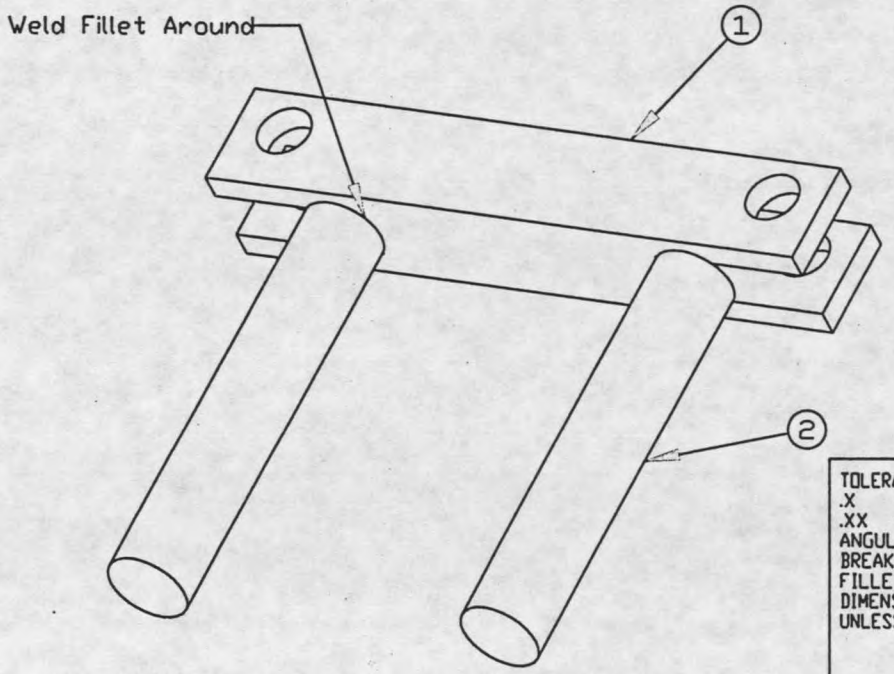
#	DESCRIPTION	PART #	QTY
1	Threaded Rod 4MM x 25.4MM	280	2
2	6.35MM x 3MM Roller Bearing	290	2
3	Assembly_Bearing_Support	300	1



667

TOLERANCES UNLESS NOTED .X = ±.5 .XX = ±.025 ANGULARITY = ±.5° BREAK CORNERS - .010 MAX FILLET RADII - .015 MAX DIMENSIONS ARE IN MM UNLESS NOTED	MATERIAL	See BOM
	FINISH	None
	Montana State University	
	Assembly_Roller_Bearing	
DRAWN A.P	SIZE A	DWG NO. 270
ENGINEER Shane Schumacher		
CREATION DATE 15-Jun-00	SCALE NTS	SHEET 9 of 11

#	DESCRIPTION	PART #	QTY
1	0.75 Cut Off Square Tubing	310	1
2	3/8" X 2 Threaded Bolt UNF	320	2



TOLERANCES UNLESS NOTED
.X = ±.50
.XX = ±.025
ANGULARITY = ±.5°
BREAK CORNERS - .010 MAX
FILLET RADII - .015 MAX
DIMENSIONS ARE IN MM
UNLESS NOTED

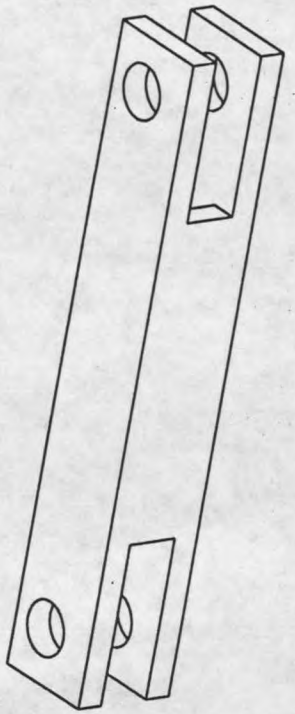
MATERIAL	See BOM
FINISH	None

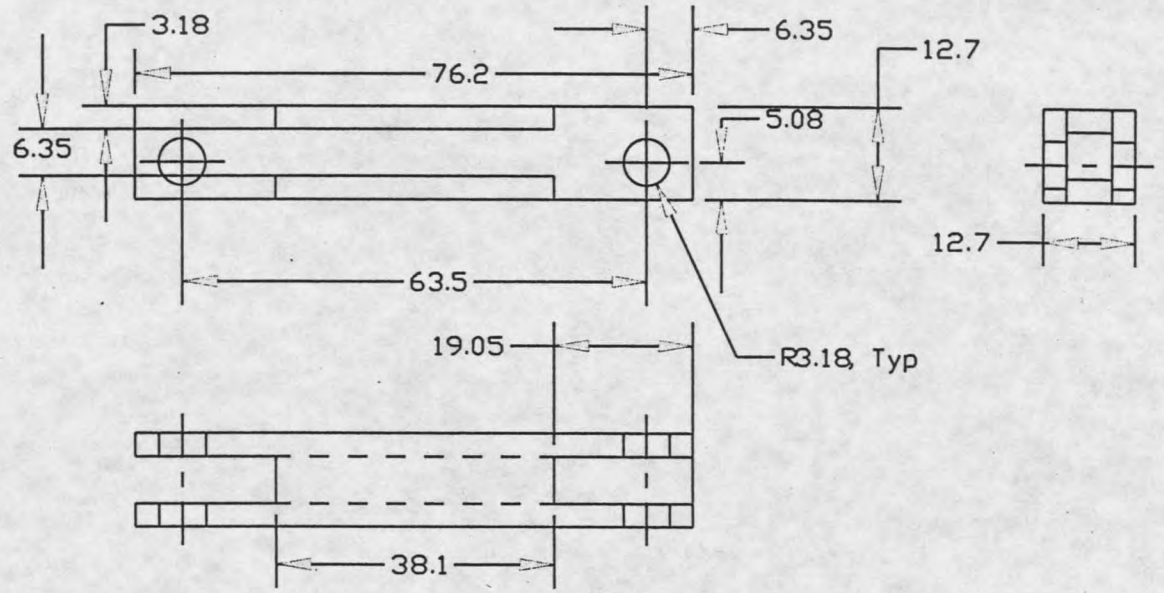
Montana State University

Assembly_Bearing Support

DRAWN A.P	SIZE A	DWG NO. 300
ENGINEER Shane Schumacher		
CREATION DATE 15-Jun-00	SCALE NTS	SHEET 10 of 11

668





TOLERANCES UNLESS NOTED .X = ±.5 .XX = ±.025 ANGULARITY = ±.5° BREAK CORNERS - .010 MAX FILLET RADII - .015 MAX DIMENSIONS ARE IN MM UNLESS NOTED	MATERIAL	.75 Square Tube
	FINISH	None
	Montana State University	
	.75 cutt off Square tube	
DRAWN A.P	SIZE A	DWG NO. 310
ENGINEER Shane Schumacher		
CREATION DATE 15-Jun-00	SCALE NTS	SHEET 11 of 11

699

APPENDIX U

Ongoing Microstructure Analysis and Model Development Based on Current Work

The experimental results obtained for Nylon 6/6 has been used for microstructure analysis and model development. Dr. Rob Winter and Isamu Kitahara performed the microstructure analysis at South Dakota School of Mines and Technology. The test specimens sent to Dr. Winter were from the preliminary testing of Nylon 6/6. The test specimens were analyzed using a Scanning Electron Microscope (SEM) and an Atomic Force Microscope (AFM). From the microstructure analysis, crazes and/or cracks have been found on the surface of the same specimens. The test specimens had been recovering (unloaded) for approximately a month before they were sent to Dr. Winter. The images are shown in Figures U.1 - 8. and a summary of the analysis is provided in Table VI.6.

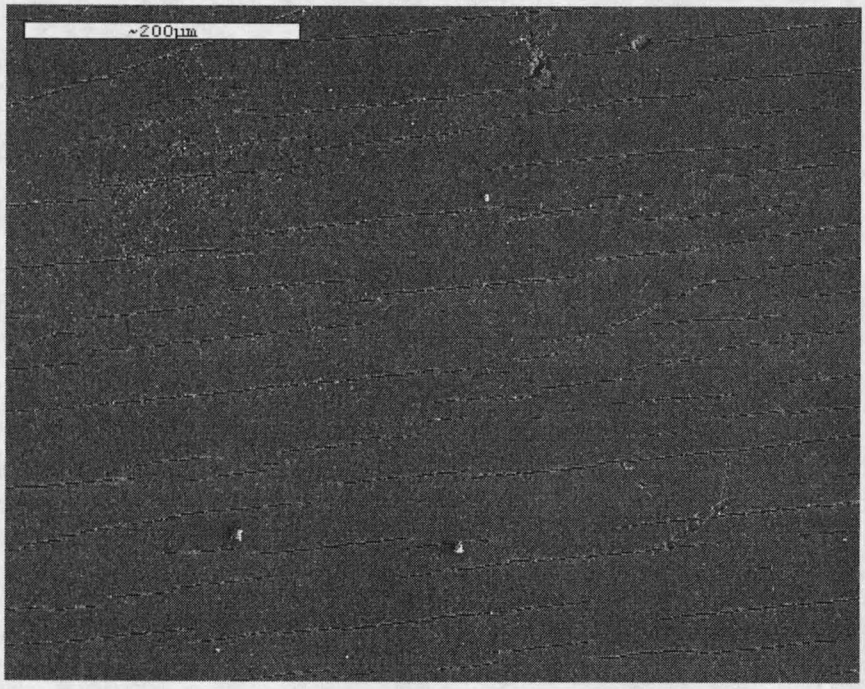


Figure U.1 SEM Image of Vibrocreep Testing at 23 °C
$(0.80\pm0.20)\sigma_y$, 20 Hz, σ_y = 70 MPa at 23 °C

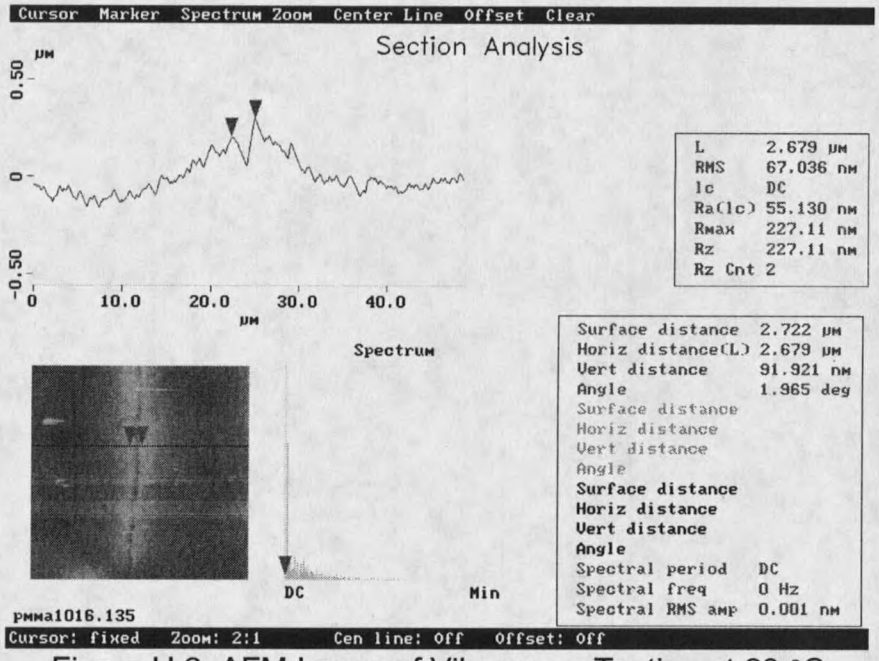


Figure U.2 AFM Image of Vibrocreep Testing at 23 °C
$(0.80\pm0.20)\sigma_y$, 20 Hz, σ_y = 70 MPa at 23 °C

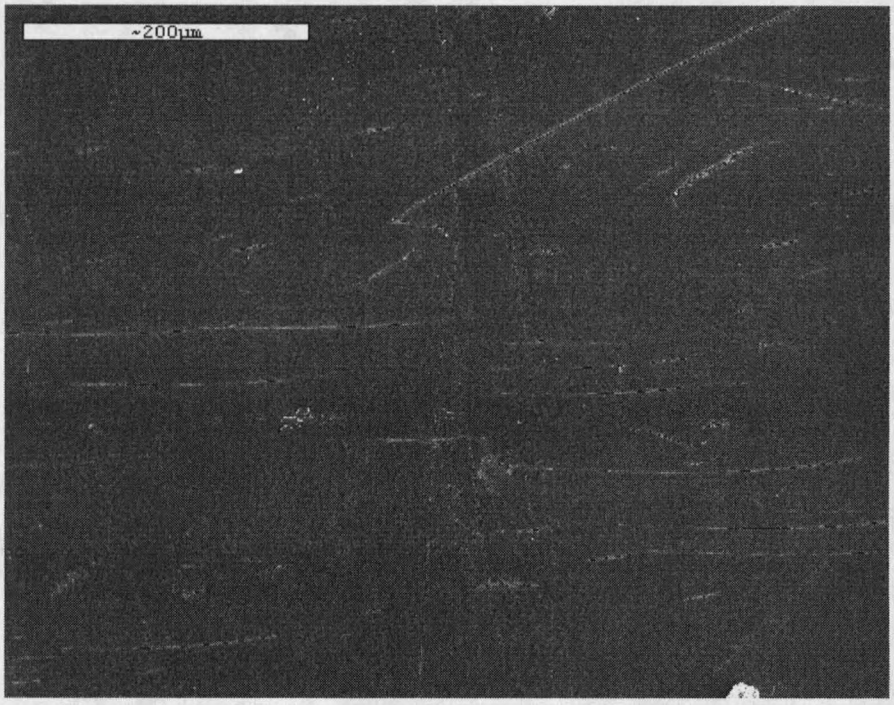


Figure U.3 SEM Image of Vibrocreep Testing at 23 °C
$(0.80\pm0.10)\sigma_y$, 20 Hz, σ_y = 70 MPa at 23 °C

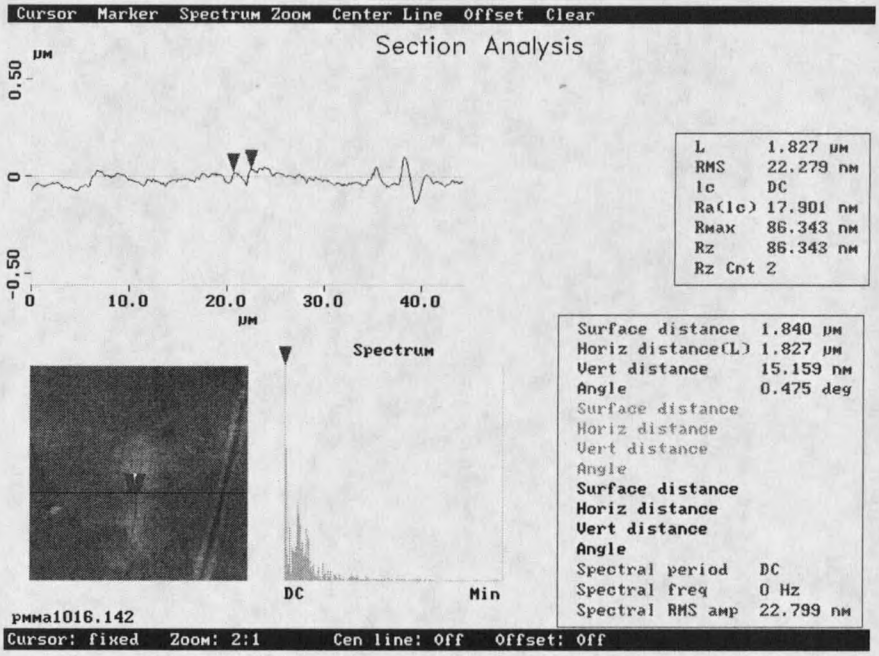


Figure U.4 AFM Image of Vibrocreep Testing at 23 °C
$(0.80\pm0.10)\sigma_y$, 20 Hz, σ_y = 70 MPa at 23 °C

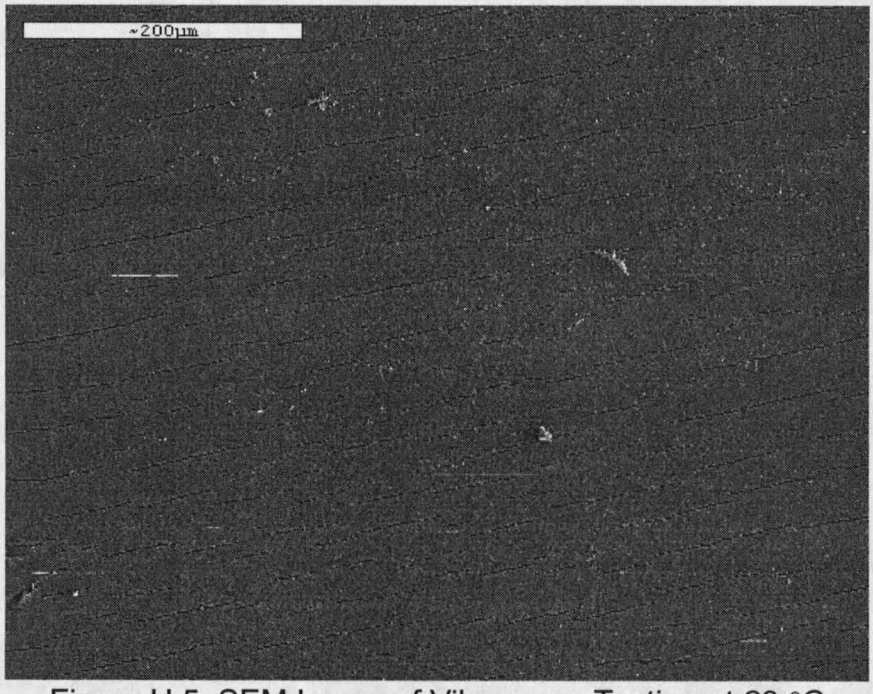


Figure U.5 SEM Image of Vibrocreep Testing at 23 °C
$(0.80\pm0.20)\sigma_y$, 10 Hz, σ_y = 70 MPa at 23 °C

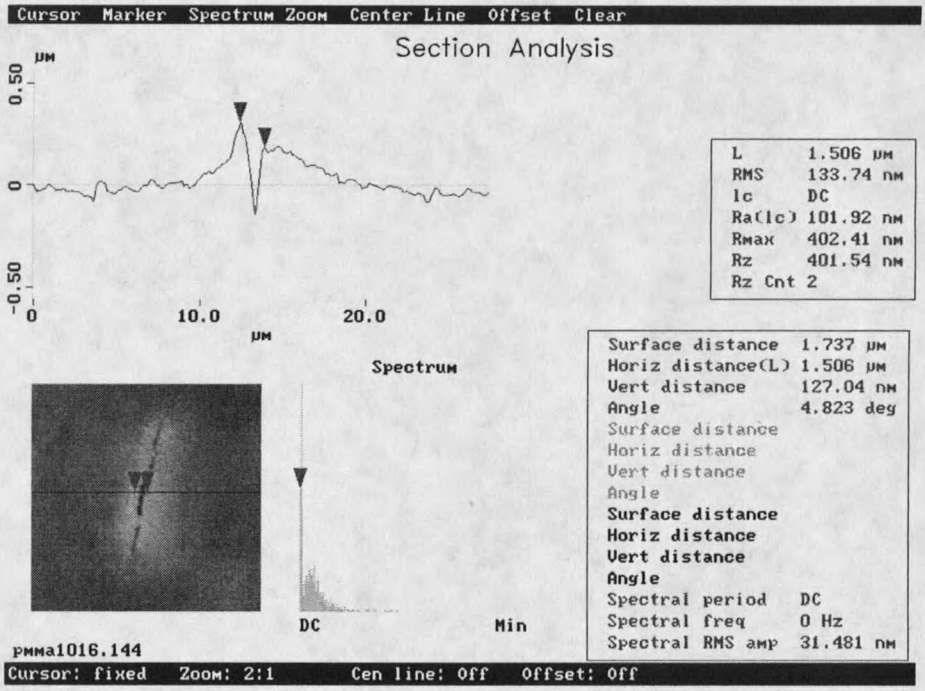


Figure U.6 AFM Image of Vibrocreep Testing at 23 °C
$(0.80\pm0.20)\sigma_y$, 10 Hz, σ_y = 70 MPa at 23 °C

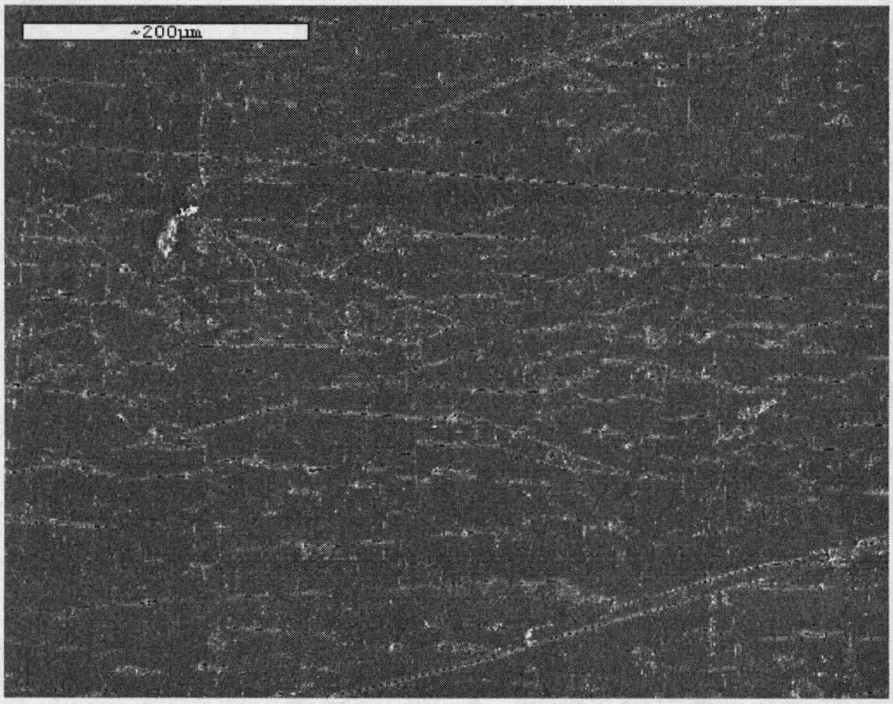


Figure U.7 SEM Image of Vibrocreep Testing at 23 °C
$(0.60\pm0.20)\sigma_y$, 10 Hz, σ_y = 70 MPa at 23 °C

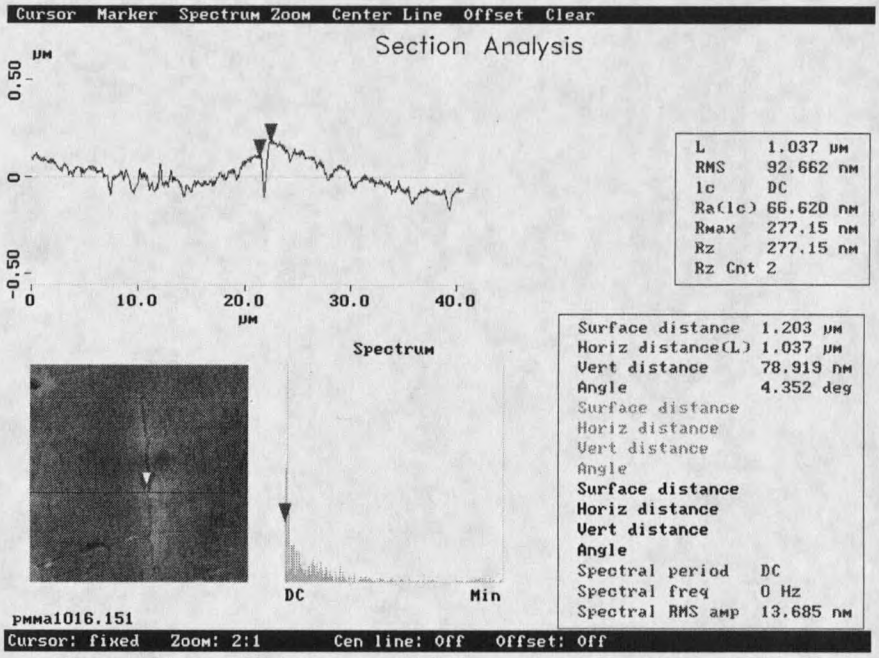


Figure U.8 AFM Image of Vibrocreep Testing at 23 °C
$(0.60\pm0.20)\sigma_y$, 0 Hz, σ_y = 70 MPa at 23 °C

Table U.1 Results of the Microstructure Analysis

Test #	Mean Stress	Amplitude	Frequency	Periodicity (μm)	Craze and/or Crack Density ($1/mm^2$)	Width (μm)
1	80%	20%	20	23.0769	540	2.679
2	80%	10%	20	42.8571	260	1.827
3	80%	20%	10	9.8361	1040	1.506
4	60%	20%	10	15.0000	680	1.037

The creep testing did not exhibit craze formations on the surface along with a few of the vibrocreep test specimens. From the microstructure analysis performed by Dr. Winter, the results were analyzed and compared on a macroscopic level by the author. Using the results from the micro to macro analysis the vibrocreep curve could be approximated from the creep curve at the end of the each test. The periodicity and density results are from the SEM

images, and the width is from the AFM images. Two methods are proposed to calculate the strain due to the crazes and/or cracks formation, one using the craze and/or crack periodicity and the second using the craze and/or crack density. The two methods are shown in Equations U.1 and U.2.

$$\frac{L_g}{P}\cdot\frac{C_w}{L_g}=\frac{C_w}{P}=\varepsilon_{Craze}$$

Equation U.1

$$\frac{L_g\cdot S\cdot D\cdot C_w}{L_g}=D\cdot S\cdot C_w=\varepsilon_{Craze}$$

Equation U.2

L_g = Gage Length (mm), S = Specimen Width (mm), C_w = Craze and/or Crack Width (μm), P = Periodicity (μm), $\varepsilon_{Craze.}$ = Strain Due To Craze and/or Crack, D = Density of Crazes and/or Cracks ($1/mm^2$)

The results are shown in Figure U.9 for a particular case and tabulated in Table VI.7-8 with error calculations. Strain values from creep or vibrocreep testing must be taken at the time at which the test is completed creep or vibrocreep. The equation used for calculation of error is shown at Equation U.3.

$$\text{Error} = \left| \frac{\text{Experimental - Calculated}}{\text{Experimental}} \right| \cdot 100$$

Equation U.3

The micro structural analysis was therefore continued and more testing was performed at the higher stress levels. The creep test specimens for the preliminary creep testing were also analyzed without evidence of surface crazing and/or cracking. The tests were performed for only a 12 hr. period rather than the 24 hr. period as with preliminary tests. The results of the microstructure analysis show that the craze and/or crack formations on the surface are most likely highly time dependent, since craze and/or crack formations were not seen after 12 hr. of testing at the same loading and environmental conditions as with the 24 hr. test with exhibited such defects.

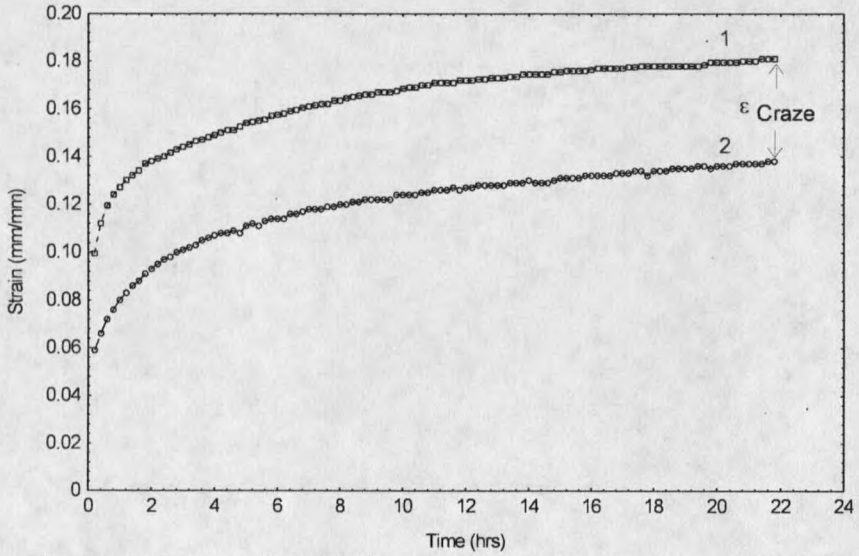


Figure U.9 Results of Vibrocreep Approximation at 23 °C
$(0.80\pm0.10)\sigma_y$, 20 Hz, σ_y = 70 MPa at 23 °C

Table U.2 Results of Equation VI.1 Micro to Macroscopic Analysis

Test #	Constant Load Creep (mm/mm)	Vibrocreep (mm/mm)	ε_{Craze}	Static + ε_{Craze}	Error (%)
1	.132	.2315	.11609	.24809	7.16
2	.138	.181	.04263	.18063	.21
3	.139	.233	.15311	.29211	25.4
4	.081	.128	.06913	.20813	62.6

Table U.3 Results of Equation VI.2 Micro to Macroscopic Analysis

Test #	Specimen Width (mm)	Constant Load Creep (mm/mm)	Vibrocreep (mm/mm)	ε_{Craze}	Static + ε_{Craze}	Error (%)
1	6.76	.132	.2315	.009779	.141779	39
2	6.26	.138	.181	.002974	140974	22.1
3	6.73	.139	.233	.01054	.14654	17.6
4	6.71	.081	.128	.00473	.08753	33

The model development to represent the vibrocreep phenomena is being performed by an exchange professor from Russia Dr. Iakov Klebanov and a fellow graduate student Carl Thrasher. A model has been developed and used to approximate Low Density Polyethylene from literature results. Currently work is being performed using the creep and vibrocreep data shown within the thesis to further support the model. The vibrocreep model is based on damage accumulation from cyclic loading. Damage accumulation is not used in creep models since damage does not exist until the tertiary creep stages, where with vibrocreep the damage is most likely initiated at the onset of the vibration loading. The verification and application to Nylon 6/6 is currently being performed. The creep test data is being used to develop a T-t and σ-t analogy.

From the creep test data, the prediction of creep test is therefore achieved. The results for 23 °C are shown in Figure VI.30. The modeling of the vibrocreep effect in Nylon 6/6 is currently being performed.

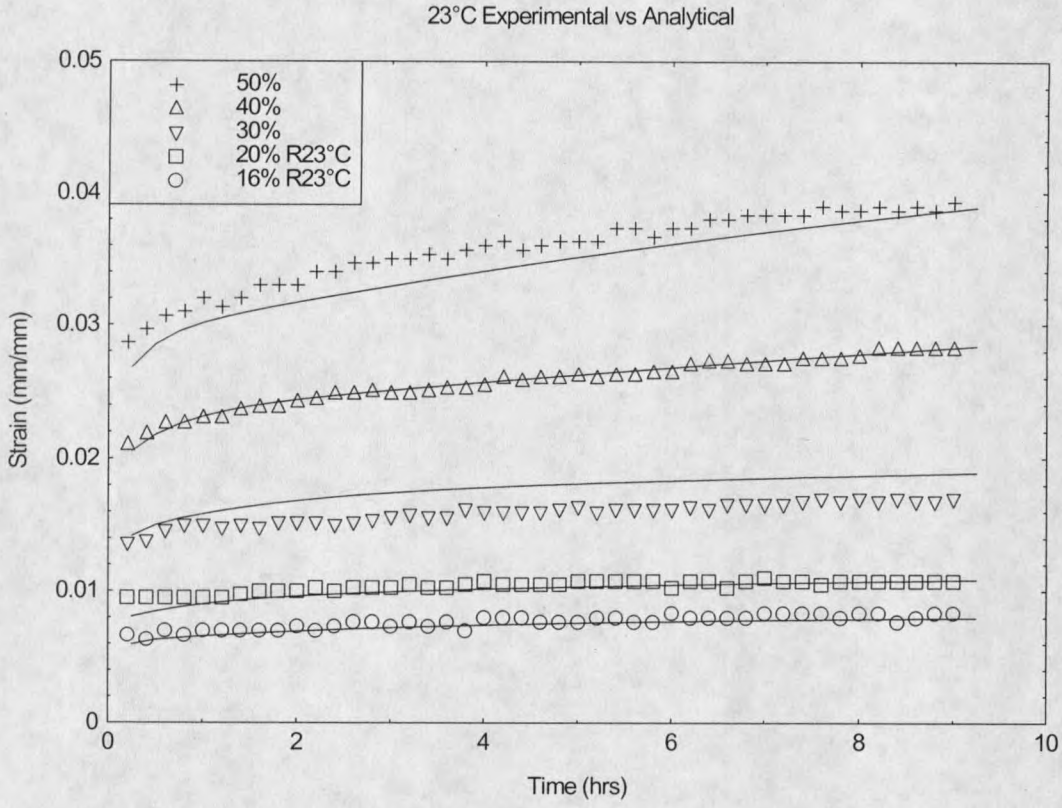


Figure U.10 Modeling results vs. Experimental Results

MONTANA STATE UNIVERSITY - BOZEMAN
3 1762 10338538 9